APPLIED COMBUSTION

Second Edition

MECHANICAL ENGINEERING
A Series of Textbooks and Reference Books

Founding Editor

L. L. Faulkner

Columbus Division, Battelle Memorial Institute
and Department of Mechanical Engineering
The Ohio State University
Columbus, Ohio

1. *Spring Designer's Handbook*, Harold Carlson
2. *Computer-Aided Graphics and Design*, Daniel L. Ryan
3. *Lubrication Fundamentals*, J. George Wills
4. *Solar Engineering for Domestic Buildings*, William A. Himmelman
5. *Applied Engineering Mechanics: Statics and Dynamics*, G. Boothroyd and C. Poli
6. *Centrifugal Pump Clinic*, Igor J. Karassik
7. *Computer-Aided Kinetics for Machine Design*, Daniel L. Ryan
8. *Plastics Products Design Handbook, Part A: Materials and Components; Part B: Processes and Design for Processes*, edited by Edward Miller
9. *Turbomachinery: Basic Theory and Applications*, Earl Logan, Jr.
10. *Vibrations of Shells and Plates*, Werner Soedel
11. *Flat and Corrugated Diaphragm Design Handbook*, Mario Di Giovanni
12. *Practical Stress Analysis in Engineering Design*, Alexander Blake
13. *An Introduction to the Design and Behavior of Bolted Joints*, John H. Bickford
14. *Optimal Engineering Design: Principles and Applications*, James N. Siddall
15. *Spring Manufacturing Handbook*, Harold Carlson
16. *Industrial Noise Control: Fundamentals and Applications*, edited by Lewis H. Bell
17. *Gears and Their Vibration: A Basic Approach to Understanding Gear Noise*, J. Derek Smith
18. *Chains for Power Transmission and Material Handling: Design and Applications Handbook*, American Chain Association
19. *Corrosion and Corrosion Protection Handbook*, edited by Philip A. Schweitzer
20. *Gear Drive Systems: Design and Application*, Peter Lynwander
21. *Controlling In-Plant Airborne Contaminants: Systems Design and Calculations*, John D. Constance
22. *CAD/CAM Systems Planning and Implementation*, Charles S. Knox
23. *Probabilistic Engineering Design: Principles and Applications*, James N. Siddall
24. *Traction Drives: Selection and Application*, Frederick W. Heilich III and Eugene E. Shube
25. *Finite Element Methods: An Introduction*, Ronald L. Huston and Chris E. Passerello
26. *Mechanical Fastening of Plastics: An Engineering Handbook*, Brayton Lincoln, Kenneth J. Gomes, and James F. Braden
27. *Lubrication in Practice: Second Edition*, edited by W. S. Robertson
28. *Principles of Automated Drafting*, Daniel L. Ryan
29. *Practical Seal Design*, edited by Leonard J. Martini
30. *Engineering Documentation for CAD/CAM Applications*, Charles S. Knox
31. *Design Dimensioning with Computer Graphics Applications*, Jerome C. Lange
32. *Mechanism Analysis: Simplified Graphical and Analytical Techniques*, Lyndon O. Barton

33. *CAD/CAM Systems: Justification, Implementation, Productivity Measurement*, Edward J. Preston, George W. Crawford, and Mark E. Coticchia
34. *Steam Plant Calculations Manual*, V. Ganapathy
35. *Design Assurance for Engineers and Managers*, John A. Burgess
36. *Heat Transfer Fluids and Systems for Process and Energy Applications*, Jasbir Singh
37. *Potential Flows: Computer Graphic Solutions*, Robert H. Kirchhoff
38. *Computer-Aided Graphics and Design: Second Edition*, Daniel L. Ryan
39. *Electronically Controlled Proportional Valves: Selection and Application*, Michael J. Tonyan, edited by Tobi Goldoftas
40. *Pressure Gauge Handbook*, AMETEK, U.S. Gauge Division, edited by Philip W. Harland
41. *Fabric Filtration for Combustion Sources: Fundamentals and Basic Technology*, R. P. Donovan
42. *Design of Mechanical Joints*, Alexander Blake
43. *CAD/CAM Dictionary*, Edward J. Preston, George W. Crawford, and Mark E. Coticchia
44. *Machinery Adhesives for Locking, Retaining, and Sealing*, Girard S. Haviland
45. *Couplings and Joints: Design, Selection, and Application*, Jon R. Mancuso
46. *Shaft Alignment Handbook*, John Piotrowski
47. *BASIC Programs for Steam Plant Engineers: Boilers, Combustion, Fluid Flow, and Heat Transfer*, V. Ganapathy
48. *Solving Mechanical Design Problems with Computer Graphics*, Jerome C. Lange
49. *Plastics Gearing: Selection and Application*, Clifford E. Adams
50. *Clutches and Brakes: Design and Selection*, William C. Orthwein
51. *Transducers in Mechanical and Electronic Design*, Harry L. Trietley
52. *Metallurgical Applications of Shock-Wave and High-Strain-Rate Phenomena*, edited by Lawrence E. Murr, Karl P. Staudhammer, and Marc A. Meyers
53. *Magnesium Products Design*, Robert S. Busk
54. *How to Integrate CAD/CAM Systems: Management and Technology*, William D. Engelke
55. *Cam Design and Manufacture: Second Edition; with cam design software for the IBM PC and compatibles*, disk included, Preben W. Jensen
56. *Solid-State AC Motor Controls: Selection and Application*, Sylvester Campbell
57. *Fundamentals of Robotics*, David D. Ardayfio
58. *Belt Selection and Application for Engineers*, edited by Wallace D. Erickson
59. *Developing Three-Dimensional CAD Software with the IBM PC*, C. Stan Wei
60. *Organizing Data for CIM Applications*, Charles S. Knox, with contributions by Thomas C. Boos, Ross S. Culverhouse, and Paul F. Muchnicki
61. *Computer-Aided Simulation in Railway Dynamics*, by Rao V. Dukkipati and Joseph R. Amyot
62. *Fiber-Reinforced Composites: Materials, Manufacturing, and Design*, P. K. Mallick
63. *Photoelectric Sensors and Controls: Selection and Application*, Scott M. Juds
64. *Finite Element Analysis with Personal Computers*, Edward R. Champion, Jr. and J. Michael Ensminger
65. *Ultrasonics: Fundamentals, Technology, Applications: Second Edition, Revised and Expanded*, Dale Ensminger
66. *Applied Finite Element Modeling: Practical Problem Solving for Engineers*, Jeffrey M. Steele
67. *Measurement and Instrumentation in Engineering: Principles and Basic Laboratory Experiments*, Francis S. Tse and Ivan E. Morse
68. *Centrifugal Pump Clinic: Second Edition, Revised and Expanded*, Igor J. Karassik
69. *Practical Stress Analysis in Engineering Design: Second Edition, Revised and Expanded*, Alexander Blake
70. *An Introduction to the Design and Behavior of Bolted Joints: Second Edition, Revised and Expanded*, John H. Bickford
71. *High Vacuum Technology: A Practical Guide*, Marsbed H. Hablanian

72. *Pressure Sensors: Selection and Application*, Duane Tandeske
73. *Zinc Handbook: Properties, Processing, and Use in Design*, Frank Porter
74. *Thermal Fatigue of Metals*, Andrzej Weronski and Tadeusz Hejwowski
75. *Classical and Modern Mechanisms for Engineers and Inventors*, Preben W. Jensen
76. *Handbook of Electronic Package Design*, edited by Michael Pecht
77. *Shock-Wave and High-Strain-Rate Phenomena in Materials*, edited by Marc A. Meyers, Lawrence E. Murr, and Karl P. Staudhammer
78. *Industrial Refrigeration: Principles, Design and Applications*, P. C. Koelet
79. *Applied Combustion*, Eugene L. Keating
80. *Engine Oils and Automotive Lubrication*, edited by Wilfried J. Bartz
81. *Mechanism Analysis: Simplified and Graphical Techniques, Second Edition, Revised and Expanded*, Lyndon O. Barton
82. *Fundamental Fluid Mechanics for the Practicing Engineer*, James W. Murdock
83. *Fiber-Reinforced Composites: Materials, Manufacturing, and Design, Second Edition, Revised and Expanded*, P. K. Mallick
84. *Numerical Methods for Engineering Applications*, Edward R. Champion, Jr.
85. *Turbomachinery: Basic Theory and Applications, Second Edition, Revised and Expanded*, Earl Logan, Jr.
86. *Vibrations of Shells and Plates: Second Edition, Revised and Expanded*, Werner Soedel
87. *Steam Plant Calculations Manual: Second Edition, Revised and Expanded*, V. Ganapathy
88. *Industrial Noise Control: Fundamentals and Applications, Second Edition, Revised and Expanded*, Lewis H. Bell and Douglas H. Bell
89. *Finite Elements: Their Design and Performance*, Richard H. MacNeal
90. *Mechanical Properties of Polymers and Composites: Second Edition, Revised and Expanded*, Lawrence E. Nielsen and Robert F. Landel
91. *Mechanical Wear Prediction and Prevention*, Raymond G. Bayer
92. *Mechanical Power Transmission Components*, edited by David W. South and Jon R. Mancuso
93. *Handbook of Turbomachinery*, edited by Earl Logan, Jr.
94. *Engineering Documentation Control Practices and Procedures*, Ray E. Monahan
95. *Refractory Linings Thermomechanical Design and Applications*, Charles A. Schacht
96. *Geometric Dimensioning and Tolerancing: Applications and Techniques for Use in Design, Manufacturing, and Inspection*, James D. Meadows
97. *An Introduction to the Design and Behavior of Bolted Joints: Third Edition, Revised and Expanded*, John H. Bickford
98. *Shaft Alignment Handbook: Second Edition, Revised and Expanded*, John Piotrowski
99. *Computer-Aided Design of Polymer-Matrix Composite Structures*, edited by Suong Van Hoa
100. *Friction Science and Technology*, Peter J. Blau
101. *Introduction to Plastics and Composites: Mechanical Properties and Engineering Applications*, Edward Miller
102. *Practical Fracture Mechanics in Design*, Alexander Blake
103. *Pump Characteristics and Applications*, Michael W. Volk
104. *Optical Principles and Technology for Engineers*, James E. Stewart
105. *Optimizing the Shape of Mechanical Elements and Structures*, A. A. Seireg and Jorge Rodriguez
106. *Kinematics and Dynamics of Machinery*, Vladimír Stejskal and Michael Valásek
107. *Shaft Seals for Dynamic Applications*, Les Horve
108. *Reliability-Based Mechanical Design*, edited by Thomas A. Cruse
109. *Mechanical Fastening, Joining, and Assembly*, James A. Speck
110. *Turbomachinery Fluid Dynamics and Heat Transfer*, edited by Chunill Hah
111. *High-Vacuum Technology: A Practical Guide, Second Edition, Revised and Expanded*, Marsbed H. Hablanian

112. *Geometric Dimensioning and Tolerancing: Workbook and Answerbook*, James D. Meadows
113. *Handbook of Materials Selection for Engineering Applications,* edited by G. T. Murray
114. *Handbook of Thermoplastic Piping System Design*, Thomas Sixsmith and Reinhard Hanselka
115. *Practical Guide to Finite Elements: A Solid Mechanics* Approach, Steven M. Lepi
116. *Applied Computational Fluid Dynamics*, edited by Vijay K. Garg
117. *Fluid Sealing Technology*, Heinz K. Muller and Bernard S. Nau
118. *Friction and Lubrication in Mechanical Design*, A. A. Seireg
119. *Influence Functions and Matrices*, Yuri A. Melnikov
120. *Mechanical Analysis of Electronic Packaging Systems*, Stephen A. McKeown
121. *Couplings and Joints: Design, Selection, and Application, Second Edition, Revised and Expanded*, Jon R. Mancuso
122. *Thermodynamics: Processes and Applications*, Earl Logan, Jr.
123. *Gear Noise and Vibration*, J. Derek Smith
124. *Practical Fluid Mechanics for Engineering Applications*, John J. Bloomer
125. *Handbook of Hydraulic Fluid Technology*, edited by George E. Totten
126. *Heat Exchanger Design Handbook*, T. Kuppan
127. *Designing for Product Sound Quality*, Richard H. Lyon
128. *Probability Applications in Mechanical Design*, Franklin E. Fisher and Joy R. Fisher
129. *Nickel Alloys*, edited by Ulrich Heubner
130. *Rotating Machinery Vibration: Problem Analysis and Troubleshooting*, Maurice L. Adams, Jr.
131. *Formulas for Dynamic Analysis*, Ronald L. Huston and C. Q. Liu
132. *Handbook of Machinery Dynamics*, Lynn L. Faulkner and Earl Logan, Jr.
133. *Rapid Prototyping Technology: Selection and Application*, Kenneth G. Cooper
134. *Reciprocating Machinery Dynamics: Design and Analysis*, Abdulla S. Rangwala
135. *Maintenance Excellence: Optimizing Equipment Life-Cycle Decisions*, edited by John D. Campbell and Andrew K. S. Jardine
136. *Practical Guide to Industrial Boiler Systems*, Ralph L. Vandagriff
137. *Lubrication Fundamentals: Second Edition, Revised and Expanded*, D. M. Pirro and A. A. Wessol
138. *Mechanical Life Cycle Handbook: Good Environmental Design and Manufacturing*, edited by Mahendra S. Hundal
139. *Micromachining of Engineering Materials*, edited by Joseph McGeough
140. *Control Strategies for Dynamic Systems: Design and Implementation*, John H. Lumkes, Jr.
141. *Practical Guide to Pressure Vessel Manufacturing*, Sunil Pullarcot
142. *Nondestructive Evaluation: Theory, Techniques, and Applications*, edited by Peter J. Shull
143. *Diesel Engine Engineering: Thermodynamics, Dynamics, Design, and Control*, Andrei Makartchouk
144. *Handbook of Machine Tool Analysis*, Ioan D. Marinescu, Constantin Ispas, and Dan Boboc
145. *Implementing Concurrent Engineering in Small Companies*, Susan Carlson Skalak
146. *Practical Guide to the Packaging of Electronics: Thermal and Mechanical Design and Analysis*, Ali Jamnia
147. *Bearing Design in Machinery: Engineering Tribology and Lubrication*, Avraham Harnoy
148. *Mechanical Reliability Improvement: Probability and Statistics for Experimental Testing*, R. E. Little
149. *Industrial Boilers and Heat Recovery Steam Generators: Design, Applications, and Calculations*, V. Ganapathy
150. *The CAD Guidebook: A Basic Manual for Understanding and Improving Computer-Aided Design*, Stephen J. Schoonmaker
151. *Industrial Noise Control and Acoustics*, Randall F. Barron

152. *Mechanical Properties of Engineered Materials*, Wolé Soboyejo
153. *Reliability Verification, Testing, and Analysis in Engineering Design*, Gary S. Wasserman
154. *Fundamental Mechanics of Fluids: Third Edition*, I. G. Currie
155. *Intermediate Heat Transfer*, Kau-Fui Vincent Wong
156. *HVAC Water Chillers and Cooling Towers: Fundamentals, Application, and Operation*, Herbert W. Stanford III
157. *Gear Noise and Vibration: Second Edition, Revised and Expanded*, J. Derek Smith
158. *Handbook of Turbomachinery: Second Edition*, *Revised and Expanded,* edited by Earl Logan, Jr. and Ramendra Roy
159. *Piping and Pipeline Engineering: Design, Construction, Maintenance, Integrity, and Repair*, George A. Antaki
160. *Turbomachinery: Design and Theory*, Rama S. R. Gorla and Aijaz Ahmed Khan
161. *Target Costing: Market-Driven Product Design*, M. Bradford Clifton, Henry M. B. Bird, Robert E. Albano, and Wesley P. Townsend
162. *Fluidized Bed Combustion*, Simeon N. Oka
163. *Theory of Dimensioning: An Introduction to Parameterizing Geometric Models*, Vijay Srinivasan
164. *Handbook of Mechanical Alloy Design*, edited by George E. Totten, Lin Xie, and Kiyoshi Funatani
165. *Structural Analysis of Polymeric Composite Materials*, Mark E. Tuttle
166. *Modeling and Simulation for Material Selection and Mechanical Design*, edited by George E. Totten, Lin Xie, and Kiyoshi Funatani
167. *Handbook of Pneumatic Conveying Engineering*, David Mills, Mark G. Jones, and Vijay K. Agarwal
168. *Clutches and Brakes: Design and Selection, Second Edition*, William C. Orthwein
169. *Fundamentals of Fluid Film Lubrication: Second Edition*, Bernard J. Hamrock, Steven R. Schmid, and Bo O. Jacobson
170. *Handbook of Lead-Free Solder Technology for Microelectronic Assemblies*, edited by Karl J. Puttlitz and Kathleen A. Stalter
171. *Vehicle Stability*, Dean Karnopp
172. *Mechanical Wear Fundamentals and Testing: Second Edition, Revised and Expanded*, Raymond G. Bayer
173. *Liquid Pipeline Hydraulics*, E. Shashi Menon
174. *Solid Fuels Combustion and Gasification*, Marcio L. de Souza-Santos
175. *Mechanical Tolerance Stackup and Analysis*, Bryan R. Fischer
176. *Engineering Design for Wear,* Raymond G. Bayer
177. *Vibrations of Shells and Plates: Third Edition, Revised and Expanded*, Werner Soedel
178. *Refractories Handbook*, edited by Charles A. Schacht
179. *Practical Engineering Failure Analysis*, Hani M. Tawancy, Anwar Ul-Hamid, and Nureddin M. Abbas
180. *Mechanical Alloying and Milling*, C. Suryanarayana
181. *Mechanical Vibration: Analysis, Uncertainties, and Control, Second Edition, Revised and Expanded*, Haym Benaroya
182. *Design of Automatic Machinery*, Stephen J. Derby
183. *Practical Fracture Mechanics in Design: Second Edition, Revised and Expanded*, Arun Shukla
184. *Practical Guide to Designed Experiments*, Paul D. Funkenbusch
185. *Gigacycle Fatigue in Mechanical Practive*, Claude Bathias and Paul C. Paris
186. *Selection of Engineering Materials and Adhesives*, Lawrence W. Fisher
187. *Boundary Methods: Elements, Contours, and Nodes*, Subrata Mukherjee and Yu Xie Mukherjee
188. *Rotordynamics*, Agnieszka (Agnes) Muszńyska
189. *Pump Characteristics and Applications: Second Edition*, Michael W. Volk
190. *Reliability Engineering: Probability Models and Maintenance Methods*, Joel A. Nachlas

191. *Industrial Heating: Principles, Techniques, Materials, Applications, and Design*, Yeshvant V. Deshmukh
192. *Micro Electro Mechanical System Design*, James J. Allen
193. *Probability Models in Engineering and Science*, Haym Benaroya and Seon Han
194. *Damage Mechanics*, George Z. Voyiadjis and Peter I. Kattan
195. *Standard Handbook of Chains: Chains for Power Transmission and Material Handling, Second Edition*, American Chain Association and John L. Wright, Technical Consultant
196. *Standards for Engineering Design and Manufacturing*, Wasim Ahmed Khan and Abdul Raouf S.I.
197. *Maintenance, Replacement, and Reliability: Theory and Applications*, Andrew K. S. Jardine and Albert H. C. Tsang
198. *Finite Element Method: Applications in Solids, Structures, and Heat Transfer*, Michael R. Gosz
199. *Microengineering, MEMS, and Interfacing: A Practical Guide*, Danny Banks
200. *Fundamentals of Natural Gas Processing*, Arthur J. Kidnay and William Parrish
201. *Optimal Control of Induction Heating Processes*, Edgar Rapoport and Yulia Pleshivtseva
202. *Practical Plant Failure Analysis: A Guide to Understanding Machinery Deterioration and Improving Equipment Reliability*, Neville W. Sachs, P.E.
203. *Shaft Alignment Handbook, Third Edition*, John Piotrowski
204. *Advanced Vibration Analysis* , S. Graham Kelly
205. *Principles of Composite Materials Mechanics, Second Edition*, Ronald F. Gibson
206. *Applied Combustion, Second Edition*, Eugene L. Keating

APPLIED COMBUSTION

Second Edition

Eugene L. Keating
Environmental Kinetics, Ltd.
Arnold, Maryland

CRC Press
Taylor & Francis Group
Boca Raton London New York

CRC Press is an imprint of the
Taylor & Francis Group, an informa business

CRC Press
Taylor & Francis Group
6000 Broken Sound Parkway NW, Suite 300
Boca Raton, FL 33487-2742

Printed in the United States of America on acid-free paper
10 9 8 7 6 5 4 3 2 1

International Standard Book Number-10: 1-57444-640-1 (Hardcover)
International Standard Book Number-13: 978-1-57444-640-1 (Hardcover)

Library of Congress Cataloging-in-Publication Data

Keating, Eugene L., 1944-
Applied combustion / Eugene Keating. -- 2nd ed.
p. cm. -- (A series of textbooks and reference books)
Includes bibliographical references and index.
ISBN-13: 978-1-57444-640-1 (alk. paper)
ISBN-10: 1-57444-640-1 (alk. paper)
1. Combustion engineering. I. Title. II. Series.

TJ254.5.K43 2006
621.402'3--dc22 2006038163

Visit the Taylor & Francis Web site at
http://www.taylorandfrancis.com

and the CRC Press Web site at
http://www.crcpress.com

Preface to Second Edition

The second edition of *Applied Combustion* will provide its readers with an expanded and updated version of the earlier edition. I anticipate that this second edition will be a source of valuable information for those whose careers involve efforts to advance applied combustion through activities in academic, industrial, and government programs. The subject matter and presentation may be valuable for use in upper-level undergraduate and graduate education, research and development, as well as professional engineering societies.

Basic precepts found in early chapters have been rearranged so that they are developed progressively and thereby utilized more efficiently in later chapters. In the initial chapters, the fundamentals of combustion thermochemistry are still formulated from general principles of chemistry, physics, and thermodynamics. A variety of subject areas are covered, including the ideal oxidation-reaction equation, fuel heat release rates, and incomplete combustion. An expanded discussion of chemical equilibrium has been provided with an extended discussion on fuel cells. The theory of detonation and thermal explosions, collision theory and chemical reactions, as well as basic flame theory have been relocated in the new edition for better continuity of text. The chapter concerning chemical kinetics of combustion now includes a presentation of the important nitrogen-oxygen reaction system. Characteristics of chemical energy resources, or fuels, such as coal, distillates derived from crude oil, alcohols, syncrudes, bio-gas, natural gas, and hydrogen, are treated in detail in the chapters that follow, including material on environmental topics related to their use. The combustion engine chapters contain added coverage of environmental aspects relating to specific combustion characteristics. A new final applied combustion chapter covers the thermal destruction of particular waste materials generated by modern industrial societies.

My career has been shaped by contributions from numerous individuals and institutions including fellow faculty members at the U.S. Merchant Marine and U.S. Naval Academies and the University of Maryland, as well as members of the Society of Automotive Engineers and American Society of Mechanical Engineers. In addition, I have benefited greatly from interaction with many of the customers, such as organizations within the Department of the Navy, with whom I have worked through Environmental Kinetics Ltd. It was while working with my colleagues in these

institutions and professional societies that much of the philosophy and specific material for this manuscript evolved. A special debt of gratitude and acknowledgment is due my wife, Doris, for her support throughout my career, and specifically for her work as both editor and typesetter on the manuscript for the second edition.

Eugene L. Keating

Preface to First Edition

Today's world requires that undergraduate engineering education produce graduates having a broad foundation in technical as well as scientific principles of energy conservation and conversion. In addition, engineers and scientists are now needed who can utilize concepts of physics and chemistry to design, develop, operate, and/or maintain current or future energy-consuming machinery. Many texts and references have been written in specific areas of energy, such as thermodynamics, internal combustion engines, gas turbines, chemical kinetics, and flame theory. Other recent publications have attempted to address, in a single volume, the entire field of current energy conversion engineering, covering topics such as solar, nuclear, geothermal, and wind energy systems. *Applied Combustion* provides its readers with a broad engineering introduction to principles of chemical energy conversion, or combustion, as well as practical applications of those laws to a variety of chemical heat engines.

In the early chapters, fundamentals of combustion are formulated from general principles of chemistry, physics, and thermodynamics. Characteristics of chemical energy resources, or fuels, such as coal, distillates derived from crude oil, alcohols, syncrudes, bio-gas, natural gas, and hydrogen, are treated in detail in the following chapters. The final chapters apply these fundamentals to several combustion engines. Basic precepts found in earlier chapters are arranged so that they are progressively developed and utilized in later chapters.

A variety of subject areas are covered in this book, including the ideal oxidation-reaction equation, fuel heat release rates, chemical equilibrium, incomplete combustion, chemical kinetics, theory of detonation and thermal explosions, as well as basic flame theory. Energy characteristics of equipment utilizing chemical fuels, including boilers, gas turbine combustors, and compression- or spark-ignition internal combustion engines, are reviewed. Example problems illustrate a proper engineering analysis and solution technique as well as important principles relevant to understanding many combustion processes and devices. Emphasis is placed on describing general performance in terms of the concept of fuel–engine compatibility, i.e., fuel consumption rates, pollution characteristics, and various energy conversion efficiency interactions of heat and power machinery.

Currently, only a few publications are available that provide as wide an engineering science introduction to the general subject of combustion as does this work. The use of dual SI and Engineers' dimensions and units, numerous key examples and exercises at the end of each chapter, as well as numerous appendixes, make this book suitable for use as a text in many engineering programs. In addition, the unique bridge between combustion science and combustion technology, thermochemical engineering data, and design formulation of basic performance relationships found in this work should make it a valuable technical reference for many personal and professional engineering libraries.

I hope that this book will stimulate its readers to pursue further this important field of study. Furthermore, I hope that this material will provide a basic foundation for those whose careers involve efforts in current and related areas of engineering activity through graduate education, research and development, and professional engineering societies. Future requirements and advances in applied combustion may have an even greater impact on the power and propulsion fields of aerospace, chemical, marine, and mechanical engineering than have many breakthroughs of the recent past.

I am indebted to numerous individuals and institutions that have contributed over many years to my career. Special acknowledgment is due to my fellow faculty members at the U.S. Merchant Marine and U.S. Naval Academies, as well as members of the Society of Automotive Engineers. It was while working with my colleagues in these institutions that much of the philosophy and specific material for this manuscript evolved.

Eugene L. Keating

About the Author

EUGENE L. KEATING, Ph.D., P.E., as founder and vice president of Environmental Kinetics, Ltd., is currently providing proprietary engineering services as an energy and environmental consultant to specific clients involved in a variety of emerging advanced heat/power concepts that are early in commercial development. He has been a consulting engineer to the Environmental Protection Branch of the U.S. Navy, Naval Surface Warfare Center, Carderock Laboratories, Maryland, providing engineering design input to a variety of environmental issues related to advanced shipboard waste disposal technology and diesel engine emissions. He has been an energy and internal combustion engine technology consultant to the David Taylor Ship Research and Development Center, an emergency diesel generator reliability consultant to the nuclear industry, and a design consultant for advanced engine technologies.

Dr. Keating taught in the thermal power program at the U.S. Merchant Marine Academy for two years prior to teaching thermodynamics, heat transfer, and combustion in the Mechanical Engineering Department at the U.S. Naval Academy for 16 years. For over 10 years Dr. Keating taught Heat Transfer at the Whiting School of Engineering Evening Program, Johns Hopkins University, Baltimore, Maryland. He is currently an adjunct faculty member in the Professional Master of Engineering Program at the University of Maryland, College Park. Dr. Keating is the author or coauthor of many journal articles and technical reports and the coauthor of two additional engineering books. He is a fellow of the American Society of Mechanical Engineers and the Society of Automotive Engineers, served on the SAE International Board of Directors 1991–1993, and is a member of the Combustion Institute. Dr. Keating received the BSME degree (1966) from the University of California, Santa Barbara; the MSME degree (1968) from the University of Michigan, Ann Arbor; and the Ph.D. degree (1973) in mechanical engineering from Drexel University, Philadelphia, Pennsylvania.

Contents

Nomenclature

a	acceleration, m/sec^2, ft/sec^2
a	specific Hemholtz function, J/kg, Btu/lbm
A	generalized chemical compound, i.e., methane, water, etc.
A	area, m^2, ft^2
A	Arrhenius rate constant prefactor
A	total Hemholtz function, J, Btu
AF	air–fuel ratio
$\bar{a}_f^0$	Hemholtz function of formation, J/kgmole, Btu/lbmole
ΔA_c	Hemholtz function of combustion, kJ/kgmole, Btu/lbmole
ΔA_f	Hemholtz function of formation, kJ/kgmole, Btu/lbmole
ΔA_r	Hemholtz function of reaction, kJ/kgmole, Btu/lbmole
$BMEP$	brake mean effective pressure
c	sonic velocity, m/sec, ft/sec
C_p	constant-pressure specific heat, J/kg·K, Btu/lbm·°R
C_v	constant-volume specific heat, J/kg·K, Btu/lbm·°R
d	diameter, m, ft
D	total differential operator
F	force, N, lbf
FA	fuel–air ratio
g	gravitational acceleration, m/sec^2, ft/sec^2
g_0	dimensional constant, 1.0 kg·m/N·sec^2, 32.1724 lbm/lbf·sec^2
g	Gibbs function, J/kg, Btu/lbm
G	total Gibbs function, J, Btu
G	mass flow per unit area, kg/m^2·sec, lbm/ft^2·sec
ΔG_c	Gibbs function of combustion, kJ/kgmole, Btu/lbmole

ΔG_f	Gibbs function of formation, kJ/kgmole, Btu/lbmole
ΔG_r	Gibbs function of reaction, kJ/kgmole, Btu/lbmole
h	specific enthalpy, J/kg, Btu/lbm
H	total enthalpy, J, Btu
h_{fg}	latent heat of vaporization, J/kg, Btu/lbm
$\bar{h}_f^0$	molar enthalpy of formation, J/kgmole, Btu/lbmole
HHV	fuel higher heating value, J/kg, Btu/lbm
ΔH_c	heat of combustion, kJ/kgmole, Btu/lbmole
ΔH_f	heat of formation, kJ/kgmole, Btu/lbmole
ΔH_r	heat of reaction, kJ/kgmole, Btu/lbmole
$IMEP$	indicated mean effective pressure, kPa, psi
k	Arrhenius elemental rate constant
k	Boltzmann's constant
K_c	equilibrium constant based on species concentrations
K_p	equilibrium constant based on partial pressures
L	length, m, ft
LHV	fuel lower heating value, J, Btu
M	total mass, kg, lbm
m_i	mass of species i, kg, lbm
mf_i	mass fraction
MW	molecular weight, kg/kgmole, lbm/lbmole
MEP	mean effective pressure, kPa, lbf
N	number of moles
N	rotational speed, rev/sec
N_m	Mach number
P	pressure, N/m^2 or Pa, $lbf/in.^2$
P_r	relative pressure
q	heat transfer per unit mass, J/kg, Btu/lbm
Q	total heat transfer, J, Btu
R	elementary reaction rate
R	specific gas constant, J/kg·K, Btu/lbm·°R
R_i	reactant species i
r_c	cutoff ratio
r_e	expansion ratio
r_p	pressure ratio
r_v	compression ratio
s	specific entropy, J/kg·K, Btu/lbm·°R
S	total entropy, J, Btu
$\bar{s}_f^0$	molar entropy of formation, J/kgmole, Btu/lbmole
ΔS_c	entropy of combustion, kJ/kgmole, Btu/lbmole
ΔS_f	entropy of formation, kJ/kgmole, Btu/lbmole
ΔS_r	entropy of reaction, kJ/kgmole, Btu/lbmole
$S.G.$	specific gravity

t	time, sec
T	temperature, °C and K, °F and °R
u	specific internal energy, J/kg·K, Btu/lbm·°R
U	total internal energy, J, Btu
$\bar{u}_f^0$	molar internal energy of formation, J/kgmole, Btu/lbmole
ΔU_c	internal energy of combustion, kJ/kgmole, Btu/lbmole
ΔU_f	internal energy of formation, kJ/kgmole, Btu/lbmole
ΔU_r	internal energy of reaction, kJ/kgmole, Btu/lbmole
v	specific volume, m^3/kg, ft^3/lbm
V	total volume, m^3, ft^3
V	velocity, m/sec, ft/sec
V_C	clearance volume, m^3/stroke, ft^3/stroke
V_D	displacement volume, m^3/stroke, ft^3/stroke
w	specific work *m*, J/kg, ft·lbf/lbm
W	total work, J, ft·lbf
W	total weight, N, lbf
$\bar{x}_i$	mole fraction of species *i*
Z	elevation, m, ft
Z_{AB}	collision frequency, number of collisions/sec
δ	differential operator
Δ	finite difference in parameters
γ	specific heat ratio
γ	specific weight, N/m^3, lbf/ft^3
λ	mean free path, cm/collision
η	efficiency (subscript will designate the particular value)
σ	molecular diameter, m^3, ft^3
Σ	summation operator
τ	torque, N·m, ft·lbf
Φ	equivalence ratio
ν	moles of species

Notes on Nomenclature Rules:

A dot over a symbol indicates a derivate with respect to time;

$\dot{Q}$	heat flux, W, Btu/hr
$\dot{W}$	power, W, hp

A bar over a symbol indicates that the parameter is on a mole basis:

$\bar{h}$	molar specific enthalpy, J/kgmole, Btu/lbmole
$\bar{R}$	universal gas constant, J/kgmole·K, Btu/lbmole·°R

An angle bracket $\langle \quad \rangle$ is an operator that implies that the quantity in question is a function of the parameters contained within:

$C_p\langle T\rangle$ constant specific heat is a function of temperature
$V\langle t\rangle$ velocity is a function of time

Subscript *i* or *j* references the quantity of a species *i* or *j*:

MW_i
mf_j

An arrow through a term in an equation means that it vanishes in that equation:

$\not{dE}$

Bibliography

THERMODYNAMICS REFERENCES

Burghardt, M. D., *Engineering Thermodynamics with Applications,* Second Edition, Harper & Row, New York, NY, 1982.

Faires, Y. M. and Simmang, C. M., *Thermodynamics,* Sixth Edition, MacMillan Publishing Co., New York, NY, 1978.

Johnston, R. M., Brockett, W. A., Bock, A. E. and Keating, E. L., *Elements of Applied Thermodynamics*, Naval Institute Press, Annapolis, MD, 1978.

Keenan, J. H., Chao, J., and Kaye, J., *Gas Tables*, John Wiley & Sons, New York, NY, 1980.

———, Keyes, F. G., Hill, P. G., and Moore, J. G., *Steam Tables*, John Wiley & Sons, New York, NY, 1969.

Smith, J. M. and Van Ness, H. C., *Introduction to Chemical Engineering Thermodynamics,* Third Edition, McGraw-Hill, New York, NY, 1975.

Stull, D. R. and Prophet, H., project directors, *JANAF Thermochemical Tables,* Second Edition, U.S. Dept. of Commerce, National Bureau of Standards, Washington, DC, 1971.

Wark, K., *Thermodynamics,* Fourth Edition, McGraw-Hill, New York, NY, 1983.

POWERPLANT ENERGY REFERENCES

Culp, A. W., Jr., *Principles of Energy Conversion*, McGraw-Hill, New York, NY, 1979.

Department of the Navy Energy Fact Book, Navy Publications and Forms Center, Philadelphia, PA, 1979.
El-Wakil, M. M., *Powerplant Technology*, McGraw-Hill, New York, NY, 1984.
Faulkner, E. A., Jr., *Guide to Efficient Burner Operation: Gas, Oil, and Dual Fuel*, Fairmont Press, Atlanta, GA, 1981.
Flack, J., Bennett, A. J. S., Strong, R., and Culver, L. J., *Marine Combustion Practice*, Pergamon Press, London, UK, 1969.
Hoogers, G. editor, *Fuel Cell Technology Handbook*, CRC Press, SAE International, Warrendale, PA, 2000.
Khartchenko, N. V., *Advanced Energy Systems*, Taylor & Francis, Washington, DC, 1998.
Krenz, J. H., *Energy Conversion and Utilization,* Second Edition, Allyn and Bacon, Boston, MA.
O'Hayre, R., Cha, S.-W., Colella, W., and Prinz, F. B., *Fuel Cell Fundamentals*, John Wiley & Sons, New York, NY, 2006.
Sionger, J. G., editor, *Combustion: Fossil Power Systems*, Combustion Engineering, Inc., Windsor, CT, 1981.
Sorensen, H. A., *Energy Conversion Systems*, John Wiley & Sons, New York, NY, 1983.
Staff of Research and Education Association, *Modern Energy Technology, Vol. I and II*, Research and Education Association, New York, NY, 1975.

GENERAL FUELS REFERENCES

Allinson, J. P., editor, *Criteria for Quality of Petroleum Products*, Halsted Press, New York, NY, 1973.
Alternative Fuels, SAE International Congress & Exposition, Detroit, MI, February 23–27, 1981, SAE Publication SP-480, SAE, Warrendale, PA, February 1981.
Alternative Fuels for Maritime Use, Maritime Transportation Research Board, National Academy of Sciences, Washington, DC, 1980.
Anderson, L. L. and Tillman, D. A., *Synthetic Fuels from Coal*, John Wiley & Sons, New York, NY, 1979.
Bastress, E. K., editor, *Gas Turbine Combustion and Fuels Technology*, ASME, New York, NY, 1977.
Benn, P. R., Edewor, J. O., and McAuliffe, C. A., *Production and Utilization of Synthetic Fuels—An Energy Economics Study*, Halsted Press, New York, NY, 1981.
Blackmore, D. R. and Thomas, A., *Fuel Economy of the Gasoline Engine, Fuel, Lubricant and Other Effects*, Halsted Press, New York, NY, 1977.
Bungay, H. R., *Energy, The Biomass Option*, John Wiley & Sons, New York, NY, 1981.
Colucci, J. M. and Gallopoulos, N. E., editors, *Future Automotive Fuels*, Plenum Press, New York, 1977.
Coordinating Research Council, *Handbook of Aviation Fuel Properties*, SAE, Warrendale, PA, 1983.
Ezra, D., *Coal and Energy*, Ernest Benn, London, UK, 1978.
Francis, W. and Peters, M. C., *Fuels and Fuel Technology*, Pergamon Press, New York, NY, 1980.
Goodger, E. M., *Alternative Fuels: Chemical Energy Resources*, Halsted Press, New York, NY, 1980.
———, *Hydrocarbon Fuels Production, Properties and Performance of Liquids and Gases*, Halsted Press, New York, NY, 1975.
Haslam, R. T. and Russell, R. B., *Fuels and Their Combustion*, McGraw-Hill, New York, NY, 1926.
Hirao, O. and Pefley, R. K., *Present and Future Automotive Fuels*, Wiley Interscience, New York, 1988.
Odgers, J. and Kretschmer, D., *Gas Turbine Fuels and Their Influence on Combustion*, Abacus Press, Cambridge, MA, 1986.

Owen, K. and Coley, T., *Automotive Fuels Handbook*, SAE, Warrendale, PA, 1990.
Paul, J. K., editor, *Ethyl Alcohol Production and Use as a Motor Fuel*, Noyes Data Corporation, Park Ridge, NJ, 1979.
———, editor, *Methanol Technology and Application in Motor Fuels*, Noyes Data Corporation, Park Ridge, NJ, 1979.
Porteous, A., *Refuse Derived Fuels*, Applied Science Publishers Ltd., London, UK, 1981.
Probstein, R. F. and Hicks, R. E., *Synthetic Fuels*, McGraw-Hill, New York, NY, 1982.
Rider, D. K., *Energy: Hydrocarbon Fuels and Chemical Resources*, John Wiley & Sons, New York, NY, 1981.
Smith, M. L. and Stinson, K. W., *Fuels and Combustion*, McGraw-Hill, New York, NY, 1952.
Smoot, L. D. and Pratt, D. T., *Pulverized-Coal Combustion and Gasification*, Plenum Press, New York, NY, 1979.
Vegetable oil fuels, in *Proceedings of the International Conference on Plant and Vegetable Oils as Fuels*, American Society of Agricultural Engineers, St. Joseph, MI, 1982.

CHEMICAL KINETICS AND GAS DYNAMICS REFERENCES

Barnard, J. A. and Bradley, J. N., *Flame and Combustion,* Second Edition, Chapman & Hall, London, UK, 1985.
Benson, S. W., *The Foundations of Chemical Kinetics*, McGraw-Hill, New York, NY, 1960.
Bowen, J. R., Manson, N., Oppenheim, A. K., and Soloukhin, R. I., editors, *Combustion in Reactive Systems*, AIAA, New York, NY, 1981.
Bowman, C. T. and Birkeland, J., *Alternative Hydrocarbon Fuels: Combustion and Chemical Kinetics*, AIAA, New York, NY, 1978.
Chigier, N., *Energy, Combustion and Environment*, McGraw-Hill, New York, NY, 1981.
Chomiak, J., *Combustion: A Study in Theory, Fact and Application*, Abacus Press, New York, NY, 1990.
Fristrom, R. M. and Westenberg, A. A., *Flame Structure*, McGraw-Hill, New York, NY, 1965.
Glassman, I., *Combustion*, Academic Press, New York, NY, 1977.
Hucknell, D. J., *Chemistry of Hydrocarbon Combustion*, Chapman & Hall, London, UK, 1985.
International Conference on Combustion in Engineering, Vol. I & II, Keble College, Oxford, UK, MEP-169 & 170, SAE, Warrendale, PA, 11–14 April, 1983.
Kondrat'ev, V. N., *Chemical Kinetics of Gas Reactions*, Pergamon Press, London, UK, 1964.
Levenspiel, O., *Chemical Reaction Engineering*, John Wiley & Sons, New York, NY, 1967.
Lewis, B., Pease, R. N., and Taylor, H. S., *Combustion Processes, Vol. II*, Princeton University Press, Princeton, NJ, 1956.
Penner, S. S., *Chemistry Problems in Jet Propulsion*, Pergamon Press, New York, NY, 1957.
Smith, J. M., *Chemical Engineering Kinetics,* Second Edition, McGraw-Hill, New York, NY, 1970.
Spalding, D. B., *Combustion and Mass Transfer,* Pergamon Press, New York, NY, 1979.
Turns, S. R., *An Introduction to Combustion—Concepts and Applications,* McGraw-Hill, New York, NY, 1996.
Zucker, R. D., *Fundamentals of Gas Dynamics*, Matrix Publishers, Portland, OR, 1977.
Zucrow, M. J. and Hoffman, J. D., *Volume I: Gas Dynamics*, John Wiley & Sons, New York, NY, 1976.

ENVIRONMENTAL REFERENCES

Chanlett, B. T., *Environmental Protection*, McGraw-Hill, New York, NY, 1979.
Chigier, N., *Energy, Combustion and Environment,* McGraw-Hill, New York, NY, 1981.

Knoll, K. E. and Davis, W. T., *Power Generation: Air Pollution Monitoring and Control*, Ann Arbor Science Publishers Inc., Ann Arbor, MI, 1976.
Patterson, D. J. and Henein, N. A., *Emissions From Combustion Engines and Their Control*, Ann Arbor Science Publishers, Inc., Ann Arbor, MI, 1981.
Perkins, H. C., *Air Pollution*, McGraw-Hill, New York, NY, 1974.
Wark, K., Warner, C. F., and Davis, W. T., *Air Pollution: Its Origin and Control*, Third Edition, Addison Wesley, New York, NY, 1998.

I.C. ENGINE REFERENCES

Benson, R. S. and Whitehouse, N. D., *Internal Combustion Engines,* Vol. I & II, Pergamon Press, New York, NY, 1979.
Blair, G. P., *The Basic Design of Two-Stroke Engines*, SAE, Warrendale, PA, 1990.
Burghardt, M. D. and Kingsley, G. D., *Marine Diesels*, Prentice Hall, Inc., Englewood Cliffs, NJ, 1981.
Calder, N., *Marine Diesel Engines: Maintenance, Troubleshooting, and Repair*, International Marine Publishing Co., Camden, MA, 1987.
Campbell, A. S., *Thermodynamic Analysis of Combustion Engines*, John Wiley & Sons, New York, NY, 1979.
Collie, M. J., editor, *Stirling Engine: Design and Feasibility for Automotive Use*, Noyes Data Corporation, Park Ridge, NJ, 1979.
Cummins, C. L., Jr., *Internal Fire*, Carnot Press, Lake Oswego, OR, 1976.
Dicksee, C. B., *The High-Speed Compression-Ignition Engine*, Blackie & Sons Ltd., London, UK, 1946.
Fenton, J., editor, *Gasoline Engine Analysis*, Mechanical Engineering Publications Ltd., London, UK, 1986.
Ferguson, C. R. and Kirkpatrick, A., *Internal Combustion Engines*, Second Edition, John Wiley & Sons, New York, NY, 2001.
Gill, P. W., Smith, J. H., Jr., and Ziurys, E. J., *Fundamentals of Internal Combustion Engines*, Naval Institute Press, Annapolis, MD, 1959.
Heywood, J. B., *Internal Combustion Engine Fundamentals*, McGraw-Hill, New York, NY, 1988.
Howarth, M. H., *The Design of High Speed Diesel Engines*, Constable & Company, London, UK, 1966.
Knak, C., *Diesel Motor Ships Engines and Machinery, Text and Drawings,* G-E-C GAD Publishers, Copenhagen, 1979.
Lichty, L. C., *Combustion Engine Processes*, McGraw-Hill, New York, NY, 1967.
Lilly, L. C. R., editor, *Diesel Engine Reference Book*, Butterworths, London, UK, 1984.
Newton, K., Steeds, W., and Garrett, T. K., *The Motor Vehicle,* Tenth Edition, Butterworths, London, UK, 1983.
Norbye, J. P., *The Wankel Engine*, Chilton Book Co., Philadelphia, PA, 1972.
Obert, E. F., *Internal Combustion Engines and Air Pollution*, Harper & Row, New York, NY, 1973.
Plint, M. and Martyr, A., *Engine Testing Theory and Practice,* Second Edition, SAE International, Warrendale, PA, 1999.
Reader, G. T. and Hooper, C., *Stirling Engines*, E. & F. N. Spon, London, UK, 1983.
Ricardo, H. R. and Hempson, J. G. G., *The High-Speed Internal-Combustion Engine*, Blackie & Sons Ltd., London, UK, 1968.
Stephenson, R. R., *Should We Have a New Engine?* Vol. I and II, Jet Propulsion Laboratory, California Institute of Technology, Pasadena, CA, 1979.
Stinson, K. W., *Diesel Engineering Handbook,* 12th Edition, Business Journals, Inc., Stamford, CT, 1972.
Stone, R., *Introduction to Internal Combustion Engines*, Macmillan Education Ltd., London, UK, 1985.

Taylor, C. F., *The Internal-Combustion Engine in Theory and Practice,* Vol. I and II, M.I.T. Press, Cambridge, MA, 1977.
Walker, G., *Stirling Engines*, Clarendon Press, Oxford, UK, 1980.
Watson, N. and Janota, M. S., *Turbocharging the Internal Combustion Engine*, John Wiley & Sons, New York, NY, 1982.

GAS TURBINE TEXTS

Cohen, H., Rogers, G. F. C., and Saravanamuttoo, H. I. H., *Gas Turbine Theory*, Longman Group Ltd., London, UK, 1974.
Dusinberre, G. M. and Lester, J. C., *Gas Turbine Power*, International Textbook Company, Scranton, PA, 1962.
Gas Turbines for Autos and Trucks (selected papers through 1980), SAE, Warrendale, PA, 1981.
Harman, R. T., *Gas Turbine Engineering*, Halsted Press, John Wiley & Sons, New York, NY, 1981.
Jennings, B. H. and Rogers, W. L., *Gas Turbine Analysis and Practice*, McGraw-Hill, New York, NY, 1953.
Lefebvre, A. W., *Gas Turbine Combustion*, McGraw-Hill, New York, NY, 1983.
Odgers J. and Kretschmer, D., *Gas Turbine Fuels and Their Influence on Combustion,* Abacus Press, Cambridge, MA, 1986.
O'Brien, J. P., editor, *Gas Turbines for Automotive Use*, Noyes Data Corporation, Park Ridge, NJ, 1980.
Saarlas, M., *Steam and Gas Turbines for Marine Propulsion*, Naval Institute Press, Annapolis, MD, 1978.
The Aircraft Gas Turbine Engine and Its Operation, United Technologies-Pratt & Whitney, Bloomfield, CT, 1982.
Whittle, F., *Gas Turbine Aero-Thermodynamics*, Pergamon Press, New York, NY, 1981.

THERMAL DESTRUCTION TEXTS

Baukal, C. E., editor, *John Zink Combustion Handbook,* CRC Press, Boca Raton, FL, 2001.
———, editor, *Oxygen-Enhanced Combustion*, CRC Press, Boca Raton, FL, 1998.
Combustion Fundamentals for Waste Incineration, ASME Research Committee on Industrial and Municipal Wastes, ASME, New York, NY, 1974.
LaGrega, M., Buckingham, P. L., and Evans, J. C., *Hazardous Waste Management*, McGraw-Hill, New York, NY, 1994.
Niessen, W. R., *Combustion and Incineration Processes*, Third Edition, Marcel Dekker, New York, NY, 2002.
Santoleri, J., Reynolds, J., and Theodore, L., *Introduction to Hazardous Waste Incineration,* Second Edition, Wiley Interscience, New York, NY, 2000.
Tchobanoglous, G., Theisen, H., and Vigil, S., *Integrated Solid Waste Management: Engineering Principles and Management Issues*, McGraw-Hill, New York, NY, 1993.

REFERENCES FOR TEXT CHAPTERS

Chapter 1

Amann, C., Trends in engine design, *Search*, G.M. Research Laboratories, Vol. 19, #1, Mar–Apr 1984.
Cohen, W., The new breed, *ASEE Prism*, 35–37, September 2000.
Huebner, G. J., Jr., Future automotive power plants, SAE Paper 760607, 1976.
Oppenheim, A. K., A rationale for advances in the technology of the I.C. engines, SAE Paper 820047, 1982.
Rain, C., Future auto engines: competition heats up, *High Technology*, Vol. 2, #3, May–June 1982.
Shoureshi, R. A. and Franke, M. E., Engineering systems face the future, *Mechanical Engineering*, 74–76, November 1996.

Chapter 3

Fuel cell power for transportation 2000, SAE Publication SP-1505, Warrendale, PA, 2000.
Gordon, S. and McBride, B. J., Computer program for calculation of complex chemical equilibrium compositions, rock performance, incident and reflected shocks, and Chapman–Jouquet detonations, NASA SP-273, 1971.
Hottel, H. and Williams, G., Charts of thermodynamic properties of fluids encountered in calculations of internal combustion engine cycles, NACA TN 1026, May 1946.
———, Williams, G., and Satterfield, C. N., *Thermodynamic Charts for Combustion Processes*, John Wiley and Sons, New York, NY, 1949.
McBride, B. J., Gordon, S. and Reno, M., Chemical Equilibrium with Transport Properties, NASA CET93/PC, 1993.
McCann, W., Thermodynamic charts for internal combustion engine fluids, NACA RB 3G28, 1943 and NACA TN 1883, July 1949.
Newhall, H. K. and Starkman, E. S., Thermodynamic properties of octane and air for engine performance calculations, *SAE Progress in Technology*, Vol. 7, 1964.
Powell, H., Applications of an enthalpy-fuel air ratio program, *ASME Trans*., Vol. 79, July 1957.
Reynolds, W., The Element Potential Method for Chemical Equilibrium Analysis: Implementation in the Interactive Program STANJAN, M. E. Department, Stanford University, Stanford, CA, 1986.
Svehla, R. A. and McBride, B. J., Fortran IV Computer Program for Calculation of Thermodynamic and Transport Properties of Complex Chemical Systems, NASA TN D-7056, 1973.

Chapter 4

Doring, W., Uber den Detonationsvorgang in Gasen, *Aannalen de Physik*, Vol. 43, 421–436, 1943.
Draper, D. S., Pressure waves accompanying detonation in the internal combustion engine, *Journal of the Aeronautical Sciences*, V5, N6, 219–226, April 1938.
Gardner, W. C., The chemistry of flames, *Scientific American*, 110–121, February, 1982.
Glassman, I., *Combustion*, Academic Press, New York, NY, 1977.
von Neuman, J., Theory of detonation waves, OSRD Report 549, 1942.
Zeldovich, Y. B., On the theory of the propagation of detonation in gaseous systems (in Russian), *Journal of Experimental and Theoretical Physics*, Vol. 10, USSR, 1940, 542. (Translated as NAXA TM 1261, November 1950.)

Chapter 5

Boccio, J. L., Weilerstein, G., and Edelman, R. B., A mathematical model for jet engine combustor pollutant emissions, NASA CR 1212083, 1973.

Cornelius W. and Agnew, W. G., editors, *Emissions from Continuous Combustion Systems*, Plenum Press, New York, NY, 1972.

Crowe, C. T., Conservation equations for vapor-droplet flows, in *Proc. 25th HTFM Inst.* (McKillop, A. A., Baughn, J. W., and Dwyer, H. A., editors), Stanford University Press, 214, 1976.

———, Vapour-droplet flow equations, Lawrence Livermore Laboratory Report No. UCRL-51877, 1977.

Gibson, M. M. and Morgan, B. B., *J. Inst. Fuel*, Vol. 43, 517, 1970.

Gouldin, F. C., *Comb. Sci. & Tech*., Vol. 9, 17, 1974.

Hinshelwood, C. N. and Williamson, A. T., *The Reaction between Hydrogen and Oxygen*, Oxford University Press, Cambridge, UK, 1934.

Launder, B. E. and Spaulding, D. B., *Mathematical Models of Turbulence,* Academic Press, London, UK, 1972.

Lilley, D. G. and Wendt, J. O. L., Modeling pollutant formation in coal combustion, *Proc. 25 HTFM Inst.* (McKillop, A. A., Baughn, J. W., and Dwyer, H. A., editors), Stanford University Press, Stanford, CA, 196, 1976.

Pratte, B. D. and Keffer, J. R., *ASME Journal of Basic Engineering*, Vol. 94, 739, Dec 1972.

Rai, C. and Siegel, R. D., editors, Air: II. Control of NO_x and SO_x emissions, *AIChE Symposium Series No. 148*, Vol. 71, 1975.

Uyehara, O. A., Sooting, burning rate as influenced by fuel structure and burning conditions, SAE Paper 850112, 1985.

Westbrook, C. K., *16th Symp. (Intl.) on Combustion*, The Combustion Institute, 1977.

Williams, F. A., *Combustion Theory*, Addison Wesley, New York, NY, 1965.

Zeldovitch, B., Sadovnikov, P., and Frank-Kamenetski, D., *Oxidation of Nitrogen in Combustion*, Academy of Sciences (USSR), Inst. of Chem. Physic, Moscow-Leningrad, 1947.

Chapter 6

ASME Steam Generating Units Power Test Codes, ASME PTC4.1-1964 and ANSI PTC4.1-1974.

Bain, R. L. et al., Biopower Technical Assessment: State of the Industry and Technology, Technical Report NREL/TP-510-33123, National Renewable Energy Laboratory, Golden, CO, March 2003.

Feldman, H. F. et al., Conversion of Forest Residues to a Methane-Rich Gas in a High Throughput Gasifier, PNL-6570/UJC-245, Columbus, OH, Battelle Columbus Laboratories for Pacific Northwest Laboratory, Richland, WA, May 1988.

Jenkins, B. N. and Ebeling, J. M., Correlation of Physical and Chemical Properties of Terrestrial Biomass with Conversion, Symposium, Energy from Biomass and Waste IX, Institute of Gas Technology, Chicago IL, 271, 1985.

Johnson, J. A. and Auth, G. H., *Fuels and Combustion Handbook*, McGraw-Hill, New York, NY, 1951.

Miles, T. R., Miles, T. R., Jr., Baxter, L. L., Bryers, R. W., Jenkins, B. M., and Oden, L. L., Alkali Deposits Found in Biomass Power Plants: A Preliminary Investigation of Their Extent and Nature, NREL/TP-433-8142, National Renewable Energy Laboratory, Golden, CO, 1996.

Risser, P. G., Agricultural and forestry residues, in *Biomass Conversion Processes for Energy and Fuels*," Soffer, S. S. and Zaborsky, O. R., editors, Plenum Press, New York, NY, 25-56d, 1981.

Sanner, W. S., Ortuglio, C., Walters, J. G., Wolfson, D. E., *Conversion of Municipal and Industrial Refuse into Useful Materials by Pyrolysis*, U.S. Bureau of Mines, RI 7428, Aug. 1970.

Steam, Its Generation and Use, 37th Edition, The Babcock & Wilcox Co, Barberton, Ohio, 1963.

Tillman, D. A., *Wood as an Energy Resource*, Academic Press, New York, NY, 1978.

Wen, C. Y., Bailie, R. C., Lin, C. Y., and O'Brien, W. S., Production of Low Btu Gas Involving Coal Pyrolysis and Gasification, *Advances in Chemistry Series*, Vol. 131, American Chemical Society, Washington, DC, 1974.

Chapter 7

Baumeister, T. and Marks, L., *Standard Handbook for Mechanical Engineers*, Seventh Edition, McGraw-Hill, New York, NY, 1967.

Burkhardt, C. H., *Domestic and Commercial Oil Burners*, Third Edition, McGraw-Hill, New York, NY, 1969.

DiBella, C. A. W., U.S. Synthetic Fuel Corporation, private communications, Conference and Workshop on Implementing Transportation Fuel Alternatives for North America Into the 21st Century, November 13–15, 1985, Washington, DC.

North American Combustion Handbook Vol. I. and Vol. II., Third Edition, North American Manufacturing Co., Cleveland OH, 1986.

Chapter 8

Faulkner, E. A., Jr., *Guide to Efficient Burner Operation: Gas, Oil, & Dual Fuel*, The Fairmont Press, Inc., Atlanta, GA, 1981.

Hammond, A. L., Metz, W. D. and Maugh, T. H., II, *Energy and the Future*, American Association for the Advancement of Science, Washington, DC, 120, 1973.

Chapter 9

1979 Annual Book of ASTM Standards, Part 47, Test Methods for Rating Motor, Diesel, Aviation Fuels, 01-47079-12, Philadelphia, PA, 1979.

Alkidas, A. C., Relationships between smoke measurements and particulate measurements, SAE Paper 840412, 1984.

Bensen, G. A., Fletcher, E. A., Murphy, T. E., and Scherrer, H. C., Knock (detonation) control by engine combustion chamber shape, SAE Paper 830509, 1983.

Bosch Automotive Handbook, Second Edition, SAE, Warrendale, PA, 1986.

Callahan, T. J., Ryan, T. W., III, and King, S. R., Engine knock rating of natural gases — methane number, ASME Paper 93-ICED-18, 1993.

Cohen, J., Emissions Standards Summary Update, US EPA Office of Air and Radiation, January 29, 1992, Ann Arbor, MI.

Federal and California Exhaust Evaporative Emission Standards for Light-Duty Vehicles and Light-Duty Trucks, EPA 420-B-00-001, February 2000.

Federal Register 33(108), Part II, 1968; 35(219), Part II, 1970; 36(128), Part II, 1971.

Halstad, L. R., Automobiles and air pollution, Conference on Universities, National Laboratories and Man's Environment, Argonne, IL, July 1969.

Lucas, S. V., Loher, D. A., and Meyer, M. E., Exhaust emissions and field trial results of a new, oxygenated, non-petroleum-based, waste-derived gasoline blending component: 2-methyltetrhydrofuran, SAE Paper 932675, 1993.

Patel, K. S. and Henein, N. A., Burning velocities in methanol-indolene air mixtures in a CFR engine, SAE Paper 850111, 1985.

Radwan, M. S., The effect of bowl-in-piston shape and geometry on detonation in spark-ignition engines, ASME Paper 92-ICE-11, 1992.

SAE Handbook, Volume 3—Engines, Fuels, Lubricants, Emissions, and Noise, SAE, Warrendale, PA, 1986.

SAE Surface Vehicle Standard Engine Power Test Code-Spark Ignition and Compression Ignition-Gross Power Rating, SAE, Warrendale, PA, June 1995.

Talwar, M., Natural gas fueled engine development & demonstration in Santa Barbara County, ASME Paper 93-ICE-16, 1993.

Treiber, P. J. H. and Sauerteig, J. E., Diesel emissions update: What's happening in Europe? *Diesel Progress Engines & Drives*, 51–55, October 1991.
Urban, C. M. and Sharp., C. A., Computing emissions from natural gas and dual-fuel engines, ASME Paper 93-ICE-29, 1993.

Chapter 10

A technical history of the automobile, Part 1, *Automotive Engineering*, Vol. 98, #6, June 1990.
A technical history of the automobile, Part 2, *Automotive Engineering*, Vol. 98, #7, July 1990.
A technical history of the automobile, Part 3, *Automotive Engineering*, Vol. 98, #8, August 1990.
Alternative fuels for spark ignition and diesel engines, SAE International Congress & Exposition, Detroit, MI, February 28–March 4, 1983, SAE Publication SP-542, SAE, Warrendale, PA, 1983.
Ashley, S., associate editor, A radical way to burn, *Mechanical Engineering*, 64–67, August 1996.
Assessment of methane-related fuels for automotive fleet vehicles: technical, supply and economic assessments, Alternative Fuels Utilization Program, U.S. Department of Energy, February 1982.
Bell, S. R., Loper, G. A., Jr., and Gupta, Manishi, Combustion characteristics of a natural gas fueled spark ignited engine, ASME Publication 93-ICE-17, 1993.
Bell, S. R. and Sekar, R., Natural gas and alterative fuels for engines, ASME Publication 93-ICE-21, 1994.
Borden, N. E. and Cake, W. J., *Fundamentals of Aircraft Piston Engines*, Hayden Book Co., Inc., Rochelle Park, NJ, 1971.
Brinkman, N. D. and Stebar, R. F., A comparison of methanol and dissociated methanol illustrating effects of fuel properties on engine efficiency—experiments and thermodynamic analyses, SAE Paper 850217, 1985.
Camden, John T., Automotive engines—A viable alternative for aircraft, SAE Paper 770466, 1977.
Cotton, K. J., A study of the potential of propane fuel to reduce utility engine exhaust emissions, SAE Paper 921696, 1992.
Dempelfeld, P. M. and Foster, D. E., Predictions of autoignition in a spark-ignition engine using chemical kinetics, SAE Paper 860322, 1986.
Flink, J. J., Innovation in automotive technology, *American Scientist*, Vol. 73, Mar–Apr 1985.
Foster, D. E. and Myers, P. S., Can paper engines stand the heat? SAE Paper 840911, 1984.
Fourth International Symposium on Automotive Propulsion Systems, NATO Committee on the Challenges of Modern Society, Washington, DC, April 17–22, 1977.
Fox, J. W., Cheng, W. K., and Heywood, J. B., A model for predicting residual gas fraction in spark-ignition engines, SAE Paper 931025, 1993.
Frank, R. M. and Heywood, J. B., The effect of piston temperature on hydrocarbon emissions from a spark-ignited direct-injection engine, SAE Paper 910558, 1991.
Fuel alternatives for the 80's, Fuels and Lubricants Meeting, Toronto, Ontario, Canada, October 18–21, 1982, SAE Publication SP-527, SAE, Warrendale, PA, 1982.
Garrett, T. K., *Automotive Fuels and Fuel Systems, Volume 1: Gasoline*, SAE, Warrendale, PA, 1991.
Gaseous fuels: technology, performance, and emissions, SAE International Fuels and Lubricants Meeting, Baltimore, MD, September 25–28, 1989, SAE Publication SP-798, SAE, Warrendale, PA, 1989.
Gavillet, G. G., Maxson, J., and Oppenheim, A. K., Thermodynamic and thermochemical aspects of combustion in premixed charge engines revisited, SAE Paper 930432, 1993.
Hottel, H. and Williams, G., Charts of thermodynamic properties of fluids encountered in calculations of internal combustion engine cycles, NACA TN 1026, May 1946.
Hottel, H. C., Williams, G. C., and Satterfield, C. N., *Thermodynamic Charts for Combustion Processes*, John Wiley & Sons, New York, NY, 1949.
Iida, N., Combustion analysis of methanol-fueled active thermo-atmosphere combustion (ATAC) engine using a spectroscopic observation, SAE Paper 940684, 1994.

Jones, C., Mack, J. R., and Griffith, M. J., Advanced rotary engine developments for naval applications, SAE Paper 851243, 1985.

Keating, E. L. and Pouring, A. A., Controlled regenerative dual cycle analysis, AIAA Paper 85-1413, 1985.

Keating, E. L. and Pouring, A. A., Internal regenerative air standard I.C. engine cycle performance, AIAA Paper 82-1281, 1982.

Keating, E. L., Pouring, A. A., and Chute, R., Internally regenerative engine cycle analysis, 83WA/AERO-3 ASME, 1983.

Klimstra, J., Carburettors for gaseous fuels—on air-to-fuel ratio, homogeneity and flow restriction, SAE Paper 892141, 1989.

Kobayashi, S., Masahiko, H., and Kim, Y. K., A comparison of thermal efficiency of carbureted and injected methanol engines by means of thermodynamic cycle simulation, SAE Paper 871673, 1987.

Koyanagi, K., Hiruma, M., Hashimoto, H., Yamane, K., and Furuhama, S., Low NOx emission automobile liquid hydrogen engine by means of dual mixture formation, SAE Paper 930757, 1993.

Lenz, H. P., *Mixture Formation in Spark-Ignition Engines*, SAE International, Warrendale, PA, 1992.

McCann, W., Thermodynamic charts for internal combustion engine fluids, NACA RB3G28, 1943, and NACA TN 1883, July 1949.

Millar, Gordon, Conference and Workshop on Implementing Transportation Fuel Alternatives for North America into the 21st Century, November 13–15, 1985, Washington, DC.

Multiple applications seen for migrating combustion chamber engine, *Diesel Progress Engines & Drives*, October, 48–49, 1989.

New developments in alternative fuels and gasolines for SI and CI engines, SAE Publication SP-958, SAE, Warrendale, PA, 1993.

Newhall, H. and Starkman, E., Thermodynamic properties of octane and air for engine performance calculations, in Digital Calculations of Engine Cycles, *SAE Progress in Technology*, Vol. 7, 38, 1964.

Nguyen, H. L., Addy, H. E., Bond, T. H., Lee, C.M., and Chun, K. S., Performance and efficiency evaluation and heat release study of a direct-injection stratified-charge rotary engine, SAE Paper 870445, 1987.

Sakurai, T., Iko, M., Okamoto, K., and Shoji, F., Basic research on combustion chambers for lean burn gas engines, SAE Paper 932710, 1993.

Sawyer, R. F., The future of the automobile, A Series of Lectures on Energy and the Future of Automotive Transportation, Meakin Interdisciplinary Studies Center, College of Engineering, U.C. Berkley, CA, 1981.

Schafer, F. and Basshuysen, R. van, *Reduced Emissions and Fuel Consumption in Automobile Engines*, SAE International, Warrendale, PA, 1995.

Shapiro, H. N. and Van Gerpen, J. H., Two zone combustion models for second law analysis of internal combustion engines, SAE Paper 890823, 1989.

Shikari, Y. A. and Bernstein, H. M., History of automotive engine development—lessons to be learned, SAE Paper 850029, 1985.

Sierens, R., A comparative test on a S.I. engine fueled with natural gas or hydrogen, ASME Paper 93-ICE-15, 1993.

Sierens, R., Barert, R., Winterbone, D. E., and Baruah, P. C., A comprehensive study of Wankel engine performance, SAE Paper 830332, 1983.

Sorenson, S. C., Myers, P. S., and Uyehara, O. A., Ethane kinetics in spark-ignition engine exhaust gases, 13th International Symposium on Combustion, Combustion Institute, Salt Lake City, UT, August 23–29, 1970.

The automotive engine, future technology, *Automotive Engineering*, Vol. 98, No. 1, 35–40, January 1990.

Thring, R. H., Gasoline engines and their future, *Mechanical Engineering*, October 1983.

Willis, E. A. and Wintucky, W. T., An Overview of NASA Intermittent Combustion Engine Research, AIAA-84-1393, AIAA/SAE/ASME 20th Joint Propulsion Conference, June 11–13, 1984, Cincinnati, Ohio.

Yamamoto, K., *Rotary Engine,* MAZ-1, SAE International, Warrendale, PA, 1981.

Yamauchi, T. and Sasayama, T., The effect of methanol-gasoline mixing ratio on performance of internal combustion engines, SAE Paper 900584, 1990.

Zeleznik, F. J. and McBride, B. J., Modeling the internal combustion engine, NASA Reference Publication 1094, March 1985.

Chapter 11

50 years of Diesel progress, *Diesel Progress*, Vol. L1, #7, ISSN 0744-0073, July 1985.

A worldwide view of diesel combustion emissions and analysis, SAE International Off-Highway Meeting & Exposition, Milwaukee, WI, September 12–15, 1983, SAE Publication P-130, SAE, Warrendale, PA, 1983.

Ahmadi, M. R., Kittelson, D. B., and Brehob, D. D., Combustion of minimally processed coal liquids in a diesel engine, SAE Paper 900399, 1990.

Alternative fuels for compression and S.I. engines, Fuels and Lubricants Meeting, Baltimore, MD, October 8–11, 1984, SAE Publication SP-587, SAE, Warrendale, PA, 1984.

Aroson, A. A. and Matula, R. A., Diesel order and the formation of aromatic hydrocarbons during the heterogeneous combustion of pure cetane in a single-cylinder diesel engine, 13th International Symposium on Combustion, Combustion Institute, Salt Lake City, UT, August 23–29, 1970.

Baker, Q. A., Expanding diesel engine cetane limits through staged injection, SAE Paper 830246, 1983.

Baumeister, T. and Marks, L., *Standard Handbook for Mechanical Engineers*, Seventh Edition, McGraw-Hill, New York, NY, 1967.

Bower, G. R. and Foster, D.E., The effect of split injection on soot and NO_x production in an engine-fed combustion chamber, SAE Paper 932655, 1993.

Bradley, J. D., Diesel fuel: problems & solutions, *Diesel Progress North American*, 10–11, June 1987.

Chevron introduces reformulated diesel fuel, *Diesel Progress Engines & Drives*, 42–43, October 1990.

Combustion emission and analysis, SAE International Congress & Exposition, Detroit, MI, February 25– March 1, 1985, SAE Publication P-162, SAE, Warrendale, PA, 1985.

Conta, L. D., Alternate fuels and the diesel engine, ASME Paper 80-DGP-37, 1980.

Diesel combustion and emissions, Part II, SAE International Congress & Exposition, Detroit, MI, February 23–27, 1981, SAE Publication SP-484, SAE, Warrendale, PA, 1981.

Diesel engine combustion and emissions, SAE Publication SP-581, SAE International Off-Highway & Powerplant Congress, Milwaukee, WI, September 10–13, 1984, SAE Publication P-581, SAE, Warrendale, PA, 1984.

Diesel combustion, emissions and exhaust aftertreatment, SAE Publication SP-931, SAE, Warrendale, PA, September 1992.

Diesel engine combustion, emissions, and particulates, SAE International Congress & Exposition, Detroit, MI, February 22–26, 1982, SAE Publication P-107, SAE, Warrendale, PA, 1982.

Diesel engines: future trends, *Automotive Engineering*, Vol. 96, No. 9, 39–46, September 1988.

Diesel exhaust emissions: particulate studies and transient cycle testing, SAE Publication SP-578, SAE International Congress & Exposition, Detroit, MI, February 27–March 2, 1984, SAE, Warrendale, PA, 1984.

Diesel particulate traps, SAE Publication P-140, SAE International Congress & Exposition, Detroit, MI, February 27–March 2, 1984, SAE, Warrendale, PA, 1984.

Ding., X. and Hill, P. G., Emissions and fuel economy of a prechamber diesel engine with natural gas dual fueling, SAE Paper 860069, 1969.

Dual fuel diesel/methane injection, *Automotive Engineering*, Vol. 97, No. 9, 17–23, September 1989.

Eberhardt, J., An overview of diesel engine emissions reduction technologies, Air Quality Compliance Workshop, American Academy of Environmental Engineers, Annapolis, MD, June 1999.

Eisenberg, W. C., Schuetzle, D., and Williams, R. L., Cooperative evaluation of methods for the analysis of PAH in extracts from diesel particulate emissions, SAE Paper 840414, 1984.

Gavillet, G. G., Maxson, J. A., and Oppenheim, A. K., Thermodynamic and thermochemical aspects of combustion in premixed charge engines revisited, SAE Paper 930432, 1993.

Karim, G. A., Jones, W., and Raine, R. R., An examination of the ignition delay period in dual fuel engines, SAE Paper 892140, 1989.

Katoh, Y., Shimauchi, T., and Nakagaki, T., SRC II in spark assisted multifuel diesel engine, SAE Paper 840003, 1984.

Kawatani, T., Kazuto, M., Fukano, I., Sugawara, K., and Koyama, T., Technology for Meeting the 1994 USA Exhaust Emission Regulations on Heavy-Duty Diesel Engine, SAE Paper 932654, 1993.

Kieser, R. D., Future trends in diesel engines, SAE Paper 880825, 1988.

Ladommatos, N. and Stone, R., Conversion of a diesel engine for gaseous fuel operation at high compression ratio, SAE Paper 910849, 1991.

Lipkea, W. H., A model of a direct injection diesel combustion system for use in cycle simulation and optimization studies, SAE Paper 870573, 1987.

Lipkea, W. H., DeJoode, A. D., and Christenson, S. R., The relationship between nitric oxide and work as influenced by engine operating conditions and combustion system parameters for a direct injection diesel engine, SAE Paper 870269, 1987.

Millar, G. H., Commercial engine development to year 2000 and beyond, SAE/IMechE Exchange Lecture, London, UK, May 1984.

Mori, M. and Arakawa, S., SRC-II combustion in prechamber diesel, SAE Paper 8840002, 1984.

Najt, P. M. and Foster, D. E., Compression-ignited homogeneous charge combustion, SAE Paper 830264, 1983.

Norris-Jones, S. R., Hollis, T., and Waterhouse, C. N. F., A study of the formation of particulates in the cylinder of a direct injection diesel engine, SAE Paper 840419, 1984.

Palumbo, J. H. and Litzinger, T. A., The effect of hydrotreatment of coal-derived synthetic fuels on DI diesel emissions and performance, SAE Paper 892132, 1989.

Plee, S. L., Ahmad, T., Meyers, J. P., and Faeth, G. M., Diesel NOx emissions — a simple correlation technique for intake air effects, 19th International Symposium on Combustion, Combustion Institute, Haifa, Israel, August 8–13, 1495–1504, 1982.

Radwan, M. S., The influence of some synfuels on the performance and thermal loading of a pre-combustion chamber diesel engine, SAE Paper 850051, 1985.

Ruiz, F. and Sepka, S., New experiments and components on the regenerative engine, SAE Paper 930063, 1993.

Ryan, T. W., III, Diesel engine injection and combustion of slurries of coal, charcoal, and coke in diesel fuel, SAE Paper 840119, 1984.

Seko, T., Hori, M., Suto, H., and Kobayashi, S., Methanol diesel engine and its application to a vehicle, SAE Paper 840116, 1984.

Spark-assisted diesels: multifuel capability? *Automotive Engineering*, 55–56, May 1981.

Szekely, G. A., Jr. and Alkidas, A. C., A two-stage heat-release model for diesel engines, SAE Paper 861272, 1986.

Thring, R. H., Homogeneous-charge compression-ignition (HCCI) engines, SAE Paper 892068, 1968.

Trevitz, S. S., Lestz, S. S., and Taylor, W. D., Single-cylinder diesel engine study of several shale and coal-derived fuels, SAE Paper 841333, 1984.

Tsao, K. C., Dong, Y., Xu, Y., Gruenwald, D., and Phillips, D., Investigation of probable combustion chamber configurations for high output D.I. diesel engines, SAE Paper 921729, 1929.

Tsao, K. C. and Han, Z., An exploratory study on combustion modeling and chamber design of natural gas engines, SAE Paper 930312, 1993.
Two-stage injection reduces diesel cetane requirements, *Automotive Engineering*, Vol. 91, No. 5, 35–38, May 1983.
Uyehara, O. A., Sooting, burning rate as influenced by fuel structure and burning conditions, SAE Paper 850112, 1985.
Vegetable oils: diesel fuel supplements? *Automotive Engineering*, Vol. 89, No. 4, 37–41, April 1981.
Wadman, B., Multi-purpose natural gas engine package, *Diesel Progress Engines & Drives*, 38–39, May 1990.
Weidmann, K. and Menrad, H., Fleet test, performance and emissions of diesel engines using different alcohol-diesel fuel blends, SAE Paper 841331, 1984.
Welch, A. B. and Wallace, J. S., Performance characteristics of a hydrogen-fueled diesel engine with ignition assist, SAE Paper 902070, 1990.
Will future medium diesels burn coal? *Automotive Engineering*, Vol. 92, No. 2, 41–45, February 1984.
Wolfer, H. H., Ignition lag in the Diesel engine, *VDI Forschung*, 1938, 392.
Yoshikawa, H., Ikeda, T., Haraguchi, K., Kawamura, T., Tanaka, M., and Yamaguchi, T., Simultaneous reduction of NOx and soot exhausted from diesel engine, SAE Paper 830509, 1983.
Yoshikawa, H., Ikeda, T., Haraguchi, K., Kawamura, T., Tanaka, M., and Yamaguchi, T., Simultaneous reduction of NO_x and soot exhausted from diesel engine, SAE Paper 940457, 1994.
Ziejewski, M., Goettler, H., and Pratt, G. L., Comparative analysis of the long-term performance of a diesel engine on vegetable oil based alternate fuels, SAE Paper 860301, 1986.

Chapter 12

Adelman, H. G. et al., Predicted exhaust emissions from a methanol and jet fueled gas turbine combustor, *AIAA Journal*, Vol. 14, No. 6, June 1976, 793–798.
Bahr, D. W., Turbine engine developers explore ways to lower NOx emission level, *ICAO Journal*, 47(8), 14–18, 1992.
Bajura, R. A. and Webb, H. A., The marriage of gas turbines and coal, *Mechanical Engineering*, 58–63, September 1991.
Brehm, N., Schilling, Th., Mack, A. and Kappler, G., NOx reduction in a fuel staged combustor by optimization of the mixing process and the residence time, RTO Applied Vehicle Technology Panel Symposium, Gas Turbine Engine Combustion, Emissions and Alternative Fuels, Lisbon, Portugal, October 1998.
Bretz, E. A., assistant editor, Examine full impact of injecting steam into gas-turbine systems, *Power*, 53–56, June 1989.
Bryan, R., Godbole, P. S., and Norster, E. R., Some observations of the atomizing characteristics of air-blast atomizers, in *Proceedings of Cranfield International Symposium, Combustion and Heat Transfer in Gas Turbine Systems*, Pergamon Press, New York, 343–356, 1969.
Burton, D. C., Combustion turbines at the crossroads, *Mechanical Engineering*, 79–85, April 1982.
Control of air pollution from aircraft and aircraft engines, *Federal Regulation*, Vol. 38, No. 136, Pt. II, Environmental Protection Agency, 1973.
Davidson, P. G. and Gray, D. C., Combustion turbines support extended dual-fuel operation, *Power*, S33–S36, April 1989.
Doerr, Th. and Hennecke, D. K., The mixing process in the quenching zone of the rich-lean-combustion concept, AGARD PEP 81st Symposium, Fuels and Combustion Technology for Advanced Aircraft Engines, CP536, 1993.
FAA Aircraft Engine Emission Database, U.S. Department of Transportation.
Fenimore, C. P., Formation of nitric oxide in premixed hydrocarbon flames, *Thirteenth Symposium (International) on Combustion*, The Combustion Institute, Pittsburgh, PA, 1971.

———, Hilt, M. B., and Johnson, R. H., Formation and measurement of nitrogen oxides in gas turbines, *Gas Turbine International*, 38–41, July–August 1971.

Fleischer, L. R., Vander Molen, R. H., and Young, W. E., Operation of gas turbines on combustion product obtained from burning municipal refuse, ASME Paper 74-WA/CD-6, 1974.

Gas Turbine Combustion and Fuels Technology, ASME Winter Annual Meeting, Atlanta, GA, November 27–December 2, 1977, ASME, NY.

Harris, S. J. and Weiner, A. M., *Combustion Science and Technology*, 31, 155–167, 1983.

Hassa, C., Carl, M., Frodermann, M., Behrendt, T., Heinze, J., Rohle, I., Boehm, N., Schilling, Th. and Doer, Th., Experimental investigation of an axially staged combustor sector with optical diagnostics at realistic operating conditions, RTO Applied Vehicle Technology Panel Symposium, Gas Turbine Engine Combustion, Emissions and Alternative Fuels, Lisbon, Portugal, October 1998.

Haupt, C. G., *Proceedings of Cranfield International Symposium, Combustion in Advanced Gas Turbine Systems*, Pergamon Press, New York, 295, 1968.

Hedman, P. O., Sturgess, G. J., Warren, D. L., Goss, L. P., and Shouse, D., Observations of flame behavior from a practical fuel injector using gaseous fuel in a technology combustor, *Tr. of the ASME J. of Engineering for Gas Turbines and Power*, 117, 441–452, July 1995.

Howard, J. B. and Kausch, W. J., Jr., Soot control by fuel additives, *Progress in Energy and Combustion Science*, 6, 263–276, 1980.

Howard, R. P. et al., Experimental characterization of gas turbine emissions at simulated flight altitude conditions, AEDC-TR-96-3, September 1996.

Hsu, K.-Y., Goss, L. P., and Roquemore, W. M., Characteristics of a trapped-vortex combustor, *J. of Propulsion and Power*, 14(1), 57, 1998.

International Civil Aviation Organization, Annex 16, Vol. II, Environmental Protection: Aircraft Engine Emissions, Second Edition, ICAO, Montreal, 1993.

Koch, R., Wittig, S., Feld, H.-J. and Mohr, H.-J., In-situ soot measurements in an operating engine gas turbine combustor, ASME Paper 91-GT-177, 1992.

Koff, B. L., Aircraft gas turbine emissions challenge, *Tr. of the ASME*, 116, 174–477, July 1994.

Kretschmer, D. and Odgers, J., Modeling of combustors: the effects of ambient conditions on performance, ASME Paper 73-W A/GT-6, 1973.

Landau, M., et al. Jet Aircraft Engine Exhaust Emissions Database Development – Year 1990 and 2015 Scenarios, NASA Contractor Report 4613, July 1994.

Lawson, R. J. and Duke, R. A., Reduction of aircraft engine emissions through stoichiometry modifications and decreased variability, AIAA Paper 94-2902, 1994.

Layne, R., This gas turbine burns sawdust, *Popular Science*, 65, November 1984.

Lefebvre, A. H., *Gas Turbine Combustion*, Series in Energy, Combustion, and Environment, McGraw-Hill, New York, NY, 1983.

Makansi, J., associate editor, External combustor enhances prospects for coal-fired gas turbine, *Power*, 63–64, January 1985.

———, senior editor, Gasifier makes coal-fired turbine a commercial powerplant, *Power*, 75–80, April 1987.

———, senior editor, Whole-tree combustion avoids fuel preparation, *Power*, 59–60, October 1989.

———, Combined-cycle power powerplants, *Power*, 91–124, June 1990.

Meijer, R. J., *The Evolution of the Stirling Engine*, Stirling Thermal Motors, Inc., Ann Arbor, MI, 1982.

Myers, P. S., Uyehara, O. A. and Newhall, H. K., Engine exhaust emissions, in *Engine Emissions — Pollutant Formation and Measurement*. Springer, G. S. and Patterson, D. J., Editors, Plenum Press, New York, NY, 1973.

Novick, A. S., Troth, D. L., and Notardanots, J., Multifuel evaluation of rich/quench/lean combustion, ASME Paper 83-GT-140, 1983.

Pandalai, R. P. and Mongia, H. C., Combustion instability characteristics of industrial engine dry low emission combustion systems, AIAA Paper 98-3379, 1998.

Roquemore, W. M., Vihinen, I., Hartrauft, J., and Mantis, P. M., Trapped Vortex Combustor for Gas Turbine Engines, Annual Report to SERDP, 1998.

Rosfjord, T. J., Sederquist, R. A., and Angello, L.C., Fuel tolerance of staged combustors, ASME Paper 82-GT-195, 1982.

SAE Aerospace Recommended Practice 1179, Aircraft Gas Turbine Engine Exhaust Smoke Measurement, Society of Automotive Engineers, New York, NY, 1970.

Schirmer, R. M., Effects of fuel composition on particulate emissions from gas turbine engines, in *Proceedings of GMRL Symposium, Emissions from Continuous Combustion Systems,* Plenum Press, New York, NY, 189–208, 1972.

Segalman, I., McKinney, R. G., Sturgess, G. J., and Hung, L.-M., Reduction of NOx by fuels in gas turbine engines—a commitment to the future, AGARD Meeting on Fuels and Combustion Technology for Advanced Aircraft Engines, AGARD-CP-536, May 1993.

———, Smith, R., Sturgess, G. J., Morford, S., and Holce, J., Engine demonstration of NOx reductions with a fuel-staged gas turbine combustor, AIAA Paper 94-2712, 1994.

Semerjian, H. C. and Ball, I., Potential reduction in NOx emissions with premixed combustors, Spring Technical Meeting, The Combustion Institute, Central States Section, NASA Lewis Research Center, Cleveland, OH, 28–30 March 1977.

Simentkosky, Michael, Mod I automotive Stirling engine mechanical development, SAE Paper 840462, 1984.

Spadaccini, L. J. and Szetela, E. J., Approaches to the prevaporized-premixed combustor concept for gas turbines, ASME Paper 75-GT-85, 1975.

Stirling Engines—Progress Towards Reality, I Mech E Conference, University of Reading, 25–26 March, 1982, UK, SAE Publication MEP-151, SAE, Warrendale, PA, 1982.

Sturgess, G. J., McKinney, R. G., and Morford, S. A., Modifications of combustor stoichiometry for reduced NOx emissions from aircraft engines, *Transactions of the ASME, Journal of Engineering for Gas Turbines and Power*, 115(3), 570–580, 1993.

———, Combustor design trends for aircraft gas turbine engines, ASME Paper 96-TA-29, Jakarta, Indonesia, 5–7 November 1996.

———, Assessment of an abbreviated jet NJP-5/JP-8 reaction mechanism for modeling gas turbine emissions, AIAA Paper 97-2709, 33rd AIANASME/SAE/ASEE Joint Propulsion Conference and Exhibit, Seattle, WA, 6–9 July 1997.

———, Trends in Gas Turbine Engine Design with Emphasis on Combustion, Seminar, University of California, Davis, May 1997.

———, An account of fuel/air unmixedness effects on NOx generation in gas turbine combustors, IECEC-98-353 Paper, 33rd Intersociety Engineering Conference on Energy Conversion, Colorado Springs, CO, 2–6 August 1998.

———, Gogineni, S., Shouse, D. T., Frayne, C., and Stutrud, J., Emissions and operability trades in the primary zones of gas turbine combustors, AIAA Paper 96-2758, 1996.

——— and Hsu, K.-Y., Combustion characteristics of a trapped vortex combustor, RTO Applied Vehicle Technology Panel Symposium, Gas Turbine Engine Combustion, Emissions and Alternative Fuels, Lisbon, Portugal, October 1998.

———, Roquemore, W. M., Hancock, R. D., Vihinen, Lt. I., Gord, J. R., and Mantz, Capt. R., Turbines, Air quality compliance workshop, American Academy of Environmental Engineers, Annapolis, MD, June 1999.

Valenti, M., associate editor, Bringing coal into the 21st century, *Mechanical Engineering*, 58–63, February 1995.

Chapter 13

Acharya, P. and Schafer, L. L., How to select an oxygen-based combustion system for rotary kiln-based hazardous waste incinerators, *1994 International Incineration Conference*, 403–412, Houston, TX, May 9–13, 1994.

Antal, M. J., Jr., Royere, C., and Vialaron, A., Biomass gasification at the focus of the Odeillo (France) 1-Mw (thermal) solar furnace, Thermal Conversion of Solid Wastes and Biomass, ACS Symposium Series 130, American Chemical Society, Washington, DC, 237–257, 1980.

Baddour, R. F. and Timmins, R. S., *The Application of Plasmas to Chemical Processing*, M.I.T. Press, Cambridge, MA, 1967.

Baukel, C. E., Romano, F. J., and Moore, G. L., Waste incineration performance improvements with oxygen-enriched combustion, 1–6, PD-Vol 39, Fossil Fuels Combustion, ASME, 1992, *16th Annual Energy-Sources Technology Conference and Exhibition*, Houston TX, January 31–February 4, 1993.

Baukal, C. E., Schafer, L. L., and Papadelis, E. P., Oxy-fuel enhances mobile incinerator performance, 335–338, *1993 International Incineration Conference*, May 3–7, 1993, Knoxville, TN.

Beaudoin, P., Charon, O., Plessier, R., Haines, A., and Schmidt, E., The use of pure oxygen in incineration processes, laboratory and pilot-scale experiments, modeling, and industrial applications, 419–423, *1994 International Incineration Conference*, Houston, TX, May 9–13, 1994.

Bennert, D. M. et al., Wastewater treatment sludge vitrification: summary of Savannah River Site M-Area surrogate demonstration, 1994 International Incineration Conference, Houston, TX, 335–341, May 9–13, 1994.

Bretz, E. assistant editor, Energy from wastes, *Power*, W1–W26, March 1989.

———, assistant editor, Energy from wastes, *Power*, S1–S10, March 1990.

Brooman, E. W. et al., Destruction of hazardous waste material using plasma arc technology, *Proceeding of the International Symposium on Environmental Technologies: Plasma Systems and Applications, Vol. I,* Atlanta, GA, 205–217, October 1995.

Brunner, C. R., *Handbook of Incineration Systems*, McGraw-Hill, New York, NY 1991.

Buekens, A. G. and Schoeters, J. G., Basic principles of waste pyrolysis and review of European processes, Thermal Conversion of Solid Wastes and Biomass, ACS Symposium Series 130, American Chemical Society, Washington, DC, 397–422, 1980.

Cage, M., Scale-up, design, and permitting of a mixed vitrification facility, *Proceedings of the 1997 International Conference on Incineration and Thermal Treatment Technologies,* Oakland, CA, 499–504, May 1997.

Carter, G. W. and Tsangaris, A. V., Plasma gasification of biomedical waste, *Proceedings of the International Symposium on Environmental Technologies: Plasma Systems and Applications, Vol. I*, Atlanta, GA, 239–250, October 1995.

———, Plasma gasification of municipal solid waste, *Proceedings of the International Symposium on Environmental Technologies: Plasma Systems and Applications, Vol. II*, Atlanta, GA, 321–332, October 1995.

Chapman, C. D. et al., Development of a plasma reactor for the treatment of incinerator ashes, *Proceedings of the International Symposium on Environmental Technologies: Plasma Systems and Applications, Vol. I*, Atlanta, GA, 129–140, October 1995.

Charles, Denis and Moreau, J. C., Prospects for oxygen incineration in a cyclone furnace of toxic waste transferred using pressurized foam, *Stabilization and Valorisation of Ultimate Waste, Plasma and Other Processes, International Symposium*, Bordeaux, France, 12–14 September 1994.

Chopra, H., Gupta, A., Keating, E. L., and White, E. B., Thermal destruction of solid wastes, *Proc. 27th Intersociety Energy Conversion Engineering Conference (IECEC)*, San Diego, CA, Vol. 1, 377–381, August 3–7, 1992.

Combustion Fundamentals for Waste Incineration, ASME Research Committee on Industrial Committee on Industrial and Municipal Wastes, Library of Congress Catalogue Number 74-19743, American Society of Mechanical Engineers (ASME), New York, NY.

Davidson, S. L., Fryer, S. R., and Ho, Min-Da, Optimization of process performance of a commercial hazardous waste incinerator using oxygen enrichment, *Proceedings of the International Incineration Conference*, Bellevue, WA , 631–636, May 8–12, 1995.

Domalski, E. S., Jobe, T. L. Jr., and Milne, T. A., *Thermodynamic Data for Biomass Materials and Waste Components*, The American Society of Mechanical Engineers, New York, NY, 210, 1987.

Donaldson, A. D. et al., A review of plasma destruction of hazardous mixed waste, *ASME Heat Transfer Division*, Vol. 161, 41, 1991.

Energy from wastes, *Power*, W1–W36, March 1988.

Falcone, P. W. and Ho, Min-Da, Control of combustion excursions in a commercial hazardous waste incinerator with oxygen-based technology, *1993 International Incineration Conference*, May 3–7, 1993, Knoxville, TN, 895–900.

Feldman, J., Waste characterization: a "need to know," *Proceedings of the 1993 Incineration Conference,* Knoxville, KN, 37–40, May 1993.

Fisher, J. C., Vavruska, J. S., and Thompson, T. K., A mass and energy balance process model for thermal treatment processes, *Proceedings of the 1996 International Conference on Incineration and Thermal Treatment Technologies,* Savannah, GA, 747–754, May 1996.

Gilder, K., Effect of temperature on the adhesion of dioxins on particles, *Proceedings of the 1996 International Conference on Incineration and Thermal Treatment Technologies,* Savannah, GA, 645–652, May 1996.

Gill, J. H. and Quiel, J. M., *Incineration of Hazardous, Toxic, and Mixed Wastes*, North American Mfg., ISBN 0-9601596-4-9, Cleveland, OH, 1993.

Gillans, R. L. et al., Mixed Waste Integrated Program Interim Evaluation Report on Thermal Treatment Technologies, Thermal Treatment Working Group Mixed Waste Integrated Program, Office of Technology Development, U.S. Department of Energy, February 1993.

Gillins, R. L. and Berry, J. B., Mixed waste integrated program thermal treatment technology development, 1993 International Incineration Conference, Knoxville, TN, 117–124, May 3–7, 1993.

——— and Poling, S. D., Plasma hearth waste treatment demonstrator for radioactive mixed waste, 1994 International Incineration Conference, Houston, TX, 25–30, May 9–13, 1994.

Green, A. E., Mahadevan, S., and Wagner, J. C., Chlorinated Benzene Formation in Incinerators, 1–10, Combustion Modeling, Cofiring, and NO_x Control, ASME FACT-Vol. 17, 1993 International Joint Power Generation Conference, Kansas City, MO, October 17–22, 1993.

Hamilton, R. A., Whittle, J. K., and Trescot, J., DC plasma arc melter technology for waste vitrification, *Proceedings of the International Symposium on Environmental Technologies: Plasma Systems and Applications, Vol. I*, Atlanta, GA, 67–76, October 1995.

Hansen, E. R., Leger, C. B., and Ho, Min-Da, Theory and practices with oxygen enrichment in a cement kiln firing waste derived fuels, *1994 International Incineration Conference*, Houston, TX, May 9–13, 1994, 397–401.

Heanley, C. P. and Chapman, C. D., Plasma arc vitrification of incinerator ash, *Proceedings of the 1998 IT3 International Conference on Incineration and Thermal Treatment Technologies,* Salt Lake City, UT, 245–252, May 1998.

Helmenstein, S. and Martin, F., Planning criteria for refuse incinerator systems, *Combustion*, 11–17, May 1974.

Ho, Min-Da and Ding, M. G., Field testing and computer modeling of an oxygen combustion system at the EPA mobile incinerator, *JAPCA*, Vol. 38, No. 9, September 1988.

Ho, Min-Da et al., Long-term field demonstration of the LINDE oxygen combustion system installed on the EPA mobile incinerator, *Proceedings of the 15th Annual EPA Research Symposium*, April 1989, Cincinnati, OH.

Igarashi, M. and Ueda, Y., Incineration and melting of sewage sludge by vortex (slagging) furnace, *Proceedings of the 1998 IT3 International Conference on Incineration and Thermal Treatment Technologies,* Salt Lake City, UT, 523–528, May 1998.

Kaiser, E. R., Physical-chemical character of municipal refuse, *Combustion*, 26–28 February 1977.

Large Incinerator Performance Test Code, PTC-33, American National Standard Institute (ANSI), American Society of Mechanical Engineers (ASME), 1978.

Lee, C. C., Plasma Systems, in *Standard Handbook on Hazardous Waste Treatment and Disposal*, McGraw-Hill, New York, NY, 8.169–8.177, 1989.

Lee, K. C., Research areas for improved incineration system performance, *JAPA*, 38, 1542–1549, December 1988.

Lewis, M. F. and Ablow, C. M., Thermodynamics of pyrolysis and activation in the production of waste or biomass derived activated carbon, Thermal Conversion of Solid Wastes and Biomass, ACS Symposium Series 130, American Chemical Society, Washington, DC, 301–317, 1980.

Lyon, D., An economic evaluation of supercritical water oxidation as an alternative to incineration, *Proceedings of the 1998 IT3 International Conference on Incineration and Thermal Treatment Technologies,* Salt Lake City, UT, 743–746, May 1998.

Massit, H. et al., Evaluation of the plasma arc centrifugal process for radioactive waste treatment, 1995 International Incineration Conference, Bellevue, WA, 517–520, May 8–12, 1995.

Mescavage, G. and Filius, K., Plasma arc technology development for application to demilitarization of pyrotechnic ordinance, *Proceedings of the International Symposium on Environmental Technologies: Plasma Systems and Applications, Vol. II*, Atlanta, GA, 597–608, October 1995.

Morris, M. and Waldheim, L., Energy recovery from solid waste fuels using advanced gasification technology, *Proceedings of the 1998 International Conference on Incineration and Thermal Treatment Technologies: Plasma Systems and Applications,* Salt Lake City, UT, 141–148, May 1998.

Niehoff, T., Dudill, R., and Baukal, C. E., Oxygen lancing to improve municipal solid waste incineration, *Proceedings of the 1996 International Conference on Incineration and Thermal Treatment Technologies*, Savannah, GA, 527–530, May 6–10, 1996.

Oden, L. I. et al., Vitrification of residue (ash) from municipal waste combustion systems, ASME, CRTD-Vol. 24, 1994.

Oppelt, E. T., Incineration of hazardous waste: a critical review, *JAPA*, 37, 558–586, May 1987.

Patterson, R. G. and Jaasund, S. A., Control of air toxic emissions from sewage sludge incinerators, *Proceedings of the1994 International Incineration Conference*, Houston, TX, 485–489, 9–13 May 1994.

Peterson, J. R. et al., The plasma energy recycle and conversion (PERC) process for processing materials resulting from demilitarization, 1995 International Incineration Conference, Bellevue, WA, 517–520, May 8–12, 1995.

Piao, G., Aono, S., Mori, S., Kondoh, M., and Yamaguchi, M., Combustion of refuse derived fuel in fluidized bed, *Proceedings of the 1998 IT3 International Conference on Incineration and Thermal Treatment Technologies,* Salt Lake City, UT, 301–304, May 1998.

Porteous, A., *Refuse Derived Fuels,* Applied Science Publishers Ltd, London, UK, Halsted Press Division, John Wiley & Sons, New York, NY, 1981.

Raghunathan, K. and Gullett, B. K., Dioxin/furan formation and control in waste combustors, *Proceedings of the 1996 International Conference on Incineration and Thermal Treatment Technologies,* Savannah, GA, 685–688, May 1996.

Risk Reduction Engineering Laboratory Office of Research and Development, U.S. Environmental Protection Agency, Evaluation of oxygen enriched MSW/sewage sludge co-incineration demonstration program, CSI Resources Systems, Inc., Boston, MA, and the Solid Waste Association of North America, Silver Spring, MA, EPA Report EPA/6007R-94/145, Cincinnati, OH 45268, September 1994.

Rivers, T. J. et al., Duration testing of the plasma arc centrifugal treatment system, 1994 International Incineration Conference, Houston, TX, 207–214, May 9–13, 1994.

Roy, K. A., Oxygen enrichment enhances hazardous waste incineration, *Hazmat World*, February 1991.

Sandahl, M. et al., The PERC process for demilitarization, *Proceedings of the International Symposium on Environmental Technologies: Plasma Systems and Applications, Vol. II*, Atlanta, GA, 393–399, October 1995.

Santolari, J., Dioxin emissions – effect of chlorine/time/temperature relationship at 300ºC, *Proceedings of the 1995 International Incineration Conference,* Bellevue, WA, 337–342, May 1995.

Sato, Y. and Ota, H., Waste liquid incinerator (water-cooled furnace), *Proceedings of the 1995 International Incineration Conference,* Bellevue, WA, 689–692, May 1995.

Schafer, L. L., Niemkiewicz, M. A., and Acharya, P., Safe use of oxygen in mobile/transportable rotary kiln-based hazardous waste incinerators, *Proceedings of the 1995 International Incineration Conference*, Bellevue, WA, 461–464, May 8–12, 1995.

Sears, J. W. et al. The plasma centrifugal furnace: a method for stabilization and decomposition of toxic and radioactive wastes, *Waste Management*, Vol. 10, 1965.

Shahani, G. H., Bucci, D. P., DeVicentis, D. M., and Goff, S. P., Oxygen enrichment for waste combustion, *Proceedings of the 1994 International Incineration Conference,* Houston, TX, 425–429, May 1994.

Simmons, W. W. and Ragland, K. W., Burning rate of millimeter sized wood particles in a furnace, *Combustion Science and Technology*, Vol. 46, 1–15, 1986.

Soelberg, N. R. et al., Arc melter vitrification of organic and chloride containing materials, *Proceedings of the International Symposium on Environmental Technologies: Plasma Systems and Applications, Vol. I*, Atlanta, GA, 227–238, October 1995.

Springer, M. D. et al., A thermal destruction and recovery process for medical waste powered by a plasma arc torch, *Proceedings of the International Symposium on Environmental Technologies: Plasma Systems and Applications, Vol. II*, Atlanta, GA, 671–682, October 1995.

Steverson, E. M. and Batdorf, J. A., The effect of oxygen enrichment on the capacity, emissions, and ash quality of a controlled air incinerator, *1994 International Incineration Conference*, Houston, TX , 413–417, May 9–13, 1994.

Stewart, B. A. and Chaney, R. L., Wastes: use or discard? *Proceedings of the 30th Annual Meeting of the Soil Conservation Society of America* (Land Use: Food and Living), San Antonio, TX, August 10–13, 1975.

Suzuki, T. et al., Melting of MSW incineration fly ash by plasma melting furnace, 13th International Symposium of Chlorinated Dioxins and Related Compounds, 1993.

Tay, J. H., Energy generation and resource recovery from refuse incineration, *J. of Energy Engineering*, Vol. 114, No. 3, 107–117, December 1988.

The Hazardous Waste Consultant, Vol. 13, No. 2, Elsevier Science Inc., New York, NY, March/April 1995.

The Plasma torch: revolutionizing the foundry fire, prepared by the Electric Power Research Institute, *EPRI Journal*, October 1986.

Topley, D. J., Comparison of thermal treatment technologies for VOC control, *Proceedings of the 1998 International Conference on Incineration and Thermal Treatment Technologies,* Salt Lake City, UT, 205–212, May 1998.

Tsuginori, I., The status of R&D of thermal plasma applications in Japan, *Proceedings of the International Symposium on Environmental Technologies: Plasma Systems and Applications, Vol. I*, Atlanta, GA, 13–35, October 1995.

Ulrich, C. R., Incinerator chlorine emission control by proper combustion air management, *Proceedings of the 1998 IT3 International Conference on Incineration and Thermal Treatment Technologies,* Salt Lake City, UT, 297–300, May 1998.

U.S. EPA Standards for the Use and Disposal of Sewage, Final Rules. *Fed. Regist*., 58, 32, February 19, 1993.

Wexell, D. R., Vitrification of municipal waste combustion flyash for hazardous element stabilization, *Proceedings of the 1993 Incineration Conference,* Knoxville, KN, 249–256, May 1993.

Whiting, K. C., A review of pyrolysis/gasification processes as applied to the disposal of wastes, *Proceedings of the 1996 International Conference on Incineration and Thermal Treatment Technologies,* Savannah, GA, 627–624, May 1996.

Zaghloul, H., Cortez, R., and Smith, E., Plasma waste remediation activities in the United States, *Proceedings of the International Symposium on Environmental Technologies: Plasma Systems and Applications, Vol. I*, Atlanta, GA, 1–12, October 1995.

1

Introduction to Applied Combustion

1.1 INTRODUCTION

The birth, growth, decay, and even ultimate death of many civilizations can be described in terms of their specific cultural understanding and application of the principles of combustion. For example, in both primitive and ancient cultures, fire was a mystery to be feared and therefore often worshiped. In such circumstances, the control of fire often provided certain groups with power either to improve or to destroy human existence. This mystical belief concerning the nature of fire, or more precisely the combustion process that caused it, was forever changed when Empedocles (ca. 490–430 B.C.) postulated his famous belief that fire was but one of four constituent elements of all matter: earth, air, fire, and water.

This idea was commonly held until the Renaissance and the Age of Enlightenment, when men such as Carnot (1796–1832) began to study the key nature of matter, energy, and combustion. In his "Reflections on the Motive Power of Fire," Carnot postulated his now-famous thermodynamic cycle, which would convert a fraction of energy transfer from a source, such as fire, into work, with the remaining energy, of necessity, being rejected into a sink. This publication provided a theoretical basis for an absolute temperature scale, contributed to the formulation of classical thermodynamics, and spurred development of practical heat engines that helped to shape the Industrial Revolution.

Tremendous progress was made by many individuals and organizations during the twentieth century to push the knowledge and application of combustion science to new limits. Many useful applications of combustion principles can be cited that have helped to make the material quality of life in America far better than any culture in the recorded history of civilization (see Figure 1.1). Applied combustion technology today helps to move mankind rapidly and efficiently over the surface of the Earth, through the air, as well as on and under the sea. The power of combustion has even taken men into orbit around the Earth and out to the surface of the moon.

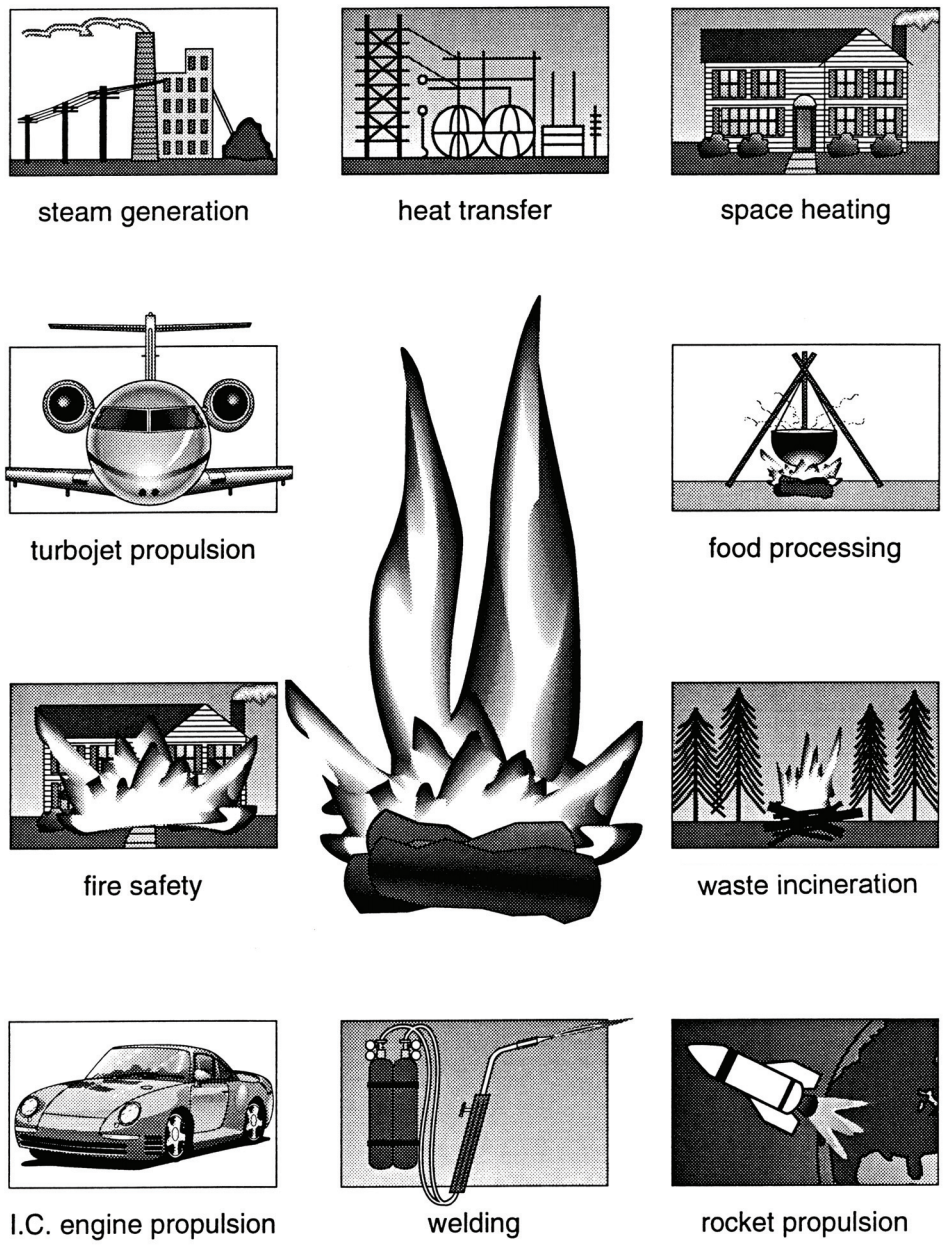

Figure 1.1 Typical applications of combustion science.

EXAMPLE 1.1 Carnot postulated an ideal thermodynamic cycle having the maximum theoretical thermal efficiency, i.e., desired work output to required heat input. The thermal efficiency η for the cycle shown below can be expressed as

$$\eta = \frac{\text{Desired energy output}}{\text{Required energy input}} = \frac{\text{Net work (power)}}{\text{Heat (flux) added}} = 1 - \frac{T_L}{T_H}$$

where

T_L = lowest cycle absolute temperature
T_H = highest cycle absolute temperature

For a T_L of 70°F calculate the required T_H for a cycle thermal efficiency of (a) 20%, (b) 40%, (c) 60%, and (d) 80%.

Solution

1. Thermal efficiency:

$$\eta = 1 - \frac{T_L}{T_H} \quad \text{where} \quad T_H = \frac{T_L}{(1-\eta)}$$

$T_L = 70 + 460 = 530°\text{R}$

	η	T_H
0.20	662.5	368.1
0.40	883.3	490.7
0.60	1,325.0	736.1
0.80	2,650.0	1,472.2
	°R	K

Comments: A high Carnot cycle efficiency implies cycle temperatures, which are consistent with the combustion process.

1.2 ENERGY AND COMBUSTION

Prior to the present age of jet travel and space exploration, energy demands were relatively low and energy was cheap. Until recent events including critical shortfalls in certain crucial fuel reserves and environmental consciousness, very little motivation, or even need, existed to develop an applied combustion engineering textbook. The material covered in this text will focus principally on an engineering study of the energy conversion aspects of combustion. *Combustion* in this dissertation will refer to any relatively fast gas-phase chemical reaction that liberates substantial energy as heat. The chemistry and physics of combustion, i.e., destruction and rearrangement of certain molecules that rapidly release energy, require temperatures of 1620–2200°C (3000–4000° F), take place within a few millionths of a second, and occur within a characteristic length of a few angstroms.

Table 1.1 Classification of Some Common Chemical Fuels

By phase		By application	
Naturally available	Synthetically produced	Heat transfer	Power
Solid		Space heating	Stationary power plants
Coal	Coke	Process heat transfer	Mobile propulsion systems
Wood	Charcoal		
Vegetation	Inorganic solid waste		
Organic solid waste			
Liquid			
Crude oil	Syncrudes		
Biological oils	Petroleum distillates		
Fuel plants	Alcohols		
	Colloidal fuels		
	Benzene		
Gas			
Natural gas	Natural gas		
Marsh gas	Hydrogen		
Biogas	Methane		
	Propane		
	Coal gasification		

Until physical and analytical tools such as the laser and modern high-speed computer became available, the microscopic nature of the very combustion process itself remained uncertain and impeded major progress in both scientific investigations and engineering applications of this most basic and universal phenomenon. Currently, combustion is a mature discipline and an integral element of diverse research and development programs, ranging from fundamental studies of the physics of flames and high-temperature molecular chemistry to applied engineering programs involved with producing clean burning coal plants and low emissions high mileage combustion engines.

Recall the classical thermodynamic concept of an energy *source* defined as an unlimited thermal energy reservoir and a *sink* as an unfillable thermal energy repository. Life cycle engineering and energy conversion technology developments today recognize that the Earth is a finite ecosphere with a delicately balanced environment that has limited terrestrial resources. To appreciate the significance of an ideal energy resource, consider a few of the conflicting requirements for a chemical fuel. It must be:

Nondepleting
Nonpolluting
Readily available
Economically viable
Politically neutral
Technically accessible
Legally valid
Socially acceptable
Aesthetically pleasing

A *fuel* can be considered as a finite resource of chemical potential energy, i.e., energy stored in the molecular structure of particular compounds that may be released via complex chemical reactions. Chemical fuels can be classified in a variety of ways, including by phase, availability, or even application (see Table 1.1). Some of the basic ideal combustion engineering characteristics of a fuel include:

High energy density (content)
High heat of combustion (release)
Good thermal stability (storage)
Low vapor pressure (volatility)
Nontoxicity (environmental impact)

Pollution from internal and external combustion systems, such as automotive engines, stationary power plants, and/or waste incinerators, results from an inability to completely rearrange fuel molecules into complete and stable products. Understanding combustion, therefore, becomes a major benefit to those in the environmental and air pollution industries. Improved combustion, i.e., an ability to oxidize certain fuels (such as solid, liquid, and gaseous hydrocarbon compounds) more completely, will impact power machinery performance characteristics, help to reduce fuel consumption, and clean emissions from stationary and mobility propulsion systems. This, in turn, could save billions of dollars in foreign oil purchases.

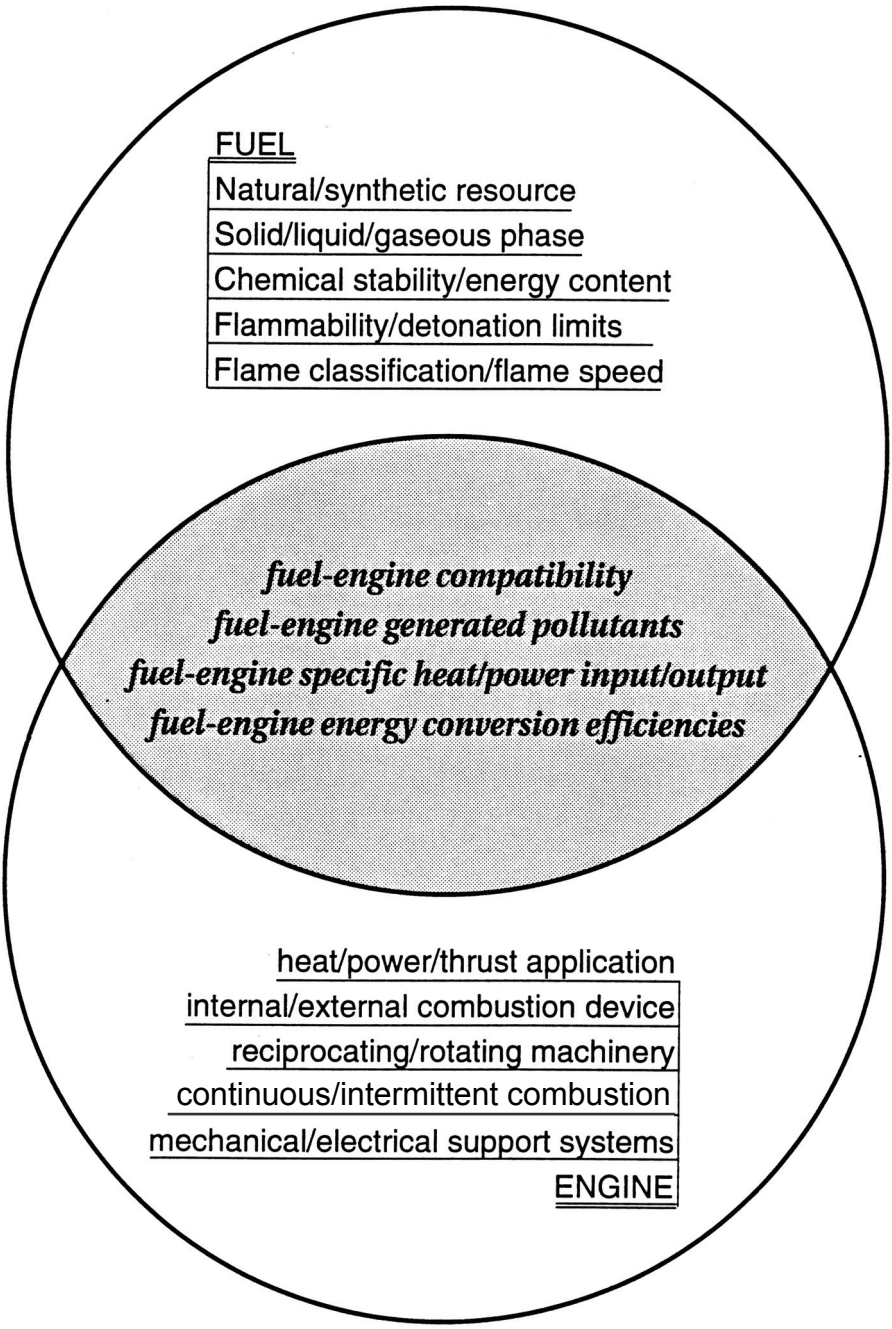

Figure 1.2 The critical fuel-engine interface.

The study of energy and combustion goes beyond a general knowledge of the physical and chemical nature of particular natural and/or synthetic fuel resources. It is an integral part of the life cycle engineering assessment of any usable fuel resource utilization starting with energy and economic issues relating to the raw materials found in the Earth and ending with the final disposal of wastes generated from their use including:

Source energy conversion penalties (drilling, mining, or growing)
Fuel preparation penalties (distillation, pyrolysis, or gasification)
Fuel distribution penalties (transportation from source to application)
Fuel storage penalties (liquefaction, compression, cooling, or required environmental controls)
Energy generation/conversion penalties (heat-transfer and power losses)
Environmental pollution control penalties (emissions reduction)

1.3 THE FUEL-ENGINE INTERFACE

Many crucial characteristics of combustion-driven heat engines are due, in fact, to their *fuel-engine interface* (see Figure 1.2), including compatibility of fuels with specific engines, pollutants generated by burning particular fuels in certain engines, general energy input/output performance characteristics of individual engines operating on a given fuel, and various interactions and efficiencies associated with those interfaces. Heat engines can be categorized in several different ways such as internal versus external combustion engines, continuous versus intermittent combustion engines, or spark- versus compression-ignition combustion engines; see Figure 1.3. The performance and emissions characteristics can differ widely between these various categories. Many outstanding reference texts have been written dealing principally with traditional topics covered in fundamentals of fuels and combustion. Other writers have produced excellent dissertations treating in detail the particulars of certain heat engines such as boilers and furnaces, spark-ignition engines, compression-ignition engines, and the gas turbine.

A need exists to improve the state of the art in engineering in a practical way in order to increase combustion and related efficiencies of current power and propulsion systems in use today as well as to develop new engines and new fuel alternatives to operate thereon. George Huebner, chairman of the Environmental Research Institute of Michigan, in an SAE paper entitled "Future Automotive Power Plants," stated: "Technical choices are being made that affect our nation's major engineering decisions for the future by those unskilled in the engineering profession and science of combustion." He further stated in the paper that "too much discussion of and consideration [is] given to alternative power plants without consideration of the fuel type." (1) As Professor Oppenheim at the University of California has so succinctly stated, "Further advances in engine technology should (a) minimize pollution emissions, (b) maximize engine efficiency, and (c) optimize tolerance to a wider variety of fuels." (2) Engineering design, development, operation, and maintenance of heat engines now require more than a cursory comprehension of fuels and engines.

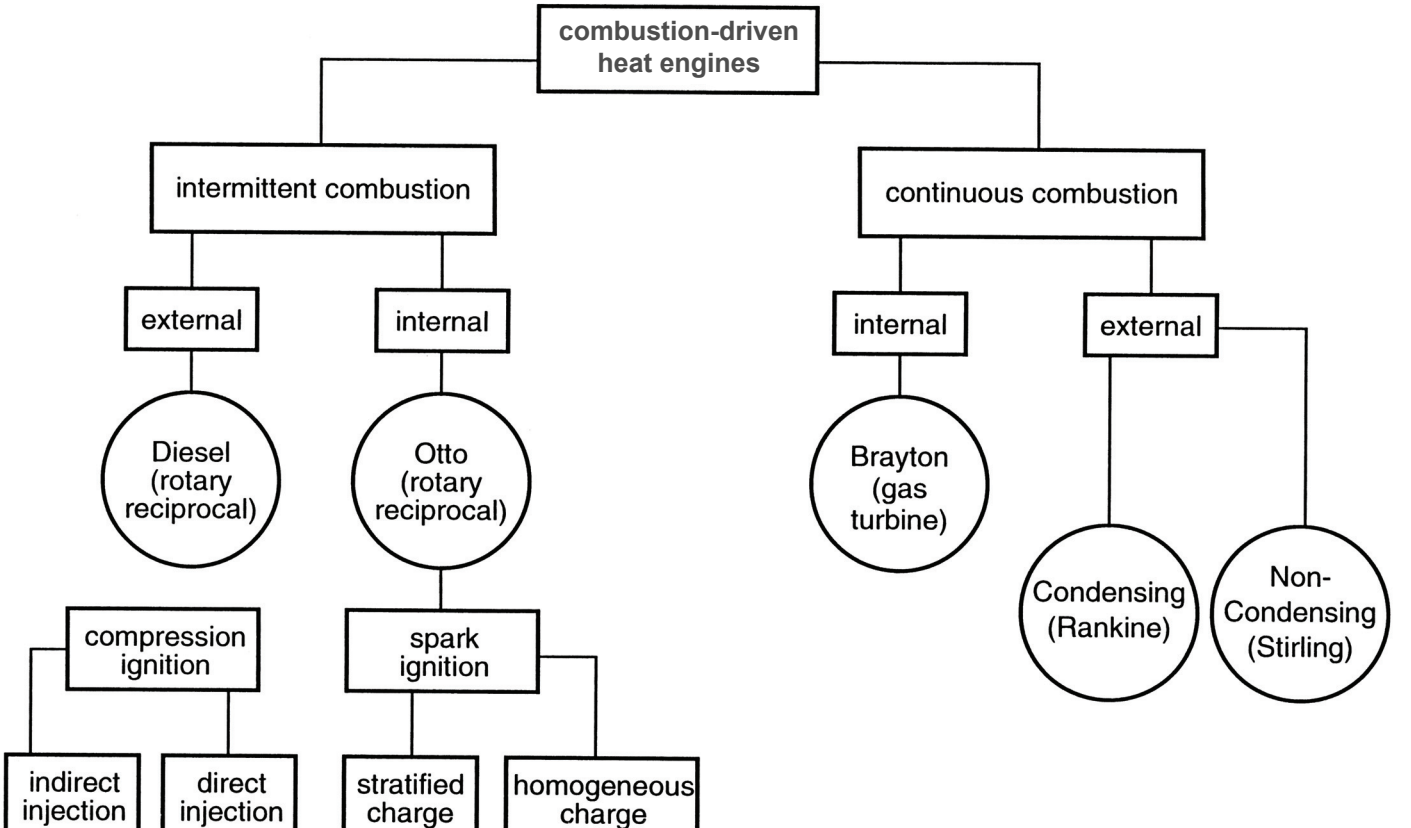

Figure 1.3 Combustion-drive heat engine family tree.

Table 1.2 Chemical Path for Fuel Combustion

Fuel (Reactants)
Storage—*compression, liquefaction*
↓
Transportation—*pumping*
↓
Preparation—*vaporization, atomization*
↓
Induction—*mixing, injection*
↓
Fuel (Products)
Ignition—*thermal, electric*
↓
Chemical conversion—*internal/external combustion*
↓
Energy transfer—*heat and/or work*
↓
Extraction—*exhaust, pollution control*

1.4 ENGINEERING SCIENCE AND COMBUSTION

The physical requirements and the thermochemical path that a fuel undergoes to produce heat and/or power will be developed in this text; see Table 1.2. In order to correctly formulate basic theories of combustion, analysis must be correct both qualitatively (physics and chemistry) and quantitatively (mathematics). Classical physics and chemistry utilize a fixed mass of material (control mass or closed system) to describe the conversion laws of mass, momentum, and energy. Consider, for example, the motion of an exhaust gas solid particulate as shown in Figure 1.4. Position and velocity of the particle are functions of space and time, and velocity $\vec{V}$ is a function (represented by $\langle\ \rangle$) of space and time $V\langle x, y, z, t\rangle$. In this instance, specific material is identified and followed using particle or *Lagrangian* analysis.

Because of the nondescript nature of fluid elements in combustion flow fields and the complexity of chemical activity therein, the unsteady three-dimensional nature of combustion is also written in *Eulerian* or field terminology. In this instance, a particular point in space is identified and observed. Note also that basic conservation laws are developed using a fixed volume (open system or control volume) system terminology. Figure 1.5 illustrates the flow of reactive gases through a stationary flame front in which the field velocity vector $\vec{V}$, in this case, describes a velocity vector at a point (x_0, y_0, z_0) in time. Mathematically, formulation of the conservation laws, such as mass conservation, will be different depending on type of analysis used, i.e., Lagrangian versus Eulerian. In addition, many problems are readily defined in terms of an infinitesimally small system using differential calculus; whereas others are more easily stated in finite geometries using integral calculus. It should be apparent that in some cases, engineering treatment of

very basic and simple physical phenomena of combustion may require very complex analytical tools; whereas, in other instances, one can use a very simple analysis to provide insight into a very complex phenomenon.

Various physical parameters, termed *dimensions,* represented with brackets, [ ], are selected to quantitatively express the physics of combustion. A base group of these defined principal or primary dimensions such as length and time are then used to express other secondary dimensions including velocity, i.e., length divided by time. Arbitrary and useful magnitudes, or *units,* for these physical parameters are established and maintained under the supervision of the General Conference on Weights and Measures. Two systems of dimensions and units will be used in this book, Système International (SI) and English Engineers. Table 1.3 lists some basic and secondary dimensions and units of combustion. Often it is necessary to change units in engineering calculations by use of identities termed *conversion factors*. Several useful conversion factors are found in Appendix A.1.

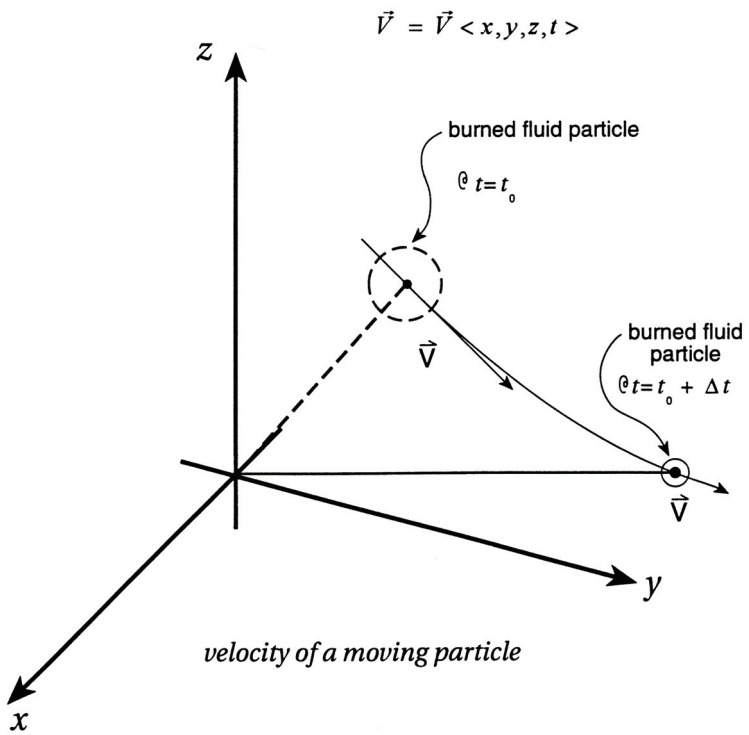

Figure 1.4 Lagrangian (particle) representation of combustion.

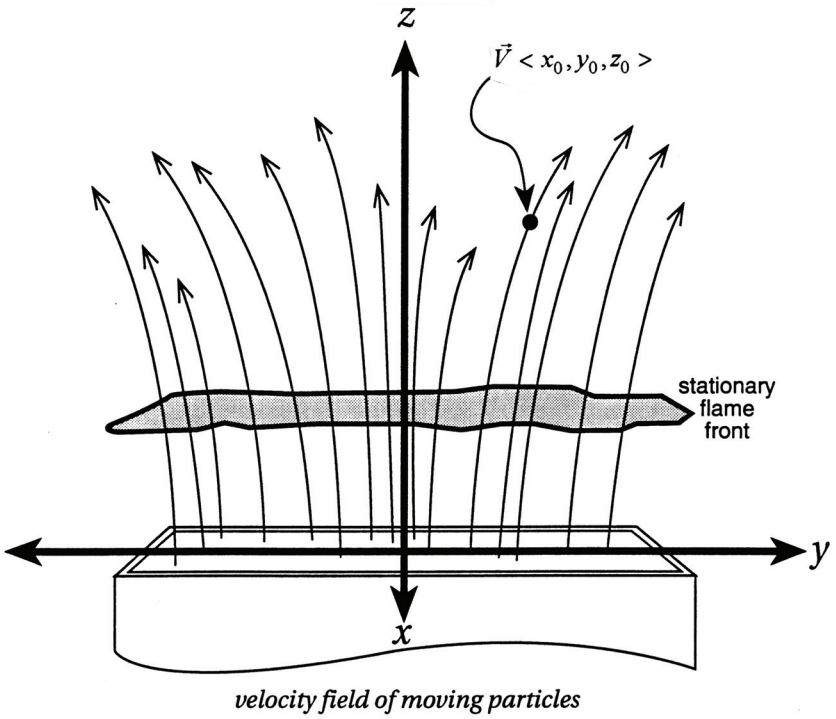

$$\vec{V} = V_x < x,y,z,t > \vec{i} + V_y < x,y,z,t > \vec{j} + V_z < x,y,z,t > \vec{k}$$

Figure 1.5 Eulerian (field) representation of combustion.

To illustrate a proper use of dimensions and units, consider Newton's second law, which describes the physical relationship between force [F], mass [M], and acceleration [a] for a fixed mass.

$$\vec{F} \sim M \cdot \vec{a} \tag{1.1}$$

where dimensionally

$$[F] \sim [M][L]/[t]^2$$

Since [F], [M], [L], and [t] are distinct dimensions, Newton's second law is more appropriately written quantitatively as

$$\vec{F} = M \cdot \vec{a}/g_0 \tag{1.1a}$$

where

$$g_0 = M \cdot \vec{a}/\vec{F} \tag{1.1b}$$

Table 1.3 Basic Dimensions and Units

Dimensions		Units			
		Système International (SI)		English System of Engineers	
Primary					
Force	$[F]$			Pound force	(lbf)
Mass	$[M]$	Kilogram	(kg)	Pound mass	(lbm)
Length	$[L]$	Meter	(m)	Feet	(ft)
Time	$[t]$	Second	(sec)	Second	(sec)
Temperature	$[T]$	Kelvin	(K)	Rankine	(°R)
Secondary					
Force	$[F]$	Newton	(kg·m/sec^2)		
Pressure	$[F]/[L]^2$	Pascal	(N/m^2)	psf	(lbf/ft^2)
Energy	$[F][L]$	Joule	(N·m)	Btu	(ft·lbf)
Power	$[F][L]/[t]$	watt	(J·sec)	horsepower or hp	(ft·lbf/sec)
Viscosity	$[M]/[L][t]$	Poises	(kg/m·sec)		(lbm/ft·sec)
Kinematic viscosity	$[L]^2/[t]$	Stokes	(m^2/sec)		(ft^2/sec)
Some principal constants					
Standard pressure		101 kPa (1 atm)		14.7 lbf/in^2 (1 atm)	
Absolute temperature		K = °C + 273		°R = °F + 460	
Standard acceleration		g = 9.8066 m/sec^2		g = 32.1740 ft/sec^2	
g_0		1.0 kg·m/N·sec^2		32.1740 ft·lbm/lbf·sec^2	

Dimensionally, the constant g_0 becomes

$$g_0 = [M][L]/[F][t]^2$$

which gives Newton's second law dimensional equality since

$$[F] = \frac{[M][L]/[t]^2}{[M][L]/[F][t]^2} = [F]$$

In SI, the primary dimensions and units are

[M] kilogram, kg
[L] meter, m
[t] second, sec

From physics, a force of 1 newton is the force that will accelerate 1.0 kg at 1.0 m/sec^2 or

$$g_0 = \frac{(1.0\text{kg})(1.0\text{m}/\text{sec}^2)}{(1\text{ N})} = 1\text{ kg}\cdot\text{m}/\text{N}\cdot\text{sec}^2$$

Now the unit of force, the newton, is a derived quantity, i.e., 1 N = 1 kg·m/sec^2, and

$$g_0 = \frac{1\text{ N}}{1\text{ N}} = 1.0$$

Note that g_0 in SI is actually dimensionless with a unit magnitude. However, using g_0, in the form 1 kg·m/N·sec^2 in equations where g_0 appears, will allow many equations to come out in correct units with ease and, therefore, g_0 will be carried throughout this text.

In Engineers units, the primary dimensions and units are

[F] pound force, lbf
[M] pound mass, lbm
[L] foot, ft
[t] second, sec

Again, from physics, 1 lbf will accelerate 1.0 lbm at 32.1740 ft/sec^2 or, in this instance,

$$g_0 = \frac{(1.0\text{ lbm})(32.1740\text{ ft}/\text{sec}^2)}{(1\text{ lbf})}$$
$$= 32.1740\text{ lbm}\cdot\text{ft}/\text{lbf}\cdot\text{sec}^2$$

Often, many problems can be understood when fundamental physical characteristics of matter, or *properties*, are stated in either dimensional or dimensionless form. In this text, capital letters generally denote extensive properties, lowercase letters imply intensive properties, and a superscript bar indicates molar properties. To illustrate, recall the concept of pressure, P, which is force/unit area or

$$[P] = [F]/[L]^2$$

Density ρ is mass/unit volume or

$$[\rho] = [M]/[L]^3$$

Specific volume v is volume/unit mass or

$$[v] = [L]^3/[M] = 1/[\rho]$$

Specific weight γ is weight/unit volume, and, since "weight" is a force due to gravity, Newton's second law can then be used to express γ as

$$[\gamma] = [F]/[L]^3 = [M]\cdot(g/g_0)/[L]^3$$

or

$$\gamma = \rho\cdot(g/g_0) \tag{1.2}$$

Specific gravity, S.G., is the density of a fluid to that of a reference fluid and is dimensionless.

EXAMPLE 1.2 Oxygen is the principal oxidant in most combustion processes. For O_2, at 25°C and 101 kPa absolute pressure, calculate (a) the specific gas constant R, J/kg·K; (b) the specific volume v, m^3/kg; (c) the density, ρ, kg/m^3; and (d) the specific weight γ, N/m^3.

Solution

1. Specific gas content:

$$R = \frac{\overline{R}}{MW} = \frac{8{,}314.34\,\text{J/kgmole}\cdot\text{K}}{32\,\text{kg/kgmole}}$$

a. $R_{O_2} = 259.82\,\text{J/kg}\cdot\text{K}$

2. Specific volume:

$$v = \frac{RT}{P} = \frac{(259.82\,\text{N}\cdot\text{m/kg}\cdot\text{K})(25+273\text{K})}{(101\text{kN/m}^2)(1{,}000\,\text{N/kN})}$$

b. $v = 0.767\,\text{m}^3/\text{kg}$

3. Density:

c. $\rho = \dfrac{1}{v} = \dfrac{1}{0.767\,\mathrm{m^3/kg}} = 1.304\,\mathrm{kg/m^3}$

4. Specific weight:

d. $\gamma = \rho\dfrac{g}{g_0} = (1.304\,\mathrm{kg/m^3})\dfrac{(9.8066\,\mathrm{m/sec^2})}{(1.0\,\mathrm{kg\cdot m/sec^2\cdot N})}$

$= 12.79\,\mathrm{N/m^3}$

Comment: Note that, in part (d), if g_0 is omitted, γ = m·kg/sec^2·m^3 and, since 1 N ≡ 1 m·kg/sec^2, γ = N/m^3. By carrying g_0 through the calculation although the quantity is unity and dimensionless, the answer comes out in correct units with ease.

Many important relations will be expressed in terms of these properties. Recall, for example, the ideal gas law that relates pressure *P*, volume *V*, mass *m* or moles *N*, and temperature *T* of a substance. Several forms are shown below.

Mass basis: $P = P\langle m, V, T\rangle$ (1.3)

$PV = mRT$ (1.3a)

$Pv = RT$ (1.3b)

$P = \rho RT$ (1.3c)

or

Molar basis: $P = P\langle N, V, T\rangle$

$PV = N\overline{R}T$ (1.4a)

$P\overline{v} = \overline{R}T$ (1.4b)

$P = \overline{\rho RT}$ (1.4c)

where the universal gas constant $\overline{R}$ is equal to

$$\overline{R} = \begin{cases} 8{,}314.34 \ \text{J/kgmole}\cdot\text{K} \\ 82.057 \ \text{atm}\cdot\text{cc/gmole}\cdot\text{K} \\ 1{,}545.3 \ \text{ft}\cdot\text{lbf/lbmole}\cdot{}^\circ\text{R} \\ 1.987 \ \text{cal/gmole}\cdot\text{K} \\ 1.987 \ \text{Btu/lbmole}\cdot{}^\circ\text{R} \end{cases}$$

Now the specific gas constant *R* can be determined as

$PV = mRT = N\overline{R}T$

or

$R = (N/m)\cdot\overline{R}$

From dimensional analysis, $[N]/[m]$ is moles per unit mass or molecular weight MW, and

$$R = \frac{\overline{R}}{MW} \tag{1.5}$$

1.5 ENGINEERING AND APPLIED COMBUSTION

Today's world makes it essential for engineers to grasp both fundamental principles (or science) and fundamental practices (or technology) in order to implement all the many diverse activities necessary to conceive, manufacture, and maintain useful products for the benefit of mankind in the 21st century. Most of the relevant engineering profession to this end can be classified into one of three distinct skill areas: theory, design, and operation; see Figure 1.6 and Table 1.4. Theory can be considered to be the part of engineering that focuses on precise formulation and development of basic principles and laws. Theory, a predominantly abstract and traditionally academic-centered activity, involves individual skills development utilized to predict specific characteristics of systems and devices. Design encompasses those segments of engineering that address the standardization and utilization of codes and practices. Many design rules have their roots in the manufacturing or operational realm of engineering. Design work is frequently accomplished using teams requiring individuals with project and/or managerial skills. Design utilizes individuals with achievements in a broad range of academic and training-centered skills in order to produce specific characteristics of systems and devices. Operation deals lastly in the field with all those aspects and actions necessary in order to protect specific characteristics of systems and devices. Operation utilizes a select group of individuals with focused training and people-centered skills having commitment to reliably maintain critical components and devices. It should be apparent that operational techniques are interrelated with both elements of theory and design.

Most undergraduate engineering curricula in the United States are based on four-year programs with emphasis on basic foundational theoretical subject matter. There is greater pressure now being placed on the university system to provide students with more design tools and experience. Operational and/or industrial experience occurs in only a few institutions that have co-op studies. Some debate exists as to whether there is sufficient time and even a need for introducing all these three skills at the college level.

The traditional notion was that engineering education and its related disciplines produced individuals whose abilities would span all three skill areas. Graduating engineers whose exposure had been predominantly to one skill area, that of theory, would have successful careers able to span all three. Another related concept was that if an individual prepared for competency in one area their preparation was sufficient for a career in the other areas. The reality and complexity of today's rapidly changing technical community, however, require engineers to be introduced to all three important and different skills in order to be prepared to choose for specialization in one. One of the key aspects of the American Board of Engineering Technology (ABET) 2000 criteria is to produce graduates with more than just technical skills.

Table 1.4 Basic Skill Areas of Professional Engineering Practice

Theory	Design	Operation
Precise formulation: engineering physics and/or chemistry	General application: engineering codes and/or rules	Specific utility: engineering tools and/or practices
Basic principles: differential and integral calculus	Complex programs: statistical and numerical analysis	Particular problems: basic math and geometry
Education-centered: requiring abstract mental skills necessary for system prediction	Educ./train-centered: requiring project managerial skills necessary for system production	Training-centered: requiring people motivational skills necessary for system protection

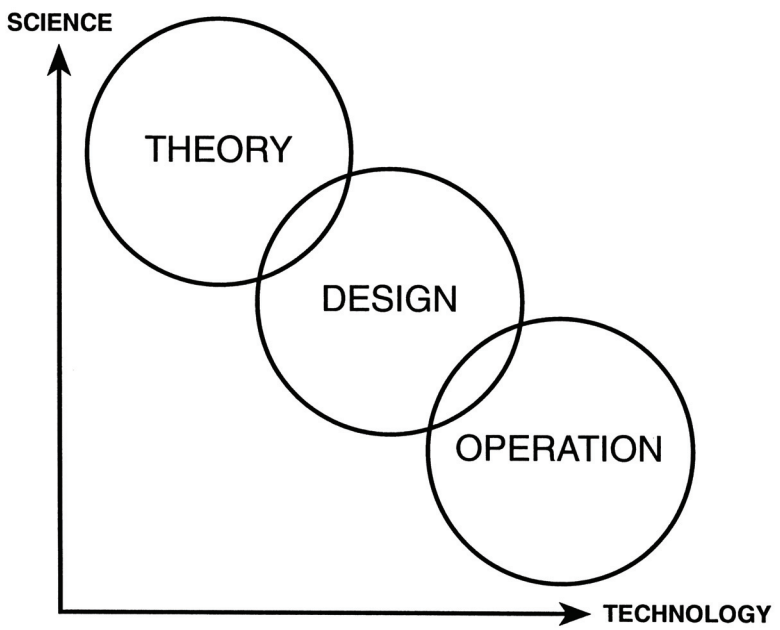

Figure 1.6 Visualization of the engineering profession.

A group of participants at the 1995 Conference of the Engineering Deans at Rensselaer Polytechnic Institute in Troy, NY, recently observed: "The engineering profession assumes that its graduates must be immediately productive and so educates them for their first job. The result is undergraduate programs that stress technical depth and an ethic that says real engineers do not stray far from their technical orientation. In reality, the careers of most engineers evolve within a few short years to include responsibility for the supervision of people, money, resources, and multidisciplinary projects. How engineers deal with these responsibilities depends on the breadth of their education and on their ability to communicate effectively." Or, as Woodrow Leake of the American Society of Engineering Education in Washington, D.C., said, "The days of rigid specialization in one discipline or sub-discipline [are gone]."

Over the years, for example, the traditions of the aerospace community have been such that areas within theory, design, and operational engineering (represented by Figure 1.6) have worked closely together on many specific projects. As such one can find instances throughout the aviation and aerospace history where the three segments have even had overlapping activities. However, through much of the history of land-based S&T engineering development not many occasions have existed where theory, design, and operational efforts were in close harmony. The three aspects shown in Figure 1.6 were often independent efforts and widely separated until recently with the appearance of activities such as concurrent engineering practices and just-in-time manufacturing, and the value chain. Table 1.5 lists critical issues of operation, design, and fundamentals presented in an integrated format, which is often useful for assessment and development purposes with these modern concurrent engineering efforts.

The U.S. industry today faces greater international competition and economic pressure to produce and operate better and environmentally benign products for public use in shorter time, for less cost, and of higher quality. Current engineering practices are being supplemented by a new paradigm of design for use through simultaneous engineering, interdisciplinary teams, new electronic engineering tools, and consortiums. Future engineers will be employed in internationally structured industries built around market-driven, goal oriented, and empowered teams. Engineering goods and services will be required to be designed, developed, and manufactured with many environmental criteria, as well as operated, maintained, and disposed of through use of concurrent engineering practices. Combustion principles and applications today will play a significant role in many important fuel-engine life cycle engineering activities.

Figure 1.7 illustrates the classic path along which successful technology developments have most frequently progressed in going from an idea or concept to a useful configuration. The process begins with a theory of physical attributes, and develops using modeling from basic laws, usually expressed in terms of simple physics and simple components. A theoretical model is translated into a design stage by passing successfully through the research laboratory, where simple testing validates or extends the initial basic theory. In the research lab, the nature of physics or the component characteristics of experiments are more complex than the original model developed from theory. Success at the research laboratory level allows a design engineer to transfer applied knowledge to industry through the development of a prototype, in which an even more complex testing establishes success or failure of the complete concept at the design level. Success at the design level results in production of a manufactured product which is then subjected to complex use, at which point success or failure is again redefined.

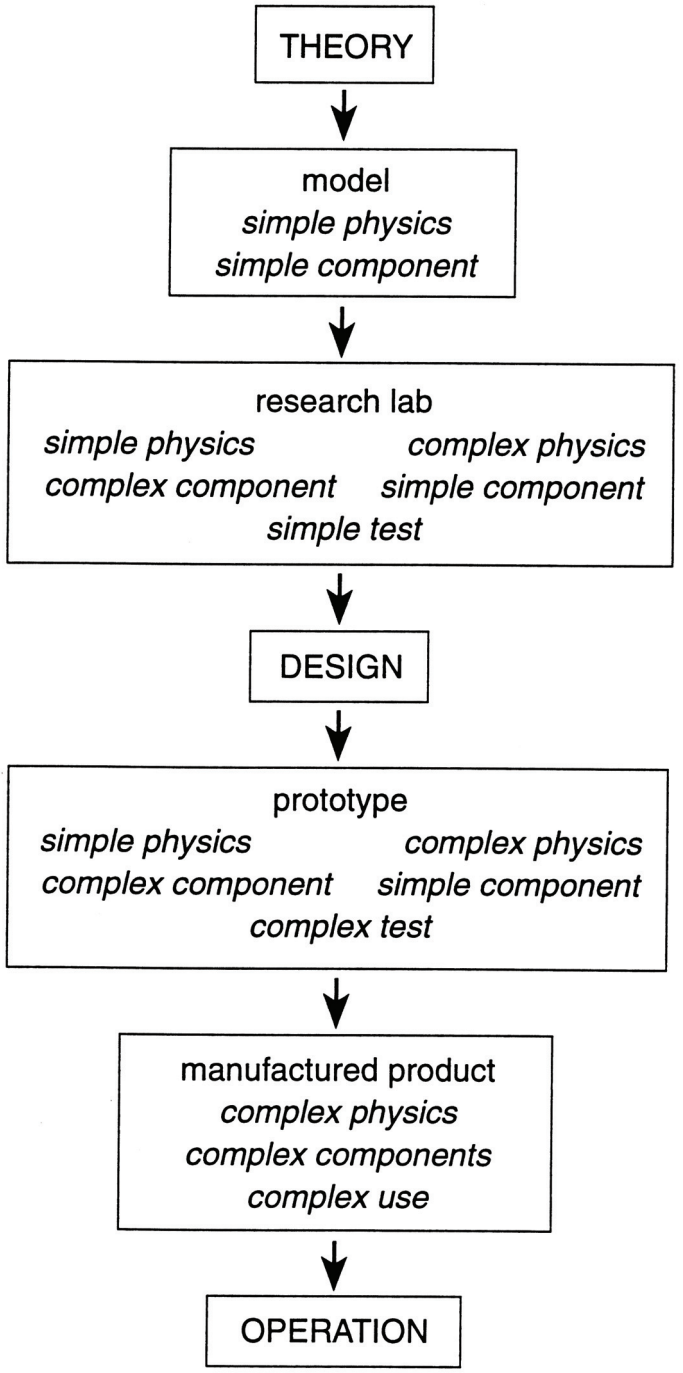

Figure 1.7 The classical path of technology development.

Table 1.5 Advanced Combustion Technologies Evaluation Issues

Operational assessment issues		Manufacturing assessment issues		Research assessment issues	
1.1	DUTY CYCLE	2.1	PRODUCT QUALITY GOALS	3.1	SCIENTIFIC MATURITY
1.1.1	run time	2.1.1	performance objectives	3.1.1	suitable patents granted
1.1.2	startup/restart	2.1.2	emission criteria	3.1.2	published records
1.1.3	shutdown	2.1.3	process control definition	3.1.3	history of technology
1.1.4	stop	2.1.4	cost of development	3.1.4	technology transfer value
		2.1.5	time to market	3.1.5	proof of basic concepts
1.2	RISK ASSESSMENT			3.1.6	breadth of scientific support
1.2.1	failure analysis	2.2	PROCESS CONTROL		
1.2.2	safety & operability	2.2.1	capability assessment	3.2	BASIC RESEARCH
1.2.3	impact on operation	2.2.2	baseline of basic unit size	3.2.1	laboratory fundamental testing
		2.2.3	technology compatibilities	3.2.2	modeling and scaling criteria
1.3	TECHNOLOGY INTEGRITY	2.2.4	technology installation impacts	3.2.3	identification of technology gaps
1.3.1	vibration	2.2.5	man-machine interface	3.2.4	chemistry/physics/biology
1.3.2	shock				
1.3.3	noise	2.3	DESIGN CONTROL	3.3	APPLIED RESEARCH
1.3.4	corrosion	2.3.1	process design	3.3.1	maturity of basic principles
1.3.5	fire & explosions	2.3.1	manufacturing design	3.3.2	alternative technology assessment
		2.3.3	assembly design	3.3.3	destruction chemistry demonstration
1.4	MAINTENANCE	2.3.4	life cycle design	3.3.4	breadboard systems
1.4.1	reliability & availability			3.3.5	solution to technology gaps
1.4.2	inspections/repair	2.4	FABRICATION RESOURCES		
1.4.3	manning requirements	2.4.1	industrial supply chain status		
		2.4.2	manufacturing materials status		
1.5	MATURITY	2.4.3	e-commerce		
1.5.1	operating history				
1.5.2	technology suitability	2.5	PRODUCT DEVELOPMENT		
1.5.3	technology acceptability	2.5.1	design of experiments		
1.5.4	operational economics	2.5.2	prototype testing		
		2.5.3	FMEA evaluation		
		2.5.4	training materials		

Figure 1.6 can also be helpful when visualizing the science and technology (S&T) of engineering technology development. Classic R&D efforts as described in Figure 1.7, for example, usually move on a tortuous path; starting from theory, and progress to the others areas, i.e., design and operation, to a final product. Today S&T of advanced technologies can be visualized as initiating within any of the three segments but then moving simultaneously through all three segments using directed and focused basic and applied R&D efforts in order to achieve successful and rapid implementation as a product. Figure 1.6 can thus be useful to illustrate and even clarify how specific interactions or lack thereof occur between theory, design, and/or operation during any given engineering S&T development effort.

Technology and literature in various fields of basic and applied combustion are expanding at an exponential rate. The professional journals and work related activities are now presenting new areas of interest not covered in many classic texts. A new approach is necessary in engineering literature to introduce important foundation and applied aspects of combustion in such a way as to develop a proper overview of major areas in the discipline, to provide basic knowledge that will enable practicing engineers to stay current in their field and to create motivation for further study. It is the author's intent that Applied Combustion provides a broader purview of the subjects and will enable the reader an ability to develop a better and broader in-depth understanding of the subject for future professional development.

PROBLEMS

1.1 Energy equivalents in various dimensions and units are often useful in combustion calculations. Determine the equivalent value of 1 hp in (a) ft·lbf/hr; (b) Btu/hr; and (c) kW.

1.2 Determine the equivalent temperature in Kelvin for an absolute temperature of (a) 500; (b) 1,000; (c) 1,500; and (d) 2,000°R.

1.3 One kg of carbon will theoretically release approximately 33,000 kJ/kg of energy by complete combustion. Calculate the amount of energy that would ideally be obtained if the carbon mass could be completely converted into nuclear energy ($E = mc^2$), kJ/kg.

1.4 The specific volume of gasoline is approximately 0.0238 ft^3/lbm. Find (a) its density, lbm/ft^3; (b) its specific weight, N/m^3; and (c) the mass of fuel in a 20-gal tank, lbm.

1.5 Standard atmospheric condition in theoretical combustion calculations is often stated as 14.7 psia. Calculate the standard atmosphere in (a) lbf/ft^2; (b) ft H_2O; (c) mm Hg; and (d) Pa.

1.6 The specific gravity of a fuel is expressed as S.G. $\langle 60°F \rangle$, indicating that both the oil and water are measured at a temperature of 60°F. A diesel fuel has a specific gravity at 60°F of 0.8762. Determine (a) the density of the fuel, lbm/ft^3; and (b) the specific weight of the fuel, lbf/gal.

1.7 A 100-liter tank is to hold H_2 gas at 25°C and 400 kPa. Calculate (a) the mass of H_2 contained in the vessel, lbm; (b) the specific volume of H_2, ft^3/lbm; and (c) the density of H_2, lbm/ft^3.

1.8 Air is to be supplied to the combustor can of a gas turbine. Inlet conditions for the air are 740°F and 174 psia. The mass flow rate of air is 9,000 lbm/min. Determine (a) the volumetric flow rate for the air, ft^3/min; and (b) the molar flow rate for the air, lbmole air/min.

1.9 An automobile will consume about 0.4 lbm fuel/hr for each horsepower of power developed. Assume that gasoline can release 19,000 Btu/lbm of energy. Determine (a) the thermal efficiency of the engine, %; and (b) heat rejection rate, Btu/hp.

1.10 A stationary steam-driven electric power plant has a thermal efficiency of approximately 35%. For a 750,000 kW unit, calculate (a) the ideal required heat addition, Btu/min; (b) the ideal amount of nuclear material required to produce this energy, lbm/yr; and (c) the amount of coal necessary to produce this energy if the coal has an energy content of approximately 12,000 Btu/lbm coal.

1.11 The ideal combustion energy content of a fuel is expressed in terms of its heating value. The approximate heating values of three important energy resources are listed below:

Natural gas	1,000 Btu/ft^3
Coal	12,000 Btu/lbm
Crude oil	138,000 Btu/gal

Determine the fuel energy equivalents of (a) natural gas to fuel oil, ft^3/gal; (b) coal to natural gas, lbm/ft^3; and (c) crude oil to coal, gal/ lbm.

1.12 The fuel energy equivalence of a natural gas and coal supply is 0.78 m^3 gas/kg coal, while the fuel energy equivalence of crude oil to coal is 0.092 m^3 oil/kg coal. If the heating value of coal is approximately 29,075 kJ/kg, determine (a) the energy equivalence of natural gas to oil, m^3 gas/m^3 oil; (b) the heating value of natural gas, kJ/m^3; and (c) the heating value of the fuel oil, kJ/m^3.

1.13 Refer to the three fuels given in Problem 1.11 and their heating values to determine the fuel economic equivalence of (a) coal, $/ton; and (b) gas, $/$ft^3$. Assume that oil is priced at $75/bbl (42 gal).

2

Combustion and Energy

2.1 INTRODUCTION

Combustion engineering requires an ability to analyze energetics of chemically reactive mixtures. Most thermodynamics texts address the general subject of energy conversion and conservation as well as cover principles of mass conservation, property relationships, equations of state, and process relationships. Classical thermodynamics provides a useful overall energy balance bookkeeping technique for describing components and processes. The particular discipline termed *thermochemistry* deals with global energy analysis associated with combustion processes. In this chapter, a basic comprehension of thermodynamics will be assumed, and a general energy balance for a chemically reactive medium will be developed.

In most cases, the conservation of energy principle is stated for changes, or *processes,* that occur between some initial stable, i.e., *equilibrium condition*, or *state,* and some final equilibrium condition; see Figure 2.1. Since thermodynamics does not address the rate at which these processes occur, it will be necessary in later chapters to develop materials that will describe the dynamic nature of combustion.

2.2 THE CONSERVATION OF MASS

The conservation of mass principle is a fundamental engineering concept. Consider the case of a fixed total mass of a chemically reactive mixture, using a *control mass* or *closed system* reference. In general, the chemical composition of such a reactive mixture will undergo change with time. The initial condition is referred to as the *reactant* state, while the final condition is termed the *product* state.

A mathematical means expressing composition change and mass conservation for reactive systems is provided by the *chemical reaction* equation, written in general form as

$$\Sigma \nu_i R_i \rightarrow \Sigma \nu_j P_j \tag{2.1}$$

where

ν_i = mass or moles of species i
R_i = reactant species i
ν_i = mass or moles of species j
P_j = product species j

All initial reactants are placed on the left-hand side of the general reaction equation, while any final products appear on the right-hand side. Indication of the type of particular reaction process, i.e., $P = c$, $V = c$, $T = c$, is shown above the process arrow.

The general mass conservation principle for a chemical reaction can be stated in terms of an *atomic mass balance*, i.e., total number of atoms of an element in the final product state, such as for example hydrogen atom, must equal the initial number of atoms of the element in the reactant state. The conservation of atomic species will yield a set of equations equal to the unique number of elements in the reactant mixture. Chemical reactions involving species containing the atoms H, C, O, and N, for example, generate four distinct atomic mass balances.

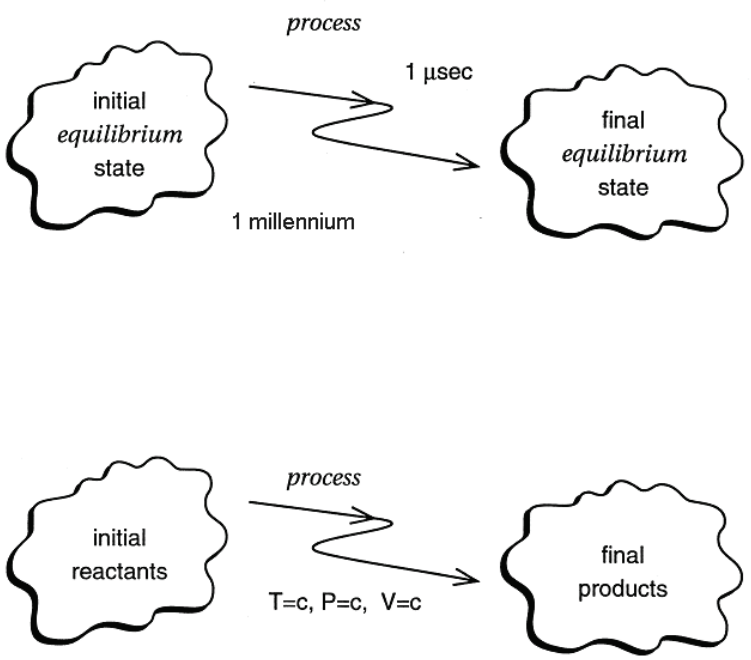

Figure 2.1 A generalized thermochemical process.

Often, it is convenient to describe chemically reactive mixtures on a *molar* basis. *Molar analysis* utilizes a relative chemical mass scale for compounds based on the periodic chart. Molar based quantities (recall the universal gas constant) will be recognized by having a bar placed over the quantity in question. For a mixture of k total chemical species, a mole fraction $\bar{x}_i$ for each i species can be expressed as

$$\bar{x}_i = \frac{N_i}{N_{\text{tot}}} \frac{\text{kgmole}_i}{\text{kgmole}_{\text{tot}}} \left(\frac{\text{lbmole}_i}{\text{lbmole}_{\text{tot}}} \right) \tag{2.2}$$

and the total moles N_{tot} is equal to

$$\sum_{i=1}^{k} N_i = N_{\text{tot}} \text{ kgmole (lbmole)} \tag{2.2a}$$

and

$$\sum_{i=1}^{k} \bar{x}_i = 1.0 \tag{2.2b}$$

A description based on mass or weight for a mixture of compounds, termed a *gravimetric analysis,* expresses the total mass of either reactant and/or product state in terms of each pure constituent. For a mixture of k total chemical species, a mass fraction mf_i for each i component species can be written as

$$mf_i \equiv \frac{m_i}{m_{\text{tot}}} \frac{\text{kg}_i}{\text{kg}_{\text{tot}}} \left(\frac{\text{lbm}_i}{\text{lbm}_{\text{tot}}} \right) \tag{2.3}$$

and the total mass m_{tot} is then equal to

$$\sum_{i=1}^{k} m_i = m_{\text{tot}} \text{ kg (lbm)} \tag{2.3a}$$

and

$$\sum_{i=1}^{k} mf_i = 1.0 \tag{2.3b}$$

Even though the total mass of a combustion process may remain constant, concentration of individual constituents such as oxygen or carbon dioxide may change during a reaction. The mass fraction of a constituent as a reactant species i may be quite different from that as a product species j.

In Chapter 1, the bridge between molar and mass analysis was shown to be molecular weight. The mole-mass relationship for species i is given as

$$m_i = N_i \cdot MW_i$$

where

m_i = mass species i, kg (lbm)
N_i = moles species i, kgmole (lbmole)
MW_i = molecular weight species i, kg/kgmole (lbm/lbmole)

For a mixture of k species, the total mass can be written

$$m_{\text{tot}} = N_{\text{tot}} MW_{\text{tot}} = \sum_{i=1}^{k} N_i MW_i \tag{2.4}$$

or

$$MW_{\text{tot}} = \sum_{i=1}^{k} \left(\frac{N_i}{N_{\text{tot}}} \right) MW_i = \sum_{i=1}^{k} \bar{x}_i MW_i \tag{2.4a}$$

EXAMPLE 2.1 Standard atmospheric conditions for many combustion calculations can be represented by the following mole fractions:

N_2 78%
O_2 21%
Ar 1%

For these conditions, determine (a) the mass fractions of N_2, O_2, and Ar; (b) the mixture molecular weight, kg/kgmole; and (c) the specific gas constant R for air, J/kg K.

Solution

1. Mole fractions:

$$\bar{x}_{N_2} = 0.78 \; x_{O_2} = 0.21 \; \bar{x}_{Ar} = 0.01$$

2. Mass fractions:

	$\bar{x}_i$	MW_i	$\bar{x}_i MW_i$	mf_i^*
O_2	0.21	32.0	6.72	0.232
N_2	0.78	28.0	21.84	0.754
Ar	0.01	40.0	0.40	0.014
	$\frac{\text{kgmole}_i}{\text{kgmole}_{\text{tot}}}$	$\frac{\text{kg}_i}{\text{kgmole}_i}$	$\frac{\text{kg}_i}{\text{kgmole}_{\text{tot}}}$	$\frac{\text{kg}_i}{\text{kg}_{\text{tot}}}$

* a. $mf_{O_2} = \dfrac{\bar{x}_{O_2}}{\Sigma \bar{x}_i MW_i} = \dfrac{6.72}{6.72+21.84+0.40} = 0.232$

$mf_{N_2} = \dfrac{21.84}{28.96} = 0.754,\ mf_{Ar} = \dfrac{0.46}{28.96} = 0.014$

b. $MW_{air} = \Sigma \bar{x}_i MW_i = 6.72 + 21.84 + 0.40 = 28.96\ \text{kg/kgmole}$

c. Specific gas constant:

$$R_{air} = \frac{\bar{R}}{MW} = \frac{8{,}314\ \text{J/kgmole} \cdot \text{K}}{28.96\ \text{kg/kgmole}} = 287\ \text{J/K} \cdot \text{kg}$$

The most prominent chemical reaction associated with power production and heat transfer is the overall *oxidation reaction*, i.e.,

"Fuel" + oxidizer $\rightarrow$ Products

Reactants and/or products of combustion may exist as a solid, liquid, and/or vapor. In addition, the contributing species may be single species, pure compounds, complex mixtures, stable molecules, and/or radicals. Traditionally, most fuels of engineering relevance have been hydrocarbon compounds, represented symbolically as C_xH_y. Furthermore, the most commonly used oxidizing agent is air. In combustion calculations, air is often assumed to be approximately 21% O_2 and 79% N_2 by volume. This theoretical air, termed *dry air,* has a molecular weight of approximately 28.96 in this text. For every mole of O_2 in air there will be an additional 3.76 moles of N_2 or 4.76 total moles of air for each mole of O_2.

For any given fuel-oxidant reaction, the actual potential combining proportions can depend on (1) the fuel, (2) the oxidant, (3) the combustion process, and/or (4) the combustion device. Ideal complete combustion of a fuel assumes formation of the most fully oxidized products. The most stable oxidized product of carbon is carbon dioxide, CO_2, while the most stable oxidized product of hydrogen is water, H_2O. Therefore, the most stable oxidized products formed from complete combustion of any hydrocarbon fuel would be only CO_2 and H_2O.

Sufficient oxidant theoretically required to support complete combustion of a particular fuel and ideally to form its most stable products can be expressed in terms of the *stoichiometric equation*. For example, consider the two stoichiometric oxidation reactions below.

$$C_S + O_2 \xrightarrow{P} CO_2$$

$$CH_4 + 2(O_2 + 3.76N_2) \xrightarrow{V} CO_2 + 2H_2O + 7.52N_2$$

For a fuel-air mixture, stoichiometric conditions are often referred to as 100% *theoretical air, TA*. It is important to note that an actual reaction having stoichiometric fuel-air proportions will not ensure complete combustion. Since stoichiometric oxidation reactions do not achieve complete combustion, many combustion systems operate using *excess air, EA*, i.e., a percentage of air over and above stoichiometric proportions. For instance, 150% theoretical air is equivalent to 50% excess air. A fuel-air mixture having excess air is termed a *fuel-lean* mixture, whereas a mixture that has excess fuel is called a *fuel-rich* mixture.

$$C_3H_8 + (5)(1.2)(O_2 + 3.76N_2) \xrightarrow{P} 3CO_2 + 4H_2O + O_2 + (6)(3.76)N_2$$

Practical engineering considerations give rise to the use of a *fuel-to-air ratio, FA,* or an *air-to-fuel ratio, AF*. These ratios can be expressed on a mass or molar basis as follows:

Mass basis:

$$AF = \frac{\text{mass of air}}{\text{mass of fuel}} \qquad \frac{\text{kg air}}{\text{kg fuel}}\left(\frac{\text{lbm air}}{\text{lbm fuel}}\right) \tag{2.5}$$

$$FA = \frac{\text{mass of fuel}}{\text{mass of air}} \qquad \frac{\text{kg fuel}}{\text{kg air}}\left(\frac{\text{lbm fuel}}{\text{lbm air}}\right) \tag{2.5a}$$

Mole basis:

$$\overline{AF} = \frac{\text{moles of air}}{\text{moles of fuel}} \qquad \frac{\text{kgmole air}}{\text{kgmole fuel}}\left(\frac{\text{lbmole air}}{\text{lbmole fuel}}\right) \tag{2.6}$$

$$\overline{FA} = \frac{\text{moles of fuel}}{\text{moles of air}} \qquad \frac{\text{kgmole fuel}}{\text{kgmole air}}\left(\frac{\text{lbmole fuel}}{\text{lbmole air}}\right) \tag{2.6a}$$

A useful dimensionless fuel-oxidant ratio, or *equivalence ratio* Φ, can be defined as

$$\Phi \equiv \frac{\left(\dfrac{\text{moles fuel}}{\text{moles oxidant}}\right)_{\text{actual}}}{\left(\dfrac{\text{moles fuel}}{\text{moles oxidant}}\right)_{\text{stoichiometric}}} \tag{2.7}$$

where

$\Phi < 1$ fuel - lean mixture
$\Phi = 1$ stoichiometric mixture
$\Phi > 1$ fuel - rich mixture

EXAMPLE 2.2 The reaction of gaseous hydrogen and oxygen to form water is well known. The combustion of carbon with oxygen forming carbon dioxide is also an important chemical reaction. Write the chemical reactions for these two oxidation reactions, and calculate (a) the reactant's molar analysis, (b) the reactant's gravimetric analysis, and (c) mass of oxygen required per mass of fuel.

Solution:

1. Stoichiometric hydrogen combustion:

$$H_2 + aO_2 \rightarrow bH_2O$$

Hydrogen atom balance	$2 = 2b$	$b = 1$
Oxygen atom balance	$2a = 1$	$a = 0.5$

$$H_2 + 0.5O_2 \rightarrow H_2O$$

2. Mole fractions:

$$\bar{x}_{H_2} = \frac{1}{1 + 0.5} = 0.667$$

$$x_{O_2} = \frac{0.5}{1.5} = 0.333$$

3. Mass fractions:

	$\bar{x}_i$	MW_i	$x_i MW_i$	mf_i[a]
H_2	0.667	2.0	1.333	0.111
O_2	0.333	32.00	10.667	0.889
	$\frac{\text{lbmole}_i}{\text{lbmole}_{tot}}$	$\frac{\text{lbm}_i}{\text{lbmole}_i}$	$\frac{\text{lbm}_i}{\text{lbmole}_{tot}}$	$\frac{\text{lbm}_i}{\text{lbm}_{tot}}$

$$MW = \Sigma \bar{x}_i MW_i = 1.333 + 10.667 = 12.00 \text{ lbm/lbmole}$$

[a] $mf_{H_2} = \frac{1.333}{12.00} = 0.111, \qquad mf_{O_2} = \frac{10.667}{12.00} = 0.889$

4. Mass O_2/H_2:

$$OF = \frac{Z \text{ lbm } O_2}{1.0 \text{ lbm } H_2} = \frac{88.9 \text{ lbm } O_2}{11.1 \text{ lbm } H_2} \qquad Z = 8.01 \frac{\text{lbm } O_2}{\text{lbm } H_2}$$

5. Stoichiometric carbon combustion:

$C_S + aO_2 \rightarrow bCO_2$
Carbon atom balance $1 = b$
Oxygen atom balancer $2a = 2$ $\qquad a = 1$
$C_S + O_2 \rightarrow CO_2$

6. Mole fractions:

$$\bar{x}_{C_S} = \frac{1}{1 + 1} = 0.50$$

$$x_{O_2} = 1 - 0.5 = 0.5$$

7. Mass fractions:

	x_i	MW_i	$\bar{x}_i MW_i$	mf_i[b]
C_S	0.50	12.00	6.00	0.273
O_2	0.50	32.00	16.00	0.727
	$\frac{\text{lbmole}_i}{\text{lbmole}_{\text{tot}}}$	$\frac{\text{lbm}_i}{\text{lbmole}_{\text{tot}}}$	$\frac{\text{lbm}_i}{\text{lbmole}_{\text{tot}}}$	$\frac{\text{lbm}_i}{\text{lbm}_{\text{tot}}}$

$$MW = \Sigma \bar{x}_i MW_i = 6.00 + 16.00 = 22.00 \text{ lbm/lbmole}_{\text{tot}}$$

[b] $mf_{C_S} = \frac{6.00}{22.00} = 0.273, \qquad mf_{O_2} = \frac{16.00}{22.00} = 0.727$

8. Mass O_2/C_S:

$$OF = \frac{Z \text{ lbm } O_2}{1.0 \text{ lbm C}} = \frac{72.7 \text{ lbm } O_2}{27.3 \text{ lbm C}} \qquad Z = 2.663 \frac{\text{lbm } O_2}{\text{lbm } C_S}$$

Comments: This problem illustrates the variations in air-fuel ratios for hydrocarbon compounds. Not only will the stoichiometric proportions vary with each particular fuel, but the ratio will differ depending on whether the results are based on a mass or molar analysis.

2.3 THERMODYNAMIC PROPERTIES

An energetic analysis of important combustion reactions will often require thermodynamic characteristics, or *properties*, of relevant constituents. Several of the more familiar include: temperature T, total pressure P, total volume V, moles N (or $\bar{x}_i$), mass M_i *(or* mf_i*)*, total internal energy U, and/or total enthalpy H. The state of a simple pure homogeneous substance can be described by specifying two independent and substance-dependent, or *intrinsic,* properties. Internal energy and pressure are examples of intrinsic properties, while kinetic and potential energies are examples of nonintrinsic, or *extrinsic,* properties.

Combustion reactions involve multiphase, multicomponent mixtures that undergo chemical transformation in both time and space. Obviously, such a complex event as chemistry cannot be characterized using a single pure homogeneous constituent. Even for most nonreactive mixtures, two independent intrinsic properties, such as temperature and total pressure, plus the chemical composition, are necessary to define a state. Considering

the many possible thermodynamic property combinations needed for combustion analysis, simply tabulating or graphing needed data is prohibitive.

Thermochemical calculations can be based on fundamental relations expressed collectively in terms of pure component species properties. Furthermore, it will be convenient to think in terms of reactant and product conditions initially as being two distinct nonreactive equilibrium mixture states. Many product mixtures can furthermore be treated as ideal-gas mixtures in part because of the heat release and high product temperatures as well as the chemical composition of most major fuels being used today.

The Gibbs-Dalton law describes the thermodynamic nature of an ideal-gas mixture in terms of each pure component species. The rule states that, *in an equilibrium mixture of ideal gases, each component acts as if it were alone in the system at* V_{tot}, T. By careful application of this law, thermodynamic state and useful thermochemical properties for a mixture can be developed.

For an equilibrium mixture of nonreactive gases A, B, C, . . . , and using the Gibbs-Dalton law, one can write the following facts:

$$V_{\text{A}} = V_{\text{B}} = V_{\text{C}} = \cdots = V_i = V_{\text{tot}} \tag{2.8}$$

$$T_{\text{A}} = T_{\text{B}} = T_{\text{C}} = \cdots = T_i = T \tag{2.9}$$

From the conservation of mass principle,

$$N_{\text{tot}} = N_{\text{A}} + N_{\text{B}} + N_{\text{C}} + \cdots = \sum_{i=1}^{k} N_i \tag{2.2a}$$

From Chapter 1, the ideal-gas equation of state was given as

$$P_{\text{tot}} V_{\text{tot}} = N_{\text{tot}} \overline{R} T \tag{1.4}$$

Combining Equations (1.4), (2.3), (2.8), and (2.9) yields

$$P_{\text{tot}} V_{tot} = \left(N_{\text{A}} + N_{\text{B}} + N_{\text{C}} + \cdots\right) \overline{R} T = \Sigma N_i \overline{R} T$$

or

$$P_{\text{tot}} = \frac{N_{\text{A}} \overline{R} T}{V_{\text{A}}} + \frac{N_{\text{B}} \overline{R} T}{V_{\text{B}}} + \frac{N_{\text{C}} \overline{R} T}{V_{\text{C}}} + \cdots = \Sigma \frac{N_i \overline{R} T}{V_i} \tag{2.10}$$

The pressure exerted by a pure component species i if it were alone in a closed system at the total volume and mixture temperature is termed its *partial pressure* P_i or

$$P_i = N_i \overline{R} T / V \tag{2.11a}$$

and

$$\frac{P_i}{P_{\text{tot}}} = \frac{N_i \overline{R} T / V}{N_{\text{tot}} \overline{R} T / V} = \frac{N_i}{N_{\text{tot}}} = \bar{x}_i$$

$$P_i = \bar{x}_i P_{\text{tot}} \tag{2.11b}$$

where

$$\Sigma P_i = \sum_{i=1}^{k} \bar{x}_i P_{\text{tot}} = P_{\text{tot}} \tag{2.11c}$$

P = pressure

i = chemical species i

k = total number of species

The total pressure is equal to the sum of partial pressures where partial pressure of a species i is equal to total pressure multiplied by its mole fraction.

Additional thermodynamic properties, such as internal energy and enthalpy, can also be evaluated by applying the Gibbs-Dalton law.

Internal energy U, for example, generally is expressed as a function of temperature, volume, and composition, i.e., $U = U\langle T, V, N_i \rangle$. Since, for ideal gases, $U = U\langle T, N_i \rangle$, the total internal energy of a mixture can be written as

Extensive:

$$U_{\text{tot}} = m_{\text{tot}} u_{\text{tot}} = \Sigma m_i u_i \qquad \text{kJ (Btu)} \tag{2.12a}$$

or

$$U_{\text{tot}} = N_{\text{tot}} \bar{u}_{\text{tot}} = \Sigma N_i \bar{u}_i \qquad \text{kJ (Btu)} \tag{2.12b}$$

Intensive:

$$u_{\text{tot}} = \sum_{i=1}^{k} \left(\frac{m_i}{m_{\text{tot}}} \right) u_i = \sum_{i=1}^{k} m f_i u_i \qquad \frac{\text{kJ}}{\text{kg mixt}} \left(\frac{\text{Btu}}{\text{lbm mixt}} \right) \tag{2.12c}$$

or

$$\bar{u}_{tot} = \sum_{i=1}^{k} \left(\frac{N_i}{N_{\text{tot}}} \right) \bar{u}_i = \sum_{i=1}^{k} \bar{x}_i \bar{u}_i \qquad \frac{\text{kJ}}{\text{kgmole mixt}} \left(\frac{\text{Btu}}{\text{lbmole mixt}} \right) \tag{2.12d}$$

Enthalpy H is generally expressed as a function of temperature, pressure, and composition, i.e., $H = H\langle T, P, N_i \rangle$. Again, for ideal gases $H = H\langle T, N_i \rangle$, and the total enthalpy of a mixture is stated as

Extensive:

$$H_{\text{tot}} = m_{\text{tot}} h_{\text{tot}} = \Sigma m_i h_i \qquad \text{kJ (Btu)} \tag{2.13a}$$

or

$$H_{\text{tot}} = N_{\text{tot}} \bar{h}_{\text{tot}} = \Sigma N_i \bar{h}_i \qquad \text{kJ (Btu)} \tag{2.13b}$$

Intensive:

$$h_{\text{tot}} = \sum_{i=1}^{k} m f_i h_i \qquad \frac{\text{kJ}}{\text{kg mixt}} \left(\frac{\text{Btu}}{\text{lbm mixt}} \right) \tag{2.13c}$$

or

$$\bar{h}_{\text{tot}} = \sum_{i=1}^{k} \bar{x}_i \bar{h}_i \qquad \frac{\text{kJ}}{\text{kgmole mixt}} \left(\frac{\text{Btu}}{\text{lbmole mixt}} \right) \tag{2.13d}$$

A constant-volume specific heat C_v is defined as

$$C_v)_{\text{tot}} = \frac{\partial u_{\text{tot}}}{\partial T} \Bigg)_v \qquad \frac{\text{kJ}}{\text{kg} \cdot \text{K}} \left(\frac{\text{Btu}}{\text{lbm} \cdot {}^\circ\text{R}} \right) \tag{2.14}$$

or for a nonreactive ideal-gas mixture using Equation (2.12c),

$$= \frac{\partial}{\partial T} \left(\frac{1}{m_{\text{tot}}} \sum_{i=1}^{k} m_i u_i \right)_v$$

$$= \frac{1}{m_{\text{tot}}} \Sigma m_i \frac{\partial u_i}{\partial T} \Bigg)_v = \Sigma m f_i C_{v_i}$$

$$C_v)_{\text{tot}} = \sum_{i=1}^{k} m f_i C_{v_i} \qquad \frac{\text{kJ}}{\text{kg} \cdot \text{K}} \left(\frac{\text{Btu}}{\text{lbm} \cdot {}^\circ\text{R}} \right) \tag{2.14a}$$

or

$$\bar{C}_v)_{\text{tot}} = \sum_{i=1}^{k} \bar{x}_i \bar{C}_{v_i} \qquad \frac{\text{kJ}}{\text{kgmole} \cdot \text{K}} \left(\frac{\text{Btu}}{\text{lbmole} \cdot {}^\circ\text{R}} \right) \tag{2.14b}$$

A constant-pressure specific heat C_p can be defined in similar fashion for a nonreactive ideal-gas mixture as

$$C_p)_{\text{tot}} = \frac{\partial h_{\text{tot}}}{\partial T} \Bigg)_p \qquad \frac{\text{kJ}}{\text{kg} \cdot \text{K}} \left(\frac{\text{Btu}}{\text{lbm} \cdot {}^\circ\text{R}} \right) \tag{2.15}$$

$$= \frac{\partial}{\partial T} \left(\frac{1}{m_{\text{tot}}} \sum_{i=1}^{k} m_i h_i \right)_p$$

$$= \frac{1}{m_{\text{tot}}} \Sigma m_i \frac{\partial h_i}{\partial T} \Bigg)_p = \Sigma m f_i C_{p_i}$$

$$C_p)_{\text{tot}} = \sum_{i=1}^{k} m f_i C_{p_i} \qquad \frac{\text{kJ}}{\text{kg} \cdot \text{K}} \left(\frac{\text{Btu}}{\text{lbm} \cdot {}^\circ\text{R}} \right) \tag{2.15a}$$

or

$$\bar{C}_p)_{\text{tot}} = \sum_{i=1}^{k} \bar{x}_i \bar{C}_{p_i} \qquad \frac{\text{kJ}}{\text{kgmole} \cdot \text{K}} \left(\frac{\text{Btu}}{\text{lbmole} \cdot {}^\circ\text{R}} \right) \tag{2.15b}$$

Enthalpy and internal energy are related by the equation $h = u + Pv$. For an ideal gas, this can be expressed as

$$h = u + RT \tag{2.16}$$

and

$$dh = du + RdT \tag{2.16a}$$

combining Equations (2.14), (2.15), and (2.16a) and noting that specific heats for an ideal gas depend only on temperature,

$$C_p dT = C_v dT + RdT$$

or

$$R_{\text{tot}} = C_{p_{\text{tot}}} - C_{v_{\text{tot}}} \quad \frac{\text{kJ}}{\text{kg}}\left(\frac{\text{Btu}}{\text{lbm}}\right) \tag{2.17}$$

and

$$R_{\text{tot}} = \sum_{i=1}^{k} mf_i C_{p_i} - \sum_{i=1}^{k} mf_i C_{v_i}$$

$$= \sum_{i=1}^{k} mf_i \left(C_{p_i} - C_{v_i}\right)$$

$$R_{\text{tot}} = \sum_{i=1}^{k} mf_i R_i$$

The specific heat ratio γ is defined as

$$\gamma \equiv \frac{C_p}{C_v} = \frac{\overline{C}_p}{\overline{C}_v} \tag{2.18}$$

Using Equations (2.17) and (2.18), one can also write

$$C_p = \frac{R\gamma}{\gamma - 1} \quad \text{or} \quad \overline{C}_p = \frac{\overline{R}\gamma}{\gamma - 1} \tag{2.19a}$$

and

$$C_v = \frac{R}{\gamma - 1} \quad \text{or} \quad \overline{C}_p = \frac{\overline{R}}{\gamma - 1} \tag{2.19b}$$

Substituting Equations (2.14b) and (2.15b) into (2.18) gives

$$\gamma_{\text{tot}} = \frac{\Sigma \bar{x}_i \overline{C}_{p_i}}{\Sigma \bar{x}_i \overline{C}_{v_i}} = \frac{\Sigma mf_i C_{p_i}}{\Sigma mf_i C_{v_i}} \tag{2.18a}$$

EXAMPLE 2.3 Consider a homogeneous mixture of ethylene, C_2H_4, and 130% theoretical air. Calculate as a function of temperature (a) the mixture gas constant R, kJ/kg; (b) the mixture constant-pressure specific heat C_p, kJ/kg·K; (c) the mixture constant-volume specific heat C_v, kJ/kg·K; and (d) the specific heat ratio γ.

Solution

1. Stoichiometric equation:

$$C_2H_4 + aO_2 \rightarrow bCO_2 + cH_2O$$

Carbon atom balance $b = 2$

Hydrogen atom balance $c = 2$

Oxygen atom balance $2a = 2(2) + 2 \qquad a = 3$

2. Actual reaction:

$$C_2H_4 + (1.3)(3)[O_2 + 3.76N_2] \rightarrow 2CO_2 + 2H_2O + 0.9O_2 + (3.9)(3.76)N_2$$

3. Mixture molecular weight:

$$\bar{x}_{C_2H_4} = \frac{1.0}{1.0 + (3.9)(4.76)} = 0.0511$$

$$\bar{x}_{air} = 1.0000 - 0.0511 = 0.9489$$

$$MW_{tot} = \Sigma \bar{x}_i MW_i = (0.0511)(28) + (0.9489)(28.97)$$

$$MW_{tot} = 28.92 \text{ kg/kgmole mixt}$$

4. Thermodynamic properties:

a. $$R = \frac{\overline{R}}{MW} = \frac{8.314 \text{ kJ/kgmole} \cdot \text{K}}{28.92 \text{ kg/kgmole}} = 0.2875 \text{ kJ/kg} \cdot \text{K}$$

and

$$C_p = \overline{C}_p / MW = \overline{C}_p / 28.92 \qquad C_p - C_v = R \qquad C_p / C_v = \gamma$$

$$\overline{C}_p = \Sigma \bar{x}_c \overline{C}_{p_i} = 0.9489\,\overline{C}_{p_{air}} + 0.0511\,\overline{C}_{p_{C_2H_4}}$$

5. From Tables B.7 and B.25 in Appendix B,

	Air		C_2H_4	
T	$\overline{C}_p$	$\overline{C}_p$	$\overline{C}_p$	$\overline{C}_p$
298	6.947	29.087	10.250	42.917
400	7.010	29.351	12.679	53.087
600	7.268	30.431	16.889	70.714
800	7.598	31.813	20.039	83.903
1,000	7.893	33.048	22.443	93.969
1,200	8.109	33.952	24.290	101.70
1,400	8.289	34.706	25.706	107.63
1,600	8.437	35.326	26.794	112.19
K	cal/gmole·K	kJ/kgmole·K	cal/gmole·K	kJ/kgmole·K

T	$\overline{C}_{p_{\text{mixt}}}$	C_p	C_v	γ
298	29.794	1.030	0.7425	1.387
400	30.564	1.057	0.7695	1.374
600	32.489	1.123	0.8355	1.344
800	34.475	1.192	0.9045	1.318
1,000	36.161	1.250	0.9625	1.298
1,200	37.414	1.294	1.0065	1.286
1,400	38.432	1.329	1.0415	1.276
1,600	39.254	1.357	1.0695	1.269
	kJ/kgmole·K	kJ/kg·K	kJ/kg·K	—

Comments: This problem illustrates that the assumption of constant specific heats and specific heat ratio may, in certain problems with a wide temperature variation, lead to serious error. Note that the specific heats C_p and C_v both increase with increasing temperature while γ decreases with increasing temperature.

The enthalpy of a single compound on a unit mole basis can be expressed as a function of temperature and pressure or

$$\overline{h}_i = \overline{h}_i\langle T, P\rangle \quad \frac{\text{kJ}}{\text{kgmole}_i}\left(\frac{\text{Btu}}{\text{lbmole}_i}\right) \tag{2.20}$$

Differential changes in enthalpy are equal to

$$d\overline{h}_i = \left(\frac{\partial \overline{h}_i}{\partial T}\right)_p dT + \left(\frac{\partial \overline{h}_i}{\partial P}\right)_T dP \tag{2.20a}$$

Since, for an ideal gas, enthalpy is independent of pressure

$$\bar{h}_i = \bar{h}_i\langle T\rangle \tag{2.21}$$

and Equation (2.15) becomes

$$d\bar{h}_i = \left(\frac{\partial \bar{h}_i}{\partial T}\right)_p dT = \bar{C}_{p_i}\langle T\rangle dT \tag{2.21a}$$

integrating Equation (2.21a) between limits

$$\Delta\bar{h}_i = \int_{h_0}^{h} d\bar{h}_i = \int_{T_0}^{T} \bar{C}_{p_i}\langle T\rangle dT \tag{2.21b}$$

where

T = system temperature
T_0 = reference datum temperature = 25°C (77°F)

Values for $\bar{C}_{p_i}$ versus T for several gases are found in Tables B.2–B.25 in Appendix B.

The temperature dependency of ideal-gas specific heats can be expressed in virial form. Consider, for example, the constant-pressure molar specific heat of a pure component i, expressed as a fitted power series in temperature as

$$\bar{C}_{p_i}\langle T\rangle = a_1 + a_2T + a_3T^2 + a_4T^3 + a_5T^4 \tag{2.22}$$

Substituting the virial form for $\bar{C}_p$ into Equation (2.21b), Equation (2.22) yields an illustrative expression for changes in enthalpy for a compound as

$$\bar{h}_i\langle T_2\rangle - \bar{h}_i\langle T_0\rangle = \int_{T_0}^{T}\left[a_1 + a_2T + a_3T^2 + a_4T^3 + a_5T^4\right]dT \tag{2.23}$$

$$= \left[a_1T + \frac{a_2}{2}T^2 + \frac{a_3}{3}T^3 + \frac{a_4}{4}T^4 + \frac{a_5}{5}T^5\right]_{T_0}^{T} \tag{2.23a}$$

Values for $\Delta\bar{h}_i\langle T\rangle$ for several gases are also found in Tables B.2–B.25 in Appendix B.

Changes in internal energy for an ideal gas can be obtained from an appropriate expression in terms of enthalpy

$$\bar{h}_i = \bar{u}_i + P_i\bar{v}_i = \bar{u}_i + \bar{R}T \tag{2.24}$$

$$\bar{u}_i = \bar{h}_i - \bar{R}T\ \frac{\text{kJ}}{\text{kgmole}}\left(\frac{\text{Btu}}{\text{lbmole}}\right)$$

and

$$\Delta\bar{u}_i + \bar{u}_i\langle T\rangle - \bar{u}_i\langle T_0\rangle = \Delta\bar{h}_i - \bar{R}\Delta T = \Delta\bar{h}_i - \bar{R}(T - T_0) \tag{2.24a}$$

EXAMPLE 2.4 A 10-kg mixture of 25% CO and 75% N_2 by weight is cooled from 1,800 to 800K. For these conditions, determine (a) Δh, kJ/kg mixture; (b) $\Delta \bar{h}$, kJ/kgmole; (c) $\Delta \bar{u}$, kJ/kgmole; and (d) Δu, kJ/kg.

Solution:

1. Mixture properties from Tables B.4 and B.18 in Appendix B:

	$\bar{h}\langle T\rangle - \bar{h}\langle T_0\rangle$[a]		$\bar{h}\langle 1{,}800\rangle - \bar{h}\langle 800\rangle$
	1,800K	800K	
N_2	49,017.2	15,056.5	33,960.7
CO	49,557.3	15,186.2	34,371.1
	kJ/kgmole		

[a]Values are equal to $4.187 \times \left[\bar{h}\langle T\rangle - \bar{h}\langle T_0\rangle\right]$ from Appendix B.

where

$$\Delta h)_{N_2} = \left.\frac{\Delta \bar{h}}{MW}\right)_{N_2} = \frac{33{,}960.7 \text{ kJ/kgmole}}{28 \text{ kg/kgmole}} = 1{,}212.9 \frac{\text{kJ}}{\text{kg}}$$

$$\Delta h)_{CO} = \left.\frac{\Delta \bar{h}}{MW}\right)_{CO} = \frac{34{,}371.1 \text{ kJ/kgmole}}{28 \text{ kg/kgmole}} = 1{,}227.5 \frac{\text{kJ}}{\text{kg}}$$

2. Mixture enthalpy:

$$\Delta h = \Sigma m f_i \Delta h_i = \left(0.25 \frac{\text{kg CO}}{\text{kg mixt}}\right)\left(1{,}227.5 \frac{\text{kJ}}{\text{kg CO}}\right) + \left(0.75 \frac{\text{kg } N_2}{\text{kg mixt}}\right)\left(1{,}212.9 \frac{\text{kJ}}{\text{kg } N_2}\right)$$

a. $\Delta h = 1{,}216.6$ kJ/kg mixt

3. Mixture molar enthalpy:

$$\Delta \bar{h}_{tot} = \Delta h_{tot} \times MW_{tot} = (1{,}216.6 \text{ kJ/kg mixt})(28 \text{ kg/kgmole})$$

b. $\Delta \bar{h} = 34{,}064.8$ kJ/kgmole

4. Mixture molar internal energy:

$$\bar{u}_i = \bar{h}_i - \bar{R} T_i$$

and

$$\Delta\bar{u}_i = \Delta\bar{h}_i - \bar{R}\Delta T$$

or

$$\Delta\bar{u} = 34{,}064.8 \text{ kJ/kgmole} - \left(8.314 \text{ kJ/kgmole} \cdot \text{K}\right)\left(1{,}000\text{K}\right)$$

c. $\Delta\bar{u} = 25{,}750.8$ kJ/kgmole

5. Mixture internal energy

$$\Delta u_{\text{tot}} = \Delta\bar{u}_{\text{tot}} / MW_{\text{tot}}$$

$$\Delta u_{\text{tot}} = \frac{25{,}750.8 \text{ kJ/kgmole}}{28 \text{ kg/kgmole}}$$

d. $\Delta u = 919.7$ kJ/kg mixt

Comments: This problem illustrates the methodology used in preparing thermodynamic tables for gas mixtures. Tables such as for air and for products of combustion of fuel with 200% theoretical air and 400% theoretical air, as well as those for particular water vapor-air mixtures, are familiar to the student of engineering thermodynamics. For complex calculations, it is convenient to store these procedures in computer codes for access and easy solution to many thermochemical problems.

Several additional properties, including entropy and Gibbs and Hemholtz functions, will be covered in Chapter 3.

2.4 HEATS OF REACTION

Thermodynamic processes will usually result in a change in temperature, pressure, and/or volume. Thermochemical processes produce additional effects, including compositional changes and release or absorption of additional energy due to chemical reactions. For the purposes of analysis, it will be convenient to model the actual energetics of combustion reactions in terms of an ideal hypothetical process.

Chemical processes can result in energy being liberated by a reaction, termed an *exothermic reaction*, or the process may require energy to be absorbed, termed an *endothermic reaction*; see Figure 2.2. Furthermore, any energy absorbed or released at the reference datum by reaction would cause temperature to change and, therefore, make it necessary to transfer energy, usually as heat, to return the final temperature to its datum value.

Consider, for example, a closed system in which a chemical reaction occurs at constant total pressure; see Figure 2.3. Experience indicates that the temperature and composition will change as reactants are converted to products. To analyze this problem, it will be assumed that all chemical reactions, i.e., mass conversions and energy release, will occur only at a datum state, i.e., conditions of constant temperature and total pressure: T_0, P_0. This idea is similar to boiling and/or condensation energy transfer, in

which T_{sat} and P_{sat} do not change but rather the energy transfer results in phase changes from liquid $\rightleftarrows$ vapor.

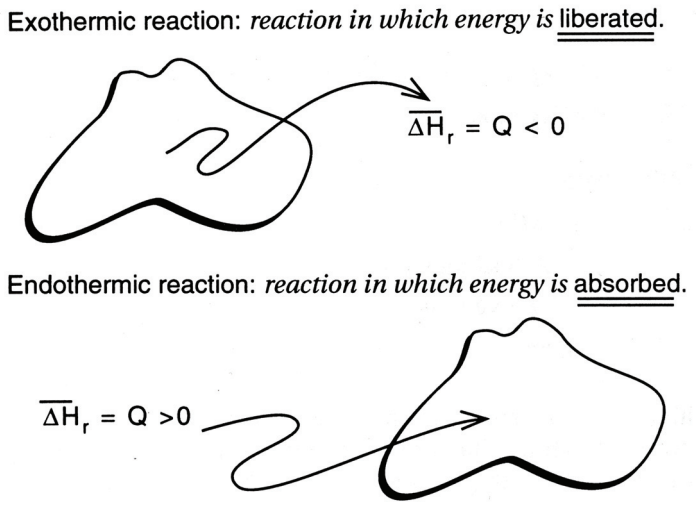

Figure 2.2 Energy of reaction.

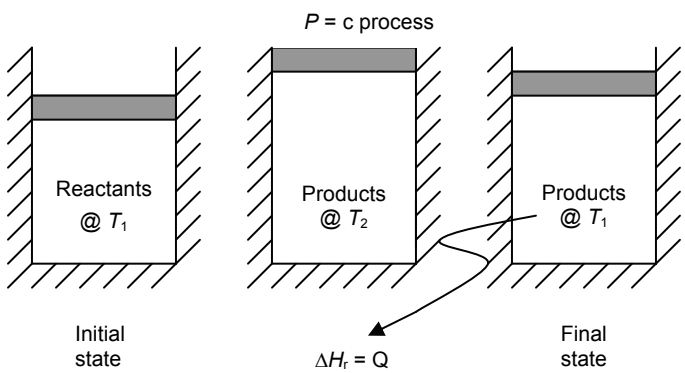

Figure 2.3 Heat of reaction.

This energy transfer is called the heat of reaction, ΔH_R, and is defined as the energy absorbed or liberated from a chemical reaction when products are brought back to the initial temperature of the reactants. Since chemical reactions involve rearrangement of chemical bonds and formation and destruction of species, it is necessary to develop a means of comparing the ideal chemical energetics of various compounds, i.e., a kind of a chemical potential energy of a species. Thus, for instance, certain compounds such as fuels have a greater capacity to react rapidly with oxygen, i.e., have high chemical potential energies, whereas product species such as CO_2 and H_2O have low chemical potential energies. This new species property, an energy of formation, will be seen to have direct bearing on the heat of reaction.

Two standard states have been used to define the datum in thermochemistry: the gaseous monatomic species datum and the natural elemental species datum. In both standards, the datum pressure and temperature are

$$P_0 = 1\,\text{atm} = 101\,\text{kPa} = 14.7\,\text{psi}$$
$$T_0 = 25°\text{C} = 298\text{K} = 77°\text{C} = 537°\text{R}$$

Standard state compounds are selected compounds that are assigned zero chemical potential energy at standard temperature and pressure (*STP*). Since our datum is for a constant-pressure process, this energy of formation is termed the *enthalpy of formation*, $\bar{h}_{f_i}^0$.

In the monatomic standard at *STP*, all monatomic species, i.e., O, H, N, etc., have $\bar{h}_{f_i}^0 = 0$. In the natural elemental standard, all natural elemental compounds have $\bar{h}_{f_i}^0 = 0$. A natural elemental compound is a species in which only one element appears and in a form in which it occurs naturally at *STP*, i.e., H_2, N_2, O_2, and *solid* carbon. Note that, for example, CO is not a natural elemental species since it contains more than one atomic species and O is also not a natural elemental species since oxygen occurs naturally as O_2 at *STP*. The natural elemental standard will be used in this text.

Two important heats of reaction warrant special attention: the heat of formation and the heat of combustion. The *heat of formation,* ΔH_f, is the *energy absorbed or liberated by a chemical reaction when the product* (a single chemical compound) *is brought back to the initial temperature of the reactants* (only natural elemental species). The heat of formation reaction for several compounds is shown below.

Elemental compounds		Single compounds
$H_2 + ½O_2$	$\xrightarrow{STP}$	H_2O
$CS + 2H_2$	$\xrightarrow{STP}$	CH_4
$C_S + O_2$	$\xrightarrow{STP}$	CO_2
$8C_S + 9H_2$	$\xrightarrow{STP}$	C_8H_{18}

Another useful heat of reaction is the heat of combustion, ΔH_c, which is the *energy liberated when a compound reacts with an oxidant to form the most oxidized form of the reactants, and is brought back to the initial reactant temperature*. Recall that, for

hydrocarbon chemistry, the most common oxidant is O_2 and the most stable oxidized products are CO_2 and H_2O; i.e.,

$$\text{Fuel} + \text{oxidant} \xrightarrow{STP} a\text{CO}_2 + b\text{H}_2\text{O}$$

If the water formed exists in the vapor state, the heat of combustion is termed *lower heating value.* If the water in the product state exists as a liquid, the heat of combustion is termed *higher heating value of the fuel.* This implies that the product mixture gave up its additional latent heat in going from a vapor to a liquid state.

Obviously, actual combustion processes do not occur at *STP*, and real combustion processes may not go to completion. It is therefore necessary to develop a means of expressing the energetics of chemical reactions in the more general case of combustion, which will be done in the following sections.

2.5 FIRST LAW FOR REACTIVE SYSTEMS

The first law of thermodynamics leads directly to an energy conservation principle. An extensive development of this concept can be found in most undergraduate thermodynamics texts. This fundamental relationship provides a statement, in general terms, of conservation and conversion of various energy forms.

From classical thermodynamics and the first law, one can obtain a *differential* form of the general energy equation for an *open system* (also termed a fixed or control volume relationship) as

$$\frac{dE}{dt} = \dot{Q} - \dot{W} + \sum_{i_{\text{in}}} \dot{m}_i e_i - \sum_{i_{\text{out}}} \dot{m}_i e_i \qquad \text{kW}\left(\frac{\text{Btu}}{\text{min}}\right) \tag{2.25a}$$

or

$$\frac{dE}{dt} = \dot{Q} - \dot{W} + \sum_{i_{\text{in}}} \dot{N}_i \dot{e}_i - \sum_{i_{\text{out}}} \dot{N}_i \bar{e}_i \tag{2.25b}$$

where

E = total system energy in C.V.
$\dot{Q}$ = rate of heat transfer to/from (+ in/– out) the C.V.
$\dot{W}$ = rate of work transfer to/from (– in/+ out) the C.V.
$\dot{m}_{i,j}$ = mass flow rate of material transferred across the C.V. boundaries
$\dot{N}_{i,j}$ = molar flow rate of material transferred across the C.V. boundaries
$e_{i,j}$ = intensive total energy per unit mass of material transferred across the C.V. boundaries
$\bar{e}_{i,j}$ = intensive total energy per unit mole of material transferred across the C.V. boundaries

This relationship can be expressed on a mass or molar basis but, in this text, will most frequently be written on a molar basis.

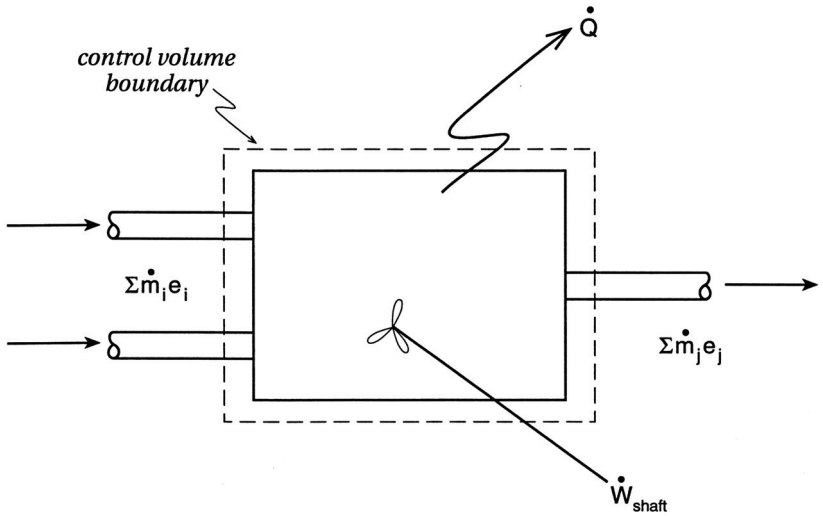

Figure 2.4 Open-system energy transfers.

Table 2.1 General Energy Equation and Applications

$$\frac{dE}{dt} = \left.\frac{\delta \dot{Q}}{dt}\right)_{C.V.} + \left.\frac{\delta W}{dt}\right)_{C.V.} + \Sigma \dot{m}_i [e_i] - \Sigma \dot{m}_j [e_j]$$

Heat exchangers	Turbines	K.E. (nozzles)
Boilers	Compressors	P.E. (hydroelectric)
Furnaces	Pump	U (steam vs. air)
Condensers	Fan	$\bar{h}_f^0$ (combustion)

Equation (2.25) shows that the total energy E of a control volume may change with time, i.e., increase, decrease, and/or remain constant. Furthermore, it indicates that the *rate of change* of total control volume energy can be the result of several influences, including heat and/or work transfer rates to and/or from an open system, as well as various energy fluxes associated with material transfer across the boundaries. Figure 2.4 and Table 2.1 illustrate the significance of this equation to certain applications.

Many specific forms of the energy equation can easily be obtained by a proper application of the general energy equation as expressed by Equation (2.25). To do so, one must: (1) understand the physics of a particular problem under consideration, (2) formulate the proper mathematical statement of the appropriate energy balance, and (3) obtain the necessary properties required for solution.

To illustrate a technique for reducing the general energy equation to a suitable specific form, consider the case in which all the properties within a C.V., as well as those transferring across the boundary, do not change with time, i.e., *steady state* and *steady*

flow. Under these restrictions, the rate of change in total C.V. energy must remain constant or

$$\frac{dE}{dt} = 0$$

Thus, the net energy flux into C.V. must equal the net energy flux out of C.V. or, when one equates transient energy forms of heat transfer and power to energy as properties crossing the boundaries due to mass transfer,

$$\dot{Q} - \dot{W} = \sum_{j_{\text{out}}} \dot{m}_j e_j - \sum_{i_{\text{in}}} \dot{m}_i e_i = \sum_{j_{\text{out}}} \dot{N}_j \bar{e}_j = \sum_{i_{\text{in}}} \dot{N}_i \bar{e}_i \tag{2.26}$$

Unsteady applications that allow mass transfer from an open system, such as in rocket propulsion systems (see Figure 2.5), are instances in which the rate of decrease in total C.V. energy is written as

$$\frac{dE}{dt} = \dot{Q} - \sum_{j_{\text{out}}} \dot{m}_j e_j = \dot{Q} - \sum_{j_{\text{out}}} \dot{N}_j \bar{e}_j \tag{2.27}$$

Consider another illustrative case in which no material is transferred across the boundary, i.e., a *closed system* (often termed a fixed or control mass). In this instance,

$$\dot{m}_i = \dot{m}_j = 0$$

and

$$\frac{dE}{dt} = \dot{Q} - \dot{W}$$

Multiplying both sides by *dt,*

$$dE = \delta Q - \delta W$$

In many engineering applications, closed systems can produce *boundary expansion work,* such as with a piston-cylinder geometry, as illustrated in Figure 2.6. In this instance, the force through a distance relationship for work takes the familiar form,

$$\delta W = PdV \tag{2.28}$$

and

$$dE = \delta Q - PdV \tag{2.29}$$

For a device that operates on a thermodynamic cycle, the initial and final states must be identical, requiring that the system must function as a closed system and integrating around the cyclic loop

$$\oint dE = 0 = \oint \delta Q - \oint \delta W$$

$$Q_{\text{net}} = W_{\text{net}} \tag{2.30}$$

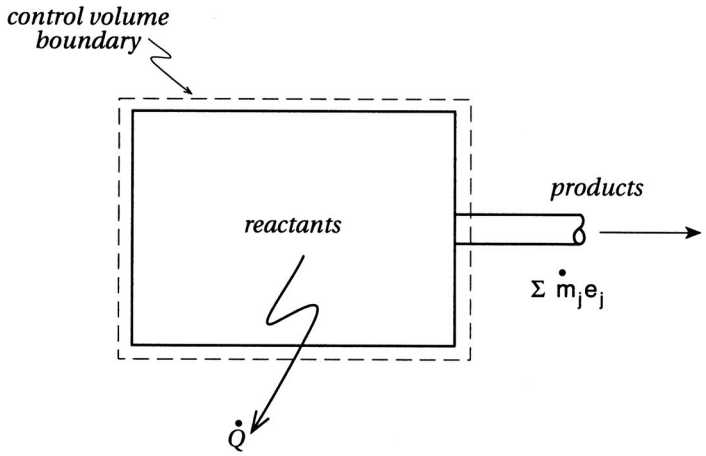

Figure 2.5 Unsteady open-system energy transfer.

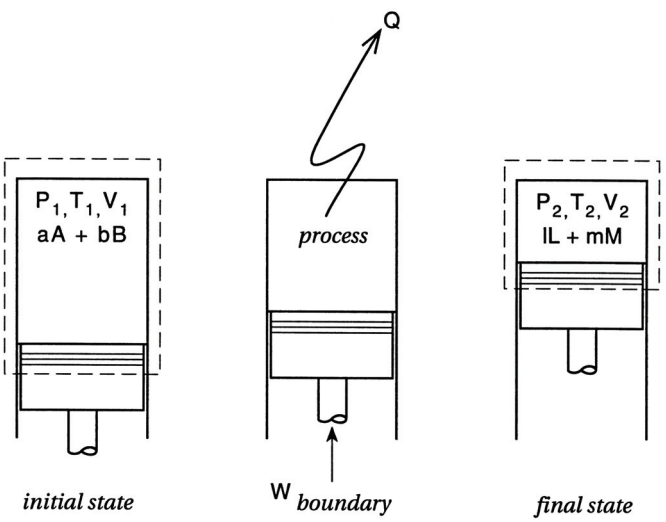

Figure 2.6 Closed-system energy transfer.

The total energy E of an ideal-gas mixture according to the Gibbs-Dalton law can be written as

$$E_{\text{tot}} = \Sigma m_i e_i = \Sigma N_i \bar{e}_i \qquad \text{kJ (Btu)} \tag{2.31}$$

or

$$e_{\text{tot}} = \Sigma m f_i e_i \qquad \text{kJ/kg (Btu/lbm)} \tag{2.31a}$$

and

$$\bar{e}_{\text{tot}} = \Sigma \bar{x}_i \bar{e}_i \qquad \text{kJ/kgmole (Btu/lbmole)} \tag{2.31b}$$

A component species i can store energy in several ways, including potential, kinetic, internal, and chemical potential energy or

$$e_i = \frac{g}{g_0} z_i + \frac{V_i^2}{2g_0} + u_i + h_{f_i}^0 \tag{2.32}$$

Neglecting kinetic and potential energy terms for the moment, the total energy of a mixture of fixed total mass equals

$$E_{\text{tot}} = U_{\text{tot}} = \Sigma N_i \left(\bar{u}_i + \bar{h}_{f_i}^0 \right) \tag{2.33}$$

Since enthalpy data are available in this text, Equation (2.33) can also be written as

$$E_{\text{tot}} = U_{\text{tot}} = \Sigma N_i \left[\bar{h}_i \langle T \rangle - \bar{R} T + \bar{h}_f^0 \right] \tag{2.34}$$

A plot of total mixture energy versus temperature for a fixed composition will yield a curve having a positive slope since both u and h increase with increasing temperature; see Figure 2.7. In addition, mixture lines representing reactants have a greater total energy value at a given temperature than corresponding curves for products because fuels have larger chemical potential energies.

In open-system applications, there is an additional energy flux term associated with pressure gradients in the flowfield termed *flow work* or *flow energy*. Flow work or energy per unit mass crossing the control volume as a result of mass transfer is equal to the local product $P_i v_i$. The total energy term associated with mass that can cross a control volume is then equal to

$$e_i = \frac{g}{g_0} z_i + \frac{V_i^2}{2g_0} + u_i + h_f^0 + p_i v_i \tag{2.35}$$

Since $h_i \equiv u_i + p_i v_i$, Equation (2.35) becomes

$$e_i = \frac{g}{g_0} z_i + \frac{v_i}{2g_0} + h_i + h_f^0 \tag{2.35a}$$

The general energy equation equates heat- and work-transfer rates to changes in energy levels of materials that undergo state changes or processes. Therefore, it is the difference between energy terms rather than their absolute values that is most important to the engineer. Since thermochemical reactants in this text assume all chemical changes occur at *STP*, it will be convenient to express internal energy and enthalpy values referenced to the *STP* state as a datum (Figure 2.8).

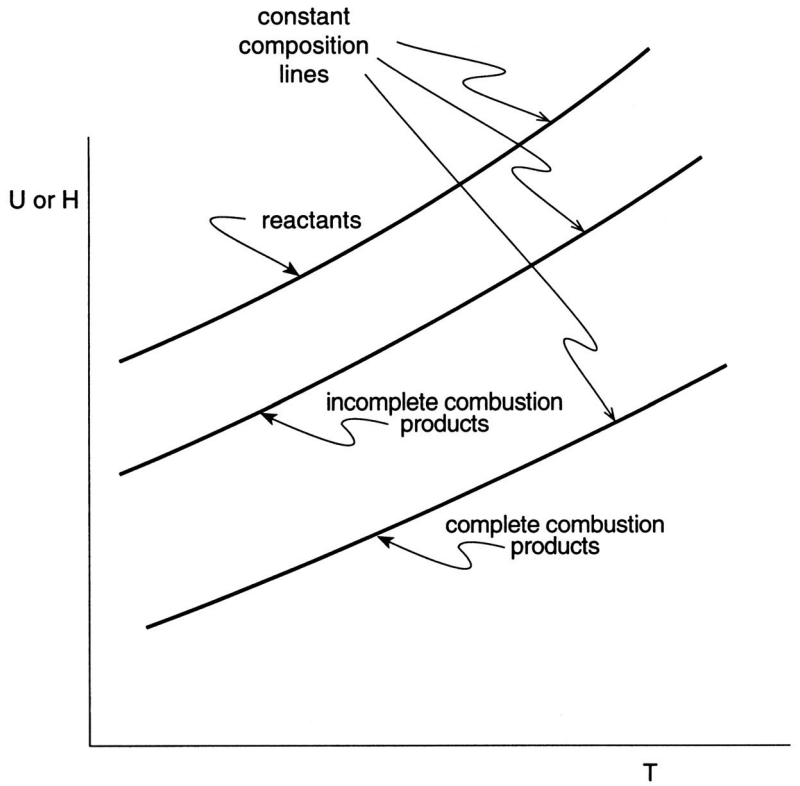

Figure 2.7 Total mixture energy lines vs. temperature.

When this approach is used, the total molar enthalpy of a species *i* may be exressed as

$$\overline{h}_i\big)_{\text{tot}} \equiv \overline{h}_i\langle T\rangle - \overline{h}_i\langle T_0\rangle + \overline{h}_{f_i}^0 \tag{2.36}$$

and the change in total enthalpy is equal to

$$\begin{aligned}\Delta H_{\text{tot}} &= H_{\text{tot}}\langle T_2\rangle - H_{\text{tot}}\langle T_1\rangle = \Sigma H_j\left\{\overline{h}_j\langle T_2\rangle - \overline{h}_j\langle T_0\rangle + \overline{h}_{f_j}^0\right\} \\ &\quad - \Sigma N_i\left\{\overline{h}_i\langle T_1\rangle - \overline{h}_i\langle T_0\rangle + \overline{h}_{f_i}^0\right\}\end{aligned} \tag{2.37}$$

Consider the case of a nonreactive gas mixture undergoing a process, i.e., $N_i = N_j$, $T_2 \neq T_1$, and

$$\begin{aligned}\Delta H_{\text{tot}} &= \Sigma N_i\left\{\overline{h}_i\langle T_2\rangle - \overline{h}_i\langle T_0\rangle + \overline{h}_{f_i}^0\right\} = \Sigma N_i\left\{\overline{h}_i\langle T_1\rangle - \overline{h}_i\langle T_0\rangle + \overline{h}_{f_j}^0\right\} \\ &\quad - \Sigma N_i\left\{\overline{h}_i\langle T_2\rangle - \overline{h}_i\langle T_1\rangle\right\}\end{aligned} \tag{2.38}$$

Equation (2.38) is the familiar form found in most introductory thermodynamics texts.

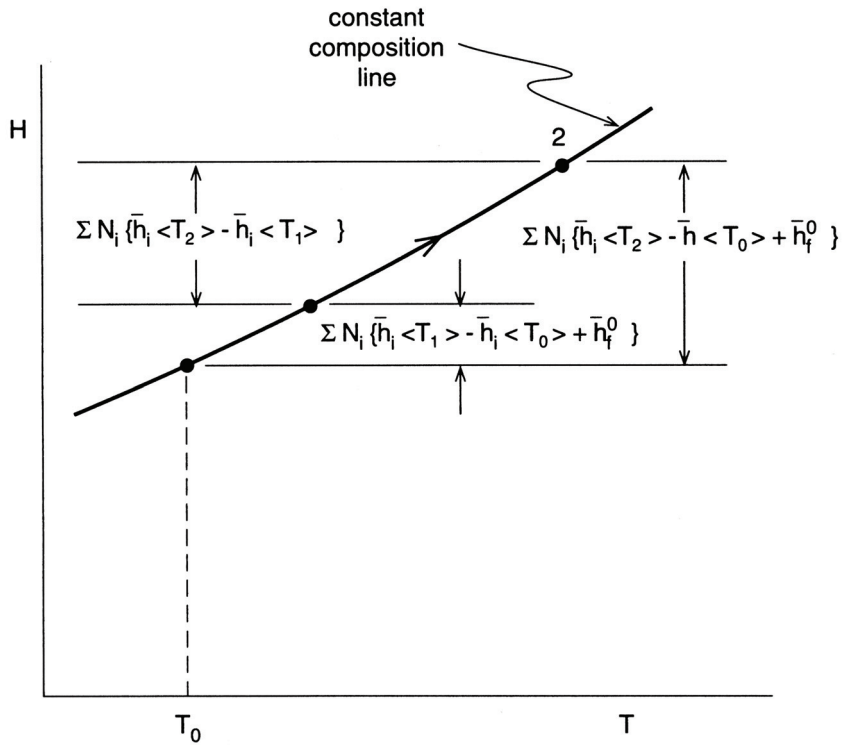

Figure 2.8 Energy vs. temperature process for fixed compositions.

Using the energy equation as developed in this chapter, an expression for various thermochemical processes pertinent to combustion can now be written. Consider the energy analysis for the heat of formation of a particular species occurring at *STP*. In this instance, $P = P_0 = \text{const}$, $T = T_0 = \text{const}$, the initial state constituents are standard elemental species, and the final state consists of a single product species. For a fixed total mass system analysis, the closed-system form of the energy equation is applicable, or

$$dE = dU_{\text{tot}} = \delta Q - PdV \tag{2.39}$$

$$\delta Q_{STP} = dU_{\text{tot}} + PdV + \cancel{VdP} = dH_{\text{tot}} \tag{2.40}$$

Integrating Equation (2.40) yields

$$Q_{STP} = \Delta H_{\text{tot}} = \sum_{\text{prod}} N_j \left[\bar{h}_f^0 + \Delta \bar{h} \right]_j - \sum_{\text{react}} N_i \left[\bar{h}_f^0 + \Delta \bar{h} \right]_i \tag{2.40a}$$

where

$$\Delta \bar{h}_{i,j} = 0 \text{ (reaction at } STP) \qquad \text{i.e., } T_2 = T_1 + T_0$$

and

$$\bar{h}_f^0\Big)_{\text{reactants}} = 0 \qquad \begin{cases}\text{product is formed from natural}\\ \text{elemental compounds at } STP\end{cases}$$

$$N_j = 1.0 \qquad \text{one product species}$$

The heat of formation Δhf is therefore given as

$$Q_{STP} = 1.0\,\bar{h}_{f_i}^0 \equiv \Delta H_{f_i} \tag{2.41}$$

Table B.1 in Appendix B lists the heat of formation at *STP* for various compounds.

Consider the energy analysis for heat of combustion of a stoichiometric hydrocarbon fuel and air mixture reaction at *STP*. Again, this process requires that $P = P_0 =$ const and $T = T_0 =$ const, with the initial state a stoichiometric fuel and air mixture and the final state consisting of most oxidized products, i.e., CO_2 and H_2O. Equation (2.40a) again applies and

$$Q = \Delta H_{\text{tot}} = \sum_{\text{prod}} N_j\left[\bar{h}_f^0 + \Delta\bar{h}\right]_j - \sum_{\text{react}} N_i\left[\bar{h}_f^0 + \Delta\bar{h}\right]_i \tag{2.40a}$$

$$Q = \left\{N_{\text{CO}_2}\left[\bar{h}_f^0 + \Delta\bar{h}\right]_{\text{CO}_2} + N_{\text{H}_2\text{O}}\left[\bar{h}_f^0 + \Delta\bar{h}\right]_{\text{H}_2\text{O}} + N_{\text{N}_2}\left[\bar{h}_f^0 + \Delta\bar{h}\right]_{\text{N}_2}\right\}_{\text{prod}}$$
$$- \left\{N_{\text{fuel}}\left[\bar{h}_f^0 + \Delta\bar{h}\right]_{\text{fuel}} + N_{\text{O}_2}\left[\bar{h}_f^0 + \Delta\bar{h}\right]_{\text{O}_2} + N_{\text{N}_2}\left[\bar{h}_f^0 + \Delta\bar{h}\right]_{\text{N}_2}\right\}_{\text{react}}$$

where

$N_{i,j}$ = determined from the stoichiometric equation

$\Delta\bar{h}_{i,j} = \text{O}$ (reaction at *STP*)

$$Q_{STP} = N_{\text{CO}_2}\left[\bar{h}_f^0\right]_{\text{CO}_2} + N_{\text{H}_2\text{O}}\left[\bar{h}_f^0\right]_{\text{H}_2\text{O}} - N_{\text{fuel}}\left[\bar{h}_f^0\right] = \Delta H_c \tag{2.42}$$

EXAMPLE 2.5 Carbon monoxide, CO, is an important product, resulting from incomplete combustion of many hydrocarbon fuels. Consider the stoichiometric reaction of carbon monoxide with oxygen. Determine (a) the constant-pressure heat of combustion of carbon monoxide at *STP,* Btu/lbm CO; (b) the constant-volume heat of combustion, Btu/lbm CO; and (c) the constant-pressure heat of combustion at 1800°R and 14.7 psia, Btu/lbm CO.

Solution:

1. Stoichiometric equation:

$$\text{CO} + a\text{O}_2 \overset{STP}{\rightarrow} b\text{CO}_2$$

Carbon atom balance: $b = 1$

Oxygen atom balance: $1 + 2a = 2b \qquad a = 0.5$

$$\text{CO} + \tfrac{1}{2}\,\text{O}_2 \rightarrow \text{CO}_2$$

2. Energy equation: $P = c$ (*STP*) using Table B.1 in Appendix B.

$$\cancel{dE} = \delta Q - \cancel{\delta W} + \Sigma N_i \bar{e}_i - \Sigma N_i \bar{e}_i$$

$$Q = \sum_{\text{prod}} N_i \left[\bar{h}_f^0 + \left\{ \bar{h}\langle T \rangle - \bar{h}\langle T_0 \rangle \right\} \right]_i - \sum_{\text{react}} N_i \left[\bar{h}_f^0 + \left\{ \bar{h}\langle T \rangle - \bar{h}\langle T_0 \rangle \right\} \right]_j$$

$$Q = 1.0\left[\bar{h}_f^0 + \cancel{\Delta \bar{h}} \right]_{CO_2} - 0.5\left[\bar{h}_f^0 + \cancel{\Delta \bar{h}} \right]_{O_2} - 1.0\left[\bar{h}_f^0 + \Delta \bar{h} \right]_{CO}$$

$$Q = \left[-94{,}054 + 26{,}416 \text{ cal/gmole} \right] \left[1.8001 \frac{\text{Btu/lbmole}}{\text{cal/gmole}} \right]$$

$$= -121{,}755 \text{Btu/lbmole CO}$$

or

a. $Q = \dfrac{-121{,}755 \text{ Btu/lbmole}}{28 \text{ lbm/lbmole}} = -4{,}348.4 \text{ Btu/lbm CO}$

3. Energy equation: $V = c$ (*STP*)

$$Q = \sum_{\text{prod}} N_i \left[\bar{h}_f^0 + \left\{ \bar{h}\langle T \rangle - \bar{h}\langle T_0 \rangle \right\} - \bar{R}T \right]_i - \sum_{\text{react}} N_i \left[\bar{h}_f^0 + \left\{ \bar{h}\langle T \rangle - \bar{h}\langle T_0 \rangle \right\} - \bar{R}T \right]_j$$

$$Q = 1.0\left[\bar{h}_f^0 + \cancel{\Delta \bar{h}} \right]_{CO_2} - 0.5\left[\bar{h}_f^0 + \cancel{\Delta \bar{h}} \right]_{O_2} - 1.0\left[\bar{h}_f^0 + \cancel{\Delta \bar{h}} \right]_{CO} - (1.0 - 0.5 - 1.0)\bar{R}T$$

$$= -121{,}755 + (0.5)(1.987)(537) = -121{,}221 \text{ Btu/lbmole CO}$$

b. $Q = \dfrac{-121{,}221}{28} = -4{,}329.3 \text{ Btu/lbm CO}$

4. Energy equation: $P = c$ $T = 1800°\text{R}$

$$Q = 1.0[-94{,}054 + 7{,}984]_{CO_2} - 0.5[0 + 5{,}427]_{O_2} - 1.0[-26{,}416 + 5{,}183]_{CO}$$

$$= -67{,}550.5 \text{ cal/gmole CO}$$

$$\text{Q} = \frac{(-67{,}550.5)(1.8001)}{28}$$

c. $Q = -4{,}342.8$ Btu/lbm CO

Comments: This problem illustrates that the heating value of a fuel at *STP* in many engineering problems is a good approximation for the heat released by combustion at conditions other than at *STP*.

Since the formation and combustion reactions both occur at *STP,* one can simply add the appropriate heats of formation via stoichiometric equations to determine heats of combustion of important fuels. Note also that addition of N_2 or excess O_2 does not change the value of heat of combustion since both those compounds are elemental species. The heat of combustion ΔH_c can be visualized on an *H–T* diagram as the vertical distance between the reactant mixture and product curves at $T = T_0$; see Figure 2.9. The heat of combustion at *STP* for various species is found in Appendix B.

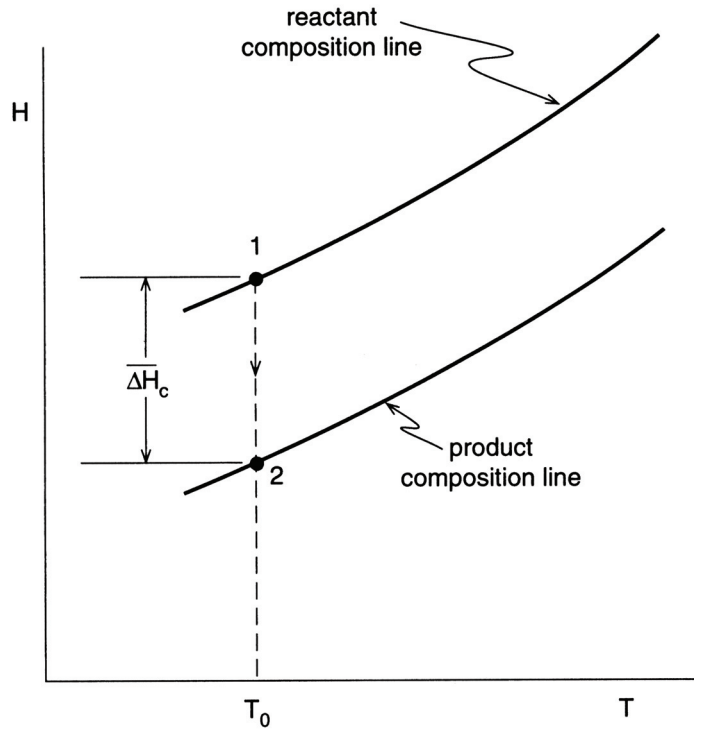

Figure 2.9 Heat of combustion H–T diagram.

EXAMPLE 2.6 A rigid vessel filled with diatomic hydrogen and air is initially at 25°C and 1 atm total pressure. Calculate the adiabatic flame temperature for ideal complete combustion for an equivalence ratio of (a) 1.0, (b) 1.4, (c) 1.8, (d) 0.6, and (e) 0.2.

Solution:

1. Stoichiometric equation:

$$H_2 + 0.5[O_2 + 3.76N_2] \xrightarrow{V} H_2O + 1.88N_2$$

2. Equivalence ratio:

$$\Phi = \frac{FA)_{\text{actual}}}{FA)_{\text{stoich}}}$$

Assume that the moles of air remain constant and vary the moles of hydrogen, giving

$$\Phi\, H_2 + 0.5[O_2 + 3.76\, N_2] \xrightarrow{V} \text{products}$$

3. Rich combustion:

$$\Phi > 1.0 \qquad \text{(excess } H_2\text{)}$$

$$\Phi\, H_2 + 0.5[O_2 + 3.76\, N_2] \rightarrow a H_2 + b H_2O + 1.88\, N_2$$

Hydrogen atom balance $\quad \Phi = a + b$

Oxygen atom balance $\quad 1 = b$

and

Φ	a	b
1.0	0	1.0
1.4	0.4	1.0
1.8	0.8	1.0

4. Energy balance:

$$\delta Q - \delta W = \cancel{\delta Q} - \cancel{P dV} = dU$$

or

$$U\langle T_2\rangle = U\langle T_1\rangle$$

$$\sum_{\text{prod}} N_i \left\{ \bar{h}^0_{f_i} + \left[\bar{h}\langle T_2\rangle - \bar{h}\langle T_0\rangle \right]_i - \bar{R} T_2 \right\}$$

$$= \sum_{\text{react}} N_j \left\{ \bar{h}^0_{f_j} + \left[\bar{h}\langle T_1\rangle - \bar{h}\langle T_0\rangle \right]_j - \bar{R} T_1 \right\}$$

5. Energy balance—rich combustion:

$$a\cancel{\left[\bar{h}^0_f + \Delta\bar{h}\right]_{H_2}} + \left[\bar{h}^0_f + \Delta\bar{h}\right]_{H_2O} + 1.88\cancel{\left[\bar{h}^0_f + \Delta\bar{h}\right]_{N_2}} - (2.88 + a)\bar{R} T_2$$

$$= \Phi\cancel{\left[\bar{h}^0_f + \Delta\bar{h}\right]_{H_2}} + 2.38\cancel{\left[\bar{h}^0_f + \Delta\bar{h}\right]_{air}} - (\Phi + 2.38)\bar{R} T_1$$

where $\bar{h}^0_f)_{H_2O_g} = -57{,}798$ cal/gmole (Appendix B)

6. For $\Phi = 1.0$, using values for $\Delta\bar{h}_{(j)}$ from Tables B.4 and B.18 in Appendix B;

$$\Delta\bar{h})_{H_2O} + 1.88\Delta\bar{h})_{N_2} - 5.723\, T_2 = 55{,}797$$

by trial and error,

$$T_2 \cong 3{,}045 \text{ K}$$

For $\Phi = 1.4$,

$$0.4\Delta\bar{h})_{H_2} + \Delta\bar{h})_{H_2O} + 1.88\Delta\bar{h})_{N_2} - 6.517\, T_2 = 55{,}560$$

by trial and error,

$T_2 \cong 2{,}805$ K

For $\Phi = 1.8$,

$$0.8\Delta\bar{h}\Big)_{H_2} + \Delta\bar{h}\Big)_{H_2O} + 1.88\Delta\bar{h}\Big)_{N_2} - 7.312\,T_2 = 55{,}320$$

by trial and error

$T_2 \cong 2{,}605$ K

7. Lean combustion: $\Phi < 1.0$ (excess air)

$$\Phi\,H_2 + 0.5[O_2 + 3.76\,N_2] \xrightarrow{V} cO_2 + dH_2O + 1.88\,N_2$$

Hydrogen atom balance $\Phi = d$
Oxygen atom balance $1 = 2c + d$

Φ	c	d
0.6	0.2	0.6
0.2	0.4	0.2

8. Energy balance—lean combustion:

$$c\left[\bar{h}_f^0 + \Delta\bar{h}\right]_{O_2} + d\left[\bar{h}_f^0 + \Delta\bar{h}\right]_{H_2O} + 1.88\left[\bar{h}_f^0 + \Delta\bar{h}\right]_{N_2} - (c + d + 1.88)\bar{R}T_2$$
$$= \Phi\left[\bar{h}_f^0 + \Delta\bar{h}\right]_{H_2} + 2.38\left[\bar{h}_f^0 + \Delta\bar{h}\right]_{air} - [\Phi + 2.38]\bar{R}T_1$$

9. For $\Phi = 0.6$,

$$0.2\Delta\bar{h}\Big)_{O_2} + 0.6\Delta\bar{h}\Big)_{H_2O} + 1.88\Delta\bar{h}\Big)_{N_2} - 5.325\,T_2 = 32{,}914$$

by trial and error,

$T_2 \cong 2{,}240$ K

For $\Phi = 0.2$,

$$0.4\Delta\bar{h}\Big)_{O_2} + 0.2\Delta\bar{h}\Big)_{H_2O} + 1.88\Delta\bar{h}\Big)_{N_2} - 4.928\,T_2 = 10{,}030$$

by trial and error

$T_2 \cong 800$ K

Comments: This problem illustrates the fact that, for most oxidation reactions, the peak flame temperature occurs at or near stoichiometric conditions. In practice, the maximum

adiabatic flame temperature may occur just on the rich side of stoichiometric proportions. This slight shift can be attributed to the reduction in specific heat of the rich combustion products with a corresponding increase in temperature. Also, in actual flame systems, incomplete combustion and heat loss to surroundings will reduce the temperature, but the above calculated trend of temperature versus Φ will still hold.

Finally, consider the control volume energy balance analysis for a burner; see Figure 2.10. For the purposes of analysis, it will be assumed that the burner system operates at steady-state, steady-flow conditions and that, in this case, no work or power transfer occurs. Also assuming negligible changes in kinetic and potential energy fluxes, one can write the energy balance for the burner as

$$\frac{dE}{dt} = \frac{\delta Q}{dt} - \frac{\delta W}{dt} + \sum_{i_{\text{in}}} \frac{dN_i}{dt}\left[\bar{h}_{\text{tot}}\langle T_1\rangle\right] - \sum_{j_{\text{out}}} \frac{dN_j}{dt}\left[\bar{h}_{\text{tot}}\langle T_j\rangle\right] \tag{2.43}$$

$$\dot{Q} = \sum_{j_{\text{out}}} \dot{N}_j\left[\bar{h}_f^0 + \left\{\bar{h}\langle T_j\rangle - \bar{h}\langle T_0\rangle\right\}\right]_j - \sum_{i_{\text{in}}} \dot{N}_i\left[\bar{h}_f^0 + \left\{\bar{h}\langle T_i\rangle - \bar{h}\langle T_0\rangle\right\}\right]_i \tag{2.44}$$

Energy transfer *from* the generated gases as heat to the surroundings due to combustion is influenced in part by (1) particular fuel burned $\left(\bar{h}_{f_i}^0\right)$, (2) particular reaction *AF* ratio (N_i and N_j), (3) reactant state (fuel and oxidant phase/temperatures), and (4) final product state (completeness of combustion and product temperature).

The general burner combustion process can also be visualized by use of the *H–T* diagram; see Figure 2.11. The actual heat release, process $1 \rightarrow 2$, can be modeled using three fictitious processes. First, if reactant conditions are offset from T_0 on the reactant line, an amount of energy is needed to "cool" reactants to *STP* conditions, i.e., process $1 \rightarrow$ a. Next, the vertical path a $\rightarrow$ b represents the heat of combustion in going from reactant to products. Finally, the product state 2 indicates that an additional amount of energy is needed to heat the product mixture from *STP* to the final state, process b $\rightarrow 2$.

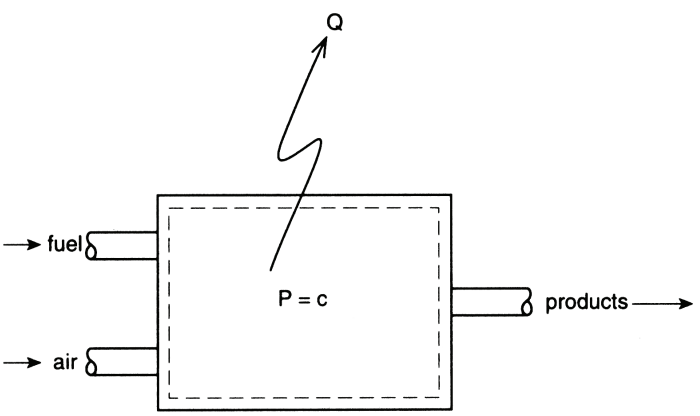

Figure 2.10 Combustor or burner schematic.

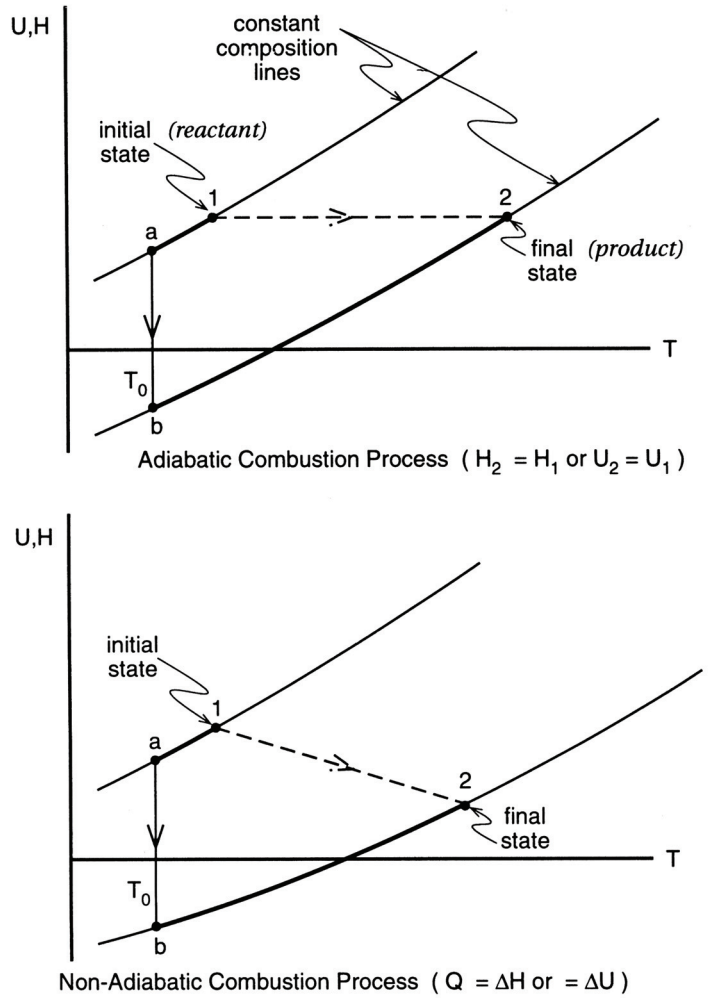

Figure 2.11 *U-T* or *H-T* diagram for chemical reaction.

EXAMPLE 2.7 Oxygen-gas combustion is being pursued for use as a supplement and/or replacment for conventional air-gas chemistry in a variety of applications. The first order design assessment in such instances is illustrated in part by the following thermochemical analysis of an acetylene cutting torch burning oxygen or air. Using ideal complete combustion of acetylene at equivalence ratio values of 1.0, 0.83333, 0.714285, 0.625, 0.55556, and 0.5, determine (a) the mass of oxidant consumed per mass of fuel burned for oxygen and air, kg oxidant/kJ fuel; (b) the adiabatic flame temperatures for acetylene in oxygen and air, K; and (c) the volume of product gas generated per mole of fuel for oxygen and air, m^3product/kgmole fuel.

Solution:

1. Stoichiometric equation for ideal combustion of acetylene in oxygen:

$$C_2H_2 + aO_2 \rightarrow bCO_2 + cH_2O$$

carbon atom balance	$b = 2$	
hydrogen atom balance	$2c = 2$	$c = 1$
oxygen atom balance	$2a = 4 + 1$	$a = 2.5$

2. Stoichiometric equation for ideal combustion of acetylene in air:

$$C_2H_2 + 2.5[O_2 + 3.76N_2] \rightarrow 2CO_2 + H_2O + (2.5)(3.76)N_2$$

3. Theoretical equation for ideal combustion of acetylene in oxygen and air:

$$\Phi C_2H_2 + 2.5O_2 \rightarrow 2\Phi CO_2 + \Phi H_2O + 2.5(1 - \Phi)O_2$$
$$\Phi C_2H_2 + 2.5[O_2 + 3.76N_2] \rightarrow$$
$$2\Phi CO_2 + \Phi H_2O + 2.5(1 - \Phi)O_2 + (2.5)(3.76)(1 - \Phi)N_2$$

or

$$C_2H_2 + (2.5/\Phi)O_2 \rightarrow 2CO_2 + H_2O + 2.5((1 - \Phi)/\Phi)O_2$$
$$C_2H_2 + (2.5/\Phi)[O_2 + 3.76N_2] \rightarrow$$
$$2CO_2 + H_2O\ 2.5((1 - \Phi)/\Phi)O_2 + (2.5)(3.76)((1 - \Phi)/\Phi)N_2$$

4. Recall the definition of equivalence ratio, Φ:

$$\Phi = (\text{moles fuel/moles oxidant})_{\text{actual}}/(\text{moles fuel/moles oxidant})_{\text{stoichiometric}}$$

for equal moles of fuel the equivalence ratio, Φ, then becomes

$$\Phi = (\text{moles oxidant})_{\text{stoichiometric}}/(\text{moles oxidant})_{\text{actual}}$$

or

$$(\text{moles oxidant})_{\text{actual}} = (\text{moles oxidant})_{\text{stoichiometric}}/\Phi$$

5. Now the concept of theoretical oxidant, *TO*, can be described as

$$(\text{moles oxidant})_{\text{actual}} = (\text{moles oxidant})_{\text{stoichiometric}} \times TO$$

by relating the two concepts of equivalence ratio and theoretical oxidant, one obtains

$$TO = (1/\Phi)100$$

Φ	*TO*	Φ	*TO*
1.0	100	0.625	160
0.83333	120	0.55556	180
0.714285	140	0.5	200

6. The mass of oxidant consumed per mass of fuel burned for oxygen and air can be determined from the moles of oxidant and fuel and their molecular weights:

TO	Moles oxidant kgmoles	MW_O kg/kgmoles	MW_f kg/kgmoles	*OF* kg/kg
		Oxygen		
100	2.5	32.00	26.04	3.072[a]
120	3.0	32.00	26.04	3.687
140	3.5	32.00	26.04	4.301
160	4.0	32.00	26.04	4.916
180	4.5	32.00	26.04	5.530
200	5.0	32.00	26.04	6.144
		Air		
100	11.90	28.97	26.04	13.24
120	14.28	28.97	26.04	15.89
140	16.66	28.97	26.04	18.53
160	19.04	28.97	26.04	21.18
180	21.42	28.97	26.04	23.83
200	23.80	28.97	26.04	26.48

[a] $OF = N_O \times MW_O/N_f \times MW_f = 2.5 \times 32/1.0 \times 26.4 = 3.072$

7. The moles of product species generated per mole of fuel for oxygen and air can be determined from the combustion equation knowing the values of the equivalence ratio:

TO	Moles CO_2 kgmoles	Moles H_2O kgmoles	Moles O_2 kgmoles	Moles N_2 kgmoles	$Moles_{total}$ kgmoles
			Oxygen		
100	2	1	0	0	3[b]
120	2	1	0.5	0	3.5
140	2	1	1.0	0	4
160	2	1	1.5	0	4.5
180	2	1	2.0	0	5
200	2	1	2.5	0	5.5

TO	Moles CO_2 kgmoles	Moles H_2O kgmoles	Moles O_2 kgmoles	Moles N_2 kgmoles	$Moles_{total}$ kgmoles
			Air		
100	2	1	0	9.40	12.40
120	2	1	0.5	11.28	14.78
140	2	1	1.0	13.16	17.16
160	2	1	1.5	15.04	19.54
180	2	1	2.0	16.92	21.92
200	2	1	2.5	18.80	24.30

[b] $N_{tot} = N_{CO_2} + N_{H_2O} + N_{O_2} + N_{N_2} = 2 + 1 + 0 + 0 = 3$

8. The mole fractions of product species generated per mole of fuel for oxygen and air can be determined knowing the moles of product species generated per mole of fuel. The molecular weight of product generated per mole of fuel for oxygen and air can be determined knowing the mole fractions and molecular weight of product species generated per mole of fuel.

Φ	$\bar{x}f_{CO_2}$	$\bar{x}f_{H_2O}$	$\bar{x}f_{O_2}$	$\bar{x}f_{N_2}$	MW_{prod}
			Oxygen		
100	0.66667[c]	0.33333	0	0	35.333[d]
120	0.57143	0.28571	0.14286	0	34.857
140	0.50000	0.25000	0.25000	0	34.500
160	0.44444	0.22222	0.33333	0	34.222
180	0.40000	0.20000	0.40000	0	34.000
200	0.36363	0.18182	0.45455	0	33.818
			Air		
100	0.16129	0.08065	0	0.75807	29.774
120	0.13532	0.06766	0.03383	0.76319	29.624
140	0.11655	0.05828	0.05828	0.76690	29.515
160	0.10235	0.05118	0.07677	0.76970	29.433
180	0.09124	0.04562	0.09124	0.77190	29.369
200	0.08231	0.04115	0.10288	0.77366	29.317

[c] $x_{prod} = N_{prod}/N_{tot} = N_{CO_2} / N_{tot} = 2/3 = 0.66667$

[d] $MW_{prod} = \Sigma \bar{x}_i MW_i = (0.66667)(44) + (0.33333)18 + (0)(32) + (0)(28)$
$= 35.333$

9. Energy balance $P = \text{c}$ $H_{\text{prod}} = H_{\text{react}}$

oxygen

$$0 = \left\{ N_{CO_2}\left[\bar{h}_f^0 + \Delta\bar{h}\right]_{CO_2} + N_{H_2O}\left[\bar{h}_f^0 + \Delta\bar{h}\right]_{H_2O} + N_{NO_2}\left[\bar{h}_f^0 + \Delta\bar{h}\right]_{NO_2} + N_{N_2}\left[\bar{h}_f^0 + \Delta\bar{h}\right]_{N_2} \right\}_{\text{prod}} - \left\{ N_{\text{fuel}}\left[\bar{h}_f^0 + \Delta\bar{h}\right]_{\text{fuel}} + N_{O_2}\left[\bar{h}_f^0 + \Delta\bar{h}\right]_{O_2} \right\}$$

or

$$\left[\bar{h}_f^0\right]_{C_2H_2} + \left(\frac{2.5}{\Phi}\right)\left[\bar{h}_f^0\right]_{O_2} = 2\left[\bar{h}_f^0 + \Delta\bar{h}\right]_{CO_2} + \left[\bar{h}_f^0 + \Delta\bar{h}\right]_{H_2O} + 2.5\left(\frac{(1-\Phi)}{\Phi}\right)\left[\bar{h}_f^0 + \Delta\bar{h}\right]_{O_2} + (-54{,}194) + \left(\frac{2.5}{\Phi}\right)[0]$$

$$= 2\left[-94{,}054 + \Delta\bar{h}\right]_{CO_2} + \left[-57{,}798 + \Delta\bar{h}\right]_{H_2O} 2.5\left(\frac{(1-\Phi)}{\Phi}\right)\left[0 + \Delta\bar{h}\right]_{O_2}$$

air

$$0 = \left\{ N_{CO_2}\left[\bar{h}_f^0 + \Delta\bar{h}\right]_{CO_2} + N_{H_2O}\left[\bar{h}_f^0 + \Delta\bar{h}\right]_{H_2O} + N_{NO_2}\left[\bar{h}_f^0 + \Delta\bar{h}\right]_{NO_2} + N_{N_2}\left[\bar{h}_f^0 + \Delta\bar{h}\right]_{N_2} \right\}_{\text{prod}} - \left\{ N_{\text{fuel}}\left[\bar{h}_f^0 + \Delta\bar{h}\right]_{\text{fuel}} + N_{O_2}\left[\bar{h}_f^0 + \Delta\bar{h}\right]_{O_2} + N_{N_2}\left[\bar{h}_f^0 + \Delta\bar{h}\right]_{N_2} \right\}_{\text{react}}$$

or

$$\left[\bar{h}_f^0\right]_{C_2H_2} + \left(\frac{2.5}{\Phi}\right)\left[\left(\bar{h}_f^0\right)_{O_2} + 3.76\left(\bar{h}_f^0\right)_{N_2}\right]$$

$$= 2\left[\bar{h}_f^0 + \Delta\bar{h}\right]_{CO_2} + \left[\bar{h}_f^0 + \Delta\bar{h}\right]_{H_2O} 2.5\left(\frac{(1-\Phi)}{\Phi}\right)\left[\bar{h}_f^0 + \Delta\bar{h}\right]_{O_2}$$

$$+ (2.5)(3.76)\left(\frac{(1-\Phi)}{\Phi}\right)\left[\bar{h}_f^0 + \Delta\bar{h}\right]_{N_2} - 54{,}194 + \left(\frac{2.5}{\Phi}\right)[0 + (3.76)(0)]$$

$$= 2\left[-94{,}054 + \Delta\bar{h}\right]_{CO_2} + \left[-57{,}798 + \Delta\bar{h}\right]_{H_2O} 2.5\left(\frac{(1-\Phi)}{\Phi}\right)\left[0 + \Delta\bar{h}\right]_{O_2}$$

$$+ (2.5)(3.76)\left(\frac{(1-\Phi)}{\Phi}\right)\left[0 + \Delta\bar{h}\right]_{N_2}$$

using the values for $\Delta\bar{h}$ from appropriate tables in Appendix B, by trial and error the values for T_2 can thus be determined for the oxygen and air cases as listed below.

TO	T_2, K	V_2, m^3/kgmole fuel
	Oxygen	
100	5,008.3	1,236.9
120	4,572.6	1,313.3
140	4,215.0	1,383.5
160	3,915.8	1,445.9
180	3,661.4	1,502.2
200	3,442.3	1,553.6
	Air	
100	2,036.7	2,072.4
120	1,803.7	2,187.6
140	1,627.4	2,291.6
160	1,489.2	2,387.8
180	1,377.6	2,477.9
200	1,285.6	2,563.5

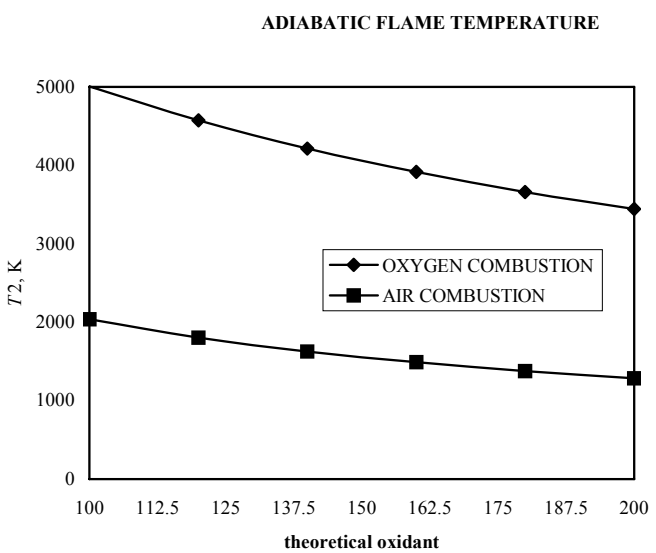

10. The final product volume V_2 can now be determined by applying the ideal gas law, Equation (1.3a), knowing the adiabatic temperature, T_2, and the total product moles N_{tot}:

$$P\overline{V} = N_{tot}\overline{R}T$$

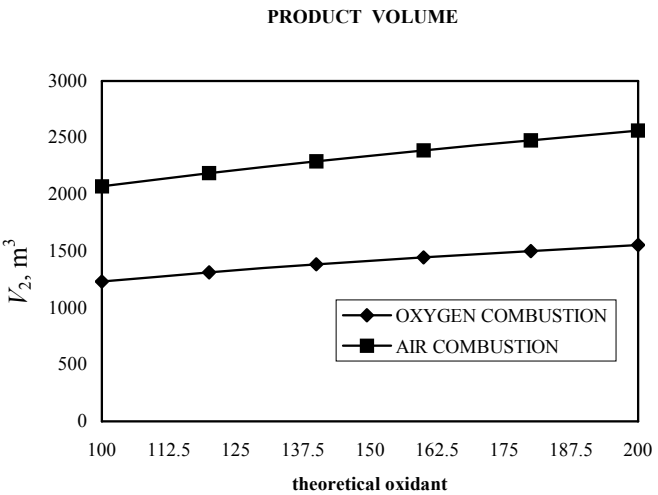

Since $P_2 = P_1$

$$\overline{V}_2 = N_{tot}\,2\overline{R}\,\frac{T_2}{P_1}$$

$$V_2 = (3\text{ kgmoles product})(8{,}314.34\text{ N}\cdot\text{m/kgmoleK})\frac{(5{,}008.3\text{K})}{(101{,}000\text{ N/m}^2)}$$

$$= 1{,}236.9\text{ m}^3/\text{kgmole fuel}$$

Comments: This problem illustrates the fact that oxygen enrichment uses less oxidant, produces a higher theoretical adiabatic flame, and less product gas volume per mole of fuel as compared to air at equal equivalence ratios. With the appearance in recent years of improved air separation technologies, applications of oxygen and oxygen-enriched combustion of industrial burners, furnaces, and certain high temperature operations, including cutting torches, have occurred. Great care should be taken however to ensure that more than simply applying energy balances are undertaken when attempting to do any oxygen enrichment design work. Among some of the more noteworthy fuel-engine oxygen enrichment impact issues are flammability limits, flame speeds, incomplete combustion, emissions, and materials that can work in high oxygen concentration and high temperature environments. In addition, economics issues such as the cost for the generation of oxygen and costs for safety-related elements of the combustion process also need to be addressed.

A combustion efficiency η_c, in similar fashion to turbine and compressor efficiency concepts introduced in thermodynamics, can be utilized to characterize actual heat release knowing the heating value of the fuel being burned; see Figure 2.12.

$$\eta_c = \frac{\text{actual heat released}}{\text{ideal heat released}} = \frac{\Delta H}{\Delta H_c} \leq 1.0 \tag{2.45}$$

For heat-transfer applications, such as in furnaces, heaters, and boilers, high combustion efficiency requires that the combustion device results in a product temperature approaching T_0, i.e., large heat transfer from the product combustion gases; see Figure 2.12. In the limit, the ideal heat release by reaction would equal the heat of combustion. For high-power gas expansion output applications, such as internal combustion and turbine engines, the need to produce a maximum combustion temperature leads to the concept of *adiabatic flame temperature,* i.e., a combustion process in which there is no heat transfer, i.e., $\Delta H = 0$ and low combustion efficiency.

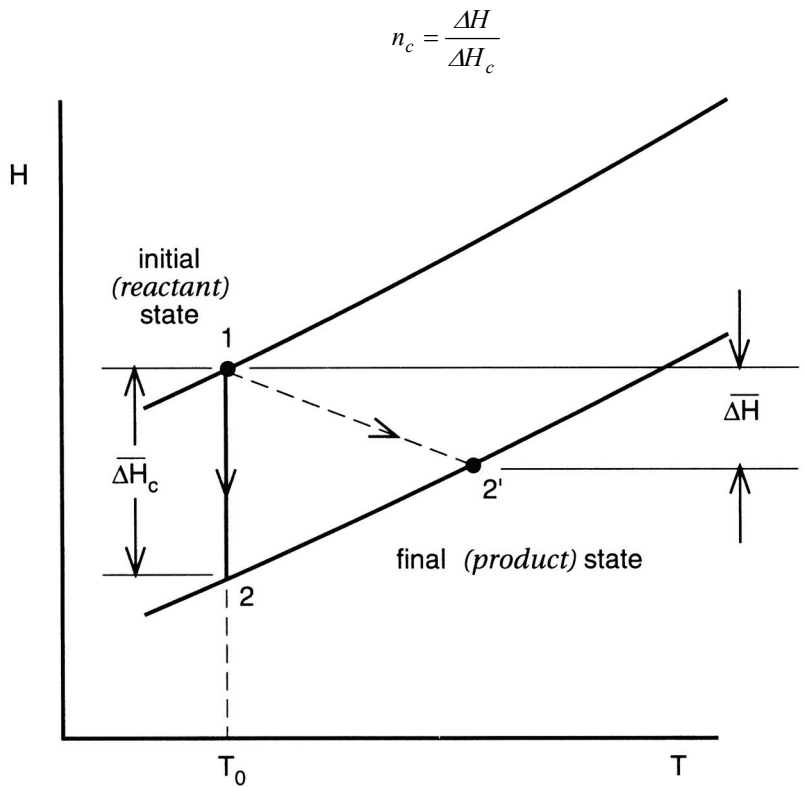

Figure 2.12 *H-T* diagram and combustion efficiency.

PROBLEMS

2.1 Consider a stoichiometric mixture of hydrogen and air. Calculate for these conditions the (a) reactant mass fractions, *mf*; (b) reactant mixture molecular weight, kg/kg mole; (c) molar $\overline{AF}$ ratio, kgmole air/kgmole fuel; and (d) mass *FA* ratio, kgfuel/kg air.

2.2 Repeat Problem 2.1 for methane, CH_4.

2.3 Repeat Problem 2.1 for propane, C_3H_8.

2.4 Repeat Problem 2.1 for iso-octane, C_8H_{18}.

2.5 Repeat Problem 2.1 for dodecane, $C_{12}H_{26}$.

2.6 Repeat Problem 2.1 for ethanol, C_2H_5OH.

2.7 An unknown hydrocarbon fuel is burned with air. The molar $\overline{AF}$ ratio for the combustion process is equal to 21.43 lbmole air/lbmole fuel, while the corresponding mass *FA* ratio is given as 0.0451 lbm fuel/lbm air. Calculate (a) fuel molecular weight, lbm/lbmole; (b) fuel structure C*x*H*y*, %; and (c) reaction excess air, % for the reaction.

2.8 A gaseous fuel having a volumetric analysis of 65% CH_4, 25% C_2H_6, 5% CO, and 5% N_2 is burned with 30% excess air. Determine (a) mass *AF* ratio, lbm air/lbm fuel; (b) mass of CO_2 produced, lbm CO_2/lbm fuel; (c) mass of water formed, lbm H_2O/lbm fuel; and (d) mass of products formed, lbm products/lbm reactants.

2.9 The dry products of combustion have the following molar percentages:

CO 2.7% O_2 5.3% H_2 0.9% CO_2 16.3% N_2 74.8%

Find, for these conditions: (a) mixture gravimetric analysis; (b) mixture molecular weight, lbm/lbmole; and (c) mixture specific gas constant *R*, ft lbf/lbm °R.

2.10 For the product conditions in Problem 2.9, assuming 1 atmosphere total pressure and a gas temperature of 1,800K, calculate: (a) mixture constant pressure specific heat, kJ/kgmole·K; (b) mixture specific heat ratio; (c) mixture enthalpy, kJ/kgmole; and (d) mixture internal energy, kJ/kgmole.

2.11 A hydrocarbon fuel, C*x*H*y*, is burned at constant pressure in air. The volumetric analysis of the products of combustion on a dry basis are:

CO 1.1% O_2 8.3% CO_2 7.8% N_2 82.8%

Determine (a) the molar carbon to hydrogen ratio for the fuel; (b) fuel mass fraction composition, %C and %H; (c) theoretical air, %; (d) mass *AF* ratio, kg air/kg fuel; and (e) dew point temperature for 1 atmospheric combustion, °C.

2.12 A homogeneous mixture of methane, CH_4, and air at *STP* has a specific heat ratio of 1.35. Obtain for this mixture (a) the reactant mixture mole fractions, %; (b) the reactant mixture molecular weight, kg/kgmole; (c) the mixture constant-pressure specific heat, kJ/kg K; (d) the mixture constant volume specific heat, kJ/kg K; and (e) the mixture density, kg/m^3.

2.13 Repeat Problem 2.12 except for enriched air using the JANAF data for O_2 and N_2 and assuming that enriched air consists of percentages of O_2 and N_2. Find, for the mixture as a function of enrichment: (a) molar specific heats $\overline{C}_p$ and $\overline{C}_v$, kJ/kg mole K; (b) mass specific heats, kJ/kg K; and (c) specific heat ratio γ for 1 atm and 300K.

2.14 Using the JANAF data for O_2 and N_2 and assuming that air consists of 1 kgmole O_2 and 3.76 kgmole N_2, find for the mixture: (a) molar specific heats $\overline{C}_p$ and $\overline{C}_v$, kJ/kgmole K; (b) mass specific heats, kJ/kg K; and (c) specific heat ratio γ for 1 atm and 300K.

2.15 Repeat Problem 2.14 for a temperature of 1,000K.

2.16 A fuel composed of 50% C_7H_{14} and 50% C_8H_{18} by weight is burned using 10% excess air. For 100 lbm of fuel, determine: (a) the volume of *STP* air required for ideal combustion, ft^3; and (b) the mass *AF* ratio, lbm air/lbm fuel.

2.17 One kg of Octane, C_8H_{18}, in gaseous state is combusted with 12 kg of air. For these proportions obtain: (a) the moles of air that react per moles of fuel, kgmoles air/kgmoles fuel; (b) moles of CO produced per mole of fuel, kgmoles CO; (c) moles of CO_2 produced per mole of fuel, kgmoles CO_2; and (d) product mole fractions.

2.18 Consider the reaction of propane, C_3H_{14}, and 120% theoretical air. Assuming ideal combustion, determine (a) product mole fractions, %; (b) product mass fractions, %; (c) product mixture molecular weight, kg/kgmole; and (d) product mixture specific gas constant, kJ/kg K.

2.19 An advanced turbine concept proposes the use of carbon dioxide as the working fluid. Inlet conditions for the turbine are 2,200K and 1,150 kPa abs. with exhaust conditions specified as 600K and 120 kPa abs. If the unit is to produce 50 kW of power outut, calculate: (a) the mass flowrate, kg CO_2/sec; (b) the inlet volumetric flowrate, m^3 CO_2/sec; and (c) the turbine work, kJ/kJ CO_2.

2.20 For a reactive mixture, the dew point temperature is defined as the saturation temperature of water corresponding to the water vapor partial pressure. Calculate (a) product mole fractions, %; (b) product water vapor partial pressure; and (c) dew point temperature, K, for the ideal constant-volume combustion of acetylene, C_2H_2, and 20% excess air. Assume that the reactants are at 14.5 psi and 77°F, while the products are at 960°R.

2.21 The lower heating value of gaseous butene, C_4H_8, is 19,483 Btu/lbm. For reaction conditions at *STP*, calculate (a) molar enthalpy of formation of butene, Btu/lbmole; (b) mass enthalpy of formation, Btu/lbm; and (c) the enthalpy of hydrogenation associated with the reaction $C_4H_{8g} + H_{2g} \rightarrow C_4H_{10g}$, Btu/lbmole H_2.

2.22 A propane torch, C_3H_8, burns lean with 120% excess air. Temperature of the flame is 1,400°R. Find (a) molar $\overline{AF}$ ratio, lbmole air/lbmole fuel; (b) ideal combustion product mole fractions, %; (c) volume of exhaust gas to volume of combustion air, ft^3 gas/ft^3 air; and (d) heat released by an ideal combustion process, Btu/lbm fuel.

2.23 A unique underwater propulsion power plant uses hydrogen peroxide, H_2O_{2l}, to oxidize gaseous hydrogen, H_2. For ideal stoichiometric gas phase thermochemistry determine (a) the reactant molecular weight, lbm/lbmole; (b) the reactant mass fractions, %; (c) the water produced, lbm H_2O/lbm reactants; and (d) the energy density at *STP*, Btu/lbm reactants.

2.24 A rigid vessel contains a mixture of one mole of methane, CH_4, and three moles of oxygen, O_2. The reactants initially are at 14.7 psia and 537°R. After complete combustion, the products are cooled to 1,080°R. Find (a) the vessel volume, ft^3; (b) the final pressure, psia; (c) the product dew point temperature, °F; (d) the heat transfer, Btu/ft^3; and (e) the product gravimetric analysis, %.

2.25 Hydrazine, N_2H_{4g}, and hydrogen peroxide, H_2O_{2g}, comprise a hyperbolic (self-igniting on contact) mixture used in special applications such as torpedo and missle propulsion. If the hydrogen peroxide is supplied in a 90% H_2O_2–10% H_2O gravimetric mixture, calculate for ideal complete combustion of the stoichiometric reaction (a) mole fractions of H_2O_2 and H_2O in oxidizing solution,%; (b) *FO* ratio, kg fuel/kg oxidant; (c) product mole fractions, %; and (d) mixture lower heating value, kJ/kg mixture.

2.26 A furnace burns 2,500 ft^3/hr of a gas having the following volumetric analysis: 90% CH_4, 7% C_2H_6, and 3% C_3H_8. Both gas and air are supplied at 25°C and atmospheric pressure. The flue gas in the exhaust has a temperature of 1,300K and passes through a stack with an inside diameter of 30 cm. Calculate (a) volumetric analysis of the ideal dry flue gas, %; (b) velocity of stack gas, cm/sec; (c) heat release for ideal combustion, Btu/hr; and (d) combustion efficiency, %.

2.27 Ethylene, C_2H_4, is to be reacted in 18% excess air in an atmosphere with changing humidity. Calculate (a) product mole fraction for dry air, %; (b) dew point temperature for dry air combustion, ºC; (c) product mole fraction for humid air with a humidity ratio ω = 18 gm H_2O/kg dry air, %; and (d) dew point temperature for the humid air combustion, ºC.

2.28 Calculate the (a) adiabatic flame temperature, K; (b) total moles of products; (c) final total pressure, kPa; and (d) product dew point temperature, °C, for the constant-volume combustion of methane, CH_4, and oxygen with a 0.75 equivalence ratio. Assume homogeneous gas-phase reactant conditions of 101 kPa and 298K.

2.29 A mixture of hydrogen and air initially at 25°C and 1 atm pressure is burned in a constant-pressure adiabatic process in which the adiabatic flame temperature is 2,800K. Assuming complete combustion in all calculations determine (a) volume of products to the volume of reactants; (b) molar $\overline{AF}$ ratio, kgmole air/kgmole fuel; (c) excess air required, %; and (d) equivalence ratio for the process.

2.30 Propane, C_3H_8, is burned in 130% theoretical air. The dry products of combustion consist of CO, CO_2, O_2, and N_2 with the oxygen percentage equal to 6.444%. For these percentages determine: (a) the Orsat combustion analysis, %; (b) the product molecular weight, kg/kgmole; (c) the mass of water produced per mass of fuel burned, kg H_2O/kg fuel; and (d) the percentage of fuel carbon converted to CO, %.

2.31 A hydrocarbon fuel C_xH_y is burned in enriched air, i.e. [O_2 + neair N_2] where 0 < neair < 3.76 is the moles of nitrogen in the synthetic atmosphere. Determine an expression in terms of neair for (a) the molecular weight of the enriched air, kg enriched air/kgmole enriched air; (b) the generalized stoichiometric equation for the combustion of one mole of fuel; (c) the molar $\overline{AF}$ ratio, kgmole enriched air/kgmole fuel; and (d) the mass *AF* ratio, kg enriched air/kg fuel.

2.32 An equimolar mixture of hydrogen and carbon monoxide is mixed with a stoichiometric quantity of air in a closed well-insulated vessel. The total initial pressure of the mixture is 5 atm and total initial temperature is 25°C. The mixture is ignited by an electric spark. Assuming the oxidation reaction to have gone to completion, determine (a) the total moles of product, kgmole products; (b) the maximum temperature, °C; and (c) the peak pressure, atm.

2.33 Reconsider Problem 2.29. Determine an expression in terms of neair for (a) the total moles of product, kgmole products; (b) the molecular weight of the products, kg

products/kgmole products; (c) the mole fractions of product species; and (d) the mass fractions of product species.

2.34 Gaseous propane, C_3H_8, and air are burned in a steady flow constant pressure process. The fuel and air are supplied at *STP* while the products are at 1,260°R. Assuming a lean adiabatic process calculate (a) the equivalence ratio required for these conditions; (b) the molar air-fuel ratio, for the reaction, lbmole air/lbmole fuel; and (c) moles of CO_2 formed per moles of propane burned.

2.35 Gaseous hydrogen and oxgen are pre-mixed in the proportion 10 parts O_2 to 1 part H_2 by weight. The mixture's initial state is at *STP*. For these reactant proportions calculate: (a) the mixture equivalence ratio; (b) the reactant mixture molecular weight, kg/kgmole; (c) the reactant mixture specific gravity; and (d) the reactant mixture lower heating value, kJ/kgfuel.

2.36 Propylene is burned in 30% excess air to provide waste heat. The combustion efficiency for the process is 80% with 60% of the carbon yield being CO_2 and 30% producing CO. Reactants are supplied to the burner at *STP*. For this process find: the *HHV*, kJ/kg fuel; (b) heat transfer, kJ/kgmole fuel; (c) moles of product, %; and (d) product temperature, K.

2.37 Methane undergoes a reaction in a constant volume combustion vessel. Complete reaction for a stoichiometric reactive mixture, initially at *STP*, results in a final reaction peak temperature of 1,200K. For these constraints find: (a) the stoichiometric reaction coefficients; (b) the peak pressure, kPa; and (c) the heat transferred during the combustion process, kJ/kgmole CH_4.

3

Combustion and Entropy

3.1 INTRODUCTION

In Chapter 2, elements of a general energy analysis for chemical reactions were developed. For any particular hydrocarbon fuel-air mixture the ideal complete combustion process only produced CO_2 and H_2O as products of reaction. In such instances, the reactant and product relationships were determined via the *stoichiometric* equation. The inability to achieve complete combustion in practice is due directly to the irreversible nature of actual high-temperature chemical reactions as well as influences and interactions within operational combustion machinery, i.e., the *fuel-engine interface.* Incomplete combustion products, or *pollutants,* are generated by internal and external combustion systems such as engines, jet aircraft, fossil-fueled stationary power plants, thermal destruction systems, as well as residential space heating systems.

Today the need to minimize and control emissions from many combustion technologies is essential. In this chapter, the product composition of incomplete combustion will be modeled thermodynamically using the concept of an equilibrium product state. In addition, second law analysis will be written for chemically reactive mixtures, and useful properties, including entropy, Gibbs, and Hemholtz functions of reaction, as well as the concept of an equilibrium constant, will be developed.

3.2 EQUILIBRIUM AND CHEMICAL REACTIONS

Since actual combustion reactions do not go to completion, it will be useful to develop characteristics that will specify an equilibrium product composition. Recall from classical thermodynamics that an isolated system, i.e., one having no mass or energy transfer with its surroundings, is in an equilibrium state if it has time-independent properties and is not capable of any spontaneous change of state. Nature tends spontaneously toward equilibrium, and systems that are not in equilibrium will try to relax to a stable state.

Non-isolated systems relax by energetically interacting with their surroundings, a rate-dependent process that is a strong function of both time and space.

Thermodynamic equilibrium implies a lack of certain potential differences, or gradients, which are expressed in terms of local thermodynamic properties. For instance, the absence of force imbalances or pressure gradients implies mechanical equilibrium, a condition that, if not in existence, would require a work transfer to achieve an equilibrium state (see Figure 3.1). Thermal equilibrium requires that no temperature gradients exist and, hence, no heat transfer. Furthermore, for pure homogeneous species, phase equilibrium means that no phase change will spontaneously occur when different phases of a pure species are in direct contact, i.e., liquid $\leftrightarrows$ vapor. Finally, chemical equilibrium requires that no spontaneous change in chemical composition occurs when different species are present together in a mixture. Full equilibrium, such as with assumed equilibrium conditions for products of combustion, would require that all the above gradient criteria would apply. Often, an assumption of partial equilibrium may be justified in many engineering calculations in that such an approach yields reasonable results.

In Chapter 2, thermochemical calculations assumed a partial equilibrium approach to combustion, i.e., complete combustion product or *frozen* composition.

Frozen thermochemistry:

Reactants in *initial* state $\rightarrow$ *Complete* products in final state

$$CH_4 + 2O_2 \rightarrow CO_2 + 2H_2O$$

Since the actual chemical path forming products of combustion involves molecular rearrangement of fuel and oxidant atoms, the potential exists for producing a wide variety of stable and unstable species. The number of possible product species in this instance may exceed the number of independent atom balances that can be written. An equilibrium product state cannot be determined from writing energy and mass conservation principles alone.

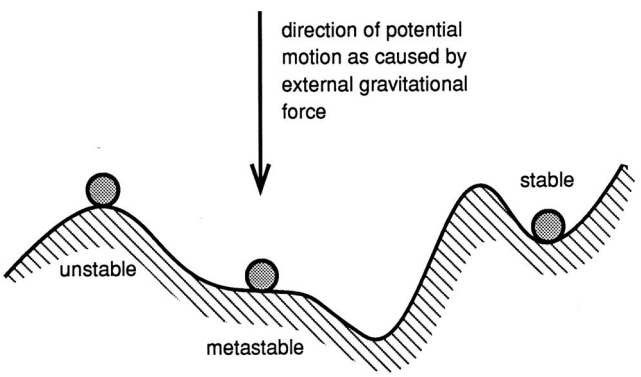

Figure 3.1 Mechanical illustration of processes and equilibrium.

Equilibrium thermochemistry:

Reactants in initial *equilibrium* state $\rightarrow$ *Actual* products in final state

$$CH_4 + 2O_2 \rightarrow aCO_2 + bCO + cC_s + dO_2 + eH_2O + fO_3 + \cdots$$

where

$$a = ?, \quad b = ?, \quad c = ?, \cdots$$

To predict a composition for equilibrium product combustion processes, additional principles beyond that of mass and energy conservation will be needed. In the next section, consequences of the second law of thermodynamics will be explored in regard to chemically reactive systems in order to determine additional information necessary to designate the equilibrium product state.

3.3 ENTROPY

Energy conversion processes have both a sense of magnitude and direction. Classical thermodynamics and the first law introduced the concept of energy conservation and the associated property energy. The second law of thermodynamics and its related property, entropy, lead to the concept of a continual entropy increase of the universe, that is, that all real processes must maintain or increase the entropy level of the universe.

The idea of perpetual motion machines, i.e., devices that violate thermodynamic principles, is first encountered in physics. Some devices, or perpetual motion machines of the first kind, do not conserve energy, while others are classified as perpetual motion machines of the second kind, i.e., entropy violators.

Natural experience dictates that combustion processes are highly irreversible and, therefore, must conserve energy but increase the total entropy of the universe. A process is assumed to be *reversible* if it can be retraced in such a way that the complete universe can be restored to its original condition without increasing the entropy of the universe. The Clausius inequality expresses the differential charge in entropy for a closed system in terms of a corresponding heat transfer as

$$TdS \geq \delta Q \qquad \text{kJ (Btu)} \tag{3.1}$$

which, for reversible heat transfer, becomes

$$T\,dS = \delta Q_{rev} \tag{3.1a}$$

and, for irreversible heat transfer, yields

$$T\,dS > \delta Q_{irrev} \tag{3.1b}$$

Consider the closed system shown in Figure 3.2 undergoing a general but differential change of state. From conservation of energy and applying Equation (2.29), for negligible kinetic and potential energy changes, the change in internal energy must be balanced by required heat and boundary expansion work transfers as

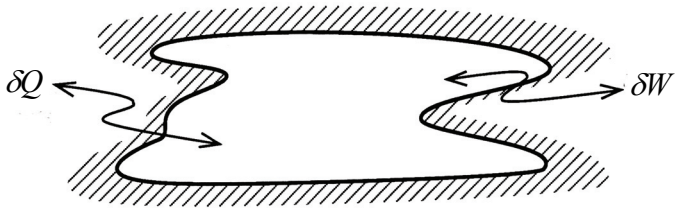

Figure 3.2 Closed system undergoing a differential change of state.

$$\delta Q = dU + P\,dV \tag{2.29}$$

If the process is assumed to be reversible, Equations (3.1a) and (2.29) can be combined to give an important *T dS* equation,

$$T\,dS = dU + P\,dV \tag{3.2a}$$

$$dS = \frac{dU}{T} + \frac{P}{T}dV \qquad \text{kJ/K (Btu/°R)} \tag{3.2b}$$

Using the definition of *enthalpy,*

$$H = U + PV \tag{3.3}$$

and differentiating gives

$$dH \equiv dU + P\,dV + V\,dP \tag{3.3a}$$

Substituting Equation (3.3a) into Equation (3.2a) yields a second important *TdS* equation

$$T\,dS = dH - P\,dV - V\,dP + PdV$$
$$TdS = dH - VdP \tag{3.4a}$$

Rearranging,

$$dS = \frac{dH}{T} - \frac{V}{T}dP \qquad \text{kJ/K (Btu/°R)} \tag{3.4b}$$

Equations (3.2b) and (3.4b) are differential equations that can be used to evaluate entropy changes for a pure component species as a function of *V* and *T* or *P* and *T*. Since thermochemical data for pure gases are tabulated in terms of enthalpies, it will be convenient to evaluate entropy in terms of the second of the *TdS* equations.

Consider evaluation of entropy for an ideal-gas species *i* having the molar equation of state, $P_i\bar{v}_i = \bar{R}T$, undergoing a differential change of state. Equation (3.4b) can be expressed in molar form as

$$d\bar{s}_i = \frac{d\bar{h}_i}{T} - \bar{R}\frac{dP_i}{P_i} \qquad \frac{\text{kJ}}{\text{kgmole}\cdot\text{K}}\left(\frac{\text{Btu}}{\text{lbmole}\cdot{}^\circ\text{R}}\right) \tag{3.5}$$

Recall that, for a pure gaseous species undergoing a process without composition change, enthalpy changes are only functions of temperature or

$$d\bar{h}_i = d[\bar{h}_f^0 + \bar{h}\langle T\rangle - \bar{h}\langle T^0\rangle] = d\bar{h}\langle T\rangle$$

and

$$d\bar{h}_i = \bar{C}_{p_i}\langle T\rangle dT \tag{2.36}$$

For a nonreactive ideal-gas species, entropy changes can now be evaluated by substituting Equation (2.36) into Equation (3.5), giving

$$d\bar{s}_i\langle T\rangle = \frac{\bar{C}_{p_i}\langle T\rangle dT}{T} - \bar{R}\frac{dP_i\langle T,P\rangle}{P_i} \tag{3.6}$$

Entropy changes are evaluated with respect to a reference datum as was done for $\bar{u}$ and $\bar{h}$ in Chapter 2 as

$$\Delta\bar{s}_i = \int_{T_0}^{T}\frac{\bar{C}_{p_i}\langle T\rangle}{T}dT - \bar{R}\int_{P_0}^{P}\frac{dP_i}{P_i} \tag{3.7}$$

where, for entropy

P_i = compound *partial* pressure < P_{tot}
P_0 = reference datum pressure = 1 atm.
T_0 = reference datum temperature = 25°C (77°F)

The first term in Equation (3.7) is defined as the *absolute standard state entropy of species i*, $\bar{s}_i^0\langle T\rangle$, and is evaluated as a function of temperature as

$$\bar{s}_i^0\langle T\rangle \equiv \int_{T_0}^{T}\frac{\bar{C}_{p_i}\langle T\rangle}{T}dT \tag{3.8}$$

Recall from Chapter 2 that molar specific heat, $\bar{C}_{p_i}$, of a pure species is temperature-dependent, and this relation was represented in virial form in Equation (2.22) as

$$\bar{C}_{p_i}\langle T\rangle = a_1 + a_2T + a_3T^2 + a_4T^3 + a_5T^4\cdots \tag{2.22}$$

Substituting Equation (2.22) into Equation (3.8) gives an expression for absolute standard state entropy of species as

$$\bar{s}_i^0\langle T\rangle = \int_{T_0}^{T}[a_1 + a_2T + a_3T^2 + a_4T^3 + a_5T^4\cdots]\frac{dT}{T} \tag{3.8a}$$

and integrating yields

$$\bar{s}_i^0\langle T\rangle = a_1\ln T + a_2T + \frac{a_3}{2}T^2 + \frac{a_4}{3}T^3 + \frac{a_5}{4}T^4 + \cdots + c_1 \tag{3.9}$$

Equation (3.9) is constrained to satisfy the requirement in keeping with the Third Law of Thermodynamics that entropy at absolute zero must be zero, i.e., $\bar{s}_i^0\langle 0\rangle = 0$. Tabulated values of $\bar{s}_i^0\langle T\rangle$ for several gases can be found in Tables B.2–B.25 in Appendix B.

A general expression for changes in entropy for an ideal-gas species can now be evaluated by combining Equations (3.9) and (3.7), giving

$$\Delta\bar{s}_i = \Delta\bar{s}_i^0 - \bar{R}\ln\left(\frac{P_i}{P_0}\right)\ \frac{\text{kJ}}{\text{kgmole}\cdot\text{K}}\left(\frac{\text{Btu}}{\text{lbmole}\cdot{}^\circ\text{R}}\right) \tag{3.9a}$$

Recall from Chapter 2 that for a closed system, reversible boundary expansion work can be evaluated by integrating Equation (2.28) or

$$\delta\bar{w}_{\text{rev}} = P\langle\bar{v}\rangle d\bar{v} \tag{2.28}$$

A $P-\bar{v}$ diagram in many instances can be used to visualize important processes, with the area under the reversible process line being equal to closed system work transfer.

Equation (3.1a) can be used to determine reversible heat transfer for a closed system as

$$\delta\bar{q}_{\text{rev}} = T\langle\bar{s}\rangle d\bar{s} \tag{3.1a}$$

and, furthermore, this relationship suggests an additional useful two-dimensional thermodynamic coordinate system, the $T-\bar{s}$ diagram. The $T-\bar{s}$ diagram can be used to visualize reversible heat transfer associated with a closed system. Figure 3.3 illustrates how several process lines for ideal gases appear on both the $P-\bar{v}$ and $T-\bar{s}$ planes.

Equations (3.2b) and (3.4b) also can be used to predict the shape of particular process lines on a $T-\bar{s}$ diagram. For example, a constant-pressure process diagram for a gas can be evaluated using Equation (3.4b), written in molar form as in Equation (3.6), as

$$d\bar{s}_i = \frac{\bar{C}_{p_i}\langle T\rangle dT}{T} - \bar{R}\frac{dP_i}{P_i} = \frac{\bar{C}_{p_i}\langle T\rangle dT}{T} \tag{3.6a}$$

Rearrangement yields an expression for the slope of a constant-pressure process curve as

$$\left(\frac{dT}{d\bar{s}_i}\right)_p = +\frac{T}{\bar{C}_{p_i}\langle T\rangle} > 0 \tag{3.10}$$

Using Equation (3.2b) and similar arguments, the slope of a constant-volume process line on a $T-\bar{s}_i$ diagram for a gas having a constant molar specific heat $\bar{C}_{v_i}$ can be shown to equal

$$\left(\frac{dT}{d\bar{s}_i}\right)_v = +\frac{T}{\bar{C}_{v_i}\langle T\rangle} > 0 \tag{3.11}$$

Since $\bar{C}_p - \bar{C}_v = \bar{R}$, then $\bar{C}_p > \bar{C}_v$ and, at a particular temperature, the slope of a constant-pressure process line will be greater than the corresponding constant-volume process line; see Figure 3.3. Furthermore, since specific heats of gases in general are temperature-dependent, the actual $P = c$ and/or $V = c$ process lines may differ from the constant molar specific heat case.

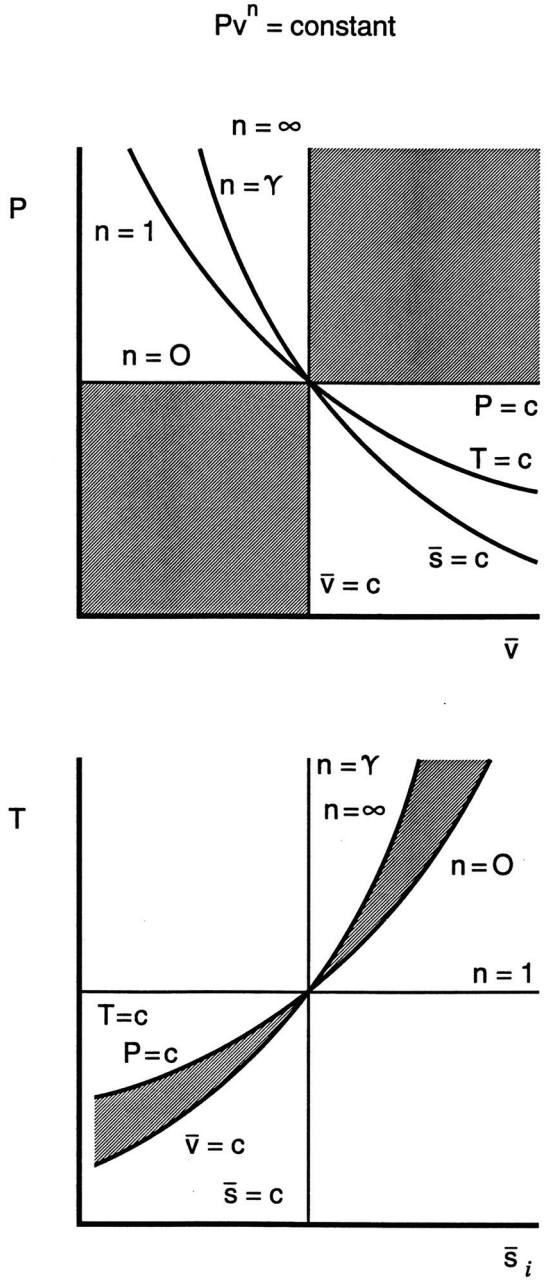

Figure 3.3 $P-\bar{v}$ and $T-\bar{s}$ ideal gas polytropic process diagrams. *Source*: Johnston, R. M., Brockett, W. A., Bock, A. E., and Keating, E. L., *Elements of Applied Thermodynamics*, 5th edition, Naval Institute Press, Annapolis, MD, 1992. With permission.

EXAMPLE 3.1 The reversible adiabatic, or *isentropic,* process is an important idealization utilized in many combustion calculations. Consider an ideal gas with constant specific heats. For a closed system, use the polytropic equation

$$Pv^n = \text{const}$$

and (a) find an expression for n in terms of $\overline{C}_p$ and $\overline{C}_v$, (b) express the change in pressure in terms of temperature and n, (c) express the change in volume in terms of temperature and n, and (d) calculate n for air at 298 and 1,200K.

Solution

1. Boundary expansion work:

$$
\begin{aligned}
{}_1w_2 &= \int_1^2 P\,dv = \int_1^2 \left(\frac{c}{v^n}\right) dv = c\int_1^2 v^{-n}\,dv \\
&= \frac{c}{1-n}\left(v_2^{1-n} - v_1^{1-n}\right) = \frac{Pv^n}{1-n}\left(v_2^{1-n} - v_1^{1-n}\right) \\
{}_1w_2 &= \frac{1}{1-n}\left(P_2v_2 - P_1v_1\right) = \frac{R}{1-n}\left(T_2 - T_1\right)
\end{aligned}
$$

2. Energy balance: $\delta Q - \delta W = dU$

$$
\begin{aligned}
-\delta w &= C_v\langle T\rangle dT = C_v dT \\
{}_1w_2 &= C_v[T_2 - T_1]
\end{aligned}
$$

3. Combining items 1 and 2,

$$
\begin{aligned}
&\left(\frac{-R}{1-n}\right)(T_2 - T_1) = C_v(T_2 - T_1) \\
&R = C_v(n-1) \\
&n - 1 = \frac{R}{C_v} = \frac{C_p - C_v}{C_v} = \frac{C_p}{C_v} - 1 \\
&n - 1 = \gamma - 1 \\
&\text{a. } n = \gamma
\end{aligned}
$$

4. Isentropic process:

$$
\begin{aligned}
P_1v_1^\gamma &= P_2v_2^\gamma \\
P_1\left(\frac{RT_1}{P_1}\right)^\gamma &= P_2\left(\frac{RT_2}{P_2}\right)^\gamma \\
\left(\frac{P_1}{P_2}\right)^{1-\gamma} &= \left(\frac{T_2}{T_1}\right)^\gamma
\end{aligned}
$$

or

$$\text{b.}\quad \frac{P_2}{P_1} = \left(\frac{T_2}{T_1}\right)^{\gamma/(\gamma-1)}$$

5. Isentropic process:

$$P_1 v_1^{\gamma} = P_2 v_2^{\gamma}$$

$$\frac{RT_1}{v_1}(v_1)^{\gamma} = \frac{RT_2}{v_2}(v_2)^{\gamma}$$

$$\left(\frac{v_1}{v_2}\right)^{\gamma-1} = \left(\frac{T_2}{T_1}\right)$$

$$\text{c.}\quad \frac{v_2}{v_1} = \left(\frac{T_2}{T_1}\right)^{1-\gamma}$$

6. From Table B.25 in Appendix B for air,

$$\overline{C}_p\langle 298\text{K}\rangle = 6.947 \qquad \overline{C}_p\langle 1{,}200\text{K}\rangle = 8.109$$

where

$$\gamma = \frac{C_p}{C_p - R} = \frac{\overline{C}_p}{\overline{C}_p - \overline{R}}$$

$$\text{d.}\quad \gamma\langle 298\text{K}\rangle = \frac{6.947}{6.947 - 1.987} = 1.40$$

$$\gamma\langle 1{,}200\text{K}\rangle = \frac{8.109}{8.109 - 1.987} = 1.32$$

Using the Gibbs-Dalton law, the entropy of a mixture of ideal gases can be expressed in terms of pure component entropy values as

$$S_{\text{tot}} = \sum_{i=1}^{k} m_i s_i \quad \text{kJ/K (Btu/°R)} \tag{3.12}$$

or

$$s_{\text{tot}} = \sum_{i=1}^{k} mf_i s_i \quad \text{kJ/kg mixt} \cdot \text{K(Btu/lbm mixt} \cdot \text{°R)} \tag{3.12a}$$

and

$$S_{\text{tot}} = \sum_{i=1}^{k} N_i \overline{s}_i \quad \text{kJ/K (Btu/°R)} \tag{3.13}$$

or

$$\bar{s}_{\text{tot}} = \sum_{i=1}^{k} \bar{x}_i \bar{s}_i \quad \text{kJ/kgmole mixt} \cdot \text{K (Btu/lbmole mixt} \cdot \text{°R)} \tag{3.13a}$$

An important process associated with the analysis of many combustion processes and devices is the *isentropic* or constant-entropy process. For a closed system containing an ideal-gas mixture undergoing an isentropic process, it is necessary that (1) no chemical change in composition occur, i.e., N_i = const, and (2) no change in total composition occur, i.e., N_{tot} = const. Thus, for an isentropic process:

$$S\langle T_2 \rangle = \Sigma N_i \bar{s}_i \langle T_2, P_2 \rangle = \Sigma N_i \bar{s}_i \langle T_1, P_1 \rangle = S\langle T_1 \rangle \tag{3.14}$$

Expressing the *STP* reference pressure P_0 in units of atmospheres, $P_0 \equiv 1$ atm, and substituting Equation 3.9 yields

$$\Sigma N_i \{\bar{s}_i^0 \langle T_2 \rangle - \bar{R} \ln(P_{i_2}/P_0)\} = \Sigma N_i \{\bar{s}_i^0 \langle T_1 \rangle - \bar{R} \ln(P_{i_1}/P_0)\}$$

or

$$\Sigma N_i \bar{R} \{\ln(P_{i_2}) - \ln(P_{i_1})\} = \Sigma N_i \{\bar{s}_i^0 \langle T_2 \rangle - \bar{s}_i^0 \langle T_1 \rangle\} \tag{3.14a}$$

Dividing by N_{tot} and using the definition of partial pressure

$$P_i = \bar{x}_i P_{\text{tot}} \tag{2.11b}$$

and rearranging gives an isentropic process relationship in terms of pressure and temperature as

$$\Sigma \bar{x}_i \bar{R} \{\ln(\bar{x}_i P_{\text{tot}_2}/\bar{x}_i P_{\text{tot}_1})\} = \Sigma \bar{x}_i \bar{R} \ln(P_{\text{tot}_2}/P_{\text{tot}_1})$$
$$= \bar{R} \ln(P_{\text{tot}_2}/P_{\text{tot}_1}) = \Sigma \bar{x}_i \{\bar{s}_i^0 \langle T_2 \rangle - \bar{S}_i^0 \langle T_1 \rangle\}$$

or

$$\left(\frac{P_2}{P_1}\right) = \frac{\exp\{\Sigma \bar{x}_i \bar{s}_i^0 \langle T_2 \rangle / \bar{R}\}}{\exp\{\Sigma \bar{x}_i \bar{s}_i^0 \langle T_1 \rangle / \bar{R}\}} \tag{3.15}$$

Using the ideal-gas equation $P\bar{v} = \bar{R}T$, Equation (3.15) can also be written as

$$\left(\frac{\bar{v}_2}{\bar{v}_1}\right) = \left(\frac{T_2}{T_1}\right) \times \left[\frac{\exp\{\Sigma \bar{x}_i \bar{s}_i^0 \langle T_1 \rangle / \bar{R}\}}{\exp\{\Sigma \bar{x}_i \bar{s}_i^0 \langle T_2 \rangle / \bar{R}\}}\right] \tag{3.16}$$

For the case of a single species, i.e., $\bar{x}_i = 1.0$, or if one is able to calculate the expression $\bar{s}^0 \langle T \rangle$ for mixtures using Equation (3.6b), the isentropic process relationship Equation (3.15) reduces to the form

$$\frac{P_2}{P_1} = \frac{\exp(\bar{s}^0 \langle T_2 \rangle / \bar{R})}{\exp(\bar{s}^0 \langle T_1 \rangle / \bar{R})} \tag{3.17}$$

Since Equation (3.17) is only a function of temperature, it is convenient to define a *relative pressure* P_r as

$$P_r\langle T\rangle \equiv \exp(\bar{s}^0\langle T\rangle/\overline{R}) \tag{3.18}$$

which yields the familiar isentropic process equation for variable specific heats,

$$\frac{P_2}{P_1} = \frac{P_r\langle T_2\rangle}{P_r\langle T_1\rangle} \tag{3.19}$$

Also, defining a *relative volume* $\bar{v}_r$ as

$$\bar{v}_r \equiv \frac{\overline{R}T}{P_r} \tag{3.20}$$

and substituting into Equation (3.19) gives the alternate isentropic process relation

$$\frac{v_2}{v_1} = \frac{v_r\langle T_2\rangle}{v_r\langle T_1\rangle} \tag{3.21}$$

If one further assumes that $\overline{C}_p$ and $\overline{C}_v$ are temperature-independent or that they may be treated as constants, the above isentropic relations can be written as follows. Combining Equations (3.8) and (3.18),

$$P_r\langle T\rangle = \exp\left\{\frac{\overline{C}_p}{\overline{R}}\int_{T_0}^{T}\frac{dT}{T}\right\} \tag{3.22}$$

$$= \exp\left\{\frac{\overline{C}_p}{\overline{R}}\ln(T/T_0)\right\}$$

$$= (T/T_0)^{\overline{C}_p/\overline{R}} \tag{3.22a}$$

Equation (3.19), the isentropic process for the constant specific heat case, then can be expressed as

$$\frac{P_2}{P_1} = \frac{P_r\langle T_2\rangle}{P_r\langle T_1\rangle} = \frac{(T_2/T_0)^{\overline{C}_p/\overline{R}}}{(T_1/T_0)^{\overline{C}_p/\overline{R}}} = \left(\frac{T_2}{T_1}\right)^{\overline{C}_p/\overline{R}} \tag{3.23}$$

Recall from Chapter 2 the expression for $\overline{C}_p$ and $\overline{R}$ in terms of γ, where $\gamma = \overline{C}_p/\overline{C}_v$, is equal to

$$\frac{\overline{C}_p}{\overline{R}} = \frac{\gamma}{\gamma - 1} \tag{2.19}$$

and, then,

$$\frac{P_2}{P_1} = \left(\frac{T_2}{T_1}\right)^{\gamma/(\gamma-1)} \tag{3.24}$$

Using the ideal-gas law $P\bar{v} = \bar{R}T$, Equation (3.24) can also be written as

$$\frac{v_2}{v_1} = \left(\frac{T_2}{T_1}\right)^{-1/(\gamma-1)} \tag{3.25}$$

and

$$\frac{P_2}{P_1} = \left(\frac{v_1}{v_2}\right)^{\gamma} \tag{3.26}$$

EXAMPLE 3.2 As indicated in Example 3.1, air has variable specific heats for the range of temperatures encountered in combustion processes. Using the JANAF air tables found in Table B.24 in Appendix B, calculate (a) the relative pressure P_r as a function of temperature and (b) the relative volume v_r as a function of temperature. Find (c) the final temperature of air, initially at 14.7 psi and 77°F when isentropically compressed to 140 psi.

Solution:

1. Relative pressure $P_r\langle T\rangle$:

$$P_r\langle T\rangle = \exp\left\{\frac{\bar{s}^0\langle T\rangle}{\bar{R}}\right\} \tag{3.18}$$

2. Relative volume $v_r\langle T\rangle$:

$$v_r\langle T\rangle = \frac{\bar{R}T}{P_r\langle T\rangle} \tag{3.20}$$

3. From the air data found in Table B.25 in Appendix B:

at $T = 537°\text{R}$ (298K)

$\bar{s}^0\langle T\rangle = 46.255$ cal/gmole·K

and

$$P_r\langle 298\text{K}\rangle = \exp\left\{\frac{46.255 \text{ cal/gmole·K}}{1.987 \text{ cal/gmole·K}}\right\} = 1.288 \times 10^{10}$$

with

$$v_r\langle 298\text{K}\rangle = \frac{(82.057 \text{ cc atm/gmole·K})(298\text{K})}{1.288 \times 10^{10}} = 1.899 \times 10^{-6}$$

Using the data for $\bar{s}^0\langle T\rangle$, a table can be generated for $P_r\langle T\rangle$ and $v_r\langle T\rangle$. Results are given in Table 3.1.

4. Isentropic process-variable specific heats:

$$\frac{P_2}{P_1} = \frac{P_r\langle T_2\rangle}{P_r\langle T_1\rangle}, \quad P_r\langle T_2\rangle = \left(\frac{140}{14.7}\right)1.288 = 12.267$$

and by interpolation

T	P_r
900	8.826
992.5	12.267
1,080	16.028

c. $T_2 = 992.5°\text{R}$

The Clausius inequality, Equation (3.1), can also be expressed in a rate form as

$$T\frac{dS}{dt} \geq \frac{\delta Q}{dt} \quad \text{kW}\left(\frac{\text{Btu}}{\text{hr}}\right) \tag{3.27}$$

or

$$\frac{dS}{dt} \geq \frac{1}{T}\frac{\delta Q}{dt}$$

A relationship, valid for closed systems, i.e., systems of fixed mass or a control mass, can be written using open-system or control-volume parameters as

$$\left.\frac{dS}{dt}\right)_{\text{C.M.}} = \left.\frac{\delta S}{\delta t}\right)_{\text{C.V.}} + \sum_{\text{out}} \dot{m}_j s_j - \sum_{\text{in}} \dot{m}_i s_i \geq \frac{\dot{Q}}{T} \tag{3.28a}$$

or

$$\left.\frac{dS}{dt}\right)_{\text{C.M.}} = \left.\frac{\delta S}{\delta t}\right)_{\text{C.V.}} + \sum_{\text{out}} \dot{N}_j \bar{s}_j - \sum_{\text{in}} \dot{N}_i \bar{s}_i \geq \frac{\dot{Q}}{T} \tag{3.28b}$$

For steady-state, steady-flow conditions and no entropy production within the control volume, Equation (3.28b) reduces to

$$\sum_{\text{out}} \dot{N}_j \bar{s}_j - \sum_{\text{in}} \dot{N}_i \bar{s}_i \geq \frac{\dot{Q}}{T} \quad \text{kW}\left(\frac{\text{Btu}}{\text{hr}}\right) \tag{3.29a}$$

and

$$\sum_{\text{out}} N_j \bar{s}_i - \sum_{\text{in}} N_k \bar{s}_i \geq \frac{Q}{T} \quad \text{kJ (Btu)} \tag{3.29b}$$

Table 3.1 Isentropic Properties for Air

T		$g^0\langle T\rangle$	$P_r\langle T\rangle \times 10^{-10}$	$v_r\langle T\rangle \times 10^{10}$
536	298	46.255	1.288	18,990
540	300	46.372	1.366	18,020
720	400	48.378	3.749	8,755
900	500	49.954	8.286	4,952
1,080	600	51.265	16.028	3,072
1,260	700	52.397	28.334	2,027
1,440	800	53.400	46.938	1,399
1,620	900	54.305	74.017	997.8
1,800	1,000	55.129	112.06	732.3
1,980	1,100	55.887	164.10	550.0
2,160	1,200	56.588	233.52	421.7
2,340	1,300	57.241	324.37	328.9
2,520	1,400	57.852	441.16	260.4
2,700	1,500	58.427	589.21	208.9
2,880	1,600	58.969	773.98	169.6
3,060	1,700	59.482	1,002.0	139.2
3,240	1,800	59.970	1,280.9	115.3
3,420	1,900	60.434	1,617.8	96.37
3,600	2,000	60.877	2,021.9	81.17
3,780	2,100	61.301	2,502.8	68.85
3,960	2,200	61.707	3,070.2	58.80
4,140	2,300	62.097	3,736.1	50.52
4,320	2,400	62.471	4,509.8	43.67
4,500	2,500	62.831	5,405.6	37.95
4,680	2,600	63.178	6,437.0	33.14
4,860	2,700	63.513	7,619.1	29.08
5,040	2,800	63.837	8,968.5	25.62
5,220	2,900	64.150	10,499	22.67
5,400	3,000	64.454	12,234	20.12
°R	K	cal/gmole·K	—	—

For an adiabatic process,

$$\sum_{\text{out}} N_j \bar{s}_j \geq \sum_{\text{in}} N_i \bar{s}_i \tag{3.30}$$

and for reversible adiabatic or isentropic processes for an open system,

$$S_{\text{out}} = S_{\text{in}} \tag{3.31}$$

which, in fact, is identical in form to the previous expressions developed in this section for ideal-gas mixture entropy analysis.

Table 3.2 Isentropic Process Relationships

Constant specific heats	
$\frac{P_2}{P_1} = \left(\frac{T_2}{T_1}\right)^{\gamma/(\gamma-1)}$	$\frac{v_2}{v_1} = \left(\frac{T_2}{T_1}\right)^{1/(1-\gamma)}$
Variable specific heats—single species	
$\frac{P_2}{P_1} = \frac{P_r\langle T_2\rangle}{P_r\langle T_1\rangle}$	$\frac{v_2}{v_1} = \frac{v_r\langle T_2\rangle}{v_r\langle T_1\rangle}$
Variable specific heats—mixture	
$\left(\frac{P_2}{P_1}\right) = \frac{\exp\{\Sigma\bar{x}_i\bar{s}_i^0\langle T_2\rangle/\bar{R}\}}{\exp\{\Sigma\bar{x}_i\bar{s}_i^0\langle T_1\rangle/\bar{R}\}}$	$\left(\frac{\bar{v}_2}{\bar{v}_1}\right) = \left(\frac{T_2}{T_1}\right) \times \left[\frac{\exp\{\Sigma\bar{x}_i\bar{s}_i^0\langle T_1\rangle/\bar{R}\}}{\exp\{\Sigma\bar{x}_i\bar{s}_i^0\langle T_2\rangle/\bar{R}\}}\right]$

Table 3.2 summarizes the various isentropic process relations applicable to nonreactive gas mixtures.

Selected reactant and/or equilibrium product mixtures charts were developed based on a unit mass and were the basis of many combustion calculations in the past; see Figures 3.4 and 3.5. Charts presented important hydrocarbon fuel-air mixtures showing values of temperature, pressure, specific volume, internal energy, enthalpy, and entropy which allowed graphical evaluation of properties in engineering calculations. When working with these combustion charts, one had to carefully note the standard state datum used. The Hottel charts, for example, were based on a 1 atm, 520°R datum with zero internal energy and entropy being assigned to CO_2, H_2O, O_2, and N_2. The Starkman-Newhall charts used a 1 atm, 537°R datum with zero energy and entropy assigned to C_{solid}, H_2, O_2, and N_2. Powell selected 1 atm and 0°R as the reference, with zero enthalpy assigned to C_{solid}, H_2, O_2, and N_2 and zero entropy in compliance with the third law. Various processes, i.e., $T = C$, $P = C$, $U = C$, etc., would be drawn directly on these charts with appropriate thermochemical properties, then read directly for analysis instead of being calculated using the basic relationships as described in this chapter.

Today many computer routines now exist, beyond the pioneering program work of Gordon and McBride at NASA Lewis, that allow routine thermochemical calculation of complex mixtures and composition to be made over a wide range of fuels and compositions. Property predictions for mixtures including pressure, temperature, and specific volume along with internal energy, enthalpy, entropy, and Gibbs free energy are determined from basic principles. This approach goes beyond techniques available in graphical form and has become more prevalent with the availability and power of the current generation of minicomputers being used by the core and related engineering disciplines involved in basic and applied combustion.

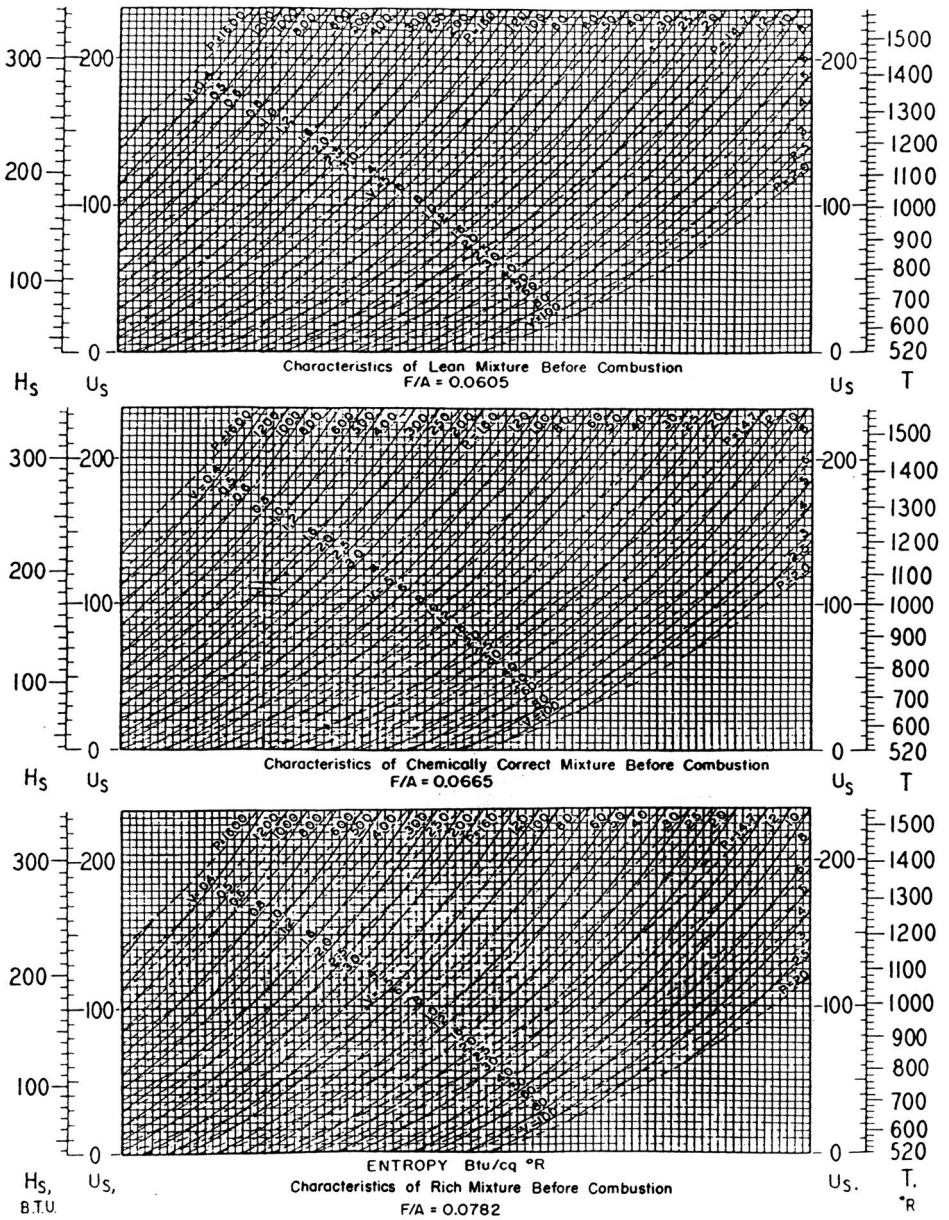

Figure 3.4 Energy-entropy diagram for hydrocarbon-air reactant mixtures. *Source*: NACA Report RB#3G28, 1943.

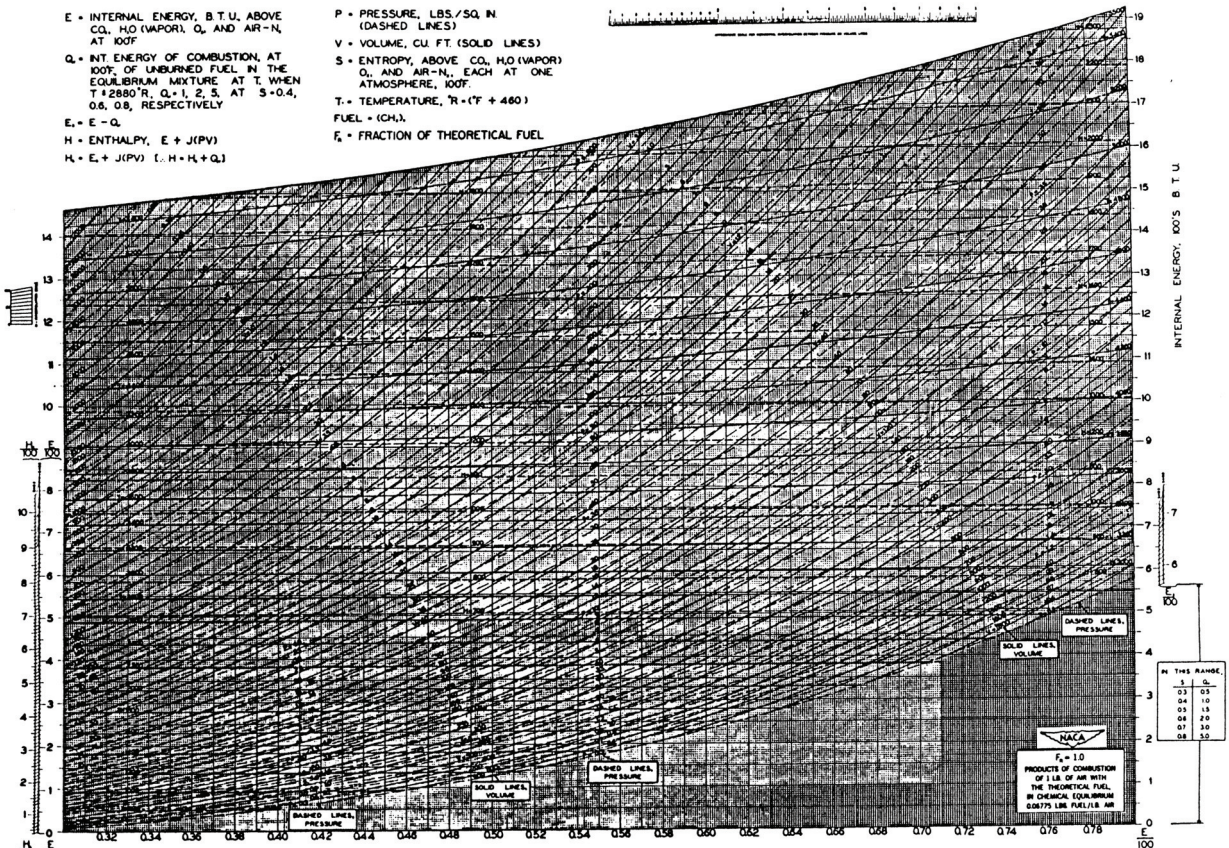

Figure 3.5 Energy-entropy diagram for hydrocarbon-air product mixture. *Source*: NACA Report RB#3G28, 1943.

3.4 GIBBS AND HEMHOLTZ FUNCTIONS

The actual exhaust gases emitted from internal or external combustion devices and processes are reactive and will not be fully oxidized. Local conditions surrounding the gases being produced as well as environmental influences, in fact, prevent complete reaction from occurring. Space-time factors such as heat transfer, free expansion, dissociation, and other irreversibilities will influence the reactive mixture. A useful concept for describing an incomplete product state in such instances is that of an exhaust gas mixture in an equilibrium condition.

Consider a fixed sample of a gas mixture such as the exhaust gases described above. Assume further that this mixture is maintained at a constant temperature and total pressure. If the mixture is not in a complete equilibrium state, composition adjustments will be necessary in order to achieve an equilibrium state. An energy balance including the potential for boundary expansion work is

$$dU = \delta Q - \delta W = \delta Q - P\,dV \tag{2.29}$$

Using Equation (3.3a) for dH and after rearranging,

$$\delta Q = dH - V dP \tag{3.32}$$

A new and useful property, the *Gibbs function G,* can now be introduced and is defined as

$$G = H - TS \qquad \text{kJ (Btu)} \tag{3.33}$$

and

$$g = h - Ts \qquad \text{kJ/kg (Btu/lbm)} \tag{3.33a}$$

or on a molar basis

$$\bar{g} = \bar{h} - T\bar{s} \qquad \text{kJ/kgmole (Btu/lbmole)} \tag{3.33b}$$

Differentiating the Gibbs function G, Equation (3.33) yields

$$dG = dH - T\,dS - S\,dT \tag{3.34}$$

Substituting Equation (3.32) for dH into Equation (3.34) gives an expression for the differential change in G as

$$dG = \delta Q + V\,dP - T\,dS - S\,dT \tag{3.35}$$

Equation (3.35) suggests that the Gibbs function for a reactive mixture can be changed by changes in T, P. Recall that it was assumed for the reactive mixture that T and P_{tot} were held constant, so that $dT = dP_{tot} = 0$ or

$$dG_{T,P} = \delta Q + V\,\cancel{dP} - T\,dS - S\,\cancel{dT} = \delta Q - T\,dS$$

From the Clausius inequality, Equation (3.1),

$$T\,dS \geq \delta Q \tag{3.1}$$

or

$$T\,dS - \delta Q \geq 0$$

and

$$\delta Q - T\,dS \leq 0$$

Substituting Equation (3.1) into Equation (3.35) gives the result

$$d\,G_{T,P} \leq 0 \tag{3.36}$$

Figure 3.6 shows a plot of Gibbs function versus changing composition at fixed temperature and total pressure. Figure 3.6 would require the equilibrium point to exist at the minimum of the curve. In other words, for a reversible differential change, i.e., at the equilibrium point, $dG = 0$ and, for all irreversible changes, dG must be <0. Equilibrium composition for a reactive mixture is therefore seen to be that composition which, at a particular temperature and total pressure, defines its minimum Gibbs function.

Recalling the Gibbs-Dalton law, the Gibbs function of a mixture of ideal gases can be expressed in terms of pure component values as

$$G_{tot} = \sum_{i=1}^{k} m_i\, g_i \quad \text{kJ (Btu)} \tag{3.37a}$$

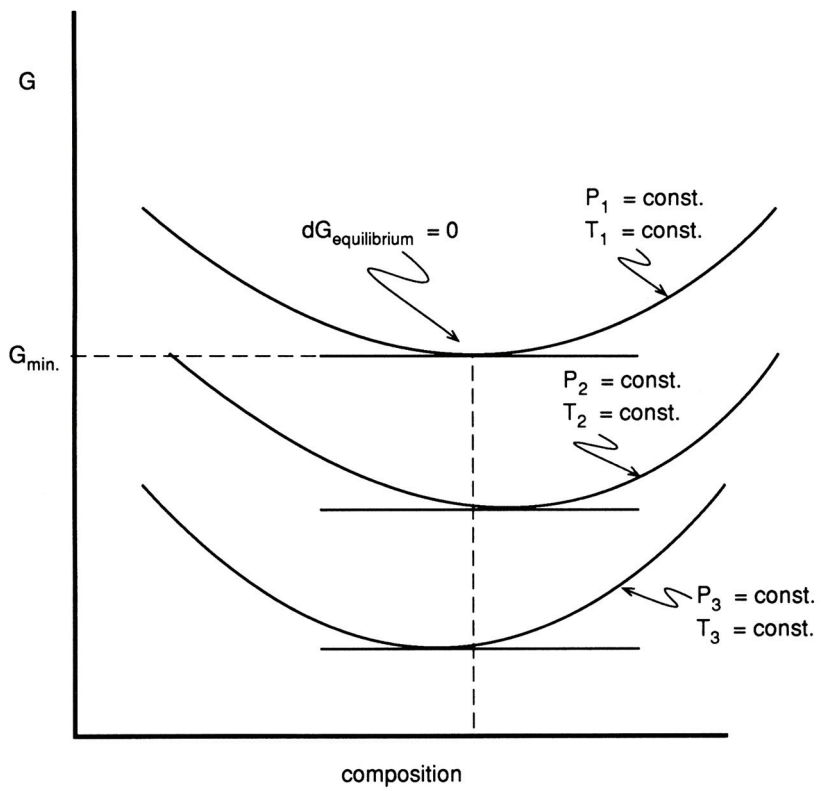

Figure 3.6 Gibbs function for a reactive mixture.

$$G_{tot} = \sum_{i=1}^{k} N_i \, \bar{g}_i \quad \text{kJ (Btu)} \tag{3.37b}$$

or

$$g_{tot} = \sum_{i=1}^{k} mf_i \, g_i \quad \text{kJ/kg mixt (Btu/lbm)} \tag{3.37c}$$

$$\bar{g}_{tot} = \sum_{i=1}^{k} \bar{x}_i \, \bar{g}_i \quad \text{kJ/kgmole mixt (Btu/lbmole)} \tag{3.37d}$$

An additional property, the *Hemholtz function A*, can be introduced and defined as

$$A = U - TS \quad \text{kJ (Btu)} \tag{3.38}$$

and

$$a = u - Ts \quad \text{kJ/kg (Btu/lbm)} \tag{3.38a}$$

or on a molar basis as

$$\bar{a} = \bar{u} - T\bar{s} \quad \text{kJ/kgmole (Btu/lbmole)} \tag{3.38b}$$

Consider now a specific sample of a reactive mixture that is maintained at constant temperature and total volume. Differentiating the expression for the Hemholtz function, Equation (3.38) gives

$$dA = dU - T\,dS - S\,dT \tag{3.39}$$

Substituting Equation (2.29) for dU yields

$$dA = \delta Q - P\,dV - T\,dS - S\,dT \tag{3.40}$$

Equation (3.40) indicates that the Hemholtz function for a reactive mixture can change by changing T, V, and/or composition. For a reactive mixture in which it is assumed that T and V are constant, $dT = dV = 0$, or

$$dA_{T,V} = \delta Q - \cancel{P\,dV} - T\,dS - \cancel{S\,dT} = \delta Q - T\,dS$$

Again, from the Clausius inequality, Equation (3.1),

$$T\,dS \geq \delta Q$$

or

$$T\,dS - \delta Q \geq 0$$

and

$$\delta Q - T\,dS \leq 0$$

Substituting Equation (3.1) yields the result that, at constant temperature and total volume,

$$dA_{T,V} \leq 0 \tag{3.41}$$

Figure 3.7 shows a plot of Hemholtz function versus changing composition at fixed T and V for a reactive system. Figure 3.7 requires the equilibrium point, similar to the case for the Gibbs function, to occur at a position of minimum Hemholtz value.

Recalling the Gibbs-Dalton law, the Hemholtz function of a mixture of ideal gases can be expressed in terms of pure component values as

$$A_{tot} = \sum_{i=1}^{k} m_i \, a_i \quad \text{kJ (Btu)} \tag{3.42a}$$

$$A_{tot} = \sum_{i=1}^{k} N_i \, \bar{a}_i \quad \text{kJ (Btu)} \tag{3.42b}$$

or

$$a_{tot} = \sum_{i=1}^{k} mf_i \, a_i \quad \text{kJ/kg mixt (Btu/lbm)} \tag{3.42c}$$

$$\bar{a}_{tot} = \sum_{i=1}^{k} \bar{x}_i \, \bar{a}_i \quad \text{kJ/kgmole mixt (Btu/lbmole)} \tag{3.42d}$$

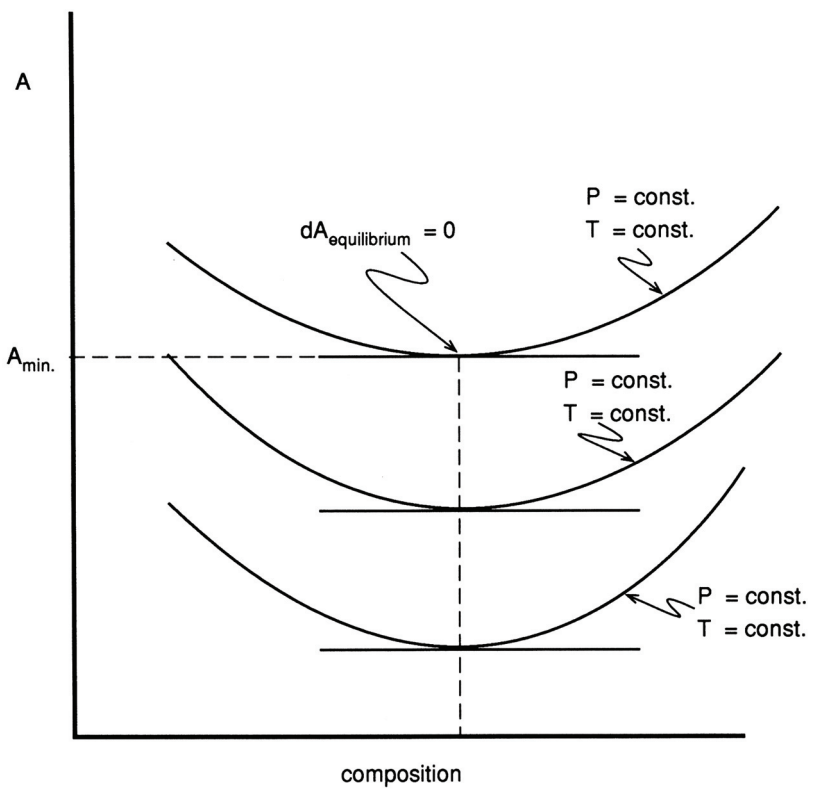

Figure 3.7 Hemholtz function for a reactive mixture.

EXAMPLE 3.3 Consider the dissociation reaction *STP*

$$\tfrac{1}{2}O_2 \overset{STP}{\rightarrow} O$$

Using JANAF data, calculate for the reaction at *STP:* (a) the enthalpy of reaction ΔH_r^0, cal; (b) the entropy of reaction ΔS_r^0, cal/K; (c) the Hemholtz function of reaction ΔA_r^0, cal; and (d) the Gibbs function of reaction ΔG_r^0, cal.

Solution:

1. Enthalpy of reaction at *STP*:

$$\Delta H_r^0\langle 25°C\rangle = \sum_{i\ \text{prod}} N_i[\bar{h}_f^0 + \Delta\bar{h}]_i - \sum_{i\ \text{react}} N_j[\bar{h}_f^0 + \Delta\bar{h}]_j$$

using the data found in Table B.1 in Appendix B for $\bar{h}_f^0$.

a. $\Delta H_r^0 = 1[59{,}559\ \text{cal/gmole}]_O - 0.5[0]_{O_2} = 59{,}559\ \text{cal}$

2. Entropy of reaction at *STP*:

$$\Delta S_r^0\langle 25°C\rangle = \sum_{i\,\text{prod}} N_i[\bar{s}_i^0\langle T\rangle - \bar{R}\ln(P_i/P_0)]_i - \sum_{j\,\text{react}} N_j[\bar{s}_j^0\langle T\rangle - \bar{R}\ln(P_j/P_0)]_j$$

using the data found in Tables B.20 and B.22 in Appendix B for $\bar{s}^0$.

b. $\Delta S_r^0 = 1[38.468\ \text{cal/gmole}\cdot\text{K}]_O - 0.5[49.004\ \text{cal/gmole}\cdot\text{K}]_{O_2}$
$= 13.966\ \text{cal/K}$

3. Hemholtz function of reaction at *STP*:

$$\bar{a}_i = \bar{u}_i - T\bar{s}_i$$

and

$$\bar{u}_i = \bar{h}_i - P\bar{v}_i = \bar{h}_i - \bar{R}T$$

or

$$\bar{a}_i = \bar{h}_i - T(\bar{s}_i + \bar{R})$$

$$\Delta A_r^0\langle 25°C\rangle = \sum_{i\,\text{prod}} N_i[\bar{h}_{f_i}^0 - T^0(\bar{s}_i\langle T^0\rangle + \bar{R})]_i - \sum_{j\,\text{react}} N_j[\bar{h}_{f_j}^0 - T^0(\bar{s}_j\langle T^0\rangle + \bar{R})]_j$$

$$= 1[59{,}559 - (298)(38.468 + 1.987)]_O - 0.5[0 - (298)(49.004 + 1.987)]_{O_2}$$

c. $\Delta A_r^0\langle 25°\text{C}\rangle = 55{,}101$ cal

4. Gibbs function of reaction at *STP*:

$$\Delta G_r^0\langle 25°\text{C}\rangle = \sum_{i\,\text{prod}} N_i[\bar{h}_{f_i}^0 - T^0\bar{s}_i^0\langle T^0\rangle]_i - \sum_{j\,\text{react}} N_j[\bar{h}_{f_j}^0 - T^0\bar{s}_j^0\langle T^0\rangle]_j$$

$$= 1[59{,}559 - (298)(38.468)]_{\text{O}} - 0.5[0 - (298)(49.004)]_{\text{O}_2}$$

d. $\Delta G_r^0\langle 25°\text{C}\rangle = 55{,}397$ cal

or, alternatively,

$$\Delta G_r^0\langle 25°\text{C}\rangle = \Sigma H_r^0\langle 25°\text{C}\rangle - T^0\Delta S_r^0\langle 25°\text{C}\rangle = 59{,}559 - (298)(13.966)$$

$$\Delta G_r^0\langle 25°\text{C}\rangle = 55{,}397 \text{ cal}$$

Sophisticated computational computer codes, such as the NASA Complex Chemical Equilibrium Programs of Gordon and McBride (1968), TRANS72 Program for Hydrocarbon-Air Mixtures by Svehla and McBride, (1973), and CET93 and CETPC, upgraded versions of the Complex Chemical Equilibrium Programs by McBride, Reno, and Gordon (1994) as well as the PC-based program STANJAN of Reynolds (1986), allow thermochemical properties of equilibrium mixtures to be determined. The various programs utilize numerical iteration and Lagrangian multiplier techniques to minimize the total Gibbs or Hemholtz free energy in order to obtain equilibrium state mixture compositions.

Consider as an example the Gibbs function for an ideal gas equilibrium mixture at T and P which can be expressed as

$$G_{tot} = \sum_{j=1}^{k} N_j \bar{g}_j \quad \text{kJ (Btu)} \tag{3.37b}$$

From Equation (3.37b) the total Gibbs function in general can be seen to be changed by changing the moles of product, N_j, and/or the specific molar Gibbs function. At equilibrium conditions of fixed T and P the differential change in total Gibbs function equals

$$dG_{T,P} = \left\{\sum_{j=1}^{k} \bar{g}_j dN_j + \sum_{j=1}^{k} N_j \cancel{d\bar{g}_j}\right\} = 0$$

where the specific molar Gibbs function, $\bar{g}_j$, is equal to

$$\bar{g}_j\langle T, P\rangle = \bar{g}_j{}^0\langle T\rangle + \bar{R}T\ln P_j \tag{3.33e}$$

or

$$\bar{g}_j\langle T, P\rangle = \bar{g}_j{}^0\langle T\rangle + \bar{R}T\ln \bar{x}_j P_{\text{tot}}$$

and by recalling that $P_0 = 1$ atm

$$\overline{g}_j\langle T,P\rangle = \overline{g}_j{}^0\langle T\rangle + \overline{R}T\ln\overline{x}_j + \overline{R}T\ln(P_{\text{tot}}/P_0)$$

Substituting the specific molar Gibbs function into the differential change in total Gibbs function at equilibrium yields the expression

$$dG_{T,P} = \sum_{j=1}^{k}\left(\overline{g}_j{}^0\langle T\rangle + \overline{R}T\ln\overline{x}_j + \overline{R}T\ln(P_{\text{tot}}/P_0)\right)dN_j = 0 \tag{3.43}$$

Now when determining the equilibrium state by minimizing total Gibbs function, the mixture composition is subject to an atom population constraint represented in general form in terms of atomic population of molecules expressed as

$$\sum_{j=1}^{k} n_{ij}N_j = p_i \qquad i = 1,2,..,a \tag{3.44}$$

where

n_{ij} – the number of atoms of element i in species j
Nj – the moles of species j
p_i – population (moles) of i atoms in the equilibrium mixture
a – number of different elements present in equilibrium mixture

Since changes in moles of equilibrium product are not all independent, relationships can be obtained by differentiating the atom population constraint and noting that the atomic numbers of element i in species j remain constant or

$$\sum_{j=1}^{k} N_j dn_{ij} + \sum_{j=1}^{k} n_{ij}dN_j = \sum_{j=1}^{k} n_{ij}dN_j = 0 \qquad i = 1,2,..,a \tag{3.44a}$$

In order to determine an equilibrium composition among k variables, only $k - a$ of the variables may be freely varied since a are constrained by the number of different defined elements present in the mixture. It is necessary to solve for the a restricted dN_j expressions in terms of the $k - a$ free dN_j ones and then substitute these relationships into the differential molar Gibbs relationship in order to express variations at the minimum point in terms of only the freely variable N_j. This substitution is equivalent to subtracting a linear combination of the differential atom balance constraint, Equation (3.44a), from the differential molar Gibbs relationship (3.43) such that the restricted dN_j drop out of the result. This subtraction yields the general expression

$$dG_{T,P} - \sum_{i=1}^{a}\lambda_i\sum_{j=1}^{k} n_{ij}dN_j$$

or

$$\sum_{j=1}^{k}\left(\overline{g}_j{}^0\langle T\rangle + \overline{R}T\ln\overline{x}_j + \overline{R}T\ln(P_{\text{tot}}/P_0)\right)dN_j - \sum_{i=1}^{a}\lambda_i\sum_{j=1}^{k} n_{ij}dN_j \quad i = 1,2,..,a$$

It is useful for mathematical convenience when numerically minimizing the molar Gibbs function at constant P and T to divide by the universal gas constant and absolute temperature giving

$$\sum_{j=1}^{k}\left(\frac{\bar{g}_j{}^0\langle T\rangle}{\bar{R}T} + \ln \bar{x}_j + \ln(P_{\text{tot}}/P_0)\right)dN_j - \frac{1}{\bar{R}T}\sum_{i=1}^{a}\lambda_i\sum_{j=1}^{k}n_{ij}\,dN_j$$

Collecting common expressions with respect to the coefficient dN_j gives

$$\sum_{j=1}^{k}\left(\frac{\bar{g}_j{}^0\langle T\rangle}{\bar{R}T} + \ln \bar{x}_j + \ln(P_{\text{tot}}/P_0) - \sum_{i=1}^{a}\frac{\lambda_i}{\bar{R}T}\sum_{j=1}^{k}n_{ij}\right)dN_j$$

In order for the restricted dN_j to drop out, the coefficient of each must be zero. Thus setting the coefficient of the dN_j term to zero one obtains the final relationship

$$\frac{\bar{g}_j{}^0\langle T\rangle}{\bar{R}T} + \ln \bar{x}_j + \ln(P_{\text{tot}}/P_0) - \sum_{i=1}^{a}\frac{\lambda_i}{\bar{R}T}n_{ij} = 0 \qquad j = 1,2\ldots k \tag{3.45}$$

The λ_i are Lagrangian multipliers which are to be determined in order to drop out the restricted set of dN_j from the equation. Using the Lagrangian multiplier approach it is necessary to obtain a solution to a set of $k + a + 1$ equations. Equation (3.45) provides set of k simultaneous equations for the unknown N_j; the atom constraint Equation (3.44) provides a additional equations. For the remaining relationship the following information is also known.

$$N_{tot} = \sum_{j=1}^{k}N_j$$

$$\bar{x}_j = \frac{N_i}{N_{tot}}$$

$$\sum_{j=1}^{k}\bar{x}_j = 1.0 \tag{3.46}$$

For initial conditions of T and V the minimization process with Lagrangian multipliers utilizes the Hemholtz function, Equation (3.34). Recalling the molar Hemholtz function is given by the expression

$$A = U - TS \tag{3.38}$$

and the molar Gibbs function given by the expression

$$G = H - TS \tag{3.33}$$

Now enthalpy is given by the expression

$$H = U + PV$$

or

$$U = H - PV$$

which, after substituting and using the molar Gibbs function, produces the following expression for the Hemholtz function:

$$A = H - PV - TS = G - PV$$

Now the Hemholtz function for an ideal gas equilibrium mixture at T and V can be expressed as

$$A_{\text{tot}} = \sum_{i=1}^{k} N_i \bar{a}_i \quad \text{kJ (Btu)} \tag{3.42b}$$

and

$$dA_{T,V} = \left\{ \sum_{j=1}^{k} \bar{a}_j dN_j + \sum_{j=1}^{k} N_j d\bar{a}_j \right\} = 0$$

One can treat the Hemholtz function in similar fashion as was done for the Gibbs function and obtain the following simultaneous equations for the λ_i Lagrangian multipliers for the condition of an ideal gas equilibrium mixture at T and V for the restricted dN_j

$$\frac{\bar{g}_j{}^0\langle T\rangle}{\bar{R}T} + \ln \bar{x}_j + \ln(\bar{R}T/P_0V) - \sum_{i=1}^{a} \frac{\lambda_i}{\bar{R}T} n_{ij} = 0 \qquad j = 1,2\ldots k \tag{3.47}$$

After obtaining the equilibrium product state for either the Gibbs or Hemholtz analysis using Lagrangian multipliers, computational routines can then determine thermochemical properties *P, V, T, U, H,* and *S* by use of equations and relations as found earlier in this chapter and in Chapter 2. Several of the aforementioned computer programs also address conditions of multiphase equilibrium thermochemistry.

3.5 EQUILIBRIUM CONSTANTS

Consider now a reactive gas mixture sample that contains species A, B, …, L, and M, all assumed to be in equilibrium at a specified temperature and total pressure but at unknown mole fractions. Furthermore, assume that these compounds were produced by the following incomplete combustion reaction:

$$\text{Reactants} \rightarrow N_1\text{A} + N_2\text{B} + N_3\text{C} + \cdots + N_i\text{L} + N_{i+1}\text{M} \tag{3.48}$$

In Section 3.4, it was shown that, for a reactive gas mixture at equilibrium, the Gibbs function is a minimum. Using the Gibbs-Dalton law for the product mixture

$$G_{\text{tot}} = \Sigma N_i \bar{g}_i\langle T,P\rangle \quad \text{kJ (Btu)} \tag{3.37b}$$

Specific molar Gibbs function for a pure species $\bar{g}_i$ can be written as

$$\bar{g}_i\langle T,P\rangle = \bar{h}_i\langle T,P\rangle - T\bar{s}_i\langle T,P\rangle \tag{3.33b}$$

while specific molar enthalpy $\bar{h}_i$ was expressed in Chapter 2 as

$$\bar{h}_i\langle T,P\rangle = \bar{h}_f^0 + [\bar{h}_i\langle T\rangle - \bar{h}_i\langle T^0\rangle] \tag{2.36}$$

An expression for specific molar entropy $\bar{s}_i$ was developed in this chapter and given as

$$\bar{s}_i\langle T,P\rangle = \bar{s}_i^0\langle T\rangle - \bar{R}\ln(P_i/P_0) \tag{3.9a}$$

Substituting Equations (2.36) and (3.9) into Equation (3.33b) and recalling that the units of atmospheres for pressure make $P_0 = 1$ yield

$$\bar{g}_i\langle T,P\rangle = \bar{h}_f^0 + [\bar{h}_i\langle T\rangle - \bar{h}_i\langle T^0\rangle] - T[\bar{s}_i^0\langle T\rangle - \bar{R}\ln P_i] \tag{3.33c}$$

Defining a standard state molar Gibbs function $\bar{g}_i^0\langle T\rangle$ as

$$\bar{g}_i^0\langle T\rangle \equiv \bar{h}_{f_i}^0 + [\bar{h}_i\langle T\rangle - \bar{h}_i\langle T^0\rangle] - T\bar{s}_i^0\langle T\rangle \tag{3.33d}$$

and the specific molar Gibbs function as

$$\bar{g}_i\langle T,P\rangle = \bar{g}_i^0\langle T\rangle + \bar{R}T\ln P_i$$

The total mixture Gibbs function can now be expressed as

$$G = \Sigma N_i[\bar{g}_i^0\langle T\rangle + \bar{R}T\ln P_i] \tag{3.49}$$

and, at equilibrium, for $T = c$, $P = c$

$$dG_{T,P} = 0 = \Sigma N_i d\bar{g}_i\langle T,P\rangle + \Sigma\bar{g}_i\langle T,P\rangle dN_i$$

or

$$0 = \Sigma[\bar{g}_i^0\langle T\rangle + \bar{R}T\ln P_i]dN_i \tag{3.50}$$

For a fixed amount of a reactive-gas mixture, one cannot independently or arbitrarily specify the concentration of each constituent and maintain equilibrium. Near an equilibrium point, the concentration relationship is expressed using the *equilibrium reaction* written in general form for the stated case above as

$$a\mathrm{A} + \mathrm{bB} \overset{T,P}{\rightleftarrows} l\mathrm{L} + m\mathrm{M} \tag{3.51}$$

Note that the equilibrium equation coefficients *a, b, 1*, and *m* are not reaction concentration coefficients *N*, given by Equation (3.48).

To illustrate, recall from chemistry the familiar equilibrium relationship for a mixture of H_2, O_2, and H_2O,

$$2\mathrm{H}_2 + \mathrm{O}_2 \rightleftarrows 2\mathrm{H}_2\mathrm{O}$$

The equilibrium equation shows that H_2 and O_2 can combine to produce H_2O, whereas H_2O can concurrently dissociate to yield H_2 and O_2. The equilibrium concentrations of H_2, O_2, and H_2O will be defined by minimum Gibbs function for the mixture at the temperature and total pressure of the gas mixture.

At high temperatures, such as those that occur in fuel-oxidant reactions, additional equilibrium reactions can be written between stable molecules and radicals. In fact, it is the endothermic dissociation effects at high temperature that work against achieving complete combustion. Examples of these types of reactions include

$$\begin{aligned} O_2 &\rightleftarrows 2O \\ CH_4 &\rightleftarrows CH_3 + H \\ N_2 &\rightleftarrows 2N \end{aligned}$$

For particular components, equilibrium equations can be written in several different but consistent forms. Consider, for example, the relationship between CO, O_2, and CO_2.

$$\begin{aligned} CO + \tfrac{1}{2}O_2 &\rightleftarrows CO_2 \\ 2CO + O_2 &\rightleftarrows 2CO_2 \\ 4CO_2 &\rightleftarrows 4CO + 2O_2 \end{aligned}$$

In the above equations, one sees any adjustment in CO, O_2, and CO_2 concentrations must be in proportion to their equilibrium coefficients. A general means of expressing the concentration adjustments required for CO, O_2, and CO_2 in terms of an *extent of reaction*

$$\begin{aligned} dN_{CO} &= \mp 2d\bar{x} \\ dN_{O_2} &= \mp d\bar{x} \\ dN_{CO_2} &= \pm 2d\bar{x} \end{aligned}$$

or

$$dN_i = \pm n_i d\bar{x}$$

Returning to the generalized equilibrium reaction equation between species A, B, …, L, and M, Equation (3.51), and substituting for minimum Gibbs function, Equation (3.50), one obtains an expression for the reaction $a\mathrm{A} + b\mathrm{B} \rightleftarrows l\mathrm{L} + m\mathrm{M}$,

$$\begin{aligned} 0 = {} & [\bar{g}_A^0\langle T\rangle + \bar{R}T\ln(P_A)]dN_A + [\bar{g}_B^0\langle T\rangle + \bar{R}T\ln(P_B)]dN_B \\ & + [\bar{g}_L^0\langle T\rangle + \bar{R}T\ln(P_L)]dN_L + [\bar{g}_M^0\langle T\rangle + \bar{R}T\ln(P_M)]dN_M \end{aligned} \tag{3.52}$$

Expressing the concentration changes in terms of the extent of reaction

$$\begin{aligned} dN_A &= \mp a\, d\bar{x} \\ dN_B &= \mp b\, d\bar{x} \\ dN_L &= \pm l\, d\bar{x} \\ dN_M &= \pm m\, d\bar{x} \end{aligned} \tag{3.53}$$

or

$$\begin{aligned} 0 = {} & \Big\{[\bar{g}_A^0\langle T\rangle + \bar{R}T\ln(P_A)](-a) + [\bar{g}_B^0\langle T\rangle + \bar{R}T\ln(P_B)](-b) \\ & + [\bar{g}_L^0\langle T\rangle + \bar{R}T\ln(P_L)](+l) + [\bar{g}_M^0\langle T\rangle + \bar{R}T\ln(P_M)](+m)\Big\}d\bar{x} \end{aligned}$$

Rearranging the above expression and noting that $d\bar{x} \neq 0$,

$$+ (a\bar{g}^0_{\mathrm{A}}\langle T\rangle + b\bar{g}^0_{\mathrm{B}}\langle T\rangle - l\,\bar{g}^0_{\mathrm{L}}\langle T\rangle - m\bar{g}^0_{\mathrm{M}}\langle T\rangle)$$
$$= -a\bar{R}T\ln(P_{\mathrm{A}}) - b\bar{R}T\ln(P_{\mathrm{B}}) + l\bar{R}T\ln(P_{\mathrm{L}}) + m\bar{R}T\ln(P_{\mathrm{M}}) \tag{3.54}$$

A *standard state Gibbs function of reaction* ΔG^0_r can be written for the reaction as

$$\Delta G^0_r\langle T\rangle = a\bar{g}^0_{\mathrm{A}}\langle T\rangle + b\bar{g}^0_{\mathrm{B}}\langle T\rangle - l\,\bar{g}^0_{\mathrm{L}}\langle T\rangle - m\bar{g}^0_{\mathrm{M}}\langle T\rangle \tag{3.55}$$

which after substituting into Equation (3.54) gives

$$\Delta G^0_r\langle T\rangle = -\bar{R}T[\ln(P_{\mathrm{A}})^a + \ln(P_{\mathrm{B}})^b - \ln(P_{\mathrm{L}})^l - \ln(P_{\mathrm{M}})^m] \tag{3.56}$$

or

$$-\Delta G^0_r\langle T\rangle = \bar{R}T\ln\left[\frac{(P_{\mathrm{A}})^a(P_{\mathrm{B}})^b}{(P_{\mathrm{L}})^l(P_{\mathrm{M}})^m}\right] \tag{3.56a}$$

and

$$\exp\left\{\frac{-\Delta G^0_r\langle T\rangle}{\bar{R}T}\right\} = \frac{(P_{\mathrm{A}})^a(P_{\mathrm{B}})^b}{(P_{\mathrm{L}})^l(P_{\mathrm{M}})^m} \tag{3.56b}$$

A constant pressure *equilibrium constant,* $K_p\langle T\rangle$, for the equilibrium reaction between ideal-gas species

$$a\mathrm{A} + b\mathrm{B} \rightleftarrows l\mathrm{L} + m\mathrm{M}$$

can be defined and written as

$$K_p\langle T\rangle = \frac{(P_i/P_0)^l_{\mathrm{L}}(P_i/P_0)^m_{\mathrm{M}}}{(P_i/P_0)^a_{\mathrm{A}}(P_i/P_0)^b_{\mathrm{B}}} \tag{3.57}$$

where

P_0 = standard state pressure = 1 atm
P_i = equilibrium partial pressure, in atmospheric units

or, for the case in which $P_{0_i} \equiv 1$ atm,

$$K_p\langle T\rangle = \frac{(P_{\mathrm{L}})^l(P_{\mathrm{M}})^M}{(P_{\mathrm{A}})^a(P_{\mathrm{B}})^b} \tag{3.58}$$

Comparing the equilibrium constant expression, Equation (3.58), to minimum Gibbs function, Equation (3.56b), one can show that the standard Gibbs free energy of reaction ΔG^0_r and equilibrium constant K_p are related as

$$\Delta G^0_r\langle T\rangle = -\bar{R}T\ln K_p\langle T\rangle$$

or

$$K_p\langle T\rangle = \exp\{-(\Delta G^0_r\langle T\rangle/\bar{R}T)\} \tag{3.59}$$

EXAMPLE 3.4 Dissociation of stable chemical compounds into active radical species occurs in many high-temperature combustion reactions. For example, diatomic oxygen O_2 can dissociate to form monatomic oxygen O, while monatomic oxygen can recombine and form diatomic oxygen. Consider the equilibrium reaction between O_2 and O:

$$O_2 \overset{P,T}{\rightleftarrows} 2O$$

Using JANAF data calculate (a) $\Delta G_r^0\langle STP\rangle$, cal/g mole; (b) $K_p\langle STP\rangle$; (c) $\log K_p\langle T\rangle$; and (d) the equilibrium mole fractions of O_2 and O at *STP*. Repeat part (d) for 1,000, 1,500, and 2,000K and 1 atm total pressure.

Solution:

1. Gibbs function of reaction from the data in Tables B.20 and B.22 in Appendix B:

$$\Delta G_r^0\langle STP\rangle = 2\Delta G_r^0\langle STP\rangle\Big)_O - \Delta G_r^0\langle STP\rangle\Big)_{O_2} = (2)(55{,}395) - 0$$

a. $= 110{,}790$ cal

2. Equilibrium constant:

$$K_p\langle STP\rangle = \exp\left\{\frac{-\Delta G_r^0\langle STP\rangle}{\bar{R}T^0}\right\} = \exp\left(\frac{-(110{,}790)}{(1.987)(298)}\right) = 5{,}5098 \times 10^{-82}$$

b. $K_p\langle 298\text{K}\rangle = 5{,}5098 \times 10^{-82}$

3. Now, JANAF value for K_p for O based on forming one mole of compound from standard state species:

$$\tfrac{1}{2}O_2 \overset{T}{\rightleftarrows} O \qquad \text{(I)}$$

and

$$\log K_p\Big)_{O_I} = \log K_p\Big)_{O_{JANAF}}$$

Original equilibrium reaction:

$$O_2 \overset{T}{\rightleftarrows} 2O \qquad \text{(II)}$$

and using the data found in Tables B.20 and B.22 in Appendix B:

$$\log K_p\Big)_{O_{II}} = 2\log K_p\Big)_{O_I} = 2\log K_p\Big)_{O_{JANAF}}$$

T	$\log K_p\Big)_I$	$\log K_p\Big)_{II}$	K_{p_0}
298	–40.604	–81.208	6.194×10^{-82}
1,000	–9.807	–19.614	2.432×10^{-20}
1,500	–5.395	–10.790	1.6218×10^{-11}
2,000	–3.178	–6.356	4.4055×10^{-7}

4. Mole fraction of equilibrium concentrations:

$$K_p\langle T\rangle = \frac{(P/P_0)^2}{(P/P_0)_{O_2}} = \frac{(\bar{x}P_0/P_0)_O^2}{(\bar{x}P_0/P_0)_{O_2}} = K_p\langle T\rangle = \frac{\bar{x}_O^2}{\bar{x}_{O_2}}$$

Let $y = x_O$, $1 - y = x_{O_2}$, or

$$K_p\langle T\rangle = \frac{y^2}{1-y}$$

$$y^2 = K_p y - K_p = 0$$

$$y = \frac{-K_p}{2} \pm \frac{1}{2}\sqrt{(K_p)^2 + 4K_p}$$

Solving for y yields

$$y = \frac{-K_p}{2} + \frac{1}{2}\sqrt{(K_p)^2 + 4K_p}$$

and

T	y	$\bar{x}_O$	$\bar{x}_{O_2}$
298	2.49×10^{-41}	0	1.0
1,000	1.56×10^{-10}	1.56×10^{-10}	~1.0
1,500	4.03×10^{-6}	4.03×10^{-6}	0.99999579
2,000	6.64×10^{-4}	6.64×10^{-4}	0.999336

Equilibrium constants for particular reactions (see Figure 3.8) can be calculated from Gibbs free energy of reaction. Values for $\log K_p$ for several compounds are found in Tables B.2–B.24 in Appendix B. In this instance, the equilibrium equations are written using natural elemental species on the left-hand side with a single compound on the right-hand side such as shown below.

$$C_s + 2H_2 \rightleftarrows CH_4$$
$$C_s + O_2 \rightleftarrows CO_2$$
$$\tfrac{1}{2}O_2 \rightleftarrows O$$

EXAMPLE 3.5 The equilibrium reaction for the combustion of carbon and oxygen can be written as

$$C_s + O_2 \overset{P_0,T}{\rightleftarrows} CO_2$$

The corresponding value of the equilibrium constant K_p for this reaction is a function of temperature. For the equilibrium reaction above at 1,000K, evaluate (a) K_p, (b) the derivative $d(\ln K_p/dT)$, and (c) the value of K_p at 1,500K using parts (a) and (b).

Solution:

1. Equilibrium constant:

$$K_p\langle T\rangle = \exp\left\{\frac{-\Delta G^0\langle T\rangle}{\bar{R}T}\right\}$$

and

$$\ln K_p\langle T\rangle = \Delta H_r^0\langle T\rangle - T\Delta S_r^0\langle T\rangle$$

2. Gibbs free energy of reaction:

$$\Delta G_r^0\langle T\rangle = \Delta H_r^0\langle T\rangle - T\Delta S_r^0\langle T\rangle$$

or

$$\ln K_p\langle T\rangle = \frac{-\Delta H^0\langle T\rangle + T\Delta S^0\langle T\rangle}{\bar{R}T}$$

$$\frac{d}{dT}\{\ln K_p\langle T\rangle\} = \frac{d}{dT}\left\{\frac{-\Delta H^0\langle T\rangle}{\bar{R}T}\right\} + \frac{d}{d}\left\{\frac{T\Delta S^0\langle T\rangle}{\bar{R}T}\right\}$$

$$= \frac{-\bar{R}T\dfrac{d\Delta H^0}{dT} - \Delta H^0\dfrac{d\bar{R}T}{dT}}{\bar{R}^2T^2} + \frac{\bar{R}T^2\dfrac{d\Delta S^0}{dT} + T\Delta S^0\dfrac{d\bar{R}T}{dT}}{\bar{R}^2T^2}$$

$$= -\frac{1}{\bar{R}T}\left\{\frac{d\Delta H^0}{dT}\frac{-\Delta H^0}{\bar{R}T^2}\right\} + \frac{1}{\bar{R}}\left\{\frac{d\Delta S^0}{dT} + \frac{\Delta S^0}{\bar{R}T}\right\}$$

3. *TdS* equation:

$$T\Delta S = \Delta H - V\Delta P \text{ since } P_0 = \text{const}$$

or

$$\frac{d}{dT}\{\ln K_p\langle T\rangle\} = \frac{-1}{\bar{R}T}\frac{d}{dT}\{T\Delta S^0\} - \frac{\Delta H^o}{\bar{R}T^2} + \frac{1}{\bar{R}}\frac{d\Delta S^o}{dT} + \frac{\Delta S^0}{\bar{R}T}$$

$$\frac{d}{dT}\{\ln k_p\langle T\rangle\} = \frac{-1}{\bar{R}}\frac{d\Delta S^0}{dT} - \frac{\Delta S^0}{\bar{R}T}\frac{dT}{dT} - \frac{\Delta H^0}{\bar{R}T^2}$$

$$\frac{1}{\bar{R}}\frac{\Delta S^0}{dT} + \frac{\Delta S^0}{\bar{R}T}$$

or

$$\frac{d}{dT}\{\ln K_p\langle T\rangle\} = \frac{-\Delta H_r^0\langle T\rangle}{\bar{R}T^2}$$

and

$$\frac{d}{d(1/T)}\left\{\ln K_p\langle T\rangle\right\} = \frac{-\Delta H_r^0\langle T\rangle}{\bar{R}T}$$

4. For the reaction $C_S + O_2 \rightleftarrows CO_2$:

$$\frac{d}{dT}\left\{\ln K_p\langle T\rangle\right\} = \frac{-\left[(\bar{h}_f^0 + \Delta\bar{h})_{CO_2} - (\bar{h}_f^0 + \Delta\bar{h})_{C_S} - (\bar{h}_f^0 + \Delta\bar{h})_{O_2}\right]}{\bar{R}T^2}$$

5. Thermochemical data found in Appendix B.1:

T	$\bar{h}_f^0)_{CO_2}$	$\bar{h})_{CO_2}$	$\bar{h}_f^0)_{C_S,O_2}$	$\bar{h})_{O_2}$	$\bar{h})_{C_S}$	$\Delta H_r^0\langle T\rangle$
500	–94,054	1,987	0.0	1,455	569	–94,091
1,000	–94,054	7,984	0.0	5,427	2,024	–93,521
1,500	–94,054	14,750	0.0	9,706	5,552	–94,562
K	$\frac{\text{cal}}{\text{gmole}}$	$\frac{\text{cal}}{\text{gmole}}$	$\frac{\text{cal}}{\text{gmole}}$	$\frac{\text{cal}}{\text{gmole}}$	$\frac{\text{cal}}{\text{gmole}}$	cal

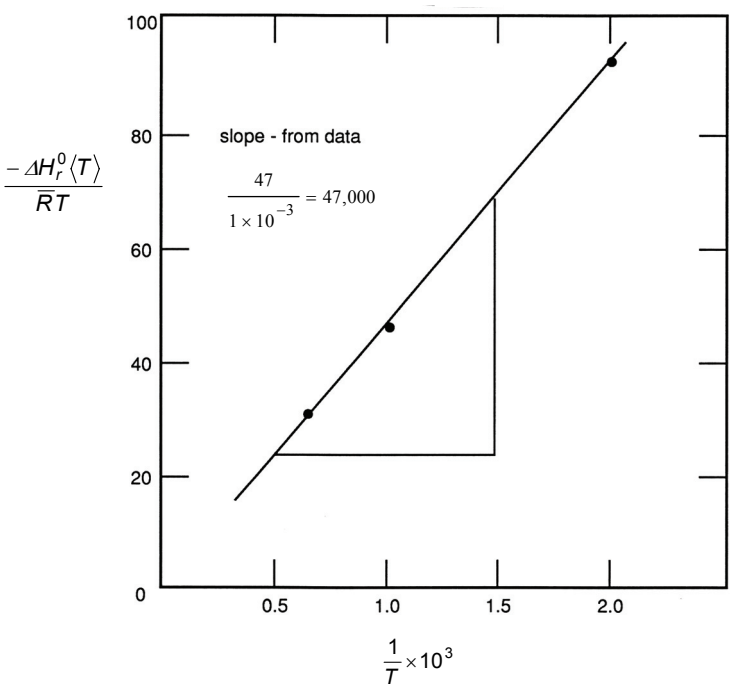

Slope, from van't Hoff's equation = +94,000/(1.986) ≅ 47,331

T	K_p	$\ln K_p$
500	1.8197×10^{41}	95.005
1,000	4.7863×10^{20}	47.617
1,500	6.3241×10^{13}	31.779

The general nature of reactive gas mixtures and chemical equilibrium can best be illustrated using a device termed a van't Hoff's equilibrium box; see Figure 3.9. Inside the box, the species A, B, … , L, and M are assumed to be in an equilibrium state. Energy transfers to and/or from the box as heat and/or work causing temperature and total pressure in the box to change. After any energy transfer, a new state will be established, and it may be necessary to adjust the species concentrations using mass transfer components shown to re-establish equilibrium. Since thermodynamics does not tell the rate of such processes, a complete analysis of the readjustment process and determination of a new equilibrium state, i.e., temperature, pressure, and composition, would require more than an application of first and second laws. Chapter 5 will introduce dynamic, i.e., time factors, or reaction kinetics, necessary to more completely describe chemical equilibrium.

3.6 THE FUEL CELL

The van't Hoff's equilibrium box shown in Figure 3.9 suggests the plausibility of a practical device that can isothermally convert chemical reactants into products while producing power rather than heat transfer. Chemical potential energy stored in a fuel effectively converted directly into electricity would provide an efficient energy conversion process, i.e., a more direct energy conversion system. By using such a reversible electrochemical process, electric power could be produced without the traditional requirement for complex generating facilities being connected to external or internal combustion heat engines. Two familiar examples of controlled chemical reactions used to generate electrical energy rather than heat are: (1) the chemical battery and (2) the fuel cell. The battery contains a fixed amount of chemicals that produce electricity until all reactive material is depleted, whereas a fuel cell will generate electricity continuously as long as reactants are supplied to the unit.

In the 1830s, Sir William Grove experimentally demonstrated that electrolysis of water was a reversible process and that H_2 and O_2 could be reacted in an electrochemical cell, or *fuel cell,* to produce power. Practical fuel cell development began with the work of Francis Bacon in the 1930s but was interrupted by World War II. By 1959, Bacon was able to develop a demonstration 6-kW H_2–O_2 fuel cell. This unit was the forerunner of fuel cells used in the U.S. space program. Many configurations and variations of fuel cells are currently being developed for potential commercial application.

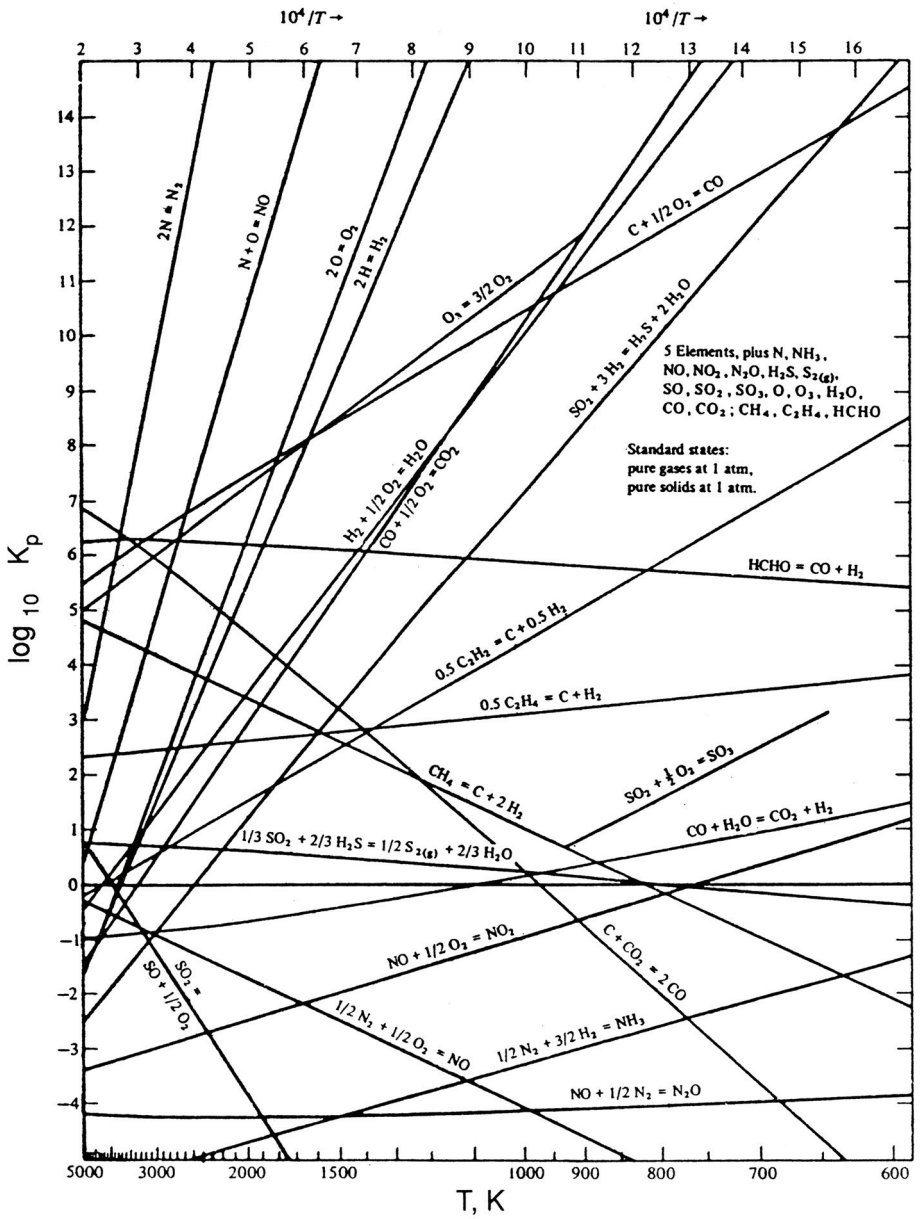

Figure 3.8 Equilibrium constants vs. temperature for various reactions. *Source*: Hottel, Hoyt C. With permission.

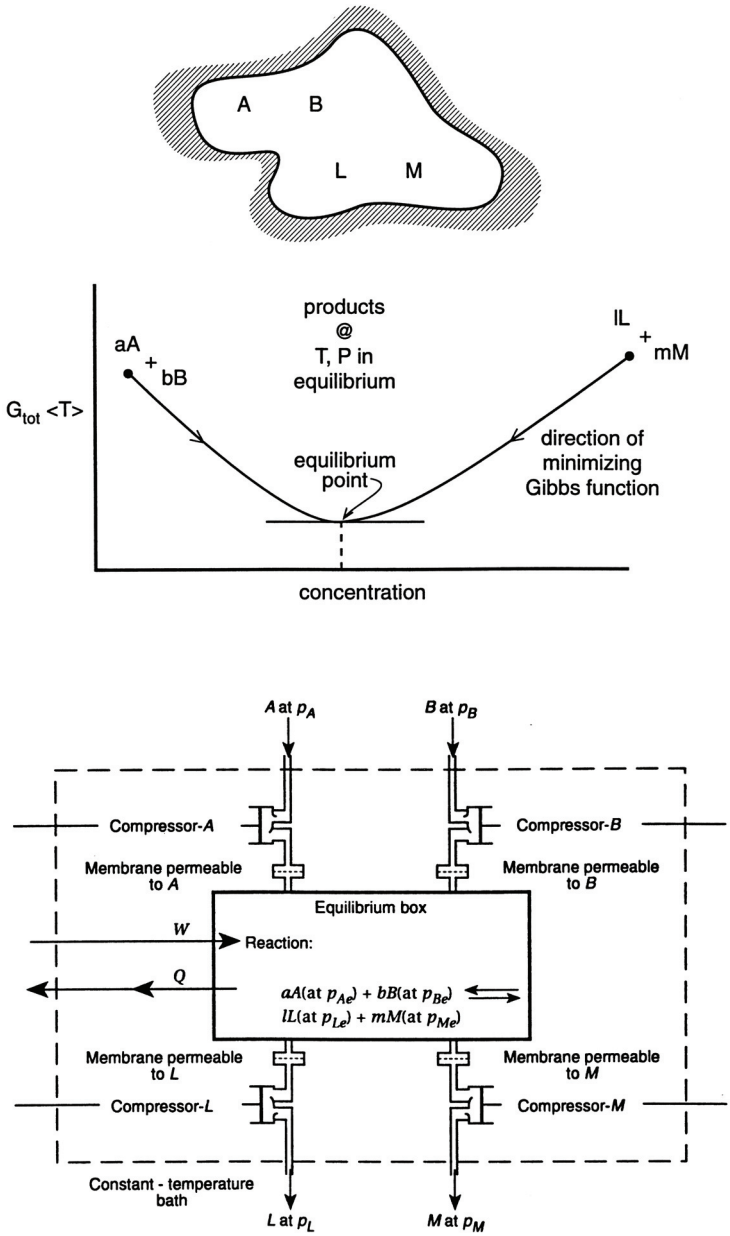

Figure 3.9 van't Hoff's equilibrium box. Adapted from Weber, H. C. and Heissner, H. P., *Thermodynamics for Chemical Engineers*, John Wiley & Sons, New York, 1957.

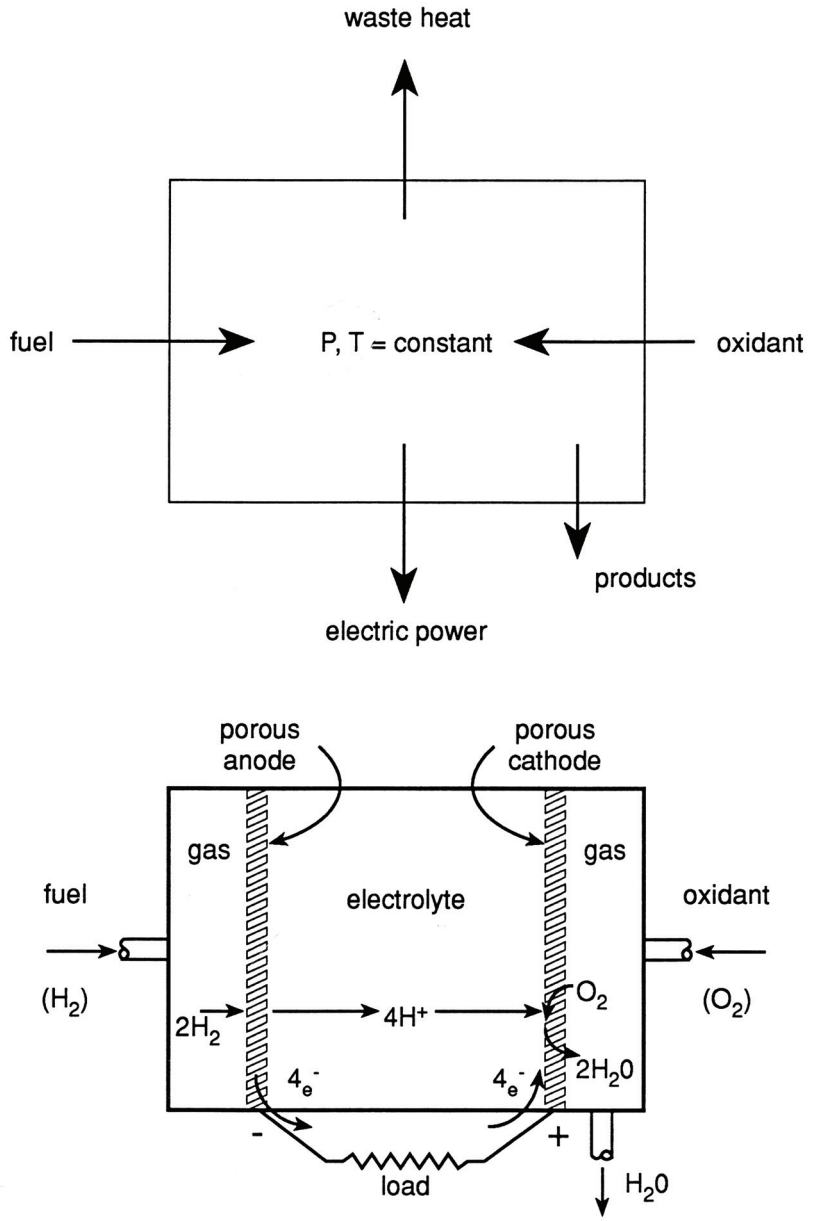

Figure 3.10 The fuel cell.

General operation of a fuel cell, illustrated schematically in Figure 3.10, requires that an easily ionized fuel, such as H_2, be fed continuously to the configuration. Hydrogen is bubbled through a porous electrode where it is reduced at an anode surface. The anode (usually made from a noble metal such as platinum) catalytically causes hydrogen to give up electrons forming hydrogen ions via an anode reaction,

$$2H_2 \rightarrow 4H^+ + 4e^- \tag{3.60}$$

Oxygen must also be continuously fed to the cell but is bubbled through a porous cathode electrode. Hydrogen ions produced at the anode pass through the electrolytic solution (potassium hydroxide as used for example in an alkaline fuel cell) in order to combine with O_2 and electrons at the cathode, producing water via an anode reaction

$$4H^+ + 4e^- + O_2 \rightarrow 2H_2O \tag{3.61}$$

The electrons produced at the anode travel to the cathode through an external circuit and an electrical load thereby producing useful electric power. Individual cells can develop about 1V and anywhere from 100–200W of power/ft^2 of electrode. Voltage can be increased by connecting individual cells in series or power increased by connecting cells in parallel.

Fuel cell thermochemistry drives the electric output. Overall fuel cell reaction is affected by mixture properties, reaction pressure, as well as cell temperature chemistry, and is ideally modeled by changes in Gibbs function. Recall the differential form of the Gibbs function

$$dG = dH - T\,dS - S\,dT = d(U + PV) - T\,dS - S\,dT \tag{3.35}$$
$$dG = dU + VdP + PdV - T\,dS - S\,dT$$

Replacing dU using the First Law relationship for a closed system, Equation 2.29, one obtains the following expression relating the differential amount of work produced to the differential change in Gibbs function as

$$dG = \delta Q - \delta W + VdP + PdV - T\,dS - S\,dT$$

Since fuel cell chemistry occurs at constant temperature and pressure, $dT = 0$ and $dP = 0$. For maximum work the assumption of reversible conditions applies with $\delta Q_{rev} = TdS$ thereby reducing the Gibbs relationship to the following form:

$$dG_{max} = -\delta W_{rev} + PdV$$

When an electrical charge moves through a voltage a fuel cell produces electrochemical work. Electrochemical work is a form of non-expansion work, $dV = 0$, and maximum reversible fuel cell work is thus seen then to be ideally equal to the negative of the change in Gibbs function for the fuel cell equilibrium chemistry or

$$W_{max\text{-}cell} = -\Delta G \tag{3.62}$$

The fuel cell reversible work can be expressed in electrical terms as electrons, with charge n_eF, moving through the cell potential, E, or

$$W_{max\text{-}cell} = -n_eFE \tag{3.63}$$

where

n_e= number of electrons transferred per mole of fuel
F = Faraday's number = charge carried by a mole of electrons
= 96,485 columbs/gmole of electrons
E = voltage difference across the electrodes

Fuel cell thermal efficiency is sometimes expressed using the First Law efficiency terminology for a heat engine, Example 1.1, as

$$\eta_{\text{thermal,cell}} = \frac{\text{Desired energy output}}{\text{Required energy input}} = \frac{\text{Net work (power)}}{\text{Heat addition (flux)}} = \frac{W_{\text{cell}}}{HV} = \frac{n_e FE}{HV} \tag{3.64}$$

The maximum thermal efficiency of a reversible fuel cell can be expressed using the Gibbs function for fuel cell work as

$$\eta_{\text{thermal,cell}} = \frac{-\Delta G_{\text{cell}}}{HV} \tag{3.65}$$

Note that the values predicted for fuel cell performance, i.e., maximum work output and thermal efficiency, will differ when heating value calculations use water in the liquid vs. vapor phase.

The maximum thermal efficiency of a reversible fuel cell can also be expressed using the Gibbs function and the standard state of reaction for fuel cell reaction as

$$\eta_{\text{thermal}} = \frac{\Delta G_{\text{cell}}}{\Delta H_{\text{cell}}} \tag{3.66}$$

EXAMPLE 3.6 Determine the ideal maximum performance characteristics for a 1 atm H_2-O_2 fuel cell assuming reversible operation. Using a Gibbs function analysis for the H_2-O_2 thermochemistry over a temperature range of 300–1400K calculate (a) the ideal maximum reversible work, kJ/gmole H_2; (b) the maximum thermal efficiency, %; and (c) repeat parts (a) and (b) for a Carnot cycle for comparison. Assume that all fuel cell reactive chemical constituents are in the gas phase for this calculation.

Solution:

1. The maximum fuel cell electrochemical work is equal to the negative of the change in Gibbs function for the fuel cell chemistry.

2. Ideal maximum fuel cell performance is based on H_2-O_2 equilibrium thermochemistry

$$H_2 + 0.5O_2 \rightleftarrows H_2O_g$$

3. The change in Gibbs function for the H_2-O_2 fuel cell equilibrium thermochemistry can be expressed in terms of the Gibbs free energy of reaction for the constituents as found in Appendix B as

$$\Delta G_{\text{cell}} = \Delta G_{H_2O_g} - 0.5 \cdot \Delta G_{O_2} - \Delta G_{H_2}$$

4. From Table B.13 for H_2 and Table B.22 for O_2 in Appendix B. $\Delta G = 0$ for all temperatures.

5. From Table B.14 for H_2O_g in Appendix B, ΔG values are listed in the table below:

T	ΔG H_2O_g	W_{cell}	η_{cell}	η_{Carnot}	W_{Carnot}
300	–54.617	228.518*	79.9+	0.7	1.906
400	–53.519	223.923	78.3	25.5	72.889
500	–52.361	219.078	76.6	40.4	115.479
600	–51.156	214.037	74.9	50.3	143.872
700	–49.915	208.844	73.1	57.4	164.153
800	–48.646	203.535	71.2	62.8	179.364
900	–47.352	198.121	69.3	66.9	191.194
1,000	–46.040	192.631	67.4	70.2	200.659
1,100	–44.712	187.075	65.4	72.9	208.402
1,200	–43.371	181.464	63.5	75.2	214.855
1,300	–42.022	175.820	61.5	77.1	220.315
1,400	–40.663	170.134	59.5	78.7	224.996
K	kcal/gmole	kJ/gmole	%	%	kJ/gmole

6. The ideal maximum reversible work is equal to the negative of the change in Gibbs free energy of reaction for the H_2-O_2 equilibrium reaction which in this instance is simply equal to the JANAF Gibbs free energy of reaction for H_2O.

$$W_{\text{rev-fuel cell}} = -\Delta G_{H_2O} = -(-54.617\,\text{kcal/gmole}\,H_2) \cdot (4.184\,\text{kJ/kcal})$$
$$= 228.518\,\text{kJ/gmole}\,H_2{}^*$$

7. Now the ΔH_r for H_2 from Table B.1 in Appendix B is

$$\Delta H_r = -68{,}317 \text{ cal/gmole } H_2$$

8. Maximum thermal efficiency for a reversible gas phase fuel cell can be determined using the Gibbs function and the ΔH_r then as

$$\eta_{\text{thermal, cell}} = \frac{\Delta G_{\text{cell}}}{\Delta H_r} = \frac{-54.617 \text{ kcal/gmole H}_2}{-68.317 \text{ kcal/gmole H}_2} = 0.797 = 79.7\%$$

9. From Example 1.1 the thermal efficiency of a Carnot cycle is found to be

$$\eta_{\text{thermal,Carnotl}} = \frac{W}{Q_H} = 1 - \frac{T_{\text{L}}}{T_H} = 1 - \frac{298}{300} = 0.007 = 0.7\%$$

10. The work output for a Carnot cycle is then equal to

$$W_{\text{cell}} = \eta_{\text{thermal,}Carnot} \cdot HHV = (0.007) \cdot (68.317 \text{ kcal/gmole H}_2) \cdot (4.184 \text{ kJ/kcal})$$
$$= 1.906 \text{ kJ/gmole H}_2$$

11. The Carnot cycle work is plotted below over a temperature range of 300–1400K for comparison to the ideal maximum work curve for the reversible H_2-O_2 fuel cell. Plots are based on results of the analysis tabulated above.

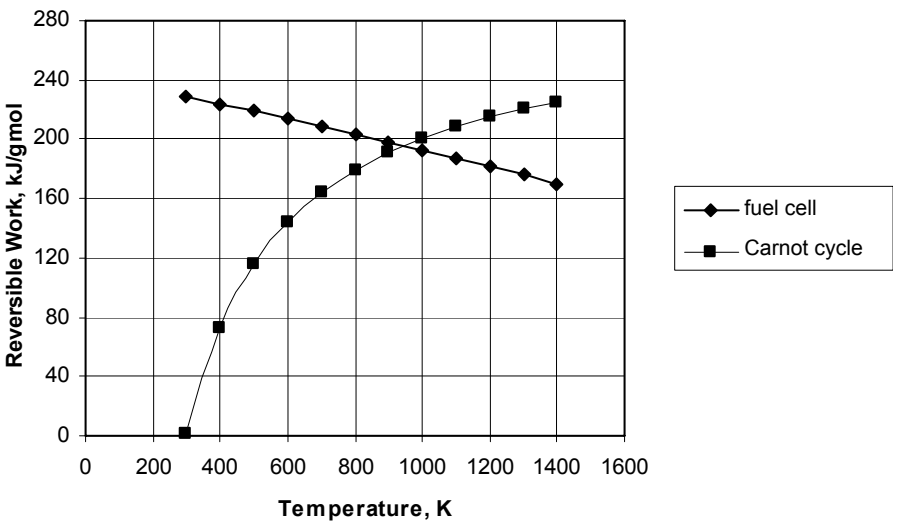

Maximum Reversible Work vs. Absolute Temperature

12. The Carnot cycle thermal efficiency is plotted below over a temperature range of 300–1400K for comparison to the ideal maximum thermal efficiency curve for the reversible H_2-O_2 fuel cell. Plots are based on results of the analysis tabulated above.

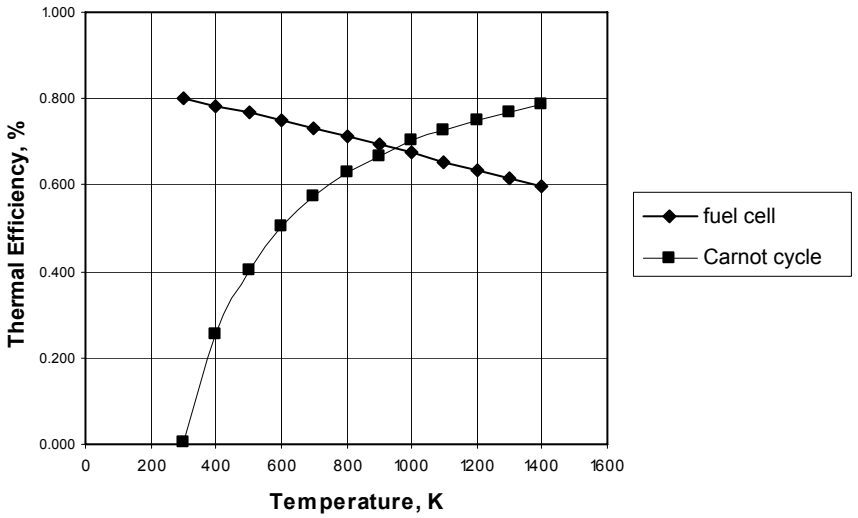

Thermal Efficiency vs. Absolute Temperature

Comments: The H_2-O_2 fuel cell maximum reversible work as well as maximum thermal efficiency both decrease with increasing absolute temperature from their highest values at low temperature, whereas the work and thermal efficiency of a Carnot cycle both increase with temperature from their lowest values at low temperature. Below 950K a H_2-O_2 fuel cell outperforms Carnot cycle conditions while above 950K H_2-O_2 fuel cell underperforms a Carnot cycle under the specifics of this case. Recall that predicted fuel cell performance, i.e., heating value, Gibbs free energy, thermal efficiency, and maximum work output, will differ for conditions when water is in the liquid vs. vapor phase. Fuel cells can operate at temperatures below typical hydrocarbon combustion reaction temperatures. The environmental impacts of a low temperature H_2-O_2 fuel cell would be less than that of conventional combustion-driven heat engines. As such, there should be less waste heat produced, i.e., lower thermal pollution of the environment. In addition, there would obviously be little or none of the high-temperature type combustion pollutants, such as carbon monoxide, unburned hydrocarbons, and nitric oxides, generated by the low-temperature fuel cell operation.

Table 3.3 Ideal Fuel Cell Reactions and Efficiency

REACTANT Half-Cell Reaction Complete-Cell Reaction	Ideal Efficiency[a] (Percent)
HYDRAZINE (aq)	
N_2H_4 (aq) + 4 OH $\rightleftarrows$ N_2 + 4 H_2O + 4 e^-	
N_2H_4 (aq) + O_2 $\rightleftarrows$ N_2 + 2 H_2O	99.4
ETHANOL (aq)	
C_2H_5OH (aq) + 3 H_2O $\rightleftarrows$ 2 CO_2 + 12 H^+ + 12 e^-	
$^{C}{}_2H_5OH$ (aq) + 3 O_2 $\rightleftarrows$ 2 CO_2 + 3 H_2O	97.5
BENZENE	
C_6H_6 + 12 H_2O $\rightleftarrows$ 6 CO_2 + 30 H^+ + 30 e^-	
$^{C}{}_6H_6$ + 7 ½ O_2 $\rightleftarrows$ 6 CO_2 + 3 H_2O	97.2
METHANOL (aq)	
CH_3OH (aq) + H_2O $\rightleftarrows$ CO_2 + 6 H^+ 6 e^-	
CH_3OH (aq) + 1 ½ O_2 $\rightleftarrows$ CO_2 + 2 H_2O	97.1
PROPYLENE	
C_3H_6 + 6H_2O $\rightleftarrows$ CO_2 + 6 H^+ + 30 e^-	
C_3H_6 + 4 ½ O_2 $\rightleftarrows$ 3 CO_2 + 3 H_2O	95.1
ACETYLENE	
C_2H_2 + 4 H_2O $\rightleftarrows$ 2 CO_2 + 10 H^+ + 10 e^-	
C_2H_2 + 2 ½ O_2 $\rightleftarrows$ 2 CO_2 + H_2O	95.0
PROPANE	
C_3H_8 + 4 H_2O $\rightleftarrows$ 3 CO_2 + 20 H^+ + 20 e^-	
C_3H_8 + 5 O_2 $\rightleftarrows$ 3 CO_2 + 4 H_2O	95.0
ETHYLENE	
C_2H_6 + 4 H_2O $\rightleftarrows$ 2 CO_2 + 12 H^+ + 12 e^-	
C_2H_6 + 3 ½ O_2 $\rightleftarrows$ 2 CO_2 + 3 H_2O	94.1
METHANE	
CH_4 + 2 H_2O $\rightleftarrows$ CO_2 + 8 H^+ + 8 e^-	
CH_4 + 2 O_2 $\rightleftarrows$ CO_2 + 2 H_2O	91.9
CARBON MONOXIDE	
CO + H_2O $\rightleftarrows$ CO_2 + 2 H^+ + 2 e^-	
CO + ½ O_2 $\rightleftarrows$ CO_2	90.9
HYDROGEN	
H_2 $\rightleftarrows$ 2 H^+ + 2 e^-	
H_2 + ½ O_2 $\rightleftarrows$ H_2O	83.0

[a]Standard-state free energy of reaction at 25°C divided by standard-state heat of reaction at 25°C.
Source: Austin, L.G., "Electromechanical Theory of Fuel Cells," pp. 22-26, in *Handbook of Fuel Cell Technology*, 1st Edition, Carl Berger, ed., Prentice-Hall, Inc., Englewood Cliffs, NJ, 1968. Adapted by permission of Pearson Education, Inc., Upper Saddle River, NJ.

At the present time a number of fuel cells are actively being pursued for their commercial advantages in the near term. SAE in a crucial Mobility Technology Forum for Technology Planning suggested that the status of getting to market with a new technology could be assisted with a time line of issues (recall Table 1.5) which would identify the effort as falling in one of three distinct phases:

Application phase – present to 3 years
Development phase – 3 to 5 years
Awareness phase – greater than 5 years

Penetration of the fuel cell industry into various segments of the power industry will require configurations having longer operational lifetimes as well as additional new high-temperature fuel cells. Specific advancements such as optimizing various component performance characteristics will result through:

Improvements in electrolyte and electrode performance
Minimizations in losses
Reductions in internal irreversibilities

A majority of present fuel cells are low temperature (<250ºC) H_2-O_2 configurations. Since hydrogen is not available in sufficient quantities as a naturally existing fuel resource, additional reactants are being considered for commercial fuel cell applications. Table 3.3 lists ideal cell reactions and standard state energy conversion efficiencies for several fuels. Efforts are focusing on developing future fuel cells that can operate with air on less expensive hydrocarbon fuels.

Table 3.4 Characteristics of Currently Developed Types of Fuel Cells

Electrolyte	Fuel Cell Type	Operating *T*	Fuel	Electric Efficiency	Power Range
KOH	Alkaline Fuel Cell (AFC)	60–120ºC	Pure H_2	35–55%	<5 kW, niche markets (military, space)
Solid Polymer	Proton Exchange Membrane Fuel Cell (PEMFC)	50–100ºC	Pure H_2 (tolerates CO_2)	35–45%	Automotive, CHP (5–250 kW), portable
Phosphoric Acid	Phosphoric Acid Fuel Cell (PAFC)	~220ºC	Pure H_2 (tolerates CO_2, ~1% CO)	40%	CHP (200 kW)
Lithium and Potassium Carbonate	Molten Carbonate Fuel Cell (MCFC)	~650ºC	H_2, CO, CH_4, other HC (tolerates CO_2)	>50%	200 kW-MW range, CHP and stand-alone
Solid Oxide	Solid Oxide Fuel Cell (SOFC)	~1000ºC	H_2, CO, CH_4, other HC (tolerates CO_2)	>50%	2 kW–MW range, CHP and stand-alone

Source: Gregor Hoogers, ed., *Fuel Cell Technology Handbook*, CRC Press, Boca Raton, FL, 2003. With permission.

Fuel cell characterization can be by many factors including their electrolytes; see Table 3.4.

Fuel cells are an ideal means for generating electrical power and can provide benefit to the stationary power sector due to their:

High efficiency in both part and full load performance
Ability to produce electrical power without combustion or rotating machinery
Capability to function with cogeneration technologies, i.e., power and thermal energy production
Low non-combustion pollution levels

These benefits must be balanced against the limitations including:

Higher capital costs
Complexity of fuel cell components
Shorter service life
Lower reliability of the present day fuel cell
Small power plant capacity in the 50–200 kW range

Three of the fuel cell systems in Table 3.4 presently have been considered for stationary power generation arrangements:

Phosphoric acid (low temperature)
Molten carbonate (intermediate temperature)
Solid oxide (high temperature)

A variety of power plant designs are being investigated that would use these available fuel cell options yet have high thermal efficiencies with favorable economics and meet the objectives for generating systems used in electric power operation. Solid oxide fuel cell power plant configurations with their high temperature operating characteristics, for example, are compatible for use in combined-cycle power plant configurations.

Currently available H_2–O_2 fuel cell arrangements require some important additional major components when being considered for electric power applications. Stationary H_2–O_2 fuel cell power plants will need (1) a separate preprocessor to convert feedstock, such as coal, oil, or natural gas, to provide sufficient purified hydrogen fuel and (2) an inverter to change the DC cell output into an AC current consistent with utility requirements for generated electrical energy output.

Non-hydrogen fuel preprocessing occurs in a reformer where, for example, natural gas or methane reacts with steam to form hydrogen and carbon dioxide as described in detail in Chapter 6.

$$CH_4 + 2H_2O \overset{T,P}{\rightleftarrows} CO_2 + 4H_2$$

There is increased public pressure for an available and applicable vehicular power plant having extremely low emission characteristics. Use of the H_2–O_2 fuel cell, with its non-combustion non-hydrocarbon chemistry, in automotive applications would eliminate many high-temperature pollutants normally associated with today's prime movers.

Several industrial suppliers are currently attempting to produce a fuel cell having appropriate power densities for mobility applications. The proton exchange membrane with its solid polymer electrolyte appears to be the leading contender for automotive usage, in part due to its

Power density being highest among the presently available types of fuel cells
Ability to deliver a large percentage of its power at ambient conditions
Capability to be easily turned on and off
Potential for mass production

Hydrogen for a commercialized market of fuel cell vehicles would need an established hydrogen fuel industry to supply and distribute fuel. In addition, on-board compact storage of pure hydrogen would be necessary either in a pressurized gaseous state, as a cryogenic liquid, in anhydrides, or in hydrogen containing fuel reforming compounds. With relatively high costs of hydrogen production, lack of any credible fuel distribution arrangement, and on-board vehicle hydrogen storage restrictions, hydrogen will probably be generated in the near term for the fuel cell from hydrogen-rich fuels. On-board reforming of hydrogen-rich fuels — such as alcohols; methanol and ethanol, or gaseous fuels; and methane and natural gas — will produce the required hydrogen for transportation fuel cell operation in the near term.

A more comprehensive coverage of the subject of fuel cells and their applications can be found in the technical literature.

PROBLEMS

3.1 An ideal-gas mixture has a molecular weight of 40 kg/kg mole and a constant-pressure specific heat of 0.525 kJ/K kg. At 480-kPa absolute pressure and 14.5-m^3 volume, the temperature of the gas is 422K. Determine for the mixture (a) the specific gas constant R, kJ/K·kg; (b) the constant-volume specific heat C_v, kJ/kg·K; (c) the specific heat ratio γ, and (d) the mass of gas in the cylinder, kg.

3.2 Air initially at 14.7 psi and 77°F is isentropically compressed until the original volume is reduced by 90%. Using constant specific heats, find (a) the final temperature, °F; and (b) the final pressure, psi. Repeat parts (a) and (b) using the isentropic tables for air based on variable specific heat analysis found in Example 3.2.

3.3 The modern compression-ignition engine injects fuel into hot compressed air. Fuel ignition occurs by contacting air that has been raised above the self-ignition temperature of the fuel. Consider air initially at 101 kPa and 30°C and a fuel with a self-ignition temperature of 600°C. Assuming an isentropic compression process for air and using constant specific heat analysis, find (a) the final pressure, kPa; (b) the final specific volume, m^3/kg; and (c) the required compression work, kJ/kg. Repeat parts (a)–(c) using the isentropic tables for air based on variable specific heat analysis found in Example 3.2.

3.4 An axial compressor is used to compress a mixture of methane, CH_4, and ethylene, C_2H_4. The mixture of 50% methane on a molar basis and compressor inlet conditions are 101 kPa, 21°C, and 0.012 m/sec. Discharge conditions from the unit

are 550 kPa and 163°C. For these conditions and assuming constant specific heats, find (a) the mixture mass flow rate, kg/sec; (b) the ideal isentropic discharge temperature; (c) the entropy increase across the compressor, kJ/K·kg; (d) the actual compressor power, kW; and (e) the compressor adiabatic efficiency, i.e., isentropic work/actual work, kW.

3.5 Gasoline can be approximated in many combustion calculations using *n*-octane. Using the JANAF data for C_8H_{18} found in Appendix B, determine the specific heat ratio at 25°C for (a) stoichiometric fuel-air mixture, (b) a fuel-rich mixture having an equivalence ratio of 0.55, and (c) a fuel-lean mixture having an equivalence ratio of 0.55. Repeat parts (a)–(c) for an average temperature between 25°C and the isentropic compression temperature for an 8:1 compression ratio.

3.6 Repeat 3.5 using methanol, CH_3OH, instead of C_8H_{18}.

3.7 Consider the reaction of formation of carbon dioxide from natural elemental species. For reaction at *STP*, determine (a) the entropy of reaction, Btu/lbmole·°R; (b) the Gibbs function of reaction, Btu/lbmole; and (c) the Hemholtz function of reaction, Btu/lbmole.

3.8 Repeat Problem 3.7 for a reaction temperature at 1,800°R.

3.9 Consider the ideal *STP* stoichiometric combustion reaction of acetylene. For these conditions, determine (a) the change in enthalpy for the reaction, kJ/kgmole; (b) the change in entropy for the reaction, kJ/kgmole·K; and (c) the change in Gibbs free energy for the reaction, kJ/kgmole.

3.10 Consider the ideal *STP* stoichiometric combustion reaction of methane. For these conditions, determine (a) the change in internal energy for the reaction, Btu/lbmole; (b) the change in entropy for the reaction, Btu/lbmole·°R; and (c) the change in Hemholtz function for the reaction, Btu/lbmole.

3.11 Consider the one-atmospheric equilibrium reaction

$$N_2 \overset{P_0,T}{\rightleftarrows} 2N$$

at 4,000K. For this condition, determine (a) the equilibrium mole fractions of N_2 and N, %; (b) the mixture Gibbs function, Btu/lbmole; and (e) whether this condition gives a minimum value to the Gibbs function.

3.12 Repeat Problem 3.11 using O_2 instead of N_2.

3.13 Many combustion processes involve products of combustion at temperatures not in excess of 2000°F. Often, the effects of dissociation of stable species are ignored for these temperatures. Is this assumption truly justified for (a) O_2, (b) N_2, (c) CO_2, or (d) H_2O?

3.14 H_2 can be commercially generated by oxidizing CO using steam via the water-gas reaction

$$H_2O_g + CO \overset{T,P}{\rightleftarrows} H_2 + CO_2$$

For this reaction, (a) write an expression for K_p for the equilibrium reaction in terms of the partial pressures of H_2, CO_2, CO, and H_2O; (b) evaluate $\log 10 K_p\langle T\rangle$ for the reaction using JANAF data for an equilibrium temperature of 2,000K; and (c) find the mole fractions of H_2, CO_2, CO, and H_2O at 2,000K using parts (a) and (b).

3.15 Hydrogen can be produced by steam-cracking methane according to the reaction

$$CH_4 + 2H_2Og \overset{T,P}{\leftrightarrows} CO_2 + 4H_2$$

An initial mixture at 1-atm total pressure and 800K consists of 50% excess steam. Determine (a) the equilibrium constant for the conversion and (b) the equilibrium mole fractions of CH_4, H_2O, CO_2, and H_2. Repeat part (b) for (c) a temperature of 1,200K and (d) a total pressure of 5 atm.

3.16 The equilibrium composition for CO_2 dissociation to form CO and O_2 at high temperatures can be described by the reaction

$$2CO_2 \overset{T,P}{\rightleftarrows} 2CO + O_2$$

For this equilibrium reaction, (a) write the JANAF equilibrium reaction and K_p for CO in terms of appropriate partial pressures; (b) repeat part (a) for CO_2; and (c) show that, for the equilibrium reaction above,

$$\log K_p\big)_{\text{reaction}} = \log K_p\big)_{CO} - \log K_p\big)_{CO_2}$$

and (d) calculate the equilibrium constant K_p, for $T = 3{,}800$K.

3.17 Solid carbon reacts with stoichiometric air at 600K and 1-atm total pressure. Assume ideal complete combustion, and determine the adiabatic flame temperature. Repeat the calculation assuming that the products consist only of CO, CO_2, O_2, and N_2.

3.18 Methane, CH_4, reacts with 90% theoretical air in a steady-flow reactor. Reactants enter at 1-atm pressure and 77°F. Assuming complete ideal combustion, determine the adiabatic flame temperature for a constant-pressure combustion process. Repeat the calculation, but assume that CO_2 and H_2O dissociation satisfies the equilibrium reaction

$$H_2O_g + CO \overset{T,P}{\rightleftarrows} H_2 + CO_2$$

Furthermore assume that no O_2 exists in the product composition.

3.19 A fuel cell thermochemical efficiency can be defined in terms of the Gibbs function of reaction and the enthalpy of reaction of the cell equilibrium reaction as

$$\eta_{FC} = \frac{\Delta G}{\Delta H}$$

Consider the fuel cell reaction $H_2 + 0.5O_2 \rightleftarrows H_2O$ at *STP* conditions, and calculate (a) the enthalpy of reaction, kJ/kgmole; (b) the Gibbs function of reaction, kJ/kgmole; and (c) the fuel cell efficiency.

3.20 Repeat Problem 3.21 for a fuel cell reaction of 800K.

3.21 Repeat Problem 3.21 for the *STP* fuel cell reaction $CO + 0.5O_2 \rightleftarrows CO_2$.

3.22 Repeat Problem 3.21 for the *STP* fuel cell reaction

$$CH_4 + 2O_2 \rightleftarrows CO_2 + 2H_2O$$

4

Fluid Mechanics

4.1 INTRODUCTION

In the first three chapters, basic thermochemical principles were developed and used to describe the ideal energetics of various combustion processes. Several important concepts were introduced, including the conservation of atomic species in reactive mixtures, standard-state heats of formation for reactive species, and the ideal heat release rates for solid, liquid, or gaseous fuels using both frozen and equilibrium product species in chemical reactions. Many facets of combustion cannot be inferred from a thermodynamic analysis of chemical energy conversion alone. For example, most high-temperature chemical reactions in combustion involve fluid motion and, thus, the necessity to understand basic fluid mechanics is obvious. In the following chapter, conservation relationships for mass and momentum, as well as energy, will be written for one-dimensional reactive fluid flow in which the particular energy released by exothermic reactions will influence the fluid properties of the flow. An extensive investigation of these three conservation equations is the subject of *gas dynamics*, which is a separate engineering area of study in and of itself. In this chapter analysis of one-dimensional chemically reactive gas dynamic relations will theoretically indicate that two distinctly different combustion wave propagation phenomena can occur. The characteristics of these two classic results will be treated in detail. An understanding of this ideal case will provide some insight into real combustion processes that occur in internal combustion engines as well as in gas turbine combustors.

4.2 BASIC CONSERVATION EQUATIONS

The concept of wave propagation is common to a variety of engineering disciplines and is important in the consideration of light physics, sound wave propagation, and shock wave formation. Characteristic analysis of an actual combustion wave propagating both spatially and over time through a reactive medium, in most instances, can be quite complex. A moving reaction zone, in general, would be propagating in an unsteady three-dimensional translation through a non-homogeneous medium. One important case is that

in which the reaction zone, or *flame front*, passes through a homogeneous premixed fuel-air mixture. The passing reaction wave in such a case would separate an unburned zone ahead of the wave front from a burned product zone behind. The actual moving region of separation is quite small, on the order of several millimeters and, to a good approximation, can be thought of as a line of discontinuity separating unburned and burned gases (Figure 4.1).

The physics associated with a one-dimensional flame front propagation can be formulated using either differential or integral calculus. Furthermore, differential or integral forms of the conservation equations can be expressed using particle, i.e., *Lagrangian,* or field, i.e., *Eulerian,* mathematics. Recall that, in Lagrangian analysis, the characteristics of a fixed mass, frequently referred to as a control mass or closed system, are described for specific material undergoing a change of state as well as location. In Eulerian analysis, characteristics of a specified volume in space, called a control volume, or open system are described in terms of a fluid flux undergoing a change of state and position.

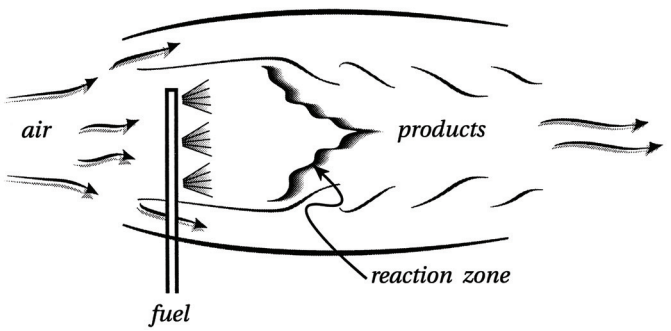

(a)

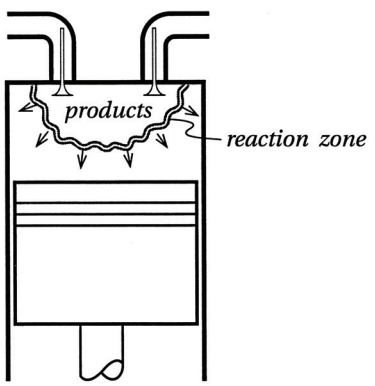

(b)

Figure 4.1 Combustion zone fluid motion: (a) continuous burner flame zone; (b) internal combustion engine flame zone.

Consider the non-accelerating one-dimensional planar reaction zone shown in Figure 4.2. In Figure 4.2a, the actual process is seen to be an unsteady wave propagation moving from left to right as time proceeds. In Figure 4.2b, a simple coordinate transformation changes the process to that of a stationary wave front through which fluid passes.

The following assumptions will be made in the analysis of the classic one-dimensional flame front propagation problem:

1. Differential formulation
2. One-dimensional stationary wave front
3. Steady-state and steady-flow conditions
4. Inviscid flow
5. Irreversible process
6. Stationary discontinuity at the wave front
7. Nonreactive homogeneous ideal-gas mixture on either side of wave

From physics, for a fixed total mass M, the conservation of mass can be stated as

$$M = \text{const} \quad \text{kg (lbm)} \tag{4.1}$$

or, for the control mass *CM,*

$$\left.\frac{DM}{Dt}\right)_{CM} = 0 \quad \frac{\text{kg}}{\text{sec}}\left(\frac{\text{lbm}}{\text{sec}}\right) \tag{4.2}$$

Written in terms of a Field control volume, CV, approach, the above conservation of mass statement can also be expressed as

$$\left.\frac{DM}{Dt}\right)_{CM} = \left.\frac{\partial M}{\partial t}\right)_{CV} + \Sigma \dot{m}_i)_{CV} = 0 \tag{4.2a}$$

where

$$\left.\frac{\partial M}{\partial t}\right)_{CV} = \text{local change of mass in } CV \text{ with time}$$

$$\Sigma \dot{m}_i)_{CV} = \text{net mass efflux out of (+) into (−) } CV$$

For steady-state, steady-flow, Equation (4.2a) reduces to

$$\cancel{\left.\frac{\partial M}{\partial t}\right)_{CV}} + \Sigma \dot{m}_i)_{CV} = 0 \tag{4.2b}$$

which, for the one-dimensional case with uniform properties in regions 1 and 2, becomes

$$\dot{m}_1 = \rho_1 A_1 V_1 = \rho_2 A_2 V_2 = \dot{m}_2 \qquad \text{kg/sec (lbm/sec)} \tag{4.3}$$

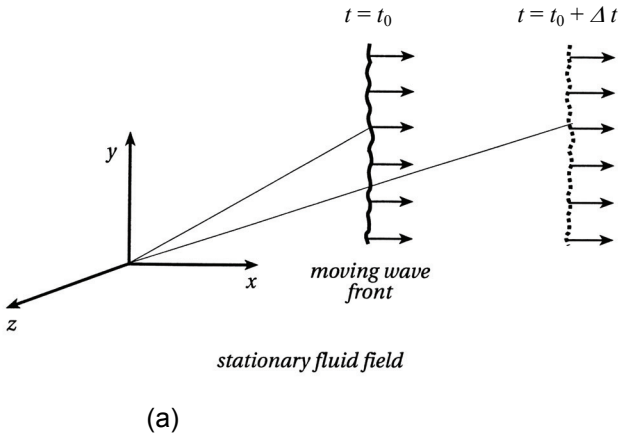

(a)

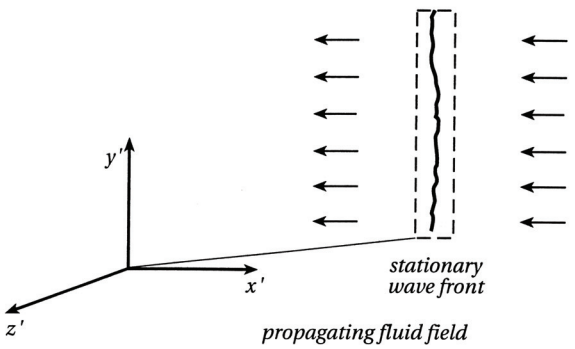

(b)

Figure 4.2 One-dimensional non-accelerating wave front: (a) propagating wave description; (b) stationary wave description.

Defining a mass flow rate per unit area, G, one obtains

$$G_1 = \rho_1 V_1 = \rho_2 V_2 = G_2 \qquad \text{kg/sec}\cdot\text{m}^2 \quad (\text{lbm/sec}\cdot\text{ft}^2) \tag{4.4}$$

Again, from physics, the conservation of momentum for a fixed total mass M is given by

$$\Sigma \vec{F} = M\vec{a})_{CM} = \frac{D}{Dt}\left\{M\vec{V}\right\}\Big)_{CM} = M\frac{D\vec{V}}{Dt}\Big)_{CM} + \vec{V}\frac{DM}{Dt}\Big)_{CM} = M\frac{D\vec{V}}{Dt}\Big)_{CM} \tag{4.5}$$

or expressed using a Field approach for forces in the x direction Equation (4.5) becomes

$$\Sigma F_x = \frac{DMV_x}{Dt}\Big)_{CM} = \frac{\partial MV_x}{\partial t}\Big)_{CV} + \Sigma_i\left(\dot{m}_x V_x\right)_i\Big)_{\text{CV}} \qquad \text{N (lbf)} \tag{4.5a}$$

where

$$\left.\frac{\partial MV_x}{\partial t}\right)_{CV} = \text{local change in } CV \text{ of } x-\text{momentum with time}$$

$$\Sigma \dot{m}_x V_x)_{CV} = \text{net } x-\text{momentum flux out of } (+) \text{ into } (-)\ CV$$

For steady-state, steady-flow conditions,

$$\Sigma F_x = \cancel{\left.\frac{\partial MV_x}{\partial t}\right)_{CV}} + \Sigma_i \left(\dot{m}_x V_x\right)_i)_{CV} \tag{4.5b}$$

and for inviscid flow, the conservation of momentum, assuming only normal pressure forces, Equation (4.5b) becomes

$$g_0\left(P_1 A - P_2 A\right) = -\left(\rho_1 A V_1\right)V_1 + \left(\rho_2 A V_2\right)V_2 \tag{4.6a}$$

$$g_0 P_1 + \rho_1 V_1^2 = g_0 P_2 + \rho_2 V_2^2 \tag{4.6b}$$

or

$$P_1 + \frac{G_1^2}{g_0 \rho_1} = P_2 + \frac{G_2^2}{g_0 \rho_2} \qquad \frac{\text{N}}{\text{m}^2}\left(\frac{\text{lbf}}{\text{ft}^2}\right) \tag{4.7}$$

Note the use of g_0 to express mass and weight in consistent dimensions and units.

EXAMPLE 4.1 The speed of sound c, through an undisturbed ideal-gas medium, can be determined using the one-dimensional formulation for compressible wave propagation. Sound can be modeled as a small-amplitude isentropic wave phenomenon. For the condition shown below, write (a) the appropriate continuity equation, (b) the momentum equation, (c) the differential equation for sonic velocity using parts (a) and (b); and (d) show that an ideal gas $c^2 = \gamma R T g_0$.

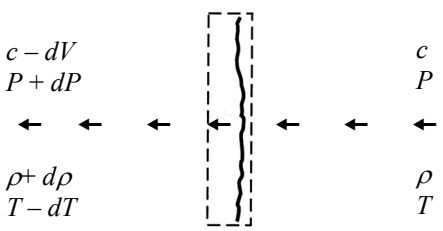

Stationary Wave

Solution:

1. Continuity:

$$G = \rho_1 V_1 = \rho_2 V_2$$

$$\rho c = \left(\rho + d\rho\right)\left(c - dV\right)$$

$$\rho c = \rho c + c\, d\rho - \rho\, dV \cancel{- d\rho\, dV}$$

or

a. $c\,d\rho = +\rho\,dV$

2. Momentum:

$$g_0\left(P_2 - P_2\right) = \rho_1 V_1^2 - \rho_2 V_2^2$$
$$g_0\left[\left(P + dP\right) - P\right] = \rho c^2 - \left(\rho + d\rho\right)\left(c - dV\right)^2$$
$$g_0 dP = \rho c^2 - \left(\rho + d\rho\right)\left(c^2 - 2c\,dV + dV^2\right)$$
$$g_0 dP = \rho c^2 - \rho c^2 + 2\rho c\,dV - c^2\,d\rho + 2c\,d\rho\,dV$$

b. $g_0 dP = 2\rho c\,dV - c^2\,d\rho$

3. Combining items 1 and 2:

$$g_0 dP = 2c\left(c\,d\rho\right) - c^2\,d\rho = c^2\,d\rho$$
$$c^2 = g_0\frac{dP}{d\rho}$$

and for small-amplitude sound waves where entropy is conserved

c. $c^2 = g_0\left.\frac{\partial P}{\partial \rho}\right)_{s=c}$

4. Sonic velocity in an ideal gas:

State	Process
$P = \rho RT$	$P\rho^{-\gamma} = \text{const} = c_1$

then, expressing $P = P\langle\rho\rangle$ using the process relationship,

$$c^2 = g_0\frac{\partial}{\partial\rho}\left[c_1\rho^{\gamma}\right]_{s=c} = g_0\left[\gamma c_1\rho^{\gamma-1}\right]$$
$$c^2 = g_0\gamma\left[P\rho^{-\gamma}\right]\rho^{\gamma-1}$$

substituting from the ideal-gas law, the equation becomes

$$= \gamma g_0\,P/\rho$$
$$c^2 = \gamma g_0 RT$$

or

$$c = \left[\gamma RTg_0\right]^{1/2}$$

In addition to the conservation of mass and momentum, the conservation of energy is needed before a discussion of the reactive wave propagation process can be considered in detail. For a fixed total mass M, the conservation of energy is equal to

$$\left.\frac{DE}{Dt}\right)_{CM} = \dot{Q} - \dot{W} \qquad \text{kJ (Btu)} \tag{4.8}$$

and, in Field CV terminology,

$$\left.\frac{DE}{Dt}\right)_{CM} = \left.\frac{\partial E}{\partial t}\right)_{CV} + \Sigma_i \dot{m}_i e_i \Big)_{CV} = \dot{Q} - \dot{W} \qquad \text{kW}\left(\frac{\text{Btu}}{\text{hr}}\right) \tag{4.9}$$

and

$$\left.\frac{\partial E}{\partial t}\right)_{CV} = \text{local change in } CV \text{ energy with time}$$
$$\Sigma \dot{m}_i e_i \Big)_{CV} = \text{net energy flux out of (+) into (–) } CV$$

Again, for steady-state, steady-flow conditions,

$$\cancel{\left.\frac{\partial E}{\partial t}\right)_{CV}} + \dot{m}_2 e_2 - \dot{m}_1 e_1 = \dot{Q} - \dot{W} \tag{4. 10a}$$

or

$$\dot{Q} - \dot{W} = \dot{m}_2\left[u_2 + \frac{P_2}{\rho_2} + \frac{V_2^2}{2g_0} + \frac{g}{g_0} z_2\right] - \dot{m}_1\left[u_1 + \frac{P_1}{\rho_1} + \frac{V_1^2}{2g_0} + \frac{g}{g_0} z_1\right] \tag{4.10b}$$

Assuming one-dimensional flow and applying conservation of mass equation (4.3), Equation (4.10b) becomes

$$u_1 + \frac{P_1}{\rho_1} + \frac{V_1^2}{2g_0} + {}_1q_2 = u_2 + \frac{P_2}{\rho_2} + \frac{V_2^2}{2g_0} + {}_1w_2 \tag{4.11}$$

or

$$h_1 + \frac{V_1^2}{2g_0} + {}_1q_2 = h_2 + \frac{V_2^2}{2g_0} + {}_1w_2 \qquad \frac{\text{kJ}}{\text{kg}}\left(\frac{\text{Btu}}{\text{lbm}}\right) \tag{4.12}$$

Equation (4.12) relates changes in flow properties to heat addition, i.e., energy released by combustion. Table 4.1 summarizes the conservation equations for the one-dimensional wave propagation process.

Table 4.1 1D Diabatic Flow Conservation Equations

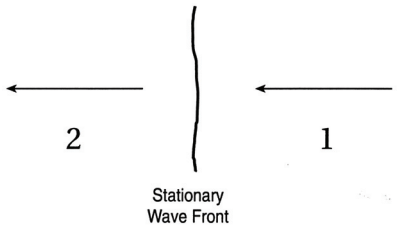

Conservation of mass:

$$G_1 = \rho_1 V_1 = \rho_2 V_2 = G_2$$

Conservation of momentum:

$$P_1 + \frac{G_1^2}{g_0 \rho_1} = P_1 + \frac{\rho_1 V_1^2}{g_0} = P_2 + \frac{\rho_2 V_2^2}{g_0} = P_2 + \frac{G_2^2}{g_0 \rho_2}$$

Conservation of energy:

$$h_1 + \frac{G_1^2}{2g_0\rho_1} + {}_1q_2 = h_1 + \frac{V_1^2}{2g_0} + {}_1q_2 = h_2 + \frac{V_2^2}{2g_0} + {}_1w_2 = h_2 + \frac{G_2^2}{2g_0\rho_2} + {}_1w_2$$

EXAMPLE 4.2 The basic conservation relationships developed in this chapter can be used to predict the local static and corresponding stagnation properties for one-dimensional homogeneous fluid flow. Recall that the local stagnation state is the condition achieved if the fluid at that point is isentropically brought to rest. For these conditions, determine an expression for the ratio of the stagnation to local values for (a) T_0/T, (b) ρ_0/ρ, (c) P_0/P. For sonic conditions in a flow, the above expressions reduce to the critical ratios. Determine the critical values for parts (a) and (c) in terms of sonic parameters T^*, P^*, ρ^*.

Solution:

1. Energy equation:

$$h_1 + \frac{V_1^2}{2g_0} + {}_1q_2 = h_2 + \frac{V_2^2}{2h_0} + {}_1w_2$$

Let state 1 ≡ the stagnation state and state 2 = the arbitrary state.

$$h_0 = h + \frac{V^2}{2g_0}$$

Assume ideal-gas mixture with constant specific heats.

$$T_0 - T = \frac{V^2}{2g_0 C_p}$$

where

$$C_p - C_v = R \qquad C_p / C_v = \gamma$$

and

$$C_p = \frac{R\gamma}{\gamma - 1}$$

$$T_0 - T = \frac{V^2(\gamma - 1)}{2g_0 R\gamma} = \frac{V^2(\gamma - 1)T}{2g_0 R\gamma T}$$

but from Example 4.1

$$c = \sqrt{g_0 R\gamma T}$$

and

$$T_0 - T = \frac{V^2(\gamma - 1)T}{2c^2}$$

Mach number, $N_m \equiv V/c$,

or

$$T_0 - T = N_m^2\left(\frac{\gamma - 1}{2}\right)T$$

$$\frac{T_0}{T} - 1 = N_m^2\left(\frac{\gamma - 1}{2}\right)$$

a. $$\frac{T_0}{T} = 1 + \left(\frac{\gamma - 1}{2}\right)N_m^2$$

2. Isentropic process, ideal-gas mixture:

$$\frac{P}{\rho^\gamma} = \text{const}$$

or

$$\frac{P}{\rho^\gamma} = \frac{P_0}{\rho_0^\gamma}$$

and

$$\frac{P}{\rho} = RT$$

$$\frac{P_0}{P} = \left(\frac{\rho_0}{\rho}\right)^{\gamma} = \left(\frac{RT}{P}\right)^{\gamma}\left(\frac{P_0}{RT_0}\right)^{\gamma}$$

$$\frac{P_0}{P} = \left(\frac{T}{T_0}\right)^{\gamma}\left(\frac{P_0}{P}\right)^{\gamma}$$

$$\left(\frac{P_0}{P}\right)^{1-\gamma} = \left(\frac{T}{T_0}\right)^{\gamma}$$

$$\left(\frac{P_0}{P}\right) = \left(\frac{T}{T_0}\right)^{\gamma/(1-\gamma)} = \left(\frac{T_0}{T}\right)^{\gamma/(\gamma-1)}$$

b. $$\left(\frac{P_0}{P}\right) = \left[1+\left(\frac{\gamma-1}{2}N_m^2\right)\right]^{\gamma/(\gamma-1)}$$

$$\frac{\rho_0}{\rho} = \left(\frac{P_0}{P}\right)^{1/\gamma} = \left(\frac{T_0}{T}\right)^{1/(\gamma-1)}$$

c. $$\frac{\rho_0}{\rho} = \left[1+\left(\frac{\gamma-1}{2}\right)N_m^2\right]^{1/(\gamma-1)}$$

3. Critical ratios, sonic conditions:

Let

$$V = c$$
$$P = P*$$
$$T = T*$$
$$\rho = \rho*$$

i.e., $N_m = 1.0$.

$$\frac{T_0}{T*} = \left[1+\left(\frac{\gamma-1}{2}\right)\right] = \frac{\gamma+1}{2}$$

or

d. $$\frac{T*}{T_0} = \left(\frac{2}{\gamma+1}\right)$$

e. $$\frac{P*}{P_0} = \left(\frac{2}{\gamma+1}\right)^{\gamma/(\gamma-1)}$$

f. $$\frac{\rho^*}{\rho_0} = \left(\frac{2}{\gamma+1}\right)^{1/(\gamma-1)}$$

Comments: One-dimensional isentropic flow for an ideal gas is seen to be a function of γ and Mach number. These dimensionless equations can be easily programmed or are tabulated as a function of N_m in sources such as the Gas Tables for use in analysis.

4.3 THE RAYLEIGH LINE

As indicated above, continuity, momentum, and energy equations are the primary gas dynamic relationships that can be used to further investigate such subjects as subsonic and supersonic compressible flow, converging-diverging nozzle performance, and normal shock wave propagation. In this chapter, interest will be limited to the problem in which heat release (combustion) and compressible flow (wave propagation) are coupled. Furthermore, the treatment will be restricted to conditions for which the following assumptions are made:

1. One-dimensional discontinuous compressible flow
2. Irreversible but inviscid flow
3. Steady stationary combustion zone (wave front)
4. Uniform properties upstream and downstream from reaction
5. Ideal gas with constant-mixture molecular weight

Two terms come into use with the general subject of reactive flow: *adiabatic* and *diabatic* flow. In *adiabatic* flow, there is no heat transfer between the fluid and surroundings, while in *diabatic* flow, heat transfer is allowed to occur. A combustion wave is an irreversible wave phenomenon with local heat release and thus can be thought of as a particular type of diabatic flow.

In one-dimensional frictionless flow with heat transfer, a relationship can be written that combines the continuity and momentum equations. The resulting expression is termed the *Rayleigh line,* and its solution often is displayed on either *P–v* or *T–s* coordinates. Recall the continuity equation and momentum relationships developed earlier and stated again as

Continuity:

$$\rho_1 V_1 = \rho_2 V_2 = G \quad \frac{\text{lbm}}{\text{ft}^2 \cdot \text{sec}}\left(\frac{\text{kg}}{\text{m}^2 \cdot \text{sec}}\right) \tag{4.4}$$

Momentum:

$$P_1 + \frac{G_1^2}{g_0 \rho_1} = P_2 + \frac{G_2^2}{g_0 \rho_2} \quad \frac{\text{N}}{\text{m}^2}\left(\frac{\text{lbf}}{\text{ft}^2}\right) \tag{4.7}$$

Combining Equations (4.4) and (4.7) yields

$$P_1 - P_2 = \frac{1}{g_0}\left(\frac{G_2^2}{\rho_2} - \frac{G_1^2}{\rho_1}\right) \tag{4.13a}$$

$$P_1 - P_2 = \frac{G^2}{g_0}\left(\frac{1}{\rho_2} - \frac{1}{\rho_1}\right) \tag{4.13b}$$

or

$$\frac{P_1 - P_2}{\left(1/\rho_2 - 1/\rho_1\right)} = \frac{G^2}{g_0} \tag{4.13c}$$

$$\frac{P_1 - P_2}{1/\rho_1 - 1/\rho_2} = \frac{P_1 - P_2}{v_1 - v_2} = -\frac{G^2}{g_0} \tag{4.14}$$

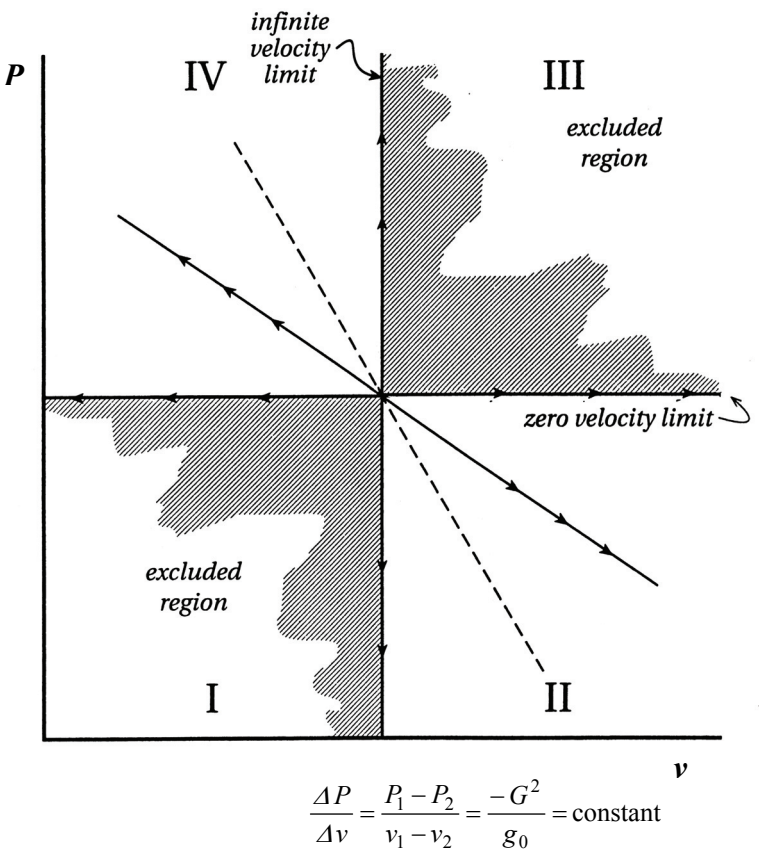

Figure 4.3 Rayleigh flow *P*–*v* diagram.

Equation (4.14) is called the *Rayleigh line.* For a fixed rate of flow, as is the case for a one-dimensional, steady-state, steady-flow problem, an inspection of Equation (4.14) indicates that

$$\frac{\Delta P}{\Delta v} = \frac{\Delta P}{\Delta(1/\rho)} = -\text{const}$$

The Rayleigh curve is therefore a straight line relation of negative slope on the *P*–*v* plane; see Figure 4.3. The steeper the slope, the greater the flow velocity. Now in the limit, at zero slope, the velocity approaches zero, while at an infinite slope, the velocity would approach an infinite value. A further inspection of Equation (4.14) reveals that two quadrants, regions I and II in Figure 4.3, are excluded regions. In other words, all points of a given flow must lie on a common Rayleigh line and can pass only through regions II and IV.

EXAMPLE 4.3 Air at a pressure of 14.7 psia and temperature of 530°R is flowing with a velocity of 800 ft/sec. Treating the flow as one-dimensional, evaluate (a) the density of the air, ρ, lbm/ft^3; (b) the specific volume v, ft^3/lbm; (e) the slope of the Rayleigh line on *P*–*v* coordinates; and (d) the conditions for Rayleigh flow for a specific volume of 5 ft^3/lbm.

Solution:

1. Continuity:

$$G = \rho_1 V_1 = \frac{P_1 V_1}{R T_1}$$

2. Density:

$$\rho_1 = \frac{(14.7\ \text{lbf/in}^2)(144\ \text{in}^2/\text{ft}^2)}{(53.34\ \text{ft}\cdot\text{lbf/lbm}\cdot{}^\circ\text{R})(530{}^\circ\text{R})}$$

$$= 0.07488\ \text{lbm/ft}^3$$

$$v_1 = 13.355\ \text{ft}^3/\text{lbm}$$

3. Mass flow:

$$G = \rho_1 V_1 = (0.07488\ \text{lbm/ft}^3)(800\ \text{ft/sec}) = 59.9 = 60\ \text{lbm/sec}\cdot\text{ft}^2$$

4. *P*–*v* Rayleigh line, *slope*:

$$\frac{\Delta P}{\Delta v} = \frac{-G^2}{g_0} = \frac{(60\ \text{lbm/sec}\cdot\text{ft}^2)^2}{(32.2\ \text{ft}\cdot\text{lbm/lbf}\cdot\text{sec}^2)}$$

$$= -111.8\frac{\text{lbm}^2/\text{sec}^2\cdot\text{ft}^4}{\text{ft}\cdot\text{lbm/lbf}\cdot\text{sec}^2}$$

$$= -111.8\left(\frac{\text{lbm}}{\text{ft}^4}\right)\left(\frac{\text{lbf}}{\text{ft}}\right)$$

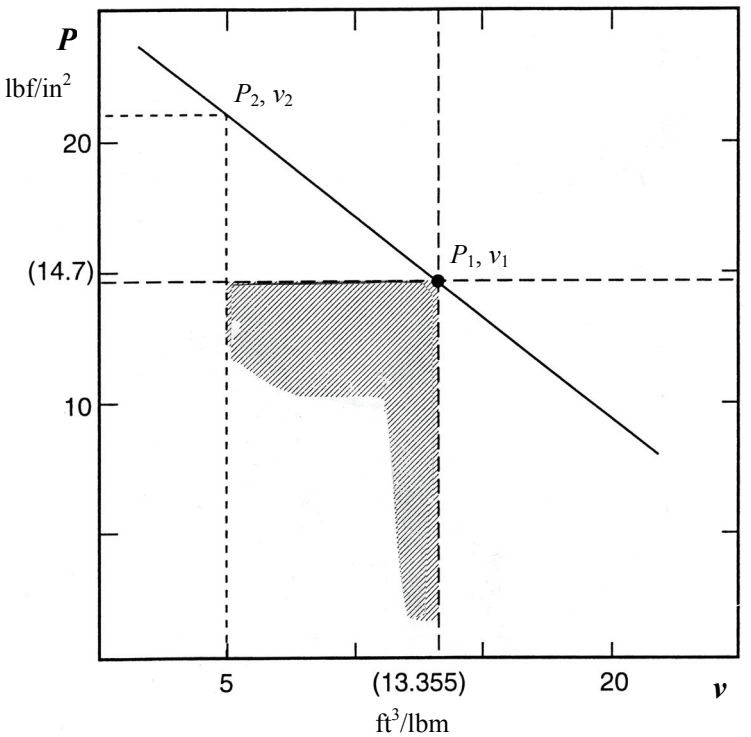

$$\frac{\Delta P}{\Delta v} = -\frac{111.8\left(\text{lbm}/\text{ft}^3\right)\left(\text{lbf}/\text{ft}^2\right)}{144\,\text{in}^2/\text{ft}^2}$$

$$= -0.78\,\frac{\text{psi}}{\text{ft}^3/\text{lbm}}$$

at $v_2 = 5\ \text{ft}^3/\text{lbm}$

$$V_2 = \frac{60\ \text{lbm}/\text{sec}\cdot\text{ft}^2}{\left(\frac{1}{5}\right)\text{lbm}/\text{ft}^3} = 300\ \text{ft}/\text{sec}$$

$$P_2 = 14.7 + 0.78(13.355 - 5) = 21.2\ \text{psia}$$

4.4 THE RANKINE-HUGONIOT CURVE

In Section 4.3, the continuity and momentum expressions developed for one-dimensional compressible flow were combined to form the Rayleigh line. An additional equation, termed the Rankine-Hugoniot curve, which is of use when modeling a combustion zone within a diabatic flow, will result from a combination of the continuity, momentum, and energy relationships. Recall that continuity is equal to

$$G = \rho V \tag{4.4}$$

and

$$\frac{1}{\rho_1} = \frac{V_1}{G_1} \tag{4.15a}$$

$$\frac{1}{\rho_2} = \frac{V_2}{G_2} \tag{4.15b}$$

The Rayleigh line, a combination of continuity and momentum, Equation (4.14), was equal to

$$\frac{P_2 - P_2}{\left(1/\rho_2 - 1/\rho_1\right)} = \frac{-G^2}{g_0} \tag{4.14}$$

Conservation of energy for a flow with no work transfer is given as

$$q + h_1 + \frac{V_1}{2g_0} = h_2 + \frac{V_2^2}{2g_0} \tag{4.12}$$

$$q = \left(h_2 - h_1\right) + \frac{1}{2g_0}\left(V_2^2 - V_1^2\right)$$

Assuming an ideal gas with constant specific heats, the above becomes

$$q = C_p\left(T_2 - T_1\right) + \frac{1}{2g_0}\left(V_2^2 - V_1^2\right) \tag{4.16}$$

$$= \left(\frac{R\gamma}{\gamma - 1}\right)\left(T_2 - T_1\right) + \frac{1}{2g_0}\left(V_2^2 - V_1^2\right) \tag{4.17}$$

and, for an ideal gas where $P = \rho RT$,

$$q = \left(\frac{\gamma}{\gamma - 1}\right)\left(\frac{P_2}{\rho_2} - \frac{P_1}{\rho_1}\right) + \frac{1}{2g_0}\left[V_2^2 - V_1^2\right] \tag{4.18}$$

Substituting the definition $G = \rho V$,

$$q = \left(\frac{\gamma}{\gamma - 1}\right)\left(\frac{P_2}{\rho_2} - \frac{P_1}{\rho_1}\right) + \frac{1}{2g_0}\left(\frac{G_2^2}{\rho_2^2} - \frac{G_1^2}{\rho_1^2}\right) \tag{4.19}$$

$$= \left(\frac{\gamma}{\gamma - 1}\right)\left(\frac{P_2}{\rho_2} - \frac{P_1}{\rho_1}\right) + \frac{1}{2g_0}\left(\frac{1}{\rho_2^2} - \frac{1}{\rho_1^2}\right)G^2$$

$$= \left(\frac{\gamma}{\gamma - 1}\right)\left(\frac{P_2}{\rho_2} - \frac{P_1}{\rho_1}\right) + \frac{1}{2g_0}\left[\left(\frac{1}{\rho_2} + \frac{1}{\rho_1}\right)\left(\frac{1}{\rho_2} - \frac{1}{\rho_1}\right)\right]G^2$$

From Equation (7.14), substitution for G^2/g_0 above yields

$$q = \left(\frac{\gamma}{\gamma - 1}\right)\left(\frac{P_2}{\rho_2} - \frac{P_1}{\rho_1}\right) + \frac{1}{2}\left[\left(\frac{1}{\rho_2} + \frac{1}{\rho_1}\right)\left(\frac{1}{\rho_2} - \frac{1}{\rho_1}\right)\right]\left[\left(\frac{-\left(P_2 - P_1\right)}{1/\rho_2 - 1/\rho_1}\right)\right] \tag{4.20}$$

$$q = \left(\frac{\gamma}{\gamma - 1}\right)\left(\frac{P_2}{\rho_2} - \frac{P_1}{\rho_1}\right) - \frac{1}{2}\left(\frac{1}{\rho_2} + \frac{1}{\rho_1}\right)(P_2 - P_1) \tag{4.20a}$$

or

$$q = (h_2 - h_1) - \frac{1}{2}(P_2 - P_1)(v_2 + v_1) \tag{4.20b}$$

Equation (4.20) is called the Rankine-Hugoniot curve and shows that the fluid flow parameters P and ρ are functions of the local *heat addition* to the reaction zone. The relation is often shown on P-v coordinates; see Figure 4.4. On this diagram, each curve corresponds to a given heat release, i.e., q = const. An adiabatic flow will lie on the curve for $q = 0$. A diabatic flow for an exothermic reaction has to move from an initial point on the $q = 0$ curve, passing through the state P_1 and v_1, and terminate on a particular Hugoniot curve where q = const. Two separate conditions along the Hugoniot curve will satisfy the diabatic flow case for P_2 and v_2. The two solutions are labeled states 2 and 2′; see Figure 4.4.

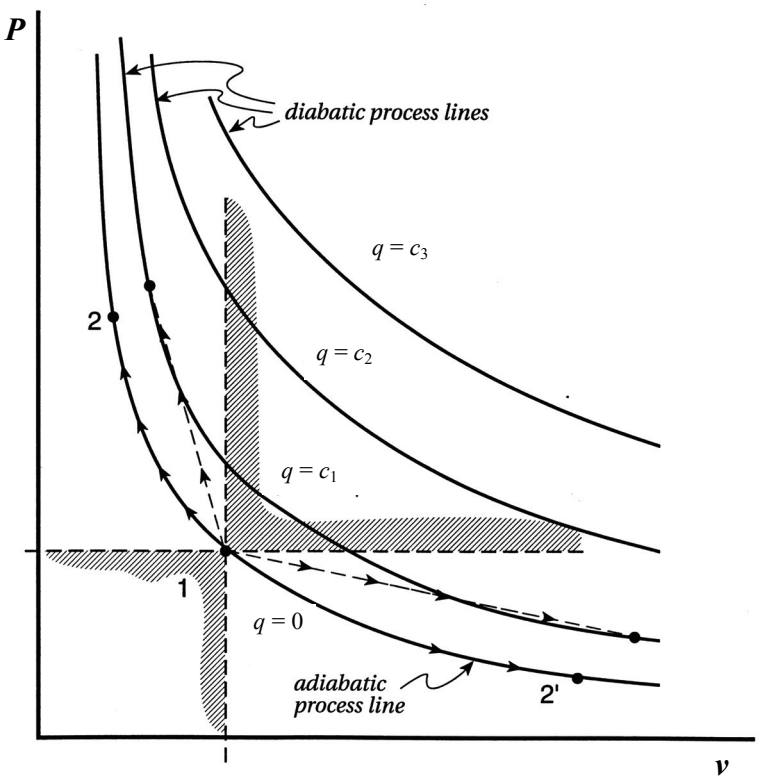

Figure 4.4 Rankine-Hugoniot curve.

For conditions at state 2, the curve indicates that the pressure behind the reaction zone, P_2, will be greater than the pressure ahead of the wave front, P_1. Also, the temperature of the burned gases, T_2, will be greater than the initial reactant temperature T_1. The specific volume of the products of combustion, v_2, will be less than the reactants v_1.

For the state defined by solution 2′, analysis shows that the pressure behind the wave front, P_2', will be less than that ahead of the reaction zone, P_1. The temperature of the combustion products, T_2', will be greater than the temperature of the initial reactants, T_1. The burned gases will have a specific volume, v_2', which will be larger than that of the original unburned mixture.

4.5 THE CHAPMAN-JOUQUET POINTS

The condition of the burned gases behind a stationary combustion zone is defined by a solution to both the Rayleigh and Hugoniot curves; see Figure 4.5. An inspection of Figure 4.5 reveals that a given Rayleigh line will intersect a particular Hugoniot curve on either its upper or lower branch. Solutions defined by points of intersection along the upper Hugoniot branch are called *detonation waves,* while lower branch solutions are termed *deflagration waves.* Recall from Section 4.3 that Rayleigh flow cannot pass into regions I and II. Conditions at 2 or 2' must therefore lie on a Rayleigh line passing through the initial state P_1, v_1, and intersecting a particular Hugoniot curve in regions II or IV for a specific q.

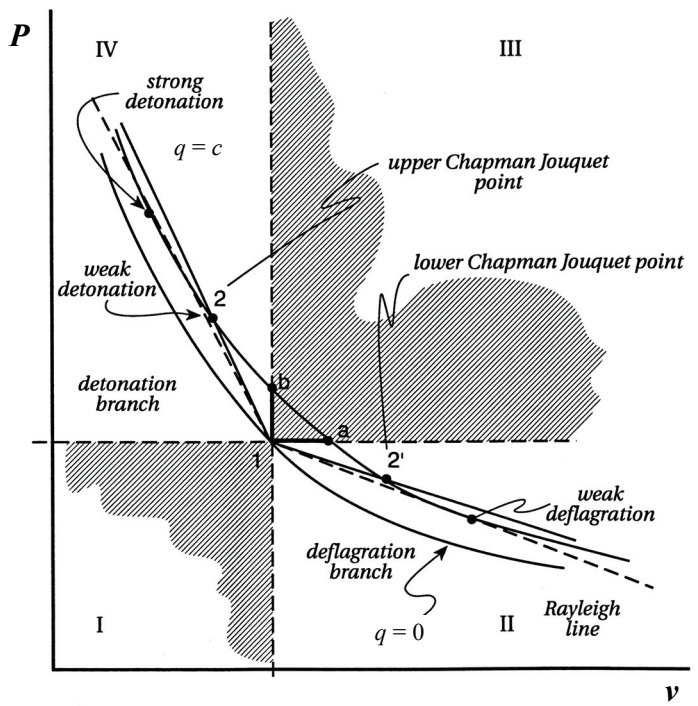

Figure 4.5 Rayleigh-Hugoniot diabatic flow analysis.

Several characteristics of the upper, or detonation, branch can be inferred from an inspection of Figure 4.5. Recall that the burned-gas temperature and pressure T_2 and P_2 must be greater than the initial values T_1 and P_1. In addition, the specific volume at state 2 will be compressed from its original value. A Rayleigh line having the smallest slope yet still intersecting a particular Hugoniot curve is seen to be a line of tangency. This unique solution is defined as the upper Chapman-Jouquet point and can be seen to be the solution with the minimum velocity at 2. Example 4.4 shows that the velocity of the gases at the Chapman-Jouquet points *relative* to the reactive wave front is at sonic speeds. Additional solutions obtained from intersections above the Chapman-Jouquet point are supersonic at state 2, with points at pressures greater than the Chapman-Jouquet point and are classified as strong detonations and those below classified as weak detonations.

EXAMPLE 4.4 The velocity V_2 of the burned gases at the Chapman-Jouquet points must satisfy both the Rayleigh line and the Hugoniot curve. For this condition, show that the velocity V_2 is equal to the sonic velocity c_2.

Solution:

1. Rayleigh line:

$$\frac{dP_2}{dv_2} = \frac{P_2 - P_1}{v_2 - v_1} = \frac{-V_2^2}{g_0 v_2^2}$$

2. Rankine-Hugoniot relationship:

$$q = (h_2 - h_1) - \tfrac{1}{2}(P_2 - P_1)(v_2 + v_1)$$

differentiating for fixed initial conditions at 1,

$$dq = 0 = d\{(h_2 - h_1) - \tfrac{1}{2}(P_2 - P_1)(v_2 + v_1)\}$$
$$dh_2 = \tfrac{1}{2}(v_2 + v_1)dP_2 + \tfrac{1}{2}(P_2 - P_1)dv_2$$

3. Using the Rayleigh line,

$$dv_2 = \frac{(v_2 - v_1)}{(P_2 - P_1)} dP_2$$

and substituting into the Hugoniot curve,

$$dh_2 = \tfrac{1}{2}(v_2 + v_1)dP_2 + \tfrac{1}{2}(P_2 - P_1)\frac{(v_2 - v_1)}{P_2 - P_1} dP_2$$

or

$$dh_2 = v_2 dP_2$$

4. Assuming an ideal gas with constant specific heats,

$$dh_2 = C_p dT_2 = \frac{\gamma R}{(\gamma - 1)} dT_2$$

and

$$P_2 v_2 = RT_2$$
$$d(P_2 v_2) = R\, dT_2$$

5. Combining parts 3 and 4,

$$\gamma R\, dT_2 = (\gamma - 1) v_2\, dP_2$$
$$\gamma[P_2\, dv_2 + v_2\, dP_2] = (\gamma - 1) v_2\, dP_2$$
$$\gamma P_2\, dv_2 = -v_2\, dP_2$$

and

$$\frac{dP_2}{dv_2} = -\gamma \frac{P_2}{v_2}$$

6. From parts 1 and 5,

$$\frac{dP_2}{dv_2} = -\gamma \frac{P_2}{v_2} = -\frac{V_2^2}{g_0 v_2^2}$$
$$V_2^2 = \gamma P_2 v_2 g_0 = \gamma RT_2 g_0$$
$$V_2 = c_2$$

Deflagration wave characteristics along the lower Hugoniot branch can also be deduced from a consideration of Figure 4.5. Again, burned-gas temperature T_2' will be greater than the initial gas temperature T_1, but the final pressure P_2' is less than the initial pressure P_1. The gas expands from the original specific volume v_1 to its final value v_2'. An inspection of Figure 4.5 reveals that the tangent Rayleigh line of smallest slope defines the lower Chapman-Jouquet point. Since the velocity at the Chapman-Jouquet points is sonic (see Example 4.4), all other deflagrations obtained from the intersections of Rayleigh and Hugoniot curves will be subsonic. Points of intersection for P_2' greater than the Chapman-Jouquet pressure are referred to as weak deflagrations, whereas values of P_2' less than the Chapman-Jouquet value are called strong deflagrations.

4.6 CALCULATION OF CHAPMAN-JOUQUET NORMAL DETONATION PARAMETERS

In Section 4.5, it was shown that the equations for mass, momentum, and energy for one-dimensional, steady compressible flow were satisfied by two different reactive wave propagations, i.e., detonations and deflagrations. Chapters 2 and 3 developed methods for predicting the ideal energy release of various chemical energy conversion processes. By combining the material in Chapters 2 and 3 with results in Section 4.5, a simplified

method for estimating upper Chapman-Jouquet properties can be obtained. The following additional assumptions will be made:

1. Nonreactive ideal-gas mixtures at states 1 and 2.
2. Conditions at state 1 are those for a homogeneous mixture of fuel and air.
3. Conditions at state 2 are based on mixture properties for the products of combustion.
4. Diabatic heat transfer is approximated by the change in enthalpy of formation between the reactants and products.
5. $P_2 \gg P_1$.

The conservation of energy equation (4.12) can be used to obtain an expression for burned-gas temperature T_2 as

$$h_2 - h_1 + \frac{V_2^2}{2g_0} - \frac{V_1^2}{2g_0} = q \tag{4.12}$$

$$C_{P_2} T_2 = C_{P_1} T_1 + q + \frac{V_1^2}{2g_0} - \frac{c_2^2}{2g_0} \tag{4.21a}$$

or

$$C_{P_2} T_2 = C_{P_1} T_1 + q + \frac{V_1^2}{2g_0} - \frac{\gamma_2 R_2 T_2}{2} \tag{4.21b}$$

Using the conservation of momentum equation (4.6b), V_1 is given by

$$\rho_1 V_1^2 = g_0 (P_2 - P_1) + \rho_2 V_2^2 \tag{4.6b}$$

$$\rho_1 V_1^2 = g_0 P_2 \left[1 - \frac{P_1}{P_2} \right] + \rho_2 V_2^2$$

and, assuming $P_2 \gg P_1$ the expression for the initial velocity becomes

$$V_1^2 = g_0 \frac{P_2}{\rho_1} + \frac{\rho_2}{\rho_1} V_2^2 \tag{4.22}$$

Substituting Equation (4.22) into Equation (4.21b) yields an expression for the burned-gas temperature T_2 solely in terms of thermodynamic properties at states 1 and 2 as

$$C_{P_2} T_2 = C_{P_1} T_1 + q - \frac{\gamma_2 R_2 T_2}{2} + \frac{1}{2g_0} \left[g_0 \frac{P_2}{\rho_1} + \frac{\rho_2}{\rho_1} V_2^2 \right]$$

$$C_{P_2} T_2 = C_{P_1} T_1 + q - \frac{\gamma_2 R_2 T_2}{2} + \frac{1}{2} \left[R_2 T_2 + \gamma_2 R_2 T_2 \right] \frac{\rho_2}{\rho_1} \tag{4.23}$$

Now, again using the momentum equation, one can write for $P_1 \ll P_2$

$$g_0 P_2\left[1 - \frac{P_1}{P_2}\right] = \rho_1 V_1^2 - \rho_2 V_2^2$$

$$\frac{\rho_1 V_1^2}{\rho_2 V_2^2} = \frac{g_0 P_2}{\rho_2 V_2^2} + 1 \tag{4.24}$$

where utilizing the conservation of mass, Equation (4.24) then becomes

$$\left(\frac{\rho_1}{\rho_2}\right)\left(\frac{\rho_2}{\rho_1}\right)^2\left(\frac{V_2^2}{V_2^2}\right) = \frac{g_0 P_2}{\rho_2 V_2^2} + 1$$

$$\frac{\rho_2}{\rho_1} = \left[\frac{g_0 P_2}{\rho_2 V_2^2} + 1\right]$$

Since the velocity of the upper Chapman-Jouquet point is sonic, the above expression reduces to

$$\frac{\rho_2}{\rho_1} = \left[\frac{1}{\gamma_2} + 1\right] = \frac{1+\gamma_2}{\gamma_2} \tag{4.25}$$

Substituting Equation (4.25) into Equation (4.22) yields

$$C_{P_2} T_2 = C_{P_1} T_1 + q - \frac{\gamma_2 R_2 T_2}{2} + \frac{R_2 T_2 \gamma_2}{2}\left[\frac{1+\gamma_2}{\gamma_2}\right]^2$$

$$T_2 = \left(\frac{C_{P_1}}{C_{P_2}}\right) T_1 + \frac{q}{C_{P_2}} - \frac{\gamma_2 R_2 T_2}{2C_{P_2}} + \frac{\gamma_2 R_2 T_2}{2C_{P_2}}\left[\frac{1+\gamma_2}{\gamma_2}\right]^2$$

Recall, for an ideal gas, the following relationships:

$$C_P - C_V = R \qquad \gamma = C_P / C_V$$

or

$$C_P = \frac{R\gamma}{\gamma - 1}$$

and

$$T_2 = \left(\frac{C_{P_1}}{C_{P_2}}\right) T_1 + \frac{q}{C_{P_2}} - \frac{\gamma_2 R_2 T_2 (\gamma_2 - 1)}{2R_2\gamma_2} + \frac{(\gamma_2 R_2 T_2)(\gamma_2 - 1)}{2R_2\gamma_2}\left[\frac{1+\gamma_2}{\gamma_2}\right]^2$$

$$T_2 = \left(\frac{C_{P_1}}{C_{P_2}}\right) T_1 + \frac{q}{C_{P_2}} + \left[\frac{\gamma_2 - 1}{2}\right] T_2 \left[\frac{1+2\gamma_2}{\gamma_2^2}\right]$$

$$\left[1 - \left(\frac{\gamma_2 - 1}{2}\right)\left(\frac{1+2\gamma_2}{\gamma_2^2}\right)\right] T_2 = \left(\frac{C_{P_1}}{C_{P_2}}\right) T_1 + \frac{q}{C_{P_2}}$$

$$T_2 = \frac{2\gamma_2^2}{\gamma_2 + 1}\left[\left(\frac{C_{P_1}}{C_{P_2}}\right)T_1 + \frac{q}{C_{P_2}}\right] \qquad \text{K(°R)} \qquad (4.26)$$

Equation (4.26) can be used to estimate the detonation temperature T_2, using only thermodynamic properties at states 1 and 2. Example 4.5 illustrates a solution technique with a specific problem.

EXAMPLE 4.5 The reaction of a combustible mixture can, under certain conditions in closed vessels, be observed to produce a detonation wave. Consider a stoichiometric mixture of methane and air initially at *STP,* and calculate (a) the detonation temperature, K; (b) the detonation pressure, atm; and (c) the detonation velocity relative to the flame front, m/sec. Assume complete combustion in your calculations.

Solution:

1. Stoichiometric reaction:

$$CH_4 + 2[O_2 + 3.76\,N_2] \rightarrow CO_2 + 2H_2O + (2)(3.76)N_2$$

2. Initial state for $T_1 = 298$K, $P_1 = 1$ atm:

$$\bar{x}_{CH_4} = \frac{1}{1 + (2)(4.76)} = 0.095$$

$$\bar{x}_{O_2} = \frac{2}{10.520} = 0.190$$

$$\bar{x}_{N_2} = 1.000 - 0.095 - 0.190 = 0.715$$

$$MW_1 = (0.095)(16) + (0.190)(32) + (0.715)(28) = 27.62 \text{ gm/gmole}$$

From Tables B.3, B.18, and B.22 in Appendix B,

$$\bar{C}_{P_1} = (0.095)(8.518) + (0.190)(7.020) + (0.715)(6.961)$$
$$= 7.120 \text{ cal/gmole} \cdot \text{K}$$

$$\gamma_1 = \frac{\bar{C}_{P_1}}{\bar{C}_{P_1} - \bar{R}} = \frac{7.120}{7.120 - 1.987} = 1.387$$

3. The heat addition can be approximated as the difference in enthalpies of formation of the initial and final mixtures. From Table B.1 in Appendix B

$$|{}_1Q_2| \cong \left|\sum_2 N_i \bar{h}_{f_i}^0\right| - \left|\sum_1 N_i \bar{h}_{f_i}^0\right|$$
$$= (1)(94{,}054) + 2(57{,}798) + (2)(3.76)(0) - (1)(17{,}895)$$
$$= 191{,}755 \text{ cal}$$

or

$${}_1\bar{q}_2 = \frac{191{,}755 \text{ cal}}{3 + (2)(3.76)} = 18{,}228 \text{ cal/gmole product}$$

4. Energy balance on a molar basis:

$$T_2 = \frac{2\gamma_2^2}{\gamma_2 + 1}\left\{\left[\frac{\overline{C}_P}{MW}\right]_1\left[\frac{MW}{\overline{C}_P}\right]_2 T_1 + \frac{{}_1\overline{q}_2}{\overline{C}_{P_2}}\right\}$$

An iterative technique is necessary since the conditions at state 2 are unknown.

5. Final state, assuming $T_2 = 3{,}200\text{K}$:

$$\bar{x}_{CO_2} = \frac{1}{3 + (2)(3.76)} = 0.095$$

$$\bar{x}_{H_2O} = \frac{2}{10.520} = 0.190$$

$$\bar{x}_{N_2} = 1.0 - 0.095 - 0.190 - 0.715$$

$$MW_2 = (0.095)(44) + (0.190)(18) + (0.715)(28) = 27.62 \text{ gm/gmole}$$

$$\overline{C}_{P_2} = (0.095)(14.930) + (0.190)(13.441) + (0.715)(8.886) = 10.326 \text{ cal/gmole} \cdot \text{K}$$

$$\gamma_2 = \frac{10.326}{10.326 - 1.987} = 1.238$$

$$T_2 = \frac{(2)(1.238)^2}{(2.238)}\left\{\left[\frac{7.120}{27.62}\right]\left[\frac{27.62}{10.326}\right](298) + \frac{18{,}228}{10.326}\right\}$$

$$T_2 = 2{,}838.5\text{K} \qquad \text{(too high a guess)}$$

6. Final state, assuming that $T_2 = 2{,}800\text{K}$:

$$\overline{C}_{P_2} = (0.095)(14.807) + (0.190)(13.146) + (0.715)(8.820) = 10.211$$

$$\gamma_2 = \frac{10.211}{10.211 - 1.987} = 1.242$$

$$T_2 = \frac{(2)(1.242)^2}{(2.242)}\left\{\left[\frac{7.120}{27.62}\right]\left[\frac{27.62}{10.211}\right](298) + \frac{18{,}228}{10.211}\right\}$$

$$T_2 = 2{,}742.4\text{K}$$

7. Assume that $T_2 = 2{,}700\text{K}$:

$$\overline{C}_{P_2} = (0.095)(14.771) + (0.190)(13.059) + (0.715)(8.800) = 10.176$$

$$\gamma_2 = \frac{10.176}{10.176 - 1.987} = 1.243$$

$$T_2 = \frac{(2)(1.243)^2}{(2.243)}\left\{\left[\frac{7.120}{27.62}\right]\left[\frac{27.62}{10.176}\right](298) + \frac{18{,}228}{10.176}\right\} = 2{,}755\text{K}$$

8. Assume that $T_2 = 2{,}750$K:

$$\overline{C}_{P_2} = (0.095)(14.789) + (0.190)(13.103) + (0.715)(8.810) = 10.194$$

$$\gamma_2 = \frac{10.194}{10.194 - 1.987} = 1.242$$

$$T_2 = \frac{(2)(1.242)^2}{(2.242)}\left\{\left[\frac{7.120}{27.62}\right]\left[\frac{27.62}{10.194}\right](298) + \frac{18{,}228}{10.194}\right\} = 2{,}747\text{K}$$

a. $T \cong 2{,}750$K

9. Relative velocity at state 2:

$$V_2 = c_2 = \sqrt{\gamma_2 R_2 T_2 g_0}$$

$$= \left[\frac{(1.242)(8{,}314\ \text{N}\cdot\text{m/kgmole}\cdot\text{sec}^2\ \text{K})(2{,}750\ \text{K})(1.0\ \text{kg}\cdot\text{m/N}\cdot\text{sec}^2)}{(27.62\ \text{kg/kgmole})}\right]^{1/2}$$

$$V_2 = 1{,}014\ \text{m/sec}$$

10. Conditions at state 2:

$$\frac{\rho_2}{\rho_1} = \frac{\gamma_2 + 1}{\gamma_2} = \frac{1.242 + 1}{1.242} = 1.805$$

$$\frac{P_2}{P_1} = \frac{\rho_2 R_2 T_2}{\rho_1 R_1 T_1} = \frac{\rho_2 MW_1 T_2}{\rho_1 MW_2 T_1}$$

$$= (1.805)\left(\frac{27.62}{27.62}\right)\left(\frac{2{,}750}{298}\right)$$

$$= 16.66$$

and

b. $P_2 = 16.66\ P_1 = 16.66$ atm

11. Detonation velocity, V_1:

c. $V_1 = (\rho_2/\rho_1)V_2 = (1.805)(1{,}014\ \text{m/sec}) = 1{,}830$ m/sec

4.7 DETONATION THEORY AND EXPERIMENTAL EVIDENCES

Experimental evidences have verified the existence of both detonation and deflagration wave propagations. Formation of detonation waves has been experimentally observed in various closed-vessel geometries and has involved a variety of fuel-air mixtures, including coal-dust mine explosions, natural gas leak explosions in buildings, and combustion knock in internal combustion engines. The potential of such phenomena will influence the design, fabrication, and operation of a variety of combustion devices. The one-dimensional Chapman-Jouquet detonation model, although somewhat an over-simplification of the actual process, does give results that are in reasonable agreement

with engineering measurements. Table 4.2 lists the order of magnitude of burned to unburned properties for a normal detonation wave, while Table 4.3 gives detonation parameters for several premixed fuel-air mixtures.

Strong detonation can occur in rare instances but is usually produced when a very strong shock wave passes through a homogeneous reactive mixture. Weak detonations also are very seldom found to occur but can be generated experimentally using special gas mixtures.

EXAMPLE 4.6 Dissociation of the combustion products can become significant for temperatures above 1,250K. This phenomenon can affect the detonation conditions calculated for different end gas conditions. Consider a stoichiometric H_2-O_2 mixture initially at *STP* and calculate the detonation temperature, K, assuming complete combustion. Repeat the calculations, assuming that the products consist of H_2, O_2, and H_2O.

Solution:

1. Stoichiometric equation:

$$H_2 + \tfrac{1}{2}O_2 \rightarrow H_2O$$

2. Initial state for $T_1 = 298$K:

$$\bar{x}_{H_2} = \frac{1.0}{1.5} = 0.667 \qquad \bar{x}_{O_2} = 0.333$$

$$MW_1 = (0.667)(2) + (0.333)(32) = 12.000 \text{ gm/gmole}$$

From Tables B.13 and B.22 in Appendix B,

$$\bar{C}_{P_1} = (0.667)(6.892) + (0.333)(7.020) = 6.935 \text{ cal/gmole} \cdot \text{K}$$

$$\gamma_1 = \frac{\bar{C}_{P_1}}{\bar{C}_{P_1} - \bar{R}} = \frac{6.935}{6.935 - 1.987} = 1.402$$

3. Heat addition can be approximated as the difference in enthalpies of formation of the products and reactants. From Table B.1 in Appendix B

$$|Q| \cong \sum_2 N_i \bar{h}_{f_i}^0 - \sum_1 N_i \bar{h}_{f_i}^0$$

$$|Q| = (1 \text{ gmole})(57{,}798 \text{ cal/gmole}) - (0.5)(0) - (1)(0)$$

$$= 57{,}798$$

and

$$|\bar{q}| = \frac{57{,}798}{1.0} = 57{,}798 \text{ cal/gmole product}$$

4. Energy balance:

$$T_2 = \frac{2\gamma_2^2}{\gamma_2 + 1}\left\{\left[\frac{\overline{C}_P}{MW}\right]_1\left[\frac{MW}{\overline{C}_P}\right]_2 T_1 + \frac{\overline{q}}{\overline{C}_{P_2}}\right\}$$

Since the condition at item 2 is unknown an iterative technique is necessary.

5. Final state from Table B.14 in Appendix B:

$$\overline{x}_{H_2O} = 1.0$$
$$MW_2 = 18.0$$
$$\overline{C}_{P_2} = \overline{C}_P\langle T_2\rangle_{H_2O}$$
$$\gamma_2 = \frac{\overline{C}_{P_2}}{\overline{C}_{P_2} - \overline{R}}$$

$(T_2)_{assumed}$	$\overline{C}_{P_2}$	γ_2	$(T_2)_{calculated}$
4,500	14.030	1.165	5,442
5,000	14.174	1.163	5,373
5,300	14.254	1.162	5,336

NOTE: $T_2 \sim 5{,}300$K.

6. Product dissociation:

$$H_2 + \tfrac{1}{2}O_2 \rightarrow aH_2 + bO_2 + cH_2O$$

Hydrogen atom balance:

$$a + c = 1$$

Oxygen atom balance:

$$2b + c = 1$$

or

$$b = \frac{a}{2} \qquad c = 1 - a$$

7. Equilibrium constant

$$H_2 + \tfrac{1}{2}O_2 \rightleftarrows H_2O$$

$$K_p = \frac{[P/P_0]_{H_2O}}{[P/P_0]_{O_2}^{1/2}[P/P_0]_{H_2}}$$

where $P_0 \equiv 1\,\text{atm}$

$$K_p = \frac{P_{H_2O}}{P_{O_2}^{1/2} P_{H_2}}$$

$$= \frac{\bar{x}_{H_2O}}{\bar{x}_{O_2}^{1/2} \bar{x}_{H_2}} (P_{tot})^{-1/2}$$

$$= \left[\frac{(1-a)}{(a/2)^{1/2}(a)}\right]\left[a + \frac{a}{2} + 1 - a\right]^{1/2} P_{tot}^{-1/2}$$

Assume that $T_2 = 4{,}000\text{K}$ and $P_2 = 18$ atm.

From Table B.14 in Appendix B for H_2O

$$\log K_p = 0.238$$

$$K_p = 1.7298$$

or

$$(1.7298)(18)^{1/2} = \frac{(1-a)([a/2]+1)^{1/2}}{(a/2)^{1/2}(a)}$$

Using numerical techniques yields:

$a = 0.280$
$b = 0.\ 140$
$c = 0.720$

8. Final state for $T_2 = 4{,}000\text{K}$:

$$\bar{x}_{H_2} = \frac{a}{a+b+c} = \frac{0.280}{0.280+0.140+0.720} = 0.2456$$

$$\bar{x}_{O_2} = \frac{b}{a+b+c} = \frac{0.140}{1.140} = 0.1228$$

$$\bar{x}_{H_2O} = \frac{c}{a+b+c} = \frac{0.720}{1.140} = 0.6316$$

$$MW_2 = (0.2456)(2) + (0.1228)(32) + (0.6316)(18) = 15.79$$

$$\bar{C}_{P_2} = (0.2456)(9.342) + (0.1228)(9.932) + (0.6316)(13.850) = 12.262$$

$$\gamma_2 = \frac{12.262}{12.262 - 1.987} = 1.193$$

$$|Q| = \Sigma N_i \bar{h}_{f_i}^0 - \Sigma N_i \bar{h}_{f_i}^0$$

$$= (0.280)(0) + (0.140)(0) + (0.720)(57.798) - (1.0)(0) - (0.5)(0) = 41{,}615\,\text{cal}$$

and

$$\bar{q} = \frac{41{,}615}{1.140} = 36{,}504 \text{ cal/gmole product}$$

$$T_2 = \frac{(2)(1.193)^2}{(2.193)} \left\{ \frac{(6.935)(15.79)}{(12.0)(12.262)}(298) + \frac{36{,}504}{12.262} \right\} = 4{,}152\text{K}$$

or

$$T_2 \simeq 4\,100\text{K}$$

The precise structure of a normal detonation wave has been modeled by Zeldovich (1950), von Neumann (1942), and Doring (1943); see Figure 4.6. A ZND detonation wave is produced by a moving shock wave traveling at the detonation velocity. Chemical reaction is initiated behind the shock front in the compression-heated mixture. Temperature continues to rise behind the moving wave front as a result of chemical reactions. Behind the short transition region, the properties *P, T,* and ρ relax to conditions of chemical equilibrium, as predicted by the Chapman-Jouquet analysis.

Table 4.2 Orders of Magnitude for Detonation/Deflagration Parameters

Parameter	Detonation	Deflagration
u_2/c_1	5–10	0.0001–0.03
u_2/u	0.4–0.7	4–16
P_2/P_1	13–55	0.98–0.976
ρ_2/ρ_1	1.4–2.6	0.06–0.25
T_2/T_1	8–21	4–16

From Friedman, R., *American Rocket Soc. J.*, Vol. 23, p. 349, 1953.

Table 4.3 Stoichiometric Detonation Velocities for Gaseous Mixtures

Mixture	P_2 atm	T_2 K	u_1, m/sec	
			Calculated	Measured
$(2H_2 + O_2)$	18.05	3,583	2,806	2,819
$(2H_2 + O_2) + 5O_2$	14.13	2,620	1,732	1,700
$(2H_2 + O_2) + 5N_2$	14.39	2,685	1,850	1,822
$(2H_2 + O_2) + 5H_2$	15.97	2,975	3,627	3,527
$(2H_2 + O_2) + 5He$	16.32	3,097	3,617	3,160
$(2H_2 + O_2) + 5Ar$	16.32	3,097	1,762	1,700
$CO + O_2$	18.6	3,500	—	(1,790)
$C_2H_2 + O_2$	44	4,200	—	(2,400)
C_2H_2 + air	19	3,100	—	(1,900)
CH_4 + air	17.2	2,736	—	(1,800)
C_3H_8 + air	18.3	2,823	—	(1,800)

NOTE: $P_1 = 1$ atm; $T_1 = 291$K.
Source: Lewis, B. and Von Elbe, G., *Combustion, Flames, and Explosions in Gases*, 2nd Edition, Academic Press, New York, 1961. With permission from Elsevier.

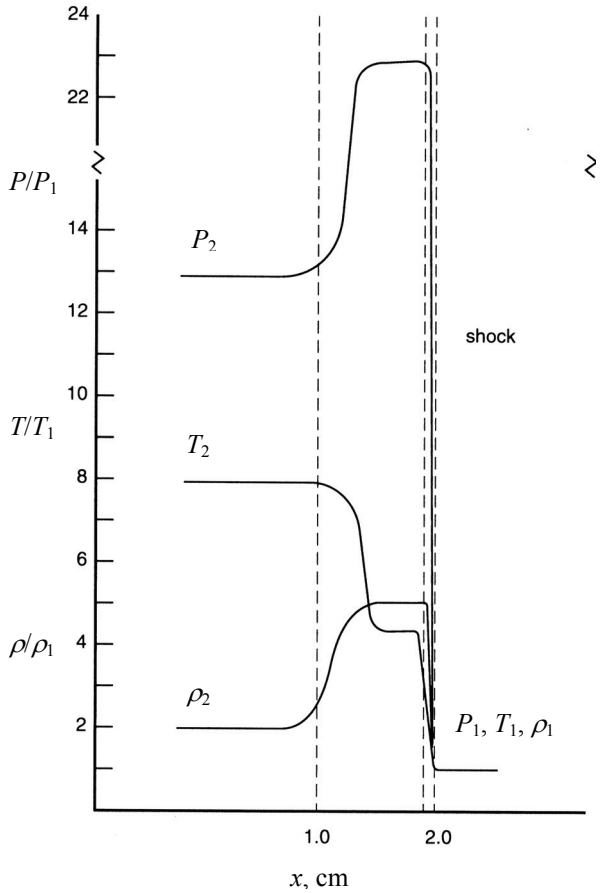

Figure 4.6 ZND detonation wave structure.

Table 4.4 Detonation Limits for Gaseous Mixtures

Mixture	% Fuel in mixture	
	Lean	Rich
$H_2 - O_2$	15	90
H_2 – air	18	59
$CO - O_2$	38	90
$NH_3 - O_2$	25	75
$C_3H_8 - O_2$	3	37

Source: Lewis, B. and Von Elbe, G., *Combustion, Flames, and Explosions in Gases*, 2nd Edition, Academic Press, New York, 1961. With permission from Elsevier.

Combustion heat release is strongly influenced by the mixture air-fuel ratio. Detonation wave parameters should thus be influenced by fuel-air mixture stoichiometry. Detonation limits are experimentally obtained using long, close-ended and narrow tubes. An explosive mixture is placed near the closed end and ignited by a small source, such as a spark. As the flame front travels a shock wave front forms in front. With the shock strengthening, the resulting rise in temperature behind the front eventually reaches a value that causes spontaneous ignition of the gas mixture. In the final transition stage the accelerating flame front chemistry changes to spontaneous ignition combustion and formation of a stable detonation wave. The techniques used to study detonations in shock tubes are well established. Table 4.4 gives the approximate detonation limits for several important reactive mixtures.

Propagation of a low-pressure subsonic reaction zone is a common occurrence. Deflagrations, called *flames*, are commonly observed in acetylene torches and spark-ignition internal combustion engines, as well as in gas turbine combustion cans. Results predicted using the one-dimensional deflagration model are not in good agreement with measured flame properties, since the simplified model developed in this chapter is inadequate and this case will be considered again in Chapter 5.

PROBLEMS

4.1 An ideal-gas mixture consists of methane, CH_4, and 120% theoretical air at *STP*. For these conditions, calculate (a) constant-pressure mixture molar specific heat, $\text{kJ/kgmole} \cdot \text{K}$; (b) constant-volume mixture molar specific heat, $\text{kJ/kgmole} \cdot \text{K}$; (c) mixture specific heat ratio at *STP*; and (d) sonic velocity at *STP,* m/sec.

4.2 A mixture of hydrogen and air at a temperature of 1,000K has a corresponding sonic velocity of 1,200 m/sec. Determine (a) equivalence ratio for the mixture; (b) mixture molecular weight, kg/kgmole; (c) mixture specific heat ratio; and (d) mixture molar specific heats, $\text{kJ/kgmole} \cdot \text{K}$.

4.3 Consider a one-dimensional steady-state and steady-sonic flow. Show that the speed of sound for these conditions can be related to the stagnation temperature by the relationship

$$c = \left[\frac{2\gamma R T_0 g_0}{\gamma + 1} \right]^{1/2}$$

4.4 A mixture of methane and air at *STP* has a specific heat ratio of 1.35. For these conditions, find (a) constant-pressure mixture molar specific, $\text{Btu/lbmole} \cdot \text{R}$; (b) reactant mixture mass fraction; (c) mixture sonic velocity at *STP,* ft/sec; and (d) mixture mass flux, $\text{lbm/sec} \cdot \text{ft}^2$.

4.5 Show that, for Rayleigh flow,

$$\frac{V_2}{V_1} = \frac{\left(1 + \gamma N_{m_1}^2\right)\left(N_{m_2}^2\right)}{\left(1 + \gamma N_{m_2}^2\right)\left(N_{m_1}^2\right)}$$

4.6 The Rankine-Hugoniot relationship can be expressed in terms of the local stagnation conditions for the gas at states 1 and 2. Show that, in this case, the Hugoniot curve is expressed as

$$\frac{q}{C_p T_1} = \left[1 + \frac{(\gamma - 1)}{2} N_{m_1}^2\right]\left[\frac{T_{02}}{T_{01}}\right]$$

4.7 Show that the ratio of the density of burned gases, ρ_2, to that of the unburned gases, ρ_1, is given as

$$\frac{\rho_2}{\rho_1} = \frac{\gamma_2 + 1}{\gamma_1}$$

4.8 The solution of the one-dimensional shock wave problem is given by the intersection of the Rayleigh line and the Rankine-Hugoniot curve for $q = 0$. Show that (a) stagnation states for points 1 and 2 are equal for the adiabatic case, i.e., $T_{0_1} = T_{0_2}$; (b) the temperature ratio across the shock wave is

$$\frac{T_2}{T_1} = \frac{1 + \left[\frac{(\gamma - 1)}{2}\right]\left(N_{m_1}^2\right)}{1 + \left[\frac{(\gamma - 1)}{2}\right]\left(N_{m_1}^2\right)}$$

and (c) the velocity ratio is given by

$$\frac{V_2}{V_1} = \frac{N_{m_2}}{N_{m_1}}\left\{\frac{1 + \left[\frac{(\gamma - 1)}{2}\right]\left(N_{m_1}^2\right)}{1 + \left[\frac{(\gamma - 1)}{2}\right]\left(N_{m_1}^2\right)}\right\}^{1/2}$$

4.9 The absolute velocity of the burned gases behind a detonation wave with respect to a stationary observer is written as

$$V_{\text{prod}} = V_1 - V_2$$

(a) Show that this velocity is given by the relation

$$V_{\text{prod}} = [1 - (\rho_1 / \rho_2)]V_1$$

(b) For a detonation, show that the above expression indicates that gas products travel behind the moving wave front but at a lower speed. (c) Show that, for a deflagration, the particular speed of the products travels in the opposite direction from the wave front. (d) Show that the absolute burned gas speed is also equal to

$$V_{\text{prod}} = [(v_1 - v_2)(P_2 - P_1)]^{1/2}$$

4.10 Show that, for an ideal-gas mixture, the Hugoniot relationship can be expressed as

$$q = u_2 - u_1 - (1/2)(P_2 - P_1)(v_1 - v_2)$$

4.11 The Rankine-Hugoniot curve for a fixed heat release is given as

$$q = h_2 - h_1 - (1/2)(P_2 - P_1)(v_2 + v_1)$$

Show that, for adiabatic flow, $P_1 v_1^{\gamma} = P_2 v_2^{\gamma} = \text{const.}$

4.12 A combustible mixture is initially at rest in a duct of constant cross-sectional area at a temperature of 500°R. A Chapman-Jouquet detonation wave propagates through the mixture, with the heat liberated by reaction equal to 960 Btu/lbm. Calculate the propagation Mach number of the detonation wave.

4.13 A Chapman-Jouquet deflagration is propagated through a combustible gaseous mixture in a duct of constant cross-sectional area. The heat release is equal to 480 Btu/lbm. The Mach number and flow velocity relative to the walls are 0.8 and 800 ft/sec in the unburned gas. Assuming that γ is 7/5 for both burned and unburned gases, estimate (a) the velocity of the flame relative to the walls, ft/sec; and (b) the velocity of the burned gas relative to the walls, ft/sec.

4.14 A mixture of H_2, O_2, and N_2 initially at rest is at 1 atm and 25°C. The heat release for the mixture is given by the reaction

$$2H_2 + O_2 + 5N_2 \rightarrow, 2H_2O + 5N_2$$

Determine (a) the detonation temperature, K; (b) the detonation pressure, atm; and (c) the detonation velocity relative to the flame, m/sec.

4.15 A mixture of H_2 and O_2 at *STP* has a constant-volume molar specific heat of 5.013 $\text{cal}/\text{gmole}\cdot\text{K}$. For these conditions, calculate (a) the reactant mixture mole fractions; (b) the mixture sonic velocity at *STP,* m/sec; (c) the mixture mass flux G at *STP*, $\text{kg}/\text{sec}\cdot\text{m}^2$; (d) the detonation temperature, K; and (e) the detonation velocity, m/sec.

4.16 Ignition of homogeneous coal dust-air mixtures confined within an enclosed space, such as mines or coal-fired steam plants, can produce explosive reactions. Consider a carbon dust-air mixture having a 0.8 equivalence ratio initially at 101 kPa and 25°C. For these conditions, calculate (a) the ideal detonation temperature, K; (b) the ideal detonation pressure, kPa; (e) the burned gas density, kg/m^3; (d) the detonation wave velocity, m/sec; and (e) the burned gas velocity, m/sec.

4.17 A detonation occurs in a stoichiometric mixture of propane and air initially at 1 atm and 25°C. The steady detonation wave speed relative to a fixed observer is 1825 m/sec, and the product gas temperature is 2,800K. Assuming ideal complete combustion, calculate (a) product specific heat ratio; (b) product velocity relative to the detonation wave, m/sec; (c) the product mass flux, $\text{kg}/\text{sec}\cdot\text{m}^2$; and (d) detonation pressure, atm.

4.18 Gasoline can audibly knock, or detonate, when burned in many spark-ignition engines. Consider that the reactants at TDC are initially at 260 psia and 1,080°R. Use one-dimensional detonation theory, and assume that gasoline can be represented by normal octane C_8H_{18}. For ideal complete combustion of a stoichiometric mixture, estimate (a) the detonation pressure, psia; (b) the detonation temperature, °R; (c) the burned gas density, lbm/ft^3; (d) the detonation wave velocity, ft/sec; and (e) the burned gas velocity, ft/sec.

4.19 Organic dust inside confined spaces and suspended in air, such as grain elevators and silos, can produce explosive reactions if accidentally ignited. Consider a stoichiometric cellulose-air mixture as a model for the dust. For these conditions, calculate (a) the ideal detonation temperature, °R; (b) the ideal detonation pressure, atm; (c) the burned-gas density, lbm/ft^3; (d) the detonation wave velocity, ft/sec; and (e) the burned-gas velocity, ft/sec.

5

Chemical Kinetics

5.1 INTRODUCTION

Heat- and/or work-producing chemical energy conversion processes have been described previously using overall chemical reaction mechanisms and time-independent energy arguments alone. Actually, combustion is a result of dynamic, or time-dependent, events that occur on a molecular level among atoms, molecules, and radicals species. Many important fuel-engine interface characteristics, therefore, cannot be understood without also introducing additional time-dependent principles of physical chemistry. The dynamic study of molecular chemistry, or *chemical kinetics,* covers subjects including kinetic theory of gases, statistical thermodynamics, quantum chemistry, and elementary reactions and reaction rate theory. In this chapter, a general but simplified overview of this area of the science of combustion will be presented in order to help the combustion engineer better understand kinetic factors that play a major role in efficiently burning any fuel for the purpose of producing heat and/or power while minimizing the formation of incomplete combustion products.

5.2 KINETIC THEORY OF GASES

A simple model for matter in the gas phase developed using kinetic theory of the microscopic world assumes that:

Matter exists as discrete particles or *molecules.*
Molecules can be treated ideally as small spheres of diameter σ.
Mean distance between molecules $\gg \sigma$.
Molecules are in continuous three-dimensional motion.
Each molecule moves in a random direction through space at a different speed.

No appreciable interatomic forces exist between gas molecules except when they collide (zero attractive and infinite repulsive force at contact).

Speed and directional characteristics for any molecule will remain constant until it interacts with another particle or a solid boundary.

Kinetic theory of gases provides both scientists and engineers with useful molecular descriptions of important ideal-gas mixture properties, including density, pressure, temperature, and internal energy. Any overall mixture property of an isolated inert gas mixture at equilibrium, i.e., $P, T, \overline{u}, \hbar,$ or $\overline{\rho},$ will remain constant, even though the kinetic characteristics of all molecules will be continuously changing. Density, or mass per unit volume, is simply total molecular mass associated with molecules contained within a given space divided by that same volume. Continuum and molecular calculations may yield quite different values for density, however, if the number of molecules and/or the volume is quite small, an important physical condition that can occur in vacuum environments or in the Earth's upper atmosphere.

Consider a differential cube *dx dy dz,* shown in Figure 5.1, having characteristic dimensions greater than molecular diameter σ and containing N_A molecules of inert gas A described by a general velocity $\vec{V}$:

$$\vec{V}\langle x, y, z\rangle = \mathrm{X}\,\vec{i} + \mathrm{Y}\,\vec{j} + \mathrm{Z}\,\vec{k}$$

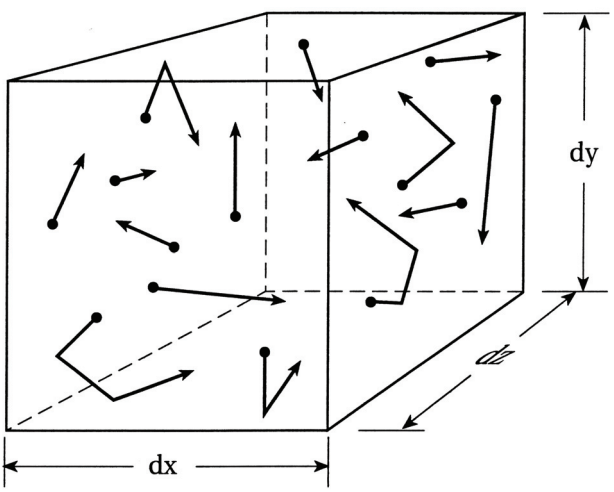

Figure 5.1 Inert gas molecules' kinetic motion in differential molecular cube.

Since the direction and speed of any particular molecule will be changing with time, all molecules do not move at the same velocity $\vec{V}$. It is more appropriate then to describe molecular motion in terms of a statistical speed distribution function ψ, developed by Maxwell in 1860 and given as

$$\psi\langle V\rangle = 4\pi\left[\frac{m}{2\pi k T}\right]^{3/2} V^2 \exp\left\{\frac{-mV^2}{2kT}\right\} \tag{5.1}$$

where

m = molecular mass of A, $m = MW/N_0$, gmole/molecule
V = molecular speed, cm/sec
N_0 = Avogadro's constant = 6.02×10^{23} molecules/mole
k = Boltzmann's constant = 1.3804×10^{-16} g·cm^2/sec^2 K

The speed distribution function ψ yields distributed molecular speeds that are functions of molecular mass m, absolute temperature T, and Boltzmann's constant k, i.e., universal gas constant per molecule. The most probable speed, the velocity magnitude associated with the maximum of the Maxwell distribution function, is found to equal

$$V_{mp} = \left[\frac{2kT}{m}\right]^{1/2} \quad \text{cm/sec} \tag{5.2}$$

while mean speed for all molecules is given as

$$V_m = \left[\frac{8kT}{\pi m}\right]^{1/2} \quad \text{cm/sec} \tag{5.3}$$

and mean square speed is found to be equal to

$$\overline{V_m^2} = \left[\frac{3kT}{m}\right]^{1/2} \quad \text{cm/sec} \tag{5.4}$$

Consider an A molecule moving through the differential volume at a mean speed V_m. The volume swept out per unit time by this molecule, i.e., base × height, would equal

$$\text{volume} = \pi\sigma^2 V_m \tag{5.5}$$

$$= \pi\sigma^2\left[\frac{8kT}{\pi m}\right]^{1/2} = \sigma^2\left[\frac{8\pi kT}{m}\right]^{1/2} \text{ cc/sec} \tag{5.6}$$

The ideal number of molecular collisions of an A molecule per unit time with all other A molecules in this swept volume is then equal to the volume swept out per unit time multiplied by the number of A molecules within the volume, or

$$\text{No. A collisions} = \sigma^2 \left[\frac{8\pi \mathcal{k} T}{m}\right]^{1/2} \left[\frac{N_A}{dx\, dy\, dz}\right]$$

$$= \sigma^2 \left[\frac{8\pi \mathcal{k} T}{m}\right]^{1/2} [\overline{A}] \qquad \text{collisions/sec} \qquad (5.7)$$

where $[\overline{A}]$ is the molar concentration of A or

$$[\overline{A}] = \left[\frac{N_A}{dx\, dy\, dz}\right] \qquad \text{molecules/cc}$$

The collision frequency Z, or total frequency of collisions between all molecules of A, then equals the number of A molecules per unit volume multiplied by the rate of collisions per molecule of A.

$$Z_{AA} = [\overline{A}][\overline{A}]\sigma^2 \left[\frac{8\pi \mathcal{k} T}{m}\right]^{1/2}$$

The *mean free path* λ, or average distance traveled by any molecule between collisions, is determined knowing the distance traveled per unit time and dividing by the number of collisions per unit time that this particle experiences or

$$\lambda = \frac{V_m}{\pi \sigma^2 V_m [\overline{A}]} = \frac{1}{\pi \sigma^2 [\overline{A}]} \qquad \text{cm/collisions} \qquad (5.8)$$

A more precise analysis of the collisional process that accounts for movement of all molecules yields a corrected expression for mean free path as

$$\lambda = \frac{1}{\sqrt{2}\pi \sigma^2 [\overline{A}]} \qquad \text{cm/collisions} \qquad (5.9)$$

The *bimolecular collision frequency Z,* or total frequency of collisions between molecules of species A and B per unit volume of gas, can be obtained from a rigorous analysis of the two-body collision process, with results found to equal

$$Z_{AB} = [\overline{A}][\overline{B}] \frac{\sigma_{AB}^2}{\delta} \left[\frac{8\pi \mathcal{k} T}{m_{AB}^*}\right]^{1/2} \qquad (5.10)$$

where

$$\sigma_{AB} = \text{average diameter} = (\sigma_A + \sigma_B)/2$$

$$m_{AB}^* = \text{reduced molecular mass} = [(m_A + m_B)/m_A m_B]$$

$$\delta = \text{symmetry factors}$$

$$= 1 \text{ if } A \neq B$$

$$= 2 \text{ if } A = B$$

EXAMPLE 5.1 Kinetic theory of gases predicts a molecular diameter of 4×10^{-8} cm for air at 0°C and 1-atm pressure. Using this information, determine the following: (a) mass of an air molecule, g/molecule; (b) molecular density, number of molecules/cc; (c) mean molecular speed, cm/sec; (d) mean free path, cm/collision; and (e) collision frequency, number of collisions/sec.

Solution:

1. Molecular mass:

$$m = \frac{MW}{N_0} = \frac{28.97 \text{ g/gmole}}{6.02 \times 10^{23} \text{ molecules/gmole}}$$

a. $m = 4.81 \times 10^{-23}$ g/molecule

2. Molecular density:

$$\rho = \frac{P}{RT} = \frac{(101{,}000 \text{ N/m}^2)(28.97 \text{ kg/kgmole})(1{,}000 \text{ g/kg})}{(8{,}314 \text{ N} \cdot \text{m/kgmole} \cdot \text{K})(273\text{K})(100 \text{ cm/m})^3}$$

$$= 1.29 \times 10^{-3} \text{ g/cm}^3$$

$$n_0 = \frac{\rho}{m} = \frac{1.289 \times 10^{-3} \text{ g/cm}^3}{4.81 \times 10^{-23} \text{ g/molecule}}$$

b. $n_0 = 2.68 \times 10^{19}$ molecules/cm^3

3. Mean molecular speed:

$$V_m = \frac{8kT}{\pi m}^{1/2} = \left[\frac{(8)(1.38 \times 10^{-16} \text{ cm}^2 \cdot \text{g/sec}^2 \cdot \text{K})(273\text{K})}{(\pi)(4.81 \times 10^{-23} \text{ g/molecule})}\right]^{1/2}$$

c. $V_m = 4.47 \times 10^4$ cm/sec

4. Mean free path:

$$\lambda = \frac{1}{\sqrt{2}\,\pi\sigma^2 n_0}$$

$$= \frac{1}{\sqrt{2}\,(\pi)(4 \times 10^{-8})^2 (2.68 \times 10^{19} \text{ molecules/cm}^2)}$$

d. $\lambda = 2.1 \times 10^{-5}$ cm/molecular collision

5. Collision frequency Z:

$$Z = \frac{V_m \langle \text{cm/sec} \rangle}{\langle \text{cm/molecular collision} \rangle}$$

$$= \frac{4.47 \times 10^{4} \text{ cm/sec}}{2.1 \times 10^{-5} \text{ cm/molecular collision}}$$

e. $Z = 2.13 \times 10^{9}$ molecular collisions/sec

Pressure within a volume can be interpreted kinetically as the net normal force at solid boundaries resulting from all individual momentum exchange processes occurring within from molecular motion. Note that the total kinetic energy and momentum of gas molecules within this volume will remain constant since all collisions are perfectly elastic. Consider again the motion of a single A molecule of mass m traveling through the original differential cube $dx\ dy\ dz$ with the mean velocity $\vec{V}_m$,

$$\vec{V}_m = X_m \vec{i} + Y_m \vec{j} + Z_m \vec{k} \tag{5.11}$$

The normal force exerted on the $dy\ dz$ wall by this A molecule is equal to its change in x momentum from $+MX_m$ to $-MX_m$ during each collision or

$$\left|F_X\right|_{\text{A}} = 2mX_m \tag{5.12}$$

An A molecule will travel the distance dx in a time interval dx/X_m and the time between repetitive collisions with the $dy\ dz$ face is equal to $2\ dx/X_m$. The number of collisions of an A molecule with the $dy\ dz$ face is, therefore, equal to $X_m/2dx$, and the change in x momentum per unit time is then the product of the number of collisions per unit time and momentum exchange per molecule or

$$mV_x)_{\text{A}} = \left[\frac{X_m}{2\ dx}\right]\left[2mX_m\right] = \frac{2mX_m^2}{2\ dx}$$

$$mV_X)_{\text{A}} = \frac{mX_m^2}{dx} \tag{5.13}$$

Table 5.1 Molecular Diameter σ, and Mean Free Path λ for Several Gases at *STP*

Gas	σ, m $\times 10^{-10}$	λ, m $\times 10^{-8}$
Argon	2.90	10.9
Helium	2.00	22.9
Nitrogen	3.50	7.46
Oxygen	2.95	10.5
Carbon dioxide	3.30	8.39
Ammonia	3.00	10.2

Source: Zucrow, M. J. and Hoffman, J. D., *Gas Dynamics, Vol. I*, © John Wiley & Sons, New York, 1976. Reprinted with permission of John Wiley & Sons, Inc.

The pressure, i.e., force per unit area, due to an A molecule is equal to

$$P_X)_{\mathrm{A}} = \frac{mX_m^2}{dx\ dy\ dz} \tag{5.14}$$

and total pressure due to all A molecules is then given as

$$P_x = \frac{\Sigma mX_m^2}{dx\ dy\ dz} = \frac{1}{dx\ dy\ dz}\Sigma mX_x^2 \tag{5.15}$$

Since pressure at equilibrium must be the same for all three faces, it follows that

$$P = P_x = P_y = P_z = \frac{1}{3\ dx\ dy\ dz}\Sigma m\left[X_m^2 + Y_m^2 + Z_m^2\right] = \frac{1}{3V}\Sigma mV_m^2$$

and

$$PV = \frac{2}{3}\left[\frac{1}{2}\Sigma mV_m^2\right] \tag{5.16}$$

A simple kinetic model for internal energy of an inert ideal gas mixture of A molecules would equal the total sum of kinetic energy of all translating A molecules or

$$\overline{U} = \Sigma\overline{E}_{\mathrm{trans}} = \frac{1}{2}\Sigma mV_m^2 \tag{5.17}$$

The ideal-gas law found in Chapter 1 was written as

$$PV = N\overline{R}T \tag{1.4}$$

Combining Equations (5.16) and (1.4) yields

$$\frac{2}{3}\left[\frac{1}{2}\Sigma mV_m^2\right] = N_{\mathrm{A}}\overline{R}T$$

or

$$T = \frac{2}{3}\left(\frac{1}{N_{\mathrm{A}}\overline{R}}\right)\Sigma mV_m^2 \tag{5.18}$$

Equation (5.18) provides a kinetic definition for the temperature of a monatomic gas. Increasing the mean molecular speed will raise both the gas temperature and the internal energy. Note also that since all collisions are elastic, two systems of the same gas at the same temperature but different pressure and/or volume could have quite different collision frequencies, but would still have the same internal energy per unit mass since internal energy of an ideal gas is only a function of temperature.

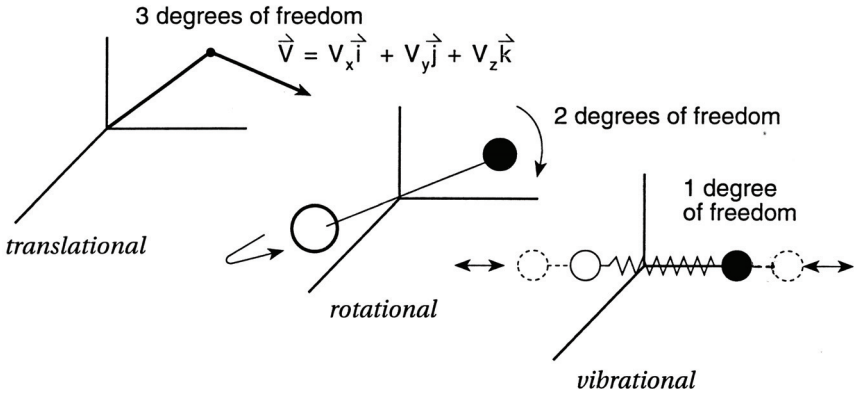

Figure 5.2 Internal energy storage modes of a gaseous diatomic molecule.

Table 5.2 C/H/N/O Molecular Bond Strengths

Bond	kcal/mole	
C–C	85.5	
C–H	98.1	
	143.0	
	194.3	
C–C	78.3	
C–N	81.0	
C–O	85.8	
C–S	63.7	
	167	(formaldehyde)
	172	(higher aldehydes)
	183	(ketones)
	210.6	
H–H	104.2	
N–N	60.0	
N–H	88.0	
	225.5	
O–O	33.1	
O–H	110.6	

Source: Penner, S., *Chemistry Problems in Jet Propulsion*, Pergamon Press, New York, 1957. With permission.

Combustion chemistry involves nonmonatomic gaseous constituents that do not remain inert, and many species that undergo significant molecular rearrangement and energy transformation during a reaction process. At temperatures associated with the process of combustion, molecules can store quantized energy in rotational, vibrational, and electronic modes in addition to that of simple translational kinetic energy; see Figure 5.2. Thus, molecular structure of reactive constituents is also an important factor in gas-phase chemical conversion processes. A complete understanding of molecular physical chemistry and combustion cannot be described using kinetic theory of gases and will require additional knowledge of subjects including statistical thermodynamics and quantum chemistry. Energy associated with an overall combustion process is not simply the kinetic molecular energy but rather a result of effective collisions between reactive molecules that can cause a disruption of molecular structure and release energy stored within molecular bonds; see Table 5.2.

EXAMPLE 5.2 Acetylene, C_2H_2, is an unsaturated hydrocarbon compound having the structure $H-C\equiv C-H$. Using the standard state reactions and bond energies found in Table 5.2, estimate the heat of formation of acetylene.

Solution:

1. Standard state reaction:

$$2C_S + H_2 \overset{STP}{\rightarrow} C_2H_2 + \Delta H_f$$

2. Carbon gas formation reaction energy, from Table B.1 in Appendix B:

$$C_S \overset{STP}{\rightarrow} C_G + 170.9 \quad \text{kcal}$$

3. Hydrogen formation reaction energy, from Table B. 1 in Appendix B:

$$H_2 \rightarrow 2H + 104.2 \ \text{kcal}$$

4. Using bond energies then for the reaction

$$2C_G + 2H \overset{STP}{\rightarrow} C_2H_2 - \Delta H_r$$

where

$$\Delta H_r = 2\times C-H \ \text{bond energy} + C\equiv C \ \text{bond energy}$$
$$= (2)(98.1) + (194.3) = 390.5 \ \text{kcal}$$

5. The standard state reaction, No. 1 above, can be determined as

$$2C_S \rightarrow 2C_G + 341.8$$
$$H_2 \rightarrow 2H + 104.2$$
$$2C_G + 2H \rightarrow C_2H_2 - 390.5$$
$$2C_S + H_2 \rightarrow C_2H_2 + \Delta H_f$$

or

$$\Delta H_f = -390.5 + 341.8 + 104.2 = 55.5 \text{ kcal}$$

This value is in reasonable agreement with the value of 54.194 found in Table B.1 in Appendix B.

5.3 COLLISION THEORY AND CHEMICAL REACTIONS

Chemical kinetics provides a means of describing dynamic events effecting changes that molecular components undergo within a reactive mixture. Reaction equations that describe actual molecular activity occurring on the microscopic level are called *elemental reactions*. For example, the elemental reaction, given by Equation (5.19) below, shows that two hydrogen atoms are produced from the dissociation of a single hydrogen molecule.

$$H_2 + M \rightarrow H + H + M \tag{5.19}$$

Equation (5.20), an overall reaction equation, however, is not an example of an elemental reaction since interaction of a single methane molecule with two oxygen molecules is not the actual kinetic mechanism for forming carbon dioxide and water.

$$CH_4 + 2O_2 \rightarrow CO_2 + 2H_2O \tag{5.20}$$

A generalized elemental reaction between atomic species A and B to form products C and D is expressed in Equation (5.21) as

$$a\text{A} + b\text{B} \rightarrow c\text{C} + d\text{D} \tag{5.21}$$

Note that atomic species A, B, C, and D may be molecules, radicals, and/or atoms. Equation (5.21) shows that only interatomic interactions between reactant species A and B occur in order to form the products C and D. Furthermore, the elemental reaction above assumes that reactants A and B are inert until they approach each other, at which point rearrangement of molecular structures to yield new species C and D occurs only when these constituents are near one another. After elemental product species C and D are formed, they separate from a molecular conversion site and remain stable until each, in turn, comes into close contact with additional molecules, atoms, radicals, and/or solid boundaries; see Figure 5.3.

A plot of species concentration versus reaction time is useful in the study of the nature of an elemental reaction rate; see Figure 5.4. The *rate of reaction R*, or change in concentration of reactive species *i* with respect to time for an elemental reaction, can be expressed as

$$R_i \equiv -\frac{d[-]_i}{dt} \tag{5.22}$$

where

R = reaction rate
$[-]$ = molar concentration, gmole/cc
t = time, sec

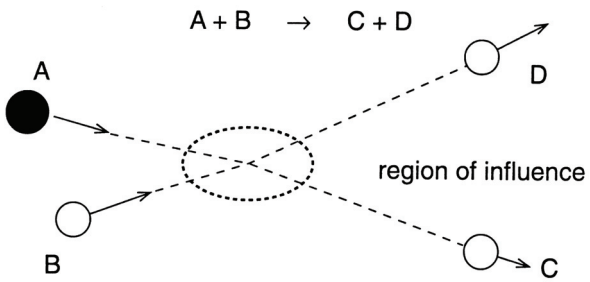

Figure 5.3 Kinetic model for molecular rearrangement via elemental reaction collisions.

Reaction rates can be thought of as a chemical velocity of reaction; i.e., higher speeds imply greater rates of conversion. The general relationships between rate of reaction of A and B and reactant species molar concentrations for the elemental reaction given by Equation (5.21) have been found to satisfy the expressions

$$R_A = \frac{-1}{a}\frac{d[\overline{A}]}{dt} = k[\overline{A}]^a[\overline{B}]^b \tag{5.23a}$$

$$R_B = \frac{-1}{b}\frac{d[\overline{B}]}{dt} = k[\overline{A}]^a[\overline{B}]^b \tag{5.23b}$$

where

k = elemental rate constant
$a,b, \ldots$ = reaction integers indicating the number of atomic members of A, B, … participating in the atomic reaction (usually 1 or 2).

The *molecularity,* or order, of an elemental reaction is the number of atomic members that participate in a reaction process; see Table 5.3 and Figure 5.5. For the general elemental reaction given by Equation (5.21),

a ≡ order of reaction with respect to A
b ≡ order of reaction with respect to B
$a + b$ ≡ overall reaction order

A reaction in which the slope of concentration versus time yields a straight line is termed a zeroth-order reaction, while a reaction in which the slope satisfies the expression

$$R_A = \frac{d[\overline{A}]}{dt} = -k[\overline{A}] \tag{5.24}$$

is called a first-order or unimolecular reaction with respect to A. Equations (5.25a) and (5.25b) are examples of bimolecular or second-order reactions, predominant reactions that occur in high-temperature combustion.

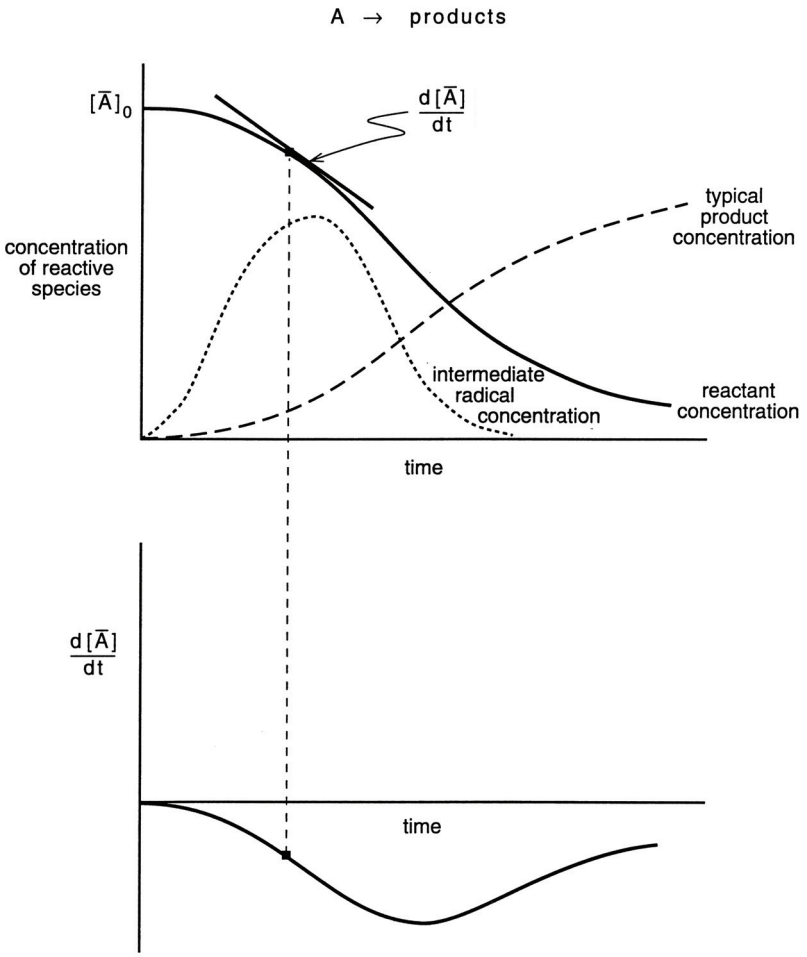

Figure 5.4 Composition-time schematic for decomposition.

$$R_A = \frac{d[\bar{A}]}{dt} = -k[\bar{A}][\bar{B}] \tag{5.25a}$$

or

$$R_A = \frac{d[\bar{A}]}{dt} = -k[\bar{A}][\bar{A}] \tag{5.25b}$$

Note that if B is inert during a bimolecular reaction, a second-order reaction may appear to be first-order in A; i.e., $[\bar{B}] = \text{const}$.

Equations (5.23a) and (5.23b) show that chemical velocity R depends on concentrations of reactive species A and B, reaction integers a and b, and a rate constant k. Elemental reaction rates do depend on absolute reaction temperature; i.e., higher reaction temperatures produce higher reaction rates, while lower temperatures result in lower reaction rates. Many experimentally measured elemental reactions will double their kinetic speed with each 10K (10°R) increase in reaction temperature.

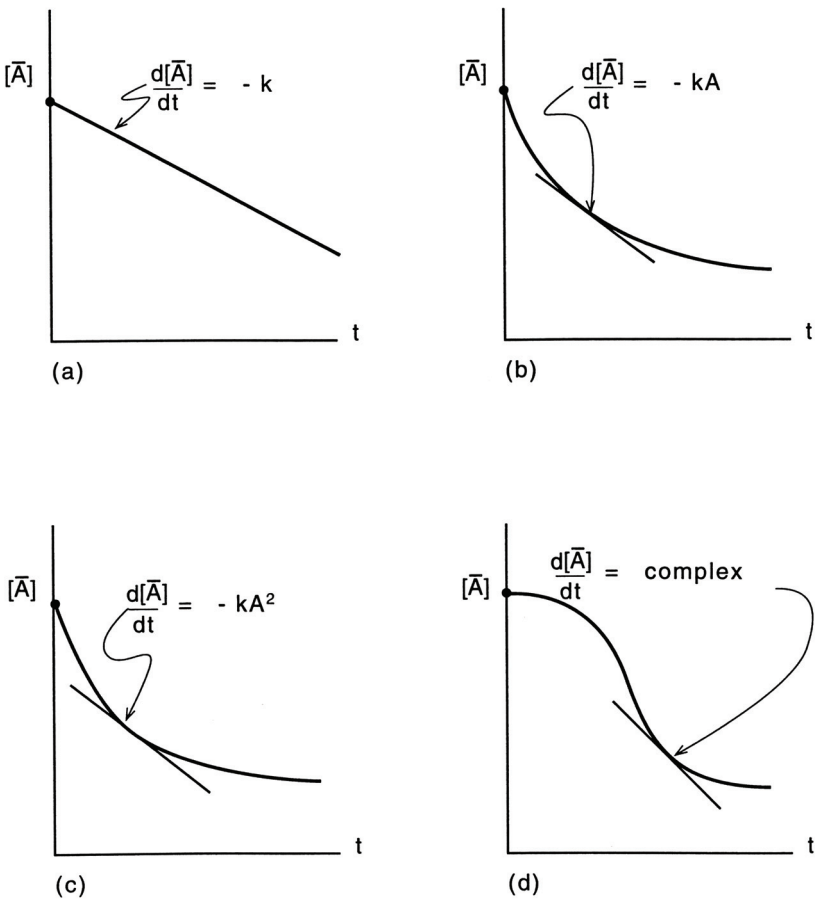

Figure 5.5 Concentration vs. time diagrams for various chemical reactions: (a) zeroth-order reaction, (b) first-order reaction, (c) second-order reaction, (d) autocatalytic oxidation reaction.

Table 5.3 Characteristics of Different-Order Reactions

Reaction order		Differential equation	Rate constant k_A from integrated equation	Half-life, $t_{1/2}$
0		$-\frac{d[\overline{\mathrm{A}}]}{dt} = k_A$	$\frac{[\overline{\mathrm{A}}]_0 - [\overline{\mathrm{A}}]}{t}$	$\frac{[\overline{\mathrm{A}}]_0}{2k_A}$
1		$-\frac{d[\overline{\mathrm{A}}]}{dt} = k_A[\overline{\mathrm{A}}]$	$\frac{1}{t}\ln\frac{[\overline{\mathrm{A}}]_0}{[\overline{\mathrm{A}}]}$	$\frac{1}{k_A}\ln 2$
2	Type I	$-\frac{d[\overline{\mathrm{A}}]}{dt} = k_A[\overline{\mathrm{A}}]^2$	$\frac{1}{t}\left(\frac{1}{[\overline{\mathrm{A}}]} - \frac{1}{[\overline{\mathrm{A}}]_0}\right)$	$\frac{1}{k_A[\overline{\mathrm{A}}]_0}$
	Type II	$-\frac{d[\overline{\mathrm{A}}]}{dt} = k_A[\overline{\mathrm{A}}][\overline{\mathrm{B}}]$	$\frac{a\ln([\overline{\mathrm{A}}]/[\overline{\mathrm{A}}]_0) \times ([\overline{\mathrm{B}}]_0/[\overline{\mathrm{B}}])}{t(b[\overline{\mathrm{A}}]_0 - a[\overline{\mathrm{B}}]_0)}$	$\frac{a}{k_A(a[\overline{\mathrm{B}}]_0 - b[\overline{\mathrm{A}}]_0)}\ln\left(2 - \frac{b[\overline{\mathrm{A}}]_0}{a[\overline{\mathrm{B}}]_0}\right)$
3	Type I	$-\frac{d[\overline{\mathrm{A}}]}{dt} = k_A[\overline{\mathrm{A}}]^3$	$\frac{1}{2t}\left(\frac{1}{[\overline{\mathrm{A}}]^2} - \frac{1}{[\overline{\mathrm{A}}]_0^2}\right)$	$\frac{3}{2k_A[\overline{\mathrm{A}}]_0^2}$
	Type II	$-\frac{d[\overline{\mathrm{A}}]}{dt} = k_A[\overline{\mathrm{A}}]^2[\overline{\mathrm{B}}]$	$\frac{-a}{t(b[\overline{\mathrm{A}}]_0 - a[\overline{\mathrm{B}}]_0)}\left(\frac{1}{[\overline{\mathrm{A}}]} - \frac{1}{[\overline{\mathrm{A}}]_0}\right) + \frac{ab}{t(b[\overline{\mathrm{A}}]_0 - a[\overline{\mathrm{B}}]_0)^2}\ln\left(\frac{[\overline{\mathrm{A}}][\overline{\mathrm{B}}]_0}{[\overline{\mathrm{A}}]_0[\overline{\mathrm{B}}]}\right)$	$\frac{-a}{k_A[\overline{\mathrm{A}}]_0(b[\overline{\mathrm{A}}]_0 - a[\overline{\mathrm{B}}]_0)} - \frac{ab\ln(2 - b[\overline{\mathrm{A}}]_0/a[\overline{\mathrm{B}}]_0)}{k_A(b[\overline{\mathrm{A}}]_0 - a[\overline{\mathrm{B}}]_0)^2}$
	Type III	$-\frac{d[\overline{\mathrm{A}}]}{dt} = k_A[\overline{\mathrm{A}}][\overline{\mathrm{B}}][\overline{\mathrm{C}}]$		
n		$-\frac{d[\overline{\mathrm{A}}]}{dt} = k_A[\overline{\mathrm{A}}]^n$	$\frac{1}{(n-1)t}\left(\frac{1}{[\overline{\mathrm{A}}]^{n-1}} - \frac{1}{[\overline{\mathrm{A}}]_0^{n-1}}\right)$	$\frac{\left(2^{n-1} - 1\right)}{k_A[\overline{\mathrm{A}}]_0^{n-1}(n-1)}$

Source: Benson, S. W., *The Foundations of Chemical Kinetics*, Robert E. Krieger Publishing Co., Malabar, FL, 1982. With permission.

EXAMPLE 5.3 The high-temperature $H_2 - O_2$ reaction involves the elementary initial reaction

$$H_2 + M \rightarrow H + H + M$$

where

$[\overline{H}_2]$ = diatomic hydrogen concentration
$[\overline{H}]$ = monatomic hydrogen concentration
$[\overline{M}]$ = total mixture concentration

(a) Write the reaction rate expression of H_2; (b) determine the relationship between $[H_2]$ and time; (c) repeat part (b) for [H]; and (d) evaluate an expression for the time it takes the concentration of H_2 to be reduced by one-half by this reaction.

Solution:

1. Reaction rate:

$$\frac{1}{1}\frac{d[\overline{H}_2]}{dt} = -k[\overline{H}_2][\overline{M}]$$

$$\frac{d[\overline{H}_2]}{[\overline{H}_2]} = -k[\overline{M}]dt$$

Assume that

$$k, [\overline{M}] \text{ are constant } [\overline{M}] \gg [\overline{H}_2]$$

Integrating yields

$$\ln\frac{[\overline{H}_2]}{[\overline{H}_2]_0} = -k[\overline{M}](t - t_0)$$

where

$[\overline{H}_2]_0$ = H_2 concentration at $t = t_0$
$[\overline{H}_2]$ = H_2 concentration at t
t_0 = initial reaction time

a. $$\frac{[\overline{H}_2]}{[\overline{H}_2]_0} = \exp\{-k[\overline{M}]t\}$$

2. Concentration versus time:

Let

$$[\overline{H}_2] = [\overline{H}_2]_0 - x$$

where

$$x = \text{extent of reaction}$$

$$[\overline{\text{H}}] = 2x$$

$$\frac{[\overline{\text{H}}]}{[\overline{\text{H}}_2]_0} = 2\left\{\frac{[\overline{\text{H}}_2]_0 - [\overline{\text{H}}_2]}{[\overline{\text{H}}_2]_0}\right\}$$

$$= 2\left\{1 - \frac{[\overline{\text{H}}_2]}{[\overline{\text{H}}_2]_0}\right\}$$

b. $$= 2\left[1 - \exp\left(-k[\overline{\text{M}}]t\right)\right]$$

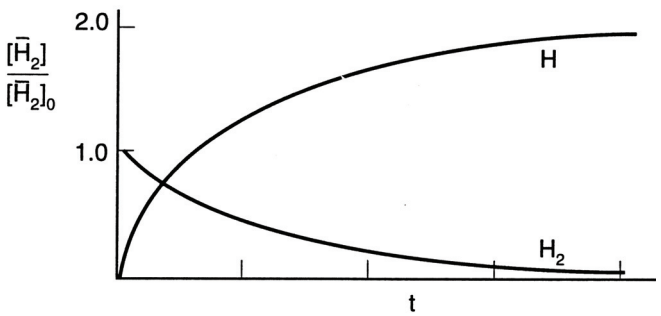

3. $[\overline{\text{H}}_2]$ half-life:

$$\frac{[\overline{\text{H}}_2]}{[\overline{\text{H}}_2]_0} = 0.5 - \exp\left\{-k[\overline{\text{M}}]t_{1/2}\right\}$$

c. $$t_{1/2} = \frac{-\ln 0.5}{k[\overline{\text{M}}]} = \frac{0.6431}{k[\overline{\text{M}}]}$$

Comments: This problem illustrates how an elementary reaction can be integrated to predict the concentration versus time in the simplest case.

Several theoretical models have been utilized to predict the observed behavior of an elemental rate constant k, including collision theory, statistical thermodynamics, and quantum mechanics. The following arguments will be based on the simple collision theory presented in Section 5.2. At first approximation, it is assumed that an elemental reaction occurs whenever appropriate reactant molecules and/or atoms collide. Recall from Section 5.2 that the frequency of collisions between two species A and B was equal to

$$Z_{\text{A–B}} = \sigma_{\text{A–B}}^2\left\{8\pi \boldsymbol{k} N_0 T\left[\frac{m_\text{A} + m_\text{B}}{m_\text{A} m_\text{B}}\right]\right\}^{1/2}[\overline{\text{A}}][\overline{\text{B}}] \qquad (5.10)$$

In this case, the ideal reaction rate for atomic species A colliding with species B would equal

$$R_A = Z_{A-B} \tag{5.26}$$

Combining Equations (5.7a), (5.8), and (5.9), and rearranging yield a collision expression for the rate constant k as

$$k = \sigma_{A-B}^2 \left\{ 8\pi \mathbf{k} N_0 T \left[\frac{m_A + m_B}{m_A m_B} \right] \right\}^{1/2} \tag{5.27}$$

The assumption that each collision results in chemical reaction yields rate constants that are unrealistically high. In fact, collisions do occur between species that do not result in chemical reaction. An engineering approximation still based on collision theory is to assume that only a fraction of these molecular collisions are capable of producing chemical reactions or

$$R_{A-B} = f \times Z_{A-B} \tag{5.28}$$

where f = fraction of collisions that result in chemical reactions; $f \ll 1.0$.

Arrhenius (1889) proposed that the temperature dependency of the rate constant k could be expressed as

$$k = C \times \exp\left\{ \frac{-\Delta \overline{E}}{\overline{R} T} \right\} \tag{5.29}$$

or

$$\ln k = \ln C - \Delta \overline{E} / \overline{R} T$$

where

C = effective conversion frequency factor
$\Delta \overline{E}$ = reaction activation energy
$\overline{R}$ = universal gas constant
T = absolute reaction temperature

Combining Equations (5.27–5.29) yields the following relationship:

$$C \exp\left\{ \frac{-\Delta \overline{E}}{\overline{R} T} \right\} = f \sigma_{AB}^2 \left\{ 8\pi \mathbf{k} N_0 T \left[\frac{m_A + m_B}{m_A m_B} \right] \right\}^{1/2} \tag{5.30}$$

The effective conversion collision frequency factor C is assumed to equal the collision frequency expression or

$$C = \sigma_{A-B}^2 \left\{ 8\pi \mathbf{k} N_0 T \left[\frac{m_A + m_B}{m_A m_B} \right] \right\}^{1/2} \tag{5.31}$$

with the fraction of collisions that result in chemical reactions then equal to

$$f = \exp\left\{\frac{-\Delta \bar{E}}{\bar{R}T}\right\} \tag{5.32}$$

EXAMPLE 5.4 Consider the elementary reaction

$$A + A \rightarrow \text{products}$$

Assume that the molecular weight of A is 50 g/gmole, the effective molecular diameter is 3.5×10^{-8} cm, and the activation energy for the reaction is 40 kcal/gmole. Determine the Arrhenius rate constant k and half-life $t_{1/2}$ using simple collision theory for (a) 500K, (b) 1000K, (c) 1500K, and (d) 2000K. Let $[A]_0 = 1$ gmole/cc.

Solution:

1. Elementary reaction:

$$A + A \rightarrow \text{products}$$

$$\frac{d[A]}{dt} = -k[A][A] = -k[A]^2$$

$$\frac{d[A]}{[A]^2} = -k\,dt$$

$$\int_{[A]_0}^{[A]} \frac{d[A]}{[A]^2} = -\int_0^t k\,dt = -k\int_0^t dt$$

$$\frac{1}{[A]} - \frac{1}{[A]_0} = -kt$$

$$t = \frac{1}{k}\left[\frac{1}{[A]} - \frac{1}{[A]_0}\right]$$

2. Half-life $t_{1/2}$:

for $t_{1/2}$

$$[A] = 0.5[A]_0$$

$$t_{1/2} = \frac{1}{k}\left[\frac{1}{0.5[A]_0} - \frac{1}{[A]_0}\right] = \frac{1}{k[A]_0}$$

3. Arrhenius rate constant:

$$k = \sigma_A^2\left\{8\pi \mathcal{k} N_0 T\left[\frac{2m_A}{m_A^2}\right]\right\}^{1/2} \exp\left\{\frac{-\Delta \bar{E}}{\bar{R}T}\right\}$$

or

$$k = \left(3.5\times10^{-8}\right)^2\left\{8\pi\left(1.38\times10^{-16}\right)\left(6.02\times10^{23}\right)\left(\frac{2}{50}\right)T^{1/2}\right\}\exp\left\{\frac{-40{,}000}{(1.987)(T)}\right\}$$

$$= 1.1195 \times 10^{-11}[T^{1/2}]\exp\left\{\frac{-20{,}131}{T}\right\} \quad \text{cc/sec}\cdot\text{molecule}$$

or since there are 6.02×10^{23} molecules/mole

$$k = 6.739 \times 10^{12} \times T^{1/2} \exp\{-20{,}131/T\}$$

and

$$t_{1/2} = 1/k$$

T, K	K, cc/sec·mole	Sec
500	4.93×10^{-4}	2.03×10^{3}
1,000	3.85×10^{5}	2.60×10^{-6}
1,500	3.87×10^{8}	2.58×10^{-9}
2,000	1.28×10^{10}	7.8×10^{-11}

Figure 5.6 shows the energy versus reaction path plot for an ideal endothermic and an exothermic elementary reaction. In both instances, heat of reaction is the difference in chemical potential energy between reactant and product states. The activation energy is seen as an energy barrier that prevents all collisions from resulting in chemical reactions. Stable molecules have intermolecular forces associated with their chemical bonding that are strong enough to hold the molecular complex together. Successful elemental reactions have sufficient collisional energy in excess of the activation energy that, when redistributed through the colliding complex at the instant of interaction, can cause dissociation or association of single-, double-, or triple-bonded molecules. Table 5.4 lists magnitudes of various elementary C/H/N/O reaction rate constants.

The rate constant k is not a true constant but is dependent on reaction temperature that must be experimentally obtained. For example, the rate constant for the general elemental reaction given by Equation (5.3) can be determined using an initial slope of a concentration versus time plot, in which case the initial reaction temperature and the initial molar concentrations $[\overline{A}]_0$ and $[\overline{B}]_0$ are known. The initial reaction rate then equals

$$R_A = \left(\frac{\Delta[\overline{A}]}{\Delta t}\right)t = 0 \tag{5.33}$$

and

$$R_A = k[\overline{A}]_0^a\,[\overline{B}]_0^b \tag{5.34}$$

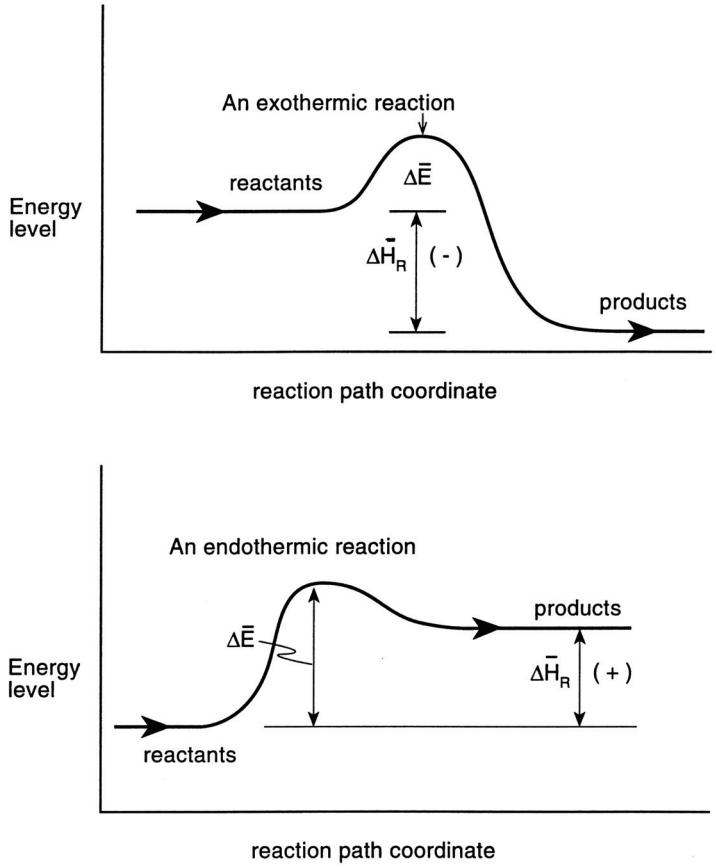

where:

$$\Delta\overline{E} = \text{activation energy}$$
$$\Delta\overline{H}_R = \text{heat of reaction}$$

Figure 5.6 Energy reaction path schematic for an elementary reaction.

Combining Equations (5.33) and (5.34) and solving for the rate constant k yield the expression

$$k = \frac{1}{[A]_0[\overline{B}]_0} \left.\frac{\Delta[\overline{A}]}{\Delta t}\right)_{t=0} \tag{5.35}$$

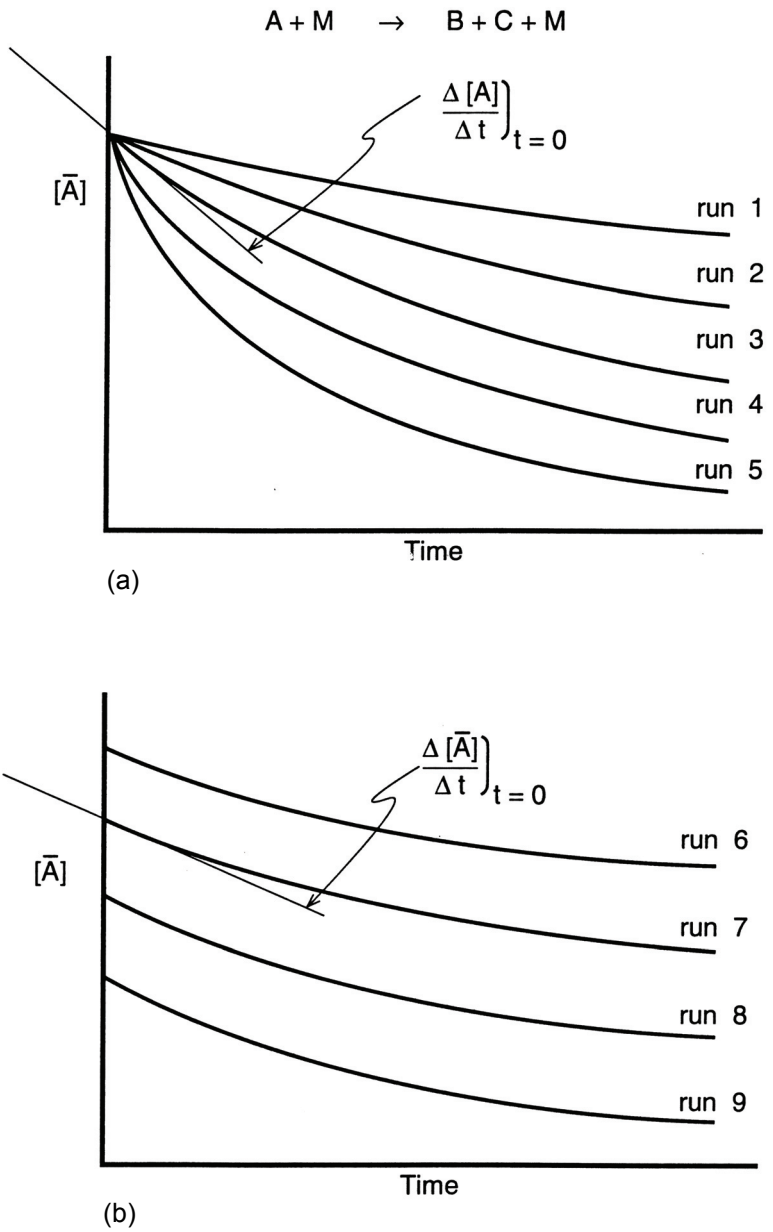

Figure 5.7 Concentration vs. time: (a) fixed initial concentration, variable initial temperatures; (b) fixed initial temperature, variable initial concentration.

Table 5.4 Fitted Elementary C/H/N/O Reaction Rate Constants, $k = A(T/T_{ref})^n \exp(-E_a/RT)$

	Reaction	A	n	E_a	RMSD*
		cm^3/molecule·sec		kcal	
1	$O + CO_2 \rightarrow CO + O_2$	5.06×10^{-12}	0.85	51.52	0.54
2	$O + CO + M \rightarrow CO_2 + M$	2.63×10^{-33}	–0.59	3.88	1.16
3	$O + H + M \rightarrow OH + M$	4.36×10^{-32}	–1	0	0
4	$O + H_2 \rightarrow H + OH$	1.74×10^{-13}	2.95	5.89	0.37
5	$O + NO \rightarrow N + O_2$	4.35×10^{-13}	1.51	38.54	1.36
6	$O + NO_2 \rightarrow NO + O_2$	5.55×10^{-12}	0.12	–0.328	0.05
7	$O + N_2 \rightarrow NO + N$	4.34×10^{-12}	1.33	70.30	0.45
8	$O + N_2O \rightarrow O_2 + N_2$	3.73×10^{-11}	0.15	23.26	1.06
9	$O + O + M \rightarrow O_2 + M$	1.95×10^{-35}	0.79	–2.3	0.69
10	$OH + H + M \rightarrow H_2O + M$	2.03×10^{-30}	–2.09	0.73	1.65
11	$OH + H_2 \rightarrow H_2O + H$	2.46×10^{-12}	1.43	3.51	0.27
12	$OH + N \rightarrow NO + H$	5.02×10^{-11}	–0.292	–0.0364	0.03
13	$OH + OH \rightarrow O + H_2O$	1.03×10^{-12}	1.26	–0.289	0.34
14	$H + CO + M \rightarrow HCO + M$	1.85×10^{-33}	–0.355	1.6	0.26
15	$H + CO_2 \rightarrow CO + OH$	5.8×10^{-10}	–0.296	27.01	0.16
16	$H + H + M \rightarrow H_2 + M$	3.27×10^{-32}	–10.5	–0.0721	2.11
17	$H + HNO \rightarrow H_2 + NO$	9.11×10^{-12}	1.14	–0.113	0.69
18	$H + NO_2 \rightarrow NO + OH$	2.18×10^{-9}	–1.47	1.69	0.13
19	$H + N_2O \rightarrow OH + N_2$	3.8×10^{-10}	–0.323	16.16	0.64
20	$H + O_2 \rightarrow O + OH$	2.91×10^{-10}	–0.0903	16.11	0.43
21	$H + O_2 + M \rightarrow HO_2 + M$	3.26×10^{-32}	–0.802	–0.0371	0.57
22	$CO + NO_2 \rightarrow NO + CO2_2$	1.61×10^{-10}	–0.0584	33.83	0.08
23	$CO + OH \rightarrow CO_2 + H$	7.55×10^{-14}	1.16	–0.441	0.24
24	$CO + O_2 \rightarrow CO_2 + O$	6.66×10^{-11}	–0.983	49.61	1.28

*RMSD = Root mean square deviation of fitted expressions from fitting data. T_{ref} = 298K

Refer to the NIST reference and the discussion in the text for more information on how these values were derived

	Reaction	A	n	E_a	RMSD*
		cm^3/molecule·sec		kcal	
25	$H + NO + M \rightarrow HNO + M$	7.65×10^{-32}	–1.01	0.33	0.21
26	$HCO + M \rightarrow H + CO + M$	2.67×10^{-9}	–1.18	17.75	0.76
27	$HCO + H \rightarrow H_2 + CO$	1.59×10^{-10}	0.07	–0.184	0.93
28	$HCO + O \rightarrow OH + CO$	4.99×10^{-11}		0	0
29	$HCO + OH \rightarrow CO + H_2O$	6.69×10^{-11}	0.16	–0.226	0.64
30	$HO_2 + CO \rightarrow CO_2 + OH$	1.01×10^{-10}	0.47	23.14	0.16
31	$HO_2 + H \rightarrow OH + OH$	1.65×10^{-10}	0.03	1.05	0.88
32	$HO_2 + H \rightarrow H_2 + O_2$	1.2×10^{-11}	0.91	0.1	0.43
33	$HO_2 + H \rightarrow O + H_2O$	3.83×10^{-11}	0.34	1.06	0.64
34	$HO_2 + HO_2 \rightarrow H_2O_2 + O_2$	1.66×10^{-11}		1	0
35	$HO_2 + H_2 \rightarrow H + H_2O_2$	4.35×10^{-16}	4.78	13.93	1.89
36	$HO_2 + NO \rightarrow OH + NO_2$	2.82×10^{-12}	0.14	–0.638	0.06
37	$HO_2 + O \rightarrow OH + O_2$	2.9×10^{-11}		–0.412	0.03
38	$HO_2 + OH \rightarrow H_2O + O_2$	6.33×10^{-11}	–0.326	–0.25	0.36
39	$H_2O_2 + M \rightarrow OH + OH + M$	6.16×10^{-3}	–5.44	53.22	0.6
40	$H_2O_2 + H \rightarrow H_2O + OH$	6.06×10^{-12}	0.85	2.9	0.36
41	$CH_3 + O_2 \rightarrow HCO + H_2O$	1.66×10^{-12}			0
42	$CH_4 + M \rightarrow CH_3 + H + M$	5.06	–5.99	107	1.75
43	$CH_4 + H \rightarrow CH_3 + H_2$	4.47×10^{-12}	1.92	9.75	1.16
44	$CH_4 + OH \rightarrow CH_3 + H_2O$	7.76×10^{-13}	2.07	2.77	0.54
45	$CH_4 + O \rightarrow CH_3 + OH$	2.18×10^{-12}	2.1	7.41	0.34
46	$CH_4 + O_2 \rightarrow CH_3 + HO_2$	2.96×10^{-12}	1.55	53.74	1.66
47	$C_2H_4 + H \rightarrow C_2H3 + H_2$	1.75×10^{-11}	1.73	13.55	0.56
48	$C_2H_4 + M \rightarrow C_2H_3 + H + M$	3.02×10^{-5}	–1.38	103	0.11

Source: NIST Chemical Kinetics Database (Web version 7.0, release 1.3), NIST Standard Reference Database 133, W. G. Mallard, F.Westley, J. T. Herron, R. F. Hampson, D. H. Frizzell, D. R. Burgess, Jr., A. Fahr, J. Hudgens, R. E. Huie, R. D. Levin, C.-Y. Lin, J. A. Manion, V. Orkin, and W. T. C. Allison, http://kinetics.nist.gov/. Values given in the table are representative of what can be produced using the fitting methods provided at the NIST web site and do not necessarily represent values reported from experimental measurements. As such, they should neither be attributed to nor considered to be endorsed by NIST.

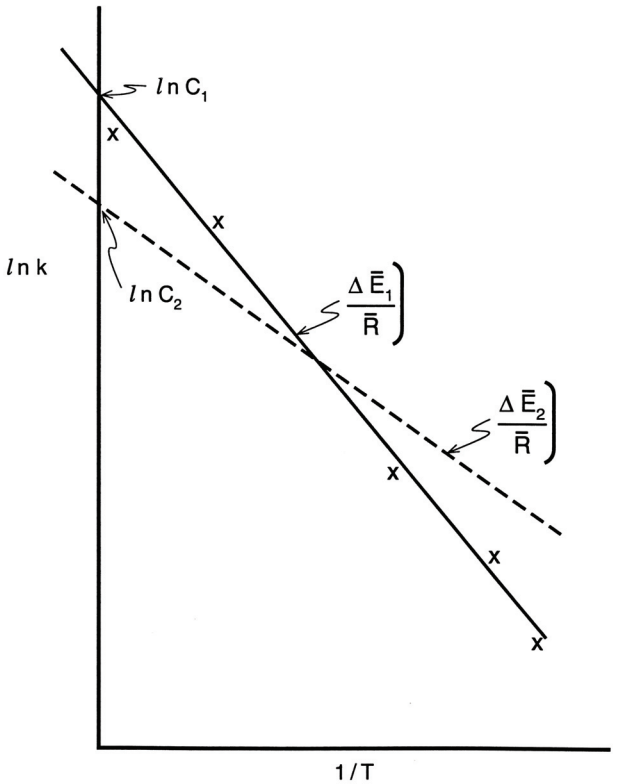

Figure 5.8 Elementary reaction Arrhenius rate constant vs. temperature (schematic diagram).

Figure 5.7 illustrates an initial slope analysis used to determine the effect of varying concentration and reaction temperature on the rate constant k for this general elemental reaction. Experimentally obtained elementary rate constant data, such as those found using Equation (5.35), should yield a straight line on natural log versus inverse temperature coordinates, as represented by Figure 5.8. The activation energy can then be obtained from the slope of the curve-fitted data and frequency factor from the abscissa intercept. Table 5.4 lists fitted Arrhenius expressions for several important elementary reactions. Expressions for the various C/H/N/O gas-phase reaction rate constants were derived by a least-squares fit of existing data selected by the author from the literature as found in the NIST Chemical Kinetics Database. The least-squares fitting was performed using a tool available on the NIST Chemical Kinetics Database web site. This technique, by careful selection and fitting, allows reported rate constant data over a selected temperature range to be represented with a single relationship.

Overall rate expressions are often written to correlate combustion of a given fuel as

$$\frac{d[\text{fuel}]}{dt} = -[\text{fuel}]^{\alpha}[\text{oxidant}]^{\beta} \tag{5.36}$$

Equation 5.36, however, is an empirical expression based on fitted experimental data and not on elemental reaction analysis.

5.4 COMPLEX CHEMICAL KINETICS MECHANISMS

Gas-phase chemical kinetics associated with most operating combustion machinery is compounded by both the complexity of the many concurrent elemental molecular reactions associated with an energy conversion process and the heterogeneous boundaries within which these chemical events are confined. No effort will be made to discuss the fuel-engine chemical kinetics interface for any particular combustion device in this chapter. Instead, only basic dynamic elements of a combustion process will be discussed. In the following section, bimolecular abstraction, association, branching, and dissociation reactions will be described, kinetic events that play a major role in high-temperature gas-phase oxidation chemistry.

EXAMPLE 5.5 Certain gas-phase chemical reactions can be experimentally studied by measuring the changes in total reaction pressure with time by using a constant-volume reaction vessel. Consider the dissociation reaction

$$A_2 \xrightarrow{k} 2A$$

(a) Determine an expression for $[A_2]$ and $[A]$ in terms of the reaction temperature and total pressure; (b) determine the rate of dissociation of A_2 using part (a); and (c) evaluate the rate constant k using parts (a) and (b).

Solution:

1. Elementary reaction:

$$A_2 \xrightarrow{k} 2A$$

where

$$\frac{d[A_2]}{dt} = -k[A_2]$$

$$\frac{d[A_2]}{[A_2]} = -k\,dt$$

or

$$\ln\frac{[A_2]}{[A_2]_0} = -kt$$

Let

$$[A_2] = [A_2]_0 - Z$$

$$[A] = [A]_0 + 2Z$$

2. The total concentration at any time is given by

$$[A_2]+[A] = \{[A_2]_0 - [A_2]_0[A_2]\} + \{2[A_2]_0 - 2[A]\}$$

$$= 2[A_2]_0 - [A_2]$$

3. Assuming an ideal-gas behavior, then,

$$P_{\text{tot}}V = N_{\text{tot}}\bar{R}T$$

or

$$\frac{N_{\text{tot}}}{V} = [\text{tot}] = \frac{P_{\text{tot}}}{\bar{R}T}$$

4. Combining items 2 and 3,

$$2[\text{A}_2]_0 - [\text{A}_2] = \frac{P_{\text{tot}}}{\bar{R}T}$$

or

$$[\text{A}_2] = 2[\text{A}_2]_0 - \frac{P_{\text{tot}}}{\bar{R}T}$$

$$\text{at } t = 0 \qquad P_{\text{tot}} = P_0$$

a. $$[\text{A}_2] = \frac{2P_0 - P_{\text{tot}}}{\bar{R}T}$$

$$[\text{A}] = \frac{P_{\text{tot}} - P_0}{\bar{R}T}$$

5. Substituting the above into item 1 yields

$$\ln\left[\frac{(2P_0 - P_{\text{tot}})\bar{R}T}{P_0\bar{R}T}\right] = -kt$$

$$\ln\left[2 - \frac{P_{\text{tot}}}{P_0}\right] = -k\,t$$

$$k = \frac{-1}{t}\ln\left[2 - \frac{P_{\text{tot}}}{P_0}\right]$$

Comment: The above analysis suggests that the total pressure versus time data for a reaction might be used to evaluate the rate constant *k*. The above expression is valid only if the reaction is the sole kinetic step and the mixture behaves as an ideal gas.

Homogeneous gas-phase combustion involves a large number and variety of different elemental reactions that: (1) begin the kinetic process; (2) produce short-lived, reactive intermediate radicals that propagate the overall mechanism; and (3) terminate the kinetic process by forming stable products of combustion; see Figure 5.9. Many of these individual reactions occur simultaneously, while others, termed *chain reactions,* are consecutive. The short-lived reactive species that propagate these interactive reactions are commonly referred to as *chain carriers.*

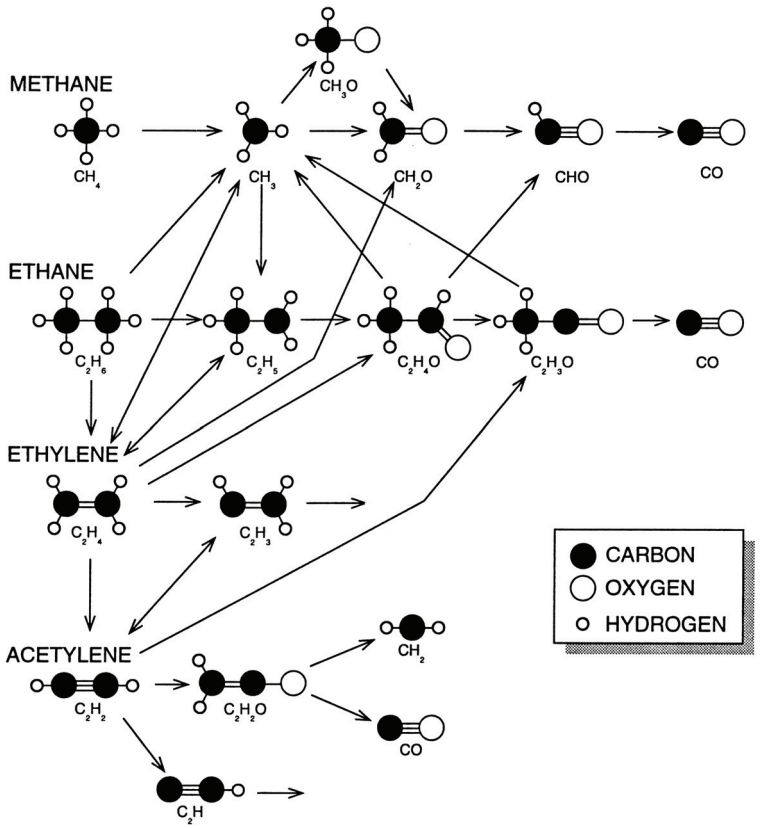

Figure 5.9 Complex elementary C/H/O reaction paths. Adapted from Gardiner, Jr., William C., The Chemistry of Flames, *Scientific American*, February 1982. With permission of Ian Worpole, illustrator.

High-temperature oxidation chemistry in premixed homogeneous fuel-air mixtures is initiated by elemental fuel pyrolysis reactions. Equation (5.37) is an example of an endothermic bimolecular *dissociation* reaction of methane in which the methyl radical CH_3 and a hydrogen atom are produced.

$$CH_4 + M \rightarrow CH_3 + H + M \tag{5.37}$$

A period of apparent inactivity can exist in the initial stages of fuel dissociation, during which significant concentrations of active radicals necessary to further propagate the overall combustion process are produced.

Equations (5.38a) and (5.38b) are examples of bimolecular *abstraction* reactions, delayed kinetic processes that require radicals such as H and O atoms and an OH radical in order to occur.

$$H + CH_4 \rightarrow H_2 + CH_3 \tag{5.38a}$$
$$OH + CH_4 \rightarrow HOH + CH_3 \tag{5.38b}$$

The reaction described by Equation (5.38a) shows a hydrogen atom abstracted by the collision of a methane molecule with a hydrogen atom to produce diatomic hydrogen and a methyl radical. In Equation (5.38b), a hydrogen atom is abstracted from the collision of a hydroxyl radical with a methane molecule to produce water and a methyl radical. Activation energies for abstraction reactions, in general, are not as great as those for bimolecular dissociation reactions.

Equations (5.39a) and (5.39b) are examples of *branching reactions,* reactions that produce more active radicals than they consume.

$$H + O_2 \rightarrow OH + O \tag{5.39a}$$
$$O + H_2 \rightarrow OH + H \tag{5.39b}$$

In Equation (5.39a), an oxygen atom and a hydroxyl radical are produced from the collision of a hydrogen atom with an oxygen molecule, whereas a hydrogen atom and a hydroxyl radical are generated from the collision of an oxygen atom with a hydrogen molecule in Equation (5.39b). Branching reactions are the chief reactions that actually control the overall rate of an oxidation process.

Equation (5.40) is an example of an *association* reaction, a bimolecular radical recombination reaction that forms a stable species, while Equation (5.41) is an example of a *termolecular,* or three-body, association reaction.

$$CH_3 + H \rightarrow CH_4 \tag{5.40}$$
$$H + H + M \rightarrow H_2 + M \tag{5.41}$$

Since the probability of a successful three-body collision is less than for a bimolecular collision, these types of reactions will have slower reaction rates but are major mechanisms for high-temperature radical recombination reactions.

EXAMPLE 5.6 Many oxidation reactions involve the dissociation of the fuel molecule to form an active radical. Consider the reaction system,

$$A_2 \underset{k_2}{\overset{k_1}{\rightleftarrows}} 2A$$

For this process, write an expression for (a) the rate of change of A_2, (b) the ratio of k_1/k_2 at equilibrium, and (c) the relationship among k_1, k_2, and the equilibrium constant K_p.

Solution:

1. Rate of change in A_2:

$$\frac{d[A_2]}{dt} = -k_1[A_2] + k_2[A]^2$$

Now, let

$$[A_2] = [A_2]_0 - x \qquad [A] = 2x$$
$$\frac{d}{dt}\{[A_2]_0 - x\} = -k_1\{[A_2]_0 - x\} + k_2(2x)^2$$

a. $$\frac{-dx}{dt} = -k[A_2]_0 + k_1 x + 4k_2 x^2$$

2. At equilibrium,

$$\frac{d[A_2]}{dt} = 0 \quad \text{or} \quad 0 = -k_1[A_2] + k_2[A]^2$$

and

$$\frac{k_1}{k_2} = \frac{[A]^2}{[A_2]}$$

3. Equilibrium constant K_c:

Define

$$K_c \equiv \frac{[A]^2/[A_0]^2}{[A_2]/[A_{2_0}]}$$

where

$$[A_{2_x}]_0 = [A]_0 \equiv 1.0$$

$$K_c = \frac{[A]^2}{[A_2]} = \frac{k_1}{k_2} \qquad \frac{k_1}{k_2} = K_c$$

4. Equilibrium constant K_p:

$$K_p = \frac{(P/P_0)_A^2}{(P/P_0)_{A_2}}$$

where

$$(P_0)_{A,A_2} = 1.0 \text{ atm}$$

$$K_p = \frac{P_A^2}{P_{A_2}}$$

and

$$P_A + P_{A_2} = P_{tot}$$

5. Assuming ideal gas behavior

$$P_A = [A]\bar{R}T \qquad P_{A_2} = [A_2]\bar{R}T$$

$$K_p = \frac{P_A^2}{P_{A_2}} = \frac{\{[A]\bar{R}T\}^2}{\{[A_2]RT\}} = \frac{[A]^2}{[A_2]}\bar{R}T$$

$$K_p = K_c\bar{R}T$$

where $\bar{R}$ = 82.057 cc·atm/gmole K

$$K_c = \frac{K_p}{\bar{R}T}$$

$$\frac{k_1}{k_2} = \frac{K_p}{\bar{R}T}$$

where $K_p \Rightarrow$ JANAF data.

The salient features of homogeneous gas-phase hydrocarbon-air combustion, i.e., initiation, branching, and termination, can be illustrated by the less complex but well-studied H_2–O_2 reaction system. Initiation of the H_2–O_2 reaction mechanism begins with the pyrolysis of hydrogen. At low temperatures, dissociation of the hydrogen molecule will be due to heterogeneous wall collisions or

$$H_2 + W \rightarrow HW + H \tag{5.42}$$

At higher temperatures, gas-phase pyrolysis of the hydrogen molecule will become important, or

$$H_2 + M \rightarrow H + H + M \tag{5.43}$$

High-temperature endothermic dissociation of the oxygen molecule will produce oxygen atoms as expressed in Equation (5.26).

$$O_2 + M \rightarrow O + O + M \tag{5.44}$$

Kinetics associated with the initial stages of an oxidation process and induction delay period are a function of initial reactant concentrations, temperature, and pressure but are not rate-controlling steps of the overall kinetic mechanisms.

Equations (5.45a) and (5.45b) are chain-branching reactions that are responsible for the rapid propagation of the H_2–O_2 reaction mechanism. These reactions are often referred to as being autocatalytic in that they create more intermediate radicals than they consume, thereby self-accelerating the reaction process.

$$H_2 + O \rightarrow OH + H \tag{5.45a}$$
$$O_2 + H \rightarrow OH + O \tag{5.45b}$$

Equations (5.46a) and (5.46b) are propagation reactions that result in the formation of stable products of combustion but require the presence of an intermediate radical species in order to occur.

$$OH + H_2 \rightarrow HOH + H \tag{5.46a}$$
$$HO_2 + H2 \rightarrow HOH + OH \tag{5.46b}$$

EXAMPLE 5.7 Complex oxidation mechanisms can involve many postulated elementary reactions. These reactions result in the formation of reactive radical species. An important assumption often applied to such a scheme is that these intermediate radicals reach a steady state, i.e., do not change with time. Consider the reaction set below for the H_2–O_2 system.

$$\text{wall} + H_2 \xrightarrow{1} 2H$$
$$H + O_2 \xrightarrow{2} OH + O$$
$$O + H_2 \xrightarrow{3} OH + H$$
$$OH + H_2 \xrightarrow{4} HOH + H$$
$$HOH + H \xrightarrow{5} OH + H_2$$
$$\text{wall} + H \xrightarrow{6} \text{removal at surface}$$
$$\text{wall} + OH \xrightarrow{7} \text{removal at surface}$$

Using these reactions (a) write an expression for the formation of H_2O; (b) for H atoms; (c) OH radical; and (d) O atoms. (e) Using the steady-state approximation for (b) → (d), express part (a) in terms of H_2 and O_2 and H steady state.

Solution:

1. Formation of H_2O:

a. $$\frac{d[H_2O]}{dt} = k_4[OH][H_2] - k_5[H_2O][H]$$

2. Formation of H:

b. $$\frac{d[H]}{dt} = k_1[H_2][W] - k_2[H][O_2] + k_3[O][H_2] + k_4[OH][H_2] - k_5[H][H_2O] - k_6[H][W]$$

3. Formation of OH:

c. $$\frac{d[OH]}{dt} = k_2[H][O_2] + k_3[O][H_2] - k_4[OH][H_2] + k_5[H_2O][H] - k_7[OH][W]$$

4. Formation of O:

d. $$\frac{d[O]}{dt} = -k_2[H][O_2] - k_3[O][H_2]$$

5. The steady-state assumption assumes that the concentration of certain radicals remains constant during reaction, or

$$\frac{d[H]}{dt} = \frac{d[OH]}{dt} = \frac{d[O]}{dt} = 0$$

6. H-atom steady state:

$$0 = k_1[H_2][W] - k_2[H][O_2] + k_3[O][H_2] + k_4[OH][H_2] - k_5[H][H_2O] - k_6[H][W]$$

7. OH steady state:

$$0 = k_2[H][O_2] + k_3[O][H_2] - k_4[OH][H_2] + k_5[H_2O][H] - k_7[OH][W]$$

8. O-atom steady state:

$$0 = k_2[H][O_2] - k_3[O][H_2]$$

or

$$\left.\frac{[H]}{[O]}\right)_{SS} = \frac{k_3[H_2]}{k_2[O_2]}$$

9. Substituting part 7 into part 6,

$$0 = k_2[H][O_2] + k_3\left(\frac{k_2[O_2][H]}{k_3[H_2]}\right)[H_2] = k_4[OH][H_2] + k_5[H_2O][H] - k_7[OH][W]$$

$$[OH]\{k_4[H_2] + k_7[W]\} = [H]\{2k_2[O_2] + k_5[H_2O]\}$$

$$\left.\frac{[OH]}{[H]}\right)_{SS} = \frac{2k_2[O_2] + k_5[H_2O]}{k_4[H_2] + k_7[W]}$$

10. Substituting parts 7 and 8 into part

$$0 = k_1[H_2][W] - k_1[H][O_2] + k_2[H][O_2] - k_5[H][H_2O] - k_6[H][W] + k_4[H_2]\left\{\frac{2k_2[O_2] + k_5[H_2O]}{k_4[H_2] + k_7[W]}\right\}[H]$$

and

$$[H]_{SS} = \frac{k_1[H_2][W]}{k_5[H_2O] + k_6[W]\dfrac{-k_4[H_2]\{2k_2[O_2] + k_5[H_2O]\}}{k_4[H_2] + k_7[W]}}$$

11. Formation of H_2O:

$$\frac{d[H_2O]}{dt} = k_4[OH]_{SS}[H_2] - k_5[H_2O][H]_{SS}$$

$$= \left[k_4[H_2] \left\{ \frac{2k_2[O_2] + k_5[H_2O]}{k_4[H_2] + k_7[W]} \right\} - k_5[H_2O] \right] [H]_{SS}$$

Comments: This problem illustrates that even the simplest kinetic mechanisms are highly complex. Numerical techniques are necessary to predict the concentration-time profiles for even the simplest conditions. In addition, the solutions to many practical combustion kinetics mechanisms are complicated by coupling of the thermodynamic, fluid mechanic, and heat transfer phenomena. Boundary conditions at the walls further influence the actual physics of high-temperature chemical kinetics.

Figure 5.10 illustrates the dynamics of the H_2–O_2 combustion process, while Table 5.5 lists the H_2–O_2 combustion mechanism postulated by Hinshelwood.

In Chapter 4, two types of ideal combustion processes were predicted that could propagate through a homogeneous premixed combustible mixture: detonations, or high-pressure supersonic reactions, and deflagrations, or low-pressure subsonic reactions. The H_2–O_2 kinetic mechanisms described in this chapter can be used to better understand the physical difference between deflagration and detonation wave propagations. Figure 5.11 illustrates a thermal explosion plot for the hydrogen-oxygen system. For H_2–O_2 mixtures below 400°C (752°F), no rapid homogeneous reaction occurs without external energy input. In this region, slow heterogeneous surface reactions dominate, and overall reaction rate is a function of material and the surface area-reaction volume ratio. For H_2–O_2 mixtures above 600°C (1,112°F), thermal explosions spontaneously occur in this region since chain-branching autocatalytic reactions cause the combustion process to run away rapidly in a fashion similar to the physics of a nuclear explosion. Between 400 and 600°C (752–1,112°F), a very different chemistry may be observed. Consider the fixed temperature line shown on Figure 5.11. Increasing pressure, i.e., collisions, will increase the overall rate of reactions but, below the first explosion limit, heat loss to walls controls the process, and radical quenching by recombination at the wall dominates. Further increases in pressure at fixed temperature raises the number of gas collisions, and the rate of energy release by gas-phase reactions becomes greater than the rate of energy loss to the walls. Increased radical formation above the first explosion limit then causes an autocatalytic explosion. Further increases in pressure will cause gas-phase radical recombination reactions to quench the process above the second explosion limit. Above the third explosion limit, additional termolecular reactions cause the reaction again to explode spontaneously.

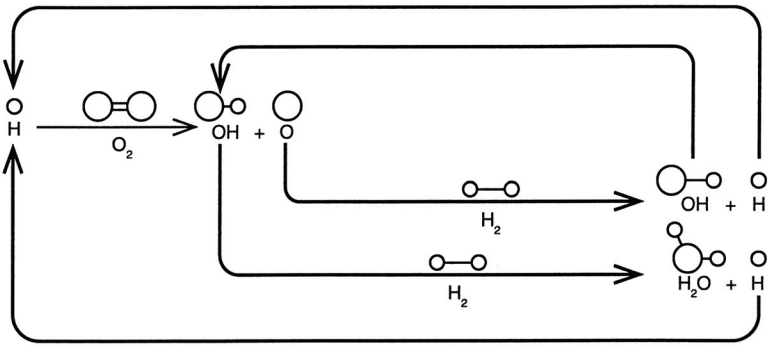

Figure 5.10 H_2–O_2 reaction mechanism. Adapted from Gardiner, Jr., William C., The Chemistry of Flames, *Scientific American*, February 1982. With permission of Ian Worpole, illustrator.

Table 5.5 H_2–O_2 Reaction Mechanism

H/O Chain Branching Reactions		
H_2 + wall	$\xrightarrow{1}$	WH + H
H + O_2	$\xrightarrow{2}$	HO + O
O + H_2	$\xrightarrow{3}$	HO + H
HO + H_2	$\underset{4}{\overset{}{\rightleftarrows}}$	HOH + H
H + O_2 + M	$\xrightarrow{5}$	HO_2 + M
H + wall	$\xrightarrow{6}$	stable species
HO_2 + wall	$\xrightarrow{7}$	stable species
HO + wall	$\xrightarrow{8}$	stable species
HO_2 + H_2	$\xrightarrow{9}$	H_2O + OH
OH + H_2	$\xrightarrow{10}$	H_2O + H
O + H_2O	$\underset{12}{\overset{11}{\rightleftarrows}}$	OH + OH

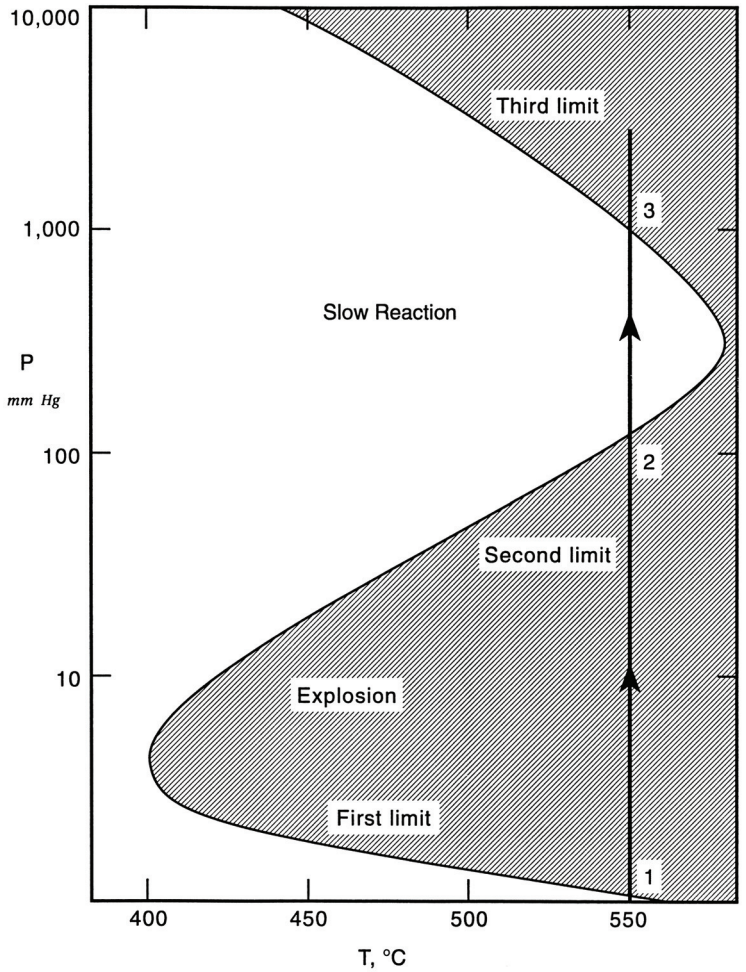

Figure 5.11 Hydrogen-oxygen thermal explosion limits. Adapted from Lewis, B. and Von Elbe, G., *Combustion, Flames, and Explosions in Gases*, 2nd Edition, Academic Press, New York, 1961. With permission from Elsevier.

Kinetic mechanisms similar to those described above can be used to model fuel ignition delay, emissions formation, and other aspects of high-temperature oxidation thermochemistry. Detailed kinetic mechanisms are developed for only a few simple combustion reactions. Most of the efforts today in this area of chemistry are directed toward better understanding the performance and emission of operating internal or external combustion systems.

5.5 NITROGEN-OXYGEN CHEMICAL KINETICS

Considerable attention is being given to fuel-engine interface generated pollutants including minimizing the environmental emissions of nitrogen-oxygen containing species. Nitrogen-oxygen containing species include: nitrous oxide (N_2O), nitric oxide (NO), nitrogen trioxide (N_2O_3), nitrogen dioxide (NO_2) and nitrogen pentoxide (N_2O_5). The two most significant toxic species of concern related to combustion are nitric oxide, NO, and nitrogen dioxide, NO_2, which are today the subject of extensive regulation. Nitrogen dioxide is the more harmful to human health, producing many negative respiratory health effects upon inhalation. The high temperature formation of these nitrogen-oxygen containing species in reactive environments requires a basic understanding of their thermochemistry but, more importantly, knowledge of the chemical kinetics of the nitrogen–oxygen reaction system.

A significant number of modern combustion processes, devices, and facilities operate at high reaction temperatures and with excess air. An important group of high temperature chemical kinetic reactions involving nitrogen, oxygen, and nitrogen-oxygen containing species occur at these conditions. These particular reactions are at the very heart of forming nitric oxide (NO) and nitrogen dioxide (NO_2), pollution constituents which are frequently combined together as NO_x emissions. Different sources of nitrogen can contribute to the formation of these oxides of nitrogen. The most obvious source comes from combustion air itself which contains 3.76 moles of diatomic nitrogen for each mole of diatomic oxygen.

Along with thermal NO_x formed from combustion air, under certain conditions NO_x can also be formed within combustion air chemistry. Phenomena such as nitrogen chemistry can occur within fuel-rich flames with active carbon-bearing fuel radical species C, CH, and CH_2 in complex kinetic processes in reactions; for example,

$$CH + N_2 \rightleftarrows HCN + N \tag{5.47}$$

Rapid nitrogen kinetic activity, even during early initial low temperature stages of combustion, with these rich intermediate hydrocarbon fuel species gives rise to the terminology of *prompt nitrogen chemistry*. Fuels with no carbon, i.e., H_2, will not be sources of prompt nitrogen. Prompt nitrogen chemistry in most cases is only a small fraction of the total NO_x production but a critical constituent in any overall control strategy needed to reach the lowest possible NO_x reductions in any combustion device.

In addition to atmospheric and prompt nitrogen, a fraction of NO_x formation can also be accounted for by combustion of fuels that contain significant nitrogen in their structure, i.e., *fuel bound nitrogen*. From an inspection of Table 5.2, the N = N molecular nitrogen bond energy is much greater than that of the C–N molecular bond energy. Thus, oxygen is seen to preferentially react with the weaker C–N bonds found in an organic compound. Fuels of principal concern recognized as contributors to fuel-bound nitrogen are fuel oil and coal. Since natural gas is essentially free of nitrogen-type compounds, it is not considered to be a fuel-bound nitrogen constituent of concern. NO_x emissions in combustion gases are scientifically classified as *thermal, prompt,* or *fuel nitrogen oxides*.

A plausible theory for thermal sources of atmospheric NO_x would simply be based on equilibrium shifts in the nitrogen and oxygen concentrations due to temperature. The equilibrium reaction for the one atmosphere formation of monatomic nitrogen atom (or oxygen) from nitrogen molecules (or oxygen) can be written as

$$0.5N_2 \rightleftarrows N \tag{5.48}$$

and

$$0.5O_2 \rightleftarrows O \tag{5.49}$$

Consider one mole of N_2 or O_2. At elevated temperatures one mole of N_2 will dissociate at equilibrium into $\bar{x}_N$ moles of N and $\bar{x}_{N_2}$ moles of N_2. Likewise one mole of O_2 will dissociate at equilibrium into $\bar{x}_O$ moles of O and $\bar{x}_{O_2}$ moles of O_2. The equilibrium constants at one atmosphere, where $P = P_0$, can then be expressed in mole fraction terms as

$$K_{P,N} = \frac{(P/P_0)_N}{(P/P_0)_{N_2}^{0.5}} = \frac{(\bar{x}_N P_0/P_0)}{(\bar{x}_{N_2} P_0/P_0)^{0.5}} = \frac{\bar{x}_N}{\bar{x}_{N_2}^{0.5}} \tag{5.50}$$

and

$$K_{P,O} = \frac{(P/P_0)_O}{(P/P_0)_{O_2}^{0.5}} = \frac{(\bar{x}_O P_0/P_0)}{(\bar{x}_{O_2} P_0/P_0)^{0.5}} = \frac{\bar{x}_O}{\bar{x}_{O_2}^{0.5}} \tag{5.51}$$

At equilibrium N and N_2 mole fractions add to unity, or

$$y = \bar{x}_N, \quad 1 - y = \bar{x}_{N_2}$$

$$K_P = \frac{y}{(1-y)^{0.5}}$$

$$K_P{}^2 = \frac{y^2}{1-y}$$

$$y^2 + K_P{}^2 y - K_P = 0$$

$$y = \frac{-K_P{}^2}{2} \pm \tfrac{1}{2}\sqrt{(K_P{}^2)^2 + 4K_P{}^2}$$

Solving for y yields

$$y = \frac{-K_P{}^2}{2} + \tfrac{1}{2}\sqrt{(K_P{}^2)^2 + 4K_P{}^2} \tag{5.52}$$

The equilibrium constant for monatomic nitrogen (or oxygen) atom formation from diatomic nitrogen (or oxygen) molecules, respectively, can be determined using JANAF data. The JANAF log K_p values for N and O atom formation as a function of temperature from 2,000–3,000K as found in Tables B.15 and B.20 in Appendix B are presented in Table 5.6. Using these values the equilibrium dissociation of one mole of N_2 and O_2 can be determined using Equation (5.52) as a function of temperature. Results from this analysis are found in Table 5.6.

Table 5.6 Equilibrium Dissociation of One Mole Oxygen or Nitrogen

T, K	2,000	2,200	2,400	2,600	2,800	3,000
$\log K_{p,\mathrm{O}}$	–3.178	–2.571	–-2.065	–1.636	–1.268	–0.949
K_p	6.637E-04	2.685E-03	8.610E-03	2.312E-02	5.400E-02	1.125E-01
$\bar{x}_{\mathrm{O}}$	6.350E-04	2.682E-03	8.573E-03	2.285E-02	5.252E-02	1.063E-01
$\bar{x}_{\mathrm{O}_2}$	9.993E-01	9.973E-01	9.914E-01	9.771E-01	9.475E-01	8.937E-01
$\log K_{p,\mathrm{N}}$	–9.046	–7.905	–6.954	–6.149	–5.457	–4.858
K_p	8.995E-10	1.245E-08	1.112E-07	7.096E-07	3.491E-06	1.387E-05
$\bar{x}_{\mathrm{N}}$	8.995E-10	1.245E-08	1.112E-07	7.096E-07	3.491E-06	1.387E-05
$\bar{x}_{\mathrm{N}_2}$	1	9.999E-01	9.999E-01	9.999E-01	9.999E-01	9.999E-01

Note that the mole fraction of atomic oxygen formed over the temperature range 2,000–3,000K is extremely small but increases with increasing temperature, whereas monatomic nitrogen values, while also increasing, are infinitesimal. Thermal dissociation of diatomic nitrogen is seen to not be a source of molecular nitrogen for forming nitric oxide.

High temperature concentrations of NO and NO_2 in combustion processes cannot be based on equilibrium predictions and analysis. The path for forming nitric oxides from nitrogen is kinetic. The generally accepted kinetic model for nitrogen reaction with oxygen occurs by the following overall free radical chain reaction mechanism proposed around 1946 by Zeldovitch. Diatomic nitrogen dissociation as seen is not a source of molecular nitrogen. Atomic nitrogen is formed by the Zeldovitch free radical chain mechanism. The dissociation of diatomic oxygen, however, is a source of monatomic oxygen in the Zeldovitch mechanism. Oxygen atoms are first formed via the elementary reaction

$$O_2 + M \rightleftarrows 2O + M \tag{5.53}$$

The Zeldovitch free radical chain mechanism consists of

$$O + N_2 \overset{k_1}{\rightleftarrows} NO + N \tag{5.54}$$

$$N + O_2 \overset{k_2}{\rightleftarrows} NO + O \tag{5.55}$$

and, in fuel-rich flames, the additional reaction is included in the model

$$OH + N \overset{k_3}{\rightleftarrows} NO + H \tag{5.56}$$

The general rate equation for NO formation via reactions (5.54) and (5.55) in terms of the general theory of complex chemical kinetics mechanisms presented in Section 5.4 is given as

Table 5.7 Zeldovitch Nitric Oxide Elementary Rate Constants

$$k_1 = 1.8 \times 10^{14} \exp\left(\frac{-76{,}241}{\bar{R}T}\right) \quad \text{cm}^3/\text{gmole}\cdot\text{sec}$$

$$k_{-1} = 3.8 \times 10^{13} \exp\left(\frac{-844}{\bar{R}T}\right) \quad \text{cm}^3/\text{gmole}\cdot\text{sec}$$

$$k_2 = 1.8 \times 10^{10} T \exp\left(\frac{-9{,}299}{\bar{R}T}\right) \quad \text{cm}^3/\text{gmole}\cdot\text{sec}$$

$$k_{-2} = 3.8 \times 10^{9} T \exp\left(\frac{-41{,}370}{\bar{R}T}\right) \quad \text{cm}^3/\text{gmole}\cdot\text{sec}$$

$$k_3 = 7.1 \times 10^{13} \exp\left(\frac{-894}{\bar{R}T}\right) \quad \text{cm}^3/\text{gmole}\cdot\text{sec}$$

$$k_{-3} = 1.7 \times 10^{14} \exp\left(\frac{-48{,}800}{\bar{R}T}\right) \quad \text{cm}^3/\text{gmole}\cdot\text{sec}$$

Adapted from Hanson, R. K. and Salimian, S., Survey of Rate Constants in the N/H/O System, Chapter 6 in *Combustion Chemistry*, W. C. Gardiner, Jr., Ed., Springer-Verlag, New York, 1984. With kind permission of Springer Science and Business Media.

$$\frac{d[\text{NO}]}{dt} = k_1[\text{O}][\text{N}_2] - k_{-1}[\text{N}][\text{NO}] + k_2[\text{N}][\text{O}_2] - k_{-2}[\text{O}][\text{NO}] \tag{5.57}$$

Table 5.7 provides the elementary rate constants for NO kinetics. Note, for clarification, k_1 and k_{-1} are the forward and reverse rate constants, respectively, for Equation (5.54). The activation energies are in cal/gmole with the appropriate universal gas constant. An inspection of the forward rate constants k_1 for reaction (5.54) and the reverse rate constant k_{-2} for reaction (5.55) reveals they have large activation energies which result in NO formation rates with strong temperature dependence.

The general rate equation for formation of N via reactions (5.54) and (5.55) is given in similar fashion as

$$\frac{d[\text{N}]}{dt} = k_1[\text{O}][\text{N}_2] - k_{-1}[\text{N}][\text{NO}] + k_{-2}[\text{NO}][\text{O}] - k_2[\text{N}][\text{O}_2] \tag{5.58}$$

The N atom concentration is assumed to be small compared to other reactive species in nitrogen-oxygen chemistry and not changing significantly over time. It is usually assumed that a steady concentration of N atoms exists. This is a fairly standard procedure whenever a species is present in very small amounts compared with other major species. N atoms in ordinary combustion processes fulfill this latter requirement, especially when $\Phi = \leq 1.2$. Using the steady state approximation of $d[\text{N}]/dt = 0$, then

$$[\text{N}]_{\text{ss}} = \frac{k_1[\text{O}][\text{N}_2] + k_{-2}[\text{NO}][\text{O}]}{k_{-1}[\text{NO}] + k_2[\text{O}_2]} \tag{5.59}$$

Applying the steady state $[\text{N}]_{\text{ss}}$ value from Equation (5.59) to Equation (5.57), after manipulation and cancellation of terms, yields the following expression:

$$\frac{d[\mathrm{NO}]}{dt} = \frac{2[\mathrm{O}]\{k_1[\mathrm{N}_2] - (k_{-1}k_{-2}[\mathrm{NO}]^2 / k_2[\mathrm{O}_2])\}}{1 + k_{-1}[\mathrm{NO}]/(k_2[\mathrm{O}_2])} \tag{5.60}$$

The JANAF equilibrium constant, $K_{p,\mathrm{NO}}$, for the formation of nitric oxide, NO, based on data found in Table B.16 in Appendix B is written in terms of diatomic oxygen, O_2, and diatomic nitrogen, N_2, as

$$0.5\mathrm{N}_2 + 0.5\mathrm{O}_2 \rightleftarrows \mathrm{NO}$$

$$K_{p,\mathrm{NO}} = \frac{(P/P_0)_{\mathrm{NO}}}{(P/P_0)^{1/2}_{\mathrm{N}_2}(P/P_0)^{1/2}_{\mathrm{O}_2}} = \frac{(\bar{x}_{\mathrm{NO}})}{(\bar{x}_{\mathrm{N}_2})^{1/2}(\bar{x}_{\mathrm{O}_2})^{1/2}} \tag{5.61}$$

Assuming ideal gas behavior one can express molar concentration of a species, [C], in terms of its partial pressure and absolute temperature as

$$P_i V = N_i \bar{R} T \tag{1.20}$$

or

$$\frac{N_i}{V} = [C] = \frac{P_i}{\bar{R}T} \tag{5.62}$$

Utilizing the expression Equation (5.62) for concentration for partial pressures in Equation (5.61) yields an expression for the equilibrium constant, $K_{p,\mathrm{NO}}$, as

$$K_{p,\mathrm{NO}} = \frac{[\mathrm{NO}]}{[\mathrm{N}_2]^{1/2}[\mathrm{O}_2]^{1/2}} \tag{5.63}$$

The forward and reverse rates of the Zeldovitch free radical chain mechanism reactions at equilibrium would be equal or

$$k_1[\mathrm{O}][\mathrm{N}_2] = k_{-1}[\mathrm{N}][\mathrm{NO}] \tag{5.64}$$

and

$$k_2[\mathrm{N}][\mathrm{O}_2] = k_{-2}[\mathrm{O}][\mathrm{NO}] \tag{5.65}$$

Combining Equations (5.64) and (5.65) yields the following expression which is seen to be similar to Equation (5.63), $K_{p,\mathrm{NO}}$, the JANAF equilibrium constant for nitric oxide, NO.

$$\frac{(k_1 / k_{-1})}{(k_{-2} / k_2)} = \frac{([\mathrm{N}][\mathrm{NO}])([\mathrm{O}][\mathrm{NO}])}{([\mathrm{O}][\mathrm{N}_2])([\mathrm{N}][\mathrm{O}_2])} = \frac{[\mathrm{NO}]^2}{[\mathrm{N}_2][\mathrm{O}_2]} = K^2_{p,\mathrm{NO}} \tag{5.66}$$

Substituting Equation (5.66) into Equation (5.60) allows the rate equation for thermal NO formation to take the following form:

$$\frac{d[\mathrm{NO}]}{dt} = \frac{2k_1[\mathrm{O}][\mathrm{N}_2]\{1 - ([\mathrm{NO}]^2 /(K^2_{p,\mathrm{NO}}[\mathrm{N}_2][\mathrm{O}_2]))\}}{1 + k_{-1}[NO]/(k_2[\mathrm{O}_2])} \tag{5.67}$$

Equation (5.67) provides an expression often used for determining the rate of formation of nitric oxide from atmospheric nitrogen in combustion processes. To determine the amount of nitric oxide formed at any time t still requires integration.

Various solution techniques for solving Equation (5.67) under a variety of conditions can be found in the literature. For example, if one further assumes

$$\frac{k_{-1}[\mathrm{NO}]}{k_2[\mathrm{O}_2]} \ll 1$$

then the denominator of Equation (5.67) is seen to approach 1 and Equation (5.67) reduces to

$$\begin{aligned}\frac{d[\mathrm{NO}]}{dt} &= 2k_1[\mathrm{O}][\mathrm{N}_2]\{1 - ([\mathrm{NO}]^2/(K_{p,\mathrm{NO}}^2[\mathrm{N}_2][\mathrm{O}_2]))\} \\ &= 2k_1[\mathrm{O}][\mathrm{N}_2] - 2k_1\{[\mathrm{O}][\mathrm{NO}]^2/(K_{p,\mathrm{NO}}^2[\mathrm{O}_2])\}\end{aligned} \tag{5.68}$$

If in the hot product gases the assumption is made that O atoms are in equilibrium with the O_2 molecules, then further simplifications can be made to Equation (5.68). Recall the equilibrium reaction between monatomic oxygen and oxygen molecules

$$0.5\mathrm{O}_2 \rightleftarrows \mathrm{O} \tag{5.49}$$

The JANAF equilibrium constant for monatomic oxygen found in Table B.20 in Appendix B can be expressed in concentration terms as

$$K_{p,\mathrm{O}} = \frac{(P/P_0)_{\mathrm{O}}}{(P/P_0)_{\mathrm{O}_2}^{0.5}} = \frac{([\mathrm{O}]\bar{R}T)}{([\mathrm{O}_2]^{0.5})(\bar{R}T)^{0.5}} = \frac{([\mathrm{O}])(\bar{R}T)^{0.5}}{([\mathrm{O}_2]^{0.5})} \tag{5.69}$$

Solving for [O] in Equation (5.69) and substituting into (5.68) yield

$$\begin{aligned}\frac{d[\mathrm{NO}]}{dt} &= 2k_1K_{p,\mathrm{O}}[\mathrm{O}_2]^{0.5}[\mathrm{N}_2]/(\bar{R}T)^{0.5} \\ &\quad - 2k_1K_{P,O}\{[\mathrm{O}_2]^{0.5}[\mathrm{NO}]^2/(K^2{}_{p,\mathrm{NO}}[\mathrm{O}_2](\bar{R}T)^{0.5})\}\end{aligned} \tag{5.70}$$

Substituting the equilibrium constant $K_{p,\mathrm{NO}}$, Equation (5.63), into the first group of terms in Equation (5.70) yields

$$\begin{aligned}\frac{d[\mathrm{NO}]}{dt} &= 2k_1K_{p,\mathrm{O}}\{[\mathrm{NO}]_e{}^2/(K^2{}_{p,\mathrm{NO}}[\mathrm{O}_2]^{0.5}(\bar{R}T)^{0.5})\} \\ &\quad - 2k_1K_{p,\mathrm{O}}\{[\mathrm{NO}]^2/(K_{p,\mathrm{NO}}^2[\mathrm{O}_2]^{0.5}(\bar{R}T)^{0.5})\} \\ &= \{2k_1K_{p,\mathrm{O}}/(K_{p,\mathrm{NO}}^2[\mathrm{O}_2]^{0.5}(\bar{R}T)^{0.5})\}([\mathrm{NO}]_e{}^2 - [\mathrm{NO}]^2)\end{aligned} \tag{5.71}$$

With this simplification the relationship Equation (5.71) reduces to the form

$$\frac{d[\mathrm{NO}]}{[\mathrm{NO}]_e{}^2 - [\mathrm{NO}]^2} = \frac{k_n}{[\mathrm{O}_2]^{0.5}}dt \tag{5.72}$$

with

$$k_n = \{2k_1 K_{p,\mathrm{O}} / (K_{p,\mathrm{NO}}^2 (\overline{R}T)^{0.5})\} \tag{5.73}$$

Integrating Equation (5.73) and assuming zero NO concentration at $t = 0$ yields

$$\frac{[\mathrm{NO}]}{[\mathrm{NO}]_e} = \frac{1 - \exp(-\alpha t)}{1 + \exp(-\alpha t)} \tag{5.74}$$

where

$$\alpha = \frac{2[\mathrm{NO}]_e k_n}{[\mathrm{O}_2]^{0.5}} \tag{5.75}$$

EXAMPLE 5.8 Calculate the equilibrium concentrations of NO and NO_2 for two cases of initial nitrogen to oxygen source conditions. Determine predicted equilibrium values at one atmosphere total pressure over a range of equilibrium temperatures from 800 to 3,000K for: (a) the standard atmospheric diatomic nitrogen to diatomic oxygen ratio of 3.76 to 1; and (b) a representative flue gas with diatomic nitrogen to diatomic oxygen ratio of 40 to 1. Consider the equilibrium NO source to be simply thermal and neglecting prompt and fuel-bound NO.

Solution:

1. Diatomic nitrogen to diatomic oxygen ratios:

   case 1: 3.76 to 1 (standard atmosphere)
   case 2: 40 to 1 (representative flue gas)

2. Oxygen to nitrogen atom balance ratios:

$$\text{case 1} \quad (2/2 \cdot 3.76) = \left(\overline{x}_{\mathrm{NO}} + 2\overline{x}_{\mathrm{O}_2} + 2\overline{x}_{\mathrm{NO}_2}\right) / \left(\overline{x}_{\mathrm{NO}} + 2\overline{x}_{\mathrm{N}_2} + \overline{x}_{\mathrm{NO}_2}\right)$$

$$\text{case 2} \quad (2/2 \cdot 40) = \left(\overline{y}_{\mathrm{NO}} + 2\overline{y}_{\mathrm{O}_2} + 2\overline{y}_{\mathrm{NO}_2}\right) / \left(\overline{y}_{\mathrm{NO}} + 2\overline{y}_{\mathrm{N}_2} + \overline{y}_{\mathrm{NO}_2}\right)$$

3. Equilibrium mole fraction summations:

$$\text{case 1} \quad \overline{\mathrm{x}}_{\mathrm{O}_2} + \overline{x}_{\mathrm{N}_2} + \overline{x}_{\mathrm{NO}} + \overline{x}_{\mathrm{NO}_2} = 1$$

$$\text{case 2} \quad \overline{\mathrm{y}}_{\mathrm{O}_2} + \overline{y}_{\mathrm{N}_2} + \overline{y}_{\mathrm{NO}} + \overline{y}_{\mathrm{NO}_2} = 1$$

4. Parts per million of equilibrium species:

$$[\mathrm{O}_2] = 1{,}000{,}000 \cdot \overline{x}_{\mathrm{O}_2} \quad \text{or} \quad 1{,}000{,}000 \cdot \overline{\mathrm{y}}_{\mathrm{O}_2}$$

$$[\mathrm{N}_2] = 1{,}000{,}000 \cdot \overline{x}_{\mathrm{N}_2} \quad \text{or} \quad 1{,}000{,}000 \cdot \overline{\mathrm{y}}_{\mathrm{N}_2}$$

$$[\mathrm{NO}] = 1{,}000{,}000 \cdot \overline{x}_{\mathrm{NO}} \quad \text{or} \quad 1{,}000{,}000 \cdot \overline{\mathrm{y}}_{\mathrm{NO}}$$

$$[\mathrm{NO}_2] = 1{,}000{,}000 \cdot \overline{x}_{\mathrm{NO}_2} \quad \text{or} \quad 1{,}000{,}000 \cdot \overline{\mathrm{y}}_{\mathrm{NO}_2}$$

5. JANAF NO equilibrium constant, $K_{p,\mathrm{NO}}$, for the formation of nitric oxide, NO, based on data found in Table B.16 in Appendix B is written in terms of diatomic oxygen, O_2, and diatomic nitrogen, N_2, as

$$0.5O_2 + 0.5N_2 \rightleftarrows NO$$

and

$$K_{p,\mathrm{NO}}\big)_J = \frac{(P_{\mathrm{NO}})}{(P_{\mathrm{O_2}})^{1/2}(P_{\mathrm{N_2}})^{1/2}} = \frac{[\bar{x}_{\mathrm{NO}}]}{[\bar{x}_{\mathrm{O_2}}]^{1/2}[\bar{x}_{\mathrm{N_2}}]^{1/2}} = \frac{[\bar{y}_{\mathrm{NO}}]}{[\bar{y}_{\mathrm{O_2}}]^{1/2}[\bar{y}_{\mathrm{N_2}}]^{1/2}} = \frac{[\mathrm{NO}]}{[\mathrm{O_2}]^{1/2}[\mathrm{N_2}]^{1/2}}$$

6. JANAF NO_2 equilibrium constant, $K_{p,\mathrm{NO_2}}$, for the formation of nitrogen dioxide, NO_2, based on data found in Table B.17 in Appendix B is written in terms of diatomic oxygen, O_2, and diatomic nitrogen, N_2, as

$$O_2 + 0.5N_2 \rightleftarrows NO_2$$

and

$$K_{p,\mathrm{NO_2}}\big)_{\mathrm{J}} = \frac{(P_{\mathrm{NO_2}})}{(P_{\mathrm{N_2}})^{1/2}(P_{\mathrm{O_2}})} = \frac{[\bar{x}_{\mathrm{NO_2}}]}{[\bar{x}_{\mathrm{N_2}}]^{1/2}[\bar{x}_{\mathrm{O_2}}]} = \frac{[\bar{y}_{\mathrm{NO_2}}]}{[\bar{y}_{\mathrm{N_2}}]^{1/2}[\bar{y}_{\mathrm{O_2}}]}$$

7. An additional equilibrium constant, $K_{p,\mathrm{NO_2}}$, for the formation of nitrogen dioxide, NO_2, can also be written in terms of diatomic oxygen, O_2, and nitric oxide, NO, as

$$0.5O_2 + NO \rightleftarrows NO_2$$

and

$$K_{p,\mathrm{NO_2}}\big)_{\mathrm{R}} = \frac{(P_{\mathrm{NO_2}})}{(P_{\mathrm{O_2}})^{1/2}(P_{\mathrm{NO}})} = \frac{[\bar{x}_{\mathrm{NO_2}}]}{[\bar{x}_{\mathrm{O_2}}]^{1/2}[\bar{x}_{\mathrm{NO}}]} = \frac{[\bar{y}_{\mathrm{NO_2}}]}{[\bar{y}_{\mathrm{O_2}}]^{1/2}[\bar{y}_{\mathrm{NO}}]}$$

8. The second nitrogen dioxide equilibrium constant, III, can be determined from the JANAF equilibrium constants, I and II, found in Tables B.16 and B.17 in Appendix B as

$$\log k_{p,\mathrm{NO_2}}\big)_{\mathrm{R}} = \log k_{p,\mathrm{NO_2}}\big)_{\mathrm{J}} - \log k_{p,\mathrm{NO}}\big)_{\mathrm{J}}$$

and

$$K_{p,\mathrm{NO_2}}\big)_{\mathrm{R}} = 10 \wedge \left(\log K_{p,\mathrm{NO_2}}\right)_{\mathrm{R}}$$

9. Results from numerical solution to these relations are provided in the tables below.

	JANAF	JANAF	JANAF	JANAF	REACTION
T, K	$\log K_{p,\mathrm{NO}}$	$K_{p,\mathrm{NO}}$	$\log K_{p,\mathrm{NO_2}}$	$\log K_{p,\mathrm{NO_2}}$	$K_{p,\mathrm{NO_2}}$
800	–5.243	0.000005715	–5.417	–0.1740	4256
1,000	–4.062	0.0000867	–5.000	–0.9380	12.56
1,200	–3.275	0.0005309	–4.721	–1.446	0.6699
1,400	–2.712	0.0019409	–4.519	–1.807	0.1153
1,600	–2.290	0.0051286	–4.367	–2.077	0.008388
1,800	–1.962	0.0109144	–4.248	–2.286	0.005176
2,000	–1.699	0.019999	–4.152	–2.453	0.003524
2,200	–1.484	0.032810	–4.074	–2.590	0.002570
2,400	–1.305	0.049545	–4.008	–2.703	0.001981
2,600	–1.154	0.070146	–3.953	–2.799	0.001588
2,800	–1.025	0.094406	–3.905	–2.880	0.001318
3,000	–0.913	0.122180	–3.864	–2.951	0.001119

	3.76 N_2/O_2			40 N_2/O_2		
T, K	$[O_2]$, ppm	[NO], ppm	$[NO_2]$, ppm	$[O_2]$, ppm	[NO], ppm	$[NO_2]$, ppm
800	212,000	2.34	.721	24,400	.882	.0922
1,000	212,000	35.4	1.88	24,400	13.4	.241
1,200	212,000	217	3.58	24,300	81.8	.457
1,400	212,000	793	5.69	24,200	298	.725
1,600	211,000	2,090	8.04	24,000	785	1.02
1,800	210,000	4,430	10.5	23,600	1,650	1.31
2,000	208,000	8,080	13.0	22,900	2,990	1.59
2,200	206,000	13,200	15.3	22,000	4,800	1.83
2,400	202,000	19,700	17.5	20,900	7,055	2.02
2,600	198,360	27,500	19.4	19,600	9,660	2.15
2,800	194,000	36,500	21.2	18,100	12,500	2.22
3,000	189,000	46,400	22.6	16,600	15,500	2.24

EQUILIBRIUM NO CONCENTRATION

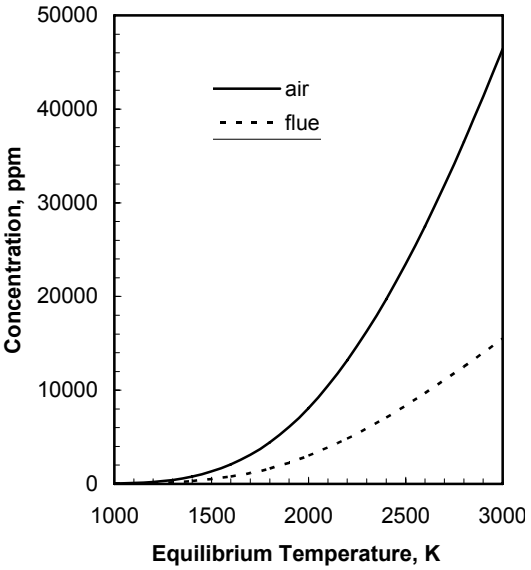

EQUILIBRIUM NO_2 CONCENTRATION

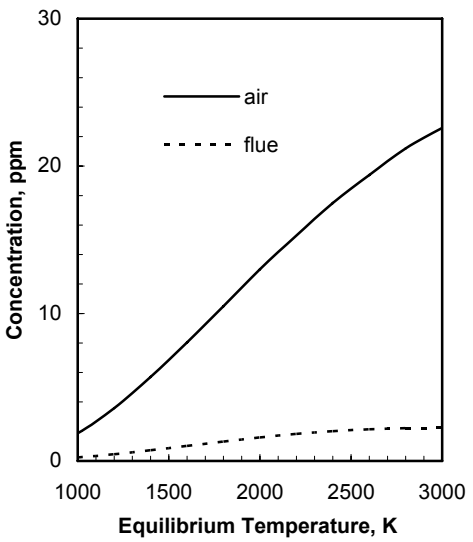

Comments: The equilibrium constant, K_p, for NO increases with equilibrium temperature but is extremely small for values below 1,000K, whereas the equilibrium constant, K_p, for NO_2 decreases with increasing equilibrium temperature. Hence above 1,000K equilibrium values for NO formation increase rapidly with temperature while values for NO_2 formation are lower becoming less favorable. Comparing results obtained for the standard atmosphere and representative flue gas conditions at similar equilibrium temperatures suggest that the amount of NO and NO_2 thermally formed also depends on the initial oxygen and nitrogen available for NO_x chemistry.

EXAMPLE 5.9 Evaluate the kinetic NO concentration in a flue gas using the simplified integrated form of the Zeldovich thermal mechanism. Estimate kinetic predictions at 2,000K for flue gas conditions found in Example 5.7 for nitric oxide concentration at 1 sec.

Solution:

1. Ratio of kinetic NO to equilibrium NO, Equation (5.74):

$$\frac{[NO]}{[NO]_e} = \frac{1 - \exp(-\alpha t)}{1 + \exp(-\alpha t)}$$

where

$$\alpha = \frac{2[NO]_e k_n}{[O_2]^{0.5}}$$

and

$$k_n = \{2k_1 K_{p,O} \big/ (K_{p,NO}^2 (\bar{R}T)^{0.5})\}$$

where the forward rate constant k_1, from Table 5.7,

$$k_1 = 1.8 \times 10^{14} \exp\left(\frac{-76{,}241}{\bar{R}T}\right) \quad \text{cm}^3/\text{gmole} \cdot \text{sec}$$

$$k_1 = 1.8 \times 10^{14} \exp\left(\frac{-76{,}241}{(1.987)(2{,}000)}\right) = 838211.5 \quad \text{cm}^3/\text{gmole} \cdot \text{sec}$$

3. The O and NO equilibrium constants:

$K_{p,O} = .0006637$ (from Table 5.6)
$K_{p,NO} = .019999$ (from Example 5.8)

4. Substituting the forward rate constant and equilibrium constants along with the appropriate universal gas constant having units of 82.057 atm·cc/gmole·K yields

$$k_n = \{(2)(838{,}211.5)(.0006637)/((.019999)^2(82.057 \cdot 2{,}000)^{0.5})\}$$
$$= 6{,}866.98 \text{ gmole/cc}$$

5. Substituting values for equilibrium concentrations of NO and O_2 and k_n,

$$\alpha = \frac{2[[\text{NO}]k_n}{[\text{O}_2]^{0.5}} = \frac{2[y_{\text{NO}}]_e k_n}{[\bar{R}Ty_{\text{O}_2}]^{1/2}} = \frac{(2)(.00299)(6{,}866.98)}{((82.057)(2{,}000)(.0229))^{1/2}}$$
$$= .670 \text{ sec}^{-1}$$

and then for $t = 1$ sec

$$\frac{[\text{NO}]}{[\text{NO}]_e} = \frac{1-\exp(-.670 \cdot 1)}{1+\exp(-.670 \cdot 1)} = 0.323$$

or

[NO] = 0.323. 2990 = 966 ppm

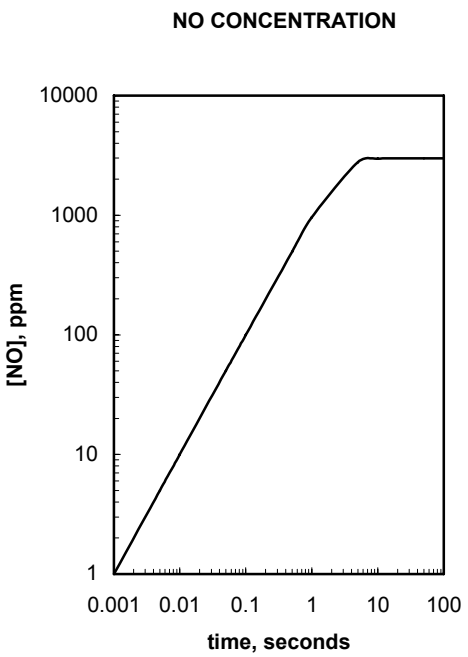

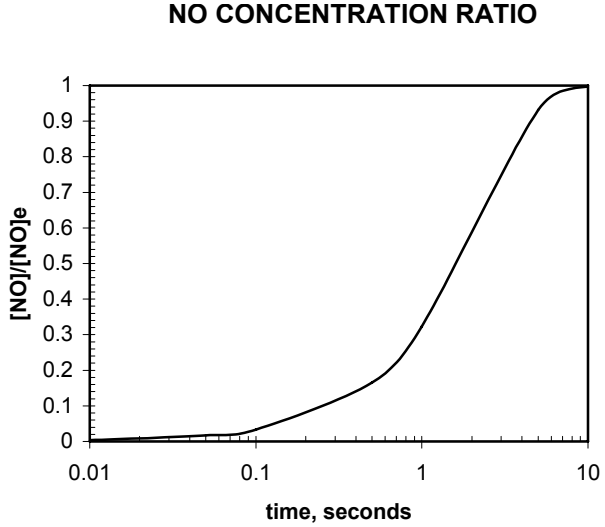

Comments: This problem demonstrates flue gas NO concentration at 2,000K predicted using the simplified Zeldovich thermal mechanism. Results indicate NO has not reached equilibrium in 1 sec. Two plots, $[NO]/[NO]_e$ ratio vs. time and [NO] vs. time, illustrate the approach to equilibrium (t > 10 sec). Values were generated with the Zeldovich mechanism for the 2,000K flue gas by simply using different reaction times. Note that for any specific internal or external combustion device actual NO characteristics may be considerably different than equilibrium predictions unless time-temperature history is such that NO has achieved equilibrium.

The Zeldovich mechanism described in this section can reasonably predict high temperature rates of thermal NO formation from N_2 and O_2. It does a poor job, however, predicting low temperature thermal NO formation rates as well as chemistry of prompt NO and/or fuel bearing NO.

The concentrations of NO are essentially frozen at the high temperature conditions where they are chiefly formed and remain at those values even when cooled. Since high temperature NO decomposition into N_2 and O_2 is a high activation energy process, it therefore is a kinetically limited slow reaction process. Thus frozen concentrations will be lower than equilibrium values predicted for peak temperatures at adiabatic flame conditions but higher than the equilibrium values predicted for cooled exhaust gas conditions.

Complete description of NO_x characteristics, in addition to the thermal mechanism, requires inclusion of fuel-air combustion chemical kinetics, prompt NO chemistry, NO formation from fuel nitrogen, as well as heating and cooling time histories of the combustion gases in specific reaction systems.

5.6 BASIC FLAME THEORY

Autocatalytic chain-branching reaction systems, as illustrated previously by the H_2–O_2 mechanism in Section 5.4, play a major role in the physics of propagating supersonic explosions or detonation waves. A subsonic reaction front that passes through a reactive gas mixture, termed a deflagration in Chapter 4, will now be referred to as a *flame.* The physics of flames is described in many ways, including specific flame reaction mechanisms, flame structures, and thermochemistry within a reactive fluid flow. Most important, flames associated with gas-phase combustion can be classified as being either *premixed,* i.e., flames that propagate through homogeneous fuel-air mixtures, or *diffusion,* i.e., flames that separate regions of pure fuel from pure oxidant.

An engineering analysis of flame physics will apply much of the thermochemical material covered in earlier chapters of this text. For example, overall flame temperature and corresponding heat release will depend on, among other factors, the nature and phase of the particular fuel being burned, total gas pressure, and reactant stoichiometry, as well as the overall reactive product gas composition. Actual peak flame temperatures closely correspond to trends predicted by adiabatic flame calculations with maximum values near stoichiometric reactant conditions. A description of physics within flames, however, is based in part on the kinetic material presented in this chapter. A bimolecular kinetic mechanism for chemistry occurring within a flame, for example, predicts characteristic reaction times on the order of bimolecular collision frequency, as well as a characteristic reaction dimension, or *flame thickness*, on the order of the molecular mean free path. Two factors will cause an actual flame to differ from the bimolecular kinetic flame model: occurrences of three-body collisions and energy loss from the flame as a result of radiation heat transfer.

Both thermal and radical-generated electromagnetic waves are produced by propagating reaction zones and often result in visible or luminous flame emissions. This apparent flame "color" is strongly affected by thermochemical properties such as the temperature, pressure, overall carbon-hydrogen atom ratio, and type of intermediate radicals produced within the flame. The major source of light emitted from within the primary reaction zone of a premixed flame is due to high concentrations of intermediate radicals present in the flame front and, therefore, is chemical kinetic in nature. Postflame emission is thermal rather than kinetic, and Planck's law for blackbody radiation generally characterizes the temperature and wavelength properties of this type of thermally excited emission.

H_2–O_2 flames produce little or no visual emission although H/O radical species such as the OH radical emit electromagnetic energy in the ultraviolet region of the spectrum. Hydrocarbon flames will, in addition, emit electromagnetic energy in the infrared region as a result of the presence of water vapor and C/O species such as CO and CO_2. Stoichiometric and lean hydrocarbon flames often appear blue in the primary zone (kinetic), while fuel-rich flames appear green. Flames with regions of high-carbon particulate concentrations will appear yellow (thermal). Soot-producing flames, having high concentrations of carbon with thermally excited blackbody radiant heat transfer, may be beneficial in certain heating and steam generation applications that require high heat transfer rates from combustion gases. Heat loss from such a flame, on the other hand, may be detrimental to the performance of propulsion machinery requiring adiabatic expansion of these high-pressure and high-temperature gases in order to produce power.

Table 5.8 Approximate Ignition Temperatures in 1-atm Air

		Temperature	
Combustile	Formula	°F	°C
Sulfur	S	470	245
Charcoal	C	650	345
Fixed carbon (bituminous coal)	C	765	405
Fixed carbon (semibituminous coal)	C	870	465
Fixed carbon (anthracite)	C	840–1,115	450–600
Acetylene	C_2H_2	580–825	305–440
Ethane	C_2H_6	880–1,165	470–630
Ethylene	C_2H_4	900–1,020	480–550
Hydrogen	H_2	1,065–1,095	575–590
Methane	CH_4	1,170–1,380	630–765
Carbon monoxide	CO	1,130–1,215	610–665
Kerosene	—	490–560	255–295
Gasoline	—	500–800	260–425

Source: Steam: Its Generation and Use, 37th edition, Babcock & Wilcox Co., Barberton, Ohio, 1963. With permission.

Premixed flames can assume many geometric structures, including flat, conical, spherical, and even cellular-shaped reaction zones. Central ignition of a quiescent gaseous fuel-air mixture contained within a spherical bomb calorimeter will produce a propagating, spherically shaped premixed flame that will travel through the reactive mixture toward the wall with unburned gases ahead of the reaction zone and burned products of combustion behind. An example of a stabilized premixed flame can be found in the inner core of the reaction zone produced by a Bunsen burner in which fuel gas, supplied to the burner base, mixes with air entering the burner tube through the side parts and base, to produce a homogeneous mixture, which then exits at the top of the burner tube.

An important premixed flame parameter is *flame speed,* the propagation rate of a flame front relative to the homogeneous reactants. Premixed flames travel in a direction normal to their flame front, burning toward unburned reactants and away from burned products. Magnitudes for a subsonic deflagration front velocity can vary anywhere from a fraction of a centimeter per second to that of the local speed of sound. Maximum flame speeds occur in stoichiometric mixtures, with speed falling off for the same fluid conditions but with leaner and/or richer mixtures. Flame speeds can be steady or unsteady or can even appear to have a zero velocity, in which event the reactive flow passes through a stabilized flame thermally attached to an appropriate flame holder. Many factors influence flame speed, including initial thermodynamic state, overall fuel-air thermochemistry, chemical kinetics, as well as the aerodynamics of flow. Basically, premixed flame speed is kinetically controlled; that is, flame speed is a function of chemical composition and of complex mechanisms and reaction rates occurring within the flame. Additional factors will also influence flame speed, such as whether the flame is traveling within a laminar or turbulent flow; whether boundary layer interactions occur, including heat transfer and friction losses at a solid wall; and whether the geometric

configuration of the flame front is one-, two-, or three-dimensional. Combustion velocities must be experimentally measured; however, experimentally reported values obtained in a combustion laboratory facility for a particular fuel-air ratio may differ from those actually produced by operational combustion heat and/or power machinery.

The minimum overall temperature at which any fuel-air mixture begins to burn is its *ignition temperature*; see Table 5.8. On a microscopic level, flame initiation and propagation occur in a very local region of a homogeneous mixture when sufficient external energy is provided, such as that supplied by an electric discharge or a spark, which raises local temperature and, hence, collision frequency in excess of that associated with the ignition temperature. *Ignitability* is a means of assessing the relative ability to initiate ignition within a given fuel-air mixture. The self-ignition temperature, or temperature at which spontaneous ignition occurs, can be considerably different from temperatures within a flame. Reactions that begin at the self-ignition temperature, in fact, often show an induction delay, i.e., time period between initiation and observable reaction (~ 1 sec), while reaction time within flames is much shorter (~ 10^{-5} sec). Ignition temperatures and ignition energy measurements are extremely sensitive to experimental facilities and techniques used to obtain these parameters, and experimentally reported values, like flame speed, obtained in a combustion laboratory facility may differ from those actually produced by heat and/or power combustion machinery. *Flammability limits* bracket the rich-to-lean fuel-air mixture range beyond which flame propagation cannot occur after an ignition source is removed, even if the mixture is at its ignition temperature; see Table 5.9. Heat loss to a solid surface and loss of active radical species can cause a premixed flame to be extinguished. The inability to completely burn a gaseous charge at the walls of a closed vessel and the inability to ignite a gas-fired burner properly using improper electrodes are two examples of *flame quenching.* Quenching characteristics of premixed flames are reported in terms of a *quenching diameter,* the minimum diameter of a tube containing a stationary gaseous mixture through which a flame can pass without extinction.

A reaction zone that separates regions of pure fuel from regions of pure oxidant and that requires mixing of these reactants with active radicals within the combustion zone in order to burn is called a *diffusion flame.* Recall that heat transfer is a result of a temperature gradient and that mass flow is a result of a pressure gradient, whereas diffusion of species is a result of a concentration gradient. Burning coal, wood fires, and candles, as well as diesel fuel droplet combustion, are examples of combustion processes that produce diffusion flames. Heat from the flame of a candle vaporizes candle wax, which then mixes by diffusion with the surrounding air to burn in a diffusion flame. It is difficult to burn just a single log or lump of coal because radiation heat loss from burning solids is quite high, and two or more reradiating surfaces are needed to reduce these heat losses. Also, burned gases within the inner core of a Bunsen burner flame mix with the surrounding air to produce a diffusion flame at the outer core of the Bunsen burner flame.

Diffusion flames are more dependent on mixing rate between reactants than on kinetic mechanisms, as is the case with premixed flames. No single parameter, such as a burning velocity, can be associated with diffusion flames because the physics for diffusion flames is considerably more complex. One-dimensional premixed flame models have been developed, but the three-dimensional nature of a diffusion flame, with its associated temperature, pressure, and concentration gradients, does not lend itself to

simple modeling. Low-speed laminar flow diffusion flames, such as those produced by a candle, are controlled by molecular diffusion. High-speed diffusion flames associated with industrial burners and gas turbine combustors depend on turbulent mixing, in which case fuel is introduced as discrete droplets and the aerodynamics of flow are critical to a proper burn.

In this chapter, basic principles of gaseous chemical kinetics and flame chemistry have been introduced. Most practical combustion machinery utilizes liquid and solid fuels. In these instances, atomization and vaporization of liquid fuels and reduction in size and dispersion of solid fuels become essential. These issues, as well as the heterogeneous chemistry of soot formation, cool flames, and safety topics such as flashback and blowoff, have not been treated. A more complete discussion of these important and other chemical kinetic subjects can be found in specific literature.

Table 5.9 Flammability Limits in Air at Ambient Temperature and 1–atm Pressure

Full	Leanest %	Richest %
Acetone (C_3H_6O)	3.10	11.15
Acetylene (C_2H_2)	2.50	80.00
Ammonia (NH_3)	16.10	26.60
Benzene (C_6H_6)	1.41	7.10
Butane (C_4H_{10})	1.86	8.41
Butyl ($C_4H_{10}O$)	1.45	11.25
Butylene (C_4H_8)	1.98	9.65
Carbon monoxide (CO)	12.50	74.20
Ethane (C_2H_6)	3.22	12.45
Ethyl (C_2H_6O)	4.25	18.95
Ethylene (C_2H_4)	3.05	28.60
Heptane (C_7H_{16})	1.00	6.70
Hexane (C_6H_{14})	1.27	6.90
Hydrogen (H_2)	4.00	74.20
Methane (CH_4)	5.00	14.00
Methyl (CH_4O)	7.10	36.50
Octane (C_8H_{18})	0.95	—
Pentane ($C_5(H_{12}$)	1.42	7.80
Propane (C_3H_8)	2.37	9.50
Propyl (C_3H_8O)	2.15	13.50
Propylene (C_3H_6)	2.40	10.30
Propylene oxide (C_3H_6O)	2.10	21.50
Toluene (C_7H_8)	1.45	6.75

Adapted from Coward, H. F. and Jones, G. W., *Limits of Flammability of Gases and Vapors,* Bureau of Mines, Bulletin 503, Washington, DC, 1952.

PROBLEMS

5.1 Equal volumes of ideal gases at equal temperatures and total pressure contain equal numbers of molecules. Using the additional fact that one mole of a gas at *STP* will occupy 22.4 liters, determine the universal gas constant for an ideal gas in units of (a) atm·liters/gmole·K; (b) ft·lbf/lbmole·°R; (c) Btu/lbmole·°R; and (d) N·m/kgmole·K.

5.2 Calculate the mean free path for the gases found in Table 8.1 at (a) 298K and 10-atm pressure; (b) 298K and 0.1-atm pressure; and (c) 1,800K and 1-atm pressure.

5.3 Consider 1 ft^3 of air at *STP*. Determine (a) the acoustic velocity, ft/ sec; (b) the most probable speed, ft/sec; and (e) the mean square speed, ft/sec. Repeat parts (a)–(c) for $T = 900°R$.

5.4 Plot the speed distribution function Ψ as a function of molecular velocity V for helium at (a) 0°C; (b) 300°C; and (e) 900°C. From your results, show that by increasing temperature, the distribution will become broader, yielding more atoms having higher velocities and, hence, greater molecular energy.

5.5 A 0.5-m^3 tank contains N_2 at 101 kPa and 298K. Calculate (a) the molecular density, molecules/cc; (b) the root mean square velocity, cm/sec; and (c) the mean molecular kinetic energy, N·m/molecule.

5.6 The Loschmidt number is defined as the number of molecules per unit volume of any gas at a given temperature and pressure. Show that this number is the same for any gas that obeys the ideal-gas law. Calculate the standard Loschmidt number for 1-atm pressure and 25°C, no./cc.

5.7 Show that the mean molecular speed can be related to the sonic velocity, c, as

$$V_m = \left[\frac{8}{\pi\gamma}\right]^{1/2} c$$

5.8 The internal energy of a monatomic gas can be treated as having an $\bar{R}T/2$ contribution for each directional degree of freedom. Using this kinetic energy model, calculate (a) the constant-volume molar specific heat, kJ/kgmole·K; (b) the constant-pressure molar specific heat, kJ/kgmole·K; and (c) the molar specific heat ratio for a monatomic gas.

5.9 The internal energy of a diatomic gas can be treated as having an $\bar{R}T/2$ contribution for each directional degree of freedom plus an $\bar{R}T/2$ contribution for each rotational degree of freedom. Using this kinetic energy model, calculate (a) the constant-volume molar specific heat, kJ/kgmole·K; (b) the constant-pressure molar heat, kJ/kgmole·K; and (c) the molar specific heat ratio for a low-temperature diatomic gas.

5.10 At high temperatures, a diatomic gas can also have an $\bar{R}T$ contribution from a vibrational energy contribution. Using this kinetic energy model, calculate (a) the constant-volume molar specific heat, kJ/kgmole·K; (b) the constant-pressure molar specific heat, kJ/kgmole·K; and (c) the molar specific heat ratio for a high-temperature diatomic gas.

5.11 Using the bond energy values in Table 5.2, calculate ΔH_f^0 for the following gaseous compounds: (a) methane, CH_4; (b) methylene, C_2H_4; (c) *n*-hexane, C_6H_{I4}; and (d) methanol, CH_3OH, kcal/gmole.

5.12 Calculate the bimolecular collision frequency between N_2 and He as compared to that for the collision frequency between N_2 and O_2, no./sec.

5.13 Determine the mean speeds for the gases found in Table 5.1 at (a) 0°C; (b) 300°C; (e) 900°C; and (d) 1200°C, m/sec.

5.14 The initiation step in most high-temperature oxidation reactions involves the thermal decomposition of the fuel. Let the pyrolysis of a fuel A be represented by the elementary reaction

$$A \rightarrow B + C$$

where
[A] = fuel concentration
[B] = radical product B concentration
[C] = radical product C concentration

For an initial concentration of A of $[A]_0$, find an expression for (a) the rate of dissociation of A; (b) the rate constant for the reaction *k*; and (c) the half-life for the process $t_{1/2}$.

5.15 Consider the elementary reaction

$$A + A \rightarrow \text{products}$$

Assume a molecular weight of 50 g/gmole for A, the effective molecular diameter is 3.5×10^{-8} cm, and the activation energy for the reaction is 40,000 cal/gmole. Determine the temperature rise needed to double the rate of reaction for an initial temperature equal to (a) 500K; (b) 1,000K; (c) 1,500K; and (d) 2,000K. (Assume $[A]_0 = 1$ gmole/cc.)

5.16 At 500K, the rate of a bimolecular reaction is 10 times the rate at 400K. Using collision theory, evaluate the activation energy ΔE of this reaction at these conditions.

5.17 The elementary reaction

$$O_2 + M \underset{k_2}{\overset{k_1}{\rightleftarrows}} O + O + M$$

has a forward rate constant

$$k_1 = 3.61 \times 10^{18}\, T^{-10} \exp\left\{\frac{-118{,}028}{\bar{R}T}\right\}$$

For a reaction temperature of 2,000K, calculate (a) the equilibrium constant K_p; (b) the equilibrium constant K_c; and (c) the reverse rate constant k_2.

5.18 The gas-phase thermal decomposition of nitrous oxide N_2O at 1,030K was studied in a constant-volume vessel at various initial pressures of N_2O. The half-life data obtained for the reactions were found to be as given below:

P_0 mm Hg	52.5	139	290	260
$t_{1/2}$sec	860	470	255	212

Determine a rate constant equation that fits these data.

5.19 The formation of many important radical species involved in certain oxidation reactions can be experimentally studied using radiation techniques. Beer's law expresses the decrease in radiation intensity of wavelength v after it passes through an absorbing medium as

$$\frac{I_1^v}{I_0^v} = \exp\{-[\mathrm{A}] l \in_v\}$$

where

I_0 = incident radiation intensity
I_1 = transmitted radiation intensity
[A] = concentration of radical, gmoles/cc
v = radiation wavelength, Å
l = radiation pathlength, cm
$\in_v$ = molar extinction coefficient

5.20 Consider the formation of radical A via the elementary reaction

$$\mathrm{A_2} + \mathrm{M} \xrightarrow{k} 2\mathrm{A} + \mathrm{M}$$

Use Beer's law to develop (a) an equation for the rate of formation of the radical A, and (b) an expression for k in terms of the initial concentrations of $[A_2]_0$ and $[A]_0$.

5.21 The maximum spectral emissive power for blackbody thermal radiation is given by Wien's displacement law

$$\lambda_{\max} T = 2{,}897\ \mu\mathrm{m\ K}$$

Determine the temperature required for maximum emission in the (a) ultraviolet ($\lambda = 0.3\ \mu$m), K; (b) visible ($\lambda = 0.5\ \mu$m), K; and (c) infrared ($\lambda = 1.2\ \mu$m), K.

5.22 Laminar premixed flame speeds S_L for fuel-air mixtures are found to fit the relationship empirically:

$$S_L = a + bT_{\text{init}}^n \quad \text{m/sec} \qquad 200 < T_{\text{init}} < 600\mathrm{K}$$

where

Gas	a	b	n
methane	0.08	1.6×10^{-6}	2.11
propane	0.10	3.4×10^{-6}	2.00
benzene	0.30	7.9×10^{-9}	2.92
isooctane	0.12	8.4×10^{-7}	2.19

Calculate the laminar flame speed for methane for an initial temperature of (a) 200K, (b) 400K, and (c) 600K, m/sec.

5.23 Repeat Problem 5.22 for (a) propane, (b) benzene, and (c) isooctane.

5.24 The pressure dependency for a laminar premixed flame is found to satisfy the relationship

$$\ln S_L = c + d \ln P \qquad \text{m/sec}$$

where

$S_L = 0.225$ m/sec at 150 kPa $\qquad$ $S_L = 0.223$ m/sec at 405 kPa

Plot (a) $\ln S_L$ versus $\ln P$, (b) S_L versus P, and (c) determine the values of c and d.

5.25 The thermal decomposition of nitrogen dioxide can be determined via the elementary initiation reaction

$$NO_2 + NO_2 \xrightarrow{k} NO + O + NO_2$$

Using the rate constants for the NO_2 reaction given below, determine the following: (a) the differential equation for NO_2 rate of decomposition; (b) the integrated expression for $[NO_2]$ versus time; (c) the reaction activation energy, cal/gmole; (d) the effective NO_2 molecular diameter, m.

$$k\langle 592\text{K}\rangle = 522\ \text{cm}^3/\text{sec}\cdot\text{gmole} \qquad k\langle 656\text{K}\rangle = 5{,}030\ \text{cm}^3/\text{sec}\cdot\text{gmole}$$

5.26 Show that when the reaction OH +N $\rightleftarrows$ NO + is included as reaction 3 in the Zeldovitch mechanism, then

$$\frac{d[\text{NO}]}{dt} = \frac{2[\text{O}][\text{N}_2]\{1 - ([\text{NO}]^2 / K_{p,\text{NO}}[\text{NO}][\text{O}_2])\}}{1 + k_{-1}[\text{NO}]/(k_2[\text{O}_2] + k_3[\text{OH}])}$$

5.27 The formation of nitric oxide (NO) can be explained using the Zeldovitch free radical chain mechanism consisting of

$$O + N_2 \rightleftarrows NO + N \tag{5.48}$$

$$N + O_2 \rightleftarrows NO + O \tag{5.49}$$

If the NO concentrations are much less than their equilibrium values, the reverse reactions can be neglected. Using the steady state approximation for N atom, show that this assumption provides the following simple rate expression for formation of nitric oxide from atmospheric nitrogen in combustion processes.

$$\frac{d[\text{NO}]}{dt} = 2k_1[\text{O}]_{eq}[\text{N}_2]_{eq}$$

6

Solid Fuels

6.1 INTRODUCTION

Any general engineering foundation in combustion, in addition to presenting principles of thermochemistry, should review several specific fuel science topics including energy characteristics of various important fuel resources. Many reasons come to mind for selecting solid fuels as the first fuel science subject covered in this text, including the historical role the solid fuel coal played in the birth of the Industrial Revolution, the relevance today solid fuels play in industrial heat and power generation, and general pollution issues associated with solid fuel combustion. In addition, solid fuel resources including coal may become viable in the future as feedstock for producing various synthetic liquid and gaseous fuels.

A significant amount of material has been written and published that addresses various subjects relating to solid fuels including the origins, the world's distribution, as well as the potential environmental impact and economics of increased use of coal. This discussion, however, will focus mainly on those particular engineering topics that are germane to industrial combustion-generated power or heat transfer applications. The following material will be limited therefore to considering technical aspects of solid fuels, the combustion machinery necessary to burn these selected reactants, and their general emissions characteristics and pollution control.

6.2 SOLID FUEL THERMOCHEMISTRY

Most naturally occurring solid fuel resources are primarily hydrocarbon-based compounds. The prominent solid phase component in these fuels is carbon. From Table B.1 in Appendix B, the heat of combustion of solid carbon is found to equal

$$\Delta\overline{H}_c = 393{,}804 \text{ kJ/kgmole} \quad (169{,}307 \text{ Btu/lbmole}) \tag{6.1}$$

or

$$\Delta H_c = 32{,}817 \text{ kJ/kg carbon} \quad (14{,}109 \text{ Btu/lbm}) \tag{6.2}$$

The heating value of hydrocarbon-based solid fuels should therefore be approximately 32,800 kJ/kg fuel (14,110 Btu/lbm).

Complex solid fuel resources, such as coal, can vary in their local material and energy characteristics. The energy released by coal obtained from various mine locations will be considerably different from the ideal heat of combustion for carbon. A practical method for determining the actual heating value of a particular solid (or liquid) fuel source employs the use of a constant-volume reaction vessel; see Figure 6.1. Results are derived by inferring the energy released from the complete combustion of a sample of source material within the vessel. The experimental techniques used to determine the heat of combustion are based on principles of *calorimetry*. In order to ensure accurate measurements of energy in a fuel sample, bomb calorimetry requires the use of standard procedures, such as those established by the American Society for Testing Materials (ASTM), skillful calibration, and repeatable operation with the facilities.

A reaction vessel containing a fuel and excess pure oxygen mixture is immersed in a water bath initially at ambient conditions, usually *STP* temperature of 25°C. Energy released by complete combustion of the reactants within the vessel is absorbed by the surrounding water bath, causing the water temperature in the jacket to rise. By burning a pure compound having a known heating value, such as benzoic acid, a thermal response, or *water equivalence,* of the apparatus can be established from the heat released by the calibration sample. After calibrating the unit, any fuel sample that releases approximately the same total energy would also cause the water jacket temperature to rise approximately the same, and by using the water equivalence, the fuel heating value can thus be determined. Using a constant-volume oxygen bomb calorimeter, heating values of solid and certain liquid fuels can be experimentally determined, using Equation (6.3) as

$$HV = \frac{W\Delta T - E_1 - E_2 - E_3 - E_4}{m} \tag{6.3}$$

where

W = water equivalent, kJ/°C (Btu/°F)
ΔT = temperature rise, °C (°F)
E_1 = correction for heat of formation of nitric acid
E_2 = correction for heat of formation of sulfuric acid
E_3 = correction for combustion of gelatin capsule (used with liquid fuel testing)
E_4 = correction for heat of combustion of firing wire
m = weight of fuel sample, kg (lbm)
HV = heating value of fuel, kJ/kg (Btu/lbm)

Accuracy requires mass measurement of the fuel sample to within ± 0.001 g and water jacket temperature to within ± 0.002°C. Ignition of premeasured fuel and excess pure oxygen is accomplished by passing current through an ignition wire. Several corrections are included in Equation (6.3) to account for extraneous experimental factors such as energy released by burning any ignition wire and energy associated with the

formation of any nitric and/or sulfuric acid. Experimental errors can arise because of improper fuel sizing or contamination with impurities during preparation. Note that, to ensure equal water equivalents, calibration and experimental runs require that fuel sample weight be carefully controlled. Improper ignition, for example, from an insufficient ignition current or misalignment or grounding of the ignition wire, or insufficient oxygen for complete combustion would also contribute to experimental error. Improper calibration or testing can result in erroneous water equivalence and/or predicted heating value.

Most natural solid fuels exist in the environment as complex organic chemical and mineral compounds that have undergone various degrees of aging and chemical conversion. Solid hydrocarbon fuel resources, beginning with wood through coal, are actually vegetation in various stages of decay and consist chiefly of carbon, hydrogen, oxygen, moisture, sulfur, carbon monoxide, methane, ethane, sulfuric acid, tars, and ammonia.

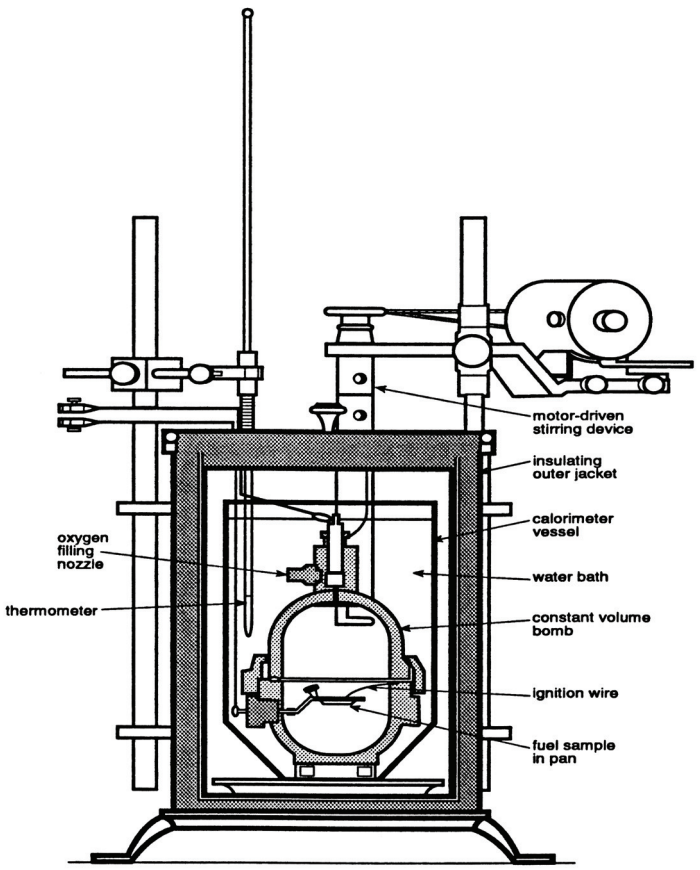

Figure 6.1 Constant-volume oxygen bomb calorimetry. Adapted from Giedt, W. H., *Thermophysics*, Van Nostrand Reinhold Company, New York, 1971. With permission of the author.

Specification of the precise energy characteristics of these solid fuels would require a complete knowledge of all constituents expressed in terms of each constituent mass fraction, i.e., an *ultimate analysis.* Often for engineering consideration a *proximate* or *fixed carbon* analysis is sufficient to define the fuel's combustion characteristics expressed as *a fixed carbon,* C*,* analysis or

$$\%\ \mathrm{C} = 100\% - \%\ \text{moisture} - \%\ \text{volatiles} - \%\ \text{ash} \tag{6.4}$$

Moisture is water trapped within a fuel sample; volatiles are constituents that evaporate during low-temperature heating of the fuel; while ash is inorganic mineral impurity or residue left when a fuel has been completely burned. The fixed carbon is a coke-like residue fuel resource left after water vapor, volatiles, and ash are removed.

EXAMPLE 6.1 A constant-volume bomb calorimeter is to be used to determine the heating value of a solid fuel. To calibrate the vessel, 0.848 g of benzoic acid, having a heating value of 26,452 kJ/kg, is completely burned by reaction with oxygen, causing the water jacket, stirrer, bomb thermometer, etc. to be heated. Precise measurement of the temperature rise of the water gives a reading of +2.49ºC. After calibration, 1.05 g of the solid fuel is then completely burned, giving a temperature increase of 4.882ºC. Neglecting the correction terms, calculate (a) the water equivalent for the bomb, kJ/ºC rise; and (b) the heating value of the fuel, kJ/kg.

Solution:

1. Water equivalence:

$$W = \frac{(HV)(m)}{\Delta T} = \frac{(26{,}452\ \text{kJ/kg})(0.848\ \text{g})}{(1{,}000\ \text{g/kg})(2.49°\text{C})}$$

   a. $W = 9.009$ kJ/°C rise

2. Heating value:

$$HV = \frac{(W)(\Delta T)}{m} = \frac{(9.009\ \text{kJ/°C})(1{,}000\ \text{g/kg})(4.882°\text{C})}{(1.05\ \text{g})}$$
$$= 41{,}888\ \text{kJ/kg}$$

   b. $HV = 41{,}890$ kJ/kg of fuel

Empirical equations, such as DuLong's formula, can be used to predict a higher heating value of solid fuels when an ultimate analysis is known.

$$HHV = 33{,}960\,C + 141{,}890\left[H - \frac{O}{8}\right] + 9{,}420\,S \quad \text{kJ/kg} \tag{6.5a}$$

$$HHV = 14{,}600\,C + 61{,}000\left[H - \frac{O}{8}\right] + 4{,}050\,S \quad \text{Btu/lbm} \tag{6.5b}$$

where

HHV = higher heating value
C = mass fraction of carbon – fuel ultimate analysis
H = mass fraction of hydrogen – fuel ultimate analysis
O = mass fraction of oxygen – fuel ultimate analysis
S = mass fraction of sulfur – fuel ultimate analysis

DuLong's formula expresses heating value in terms of major solid fuel constituents, their heating value, and corresponding mass fractions.

The lower heating value of a solid fuel can be determined from higher heating value of the fuel and knowledge of the mass of water formed by combustion to the mass of fuel as

$$LHV = HHV - Wh_{fg} \qquad \text{kJ/kg (Btu/lbm)} \qquad (6.6)$$

where

LHV = lower heating value
W = mass of water formed/mass of fuel burned
h_{fg} = latent heat of vaporization for water at heating value conditions

6.3 COAL AND OTHER SOLID FUEL RESOURCES

The world's most prominent natural solid fuel resource is coal. Coal, remnants of plants and other vegetation that have undergone varying degrees of chemical conversion in the biosphere, is not a simple homogeneous material but rather is a complex substance having varying chemical consistency. Energy characteristics of coal obviously depend on many factors, including particular composition of the original vegetation, amount and type of inorganic materials present in the debris, and the specific history that these local materials have undergone during regional deposition and conversion.

Plant life first began to decay by anaerobic, or bacterial, action, often in swamps or other aqueous environments, producing a material known as *peat.* The decomposing material was next covered and folded into the Earth's crust via geological action that provided extreme hydrological pressure and heating required for the coal conversion process, as well as an environment that drove off volatiles and water. This complex transformation, or *coalification process,* resulted in change, or *metamorphosis,* over great periods of time and in a variety of fuels ranging from peat, which is principally cellulose, to hard, black coal, which is principally amorphous carbon.

Standards for coal classification have been established by the ASTM and allow coal to be identified by rank and grade. *Rank* is a measure of the time period for coal conversion; i.e., a low rank has less carbon, whereas a high rank coal is mostly carbon. *Grade* is a measure of the degree of fixed carbon in a coal sample. Four grades of coal commonly specified, starting from lowest to highest, are: lignite, subbituminous, bituminous, and anthracite. Table 6.1 gives typical energy characteristics of coal.

Table 6.1a Properties of Coal

Coal grade	Approximate heating value	
Anthracite	30,240–33,730	13,000–14,500
Bituminous	27,910–34,420	12,000–14,800
Subbituminous	19,310–23,620	8,300–10,000
Lignite	13,260–17,450	5,700– 7,500
	kJ/kg coal	Btu/lbm coal

Table 6.1b Proximate Analysis of Typical U.S. Coal Samples

		Proximate analysis, %				Nominal heating value	
Coal grade	Source	Moisture	Volatile matter	Fixed carbon	Ash	kJ/kg	Btu/lbm
Anthracite	PA	4.4	4.8	81.8	9.0	30,540	13,130
Bituminous							
Low-volatile	MD	2.3	19.6	65.8	12.3	30,750	13,220
Medium-volatile	AK	3.1	23.4	63.6	9.9	31,470	13,530
High-volatile	OH	5.9	43.8	46.5	3.8	30,590	13,150
Subbituminous	WA	13.9	34.2	41.0	10.9	24,030	10,330
	CO	25.8	31.1	38.4	4.7	19,960	8,580
Lignite	ND	36.8	27.8	30.2	5.2	16,190	6,960

Source: U.S. Bureau of Mines Technical Bulletin, 1970, Washington, DC.

EXAMPLE 6.2 Cellulose, $C_6H_{10}O_5$, is a major constituent of both organic and inorganic waste material. The higher heating value of cellulose is approximately 7,500 Btu/lbm. (a) Determine the stoichiometric reaction for the ideal combustion of cellulose; (b) estimate the heat of formation at *STP*, Btu/lbmole; (c) find the heat released from burning cellulose with 140% theoretical air in an atmospheric burner, assuming the stack temperature to be 1,520ºF; and (d) find the ratio of cellulose to that of carbon required to produce the same ideal heat release.

Solution:

1. Stoichiometric equation:

$$C_6H_{10}O_5 + aO_2 \rightarrow bCO_2 + cH_2O_g$$

Carbon atom balance:

$$b = 6$$

Hydrogen atom balance:

$$c = 5$$

Oxygen atom balance:

$$5 + 2a = 12 + 5$$
$$a = 6$$

or

$$C_6H_{10}O_5 + 6[O_2 + 3.76\,N_2] \rightarrow 6CO_2 + 5H_2O + (6)(3.76)N_2$$

2. Energy balance (*STP*) using $\bar{h}_f^0$ from Table B.1 in Appendix B:

$$Q = \sum_{\text{prod}} N_j\left[\bar{h}_f^0 + \Delta\bar{h}\right]_j - \sum_{\text{react}} N_i\left[\bar{h}_f^0 + \Delta\bar{h}\right]_i$$
$$= [6(-94{,}054)(1.8)_{CO_2} + 5(-68{,}317)(1.8)_{H_2O}] - \bar{h}_f^0\Big)_{C_6H_{10}O_5}$$

and

$$Q = [(6)(12) + (10)(1) + (5)(16)][-7500] = -1{,}215{,}000 \text{ Btu/lbmole fuel}$$

or

$$\bar{h}_f^0\Big)_{C_6H_{10}O_5} = +1{,}215{,}000 - 6(94{,}054)(1.8) - 5(68{,}317)(1.8)$$

b. $$= -415{,}640 \text{ Btu/lbmole}$$

3. 140% theoretical air combustion with $T_2 = 1980°R$:

$$C_6H_{10}O_5 + (1.4)(6)[O_2 + 3.76\,N_2] \overset{P}{\rightarrow}$$
$$6CO_2 + 5H_2O + (0.4)(6)O_2 + (1.4)(6)(3.76)\,N_2$$

$$Q = [\{6(-94{,}054 + 9{,}296)_{CO_2} + (5)(-57{,}798 + 7{,}210)_{H_2O_g} + (0.4)(6)(O + 6{,}266)_{O_2} + (1.4)(6)(3.76)(O + 5{,}917)_{N_2}\}(1.8) - 1.0(-415{,}640 + O)_{C_6H_{10}O_5}]$$

$$Q = -5.92 \times 10^5 \text{ Btu/lbmole cellulose}$$

or

c. $$|q| = \frac{5.92 \times 10^5 \text{ Btu/lbmole}}{162 \text{ lbm/lbmole}} = 3{,}654 \text{ Btu/lbm cellulose}$$

4. Heat flux—using the higher heating value:

Cellulose:

$$\dot{Q}\langle STP\rangle = \dot{m} \times 7{,}500 \text{ Btu/lbm cellulose}$$

Carbon:

$$\dot{Q}\langle STP\rangle = \dot{m} \times 14{,}095 \text{ Btu/lbm carbon}$$

or

d. $$\frac{m\langle \text{lbm cellulose}\rangle}{m\langle \text{lbm carbon}\rangle} = \frac{14{,}095}{7{,}500} = 1.88$$

Lignite, the lowest grade of coal, takes its name from the Latin word for wood, *lignum*. Since this material is in the early stages of coalification, it often has a woodlike structure and is high both in moisture content and volatile components. Lignite has a low heat of combustion, nearly equal that of cellulose.

Subbituminous, the next highest grade, is often referred to as black lignite. U.S. subbituminous coal reserves are large; and, in general, this type of coal has a higher fixed carbon content than lignite but might still have a high degree of moisture as well as considerable ash content. Subbituminous is often not preferred as a natural fuel resource; but its low sulfur content, relatively free-burning, non-caking characteristics, and relatively low energy density make it a candidate for combustion in coal-burning systems in which sulfur content may be critical.

Bituminous coal, the next highest grade, is a soft coal having high sulfur content. It will produce significant smoke when burned and is therefore also not usable as a natural fuel. The largest U.S. coal reserves are bituminous; and, in general, this class of coal will have a lower fixed carbon but higher volatile concentration than the highest grade of coal. Bituminous coal, because of its high volatile content, is a good potential candidate solid fuel for use as a feedstock for producing synthetic liquid and gaseous fuels. It will burn easily in a pulverized or powdered form since, when heated, it tends to reduce to a cohesive, sticky mass.

Anthracite, the highest grade of coal, is a brittle, homogeneous and hard, black substance having a high fixed carbon content (usually above 90%) and a low percentage of volatiles (less than 15%). It is a dense material, bordering on graphite, having a high energy density, low sulfur content, but the lowest known U.S. reserves of the four grades of coal. Anthracite is a slow-burning coal that is difficult to ignite and tends not to cake.

The composition and location of anthracite have made it an energy resource heavily used in the steel industry.

The most important renewable solid fuel resource, which has been used in many cultures for millennia, is wood. Timber is a natural solar energy storage medium, having a reproduction rate that can vary anywhere from 25 to 100 years, depending on the type of tree. Wood was a major energy source in the early history of the United States, and at the turn of the nineteenth century, it accounted for one-fourth of the nation's total energy supply. U.S. timber resources could yield about the same energy as that available in proven U.S. natural gas reserves, about a third more energy than that in proven oil reserves, and less than 10% of energy potential in proven coal reserves. Estimates further indicated that a region of approximately 30% of the total farming acreage in the United States could theoretically meet energy input requirements of all installed electric generating capacity in the United States.

Proper use of wood as a fuel could contribute to development of forested regions as long as its burning rate does not ecologically and aesthetically exceed the growth rate in the region. History tells of what occurs when this principle is violated. Mediterranean forests were cut down during the years of the Roman Empire to provide fuel for smelting iron. Toward the end of the Roman Empire, local forests were so depleted that the Empire had to resort to moving their iron works north to German forests and importing iron from the provinces. The large water requirements for biomass production also tend to limit pursuing use of timber as a major fuel resource. Some consideration, however, has been given to producing liquid and gaseous fuels from biomass growing in aqueous environments such as the ocean. Biomass fuels generated from vegetation will be discussed in later chapters.

Although the industrial and commercial use of trees and other forms of vegetation as a solid biomass fuel is not as extensive today as in the past, its use as a general-purpose or supplementary source of energy for domestic heating and cooking is still significant in specific applications and local areas. In certain regions, steam power plants purchase chipped wood as a fuel. Commercial use of wood and wood wastes is more common in the lumber industry. Wood waste left from manufacturing of lumber can be as high as 50% of the original logging and consists of unusable side slabs, bark, shavings, and sawdust. The larger pieces of this waste material are reduced in size for proper burning using a device termed a *hog.* Sized chips, shavings, and sawdust are mixed to yield a wood fuel commonly referred to as *hog fuel.* Sawmills produce energy while using burning as a means of eliminating this waste material. Paper mills also burn their wet wood by-products as a means of disposal.

EXAMPLE 6.3 The ultimate analysis of a coal as fired is reported to be as listed below.

As-fired constituent	*Percentage*	*As-fired constituent*	*Percentage*
C_S	72.8	H_2O	3.5
H_2	4.8	S	2.2
O_2	6.2	ash	9.0
N_2	1.5		

Assuming ideal complete combustion of the coal at *STP,* calculate (a) the molar air-fuel ratio; (b) the mass air-fuel ratio; (c) the higher heating value of the coal using DuLong's formula, kJ/kg fuel; and (d) the higher heating value of the coal using JANAF data, kJ/kg fuel.

Solution:

1. Mole fraction fuel sample, ashless

	mf_i	MW_i	mf_i/MW_i	$\bar{x}_i$
C_S	0.8000	12.0	0.06667	0.6760
H_2	0.0527	2.0	0.02635	0.2672
O_2	0.0681	32.0	0.002128	0.02158
N_2	0.0165	28.0	0.000589	0.005972
H_2O	0.0385	18.0	0.002139	0.02169
S	0.0242	32.0	0.000756	0.007665
	$\frac{\text{kg}_i}{\text{kg}_{\text{tot}}}$	$\frac{\text{kg}_i}{\text{kg}_{\text{mole}}}$	$\frac{\text{kg}_{\text{mole}_i}}{\text{kg}_{\text{tot}}}$	$\frac{\text{kg}_{\text{mole}_i}}{\text{kg}_{\text{mole}_{\text{tot}}}}$

where, for example, for carbon

$$mf_i = \frac{72.8}{100 - 9.0} = 0.8000$$

$$\Sigma\left(\frac{mf}{MW}\right)_i = 0.06667 + 0.02635 + 0.002128 + 0.000589 + 0.002139 + 0.000756 = 0.09863 \text{ kgmole/kg})_{\text{tot}}$$

$$\bar{x}_i = \frac{0.06667 \text{ kgmole}_i/\text{kg}_{\text{tot}}}{0.09863 \text{ kgmole}_{\text{tot}}/\text{kg}_{\text{tot}}} = 0.6760 \frac{\text{kgmole}_i}{\text{kgmole}_{\text{tot}}}$$

2. Stoichiometric equation:

$$[0.6760\ C_S + 0.2672\ H_2 + 0.0216\ O_2 + 0.0060\ N_2 + 0.02169\ H_2O + 0.00767\ S] + a[O_2 + 3.76\ N_2] \rightarrow bCO_2 + cH_2O + dSO_2 + eN_2$$

Carbon atom balance:

$b = 0.676$

Hydrogen atom balance:

$2(0.2672 + 0.02169) = 2c$ $\qquad c = 0.28889$

Sulfur atom balance:

$d = 0.00767$

Oxygen atom balance:

$2(0.0216) + 0.02169 + 2a = 2(0.676) + 0.28889 + 2(0.00767)$

$a = 0.7957$

Nitrogen atom balance:

$e = (0.7957)(3.76) + 0.0060 = 2.998$

3. Air-fuel ratio:

Molar:

a. $\overline{AF} = \dfrac{(0.7957)(4.76)\ \text{kgmole air}}{1.0\ \text{kgmole fuel}} = 3.7875$

Mass:

$$AF = \frac{(3.7875\ \text{kgmoles air})(28.96\ \text{kg/kgmole air})}{(1.0\ \text{kgmole fuel})(0.09863\ \text{kgmole fuel/kg})^{-1}}$$

b. $AF = 10.818$

4. DuLong's formula:

$$HHV = 33{,}960\ C + 141{,}890\left[H - \frac{O}{8}\right] + 9{,}420\ S$$

or

$HHV = 33{,}960(0.728) + 141{,}890[0.048 - (0.062/8)] + 9{,}420(0.0222)$

c. $HHV = 30{,}640$ kJ/kg coal

5. Energy balance:

$$Q = \sum_{\text{prod}} N_i[\bar{h}_f^0 + \Delta\bar{h}]_i - \sum_{\text{react}} N_j[\bar{h}_f^0 + \Delta\bar{h}]_j$$

where, using appropriate values from Appendix B,

$$\sum_{\text{prod}} N_i\bar{h}_{f_i}^0 = [0.676(-94{,}054)_{CO_2} + 0.28889(-68{,}317)_{H_2O} + 0.00767(-70{,}947)_{SO_2} + 2.998(0)_{N_2}]\text{cal/gmole} = -83{,}860\ \text{cal/gmole}$$

$$\sum_{\text{react}} N_j\bar{h}_{f_j}^0 = [0.676(0)_{C_S} + 0.2672(0)_{H_2} + 0.0216(0)_{O_2} + 0.006(0)_{N_2} + 0.02169(-68{,}317)_{H_2O} + 0.00767(0)_S] = -1{,}482\ \text{cal/gmole}$$

$$Q = [-83{,}860 - (-1{,}482)\ \text{cal/gmole}]\left[4.187\ \frac{\text{kJ/kgmole}}{\text{cal/gmole}}\right]$$

$$= 344{,}917\ \text{kJ/kgmole}$$

d. $HHV = (344{,}917\ \text{kJ/kgmole fuel})(0.09863\ \text{kgmole fuel/kg})$

$$= (34{,}020\ \text{kJ/kg ashless})\left(\frac{91\ \text{kg ashless}}{100\ \text{kg coal}}\right) = 30{,}960\ \text{kJ/kg coal}$$

Table 6.2 Typical Analyses of Dry Wood

Type	Wt %							*HHV*		Reference
	C	H	N	S	O	Cl	Ash	MJ/kg	Btu/lbm	
Softwoods*										
Cedar, white	48.80	6.40	—	—	44.40	—	0.40	18.61	8,018	Johnson & Auth
Cypress	55.00	6.50	—	—	38.10	—	0.40	22.96	9,892	Johnson & Auth
Douglas fir	52.3	6.3	0.1	0.0	40.5	—	0.8	21.01	9,050	Tillman 1978
Hemlock, western	50.4	5.8	0.1	0.1	41.4	—	2.2	20.01	8,620	Tillman 1978
Pine	51.27	6.19	0.13	0.13	42.13	0.02	0.13	20.3	8,748	Feldman et. al.
white	52.60	6.10	—	—	41.20	—	0.10	20.7	8,919	Johnson & Auth
yellow	52.60	7.00	—	—	52.60	—	1.31	22.44	9,668	Risser
Redwood	53.5	5.9	0.1	0.0	40.3	—	0.2	20.98	9,040	Tillman 1978
Hardwoods*										
Ash, white	49.70	6.90	—	—	43.00	—	0.30	20.75	8,940	Johnson & Auth
Beech	51.6	6.3	0.0	0.0	41.5	—	0.6	20.33	8,760	Tillman 1978
Birch, white	49.80	6.50	—	—	43.40	—	0.30	20.12	8,669	Johnson & Auth
Elm	50.40	6.60	—	—	42.30	—	0.70	20.98	9,039	Johnson & Auth
Hickory	49.7	6.5	0.0	0.0	43.1	—	0.7	20.12	8,670	Tillman 1978
Maple	50.6	6.0	0.3	0.0	41.7	—	1.4	19.91	8,580	Tillman 1978
Oak	49.83	5.87	0.32	0.04	41.82	0.03	2.09	19.43	8,373	Feldman et al.
red	49.34	5.93	0.07	0.13	41.74	0.03	2.76	19.08	8,220	Feldman et al.
white	49.48	6.38	0.35	0.01	43.13	—	1.52	19.42	8,367	Jenkins & Ebeling
Poplar	51.6	6.3	0.0	0.0	41.5	—	0.6	20.7	8,920	Tillman 1978

*Softwoods belong to the botanical group having needle or scalelike leaves, whereas hardwoods belong to the group that are broad-leaved; neither of which refer to the actual hardness of the wood, according to the *Wood Handbook*, Forest Products Laboratory of the U.S. Department of Agriculture.
Source: R. L. Bain and W. A. Amos, National Renewable Energy Laboratory and M. Downing and R. L. Perlack, Oak Ridge National Laboratory, *Technical Report: Biopwer Technical Assessment: State of the Industry and Technology*, National Renewable Energy Laboratory, Department of Energy Laboratory, Golden, CO, 2003.

Burning wood is also a good means of utilizing diseased timber, trees downed by wind, as well as cull trees, i.e., those so twisted that they have no lumber value and ash left from burning can be used in a garden. The worldwide energy crisis of the late twentieth century motivated many Americans again to try to use wood for domestic heating. Burning wood in suitable wood-burning stoves might provide an auxiliary source of heat when an appropriate high energy density, slow-burning, low-creosote timber is locally available. Also, not all wood-burning stoves and fireplaces are efficient space heaters. Many homes heated using wood actually lose more energy than is released by combustion since even good wood-burning stoves have efficiencies on the order of only 50%.

Wood has a variable consistency and, like coal, is actually a heterogeneous fuel source; see Table 6.2. The major fuel component in wood is Cellulose $(C_6H_{10}O_5)_n$, with trace amounts of lignin, resins, gum, water, and ash. Water content in wood, a critical parameter in its ability to burn properly, ranges from 30–50% by weight in green wood to 18–25% in air-dried lumber. Even burning various types of dried timber will release a different energy per unit mass because of the non-uniform concentrations of the resins, gums, and other trace combustible components in wood. Since Dulong's formula does not include heat released by these trace constituents, predicting heating value with this relationship can predict improper heats of combustion for wood.

Coal or wood can be upgraded as a fuel suitable for certain applications simply by driving off the volatiles and moisture content of the raw material. Destructive distillation, accomplished by limited combustion in an oxygen-deficient atmosphere, or *pyrolysis,* produces a solid carbonaceous residue, *or char,* that can subsequently be burned. Char produced using coal resources is called *coke* which, because it is purer than raw coal, is a processed fuel that the metallurgical industry uses in the production of iron and steel. Char produced using wood is referred to as *charcoal* and is used, among other things, as a filtering medium.

Certain by-products of the food processing industry can also produce a useable solid fuel. As examples, nut shells, rice hulls, coffee grounds, and corn husks are burnable and can be used to provide some of the necessary heating in fruit and vegetable processing plants. Sugarcane grows abundantly in Central America and the tropics and, on a moisture- and ash-free basis, consists of 83–90% sugar and 17–10% cellulose by weight. After extracting the sugar by shredding, rolling, and steam heating, the wasteful fibrous cane by-product, termed *bagasse,* can be burned in a suitable boiler used to generate steam required to extract sugar from the cane.

Modern industrialized societies tend to produce an abundance of both organic and inorganic solid wastes. The traditional means for disposing of these high-technology waste by-products is by burial in sanitary landfills. Many constituents of *municipal solid waste,* or MSW, are not inert and, when buried, will begin a process of biodegradation that can produce potentially explosive pockets of gas consisting of approximately 50% methane-50% carbon dioxide by volume. In addition, toxic compounds such as chlorine, fluorine, and other trace substances present in raw MSW can leach into the water table surrounding a landfill site. The continued introduction of non-inert MSW into a limited number of suitable landfill sites is therefore a serious environmental issue that many growing urban centers are now facing.

An alternate means of MSW disposal, since those materials by weight consist of 50–80% combustibles, is incineration. After burning, original waste material is transformed into a sterile, solid burned-out residue that is reduced to 5% of the original volume or 17% of its original mass. Incineration has been used chiefly as a means of

volume reduction of MSW prior to burial in landfills. Mass burning of trash does release energy in a form as heat that could be recovered if appropriate steam-generating systems are utilized. Incinerators with waste heat boilers have been used to provide steam for heating purposes in both the United States and Europe. Direct combustion of 10–20% MSW, 90–80% coal mixtures by weight, has been successfully burned using particular coal-burning equipment. Use of MSW as a suitable solid fuel does raise some engineering concerns and constraints, such as generation of unhealthy levels of hazardous air pollution, significant airborne ash; presence of highly explosive constituents, such as gas cans, fireworks, TNT; unacceptably high moisture content; long-term instability due to the biodegradable nature of MSW; and production of pungent odors. Incineration-fired steam generators tend to have abnormally corrosive flue gases that attack heat transfer surfaces in a unit because of the presence of chlorine, fluorine, sulfur, and chlorinated plastics in the waste stream. Incinerators for MSW reduction have been curtailed as emission control requirements have become more stringent. Modern refuse disposal combustion facilities that are environmentally safe are under design and construction in the United States as well as overseas in Europe and Japan. The Europeans and the Japanese, because of their limited land, energy, and economic resources, were concerned with resource recovery systems before major U.S. efforts began after the energy crisis of the 1970s. Thermal Destructors will be discussed in detail in Chapter 13.

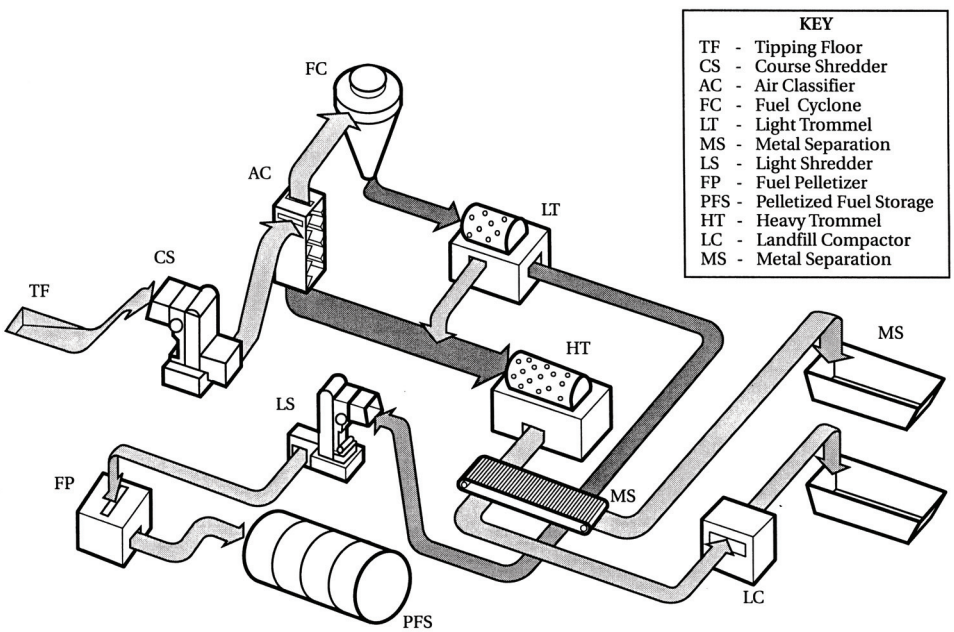

Figure 6.2 Schematic of a municipal solid waste (MSW) fuel processing plant.

Table 6.3 Typical Dry Analysis of Solid Fuels and Biomass Materials

Material	Wt %							*HHV*		Reference
	C	H	N	S	O	Cl	Ash	MJ/kg	Btu/lbm	
Charcoal	80.3	3.1	0.2	0.0	11.3	—	3.4	31.03	13,370	Tillman 1978
Pittsburgh seam coal	75.5	5.0	1.2	3.1	4.9	—	10.3	31.68	13,650	Tillman 1978
Bagasse	48.64	5.87	0.16	0.04	42.85	0.03	2.44	18.95	8,166	Miles et al. 1995
Hog fuel	45.36	5.63	0.18	0.02	42.13	0.03	16.89	17.83	7,681	Feldman et al.
Mixed waste paper	47.99	6.63	0.14	0.07	36.84	—	8.33	20.74	8,934	Miles et al. 1995
Municipal solid waste	47.6	8.0	1.2	0.3	32.9	—	12.0	19.84	8,546	Sanner et al. 1970
RDF-Tacoma WA	39.70	5.78	0.80	0.35	27.24	—	26.13	15.5	6,679	Miles et al. 1995
Sawdust pellets	47.2	6.5	0.0	0.0	45.4	—	1.0	20.46	8,814	Wen et al. 1974
Urban wood waste	48.77	5.76	0.27	0.07	39.59	0.05	2.50	19.41	8,361	Miles et al. 1955
Wood bark	47.27	5.20	0.40	0.05	37.68	0.03	9.37	17.92	7,721	Feldman et al.

Source: R. L. Bain and W. A. Amos, National Renewable Energy Laboratory and M. Downing and R. L. Perlack, Oak Ridge National Laboratory, *Technical Report: Biopwer Technical Assessment: State of the Industry and Technology*, National Renewable Energy Laboratory, Department of Energy Laboratory, Golden, CO, 2003.

Efforts have been made to try to use MSW as a feedstock for commercially produced synthetic solid, liquid, and/or gaseous fuels. Liquid and gaseous fuel resource characteristics will be considered in Chapters 7 and 8, and so the following material will deal only with the technology necessary for producing a solid *refuse-derived fuel,* or RDF. Successfully operating RDF facilities demonstrate that the concept is viable. However, since such facilities are complex, design and operation of an RDF-producing plant must be in the hands of experts knowledgeable in both the characteristics of waste-generated fuel combustion and the particular heat engines necessary to utilize these materials. Operational RDF-producing facilities consist of the following major components:

Staging/sorting area
Shredders
Air classifiers
Metal magnetic separators
Sizing devices
Bag houses
Fuel densifiers
Transfer mechanisms

Arrangement of these components can be varied to optimize a facility for local conditions of refuse, fuel form desired, and local environmental and social requirements. The following discussion describes a general flow of MSW through such an RDF plant; see Figure 6.2.

Solid RDF production facilities should generate minimal airborne pollutants. Dust and potential explosion of certain waste items are hazards when RDF facilities are in operation. Mechanical shredding, waste stream separation or classifying, and suitable processing of raw MSW yield a paperlike substance that can be burned directly. Additional steps will allow long-term storage and use of RDF as a clean-burning, renewable, low-sulfur solid fuel that can supplement coal in the generation of steam and/or electricity. Removal of metals and glass from MSW prior to RDF production purifies as well as energetically upgrades the fuel on a mass basis.

Municipal waste is initially delivered to a plant at the staging/sorting area. This area should be enclosed for aesthetic, environmental, and operational benefits. Visual inspection of MSW being dumped allows plant operators to remove any massive and/or hazardous objects prior to its being fed to the RDF plant. Continuous feed and control of this supply stream occur at the staging area.

Two successful techniques of staging/sorting are used: tipping floor transfer or a recessed floor transfer configuration. With the tipping floor, refuse delivery trucks drive onto a large, flat floor, dump their waste, and then leave. Material being fed to the plant is transferred and sorted by front-end loaders. With the recessed floor configurations, refuse trucks back up to a large on-grade floor, dump their waste, and then leave. Hydraulic pickers, overhead cranes, or front-end loaders then transfer material to the RDF-producing plant feed lines. Long-term storage of material at the staging/sorting area is not desirable.

Typically, MSW is continually fed to a shredder, mill, or hammer system that reduces the waste stream to small pieces. The operation, wear, and energy input required by any shredder are a strong function of a specific waste-stream composition, i.e., the

presence of abrasive and potentially explosive constituents. Separation of metals, glass, stones, and ceramics from the flow prior to shredding could prolong the life of the mill hammers. Removal of potentially explosive materials, such as gas cans, TNT, and fireworks, would also increase safe operation of the shredder. The required specific energy input per mass of fuel produced is greatly affected by this separation process. This size reduction step, however, does not segregate, separate, or select waste stream components.

The air classifier is the major component that separates light organic and inorganic combustible materials from remaining heavy objects. This unit, which is often several stories tall, uses high-velocity air supplied by fans to separate out pulverized waste. Light materials, consisting mainly of paper, plastics, wood chips, and other combustibles, are drawn out the top while heavier particles, chiefly metal, glass, and ceramics, fall to the bottom.

A magnetic system can extract ferrous metals from the waste stream for resale as scrap. An "aluminum magnet" using eddy current separation techniques can also be used to remove aluminum for recycling. Glass, stones, and ceramics are removed from the heavy fraction by a sizing device. This unit can be either a trommel or a vibrating screen, which allows smaller materials to pass through a fine mesh while restricting the passage of larger pieces. Abrasives, such as fine sand, glass, and grit, are separated by this technique either for further processing or transfer to a sanitary landfill.

Dust generated by the operation of an RDF-producing facility is collected by the bag house. The collection system consists of pickup hoods that draw dusty air from various points around the plant, i.e., shredders and conveyor transfer points. A series of cyclone separators removes dust, after which the air is filtered, cleaned, and discharged to the environment.

The light combustible stream can be transferred for direct combustion or further processing. Compacting and extrusion of processed RDF product to form cubettes, sheets, or pellets heat the material to temperatures that kill bacteria, which normally would cause MSW to decompose. The long-term storage of RDF is thereby enhanced as long as the material is kept dry. The compactor is the plant component that densifies this stream and produces the final form of storable RDF. Also, if the light stream is chemically treated with an embrittling agent, this material can be ground to a powder or dust in a mill to make a fine mesh pulverized RDF.

When properly processed, highly refined RDF can be transferred, stored, and burned with high efficiency in a variety of compatible systems. In addition, potential recovery of metals and glass, as well as reduced landfill volumes, makes RDF processing more acceptable than other solid waste utilization schemes. Conversion of MSW into fuel-grade RDF offers the following benefits:

1. A long-term energy source since industrial and urban waste will continue to be generated.
2. Established and successful technology beyond the pilot plant stage.
3. Minimal environmental impact on air pollution standards of all waste recovery techniques.
4. Maximum utilization of waste materials, i.e., fuel production, as well as proven recovery of metals and glass.
5. Minimum required landfilling of inert material.
6. Commercial viability and replicability throughout the United States in the near term.

7. RDF is a low-ash, low-sulfur, low-slagging, odorless, higher-Btu fuel source than raw MSW.
8. RDF technology can produce a variety of different fuels for a variety of applications:
   a. Densified RDF
   b. Pulverized RDF
   c. Coal-RDF mixture
   d. Waste oil-impregnated RDF
   e. RDF-derived alcohol
9. Compatibility with existing boilers and demonstrated efficient combustion therein.

The technology of refuse-derived fuel could achieve the goals set forth above if successes and failures of previous fuel processing and combustion systems are fully understood. Producing fuels using solid wastes in the future is as much an economic as an engineering issue. Economics and engineering issues dictate that each plant be uniquely designed for local conditions. Municipal solid waste is a seasonally changing, nonhomogeneous mixture containing a variety of combustible and recyclable materials in various sizes and shapes. As such, knowledge of local area waste stream time-dependent composition is essential. Any emerging RDF technology does raise several negative economic points, including: social cost required to produce these fuels in a usable, environmentally and socially acceptable manner; economics of scale necessary to ensure successful operation of an RDF processing plant; and the requirement that resources other than gas and oil be utilized in RDF production. Positive economic benefits result from RDF technology commercialization, including the cost benefit of producing RDF over the cost of MSW landfill disposal; the cost benefit of replacing oil and gas with RDF for use in certain suitable applications; and the cost benefit of revenue-producing recycling of scarce materials as recovered during RDF production. The ultimate analysis of various solid fuels and biomass material on a dry basis are compared in Table 6.3.

6.4 SOLID FUEL COMBUSTION

Burning solid fuels, such as coal, requires both proper machinery and sufficient preparation of reactants in order to achieve and control the chemical energy conversion processes during combustion. An understanding of major solid fuel-heat engine interface characteristics is essential in discussions of direct combustion of the chemical energy resources presented in earlier sections of this chapter. For example, because of the structure, rank, chemical composition, caloric value, porosity, and caking nature of various grades of coal, different methods of firing are required. Also, the nonuniform nature of these reactive materials influences, among other factors, the required fuel-air ratio necessary to sustain complete combustion, the amount of energy released, and the type of critical emissions present in the effluent product stream. Coal generally burns as either a *caking* or *free-burning* solid fuel. Caking coals, when heated, tend to fuse and form a semicoke substance that is impervious to the passage of air and combustion gases. Free-burning coals (FBCs), however, tend to crumble into smaller pieces when heated, which then burn separately.

Efficient solid fuel combustion systems will be successful only if they provide a proper distribution and flow rate of reactants, proper ignition, and a proper firing temperature. Solid fuel combustion systems therefore must (1) prepare fuel for burning, (2) transfer energy released by the complex chemical reactions as either heat or work, (3) minimize incomplete combustion and losses, as well as (4) control formation and removal of emissions. Solid fuels used with heat engines traditionally are generally large and have been steam generators that are used for heat and power applications. Coal-burning steam-generating facilities, in addition to firing, must store, handle, and crush or pulverize coal. Coal-fired units are designed to burn a reasonable range of statistically varying coal supplies. Dust and bottom ash collection, as well as stack systems that remove soot and fly ash, is also needed to lessen the environmental impact of these by-products.

Three general methods for traditionally burning coal have been used: stoker systems, pulverized coal systems, and cyclone-firing systems. Stoker systems, limited to small capacity boilers of less than 181,440 kg/hr (400,000 lbm/hr) steam flow rates, were developed in the late nineteenth century and used predominantly until the 1920s. In the 1920s, pulverized coal firing was introduced, allowing coal to be burned in boilers having greater capacities, with steam flow rate of 181,440 kg/hr (400,000 lbm/hr), and is still the chief means of burning coal to produce power commercially. Cyclone-fired furnaces, developed in the 1940s, provided an improvement in efficient coal burning over either stoker or pulverized coal-firing systems. Considerable efforts are underway to try to commercialize fluidized bed combustion as a fourth coal-burning technique. Coal-fired fluidized bed combustors would improve combustion efficiency of coal-fired steam generators, lower sulfur oxide emissions of commercial power plants, and eliminate ash slagging and fouling of steam-generating systems.

The first mechanical coal-firing technique to replace hand firing was the *stoker* coal-fired unit. Three general classes of mechanical stokers, overfeed, spreader, and underfeed systems, have been used. Mechanical stokers are limited to low-capacity steam generation but are relatively simple, are economical, and can be designed to accommodate a wide range of unsized solid fuels ranging from all ranks of coal to wood, bagasse, and even RDF.

Coal combustion using stokers involves three phases of reaction: drying, distillation of volatiles, and burning of fixed carbon on a burning bed; see Figure 6.3. When firing, crushed coal is admitted from a storage hopper through a regulating coal feeder and introduced onto a moving grate. Various overfeed grate designs have been utilized, such as the chain and traveling grate systems and the vibrating and oscillating grate systems. Stoker feed furnaces burn both fine and coarse coal in a burning bed that moves away from the coal injection point. The larger particles lie on the grate and react with the underfire primary air supply while smaller particles are held in suspension over the grate and are ignited by the overfire secondary air and hot product gases. Size distribution is critical in that large or coarse coal does not provide as great a total surface area for complete combustion as smaller pieces would. Too fine a coal bed would require a very fine grate opening, which would make it difficult for combustion air to pass through. The layer of coal on a moving grate is heated, dried, pyrolyzed, and ignited by radiation from furnace gases directly above the bed. Fine coal burns together in suspension above the grate in the overfire gases, along with hydrocarbons, and other combustible gases driven off the coal bed by distillation, as well as products of incomplete combustion such as CO. The moving bed becomes thinner as it proceeds until, ideally, at the end of travel, all that remains is ash, which is dumped as bottom ash into an ash hopper.

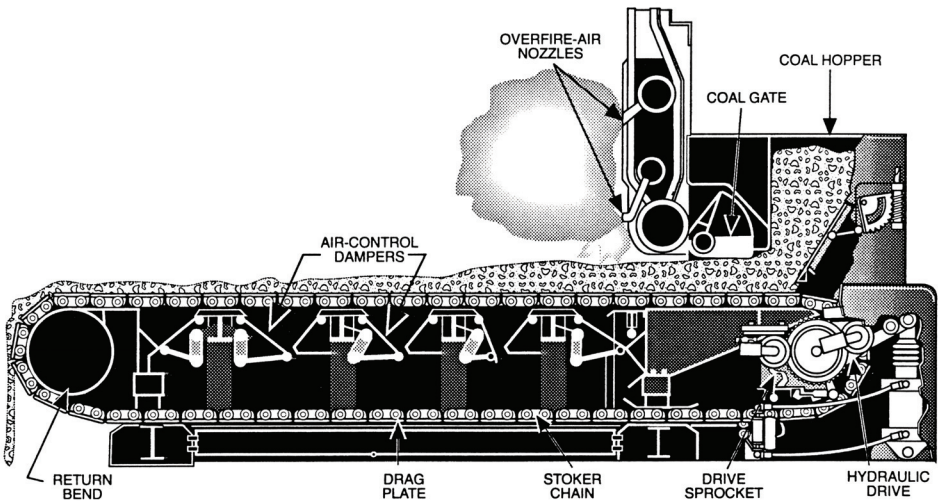

Figure 6.3 Stoker-fed coal combustion system schematic. Adapted from *Steam: Its Generation and Use*, 37th Edition, Babcock and Wilcox Co., Barberton, Ohio, 1963. With permission.

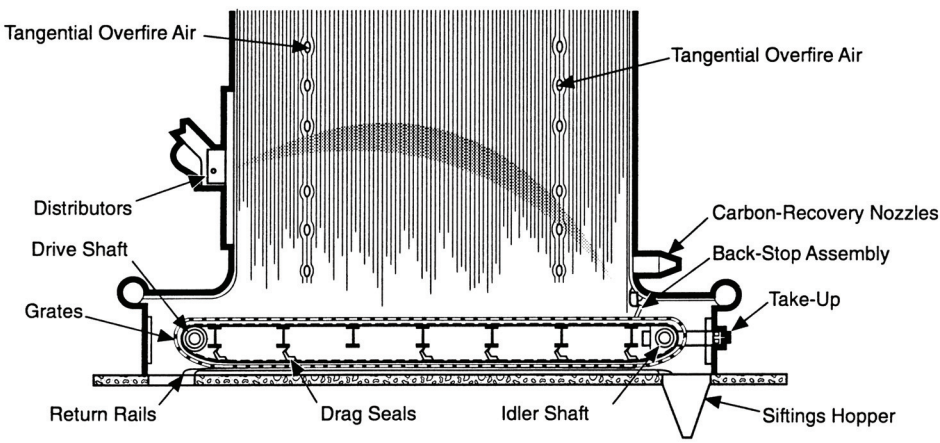

Figure 6.4 Spreader-fed coal combustion system schematic. Adapted from Singer, J. G., editor, *Combustion Fossil Power Systems*, 3rd Edition, Combustion Engineering, 1981. Reproduced with the permission of ALSTOM Power, Inc., Windsor, CT.

Spreader stokers fire coal in much the same way as a traveling grate overfeed stoker. The essential difference between spreader and moving grate stokers is that a spreader system uses a combination of suspension burning and a thin, fast-burning fuel bed, whereas overfeed systems utilize chiefly a mass-bed burning approach. In spreader firing, coal is uniformly spread over a burning coal bed by means of a distributor; see Figure 6.4. Spreader coal firing can be used with either a stationary or moving bed.

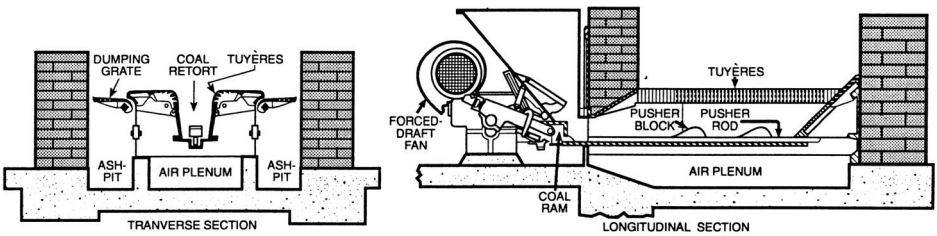

Figure 6.5 Underfeed stoker coal combustion schematic. Adapted from *Steam: Its Generation and Use*, 37th Edition, Babcock and Wilcox Co., Barberton, Ohio, 1963. With permission.

Underfire stokers operate by feeding crushed coal through a channel, or *retort,* below the burning bed; see Figure 6.5. When the passage is filled, the coal is pushed up and over on two sides, forming and feeding the burning fuel bed. Combustion air passes up through tuyeres with a burning bed, which is being pushed toward ash dumps by retorted coal. Underfeed stokers are best for burning caking coals, spreader stokers will burn all ranks of coal except anthracite, and traveling stokers will fire all but strongly caking bituminous coals.

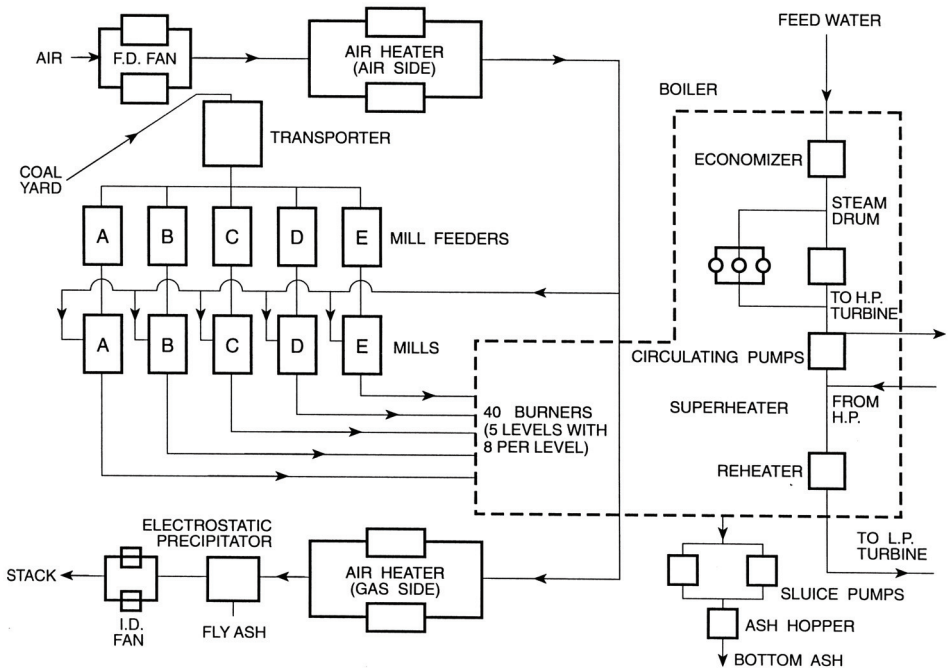

Figure 6.6 Pulverized coal combustion system schematic.

Commercial operation of large coal-fired steam generators producing 453,600–1,814,400 kg/hr (100,000–4,000,000 lbm/hr) steam began in the 1920s with the introduction of pulverized coal firing. The added cost of operating pulverized coal plants, in terms of increased complexity and plant size in these units, is offset by gains in steam generation and reduction in labor over stoker-fired, coal-fired boiler installations. Essential combustion elements of a pulverized coal facility are shown in Figure 6.6.

Coal is moved from a supply yard to the furnace on a *transporter* that fills *mill feeders,* i.e., containers that are used to store and meter proper amounts of coal for burning. Gravity-fed coal is delivered from a silo, hopper, or bin mill feed system to coal grinding components, or *mills.* Coarse coal is pulverized into a fine dust having particle dimensions of a few thousandths of a centimeter, or approximately 200 mesh size. Environmental air is supplied for combustion using a *forced-draft fan.* Hot exhaust gases from the furnace are used to preheat air in a heat exchanger, termed an *air preheater.* Approximately 20% of the air flow is used to dry and blow pulverized coal from mills into the furnace, as *primary air,* while the remaining air is supplied directly to the furnace, as *secondary* air, to promote complete combustion.

Various methods are utilized to inject fuel and air into the furnace while producing turbulence and promoting combustion. These techniques fire pulverized coal using a series of separate coal burners that generate a number of distinct flame zones inside the furnace; see Figure 6.7. In one method, Figure 6.7(a), multiple rows of individual coal burners are located in the furnace wall, admitting primary air with pulverized coal to the furnace along with separate secondary air flow. Two-wall firing is also utilized in which case burners are located on both front and rear walls, referred to as *opposed firing*. In a variation, multiple rows of individual coal burners are located in the furnace wall, allowing pulverized coal with primary air to be introduced to the furnace but secondary air flow is introduced separately as overfire air above the coal burners. In another firing approach, Figure 6.7(b), multiple rows of individual coal burners are located at corners of the furnace walls in such a way that allow coal and primary air to be injected into the furnace using *tangential firing*. Separate secondary air nozzles are provided above each coal nozzle with limited movement to provide operational flexibility for burning a range of coals.

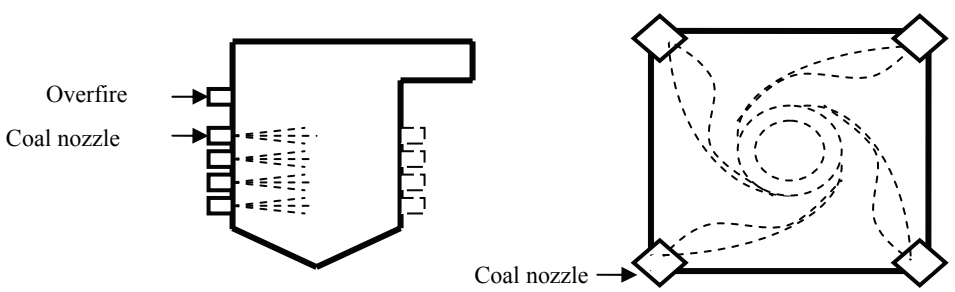

(a) vertical furnace wall firing (b) horizontal tangential firing

Figure 6.7 Pulverized coal firing techniques.

Pulverized coal particles burn in suspension within the furnace. The smaller size, increased surface area, and longer residence time of pulverized coal particles confined within the fireball make this technique of firing very fuel-insensitive. The homogeneous fine coal-air stream burns much like a gaseous torch. Radiant distillation of coal particles blown into the furnace leaves a coke particle that then burns by diffusion of oxygen through the CO, CO_2, and N_2 atmosphere surrounding the particles. An *induced-draft* fan extracts products of combustion from the furnace, through the hot side of the air preheater, and to the environment. Appropriate air pollution control of the exhaust gas, often referred to as *flue* or *stack* gas, is required prior to discharge. Pollution control includes appropriate fly ash removal machinery as well as control devices for oxides of sulfur and nitrogen.

The cyclone-fired coal burner, introduced in the 1940s, improved certain negative features of pulverized coal combustion systems; see Figure 6.8. Coal feed is similar to pulverized coal units except that coal is not crushed as fine, only four mesh, thereby requiring less power for grinding. Cyclone coal firing uses a small horizontal water-cooled burner, which requires less furnace volume than that used in pulverized coal plants. Crushed coal is admitted to a horizontal burner, with combustion air entering tangentially, inducing swirl and greater turbulence, which promotes better burning. Cyclone burners allow higher gas temperatures, 1,650°C (3,000°F), enabling quick firing and complete combustion to occur. In addition, high firing rates melt 30–50% of ash, forming a liquid slag that can be removed as a liquid bottom. Pulverized coal units generate 10–30% ash as bottom ash and 90–70% as fly ash. Cyclone units, however, generate only 50–70% of the ash as fly ash. Also, cyclone furnaces do not require the combustion space that pulverized coal combustion systems do, so that cyclone coal combustion plants need not be as large.

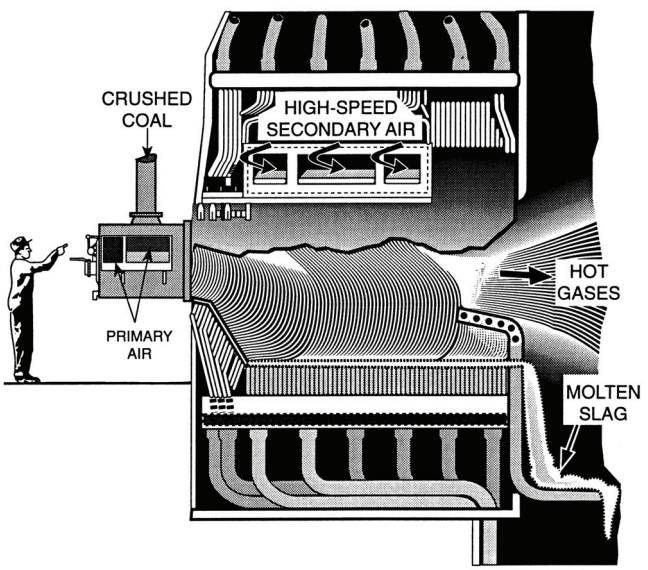

Figure 6.8 Cyclone combustor schematic. Adapted from *Steam: Its Generation and Use*, 37th Edition, Babcock and Wilcox Co., Barberton, Ohio, 1963. With permission.

The *fluidized bed combustor,* or FBC, a more recent solid fuel combustion technology, is currently being introduced into commercial use around the world; see Figure 6.9. Combustion occurs within a unique bed consisting chiefly of sand, with lesser amounts of limestone, ash, and only about 1% fuel. Air with a nominal velocity of 122–366 cm/sec (4–12 ft/sec) passes up through the bottom of the furnace to provide: (1) satisfactory momentum for the bed to levitate and overcome its static weight; (2) significant turbulent action to cause the solid bed to behave much like a boiling liquid; and (3) sufficient oxygen for complete combustion. Too high a flow rate would cause the reacting bed to blow away, whereas too low a velocity would make the bed slump and not burn properly.

Turbulent mixing maintains a fairly uniform operating temperature of approximately 680–870°C (1,150–1,600°F) throughout the burning bed. These reaction temperatures are generally below ash melting temperatures, so that the slagging and fouling normally associated with coal-fired steam generators is largely eliminated. This means low ash fusion temperature coals can be burned using FBC technology with less difficulty and minimal slagging problems. Since coal combustion occurs in the FBC, most of the ash is also entrained within the active bed, thus reducing fly ash.

Furthermore, at the FBC temperatures, hot corrosion problems associated with normal steam-generating tubes are minimized, thus allowing tubes to be buried directly in the combustion bed. Submersion of the steam generating tubes directly into the fluidized bed produces solid to solid heat transfer. Steam generation using the solid bed heat transfer process provides greater heat transfer rates, which translates directly into greater steam generation rates, less required surface area, lower unit weight, and reduced capital cost for FBC steam generating systems.

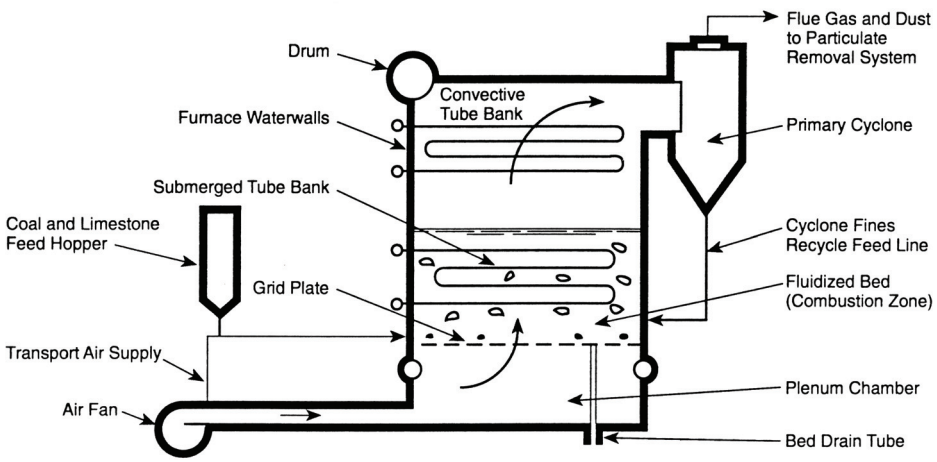

Figure 6.9 Fluidized bed combustor (FBC) schematic. Adapted from Singer, J. G., editor, *Combustion Fossil Power Systems*, 3rd Edition, Combustion Engineering, 1981. Reproduced with the permission of ALSTOM Power, Inc., Windsor, CT.

Many design problems are being solved in order to successfully commercialize FBC, including development of better coal feed and bed waste removal systems, suitable scaling of pilot plants to commercial size, and integrating FBC technology as the combustor portion of advanced combined cycle power plant configurations, to name but a few. Higher carbon burnout can be achieved by recirculation of bed material entrained in discharge gases from an FBC. Operating an FBC combustor as a pressurized configuration allows hot exhaust gases, after cleanup, to provide additional expansion work in combined cycle applications. Advanced fluidized bed combustion technology configurations are found being adopted around the world for utility applications and use of coal including:

Atmospheric fluidized bed combustion
Atmospheric recycled fluidized bed combustion
Pressurized fluidized bed combustion
Pressurized recycled fluidized bed combustion

FBC steam generation power plants can potentially burn coal as well as a variety of the solid fuels described earlier in this chapter with acceptable environmental impact. Unique control techniques for critical by-products of solid fuel combustion such as ash, sulfur dioxide, and nitric oxides are provided with FBC technology.

6.5 SOLID FUEL COMBUSTION POLLUTION CONTROL

The environmental impact of increased solid fuel combustion requires a greater degree of pollution control. The resurgence of coal-fired electric power generation and cogeneration, i.e., combined electric and steam production, escalating amounts of MSW, and its incineration, landfilling, or processing to produce RDF have made improvements in combustion efficiency and emissions control both a local and a federal matter. Engineers today and in the future will need to make major fuel-engine design decisions for solid fuel combustion units, choices that will concurrently influence selection of fuel options, method of firing, and means of controlling emissions. Table 6.4 lists some excess air requirements for fuel-burning equipment.

The carbon-to-hydrogen atom ratio of any hydrocarbon fuel is one of many important parameters that affect energy content, density, and other combustion properties. Coal and many of the solid fuel resources discussed in this chapter have a high carbon-to-hydrogen ratio and therefore will produce a greater proportion of carbon dioxide than other hydrocarbon fuels. In fact, CO_2 produced per unit of thermal energy release is greater for coal than for other liquid and/or gaseous hydrocarbon fuels. In the limit, ideal combustion of pure carbon yields only CO_2 or

$$C_S + O_2 \rightarrow CO_2$$

Table 6.4 Usual Amount Excess Air Supplied to Fuel-Burning Equipment

Fuel	Type of furnace or burner	Wt. % excess air
Pulverized coal	Completely water-cooled furnace for slag tap or dry ash removal	15–20
	Partially water-cooled furnace for dry ash removal	15–40
Crushed coal	Cyclone furnace pressure or suction	10–15
Coal	Stoker-fired, forced-draft, B&W chain grate	15–50
	Stoker-fired, forced-draft, underfeed	20–50
	Stoker-fired, natural draft	50–65
Fuel oil	Oil burners, register type	5–10
	Multifuel burners and flat flame	10–20
Natural, coke oven, and refinery gas	Register-type burners	5–10
	Multifuel burners	7–12
Blast furnace gas	Intertube nozzle-type burners	15–18
Wood	Dutch oven (10–23% through grates) and Hofft type	20–25
Bagasse	All furnaces	25–35

Source: Steam: Its Generation and Use, 37th Edition, Babcock and Wilcox Co., Barberton, Ohio, 1963. With permission.

and

$$1 \text{ kgmole carbon} \rightarrow 1 \text{ kgmole carbon dioxide}$$
$$(1 \text{ lbmole C}) \rightarrow (1 \text{ lbmole } CO_2)$$

or

$$1 \text{ kg carbon} \rightarrow 44 \text{ kg carbon dioxide}$$
$$(1 \text{ lbm C}) \rightarrow (44 \text{ lbm } CO_2)$$

It has been documented by groups such as the National Oceanic and Atmospheric Administration and the National Academy of Sciences that the world's atmospheric CO_2 level has been steadily increasing. Although only a part of atmospheric CO_2 results from combustion sources, increased coal combustion would accelerate this growth at a greater rate. Certain gases, such as CO_2 and water vapor, are known to absorb high-temperature thermal radiation in the infrared region of the electromagnetic spectrum. These gases are opaque to low-temperature radiation in the infrared region, while gases such as oxygen and nitrogen are transparent throughout the spectrum. This ability of CO_2 and H_2O in the atmosphere to pass solar energy to the Earth but block environmental radiation back into space is commonly referred to as the *greenhouse effect.* Predictions suggest that a continued increase in atmospheric CO_2 could raise the Earth's air temperature an average of 2–4°C by the next century. The delicate balance in the Earth's biosphere requires a greater understanding of, and concern for the generation of CO_2 and its consumption by vegetation and the ocean, as well as geothermal impact of these parameters on the Earth's weather.

Other solid fuel combustion products, in addition to CO_2, may also have potential long-term biological and geological impact on the Earth's ecosystem. As an example, certain exhaust gas species can interact with moisture and, given proper conditions, produce a dilute acidic solution; i.e., CO_2 can form carbonic acid, sulfur dioxide can form

sulfuric acid, and nitric oxide can form nitric acid. Acid corrosion within coal-fired steam generators is well known, but concern is growing about the effects these species have on the environment when they precipitate in the form of acid rain.

The Clean Air Act Amendments of 1977 set air-quality standards for the United States that limit pollution from combustion of coal and other solid fuels. Solid fuels, when burned, generate three major pollutants that are regulated and controlled by this law: sulfur oxides, SO_x; nitrogen oxides, NO_x; and particulates. Fossil-fueled power plants annually produce approximately 65% of the total sulfur oxides, 29% of the nitric oxides, and 24% of the particulate emissions, with almost two-thirds of these pollutants coming from coal-fired plants alone.

The Environmental Protection Agency (EPA) has produced national emission or performance standards, referred to as New Source Performance Standards (NSPS), for a number of important industrial processes. The complete listing for each NSPS text is available in the Code of Federal Register (40 CFR Part 60). NSPS with emissions exist for various large solid fuel combustors, such as fossil fuel steam electric power plants and existing municipal waste incinerators.

A general control removal efficiency relationship that relates the emission guideline characteristic to the uncontrolled discharge characteristic for a particular pollutant to be controlled is given as

$$\text{Removal efficiency} = \left[\frac{\text{performance} - \text{standard}}{\text{performance}}\right] \times 100\,\% \tag{6.7}$$

where

performance – uncontrolled discharge characteristic for pollutant to be controlled
standard – emission guideline characteristic for pollutant to be controlled

Sulfur present in solid fuels, such as coal, will form sulfur oxides, or SO_x during combustion, or

$$S + aO_2 \rightarrow bSO_2 + cSO_3$$

These oxides and other pollutants, along with the products of combustion CO_2 and H_2O, are released into the atmosphere by a power plant. Sulfur oxides can precipitate in rain or snow as acid rain or as dry SO_x particles that settle on trees and soil, which then interact with rain or snow to produce sulfuric acid:

$$SO_x + aH_2O \rightarrow bH_2SO_4 + cH_2SO_3$$

Sulfur dioxide control can be accomplished prior to combustion by choosing to burn only low-sulfur coal. Burning low-sulfur coals may involve an engineering design trade-off since most low-sulfur coals are low-energy coals. In addition, most U.S. coal reserves are high-sulfur fuels. Benefication, or coal cleaning, to alter sulfur, ash, and moisture content prior to burning, can produce harmful by-products and waste that are as difficult to dispose of as the original sulfur. Controlling sulfur dioxide emissions during combustion may be possible using a fluidized bed combustion system. Flue gas desulfurization techniques are necessary to control SO_x after combustion, as in pulverized coal units.

Current practice for desulfurizing flue gases utilizes a scrubbing agent such as water and/or an alkaline material like lime or limestone. Commercial wet systems use a variety of geometries for capturing SO_2, including spray towers, packed towers, and spray chambers. Wet scrubbing provides several benefits, including the ability to

efficiently scrub a variety of flue gases, the ability to remove some particulates, little or no restrictions from flue gas temperature or moisture, and desulfurization within a small region of space. There are also some disadvantages of wet systems such as problems associated with disposal of the sludge produced from flue gas cleaning, acidic misting, and high power requirements of the process.

Dry absorption systems and regenerative techniques are currently focused on efforts that would allow material to recover sulfur reversibly. For example, a fluidized bed combustor allows for the removal of sulfur within the suspended mixture during combustion using coal and limestone. Crushed dolomite or limestone is mixed with crushed coal into the fluidized bed. Limestone calcinations occur in the suspended mixture via the reaction

$$CaCO_3 + \text{heat} \rightarrow CaO + CO_2$$

Capture of sulfur dioxide produced by combustion then occurs via the reaction

$$SO_2 + CaO + \tfrac{1}{2}O_2 \rightarrow CaSO_4$$

The FBC sulfur removal method is compatible with burning high-sulfur coal. Fuel sulfur oxidizes to form sulfur dioxide, SO_2, but limestone, dolomite, or other absorbent particles present in the bed react with generated sulfur dioxide to form calcium sulfate. This stable material can then be removed from the bed and either be sent to a landfill or used as a feedstock to produce sulfur. Flue gas scrubbing systems are used with non-FBC solid fuel combustors.

The NO_x emissions associated with solid fuel combustion are a direct result of several fuel-engine parameters, such as means of preparing and particle sizing of solid fuel being burned, percent excess air used in firing, actual reaction temperatures, and percent nitrogen originally present in the fuel. Burning solid fuels, such as coal, can therefore generate both thermal NO_x because of high-temperature N-O thermochemistry, and fuel NO_x because of the presence of fuel bound nitrogen. Any alteration in solid fuel burner design and/or operational technique that favorably shifts reaction temperatures and partial pressures of O and N via the Zeldovitch free radical reaction mechanism (see Chapter 5) will contribute to a reduction in thermal NO_x emissions.

Deposits from coal combustion, such as ash, make heat-absorbing surfaces in steam generating units ineffective, increase flue gas temperatures, and thereby contribute to formation of NO_x. Controlling the highly oxidizing primary combustion stage by reducing air preheat and promoting off-stoichiometric burning are used to control fuel NO_x. The success of in-situ techniques depends to a great degree on the type of fuel and firing utilized, i.e., tangential versus horizontal configuration. Several in-situ techniques are presently being utilized to control NO_x from solid fuel fired utility configurations including

Using overfire air for air staging
Using fuel staging (reburn)
Using low NO_x burners to slow the rate of fuel air mixing
Using low excess air operation
Using furnace or burner flue gas recirculation

Adjusting primary air in the coal nozzles to promote substoichiometric fuel-rich first stage combustion in the furnace's main combustion zone will reduce the intermediate flame temperature and hence lower NO_x formation. Air staging using overfire air and separated multilevel injection ports achieves burnout at a lower final temperature and prevents additional NO_x formation. This technique should not be used, however, in boilers with slagging furnaces. Reducing conditions inside a furnace can accelerate evaporator tube corrosion in dry bottom coal-fired boilers.

In fuel staging, pulverized coal and primary air are introduced using fuel nozzles with different stoichiometries at various levels of the furnace's main combustion zone. A majority of the coal is admitted in the lower portions of the furnace under fuel-rich conditions. The remaining coal is injected in the upper portions under fuel-lean conditions. Staged fuel combustion is completed by introducing secondary air using overfire air locations at the top of the furnace to complete reaction at a lower final temperature to insure no additional NO_x is being formed.

Specially designed low NO_x burners are also being utilized to provide in-situ NO_x combustion control. Most pulverized coal low-NO_x burners also employ air staging. Complications arising from low NO_x burner use include increases in carbon content in fly ash, CO emissions levels, and furnace discharge temperature. Low excess air operation to limit oxygen availability can provide limited NO_x reduction constrained by flame stability and CO emissions regulations and is therefore utilized in conjunction with other NO_x control techniques.

Reburning utilizes a reducing fuel, such as natural gas or methane, as an agent to reduce NO_x to molecular nitrogen. Reburned fuel is injected over the primary combustion zone to form a fuel-rich second stage where NO_x is reduced to molecular nitrogen. The use of a reburning fuel can produce high NO_x reduction values. On the other hand flue gas recirculation techniques can return a fraction of the gas either to the furnace or into the coal burners in order to reduce NO_x. Recirculating flue gas can also be added to low NO_x burners in order to reduce available oxygen and thereby lower flame temperature.

Post combustion NO_x control approaches take oxygen away from the NO_x chemistry by adding a reducing agent to the exhaust. A number of potential gaseous reducing agents have been considered, e.g., CO, CH_4, NH_3, and urea $CO(NH_2)_2$. *Selective noncatalytic reduction* (SNCR) technology utilizes ammonia, or urea, for thermal de-NO_x in an oxygen environment. SNCR operates within a narrow temperature zone of 870–1,150ºC (1,600–2,100ºF) producing N_2 and water. Selective reduction of NO_x by ammonia occurs in an oxygen environment via the reactions

$$4NH_3 + 4NO + O_2 \rightarrow 4N_2 + 6H_2O$$

and

$$8NH_3 + 6NO_2 \rightarrow 7N_2 + 12H_2O$$

Higher removal efficiencies, greater than 90%, are achieved for these reactions using *selective catalytic reduction* (SCR) technology. SCR in an oxygen environment introduces ammonia upstream of a catalyst in the NO_x reduction process. SCR technology, depending on the specific catalyst used, operates over a lower temperature range between 200–500ºC (550–750ºF).

Catalysts are active material consisting of a precious metal, a base metal oxide, or a zeolite.

A majority of solid fuel combustion processes described in Section 6.4 will also discharge their solid fuel ash content as either *bottom ash* or *fly ash*. Specific ash temperatures important to discharge characteristics from the combustion environment of coal ash include: (1) ash melting point temperature which limits the burning rate on hearths/grates, and (2) ash fusion temperature which defines onset of slagging and fouling. Since ash can slag and build up on heat absorbing surfaces of a solid fuel combustor furnace and steam generator, chemical testing with coal samples according to ASTM standards can provide useful data to help understand the nature of the actual ash discharge, coal-ash slag characteristics, and other facets of the solid fuel ash-combustor interface. A large amount of molten slag from low ash fusion temperature coals can adhere to internal surfaces but, due to the weight from buildup or by changing operating conditions, the buildup can break off and drop to the substructure of the furnace as bottom ash where it can be collected and removed. Approaches to bottom ash handling include dry and wet as well as intermittent and continuous collection and removal techniques. Fly ash is entrained with the flue gas stream and removed prior to the stack discharge in the air pollution control section. There have been efforts to combine the two collected ash waste streams, the fly ash with the bottom ash, to form a single disposal product if the two can be environmentally and economically mixed.

Notable environmental issues relate to handling ash during its ultimate disposal and include concerns over discharging any uncombusted materials commingled with the discharged ash, stability characteristics of the discarded ash, and potential groundwater contamination from the ash disposal process. Solid fuel ash, other than standard boiler ash from coal, may generate a hazardous waste. Toxic ash may result from a solid hazardous waste incinerator operation or from firing certain solid fuels, for example, particular MSW or RDF fuels using solid fuel combustors. These residual materials may require testing to determine if the ash contains toxic and/or hazardous waste having excessive limits in regulated levels of heavy metals, volatiles, and/or semivolatiles. Such ash must pass explicit environmental tests before being allowed to be disposed of in municipal waste landfills or be used as a by-product for industrial applications. Otherwise it must be disposed of in hazardous waste landfills. For example, ash stability is measured using the toxicity characteristic leaching procedure (TCLP). Before final disposal, ash may need to be further processed by being mixed with solidifying and stabilizing material.

Solid fuel combustion can generate a high level of fly ash and uncontrolled particulates. Particulate levels are a result of the type of solid fuel being burned and the method of firing. For example, RDF is a greater source of fly ash than coal. Also, stoker and spreader firing produce greater particulates than pulverized burners which, in turn, produce more particulates than cyclone or FBC systems. These fine particles consisting of inert materials, finely divided carbon particles resulting from incomplete combustion or *soot,* and trace toxic metals such as cadmium and arsenic are of current concern because:

They are principal carriers of toxic and carcinogenic trace metals.
They are more easily inhaled.
Their greater surface area increases reactive or absorptive capacity.
Articles in the size range 0.1–1.0 μ scatter or absorb sunlight, lowering visibility.
Increases in consumption of coal could significantly increase the amount of fine particles in the atmosphere.

Particulate resulting from incomplete combustion exists mainly as finely divided aerosol particles, i.e., dispersed solid or liquid material constituents in which the individual aggregates are larger than single small molecules but smaller than 500 μ. Combustible aerosol constituents are best controlled prior to reaching the air emission control equipment by the classic "3 T's":

Increasing residence time (Time)
Providing better air distribution (Turbulence)
Operating at higher combustion temperatures (Temperature)

A variety of methods are utilized to remove particles from an exhaust gas stream including mechanical collectors, wet collectors, electrostatic precipitators, and filters. Centrifugal collectors, or cyclones, use a vortex motion and inertia to collect particulates. Cyclones typically are the first component in a dry off-gas system and provide gross particle capture by centrifugal separation. The performance of a cyclone system is a function of gas volume handled, particulate loading, cyclone inlet conditions, gas velocity, and cyclone geometry. Cyclones are simple, low-cost devices having no moving parts, but are ineffective with small size particulates and are subject to erosion. Particle removal efficiencies of 85% can be achieved on >10-μ. particulate but efficiencies drop off rapidly to about 20% on particulate <1 μ.. Cyclones are also used in applications where the particulate content of the exhaust gas is high. A common application of cyclones is with a FBC where they are used to recycle material to the FBC bed.

The electrostatic precipitator (ESP) utilizes a high-voltage DC discharge between emitting and collecting electrodes to electrically charge and remove particles from a particle laden off-gas passing between two plates. Collected material can be periodically removed from the charged collecting plate of these highly efficient and reliable collectors. Configurations can be operated as high as 370ºC (698ºF) and with small pressure and temperature drops across the unit. An ESP has no gaseous pollutant removal capabilities and if acid gases are produced in a system using an ESP, gas scrubbing must be employed upstream of the ESP to protect the unit from corrosion. ESP installations are costly to operate but are frequently used with pulverized coal units for <1-μ-size fine particulate scrubbing. ESP effectiveness however is considerably reduced with a fly ash that has a high electrical resistivity. Combustion of low-sulfur coal will usually result in high resistivity fly ash.

Baghouses use fabric filters to collect fine particulate and can circumvent ESP problems associated with low-sulfur coal. The fabric filter used in a baghouse reduces particulate emissions from the flue gas to the lowest regulatory levels. With any fabric filter type collector, a relatively narrow temperature window is required for proper operation. Thermal damage to the bag material can occur from too high a flue gas temperature while condensation, with attendant bag blinding, i.e., plugging the pores with irremovable material, can result from too low a flue gas temperature. Some fabrics used in bags include Teflon, fiberglass, wool, nylon, Dacron, and ceramics. The type of fiber used depends on the application and is usually governed primarily by the temperature and acid content of the gas as well as the size and chemical properties of the particulate.

EXAMPLE 6.4 Municipal solid waste (MSW) is to be utilized as an alternate fuel for steam generation. The fuel composition on a weight basis is given as

C_S	25.0%	H_2	3.3%	N_2	0.5%
H_2O	28.0%	O_2	21.1%	S	0.1%
Glass, metals, ash	22%				

The material stream is treated to remove the noncombustibles for recycling. Air enters the burner at 25°C and 104 kPa, and the dry exhaust gases leave the boiler at 500K and 101 kPa, with the following stack analysis:

CO_2	13.6%	O_2	4.4%
CO	3.4%	SO_2	0.02%

Find: (a) excess air, %; (b) stack dew point temperature, °C; (c) sulfur dioxide production, kg SO_2/kg fuel; (d) boiler combustion efficiency, %; and (e) removal efficiency for a 30 ppm SO_2 required discharge.

Solution:

1. Fuel mole fractions:

	mf_{orig}	mf_i	MW_i	$(mf/MW)_i$	$\bar{x}_i$
C_S	0.250	0.3205	12	0.026708	0.3490
H_2O	0.280	0.3590	18	0.019944	0.2606
H_2	0.033	0.0423	2	0.021150	0.2764
O_2	0.211	0.2705	32	0.008453	0.1105
N_2	0.005	0.0064	28	0.000229	0.0030
S	0.001	0.0013	32	0.000041	0.0005
Waste	0.220	—	—	—	—

$\Sigma(mf/MW)_i = 0.0765251$
or $MW = 13.068$ kg/kgmole

2. Stoichiometric equation:

$$[0.349C_S + 0.2606H_2O + 0.2764H_2 + 0.1105O_2 + 0.0030N_2 + 0.0005S] + aO_2 \rightarrow bCO_2 + cH_2O + dSO_2$$

Carbon: $b = 0.349$

Hydrogen: $c = (0.02606 + 0.2764) = 0.537$

Sulfur: $d = 0.0005$

Oxygen: $0.2606 + (2)(0.1105) + 2a = (2)(0.349) + 0.537 + (2)(0.0005)$

$a = 0.3772$

3. Actual equation:

$$[0.349C_S + 0.2606H_2O + 0.2674H_2 + 0.0030N_2 + 0.1105O_2 + 0.0005S] + a[0.3772][O_2 + 3.76N_2] \rightarrow b[0.136CO_2 + 0.034CO + 0.044O_2 + 0.002SO_2 + 0.7858N_2] + cH_2O$$

Carbon: $0.349 = b(0.136 + 0.034)$

$b = 2.053$

Hydrogen: $0.2606 + 0.2764 = c = 0.537$

Nitrogen: $0.003 + (a)(0.3772)(3.76) = (2.053)(0.7858)$

$a = 1.135$

4. Excess air, %:

113.5% theoretical air or 13.5% excess air

5. Dew point T:

$$\bar{x}_{H_2O} = \frac{0.537}{2.053} = 0.2616$$

$$P_{H_2O} = (0.2616)(101) = 26.4 \text{ kPa}$$

$$T_{sat}\langle 26.4 \text{ kPa}\rangle = T_{db} \cong 66°C$$

6. SO_2 production:

$$\frac{m_{SO_2}}{m_{fuel}} = \frac{(2.053)(0.0002)(32) \text{ lbm } SO_2}{(1.0)(13.068) \text{ kg fuel}} = 1.0 \frac{\text{kg } SO_2}{\text{kg fuel}}$$

but there is 0.78 lbm fuel/1.0 lbm of fuel + waste, or

$$\frac{m_{SO_2}}{m_{fuel}} = \left(0.78 \frac{\text{kg fuel}}{\text{kg MSW}}\right)\left(1.0 \frac{\text{kg } SO_2}{\text{kg fuel}}\right) = 0.78 \frac{\text{kg } SO_2}{\text{kg MSW}}$$

7. Boiler combustion efficiency:

$$Q = \sum_{i_{prod}} N_i[\bar{h}_f^0 + \Delta\bar{h}] - \sum_{react} N_j[\bar{h}_f^0 + \Delta\bar{h}]$$

$$\begin{aligned} Q = {} & (2.053)(0.136)[\bar{h}_f^0 + \Delta\bar{h}]_{CO_2} + (2.053)(0.034)[\bar{h}_f^0 + \Delta\bar{h}]_{CO} \\ & + (2.053)(0.044)[\bar{h}_f^0 + \Delta\bar{h}]_{O_2} + (2.053)(0.0002)[\bar{h}_f^0 + \Delta\bar{h}]_{SO_2} \\ & + (0.7858)(2.053)[\bar{h}_f^0 + \Delta\bar{h}]_{N_2} + (0.537)[\bar{h}_f^0 + \Delta\bar{h}]H_2O_g \\ & - (1.135)(0.3772)[\bar{h}_f^0 + \Delta\bar{h}]_{O_2} - (1.135)(3.76)(0.3772)[\bar{h}_f^0 + \Delta\bar{h}]_{N_2} \\ & - (0.0005)[\bar{h}_f^0 + \Delta\bar{h}]_S - (0.1105)[\bar{h}_f^0 + \Delta\bar{h}]_{O_2} - (0.003)[\bar{h}_f^0 + \Delta\bar{h}]_{N_2} \\ & - (0.2764)[\bar{h}_f^0 + \Delta\bar{h}]_{H_2} - (0.349)[\bar{h}_f^0 + \Delta\bar{h}]_{C_S} - (0.2606[\bar{h}_f^0 + \Delta\bar{h}]_{H_2O} \end{aligned}$$

$$Q = (2.053)(0.136)(-94{,}054 + 958)_{CO_2} + (2.053)(0.034)(-26{,}417 + 711)_{CO}$$
$$+ (2.053)(0.044)(724)_{O_2} + (2.053)(0.0002)(-20{,}947 + 1{,}016)_{SO_2}$$
$$+ (0.7858)(2.053)(710)_{N_2} + (0.537)(-57{,}798 + 825)_{H_2O}$$
$$- (0.2606)(-68{,}317)_{H_2O} = -39{,}396.5 \text{ cal/gmole of fuel}$$

$$LHV = Q\langle \text{stoichiometric without the } \Delta\bar{h} \rangle$$
$$= (0.349)(-94{,}054)_{CO_2} + (0.0005)(-70{,}947)_{SO_2}$$
$$+ (0.537)(-57{,}798)_{H_2O_g} - (0.2606)(-68{,}317)$$
$$= -46.094.4 \text{ cal/gmole fuel}$$

$$\eta_{\text{boiler}} = \frac{-39{,}396.5 \text{ cal/gmole fuel}}{-46{,}094.4 \text{ cal/gmole}} = 0.855$$
$$= 85.5\%$$

8. Sulfur dioxide removal efficiency:

total moles of product

$$N_{\text{prod}} = (2.053)(0.136 + 0.034 + 0.044 + 0.002 + 0.7858) + 0.537$$
$$= 0.279208 + 0.069802 + 0.090332 + 0.004106 + 1.6132474 + 1.102461$$
$$= 3.1591564$$

To express products as 1 million moles, multiply the total moles of product above by 1000000/3.1591564 or

$$N_{\text{prod}} = 88{,}380.556 + 22{,}095.139 + 28{,}593.709 + 1{,}299.714$$
$$+ 510{,}657.655 + 34{,}893.226 = 1{,}000{,}000$$

or 1,299.714 ppm SO_2

$$SO_x \text{ removal efficiency} = \left[\frac{1{,}299.714 - 30}{1{,}299.714}\right] \times 100 = 97.69\%$$

6.6 BOILER ENERGY BALANCE

The combustion of many solid fuels described in this chapter is compatible with steam-generating systems used for industrial heating and/or production of power; see Figure 6.10. Several important energy characteristics of such external combustion configurations can be determined from knowledge of the following items:

1. Energy available in the fuel as fired
2. Energy absorbed by generated steam
3. Energy loss due to dry flue gas conditions
4. Energy loss due to moisture in fuel

5. Energy loss due to moisture in combustion air
6. Energy loss due to moisture formed from burning hydrogen in fuel
7. Energy loss due to incomplete combustion
8. Energy loss due to radiation heat transfer and other unaccounted effects

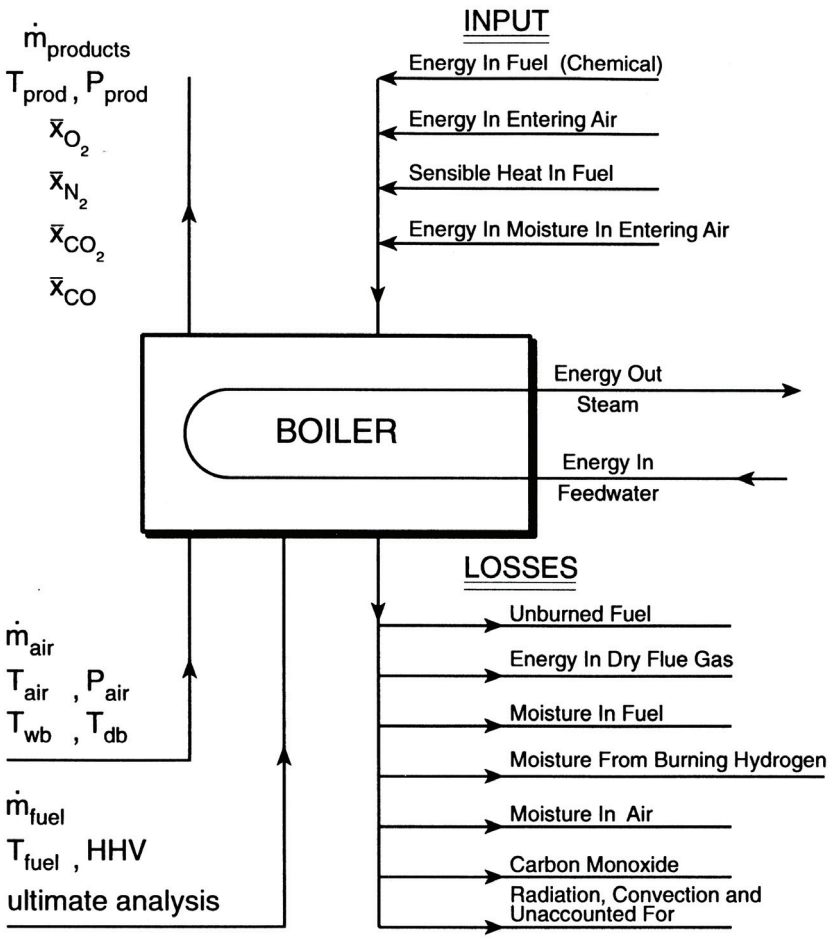

$$\text{OUTPUT} = \text{INPUT} - \text{LOSSES}$$

$$\text{EFFICIENCY} = \frac{\text{OUTPUT}}{\text{INPUT}} = \frac{Q_b}{\text{HHV}}$$

Figure 6.10 Elements of a boiler energy balance.

In order to quantify the performance of a steam generator or boiler, several measurements are required to be made during any standard test. It is important first that the unit must achieve steady-state conditions and that these conditions are maintained throughout the entire test period. Often test codes, such as the ASME Power Test Codes, are used to determine a *boiler heat balance.* These procedures have been developed and published in engineering literature. Based on published procedures and practices included in these codes, the following items are found to be needed for predicting combustion aspects of a steam generator.

1. Ultimate analysis of the fuel along with its higher heating value
2. Mass of fuel fired during the test
3. Fuel temperature entering the burner
4. Relative humidity, barometric pressure, and dry bulb temperature of combustion air
5. Total mass of steam generated during the test
6. Average temperature and pressure of both the feedwater and the generated steam
7. Flue gas temperature measured just at the exit of the heat exchanger
8. Average flue gas analysis as sampled just at the heat exchanger exit, i.e., mole fractions of CO, CO_2, O_2, and N_2

Recall from Chapter 2 that the ideal energy released by a fuel-air mixture can be predicted using the heating value of the fuel. Therefore, if a boiler could operate such that (1) ideal complete combustion occurred, (2) reactants and stack temperature were both at *STP,* and (3) water in the exhaust gases formed by combustion was a liquid, then the heat released would be a maximum and equal to the higher heating value of the fuel. If the generated steam could absorb all this chemical potential energy of the fuel released by combustion, the ideal heat transfer for making steam would equal

$$\dot{Q} = \dot{m}_{H_2O}(h_2 - h_1) \qquad \text{kW (Btu/hr)} \tag{6.8a}$$

and

$$\dot{Q} = \dot{m}_f HHV \qquad \text{kW (Btu/hr)} \tag{6.8b}$$

where

$\dot{m}_{H_2O}$ = feedwater mass flow rate
$\dot{m}_f$ = fuel mass flow rate
HHV = fuel higher heating value
h_2 = steam boiler or superheater generated outlet enthalpy
h_1 = feedwater enthalpy

A *boiler combustion efficiency* η_b can be defined as the actual energy absorbed by the feedwater to the ideal chemical potential energy available in the fuel, or

$$\eta_b = \frac{\dot{m}_{H_2O}(h_2 - h_1)}{\dot{m}_f HHV} < 1.0 \tag{6.9}$$

Since combustion, heat transfer, and other irreversible events take place in a boiler, losses occur and boiler combustion efficiency will not be 100%. It is useful to calculate these losses in terms that then will allow a direct comparison to be made to the heating value of a fuel being fired.

The energy actually absorbed by the feedwater as it is converted into steam measured per mass of fuel is equal to

$$Q_1 = M_s(h_2 - h_1) \quad \text{kJ/kg fuel (Btu/lbm)} \tag{6.10}$$

where M_s = the mass of steam generated per mass of fuel fired, and

$$M_s = \frac{\dot{m}_{H_2O}}{\dot{m}_f} \tag{6.11}$$

Frequently, actual air temperature as supplied to the burner is not at standard state or even ambient conditions. This is due to air having passed through auxiliary machinery that is required to supply air to the boiler and that precludes corrosion, such as fans and heaters. In actual operation, then, the boiler stack temperature will be considerably in excess of ambient conditions. It is also reasonable to assume that, in the boiler, complete combustion will not have occurred. All these factors will cause boiler efficiency to be less than 100%.

The amount of energy loss due to dry flue gas can now be expressed as

$$Q_2 = M_g C_p(T_4 - T_3) \quad \text{kJ/kgfuel (Btu/lbm)} \tag{6.12}$$

where M_g = mass of dry flue gas per mass of fuel fired, and

$$M_g = \frac{\dot{m}_g}{\dot{m}_f} \tag{6.13}$$

C_p = mean constant pressure specific heat of dry flue gases evaluated at conditions between air supply and flue gas temperatures
T_4 = flue gas temperature measured at the heat exchanger exit
T_3 = air supply dry bulb temperature

Any water formed or present in the exhaust gases should be above its corresponding dew point temperature and therefore vaporized by the flue gases. The latent heat of vaporization associated with this process will not then be available to generate steam. Several factors contribute to the presence of moisture in the combustion process and the resulting energy loss, including the combustion of hydrogen in the fuel, moisture present in the fuel, and moisture existing in the combustion air supply.

Recall from Chapter 2 that, ideally, 2 moles H_2 form 2 moles H_2O or 4 mass units H_2 produce 36 mass units H_2O. Therefore, 9 mass units of water are produced by each mass unit of H_2. The loss due to moisture produced from hydrogen in the fuel is then given as

$$Q_3 = \frac{9H}{100}[h_6 - h_5] \qquad \text{kJ/kg fuel (Btu/lbm)} \tag{6.14}$$

where

H = H_2 ultimate analysis in fuel, %
h_6 = enthalpy of superheated steam at low pressure (10 kPa, 1 psi) and flue gas temperature measured at the heat exchanger exit
h_5 = enthalpy of saturated liquid at fuel supply temperature

The loss associated with vaporization of moisture in the fuel is determined in similar fashion to hydrogen loss above as

$$Q_4 = \frac{M_1}{1 - M_1}(h_6 - h_5) \quad \text{kJ/kg fuel (Btu/lbm)} \tag{6.15}$$

where M_l = mass of fuel moisture per mass of fuel fired.

The loss due to vaporization of moisture in the air supplied for combustion can also be evaluated and is equal to

$$Q_5 = M_a M_v (h_6 - h_7) \qquad \text{kJ/kg fuel (Btu/lbm)} \tag{6.16}$$

where

M_a = mass of air supplied per mass of fuel
M_v = mass of moisture per mass of dry air

$$M_a = \frac{\dot{m}_a}{\dot{m}_f} \tag{6.17}$$

$$M_v = \frac{\dot{m}_v}{\dot{m}_a} \tag{6.18}$$

h_7 = enthalpy of superheated steam at air supply temperature and water vapor partial pressure

Incomplete combustion of carbon in the fuel to form CO instead of CO_2 also will result in less energy being available to generate steam. The energy released by oxidation of CO to form CO_2, a measure of this loss, is given by the heating value of CO or

$$Q_6 = HV_{CO}\left\langle \frac{\text{energy release}}{\text{unit mass CO}} \right\rangle \tag{6.19}$$

From a boiler flue gas analysis, major dry exhaust gas constituents are found, in general, to be CO, CO_2, O_2, and N_2. By measuring concentrations of these species, their mole fractions in dry gas mixture can be determined. Obviously, the presence of nitric oxides, sulfur, ash, and other trace elements influence boiler performance, but these components do not have a pronounced effect on a boiler energy analysis. The mass of CO formed per mole of dry exhaust gas is therefore equal to the molecular weight of CO multiplied by the mole fraction of CO or

$$28\,\bar{x}_{CO}\left\langle \frac{\text{mass CO}}{\text{moles dry gas}} \right\rangle \tag{6.20}$$

As previously indicated, carbon, when oxidized, will form carbon monoxide and carbon dioxide, and the mass of carbon per moles of dry exhaust gas is given by the expression

$$12[\bar{x}_{CO} + \bar{x}_{CO_2}]\left\langle \frac{\text{mass carbon}}{\text{moles dry gas}} \right\rangle \tag{6.21}$$

The mass of carbon per mass of fuel fired, C, can be obtained from the fuel gravimetric analysis. Combining Equations (6.19–6.21) yields an expression for energy loss due to incomplete combustion of carbon per unit mass of fuel as

$$Q_6 = \left[\frac{28\ C}{12}\right]\left[\frac{\bar{x}_{CO}}{\bar{x}_{CO} + \bar{x}_{CO_2}}\right] HV_{CO} \qquad \text{kJ/kg fuel (Btu/lbm)} \tag{6.22}$$

The energy loss to radiation and convective heat transfer as well as other unaccounted-for losses can now be expressed in terms of the heating value of the fuel and the losses evaluated above as

$$Q_7 = HHV - \sum_{i=1}^{6} Q_i \qquad \text{kJ/kg fuel (Btu/lbm)} \tag{6.23}$$

The above items are often expressed alternatively as percentages of heating value. In general, acceptable test results require that unaccounted-for losses should be less than 2%. Additional minor losses could also be considered if information is available and might include losses due to unburned carbon in the bottom and fly ash.

EXAMPLE 6.5 The following data were obtained during a standard boiler test:

1.	Duration of test	1 hr
2.	Steam delivered by boiler	200,000 lbm
3.	Average steam temperature at superheater outlet	760°F
4.	Average steam pressure at superheater outlet	600 psia
5.	Feedwater temperature	240°F
6.	Feedwater pressure	700 psia
7.	Fuel fired	15,385 lbm
8.	Flue gas temperature leaving last heat transfer passage	450°F
9.	Dry bulb temperature of air supplied for combustion	80°F
10.	Wet bulb temperature of air supplied for combustion	70°F
11.	Barometric pressure at test location	29.92 in. Hg
12.	Temperature of fuel supplied to burners	80°F
13.	Ultimate analysis of fuel on an as-fired basis:	
	Carbon	0.8095 lbm/lbm fuel
	Hydrogen	0.1143 lbm/lbm fuel
	Nitrogen	0.0048 lbm/lbm fuel
	Sulfur	0.0143 lbm/lbm fuel
	Oxygen	0.0095 lbm/lbm fuel
	Moisture	0.0476 lbm/lbm fuel
	Ash	0.0000 lbm/lbm fuel
		1.0000

14. Volume analysis of flue gases in percent (Orsat):
    CO_2 = 11.34%
    CO = 00.71
    O_2 = 5.06
    N_2 = 82.89
    100.00%
15. Higher heating value of fuels is 19,500 Btu/lbm dry fuel

Calculate an energy balance for the tested boiler.

Solution:

1. Fuel analysis, dry basis gravimetric analysis:

	mf_i	$mf_{i)_{\text{I}}}$	$mf_{i)_{\text{II}}}$
C_S	0.8095	0.8095	0.8500
H_2	0.1143	0.1143	0.1200
O_2	0.0048	0.0048	0.0050
S	0.0143	0.0143	0.0150
N_2	0.0095	0.0095	0.0100
Moisture	0.0476	—	—
	$\frac{\text{lbm}_i}{\text{lbm}_{\text{tot}}}$	$\frac{\text{lbm}_i}{\text{lbm}_{\text{tot}}}$	$\frac{\text{lbm}_i}{\text{lbm}_{\text{tot}}}$

$\Sigma\, mf_{i)_{\text{I}}} = 0.9524$

2. Flue gas analysis, gravimetric:

	$\bar{x}_i$	MW	$\bar{x}_i MW_i$	mf_i
CO_2	0.1134	44	4.9896	0.1662
CO	0.0071	28	0.1988	0.0066
O_2	0.0506	32	1.6192	0.0539
N_2	0.8289	28	23.2092	0.7733
	$\frac{\text{lbmole}_i}{\text{lbmole}_{\text{tot}}}$	$\frac{\text{lbm}_i}{\text{lbmole}_i}$	$\frac{\text{lbm}_i}{\text{lbmole}_{\text{tot}}}$	$\frac{\text{lbm}_i}{\text{lbm}_{\text{tot}}}$

$MW = \Sigma \bar{x}_i MW_i = 30.0168$ lbm/lbmole

3. Energy absorbed by water:

$$Q_1 = M_S(h_2 - h_1)$$

$$= \left(\frac{200{,}000 \text{ lbm steam}}{15{,}385 \text{ lbm fuel}}\right)\left[(1{,}385.1 - 209.9)\frac{\text{Btu}}{\text{lbm steam}}\right]^*$$

$$= 15{,}277.2 \text{ Btu/lbm fuel}$$

4. Energy loss to dry flue gases:

$$Q_2 = M_g C_p (T_2 - T_1)$$

where

$$M_g = \frac{0.85 \dfrac{\text{lbm carbon}}{\text{lbm fuel}}}{\left[\left(\dfrac{12}{44}\right)(0.1662) + \left(\dfrac{12}{28}\right)(0.0066)\right]\dfrac{\text{lbm carbon}}{\text{lbm gas}}}$$

$$= 17.65 \text{ lbm gas/lbm fuel}$$

$$Q_2 = (17.65 \text{ lbm gas/lbm fuel})(0.24 \text{ Btu/lbm gas} \cdot °\text{R})(450 - 80°\text{R})$$

$$= 1{,}567.3 \text{ Btu/lbm fuel}$$

5. Energy lost to moisture from burning hydrogen:

$$Q_3 = \frac{9H}{100}(h_4 - h_3)$$

$$= \left(\frac{9 \text{ lbm } H_2O}{\text{lbm } H_2}\right)\left(\frac{12 \text{ lbm } H_2}{100 \text{ lbm fuel}}\right)[1{,}265.1 - 48.09] \text{ Btu/lbm } H_2O$$

$$= 1{,}314.3 \text{ Btu/lbm fuel}$$

6. Energy lost to moisture accompanying fuel:

$$Q_4 = \frac{M_l}{1 - M_l}(h_4 - h_3) = \left(\frac{0.0476}{1 - 0.0476}\right)[1{,}265.1 - 48.09]$$

$$= 60.8 \text{ Btu/lbm fuel}$$

*Keenan, J. H., Keyes, F. G., Hill, P. G., and Moore, J. G., *Steam Tables* (English Units), © John Wiley & Sons, Inc., New York, 1969, 1978.

7. Energy loss to moisture in air:

$$Q_5 = M_a M_v (h_4 - h_5)$$

$$M_a = \frac{\left(0.7732 \frac{\text{lbm N}_2}{\text{lbm gas}}\right)\left(0.8500 \frac{\text{lbm C}}{\text{lbm fuel}}\right)\left(1.3040 \frac{\text{lbm air}}{\text{lbm N}_2}\right)}{\left[\left(\frac{12}{44}\right)(0.1662) + \left(\frac{12}{28}\right)(0.0066)\right]\frac{\text{lbm C}}{\text{lbm gas}}}$$

$$= 18.10 \text{ lbm air/lbm fuel}$$

M_v = 0.0134 lbm moisture/lbm dry air from psychometric chart @ 80°F dry bulb and 70°F wet bulb

$h_5 = h_g(T = 80°\text{F}) = 1{,}096.4$ Btu/lbm

$$Q_5 = \left(18.10 \frac{\text{lbm air}}{\text{lbm fuel}}\right)\left(0.0134 \frac{\text{lbm moisture}}{\text{lbm air}}\right)(1{,}265.1 - 1{,}096.4)$$

$$= 40.92 \text{ Btu/lbm fuel}$$

8. Energy loss to incomplete combustion:

$$Q_6 = \left[\frac{28\ C}{12}\right]\left[\frac{\bar{x}_{CO}}{\bar{x}_{CO} + \bar{x}_{CO_2}}\right] HV_{CO}$$

$$= (28/12)(0.85)\left[\frac{0.0071}{0.1134 + 0.0071}\right]\left[\frac{(67{,}636)(1.8001)}{(28)}\right]$$

$$= 508.1 \text{ Btu/lbm fuel}$$

9. Energy loss to radiation and unaccounted-for losses:

$$Q_7 = HHV - (Q_1 + Q_2 + Q_3 + Q_4 + Q_5 + Q_6)$$

$$= 19{,}500 - (15{,}277.2 + 1{,}567.3 + 1{,}314.4 + 60.8 + 40.9 + 508.1)$$

$$= 731.3 \text{ Btu/lbm dry fuel}$$

10. Boiler energy balance summary:

No.	Item	Btu/lbm	%
1	Gain by water and steam	15,277.2	78.34
2	Loss to dry flue gases	1,567.3	8.04
3	Loss to moisture from burning H_2	1,314.4	6.74
4	Loss to moisture in fuel	60.8	0.31
5	Loss to moisture in air	40.9	0.21
6	Loss to incomplete combustion	508.1	2.61
7	Radiation and unaccounted losses	731.3	3.75
8	Higher heating value of fuel	19,500.0	100.00

Additional terminology and definitions are commonly used when evaluating boiler combustion systems. *Capacity* C_b is the heat absorption rate of a boiler and its feedwater and generated steam

$$C_b = \dot{m}_s(h_2 - h_1) \qquad \text{kW (mBtu/hr)} \tag{6.24}$$

where m_s = steam mass flow rate, kg/sec (lbm/hr).

Heat rate HR compares the boiler heat addition to the net power plant output, an inverse of thermal efficiency η or

$$HR = \eta^{-1} \tag{6.25}$$

and

$$HR = \frac{3{,}413}{\eta} \qquad \frac{\text{Btu}}{\text{kW} \cdot \text{hr}}$$

$$HR = \frac{2{,}544}{\eta} \qquad \frac{\text{Btu}}{\text{hp} \cdot \text{hr}}$$

The heat rate per unit volume of furnace space is termed the *furnace rating FR* or

$$FR = \frac{\dot{m}_f \; HHV}{\text{Furnace volume}} \qquad \text{kW/m}^3 \text{ (Btu/ft}^3 \text{ hr)} \tag{6.26}$$

A more complete discussion of boiler equipment and the general subject of steam generation can be found in the literature.

PROBLEMS

6.1 An anthracite coal sample has the following dry-basis ultimate analysis:

C_s	83.73%	S	0.48%	N_2	0.80%
H_2	2.14%	O_2	1.92%	Ash	10.93%

For this solid fuel, (a) write the stoichiometric equation for the ideal combustion reaction; (b) determine the mass *AF* ratio on a dry basis, lbm air/lbm fuel; and (c) calculate the amount of carbon dioxide formed per unit of fuel fired, lbm CO_2/lbm coal.

6.2 Two hundred pounds of coal/min having the following ultimate analysis is burned in a boiler:

C_s	74.17%	S	1.95%	N_2	2.40%
H_2	5.64%	O_2	9.02%	Ash	6.82%

Determine, for the unit: (a) the rating for a forced-draft fan designed to supply 35% excess air at 90°F and 14.7 psia, ft^3/min; and (b) the mass flow rate of dry flue gas resulting from combustion if the Orsat analysis yields 11.95% CO_2, 6.20% O_2, and 1.33% CO, lbm/min.

6.3 The ultimate analysis of a bituminous coal sample is reported to be:

C_s	76.3%	S	1.4%	N_2	2.3%
H_2	4.8%	O_2	4.1%	H_2O	4.1 %
Ash	7.0%				

Determine the following: (a) fuel analysis on a dry basis, %; (b) fuel analysis on a dry and ashless basis, %; and (c) the amount of refuse from combustion to be handled if this fuel is burned at a rate of 200 tons/hr as received and the refuse is found to be 10% carbon in ash, lbm refuse/hr.

6.4 Ten pounds mass of coal/min having an ultimate analysis as given below is completely burned in a small power boiler.

C_s	79.5 %	S	1.2%	N_2	2.7%
H_2	4.1%	O_2	6.6%	Ash	5.9%

Twenty-five percent excess air is supplied at 70°F and 28-in. Hg. Flue gas leaves the unit at 155°F and 28-in. Hg. For complete combustion, find (a) the ideal *AF* ratio, lbm air/lbm fuel; (b) the mass flow rate of CO_2, lbm/min; (c) the flue gas volumetric flow rate, ft^3/min; (d) the percent O_2 in dry flue gas analysis, %; and (e) exhaust dew point temperature, °F.

6.5 Fifty kilograms of coal/sec having the ultimate analysis as given below is burned in a boiler.

C_s	78.2%	O_2	6.4%	H_2	5.2%
N_2	1.6%	S	1.3%	Ash	7.3%

One hundred and twenty percent theoretical air is supplied at 70°C and 101 kPa. The flue gases leave the unit at 327°C and 101 kPa. Calculate (a) the *MW* of the coal, kg/kg mole; (b) Orsat analysis if 10% of the ideal CO_2 is CO, %; (c) the dry flue gas *MW*, kg/kg mole; (d) the dry flue gas volumetric flow rate, m^3/sec; and (e) the exhaust dew point temperature, °C.

6.6 Pulverized coal is fired at a rate of 100 tons/hr in a stationary power plant. The analysis of the coal is reported to be:

C_s	72.6%	H_2O	4. 1 %	N_2	3.2%
H_2	6.9%	O_2	8.7%	Ash	4.5%

The stack gas analysis on a volumetric basis yields the following:

CO_2	10.38%	O_2	7.55%	CO	1.83%	N_2	80.24%

Refuse pit analysis on a mass basis yields:

C_s	23%
Ash	77%

Determine the following: (a) volume of air supplied measured at 14.7 psia and 90ºF, ft^3/hr; (b) refuse collection rate, lbm/hr; and (c) the volume of dry products measured at a total pressure of 14.7 psia and stack temperature of 310ºF.

6.7 A sample of dry wood has the following ultimate analysis:

C_s	53.6%	S	0.1%	N_2	29.8%	H_2	6.4%	O_2	7.2%	Ash	2.9%

Calculate (a) the stoichiometric equation; (b) the *AF* ratio, kg air/kg wood; and (e) the higher heating value, kJ/kg wood.

6.8 Consider the dry wood in Problem 6.7. For 0, 20, 40, and 80% moisture, calculate (a) the net heating value of the wood, kJ/kg; (b) the mass of water to mass of dry wood, %; (c) the heat required to vaporize the water, kJ/kg of dry wood; and (d) the percentage of water at which the ideal net heat of combustion would be zero, %.

6.9 A processed coal, consisting only of carbon and ash, is burned at a rate of 30,000 kg/hr. The combustion occurs with 20% excess air, and the entire ash is collected after combustion at a rate of 4,500 kg/hr. Determine (a) the ultimate analysis of the coal, (b) the *AF* ratio, kg air/kg fuel; (c) the volume of air supply required at 101 kPa and 27°C; and (d) the higher heating value of the coal, kJ/kg.

6.10 Municipal solid waste (MSW) is being utilized as an alternate fuel for steam generation. The fuel composition on a weight basis is:

C_s	25.0%	O_2	21.1%	H_2	3.3 %
H_2O	28.0%	N_2	0.5 %	S	0.1%

Glass, metals, ash 22.0%

Dry exhaust gases leave the boiler at 500K and 101 kPa with the following stack analysis:

CO_2	13.6%	O_2	4.4%
CO	3.4%	SO_2	0.02%

Air enters the burner at 25°C and 104 kPa. Determine (a) the excess air, %; (b) the stack dew point temperature, °C; (c) the sulfur dioxide production rate, kg SO_2/kg fuel; and (d) the boiler efficiency, %.

6.11 A small one-room cabin is to be heated during the winter using a wood-burning stove having a 60% combustion efficiency. The room will require on the average about 8,000 Btu/hr of heat from the stove. Specifications for a given wood supply on a weight basis are given below:

C_s	44.00%	S	0.10%	N_2	0.25%
H_2	5.60%	O_2	36.15%	H_2O	12.00%
Inerts	1.90%	(Density = 30 lbm/ft^3)			

Estimate the following: (a) minimum required cords of wood burned/hr (1 cord = 4 x 4 x 8 ft = 128 ft^3), cords/hr; (b) equivalent gallons of fuel oil saved if fuel oil has a higher heating value of 19,000 Btu/lbm, gal/hr; and (c) the economic equivalency of these two fuels on a Btu basis for a fuel price of $1.50/gal, $/cord.

6.12 The stoichiometric combustion of an unknown ashless coal sample yields a 17.44% CO_2, 1.94% CO, and 0.97% O_2 dry flue gas analysis. The molar $\overline{AF}$ ratio for this reaction is 4.286 lb mole air/lb mole fuel while producing 0.2815 lbm H_2O/lbm ashless coal. The product molecular weight is 30.351 lbm/lb mole. For this ashless coal, find (a) the stoichiometric equation; (b) mass fractions of the coal sample, %; (c) molecular weight of the coal, lbm/lb mole; and (d) the mass *FA* ratio, lbm coal/lbm air.

6.13 A power plant, rated at 500 MW and 39% thermal efficiency, is to be switched over to the low-sulfur coal having the ultimate analysis shown below.

	Original coal	Low-sulfur coal
C_s	68.87%	83.84%
H_2	20.41%	4.65%
S	1.38%	0.47%
O_2	2.32%	5.36%
N_2	0.59%	1.17%
Ash	6.43%	4.51%

Assume that the volumetric flow rate and air supply conditions to the burners remain constant and that the original combustion requires 130% theoretical air. Find (a) the change in coal mass flow rate, %; (b) the reduction in SO_2 emissions, %; (c) the change in moisture in the exhaust, %; and (d) the change in CO_2 level in the stack, %.

6.14 The fuel for the preliminary design of a 500,000-kW steam power plant with a 40% thermal efficiency is to be coal at 5 $/ton. The as-fired gravimetric analysis of the coal for the initial design analysis is given below:

C_s	74.79%	S	3.42%	N_2	1.20%		
H_2	4.98%	O_2	6.42%	H_2O	1.55%	Ash	7.82%

Calculate, for the unit: (a) the specific fuel consumption, kg/kW hr; and (b) the fuel cost for operation, $/hr.

6.15 A western U.S. coal has the following ultimate analysis:

C_s	72.3%	S	0.5%	N_2	1.3%
H_2	5.8%	O_2	14.9%	Ash	5.2%

Estimate (a) the higher heating value of the coal, kJ/kg; (b) the dry SO_2 in the stack if the flue gas is 3% O_2, %; (c) the NO_x concentration as NO, assuming all the chemically bound nitrogen is converted to NO, %; and (d) repeat parts (b) and (c) product analysis, kg product/million kJ fuel.

6.16 A fuel plant is designed to convert municipal solid waste (MSW) into a refuse-derived fuel (RDF). The plant is supplied with MSW, having the ultimate analysis shown below at a rate of 1200 tons/day.

C_s	25.2%	S	0.1%	H_2O	28.0%
H_2	3.3%	O_2	21.1%	Ash	5.6%
Glass	9.3%	Metal	7.4%		

For ideal conversion, determine the following: (a) mass flow rate of recoverable glass and metal, kg/day; (b) mass flow of landfill inerts, kg/day; (c) mass flow of RDF, kg/day; (d) higher heating value of MSW, kJ/kg; and (e) higher heating value of RDF, kJ/kg.

6.17 Determine the adiabatic flame temperature of the anthracite coal in Problem 6.1 when burned at constant pressure with 130% theoretical air. Assume that both the fuel and air are initially at 1 atm and 25ºC.

6.18 A 1-g sample of solid carbon is burned in 200% excess air in a bomb calorimeter. The initial fill conditions are 62°F and 15 psia. After combustion in the constant-volume vessel, determine (a) the product mole fractions for complete combustion;

(b) the adiabatic flame temperature, ºR; and (e) the rise in temperature of a water jacket from this process if the mass of the water is 5 lbm.

6.19 The following data were obtained during the operation of a coal-fired steam generator:

Fuel analysis		*Stack analysis*	
C_s	63.70%	CO_2	14.8%
H_2	4.78%	CO	0.0%
N_2	1.40%	O_2	4.5%
O_2	9.42%	N_2	80.7%
H_2O	8.10%	Ash	12.60%

Barometer	1 atm	Coal feed	3,400 lbm/hr
Flue gas *T*	500°F	Steam rate	30,600 lbm/hr
Air supply	82°F	Refuse	445 lbm/hr
Feedwater	208°F	Sat vap at	150 psia

Determine, for the unit: (a) the excess air supplied for combustion, %; and (b) steam generator efficiency, %. Assume the refuse is composed of ash and carbon alone.

6.20 A boiler is being designed to burn a coal-water slurry that is 80% carbon (coal) and 20% water by weight. Assume that the fuel and air is supplied at *STP* and that ideal products of combustion leave the boiler at 127ºC. The burner requires 20% excess air by weight. Calculate the following: (a) the fuel-air ratio, kg fuel/kg air; (b) the ideal heat release, kJ/kg air; (c) the actual heat release, kJ/kg air; and (d) the combustion efficiency, %.

6.21 A 950-MW power plant has the following ultimate analysis:

C_s	78.6%	S	2.2%	N_2	1.6%		
H_2	4.3%	O_2	3.2%	H_2O	1.3%	Ash	8.8%

Overall plant thermal efficiency	40%
Overall boiler efficiency	91%
Overall allowable sulfur dioxide emissions	7%
Overall ESP efficiency	99%

Calculate for these conditions: (a) the fuel rate, kg fuel/hr; (b) the annual CO_2 production rate, kg/yr; (c) the sulfur dioxide release with collection rates, kg/hr; (d) the mass of adsorbent limestone ($CaCO_3$) required with mass of by-product $CaSO_3$ produced; and (e) mass of annual ash produced with annual particulate emissions, kg/yr.

6.22 A power plant burns 86,400 kg/hr of lignite coal and utilizes advanced post combustion NO_x catalytic reduction technology to remove 91% of the NO from the flue gas. The wet flue gas flowrate is 4.5 m^3 per kg of coal and the initial NO concentration prior to cleanup is 1,200 mg per m^3 of flue gas. Determine (a) the flue gas flowrate, m^3/hr; (b) the mass ratio of ammonia, NH_3, to NO, mg/mg; (c) the final flue gas NO concentration after treatment, mg/m^3; and (d) required hourly ammonia input to the unit, kg/hr.

6.23 A stationary power plant burns coal with an ash content of 7.4% and higher heating value of 11,420 Btu/lbm in a pulverized coal-fired dry bottom wall-fired utility boiler. Using the New Source Performance Standards (NSPSs) particulate emissions factor of 10 × (% ash), lbm/ton of coal and electric utility steam generating unit particulate emission standard of 0.03 lbm/10^6 Btu, determine: (a) the emissions factor, lbm/ton of coal; (b) ash emissions, lbm/10^6 Btu; (c) the collector efficiency necessary to meet the NSPS standard for particulate matter, %; (d) repeat (a) – (c) if only 60% of the total ash results in flash.

7

Liquid Fuels

7.1 INTRODUCTION

Energy characteristics of specific solid fuel resources and the combustion systems they require for power generation were considered in some detail in Chapter 6. In this chapter, however, attention will be given to general energy properties of important liquid fuel resources. Availability of crude oil reserves, ease of storage and handling of distillate liquid fuels, along with the broad utilization of oil-fired combustion systems have contributed to making liquid hydrocarbon fuels a major energy resource in today's world economy. The critical dependency on petroleum-based fuels of mobility propulsion systems such as spark and compression engines, as well as gas turbine engines, is basic to their present state of development. The combustion characteristics and specific nature of each of these three liquid fuel-engine interfaces will be treated in detail separately in later chapters. With the projected shortage in future oil reserves, power and propulsion engineering will require a greater emphasis on utilizing liquid fuel alternates and potential application of synthetic liquid fuels.

In this chapter, various liquid fuel resources derived from crude oil reserves, as well as those produced from synthetic stocks, will be reviewed. An understanding of liquid fuel science and engineering requires some background in chemistry and fluid mechanics. The use of liquid fuels to produce heat and power depends on their particular properties, but additional characteristics do result from the specific application or unique nature of each fuel-engine interface. For example, the explosive nature, or detonation, of spark-ignition engine fuels is defined by a fuel-engine parameter, the *octane rating.*

EXAMPLE 7.1 Kerogen, or shale oil, has been proposed as a potential liquid fuel source. The ultimate analysis of a typical 1-ton sample of raw shale is given below.

Raw shale constituent	Percentage
Ash	65.7
CO_2	18.9
Organic carbon	12.4
H2	1.8
N_2	0.4
Sulfur	0.6
H_2O	0.2

Using these percentages, determine (1) the dry and ashless gravimetric analysis of the shale; (b) the gravimetric analysis for part (a) on an oxygen-free basis; (c) the mass of part (a) as derived from 1 ton of raw shale, and (d) the mass of part (b) as derived from one ton of raw shale.

Solution:

1. Gravimetric analysis, dry and ashless basis:

$$mf_i = \frac{\text{lbm component } i}{\text{lbm mixture}}$$

a. Mass fraction, where lbm mixt = lbm total – lbm H_2O – lbm ash

$$mf_{CO_2} = \frac{0.189}{1.00 - 0.657 - 0.002} = 0.5543 \text{ or } 55.43\%$$

$$mf_{C_S} = \frac{0.124}{0.341} = 0.3636 \text{ or } 36.36\%$$

$$mf_{H_2} = \frac{0.018}{0.341} = 0.0528 \text{ or } 5.28\%$$

$$mf_{N_2} = \frac{0.004}{0.341} = 0.0117 \text{ or } 1.17\%$$

$$mf_S = \frac{0.006}{0.341} = 0.0176 \text{ or } 1.76\%$$

2. Oxygen-free basis:

$$12 \text{ lbm } C_s + 32 \text{ lbm } O_2 \rightarrow 44 \text{ lbm } CO_2$$

or for each lbm CO_2 on a mass basis:

$$\%\, C_S = \frac{12 \text{ lbm carbon}}{44 \text{ lbm } CO_2}$$

$$\%\,O_2 = \frac{32\ \text{lbm}\,O_2}{44\ \text{lbm}\,CO_2}$$

Mass fraction of dry, ashless sample:

$$mf_{C_S} = \left(\frac{12}{44}\right)(0.5543) = 0.1512$$

$$mf_{O_2} = \left(\frac{32}{44}\right)(0.5543) = 0.4031$$

$$mf_{C_S} = 0.3636$$

$$mf_{H_2} = 0.0528$$

$$mf_{N_2} = 0.0117$$

$$mf_S = 0.0176$$

b. Mass fraction, dry, ashless, oxygen-free:

$$mf_{C_S} = \frac{0.1512 + 0.3636}{1.0000 - 0.4031} = 0.8625 \text{ or } 86.25\%$$

$$mf_{H_2} = \frac{0.0528}{0.5969} = 0.0885 \text{ or } 8.85\%$$

$$mf_{N_2} = \frac{0.0117}{0.5969} = 0.0196 \text{ or } 1.96\%$$

$$mf_S = \frac{0.0176}{0.5969} = 0.294 \text{ or } 2.94\%$$

3. Total mass of dry, ashless sample now from 1.

$$m_{tot} = \left(0.341\frac{\text{lbm dry, ashless sample}}{\text{lbm raw shale}}\right) \times (2000\ \text{lbm raw shale})$$

c. $m_{tot} = 682$ lbm (0.341 ton)

4. Total mass of dry, ashless, oxygen-free sample now from 2.

$$m_{tot} = \left(0.5969\frac{\text{lbm dry, ashless, } O_2\text{ - free}}{\text{lbm dry, ashless}}\right) \times (682\ \text{lbm})$$

d. $m_{tot} = 407$ lbm (0.2035 ton)

Comments: This problem illustrates the fact that potential oil production from shale sources, such as kerogen, generates high levels of waste with low yields of fuel. To separate the waste material from a viable fuel source may require high levels of energy and potentially significant environmental penalties.

7.2 LIQUID FUEL PROPERTIES

In the following section, a few major liquid fuel properties that influence their combustion are covered. Standard tests for liquid fuels are established by engineering societies such as the American Petroleum Institute (API), American Society for Testing Materials (ASTM), American Society of Mechanical Engineering (ASME), and the Society of Automotive Engineers (SAE).

Liquid hydrocarbon fuels basically are mixtures of specific compounds from the following inorganic families:

Paraffins
Olefins
Naphthenes
Aromatics

Many liquid fuel chemical and combustion characteristics are a direct result of the particular nature of those hydrocarbon groups. General naming and classifying of particular species follow rules established in inorganic chemistry. For example, each hydrocarbon compound is named in terms of the number of carbon atoms per molecule by using the basic carbon atom prefixes given below; see Figure 7.1.

No. C atoms	Prefix
1	meth-
2	eth-
3	prop-
4	but-
5	pent-
6	hex-
7	hept-
8	oct-
9	non-
10	dec-
16	hexadec-

Paraffins are hydrocarbon compounds having open saturated carbon chain structures with only single carbon atom bonds. Saturated structures are those in which each bond is made with a separate C-C or C-H atom-to-atom bond. Every carbon atom has four single valence bonds available. Paraffins can be represented chemically as C_xH_{2x+2} and are recognized by their common suffix *-ane*. For example, if $x = 4$, then C_4H_{10} is termed but*ane*; whereas, if $x = 10$ then $C_{10}H_{12}$ is called dec*ane*. Paraffins are major constituents in most crude oil base liquid fuels.

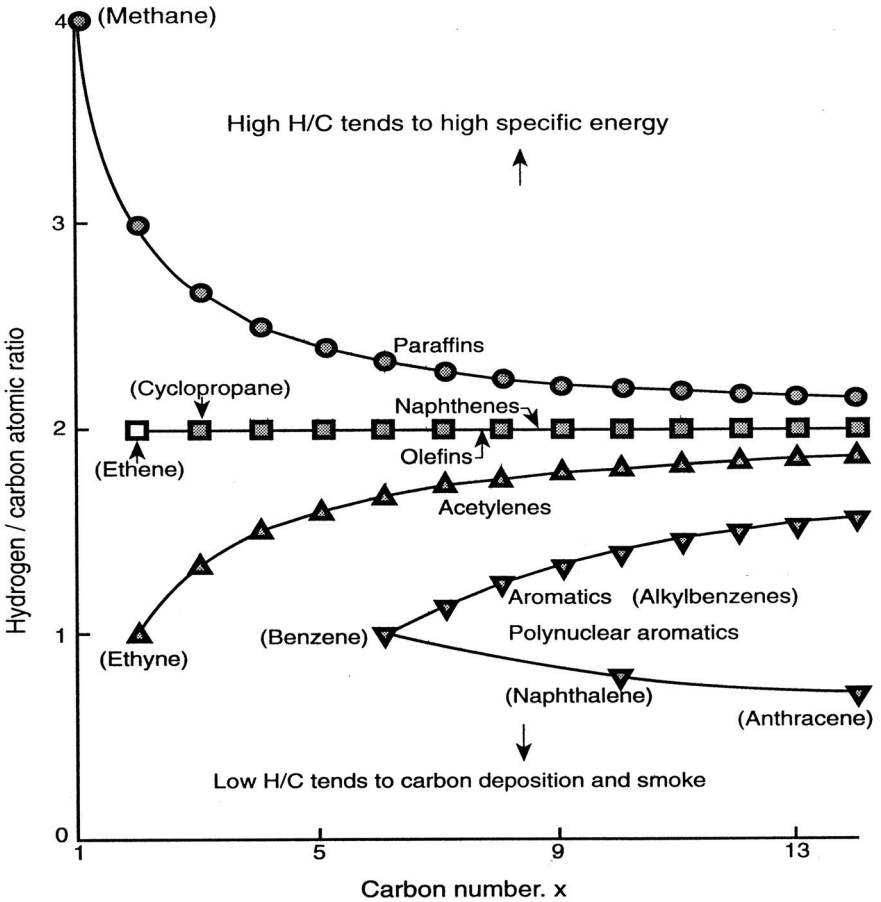

Figure 7.1 H:C atomic ratio of various inorganic hydrocarbon compounds. *Source*: Goodger, E. M., *Alternate Fuels: Chemical Energy Sources*, Halsted Press, New York, 1980. Reproduced with permission of Palgrave Macmillan.

methane (CH_4), ethane (C_2H_6) } natural gas components

propane (C_3H_8), butane (C_4H_{10}) } liquid petroleum gas compounds

octane (C_8H_{18}) gasoline component

Paraffins can have the same total carbon-to-hydrogen ratio but may assume considerably different structures. Open, straight chain structures, termed normal paraffins, are written as n-C_xH_{2x+2}, whereas branched chain structures, termed *isomers,*

are designated *iso*- C_xH_{2x+2}. Radicals other than a single hydrogen atom can be bonded to the basic carbon chain, i.e., additional carbon atoms or even radicals such as the *methyl* radical CH_3.

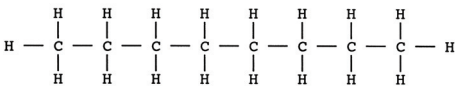

n-octane

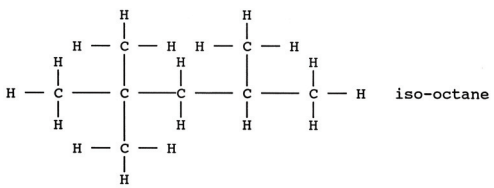

iso-octane

Branched hydrocarbon structures can be named using alternative nomenclatures. The isooctane structure above is also termed 2, 2, 4-trimethylpentane since pentane is the principal root; i.e., the basic chain consists of five carbon atoms. Trimethyl is used because there are three methyl radicals attached to the chain, and 2, 2, 4 is used to identify that the branched radicals are attached to the second, second, and fourth carbon atoms of the basic chain.

Several general thermochemical characteristics of paraffin fuels can be cited that are a result of their structure.

Maximum hydrogen atom/carbon atom ratio
Highest heating values per unit mass of liquid hydrocarbon fuels
Lowest densities
Lowest heating values per unit volume of liquid hydrocarbon fuels
Clean burning
Stable when stored

Olefins are hydrocarbon compounds having open unsaturated carbon chain structures with both single and double carbon atom bonds. Olefins, termed alkenes, that have one double carbon bond are written chemically as C_xH_{2x} and are identifiable by their common suffix -*ene.* As an example, for $x = 5$, C_5H_{10} is pent*ene*, while if $x = 8$, C_8H_{16} would be oct*ene*. For compounds having more than one double bond, *diolefins,* the chemical structure is C_xH_{2x-2}, and the suffix is -*diene.* Olefins are formed predominantly by cracking heavy paraffin compounds.

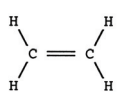

Ethene

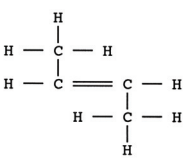

Isobutene

Olefins, like paraffin fuels, have certain thermochemical characteristics that are a result of their structure:

Fewer hydrogen atoms than for paraffins having the same number of total carbon atoms
Unstable when formed
Can form residue or gum when exposed to O_2
Fairly clean-burning fuel

Naphthenes are hydrocarbon ring compounds having saturated carbon chain structures with only single carbon atom bonds. Chemically, naphthenes are similar in character to normal paraffins and isoparaffins. Structurally, they are represented by the use of their common prefix *cyclo-* and the corresponding paraffin suffix. As an example, C_5H_{10} is termed *cyclo*pentane.

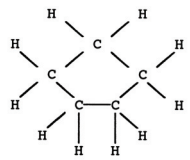

Cyclopentane

Aromatics are hydrocarbon ring structures having unsaturated carbon ring structures with both single and double carbon atom bonds. Aromatic hydrocarbons are recognized by their basic six carbon atom benzene ring structure.

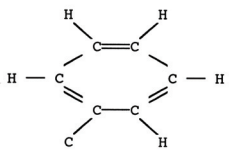

Benzene

Aromatics having single-ringed structures have the general formula C_xH_{2x-6}, and double-ringed species have the formula C_xH_{2x-12}.

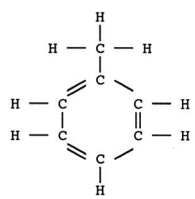

Toluene

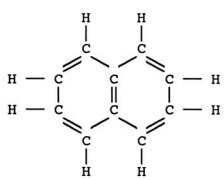

naphthalene

Aromatic hydrocarbons also have thermochemical characteristics that are a result of their structures:

Compact molecular structure
Stable when stored

Smoky combustion process
Highest fuel distillate densities
Highest heating values per unit volume of liquid hydrocarbon fuels
Lowest heating values per *unit mass* of liquid hydrocarbon fuels

Aromatic compounds are found in gasoline and diesel fuels as well as predominant products of coal-based distillate fuels. These particular fuel constituents are of a major concern in terms of incomplete combustion and their *carcinogenic,* or cancer-causing, products of incomplete combustion.

Acetylenes are unsaturated carbon chain compounds having triple carbon atom bonds. They have the same formula as diolefins and are recognized by the suffix *-yne.*

Acetylene

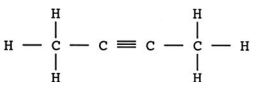

Butyne-2

Partially oxidized hydrocarbon compounds having saturated carbon structures are known as *alcohols.* Alcohols are recognized by a common suffix *-ol* and have the chemical formula $C_xH_{y\text{-}1}OH$ where a hydrogen atom has been replaced by the OH hydroxyl radical. Alcohols have been synthesized from vegetable matter and produced from wood or grain sources, i.e., ethanol. Much attention has been given to try and produce fuel grade methanol from natural gas or coal. The discussion of alcohol fuels and their utilization depends greatly on successful commercialization of technology with favorable economics and energetics; i.e., one cannot use 10 units of energy and/or monetary value to produce a fuel with 5 units of energy and/or monetary value, or one cannot successfully market a fuel resource that costs twice that of competitive resources.

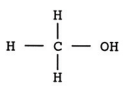

Methanol

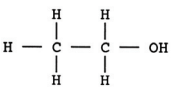

Ethanol

A number of fluid properties of liquid hydrocarbon fuels are important when determining their combustion characteristics. Liquid fuel densities can be expressed in dimensionless form in terms of their *specific gravity,* that is, density of the liquid at a specified temperature and pressure to a reference liquid (usually water) also at the specified temperature and pressure. The measurements for specific gravity, *SG*, are taken at barometric conditions and are written

$$SG = \frac{\rho_{\text{fuel}}\langle T \rangle}{\rho_{\text{fuel}}\langle T \rangle} \tag{7.1}$$

Often, the fuel and water reference temperatures are taken as 15.8°C (60°F), and then specific gravity is equal to $SG\langle 60°\text{F}/60°\text{F}\rangle$. The American Petroleum Industry has developed the *API* gravity scale reading, which can be expressed in terms of specific gravity as

$$API \text{ gravity} = \frac{141.5}{SG\langle 60/60 \rangle} - 131.4 \tag{7.2}$$

API hydrometer readings at temperatures other than 15.8°C (60°F) can be corrected to the reference temperature as

$$API°\langle 60\rangle = \left[0.002\left(60 - \text{observed°F}\right) + 1\right] \times \left[\text{observed } API°\right] \tag{7.3}$$

Note that a fuel having a low specific gravity will have a high *API* reading and vice versa.

Hydrocarbon liquid densities are related to their molecular structure and molecular weight by their carbon atom-to-hydrogen atom ratio. Recall that hydrogen per carbon atom is greatest for paraffin fuels; therefore, these liquids would be lighter such that specific gravity of liquid fuels will range from their lowest value (~0.8) for paraffinic compounds to ~1.0 for naphthenic materials.

Specific gravity is also a convenient means for empirically expressing the heating value of liquid hydrocarbon fuels; see Figure 7.2 and Appendix C.

SI:

Fuel oil	$HHV = 43{,}380 + 93\ (API - 10)$ kJ/kg	(7.4a)
Kerosene	$HHV = 42{,}890 + 93\ (API - 10)$ kJ/kg	(7.4b)
Gasoline	$HHV = 42{,}612 + 93\ (API - 10)$ kJ/kg	(7.4c)
Heavy cracked fuel	$HHV = 41{,}042 + 126 \times API$ kJ/kg	(7.4d)

Engineers:

Fuel oil	$HHV = 18{,}650 + 40\ (API - 10)$ Btu/lbm	(7.5a)
Kerosene	$HHV = 18{,}440 + 40\ (API - 10)$ Btu/lbm	(7.5b)
Gasoline	$HHV = 18{,}320 + 40\ (API - 10)$ Btu/lbm	(7.5c)
Heavy cracked fuel	$HHV = 17{,}645 + 54 \times API$ Btu/lbm	(7.5d)

Note that the greater the percentage of hydrogen in a fuel, the higher the heating value will be since the heating value of hydrogen per unit mass is approximately four times that for carbon. Therefore, fuels with lower specific gravities, i.e., lighter fuels, will generally have greater heating values per unit mass.

EXAMPLE 7.2 The specific gravity of #2 diesel fuel measured at 60°F is found to be 32.5 *API*. For conditions of 75°F, calculate (a) the specific gravity, *API;* (b) the density of the fuel, lbm/ft^3; (c) the higher heating value of the fuel using Equation (7.2a); (d) the higher heating value using Appendix C; and (e) the heating value using Figure 7.2.

Solution:

1. Specific gravity, Equation (7.3):

$$API\langle 60\rangle = 32.5$$

$$API\langle 75\rangle = \frac{32.5}{\left[0.002(60 - 75) + 1\right]} = 33.5$$

2. Density of fuel, from Appendix C, *API* = 33.5 *SG* = 0.8576:

$$\rho_{\text{fuel}}\langle 75°\text{F}\rangle = SG \times \rho_{\text{H}_2\text{O}}\langle 75°\text{F}\rangle$$

from Appendix D, $\rho_{H_2O}\langle 75°F\rangle = 62.253$ lbm/ft^3

b. $\rho_{fuel} = (0.8576)(62.253) = 53.388$ lbm/ft^3

3. *HHV*—from Appendix C:

c. *HHV* = 19,520 + 0.5(40) = 19,540 Btu/Ibm

4. *HHV*, Equation (7.2a):

$$HHV = 18{,}650 + 40(API - 10)$$
$$= 18{,}560 + 40(33.5 - 10)$$

d. *HHV* = 19,590 Btu/Ibm

5. *HHV,* Figure 7.2:

API = 33.5

e. *HHV* = 19,530 Btu/ibm

Every pure compound has a unique liquid-vapor relationship identified by its particular saturation temperature-pressure curve; see Figure 7.3. Recall from thermodynamics that saturation temperature and pressure are dependent properties; that is, for a pure species, any saturation pressure corresponds to a unique saturation temperature. The liquid-to-vapor transition for a pure liquid such as benzene, methyl, or ethyl alcohol will, therefore, occur at the saturation temperature corresponding to its fuel saturation pressure. The energy required to vaporize a liquid fuel prior to combustion is equal to its *latent heat of vaporization.*

A blend of pure liquids, however, will boil off at a more complex rate, which will depend on composition as well as temperature and pressure. The vaporizing characteristic of liquid fuels, expressed as a percent of volume distilled for a fixed total pressure and variable distillation temperature, is referred to as its *volatility.* Volatility curves for several liquid fuels are shown in Figure 7.4. The ASTM has established an atmospheric distillation test to determine the volatility characteristics of liquid fuels. In this test, a sample is placed in a 100-ml flask and thermally distilled by external heating. Fuel begins to vaporize at the fuel initial vaporization, or *bubble point* temperature, and, with further heating, will finally become completely vaporized at the terminating vaporization, or *dew point,* temperature. By collecting and measuring the liquid volume of recondensed vapor during this process, the volatility curve for any liquid fuel can be experimentally determined. The process will not completely distill the original fuel sample chiefly because of the loss of vapor during distillation and/or the presence of impurities, which will remain as residue.

The ASTM distillation test measures fuel volatility in a liquid-vapor fuel atmosphere. Since combustion occurs not in a fuel atmosphere but in a fuel-air environment, additional tests such as the equilibrium air distillation and Reid vapor tests have been developed to measure volatility of liquid fuels in air. In the Reid test, for example, liquid fuel is placed within a chilled fuel sample chamber, which connects below an air chamber having a volume four times that of the fuel sample. The entire unit is assembled along with a pressure gauge attached at the top of the air chamber and immersed in a 38°C (100°F) water bath. The pressure increase, due to heating, creates an air-water-vapor-fuel vapor mixture that is characteristic of fuel vaporization in air for the configuration.

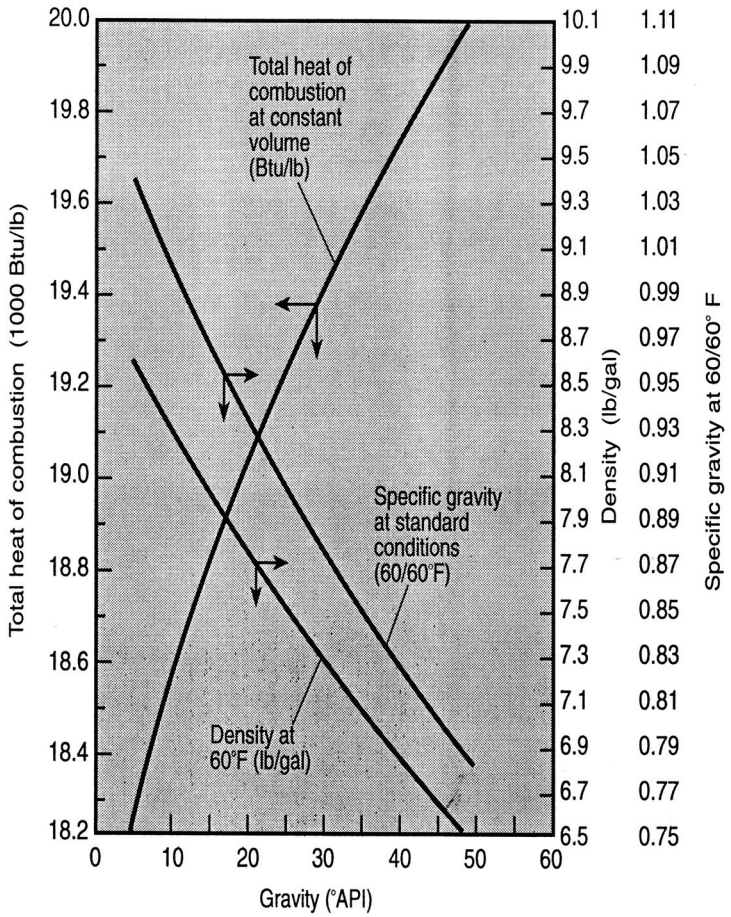

Figure 7.2 Distillate fuel properties as a function of specific gravity. *Source*: *Steam: Its Generation and Use*, Babcock and Wilcox Co., Barberton, Ohio, 1972. With permission.

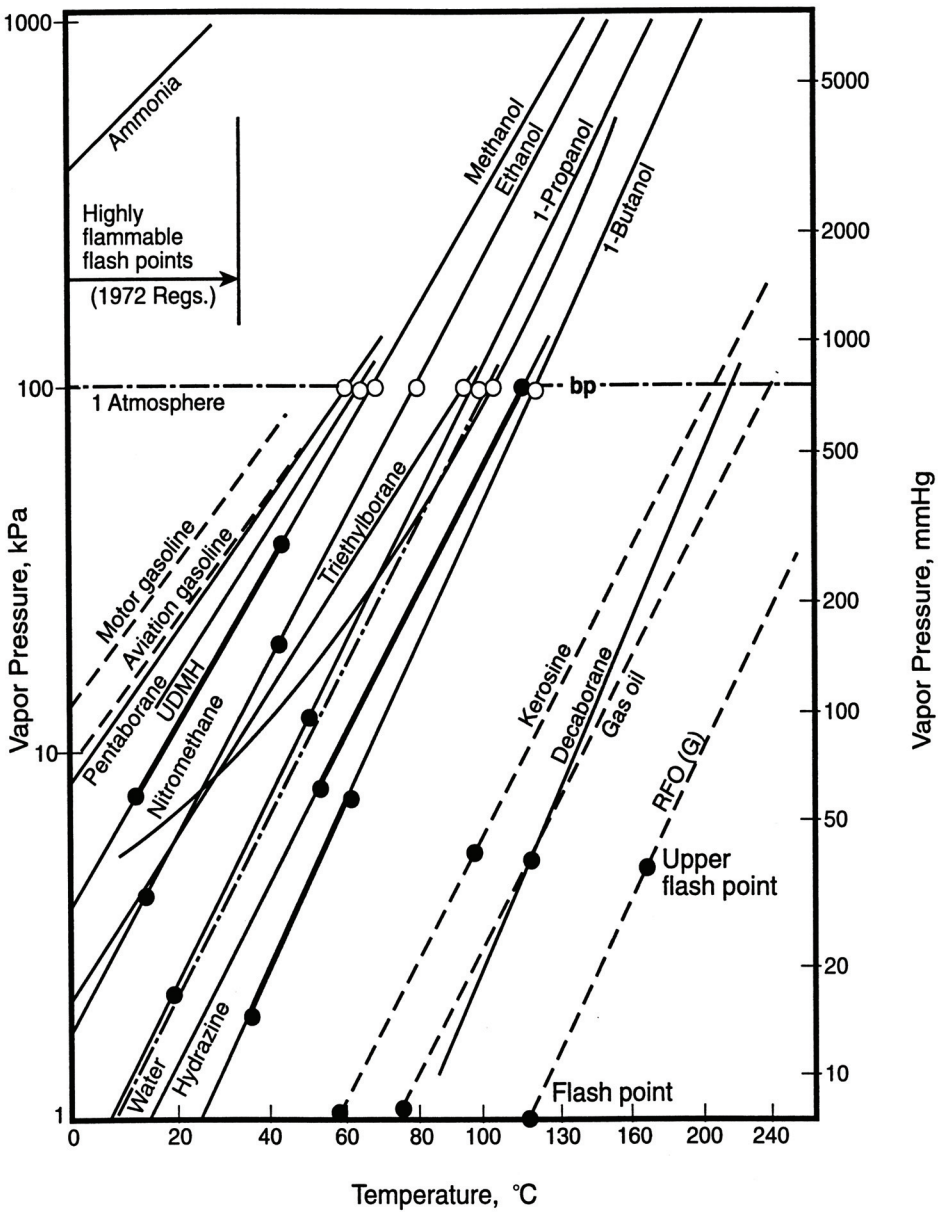

Figure 7.3 Saturation pressure-temperature curves for various petroleum and alternate liquid fuels. *Source*: Goodger, E. M., *Alternate Fuels: Chemical Energy Sources*, Halsted Press, New York, 1980. Reproduced with permission of Palgrave Macmillan.

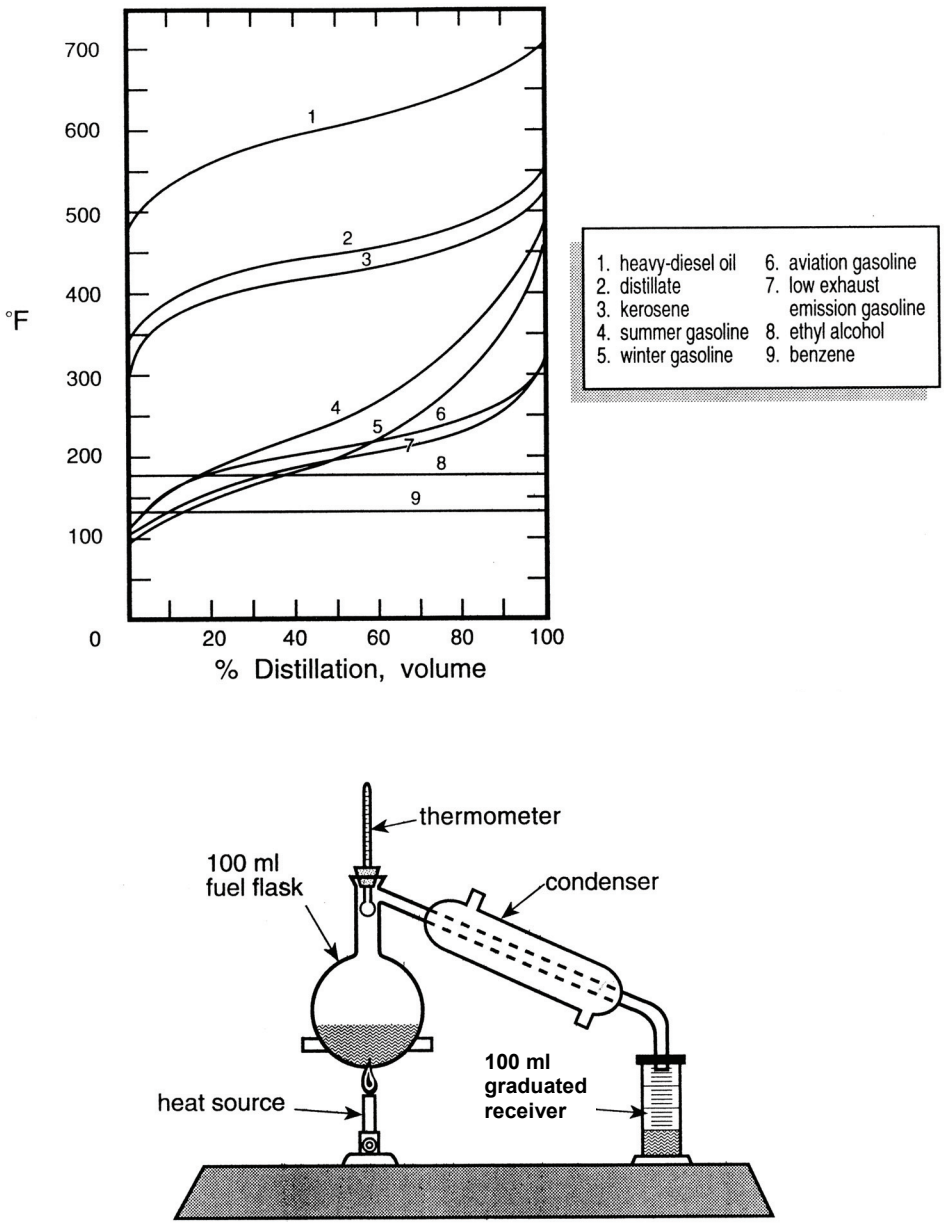

Figure 7.4 Typical ASTM petroleum distillation test facility and distillation curves. Adapted from Taylor, C. F., *The Internal-Combustion Engine in Theory and Practice, Vol. 2: Combustion, Fuels, Materials, Design*, The M.I.T. Press, Cambridge, Massachusetts, 1977. With permission.

Table 7.1 Thermodynamic Properties of Various Hydrocarbon Compounds

Compound		Formula	Molecular weight	API gravity 60°F	Specific gravity 60/60°F	Freezing point °F[a]	Boiling point °F[b]	H_{fg} Btu/lbm[c]
n-Paraffins & Isoparaffins								
Methane	*g*	CH_4	16.04	—	—	–296.5	–258.7	—
Ethane	*g*	C_2H_6	30.07	—	—	–297.8	–127.5	—
Propane	*g*	C_3H_8	44.09	147.0	0.508	–305.8	–43.7	147.1
n-Butane	*g*	C_4H_{10}	58.12	110.8	0.584	–217.0	+31.1	155.8
Isobutane	*g*	C_4H_{10}	58.12	119.8	0.563	–255.3	10.9	141.4
n-Pentane	*ℓ*	C_5H_{12}	72.15	92.7	0.631	–201.5	96.9	157.5
2-Methylbutane	*ℓ*	C_5H_{12}	72.15	94.9	0.625	–255.8	82.1	146.6
n-Hexane	*ℓ*	C_6H_{14}	86.17	81.6	0.664	–139.6	155.7	157.4
2,2-Dimethylbutane	*ℓ*	C_6H_{14}	86.17	84.9	0.654	–147.5	121.5	138.1
n-Heptane	*ℓ*	C_7H_{16}	100.20	74.2	0.688	–131.1	209.2	156.8
2,2,3-Trimethylbutane	*ℓ*	C_7H_{16}	100.20	72.4	0.694	–12.9	177.6	137.5
n-Octane	*ℓ*	C_8H_{18}	114.22	68.6	0.707	–70.2	258.2	156.1
4-Methylheptane	*ℓ*	C_8H_{18}	114.22	68.1	0.709	–185.7	243.9	149.3
2,2,4-Trimethylpentane	*ℓ*	C_8H_{18}	114.22	71.8	0.696	–161.3	210.6	132.2
n-Nonane	*ℓ*	C_9H_{20}	128.25	64.5	0.722	–64.5	303.4	155.7
2,2,4,4-Tetramethylpentane	*ℓ*	C_9H_{20}	128.25	63.9	0.724	–87.8	252.1	127.8
n-Decane	*ℓ*	$C_{10}H_{22}$	142.28	62.3	0.730	–22	345	155
n-Dodocane	*ℓ*	$C_{12}H_{26}$	170.33	57.5	0.749	15	421	110
n-Tetradecane	*ℓ*	$C_{14}H_{30}$	198.38	54.0	0.763	+42	484	154
n-Hexadecane	*ℓ*	$C_{16}H_{34}$	226.43	51.5	0.774	65	536	154
n-Pentatriacontane	*ℓ*	$C_{35}H_{72}$	492.93	49.5	0.781	176	628	—

Olefins								
Ethylene	*g*	C_2H_4	28.05	—	—	–272.5	–154.7	—
Propylene	*g*	C_3H_6	42.08	139.6	0.522	–301.5	–53.9	—
Isobutene	*g*	C_4H_8	56.10	104.3	0.600	–220.6	+19.6	157.7
Pentene	*ℓ*	C_5H_{10}	70.13	87.5	0.646	–265.4	86.0	—
Hexene	*ℓ*	C_6H_{12}	84.16	77.2	0.678	–218	146.4	—
Octene	*ℓ*	C_8H_{16}	112.21	65.0	0.720	–152.3	250.3	158.0
Hexadecene	*ℓ*	$C_{16}H_{32}$	224.42	49.2	0.783	+39	527	—
Naphthenes								
Cyclopentane	*ℓ*	C_5H_{10}	70.13	57.2	0.750	–136.8	120.7	174.7
Cyclohexane	*ℓ*	C_6H_{12}	84.16	49.2	0.783	+43.8	177.3	168.8
Ethylcyclohexane	*ℓ*	C_8H_{16}	112.21	47.1	0.792	–168.3	269.2	155.1
Aromatics								
Benzene	*ℓ*	C_6H_6	78.11	28.4	0.885	+42.0	176.2	186.3
Toluene	*ℓ*	C_8H_{10}	106.16	28.4	0.885	–13,3	282,9	165.8
Alcohols								
Methyl	*ℓ*	CH_3OH	32.0	47.2	0.792	–144	149	502
Ethyl	*ℓ*	C_2H_5OH	46.0	48.8	0.785	–179	172	396
Propyl	*ℓ*	C_3H_7OH	60.0	45.6	0.799	—	208	295
Butyl	*ℓ*	C_4H_9OH	74.1	44.2	0.805	+26	244	254
Acetylene	*g*	C_2H_2	26.04	—	—	+114	+114	—

Source: Most of these data were obtained from "Selected Value of Properties of Hydrocarbons," National Bureau of Standards, Circular C461, API Research Project 44.

[a]In air, 1 atm.

[b]At 1 atm.

[c]Latent heat of fuel at constant pressure, 77°F.

Volatility characteristics of a liquid fuel will affect its suitability in particular combustion systems. Some of the more general combustion factors associated with volatility include:

Potential evaporative fuel loss during storage
Potential fire hazard associated with highly volatile fuels
Proper fuel-air preparation requirements prior to combustion, i.e., atomization, and distribution
Ambient influences on fuel volatility, i.e., cold start limitations, potential vapor lock

The *flash point* temperature, a measure of the lean ignitable limit for a fuel vapor-air mixture formed above a liquid fuel, is important in relation to the potential hazards of handling flammable fuel vapors. On the other hand, the *spontaneous ignition* temperature is the minimum temperature to which a fuel vapor-air mixture must be heated in order to promote combustion without an external ignition source. This temperature is much greater than the flash point temperature of a fuel and, for hydrocarbon fuels, is generally within the ranges of 260–116°C (500–700°F). The *cloud point* is the temperature at which, when a fuel is cooled, a hazy or waxy crystallization begins to appear in the fuel. The *pour point temperature* measures the lowest temperature to which a fuel can be cooled without impeding the free flow of liquid, while the *freezing point* is the state at which a fuel is completely frozen. Liquid fuel properties are found in Table 7.1.

Viscosity, a measure of fluid resistance to internal shearing, is an important property that influences pumping, lubricity, and atomization characteristics of liquid fuels. Viscosity is also a major factor in selecting suitable lubricating oils. The SAE has established a worldwide viscosity numbering system for both lubricating and transmission oils.

Additional conditions of liquid fuels, such as impurities, oxidation stability, and combustion residue, are also important in assessing their nature during combustion. For example, trace amounts of materials such as ash, sulfur, water, and metals like vanadium can influence or even limit use of liquid fuels unless they do not exceed defined concentrations. *Carbon residue*, for example, provides a means of quantifying the carbon-forming propensities of liquid fuels on fuel nozzles.

Table 7.2 Major Liquid Distillate Fuels Derived from a Barrel of Crude Petroleum

Distillation product	Principal hydrocarbon families	Number of carbon atoms	% of barrel
Gasoline	Paraffins, aromatics, naphthenes	C_4–C_{10}	44
Kerosene	″	C_{10}–C_{13}	5
Distillate fuel oil	″	C_{13}–C_{18}	24
Lubricating oil	″	C_{18}–C_{45}	2
Residual fuel oil	Aromatics, naphthenes, other very complex compounds	C_{45}	9
Asphalt and refinery fuel			16

Source: *Steam: Its Generation and Use*, 37th Edition, Babcock & Wilcox Co., Barberton, Ohio,1963. With permission.

7.3 CRUDE OIL AND DISTILLATE FUELS

The world's most prominent natural liquid fuel resources are found within *crude oil*; see Table 7.2. Crude oil, or *petroleum,* was originally marine life, which has been converted over time, much like coal, into a mixture of various hydrocarbon compounds. Petroleum reserves are located within nonhomogeneous underground pools containing a variety of compounds that, depending on location, can range from heavy tarlike components to gases. Most petroleum, however, on a mass basis, consists chiefly of the following elements:

Element	Mass fraction, %
Carbon	84–87
Hydrogen	11–14
Sulfur	0–2
Nitrogen	0–0.2

The geographical location of oil reserves, such as those found in the Middle East, has played a major role in the recent history of modern civilization. Current projected decline in oil resources along with the growing worldwide demand for more fuel oil and refined products necessitates efforts to (1) increase the yield of existing oil fields using enhanced recovery techniques; (2) explore and discover new fields, such as those found offshore; and (3) successfully commercialize alternative natural petroleum resources, such as tar sands and oil shale.

Only a small percentage of crude petroleum can be directly used as natural liquid fuels; but through further chemical processing, or *refining,* crude petroleum can yield a variety of useful fuels as well as several nonfuel products, such as greases, lubricants, and other petrochemical by-products. Any refined fuel oil or *distillate* fuel produced by a refinery will actually be a blend of many different inorganic compounds. For example, gasoline, which is not a single chemical compound but rather a blend of over 50 different identifiable hydrocarbon compounds, is often written chemically as C_xH_y. Often a single major constituent, such as isooctane C_8H_{18}, is used in thermodynamic calculations to approximate the energy characteristics of gasoline.

Any hydrocarbon compound, as with all pure chemical species, has a specific boiling curve. Recall saturation pressure is a unique function of saturation temperature. For hydrocarbons, boiling point temperatures generally increase with the number of carbon atoms in the compound; i.e., lower molecular weight components will boil at lower temperatures, followed at higher temperatures by heavier constituents. Major distillate fuels from crude can be classified by their volatility and, in order of increasing boiling point temperature, are:

Low molecular weight hydrocarbons
Gasolines
Naphthas
Kerosenes

Diesel fuels
Lubricating oils
Residuals

A major step in the refining of crude is thermal separation, which is achieved in the fractionating distillation tower, illustrated in Figure 7.5. Crude, after pretreatment to remove gross impurities, is heated to 927ºC (700ºF), then passed through the tower for component separation by boiling at atmospheric pressure (*atmospheric distillation*). A thermal gradient is maintained along the tower so that higher temperatures are at the bottom and lower temperatures are at the top of the unit. Compounds boil off in a specific temperature range and major products are thus separated by condensing vapors at different tower locations. In the column, the hydrocarbon vapors with the lowest boiling points – propane and butane – rise and flow out the top in the overhead stream. The straight run gasoline, kerosene, and diesel fuel cuts are drawn off at successively lower sidestream positions in the tower. Hydrocarbons with boiling points higher than diesel fuel are not vaporized. They remain in liquid form and flow out the bottom of the tower as atmospheric residue.

The atmospheric distillation yield is determined solely by the quantity of hydrocarbons condensed within each particular boiling range. Atmospheric distillation cannot produce additional amounts of particular product for meeting demands of a changing marketplace, such as more gasoline. In addition, the quality requirements for particular fuels, such as automotive, diesel, aviation, and fuel heating oils, cannot be met by atmospheric thermal distillation of crude oil. Additional refining of thermally partitioned crude is necessary to provide products that will meet these particular fuel usage specification characteristics.

EXAMPLE 7.3 Gasoline can be represented by the formula C_8H_{16}. Determine (a) *AF* ratio and *FA* ratio for the stoichiometric combustion of gasoline and air on a molar basis; (b) repeat part (a) on a mass basis; and (c) calculate the gravimetric and mole fractions for the stoichiometric reactants of gasoline and air.

Solution:

1. Stoichiometric reaction:

$$C_8H_{16} + aO_2 \rightarrow bCO_2 + cH_2O$$

Carbon atom balance:

$$b = 8$$

Hydrogen atom balance:

$$2c = 16 \qquad c = 8$$

Oxygen atom balance:

$$2a = 16 + 8 \qquad a = 12$$

$$C_8H_{16} + 12[O_2 + 3.76N_2] \rightarrow 8CO_2 + 8H_2O + (12)(3.76)N_2$$

2. Molar *AF* and *FA* ratios:

a. $$\overline{AF} = \frac{(12)(4.76)\text{ moles air}}{1.0\text{ mole fuel}} = 57.12$$

$$\overline{FA} = (57.12)^{-1} = 0.0175$$

3. Mass *AF* and *FA* ratios:

b. $$AF = \frac{(12)(4.76\text{ moles air})(28.96\text{ lbm/lbmole air})}{(1.0)(96 + 16)\text{lbm fuel}} = 14.770$$

$$FA = (14.770)^{-1} = 0.0677$$

4. Fuel-air mole fraction analysis:

c. $$\bar{x}_{C_8H_{16}} = \frac{1}{1.0 + (12)(4.76)} = 0.0172 \text{ or } 1.72\%$$

$$\bar{x}_{O_2} = \frac{12}{58.12} = 0.2065 \text{ or } 20.65\%$$

$$\bar{x}_{N_2} = \frac{(12)(3.76)}{58.12} = 0.7763 \text{ or } 77.63\%$$

5. Fuel-air gravimetric analysis:

i	$\bar{x}_i$	MW_i	$\bar{x}_i MW_i$	mf_i
C_8H_{16}	0.0172	112.0	1.9264	0.0636
O_2	0.2065	32.0	6.6080	0.2183
N_2	0.7763	28.0	21.7364	0.7181
	$\frac{\text{lbmole}_i}{\text{lbmole}_{tot}}$	$\frac{\text{lbm}_i}{\text{lbmole}_i}$	$\frac{\text{lbm}_i}{\text{lbmole}_{tot}}$	$\frac{\text{lbm}_i}{\text{lbm}_{tot}}$

$$MW = \Sigma \bar{x}_i MW_i = 30.271 \text{ lbm/lbmole}$$

where, for example,

$$mf_i = \bar{x}_i\, MW_i / MW$$

$$mf_{C_8H_{16}} = \frac{1.9264}{30.271} = 0.0636$$

An initial technique used for producing additional hydrocarbon fuel constituents, such as gasoline, was *cracking*, i.e., breaking larger molecules into smaller species. *Thermal cracking* is a high-temperature [540°C (1,000°F)] and high-pressure [6,870–10,306 kPa (1,000–1,500 psi)] conversion process in which higher boiling hydrocarbons are broken down into lower boiling hydrocarbons. In the early 1900s this method was used to treat the atmospheric distillation residue in order to increase the gasoline fraction yield from crude. Thermally cracked gasoline contains a lot of olefins that have higher octane number than straight run gasoline but are unstable and can oxidize causing engine deposits (gums). By today's standards, the quality and performance of early thermal cracked gasoline was low, but sufficient for the engines of that day.

Initially there was no market for the higher boiling material produced by atmospheric distillation. Atmospheric residue was used for paving and sealing. Later it was found that it could yield higher value products like lubricating oil and paraffin wax when further distilled in a vacuum. *Visbreaking*, another form of thermal cracking, reduces the viscosity of extra heavy vacuum residues using heat and mild pressure. The main product of visbreaking is a lower viscosity residue. Naphtha and gasoil are also produced as side products. It is an economically viable method for converting a portion of excess fuel oil into more profitable distillate.

Coking is a thermal cracking process used to convert vacuum residues and petroleum tars into lighter products and coke. Coke cracking processes produce some amounts of gasoil. The properties of these gasoil streams are not very good of themselves, but are used as blending components in the overall refinery process. Two coking processes are utilized today, *delayed coking* and *fluid coking*.

Catalytic cracking has become the preferred method for breaking larger molecules in most modern refineries. Catalytic cracking is a lower-temperature and lower-pressure conversion process used for gasoline production (not for diesel fuel). A catalyst such as aluminum silicate (zeolite) is used to produce a gasoline of higher quality than thermal cracking. Because of its greater yield, improved product quality, and superior economics catalytic cracking has superseded conventional thermal cracking for gasoline. There are many variations on catalytic cracking, fixed, moving, and fluidized bed; but *fluidized bed catalytic cracking* is the main process for gasoline production in most modern refineries. *Catalytic reforming* utilizes a catalyst such as platinum to increase the antiknock properties of gasoline.

Hydrocracking is similar to catalytic cracking in that it utilizes a catalyst, but the catalyst operates in a hydrogen atmosphere. It is necessary to produce the cracking hydrogen atmosphere using steam reforming of natural gas (methane) or other light hydrocarbons (such as LPG or naphtha) since the process hydrogen requirement is substantial. Hydrocracking can break down hydrocarbons that are resistant to catalytic cracking alone. Cracking done in a hydrogen gas atmosphere, or *hydrogenation,* allows unsaturated hydrocarbon compounds to pick up additional hydrogen atoms to become saturated. The presence of hydrogen saturates the olefins produced from the cracking processes. It is more commonly used to produce diesel fuel than gasoline. Hydrocracking is used to upgrade heavy vacuum distillates to very good quality gasoil streams. Hydrocrackers are operating at very high pressures [up to 2,070 kPa (3,000 psi)] and temperatures [427°C (800°F)].

Specific secondary refining processes can combine smaller hydrocarbon molecules and compounds to produce larger ones, i.e., *polymerization:*

$$a\mathrm{C_3H_6} + b\mathrm{C_2H_6} + c\mathrm{C_2H_4} + d\mathrm{CH_4} \overset{T,P}{\rightleftarrows} \mathrm{C_3H_8}$$

Lighter members of particular hydrocarbon families can be reformed by *alkylation* to yield heavier compounds of another family. For example, light olefins and isoparaffins can combine to form higher molecular weight isoparaffins. Natural crude oil vapors can be combined with kerosene or light fuel oil by *absorption* to yield additional species. Precipitation of heavier compounds formed by absorption yields natural gasoline, while compression of lighter fractions produces *liquid petroleum gas* (LPG).

$$\mathrm{C_{12}H_{26}} \overset{T,P}{\rightleftarrows} e\mathrm{C_5H_{12}} + f\mathrm{C_4H_8} + g\mathrm{C_3H_6}$$

Crude oil refineries have changed through the years in response to changing market demands and shifts in crude resources being processed. For example, U.S. refineries initially were more concerned with producing kerosene from American reserves; gasoline was an unwanted by-product. Today, gasoline is a major product of refining, and crude oil from all parts of the world is used as feedstock. By blending various streams mentioned previously, a refinery can more successfully meet specific fuel requirements. The complex modern oil refinery allows crude oil to be distilled (*separated*); to be altered structurally to produce different molecules (*converted);* to be changed molecularly while retaining the general boiling range *(upgraded);* to be processed to remove contaminants such as sulfur, nitrogen, and oxygenated species (*hydrotreated*); and to be combined (*blended*) in various refinery fractions to yield a particular product.

A simplified schematic layout of a refinery is shown in Figure 7.5. Crude oil is fed to the fractionation distillation column tower where straight run light and heavy naphtha, jet, and diesel are separated at atmospheric pressure. Straight run jet and diesel are usually acceptable as they are, but the straight run naphthas require more processing to convert them into gasoline blending components. The straight run light naphtha may be isomer-ized to increase octane, or hydrotreated to convert benzene into cyclohexane so that the final gasoline blend will meet a benzene specification limit, or both. The straight run heavy naphtha is hydrotreated to remove sulfur and then reformed to improve octane and generate hydrogen for the hydrotreaters.

Gasolines are crude oil constituents that boil in the 30–200°C (85–390°F) range and are used chiefly as spark-ignition engine fuels. These refinery products must be compatible with many different types of spark-ignition engines, ranging from automotive to aviation machinery, and are required to burn in a variety of conditions, ranging from summer to winter environments. Straight run gasolines contain 5–8 carbon atoms per molecule, have a large percentage of paraffins, and are poor-quality spark-ignition engine fuels. Additional and upgraded gasoline supplies come from the refinery as a blend of straight run gasolines, cracked gasolines (often formed in the presence of hydrogen), and/or reformed gasolines (often catalytically processed in the presence of platinum).

Naphthas are crude oil constituents that distill in the 95–315°C (200–600°F) range. The major use of these refinery by-products, which distill between gasoline and kerosene range, is not as fuels but rather as a feedstock for producing industrial solvents.

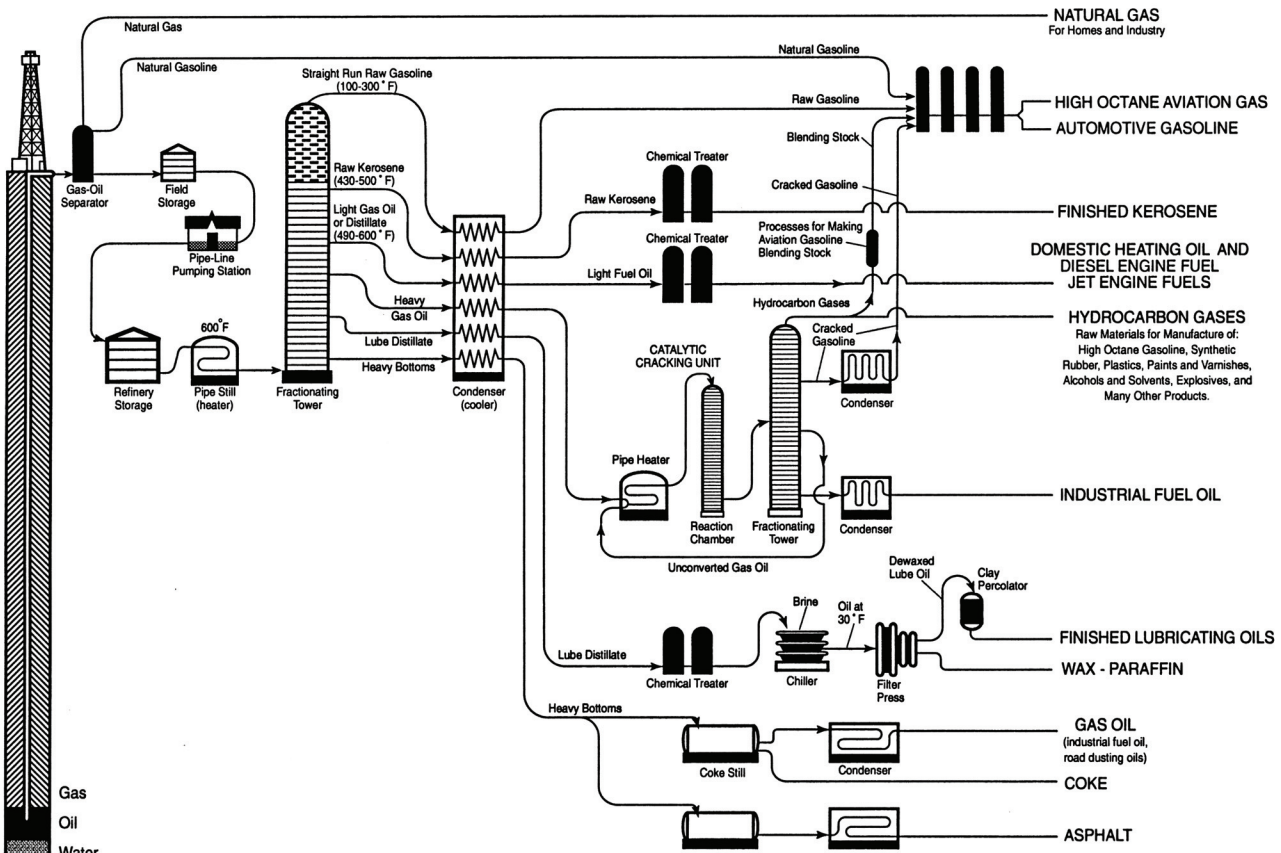

Figure 7.5 Simplified petroleum distillation refinery schematic. Reproduced courtesy of the American Petroleum Institute.

Kerosenes, crude oil constitutents that boil in the 140–250°C (285–481°F) range, are used mainly as a burning oil in lamps, heaters, and stoves. Kerosene is a colorless hydrocarbon blend consisting of from 12–16 carbon atoms per molecule having a higher percentage of hydrogen per molecule and a greater heating value; it is lighter than gasoline. Burning oil-kerosene blends, often represented thermodynamically as dodecane, $C_{12}H_{26}$, are high in paraffins with smaller percentages of naphthalenic and aromatic constituents. Power kerosenes are higher in aromatics and can be approximated by tridocane, $C_{13}H_{28}$. A gas turbine fuel, such as JP5, is an example of a straight power kerosene distillate fuel, while JP4 is an example of a gasoline-kerosene gas turbine fuel blend.

Diesel fuels, distillate fractions that boil in the range 240–370°C (465–700°F), are used primarily in compression-ignition internal combustion engines. The diesel is a broad-cut fuel combustion engine and, depending on engine size, speed, and load, can burn fuels that fall between kerosenes and heavy residuals. In general, high-speed automotive-type diesels require light kerosene-type distillates, medium-speed diesels use fuel oil-grade distillate, while low-speed marine engines can burn heavy residual fuels. Various diesel fuel grades have been established that reflect the stringent flash point, viscosity, sulfur, ash, and moisture fuel quality limits set for distillates used in compression-ignition engines.

Fuel oil, or oil burner fuel, consists of crude oil fractions that boil in the 340-420°C (640–590°F) range. Six grades of fuel oil have been established covering the requirements of atomization, smoke, and heat release of various burner fuels. The larger the fuel oil's specific gravity for a fixed boiling point temperature, the greater will be the concentration of condensables, such as naphthenes, aromatics, and melting compounds, whereas a lower specific gravity implies higher percentages of open-chained paraffins. For example, fuel oils #1 and #2 are light and medium domestic fuel oils, respectively, while #6 (termed Bunker C) is a heavy residual oil that requires preheating to burn properly. Heavy fuel oils and diesel fuels are similar and consist of hydrocarbons with 12 to 16 or more carbon atoms per molecule. Some of the general thermodynamic properties of major distillate fuels are found in Table 7.3.

Today, refineries squeeze as much high value product as possible from every barrel of crude. Previously, vacuum residue might have been used as low value, high sulfur fuel oil for power generation or marine fuel, i.e., bunker. As a result, the vacuum residue is sent to a residue conversion unit, such as a residue cracker, solvent extraction unit, or coker. These units produce more transportation fuel or gasoil, leaving an irreducible minimum amount of residue or coke. The residue-derived streams require further processing and/or treating before they can be blended into light fuels like gasoline or diesel. The economics and energetics of petroleum refining are considered in detail in chemical and petroleum fuel engineering.

Table 7.3 Thermodynamic Properties of Major Distillate Fuels

	SG		T_{boil}		Heat of vaporization		
Gasoline	60	138	280	270	75,250	116	715
Naptha	40	171	340	240	6,690	103	670
Kerosene	30	227	440	200	5,575	86	595
Fuel oil	*API*	304	580	156	4,350	67	490
		C	°F	kJ/kg	kJ/m^3	Btu/lbm	Btu/gal

	Gasoline	Kerosene	Diesel	Fuel oil
API @ 60°	54–72	50–35	47–11	42–19
Specific gravity	0.70–0.78	0.78–0.85	0.80–0.99	0.815–0.940
Proximate analysis				
% carbon	84–86	85–88	85.7–84.9	86.1–85.0
% hydrogen	16–14	15–12	13.4–11.5	13.1–12.7
% sulfur	0.3	0.5	6.9–4.6	0.1–2.3
HHV = kJ/kg	46,520–48,265	45,125–46,985	43,030–46,520	46,100–42,565
Btu/lbm	20,000–20,750	19,400–20,200	18,500–20,000	19,818–18,300
Approximate chemical formula	C_8H_{16}	$C_{11.6}H_{23.2}$	$C_{12}H_{26}$	—

Source: National Bureau of Standards, Misc. Pub. 97, 1929, 34.

EXAMPLE 7.4 A fuel oil having the ash and moisture-free analysis below is used in an oil-fired boiler. The dry analysis of the exhaust gases was measured and found to be as listed below:

Reactant analysis			Product analysis	
Fuel oil constituent	Gaseous component	Percentage	Gaseous component	Percentage
C_S	CO_2	87.0%	CO_2	11.2%
H_2	CO	12.0%	CO	2.2%
N_2	O_2	0.2%	O_2	4.1%
S	N_2	0.2%	N_2	82.5%
O_2		0.6%		

For these conditions, calculate (a) the mass of dry flue gas, lbm/lbm fuel; (b) the mass of air supplied, lbm/lbm fuel; (c) the air required for ideal complete combustion, lbm/lbm fuel; and (d) the percent excess air supplied, %.

Solution:

1. Fuel molar analysis:

i	mf_i	MW_i	mf_i/MW_i	$\bar{x}_i$
C	0.870	12.0	0.07250	0.5459
H_2	0.120	2.0	0.06000	0.4517
N_2	0.002	28.0	0.00007	0.0005
S	0.002	32.0	0.00006	0.0005
O_2	0.006	32.0	0.00019	0.0014
	$\frac{\text{lbm}_\text{i}}{\text{lbm}_\text{tot}}$	$\frac{\text{lbm}_i}{\text{lbmole}_i}$	$\frac{\text{lbmole}_i}{\text{lbm}_\text{tot}}$	$\frac{\text{lbmole}_i}{\text{lbmole}_\text{tot}}$

$$\sum \frac{mf}{MW}\Big)_i = 0.07250 + 0.0600 + 0.00007 + 0.00006 + 0.00019$$

$$= 0.13282 \ \text{lbmole}_\text{tot} / \text{lbm}_\text{tot}$$

$$MW = \left(\sum \frac{mf}{MW}\right)_i^{-1} = (0.13282)^{-1} = 7.529 \ \text{lbm/lbmole}$$

2. Actual combustion equation:

$$[0.5459C_S + 0.4517H_2 + 0.0005N_2 + 0.0005S + 0.0014O_2] + a[O_2 + 3.76N_2] \rightarrow bH_2O + cSO_2 + d[0.112CO_2 + 0.022CO + 0.041O_2 + 0.825N_2]$$

Carbon atom balance:

$0.5459 = (0.112 + 0.022)d$ $\quad d = 4.074$

Hydrogen atom balance:

$(2)(0.4157) = 2b$ $\quad b = 0.4157$

Nitrogen atom balance:

$(2)(0.0005) + (2)(3.76)a = (2)(0.825)(4.074)$

$a = 0.894$

Sulfur atom balance: $\quad c = 0.0005$

Oxygen atom balance: $\quad (0.0014)(2) + (2)(0.894) = 1.790$

$0.4157 + (2)(0.0005) + 4.044\ (0.228 + 0.021 + 0.084) = 1.790$

3. Molecular weight dry flue gas:

$$MW = (0.112)(44) + (0.022)(28) + (0.041)(32) + (0.825)(28)$$
$$= 29.96 \text{ lbm/lbmole}$$

4. Mass dry flue gas/mass fuel:

$$= \left[\frac{(4.074 \text{ lbmole gas})}{(1.0 \text{ lbmole fuel})}\right] \times \left[\frac{(29.96 \text{ lbm/lbmole gas})}{(7.529 \text{ lbm/lbmole fuel})}\right]$$

a. $\dfrac{m_g}{m_f} = 16.21$ lbm gas/lbm fuel

5. Actual mass air/fuel ratio:

$$AF_a = \left[\frac{(0.894)(4.76) \text{ lbmoles air}}{(1 \text{ lbmole fuel})}\right] \times \left[\frac{(28.96 \text{ lbm/lbmole air})}{(7.529 \text{ lbm/lbmole fuel})}\right]$$

b. $AF_a = 16.37$ lbm air/lbm fuel

6. Stoichiometric reaction:

$$[0.5459C_S + 0.4517H_2 + 0.0005N_2 + 0.0005S + 0.0014O_2] + aO_2 \rightarrow bCO_2 + cH_2O + dSO_2$$

Carbon atom balance: $\quad b = 0.5459$

Hydrogen atom balance:

$(2)(0.4517) = (2)c$ $\qquad c = 0.4517$

Sulfur atom balance: $\qquad d = 0.0005$

Oxygen atom balance:

$(2)(0.0014) + 2a = (2)(0.5459) + 0.4517 + (2)(0.0005)$

$a = 0.771$

7. Stoichiometric mass air/fuel ratio:

c. $$AF_s = \frac{(0.771)(4.76)(28.96)}{(1.0)(7.529)} = (14.12) \text{ lbm air/lbm fuel}$$

8. Percent excess air:

$$\% = \frac{(0.894 - 0.771)(4.76)}{(0.771)(4.76)} = 16.0\%$$

7.4 SYNTHETIC LIQUID FUELS

Crude oil has been the major resource base for producing a variety of primary liquid fuels for use in boilers and heaters, as well as internal and external combustion engines. Projected crude oil shortfalls and the ensuing cost of using these finite resources may cause industrial nations to look seriously in the near future for acceptable long-term replacement liquid fuel options. At present, combustion machinery such as the spark-ignition engine is being designed to burn specific liquid petroleum-based fuels. In the future, these engines will be required to burn not only those fuels more efficiently but fuel alternatives as well. Synthetic fuels are manufactured, or processed, non petroleum-based liquid fuels that potentially can substitute for petroleum-derived fuels. Fuel alternatives are then all the various acceptable liquid fuels derived from naturally occurring or synthetically derived crudes available for use; see Table 7.4. Fuel alternates should provide performance equivalent to that by the primary fuel in a particular application. The various fuel alternates may not be used at present, in part, because of logistic and/or economic considerations.

From Chapter 6, coal was seen to have several characteristics that make it somewhat unsuitable for direct use as a mobility fuel; for example, it exists naturally as a solid, it has a low H:C ratio (approximately 0.9:1 for coal versus 2:1 for crude oil), and it has high concentrations of moisture, ash, sulfur, and nitrogen. The large known U.S. reserves of coal, however, could make it a logical candidate for consideration in producing synthetic liquid fuels, i.e., *syncrudes.* To produce a useful synoil from coal, any successful conversion must however show favorable economics; use minimal non-oil energy input; increase H:C ratio; reduce mineral, sulfur, and nitrogen content; and break down coal molecularly to allow carbon-hydrogen atoms to be restructured to yield a suitable liquid.

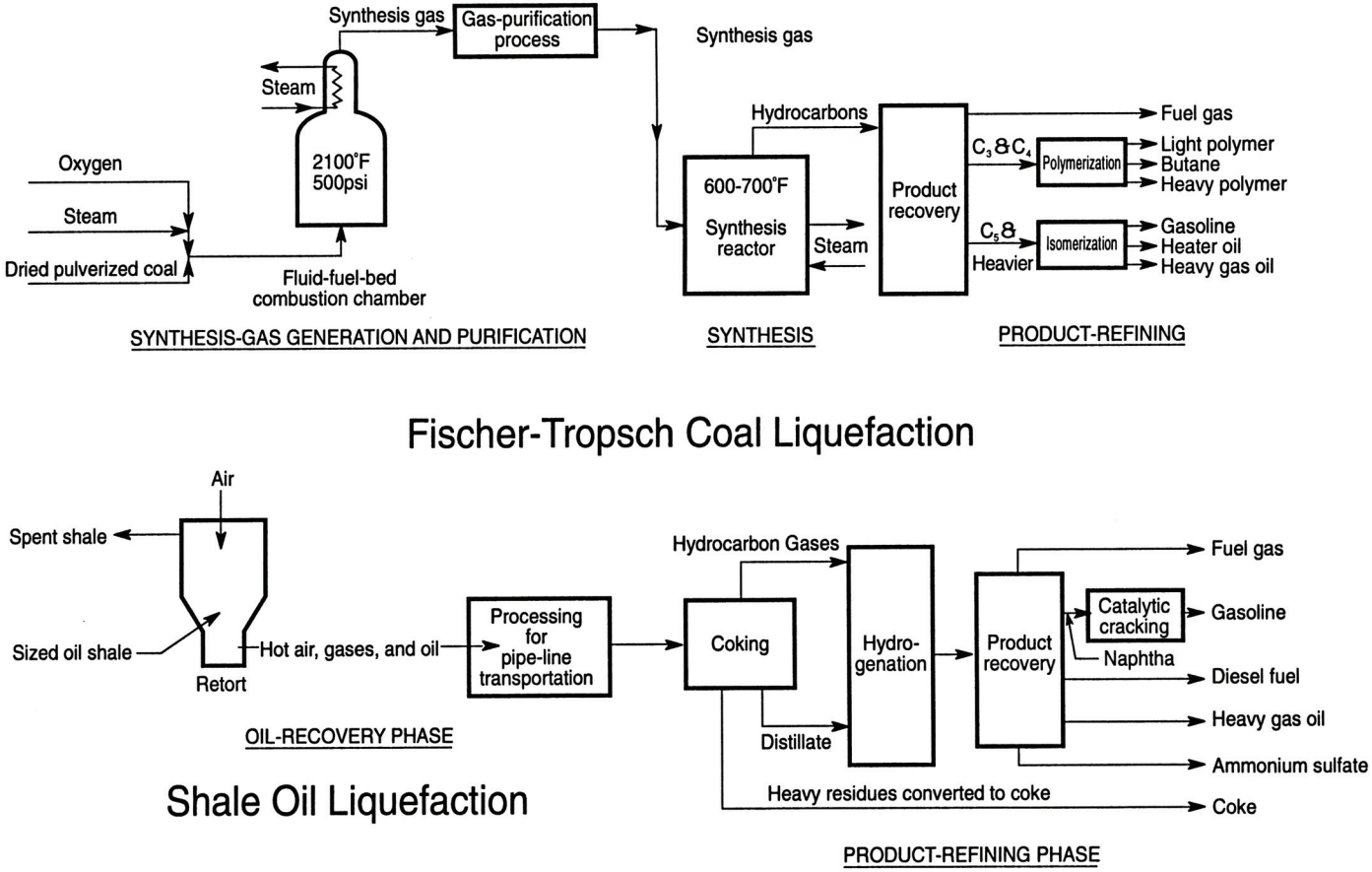

Figure 7.6 Synthetic liquid fuel recovery from coal and shale oil.

Table 7.4 Simplified Synthetic Fuel Processes

(Δ = HEAT, CAT = CATALYST, H_2 = HYDROGEN)

COAL:	
Direct	$\text{COAL} \xrightarrow[\Delta,\ (\text{CAT})]{H_2} \text{COAL LIQUIDS} \xrightarrow[\Delta,\ \text{CAT}]{H_2} \text{SYNCRUDE} \xrightarrow[\text{REFINERY}]{} \text{PRODUCTS}$
Indirect (Gasification)	$\text{COAL} \xrightarrow[\Delta]{H_2O} \underset{(\text{SYNGAS})}{\text{CO} + \text{H}} \xrightarrow[\Delta,\text{CAT}]{} \text{INDIRECT LIQUIDS} \xrightarrow{\text{PURIFY}} \text{PRODUCTS}$
Pyrolysis	$\text{COAL} \xrightarrow[\Delta]{} \begin{matrix}\text{LIQUIDS}\\ + \text{COKE}\downarrow\end{matrix} \xrightarrow[\Delta,\ \text{CAT}]{H_2} \text{SYNCRUDE} \xrightarrow[\text{REFINERY}]{} \text{PRODUCTS}$
SHALE:	$\text{OIL SHALE} \xrightarrow[\Delta]{} \text{RAW SHALE OIL} \xrightarrow[\Delta,\ \text{CAT}]{H_2} \text{SYNCRUDE} \xrightarrow[\text{REFINERY}]{} \text{PRODUCTS}$
TAR SANDS:	
Near-Surface	$\begin{matrix}\text{TAR SAND}\\ \text{ORE}\end{matrix} \xrightarrow[\text{EXTRACT}]{} \text{TAR} \xrightarrow[\text{REFINERY}]{} \text{PRODUCTS}$
Deep	$\begin{matrix}\text{TAR SAND}\\ \text{RESERVOIR}\end{matrix} \xrightarrow[\text{WELLS},\ \Delta]{} \text{TAR} \xrightarrow[\text{REFINERY}]{} \text{PRODUCTS}$

Source: United States Synthetic Fuels Corporation.

Coal is well suited for direct combustion in stationary power applications, and pulverized coal-liquid slurries have been proposed as a method of transporting coal from the mine to the utility site, where it could be separated and burned in coal-fired boilers. Another use for coal slurry would be to burn the entire mixture directly in residual fuel oil-fired boilers. Coal slurries such as coal-oil, coal-water, and/or coal-alcohol mixtures, with as high as 40–75% coal by weight, have been burned in suitable oil burners. Burning coal-oil mixtures as a substitute liquid fuel could be a means of stretching oil reserves at certain existing oil-fired power plants as well as postponing their replacement with either a new coal or nuclear unit. However, oil-fired burner specifications and coal slurry properties do result in several adverse interface characteristics, including a need for additives due to settlement and separation of coal in nonhomogeneous slurry mixtures, increased burner abrasion, stack sooting when burning coal slurries, a reduction in heat rate of oil-fired units burning coal-liquid slurries, and change in pollution characteristics of the configuration.

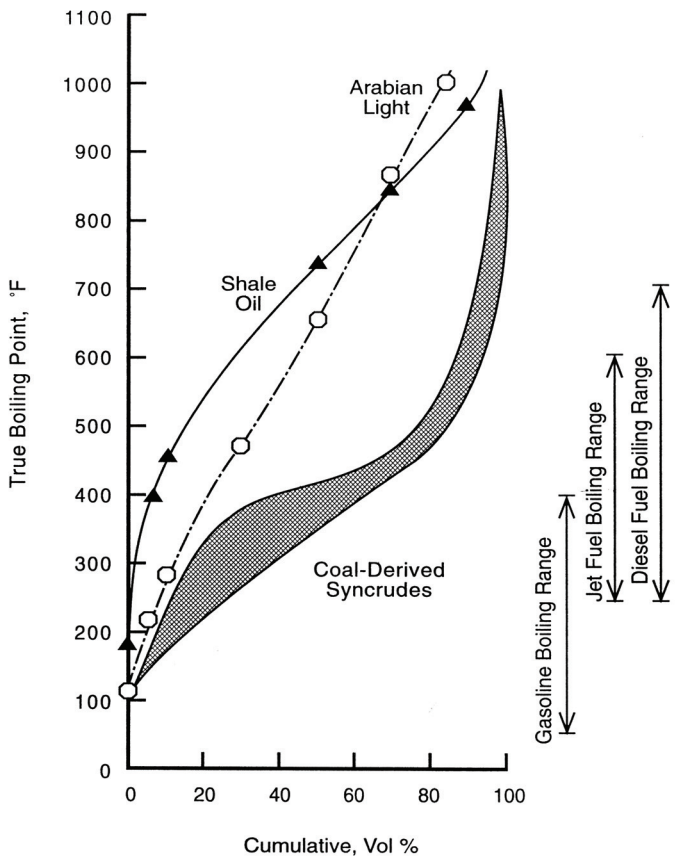

Figure 7.7 True boiling point distillation curves for Arabian light crude, shale oil, and coal-derived syncrudes. Source: United States Synthetic Fuels Corporation.

Any long-range future of coal-derived syncrudes requires far more than simply supplementing residual fuel oils with pulverized coal slurries. Marketable processes must be developed and scaled up to supply a wide range of liquid fuels. Although many methods for making synoil from coal have been attempted, at present only a few hold promise. In fact, current successful coal liquefaction technology has its origins in work pioneered by German scientists in the 1930s prior to World War II.

Coal liquefaction techniques are needed that can remove sulfur as well as extract carbon, and/or add hydrogen to increase the H:C ratio of the liquid product. *Carbonization,* or destructive thermal distillation of coal by pyrolysis, yields a carbon-rich solid char, a hydrogen-rich liquid tar, and coal gas. The low liquid yields of coal pyrolysis have properties similar to those of low-sulfur heavy crude oil, but this effluent may be processed further to yield more desirable liquid fuels. Some of the volatiles driven off by coal carbonization can also be condensed out to yield additional coal liquids.

Coal-derived syncrudes can be upgraded further and be refined in much the same manner as crude oil, to produce a wider range of useful middle-cut distillate fuels. Hydrogenation in the coal conversion process uses direct hydrogen addition via a hydrogen-rich gas and/or a hydrogenated solvent-rich donor, such as Solvent Refined Coal (SRC). In direct pyrolysis, no additional hydrogen source other than hydrogen in coal itself is provided whereas, in hydropyrolysis or hydrocarbonization, tar is hydrotreated to further increase the quality of the syncrude. Pulverized coal, in this instance, is fed to a hydrogen-rich gas and recycled coal-derived liquid slurry at elevated temperature and pressure to shift the H:C ratio of the liquid. The resulting products of hydrogenated coal are solid, gas, and liquid, and the HC shift process may require catalysis, depending on the type of coal and ash content. This technique may be the most probable source of future coal-derived liquid fuels.

Indirect hydrogenation uses coal-derived syngas to produce methanol and/or further conversion of methanol into gasoline. The shift of synthesis gas into low-octane gasoline and other liquids is by means of a Fisher-Tropsch catalytic converter technology developed by Franz Fischer and Hans Tropsch prior to World War II. The technology generates a large amount of intermediate or high-Btu gas along with separated liquid products.

The most successful coal liquefaction program was developed by the Germans during World War II, in which Fischer-Tropsch catalytic conversion, along with Bergius hydrogeneration and catalytic hydrorefining of coal at 15–500°C (60–930°F) and 200–680 atm pressure, was used to produce gasoline and aviation fuels; see Figure 7.6. At present, no full-scale successful coal liquefaction industry is economically viable. Many methods that use basically the techniques discussed or combinations of various methods mentioned are being explored.

Synthetic oil can also be produced from shale, a sedimentary rock marbled with a complex solid substance called *kerogen.* Kerogen consists chiefly of carbon, hydrogen, nitrogen, oxygen, and sulfur. Shale oil is found in rock deposits as well as in marine and coal beds and is potentially a large liquid fuel resource. Since shale oil does not exist naturally as a liquid, as does crude oil, it must be made by pyrolyzing kerogen at 480°C (900°F) to yield a synthetic liquid crude. Crude shale oil is a highly viscous liquid that is difficult to pump below 2–32°C, making transportation and storage difficult. In addition, it has a high pour point, high nitrogen but moderate sulfur content, as well as a petroleum wax base. Shale oil can be burned as a boiler fuel or used as a refinery feedstock to yield middle-cut distillate fuels. True point distillation curves for these petroluem liquid fuel alternatives are found in Figure 7.7.

Table 7.5 Thermodynamic Properties of Arabian Light Crude, Shale Oil, and Coal-Derived Oil

	Arabian light crude	Shale oil	Coal-derived oil
Physical appearance	Viscous liquid	Waxy liquid	Liquid
Gravity, °*API*	33.4	20.2	18.6
Pour point, °F	–15	+90	<–80
Sulfur, wt %	1.7	0.7	0.3
Oxygen, wt %	0.1	1.2	3.8
Total nitrogen, wt %	0.1	2.2	0.9
Iron, ppm	<3	70	8
Arsenic, ppm	—	28	—
Hydrogen/carbon atom ratio	1.84	1.60	1.47
Boiling range, *LV* %			
St-400°F	31	4	37
400–1000°F	53	86	63
1000°F+	16	10	0

Source: United States Synthetic Fuels Corporation.

Shale oil is expensive, and many factors contribute to its high cost, including low organic content in shale, remoteness of the resource, as well as the capital and labor required to produce crude shale oil. Additional factors, such as air pollution from blasting, mining, crushing, transporting, and retorting shale and large quantities of polluted water associated with shale oil processing and cooling, as well as required handling of solid residue, place stringent environmental limits on shale oil production.

Shale oil technology generates a high level of waste and yields low amounts of oil per unit mass of raw material. Raw shale must first be mined or fractured in place, crushed, and then heated to yield a useful liquid. Both surface and in situ recovery techniques are means of retorting shale to produce syncrudes. In surface retorting, raw shale is fed into a large kiln where it is mixed and heated to produce oil, gas, and solid residue. Shale oil can be as rich as 35% by weight aromatics; however, it is still closer to crude oil in nature than coal-derived liquids and therefore has a potential as a feedstock for producing gasoline, diesel fuel, and boiler and heating oil. Properties of various oils are found in Table 7.5.

EXAMPLE 7.5 An internal combustion engine uses liquid octane fuel. The air-fuel mixture enters the engine at 25°C and 101 kPa. The mixture, 150% theoretical air, leaves the engine at 550 K. Assuming complete combustion and that the heat loss by the engine is equal to 20% of the net work produced, calculate (a) the mass air-fuel ratio, (b) the mass flow rate of fuel required to produce 375-kW power, and (c) the corresponding mass flow rate of CO_2 produced by the engine.

Solution:

1. Stoichiometric equation:

$$C_8H_{18} + aO_2 \rightarrow bCO_2. + cH_2O$$

Carbon atom balance:

$b = 8$

Hydrogen atom balance:

$2c = 18 \qquad c = 9$

Oxygen atom balance:

$2a = (2)(8) + 9 \qquad a = 12.5$

2. Ideal reaction (150% theoretical air):

$$C_8H_{18} + (1.5)(12.5)(O_2 + 3.76N_2) \rightarrow 8CO_2 + 9H_2O + 6.25O_2 + 70.5N_2$$

3. Air-fuel ratio *(mass basis):*

$$AF = \frac{(1.5)(12.5)(4.76 \text{ moles air})(28.97 \text{ kg/kgmole air})}{(1 \text{ mole fuel})(114 \text{ kg/kgmole fuel})}$$

a. = 22.68 kg air/kg fuel

4. Energy balance (*open system*)*:*

$$Q - W = \sum_{\text{out}} N_j \left[\bar{h}_f^0 + \left\{\bar{h}\langle T_j\rangle - \bar{h}\langle T_0\rangle\right\}\right]_j - \sum_{\text{in}} N_i \left[\bar{h}_f^0 + \left\{\bar{h}\langle T_i\rangle - \bar{h}\langle T_0\rangle\right\}\right]_i$$

where values obtained from Appendix B

$$T_i = 298\text{K} \qquad T_j = 550\text{K}$$

$$\sum_{\text{out}} N_j \bar{e}_j = 8[-94{,}054 + 2{,}537]_{CO_2} + 9[-57{,}798 + 2{,}082]_{H_2O_g} + 6.25[1{,}833]_{O_2} + 70.5[1{,}769]_{N_2}$$

$$= -1097{,}409 \text{ cal} = (-1{,}097{,}409)(4.187) = -4{,}594{,}852 \text{ kJ}$$

$$\sum_{\text{in}} N_i e_i = (1)(-59{,}740)(4.187) = -250{,}131 \text{ kJ}$$

and, since the heat loss equals 20% of the net work in magnitude,

$$-0.2W - W = -4{,}594{,}852 + 250{,}131$$

$$W = 3{,}829{,}040 \text{ kJ}$$

$$w = 3{,}829{,}040 \text{ kJ/kg fuel}$$

$$w = \frac{3{,}892{,}040 \text{ kJ/kg fuel}}{114 \text{ kg/kgmole fuel}}$$

$$w = 33{,}590 \text{ kJ/kg fuel}$$

and

$$\dot{W} = \dot{m}_f w$$

or

b. $$\dot{m}_f = \frac{375 \text{ kN} \cdot \text{m/sec}}{33{,}590 \text{ m} \cdot \text{kN/kg fuel}} = 0.0112 \text{ kg fuel/sec} = 40.3 \text{ kg fuel/hr}$$

5. Carbon dioxide:
From item 1, there are 8 moles of CO_2 per mole of C_8H_{16}, or

$$\dot{m}_{CO_2} = \left[\frac{8 \text{ kgmoles } CO_2}{1 \text{ kgmole } C_8H_{16}}\right]\left[\frac{44 \text{ kg/kgmole } CO_2}{114 \text{ kg/kgmole } C_8H_{16}}\right]\left(40.3 \frac{\text{kg fuel}}{\text{hr}}\right)$$

c. $$\dot{m}_{CO_2} = 124.4 \text{ kg } CO_2 / \text{hr}$$

Large reserves of tar sands and heavy oil are yet additional potential resources for long-term production of syncrude. Bitumen, a hydrocarbon substance that can exist as either a solid or a heavy liquid, can be found in tar sands, sandstone, limestone, and oil-impregnated rock. Because of the cohesive nature of these materials to sand and rock, they have traditionally been used to make asphalt. Petroleum techniques used to recover crude oil, such as drilling, cannot be used to recover this very viscous material. Tar sand oils have specific gravities of less than 10–15°*API* but, much like shale oil, they can be recovered, upgraded, and used to produce petroleum products. Problems associated with mining and processing of tar sands are similar to those identified with shale oil recovery. Some bitumen can be separated by hot water, while other sources require light hydrocarbon and aromatic solvent extraction. In solvent extraction systems, some solvents will remain in the solid residue. Heavy oil (10–15°*API*) and tar sands are often considered synonymous since classification and quantification of tar sands and heavy oil are difficult.

U.S. domestic syncrude resources, particularly coal and oil shale, are vast and could, therefore, supply all transportation fuel needs for centuries. Crude oil for mobility fuels will be available into the new century, while synthetic fuel technology could begin to be available later in the century. With reduced reserves and greater oil costs may come an impetus for improved fuel economy, wider fuel tolerance, and improved combustion performance in liquid fuel combustion systems with both current fuels and the liquid fuel alternatives. When syncrude options provide viable solutions to the engineering, economic, and environmental hurdles confronting their production, a long-term future for a synthetic fuel industry could become a reality.

7.5 UNCONVENTIONAL LIQUID FUELS

Considerable effort has been given in recent years to developing potentially a renewable liquid biofuel alternative to supplement depleting world oil supplies. Solid biomass resources were considered in Chapter 6, and gaseous biofuels will be dealt with in Chapter 8. Animal fats, such as beef tallow and whale oil, and vegetable oils, such as peanut oil and those derived from sunflower seeds, soy, and cottonseed, have all been used as combustibles. In the past these materials have had limited use in certain specific applications, such as oil for illumination. These resources, termed *triglyceride fuels,* are

hydrocarbon compounds consisting of various esters, i.e., products of alcohol and acids, such as glycerine molecules attached to long-chain fatty acids.

Photosynthesis in vegetation produces *carbohydrates* or glucose polymers, i.e., C/H/O compounds, such as sugar, starch, and/or cellulose. These materials can be converted into alcohol. A few natural plants, such as the milkweed, the rubber tree, the petroleum nut tree of the Philippines, and the gopher weed, actually produce hydrocarbons rather than carbohydrates. The source of liquid hydrocarbon in these plants is often concentrated in a milky, viscous sap, called *latex,* which can be tapped and, in some cases, used directly as a fuel. Those plants that cannot be milked are first dried to remove water, reduced in size by grinding, and boiled in a solvent such as heptane to extract a liquid biocrude, which then can be processed further using current refinery technology to produce useful fuels.

Since liquid biomass fuels produced from these various feedstocks are partially oxygenated hydrocarbons, they will have a lower heating value, higher moisture content (approximately 50% by weight in fresh plants), and lower sulfur, ash, and nitrogen percentage than comparable liquid hydrocarbon fuels produced from crude oil. Liquid fuels derived from biomass are actually renewable forms of solar energy. Several major issues impact any successful industrial development from these fuel alternatives, including the limited magnitude of resources available, food versus fuel debate, cost, energetics required to produce these fuels, and their compatibility with present and future power systems.

EXAMPLE 7.6 Methanol, CH_3OH, is to be used as an automotive engine alternative fuel. An air-fuel mixture, having an equivalence ratio of 1.2 after compression, is at a total pressure of 1,850 kPa abs and 680K. The combustion process occurs at constant volume, and the peak reaction temperature is 2,800K. Assuming that the products of combustion contain CO, CO_2, H_2, H_2O_g, and N_2, determine (a) the combustion product's volumetric analysis and (b) the peak pressure, kPa abs.

Solution:

1. Equivalence ratio:

$$\Phi = \frac{\left(\dfrac{\text{moles fuel}}{\text{moles oxidant}}\right)_{\text{actual}}}{\left(\dfrac{\text{moles fuel}}{\text{moles oxidant}}\right)_{\text{stoichiometric}}}$$

$$= 1.2$$

2. Stoichiometric equation:

$$CH_3OH + aO_2 \rightarrow bCO_2 + cH_2O$$

Carbon atom balance:

$$b = 1$$

Hydrogen atom balance:

$$2c = 4 \qquad c = 2$$

Oxygen atom balance:

$$2a + 1 = 2b + c$$
$$2a = 2 + 2 - 1$$
$$a = 1.5$$
$$CH_3OH + 1.5(O_2 + 3.76N_2) \rightarrow CO_2 + 2H_2O + (1.5)(3.76)N_2$$

3. Actual combustion:
Now, for stoichiometric reaction,

1 mole fuel/(1.5)(4.76) moles air

and

$$\Phi = 1.2 = \frac{x \text{ moles fuel}/(1.5)(4.76) \text{ moles air}}{1 \text{ mole fuel}/(1.5)(4.76) \text{ moles air}}$$
$$x = \left(\frac{1 \text{ mole fuel}}{(1.5)(4.76) \text{ moles air}} \right) \times (1.5)(4.76 \text{ moles air}) \times 1.2$$
$$x = 1.2$$

or

$$1.2CH_3OH + 1.5(O_2 + 3.76N_2) \xrightarrow{V}$$
$$aCO + bCO_2 + cH_2 + dH_2O + eN_2$$

4. Atomic mass balances:
Nitrogen:

$(1.5)(3.76) = e = 5.64$

Carbon:

$1.2 = a + b$

Oxygen:

$1.2 + 3.0 = 4.2 = a + 2b + d$

Hydrogen:

$4.8 = 2c + 2d$

5. Equilibrium criteria: Since the products CO, CO_2, H_2, H_2O, and N_2 *are assumed to be in equilibrium,* we can write an equilibrium relation between these species. For example,

$$CO_2 + H_2 \rightleftarrows CO + H_2O$$

and

$$K_p = \frac{\left(\frac{P_i}{P_0}\right)_{CO}\left(\frac{P_i}{P_0}\right)_{H_2O}}{\left(\frac{P_i}{P_0}\right)_{CO_2}\left(\frac{P_i}{P_0}\right)_{H_2}}$$

$$= \frac{P_{CO}P_{H_2O}}{P_{CO_2}P_{H_2}}(P_0)^{2-2}$$

$$= \frac{\bar{x}_{CO}\bar{x}_{H_2O}}{\bar{x}_{CO_2}\bar{x}_{H_2}}$$

$$K_p = \frac{a\,d}{b\,c}$$

6. From the atomic mass balances in item 4,

$$a = 1.2 - b$$
$$d = 4.2 - (1.2 - b) - 2b$$
$$c = 2.4 - (3.0 - b)$$
$$c = b - 0.6$$

or

$$K_p = \frac{(1.2 - b)(3.0 - b)}{(b)(b - 0.6)}$$

$$K_p = \frac{3.6 - 3b - 1.2b + b^2}{b^2 - 0.6b}$$

$$K_p(b^2 - 0.6b) = 3.6 - 4.2b + b^2$$

$$(K_p - 1)b^2 + (4.2 - 0.6K_p)b - 3.6 = 0$$

7. Equilibrium constant K_p:

$$\log K_p = \sum_{\text{prod}}{}_i \log K_{p_i}\langle T\rangle - \sum_{\text{react}}{}_j \log K_{p_j}\langle T\rangle$$

or

$$\log K_p = \left[\log K_p\langle T\rangle\right]_{CO} + \left[\log K_p\langle T\rangle\right]_{H_2O} - \left[\log K_p\langle T\rangle\right]_{CO_2} - \left[\log K_p\langle T\rangle\right]_{H_2}$$

for $T_2 = 2800$ K

$$\log K_p = 6.649 + 1.833 - 7.664 - 0.00$$
$$\log K_p = 0.818$$
$$K_p = 6.5766$$

8. Solving for b:

$$5.5766b^2 + [(4.2) - (0.6)(6.5766)]b - 3.6 = 0$$
$$5.5766b^2 + 0.254b - 3.6 = 0$$
$$b = \frac{-0.254}{(2)(5.5766)} \pm \frac{1}{(2)(5.5766)}\sqrt{(0.254)^2 + (4)(5.5766)(3.6)}$$
$$b = 0.781$$
$$a = 1.2 - 0.781 = 0.419$$
$$d = 3.0 - 0.781 = 2.220$$
$$c = 0.781 - 0.6 = 0.181$$

Check:

$$K_p = \frac{a\,d}{b\,c} = \frac{(0.419)(2.220)}{(0.781)(0.181)}$$
$$= 6.58$$

9. Mole fractions:

$$\bar{x}_{CO} = \frac{a}{a + b + c + d + e} = \frac{0.419}{9.241} = 0.04534$$
$$\bar{x}_{CO_2} = \frac{b}{a + b + c + d + e} = \frac{0.781}{9.241} = 0.08451$$
$$\bar{x}_{H_2} = \frac{c}{a + b + c + d + e} = \frac{0.181}{9.241} = 0.01959$$
$$\bar{x}_{H_2O} = \frac{d}{a + b + c + d + e} = \frac{2.220}{9.241} = 0.2402$$
$$\bar{x}_{N_2} = \frac{e}{a + b + c + d + e} = \frac{5.64}{9.241} = 0.6103$$

10. Peak pressure: $V = C$ combustion

$$P_1V_1 = N_1\bar{R}T_1 \qquad P_2V_2 = N_2\bar{R}T_2$$
$$P_2 = \frac{N_2\bar{R}T_2}{V} = \frac{N_2\bar{R}T_2}{N_1\bar{R}T_1}P_1 = \frac{N_2T_2}{N_1T_1}P_1$$

$$P_3 = \frac{(9.241)(2{,}800)(1{,}850\ \text{kPa})}{[1.2 + (1.5)(4.76)](680)} = 8{,}441\ \text{kPa abs}$$

Methanol, CH_3OH, is produced primarily from natural gas; however, other carbonaceous feeds such as coal or wood can be used after conversion to a syngas (carbon monoxide and hydrogen). The reactions for methanol production are:

$$CH_4 + 0.5O_2 \rightarrow CO + 2H_2$$
$$CO + 2H_2 \rightarrow CH_3OH$$

Fuel-grade ethanol, C_2H_5OH, can be produced on a commercial scale either by synthesis or fermentation reactions. The chemical industry has generated ethyl alcohol, using ethylene as feedstock by mixing ethylene with steam at 60–70 atm and 300ºC (572ºF) over a phosphoric-acid catalyst. The reaction for ethanol production is:

$$C_2H_4 + H_2O \rightarrow CH_3CH_2OH$$

Several renewable biomass resources have been considered as feedstocks for commercially fermented fuel alcohol production. These materials, which are principally carbohydrates, can be chemically converted by enzyme action into alcohol, carbon dioxide, protein, and various secondary products. Potentially, any biomass material is a source of alcohol production, but the most readily available materials commercially viable on a large scale at present are sugar or starch sources. Sugar sources include sugarcane, sugar beets, and molasses, as well as fruits and their juices. Starch sources include grains, potatoes, and other root crops. The technology for cellulose enzyme conversion is not yet developed to a commercial scale.

Sugar stocks are principally sucrose, $C_{12}H_{22}O_{11}$, which, under catalysis of invertase enzyme, produces glucose, $C_6H_{12}O_6$, and fructose, $C_6H_{12}O_6$, via the sucrose hydrolysis reaction.

$$\underset{\text{Sucrose}}{C_{12}H_{22}O_{11}} + H_2O \xrightarrow{\text{Intertase}} \underset{\text{Glucose}}{C_6H_{12}O_6} + \underset{\text{Fructose}}{C_6H_{12}O_6}$$

Invert sugars, i.e., glucose and fructose, are next converted by fermentation into equal moles of ethyl alcohol, C_2H_5OH, and carbon dioxide by the enzyme zymase.

$$\underset{\text{Invert sugars}}{C_6H_{12}O_6} \xrightarrow{\text{Zymase}} \underset{\text{Ethanol}}{2CH_3CH_2OH} + \underset{\text{Carbon dioxide}}{2CO_2}$$

Secondary by-products are produced from invert sugars and include aldehydes, esters such as ethyl acetate, higher molecular weight alcohols called fusel oils, fatty acids, and trace amounts of aromatics. These compounds are referred to as *congeners*.

Starch sources must be cooked to form a gel and prepared differently than sugar sources. Starch is mixed with malt, i.e., sprouted barley, which contains the diastase enzyme. This enzyme converts starch, $(C_6H_{10}O_5)_n$, into maltose sugar, $C_{12}H_{22}O_{11}$.

$$\underset{\text{Starches}}{(C_6H_{10}O_5)_n} \xrightarrow[\substack{\text{Malt}\\ \text{enzyme}\\ \text{diastase}}]{H_2O} \underset{\substack{\text{Maltose}\\ \text{sugar}}}{C_{12}H_{22}O_{11}}$$

Glucose is converted to ethyl alcohol and CO_2 by fermentation with zymase enzymes as was the case for sugar stocks.

The technology for commercial ethanol production is available, and facilities currently in operation or near operational status demonstrate concept viability. Since a major and most stable grain feedstock in the United States is corn, the following facility will describe specifically with fermentation of cornstarch to produce fuel-grade ethanol. The production of grain alcohol fuel consists of the following major steps:

1. Corn cleaning and milling
2. Corn mill cooking
3. Saccharification
4. Fermentation
5. Distillation
6. Azeotropic drying
7. Protein by-product drying

The principle of anaerobic fermentation and distillation are specific processes currently in use in related fields such as the beverage alcohol and petrochemical industries. Operational experience and data from a growing alcohol fuel industry indicate that successful alcohol plants must be designed and operated on the basis of favorable energy balances, i.e., energy output > energy input. Successful 200-proof ethanol production requires use of nonpetroleum energy sources as well as strong regional and local availability of grain input and marketability of product output. Commercially viable ethanol-producing plants should:

1. Utilize no petroleum in the production of alcohol fuels and protein by-products
2. Reduce foreign oil energy consumption in the United States and contribute to U.S. energy independence
3. Produce a fuel-grade alcohol that can be used as a fuel or an octane booster in unleaded gasoline
4. Produce a usable protein by-product that can meet farm-customer requirements
5. Develop the technology of alternate energy in the production of biosynthetic fuel resources

A process flow diagram for a corn-to-ethanol facility is shown in Figure 7.8. Corn is transported by rail and/or truck to the feedstock delivery where each load is recorded at a weighing station. The corn is then dumped into a transfer pit, and the delivery vehicle exits the site.

Grain is transferred from the delivery site to storage facilities and/or the main plant. The corn is first transported to a grain cleaner, where foreign material such as sand, glass, and metals are removed from the grain. Cleaned grain drops by gravity feed into a discharge hopper, where a bucket elevator transfers it to a cleaned-grain storage bin. A feed system transfers the corn to a hammermill, where corn is continuously milled to a 20-mesh screening. After milling, the grain is carried pneumatically through a flow meter for inventory control and directed to a surge hopper.

The grain delivery, storage, and milling operations are located away from alcohol-generating portions of the plant. This isolation ensures that dust from these components does not interfere with the activities required to generate anhydrous alcohol. Dust-collecting facilities are provided to remove dust from these processes and transfer the material to a baghouse area.

Starch in milled corn can be commercially converted into fermentable sugars by acid or enzymatic hydrolysis. Enzyme conversion requires cooking to gelatinize the material prior to reduction to soluble dextrins. Choice of high- or low-temperature cooking will be dictated by plant size and the energetics of its specific configuration. Cooking can be done on a batch or continuous basis, as well as by extrusion and/or direct steam injection. Large-scale facilities favor high-temperature continuous cooking using extrusion and steam injection systems in order to conserve energy, shorten cooking time, and be compatible with continuous production of alcohol. Saccharification converts dextrin into simple fermentable sugars. This process requires a lower temperature and different enzyme action than the cooking step.

Next, clean, dry, milled corn is continuously fed through the corn cooker extruder. Cooked corn leaves the process at 150°C (300°F) and is fed to an attrition mill, where material is reduced to 20-mesh screening. Extruder cooking greatly reduces the required amount of process heat over conventional steam-jacketed cooking tanks. Heat generated by friction, in addition to steam injected directly in the corn extrusion process, provides heat needed for cooking.

Material from the corn cooker extruder facility is next fed to a pre-saccharification mixer. At this stage, water, enzymes, thin stillage, and pH controls (such as sodium hydroxide for low water pH or concentrated sulfuric acid for high water pH) are added to the tank and continuously mixed. Residence time in the premixing tank is approximately 2 minutes. Sufficient liquid input to the premixing process produces approximately 30 gallons of mash per bushel of grain input. Cooling water is provided to ensure that the mash mixture is at 66°C (150°F) at discharge. The mash consists of approximately 33% solids.

The mash is pumped from the mixing tank by means of a mash transfer pump through a continuous-pipe saccharification process. In this process, mash starch mixture is converted into fermentable sugars at 60°C (140°F). Residence time in the unit is approximately 7 minutes. After the saccharification process, mash passes through a mash cooler, where it is cooled to 27°C (80°F) by water.

Saccharificated corn mash is next transferred to alcohol fermentation tanks. Mash is pumped into a tank while fermentation yeast is concurrently added. Multiple tank sections allow continuous feed to be maintained so that one tank is being cleaned and filled, one tank is being discharged, and the remaining fermenters are kept at 27°C (80°F). Fermentation converts sugar produced by cooking and saccharification into a alcohol-water wet mash mixture, termed *beer*. The beer, a 6–12% ethanol + water mixture, can be commercially produced using batch or continuous processes at room temperature over a 36–48-hour period. Techniques using advanced enzymes, which may accelerate this step, are still in developmental stages.

Each tank has a provision for venting carbon dioxide generated during fermentation. The CO_2 is vented to a scrubber, where alcohol is stripped from the gases and redirected to the beer well. After fermentation, the beer is pumped from the tank to a solid separation system.

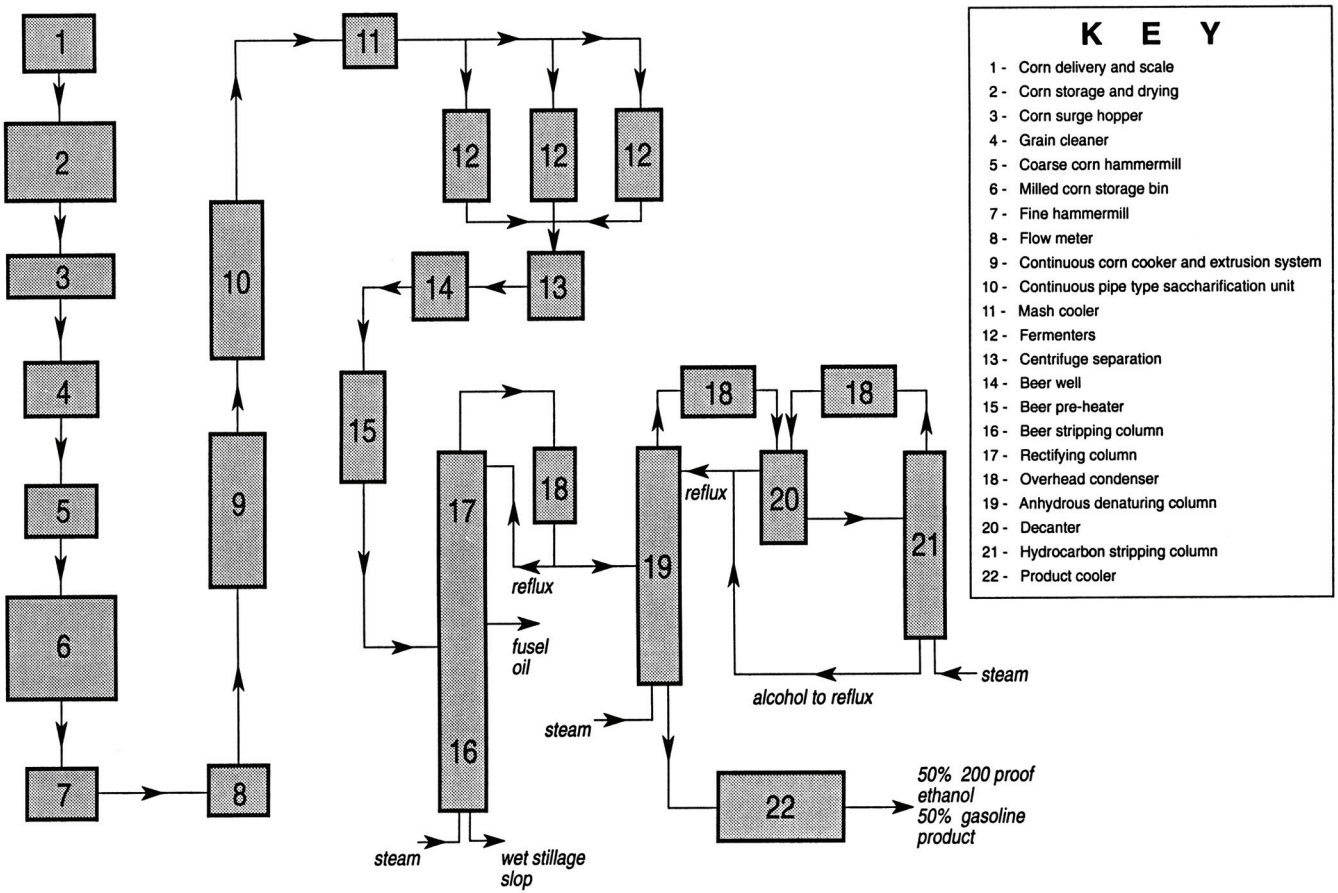

Figure 7.8 Simplified grain ethanol process schematic.

After leaving the fermenter, a discharge of water, ethanol, and solids passes through a centrifuge, which separates heavy solids from the alcohol-water stream for removal, treatment, and recovery of distiller dried grains with solids (DDGS) for separate marketing. The water-alcohol mixture, which is approximately 10% alcohol, is pumped to the beer well.

Alcohol recovery and stillage separation of a dilute alcohol-water-solids beer mixture occur in the distillation and drying section of the plant. Beer is pumped from a beer well to distillation columns through a beer preheater, where it is heated from 33°C (90°F) to 93°C (199°F). Saturated beer having an alcohol concentration of 6–12% enters the distillation column for product separation.

Steam distillation of the alcohol-water mixture will produce an azeotropic mixture of approximately 96% ethanol. Further drying of the product produces a 200-proof anhydrous ethanol product, which can be denatured and blended with gasoline to produce a fuel-grade blend of 10% alcohol–90% gasoline, commercially termed *gasohol.*

Alcohol is stripped from the water and solids by the rectifying column. The column produces an overhead azeotropic mixture having a 95.7% alcohol content at 79°C (173°F). The overhead vapor passes through a rectifying condenser. A fraction of the condensed product is sent to a denaturing and drying column for further drying and handling.

Higher molecular weight alcohols, termed fusel oils, are produced in the fermentation stage. These components must be removed from the upper section of the rectifying column by side extraction, and then cooled, washed, and stored.

Stillage is removed from the beer in the beer stripping column below the rectifying section. The column produces a bottom slop having approximately 8% solids and less than 0.05% ethanol. The wet stillage leaves the column at approximately 100°C (212°F). This material is pumped to the distillers dried grain recovery section of the plant.

The azeotropic alcohol-water product is pumped to an anhydrous denaturing column. The column produces an anhydrous ethanol-unleaded gasoline blend, which is pumped to a tank and cooled for storage. Steam supplied at the base produces a tertiary azeotrope of hydrocarbon alcohol and water. After condensing, the overhead is fed to a decanter, where material separates into a top hydrocarbon-rich layer and a bottom alcohol-hydrocarbon-water mixture. The upper section is pumped as reflux back into the drying column. The bottom of the decanter is pumped to the hydrocarbon stripping column, where alcohol and hydrocarbon are separated.

A major by-product of the main plant will be a high-protein livestock feed of dark distillers dried grains (DDDG). Nonsoluble grain residuals are separated from dissolved solids, i.e., sugars, in the protein by a product drying system. These grain residuals are further dewatered to produce a DDDG having at least 30–50% solids. Energy for drying these grains is expensive, and stack gases from the steam generation system could be used to further dry the product. Liquid waste from this process, after partial recirculation to the plant processing, would be environmentally treated and passed to a waste stream discharging from the plant to a sewer system.

7.6 LIQUID FUEL COMBUSTION AND BURNERS

Combustion of the liquid fuels described in Chapter 7 occurs in the vapor phase. Therefore in order to initiate and sustain proper liquid fuel-air mixture chemistry, specific fuel preparation steps are necessary. A continuously flowing liquid fuel stream within a few milliseconds must be: (1) correctly reduced in size in order to rapidly mix with air; (2) spatially distributed properly with ample momentum as a fuel-air mixture; as well as (3) sufficiently heated and vaporized in order to ignite and burn. Liquid fuel preparation and delivery technologies differ for heat transfer versus power applications, continuous versus intermittent combustion configurations, and/or low pressure versus high pressure operation. It is essential that a proper comprehension of fuel-engine fuel preparation interfaces be understood when using liquid fuels to produce heat or power.

In heat transfer applications, such as boilers and furnaces, the *burner* is the component designed to prepare and mix liquid fuels with air prior to burning. Liquid fuel enters the burner where *atomization* shatters the fluid feed stream into a fine mist of droplets. Droplet sizes are of an order of a few microns in order for fuel to mix, quickly vaporize, and burn. Combustion air is supplied to the burner through two distinct paths: (1) introduced with the fuel or along with the fuel as *primary air* or (2) introduced to the flame zone or post combustion zone after the flame as *secondary air*. The amount of primary air relative to secondary air is determined by combustion requirements as well as particularities of individual burner designs.

There are three principal means of atomization used with liquid fuels: mechanical atomization, fluid atomization, and/or steam atomization. Atomization by mechanical means utilizes a spray of liquid droplets produced by pumping fuel oil through a fine nozzle or jet. The atomized film is usually discharged as a hollow cone which then mixes with air to burn. Output is controlled by pressure and temperature-dependent fuel viscosity. Ratio of rated output to minimum operable output, called "*turn-down*" ratio, with simple pressure jet burners, is low, i.e. 2:1. Modified single fluid pressure jet burners provide turn-down ratios >2:1.

The rotary cup burner, a mechanical means of atomization, is capable of use with a variety of liquid feeds without requiring major burner modification. Oil is fed through a hollow shaft into the narrow end of the open cup, which is rotating 4000–6000 rpm about its shaft axis. A film of oil travels along the cup surface and is thrown off the wide end of the cup periphery by centrifugal force as oil droplets. Oil droplets being ejected from the rotating cup are broken up into a fine mist after colliding with a stream of high velocity primary air directed axially around the cup. A fan and/or a separate compressor supplies the high velocity air stream that shapes the emerging oil film into a cone. Advantages of mechanical atomization include operational and control simplicity, no need for an additional atomizing fluid with its needed delivery components. Advantages of the rotary cup burner atomization over simple pressure jet atomization include turn-down ratio up to 5:1, ability to handle high viscosity oils, and more economical operation in oil preheat mode. Disadvantages of mechanical atomization include higher fuel oil operational temperature and pressure requirements and inflexibility to changing fuel oil with fixed configuration. A major disadvantage of the rotary cup burner is its greater susceptibility to fouling by carbon.

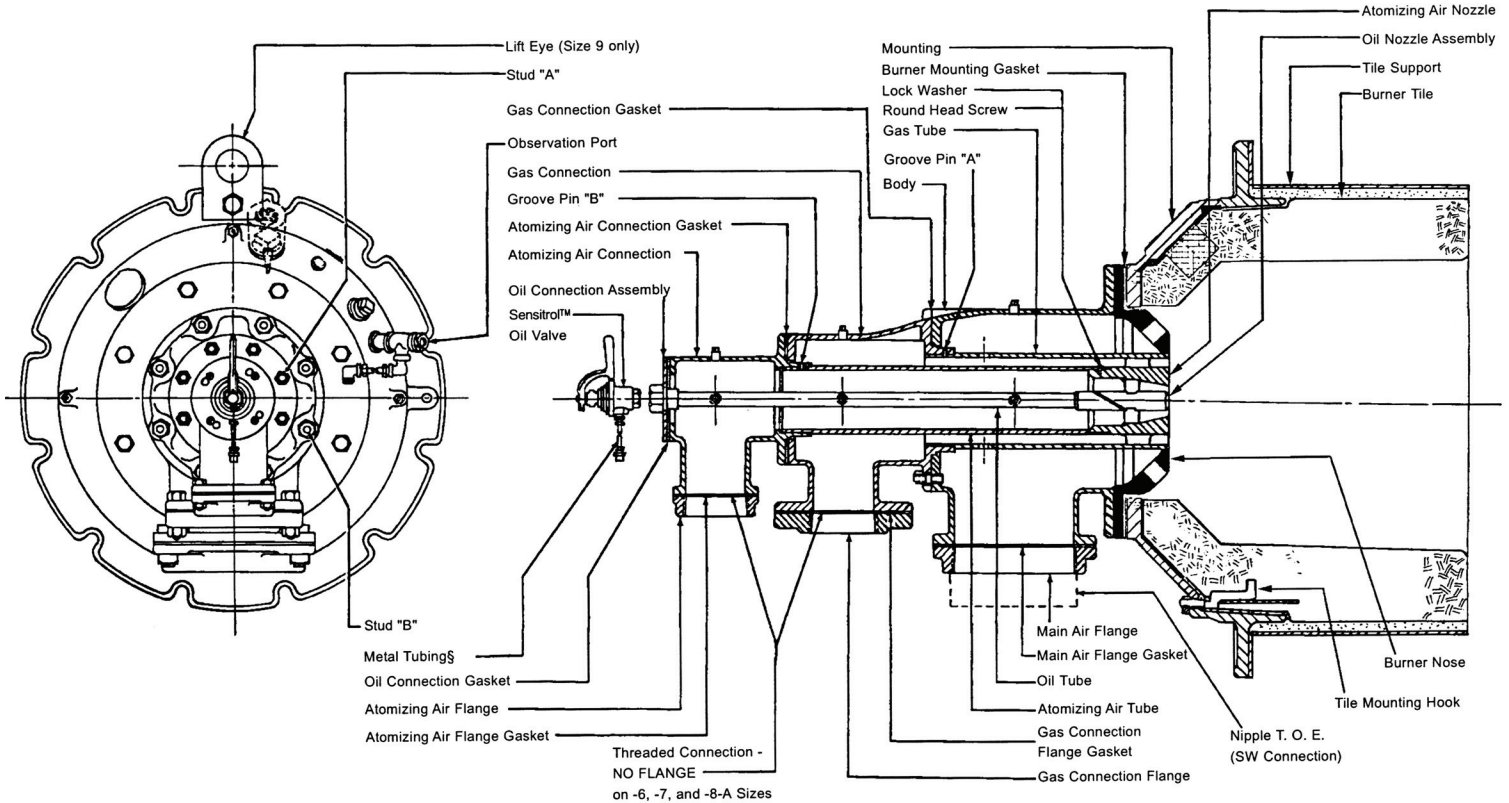

Figure 7.9. North American Manufacturing Company Series 6514-10 and 6514-10-L Dual-Fuel™ Burners. Reproduced with the permission of The North American Manufacturing Company, Ltd., Cleveland, OH.

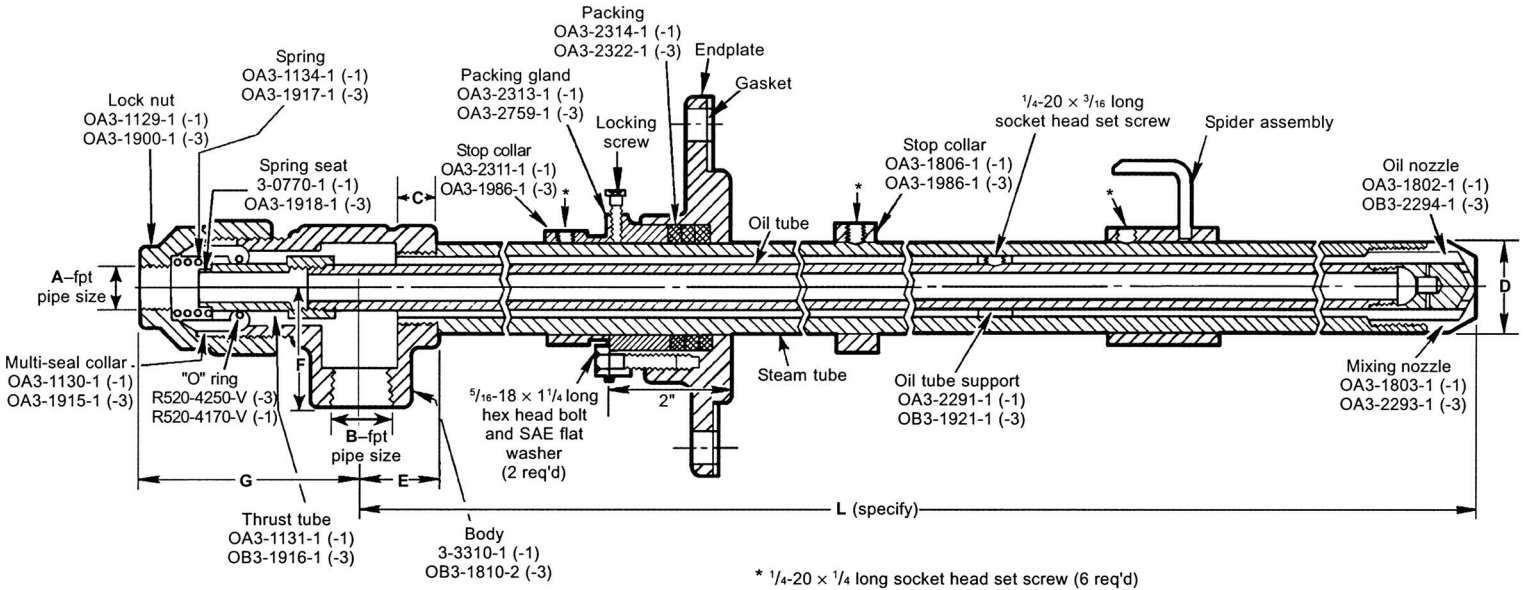

Figure 7.10. North American Manufacturing Co. Series 5643 Steam Atomizers. Reproduced with the permission of The North American Manufacturing Company, Ltd., Cleveland, OH.

Atomization by means of an atomizing fluid results from the shearing effect of a high-velocity stream acting on a liquid fuel. Atomization thus occurs through momentum exchange between two streams, i.e., fuel and air or steam; see Figures 7.9 and 7.10. For the vast majority of two-fluid applications at low, medium, or high pressures, air is the atomizing fluid. For high viscosity fuels and residual fuel oils, steam is a preferred atomizing fluid because, in addition, it supplies both heat and pressure. Steam atomization reduces flame temperature. An advantage of atomization by fluids over mechanical atomization includes increased turn-down ratio, i.e., 10:1, while a major disadvantage is the cost and complexity of supplying the atomizing fluid under pressure.

After ignition, heat is supplied to burning droplets by the flame and surrounding heated surfaces. These droplets, in turn, are related to fuel-atomizer or orifice geometry and cleanliness, as well as to the pressure, viscosity, and surface tension of the oil. Droplet combustion, as described in Chapter 5, burns as a diffusion flame. Distillation occurs at the droplet surfaces, leaving carbon particles that burn with a luminous flame. This destruction process is further complicated by the shape the oil mist assumes as a result of the discharge air pattern of the burner. The shape and size of flame affect combustion efficiency. The process depends on the liquid fuel, the design of the burner, the amount of air supplied, and its mode of distribution. A more complete discussion of liquid fuel atomization and droplet combustion physics requires discussion of fluid mechanics and heat transfer.

PROBLEMS

7.1 Consider the stoichiometric combustion of the paraffin fuel C_xH_{2x+2} and air. Find an expression in terms of x for (a) the molar $\overline{FA}$ ratio, kgmole fuel/kgmole air; (b) the AF ratio, kg air/kg fuel; (c) the air-fuel mixture molecular weight, kg/kgmole; and (d) the ideal product mole fractions.

7.2 NASA has developed a thermodynamic model for gasoline. The analysis approximates gasoline as a mixture of 25% benzene, 25% octane, and 50% dodecane, by weight. For this hypothetical fuel, calculate (a) the molar $\overline{FA}$ ratio, lbmole fuel/lbmole air; (b) the AF ratio, lbm air/lbm fuel; (c) the fuel molecular weight, lbm/lbmole; and (d) the fuel higher heating value, Btu/lbm.

7.3 Gasohol, developed as an alternative unleaded gasoline fuel, can be represented as a liquid mixture of 90% octane and 10% ethanol by weight. For this fuel, determine (a) the stoichiometric AF ratio, lbm air/lbm fuel; (b) the fuel molecular weight, lbm/lbmole; (c) the fuel higher heating value, Btu/lbm fuel; and (d) the gasohol-to-n-octane mass ratio necessary ideally to produce equal STP heat releases burning in equal amounts of air.

7.4 Fuel oil is often represented chemically using a single hydrocarbon surrogate compound such as dodecane, $C_{12}H_{26}$. Determine the following assuming complete combustion of dodecane with 50% excess air: (a) the FA, lbm fuel/lbm air; (b) mole fraction of moisture in ideal products, %; and (c) mass of moisture produced per mass of fuel, lbm water/lbm fuel.

7.5 A fuel rich combustion process burns liquid n-butane, C_4H_{10}, such that no CO_2 is formed, only CO. For this reaction calculate: (a) the theoretical air required, %; (b)

the equivalence ratio for the reaction; (c) the $\overline{fa}$ ratio for the reaction, kgmole fuel/kgmole air; and (d) the *FA* ratio for the reaction, kg fuel/kg air.

7.6 Iso-octane is used as a standard fuel in rating spark-ignition engine fuels. For iso-octane, calculate (a) the higher heating value for this liquid fuel, Btu/lbm; (b) the lower heating value, Btu/lbm; (c) the higher heating value, Btu/gal; and (d) lower heating value, Btu/gal.

7.7 A #4 fuel oil has an *API* gravity at 60ºF of 24. For this fuel find: (a) fuel density, lbm/gal; (b) higher heating value, Btu/gal; and (c) lower heating value, Btu/gal.

7.8 The *API* gravity of a distillate fuel oil at 78°F is 64.5. Determine (a) the *API* gravity at 60°F; (b) the specific gravity at 60°F; (c) the density at 60°F, lbm/ft^3; and (d) the density at 78°F, lbm/gal.

7.9 A gasoline blend has a specific gravity of 0.707 at 15°C. Calculate (a) the specific gravity, *API*; (b) the fuel density, kg/m^3; (c) the fuel lower heating value, kJ/kg; and (d) the fuel higher heating value, kJ/m^3.

7.10 Fuel oil can be represented chemically as $C_{16}H_{32}$. For complete combustion of fuel obtain the following: (a) the stoichiometric reaction equation; (b) the *FA* for 50% excess air, lbm fuel/lbm air; and (c) the mass of moisture produced per mass of fuel burned, lbm water/lbm fuel.

7.11 Gasoline, having 85 wt % carbon and 15 wt % hydrogen, has a density of 6 lbm/ft^3 and a higher heating value of 20,700 Btu/lbm. For ideal complete combustion and $\Phi = 0.8$, find (a) the ratio of dry moles of product to moles of reactant; (b) the *AF* ratio, lbm air/lbm fuel; (e) the ratio of water formed to fuel burned, gal H_2O/gal fuel; and (d) the approximate overall chemical formula of the fuel, C_xH_y.

7.12 A proposal has been made to replace fuel oil by combustion of a liquid methanol and pulverized coal mixture. For a fuel having a gravimetric analysis of 50% liquid and 50% solid (represented by pure carbon), find (a) the stoichiometric equation; (b) the *AF* ratio, kg air/kg fuel; (c) the fuel molecular weight, kg/kgmole; (d) the fuel lower heating value, kJ/kgmole fuel; and (e) the fuel higher heating value, kJ/kg fuel.

7.13 The gravimetric analysis of a liquid marine boiler fuel on an ash- and moisture-free basis is given as:

Carbon	86.63%	Oxygen	0.19%	Sulfur	1.63%
Hydrogen	11.27%	Nitrogen	0.28%		

Calculate (a) the stoichiometric equation for ideal complete combustion of the fuel; (b) the ratio of weight of water formed to weight of fuel burned, lbm H_2O/lbm fuel; and (c) the higher heating value of the fuel, Btu/lbm fuel.

7.14 A fuel oil has the following gravimetric ash and moisture-free analysis:

Carbon	87.0%	Oxygen	0.7%	Sulfur	0.2%
Hydrogen	12.0%	Nitrogen	0.1%		

The dry exhaust gas volumetric analysis is found to be:

CO_2	12%	O_2	8%
N_2	78%	CO	2%

For constant-pressure combustion at 1-atm pressure, calculate (a) the mass of water formed per mass of fuel burned, kg H_2O/kg fuel; (b) the dew point temperature of the stack gases, °C; (c) the mass of CO_2 produced per mass of fuel burned, kg CO_2/kg fuel; and (d) the percent of excess air required for combustion, %.

7.15 A boiler burns 50 lbm/hr of *n*-decane in 130% theoretical air. If both fuel and air are supplied at 60°F, find (a) the required fuel flow rate, gal fuel/hr; (b) the required air flow rate, ft^3 air/min; (e) the required stack gas condensation rate for removal of water, lbm H_2O/hr; and (d) the dry exhaust gas flow rate for exhaust gases at 300°F, ft^3/hr.

7.16 An iso-pentane and 135% theoretical air mixture ignites and burns at constant pressure. Both liquid fuel and air are supplied to the unit at 27°C and 103 kPa. Exhaust gases leave the unit at 327°C. Calculate (a) the energy released by ideal combustion, kJ/kgmole fuel; (b) the exhaust dew point temperature, °C; (c) the specific heat ratio of dry exhaust gases, kJ/kg C; and (d) the combustion efficiency for a product temperature of 127°C, %.

7.17 An internal combustion engine runs on liquid octane and 150% theoretical air. At steady-state operation, the fuel-air mixture enters the engine at 25°C and 101 kPa. The heat loss from the engine combustion is equal in magnitude to 20% of the work output. Assuming complete combustion of the mixture and the exhaust T = 600K, find (a) the reaction equivalence ratio; (b) the net work, kJ/kgmole fuel; (c) the engine thermal efficiency, %; and (d) the fuel consumption required to produce 100 kW, kg/sec.

7.18 A synthetic colloidal fuel is to be made using pulverized coal and liquid methanol. The fuel contains 80% methanol and 20% pulverized coal on a mass basis. Assume that the liquid slurry can be represented as $\left[\alpha C_S + \beta CH_3OH\right]$, where α and β are mole fractions of carbon and methanol, respectively. For this fuel, determine (a) the values of α and β; (b) the ideal stoichiometric combustion reaction; (c) the *FA* ratio, lbm fuel/lbm air; and (d) constant-pressure combustion efficiency for stoichiometric conditions with reactants @ 77°F and products at 1,080°R, %.

7.19 Liquid butane is being used as a fuel for space heating. The required energy from combustion is 50 kW. Design specifications require that the exhaust gas temperature not exceed 400K. The dew point temperature of the exhaust is 41.5°C, while both fuel and air are supplied at 1-atm pressure and 25°C. Calculate (a) the percent of excess air, %; (b) the ideal minimum fan power required for the air supply, kW; (c) the fuel rate of consumption, kg fuel/hr; and (d) the maximum volumetric flow rate of dry exhaust gases, m^3/hr.

7.20 A 10.0 kg/hr blend of 25% benzene –75% liquid dodecane is to be burned in 20% excess air. Determine (a) the dry air required @ 25ºC and 101 kPa for complete combustion, m^3/hr; (b) the adiabatic flame temperature, K; (c) the product gas analysis, %; and (d) the product gas volume @ final T and 101 kPa, m^3/hr.

7.21 A portable kerosene burner is being used for the purpose of providing space heating. The heater delivers 15,200 Btu/hr of thermal energy and uses kerosene having a specific gravity @ 60°F of 0.8. For the unit, determine (a) the higher heating value of the kerosene, Btu/lbm; (b) the density of the fuel, lbm/gal; and (c) the steady burn period for the space heater if the unit has an 85% combustion efficiency and a 2-gal fuel tank, hr.

7.22 An oil-fired boiler has an 80% boiler efficiency. Cold water enters the tank at 65°F and leaves at 165°F. The heater, when running at steady-state and steady-flow conditions, produces 200 gal H_2O/hr. The burner is fired using liquid benzene and 115% theoretical air. Fuel supply is at 77°F, while the air enters the burner at 100°F. Find (a) the exhaust flue gas temperature for complete combustion, °F; (b) the fuel consumption, gal fuel/hr; (c) the minimum fan power for the air supply, hp; and (d) the combustion efficiency, %.

7.23 A steam generator in a turboelectric plant uses fuel oil and produces the following performance results:

Fuel analysis			*Stack analysis*
$C_{12}H_{26}$		CO_2	12.01%
184,000	lbm/hr	O_2	3.71%
T_{inlet}	80°F (fuel and air)	T_{outlet}	450°F

feedwater @	570°F
sat steam @	2,400 psia
steam flow	3,500,000 lbm/hr

For the unit, estimate (a) the amount of excess air used, %; and (b) the thermal efficiency of this steam generator, %.

7.24 Liquid dodecane, $C_{12}H_{26}$, and 120% theoretical air are supplied to a constant-pressure atmospheric combustor. Fuel is supplied at 77°F, and the product adiabatic flame temperature is 4,500°R. Calculate (a) required air preheat temperature, °R; (b) heat release, Btu/lbm fuel; and (c) dry exhaust gas volumetric flow rate for a fuel mass flow rate of 1 lbm/hr.

7.25 A liquid fuel consists of 40% C_6H_{14} and 60% C_8H_{18} by weight. The reactants are burned in 15% excess air at *STP*. For this reaction calculate: (a) the mole fraction of the fuel constituents, %; (b) the mole fraction of the ideal products of combustion, %; (c) the volumetric flow rate of dry air to burn 100 lbm/hr of fuel, ft^3/hr; and (d) the adiabatic flame temperature for ideal complete combustion, K.

7.26 Liquid butane is burned in 180% theoretical air with the equilibrium products of combustion consisting of only CO_2, O_2, H_2O, N_2, NO, and NO_2. For reaction at 1 atm and 1,600K find: (a) the molar ratio $\underline{fa}$ for the reaction, kgmole fuel/kgmole air; (b) equilibrium reactions for the product state; (c) equilibrium constants, K_P, for the product state; and (d) the equilibrium product composition, %.

8

Gaseous Fuels

8.1 INTRODUCTION

Solid and liquid fuels, along with their general thermochemical properties and combustion characteristics, were treated separately in Chapters 6 and 7. In this chapter, the remaining fuel category by phase, i.e., gaseous fuels, will be discussed. Depending on temperature and pressure, every pure compound can exist as a gas, liquid, and/or a vapor, and, obviously, gases can be liquefied. Many fuel gases, in fact, can be condensed simply by compression. Some, such as liquefied natural gas (LNG) and liquid hydrogen, require a supercold, or *cryogenic,* state in order to exist and will not remain in this condition without extreme refrigeration and insulation. For the sake of this discussion, therefore, a fuel will be considered to be a gas if it is noncondensable over normal temperatures and pressures. Examples of gaseous fuels include hydrogen gas, methane, and natural and synthetic natural gas (SNG). Vapors such as propane, butane, and liquefied petroleum gas (LPG) are fuels that are condensable over normal temperatures and pressures. Organizations such as the American Gas Association (AGA) are involved in supporting many aspects of fuel gas technology, including research and development within the natural gas industry, production of synthetic gas via coal gasification, and development of biomass-generated methane systems. Gaseous fuel science will continue to play an important role in combustion engineering in part because of the clean-burning nature of these energy resources, the fact that most fuels actually burn in the gas phase, and insights into the complex nature of general combustion processes that studies of simple gas-phase molecular reactions provide.

EXAMPLE 8.1 The specific gravity (*SG*) of gaseous fuels is expressed as the density, or specific weight, of the fuel at 15.56°C and 1 atm to that of air at 15.56°C and 1 atm. For these conditions, determine (a) the density of methane, CH_4, kg/m^3; (b) the density of propane, C_3H_8, kg/m^3; (e) the specific gravity of methane; and (d) the specific gravity of propane.

Solution:

1. Density:

$$P = \rho RT = \rho\left(\frac{\overline{R}}{MW}\right)T, \quad \rho = \left(\frac{MW}{\overline{R}}\right)\frac{P}{T}$$

CH_4:

$$\text{a. } \rho = \frac{(16 \text{ kg/kgmole})(101 \text{ kN/m}^3)}{(8{,}314 \text{ kN}\cdot\text{m/kgmole}\cdot\text{K})(288.56\text{K})} = 6.736 \times 10^{-4} \text{ kg/m}^3$$

C_3H_8:

$$\text{b. } \rho = \frac{(44)(101)}{(8{,}314)(288.56)} = 1.852 \times 10^{-3} \text{ kg/m}^3$$

2. Specific gravity of gases:

$$SG\langle 15.56°\text{C}\rangle = \frac{\rho_{\text{gas}}\langle 15.56°\text{C},\ 1\,\text{atm}\rangle}{\rho_{\text{air}}\langle 15.56°\text{C},\ 1\,\text{atm}\rangle} = \frac{MW_{\text{gas}}}{MW_{\text{air}}}$$

$$\rho_{\text{air}} = \frac{(28.96)(101)}{(8{,}314)(288.56)} = 1.22 \times 10^{-3} \text{ kg/m}^3$$

$$\text{c. } SG_{CH_4} = \frac{6.736 \times 10^{-4}}{1.220 \times 10^{-3}} = \frac{16}{28.97} = 0.552$$

$$\text{d. } SG_{C_3H_8} = \frac{1.852 \times 10^{-3}}{1.220 \times 10^{-3}} = \frac{44}{28.97} = 1.519$$

Comments: Since the specific gravity of methane is less than 1, a methane leak will fill an entire enclosed space, while propane, with a specific gravity greater than 1, tends to settle to the bottom of the space. This effect produces fire hazards associated with methane leaks to be different from those for propane in an enclosed area. For methane, a spark anywhere could ignite an entire closed room, whereas for propane, the ignition would have to occur near the floor.

8.2 GASEOUS FUEL PROPERTIES

Recall from Chapters 1 and 7 that the specific gravity (*SG*) of gases and liquids is equal to the ratio of density for a particular fluid of interest to that of a reference compound. For liquids, the reference fluid is water; however, the reference for gases is air. Liquid density is only a function of temperature but, for gases, density is a function of both temperature and pressure and, therefore, the specific gravity of a gas is given as

$$SG_{\text{gas}} = \frac{\rho_{\text{fuel}} \langle 1 \text{ atm, } 15.56°\text{C } (60°\text{F}) \rangle}{\rho_{\text{air}} \langle 1 \text{ atm, } 15.56°\text{C } (60°\text{F}) \rangle} \tag{8.1}$$

If ideal-gas behavior is assumed, the molar density $\overline{\rho}$ of fuel gases is then equal to

$$\overline{\rho} = \frac{P}{\overline{R}T} \frac{\text{kgmole}}{\text{m}^3} \left(\frac{\text{lbmole}}{\text{ft}^3} \right) \tag{8.2}$$

and the specific gravity of these fuels is, therefore, equal to

$$SG_{\text{gas}} = \left[\left(\frac{MW}{\overline{R}} \right) \left(\frac{P}{T} \right) \right]_{\text{gas}} \left[\left(\frac{MW}{\overline{R}} \right) \left(\frac{P}{T} \right) \right]_{\text{air}} = \frac{MW_{\text{gas}}}{MW_{\text{air}}} \tag{8.3}$$

Equation (8.3) shows that a gaseous fuel having a specific gravity of less than 1.0 is lighter than air, whereas a fuel having a specific gravity greater than 1.0 is heavier than air. This property can be an important factor in the safety requirement for storing, handling, and even leakage considerations of a gaseous fuel; see Example 8.1. Table 8.1 lists specific gravities and critical constants for several gaseous fuels.

Constant-volume solid and liquid fuel bomb calorimetry, described in Chapter 6, is not used with gaseous fuels. Instead, gaseous fuel heating values are experimentally determined using the constant-pressure flow calorimeter shown in Figure 8.1. Gas and air are supplied at room temperature to the calorimeter unit. Energy released by burning gases is absorbed by cooling water flowing through a water jacket surrounding the burner. Regulated cooling water mass flow rate ensures that products of combustion exhaust from the calorimeter at room temperature. Precise measurement of the cooling water temperature rise and water mass flow rate allows experimental determination of the fuel energy release rate, i.e., kJ/sec (Btu/min). Gaseous fuel volumetric flow rates are obtained by use of a wet test meter. Flow calorimeters can experimentally measure heating values in a 3.7–120 MJ/m^3 (100–3,200 Btu/ft^3) range. An inability to maintain steady-state and steady-flow conditions, caused, for example, by fluctuations in water and/or gas source supply conditions as well as gas leaks within the calorimeter, can introduce significant experimental error and, hence, can predict erroneous heating values for a gaseous fuel.

The molar heat of combustion of methane, a major gaseous fuel constituent, is found in Table B.1 in Appendix B to equal

$$\overline{HHV}_{\text{CH}_4} = (212{,}800 \text{ cal/gmole})(4.187) = 890{,}994 \text{ kJ/kgmole} \tag{8.4a}$$

or

$$= (212{,}800 \text{ cal/gmole})(1.8001) = 383{,}040 \text{ Btu/lbmole} \tag{8.4b}$$

The molar density of methane at *STP* can be obtained from Equation (8.2) and is equal to

$$\overline{\rho}_{\text{CH}_4} = \frac{(101{,}000 \text{ N/m}^2)}{(8{,}314 \text{ N} \cdot \text{m/kgmole} \cdot \text{K})(298\text{K})} = 0.0408 \text{ kgmole/m}^3 \tag{8.5a}$$

Table 8.1 Gaseous Fuel Specific Gravities

		Critical constants		
			T	
	SG	*P*, atm	°C	(°F)
Paraffins				
Methane	0.554	45.8	–81.9	–116
Ethane	1.049	48.2	32.5	90
Propane	1.562	42.0	97.0	206
Butane (iso)	2.066	36.0	135.3	275
Butane (N)	2.066	37.5	152.6	306
Pentane (nee) 2.2-dimethyl propane	2.487	31.6	160.9	321
Pentane (iso) 2-methylbutane	2.487	32.9	188.1	370
Pentane (N)	2.487	33.3	197.0	386
Hexane (nee) 2.2-dimethylbutane	2.973	30.7	216.4	421
Hexane 2.3-dimethylbutane	2.973	30.9	227.6	441
Hexane (iso) 2-methylpentane	2.973	29.9	225.3	437
Hexane 3-methylpentane	2.973	30.8	231.4	448
Hexane (N)	2.973	–29.9	234.8	454
Heptane 2.2.3-dimethylbutane	3.459	–29.7	258.7	497
Heptane (iso) 2-methylhexane	3.459	27.2	258.1	496
Heptane (N)	3.459	27.0	267.6	513
Octane (iso) 2.2.4-trimethylpentane[a]	3.944	25.5	271.4	520
Octane 2.5-dimethylhexane	3.944	25.0	279.2	534
Octane (N)	3.944	24.6	296.4	565
Nonane (N)	4.428	22.5	322.0	611
Decane (N)	4.915	20.8	345.9	654
Naphtenes				
Cyclopropane	1.451	—	—	—
Cyclobutane	1.938	—	—	—
Cyclopentane	2.422	—	—	—
Cyclohexane	2.905	40.4	281.4	538
Olefins				
Ethylene-ethene	0.974	50.5	259.2	498
Propylene-propane	1.451	45.4	92.0	197
Butylene (iso) 2-methylpropane	1.934	39.5	145.3	293
Butylene (a) butene 1	1.934	39.7	147.0	296
Butylene (b) butene 2	2.004	40.8	155.3	311
Amylene (N) pentene 1	2.420	39.9	201.4	394
Diolefins				
Butadiene 1.3	1.869	42.7	152.6	306
Butadiene 1.2	1.869	—	—	—
Acetylene				
Acetylene-ethyne	0.911	61.6	36.4	97
Aromatics				
Benzene	2.692	48.6	289.8	553
Toluene-methylbenzene	3.176	40.1	321.4	610

Table 8.1 Continued

		Critical constants		
			T	
	SG	*P*, atm	°C	(°F)
Miscellaneous gases				
Air	1.000	37.2	–140.0	–221
Ammonia	0.596	111.5	132.6	270
Carbon monoxide	0.967	35.0	–138.6	–218
Carbon dioxide	1.528	72.9	31.4	88
Chlorine	2.449	76.0	144.2	291
Hydrogen	0.0696	12.8	–239.7	–400
Hydrogen sulfide	1.190	88.8	100.9	213
Nitrogen	0.972	33.5	–146.9	–233
Oxygen	1.105	49.7	–118.6	–182
Sulfur dioxide	2.44	77.8	157.6	315

[a]Refers to isooctane, used as a standard in fuel testing. Organic chemists apply the same name to 2-methylheptane.

Source: Cusick, C. F., Ed., *Flow Meter Engineering Handbook,* 3rd Edition, Minneapolis-Honeywell Regulator Company, Philadelphia, PA, 1961. With permission.

or

$$= \frac{(14.7\ \text{lbf/in}^2)(144\ \text{in}^2/\text{ft}^2)}{(1{,}454\ \text{ft}\cdot\text{lbf/lbmole}\cdot\text{R})(537\ ^\circ\text{R})} = 0.00255\ \text{lbmole/ft}^3 \tag{8.5b}$$

By combining Equations (8.4) and (8.5), the volumetric heating value for methane is given as

$$HHV_{CH4} = (890{,}994\ \text{kJ/kgmole})(0.0408\ \text{kgmole/m}^3) = 36{,}350\ \text{kJ/m}^3 \tag{8.6a}$$

$$= (383{,}040\ \text{Btu/lbmole})(0.00255\ \text{lbmole/ft}^3) = 977\ \text{Btu/ft}^3 \tag{8.6b}$$

The heating value of solid and liquid fuels is usually expressed in terms of a unit mass of fuel, whereas gaseous fuel heating values are most often specified on a per-unit volume basis. It is essential that energy reported for different fuels are compared on a consistent basis, i.e., per unit mole, unit volume, or unit mass. To illustrate, consider the molar heating values of methane and hydrogen:

$$\overline{HHV}_{CH_4} = 890{,}994\ \text{kJ/kgmole}\quad (383{,}040\ \text{Btu/lbmole}) \tag{8.7a}$$

and

$$\overline{HHV}_{H_2} = 286{,}043\ \text{kJ/kgmole}\quad (122{,}977\ \text{Btu/lbmole}) \tag{8.7b}$$

Equations (8.7a) and (8.7b) clearly show that, on a molar basis, methane has a greater heating value than hydrogen.

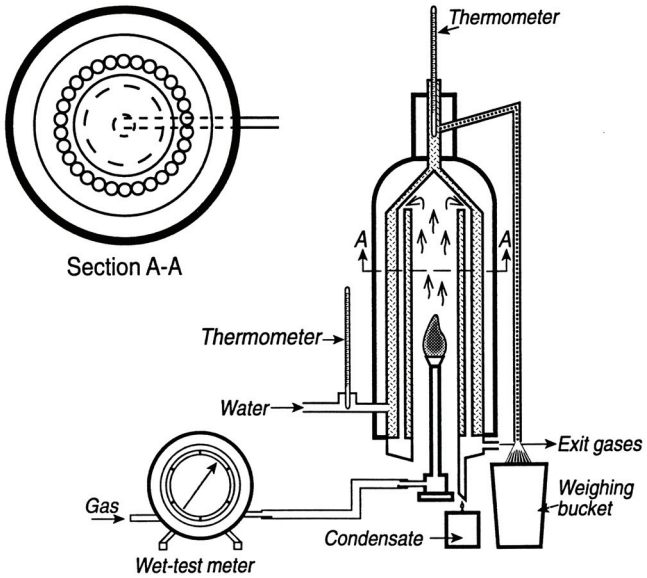

Figure 8.1 Constant-pressure flow calorimeter. Adapted from Smith, M. L. and Stinson, K. W., *Fuels and Combustion*, McGraw Hill Co., New York, 1952.

The heating value for these two fuels on a volumetric basis is equal to

$$HHV = \overline{HHV}\,\overline{\rho} \tag{8.8}$$

and

$$HHV_{CH_4} = (890{,}994)(0.0408) = 36{,}350 \text{ kJ/m}^3 \quad (977 \text{ Btu/ft}^3) \tag{8.8a}$$

$$HHV_{H_2} = (286{,}043)(0.0408) = 11{,}670 \text{ kJ/m}^3 \quad (314 \text{ Btu/ft}^3) \tag{8.8b}$$

Equations (8.8a) and (8.8b) show that, on a unit volume basis, methane also has a greater heating value than hydrogen.

Finally, the heating value for these two fuels on a mass basis is equal to

$$HHV = \frac{\overline{HHV}}{MW} \tag{8.9}$$

with

$$HHV_{CH_4} = 890{,}994/16 = 55{,}687 \text{ kJ/kg} \quad (23{,}940 \text{ Btu/lbm}) \tag{8.9a}$$

and

$$HHV_{H_2} = 286{,}043/2 = 143{,}022 \text{ kJ/kg} \quad (61{,}489 \text{ Btu/lbm}) \tag{8.9b}$$

Equations (8.8a) and (8.8b) indicate that, on a unit mass basis, however, hydrogen has a greater heating value than methane.

Propulsion heat engine fuel utilization usually involves vehicle weight and/or volume design restrictions. In these instances, the fuel-engine energy density requirements of such machinery may dictate the use of fuels having high heats of combustion on both a unit mass and volume basis. This suggests that gaseous fuels in *virgin form* may not be best suited to mobility power requirements but, instead, are more compatible with heating and stationary power needs. Hydrogen has been successfully stored in hydride form for mobility use.

When combustion characteristics of gaseous fuels are matched with a particular gas burner, the fuel-engine energy interface requirements cannot be based on simply selecting fuels having an equal heating value or specific gravity alone. In fact, in order to pass a constant energy rate through a given burner orifice, gaseous fuels with equal operating gas pressure levels and pressure drop across the orifice must have an equal *Wobble number,* W_0, where

$$W_0 = \frac{\text{higher heating value of gaseous fuel}}{\sqrt{SG}} \tag{8.10}$$

EXAMPLE 8.2 Hydrogen has been suggested to be a potential long-term replacement for natural gas. Considering methane to represent natural gas, calculate the heating value per unit volume, kJ/m, specific gravity, and Wobble number, kJ/m^3, for (a) 100% CH_4, (b) 75% CH_4–25% H_2, (e) 50% CH_4–50% H_2, (d) 25% CH_4–75% H_2, and (e) 100% H_2 on a volumetric basis.

Solution:

1. Molar density for $P = \bar{\rho}\bar{R}T$:

$$\bar{\rho} = 101{,}000 \text{ N/m}^2 / (8{,}314 \text{ N} \cdot \text{m/kgmole} \cdot \text{K})(298\text{K})$$
$$= 0.04077 \text{ kgmole/m}^3$$

2. Heating value for CH_4-H_2 mixture, using Table B.1 in Appendix B:

$$\overline{HHV}_{CH_4} = 212{,}800 \text{ cal/gmole} \qquad \overline{HHV}_{H_2} = 68{,}317 \text{ cal/gmole}$$

and

$$HHV_{CH_4} = (212{,}800)(4.187 \text{ kJ/kgmole})(0.04077 \text{ kgmole/m}^3)$$
$$= 36{,}320 \text{ kJ/m}^3$$
$$HHV_{H_2} = (68{,}317)(4.187)(0.4077) = 11{,}660 \text{ kJ/m}^3$$

where

$$HHV_{mixt} = \bar{x}_{CH_4} HHV_{CH_4} + (1 - \bar{x}_{CH_4}) HHV_{H_2}$$

a.

$\bar{x}_{CH_4}$	$\bar{x}_{H_2}$	$HHV\left\langle \mathrm{kJ/m^3} \right\rangle$
1.00	0	36,320
0.75	0.25	30,155
0.50	0.50	23,990
0.25	0.75	17,825
0	1.00	11,660

3. Specific gravity for CH_4-H_2 mixture:

$$SG = [MW_{\text{mixt}} / MW_{\text{air}}]$$

where

$$MW_{\text{mixt}} = \bar{x}_{CH_4} MW_{CH_4} + (1 - \bar{x}_{CH_4}) MW_{H_2}$$

b.

$\bar{x}_{CH_4}$	$\bar{x}_{H_2}$	MW	SG
1.00	0	16.0	0.552
0.75	0.25	12.5	0.432
0.50	0.50	9.0	0.311
0.25	0.75	5.5	0.190
0	1.00	2.0	0.069

4. Wobble number for CH_4-H_2 mixture:

$$W_0 = HHV / \sqrt{SG}$$

c.

$\bar{x}_{CH_4}$	$\bar{x}_{H_2}$	W_0
1.00	0	48,890
0.75	0.25	45,880
0.50	0.50	43,020
0.25	0.75	40,890
0	1.00	44,390

Comments: A review of these results shows that the energy density per unit volume decreases as hydrogen is substituted for methane to almost one-third the original value; the specific gravity also drops as hydrogen substitution increases. However, the Wobble number remains fairly constant for the different CH_4-H_2 mole fractions.

Gaseous fuels have a greater role as a stationary power fuel because of environmental benefits associated with their clean burning benefits, but must be weighed against the energy costs placed on economic premiums of all fuel alternatives. The concentrations of CO, CO_2, and O_2 in the exhaust from natural gas and even oil-fired boilers and furnaces were historically measured by chemical absorption devices such as the classic Orsat analyzer shown in Figure 8.2. Many boiler applications can maintain efficient burner stoichiometry for operation by major exhaust, or flue gas composition measurements via an Orsat in conjunction with the boiler energy balance presented in Chapter 6.

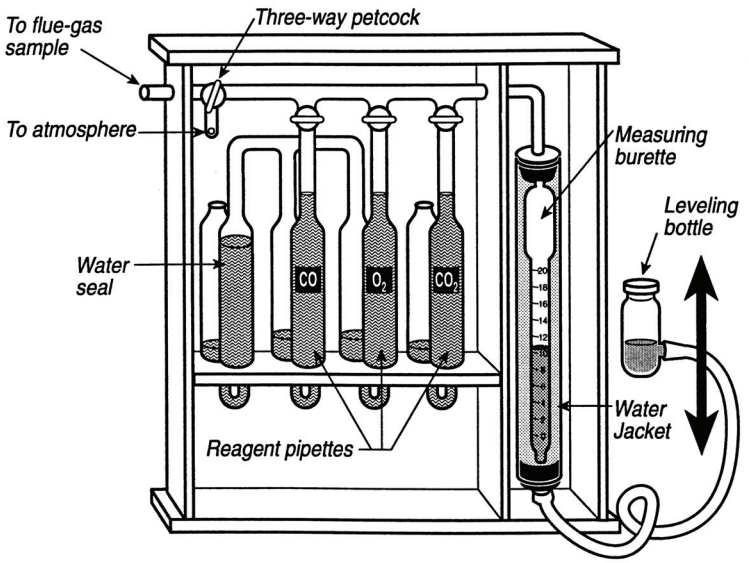

Figure 8.2 Orsat flue gas analyzer. Adapted from Smith, M. L. and Stinson, K. W. *Fuels and Combustion*, McGraw Hill Co., New York, 1952.

A 100-ml flue gas sample can be drawn into an Orsat apparatus for analysis by lowering a displacing water bottle, which changes the hydrostatic head in the sampling loop. During fill, all the reagent bottle valves, as well as the atmospheric vent line valves, are closed. After the 100-ml volume is filled with exhaust, the sample line is closed, and the valve to the CO_2 absorbent is then opened. The water-leveling bottle is raised until 100 ml of gas is passed into the CO_2 absorbent, a 20% aqueous solution of potassium hydride. When the water-leveling bottle is returned to its original position, the reduction in the original 100-ml volume can be measured and is equal to the volume of CO_2 in the original gas mixture sample. This process is repeated several times to ensure complete CO_2 removal. Next, oxygen is removed by passing the gas sample back and forth several times between the 100-ml sample volume and the second reagent bottle, which contains an aqueous alkaline solution of pyrogallic acid. The percentage of oxygen by volume in the original gas sample is determined by noting an additional reduction of the remaining gas contained in the 100-ml sample volume. The last reagent pipette contains an aqueous solution of cuprous chloride, which absorbs CO and allows the volume percentage of CO in the sample to be determined as well. This order of absorption is critical to ensure

reliable results. The Orsat analysis yields a dry product analysis, as shown in Example 8.3, and assumes that the remaining gas is N_2. More complex and sensitive methods of detection, such as ultraviolet and infrared emissions spectroscopy, ultraviolet absorption spectroscopy, and mass spectrometry, which are used to determine the presence of minute amounts of unburned hydrocarbons and nitric oxides, are used.

EXAMPLE 8.3 An exhaust gas sample consists of the following numbers of moles of gaseous species:

Moles $CO_2 = N_1$
Moles $CO = N_2$
Moles $H_2O = N_3$
Moles $O_2 = N_4$
Moles $N_2 = N_5$

The sample is analyzed using an Orsat analyzer. Show that the actual volumetric analysis for CO_2 (using an Orsat apparatus) equals the sample volume of CO_2, based on a dry analysis of the products.

Solution:

1. Initial total gas sample volume:

$$P_{\text{tot}}V_{\text{tot}} = N_{\text{tot}}\overline{R}T$$

where

$$\begin{aligned} P_{\text{tot}} &= 1\,\text{atm} = \text{constant during the analysis} \\ T &= \text{constant during analysis} \\ V_{\text{tot}} &= 100 \text{ units} \\ N_{\text{tot}} &= N_1 + N_2 + N_3 + N_4 + N_5 \\ P_{\text{tot}}V_{\text{tot}} &= (N_1 + N_2 + N_3 + N_4 + N_5)\overline{R}T \end{aligned}$$

2. Since liquid and water vapor are in direct contact during the entire analysis, the partial pressure of the water vapor remains constant in the apparatus, or

$$P_{H_2O} = P_{\text{sat}}\langle T\rangle = \text{const}$$

thus,

$$\overline{x}_{H_2O} = \frac{P_{H_2O}}{P_{\text{tot}}} = \frac{N_3}{N_1 + N_2 + N_3 + N_4 + N_5} = \frac{N_3'}{N_2 + N_3' + N_4 + N_5}$$

NOTE: N_{tot} is changing because of the absorption of CO_2 and, thus, the moles of water vapor, N_{H_2O}, also have to change.

3. Total gas sample after removal of CO_2:

$$P_{tot}V_1 = (N_2 + N_3' + N_4 + N_5)\overline{R}T$$

where

$$N_3' = \text{moles of } H_2O \text{ after } CO_2 \text{ analysis} \neq N_3$$

4. Volume percent associated with CO_2 removal:

$$\%\,CO_2 = \left[\frac{V_{tot} - V_1}{V_{tot}}\right] \times 100$$

$$V_{tot} = \frac{[N_1 + N_2 + N_3 + N_4 + N_5]\overline{R}T}{P_{tot}}$$

and

$$V_1 = \frac{[N_2 + N_3' + N_4 + N_5]\overline{R}T}{P_{tot}}$$

where

$$\left[\frac{V_{tot} - V_1}{V_{tot}}\right] = \frac{(N_1 + N_2 + N_3 + N_4 + N_5) - (N_2 + N_3' + N_4 + N_5)}{(N_1 + N_2 + N_3 + N_4 + N_5)}$$

$$\left[\frac{V_{tot} - V_1}{V_{tot}}\right] = \frac{N_1 + N_3 - N_3'}{(N_1 + N_2 + N_3 + N_4 + N_5)}$$

$$= \frac{N_1 + N_3 - [(N_2 + N_4 + N_5)/(N_1 + N_2 + N_4 + N_5)]N_3}{(N_1 + N_2 + N_3 + N_4 + N_5)}$$

$$= \frac{N_1(N_1 + N_2 + N_3 + N_4 + N_5)/(N_1 + N_2 + N_4 + N_5)}{(N_1 + N_2 + N_3 + N_4 + N_5)}$$

$$= \frac{N_1}{N_1 + N_2 + N_4 + N_5} = \bar{x}_{CO_2}\Big)_{\text{dry basis}}$$

Table 8.2 Gaseoues Fuel Characteristics

Type	CO_2	O_2	N_2	CO	H_2	CH_4	C_2H_6	C_3H_8	C_4H_{10}	Illumi-nants and Others	*SG*	Heating Value kJ/m^3 Gross	Heating Value kJ/m^3 Net	Heating Value Btu/ft^3 Gross	Heating Value Btu/ft^3 Net
Natural	....	....	5.0	....	....	90.0	5.0	....	....	....	0.60	37,300	33,680	1,002	904
Natural	....	....	0.8	....	....	83.4	15.8	....	....	....	0.61	42,060	38,030	1,129	1,021
Natural	6.5	....	....	....	....	77.5	16.0	....	....	....	0.70	39,970	36,170	1,073	971
Natural	0.8	....	8.4	....	....	84.1	6.7	....	....	....	0.63	36,280	32,740	974	879
Natural	....	....	....	....	....	36.7	14.5	23.5	14.9	10.4*	1.29	79,460	72,980	2,133	1,959
Propane	....	....	....	....	....	....	2.2	97.3	0.5	....	1.55	95,290	87,840	2,558	2,358
Propane	....	....	....	....	....	....	2.0	72.9	0.8	24.3#	1.77	93,280	86,280	2,504	2,316
Butane	....	....	....	....	....	....	....	6.0	94.0	....	2.04	119,580	110,300	3,210	2,961
Butane	....	....	....	....	....	....	....	5.0	66.7	28.3§	2.00	118,610	109,300	3,184	2,935
Refinery oil	....	0.2	0.6	1.2	6.1	4.4	72.5	....	....	....	1.00	61,470	56,770	1,650	1,524
Refinery oil	0.2	0.2	0.5	1.2	13.1	23.3	21.9	....	....	39.6	0.89	54,950	50,330	1,475	1,351
Oil gas	1.2	0.5	2.4	7.7	54.2	30.1	....	....	....	3.9	0.37	21,230	19,000	570	510
Coal gas	2.4	0.8	11.3	7.4	48.0	27.1	....	....	....	3.0	0.47	20,190	18,100	542	486
Coal gas	1.7	0.8	8.1	7.3	49.5	29.2	....	....	....	3.4	0.47	22,310	20,120	599	540
Coal gas	2.1	0.4	4.4	13.5	51.9	24.3	....	....	....	3.4	0.42	19,370	17,360	520	466
Coke oven	2.2	0.8	8.1	6.3	46.5	32.1	....	....	....	4.0	0.44	21,200	18,960	569	509
Producer	8.0	0.1	50.0	23.2	17.7	1.0	....	....	....	....	0.86	5,330	4,950	143	133
Producer	4.5	0.6	50.9	27.0	14.0	3.0	....	....	....	....	0.86	6,070	5,700	163	153
Blast furnace	11.5	....	60.0	27.5	1.0	....	....	....	....	....	1.02	3,430	3,430	92	92
Blue gas (water gas)	5.4	0.7	8.3	37.0	47.3	1.3	....	....	....	....	0.57	10,690	9,760	287	262
Blue gas (water gas)	5.5	0.9	27.6	28.2	32.5	4.6	....	....	....	0.7	0.70	9,690	8,900	260	239
Carbureted water	3.6	0.4	5.0	21.9	49.6	10.6	2.5	....	....	6.1	0.54	19,970	17,170	536	461
Carbureted water	6.0	0.9	12.4	26.8	32.2	13.5	....	....	....	8.2	0.66	19,740	16,800	530	451
Carbureted water	0.7	0.3	5.8	11.7	28.0	36.1	....	....	....	17.4	0.63	31,290	28,680	840	770
Sewage	22.0	....	6.0	....	2.0	68.0	....	....	....	....	0.79	25,700	23,130	690	621

Source: American Gas Association, 1948. Used by permission of the copyright holder.

*C_5H_{12} #C_3H_6 §C_4H_8 ‖ At 60 and 30 in. Hg.

8.3 NATURAL GAS

The world's most readily available and abundant gaseous fuel resources are found in *natural gas* reserves. Gaseous fuels have been used for centuries in China and for over 100 years in both the United States and Europe. In the United States, when natural gas was originally discovered at oil wells, it was burned, or *flared off*, as a useless by-product of oil production. Today, natural gas is a major industry that transports fuel throughout the United States by a complex interstate pipeline network. Natural gas was formed by *anaerobic,* or bacterial-assisted, decomposition of organic matter under heat and pressure and, therefore, like coal and crude oil, is a variable-composition hydrocarbon fuel. Table 8.2 lists properties of certain natural and synthetic gas resources. Synthetic natural gas (SNG) production and anaerobic digester technology will be discussed in Sections 8.4 and 8.5.

Natural gas consists chiefly of methane, ranging anywhere from 75% to 99% by volume, with varying concentrations of low molecular weight hydrocarbons, CO, CO_2, He, N_2, and/or H_2O. Conventional gas well drilling has proved successful in or near oil fields. New and additional unconventional drilling methods are finding reserves in deep wells and coal beds, as well as in shale and tar sands. Natural gas is practically colorless and odorless and, for safety reasons, is "soured" with the familiar rotten egg odor by adding hydrogen sulfide, H_2S. The American Gas Association classifies natural gas as sweet or sour gas and, additionally, as being associated or nonassociated gas. Associated, or *wet,* gas is either dissolved in crude oil reserves or confined in pressurized gas caps located on the top of oil ponds. Wet gas has appreciable concentrations of ethene, butene, propane, propylene, and butylenes. Nonassociated, or *dry,* gas can be found in gas pockets trapped under high pressure that have migrated from oil ponds or are the results of an early coalization gasification stage. Natural gas, like coal and oil, has regional characteristics. For example, western U.S. natural gas fields generally contain substantial amounts of CO_2, Midwestern reserves have higher N_2 concentrations and some He, and eastern gas is high in paraffins. European gas reserves are basically high in CO_2, H_2, and olefinic hydrocarbons.

Liquid petroleum gas, or LPG, consists of condensable hydrocarbon vapors recovered by expansion of wet gas reserves. By compressing the condensable fractions, liquefied fuel vapors, such as commercial propane and butane, can be stored and transported at ambient temperatures as a liquid. Liquefied natural gas, LNG, is the condensed state of dry natural gas but requires a cryogenic refrigeration for storage and handling at –102°C (–260°F). Efficient transportation of large Middle Eastern natural gas to the United States, Europe, and Asia by sea would require use of specially designed LNG tankers.

EXAMPLE 8.4 A natural gas has a volumetric analysis of 95% CH_4, 3% C_2H_6, and 2% CO_2. For conditions of 14.7 psia and 77°F, calculate (a) the higher heating value of the fuel, Btu/ft^3 of gas; and (b) the lower heating value of the fuel, Btu/ft^3 of gas.

Solution:

1. Stoichiometric equation:

$$[0.95\ CH_4 + 0.03\ C_2H_6 + 0.02\ CO_2] + a[O_2 + 3.76\ N_2] \rightarrow bCO_2 + cH_2O + d\,N_2$$

Carbon atom balance:

$$0.02 + 0.95 + 0.06 = b = 1.03$$

Hydrogen atom balance:

$$(4)(0.95) + (6)(0.03) = 2c \qquad c = 1.99$$

Oxygen atom balance:

$$(2)(0.02) + 2a = (2)(1.03) + 1.99 \qquad a = 2.005$$

Nitrogen atom balance:

$$d = 3.76a = (3.76)(2.005) = 7.539$$

2. Energy balance:

$$Q = \sum_{i=\text{prod}} N_i[\bar{h}_f^0 + \Delta\bar{h}]_i = \sum_{j=\text{react}} N_j[\bar{h}_f^0 + \Delta\bar{h}]_j$$

or

$$\begin{aligned} Q = {} & 1.03[\bar{h}_f^0 + \Delta\bar{h}]_{CO_2} + 1.99[\bar{h}_f^0 + \Delta\bar{h}]_{H_2O_l} \\ & + (3.76)(2.005)[\bar{h}_f^0 + \Delta\bar{h}]_{N_2} - 0.95[\bar{h}_f^0 + \Delta\bar{h}]_{CH_4} \\ & - 0.03[\bar{h}_f^0 + \Delta\bar{h}]_{C_2H_6} - 0.02[\bar{h}_f^0 + \Delta\bar{h}]_{CO_2} \\ & - 2.005[\bar{h}_f^0 + \Delta\bar{h}]_{O_2} - (2.005)(3.76)[\bar{h}_f^0 + \Delta\bar{h}]_{N_2} \end{aligned}$$

Recall that the higher heating value assumes water in the products is a liquid.

From Table B.1 in Appendix B,

$$\begin{aligned} Q = {} & (1.03)(-94{,}054) + 1.99(-68{,}317) - 0.95(-17{,}889) \\ & - 0.03(-20{,}236) - 0.02(-94{,}054) = -213{,}344 \end{aligned}$$

$$\begin{aligned} \overline{HHV} &= 213{,}340 \text{ cal/gmole} \\ &= (213{,}340 \text{ cal/gmole})(1.8001 \frac{\text{Btu/lbmole}}{\text{cal/gmole}}) \\ &= 384{,}033 \text{ Btu/lbmole} \end{aligned}$$

3. Density, *fuel*:

$$\overline{\rho} = \frac{P}{\overline{R}T} = \frac{(14.7\ \text{lbf/in}^2)(144\ \text{in.}^2/\text{ft}^2)}{(1{,}545\ \text{ft}\cdot\text{lbf/lbmole}\cdot°\text{R})(537°\text{R})}$$
$$= 0.00255\ \text{lbmole/ft}^3$$

4. Higher heating value, *water as liquid in product*:

$$HHV = (384{,}033\ \text{Btu/lbmole})(0.00255\ \text{lbmole/ft}^3)$$

a. $HHV = 980\ \text{Btu/ft}^3$

5. Lower heating value, *water as vapor in product*:

$$LHV = HHV - 1.99\, h_{fg}\langle 68°F\rangle$$
$$LHV = +384{,}033\ \text{Btu/lbmole fuel}$$
$$- \left(1.99\frac{\text{lbmole } H_2O}{\text{lbmole fuel}}\right)\left(1{,}054\frac{\text{Btu}}{\text{lbm } H_2O}\right)\left(18\frac{\text{lbm}}{\text{lbmole } H_2O}\right)$$

b. $LHV = 346{,}279\ \text{Btu/lbmole}$

8.4 COAL-DERIVED GASEOUS FUELS

Synthetic, or manufactured, gaseous fuels have been generated using coal resources for more than 100 years. *Coke* and *coke gas,* by-products of coal used in the iron industry, were produced as early as the eighteenth century. *Towngas,* a commercial and residential grade "low-Btu" fuel, was used during the late nineteenth and early twentieth centuries until replaced by electric power as well as by the oil and natural gas industries. Most coal-derived fuel gas technologies fall into one of three general categories: coal pyrolysis, coal gasification, or coal catalytic synthesis. Today, many factors point toward a need for redeveloping a coal-derived syngas industry. These factors include:

Large U. S. coal reserves ill suited for direct combustion
Environmental pressure for greater coal combustion pollution abatement
Sulfur removal as H_2S during gasification versus sulfur generation as SO_2 during combustion
Market for clean-burning, coal-based fuel gas in stationary power plants
Transportable
Synthetic gaseous fuel via pipelines

Coal is a poor feedstock, however, for making a commercially viable gaseous fuel, in part because of the following properties:

Natural occurrence as a solid
Variable and nonuniform nature
Poor conversion energetics and economics
Lower overall gasification energy efficiencies as compared to direct combustion efficiencies

Carbonization, or pyrolysis, is a destructive thermal distillation process in which volatile combustible fractions contained in raw coal or coke (such as hydrogen, methane, ethyene, and carbon monoxide) are driven off. Yields are relatively low with 70 wt % of the original coal remaining as a solid residue after devolatilization. To release gases, coal or coke is placed in a closed vessel, or *retort,* and heated by external coal combustion to a temperature range of 530–1,000ºC (985–1,830ºF). Coal and coke gas have properties that are a function of the particular coal supply, actual pyrolysis temperature, specific type of retort being used, and total residence time of reactants within the vessel. These gas energy volumes cover the range 18,630–24,220 kJ/m^3 (500–650 Btu/ft^3).

An alternate means of producing syngas is by partial combustion and thermal cracking of an incandescent solid fuel bed of coal, coke, peat, or even wood with air. *Producer gas,* for example, is generated by fuel-lean combustion, which occurs in a reacting bed of coal or coke. The initial stages of gasification result from partial combustion of the bottom coal to yield carbon dioxide and heat (see Figure 8.3). Thermodynamically, this process can be represented by the reaction

$$C_S + O_2 \rightarrow CO_2 + \text{heat} \tag{8.11}$$

Exothermic reactions within the remaining coal bed with carbon dioxide and heat then produce carbon monoxide or

$$\text{Heat} + C_S + CO_2 \rightarrow 2CO \tag{8.12}$$

Overall, then, the gasification of coal can be expressed as

$$2C_S + O_2 \rightarrow 2CO \tag{8.13}$$

Producer gas has a low energy volume of 5,220–6,700 kJ/m^3 (140–180 Btu/ ft^3) because of a high percentage of nitrogen present in the gas, approximately 50 vol %.

The low yields of gas resulting from coal pyrolysis and the relatively low energy content of producer gas, approximately 10–20% that of natural gas, limit their use to special applications at local production sites. One means of upgrading producer gas, for example, would be to reduce the mole fraction of nitrogen in product gas by using oxygen instead of air. Steam-cracking coal at elevated temperature and pressure generates *carbureted water gas,* a synthesis gas that also has a lower nitrogen content and, therefore, greater energy volume than producer gas. Carbureted water gas production is initiated by blowing pyrolysis air through coal for 1–2 min, followed in turn by a 2–4 min blast of steam through the incandescent bed to hydrogasify the coal. This entire process is repeated continuously to produce a steady stream of gas having an energy volume of approximately 10,060 kJ/m^3 (270 Btu/ft^3) (see Figure 8.4). Steam cracking or reforming of coal can be represented thermodynamically by the equilibrium reaction

$$C_S + H_2O \overset{T,P}{\leftrightarrows} CO + H_2 \tag{8.14}$$

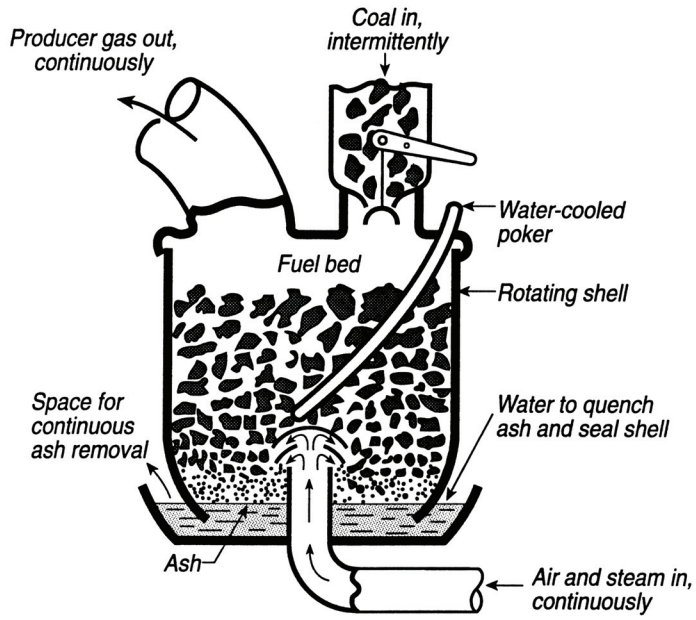

Figure 8.3 Producer gas generator. Adapted from Smith, M. L. and Stinson, K. W., *Fuels and Combustion*, McGraw Hill Co., New York, 1952.

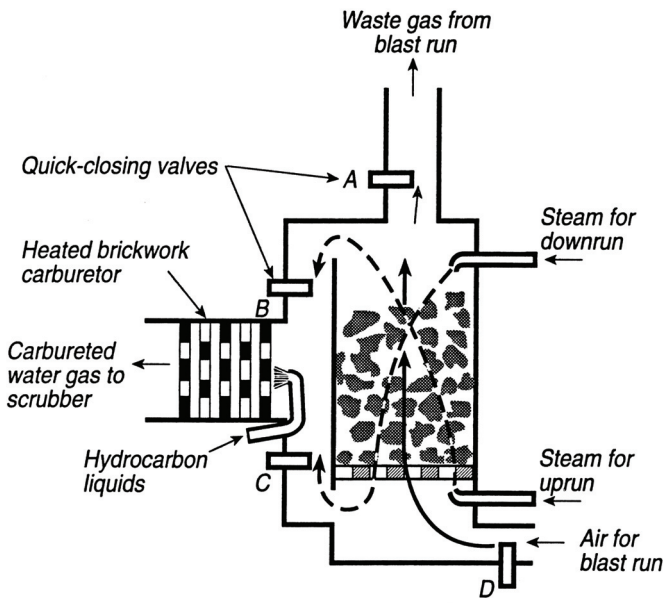

Figure 8.4 Carbureted water gas generator. Adapted from Smith, M. L. and Stinson, K. W., *Fuels and Combustion*, McGraw Hill Co., New York, 1952.

Oil gas or fuel oil can be sprayed into carbureted water gas during processing to further raise the heating value to 18,630–22,350 kJ/m^3 (500–600 Btu/ft^3). Carbureted water gas is often referred to as *blue gas* since carbon monoxide in this gaseous fuel burns with a characteristic short blue flame.

Russian engineering in the 1930s pioneered underground hydrogasification of coal by injecting steam directly into coal beds. By 1938, this technique was supplying coal gas on a commercial basis within the Soviet Union. This technology has been considered by the U.S. coal industry as a potential method for utilizing the vast reserves of relatively low-grade, environmentally unburnable western coal. However, because of the large amount of water required, the limited availability of usable water resources in the region, and the world's growing critical water crisis, this is a questionable technology for gasifying U.S. coal.

Producer gas, a "low-Btu" coal gas made with nineteenth-century coal conversion technology, cannot be economically transported and, therefore, is not a viable substitute for natural gas. A full-scale commercial industry that could supply a coal-derived *synthetic natural gas,* SNG, would require large water and energy inputs, along with development of more complex and yet unproven commercialized technologies. Environmental concerns over burning high-sulfur coal may spur development of this alternate coal utilization even though SNG will be more expensive and less efficient than direct combustion of coal. In addition, future depletion of both proven and projected natural gas reserves would impact existing gas supplies and pipeline distribution.

EXAMPLE 8.5 One mole of CO and 220% theoretical oxygen, both at 25ºC, undergo a steady flow reaction at 1-atm pressure. Neglecting dissociation of O_2, determine (a) the final equilibrium composition, and (b) the final temperature if the process is adiabatic.

Solution:

1. Stoichiometric reaction:

   $$CO + \tfrac{1}{2}\, O_2 \rightarrow CO_2$$

2. Actual reaction:

   $$CO + (2.2)(0.5)O_2 \rightarrow aO_2 + bCO + cCO_2$$

   Carbon atom balance:

   $$1 = b + c$$

   Oxygen atom balance:

   $$3.2 = 2a + b + 2c$$
   $$3.2 = 2a - b + 2$$
   $$1.2 = 2a - b$$

3. Energy balance for $P = C$ (adiabatic):

   $$dE = \delta Q - \delta W + \Sigma N_i \bar{e}_i - \Sigma N_j \bar{e}_j$$
   $$\Sigma N_i \bar{e}_i = \Sigma N_j \bar{e}_j$$

$$[\bar{h}_f^0 + \Delta\bar{h}]_{CO} + 1.1[\bar{h}_f^0 + \Delta\bar{h}]_{O_2} = a[\bar{h}_f^0 + \Delta\bar{h}]_{O_2} + b[\bar{h}_f^0 + \Delta\bar{h}]_{CO} + c[\bar{h}_f^0 + \Delta\bar{h}]_{CO_2}$$

4. Equilibrium constant:

$$CO + \tfrac{1}{2}O_2 \leftrightarrows CO_2$$

$$\log K_p = \log K_P)_{CO_2} - \tfrac{1}{2}\log K_p)_{O_2} - \log K_p)_{CO}$$

and

$$K_P = \frac{[P/P_0]_{CO_2}}{[P/P_0]_{O_2}^{1/2}[P/P_0]_{CO}} = \left[\frac{P_{CO_2}}{P_{O_2}^{1/2}P_{CO}}\right]P_0^{-1/2}$$

Now,

$$P_0 \equiv 1 \text{ atm} = P_{tot}$$

and

$$P_i = \bar{x}_i P_{tot}$$

$$\bar{x}_{O_2} = \frac{a}{a + b + c}$$

$$\bar{x}_{CO} = \frac{b}{a + b + c}$$

$$\bar{x}_{CO_2} = \frac{c}{a + b + c}$$

or

$$K_p = \frac{(c)(a + b + c)^{1/2}}{(a)^{1/2}(b)}$$

5. From item 2, then, one can eliminate b and c, obtaining

$$a = a$$

$$b = 2a - 1.2$$

$$c = 2.2 - 2a$$

and

$$K_p = \frac{(2.2 - 2a)(a + 1)^{1/2}}{a^{1/2}(2a - 1.2)}$$

6. Since the final state is unknown, i.e., T_2, *a, b,* and *c*, an iterative technique is required for solution.

7. Initial guess for $T_2 = 2{,}800$K:
Energy balance using data found in Table B.1 in Appendix B:

$$-26{,}416 = a(+21{,}545) + (2a - 1.2)(-26{,}416 + 20{,}582) + (2.2 - 2a)(-94{,}051 + 33{,}567)$$

or

$$a = 0.762$$

Equilibrium constant:

$$K_p = \frac{[(2.2) - (2)(0.762)][1.762]^{1/2}}{[0.762]^{1/2}[(2)(0.762) - 1.2]} = 3.173$$

From Tables B.4 and B.5 in Appendix B,

$$\log K_p = 7.388 - 6.563 = 0.825$$
$$K_p = 6.683$$

8. Second estimation for $T_2 = 3{,}000$K:

$$-26{,}416 = a(23{,}446) + (2a - 1.2)(-26{,}416 + 22{,}357) + (2.2 - 2a)(-94{,}051 + 36{,}535)$$
$$a = 0.731$$

Equilibrium constant:

$$K_p = \frac{[2.2 - (2)(0.731)][1.731]^{1/2}}{[0.731]^{1/2}[(2)(0.731) - 1.2]} = 4.335$$
$$\log K_p = 6.892 - 6.407 - 0.485$$
$$K_P = 3.055$$

9. Third estimation for $T_3 = 2{,}900$K:

$$-26{,}416 = a(22{,}493) + (2a - 1.2)(-26{,}416 + 21{,}469) + (2.2 - 2a)(-94{,}051 + 35{,}049)$$
$$a = 0.746$$

Equilibrium constant:

$$K_p = \frac{[2.2 - (2)(0.746)][1.746]^{1/2}}{[0.746]^{1/2}[(2)(0.746) - 1.2]} = 3.709$$
$$\log K_p = 7.132 - 6.483 = 0.649$$
$$K_p = 4.46$$

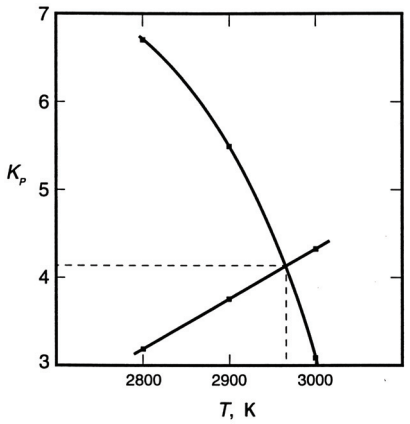

10. From the graph, $T_2 \sim 2{,}970$K:

$a \sim 0.740$
$b \sim 0.280$
$c \sim 0.720$

or

$$CO + 2.2\ O_2 \rightarrow 0.740\ O_2 + 0.280\ CO + 0.72\ CO_2$$

There are no known direct coal-methanization conversion processes. The overall equilibrium reaction

$$C_S + 2H_2O_g \leftrightarrows CH_4 + CO_2 \tag{8.15}$$

suggests favorable thermodynamics in that the heat of reaction is approximately zero, but no catalyst has been found that will allow this overall process to occur. Bioconversion of cellulose and other organic materials, covered in the next section, can generate methane directly.

Current and conversion technologies require pretreatment gasification and methanization in order to produce a pipeline-quality SNG (Figure 8.5). Development and application of various designs will differ in their coal selection as well as the means they use to introduce coal and either air or oxygen into the gasifier. Pretreatment of coals that cake requires mild oxidation to prevent caking during gasification. Gasification begins with heating and drying of the coal. Devolatilization or distillation will drive off evolved gases, with the initial heating raising the coal to near its softening temperature. Chemical conversion reacts coal with oxygen, or air, and steam. Recall that this chemical conversion will yield a low-Btu product if air is used, while a low-nitrogen or medium-Btu gas will be produced with the use of oxygen or water. The degree of chemical conversion is related to equilibrium shifts in the products CO, CH_4, and H_2 or

$$2C + O_2 \leftrightarrows 2CO_2 \tag{8.16}$$

$$C + H_2O \leftrightarrows CO + H_2 \tag{8.17}$$

$$C + CO_2 \leftrightarrows 2CO \tag{8.18}$$

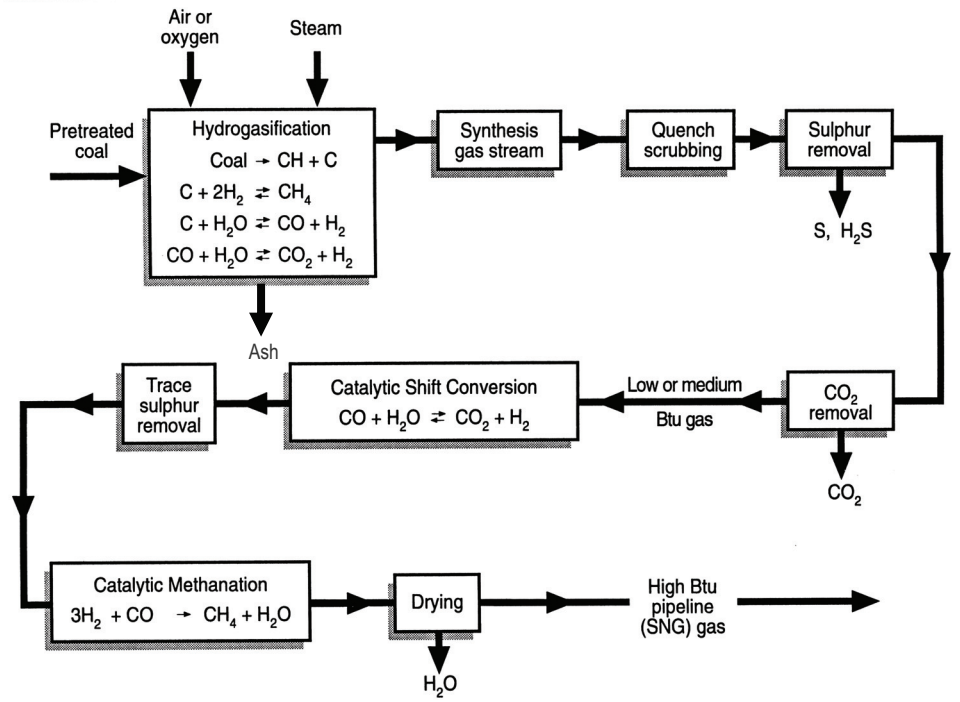

Figure 8.5 Coal gasification schematic. Adapted from *Department of the Navy Energy Fact Book*, Report No. TT-A-6054-79-403, 1979.

Several coal gasifiers are being commercially developed and include fixed or moving beds, entrained flow, fluidized beds, and molten bed systems. The Lurgi fixed-bed gasification technique feeds coal at the top of a gasifier, with steam or air supplied at the bottom, allowing gasification to occur as the coal passes down through the gasifier; see Figure 8.6. The Kopper, an entrained flow system, feeds a mixture of pulverized coal and air/steam or oxygen/steam to the gasifier. Gasifiers can be further categorized as either slagging or dry, depending on whether they are operated above or below ash fusion temperature. Coal gasification chemically reduces sulfur to hydrogen sulfide, H_2S, during the pyrolysis stage. Extraction of H_2S yields a sulfur-free synthesis gas.

Catalytic methanization of synthesis gas is required to produce an SNG of approximately 95–98% methane and occurs via the reaction

$$CO + 3H_2 \rightleftarrows CH_4 + H_2O \tag{8.19}$$

The major thrust of current coal gasification programs is to optimize methane production by conducting hydrogasification at much higher pressures and temperatures than those used in traditional coal gas production. Future technological breakthroughs are hampered by the very complex, non-uniform, and variable composition of U.S. coal resources. Development of coal-based SNG having pipeline quality will be strongly influenced by the going price of energy alternatives and the ready availability of alternate gas resources.

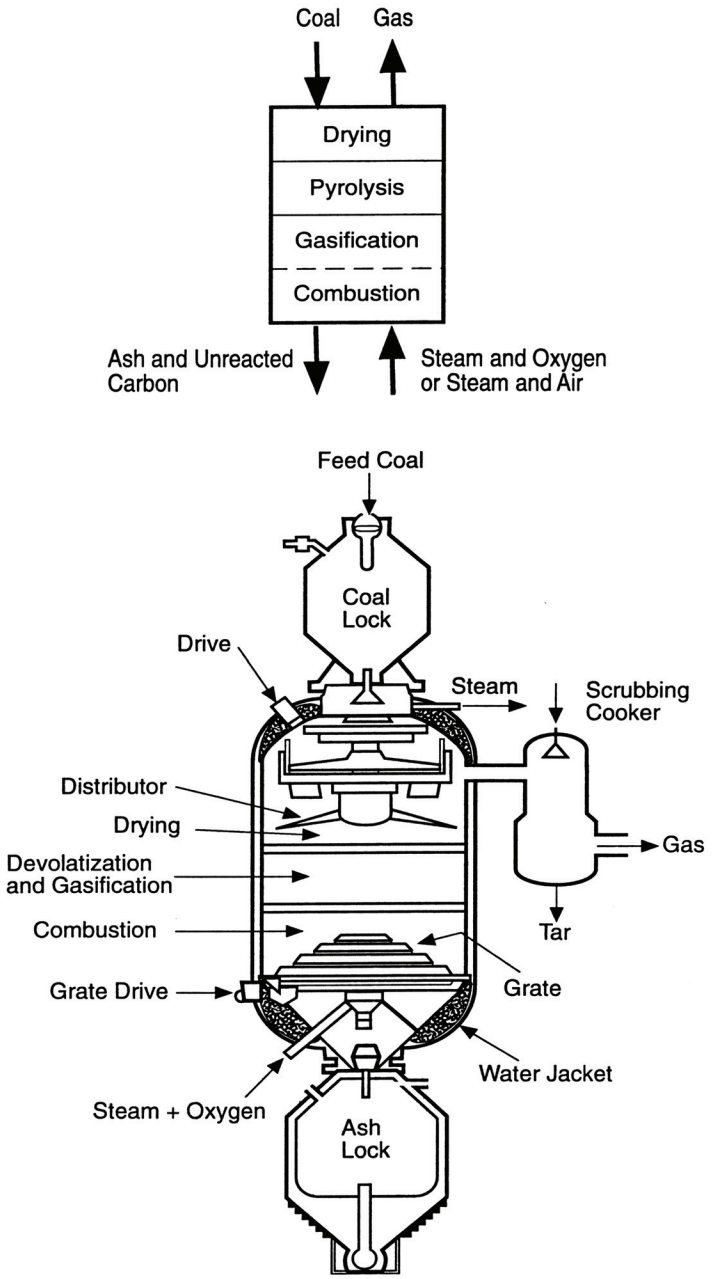

Figure 8.6 Lurgi coal gasification. *Source*: Hammond, A. L., Metz, W. D., and Maugh II, T. H., *Energy and the Future*, American Association for the Advancement of Science, Washington, DC, 1973, 120. With permission of author.

8.5 BIOMASS AND SYNTHETIC NATURAL GAS

Resources other than coal or crude oil can be used as feedstock for generating a synthetic gaseous fuel. This synthetic natural gas, or *biogas,* can be produced from a variety of organic materials, including vegetation, animal and plant residue, and municipal solid wastes (MSW). A renewable methane fuel resource can be derived from solar energy stored in naturally occurring organic materials, as well as from certain wasteful by-products of modern industrialized civilizations by microbiological conversion processes, direct material pyrolysis, or thermochemical technologies.

Microbiological conversion, based on the metabolic process of certain bacteria, can consume cellulose found in vegetation or manures produced by livestock and yield methane, carbon dioxide, and undecomposable or digested sludge as their by-products. *Marsh gas* is a natural methane produced from decayed organic matter submerged in stagnant water and is itself the source of the ghostly will-o'-the wisp observed in swampy areas. Bacteria required for natural or commercial microbiological methane conversion processes need oxygen to reproduce. *Anaerobic* bacteria are those that thrive on chemically combined oxygen, while *aerobic* bacteria can exist only on dissolved oxygen and are therefore referred to as being oxygen-free (Figure 8.7).

Moist biomass feedstock is first converted by acid-forming, or aerobic, bacteria to simple organic compounds, chiefly organic acids and carbon dioxide. These intermediate products are then fermented by anaerobic bacteria, yielding methane and additional carbon dioxide as by-products. This *anaerobic digester* gas product is approximately 50–67% methane, 50–33% CO_2 by volume with approximately 10–40 ppm hydrogen sulfide.

Specially designed digestion tanks, or *digesters,* are used commercially to accomplish this anaerobic biomass conversion process. In order to sustain a conversion process within an artificial digester environment, bacteria health and growth require precise monitoring and control of the following:

Proper balance between acid-forming and methane-forming bacteria
Proper solids-to-liquid ratio (7–9% solids):

$$\left.\begin{array}{r} \textit{sewage}\ (5\%\ \text{solids}) \\ \textit{animal manure}\ (18\%\ \text{solids}) \\ \textit{vegetable wastes}\ (30-40\%\ \text{solids}) \end{array}\right\} \text{raw stock percentages}$$

Proper pH between 7.5 and 8.5 or near neutral (7)
Proper phosphorus, nitrogen, and other nutrients levels
Proper digester temperature of 20–60°C (68–140°F)
The anaerobic mesophilic bacteria, which can exist between 20 and 40°C (68 and 104°F), require 20 days to digest, while the aerobic thermophilic bacteria can exist in a 49–60°C (120–140°F) environment and require only 7–8 days for conversion.

Methane digester history can be traced back to ancient China, where methane was produced in sewage lagoons, and to nineteenth-century England, where sewer gas was used to supply *lamp gas* for street illumination in London. Small-scale digester technology applications can be found throughout the world today, including areas of India, France, Germany, and the United States.

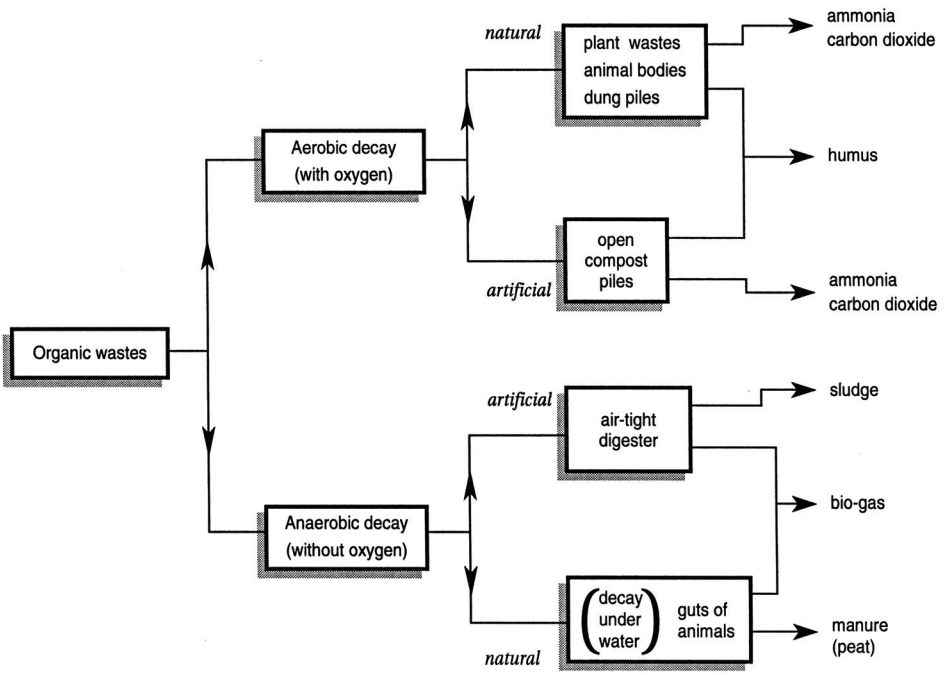

Figure 8.7 Aerobic and anaerobic biogas production.

Large land acreage suitable for farming would be required to grow sufficient photosynthetic fuel crops necessary to sustain a viable biomass industrial gas industry. Such an industry, which must also need water for the biomass conversion process, would therefore compete directly with the current utilization of fertile land and water resources for producing food. Regions of humid tropics and temperate zones where large parcels of uncultivated lands and low per capita energy consumption exist hold greater promise for biomass fuel production and use.

Aerobic destruction, or *composting,* converts organic wastes into a stable humuslike product, the chief value of which is its use as a soil conditioner and fertilizer. Composting will not generate a gaseous fuel but can stabilize and neutralize organic wastes prior to their disposal. Suitable geological conditions at landfill sites where untreated organic and municipal wastes have been buried, however, can promote anaerobic methane generation. Methane in old sanitary landfills is often vented and/or flared off to minimize the explosive risks of gas pockets building up within disposal sites. At selected dump sites, unnatural or landfill gas can be drilled, piped, and treated to remove carbon dioxide, moisture, hydrogen sulfide, and other contaminants and can yield a pipeline-quality gas.

Several biomass gasification techniques for producing a commercial fuel gas are in various stages of research and development today. Biomass gasification is difficult as a result of, among many factors, the nonhomogeneous and fibrous complexity of these organic materials. As such, proposed conversion technologies differ in their design approach to selecting operating pressure, temperature, biomass preparation, and time needed for the conversion reaction. Endothermic destructive distillation, or pyrolysis, of

organic materials at 430–450°C (805–841°F) can yield a gas having an energy density near that of a coal-derived medium-Btu gas. Municipal solid waste, for example, can be used to produce a low [3.73–5.59 MJ/m^3 (100–150 Btu/ft^3)] to medium [11.2–14.9 MJ/m^3(300–400 Btu/ft^3)] gas by pyrolysis. Thermal decomposition of these organic wastes in substoichiometric or oxygen-deficient atmospheres will shift from gas product mixtures rich in methane-carbon dioxide to mixtures rich in hydrogen-carbon monoxide as pyrolysis temperature increases. In addition to *pyrogas,* small amounts of oil, charred metals, solid materials containing glassy aggregate, carbon char, and considerable bottom and fly ash will result from municipal waste pyrolysis. Gasification techniques differ in degree of carbon gasification and amount of air utilized per unit of organic mass converted. Catalytic hydrogenation uses a hydrogen-rich environment, which is heated to temperatures in excess of 300°C (908°F) for biomass gasification. Newer gasification systems utilizing fixed-bed and/or fluidized-bed reactors, similar to the solid fuel combustion systems described earlier in this text, are currently being evaluated and pursued.

Waste in a landfill, once covered to restrict the inward diffusion of oxygen, can generate methane in the presence of moisture and heat by anaerobic bacteria activity. Biodegradation yields a raw gas containing nominally 45–60% CH_4 with 35–50% CO_2 by volume. The remaining constituents consist of N_2, O_2, trace hydrocarbons, and hydrogen sulfide.

Landfill gas recovery operations are similar to those at a natural gas field except that collection up to the compressor is under vacuum. Wells drilled into the landfill site to extract gas remove a substantial amount of water along with the gas under the vacuum abstraction process. This water, along with nonmethane hydrocarbon compounds, must be removed after the collection and compression process. Benefits for recovering landfill gas include:

- Provides a gaseous fuel resource which, after treatment, is comparable to natural gas
- Reduces buildup of trapped gas generated in landfills from dangerous levels with the potential for explosion
- Produces a cleaner burning gas fuel than natural gas

To provide a high-Btu (i.e., pipeline quality) gas, any CO_2 and hydrogen sulfide must be removed. Successful landfill gas recovery is dependent on the location and age of each particular site. Profitable recovery is highly reliant on favorable economics driven by the recovery process characteristics, desired end product quality, and particular nature of the end use of the fuel product.

In the previous sections, several alternative and potential substitutes for natural gas were considered. The viability and development of any and all of these synthetic gaseous fuel alternatives will depend on numerous factors including:

- Successful economics of scale in their development and commercialization
- Ability to compete successfully against other alternatives
- Environmental impact of their fuel production process and combustion characteristics

8.6 HYDROGEN

Alternatives are apparently available to substitute for any major worldwide natural gas shortage in the near-term future. The long-term gaseous alternative fuel resource of the future is considered by many to be hydrogen. Environmentally, diatomic hydrogen is the cleanest-burning fuel since its combustion produces only water and oxides of nitrogen.

$$H_2 + a[O_2 + 3.76N_2] \rightarrow bH_2 + cH_2O + dO_2 + eN_2 + fNO_x. \quad (8.20)$$

Hydrogen, therefore, holds promise as a long-term fuel option because, when burned in air, it also generates no unburned hydrocarbons or carbon dioxide, a compound that contributes significantly to the greenhouse effect of the Earth's upper atmosphere.

Certain properties of diatomic hydrogen gas give it its unique fuel characteristics. The specific gravity of gaseous hydrogen, for example, is approximately 0.07, meaning that it is less dense than methane, is lighter than air, and requires a greater normal storage volume than natural gas. Hydrogen burns differently than natural gas, partly because of its lower ignition energy, higher laminar flame speed, invisible but hotter flame, and broader explosive fuel-air mixture limits. Furthermore, the heat of combustion for gaseous hydrogen on a volumetric basis of 12.0 MJ/m^3 (320 Btu/ft^3) is approximately one-third that for natural gas, whereas the heat of combustion on a mass basis is 2.75 times that of most hydrocarbon fuels. Hydrogen's high diffusivity also means that it has a greater leak rate than natural gas, is able to embrittle metals, and can be "absorbed" by certain solid materials termed *hydrides*. The saturation state for hydrogen at 1 atm of –253ºC (–424ºF) requires that liquid storage must be at *cryogenic* conditions, a state that cannot be achieved by simply compressing and cooling hydrogen gas.

Producing heat by hydrogen combustion with air or oxygen can result in both high temperatures and high NO_x emissions. On the other hand, the nature of the hydrogen flame allows hydrogen to be burned at conditions even as low as 500ºC (932ºF) in a low temperature flameless catalytic burner. Low NO_x emissions can thereby be achieved in heating applications in the 800–1,500ºC (1,472–2,732ºF) temperature range by use of the low-temperature flameless catalytic combustion of hydrogen.

Currently hydrogen generation is predominantly for use in crude oil refining, ammonia production, as well as other industrial operations. An infrastructure to potentially supply enough hydrogen capacity for a national transportation network, however, is presently unavailable and currently unachievable.

Unfortunately, hydrogen gas does not occur naturally and, hence, must be generated, which requires both a source material and an energy input. Hydrogen, however, is an abundant element contained in many different substances including gases like methane and ammonia, liquids such as crude oil and water, and solids like coal and shale. In the short term, hydrogen can be produced by steam-reforming natural gas via the *water-gas* reaction or

$$CH_4 + 2H_2O \overset{T,P}{\leftrightarrows} CO_2 + 4H_2 \quad (8.21)$$

and by steam-reforming coal via the *carbureted water-gas* reaction

$$C_S + H_2O \overset{T,P}{\leftrightarrows} CO + H_2 \quad (8.22)$$

Steam reforming, the most prevalent commercial means of producing hydrogen, utilizes a hydrogen-rich donor such as natural gas. Refineries make use of on-site hydrocarbon feedstocks, i.e., natural gas (methane) or other light hydrocarbons (such as LPG or naphtha) to generate hydrogen by steam reforming for use in the crude oil refining process. Steam reforming as well as gasification of nonhydrocarbon sources such as coal can also produce hydrogen by use of the technologies described previously in Section 8.4. Gasification and pyrolysis of biomass sources have also been considered as a potential source for producing hydrogen. Processing coal to produce hydrogen raises by-product and pollution issues and current projected production methods are not even cost competitive with steam reforming methane. Note also that many of these resources are also considered suitable feedstock for producing alternate liquid and gaseous synfuels.

In the long term, hydrogen can be generated by the electrolysis of water.

$$2H_2O \overset{T,P}{\leftrightarrows} H_2 + O_2 \tag{8.23}$$

Any use of electrical energy to make hydrogen via water electrolysis competes with the direct utility use of electricity. Hydrogen production and electric power generation could be combined during off-peak hours of electrical power demand, though, as a means of load leveling and energy storage at utility power plants. An unusual concept, shown in Figure 8.8, uses heat generated from fissionable radioactive waste to produce steam which, in turn, generates electricity required for water electrolysis. Eventually, a solar electrical energy/hydrogen economy would be independent of any petrochemical, coal, or even nuclear energy systems.

Several positive reasons for developing a viable hydrogen fuel industry can be identified, including the obvious fact that it is the long-term renewable fuel of the future. Hydrogen is a clean-burning fuel that could become a viable long range alternative to depleted crude oil based hydrocarbon reserves and if the processing of coal-derived fuels are environmentally restrictive. Hydrogen is also an essential ingredient required to upgrade many of the liquid syncrudes mentioned in Chapter 7. However, when discussing the environmental benefits of hydrogen as a fuel, one must also address the pollution issues associated with any hydrogen generating process.

Hydrogen, like electricity, is an energy carrier that could be transported from production to particular sites by pipelines for specific uses. Some have therefore suggested hydrogen as a possible replacement for natural gas, but there appears to be sufficient new natural gas resources, as well as additional syngas resources, that would be able to meet current natural gas needs. Finally, a hydrogen fuel industry would have to be established and the world's entire energy infrastructure drastically changed in order to effectively transition to hydrogen utilization as a major new fuel resource.

Spark-ignition engines have been demonstrated that can use hydrogen as a fuel but, with on-board vehicle fuel storage restrictions, relatively high cost of the fuel, lack of any available fuel distribution, and poor public acceptance, this capability of hydrogen has made limited commercial advancement. Transportation uses of hydrogen fueled engines are severely limited by their need for compact H_2 storage, either as a cryogenic liquid, in anhydrides like iron titanium hydride $FeTiH_2$, in pressurized gaseous state, or in hydrogen-containing fuel-reforming compounds like methanol. Today there is an increasing environmental motivation for development and use of hydrogen-fueled vehicles in certain high-pollution density metropolitan areas.

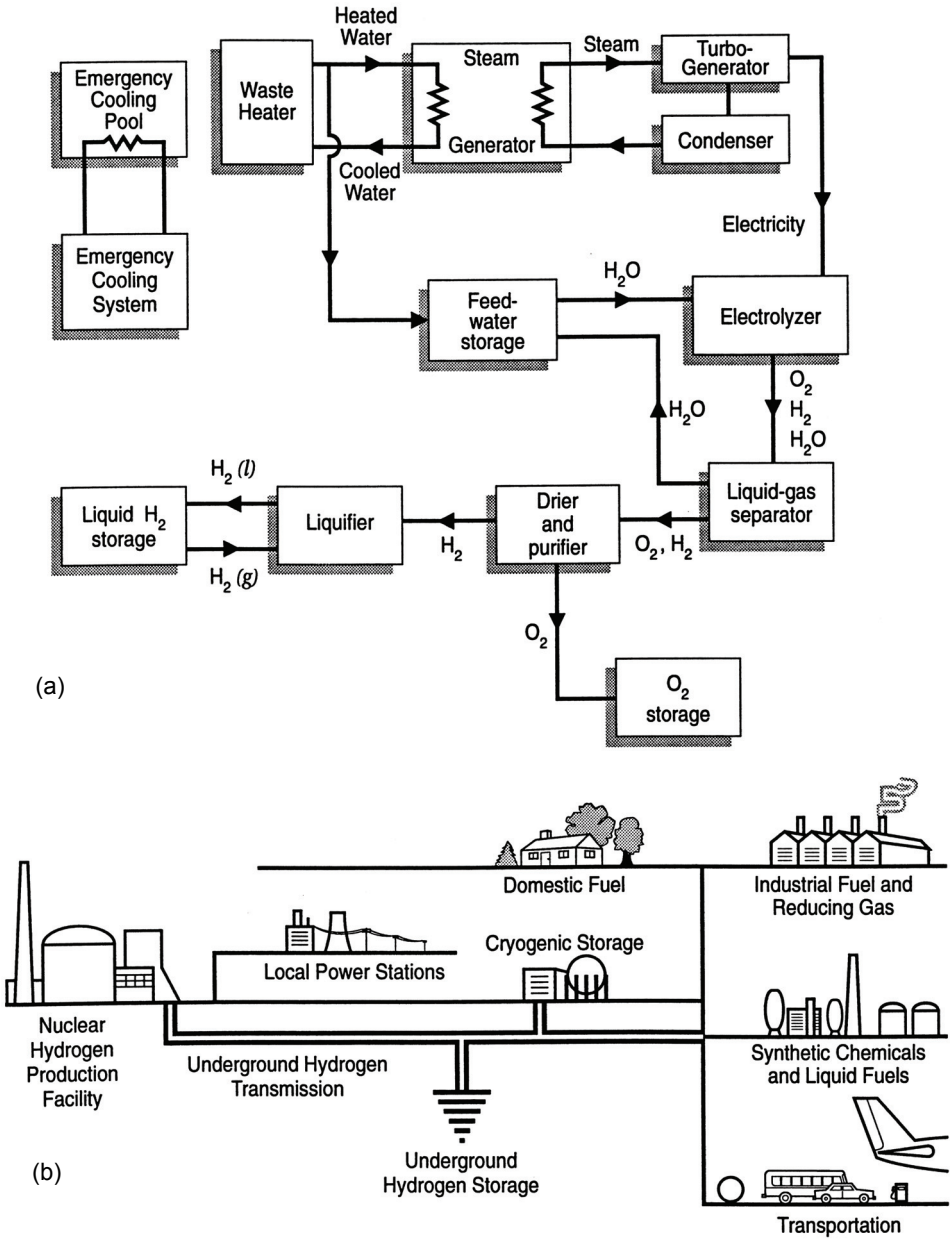

Figure 8.8 The hydrogen economy: (a) production, from Nelson, M. E., Keating, E. L., Govan, D. R., Banchak, R. J., and Corpus, J. R., *Int. J. Hydrogen Energy*, 5, 383-399, 1980. With permission; (b) distribution, from Hammond, A. L., Metz, W. D., and Maugh II, T. H., *Energy and the Future*, American Association for the Advancement of Science, Washington, DC, 1973, 120. With permission of author.

Another potential use of hydrogen comes from active H_2-O_2 fuel cell technology being developed for use in advanced stationary power and vehicle power applications. Fuel cell stationary power plant applications can incorporate H_2 generating components, such as steam reforming utilizing natural gas, to supply hydrogen. Fuel cell in vehicle applications, much like the hydrogen-fueled engines, need compact H_2 storage either as a cryogenic liquid, in anhydrides like iron titanium, or in hydrogen-containing fuel-reforming compounds like methanol.

Hydrogen has been a part of the aerospace energy inventory and successfully employed as a rocket fuel. In addition, hydrogen in liquid form appears to be a leading fuel contender for future commercial aviation applications, a field in which weight is a critical factor. In summary, hydrogen was seen in the recent past as not being a major fuel option, but it will begin to play a role in the coming decades.

Some of the more prominent negative aspects of a hydrogen fuel technology are economic, including the costs of production, transportation, storage, safety, and public acceptance. The fateful accident at Lakehurst, New Jersey, in 1937, when the hydrogen-filled German zeppelin *Hindenburg* caught fire and burned, has created public rejection of hydrogen, termed the *Hindenberg syndrome.* Many now believe, however, that the explosion and accident were associated with diesel fuel and not hydrogen. In fact, when a hydrogen leak occurs, it tends to escape rapidly, to rise vertically into the atmosphere and, if it catches fire, to provide little or no radiative heating because of the absence of carbon.

Fuel requirements in the new century will not be met by utilizing any one resource such as petroleum, coal, synfuels, or hydrogen. In fact, future energy needs will be based on a mix of all the fuels discussed in the last three chapters. The applied combustion engineer will, therefore, require a broad overview of fuel science in order to understand and to utilize most effectively the appropriate fuel option in each specific heat/power application.

8.7 GASEOUS FUEL BURNERS

Gaseous fuels do not require the charge preparation that liquid fuels do since they already exist naturally in a reactive state. The primary function of a gas burner is therefore to introduce a fuel-air mixture to the reaction zone at a proper *AF* ratio in order to sustain proper combustion. Essential components of a gas burner consist of a section for delivering reactants, a nozzle, and a flame holder. Gas burners operate as either low or high pressure configurations.

Natural gas systems that are used in domestic applications, such as cooking and heating, generally are low pressure units with many utilizing processes based on the classic Bunsen burner shown in Figure 8.9.

Suction induced by a jet of fuel gas delivered to base of burner draws primary air through a variable area.

Primary fuel-air mixture travels up the burner tube at an adequate velocity to prevent the flame from stroking back down the tube.

Fuel-air mixture burns with secondary air at the top of the burner in a diffusion flame.

Secondary air supply is provided by entrainment at outer envelope of flame at the top of the burner.

If primary air is delivered at a velocity much greater than maximum mixture flame speed the flame can be blown off and the burner extinguished.

Natural gas burners often use multi-jet arrangement, such as a ring configuration, to discharge fuel gas vertically into the required combustion space, such as near the floor level of a hot water heater or a furnace. Fuel-air ignition and combustion occur above the gas burner orifice.

Gaseous fuels due in part to their thermochemical properties and clean burning nature have replaced and/or supplemented many solid and liquid hydrocarbon fuels in heating and/or stationary power applications. Note that gaseous fuel preparation and burner components will be simpler than comparable systems used with solid and liquid fuels described in Chapters 6 and 7. In certain instances particular facilities are operated using dual-fuel burners, i.e., burners that can utilize either gas fuels, liquid fuels, or both types of fuels concurrently. This particular class of burners is found in use, for example, on waste incinerators where low energy liquid wastes that are difficult to thermally destroy are burned together with natural gas or oil.

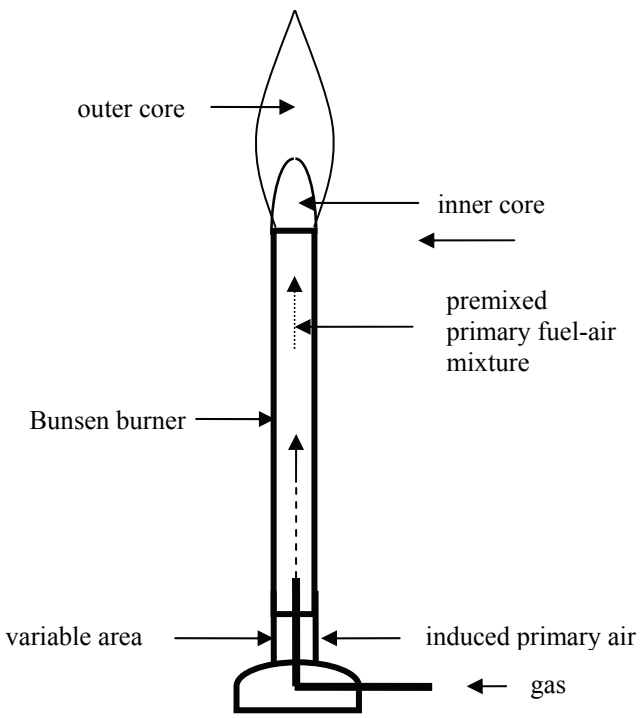

Figure 8.9 Elements of a Bunsen burner.

Current industrial gas burners are classified in a variety of ways including according to the manner in which the fuel and air are combined. *Fully premixed gas burners* completely combine both fuel and oxidant (i.e., air or oxygen) prior to reaching the combustion zone. *Partially premixed gas burners* combine both fuel and oxidant as a flammable fuel-rich reactive mixture prior to the combustion zone. Secondary air is then introduced around the flame holder. Partially premixed burners have flame lengths, temperatures, and heat flux distributions that fall between the fully premixed and diffusion flames. In a *diffusion-mixed burner* both fuel and oxidant travel separately through the burner and exit unmixed prior to diffusion mixing in the combustion zone (recall a candle, the classic example of a diffusion flame). *Nozzle mix gas burners* also provide for both fuel and oxidant to travel separately through the burner prior to exiting unmixed into the combustion zone and mix rapidly or slowly allowing for a wide variation in flame shapes and swirl. *Staged gas burners* inject a portion of the fuel and/or air into the flame zone downstream of the principal flame using *air staged burners* or *fuel staged burners*. Staging is usually done to produce a longer flame with lower peak temperature and hence lower NO_x with a more uniform heat flux distribution than non-staged flames.

Low temperature combustion of fully premixed gaseous fuel-air mixtures within certain porous materials, such as ceramic filaments and special metal alloy screens, has led to the development of the *surface combustion burner*. These solids, acting as flame holders and heat sinks, allow energy to be transferred by the combustion process to an application through heat transfer from the surface of the material. Surface combustion burners have the added benefit of being able to be contoured to match the heat transfer profile of an application.

Bluff body, swirl, and combinations are utilized predominantly as stabilizing mechanisms for gas burners. Air-swirl (strong rotary motion) provides greater stability to low energy content gaseous fuels because of their low flame speeds. Likewise air-swirl shortens the flame of high energy value fuel thereby providing greater control.

PROBLEMS

8.1 A homogeneous gaseous mixture of iso-octane and air has a specific gas constant of 51.255 ft lbf/lbm °R. For the mixture, find (a) the % theoretical air; (b) the *STP* mixture density, kg/m^3; (c) the equivalence ratio; and (d) the reaction mass *FA* ratio, lbm fuel/lbm air.

8.2 A homogeneous mixture of methane and air at *STP* has a specific heat ratio of 1.35. For this mixture, find (a) the molar constant pressure specific heat, kJ/kgmole·K; (b) the reactant mole fractions, %; (c) the mixture density, kg/m^3; and (d) the mixture specific gravity.

8.3 A natural gas supply is composed of 20% CH_4, 40% C_2H_6, and 40% C_3H_8, where all percentages are by volume. The Orsat analysis of dry combustion products yields 10.6% CO_2, 3.0% O_2, and 1.0% CO. Determine (a) the gravimetric fuel analysis, %; (b) the required theoretical *AF* ratio, kg air/kg fuel; (c) the reaction excess air, %; and (d) the mass of dry exhaust gases to mass of fuel fired, kg gas/kg fuel.

8.4 The limits of inflammability of ethane, C_2H_6, based on % volume of fuel vapor in reactive mixture are as follows:

Lower limit	3.22%
Stoichiometric	5.64%
Upper limit	12.45%

Determine the *AF* corresponding to these three limits of inflammability, kg air/kg fuel.

8.5 The volumetric analysis of a natural gas supply is 22.6% C_2H_6 and 77.4% CH_4. Find (a) the mass stoichiometric *FA* ratio, lbm fuel/lbm air; (b) the mass of CO, and H_2O formed per mass of fuel, lbm gas/lbm fuel; (e) the gravimetric percentages of C and H_2 in the fuel, %; (d) the dew point temperature for ideal stoichiometric combustion, °F; and (e) the specific gravity of the dry exhaust gases for this natural gas.

8.6 A gaseous fuel having a volumetric analysis of 65% CH_4, 25% C_2H_6, 5% CO, and 5% N_2 is burned with 30% excess air. Find (a) the ideal mass of air supplied per unit mass of fuel, kg air/kg fuel; (b) the volumetric flow rate of *STP* air to that of gaseous fuel at *STP* conditions; (c) the reaction equivalence ratio; and (d) the moles of CO_2 produced per mole of fuel.

8.7 A natural gas supply is to be augmented using a mixture of methane and propane. The supplier indicates that the specific gravity of the gas at *STP* conditions is 1.0. For this fuel, determine (a) the mole fractions of methane and propane, %; (b) the fuel density at *STP,* kg/m^3; (c) the fuel higher heating value at *STP*, kJ/kg; and (d) the ratio of the answer to part (c) to the higher heating value of methane.

8.8 Propane, an LPG fuel resource, is supplied to a constant-pressure atmospheric burner at 77°F. For a combustion efficiency of 87%, calculate (a) the ideal burner exhaust gas temperature, °F; (b) the excess air, %; (c) the dry exhaust gas mole fractions, %; and (d) the dew point stack temperature, °F.

8.9 A synthetic natural gas, or SNG, is to be generated using methane and propane. The lower heating value of the fuel at *STP* has a value of 37.25 MJ/m^3. Calculate (a) the mixture molar density, kg mole/m^3; (b) the fuel component mole fractions, %; (c) the fuel density at *STP,* kg/m^3; and (d) the specific gravity of the fuel.

8.10 Gas burners can be fired with different gaseous fuels yet produce an equivalent performance as long as the gases have equal Wobble numbers. Consider a gaseous fuel mixture of 85% methane–15% butane at *STP,* by volume. For stoichiometric combustion, find (a) the molar $\overline{FA}$ ratio, m^3 fuel/m^3 air; (b) the fuel specific gravity; (e) the fuel density, kg/m^3; (d) the fuel *HHV,* MJ/m^3; and (e) the fuel Wobble number, MJ/m^3.

8.11 A cigarette lighter uses butane combustion in 200% theoretical air. Both fuel and air are at 25°C, and the complete combustion products are at 127°C. The gas-phase combustion occurs at 101 kPa. Determine (a) the molar *AF*, kgmole air/kgmole fuel; (b) the equivalence ratio; (c) the reactant mass fractions, %; (d) the dew point temperature, °C; and (e) the heat released during combustion, kJ/kg fuel for the butane combustion.

8.12 A flow calorimeter is used to measure the higher heating value of a natural gas. The gas is delivered to the calorimeter at 14.7 psi and 77°F. The water supplied to the calorimeter has a mass flow rate of 1.3 lbm/min, with a corresponding temperature rise of 8.3°F. The volume flow rate of the gas, measured using a wet test meter, is 0.01 ft^3/min. Find (a) the heat absorbed by the water jacket, Btu/min; and (b) the higher heating value of the fuel, Btu/ft^3.

8.13 A gaseous fuel has a specific gravity of 2.066 and a higher heating value at *STP* of 49,535 kJ/kg. Find: (a) the molecular weight of the fuel, kg/kgmole; (b) the density of the fuel, kg/m^3; and (c) the higher heating value of the fuel, kJ/m^3.

8.14 A gas furnace burns 2.5 ft^3/hr of a gaseous fuel in 25% excess air. The fuel volumetric analysis yields 90% CH_4, 7% C_2H_6, and 3% C_3H_8. Both fuel and air enter the atmospheric burner at 77°F, while flue gases exit at a temperature of 1,880°F. Assuming ideal combustion, calculate (a) the dry flue gas analysis, %; (b) the product volumetric flow rate, ft^3/hr; (c) heat release, Btu/hr; and (d) the furnace efficiency, %.

8.15 A portable furnace burns a propane-air mixture having a 0.8 equivalence ratio. The fuel-air supply to the burner is at 25°C and 101 kPa, with the gases leaving the stack at 127°C. Assuming ideal complete combustion, find (a) the ideal flue gas molecular weight, kg/kgmole; (b) the exhaust dew point temperature, °C; (c) the mass of CO_2 produced per mass of fuel supplied, kg gas/kg fuel; and (d) the furnace efficiency, %.

8.16 Methane and air are supplied to a constant-pressure burner at 108 kPa and 25°C. The dry products of combustion mole fractions are 6.95% CO_2, 3.02% O_2, and 90.00% N_2. The dew point temperature of the products is 100°C. Determine (a) the molar *AF* ratio, kgmole air/kgmole fuel; (b) the exhaust gas molecular weight, kg/kgmole; (c) the combustion heat transfer if the exhaust gases are at 100°C; and (d) the combustion efficiency, %.

8.17 A fuel gas mixture is supplied to a furnace at 15 psia and 77ºF. The mixture, burned in 15% excess air, consists of the following constituents by volume:

CH_4	60%	C_2H_6	30%	CO	10%

If air is supplied at 14.7 psia and 80ºF calculate: (a) the ft^3 air/ft^3 fuel; and (b) the fan power required when burning fuel at a rate of 100,000 ft^3/hr, hp.

8.18 Acetylene is burned using a constant-pressure water-cooled burner. Fuel is supplied at 200 kPa and 15°C, while air supply enters the burner at 200 kPa and 20°C. The products leave the unit at 150°C. Water supplied at a flow rate of 0.25 kg/sec enters the jacket at 20°C and leaves at 120°C. Calculate (a) the heat transfer rate to cooling water, W; (b) the total mass flow rate of fuel and air, kg/see; (c) the volumetric flow rate of dry exhaust gases, m^3/sec; and (d) the rate of condensation of water in the exhaust, kg/sec.

8.19 A hot water heater receives feed water at 60°F and produces hot water at 120°F. The gas-fired unit produces 30-gal water/hr and burns methane at *STP* reactant conditions. The burner design requires 130% theoretical air combustion. Calculate (a) the required heat transfer rate to the water, Btu/hr; (b) the gas flow rate, ft^3/min; (c) the dew point temperature, °F; and (d) the boiler efficiency, %.

8.20 Methane is burned initially at 1 atm and 25°C in 20% excess air. The adiabatic flame temperature for the constant-pressure combustion process is 2500K. For complete combustion, calculate (a) the ideal reaction equivalence ratio; (b) the frozen product mole fractions, %; and (c) the air preheat temperature needed to produce these results, K.

8.21 A furnace designed to burn coal gas in 60% excess air is to be converted to a biomass methane gas. Design requirements are to provide the same energy transfer, using the same volumetric supply rate of air. Fuel and air are supplied at *STP*. Composition of the two gaseous fuels are:

Coal gas	Biogas
30.0% CH_4	90.0% CH_4
3.6% C_2H_4	2.0% CO_2
8.0% CO	8.0% N_2
52.0% H_2	
0.4% O_2	
2.0% CO_2	
4.0% N_2	

For these conditions, determine (a) the maximum energy release rate for 100 m^3/sec of air, kW; (b) the excess air requirements for the converted burner, %; (c) the ratio of volumetric fuel flow rates; and (d) the Wobble number for the two fuels, mJ/m^3.

8.22 A mixture of 1 part by volume of ethylene to 50 parts by volume of air is ignited in a closed rigid vessel. The initial pressure and temperature of the charge mixture is 10 atm and 300K. Calculate (a) the mixture equivalence ratio; (b) the maximum adiabatic temperature, K; and (c) the maximum adiabatic pressure, atm.

8.23 A carbureted water gas has the following composition:

16.0% C_2H_4	32.3% H_2	2.9% CO_2
19.9% CH_4	26.1% CO	2.8% N_2

Flue gas analysis of the combustion process yields:

11.83% CO_2	4.53% O_2
83.24% N_2	0.4% CO

For combustion at *STP*, compute (a) the volumetric flow rate of air to the volumetric flow rate of fuel, ft^3 air/ft^3 fuel; (b) the volumetric flow rate of flue gases at 620°F to flow rate of fuel, ft^3 gas/ft^3 fuel; (c) the equivalence ratio for the reaction; and (d) the ideal combustion efficiency for the reaction with the stack gases at 620°F.

8.24 Methane and air at an equivalence ratio of 0.9 are supplied to a boiler at *STP*. Compute the following under the assumption of complete combustion: (a) dew point temperature for the reaction, ºF; (b) heat release per mole of fuel assuming T_{prod} = 720ºR; and (c) boiler efficiency for part (b), %.

8.25 A hot water heater receives feed water at 60°F and produces hot water at 120°F. The gas-fired unit burns 0.73 lbm/hr of methane, CH_4, and produces 30 gal/hr of hot water. If the heater is supplied with fuel and air at *STP*, calculate (a) the required heat transfer to the water, Btu/hr; (b) the boiler efficiency, %; (c) the gas consumption, ft^3/min; (d) the ideal dry flue gas analysis for 130% theoretical air combustion; and (e) the product dew point temperature, °F.

8.26 The preliminary design for a low-pollution steam power plant is required to satisfy the following design specifications: 1×10^6-kW net power plant output; 40% steam cycle thermal efficiency; CH_4 fuel source; 15% excess air for combustion; 1 atm and 25°C burner air supply; 1 atm and 227°C flue gas conditions. For complete ideal combustion, determine (a) the ideal Orsat analysis, %; (b) the dew point temperature, °C; (c) the fuel mass flow rate for a stack temperature that is 10°C greater than the dew point temperature, kg fuel/hr; and (d) the combustion efficiency, %.

8.27 The following dry product analysis is for methane and air constant pressure combustion at T_{prod} = 1,200K:

O_2	4.6%
N_2	85.46%
CO	1.14%
CO_2	8.33%
H_2	0.47%

Using these data determine the following: (a) percent theoretical air for the reaction, %; (b) *AF* ratio, kg air/kg fuel; (c) dew point temperature, ºC; and (d) heat released by the reaction ${}_1Q_2$, kJ/m^3 CH_4.

8.28 Catalytic methanization of synthesis gas is necessary to produce an SNG of approximately 90–98% methane and occurs via the reaction

$$CO + 3H_2 \leftrightarrows CH_4 + H_2O$$

For the SNG methanization process with a H_2/CO molar feed ratio of 3 to 1, at a pressure and temperature of 1 atm and 1,000K, obtain: (a) the equilibrium constant, K_P, for the methanization reaction in terms of the definition and the constituents; (b) the equilibrium constant, K_P, for the methanization reaction in terms of JANAF data for the constituents for the reaction; and (c) the equilibrium composition mole fractions for mixture at a pressure and temperature of 1 atm and 1,000K.

9

Combustion Engine Testing

9.1 INTRODUCTION

In the first eight chapters, considerable time was devoted to several significant engineering aspects of combustion and fuel science. Obviously, these topics relate to the general performance of any internal combustion engine. Even so, proper design and operation of spark- and compression-ignition engines cannot be based on combustion modeling and theoretical considerations alone. Much of what is known today concerning these devices has been developed by laboratory testing. Before turning to the fuel-engine energy characteristics of particular *internal combustion* (IC) engines in coming chapters, the general subject of engine testing will first be covered. In this chapter, therefore, useful definitions and standard engine testing terminology will be reviewed. Emphasis will be given to piston-cylinder devices.

9.2 INTERNAL COMBUSTION ENGINE NOMENCLATURE

Successful commercial development of IC engines has been due, in part, to the reciprocating piston-cylinder configuration; see Figure 9.1. Also, the operation of various alternative prime movers, such as the Stirling engine, will require the use of positive displacement geometry. By referring to Figure 9.1, some useful terms pertinent to such machines can better be understood.

The piston diameter D is termed the *bore,* while the piston travel in one direction, L, is called the *stroke.* An expansion stroke motion requires that a piston travel from its piston upper limit of travel, i.e., *top dead center* (TDC), to its piston lower limit of travel, i.e., *bottom dead center* (BDC). Common engineering practice is to state a given engine geometry in terms of its bore and stroke as $D \times L$. The volume swept by a piston during one stroke, V_D, is referred to as cylinder *displacement volume,* described in terms of bore and stroke as

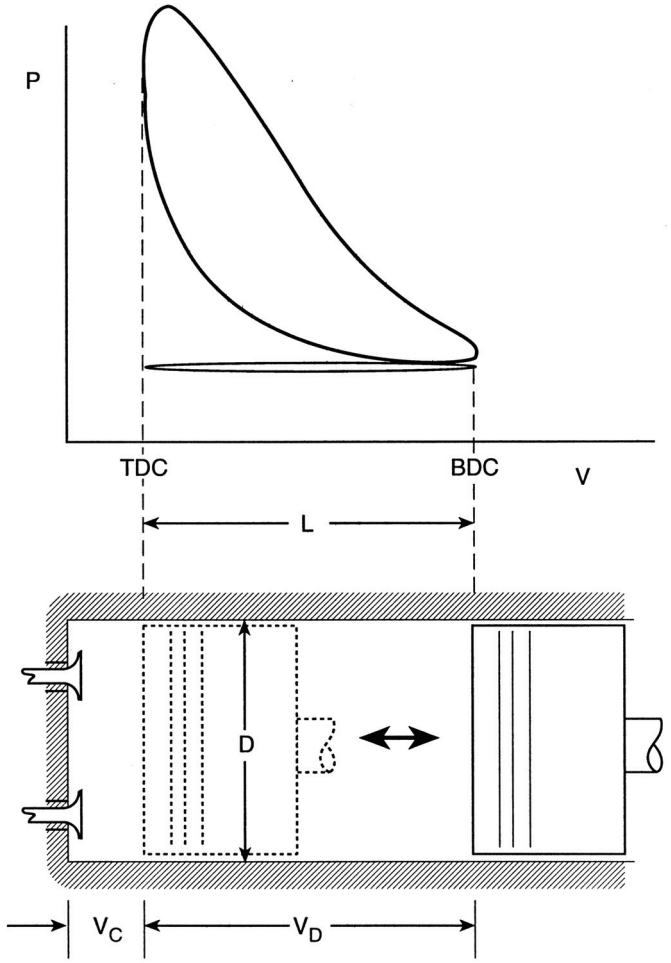

Figure 9.1 Internal combustion engine reciprocating piston cylinder configuration. *Source*: Johnston, R. M., Brockett, W. A., Bock, A. E., and Keating, E. L., *Elements of Applied Thermodynamics*, 5th edition, Naval Institute Press, Annapolis, MD, 1992. With permission.

$$V_D = \frac{\pi}{4} D^2 L \quad \frac{\text{m}^3}{\text{stroke}} \left(\frac{\text{ft}^3}{\text{stroke}} \right) \tag{9.1}$$

Volume above the piston at the TDC location is referred to as the *clearance volume,* V_C, and is often expressed as a percentage of the displacement volume c, where $0 < c < 1.0$:

$$V_C = cV_D \qquad \text{m}^3 \, (\text{ft}^3) \tag{9.2}$$

The geometric ratio of the volume at BDC to that at TDC is termed the *compression ratio,* r_v, or

$$r_v = \frac{\text{volume at BDC}}{\text{volume at TDC}} > 1.0 \tag{9.3a}$$

and, in terms of the clearance and displacement volumes, is expressed as

$$r_v = \frac{V_C + V_D}{V_C} = 1 + \frac{V_D}{V_C} = 1 + \frac{1}{c} \tag{9.3b}$$

Another useful parameter is the *pressure ratio* r_p which, for the piston-cylinder case, is given by the expression

$$r_p = \frac{\text{pressure at TDC}}{\text{pressure at BDC}} > 1.0 \tag{9.4}$$

EXAMPLE 9.1 A 4 × 5-in. single-cylinder engine is being used as a research engine. The engine, a four-stroke IC engine, is running at 1,800 rpm with inlet conditions of 73°F and 14.5 psia. Determine (a) the displacement volume V_D, ft^3; (b) the clearance volume V_C for an 8:1 compression ratio, ft^3; (c) the ideal volumetric flow rate $\dot{V}$, ft^3/min; and (d) the ideal air mass flow rate $\dot{m}$, lbm/min.

Solution:

1. Displacement volume:

$$\text{a. } V_D = \frac{\pi D^2}{4} \times L = \frac{\pi}{4}\left(\frac{4}{12}\text{ ft}\right)^2 \times \left(\frac{5}{12}\text{ ft}\right) = 0.0364 \text{ ft}^3/\text{stroke}$$

2. Clearance volume:

$$\text{b. } V_C = \frac{V_D}{r_v - 1} = \frac{0.0364}{7} = 0.00520 \text{ ft}^3/\text{stroke}$$

3. Ideal volumetric flow rate:

$$\dot{V} = \frac{V_D\langle \text{ft}^3/\text{power stroke}\rangle N\langle \text{rev/min}\rangle}{n\langle \text{revolutions/power stroke}\rangle} = \frac{(0.0364)(1{,}800)}{2}$$

$$\text{c. } \dot{V} = 32.76 \text{ ft}^3/\text{min}$$

4. Mass flow rate, assuming induced charge is air alone:

$$\dot{m} = \frac{P\dot{V}}{RT} = \rho\left\langle\frac{\text{lbm}}{\text{ft}^3}\right\rangle \times \dot{V}\left\langle\frac{\text{ft}^3}{\text{min}}\right\rangle$$

$$\text{d. } \dot{m} = \frac{(14.5 \text{ lbf/in.}^2)(144 \text{ in.}^2/\text{ft}^2)(32.76 \text{ ft}^3/\text{min})}{(1545/28.96 \text{ ft}\cdot\text{lbf/lbm}\cdot°\text{R})(533°\text{R})} = 2.41 \text{ lbm/min}$$

Comments: In an actual engine, the irreversible nature of the intake and exhaust processes prevents an ideal induction process from occurring. This discrepancy is due to thermal and fluid effects such as residual gas composition, temperature, and pressure; charge air-fuel ratio; inlet pressure and temperature; fluid viscosity; and losses due to mixing and fluid flow through valve openings.

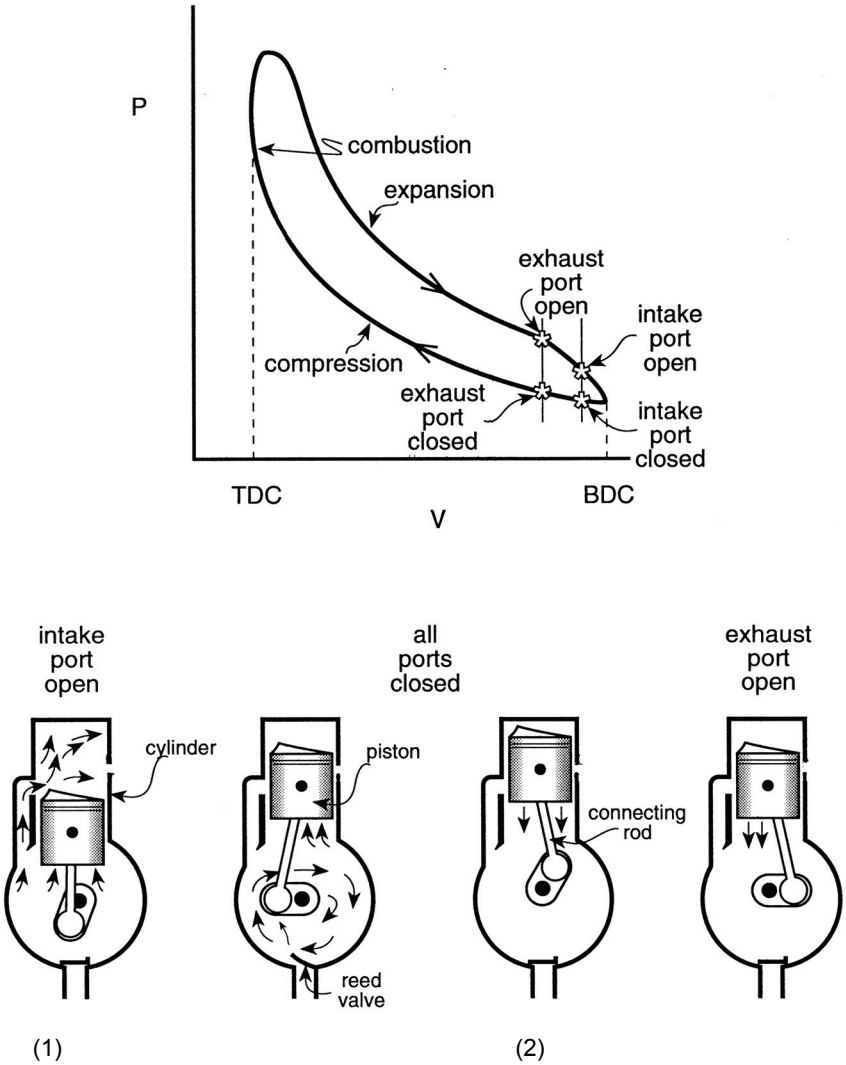

Figure 9.2 Two-stroke IC engine: (1) intake-compression stroke; (2) power-exhaust stroke.

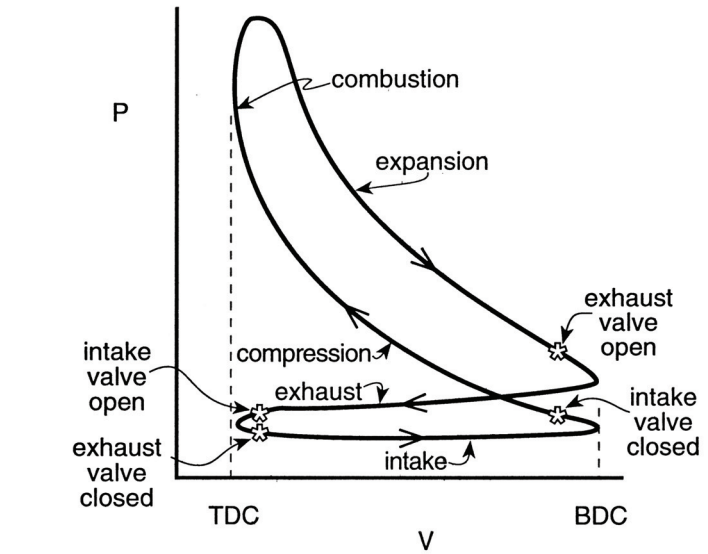

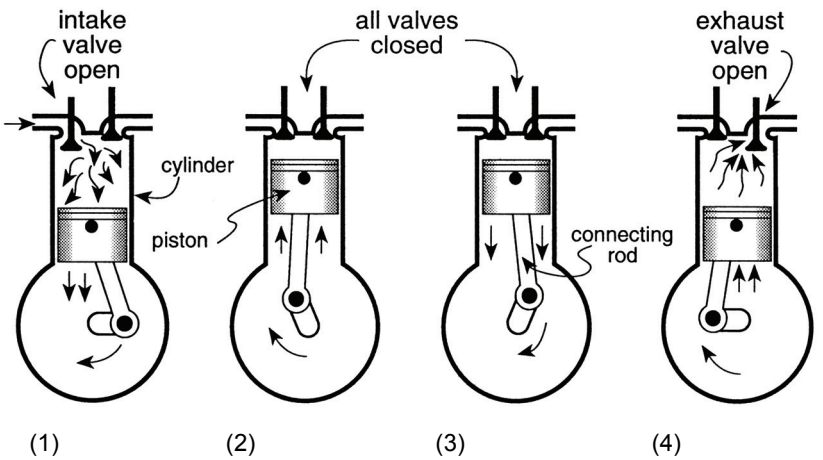

Figure 9.3 Four-stroke IC engine: (1) intake stroke; (2) compression stroke; (3) power stroke; and (4) exhaust stroke.

Each mechanical cycle of a reciprocating IC engine involves an intake, compression, combustion, expansion, and exhaust of a (fuel)-air mixture. In a *two-stroke engine,* shown in Figure 9.2, two strokes, i.e., an intake-compression stroke and a power-exhaust stroke, repeat each mechanical cycle. In a *four-stroke engine,* shown in Figure 9.3, each mechanical cycle consists of separate intake, compression, power, and exhaust strokes.

It is evident that it will be impossible to fill the entire volume at the TDC position after an exhaust stroke on intake with a fresh charge. This is due in part to the fact that each cylinder will contain trapped products of combustion in the clearance volume, called *residuals*. A larger clearance volume would therefore increase the dilution of the intake and, because of gas dynamic and thermal effects, the actual volumetric intake may be less than the ideal volumetric intake. The *volumetric efficiency* η_v relates the actual and ideal induction performance of an engine intake process as

$$\eta_v = \frac{\text{mass (volume) actually induced at inlet } P \,\&\, T}{\text{engine displacement mass (volume)}} \times 100 \tag{9.5}$$

Several of these definitions have direct bearing on the energy characteristics of reciprocating piston-cylinder geometries.

9.3 INDICATED ENGINE PERFORMANCE

When performing an energy analysis on any particular IC engine, it is essential to clearly understand the system boundaries being defined for the analysis. For example, considering the (fuel)-air mixture as a system, the thermodynamic description is termed an *indicated engine analysis* and deals with the heat/work transfers to/from the gases within an engine. Consideration of the complete engine as a thermodynamic system is termed a *brake engine analysis* and deals with the heat/work transfers to/from the engine.

Indicated performance predictions ideally can be based on thermodynamic arguments alone. Results produced from an indicated *air standard cycle analysis* can be found in most engineering thermodynamic textbooks. Using this approach, a closed system consisting of only air replaces the actual fuel-air mixture, and the intake and exhaust strokes are replaced by heat transfer processes. A *cold air* cycle approach uses a room-temperature specific heat ratio ($\gamma = 1.4$) in performance calculations, while a *hot air* cycle with $\gamma = 1.3$ is often used to more realistically represent actual IC engine energetics.

Thermodynamic analyses of air standard cycles often utilize a pressure-volume, or *P-V*, diagram to visualize the engine-energy transfer process. Theoretical or *ideal indicated P-V* diagrams can be drawn from first principles for Otto, Diesel, and/or Stirling engines. From a basic energy analysis, ideal peak pressure, net work, and thermal efficiency for those classic heat engines can be predicted. Direct experimental in-cylinder measurement using *P-V* history of an actual operating engine, either by mechanical or electronic techniques, produces an *indicator diagram.* Figures 9.2 and 9.3 show generalized indicated *P-V* diagrams for representative two- and four-stroke IC engines. Obviously, considerable differences will distinguish between ideal and actual indicator diagrams for both spark- and compression-ignition engines.

Closed system boundary expansion work for the piston cylinder configuration equals the summation of the infinitesimal force (PA) through displacement (dL) over the mechanical cycle. The indicated work during the cycle can be evaluated thus as an integration in pressure and volume as

$$W_I = \int P\,dV \qquad \frac{\text{N}\cdot\text{m}}{\text{stroke}}\left(\frac{\text{ft}\cdot\text{lbf}}{\text{stroke}}\right) \tag{9.6}$$

where

W_I = indicated work	N·m/stroke (ft·lbf/stroke)
P = cylinder pressure	N/m^2 (lbf/ft^2)
V = cylinder volume	m^3/stroke (ft^3/stroke)

Defining an average or *mean effective pressure* $\overline{P}$, one can calculate indicated cycle work during the power stroke as

$$W_I = \int \overline{P}\,dV = \overline{P}\int dV = \overline{P}(V_{\text{BDC}} - V_{\text{TDC}}) = \overline{P}V_D \tag{9.7a}$$

or

$$\overline{P} = \frac{W_I}{V_D} \qquad \frac{\text{N/m}^2}{\text{stroke}}\left(\frac{\text{lbf/ft}^2}{\text{stroke}}\right) \tag{9.7b}$$

Indicated mean effective pressure (*IMEP*) is thus seen as an "average" pressure that, if acting over the power stroke, would produce the same work as the actual cycle. Using the definition for displacement volume, indicated work per cylinder can be expressed as

$$W_I = \overline{P}\left(\frac{\pi}{4}\right)D^2L = \overline{P}AL \tag{9.8}$$

Note that an *ideal* indicated mean effective pressure can be determined from classic cycle analysis, whereas an *actual* indicated mean effective pressure must be obtained directly from numeral integration of an indicator diagram or card obtained from an operating engine.

EXAMPLE 9.2 The mechanical or electronic measurement of an actual IC engine pressure-volume diagram is termed an engine indicator diagram. The recorded experimental information can be used to determine indicated power produced by the combustion gases in the cylinder. Consider an idealized indicator card diagram of a 3-in. × 5-in. four-stroke engine operating at 1,400 rpm shown below.

Using the idealized diagram shown, calculate (a) peak cycle pressure, psi; (b) the indicated mean effective pressure, psi; and (c) the indicated engine power, ihp.

Solution:

1. Peak pressure from the diagram:

   a. $P_{\text{max}} = 400$ psia

2. Net work/power stroke from the diagram:

$$W_{\text{net}} = \oint P\,dV$$

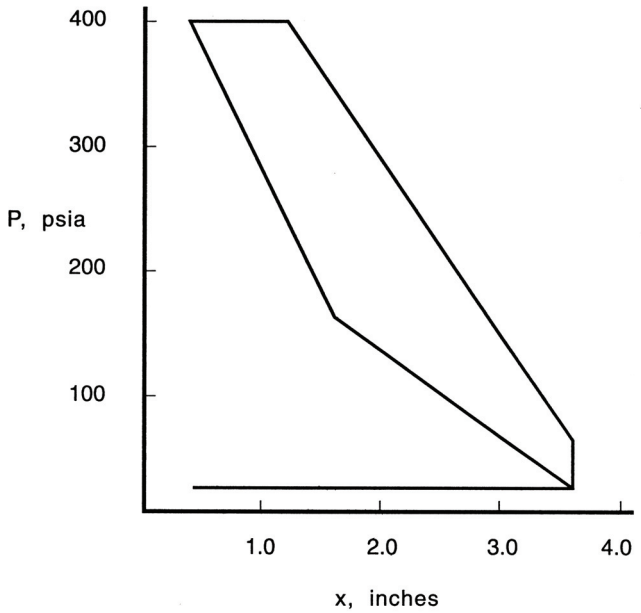

The net work is given by the enclosed area.

$$A_{\text{net}} = (400 - 20 \text{ psia}) \times (3.6 - 0.4 \text{ in.})$$
$$- \tfrac{1}{2}(400 - 60) \times (3.6 - 1.2) - \tfrac{1}{2}(160 - 20) \times (3.6 - 1.6)$$
$$- \tfrac{1}{2}(400 - 160) \times (1.6 - 0.4) - (160 - 20) \times (1.6 - (0.4)$$
$$= 356 \text{ psi in.}$$

This area is assumed to equal the product of the mean effective pressure and the *diagram* displacement length.

$$A_{\text{net}} = \overline{P} X_{\text{base}} = 356 \text{ psi} \cdot \text{in.}$$

or

$$\text{b. } \overline{P} = \frac{356 \text{ psi} \cdot \text{in.}}{(3.6 - 0.4) \text{ in.}} = 111.25 \text{ psi}$$

3. Ideal engine power:

$$\dot{W}_I = \frac{\overline{P}\langle \text{lbf/ft}^2 \rangle L\langle \text{ft} \rangle A\langle \text{ft}^2 \rangle N\langle \text{rev/min} \rangle C\langle \text{no. cylinders} \rangle}{(33{,}000 \text{ ft} \cdot \text{lbf/hp} \cdot \text{min}) n\langle \text{rev/power stroke} \rangle}$$

and

$$\dot{W}_I = \frac{(111.25 \text{ lbf/in.}^2)(144 \text{ in.}^2/\text{ft}^2)(5/12)(\pi/4)(3/12)^2(1{,}400)}{(33{,}000)(2)}$$

c. = 6.95 ihp/cylinder

Comments: An experimentally recorded indicator card can be integrated by digital or planimetric techniques to determine the actual indicated mean effective pressure. Note also that the mechanically or electrically produced illustrations require a linear vertical scale, "pressure per unit vertical displacement," and a horizontal linear scale, "linear displacement per unit volume." Such a figure allows the *IMEP* to be obtained without recourse to thermodynamic or engine information.

Practical considerations of an IC engine more frequently are in terms of the *rate* at which work is being produced, i.e., power. The *indicated engine power* can be obtained from *IMEP* in SI as:

$$\dot{W}_I = \frac{\overline{P}\left\langle \frac{\mathrm{N/m^2}}{\mathrm{stroke}} \right\rangle L\langle \mathrm{m} \rangle A\left\langle \mathrm{m^2} \right\rangle N\left\langle \frac{\mathrm{rev}}{\mathrm{min}} \right\rangle C\langle \text{no. cylinders} \rangle}{\left(60\frac{\mathrm{sec}}{\mathrm{min}}\right)\left(1{,}000\frac{\mathrm{N \cdot m}}{\mathrm{kW \cdot sec}}\right) n\left\langle \frac{\text{revolutions}}{\text{power stroke}} \right\rangle} \ \mathrm{kW} \tag{9.9a}$$

Indicated power is expressed in Engineers' units as:

$$\dot{W}_I = IHP = \frac{\overline{P}\left\langle \frac{\mathrm{lbf/ft^2}}{\mathrm{stroke}} \right\rangle L\langle \mathrm{ft} \rangle A\left\langle \mathrm{ft^2} \right\rangle N\left\langle \frac{\mathrm{rev}}{\mathrm{min}} \right\rangle C\langle \text{no. cylinders} \rangle}{\left(33{,}000\frac{\mathrm{ft \cdot lbf}}{\mathrm{hp \cdot min}}\right) n\left\langle \frac{\text{revolutions}}{\text{power stroke}} \right\rangle} \ \mathrm{hp} \tag{9.9b}$$

Engine power is a result of energy released during particular chemical reactions occurring near TDC. In thermodynamic considerations of ideal indicated cycle performance, heat addition is used to approximate this process. The maximum or ideal theoretical heat added to any cycle can be expressed in terms of the heating value of the fuel used as

$$\dot{Q} = \dot{m}_{\text{fuel}} \times LHV_{\text{fuel}} \quad \frac{\mathrm{kJ}}{\mathrm{sec}}\left(\frac{\mathrm{Btu}}{\mathrm{min}}\right) \tag{9. 10}$$

where

$$\dot{m}_{\text{fuel}} = FA \times \dot{m}_{\text{air}} \quad \frac{\mathrm{kg \cdot fuel}}{\mathrm{sec}}\left(\frac{\mathrm{lbm}}{\mathrm{min}}\right) \tag{9.11}$$

with

$$\dot{m}_{\text{air}} = \left(\frac{P\dot{V}_D}{R_{\text{air}}T}\right)_{\text{inlet}} \quad \frac{\mathrm{kg \cdot air}}{\mathrm{sec}}\left(\frac{\mathrm{lbm}}{\mathrm{min}}\right) \tag{9.12}$$

Indicated thermal efficiency η_{thermal} for an air standard thermodynamic cycle can be written as

$$\eta_{\text{thermal}} = \frac{\text{net work (power) output}}{\text{net heat (flux) addition}} \tag{9.13a}$$

In SI:

$$\eta_{\text{thermal}} = \frac{\dot{W}_I \langle \text{kW} \rangle}{\dot{m}_{\text{fuel}} \langle \text{kg/sec} \rangle LHV \langle \text{kJ/kg} \rangle} \times 100 \tag{9.13b}$$

and in Engineers' units:

$$\eta_{\text{thermal}} = \frac{IHP \langle \text{hp} \rangle (2{,}545 \text{ Btu/hp} \cdot \text{hr})}{\dot{m}_{\text{fuel}} \langle \text{lb/hr} \rangle LHV \langle \text{Btu/lbm} \rangle} \times 100 \tag{9.13c}$$

Indicated heat rate (IHR) expresses the heat addition required per unit of power produced and, as such, is an "inverse" of thermal efficiency, or

$$IHR = \frac{\dot{Q}}{\dot{W}_I} = \frac{\dot{m}_{\text{fuel}} HV}{\dot{W}_I} \quad \frac{\text{kJ}}{\text{kW} \cdot \text{sec}} \left(\frac{\text{Btu}}{\text{hp} \cdot \text{min}} \right) \tag{9.14}$$

The indicated specific fuel consumption *(ISFC)* determines a normalized fuel consumption rate to the indicated engine power output as

$$ISFC = \frac{\dot{m}_f}{\dot{W}_I} \quad \frac{\text{kg} \cdot \text{fuel}}{\text{kW} \cdot \text{sec}} \left(\frac{\text{lbm}}{\text{hp} \cdot \text{min}} \right) \tag{9.15}$$

Specific fuel consumption can be considered as a statement of fuel consumption per unit of engine output. Smaller values for specific fuel consumption imply that less fuel is necessary to produce a unit of power output.

It is essential to recognize that the central aspect of any engine operation or design begins with understanding fundamental processes that occur within the engine combustion chamber. The magnitude of each of these indicated engine performance parameters will vary as a function of engine type, load, fuel-air ratio, fuel type, piston speed, and a variety of additional factors.

9.4 BRAKE ENGINE PERFORMANCE

The second law of thermodynamics predicts that energy in transition degrades as a result of irreversible processes. From such principles of irreversibility as entropy production and friction, it is apparent that any energy transfer associated with gases within the piston-cylinder geometry, i.e., indicated engine performance, will be considerably different from those resulting energy transfers by the engine drive train, i.e., *brake engine performance.* Because of mechanical and thermal energy losses within and from an engine, its brake work, or power, will therefore be less than the corresponding indicated work or power

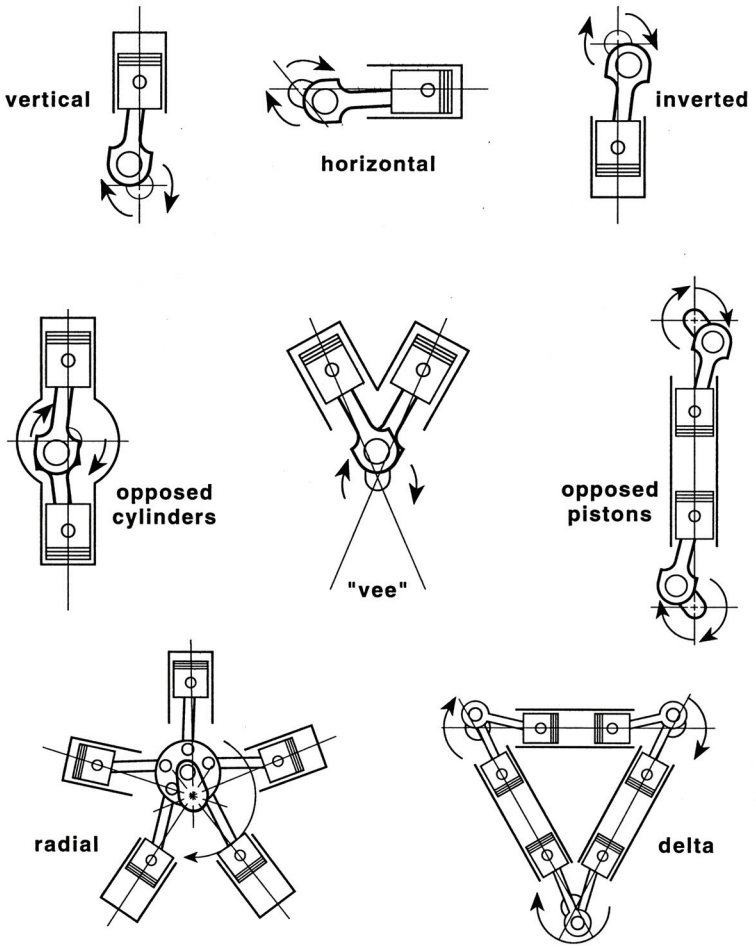

Figure 9.4 Various IC engine cylinder arrangements.

$$\dot{W}_I > \dot{W}_B \quad \text{kW (hp)} \tag{9.16}$$

and

$$\dot{W}_I = \dot{W}_B + \dot{W}_F \quad \text{kW (hp)} \tag{9.17}$$

where

$\dot{W}_I$ = indicated power (generated)
$\dot{W}_B$ = brake power (delivered)
$\dot{W}_F$ = friction power (lost)

The engine *mechanical efficiency,* η_{mech}, provides a means of determining how effective a particular engine is at reducing internal losses.

$$\eta_{\text{mech}} = \frac{\dot{W}_B}{\dot{W}_I} \times 100 \tag{9.18}$$

Most commercial IC engines, except for certain research applications, are produced in multi-cylinder configurations. Figure 9.4 illustrates a few particular arrangements that have been used in engine development to satisfy specific design requirements, such as vibrational, inertial, and/or frictional influences, while at the same time optimize criteria such as power, torque, and/ or engine size and arrangement.

Internal combustion engine power is transmitted through mechanical gearing, electric generators, or propeller shafting. These added energy transfers will result in further reductions in actual delivered power. Such losses can be accounted for by introducing transmission, generator, and/or propeller efficiencies.

Brake engine performance, unlike ideal indicated performance, cannot be determined from basic theory and therefore requires experimental measurements in the test laboratory. Brake characteristics are often obtained by means of a power absorption device termed a *dynamometer*. The simplest and earliest means of measuring brake performance was by use of a *friction* dynamometer or brake, shown in Figure 9.5. Engine power is dissipated by friction loading a prony brake absorption band. Since mechanical work can be described as the product of force acting through a distance, the brake work during one revolution is given by the expression

$$W_B = \text{distance} \times \text{force} = (2\pi r) \times f \tag{9.19}$$

where

W_B = brake working during one revolution, N·m (ft·lbf)
r = drive shaft wheel radius, m (ft)
f = friction force, N (lbf)

Brake torque, τ, is the product of a moment arm and corresponding brake force or,

$$\tau = rf \quad \text{N·m (ft·lbf)} \tag{9.20a}$$

The drive shaft torque is absorbed by an opposing dynamometer measuring torque and at dynamic equilibrium,

$$\tau = rf = RF \quad \text{N·m (ft·lbf)} \tag{9.20b}$$

where

R = measuring moment arm, m (ft)
F = measuring load as determined by a scale, N (lbf)

Torque is a statement of the amount of work a prime mover can produce and is therefore a measure of how large a load a given engine is capable of pulling. Since engine power is a *rate* of work term, it will specify how fast a particular engine will pull a given load. *Brake power* $\dot{W}_B$ can be determined from torque in SI as:

$$\dot{W}_B = \frac{2\pi R\langle \text{m/rev} \rangle F\langle \text{N} \rangle N\langle \text{rev/sec} \rangle}{(1{,}000 \ \text{N} \cdot \text{m/kW} \cdot \text{sec})} \ \text{kW} \tag{9.21a}$$

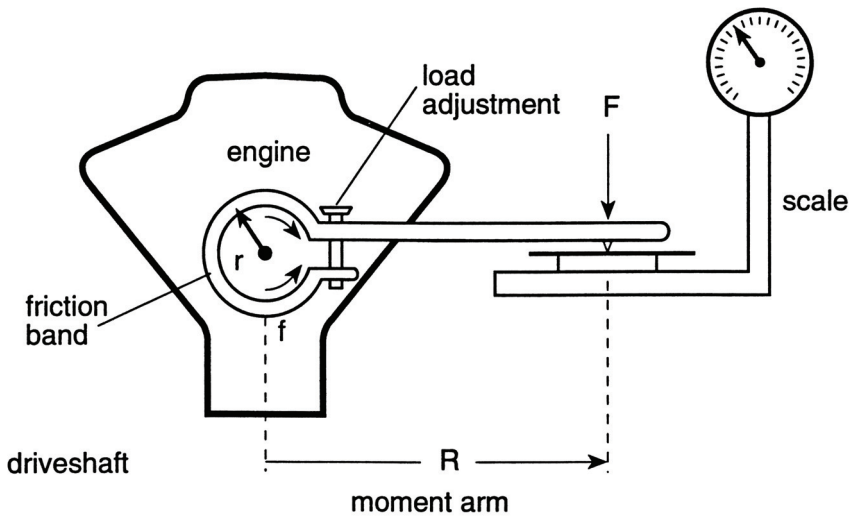

Figure 9.5 Friction band engine dynamometer schematic.

In Engineers' units brake power is expressed as:

$$\dot{W}_B = BHP = \frac{2\pi R\langle \text{ft/rev}\rangle F\langle \text{lbf}\rangle N\langle \text{rev/min}\rangle}{(33{,}000\ \text{ft}\cdot\text{lbf/hp}\cdot\text{min})}\ \text{hp} \tag{9.21b}$$

Notice that brake power, unlike indicated power, is not modified by the number of power strokes per revolution or number of cylinders.

A *brake mean effective pressure (BMEP)* can be obtained from the brake power equation (9.21) and the indicated power equation (9.9) in SI as:

$$BMEP = \frac{\dot{W}_B\langle \text{kW}\rangle\left(1{,}000\dfrac{\text{N}\cdot\text{m}}{\text{kW}\cdot\text{sec}}\right)\left(60\dfrac{\text{sec}}{\text{min}}\right)n\left\langle\dfrac{\text{rev}}{\text{power stroke}}\right\rangle}{L\left\langle\dfrac{\text{m}}{\text{stroke}}\right\rangle A\langle \text{m}^2\rangle N\left\langle\dfrac{\text{rev}}{\text{min}}\right\rangle C\langle\text{no. cylinders}\rangle}\ \text{N/m}^2 \tag{9.22a}$$

Engineers' units:

$$BMEP = \frac{\dot{W}_B\langle \text{hp}\rangle\left(33{,}000\dfrac{\text{ft}\cdot\text{lbf}}{\text{hp}\cdot\text{min}}\right)n\left(\dfrac{\text{rev}}{\text{power stroke}}\right)}{L\left\langle\dfrac{\text{ft}}{\text{stroke}}\right\rangle A\langle \text{ft}^2\rangle N\left\langle\dfrac{\text{rev}}{\text{min}}\right\rangle C\langle\text{no. cylinders}\rangle}\ \text{lbf/ft}^2 \tag{9.22b}$$

Combining Equations (9.9), (9.22), and (9.17), mechanical efficiency can be expressed in terms of mean effective pressures as

$$\eta_{\text{mech}} = \frac{\dot{W}_B}{\dot{W}_I} \times 100 = \frac{BMEP}{IMEP} \times 100 \tag{9.23}$$

Brake thermal efficiency, η_{brake}, for an engine can be determined using Equation (9.13a) in terms of engine brake power output.

SI:

$$\eta_{\text{brake}} = \frac{(1{,}000\ \text{N}\cdot\text{m/kW})\dot{W}_B\langle\text{kW}\rangle}{\dot{m}_{\text{fuel}}\langle\text{kg/sec}\rangle HV\langle\text{kJ/kg}\rangle} \times 100 \tag{9.24a}$$

Engineers' units:

$$\eta_{\text{brake}} = \frac{(2{,}545\ \text{Btu/hp}\cdot\text{hr})BHP\langle\text{hp}\rangle}{\dot{m}_{\text{fuel}}\langle\text{lbm/hr}\rangle HV\langle\text{Btu/lbm}\rangle} \times 100 \tag{9.24b}$$

Brake heat rate (*BHR*), an inverse of brake thermal efficiency, expresses the ideal fuel-air energy addition required by an engine per unit of brake power output as

$$BHR = \frac{\dot{Q}}{\dot{W}_B} = \frac{\dot{m}_{\text{fuel}}HV}{\dot{W}_B} \qquad \frac{\text{kJ}}{\text{kW}\cdot\text{sec}}\left(\frac{\text{Btu}}{\text{hp}\cdot\text{min}}\right) \tag{9.25}$$

Brake specific fuel consumption (*BSFC*) expresses the normalized fuel consumption to the brake engine power output as

$$BSFC = \frac{\dot{m}_f}{\dot{W}_B} \qquad \frac{\text{kg}\cdot\text{fuel}}{\text{kW}\cdot\text{sec}}\left(\frac{\text{lbm}}{\text{hp}\cdot\text{min}}\right) \tag{9.26}$$

EXAMPLE 9.3 An 11.5 × 12.75-cm six-cylinder, two-stroke marine diesel delivers 170 bkW at 2,100 rpm. The engine burns 50.9 kg fuel/hr. The indicated engine power is 205 ikW. For these conditions, calculate (a) the engine torque, N·m; (b) *BMEP,* kPa; (c) brake specific fuel consumption, kg/bkW·hr; (d) *IMEP,* kPa; (e) indicated specific fuel consumption, kg/ikW·hr; (f) mechanical efficiency; and (g) friction power, fkW.

Solution:

1. Brake engine torque:

$$\text{a.}\quad \tau_B = \frac{(1{,}000\ \text{N}\cdot\text{m/kW}\cdot\text{sec})(170\ \text{bkW})(60\ \text{sec/min})}{2\pi(2{,}100\ \text{rev/min})} = 773\ \text{N}\cdot\text{m}$$

2. *BMEP:*

$$\overline{P} = \frac{W_B 1{,}000n}{LANC} = \frac{(170\ \text{bkW})(1{,}000\ \text{N}\cdot\text{m/kW}\cdot\text{sec})(1)(60\ \text{sec/min})}{(0.1275\ \text{m})(\pi/4)(0.115\ \text{m})^2(2{,}100\ \text{rev/min})6}$$

$$\text{b.}\quad \overline{P}_B = 6.113 \times 10^5\ \text{N/m}^2 = 611\ \text{kPa}$$

3. Brake specific fuel consumption:

$$\text{c.}\quad BSFC = \frac{50.9\ \text{kg fuel/hr}}{170\ \text{bkW}} = 0.299\ \text{kg/bkW}\cdot\text{hr}$$

4. *IMEP:*

$$\text{d.}\quad \frac{IMEP}{BMEP} = \frac{\dot{W}_I}{\dot{W}_B} \quad \text{or} \quad \overline{P}_I = \frac{(205)}{(170)}(611) = 737 \text{ kPa}$$

5. Indicated specific fuel consumption:

$$\text{e.}\quad ISFC = \frac{50.9 \text{ kg fuel/hr}}{205 \text{ ikW}} = 0.248 \text{ kg/ikW} \cdot \text{hr}$$

6. Mechanical efficiency:

$$\text{f.}\quad \eta_{\text{mech}} = \frac{\dot{W}_B}{\dot{W}_I} = \frac{170}{205} = 0.829 = 83\%$$

7. Friction power:

$$\text{g.}\quad \dot{W}_F = \dot{W}_I - \dot{W}_B = 205 - 170 = 35 \text{ fkW}$$

As discussed earlier, a dynamometer can be used to investigate a given engine experimentally under various operational conditions. A brief description of engine dynamometers is given in the following section. A more complete discussion of these devices can be found in the engineering literature.

The *prony brake* is the simplest and most inexpensive measuring system; see Figure 9.5. A brake drum is attached to an engine, and a friction band lined with asbestos is then used to load the engine. A constant resisting torque is developed for a given friction band pressure. Engine load can be changed by varying band pressure. The sliding resistance between the brake liner and the brake drum dissipates the engine power as heat. Too severe or too rapid a change in this mechanical braking can result in a loss of engine speed or even cause the engine to stall. This type of dynamometer is difficult to maintain at a constant load over a long testing period because of the heat generated by friction loading. Brake cooling is required and is provided by water. If water gets on the brake drum lining, it can influence brake performance and ensuing engine measurements. In general, characteristics of prony brake dynamometers limit its use to testing small, low-speed engines.

The *water brake* dynamometer is a hydraulic or fluid power absorption system. Basically, this type of loading utilizes a pump driven by an engine. Engine torque is transmitted through the pump utilizing the viscous nature of water. As the pump impeller rotates, a torque will be transmitted through the water and will be resisted by the pump casing. The pump casing is allowed to move or rotate, permitting casing torque to be measured using a brake arm and scale technique similar to the prony brake mentioned previously. Constant water flow rate will maintain a constant load as long as the viscosity (water temperature) is kept constant, whereas variations in loading can be accomplished by adjusting the water flow rate through the brake. This type of dynamometer is compatible with a wide range of engine speeds and sizes. It is a more stable system than a prony brake and will not stall as easily as the prony when a load is varied.

A fan brake dynamometer is also a fluid, power absorption system. The viscous resistance of air, as opposed to water, is used in fan dynamometers to load a given IC engine. A fan is attached to an engine, and air resistance to the rotating fan blades absorbs

the engine power. In this device, a specially calibrated fan is used to load the engine. Adjustments for load variations require change in fan blade radius, diameter, and/or pitch. Typically, a particular blade is used for a specific load and then replaced for different loads. Fan dynamometers are not very accurate and are most frequently used to test an engine in a very long test over several hours at a given condition.

Several dynamometers are available for engine testing that use electrical as opposed to mechanical means of loading. The *electric generator* dynamometer is a power absorption system in which the engine is connected to an electric motor/generator set. An engine-generated torque is developed by a rotating stator and a fixed armature, which is resisted by an electro-magnetic field. This electrically generated torque can be measured by allowing the generator housing to move or rotate, and connection of this to a brake arm and scale permits engine power measurement similar to that by prony brake and water brake systems. This type of dynamometer is governed by its electric generator efficiency. In addition, generated power may be dissipated through joule heating of resistance coils or a light bulb load bank, but a generator can also be run as a motor to measure engine friction power. These units are expensive and are most frequently matched with low-power and high-speed IC engines.

The *electric current* dynamometer is similar to an electric generator system. It is an electromagnetic power absorption device in which an engine drives a disk or rotor inside an electric coil. The engine torque is resisted by a torque produced by the electromagnetic field. Brake load is varied by changing the DC current in the coil.

The engine chasis dynamometer is another type of dynamometer. These devices place an entire vehicle on a treadmill for the purpose of loading the vehicle for testing. This is more precisely termed a *vehicle* versus an engine dynamometer.

9.5 ENGINE PERFORMANCE TESTING

In practice, IC engines are designed for use over a wide operating range and therefore require testing to determine their particular performance characteristics over such conditions. Several reasons come to mind for such sophisticated testing, including: evaluating an engine to determine whether it meets design parameters predicted by the manufacturer; research and development programs involving modified or new engine concepts; and laboratory exercises used to illustrate engine principles to engineering students. Standard tests have been established and maintained by engineering societies such as the Society of Automotive Engineers (SAE), American Society of Mechanical Engineers (ASME), and the American Society of Testing Materials (ASTM).

Engine testing typically provides information such as brake performance parameters, fuel-engine interface sensitivity, and/or exhaust gas emission characteristics. In general, this type of information can be quite complex and often is unit-sensitive, which is to say, a function of engine type, size, load, speed, fuel, and ambient environment.

EXAMPLE 9.4 The following two-stroke diesel engine data were obtained during a standard engine test.

1.	Fraction of fuel load, %	25	50	75	85	100
2.	100-cc fuel consumption time, sec	77	65	52	47	43
3.	Fuel specific gravity at 70°F, °API	45	45	45	45	45
4.	Air supply mass flow rate, lbm/min	11	11	11	11	11
5.	Air supply inlet temperature, °F	70	71	71	71	72
6.	Cooling water mass flow rate, lbm/min	13.5	13.5	13.5	13.5	13.5
7.	Cooling water inlet temperature, °F	60	60	60	60	60
8.	Cooling water outlet temperature, °F	115	130	150	160	170
9.	Exhaust gas temperature, °F	315	392	465	476	560
10.	Dynamometer load voltage, V	120	120	120	120	120
11.	Dynamometer load current, A	40	70	125	140	165

Determine the following: (a) rate of energy being supplied by the fuel, Btu/min; (b) rate of energy delivered by the engine to the dynamometer, Btu/min; (e) rate of energy lost to coolant, Btu/min; (d) rate of energy lost to exhaust gases, Btu/min; and (e) rate of unaccounted-for energy lost by radiation, oil coolant, etc., Btu/min.

Solution:

1. Energy balance, fuel input:

   Fuel specific gravity:

$$API\langle 60\rangle = [0.002(60 - 70) + 1]\ 45°\text{API} = 44°\text{API} \tag{5.7}$$

   From Appendix C,

   At 44°API $SG = 0.8063$ $LHV = 18{,}600$ Btu/lbm

Fuel density:

$$\rho_{\text{fuel}} = (SG)(\rho_{H_2O})$$
$$= (0.8063)(62.4 \text{ lbm/ft}^3) = 50.313 \text{ lbm/ft}^3$$

Fuel mass flow, 25% load:

$$\dot{m}_{\text{fuel}} = \frac{(50.313 \text{ lbm/ft}^3)(100 \text{ cc})(60 \text{ sec/min})}{(77 \text{ sec})[(2.54 \text{ cm/in.})(12 \text{ in./ft})]^3} = 0.138 \text{ lbm fuel/min}$$

Fuel energy supply to engine, 25% load:

a. $$\left|\dot{Q}_{\text{fuel}}\right| = \dot{m}_{\text{fuel}} \times LHV = (0.138 \text{ lbm/min})(18{,}600 \text{ Btu/lbm})$$
$$= 2567 \text{ Btu/min}$$

2. Energy balance, dynamometer load:

$$\dot{W}_{\text{brake}} = I^2R = VR$$

Brake load, 25%

b. $$\dot{W}_{\text{brake}} = (120 \text{ V})(40 \text{ A}) = 4{,}800 \text{ W}$$
$$= (4.8 \text{ kW})(56.87 \text{ Btu/kW} \cdot \text{min}) = 273 \text{ Btu/min}$$

3. Energy balance, cooling water:

$$\left|\dot{Q}_{H_2O}\right| = \left(\dot{m}_{H_2O} C_p \Delta T\right)_{H_2O}$$

Coolant loss, 25% load:

c. $$\left|\dot{Q}_{H_2O}\right| = (13.5 \text{ lbm/min})(1.0 \text{ Btu/lbm°R})(115 - 60°\text{R})$$
$$= 742.5 \text{ Btu/min}$$

4. Energy balance, combustion gases:

$$\left|\dot{Q}_{\text{gas}}\right| = (\dot{m}_{\text{fuel}} + \dot{m}_{\text{air}}) C_{p/\text{gas}} T_{\text{gas}} - (\dot{m} C_p T)_{\text{air}} - (\dot{m} C_p T)_{\text{fuel}}$$

The specific heats for the air and exhaust gases will depend on both temperature and composition. For this calculation, use the properties of air for first estimation.

From Table B.25 in Appendix B

$$C_p\langle \text{Btu/lbm°R} \rangle = \frac{\overline{C}_p\langle \text{cal/gmole} \cdot \text{K} \rangle \times 1.8001}{MW_{\text{air}} \times (9\text{K}/5°\text{R})}$$

T, °R	$\overline{C}_p$, cal/gmole · K	C_p, Btu/lbm°R
530	6.947	0.240
775	7.044	0.243
852	7.092	0.245
925	7.142	0.246
936	7.151	0.247
1,020	7.219	0.249

Gas loss, 25% load:

d. $\left|\dot{Q}_{\text{gas}}\right| = (0.138 + 11 \text{ lbm/min})(0.243 \text{ Btu/lbm°R})(775°\text{R}) - (11)(0.240)(530) = 698 \text{ Btu/min}$

5. Energy balance, miscellaneous losses:

$$\dot{E}_{\text{fuel}} = \dot{W}_{\text{brake}} + \dot{Q}_{\text{H}_2\text{O}} + \dot{Q}_{\text{gas}} + \dot{Q}_{\text{misc}}$$

or

$$\dot{Q}_{\text{misc}} = \dot{E}_{\text{fuel}} - \dot{W}_{\text{brake}} - \dot{Q}_{\text{H}_2\text{O}} - \dot{Q}_{\text{gas}}$$

Miscellaneous losses, 25% load:

e. $\dot{Q}_{\text{misc}} = 2567 - 273 - 742.5 - 698 = 853.5 \text{ Btu/min}$

6. Energy balance summary:

% Load	$\dot{Q}_{\text{fuel}}$	$\dot{W}_{\text{B}}$, Btu/min	$\dot{Q}_{\text{H}_2\text{O}}$, Btu/min	$\dot{Q}_{\text{gas}}$	$\dot{Q}_{\text{misc}}$
25	2,567	273	742.5	698	854
50	3,050	478	945.0	931	696
75	3,813	853	1,215.0	1,150	595
85	4,222	955	1,350.0	1,196	721
100	4,613	1,126	1,485.0	1,458	544

7. Diesel energy utilization on a percentage basis, or

$$\%\ \text{Power} = \frac{\dot{W}_B}{\dot{E}_{\text{fuel}}} \times 100 \qquad \%\ \text{Exhaust} = \frac{\dot{Q}_{\text{gas}}}{\dot{E}_{\text{fuel}}} \times 100$$

$$\%\ \text{Coolant} = \frac{\dot{Q}_{\text{H}_2\text{O}}}{\dot{E}_{\text{fuel}}} \times 100 \qquad \%\ \text{Misc} = \frac{\dot{Q}_{\text{misc}}}{\dot{E}_{\text{fuel}}} \times 100$$

% Load	% Power	% Coolant	% Exhaust	% Misc
25	10.63	28.92	27.20	33.25
50	15.67	30.98	30.52	22.82
75	22.37	31.86	30.16	15.60
85	22.62	31.98	28.33	17.03
100	24.40	32.19	31.61	11.79

Engine evaluations involve many critical measurements, including fuel and air mass (or volume) flow rates, cylinder pressure, power output, speed, and emission characteristics. Pressure indicators using in-cylinder measurements can provide useful pressure-time (crank angle), pressure-volume, and/or indicated performance diagrams. Low-speed engines are compatible with piston spring measurements, while pressure transducers are useful with high-speed engine movements. Engine speed can be monitored using flywheel measurements such as tachometers, magnetic signals, or stroboscopic techniques. Brake power output can be absorbed using engine dynamometers, as discussed in Section 9.4.

The performance of an IC engine depends on consumption and combustion of fuel and air. Accurate fuel and air flow measurements are generally required when investigating an engine's operating characteristics in a test environment. The most reliable fuel consumption data, cumulative, can be determined by continuously measuring fuel usage while running an engine under steady test conditions. Collecting fuel flow under such circumstances helps to minimize instabilities such as short-term engine torque and speed fluctuations, which are normally encountered during transient engine testing. Fuel data can be gathered using either volume or weight measuring techniques. A specific gravity correction will be required with any fuel consumption result derived from a volume measuring method and inherently introduces an additional uncertainty into the analysis.

A simple volumetric measuring method to determine fuel consumption utilizes clear marked glass bulbs or cylindrical vessels of known internal volumes. The time an engine takes to consume fuel contained within the known volume is determined with a timer such as a stop watch. Various volumetric fuel measuring arrangements using glass bulbs of different capacity are often used with engine test facilities. The configuration shown in Figure 9.6 consists of two marked glass bulbs connected to the test engine fuel line via a three way cock valve so that fuel can be fed from either one of the bulbs while the other is being filled with fuel. A second three way cock located between the fuel tank and the two bulbs completes the connection in order to either isolate or fill the bulbs. Fuel volumetric flow rate for each bulb is obtained by dividing the known fixed volumes by their respective recorded consumption times.

Special photocell fuel burette instruments have been developed to automatically make measurements and regulate fuel flow to a test engine. These photocell fuel burette arrangements eliminate the human error of reading fuel level markings required with the conventional volumetric flow method. At proper high/low burette fuel levels, lamps automatically switch valves on/off regulating fuel flow between the engine and burette measurement circuit and/or fuel tank. During fueling from the measurement circuit the instrumentation also triggers recording of the time required to consume fuel which had automatically been delivered from the specified burette volume. Some flow meters which use a light beam in their operation, however, can have fuel color affect their performance.

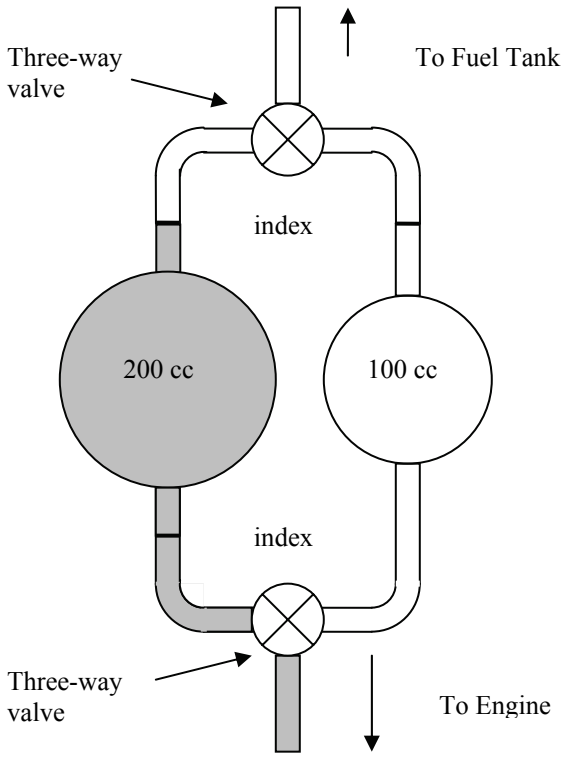

Figure 9.6 Volumetric method for measuring liquid fuel consumption.

Flow meters fitted with pre-calibrated orifice plates are also used in particular circumstances which allow continual delivery of a fixed volume of liquid fuel per unit time. Configurations are available for these applications that permit interchange and use of different size orifices in order to cover a range of fixed flow rates.

Gravimetric fuel gauges meter flow on a mass basis rather than volume. A simple method for measuring mass fuel consumption makes use of a transfer container, such as a glass beaker. Placing the transfer container on a scale or load cell allows fuel to be weighed directly as the transfer container is being filled with fuel and then as fuel is drawn off by the engine. The time the engine takes to draw, or siphon off, fuel from the transfer container is ascertained by means of a timer or stop watch. This technique can be incorporated into automated configurations with appropriate valving so that the engine can be run while measuring the mass rate of fuel supply or run being fueled directly from the fuel tank.

Engines utilizing fuel injection systems all have the common problem of fuel spillback. Fuel spillback from injection must be properly returned to the fueling system to prevent spillback from incorrectly contributing to fuel consumption measurements.

Particular fuel determinations may imply cumulative as well as instantaneous rate measurements during steady state and/or transient engine laboratory work. In such instances, selecting an appropriate fuel metering device(s) becomes important. Various volumetric or gravimetric configurations are available from manufacturers with specific attributes for appropriate use in the test cell environment.

The density of air, the predominant intake charge component of an IC engine, is a function of both pressure and temperature. The interrelationship between pressure, P, absolute temperature, T, and density, ρ, of air (see Table 9.1) can be determined using the ideal gas law written as

$$\rho = P/RT \tag{1.3c}$$

A sharp-edged orifice is an inexpensive but accurate technique used in many applications to determine steady flow characteristics of a compressible fluid, such as air. Flow information is obtained by recording the pressure drop across the orifice as fluid passes through the measuring device. Trying to position an orifice directly within an engine's intake in order to obtain inducted air flow usually proves unsuccessful since the actual intake process produces an unsteady pulsating flow. The inducted pulsating fluid motion results from the cyclic operating nature of the IC engine's piston-cylinder configuration.

Test measurements of intake air flow to an engine can be made with a sharp-edged orifice, however, if connections are accommodated using an *airbox* as shown in Figure 9.7. The airbox is a box or cylinder with sufficient volume to dampen out engine inlet intake pulsations from being propagated back to an orifice mounted in the chamber intake. Also the airbox engine connection is kept as short as possible to help minimize pressure pulsations. Every airbox volume has a design size, which amongst other factors, depends on test engine criteria including type, size, number of cylinders, and operating speed. An airbox's swept volume must be much greater than the test engine's displacement volume, with largest swept volume increases required for single cylinder applications and less swept volume increases needed for multi-cylinder applications. Multi-cylinder and turbocharged engines show less sensitivity to pulsations with the airbox orifice technique than a single cylinder engine.

Table 9.1 Ideal Gas Relationship for Air

Property	SI	English Engineers
ρ	kg/m^3	lbm/ft^3
P	N/m^2	lbf/ft^2
T	K	°R
R	287 J/kg·K	53.34 ft·lbf/lbm °R

The ideal fluidic relationship for ambient air flowing through an orifice mounted in an airbox having discharge velocity, V, due to a pressure difference, ΔP, is given as

$$\frac{\rho V^2}{2g_0} = \Delta P \tag{9.27a}$$

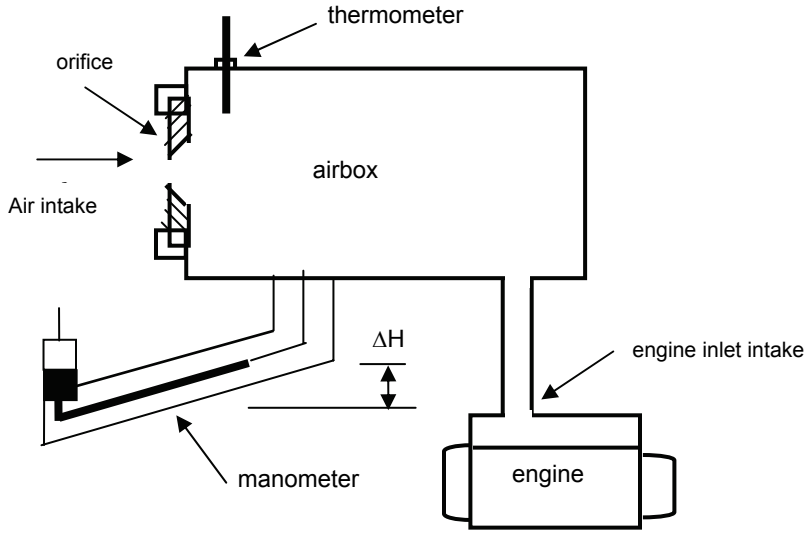

Figure 9.7 Airbox method for measuring air flow.

where

Property	SI	English Engineers
ρ	kg/m^3	lbm/ft^3
V	m/sec	ft/sec
P	N/m^2	lbf/ft^2
g_0	1.0 kg·m/N·sec^2	32.174 ft·lbm/lbf·sec^2

or

$$V = \sqrt{\frac{2g_0 \Delta P}{\rho}} \tag{9.27b}$$

Actual volumetric flow rate through the orifice, Q, is given as the product of velocity and orifice area (orifice diameter d) and the corresponding orifice coefficient of discharge, C_d, which accounts for the area effects (*vena contracta*) and velocity effects (velocity coefficient).

$$Q = C_d\left(\frac{\pi d^2}{4}\right)\sqrt{\frac{2g_0 \Delta P}{\rho}} \tag{9.28}$$

Measuring the orifice pressure drop with a manometer as a height, h, and assuming the density of air as given by Equation 1.3c, the orifice volumetric flow rate then becomes

$$Q = C_d\left(\frac{\pi d^2}{4}\right)\sqrt{\frac{2g_0 hRT}{P}} \tag{9.29}$$

To determine the air mass flow rate recall that mass flow rate is the product of density, area, and velocity or density and volumetric flow rate,

$$\dot{m} = \rho Q = C_d\left(\frac{P}{RT}\right)\left(\frac{\pi d^2}{4}\right)\sqrt{\frac{2g_0 hRT}{P}} = C_d\left(\frac{\pi d^2}{4}\right)\sqrt{\frac{2g_0 hP}{RT}} \tag{9.30}$$

Expressing the orifice pressure drop manometer height, h, in units of mm H_2O and substituting the ideal gas law in either SI or Engineers' units along with the appropriate values for g_0 and appropriate conversion factors, the following relationships for volumetric and mass flow rate relationships are obtained:

SI

$$Q = 0.1862 \cdot C_d \cdot d^2\sqrt{\frac{hP}{T}} \qquad \dot{m} = 64.89 \cdot C_d \cdot d^2\sqrt{\frac{hP}{T}}$$

English Engineers

$$Q = 0.01204 \cdot C_d \cdot d^2\sqrt{\frac{hP}{T}} \qquad \dot{m} = 0.03252 \cdot C_d \cdot d^2\sqrt{\frac{hP}{T}}$$

where

Property	SI	English Engineers
Q	m^3/sec	ft^3/sec
m	kg/sec	lbm/sec
ρ	kg/m^3	lbm/ft^3
P	N/m^2	lbf/ft^2
T	K	°R
d	mm	in.
h	$mm{\cdot}H_2O$	$mm{\cdot}H_2O$

Various non-orifice intake air flow measurement methods are available for use during engine testing, each with particular benefits and limitations, including the following:

Critical flow nozzle – Flow rate depends linearly on delivery pressure to a venturi nozzle but is independent of pressure in the airbox. An external compressor is required to ensure flow rate is choked.

Turbine and positive displacement air flow meters – Flow rate depends linearly on the rotational speed of the flow meter. Positive displacement versions are available that operate on the principle of the Roots blower.

Hot wire anemometer – Flow rate is proportional to the measured centerline velocity in the flow meter. Hot wire anemometry can be used to measure both steady state and instantaneous mass flow rates.

Laminar viscous air flow meter – Flow rate depends linearly on pressure drop across the meter rather than its square root as with an orifice measurement. Measuring element consists of a bundle of small non-circular tubes sized such that the Reynold's number in each passage is well within the laminar regime. No airbox damping is required and as such, provides a more compact measurement device.

With each of these air flow measurements, local temperature and pressure measurements are still required. It is also still important to take into consideration unsteady pulsating intake air flow effects even when utilizing devices, such as the hot wire anemometer, to make transient and instantaneous measurements.

Now an actual atmosphere contains water vapor which means, unlike air, it cannot be described by the ideal gas law. Humid air conditions can be determined from psychometrics using wet- and dry-bulb temperatures in conjunction with the psychometric chart. One expression reports moisture content in the atmosphere using *relative humidity*, ϕ, the ratio of partial pressure of water present at temperature to the saturation pressure of water at the same temperature. Alternatively moisture content can be reported as *humidity ratio*, ω, the ratio of mass of water to mass of dry air.

Since different engines are investigated under various test conditions, correcting to a standard reference enables direct comparison of dissimilar results. Intake ambient atmosphere for an IC engine is frequently corrected to a reference state, such as the Reference Atmosphere shown in Table 9.2. Total atmospheric pressure of the Reference Atmosphere consists of the partial pressure of dry air and the partial pressure of water vapor or

$$P_{\text{atm}} = P_{\text{air}} + P_{\text{water}} \tag{9.31}$$

Table 9.2 Reference Atmospheric Properties

Property	Standard	SI	English Engineers
P_{ref}	1 bar	100,000 N/m^2	14.50382 psi
T_{ref}	25°C	25°C	77°F
ϕ_{ref}	30%	30%	30%

Table 9.3 Water Saturation Pressure as a Function of Relative Humidity & Temperature

T	ϕ, %				
°C	20	40	60	80	100
0	0.000122	0.000244	0.000366	0.000488	0.00061
10	0.002454	0.004908	0.007362	0.009816	0.01227
20	0.004678	0.009356	0.014034	0.018712	0.02339
30	0.008492	0.016984	0.025476	0.033968	0.04246
40	0.014768	0.029536	0.044304	0.059072	0.07384

Table 9.3 shows the partial pressure of water vapor in the Reference Atmosphere expressed in bars for different values of relative humidity and temperature. Values were created as a function of temperature using the definition of relative humidity, ϕ, and the saturation pressure of water obtained from Appendix C.

Table 9.4 shows the partial pressure of air in the Reference Atmosphere expressed in bars for different values of relative humidity and temperature using Equation 9.31 and Table 9.3.

Figures 9.8 and 9.9 illustrate the results of the computations shown in Tables 9.3 and 9.4. An inspection of Figure 9.9 reveals that at the Reference Atmosphere (1 bar, 25°C and 30% relative humidity), the partial pressure of air equals 0.99 bars (99,000 N/m^2 or 14.35878 psi). A further inspection of Figure 9.9 indicates that at about 8°C and 100% relative humidity the partial pressure of air also equals 0.99 bars suggesting that below this temperature barometric corrections are perhaps not significant. From Figure 9.9 humidity corrections are seen to be temperature dependent and above the standard conditions strongly dependent on relative humidity. For example, at 40°C and 100% relative humidity the partial pressure of air equals 0.926 bar, a 6.46% reduction in value from reference atmosphere conditions.

Table 9.4 Partial Pressure of Air as a Function of Relative Humidity & Temperature

T	ϕ, %				
°C	20	40	60	80	100
0	0.999878	0.999756	0.999634	0.999512	0.99939
10	0.997546	0.995092	0.992638	0.990184	0.98773
20	0.995322	0.990644	0.985966	0.981288	0.97661
30	0.991508	0.983016	0.974524	0.966032	0.95754
40	0.985232	0.970464	0.955696	0.940928	0.92616

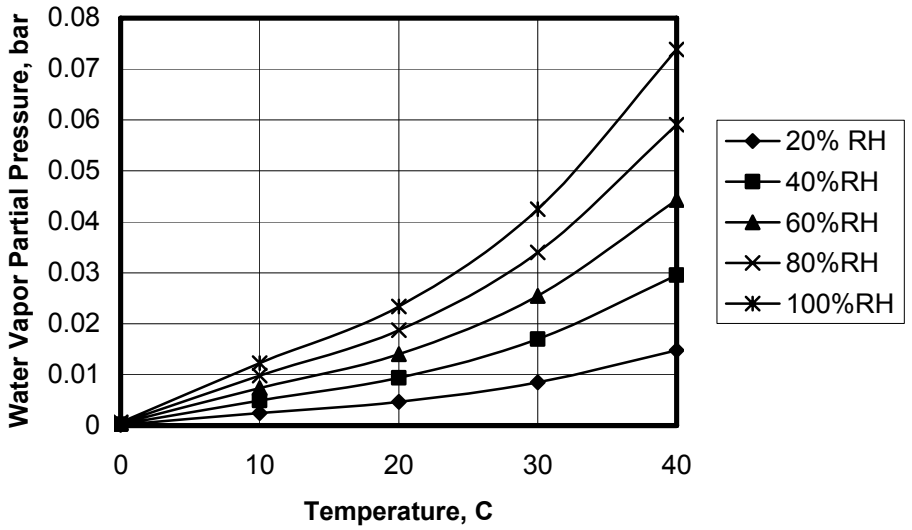

Figure 9.8 Saturation pressure of water as a function of relative humidity and temperature.

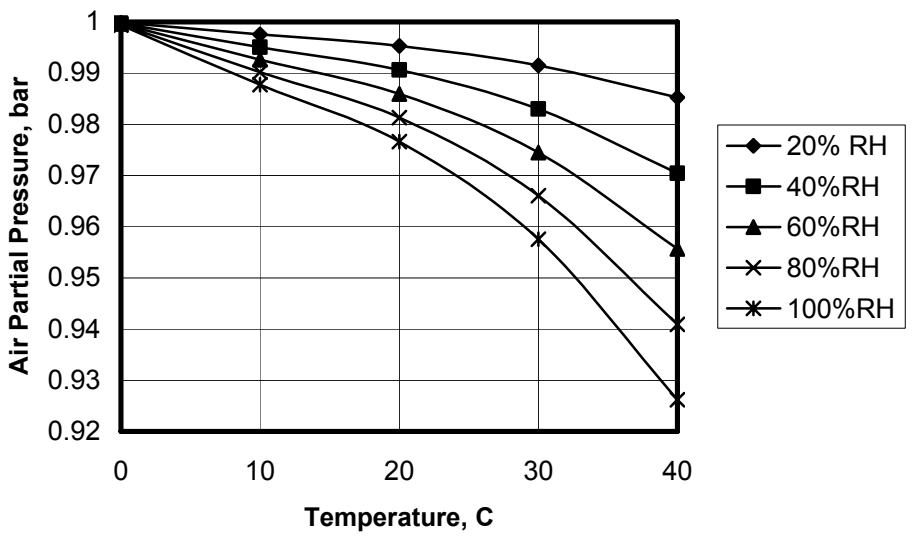

Figure 9.9 Partial pressure of air as a function of relative humidity and temperature.

When performing intake air flow analysis, the air pressure should be based on a dry air value.

$$P_{\text{dry-air}} = P_{\text{atm}} - P_{\text{water-vapor}} \tag{9.32}$$

From Equation (1.3c) dry air density is seen to vary inversely with absolute temperature and directly with absolute pressure. Using the ideal gas law for air the expression to adjust air density from test conditions to reference conditions can be shown to be

$$\rho_{\text{ref}} = \rho_{\text{test}}(P_{\text{dry-air-ref}} / P_{\text{dry-air-test}})\,(T_{\text{test}}/T_{\text{ref}}) \tag{9.33}$$

where

$\rho_{\text{dry-air-ref}}$ = dry air density at reference conditions
$\rho_{\text{dry-air-test}}$ = dry air density at test conditions
$P_{\text{dry-air-ref}}$ = dry air partial pressure at reference conditions
$P_{\text{dry-air-test}}$ = dry air partial pressure at test conditions
$T_{\text{dry-air-ref}}$ = dry air temperature at reference conditions
$T_{\text{dry-air-test}}$ = dry air temperature at test conditions

Equation (9.30) can be used to obtain a relation to adjust the air mass flow rate for a spark-ignition engine at wide-open throttle from test conditions to reference conditions. In SI

$$\dot{m} = 64.89 \cdot \mathrm{C_d} \cdot \mathrm{d}^2 \sqrt{\frac{\mathrm{h}P}{T}} = \mathrm{c}_1 \sqrt{\frac{\Delta P \cdot P}{T}} = \mathrm{c}_1 \sqrt{\frac{\mathrm{c}_2 P \cdot P}{T}}$$

or

$$\dot{m} \approx (P)(T)^{-0.5} \tag{9.34}$$

Equation (9.34) indicates that the air mass flow rate is proportional to local test atmospheric pressure and inversely proportional to the square root of local temperature. The air mass flow rate correction for a test engine at wide-open throttle to standard reference conditions in SI units would then be equal to

$$\dot{m}_{\text{ref}} = \dot{m}_{\text{test}} \left[\left(\frac{P_{\text{dry-air-ref}}}{P_{\text{dry-air-test}}} \right) \left(\frac{t_{\text{test}} + 273}{298} \right)^{0.5} \right] \tag{9.35}$$

where

$P_{\text{dry-air-ref}}$ = dry air partial pressure at reference conditions, bar or kPa
$P_{\text{dry-air-test}}$ = dry air partial pressure at test conditions, bar or kPa
t_{test} = air temperature at test conditions, °C
m = mass flow rate, kg/sec

Recall that volumetric efficiency, Equation (9.5), relates actual and ideal induction performance of an engine intake process as

$$\eta_v = \frac{\text{mass (volume) actually induced at inlet } P \text{ \& } T}{\text{engine displacement volume mass (volume)}} \times 100$$

Volumetric efficiency for a four-stroke engine with displacement volume, V_D, running at engine speed, N, can be expressed in terms of the volume flow rate of intake air as

$$\eta_v = \frac{2 \cdot \dot{m}_{\text{dry-air}}}{\rho_{\text{dry-air}} \cdot V_D \cdot N} = \frac{m_{\text{dry-air}}}{\rho_{\text{dry-air}} \cdot V_D} \tag{9.36}$$

where

2 = 2 rev/intake stroke
$m_{\text{dry-air}}$ = air mass flow rate kg/sec/cyl (lbm/sec/cyl)
$m_{\text{dry-air}}$ = air mass inducted per cylinder per cylinder, kg/intake/cyl (lbm/intake/cyl)
$\rho_{\text{dry-air}}$ = air density, kg/m^3 (lbm/ft^3)
V_D = displacement volume per cylinder, m^3/intake/cyl (ft^3/intake/cyl)
N = engine speed, rev/sec

A correction factor, CV, for adjusting volumetric efficiency at test values to standard reference conditions can be expressed using Equations (9.26) and (9.27) which reduces to the following relation equal to a ratio of only temperatures.

$$\text{CV} = \frac{\eta_{\text{dry-air-std}}}{\eta_{\text{dry-air-test}}} = \left(\frac{T_{\text{dry-air-std}}}{T_{\text{dry-air-test}}} \right)^{0.5} \tag{9.37}$$

Temperature, pressure, and relative humidity influence the local ambient intake atmosphere of an IC engine which in turn, for any given speed, will affect output and performance. Specific relationships are recommended for particular SI and CI engines that include correction factors similar to the general standard reference atmospheric state relationships shown above. Specific relationships may be found in detail in SAE and other technical standards.

Engine performance maps provide a means of representing complete engine characteristics over a wide range of speed, power, and torque. The general nature of these curves can be ascertained from relations developed in this chapter.

Internal combustion engine power is directly related to its fuel-air mixture and, for a particular engine geometry and specific fuel-air ratio, the ideal charge per cylinder per cycle should be independent of speed. In Section 9.2, the ideal and actual induction processes were related by the use of a volumetric efficiency η_v. Volumetric efficiency is strongly influenced by heat transfer, fuel parameters, the thermodynamic state of both intake charge and residual gases, and engine parameters such as intake and exhaust manifolds and valve design. For a particular condition of engine load, valve timing, and fuel-air input, the actual volumetric efficiency versus engine speed yields the characteristic curve shown in Figure 9.10. At low engine (piston) speed, an incoming charge has little kinetic energy influence on the intake process, i.e., *ramming.* At higher speeds, inertial ramming will increase the charge input to a maximum valve but, as speed is increased, frictional effects will tend to reduce the magnitude of η_v from its midspeed optimum valve. Changing engine operational regime may shift the volumetric efficiency curve.

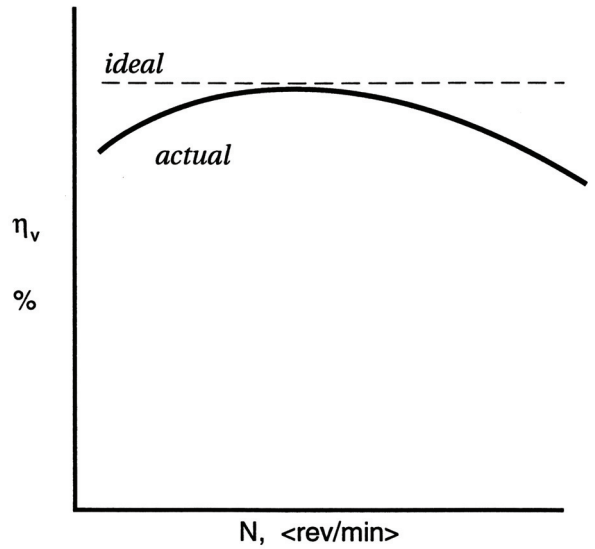

Figure 9.10 Volumetric efficiency vs. engine speed.

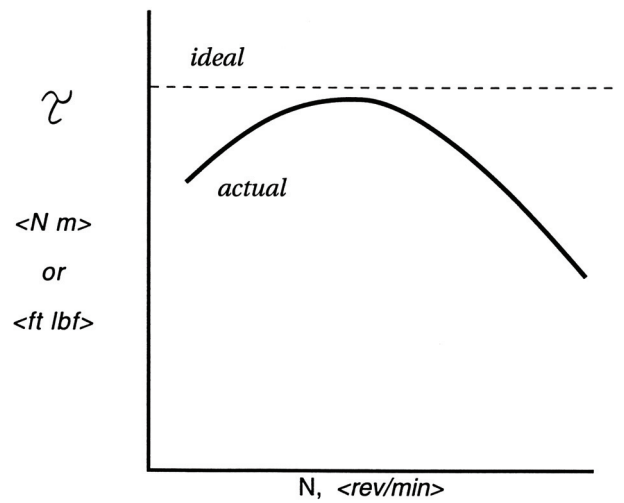

Figure 9.11 Engine torque vs. engine speed.

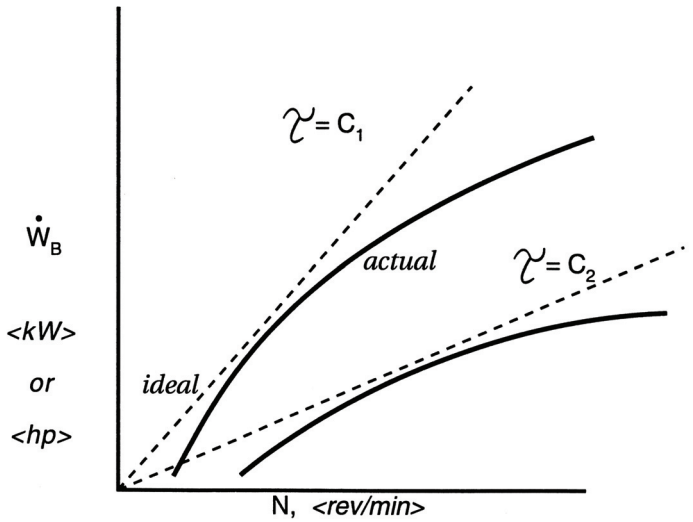

Figure 9.12 Brake power vs. engine speed.

At constant load, Equation (9.20) shows that, ideally, engine torque, $\tau = rf$, is independent of speed. Since power results from the combustion of a fuel-air mixture, an actual torque curve, like volumetric efficiency, will fall off at high and low engine speeds; see Figure 9.11. Equation (9.21) relates brake power, torque, and engine speed as

$$\dot{W}_B = C_1 \times \tau \times N \tag{9.38}$$

Brake power versus engine speed for fixed load should ideally yield a straight line having a constant slope; see Figure 9.12. Actual brake power will fall off at low and high speeds because of the speed dependency of the torque curve.

Brake mean effective pressure, *BMEP,* is calculated knowing brake power and speed, using Equation (9.22) or

$$BMEP = C_2 \times \frac{\dot{W}_B}{N} \tag{9.39}$$

or combining Equations (9.38) and (9.39)

$$BMEP = C_2 \times C_1 \times \tau \times \frac{N}{N} = C_3 \times \tau \tag{9.40}$$

Ideally, *BMEP* versus speed plots as a straight line having a positive slope and passes through the origin; see Figure 9.13. Again, as with brake power, a speed-dependent torque relation will produce an actual *BMEP* curve having low- and high-speed fall-off regions.

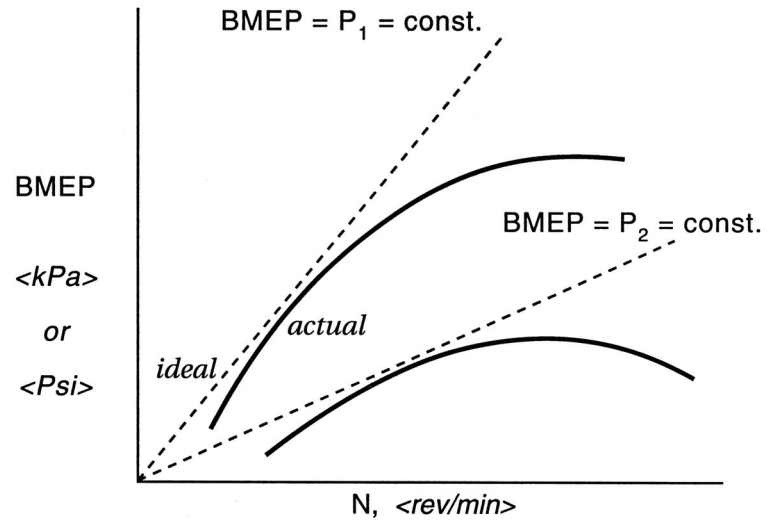

Figure 9.13 Brake mean effective pressure vs. engine speed.

Brake specific fuel consumption, BSFC, Equation (9.26), a measure of fuel consumed per unit of brake power, can be related to the induced air and brake power as

$$BSFC = \frac{\dot{m}_f}{\dot{W}_B} = \frac{\dot{m}_{\text{air}} FA}{\dot{W}_B} = C_4 \times \frac{\dot{m}_{\text{air}}}{\dot{W}_B} \tag{9.41}$$

For a fixed load and air-fuel ratio, the volumetric efficiency and brake power curves show that specific fuel consumption versus engine rpms would produce large values at low and high rpms, with a minimum rather than a maximum valve at midrange speed; see Figure 9.14. Brake thermal efficiency, Equation (9.24), i.e., the ratio of brake power to fuel consumption, should be inversely proportional to the brake specific consumption curve as shown in Figure 9.14.

As stated earlier, friction power $\dot{W}_F$, a measure of engine losses, increases with speed. Mechanical efficiency, Equation (9.42), defined as the ratio of brake to indicated power,

$$\eta_{\text{mech}} = \frac{\dot{W}_B}{\dot{W}_I} = \frac{\dot{W}_B}{\dot{W}_B + \dot{W}_F} \tag{9.42}$$

will tend to decrease with speed since friction power tends to increase at a greater rate than the sum of brake and friction power; see Figure 9.14.

Additional aspects of IC engine testing, such as matching load and output or correcting for nonstandard barometric testing, can be found in many IC engine textbooks and in the standards literature for engine testing established by relevant engineering societies mentioned at the beginning of Section 9.5.

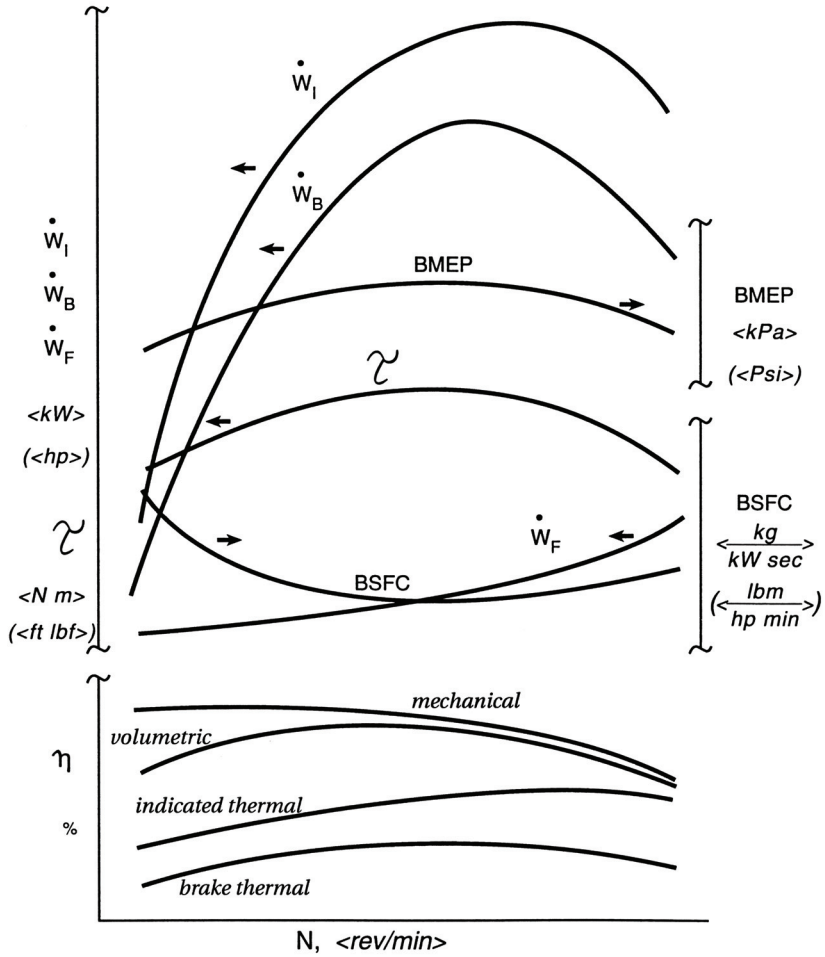

Figure 9.14 Typical IC engine performance map.

9.6 THE COOPERATIVE FUEL RESEARCH (CFR) ENGINE

The design and development of more efficient internal combustion engines will require a fuller understanding of the general characteristics of fuel-engine compatibility. As described in previous sections of this chapter, many important brake and indicated performance parameters for a variety of engine types and sizes are determined in the engine test cell.

One significant fuel-engine interaction not mentioned in earlier sections but worthy of attention is the tendency of fuel-air mixtures to detonate at certain conditions in both spark-ignition (SI) and compression-ignition (CI) engines. This explosive nature is termed *autoignition,* or *knock.* Knock characteristics are a function of the chemical nature of a fuel and the combustion processes in a particular engine. Since knock performance of fuels must be determined experimentally, a variety of standardized tests for both SI and CI fuels have been established by the American Society for Testing Materials (ASTM). These tests involve the use of specific engines and include research, motor, or vehicle tests.

The research method for testing SI and CI fuels for knock uses a single-cylinder *Cooperative Fuel Research* (CFR) engine. This unique 3.25 in × 4.5 in. four-stroke engine has several parameters that can be varied while the engine is in operation, including the compression ratio (3:1 to 15:1), air-fuel ratio, and/or fuel type. Variable compression is accomplished by means of a hand crank and worm gear mechanism, which allows the cylinder and head assembly to be raised or lowered with respect to the crankshaft. A unique overhead valve design maintains constant-volume clearance with varying compression ratio.

Three separate gravity-fed fuel bowls are connected to a horizontal draft, air-bled jet carburetor, allowing any of three different fuels to be used and/or interchanged while the engine is running. The fuel-air ratio can also be changed by simply raising or lowering each of the three fuel bowls.

Engine speed is maintained at 900 rpm by means of an engine-belted, synchronous AC power generator. Also, particular SI versions of the CFR engine have components that allow spark timing to be changed, while CI configurations have the capability of varying fuel injection rate and timing.

Recall from Chapter 7 that liquid hydrocarbon fuel characteristics are a function of their distillation curves. Since most commercial fuels are a mixture of many compounds of varying volatility, the knock characteristics will, in general, relate to their distillation curves. Detonation, or knock, in an engine will result in a rapid rise in peak engine pressure. Cylinder pressure in the research test is measured using a pressure transducer with filtered voltage output displayed on a knock meter. The knock rating of a particular fuel is obtained by matching the knock intensity of a sample at fixed operating conditions to that produced by blends of reference fuels.

Four primary fuels are used as standards for making mixtures of reference blends. Spark-ignition engine fuel ratings are measured in terms of an *octane* rating, while compression-ignition engine fuel ratings are specified by a *cetane* scale. Octane numbers are based on isooctane having an octane value of 100 and *n*-heptane having an assigned value of 0 octane. Thus, a 90-octane reference blend would be 90% isooctane and 10% *n*-heptane mixture by volume or

Reference octane no. = % isooctane + % *n*-heptane

Cetane numbers are based on *n*-cetane (nexadecane) having a cetane value of 100 and n-methylnaphthalene ($C_{11}H_{10}$) having an assigned value of 0 cetane. The octane scale for a reference blend by volume is given as

Reference cetane no. = % *n*-cetane + % $C_{11}H_{10}$

In general, the higher the octane rating, the lower the tendency for the fuel-air mixture to autoignite in an SI engine. Also, the higher the cetane rating of a fuel, the greater the tendency for autoignition in a CI engine. Thus, a high-octane fuel will be a low-cetane fuel, and a low-octane fuel will have a high cetane index.

Knock rating of IC engine fuels based on the research test method is often different from values obtained using the motor method. Octane and/or cetane rating variations according to knock testing by research and motor methods are specified by *fuel sensitivity*. In general, the research method yields octane ratings higher than those obtained from the motor test. Current practice requires that automotive fuels be based on an average of the research and motor octane numbers.

Fuel	Old scale	New scale
Unleaded	91	87
Regular	94	89
Midpremium	96	91.5
Premium	99	94

Additives, such as tetraethyl lead (TEL), were used in the past to raise the octane values of gasoline, but environmental impact forced the development of unleaded fuels and alternate octane boosters, such as the efforts with anhydrous ethanol-gasoline blends, or gasohol. In addition, some fuels may actually yield octane numbers in excess of 100.

9.7 ENGINE EMISSIONS TESTING

In Sections 9.5–9.6 standard tests necessary to determine several critical fuel-engine interfaces of IC engines were discussed. Current engine testing also requires activities that discern the nature of certain species emitted with the exhaust from IC engines. Over 90% of the typical exhaust gas composition for today's internal combustion engines, on a volumetric basis, consist chiefly of CO_2, H_2O, and N_2. However, over 200 specific trace chemical compounds have been identified in various engine exhausts, including carbon monoxide, CO; nitric oxides, NO_x; unburned hydrocarbons, UHC; partially oxidized hydrocarbons, PHC; sulfur dioxide, SO_2; as well as particulates and smoke; see Figure 9.15 and Table 9.5.

The concentrations of these engine pollutants, i.e., exhaust products other than O_2, H_2O, and N_2, are very small and cannot be inferred using the boiler or furnace stack sampling techniques such as the Orsat discussed in earlier chapters. Engine exhaust gas instrumentation must generally be designed to detect 1 part per million (ppm) of a particular species in a mixture.

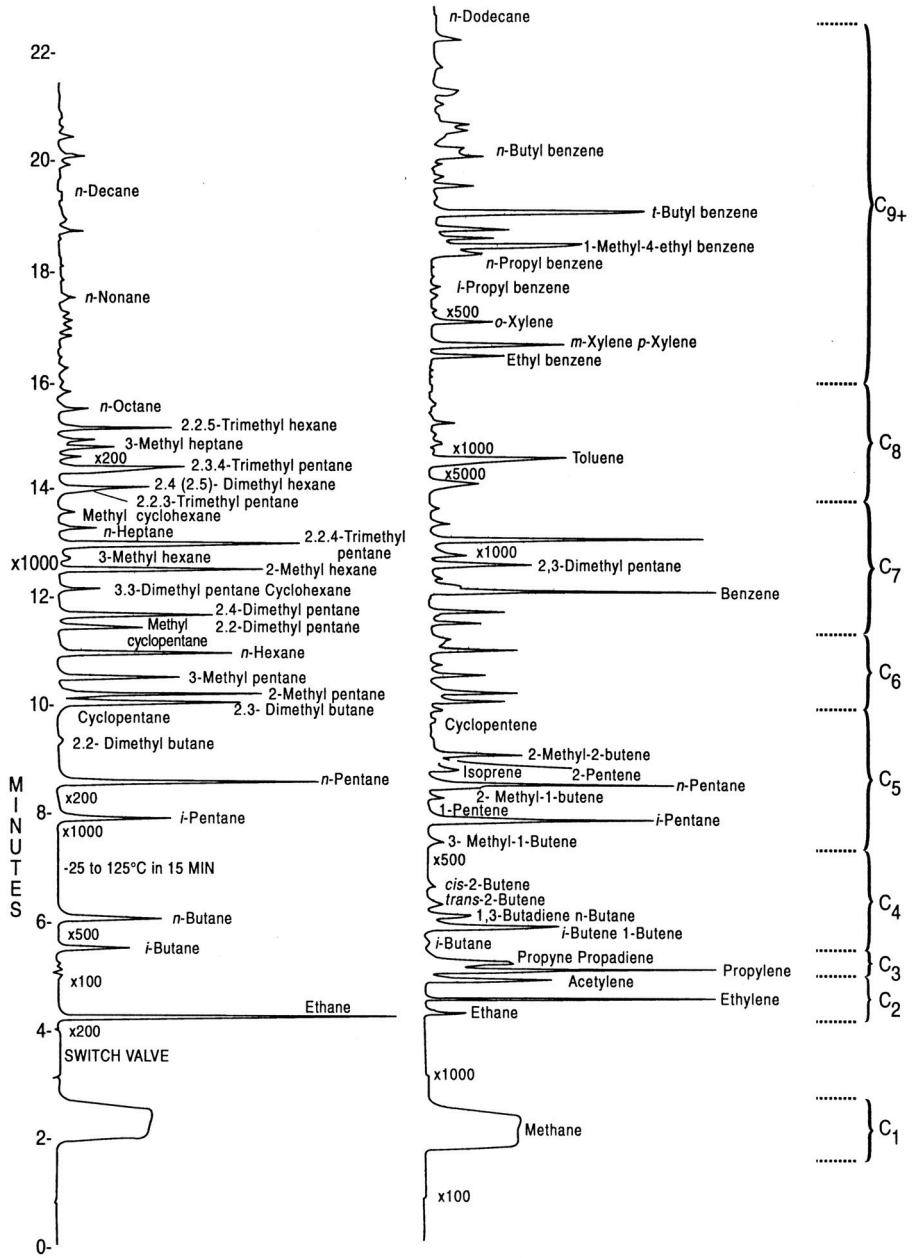

Figure 9.15 Typical gas chromatograph of exhaust gas emissions. *Source*: Hafstad, L. R., Argonne Universities Association Conference on Universities, National Laboratories, and Man's Environment, July 27–29, 1969, Chicago, IL, U.S. Atomic Energy Commission, Division of Technical Information.

Table 9.5 Internal Combustion Engine Exhaust Gas Emissions

Carbon Monoxide (CO): CO, odorless, toxic gas (0.3% CO in air is lethal within 30 min), product of incomplete combustion.
Unburned Hydrocarbons (UHC): C_xH_y, paraffins, olefins, and aromatics (odor and carcinogenic constituents), products of incomplete combustion.
Partially Burned Hydrocarbons (PHC): C_xH_y·CHO, aldehydes; C_xH_y·CO, ketones; and C_xH_y·COOH, carboxylic acids; quenched products of low-temperature combustion.
Nitric Oxides (NO_x): NO, nitric oxide, colorless and odorless gas; NO_2, nitrogen dioxide, reddish orange gas, corrosive and toxic; N_2O, nitrous oxide, colorless, odorless laughing gas. High-temperature by-products of lean combustion dissociation in excess air, major contributor to photochemical smog.
Sulfur Oxides (SO_x): SO_2, sulfur dioxide, nonflammable colorless gas, source of sulfuric acid (H_2SO_4) and acid rain, product of combustion of sulfur impurities in hydrocarbon fuels.

The ability to absorb or emit radiation is one means of characterizing or identifying particular chemical compounds. Spectroscopy characterizes the interactions of electromagnetic radiation and matter. Absorption spectroscopy utilizes the ability of matter to absorb radiation, whereas emission spectroscopy involves the radiant energy emitted by matter. No chemical species absorbs or emits radiation throughout the entire electromagnetic spectrum from ultraviolet to infrared. The distinct absorption or emission spectrum for a given compound is determined by its molecular structure and quantized internal energy levels. Energy is stored in a molecule as translational, rotational, vibrational, electronic, and chemical energy. The infrared spectrum can be related, for example, to rotational and vibrational state changes in a molecule, whereas ultraviolet radiation can be associated with electronic state changes in a molecule.

Electromagnetic radiation via quantum mechanics principles is converted by the spectroscopic emission detector into a measurable quantity, such as an electric current or voltage. Among the requirements for a useful spectroscopic detector are: (1) a high sensitivity to measured radiation with a low background noise level, (2) a fast time response to changes in radiation flux, (3) a low fatigue level, and (4) a measurable detection signal.

Ultraviolet and visible photons can cause photoejection of electrons from certain specially treated surfaces. Incorporation of these photosensitive materials into the construction of certain detectors, termed *photoelectric detectors,* allows conversion of radiant photon flux into an electric current. Infrared radiation can cause a decrease in the resistance of certain materials that are poor electric conductors. Application of these materials in designing certain exhaust gas detectors allows conversion of an infrared photon flux into measurable voltages. This internal photoconductive effect, since no electron ejection occurs as in phototube-type detectors, is found in certain metallic sulfides, certain element semiconductors such as silicon or germanium, and many compound semiconductors such as indium antimonide (InSb).

EXAMPLE 9.5 An automobile consumes 3.33 gal/hr of fuel while running at a constant speed of 50 mph on an engine dynamometer test facility. The spark-ignition engine burns a rich isooctane mixture. Exhaust gas analysis, on a dry volumetric basis, gives the following results:

9.54%	CO_2	0.84%	H_2
4.77%	CO	2.8%	O_2
3.15%	CH_4	78.9%	N_2

The specific gravity of isooctane is 0.702. Calculate (a) the fuel-air equivalence ratio; (b) the air-fuel ratio on a mass basis; (c) the fuel density, lbm/gal; (d) the fuel consumed, mpg; and (e) the grams of CO produced per mile.

Solution:

1. Reaction equation:

   Stoichiometric:

   $$C_8H_{18} + 12.5[O_2 + 3.76N_2] \rightarrow 8CO_2 + 9H_2O + 47N_2$$

   Actual:

   $$\Phi C_8H_{18} + 12.5[O_2 + 3.76N_2] \rightarrow a[0.0954CO_2 + 0.0477CO + 0.0315CH_4 + 0.0084H_2 + 0.028O_2 + 0.789N_2] + bH_2O$$

   Nitrogen balance:

   $$(25)(3.76) = (0.789)(2)a \qquad a = 59.569$$

   Carbon balance:

   $$8\Phi = [0.0954 + 0.0477 + 0.0315](59.569)$$

   a. $\Phi = 1.30$

   Oxygen balance:

   $$25 = (59.569)[(2)(0.0954) + 0.0477 + 0.056] + b$$
   $$b = 7.457$$

   Hydrogen balance (check):

   $$(18)(1.30) = 23.4$$
   $$59.569[(4)(0.0315) + 0.016] + (2)(7.457) = 23.4$$

2. Mass air-fuel ratio:

   b. $$AF = \frac{[(12.5)(4.76)\,\text{lbmoles air}][(28.97)\,\text{lbm/lbmoles air}]}{[(1.3)\,\text{lbmoles fuel}][(114)\ \text{lbm/lbmole fuel}]} = 11.6\,\frac{\text{lbm air}}{\text{lbm fuel}}$$

3. Mass of fuel consumed per hour:

$$\rho_{\text{fuel}} = (0.702)(62.4 \text{ lbm/ft}^3) = 43.8 \text{ lbm fuel/ft}^3$$
$$= (43.8 \text{ lbm fuel/ft}^3)(231 \text{ in.}^3/\text{gal})(1728 \text{ in.}^3/\text{ft}^3)^{-1}$$

c. $\rho_{\text{fuel}} = 5.855$ lbm fuel/gal

$$\dot{M}_{\text{fuel}} = (5.855 \text{ lbm fuel/gal})(3.33 \text{ gal/hr}) = 19.5 \text{ lbm fuel/hr}$$

where

$$Z\langle\text{mpg}\rangle = (50 \text{ mph})/(3.33 \text{ gal/hr})$$

d. $Z = 15$ mpg

4. Grams of CO produced per mile:

$$\frac{M_{\text{CO}}}{M_{\text{fuel}}} = \frac{[(59.569)(0.0477) \text{ lbmole CO}][(28) \text{ lbm/lbmole CO}]}{[(1.3) \text{ lbmoles fuel}][(114) \text{ lbm/lbmole fuel}]} = 0.5368 \frac{\text{lbm CO}}{\text{lbm fuel}}$$

or

$$\dot{M}_{\text{CO}} = \frac{\left(0.5368 \frac{\text{lbm CO}}{\text{lbm fuel}}\right)\left(19.5 \frac{\text{lbm fuel}}{\text{hr}}\right)\left(0.45359 \frac{\text{kg}}{\text{lbm}}\right)\left(1000 \frac{\text{g}}{\text{kg}}\right)}{(50 \text{ mph})}$$

e. $\dot{M}_{\text{CO}} = 94.96 = 95.0$ g CO/mi

It is often necessary to separate various exhaust gas emission species from each other prior to their detection and analysis. Gas chromatography is a material separation phenomenon in which given exhaust gas/vapor mixture species are segregated into pure samples contaminated only by an inert carrier gas. These segregated compounds are then detected, giving a quantitative analysis of the gas mixture. The column, the heart of the chromatograph, is a component that isolates and partitions the various chemical species in a given exhaust sample. The detector provides the means of quantizing the column effluent. Several types of detectors are currently used, among them the infrared analyzer, the mass spectrometer, the flame ionization detector, and the thermal conductivity cell. The detector is designed to produce a signal that is proportional to the mass of the unknown sample. The voltage generated by the detector, often after suitable amplification, is recorded as a function of time; see Figure 9.15.

Exhaust gas, or *emissions*, analysis is an important engine performance activity because of the increasing environmental impact of worldwide IC engine operation. Today IC engine testing and performance evaluation include emissions testing not only during new engine development and certification but also as a standard part of regulation and monitoring of older used vehicles. Standard emissions test programs, such as established by state, U.S. Federal, and European International Standards Organization ISO, are used to measure the pollution levels of new vehicles. Emission issues began to be an environmental issue in the 1950s when concentrated engine discharges affected specific geographical areas and unique local climates, such as the Los Angeles basin.

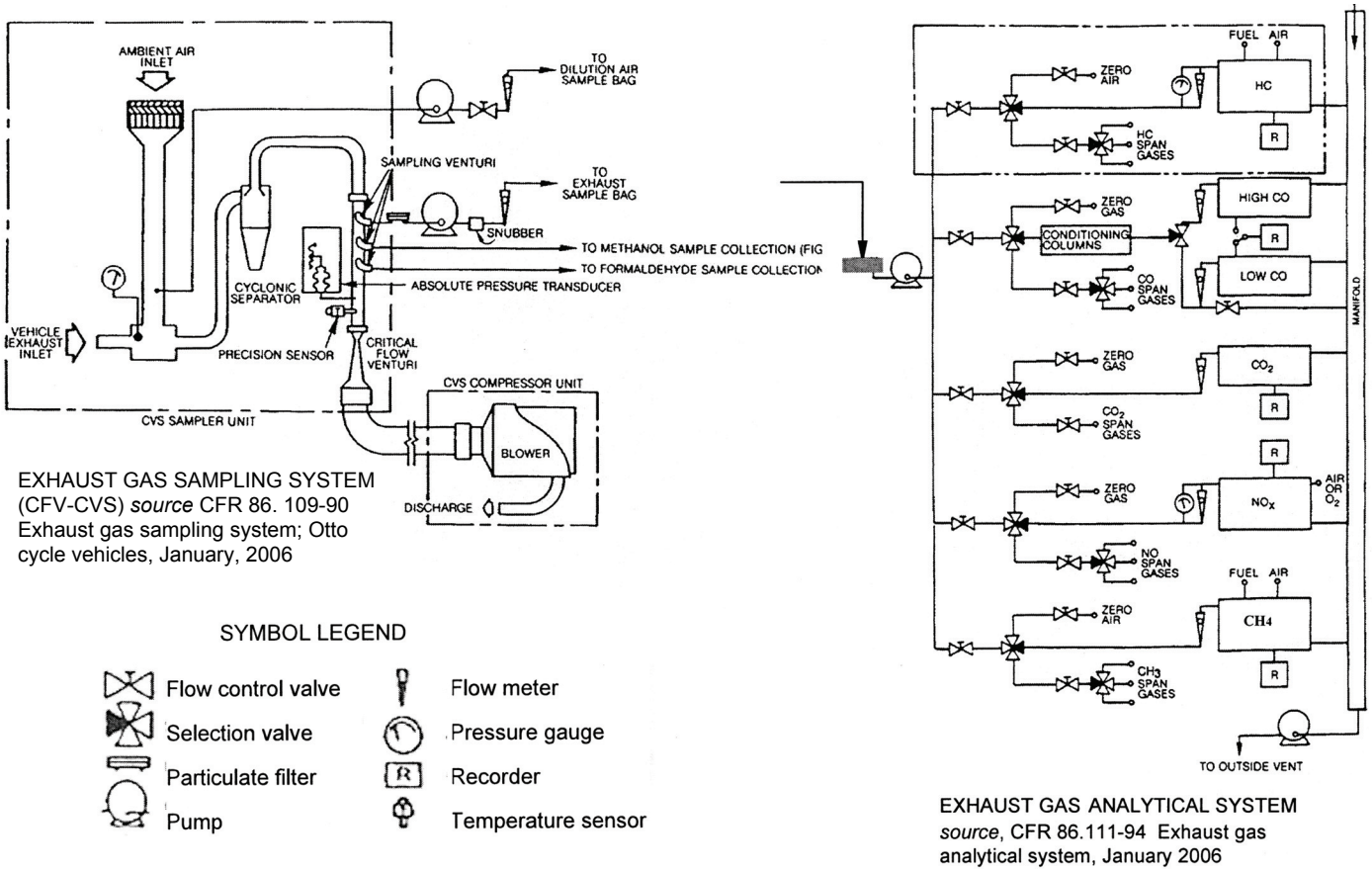

Figure 9.16 Constant-volume IC engine exhaust gas emission sampling and analysis system schematic.

Table 9.6 U.S. Light Duty Vehicle Emissions Standards

Model Year	Test Procedure	Useful Life	[CO] gpm	$[HC]_1$ gpm	$[HC]_2$ gpm	$[HC]_3$ g/test	$[NO_x]$ gpm	[PM] gpm
Pre-Control	7-mode		3.4%	850 ppm	—	—	1000 ppm	—
Pre-Control	7-mode		80	11	—	—	4	—
Pre-Control	CVS-75		87.0	8.8	—	—	3.6	—
1968–69	7-mode							
	50-100 CID		2.3%	410 ppm	—	—	—	—
	101-140		2.0%	350 ppm	—	—	—	—
	Over 140		1.5%	275 ppm	—	—	—	—
1970	7-mode		23	2.2	—	—	—	—
1971	7-mode		23	2.2	—	6	—	—
1972	CVS-72		39	3.4	—	2	—	—
1973–74	CVS-72		39	3.4	—	2	3.0	—
1975–76	CVS-75		15	1.5	—	2	3.1	—
1977	CVS-75		15	1.5	—	2.0	2.0	—
1978–79	CVS-75		15	1.5	—	6.0	2.0	—
1980	CVS-75		7.0	0.41	—	6.0	2.0	—
1981	CVS-75		3.4	0.41	—	2.0	1.0	—
1982	CVS-75		3.4	0.41	—	2.0	1.0	0.6 (D)
			(7.8)	(0.57)	—	(2.6)	(1.0)	—
1983	CVS-75		3.4	0.41	—	2.0	1.0	0.6 (D)
			(7.8)	(0.57)	—	(2.6)	(1.0)	—
1984	CVS-75		3.4	0.41	—	2.0	1.0	0.6 (D)
			(7.8)	(0.57)	—	(2.6)	(1.0)	—
1985–86	CVS-75		3.4	0.41	—	2.0	1.0	0.6 (D)
1987–93	CVS-75	5 yrs/ 50,000 mi	3.4	0.41	N/A	2.0	1.0	0.2 (D)
1994	CVS-75	5 yrs/ 50,000 mi	3.4	0.41	0.25	2.0	0.4 (ND) 1.0 (D)	0.8
		10 yrs/ 100,000 mi	4.2	N/A	0.31	2.0	0.6 (ND) 1.25 (D)	0.1
2000	FTP-75	5 yrs/ 50,000 mi	3.4	0.41	0.25		0.4 (ND) 1.0 (D)	0.08
		10 yrs/ 100,000 mi	4.2	N/A	0.31		0.6 (SI) 1.25 (D)	0.10

HC = unburned hydrocarbons; CO = carbon monoxide; NO_x = nitric oxides
$[HC]_1$ = Standard HC; $[HC]_2$ = Non-methane HC; $[HC]_3$ = Evaporative HC
(ND) = Non Diesel; (D) = Diesel
Source: U.S. Environmental Protection Agency (EPA) Emissions Standards Summary Update, Ann Arbor, Michigan, 1992, Federal and California Exhaust and Evaporative Emission Standards for Light Duty Vehicles and Light Duty Trucks, EPA 420-B-00-001, February 2000.

The first regulation designed to help reduce air pollution was issued in 1959 by the Los Angeles County Board of Supervisors. In 1971, this regulating responsibility was taken over by the California Air Resources Board (CARB). The U.S. Clean Air Act of 1963 and amendments following from 1965 through the 1990s provided the major legal basis for air pollution laws, including for U.S. vehicles. In the 1970s the EPA intentionally became a technology forcing agency, i.e., emissions levels could not be met by existing technology and solutions were required to come from a push–pull approach. The National Low Emission Vehicle Program, for example, appeared in December, 1997, and Portable Emissions Measurement Systems (PEMS) with on-board vehicle applications are to begin in the near future. Today worldwide emission standards for spark- and compression-ignition IC engines are continually under revision, with stricter requirements being developed as illustrated by the trends seen in Table 9.6.

The Clean Air Act Amendments (CAAA) of 1990 expanded emission activities by introducing two sets of standards for IC engine powered vehicles: Tier 1 and Tier 2. All new light duty vehicles (LDV), a category including all gasoline- and diesel-fueled vehicles of less than 8,500 gross vehicle weight, were subject to the Tier 1 standards. Tier 1 light-duty vehicle regulations were published on June 5, 1991 and fully implemented in 1997, whereas the Tier 2 standards were adopted on December 21, 1999 and phased in beginning in 2004. LDV Tier 1 standards, progressively introduced between 1994 and 1997, introduced more aggressive emission testing with the Federal Test Procedure (FTP) and Supplemental Federal Test Procedure (SFTP). LDV Tier 1 standards will be expanded to some of the heavier Tier 2 vehicles. This emission reduction effort is being phased in between 2004 and 2009.

Standard tests, such as the U.S. Federal, California, and European programs, are used to evaluate the pollutant emission levels of new vehicles. Vehicle emissions are determined in laboratories equipped with appropriate chassis dynamometers and suitable emission instrumentation. Most current results are based on a constant-volume sampling (CVS) system; see Figure 9.16. During a programmed test period exhaust gases are accumulated in a bag using either older positive displacement pump (PDP-CVC) systems or newer critical flow venturi (CFV-CVS) systems. The vehicle is run using a standard test fuel, such as indolene, as a spark-ignition engine fuel and is made to operate over a specified driving cycle consisting of various cruise, acceleration, and deceleration modes. An experimental recording of the engine speed versus test time is made and compared to the precise speed versus time requirement of the standard test. Exhaust gases collected during the driving cycle are diluted with filtered ambient air supplied by a compressor running at a constant delivery rate. Dilution with excess air ensures that the water in the exhaust will not condense. After driving the cycle, a small fixed sample is withdrawn from the collection bag and analyzed. Emissions analysis is then reported, usually in terms of a million moles of product or grams of sample per mile.

PROBLEMS

9.1 The Cooperative Fuel Research (CFR) engine is used in the octane rating of gasolines. This unique four-stroke single-cylinder engine runs at a constant speed of 900 rpm and has a variable compression ratio that can be adjusted from 3:1 to 15:1 while the engine is in operation. The 3.25-in. × 4.5-in. engine geometry maintains a constant displacement volume while the clearance volume can be adjusted. Calculate (a) the displacement volume, ft^3; (b) the clearance volume, ft^3;

(c) the ideal volumetric airflow rate, ft^3/min; and (d) the ideal mass flow rate of air for the engine as a function of compression ratio, lbm/min. Assume that air enters the engine at *STP* conditions.

9.2 A six-cylinder, four-stroke spark-ignition engine is running at 1,800 rpm. The 10-cm × 11.5-cm engine has an 8:1 compression ratio and burns an isooctane air mixture having an equivalence ratio of 0.8. Inlet conditions are 23°C and 100 kPa abs. Determine the ideal mass flow rate of fuel-air mixture to the engine for a volumetric efficiency of (a) 100%, (b) 95%, (c) 90%, and (d) 85%, kg/min.

9.3 The surface-to-volume ratio at TDC is important in achieving the optimum combustion process in any IC engine. Four possible geometries are shown below, and each configuration has a bore and stroke of 3 in. × 4 in. For these geometries, calculate, for an 8:1 compression ratio, (a) geometric parameters for the combustion chambers; (b) the surface-to-volume ratios at TDC; and (c) the mass of air at *STP* that could occupy the four clearance volumes, kg.

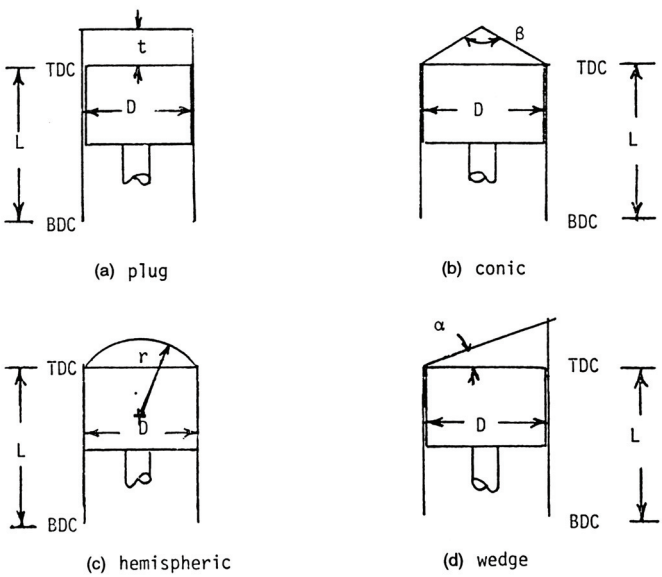

9.4 An internal combustion engine cannot be fully charged with fresh reactants during the intake stroke. At BDC, the displacement volume of an engine would ideally be filled with the fresh charge while the clearance volume would contain residual exhaust gases. For this condition, (a) show that the mass of gas in the displacement volume, M_c, can be determined from the total mass of air that could fill the entire volume, M_t, and the compression ratio, r_v, as

$$M_c = M_t\left[1 - \frac{1}{r_v}\right]$$

(b) Show that the ideal mass flow rate of air induced by the engine in terms of engine speed N and strokes per cycle n would become

$$\dot{M}_a = (M_t N / n)\left[1 - \frac{1}{r_v}\right]$$

(c) Show that the ideal mass flow rate of fuel induced by the engine in terms of engine speed N and strokes per cycle n would become

$$\dot{M}_f = (M_t N / nAF)\left[1 - \frac{1}{r_v}\right]$$

9.5 Internal combustion engine compression and expansion processes are thermodynamically modeled using the polytropic process relationship

$Pv^n = \text{const}$

The value of n for a particular engine can be obtained by plotting the experimental expansion and compression P-V data on a log P versus log V graph, which results in straight line relationships; the slope is n. Demonstrate the technique by considering a 3-in. × 5-in. diesel engine with an 18:1 compression ratio and inlet conditions of 14.8 psi and 72°F. Plot the polytropic process log P versus log V diagram for n = (a) 1.4, (b) 1.35, and (c) 1.30.

9.6 The indicated mean effective pressure and indicated work per cycle can be obtained from an experimental measurement and integration of the cylinder pressure versus swept cylinder volume diagram for an engine. An equivalent indicated heat transfer to the working fluid within the cylinder as a result of combustion can be obtained from the pressure and crank data. Show that the first law for a closed system, i.e., the working fluid in the cylinder, can be related to the crank angle θ as

$$\frac{\delta Q\langle\theta\rangle}{d\theta} = P\langle\theta\rangle\frac{dV}{d\theta} + \frac{dU}{d\theta}$$

If the gases within the engine can be treated as an ideal gas, show that

$$\frac{mR\,dT}{d\theta} = \frac{P\,dV}{d\theta} + \frac{V\,dP}{d\theta}$$

Assuming constant specific heats for the gas within the cylinder, show that the heat transfer as a function of crank angle can be written as

$$\frac{\delta Q\langle\theta\rangle}{d\theta} = \frac{\gamma}{\gamma - 1}P\langle\theta\rangle\frac{dV}{d\theta} + \frac{1}{\gamma - 1}V\langle\theta\rangle\frac{dP}{d\theta}$$

9.7 A four-stroke, six-cylinder IC engine operates at a constant speed of 1,600 rpm. The 12-cm × 20-cm engine produces a mechanical indicator card having a total area of 3.25 cm^2 and a length of 1.0 cm. The spring constant for the indicator is given as 1,082 kPa/cm of deflection. Calculate (a) the indicated mean effective pressure per

cylinder, kPa; (b) the indicator card height for a maximum cylinder pressure of 12,120 kPa, cm; and (c) the indicated engine power, kW.

9.8 A 4-in. × 5-in. single-cylinder engine is being used as a research engine. The engine, a four-stroke IC engine, is running at 1,800 rpm, with inlet conditions of 73°F and 14.5 psia. Find (a) the displacement volume, $in.^3$; (b) the clearance volume, $in.^3$; (c) the ideal volumetric flow rate, ft^3/min; and (d) the ideal mass flow rate for an engine with an 8:1 compression ratio, lbm/min.

9.9 A four-stroke CI engine is delivering 600 bhp while running at 2,400 rpm. The total engine piston displacement is 1,650 $in.^3$ and the mass *AF* ratio is 22:1. The engine uses 69.5 lbm air/min. Determine (a) the brake mean effective pressure, psi; (b) the brake torque, ft·lbf; and (c) the brake specific fuel consumption, lbm fuel/hp hr.

9.10 A six-cylinder IC engine is being performance-tested on an electric dynamometer. At full load, the experimental data obtained are as follows:

Engine rpm	N	1,500 rpm
Dynamometer load	F	64.5 lbf
Brake arm	R	2 ft
Friction power	FHP	2.5 hp
Fuel flow rate	M_f	0.245 lbm fuel/min
Heating value	LHV	12,000 Btu/Ibm

Determine (a) the brake power delivered to the dynamometer, hp; (b) the engine mechanical efficiency, %; and (c) the engine brake thermal efficiency, %.

9.11 A four-stroke 4.75-in. × 6.5-in. four-cylinder diesel yields the following test data:

Engine rpm	N	1,160 rpm
Dynamometer load	F	120 lbf
Brake arm	R	1.75 ft
Friction power	FHP	57.3 hp
Mass *AF* ratio		13.5:1
Fuel oil specific gravity		0.82
Ambient air conditions		14.7 psia, 68°F
Fuel flow rate		21 lbm/hr

Calculate (a) the fuel lower beating value, Btu/gal; (b) the engine *BHP, FHP,* and *IHP,* hp; (c) the engine mechanical efficiency, %; (d) the brake specific fuel consumption, lbm/hp hr; (e) the brake mean effective pressure, psi; (f) the engine brake torque, ft·lbf; and (g) the brake thermal efficiency, %.

9.12 An engine is using 9.1 lbm air/min while operating at 1,200 rpm. The engine requires 0.352 lbm fuel/hr to produce 1 hp of indicated power. The *AF* ratio is 14:1, and the indicated thermal efficiency is 38%. For a mechanical efficiency of 82%, find (a) the engine brake power, hp; and (b) the fuel heating value, Btu/lbm fuel.

9.13 A four-cylinder, 20-cm × 30-cm two-cycle engine has an indicated mean effective pressure of 61.0 kN/m^2 and a mechanical efficiency of 83%. For operation at 2100 rpm, determine (a) the brake power, kW; (b) the brake torque, N·m; and (c) the brake specific fuel consumption for a 78% volumetric efficiency for the engine, kg/kW sec.

9.14 A compression-ignition engine has a brake power output of 2,900 kW and burns diesel fuel having an *API* value of 30. For a brake thermal efficiency of 37.6%, calculate (a) the lower heating value of the fuel, kJ/kg fuel; and (b) the brake specific fuel consumption, kg/kW sec.

9.15 A six-cylinder, four-stroke IC engine is running at 2,680 rpm. The 11.5 cm × 13 cm produced an indicator card diagram having an upper power loop area of 7.25 cm^2 and a lower pumping loop area of 0.38 cm^2. The indicator card has a displacement length of 7.45 cm and a vertical peak deflection of 3.5 cm. A spring scale of 1000 kPa/cm displacement is required for the pressure measurement. From this information, find (a) the peak pressure, kPa; (b) the indicated mean effective pressure, kPa; and (c) the indicated power, kPa.

9.16 A performance map for a four-stroke IC engine shows a minimum *BSFC* of 0.338 kg/kW hr when operating at 80% of the rated engine speed. Brake power output of 128 kW, volumetric efficiency of 95%, and an *AF* ratio of 15:1 are measured at this condition. If the engine is operated at 120% of its rated speed, the brake power output is found to be 158 kW, with a *BSFC* of 0.398 kg/kW hr. If the volumetric efficiency remains the same, what is the new *AF* ratio? Determine the volumetric efficiency if the same *AF* ratio is maintained.

9.17 A six-cylinder, 4.3-in. × 4.125-in. automotive engine burns 25.5 lbm/hr of gasoline while running at 3,000 rpm and producing half-load on a dynamometer. If this engine is used in a vehicle at the same rpm and load and the engine-to-rear-axle speed ratio is 3.75:1, determine (a) the vehicle speed, mph; and (b) the fuel consumption, mpg. (Assume a rear-tire radius of 14 in.)

9.18 Dodecane is used as a standard fuel in rating compression-ignition engine fuels. For dodecane, calculate (a) the higher heating value of this fuel, kJ/kg; (b) the higher heating value, kJ/m^3; (e) the lower heating value, kJ/kg; and (d) the lower heating value, kJ/m^3.

9.19 Indolene, a standardized blended fuel often used in spark ignition engine emission testing, can be represented as $C_7H_{13.02}$. For ideal complete stoichiometric combustion determine (a) the product molecular weight, kg/kgmole; (b) the amount of each product, ppm; and (c) the mass of products to mass of reactants, kg/kg.

9.20 Indolene, $C_7H_{13.02}$, is used extensively in CVC emissions testing of SI engines. Fuel economy can be calculated using a carbon balance on the measured engine emissions. For indolene, determine (a) the H/C mass ratio; (b) the grams of carbon per gallon of fuel (SG = 0.7404); and (e) the mass fraction of carbon in indolene, CO_2, and CO. Using parts (a), (b), and CO, show also that the miles per gallon of fuel consumed during testing can be determined to equal

$$\text{MPG} = \frac{2{,}426\langle \text{g} \cdot \text{C/gal fuel} \rangle}{\{0.866[\text{HC}] + 0.273[\text{CO}_2] + 0.429[\text{CO}]\}\langle \text{g} \cdot \text{C/mi} \rangle}$$

where [ ] = measured emission in g/mi

9.21 A CVC test on a four-cylinder, four-stroke engine yields 1.52 g/mi UHC, 2.92 g/mi NO_x, 10.54 g/mi CO, and 565.17 g/mi CO_2. Using the results of Problem 9.20, estimate fuel economy for the test run, mpg.

10

Spark-Ignition Engine Combustion

10.1 INTRODUCTION

Early internal combustion engine technology was a result of efforts by many individuals from around the world as well as a variety of important historical factors. Several names are frequently associated with the development of the spark-ignition IC engine, including Lenoir, who patented the first commercially successful internal combustion engine in 1860. Nicolaus Otto has been credited with producing the four-stroke, spark-ignition gas engine in 1876; however, his contribution was based on a cycle proposed 14 years earlier by Beau de Rochas.

In 1895, Charles E. and J. Frank Duryea built the first successful gasoline automobiles in the United States but, by 1898, there were still less than 1000 automobiles in use. Ten years later, Henry Ford offered his first Model T Ford and, by 1911, there were more than a half-million cars in the country. When the highly successful Model T was withdrawn from production in 1927, over 15 million units had been produced, and its unit cost had dropped from an initial price of $825 to only $290. The early growth of a U.S. automotive industry was due in part to the concurrence of several unique historical factors, including: (1) a westward population migration that required an ability to move easily between vastly separated and dispersed low-density population centers; (2) the greater per capita income and purchasing power of Americans relative to the rest of the world; and (3) the availability of gasoline, a suitable and relatively cheap motor fuel.

The question: Which came first—better engines or better fuels? is reminiscent of the proverbial dilemma of the chicken and the egg. Actually, the history of automotive combustion engine development cannot be separated from the growing and developing U.S. oil industry. At the end of the nineteenth century, kerosene, which was used chiefly to enrich coal gas, began to lose its value as a result of Edison's invention of the electric light. By the turn of the century, the emerging gasoline-powered automotive engine was still competing with electric- and even steam-powered vehicles, but the gasoline engine won out in America, in large measure because of the needs of an expanding and mobile population and the American oil industry's ability to shift from supplying its kerosene

product to cheap gasoline. In 1911, the Standard Oil Companies, for the first time, sold more gasoline than kerosene.

Early straight-run low-octane gasolines, however, knocked in the 4.1:1 compression ratio engines of that day. As early as 1913, efforts were under way to find compounds that would improve gasoline octane ratings. In 1923, after testing over 30,000 compounds, Drs. Midgley and Boyd found that a teaspoon of tetraethyl lead mixed with a gallon of gasoline raised the fuel octane rating from 75 to 85, which satisfactorily eliminated knock in low-compression ratio engines of those days. Modern spark-ignition (SI) engines need gasoline having an ignition quality, or *octane rating,* that is in the mid to upper 90 range; see Chapter 9.

Professor R. F. Sawyer from University of California, Berkeley, stated, in an essay found in the *Future of the Automobile,* that "the automobile engine persisted through 100 years with no significant changes from its original design." From its very start, the growth of the American automotive industry was based on a successful marketing strategy that did not require scientific innovation to nurture basic spark-ignition combustion research and development. For example, most major engine technology that distinguished post-World War II gasoline engines from the turn-of-the-century engines had been achieved by the late 1920s.

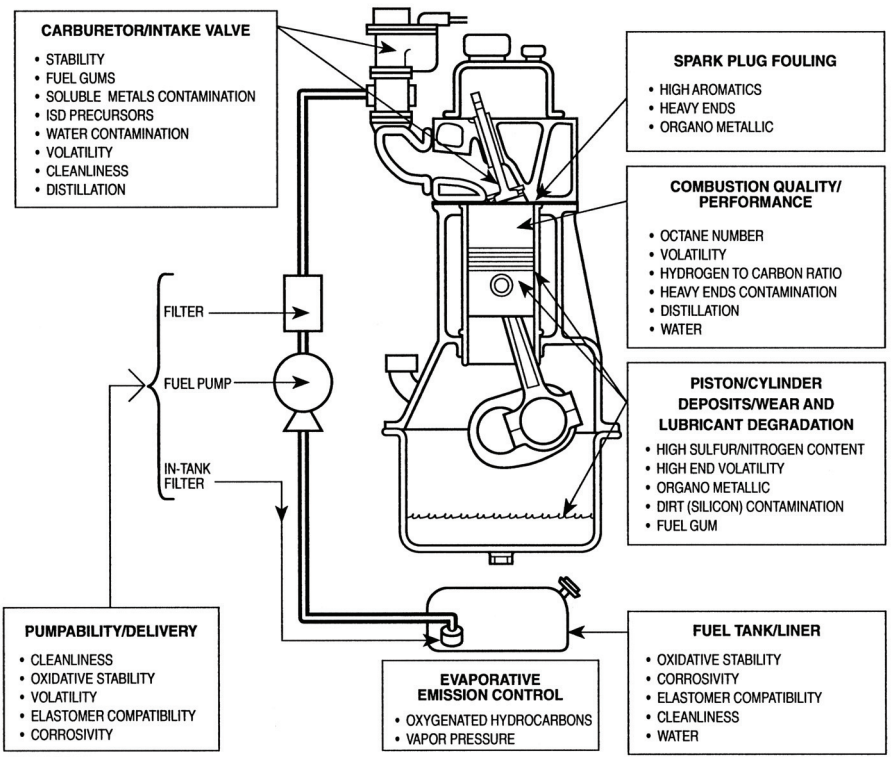

Figure 10.1 Basic spark-ignition fuel-engine interface. After Sid Lestz, Report No. AFLRL-164, "Engines/Fuels Workshop," Mann, David M.; Lepera, M. E.; Glance, Paul C.; Munt, Richard; and Mularz, Edward J.; SwRI Fuels and Lubricants Research Lab, San Antonio, TX, 6–8 December 1982.

Since the environmental and fuel crises of the 1960s and 1970s, IC engine combustion research activities have continued on a worldwide level. Critical fuel-engine interactions for SI engines are illustrated in Figure 10.1. Institutions and individuals in industrial, university, and government centers of excellence are directing their efforts and work in fundamental and applied combustion toward the following goals:

To develop engines that will show a substantial increase in useful power output and a decrease in required fuel consumption
To design engines that will improve combustion efficiency and reduce generation of harmful pollutant by-products
To produce spark-ignition engines having wider tolerances to a variety of fuel alternatives

10.2 THERMODYNAMICS AND SPARK-IGNITION ENGINE MODELING

Spark-ignition, or SI, engines are internal combustion engines in which fuel-air mixture chemical kinetics are initiated by a local electric discharge. Successful ignition occurs only if the spark process provides sufficient energy within a very small region of the fuel-air mixture to ensure that (1) this local charge is above its self-ignition temperature and (2) initial local heat release by combustion within this local charge is greater than any instantaneous heat loss. Otto's spark-ignition engine required fuel-air ignition near TDC followed by rapid combustion prior to the expansion stroke.

Several levels of thermochemical modeling can be used to predict theoretical energy conversion characteristics of SI engines, including air standard thermodynamic cycle analysis, fuel-air cycle analysis, and full engine simulations. Professors D. Foster and P. Myers in an SAE paper entitled "Can Paper Engines Stand the Heat?" indicated that IC engine models:

Are a mathematical catalogue of the most current physical information of IC engine energy characteristics
Provide a framework to systemize thinking about fundamental variables and mechanisms affecting engine performance
Give physical insight into engine chemistry and identify areas where fundamental information is needed
Provide a quantitative description of intermediate steps between measured data points
Cannot be the sole basis for designing engines but can go hand in hand with experimentation to achieve this end

A zeroth-order SI engine model is provided by the air standard Otto cycle, covered in most classical thermodynamics texts, in which the charge is assumed to consist of a fixed amount of air alone. Since this mass is constant, combustion and exhaust processes are replaced with heat transfer and, using classical thermodynamics, with either constant or variable specific heats; calculations can be made to predict ideal cycle indicated state parameters such as pressure, temperature, and density, as well as indicated energy

parameters, including work, heat transfer, and thermal efficiency. An air standard Otto cycle consists of the following four ideal processes:

1–2 Isentropic compression from BDC to TDC
2–3 Constant-volume heat addition at TDC
3–4 Isentropic expansion from TDC to BDC
4–1 Constant-volume heat rejection at BDC

A dimensionless analysis based on a technique used by Walker in his Stirling engine work can be written for an ideal Otto cycle and utilizes the following dimensionless parameters:

τ = T_3/T_1 = maximum cycle temperature ratio
r_v = V_1/V_2 = compression ratio
r_e = V_4/V_3 = expansion ratio
α = $T_3/T_2 = P_3/P_2$ constant volume heating temperature ratio
ρ = $T_4/T_1 = P_4/P_1$ constant volume cooling temperature ratio
$IMEP$ = indicated mean effective pressure
ξ = $IMEP/P_1$ = dimensionless specific work

For a constant specific heat analysis, and using the dimensionless parameters listed above, the following expressions for temperature can be written:

$$T_2 = T_1 r_v^{\gamma-1}$$
$$T_3 = \alpha T_2 = \alpha r_v^{\gamma-1} T_1 = \tau T_1$$
$$T_4 = \rho T_1 = (1/r_e)^{\gamma-1} T_3$$

Now, for an Otto cycle, $v_2 = v_3$ and $v_4 = v_1$, which means that compression and expansion ratios are equal or

$$r_v = v_1/v_2 = v_4/v_3 = r_e$$

and

$$\rho = \tau / r_v^{\gamma-1}$$

where

$$T_4 = (\tau / r_v^{\gamma-1}) T_1$$

The net cycle work on a unit mass basis is given as

$$w_{\text{net}} = {}_1w_2 + {}_2w_3 + {}_3w_4 + {}_4w_1 = u_1 - u_2 + u_3 - u_4$$
$$= C_v(T_1 - T_2 + T_3 - T_4)$$

or

$$w_{\text{net}} = \frac{RT_1}{(\gamma - 1)}\left[1 - r_v^{\gamma-1} + \tau - \frac{\tau}{r_v^{\gamma-1}}\right] \tag{10.1}$$

The net work divided by displacement volume, i.e., indicated mean effective pressure (*IMEP*), is then equal to

$$\begin{aligned} IMEP &= \frac{w_{\text{net}}}{v_1 - v_2} = \frac{w_{\text{net}}}{v_1 - (v_1/r_v)} = \frac{w_{\text{net}}}{v_1[1 - (1/r_v)]} \\ &= \frac{RT_1[(1 - r_v^{\gamma-1}) + \tau - \tau/r_v^{\gamma-1}}{v_1(\gamma - 1)[1 - 1/r_v]} \end{aligned} \tag{10.2}$$

Specific work ξ, *IMEP* in dimensionless form, is written as

$$\xi = \frac{IMEP}{P_1} = \frac{[(1 - r_v^{\gamma-1}) + \tau - \tau/r_v^{\gamma-1}}{(\gamma - 1)[1 - 1/r_v]} \tag{10.3}$$

External heat addition per unit mass, q_H, is

$$\begin{aligned} q_H &= {}_2q_3 = C_v[T_3 - T_2] = C_vT_1[\tau - r_v^{\gamma-1}] \\ \frac{q_H}{C_vT_1} &= \tau - r_v^{\gamma-1} \end{aligned} \tag{10.4}$$

Indicated thermal efficiency η is, therefore, given as

$$\begin{aligned} \eta &= \frac{w_{\text{net}}}{q_H} = \frac{[RT_1/(\gamma - 1)][1 - r_v^{\gamma-1} + \tau - \tau/r_v^{\gamma-1}]}{C_vT_1[\tau - r_v^{\gamma-1}]} \\ &= \frac{1 - r_v^{\gamma-1} + \tau(1 - 1/r_v^{\gamma-1})}{\tau - r_v^{\gamma-1}} = \frac{\tau - r_v^{\gamma-1} + 1 - \tau/r_v^{\gamma-1}}{\tau - r_v^{\gamma-1}} \\ &= 1 + \frac{1 - \tau/r_v^{\gamma-1}}{\tau - r_v^{\gamma-1}} = 1 + \frac{(r_v^{\gamma-1})[1 - \tau/r_v^{\gamma-1}]}{(r_v^{\gamma-1})[\tau - r_v^{\gamma-1}]} \\ &= 1 + \frac{1}{r_v^{\gamma-1}}\frac{[r_v^{\gamma-1} - \tau]}{[\tau - r_v^{\gamma-1}]} = 1 - \left(\frac{1}{r_v}\right)^{\gamma-1} \end{aligned} \tag{10.5}$$

EXAMPLE 10.1 Using the dimensionless Otto cycle analysis developed in this chapter, determine the value for specific work as a function of compression ratio for the following constraints: (a) fixed peak temperature ratio, $\tau = 10$; (b) fixed peak pressure ratio, $P_3/P_1 = 30$; and (c) fixed heat addition per unit mass, $q_H/C_vT_1 = 10$. For each of these conditions, determine (d) the corresponding values of τ, P_3/P_1, and q_H/C_vT_1. Assume that $\gamma = 1.4$.

Solution:

1. Specific work:

$$\xi = \frac{[(1 - r_v^{\gamma-1}) + \tau - \tau / r_v^{\gamma-1}}{(\gamma - 1)[1 - (1/r_v)]}$$

2. External heat addition per unit mass:

$$\frac{q_H}{C_v T_1} = \tau - r_v^{\gamma-1}$$

3. Maximum pressure ratio, P_3/P_1:

$$\frac{P_3}{P_1} = \left(\frac{P_3}{P_2}\right)\left(\frac{P_2}{P_1}\right) = \left(\frac{T_3}{T_2}\right) r_v^{\gamma} = \alpha r_v^{\gamma}$$

4. $V = c$ heating temperature ratio α:

$$\alpha = \tau / r_v^{\gamma-1}$$

5. Fixed peak temperature ratio τ:

a.

r_v	τ	q_H/C_vT_1	P_3/P_1	ξ
2	10	8.6805[a]	20[a]	10.5095[a]
3	10	8.4482	30	11.2658
4	10	8.2589	40	11.7180
5	10	8.0963	50	12.0103
6	10	7.9523	60	12.2062
7	10	7.8221	70	12.3390
8	10	7.7026	80	12.4281
9	10	7.5918	90	12.4856
10	10	7.4881	100	12.5196

[a] $\frac{q_H}{C_v T_1} = 10 - 2^{0.4} = 8.6805$

$$\frac{P_3}{P_1} = \alpha r_v^{\gamma} = \left(\frac{\tau}{r_v^{\gamma-1}}\right) r_v^{\gamma} = \tau r_v = (10)(2) = 20$$

$$\xi = \frac{1 - 2^{0.4} + 10 - (10/2^{0.4})}{(0.4)[1 - (1/2)]} = 10.5095$$

6. Fixed peak pressure ratio P_3/P_1:

b.

r_v	P_3/P_1	τ	q_H/C_vT_1	ξ
2	30[a]	15[a]	13.6805	16.5631[a]
3	30	10	8.4482	11.2658
4	30	7.5	5.7589	8.1709
5	30	6.0	4.0963	6.0766
6	30	5.0	2.9523	4.5316
7	30	4.286	2.1078	3.3250
8	30	3.75	1.4526	2.3438
9	30	3.33	0.9251	1.5215
10	30	3.0	0.4881	0.8161

[a] $\dfrac{P_3}{P_1} = \alpha r_v^{\gamma} = \left(\dfrac{\tau}{r_v^{\gamma-1}}\right) r_v^{\gamma} = \tau r_v$

$$\tau = \frac{P_3/P_1}{r_v} = \frac{30}{2} = 15$$

$$\frac{q_H}{C_vT_1} = 15 - 2^{0.4} = 13.6805$$

$$\xi = \frac{1 - 2^{0.4} + 15 - (15/2^{0.4})}{(0.4)[1 - (1/2)]} = 16.5631$$

7. Fixed specific heat addition, q_H / C_vT_1 :

c.

r_v	q_H/C_vT_1	τ	P_3/P_1	ξ
2	10	11.3195[a]	22.6390[a]	12.1071[a]
3	10	11.5518	34.6555	13.3352
4	10	11.7411	46.9644	14.1884
5	10	11.9037	59.5183	14.8342
6	10	12.0477	72.2860	15.3492
7	10	12.1780	85.2453	15.7746
8	10	12.2974	98.3792	16.1350
9	10	12.4082	111.6740	16.4463
10	10	12.5119	125.1189	16.7192

[a] $\tau = (q_H / C_vT_1) + r_v^{\gamma-1} = 10 + 2^{0.4} = 11.3195$

$$P_3/P_1 = \tau r_v = (11.3195)(2) = 22.6390$$

$$\xi = \frac{1 - 2^{0.4} = 11.3195 - (11.3195/2^{0.4})}{(0.4)[1 - (1/2)]} = 12.1071$$

Comments: This problem illustrates the usefulness of the constant specific heat dimensionless relationships when characterizing variations in Otto cycle performance. Results from parametric investigations can be plotted in dimensionless form as functions of compression ratio as shown in Figure 10.2.

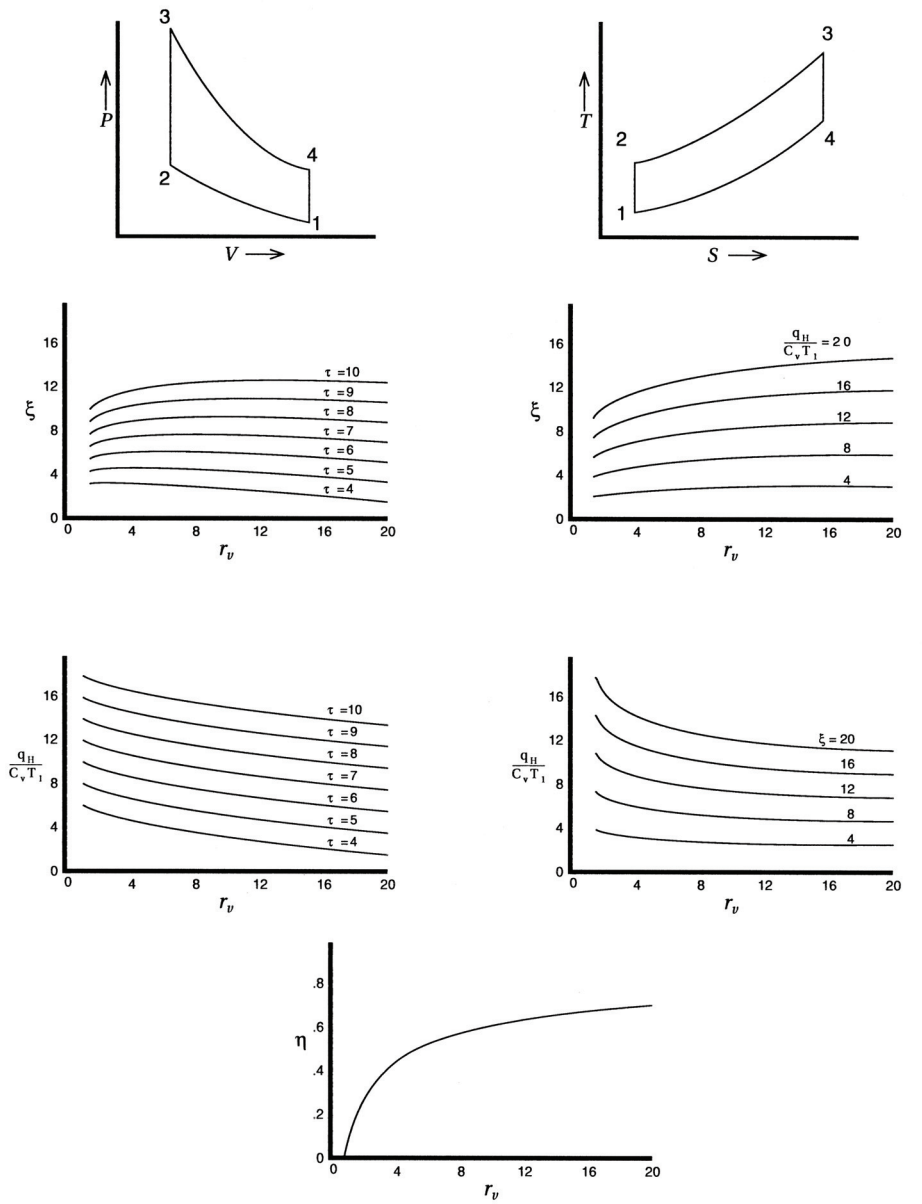

Figure 10.2 Ideal air standard Otto cycle thermodynamic characteristics.

Now air standard Otto cycle predictions would appear to be of limited value since any operating SI engine (1) does not operate as a closed system, (2) does not actually consume air but requires a fuel-air mixture, and (3) does not operate with an external heat transfer process but utilizes complex combustion processes that occur within a piston-cylinder geometry. Thermodynamic arguments are based on time-independent and equilibrium principles, and they are not expected to address many important time-related engine effects such as engine friction, kinematics, spark timing influences, heat transfer losses, and chemical kinetics of fuel oxidation and engine emissions formation. Thermodynamic predictions for indicated efficiency and indicated specific work as functions of compression ratio, however, follow the general performance trends of actual SI engines.

The zeroth-order air standard Otto cycle can be extended to include ideal exhaust and intake processes, in which case valve dynamics and blowby of gases through valve orifices are neglected. It will be assumed, however, in this first order open cycle engine approach that the working substance consumed by the engine is still air. In the zeroth-order air standard open cycle Otto analysis the charge undergoes isentropic compression from BDC to TDC (1–2), is externally heated by heat addition at TDC (2–3), and undergoes isentropic expansion from TDC to BDC (3–4). Exhaust and intake processes distinguish the open cycle from the closed cycle analysis.

For a four-stroke engine, the ideal exhaust process would begin at the end of the power stroke at BDC (4) and would continue until the piston again reaches TDC position (5), at which point it is assumed that both exhaust and intake pressures are equal. At TDC after the exhaust stroke is ended, there will be a certain quantity of trapped hot exhaust gases remaining in the cylinder, described by a *residual factor f*. The residual *f* is defined as the mass of clearance gases contained in the cylinder at the end of the exhaust stroke at TDC (5) divided by the total mass of residual and intake gases in the cylinder at the beginning of the compression stroke (1) at BDC (1). Referring to Figure 10.3 and assuming a total unit mass of charge confined during compression, combustion, and expansion, it follows that

$$m_{\text{tot}} = m_{\text{air}} + m_{\text{res}} = m_1 = m_2 = m_3 = m_4 = 1.0$$

with

$$f = \frac{m_5}{m_1} < 1.0$$

For the exhaust blowdown, then,

Initial state	Final state
$P = P_4$	$P = P_5 = P_1$
$T = T_4$	$T = T_5 \neq T_6 \neq T_1$
$V = V_{\text{BDC}}$	$V = V_{\text{TDC}}$
$m = m_{\text{tot}} = 1$	$m = m_{\text{res}} = f$

The conservation of mass can be expressed for a control volume around the piston-cylinder configuration during the exhaust process using Equation (7.2a) in which no mass enters; one exhaust stream exits as

$$\left.\frac{Dm}{Dt}\right)_{\text{CM}} = \left.\frac{\partial m}{\partial t}\right)_{\text{CV}} + \sum_{\text{out}} \dot{m}_j - \cancel{\sum_{\text{in}} \dot{m}_i} = 0 \tag{7.2a}$$

$$\left.\frac{dm}{dt}\right)_{\text{CV}} = -\dot{m}_{\text{exh}}$$

or

$$dm = -\dot{m}_{\text{exh}}\, dt \tag{10.6}$$

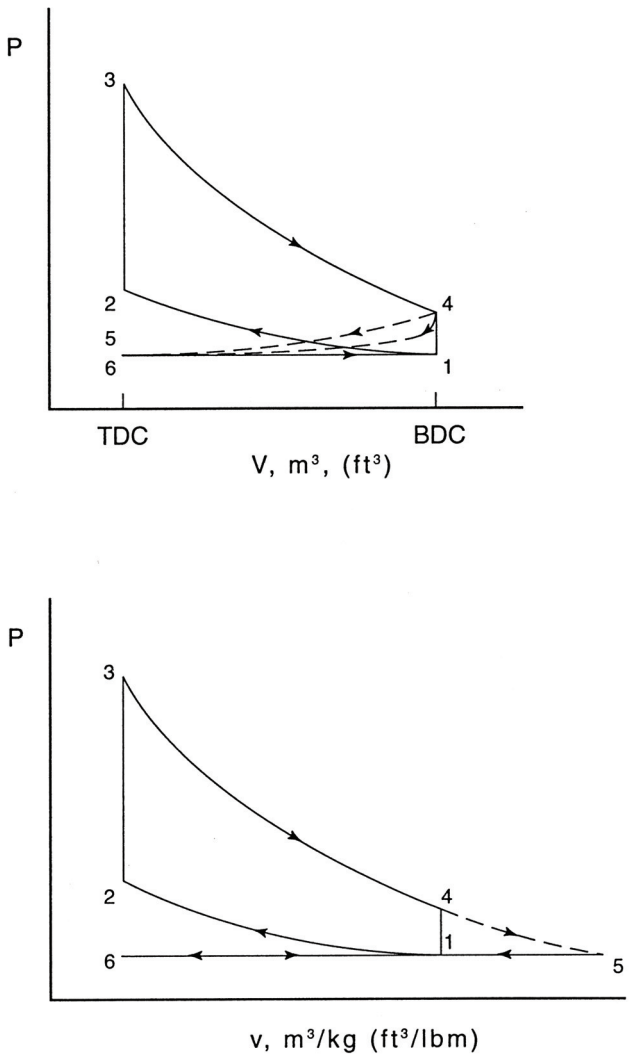

Figure 10.3 Indicator diagram for the four-stroke Otto cycle.

The conservation of energy for the piston-cylinder control volume can be expressed in similar fashion using Equation (7.9) as

$$\left.\frac{DE}{Dt}\right)_{\text{CV}} = \left.\frac{\partial E}{\partial t}\right)_{\text{CV}} + \sum_{\text{out}} \dot{m}_j e_j - \cancel{\sum_{\text{in}} \dot{m}_i e_i} = \dot{Q} - \dot{W} \tag{7.9}$$

which, for adiabatic exhaust blowdown, is expressed simply as

$$\left.\frac{d(me)}{dt}\right)_{\text{CV}} = -\dot{W} - \dot{m}_{\text{exh}} e_{\text{exh}}$$

and

$$\left.\frac{d(me)}{dt}\right)_{\text{CV}} = \left.\frac{d(mu)}{dt}\right)_{\text{CV}} = \left. m\frac{du}{dt}\right)_{\text{CV}} + \left. u\frac{dm}{dt}\right)_{\text{CV}}$$
$$= \left. m\frac{du}{dt}\right)_{\text{CV}} - \dot{m}_{\text{exh}} u$$

or

$$\left. m\frac{du}{dt}\right)_{\text{CV}} - \dot{m}_{\text{exh}} u = -\dot{W} - \dot{m}_{\text{exh}} e_{\text{exh}} = -\dot{W} - \dot{m}_{\text{exh}} h_{\text{exh}}$$
$$m\,du = -dW + \dot{m}_{\text{exh}}(u - h)\,dt$$
$$m\,du = -P\,dV + \dot{m}_{\text{exh}}(u - h)\,dt$$
$$m\,du = -P\,dV - (u - h)dm \tag{10.7}$$

For an ideal gas having constant specific heats, Equation (10.7) becomes

$$mC_v\,dT = -P\,dV - (C_v - C_p)T\,dm = -P\,dV + RT\,dm$$

where

$$PV = mRT \tag{1.3}$$
$$P\,dV + V\,dP = RT\,dm + Rm\,dT$$

Substituting $RT\,dm$ from this expression into Equation (10.7) yields

$$mC_v\,dT = -P\,dV + [P\,dV + V\,dP - Rm\,dT] = V\,dP - Rm\,dT$$

which after rearranging, gives

$$m(C_v + R)\,dT = +V\,dP$$

or

$$\left(\frac{C_P}{R}\right)\frac{dT}{T} = \frac{dP}{P} \tag{10.8}$$
$$\left(\frac{T_{\text{fin}}}{T_{\text{init}}}\right)^{C_p/R} = \left(\frac{P_{\text{fin}}}{P_{\text{init}}}\right)$$

and

$$\frac{T_{\text{fin}}}{T_{\text{init}}} = \left(\frac{P_{\text{fin}}}{P_{\text{init}}}\right)^{(\gamma-1)/\gamma} = \left(\frac{V_{\text{fin}}}{V_{\text{init}}}\right)^{1-\gamma} \tag{10.9}$$

Equation (10.9) shows that the ideal exhaust blowdown process is isentropic, in which case gas temperature at the end of an exhaust stroke is given as

$$T_5 = \left(\frac{1}{r_v}\right)^{1-\gamma} T_4 = (r_v)^{\gamma-1} T_4 \tag{10.10}$$

and a residual fraction f can then be expressed as

$$\begin{aligned} f = \frac{m_5}{m_1} = \frac{m_5}{m_4} &= \left(\frac{P_5 V_5}{R T_5}\right)\left(\frac{R T_4}{P_4 V_4}\right) = \left(\frac{V_5}{V_4}\right)\left(\frac{P_5}{P_4}\right)\left(\frac{T_4}{T_5}\right) \\ &= \left(\frac{1}{r_v}\right)\left(\frac{P_5}{P_4}\right)\left(\frac{P_4}{P_5}\right)^{(\gamma-1)/\gamma} = \left(\frac{1}{r_v}\right)\left(\frac{P_5}{P_4}\right)^{1/\gamma} \\ &= \left(\frac{1}{r_v}\right)\left(\frac{P_1}{P_4}\right)^{1/\gamma} \end{aligned} \tag{10.11}$$

For an ideal isobaric and adiabatic intake process, the piston begins the intake stroke at TDC, with ambient air entering the piston-cylinder configuration at P_6 and T_6 and mixing with the remaining residual gases at P_5 and T_5. As was done for the exhaust analysis, inlet valve dynamics and gas dynamics of flow through an intake orifice will be neglected. The intake process ends at BDC, with conditions in the control volume identified as state 1. Thus, for an ideal intake process,

Initial state	Final state
$P = P_5 = P_1$	$P = P_1$
$T = T_5 \neq T_1$	$T = T_1$
$V = V_{\text{TDC}}$	$V = V_{\text{BDC}}$
$m = m_{\text{res}} = f$	$m = m_{\text{tot}} \neq m_{\text{res}} = 1$

The conservation of mass for a control volume around the piston-cylinder configuration during an adiabatic intake process for one inlet stream can be written as

$$\left.\frac{Dm}{Dt}\right)_{\text{CM}} = \left.\frac{\partial m}{\partial t}\right)_{\text{CV}} + \sum_{\text{out}} \dot{m}_j - \sum_{\text{in}} \dot{m}_i = 0 \tag{7.2a}$$

$$\left.\frac{dm}{dt}\right)_{\text{CV}} + + \dot{m}_{\text{tot}}$$

or

$$dm = + \dot{m}_{\text{int}} dt$$

The conservation of energy for the adiabatic intake process can be stated as

$$\left.\frac{DE}{Dt}\right)_{\text{CM}} = \left.\frac{\partial E}{\partial t}\right)_{\text{CV}} + \sum_{\text{out}} \dot{m}_j e_j - \sum_{\text{in}} \dot{m}_i e_i = \dot{Q} - \dot{W}$$

$$\left.\frac{d(me)}{dt}\right)_{\text{CV}} = -\dot{W} + \dot{m}_{\text{int}} e_{\text{int}}$$

or

$$d(me)_{\text{CV}} = -\dot{W}\, dt + dm_{\text{CV}} h_{\text{intake}} \tag{10.12}$$

Integration of Equation (10.12) for a constant-pressure intake process yields

$$(m_{\text{fin}} u_{\text{fin}} - m_{\text{init}} u_{\text{init}}) = -P[V_{\text{BDC}} - V_{\text{TDC}}] + (m_1 - m_5) h_6$$

or

$$\begin{aligned} u_1 - f u_5 &= P[V_{\text{TDC}} - V_{\text{BDC}}] + (1 - f) h_6 \\ u_1 - f u_5 &= f R T_5 - R T_1 + (1 - f) h_6 \\ u_1 + R T_1 &= f(u_5 + R T_5) + (1 - f) h_6 \\ h_1 &= f h_5 + (1 - f) h_6 \end{aligned} \tag{10.13}$$

Equation (10.13) requires that conditions at both 5 and 6 be known in order to determine conditions at 1 prior to compression. Note that properties at 1 are influenced by residual gas conditions at 5 and the intake state at 6. However, to determine state point 5 at the end of the exhaust stroke, one must know conditions at states 4, 3, 2, and 1; hence, a trial-and-error solution is necessary to calculate clearance gas weight fraction f and temperature T_1 at the beginning of compression.

An ideal open system SI engine analysis in which inlet and exhaust pressures are equal is commonly referred to as an *unthrottled* engine. *Supercharging*, a technique for power-boosting a particular engine design, raises charge delivery pressure above ambient by the use of an engine-driven compressor. *Turbocharging*, on the other hand, is a specific method of engine super-charging using hot-gas expansion through an exhaust gas-driven turbine, charge-compression compressor set to provide the required charge preparation. Figure 10.4 shows ideal indicator diagrams for SI engines.

Extended air standard Otto cycle analysis will not predict how fuel-air charge induction, product gas composition, or even combustion process impact indicated engine performance predictions. Development of a fuel-air cycle analysis, however, allows additional fuel-air physics to be included in IC engine modeling. At this next level, specific heat variations, real gas mixture thermochemistry, and dissociation effects are considered. Performance calculations approximate a finite burn rate with an instantaneous combustion process. Classical analysis used suitable energy-entropy charts with particular equivalent ratios for several useful hydrocarbon fuels. Both Hottell and Starkmann published charts for rich, lean, and stoichiometric frozen isooctane-air mixtures, as well as corresponding charts for their equilibrium products of combustion; see Chapter 3. Property values for charted fuel vapor-dry air mixtures were based on ideal-gas mixture predictions, assuming variable specific heats and no residual gas present. Property values for product charts are based on frozen complete combustion composition for temperatures below 1,700K (3,060ºR) and equilibrium composition for temperatures above 1,700K (3,060ºR). Several classic texts, such as those by C.F. Taylor

(1966) and John B. Heywood (1988), give a more complete discussion of the use of these charts in SI and IC engine calculations.

The fuel-air Otto analysis assumes a fuel-air mixture with frozen charge composition and an isentropic compression process from BDC to TDC. Combustion at TDC is approximated as a constant-volume adiabatic flame process in which products of combustion are assumed to have either a frozen complete reaction composition for temperatures less than 1,700K (3,060ºR) or an equilibrium reaction composition for conditions above 1,700K (3,060ºR). Expansion from TDC is treated as an isentropic and frozen product composition process to BDC. Reactant and product charts can also be used in a fuel-air analysis that includes exhaust residual gas recirculation analysis.

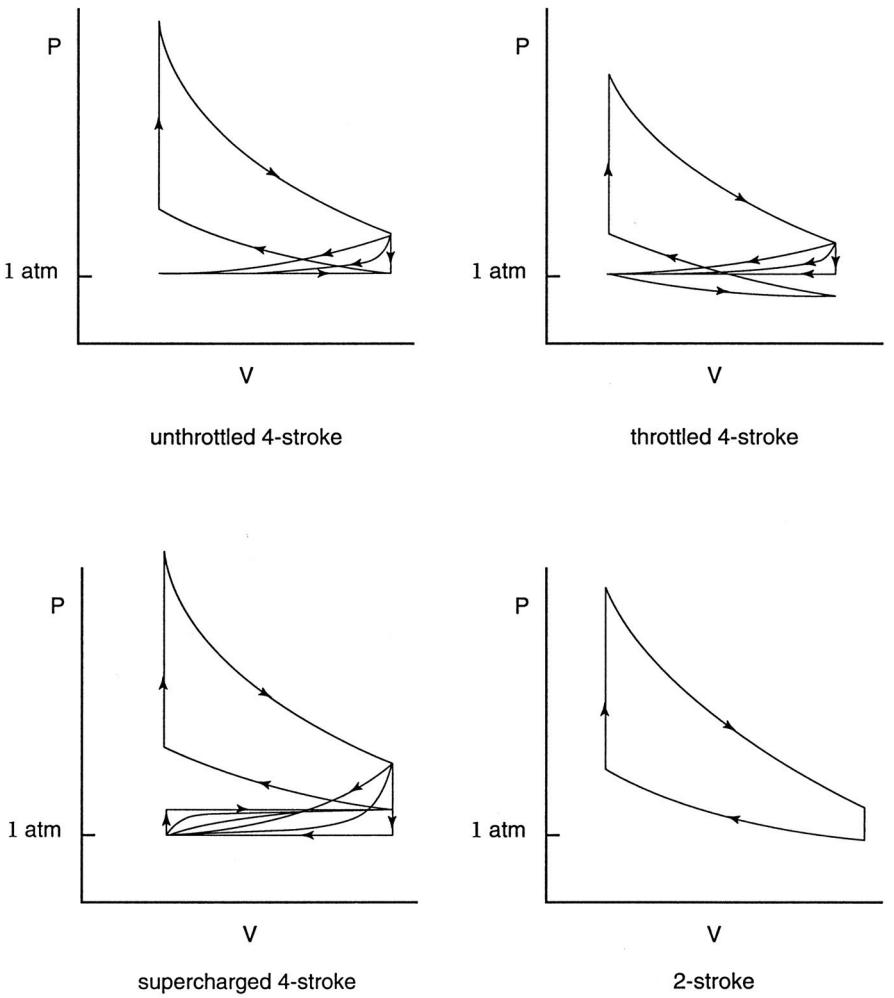

Figure 10.4 Various indicator diagrams for SI engine operation.

EXAMPLE 10.2 A four-cylinder SI engine with a total displacement of 820 cc and having 8:1 compression ratio is to be analyzed using an air standard Otto cycle analysis. Conditions at BDC are assumed to be 105 kPa abs and 27°C. For a total heat addition of 2.5 kJ, calculate the following, assuming constant specific heats: (a) the maximum cycle temperature and pressure, K and kPa; (b) the ideal indicated thermal efficiency, %; and (c) the indicated mean effective pressure, kPa. Repeat parts (a)–(c), assuming variable specific heats and using JANAF data for air.

Solution:

1. Conditions at BDC state 1, assuming charge is air alone:

$$V_D = \frac{V_{\text{tot}}}{4} = V_1 - V_2 = V_1\left[1 - \left(\frac{1}{r_v}\right)\right]$$

$$V_1 = \left(\frac{8}{7}\right)\left(\frac{0.00082\ \text{m}^3}{4}\right) = 0.000234\ \text{m}^3/\text{cyl}$$

$$m = \frac{P_1 V_1}{RT_1} = \frac{(105{,}000\ \text{N/m}^2)(0.000234\ \text{m}^3/\text{cyl})}{(8{,}314\ \text{N}\cdot\text{m/kg}\cdot\text{K}/28.97)(300\text{K})} = 0.000285\text{kg/cyl}$$

2. Process 1 → 2 isentropic compression $S_1 = S_2$ for constant specific heats, from Table B.25 in Appendix B for air at 300K:

$$C_p\Big)_{\text{air}} = \frac{(6.949\ \text{cal/gmole}\cdot\text{K})\left(4.187\dfrac{\text{kJ/kgmole}}{\text{cal/gmole}}\right)}{(28.97\ \text{kg/kgmole})} = 1.0043\ \text{kJ/kg}\cdot\text{K}$$

$$C_v = C_p - R = 1.0043 - 0.287 = 0.7173\ \text{kJ/kg}$$

$$\gamma = \frac{C_p}{C_v} = \frac{1.0043}{0.7173} = 1.400$$

Constant specific heats (Cold air standard)	Variable specific heats (Use Example 3.2)
$r_v = \dfrac{V_{\text{BDC}}}{V_{\text{TDC}}} = \left(\dfrac{T_2}{T_1}\right)^{1/\gamma-1}$	$r_v = \dfrac{V_{\text{BDC}}}{V_{\text{TDC}}} = \dfrac{V_r\langle T_1\rangle}{V_r\langle T_2\rangle}$
	$V_r\langle T_2\rangle = (18{,}020)/8 = 2252$
$T_2 = (8)^{0.4}(300) = 689\text{K}$	$T_2 = 678.5\text{K}$

3. Process 2 → 3, V = constant heat addition:

$$_2Q_3 = m(u_3 - u_2)$$

Constant specific heats:

a. $T_3 = T_2 + \dfrac{{}_2Q_3}{mC_v} = 689 + \dfrac{(2.5 \text{ kJ}/4)}{(0.000285 \text{ kg})(0.7173 \text{ kJ/kg} \cdot \text{K})} = 3{,}746\text{K}$

$$P_3 = \frac{mRT_3}{V_3} = \frac{(0.000285 \text{ kg})(8{,}314 \text{ N} \cdot \text{m/kg} \cdot \text{K})(3{,}746\text{K})(8)}{(28.97)(0.000234 \text{ m}^3)}$$

$$P_3 = 10{,}474{,}861 \text{ N/m}^2 = 10{,}475 \text{ kN/m}^2$$

Variable specific heats using Table B.25 in Appendix B:

$${}_2\bar{q}_3 = [\Delta\bar{h}\langle T_3\rangle - \bar{R}T_3] - [\Delta\bar{h}\langle T_2\rangle - \bar{R}T_2]$$

where

$$\bar{q} = \frac{(2.5 \text{ kJ}/4)(28.97 \text{ kg/kgmole})}{\left(4.187 \dfrac{\text{kJ/kgmole}}{\text{cal/gmole}}\right)(0.000285 \text{ kg})} = 15{,}173 \text{ cal/gmole}$$

$$T_2 = 678.5\text{K} \qquad \Delta\bar{h}\langle T_2\rangle = 2{,}735 \text{ cal/gmole}$$

or

$$\Delta\bar{h}\langle T_3\rangle - 1.987 \cdot T_3 = 15{,}173 + [2735 - (1.987)(678.5)]$$

$$= 16{,}560 \text{ cal/gmole}$$

by trial and error, $T_3 = 3{,}023\text{K}$

$$\Delta\bar{h}\langle T_3\rangle = 22{,}567 \text{ cal/gmole}$$

$$P_3 = \frac{(0.000285)(8{,}314)(8)(3{,}023)}{(28.97)(0.000234)(1{,}000)} = 8{,}453 \text{ kPa}$$

4. $3 \rightarrow 4$, isentropic expansion $S_3 - S_4$:

Constant specific heats

$$\frac{T_4}{T_3} = \left(\frac{V_{\text{TDC}}}{V_{\text{BDC}}}\right)^{\gamma - 1}$$

$$T_4 = (1/8)^{0.4}(3746)$$

$$= 1{,}630\text{K}$$

Variable specific heats
(Use Example 3.2)

$$V_r\langle T_4\rangle = 8V_r\langle T_3\rangle = (8)(20.06)$$

$$V_r\langle T_4\rangle = 160.48$$

$$T_4 = 1{,}630\text{K}$$

5. Indicated thermal efficiency:

$$\eta = \frac{\text{desired energy output}}{\text{required energy output}} = \frac{w_{\text{net}}}{q_{\text{add}}} = 1 + \frac{{}_4q_1}{{}_2q_3}$$

Constant specific heats:

$$\text{b. } \eta = 1 - \left(\frac{T_1}{T_2}\right) = 1 - \left(\frac{300}{689}\right) = 0.565 = 56.5\%$$

Variable specific heats using Table B.25 in Appendix B:

$$\eta = 1 - \left[\frac{\bar{u}\langle T_4\rangle - \bar{u}\langle T_1\rangle}{\bar{u}\langle T_3\rangle - \bar{u}\langle T_2\rangle}\right] = 1 - \left[\frac{\Delta\bar{h}\langle T_4\rangle - \Delta\bar{h}\langle T_1\rangle - \bar{R}(T_4 - T_1)}{\Delta\bar{h}\langle T_3\rangle - \Delta\bar{h}\langle T_2\rangle - \bar{R}(T_3 - T_2)}\right]$$

$$= 1 - \left[\frac{10{,}363 - 35 - (1.987)(1{,}630 - 300)}{22{,}567 - 2{,}735 - (1.987)(3{,}023 - 679)}\right] = 0.494 - 49.4\%$$

6. Indicated mean effective pressure:

$$IMEP = \frac{W_{\text{net}}}{V_D} = \frac{\eta_2 Q_3}{[V_1 - V_2]}$$

Constant specific heats:

$$\text{c. } IMEP = \left[\frac{(0.565)(2.5/4 \text{ kN}\cdot\text{m})}{(0.00082 \text{ m}^3/4)}\right] = 1{,}722.6 = 1{,}723 \text{ kPa}$$

Variable specific heats:

$$IMEP = \left[\frac{(0.494)(2.5/4)}{(0.00082/4)}\right] = 1{,}506.1 = 1{,}506 \text{ kPa}$$

Comments: The influence of specific heat on the predicted air standard Otto cycle is seen in this example. For the same geometry and heat input, the assumption of constant heats yields too large an indicated thermal efficiency, indicated mean effective pressure, and indicated peak temperature. The hot-air standard value of 1.3 gives values that are closer to those obtained using the air tables. Further realism results from using fuel-air cycles, open system analysis, and equilibrium thermochemistry.

Executable fuel-air cycle analyses and solutions can now be based on first principle arguments that can be supported by modern computers and numerical techniques that are able to go beyond the solution range available using classical hydrocarbon fuel-air charts. From First Law energy considerations found in Chapter 2, one can obtain the following general relationship for an adiabatic constant volume closed system.

Energy balance:

$$\delta Q - \delta W = \delta Q - P\,dV = dU$$

or

$$U\langle T_3\rangle = U\langle T_2\rangle$$

$$\sum_{\text{prod}} N_i \left\{\bar{h}_{f_i}^0 + \left[\bar{h}\langle T_3\rangle - \bar{h}\langle T_0\rangle\right]_i - \bar{R}T_3\right\}$$

$$= \sum_{\text{react}} N_j \left\{\bar{h}_{f_j}^0 + \left[\bar{h}\langle T_2\rangle - \bar{h}\langle T_0\rangle\right]_j - \bar{R}T_2\right\} \qquad (10.14)$$

Consider the combustion reaction shown below in Equation (10.15) to represent the generalized TDC fuel-air equilibrium in-cylinder chemistry. The SI engine fuel-air equilibrium reaction applies to the general energy balance at TDC given by Equation (10.14). Now equilibrium product state composition, such as for the implied conditions at TDC, is complex and a function of a particular fuel, total pressure, P, absolute temperature, T, and equivalence ratio, Φ.

$$C_xH_yO_zN_w + (a_s/\Phi)[O_2 + 3.76N_2] \overset{V}{\rightarrow} n_1CO_2 + n_2H_2O + n_3N_2 + n_4O_2 + n_5CO + n_6H_2 + n_7H + n_8O + n_9OH + n_{10}NO + n_{11}N \quad (10.15)$$

where

$C_xH_yO_zN_w$ – one mole of generalized fuel
a_s – molar stoichiometric coefficient
Φ – equivalence ratio

Atom balances based on a mole of fuel yields the following results:

Carbon atom balance:

$$x = (n_1 + n_5)$$

Hydrogen atom balance:

$$y = (2n_2 + 2n_6 + n_7 + n_9)$$

Oxygen atom balance:

$$z + \frac{2a_s}{\Phi} = (2n_1 + n_2 + 2n_4 + n_5 + n_8 + n_9 + n_{10})$$

Nitrogen atom balance:

$$w + \frac{7.52a_s}{\Phi} = (2n_3 + n_{10} + n_{11})$$

and

Molar FA ratio:

$$\overline{FA} = \frac{\Phi}{4.76a_s}$$

Since the SI Otto constant volume equilibrium reaction occurs at TDC, the total moles of reactants, N_R, and products, N_P, can be related to conditions at reaction temperatures in the cylinder by assuming ideal gas law behavior. Now the total moles of reactants after variable specific heat isentropic compression of a fuel-air mixture from BDC to TDC is given by

$$N_R = \frac{P_2V_{TDC}}{\overline{R}T_2} \text{ kgmole reactants (lbmole reactants)} \quad (10.16)$$

where

P_2 – pressure of fuel-air mixture at TDC kPa (lbf/in^2)
T_2 – temperature of fuel-air mixture at TDC K (ºR)

with

$$\bar{x}_{\text{fuel}} = \left[\frac{1}{1 + (4.76a_s/\Phi)}\right]$$

or

$$N_{\text{fuel}} = \left[\frac{1}{1 + (4.76a_s/\Phi)}\right]N_{\text{R}}$$

$$N_{\text{fuel}} = \bar{x}_{\text{fuel}}N_R \quad \text{kgnole fuel (lbmole fuel)} \tag{10.17}$$

and

$$\bar{x}_{\text{air}} = \left[\frac{4.76a_s/\Phi}{1 + (4.76a_s/\Phi)}\right]$$

or

$$N_{\text{air}} = \left[\frac{4.76a_s/\Phi}{1 + (4.76a_s/\Phi)}\right]N_{\text{R}} \quad \text{kgmole air (lbmole air)} \tag{10.18}$$

The ideal gas relationship for product conditions yields

$$N_{\text{P}} = \frac{P_3V_{\text{TDC}}}{\bar{R}T_3} \quad \text{kgmole products (lbmole products)} \tag{10.19}$$

Now expressing Equation (10.15) to reflect the actual total moles of reactants, N_{R}, and products, N_{P}, at TDC yields

$$\begin{aligned} N_R\{\bar{x}_{\text{fuel}}\text{C}_\text{x}\text{H}_\text{y}\text{O}_\text{z}\text{N}_\text{w} + \bar{x}_{\text{air}}[\text{O}_2 + 3.76\text{N}_2]\} \xrightarrow{V} N_{\text{P}}[\bar{x}_1\text{CO}_2 + \bar{x}_2\text{H}_2\text{O} \\ + \bar{x}_3\text{N}_2 + \bar{x}_4\text{O}_2 + \bar{x}_5\text{CO} + \bar{x}_6\text{H}_2 + \bar{x}_7\text{H} + \bar{x}_8\text{O} + \bar{x}_9\text{OH} \\ + \bar{x}_{10}\text{NO} + n_{11}\text{N}] \end{aligned} \tag{10.20}$$

Atom balances based on total moles yield the following:

Carbon atom balance:

$$\text{x} = (N_{\text{P}}/\bar{x}_{\text{fuel}}N_{\text{R}})(x_1 + x_5)$$

Hydrogen atom balance:

$$\text{y} = (N_{\text{P}}/\bar{x}_{\text{fuel}}N_{\text{R}})(2x_2 + 2x_6 + x_7 + x_9)$$

Oxygen atom balance:

$$\bar{x}_{\text{fuel}}\text{z} + 2 \cdot 0.21 \cdot \bar{x}_{\text{air}} = (N_{\text{P}}/N_{\text{R}})(2\bar{x}_1 + \bar{x}_2 + 2\bar{x}_4 + \bar{x}_5 + \bar{x}_8 + \bar{x}_9 + \bar{x}_{10})$$

Nitrogen atom balance:

$$\bar{x}_{\text{fuel}}\text{w} + 2 \cdot 0.79 \cdot \bar{x}_{\text{air}} = (N_{\text{P}} / N_{\text{R}})(2\bar{x}_3 + \bar{x}_{10} + \bar{x}_{11})$$

Combustion analysis has been expressed in terms of moles per fuel. In engine analysis, however, it is often more useful to present information based on a unit (mole or mass) of air. By recalling the engineering percentages for one mole of air presented in Chapter 2 of 21% O_2 and 79% N_2, Equation (10.15) can be rewritten on a per mole of air as shown below in Equation (10.21). The engineering fuel-air cycle analysis would then be developed starting with Equation (10.21).

$$(\Phi/a_s)\text{C}_x\text{H}_y\text{O}_z\text{N}_w + [0.21\text{O}_2 + 0.79\text{N2}] \rightarrow n'_1\text{CO}_2 + n'_2\text{H}_2\text{O} + n'_3\text{N}_2$$
$$+ n'_4\text{O}_2 + n'_5\text{CO} + n'_6\text{H}_2 + n'_7\text{H} + n'_8\text{O} + n'_9\text{OH} + n'_{10}\text{NO} + n'_{11}\text{N} \qquad (10.21)$$

To evaluate the product state of Equation (10.15) or (10.21), it is necessary to determine T_3, ($U\langle T_3\rangle = U\langle T_2\rangle$) and the eleven mole fractions, $\bar{x}_i$. Since there are more equilibrium product species than conservation of atomic mass balances, additional relations are necessary in order to determine a solution. Because products are assumed to be in equilibrium with each other, one can try to write additional equilibrium relationships in order to obtain a final solution. Significant effort was spent in Chapter 3 describing methodologies to determine equilibrium characteristics of hydrocarbon combustion products.

Olikara and Borman developed a computational program for solving the general equilibrium thermodynamics represented by the reaction given by Equation (10.15). Their numerical technique enables gas phase equilibrium mole fractions for the products of combustion, amongst other product parameters, to be determined with respect to temperature, pressure, and equivalence ratio. The program utilizes Newton-Raphson iteration of the nonlinear differential equations in order to determine a numerical solution. Seven non-redundant equilibrium relationships were written as a part of the solutions set involving the selected product species, shown in Equations (10.22a)–(10.22g).

$$\tfrac{1}{2}\text{H}_2 \rightleftarrows \text{H} \qquad K_{p1} = \frac{\bar{x}_7 P^{1/2}}{\bar{x}_6^{1/2}} \qquad (10.22a)$$

$$\tfrac{1}{2}\text{O}_2 \rightleftarrows \text{O} \qquad K_{p2} = \frac{\bar{x}_8 P^{1/2}}{\bar{x}_4^{1/2}} \qquad (10.22b)$$

$$\tfrac{1}{2}\text{N}_2 \rightleftarrows \text{N} \qquad K_{p3} = \frac{\bar{x}_{11} P^{1/2}}{\bar{x}_3^{1/2}} \qquad (10.22c)$$

$$\tfrac{1}{2}\text{H}_2 + \tfrac{1}{2}\text{O}_2 \rightleftarrows \text{OH} \qquad K_{p4} = \frac{\bar{x}_9}{\bar{x}_4^{1/2}\bar{x}_6^{1/2}} \qquad (10.22d)$$

$$\tfrac{1}{2}\text{O}_2 + \tfrac{1}{2}\text{N}_2 \rightleftarrows \text{NO} \qquad K_{p5} = \frac{\bar{x}_{10}}{\bar{x}_4^{1/2}\bar{x}_3^{1/2}} \qquad (10.22e)$$

$$\text{H}_2 + \tfrac{1}{2}\text{O}_2 \rightleftarrows \text{H}_2\text{O} \qquad K_{p6} = \frac{\bar{x}_2}{\bar{x}_4^{1/2}\bar{x}_6 P^{1/2}} \qquad (10.22f)$$

$$\text{CO} + \tfrac{1}{2}\text{O}_2 \rightleftarrows \text{CO}_2 \qquad K_{p7} = \frac{\bar{x}_1}{\bar{x}_5\bar{x}_4^{1/2} P^{1/2}} \qquad (10.22g)$$

Table 10.1 Constant Pressure Equilibrium Curve-Fit Correlation Coefficients

i	A_i	B_i	C_i	D_i	E_i
1	0.432168E + 00	–0.112464E + 02	0.267269E + 01	–0.745744E – 01	0.242484E – 02
2	0.310805E + 00	–0.129540E + 052	0.321779E + 01	–0.738336E – 01	0.344645E – 02
3	0.389716E + 00	–0.245828E + 02	0.314505E + 01	–0.963730E – 01	0.585643E – 02
4	–0.141784E + 00	–0.213308E + 01	0.853461E + 00	0.355015E – 01	–0.310227E – 02
5	0.150879E – 01	–0.470959E + 01	0.646096E + 00	0.272805E – 01	–0.154444E – 02
6	–0.752364E + 00	0.124210E + 02	–0.260286E + 01	0.259556E – 00	–0.162687E – 01
7	–0.415302E – 02	0.148627E + 02	–0.475746E + 01	0.124699E – 00	–0.900227E – 02

So*urce*: Olikara, Cherian and Borman, Gary L., A Computer Program for Calculating Properties of Equilibrium Combustion Products with Some Applications to I.C. Engines, University of Wisconsin, SAE Paper 750468, SAE International, Warrendale, PA, 1975. With permission.

Constant pressure equilibrium data for each of the above eleven individual species was obtained from JANAF Thermochemical Tables. Constant pressure equilibrium constants for each of the seven equilibrium reactions shown, where pressure is in atm and standard state pressure is 1atm, were then obtained as a function of temperature using JANAF data as

$$\log K_p\langle T\rangle\Big)_{\text{reaction}} = \sum_{\text{products}} n_e \log K_p\langle T\rangle\Big)_{\text{JANAF}} - \sum_{\text{reactannts}} n_e \log K_p\langle T\rangle\Big)_{\text{JANAF}} \tag{10.23}$$

where

$K_p\langle T\rangle$ – constant pressure equilibrium constant
P – pressure
n_e – equilibrium equation molar coefficient

Equilibrium constant data for each of the seven reactions obtained with Equation (10.23) were fitted to temperatures over the range 600–4,000K (1,080–7,200ºR) using the general functional relationship

$$\log K_p\Big)_{reaction} = A\ln T_A + \frac{B}{T_A} + C + DT_A + ET_A^{\,2} \tag{10.24}$$

Coefficients for the seven reactions of Equations (10.22a)–(10.22g) fitted by Equation (10.24) are listed in Table 10.1. For SI analysis, Equation (10.24) utilizes a transformation temperature, T_A, expressed as (T/1,000), with T in K. For engineers units, a transformation temperature, T_A, is defined as (0.005T/9), where T is in ºR.

Equilibrium product state composition, as indicated previously, is complex and a function of the particular fuel composition, total pressure, P, absolute temperature, T, and equivalence ratio, Φ. For low temperatures and lean hydrocarbon fuel stoichiometries, $\Phi < 1$, based on evidences such as SI combustion engine exhaust measurements and extensive equilibrium studies, it is reasonable to assume that equilibrium products for these conditions contain no CO, H_2, or NO as well as dissociation species H, O, N, or OH. This reduction in the number of product species from eleven to four enables the equilibrium product compositions to be determined from the four C/H/O/N atom balances.

For low temperatures and rich hydrocarbon fuel stoichiometries, $\Phi > 1$, it is reasonable again, based on evidences such as SI combustion engine exhaust measurements and extensive equilibrium studies, to assume that equilibrium products for these conditions contain no O_2 or NO as well as dissociation species H, O, N, or OH. This reduction in the number of equilibrium species from eleven to five means the four C/H/O/N atom balances in this instance are insufficient by one equation to establish the equilibrium product compositions. In this instance a fifth additional relationship can be provided via the water gas equilibrium reaction and products CO, CO_2, H_2, and H_2O; see Example Problem 5.6.

$$CO_2 + H_2 \rightleftarrows CO + H_2O$$

where

$$K_p\langle T\rangle = \frac{\bar{x}_5\,\bar{x}_2}{\bar{x}_1\,\bar{x}_6} \tag{10.25}$$

For low temperature rich hydrocarbon fuel combustion, a temperature-dependent constant pressure water gas equilibrium reaction relationship can be developed using Equations (10.23) and (10.24). Constant pressure JANAF equilibrium data are required for CO_2, H_2, CO, and H_2O.

For higher product temperatures, relevant chemical kinetic and equilibrium studies show that the equilibrium product dissociation species H, O, and OH begin to become noteworthy. Zeleznik and McBride at NASA developed a flexible five-level program for the SI internal combustion engine ranging from simple models requiring only thermodynamic properties to complex models requiring full combustion kinetics input. Among many features of the modeling included heat transfer, valve timing, supercharging, motoring, finite burn rates, cycle-to-cycle variation in air-fuel ratio, residuals, and recirculated exhaust gas. This sophisticated engine coding utilized the extensive NASA thermochemical property program written by Gordon and McBride (see Chapter 3) to evaluate the required in-cylinder fuel-air thermochemistry and equilibrium properties. The NASA equilibrium solution is not limited to the eleven species assumed in Equation (10.15), does not require the use of equilibrium constants, but rather utilizes the minimization of the total Gibbs free energy of the product state to define the solution for the equilibrium mixture, as described in Chapter 3.

NO equilibrium concentration predicted for high product combustion temperatures at TDC does not correlate with tailpipe NO measurements. Recall from Chapter 5 that NO_x formation was chemical kinetic in nature and, therefore, the concentrations of NO are essentially frozen at their high temperature formation values and remain so even when cooled by expansion during the power stroke. NO decomposition into N_2 and O_2 is a kinetically limited, high activation energy, slow reaction process. Thus frozen concentrations will be lower than equilibrium values predicted for peak temperatures at adiabatic flame conditions but higher than the equilibrium values determined for cooled exhaust gas conditions.

Various numerical techniques and computational devices are now available and are being utilized to develop a variety of extensive and realistic SI fuel-air engine models. With the current advances in computational power of high-speed computers and personal programmable PCs to iteratively and numerically solve nonlinear equations, engineers can now predict indicated performance with executable codes that can change

The specifics of an engine geometry
The fuel being introduced with the charge
The characteristics of the exhaust and intake process
The thermochemistry of the fuel-air constituents
The combustion characteristics near TDC

Programming flexibility permits introduction of time-dependent aspects of engine parameters (rpm, valve timing), greater range and choices in *FA* ratios (more than the three choices of the charts), wider selection and specification of SI fuel alternatives (gasoline, methane, alcohol, and/or hydrogen), and greater capability in manipulating large thermochemical data bases (curve fitted data and/or other critical property correlations). Fuel-air model can include the following in-cylinder processes:

1–2 Variable specific heat fuel-air mixture isentropic compression from BDC to TDC
2–3 Adiabatic constant volume fuel-air equilibrium combustion reaction (equilibrium constants, such as described above, or minimization of the product Gibbs free energy, as described in Chapter 3)
3–4 Variable specific heat equilibrium product mixture isentropic expansion from TDC to BDC

Analytical modeling can also include intake, exhaust and residual gas effects such that engineers and scientists are able to investigate fundamental factors in SI engine combustion that influence

The final gas composition at TDC
The combustion process near TDC
The peak T and P at TDC
The indicated net power, *MEP*, and thermal efficiency

Instantaneous piston speed, internal fluid turbulence, real intake and exhaust gas exchange rates, heat transfer, friction, and transient engine speeds are but a few of the dynamic engine effects that influence actual SI engine operation (see Figure 10.5). The probabilistic and spatially resolved physics of periodic ignition phenomena, misfire, the complex chemical kinetics of combustion, and the generation of pollution by-products are examples of dynamic chemistry that also impact SI engine performance. Complex and sophisticated programs can extend further the realism of fuel-air cycle models by covering additional elements including

Heat transfer
Fluid mechanics
Chemical kinetics
Three-dimensional geometry

Texts such as by Campbell (1979), Blair (1990), as well as Ferguson and Kirkpatrick (2001), provide a more thorough treatment of computer programming and IC engines.

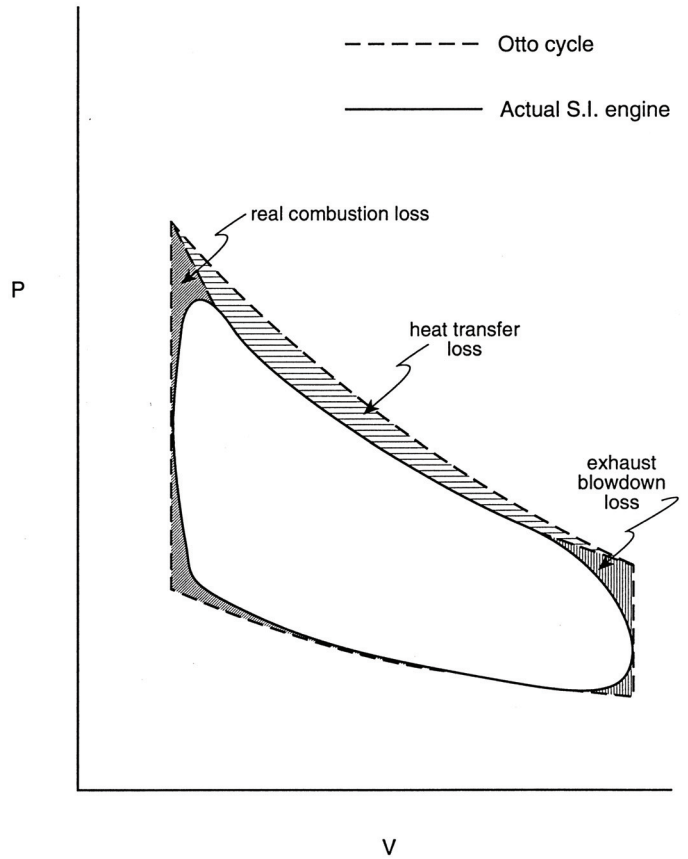

Figure 10.5 Effects of time-related losses on SI indicator card.

10.3 FUEL THERMOCHEMISTRY AND SPARK-IGNITION ENGINES

Today, proper charge preparation is essential to good SI engine performance. Precise fuel-air control allows SI engines to run over a wide range of loads and speeds. Fuel metering and control were most frequently accomplished prior to fuel injection by carburetion; see Figure 10.6. Both manifold and throttle-body fuel injection techniques are now being utilized in order to develop engines having better cylinder-to-cylinder fuel distribution, fuel economy, power output, emissions control, and/ or a broader tolerance to fuel alternatives. Note, however, that charge preparation and mixture control are quite different for carbureted and fuel-injected engines. Power and torque demands for SI engines are met by varying the mixture fuel-air ratio. For example, engines built to operate on gasoline can have an air-fuel ratio that may vary while running from approximately 8:1 (rich limits) to 20:1 (lean limits). Too lean a mixture makes it difficult to ignite, while too rich a mixture yields unburned hydrocarbon and carbon monoxide levels that may be in excess of acceptable limits. Fuel-air limits usually fall within fuel-air mixture flammability limits.

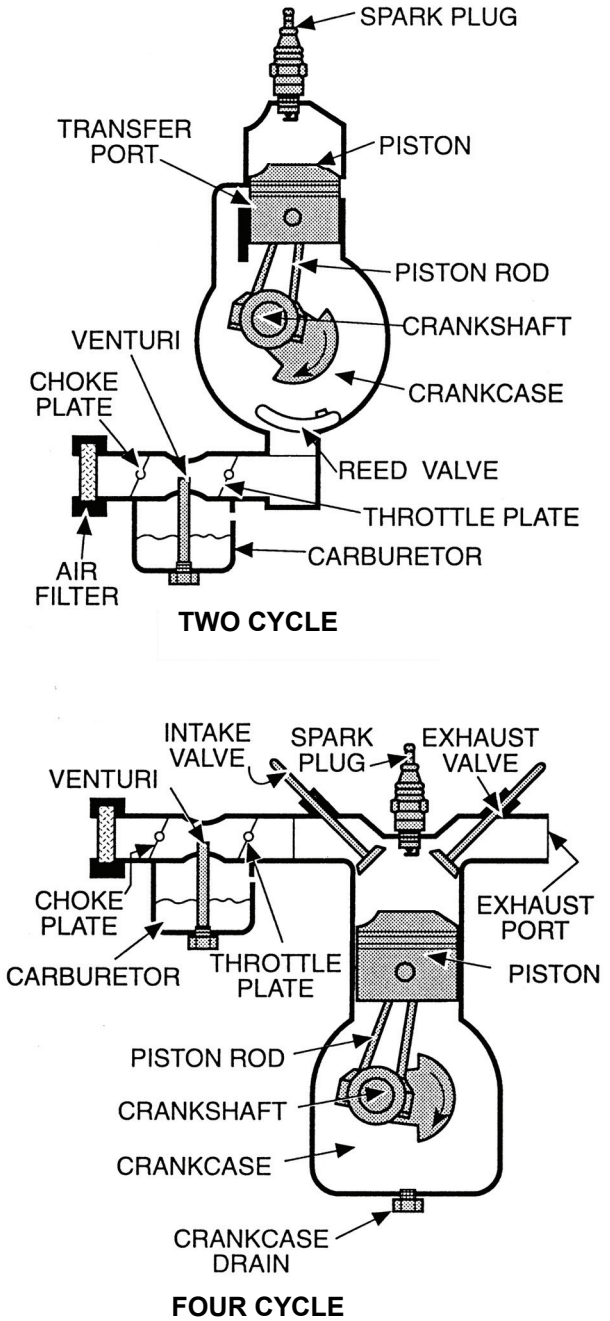

Figure 10.6 Charge preparation and the classic carbureted SI engine. After Stephenson, G. E., *Small Gasoline Engines*, Van Nostrand Reinhold Co., New York, 1978.

Many basic fuel properties are important to proper charge preparation and engine operation. For example, complete vaporization and mixing of a liquid fuel in air prior to compression is an essential element of SI charge preparation. Fuel-air delivery systems, such as those used in direct injected induction mechanisms, and standard classic carbureted manifold, require the use of liquid fuel blends having appropriate low-temperature distillation curves; recall Chapter 5. Note that this fuel-engine nature of volatility will mean that a lower effective fuel distillation temperature is needed during start-up and warm-up than when an engine is running. A distillation temperature that is too low may, in some instances, cause fuel to vaporize in the fuel delivery system, resulting in *vapor lock*, a severe situation in which liquid fuel flow to an engine is blocked. Vapor lock can be crucial in aircraft fuel applications where high-altitude flight will mean a lower fuel boiling point temperature than at sea level. Seasonal atmospheric temperature fluctuations create a need for supplying both summer and winter fuel blends. Note also that unvaporized fuel-air mixtures admit liquid fuel droplets into an engine, diluting and scrubbing lubricating oil film from cylinder walls and increasing friction. Preheating an intake manifold can help to reduce the amount of liquid fuel that reaches cylinder walls, but this would also reduce indicated power output due to the expansion of, and reduction in, the heated charge actually inducted into the engine.

The more volatile a fuel, the greater will be the amount vaporized in the fuel process, and the potentially larger will be the temperature drop within a carburetor, a condition that may cause any moisture in air to condense and ice the carburetor. Less volatile fuels will prevent icing but can make warm-up of the engine more difficult. Volatility requirements for an SI engine designed to run on pure compounds, such as alcohols or propane, are even more unmanageable during cold start since these fuels are not blends but rather are substances that have fixed saturation temperatures for a given saturation pressure. Cold starts often necessitate some additional fuel enrichment to ensure sufficient vaporized fuel for proper ignitability, which traditionally is provided in carbureted engines by the choke. Choking can also prevent hesitation, stumble, stall, and backfire during cold starting. Uniform fuel-air distribution is hard to achieve in multicylinder carbureted engines. Complete vaporization is formidable, and liquid droplets may enter the intake manifold. The momentum of airflow and that of liquid fuel droplets are considerably different, resulting in uneven fuel distribution between cylinders. Cylinder-to-cylinder *FA* ratio variations can also occur under transient operation, causing a time variation, or lag, during charge induction. The poor part-load efficiency of SI engines is primarily an inability to maintain cylinder-to-cylinder mixture quality control. Improvements in fuel control and distribution have resulted from the development and implementation of direct manifold and cylinder-injected engines.

Energy is required to vaporize liquid fuel during charge preparation and induction prior to combustion. Both latent heat of vaporization and ignition energy of SI fuels are functions of mixture composition within any cylinder. Mixture ignition temperatures must be lower than their fuel-air self-ignition temperatures to prevent preignition during compression. Internal combustion engine chemistry produces gases in the exhaust gas stream at temperatures in which water will most probably be a vapor and, thus, the heat of combustion for a particular fuel should be based on its lower heating value. Condensation of this moisture in the exhaust line occurs when the engine is shut off, which can cause rusting of engine exhaust components. There also can be an appreciable quantity of dissociated products of combustion in the burned charge resulting from high-temperature endothermic reactions. These energy-absorbing reactions will lower the total

overall exothermic energy released by the fuel, and the actual temperature rise at TDC will be less than that predicted if dissociation is ignored.

Full power means heavy loads and rich mixture combustion. Maximum air mass must be inducted into the cylinders. Minimum intake resistance for a carbureted engine requires conditions of wide open throttle, or WOT. The influences of residual gases remaining from a previous mechanical cycle are low when operating at WOT. This high power output regime utilizes a rich mixture in each cylinder and produces the greatest values for both peak and mean effective pressures. Excess fuel in the cylinders also can help to prevent overheating of exhaust valves and inhibit the tendency of SI fuels to knock during combustion. Engines run at full power at their best power point.

Idle, or no-load, operation also requires rich mixtures in order to overcome friction and sustain power. With a carbureted engine, this is accomplished with a nearly closed throttle setting, but throttling produces a lower induction cylinder pressure (vacuum) and less air intake. This means that the quantity and condition of hot residual gases left in the clearance volume have a more significant influence on charge induction and preparation. With a lower total charge, peak pressure and indicated mean effective pressures will be greatly reduced.

Cruise performance means a partially opened throttle setting and lean stoichiometry. The intake charge inducted has less dilution by hot residuals. Only enough energy is needed from combustion to overcome both engine friction and vehicle drag. This reduction in power output means that steady cruise operation can burn a lean mixture and operation of the engine is at the point of best economy (see Figure 10.7).

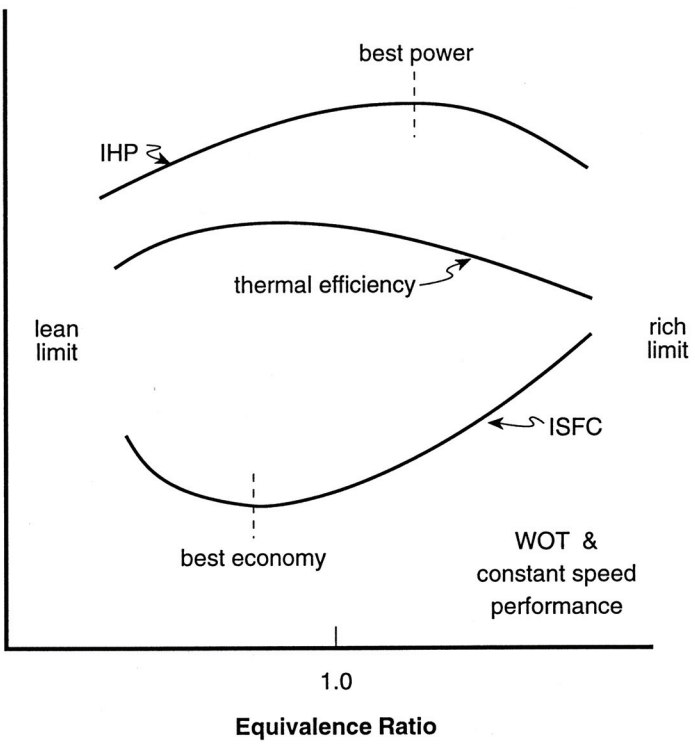

Figure 10.7 Stoichiometry and SI indicated engine performance.

10.4 SPARK-IGNITION I.C. ENGINE COMBUSTION CHEMISTRY

Spark-ignition combustion processes can be classified as normal, i.e., a spark-initiated process; abnormal, i.e., preignition via hot-spot processes, such as carbon deposits or hot spark plugs; and self-ignition, i.e., auto-catalylic detonation processes. Historic SI engine combustion requires a homogeneous combustion process, while current efforts are directed toward nonhomogeneous or stratified charge engine chemistry.

Basic design objectives of classic spark-ignition combustion include:

Developing a high level of turbulence within the charge
Promoting a rapid but smooth rise in pressure versus time (crank angle) during burn
Achieving peak cylinder pressure as close to TDC as possible
Establishing the maximum premixed flame speed
Burning the greatest portion of the charge early in the reaction process
Attaining complete fuel-air charge mixture combustion
Precluding the occurrence of detonation or knock
Minimizing combustion heat loss

Today, most SI engines are designed to operate within the 1,000–6,000-rpm range with spark firing required from 8 to 50 times each second. Engine power results from spark-initiated chemical kinetic and related thermochemical events occurring with a given piston-cylinder head configuration. Spark-ignition engine output, therefore, is strongly influenced by the TDC combustion chamber geometry. Some of these more obvious shape factors include:

TDC surface-to-volume configuration characteristics that allow heat loss and reduce power output
Combustion chamber configurations during burn that can promote the development of detonation waves and combustion knock
Particular configurations with crevice and cold wall quench zones that cause incomplete combustion

Flame speed, a characteristic of fuel-engine interactions, is a maximum near stoichiometric proportions that for gasoline engines can achieve values in the range of 20–40 m/sec (66–131 ft/sec). Increasing engine speed will promote greater turbulence and higher flame speeds, but spark-ignition must be advanced to maintain combustion near the TDC position. Spark advance is also required at part-load operation, a regime characterized by lower power output, lower total energy release, and lower flame speed. Part-load performance, with its greater residual gas containing charge and hotter running cylinders, makes the engine more sensitive to spark knock. Flame speed for extremely lean burn can be so slow that a flame may still be progressing through the chamber when inlet valves open, leading to backfire into the inlet manifold. Spark advance is set at minimum ignition advance for best torque (MBT).

A spherical combustion chamber having a radius r_0 can be used to describe essential elements of SI premixed homogeneous charge combustion. Assume that such a geometry contains reactants initially at uniform conditions T_2 and P_2. Central ignition of this fuel-air mixture produces a spherically shaped premixed flame front that burns outward toward the combustion chamber wall. Recall from Chapter 5 that a premixed

flame speed depends on the initial thermodynamic state, fuel-air ratio, chemical kinetics of the fuel-air mixture, and aerodynamics of flow.

Initial rates of chemical reactions and flame propagation at the center of the constant-volume chamber will be relatively slow because of low turbulence, initial temperature, and pressure within the original charge. This is why efforts are made to initiate swirl and turbulence within a cylinder during charge induction and prior to charge ignition. Too much turbulence, however, could contribute to increased convective heat transfer loss, flame extinction, and/or reduction in indicated power output.

As the flame front progressively burns through the charge, burned gas product temperature T_3, pressure P_3, and specific volume v_3 behind the flame front will be greater, causing thermal compression of the remaining unburned charge ahead of the flame. In addition, heat transfer and diffusion of some reactive radical elements across the traveling reaction zone from the burned product gases will raise local temperature and reactivity in the charge ahead of the flame. This means that flame speed will increase as it moves into these gases. Note that this differs from the one-dimensional steady-state and steady-flow subsonic reaction propagation process described in Chapter 4. In Chapter 4, a reaction front was burning in an open duct with constant upstream conditions; whereas, in an SI engine, flame propagation occurs within confined spaces having upstream conditions that are not constant.

The highest kinetic rates, gas temperatures, and hence flame speeds are achieved in the middle region of the sphere. Since flame speeds are greatest in this area, the largest part of the charge is burned during this stage of combustion. Thermal compression of the unburned charge ahead of the flame, however, continues during this portion of the reaction.

Flame extinction and termination of combustion occur near the wall. High heat transfer rates between the moving flame front and cold wall cause rapid reduction in gas temperature and flame speed approaching the cavity wall. Quenching of the flame occurs prior to its arrival at the wall, leaving a boundary layer region of incomplete reaction within the volume. Note that flame quench in narrow gaps and crevice geometries of an actual chamber can play a major role in emissions formation in an operating engine.

Recall from Chapter 5 that increasing values of reaction temperature and pressure caused the hydrogen-oxygen system to shift from a subsonic flame to a supersonic detonation wave. Higher temperatures and pressures are found in the unburned charge at the end of burn as a result of thermal compression and heating. The potential for knock, or detonation, therefore, exists in a spherical cavity near the end of burn, where conditions may allow gas phase autocatalytic reactions to propagate at a rate that causes oxidation chemistry to self-accelerate. This phenomenon of engine knock can be observed by the use of a cylinder pressure-crank-angle diagram; see Figure 10.8.

Central ignition and combustion of a homogeneous fuel-air charge using a constant-volume spherical chamber produces the following general traits:

Low initial burn rate with little flame expansion and turbulence
An intermediate burn rate having the greatest flame speed, percent of burn, and distance of travel
Terminal burn rate having the maximum flame front area and a thermally compressed end charge that can potentially detonate

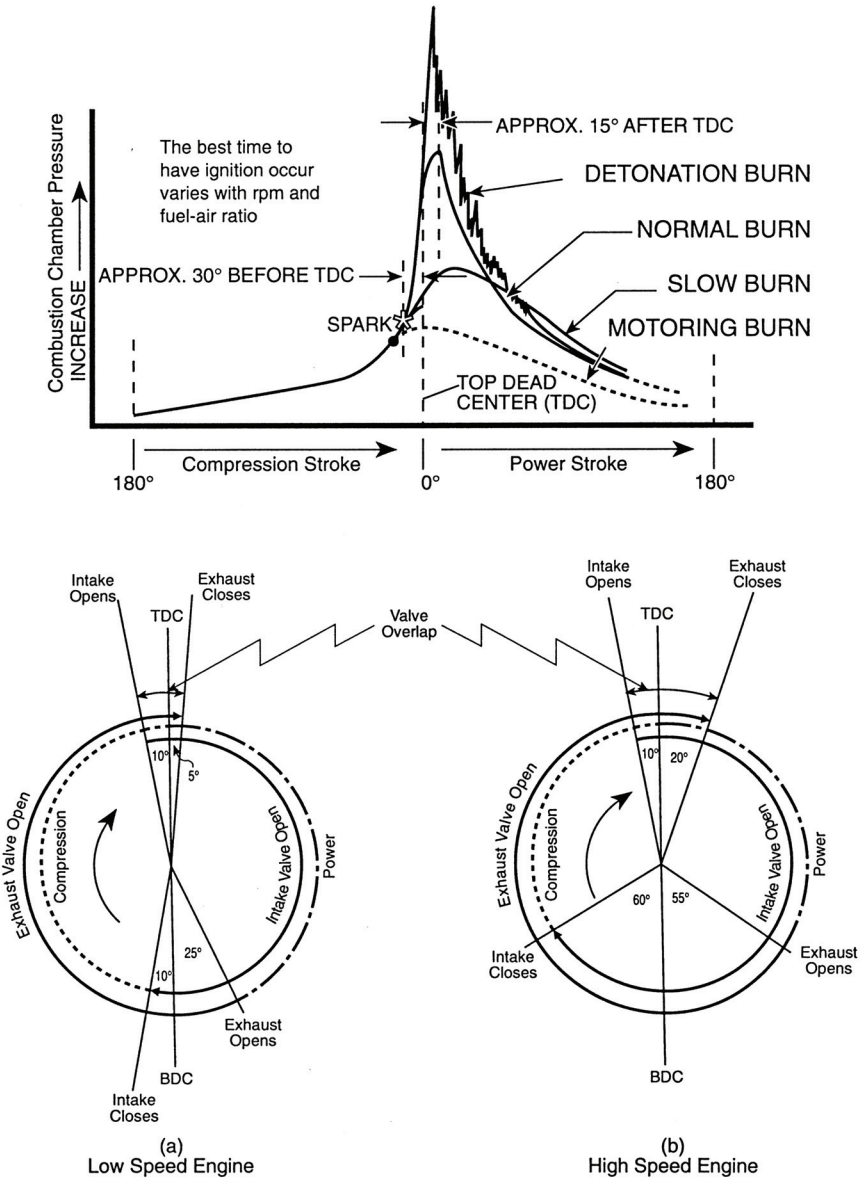

Figure 10.8 Spark-ignition combustion-pressure-crank angle diagram. Adapted from Gill, P. W., Smith, J. H., Jr., and Ziurys, E. J., *Internal Combustion Engines*, 4th Edition, U.S. Naval Institute, 1959. With permission.

Figure 10.9 graphically illustrates these results. The flame front-time plot is often referred to as the classic premixed S combustion curve. The classic S heat release curve is often incorporated in SI engine modeling to relate heat addition as heat release as a function of crank angle near TDC.

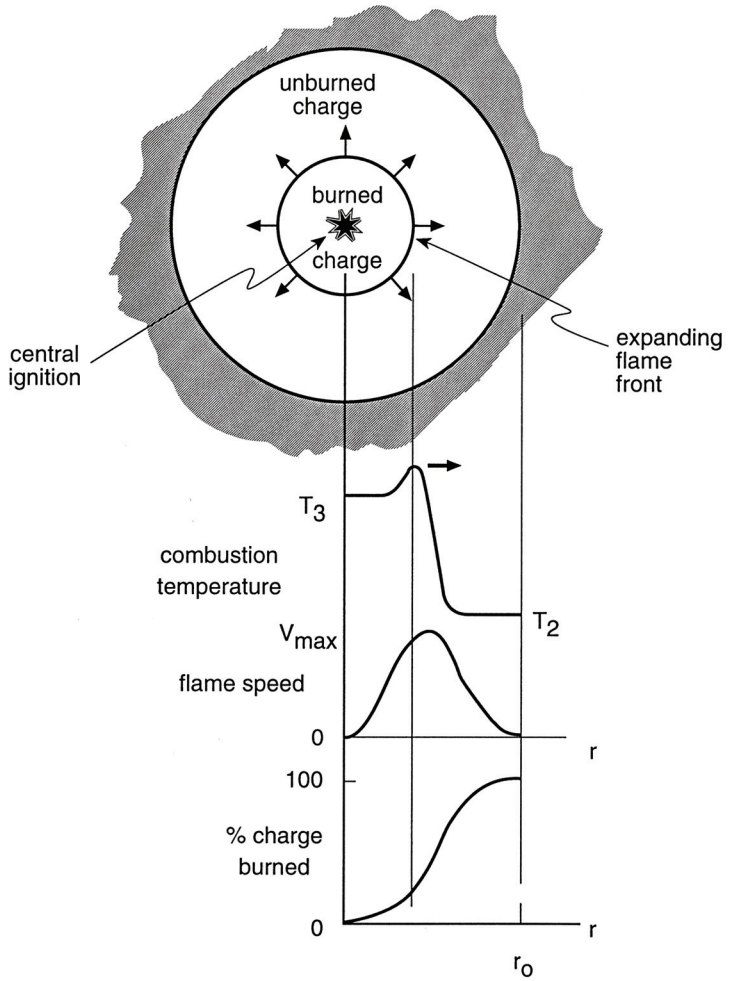

Figure 10.9 Spark-ignition constant-volume combustion characteristics.

Control or limitation of knock in SI engines is a key goal of engine research and development. A given CFR octane-rated fuel will burn differently in the many types of engine internal configurations that are now available. It should be noted that volume is not necessarily constant during combustion in an actual SI engine. Efforts are being made to improve the knock limitations through combustion chamber design and/or basic fuel science research to develop fuels having higher octane ratings. To illustrate, consider side ignition of the spherical charge previously described. The final flame front area is reduced, but the distance the flame would have to travel is increased, i.e., $2r_0$ versus r_0. This added distance could increase thermal compression of end gases and promote knock. A simple cone- or wedge-shaped chamber, rather than a cylinder, with spark ignition at the base would yield an initially large burn rate and flame front, with reduced area and mass at the end of burn. This is a technique used to control knock, but the total charge in

this instance may be less than for a sphere. Many geometric configurations and SI combustion techniques are pursued in an attempt to achieve optimal engine performance.

Thermodynamic and time-related factors both play a role in controlling SI engine knock. Lower-reaction thermal conditions and shorter periods of time for reaction will reduce the tendency for spark knock. Hence, thermodynamic factors that can reduce the potential for knock include:

Reducing the charge by throttling (heat release)
Raising the combustion chamber wall temperature (heat loss)
Operating with an excessively rich or lean mixture (lower peak temperature)
Charge dilution
Lowering the inlet air temperature
Increasing the air inlet humidity
Raising the octane number of the fuel

Time factors that can reduce the potential for knock include the following:

Increasing cylinder turbulence (flame speed)
Increasing engine speed
Decreasing flame travel distance
Retarding spark timing

Indirect methods that can help control knock include:

Promotion of combustion chamber swirl (turbulence)
Exhaust gas recirculation (temperature)
Manifold and/or cylinder-injected combustion
Nonhomogeneous combustion

Efforts have been directed at trying to develop commercially successful engines that *stratify* the charge, i.e., replace the homogeneous charge with a mixture that is richer during the middle stages of reaction and leaner during termination of flame propagation. This type of burn could not only help control knock but would promote more complete combustion of a fuel-air charge and reduce fuel consumption. Development of suitable additives to increase the octane rating of gasoline could also be a means of decreasing the fuel-engine knock sensitivity.

Figure 10.10 shows several SI combustion chamber geometries that have been used in an attempt to achieve a specific design goal such as controlling detonation (wedge), increasing power (hemispherical), and reducing emissions (stratified charge). Other chambers provide examples of unique SI combustion processes (jet valve and pulse bum) that have also been developed in an effort to improve SI engine performance. The cylinder head must provide more than just a cover for the piston crown at TDC and definition for the chamber volume. For example, the spark plug and the exhaust valve are most frequently located near each other and away from the end gas, while the end gas is located in a cool region of the chamber to minimize detonation.

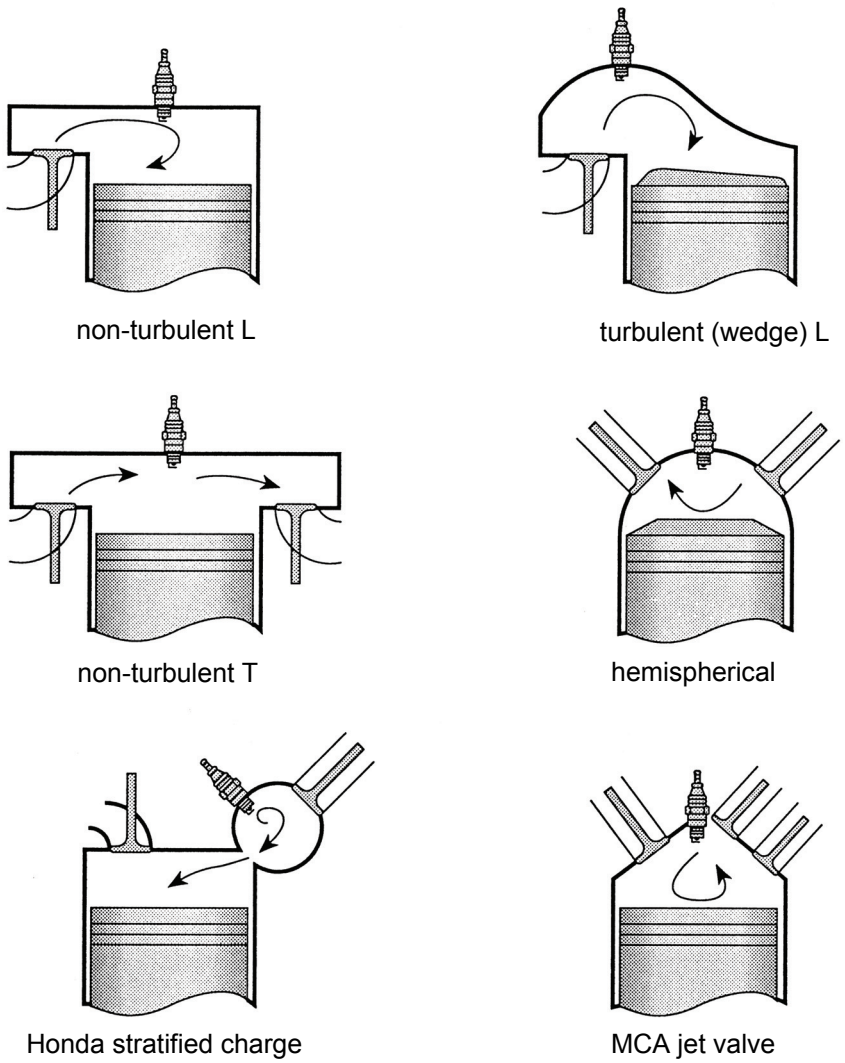

Figure 10.10 Various SI combustion chamber designs.

EXAMPLE 10.3 An ideal open system air standard Otto engine has a compression ratio of 9:1. Charge intake conditions are given as 80ºF and 14.7 psi with combustion approximated by a heat addition of 650 Btu/lbm. Using a constant specific heat analysis and residual gas recirculation, determine the following: (a) charge temperature at BDC prior to compression; (b) peak cycle temperature; (c) residual gas temperature at TDC after exhaust; and (d) residual gas fraction *f*. Compare these results to those for an equivalent Otto cycle.

Solution:

1. Properties of air, from Table B.24 in Appendix B at *STP*:

$$\overline{C}_p\langle T_0\rangle = 6.947 \text{ cal/gmole}\cdot\text{K}$$

or

$$C_p = \frac{(6.947)(1.8001 \text{ Btu/lbmole}\cdot\text{K})(5\text{K})}{(9°\text{R})(28.97 \text{ lbm/lbmole})} = 0.24\frac{\text{Btu}}{\text{lbm}\cdot°\text{R}}$$

$$\overline{C}_v = \overline{C}_p - \overline{R} = 6.947 - 1.987 = 4.960 \text{ cal/gmole}\cdot\text{K}$$

$$C_v = \frac{(4.960)(1.8001)(5)}{(9)(28.97)} = 0.171\frac{\text{Btu}}{\text{lbm}\cdot°\text{R}}$$

$$\gamma = \frac{C_p}{C_v} = \frac{0.24}{0.171} = 1.4$$

2. Otto cycle analysis, no intake/exhaust/recirculation:

$$T_1 = 80°\text{F} \qquad P_1 = 14.7 \text{ psi}$$

$$v_1 = \frac{(53.34 \text{ ft}\cdot\text{lbf/lbm}\cdot°\text{R})(540°\text{R})}{(14.7 \text{ lbf/in.}^2)\left(144 \text{ in.}^2/\text{ft}^2\right)} = 13.607\frac{\text{ft}^3}{\text{lbm}}$$

$$T_2 = T_1\left(\frac{v_1}{v_2}\right)^{\gamma-1} = 540(9)^{0.4} = 1{,}300.4°\text{R}$$

$$T_3 = T_2 + \frac{q}{C_v} = 1{,}300 + (650/0.171) = 5{,}101.2°\text{R}$$

$$T_4 = T_3\left(\frac{v_3}{v_4}\right)^{\gamma-1} = 5{,}101\left(\frac{1}{9}\right)^{0.4} = 2{,}118.1°\text{R}$$

3. Open cycle analysis—assume $T_1 = 560°\text{R}$, $f = 0.03$:

$$v_1 = \frac{(53.34)(560)}{(14.7)(144)} = 14.11 \text{ ft}^3/\text{lbm}$$

4. Compression process:

$$T_2 = T_1\left(\frac{v_1}{v_2}\right)^{\gamma-1} = 560(9)^{0.4} = 1{,}348.6°\text{R}$$

$$P_2 = P_1\left(\frac{v_1}{v_2}\right)^{\gamma} = (14.7)(9)^{1.4} = 318.6 \text{ psia}$$

5. Heat addition, $q(1-f) = C_v(T_3 - T_2)$:

$$T_3 = T_2 + (1-f)q/C_v = 1{,}348.6 + \frac{(1.0 - 0.03)(650)}{0.171} = 5{,}035.7\,°\text{R}$$

$$T_3 = 5{,}035.7°\text{R}$$

$$P_3 = \frac{(53.34)(5{,}035.7)(9)}{(14.11)(144)} = 1{,}189.8 \text{ psi}$$

6. Expansion and exhaust:

$$f = \left(\frac{1}{r_v}\right)\left(\frac{P_1}{P_4}\right)^{1/\gamma} = \left(\frac{1}{r_v}\right)\left(\frac{P_1}{P_3}\right)(r_v)^{\gamma} = \left(\frac{1}{9}\right)\left(\frac{14.7}{1{,}189.8}\right)(9)^{1.4} = 0.0298$$

7. Residual gas temperature:

$$T_5 = T_3\left(\frac{P_5}{P_3}\right)^{\gamma-1/\gamma} = (5{,}035.7)\left(\frac{14.7}{1{,}189.8}\right)^{0.4/1.4} = 1{,}435.1°\text{R}$$

8. Intake and mixing process, $P = c$ (adiabatic):

$$C_pT_1 = f\,C_pT_5 + (1 - f)C_pT_6$$

$$T_1 = f\,T_5 + (1 - f)T_6$$

$$= (0.0298)(1{,}435.1) + (1 - 0.0298)(540)$$

$$= 566.7°\text{R}$$

9. Return to step 3 and choose a new T_1 and f, and repeat steps 3–8. By iteration, one finds that

Part		Otto cycle
a	$T_1 = 567.1°\text{R}$	(540°R)
b	$T_3 = 5{,}053°\text{R}$	(5,101.2°R)
c	$T_5 = 1{,}444°\text{R}$	
d	$f = 0.0300$	

Comments: This problem illustrates how the residual gas influences SI engine indicated cycle characteristics. These calculations did not include the temperature dependency of γ, the impact fuel-air composition, and losses such as heat, friction, and pumping volumetric efficiency.

10.5 SPARK-IGNITION I.C. ENGINE EMISSIONS

Incomplete combustion is a natural consequence of SI engine operation and results from the unique nature of each particular fuel-engine interface; i.e., the quality of fuel used, the specific geometry of an engine's combustion chamber, and the particular means of ignition and burn utilized to produce power. The major by-products of incomplete

combustion, or *engine pollutants*, associated with SI chemistry are carbon monoxide, or CO; unburned hydrocarbons, or UHC; and nitric oxides, or NO_x. Equilibrium product predictions using first and second law analysis as described in Chapter 3 cannot predict levels of certain engine emissions measured using techniques described in Chapter 9. Equilibrium thermochemistry is independent of time, but the process of combustion in an SI engine is, of necessity, time-bounded. An understanding of emissions cannot be based on simple thermochemical calculations but rather requires a knowledge of both fuel and engine characteristics.

Carbon monoxide, an intermediate product of combustion of any hydrocarbon fuel, is a rich SI combustion product produced at both full-load and idle operation. At idle, 0.3 vol % CO is lethal and can cause death in confined spaces within 30 min. The major source of CO is a result of chemical kinetics within the bulk gas; however, CO is also produced by partial oxidation of UHC during the exhaust stroke as well as dissociation of CO_2 produced during combustion. The rapid drop in gas temperature during expansion will freeze CO concentrations at levels different from those predicted on the basis of equal temperatures and equilibrium composition calculations. Control of CO is chiefly by improved *FA* management and lean burn, such as with a stratified engine. Additional CO reduction is obtained using exhaust gas afterburning management via catalyst.

Unburned hydrocarbons, or UHC, can be found in the boundary layer around the combustion walls, where convective and radiative heat transfer have quenched the reaction at the end of flame travel. Additional sources of UHC can include fuel pyrolyzed during burn, lean operation misfire, rich combustion during start-up, and *FA* variation between cylinders. Non-combustion UHC emissions include desorbed or outgassed fuel that had undergone oil film loading early in the charge induction process and gases trapped in small quench zones and crevice volumes formed by the piston crown, top ring, and cylinder walls.

Early efforts to reduce and control UHC in SI engines used fuel injection to replace carburetion, adjustments in spark timing, and careful attention to minimize the surface-to-volume ratio in the design of a combustion chamber. Lean burn combustion, a technique for CO management, has also been used as a technique for controlling UHC emissions. Recall that stratified combustion is based on having the ability to burn rich during that portion of the reaction in which the greatest fraction of charge is consumed. A lean burn design approach produced engines having poor fuel economy with unacceptable performance, which required increased maintenance. Most current UHC control systems now incorporate catalytic reduction of the UHC exhaust. Oxidizing catalytic converters, containing materials such as platinum, reduce both CO and UHC without interfering with engine operation but require the use of unleaded gasoline to prevent catalyst poisoning.

In-cylinder NO_x formation within SI engines is by a different chemical kinetic mechanism than either CO and/or HC processes. Recall from Chapter 5 that NO_x is generated at high temperatures by reactions that occur between nitrogen and oxygen. The production of NO_x is increased by higher combustion temperatures and the presence of oxygen such as occurs under fuel lean conditions. Thus, NO_x formation in SI engines is influenced by the *AF* ratio and by engine design parameters that affect peak temperature, including compression ratio, spark timing, and cooling. In-cylinder control techniques attempt to lower the peak temperature and include external and internal circulation techniques. With external circulation, exhaust gas recirculation (EGR) returns a small fraction of exhaust, i.e., products of combustion, to dilute the intake charge and

thereby reduce the peak temperature and thus lower the amount of NO_x formed. With internal circulation, valve timing is controlled such that during intake there is an overlap period in which the exhaust valve is still opened along with the intake valve allowing internal exhaust gas recirculation.

Three-way catalyst systems are also used to effectively reduce spark-ignition exhaust emissions by oxidizing CO and HC as well as providing for NO_x reduction. However, the discharge control method requires stoichiometric or oxygen-deficient exhaust gas composition to work. A computer controlled closed loop air-fuel ratio feedback control system upstream of the three-way catalysts is required to monitor the oxygen content, i.e., stoichiometric conditions.

Figure 10.11 illustrates the general relationship among CO, UHC, and NO_x emission concentrations and fuel-air mixture equivalence ratio for an SI engine operating on a hydrocarbon fuel such as gasoline. Non-engine UHC emissions include fuel tank, crankcase, and carburetor evaporative losses.

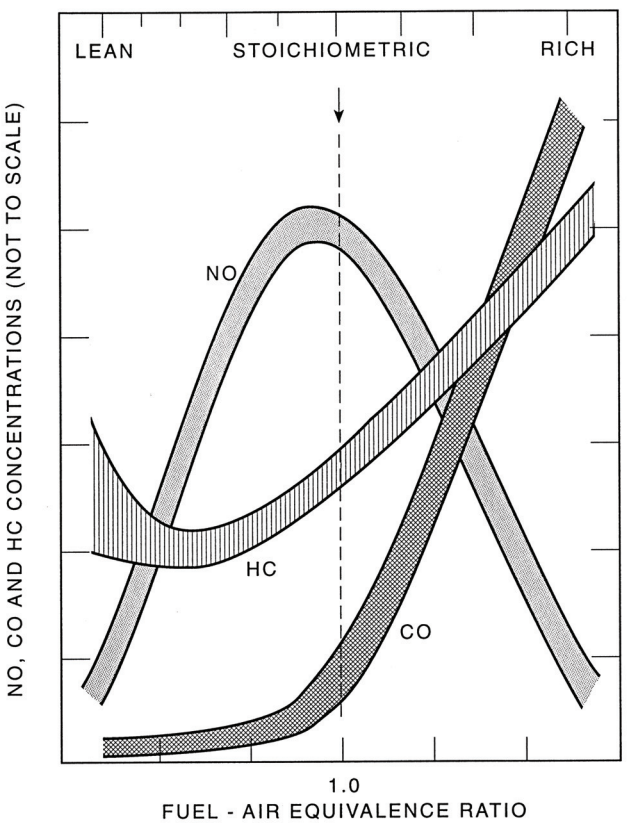

Figure 10.11 Spark-ignition emissions vs. equivalence ratio.

EXAMPLE 10.4 An automotive SI engine burns liquid octane at the rate of 0.0006 kg/sec. Both air and fuel are assumed to enter the engine at 25ºC and 1 atm. The exhaust gases leave the engine at 900K and 1 atm. Steady-state operation results from an equivalence ratio of 0.833, with 88% of the carbon in the fuel burning to form carbon dioxide and the remaining 12% forming carbon monoxide. Measurements show that the indicated heat loss from the engine is equal to 80% of the indicated work output of the engine. Using this information, obtain the following: (a) fuel-air ratio, kg fuel/kg air; (b) combustion product composition, ppm; (c) exhaust gas dew point temperature, K; (d) indicated engine power output, ikW; and (e) indicated specific fuel consumption, kg/ikW sec.

Solution:

1. Stoichiometric equation:

$$C_8H_{18} + 12.5[O_2 + 3.76N_2] \rightarrow 8CO_2 + 9H_2O + (12.5)(3.76)N_2$$

2. Actual reaction:

$$0.833C_8H_{18} + 12.5O_2 + 3.76N_2] \rightarrow$$
$$0.833[(0.88CO_2 + 0.12CO)8 + 9H_2O] + 2.49O_2 + (12.5)(3.76)N_2$$

3. Fuel-air ratio:

$$FA = \frac{(0.833 \text{ kg/mole})(114 \text{ kg/kgmole})}{(12.5)(4.76 \text{ kgmole})(28.97 \text{ kg/kgmole})}$$

a. $= 0.055$ kg fuel/kg air

4. Exhaust gas analysis:

$$\bar{x}_{CO_2} = \frac{(0.833)(8)(0.88)}{14.16 + 2.49 + 47} = 0.0921 \text{ (92,100 ppm)}$$

$$\bar{x}_{CO} = \frac{(0.833)(8)(0.12)}{63.65} = 0.0126 \text{ (12,600 ppm)}$$

$$\bar{x}_{H_2O} = \frac{(0.833)(9)}{63.65} = 0.1178 \text{ (117,800 ppm)}$$

b. $$\bar{x}_{O_2} = \frac{2.49}{63.65} = 0.0391 \text{ (39,100 ppm)}$$

$$\bar{x}_{N_2} = \frac{(12.5)(3.76)}{63.65} = 0.7384 \text{ (738,400 ppm)}$$

5. Exhaust gas dew point T:

$$P_{H_2O} = \bar{x}_{H_2O} P_{tot} = (0.1178)(101 \text{ kPa})$$
$$= 11.89 = 11.9 \text{ kPa}$$

c. $T_{sat}\langle 11.9 \text{ kPa}\rangle = 322\text{K}$

6. Energy balance:

$$\frac{dE}{dt} = \frac{\delta Q}{dt} - \frac{\delta W}{dt} + \sum \dot{N}_i \bar{e}_i - \sum \dot{N}_j \bar{e}_j$$

or

$$0 = Q - W + \sum N_i \bar{e}_i - \sum N_j \bar{e}_j$$

$$W - (0.8)(W) = \sum N_i \bar{e}_i - \sum N_j \bar{e}_j$$

$$0.2W = \{(12.5)(3.76)[\bar{h}_f^0 + \Delta\bar{h}\langle 900\rangle]_{N_2} + (2.49)[\bar{h}_f^0 + \Delta\bar{h}\langle 900\rangle]_{O_2}$$

$$+ (0.833)(9)[\bar{h}_f^0 + \Delta\bar{h}\langle 900\rangle]_{H_2O_g} + (0.833)(8)(0.12)[\bar{h}_f^0 + \Delta\bar{h}\langle 900\rangle]_{CO}$$

$$+ (0.833)(8)(0.88)[\bar{h}_f^0 + \Delta\bar{h}\langle 900\rangle]_{CO_2}\}$$

$$- \{(12.5)[\bar{h}_f^0 + \Delta\bar{h}\langle 298\rangle]_{O_2} + (12.5)(3.76)[\bar{h}_f^0 + \Delta\bar{h}\langle 298\rangle]_{N_2}$$

$$+ (0.833)[\bar{h}_f^0 + \Delta\bar{h}\langle 298\rangle]_{C_8H_{18}}\}$$

$$0.2W = \{(12.5)(3.76)[4{,}355] + (2.49)[4{,}600]$$

$$+ (0.833)(9)[-57{,}798 + 5{,}240] + (0.833)(8)(0.12)[-26{,}417 + 4{,}397]$$

$$+ (0.833)(8)(0.88)[-94{,}054 + 6{,}702]\} - \{(0.833)[-59{,}740]\}$$

$$0.2W = -657{,}993.9 \text{ cal/gmole}$$

$$W = -3{,}289{,}969 = -3{,}290{,}000 \text{ cal/gmole}$$

and

$$\dot{W} = \frac{\left(3.29\times10^6 \text{ cal/gmole}\right)\left(4.187\,\frac{\text{kJ/kgmole}}{\text{cal/gmole}}\right)(0.0006 \text{ kg/sec})}{(114 \text{ kg/kgmole})}$$

d. $\dot{W} = 72.5$ kJ/sec $= 72.5$ikW

7. Indicated specific fuel consumption:

$$ISFC = \frac{\dot{m}_{\text{fuel}}}{\dot{W}_I} = \frac{0.0006 \text{ kg/sec}}{72.5 \text{ ikW}}$$

e. $= 8.28\times10^{-6} = 8.3\times10^{-6}$ kg/ikW·sec

10.6 SPARK-IGNITION ENGINE FUEL ALTERNATIVES

Mobility in today's world is due, in part, to the historic and successful relationship that has existed between gasoline and the SI engine. Future SI engine manufacturers will be required to provide improved engine technology in the long run that can utilize a wider

range of fuel alternatives other than just unleaded gasoline, including non-gasoline petroleum-based distillate fuel fractions, non-petroleum-based fuels produced from resources such as biomass compounds, and alcohols, as well as alcohol-petroleum blends, coal-derived liquid fuels, tar sands, and shale oil. Table 10.2 summarizes nominal properties for certain of these fuel choices. Dr. Gordon Millar, a former president of SAE, has observed that an omnivorous engine must be produced in order to use these fuels effectively, a design goal that raises many new challenges in materials-fuel interactions for the engine designers and manufacturers who will build these improved machines. A variety of complex and interactive factors will influence the success or failure of these new prime movers including: economics; a viable industrial base for providing suitable fuel alternatives; acceptable performance characteristics for the next generation of mobility propulsion hardware, including better fuel economy and emissions control; and overall fuel-engine systems with greater durability, reliability, and efficiency.

The ideal energy characteristics for any SI engine fuel should include:

Storage as a stable liquid at ambient temperature
Low vapor pressure to prevent vapor lock but with light fractions for easy vaporization during cold start
High energy content per unit mass and a fuel density at ambient conditions for both good fuel economy and power
High octane number to allow increased compression ratio operation for better thermal efficiency
Chemical constituents that minimize the generation of polluting engine emissions
Environmentally safe fuel-handling characteristics
Antioxidant, anti-icing, ignition control, cleansers, antiknock, and other required fuel additives

In the past, leaded gasoline, which was the principal commercial spark-ignition engine fuel, best met the greatest number of these important fuel criteria. Today, however, with concern about the impact of lead on the environment unleaded gasolines are required to be produced and utilized. Efforts continue to be under way to discover suitable new octane boosters for unleaded gasoline and to extend and expand current crude oil gasoline resources in an attempt to be able to produce a world supply of usable unleaded fuel. Gasolines can also be distilled from several of the solid and liquid fuel resources discussed in Chapters 6 and 7. Gasoline fractions from shale oil and coderived distillates may have distillation curves similar to those produced from crude oil but may differ widely in their specific properties, such as carbon-to-hydrogen ratio, ignition temperature, viscosity, ultimate analysis, and even molecular structure. Oil shale gasoline, for example, is highly paraffinic and has a low octane number, whereas coal-derived distillate gasoline is generally highly aromatic and has a high octane number. Germany produced 10,000 bbl/day of high octane fuel from coal during World War II, a technology used in recent years in South Africa; see Chapter 7. Hydrogenation of these gasolines may be necessary to make them more suitable for use with present SI engine designs. The performance of engines burning these various gasolines will depend strongly on how closely they compare to the current grades of gasoline being refined from crude oil.

Alcohol is another resource that has been used as an SI engine fuel. The two most practical power alcohol fuels are methanol, which can be produced from coal and/or natural gas, and ethanol, which can be produced from fermentation of certain biomass

materials; see Chapter 7. American farmers burned a grain alcohol fuel called argol in their tractors during the depression, while Germany used alcohol as a military fuel during World War II when gasoline supplies were cut off. Post-World War II French vehicles burned a 50/50 gasoline-alcohol blend and, during the energy crisis of the 1970s, Americans were encouraged to use gasohol, a 90% gasoline-10% ethanol fuel blend in which the alcohol acted chiefly as a political additive. Activities such as in Brazil, where ethanol production can be based on its sugarcane industry, and in Canada, where methanol produced from natural gas is feasible, strongly suggest that alcohol fuels may be a reasonable choice for the future mix of worldwide SI fuel options.

Several properties of neat alcohol do make it unsuitable for direct use with current engine technology, a situation that cannot be easily circumvented without some major redesign. Alcohols have a higher latent heat of vaporization and lower vapor pressure than gasoline and will require a modified intake and charge preparation technique for successful consumption. Alcohol, unlike gasoline blends, has a simple saturation temperature-pressure relationship and, therefore, preheating is essential to eliminate cold-start difficulties. These same characteristics make alcohol fuels less likely to vapor-lock and, with their greater latent heats of vaporization, yield higher volumetric efficiencies as a result of charge cooling during induction. Alcohol-fueled racing engines have used this property successfully to provide a greater mass of charge and thus increase the indicated torque and power output of their vehicles. These engines run rich, an impractical condition for consumer operation given the current stringent requirements on emissions and fuel economy. Efforts to improve fuel economy are further aggravated with alcohol since the heating value, on a mass basis, for both methanol and ethanol is less than that of gasoline or, in other words, more gallons of fuel are burned per mile. Also, stoichiometric fuel-air ratios for alcohol combustion are greater than those for gasoline-air, meaning that, for equal amounts of air, more alcohol fuel is needed. A standard carburetor cannot meter sufficient fuel for stoichiometric combustion and, in fact, will cause the engine to run lean. Thermochemically, Table 10.2 would suggest that ethanol is more favorable than methanol, i.e., has higher heat of combustion and lower latent heat of vaporization. However, it should be recalled that the successful fuel-engine interface design involves more issues than just thermodynamic properties of a given fuel. Alcohol-air mixtures have wide flammability limits, high flame speed, and low flame luminosity, i.e., less radiation heat loss, which suggests potentially better part-load performance. Octane numbers of ethanol and methanol are higher than gasoline and have even been considered as blending agents to raise the octane number of unleaded gasoline. The higher octane number for pure ethanol may allow an engine to be designed having a 12:1 compression ratio.

Alcohol motor fuels are more susceptible to hot-spot preignition, but this can be alleviated somewhat by using a spark plug having a lower heat range. Emissions of UHC, CO, and NO_x should be lower for alcohol-fueled engines, but partially oxidized aldehyde emissions will generally be greater because of their lower charge temperature and lean operation limits. Alcohol motor fuels will not degrade over time as certain gasoline constituents do, but they do absorb water, and alcohol-water mixtures will separate when stored. Alcohols are also more corrosive when in contact with metals such as copper and brass, in addition to certain plastics and gasket materials. Alcohol provides less natural lubricity than gasolines and results in lower engine component durability, greater wear, and possibly greater rust because of its affinity for water.

Table 10.2 Nominal Properties for Certain SI Fuels[a]

Compound	Hydrogen	Methane	Propane	Methanol	Ethanol	"Gasoline"
Formula	H_2	CH_4	C_3H_8	CH_3OH	C_2H_5OH	C_8H_{17}
Phase	gas	gas	lpg	liquid	liquid	liquid
Molecular weight	2.0	16.04	44.09	32.0	46.0	variable
Stoichiometric *AF*	34.19:1	17.19:1	15.63:1	6.45:1	8.98:1	~14.6:1
Specific gravity	0.0696	0.554	0.508	0.792	0.785	~0.7
h_{fg}						
MJ/kg	—	—	0.342	1.17	0.93	~0.18
(Btu/lbm)	—	—	147.1	502	396	~77.4
Boiling point, *T*						
°C	—	–162	–42	65	78	35–210
(°F)	—	–259	–44	149	172	95–410
LHV						
MJ/kg	120.0	50.0	46.0	19.9	26.8	~42.7
(Btu/lbm)	51,600	21,520	19,790	8,570	11,540	~18,400
Octane number						
RON	—	120	111	109	109	90–100
MON	—	120	100	89	90	80–90

[a]Data based on Table 7.1 Thermodynamic Properties of Various Hydrocarbon Compounds, Table 8.1 Gaseous Fuel Specific Gravities, Table B.1 Standard State of Heats of Formation and Combustion for Various Compounds, as well as data reprinted with permission from *Automotive Fuels Handbook*, © 1990 SAE International.

Methane is also a cleaner-burning fuel than gasoline. Charge preparation techniques must be modified when burning methane in order to accommodate its larger required fuel volumetric flow rate and the resulting reduction in volumetric efficiency. Charge preparation is somewhat simplified in that methane is already a vapor, a benefit when cold-starting an engine. One hundred cubic feet of methane gas is approximately equal to one gallon of gasoline in terms of stored chemical energy content, but operation with methane requires ignition timing adjustments because of its lower flame speed. Methane has a high octane number and is easily ignited but has a higher ignition temperature than gasoline.

Liquefied natural gas (LNG), compressed natural gas (CNG), synthetic natural gas (SNG), and even producer gas can all be used as SI fuels. Sulfur impurities in these fuels, however, can cause extensive engine component corrosion. Liquefied petroleum gas (LPG), such as butane and/or propane, is also a suitable automotive fuel that has been used in certain limited dual-fuel applications. High-pressure gas can be stored in heavy cylinders and then be throttled, metered, and supplied by means of a pressure regulator, fuel flow gauge, and fuel-air mixer. A fuel solenoid shutoff valve is necessary for safety when the engine is not running.

The cleanest-burning SI fuel is hydrogen, i.e., no CO, CO_2, or UHC. Products of hydrogen-air engine combustion have less dissociation and a higher specific heat ratio than those for gasoline-air chemistry. Indicated thermal efficiency of a gasoline engine when it is switched to operate on hydrogen is comparable to that using gasoline, but the engine does require modifications. For example, a piston-ring redesign may be necessary to limit hydrogen gas blowby. Hydrogen combustion has some unique characteristics that would influence its use as an SI fuel, including wider flammability limits, higher flame speed, lower ignition temperature, and higher detonation tendency than gasoline-air mixtures. Spark-ignition engines that burn hydrogen also have a greater tendency to preignite, backfire, and spark-knock during operation than when running on gasoline. Smaller quenching distances are found for hydrogen-air combustion. This allows a flame front to pass through smaller areas, such as when valves open, causing backfiring. Conversion of an existing engine to stoichiometric hydrogen combustion would result in a lower indicated power output than when the engine is burning gasoline, but an ability to run lean (wider flammability limits), along with increasing compression ratio, can recover this loss in power. The high NO_x emissions level, peak temperature, and flame speed can all be reduced by lean operation, use of exhaust gas recirculation (EGR), or recycling exhaust moisture.

Efficient fuel storage in vehicle applications is a major disadvantage since hydrogen must be stored either as a liquid or as a gas using metal hydride absorption, but these solutions introduce severe weight and volume penalties to the vehicle. In addition, hydrogen is not naturally occurring and is, therefore, truly an exotic SI fuel option that may be practical in the near term only in large metropolitan areas where severe environmental constraints on pollution levels now exist.

EXAMPLE 10.5 The influence of variable specific heats and gas composition is incorporated in the fuel-air thermochemical SI engine analysis. Consider a stoichiometric mixture of gaseous octane-air and, using JANAF data found in Appendix B, find (a) the mixture relative pressure P, and (b) the mixture relative volume v_r as functions of temperature. Repeat parts (a) and (b) for (c) ideal complete combustion products.

Solution:

1. Stoichiometric equation:

$$C_8H_{18} + 12.5(O_2 + 3.76N_2) \rightarrow 8CO_2 + 9H_2O + 47N_2$$

2. Reactant mole fractions:

$$\bar{x}_{C_8H_{18}} = \frac{1}{1 + (12.5)(4.76)} = 0.01653$$

$$\bar{x}_{O_2} = \frac{12.5}{1 + (12.5)(4.76)} = 0.20661$$

$$\bar{x}_{N_2} = \frac{(12.5)(3.76)}{1 + (12.5)(4.76)} = 0.77686$$

3. Product mole fractions:

$$\bar{x}_{CO_2} = \frac{8}{17 + 47} = 0.12500$$

$$\bar{x}_{H_2O} = \frac{9}{17 + 47} = 0.14063$$

$$\bar{x}_{N_2} = \frac{47}{17 + 47} = 0.73437$$

4. Reactant mixture entropy (Tables B.8, B.18, and B.22 from Appendix B):

$$\bar{s}^0\langle T\rangle = \Sigma \bar{x}_i \bar{s}_i^0\langle T\rangle$$

T		cal/gmole·K			
K	°R	$\bar{s}^0_{C_8H_{18}}$	$\bar{s}^0_{O_2}$	$\bar{s}^0_{N_2}$	$\bar{s}^0\langle T\rangle$
298	536	111.807	49.004	45.770	47.5298
300	540	111.853	49.047	45.815	47.5744
400	720	126.555	51.091	47.818	49.7960
500	900	140.574	52.722	49.386	51.5826
600	1,080	153.816	54.098	50.685	53.0949
700	1,260	166.387	55.297	51.806	54.4213
800	1,440	178.320	56.361	52.798	55.6090
900	1,620	189.540	57.320	53.692	56.6870
1,000	1,800	200.202	58.192	54.507	57.6767

5. Reactant relative pressure and volume:

$$P_r\langle T\rangle = \exp\{\bar{s}^0\langle T\rangle / \bar{R}\} \qquad v_r\langle T\rangle = \bar{R}T / P_r\langle T\rangle$$

T			
K	°R	$P_r \times 10^{-10}$	$v_r \times 10^{+10}$
298	536	2.4462	242.1
300	540	2.5017	238.3
400	720	7.6526	103.86
500	900	18.806	52.829
600	1,080	40.257	29.615
700	1,260	78.479	17.723
800	1,440	142.67	11.142
900	1,620	245.45	7.286
1,000	1,800	403.90	4.920

6. Product mixture entropy (Tables B.5, B.14, and B.18 from Appendix B):

$$\bar{s}^0\langle T\rangle = \Sigma \bar{x}_j \bar{s}_j^0 \langle T\rangle$$

T		cal/gmole·K			
K	°R	$\bar{s}^0_{CO_2}$	$\bar{s}^0_{H_2O}$	$\bar{s}^0_{N_2}$	$\bar{s}^0\langle T\rangle$
1,800	3,240	72.391	61.965	59.320	61.3258
1,900	3,420	73.165	62.612	59.782	61.8529
2,000	3,600	73.903	63.234	60.222	62.3557
2,100	3,780	74.608	63.834	60.642	62.8366
2,200	3,960	75.284	64.412	61.045	63.2984
2,300	4,140	75.931	64.971	61.431	63.7413
2,400	4,320	76.554	65.511	61.802	64.1676
2,500	4,500	77.153	66.034	62.159	64.5782
2,600	4,680	77.730	66.541	62.503	64.9742
2,700	4,860	78.286	67.032	62.835	65.3566
2,800	5,040	78.824	67.508	63.155	65.7258
2,900	5,220	79.344	67.971	63.465	66.0836
3,000	5,400	79.848	68.421	63.765	66.4301
3,100	5,580	80.336	68.858	64.055	66.7656
3,200	5,760	80.810	69.284	64.337	67.0918

7. Product relative pressure and volume:

T			
K	°R	$P_r \times 10^{-10}$	$v_r \times 10^{+10}$
1,800	3,240	2,534.3	1.411
1,900	3,420	3,304.2	1.143
2,000	3,600	4,255.6	0.9338
2,100	3,780	5,420.8	0.7698
2,200	3,960	6,839.1	0.6392
2,300	4,140	8,546.8	0.5347
2,400	4,320	10,592	0.4502
2,500	4,500	13,023	0.3814
2,600	4,680	15,896	0.3250
2,700	4,860	19,269	0.2784
2,800	5,040	23,203	0.2398
2,900	5,220	27,782	0.2074
3,000	5,400	33,074	0.1802
3,100	5,580	39,158	0.1573
3,200	5,760	46,144	0.1378

EXAMPLE 10.6 A 4-in. × 4-in. four-stroke IC engine having a 0.571-in. clearance operates at a constant piston speed of 1,300 rpm. The six-cylinder engine burns a stoichiometric mixture of octane and air. Conditions at BDC after intake can be taken to a vaporized fuel-air mixture at 14.7 psi and 80ºF. Based on the fuel air Otto cycle and JANAF data for the engine thermochemistry, determine (a) the ideal indicated net work, ft·lbf; (b) the ideal indicated mean effective pressure, psi; (c) the ideal indicated thermal efficiency; and (d) the ideal indicated specific fuel consumption.

Solution:

1. Engine geometry:

$$V_{\text{clearance}} = \frac{\pi}{4}\left(\frac{0.571}{12}\text{ ft}\right)\left(\frac{4}{12}\text{ ft}\right)^2 = 0.0041524\ \text{ft}^3$$

$$V_{\text{displacement}} = \frac{\pi}{4}\left(\frac{4}{12}\text{ ft}\right)\left(\frac{4}{12}\text{ ft}\right)^2 = 0.0290888\ \text{ft}^3$$

or

$$V_{\text{TDC}} = 0.0041524\ \text{ft}^3$$

$$V_{\text{BDC}} = 0.0041524 + 0.0290888 = 0.332412\ \text{ft}^3$$

$$r_v = \frac{V_{\text{BDC}}}{V_{\text{TDC}}} = \frac{0.0332412}{0.0041524} = 8.00:1$$

2. Stoichiometric equation, ideal combustion:

$$C_8H_{18} + 12.5[O_2 + 3.76N_2] \rightarrow 8CO_2 + 9H_2O + (12.5)(3.76)N_2$$

Reactant mole fractions:

$$\bar{x}_{C_8H_{18}} = \frac{1.0}{1.0 + (12.5)(4.76)} = 0.01653$$

$$\bar{x}_{O_2} = \frac{12.5}{60.5} = 0.20661 \qquad \bar{x}_{N_2} = \frac{(12.5)(3.76)}{60.5} = 0.77686$$

Product mole fractions:

$$\bar{x}_{CO_2} = \frac{8}{8 + 9 + (12.5)(3.76)} = 0.1250$$

$$\bar{x}_{H_2O} = \frac{9}{64} = 0.1406 \qquad \bar{x}_{N_2} = \frac{47}{64} = 0.7344$$

3. Conditions at BDC, state 1:

$$T_1 = 540°\text{R} = 300\text{K}$$

$$N_{\text{tot}} = \frac{P_1V_1}{\bar{R}T_1} = \frac{(14.7\ \text{lbf/in.}^2)(144\ \text{in.}^2/\text{ft}^2)(0.0332413\ \text{ft}^3)}{(1{,}545\ \text{ft}\cdot\text{lbf/lbmole°R})(540°\text{R})}$$

$$= 8.434 \times 10^{-5}\ \text{lbmoles}$$

$$\bar{U}_{\text{tot}}\langle T_1\rangle = \sum_{i=1} \bar{x}_i N_{\text{tot}}[\bar{h}_f^0 + \Delta\bar{h}\langle T_1\rangle - \bar{R}T_1]_i$$

Using Tables B.8, B.18, and B.22 from Appendix B,

$$U_{\text{tot}}\langle 300\text{K}\rangle = \left\{(8.434 \times 10^{-5}\ \text{lbmole})\left[1.8001\frac{\text{Btu/lbmole}}{\text{cal/gmole}}\right]\right\} \times$$

$$\{(0.20661)[0 + 13 - (1.987)(300)]_{O_2}$$

$$+ (0.77686)[0 + 13 - (1.987)(300)]_{N_2}$$

$$+ (0.01653)[-49{,}820 + 82 - (1.987)(300)]_{C_8H_{18}}\}\ \text{cal/gmole}$$

$$U_1\langle 300\text{K}\rangle = -0.21338\ \text{Btu}$$

4. Process 1–2 isentropic compression of reactants:

$$\frac{V_2}{V_1} = \frac{v_r\langle T_2\rangle}{v_r\langle T_1\rangle} = \frac{1}{8}$$

From Example 10.5,

$$v_r\langle 300\text{K}\rangle = 238.3 \times 10^{-10}$$

or

$$v_r\langle T_2\rangle = \frac{238.3 \times 10^{-10}}{8} = 29.79 \times 10^{-10}$$

and

$$T_2 = 600\text{K} = 1{,}080\,^\circ\text{R}$$

5. Conditions at TDC, state 2:

$$T_2 = 600\text{K} = 1{,}080^\circ\text{R}$$

$$P_2 = \frac{N_{\text{tot}}\bar{R}T_2}{V_2} = \frac{(8.434\times10^{-5}\ \text{lbmoles})(1{,}545\ \text{ft}\cdot\text{lbf/lbmole}\,^\circ\text{R})(1{,}080\,^\circ\text{R})}{(0.0041524\ \text{ft}^3)(144\ \text{in.}^2/\text{ft}^2)}$$

$$= 235.36\ \text{psi}$$

$$U_{\text{tot}}\langle T_2\rangle = \sum_{i=1} \bar{x}_i N_{\text{tot}}[\bar{h}_f^0 + \Delta\bar{h}\langle T_2\rangle - \bar{R}T_2]_i$$

Using Tables B.8, B.18, and B.22 from Appendix B,

$$U_{\text{tot}}\langle 600\text{K}\rangle = \{(8.434 \times 10^{-5})(1.8001)\} \times$$
$$\{(0.20661)[0 + 2{,}210 - (1.987)(600)]_{\text{O}_2}$$
$$+ (0.77686)[0 + 2{,}125 - (1.987)(600)]_{\text{N}_2}$$
$$+ (0.01653)[-49{,}820 + 18{,}813 - (1.987)(600)]_{\text{C}_8\text{H}_{18}}\}$$
$$U_2\langle 600\text{K}\rangle = 0.061137\ \text{Btu}$$

6. Process 2–3 V = constant adiabatic flame; assume complete combustion:

$$\delta Q - P\,dV = dU \qquad U\langle T_3\rangle = U\langle T_2\rangle$$
$$U\langle T_2\rangle = \sum_{\text{rreact}} \bar{x}_i N_{\text{tot}}[\bar{h}_f^0 + \Delta\bar{h} - R\bar{T}]_i = 0.61148\ \text{Btu}$$
$$U\langle T_3\rangle = \sum_{\text{prod}} N_j[\bar{h}_f^0 + \Delta\bar{h} - R\bar{T}]_j$$

or using Tables B.5, B.14, and B.18 from Appendix B,

$$0.061137 = \{0.1394 \times 10^{-5}\ \text{lbmole}\ \text{C}_8\text{H}_{18})(1.8001)\} \times$$
$$\{[-94{,}054 + \Delta\bar{h}\langle T_3\rangle - 1.987\,T_3]_{\text{CO}_2}(8\ \text{lbmole}\ \text{CO}_2/\text{lbmole}\ \text{C}_8\text{H}_{18})$$
$$+ [-57{,}798 + \Delta\bar{h}\langle T_3\rangle - 1.987\,T_3]_{\text{H}_2\text{O}}(9\ \text{lbmole}\ \text{H}_2\text{O}/\text{lbmole}\ \text{C}_8\text{H}_{18})$$
$$+ [0 + \Delta\bar{h}\langle T_3\rangle - 1.987\,T_3]_{\text{N}_2}(12.5)(3.76\ \text{lbmole}\ \text{N}_2/\text{lbmole}\ \text{C}_8\text{H}_{18})\}$$

Rearranging yields

$$(8\Delta\bar{h}\langle T_3\rangle)_{\text{CO}_2} + (9\Delta\bar{h}\langle T_3\rangle)_{\text{H}_2\text{O}} + 47\Delta\bar{h}\langle T_3\rangle_{\text{N}_2} - 127.168\,T_3 = 1{,}296{,}978$$

By trial and error,

$$T_3 = 3{,}137\text{K} = 5{,}647^\circ\text{R}$$

Also,

$$P_3 = \frac{(0.1394 \times 10^{-5})(8 + 9 + 47)(1{,}545)(5{,}647)}{(0.0041524)(144)} = 1{,}302 \text{ psi}$$

7. Process 3–4 isentropic expansion of products:

$$\frac{V_4}{V_3} = \frac{v_r\langle T_4\rangle}{v_r\langle T_3\rangle} = 8$$

Again, using the results from Example 10.5,

$$v_r\langle T_3\rangle = 0.150 \times 10^{-10}$$

with

$$v_r\langle T_4\rangle = (8)(0.150 \times 10^{-10}) = 1.20 \times 10^{-10}$$

and

$$T_4 = 1{,}880\text{K} = 3{,}384°\text{R}$$

8. Conditions at BDC, state 4:

$$T_4 = 1{,}880\text{K} = 3{,}384°\text{R}$$

$$P_4 = \frac{(0.1394 \times 10^{-5})(8 + 9 + 47)(1{,}545)(3{,}384)}{(0.0332413)(144)} = 97.445 \text{ psi}$$

$$U_{\text{tot}}\langle T_4\rangle = \sum N_j[\bar{h}_f^0 + \Delta\bar{h}\langle T_4\rangle - \bar{R}T_4]_j$$

Using Tables B.5, B.14, and B.18 from Appendix B yields

$$U_4\langle 1{,}880\text{K}\rangle = \{(0.1394 \times 10^{-5})(1.8001)\}$$
$$\times \{(8)[-94{,}054 + 20{,}132 - (1.987)(1{,}880)]_{CO_2}$$
$$+ (9)[-57{,}798 + 15{,}921 - (1.987)(1{,}880)]_{H_2O}$$
$$+ (12.5)(3.76)[12{,}389 - (1.987)(1{,}880)]_{N_2}\}$$
$$= -1.5685 \text{ Btu}$$

9. Ideal indicated net work per cylinder:

$$W_{\text{net}} = {}_1W_2 + {}_2W_3 + {}_3W_4 + {}_4W_1$$

With process $i \rightarrow j$:

$$\delta Q - \delta W = dU$$
$${}_1W_2 = U\langle T_1\rangle - U\langle T_2\rangle$$
$${}_3W_4 = U\langle T_3\rangle - U\langle T_4\rangle$$
$$W_{\text{net}} = U\langle T_1\rangle - U\langle T_2\rangle + U\langle T_3\rangle - U\langle T_4\rangle$$

but

$$U\langle T_3\rangle = U\langle T_2\rangle \qquad \text{(see step 6)}$$

$$W_{net} = -0.21338 + 1.5685 = 1.355 \text{ Btu/cyl}$$

a. $W_{net} = (1.355)(778) = 1{,}054 \text{ ft} \cdot \text{lbf/cyl}$

10. Ideal indicated mean effective pressure:

b. $$IMEP = \frac{W_{net}}{V_D} = \frac{(1{,}054 \text{ ft} \cdot \text{lbf/cyl})}{(0.0290888 \text{ ft}^3)(144 \text{ in.}^2/\text{ft}^2)} = 252 \text{ psi/cyl}$$

11. Ideal indicated thermal efficiency:

$$\eta = \frac{W_{net}}{\dot{M}_{fuel} HV}$$

$$= \frac{1.355 \text{ Btu/cyl}}{(1{,}317{,}440 \times 1.8001 \text{ Btu/lbmole fuel})(0.1394 \times 10^{-5} \text{ lbmole fuel/cyl})}$$

c. $\eta = 0.410 = 41.0\%$

12. Ideal indicated engine power, Equation (9.9b):

$$\dot{W}_I = \frac{\overline{P} LANc}{33{,}000\, n} = \frac{(252 \text{ psi/cyl})(4/12 \text{ ft/stroke})(\pi)(4 \text{ in.})^2 (1{,}300 \text{ rpm})(6 \text{ cyl})}{(4)(33{,}000 \text{ ft} \cdot \text{lbf/hp} \cdot \text{min})(2 \text{ rev/power stroke})}$$

$$= 125 \text{ ihp}$$

13. Ideal indicated specific fuel consumption:

$$\dot{M}_{fuel} = \left(114 \times 0.1394 \times 10^{-5} \frac{\text{lbm fuel}}{\text{intake}}\right)\left(1{,}300 \frac{\text{rev}}{\text{min}}\right)\left(\frac{1 \text{ intake}}{2 \text{ rev}}\right)(6 \text{ cyl})$$

$$= 0.6198 \text{ lbm fuel/min}$$

and

$$ISFC = \frac{\dot{M}_{fuel}}{W_I} = \frac{(0.6198 \text{ lbm fuel/min})(60 \text{ min/hr})}{(125 \text{ ihp})}$$

d. $= 0.2975$ lbm/ihp·hr

10.7 THE WANKEL ROTARY ENGINE

The Wankel rotary engine design, developed and patented by Felix Wankel in Germany (ca. 1960), was the result of his efforts to perfect rotary valve sealing. Mechanically, the Wankel rotary engine (see Figure 10.12) is quite different from the reciprocating piston-cylinder positive displacement engine geometry normally used in SI internal combustion engine applications. Rather than a piston, the Wankel has a three-sided rotor that rotates

within an apitrochoidal (somewhat oval) housing. The working fluid is confined within three spaces between faces of the rotors and housing by apex and side seals on the rotor. Three expansion processes per rotor revolution occur since each rotation of the rotor allows three separate charges to move through the engine per lobe.

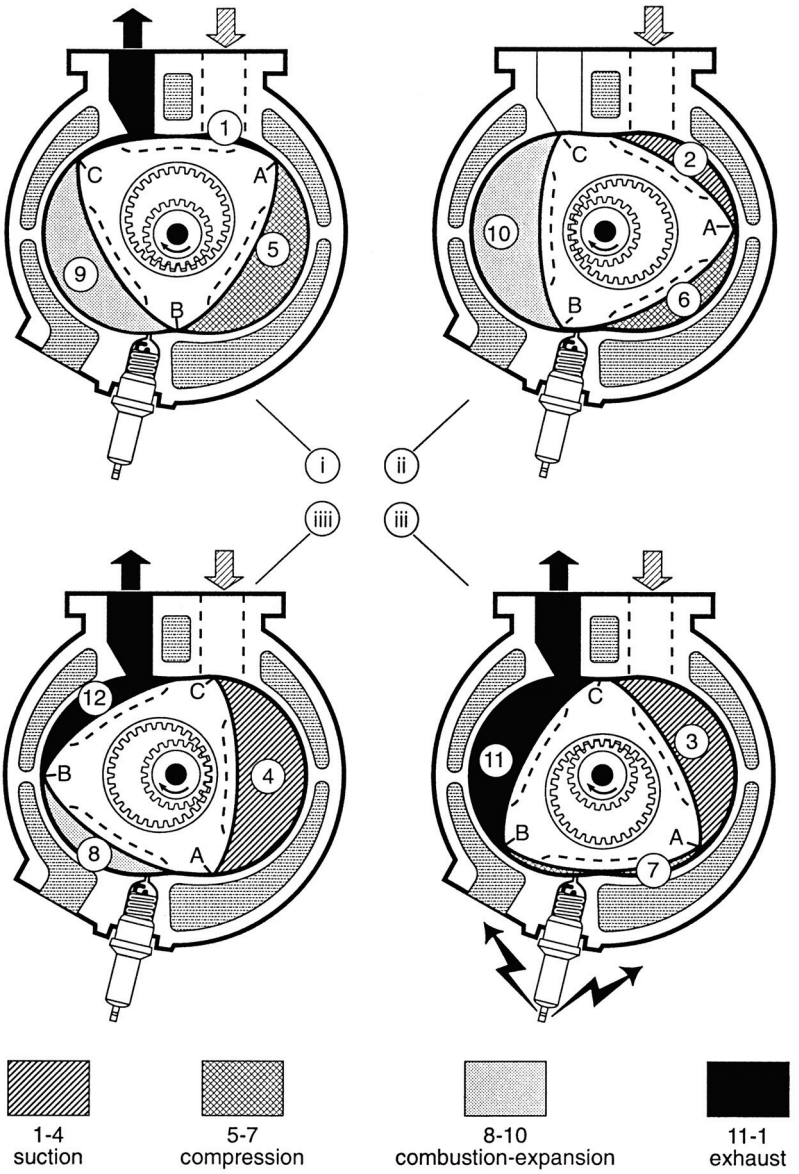

Figure 10.12 The Wankel rotary SI engine. Adapted from Taylor, C. F., *The Internal Combustion Engine in Theory and Practice*, Vol. 2, The M.I.T. Press, Cambridge, Massachusetts, 1977. With permission.

The Wankel rotary engine is, in effect, a "four-stroke" spark-ignition engine that requires the following events per rotor rotation (see Figure 10.12):

1. Intake (1–4): Volume increase because of rotor rotation and the resulting fuel-air suction through the intake port
2. Compression (5–7): Volume sealing and reduction, with resulting increased confined gas pressure and temperature
3. Combustion (6–7): Electrical spark ignition of fuel-air mixture at minimum volume and rapid heat release, raising both pressure and gas temperature
4. Power (8 –10): Volume increase with rotor rotation because of work done by the expanding high-pressure gas on the rotor lobe
5. Exhaust (11–1): Volume decrease and exhaust resulting from rotor rotation and the exposure of the exhaust port

The Wankel configuration offers several potential advantages over the piston engine, some of which are:

Considerably fewer parts. For example, a typical V8 engine has over 1,000 total parts, of which 390 are moving parts. A Curtis-Wright 185-hp Wankel has only 633 parts, of which 154 are moving. This offers advantages such as lighter and smaller engines, increased power density, i.e., power output per unit engine weight, and lower production costs.

Less friction. Fewer moving parts suggest less friction. Less power is lost to friction since fewer parts are subject to wear. This allows a rotary engine to operate at high speeds and, therefore, higher power output.

Less vibration. Rotary engine motion is rotational rather than reciprocating; thus, a rotary-engine vehicle generally runs more smoothly than a piston-engine vehicle, providing smooth output torque characteristics.

Advantages of a two-stroke engine with a four-step (stroke) power sequence. The Wankel is designed so that its rotor rotates once for every three shaft rotations, and the three-sided rotor allows three complete power cycles with each rotor rotation. Each lobe therefore experiences a power cycle on every rotation much like a single-cylinder two-stroke piston engine.

Lower NO_x emissions. Although an advantage in itself, this is actually a result of poor engine combustion efficiency and lower peak temperature. (Recall that NO_x formation is a result of high-temperature $N_2 \leftrightarrows O_2$ thermochemistry.)

Greater knock insensitivity. This, too, is a result of the poor combustion for these engines but does allow the use of lower octane fuels than piston engines.

The Wankel has some disadvantages when compared to the piston engine configuration. These include:

Poor long-term rotor-sealing integrity. The Wankel uses a rotor assembly with apex and side seals that are subject to significant wear. Note that, in reciprocating engines, ring velocities are low at TDC during combustion, whereas in a Wankel engine rotor speed remains high during the development of peak pressure. As a

result, gas seals tend to fail after a relatively short time. Simple and effective solutions for the Wankel have not been as effective as improved ring designs have been for reciprocating piston engines.

Greater heat transfer losses. Because of combustion chamber geometry, the Wankel has a much higher surface area-to-volume ratio than a piston engine. As a result, more energy released by combustion is lost as heat, resulting in lower engine efficiencies. This heat loss is a contributor to a Wankel's poor combustion efficiency.

Inefficient combustion. The Wankel produces emissions that are high in unburned hydrocarbons (UHCs). The fuel rate and oil consumption for Wankel engines are somewhat greater than for comparable reciprocating engines.

Uneven heating. Unlike the piston engine, the same area of the Wankel housing is always exposed to hot combustion gases. This area never gets cooled by fuel-air intake charge, as is the case in a reciprocating engine, and therefore remains hot while other parts of the housing are cooler. This condition causes engine cooling, distortion, and material problems.

PROBLEMS

10.1 The Lenoir cycle, a forerunner of the modern spark-ignition engine, had combustion without compression of the charge. The air standard cycle for this engine consists of the following ideal processes:

1–2	$P = c$	cooling from BDC to TDC
2–3	$V = c$	heat addition at TDC
3–1	$s = c$	expansion from TDC to BDC

Assuming constant specific heats, derive expressions for the following in terms of γ, T_1, T_2, and T_3: (a) compression ratio; (b) net *IMEP*; (c) heat additions; and (d) indicated thermal efficiency.

10.2 Repeat Example Problem10.1 for (a) $\gamma = 1.67$; (b) $\gamma = 1.3$; and (c) $\gamma = 1.2$.

10.3 Conditions at the beginning of compression in an SI engine with an 8.5:1 compression ratio are 14.7 psia and 77ºF. Determine the conditions at the end of ideal compression, assuming properties for the charge to be (a) air with constant specific heats at T_0; (b) air with constant specific heats at the average temperature for part (a); (c) air with variable specific heats; (d) stoichiometric C_8H_{18}-air mixture with constant specific heats at T_0; and (e) stoichiometric C_8H_{18}-air mixture with variable specific heats.

10.4 Use the results of Problem 10.3, and calculate the ideal compression work per unit mass of charge, assuming the properties for the charge to be (a) air with constant specific heats at T_0; (b) air with constant specific heats at the average temperature for part (a); (c) air with variable specific heats; (d) stoichiometric C_8H_{18}-air mixture with constant specific heats at T_0; and (e) stoichiometric C_8H_{18}-air mixture with variable specific heats via combustion charts.

10.5 Conditions at the beginning of expansion in an SI engine having an 8.5:1 compression ratio are 4,320ºR and 920 psia. Determine the conditions at the end of ideal expansion, assuming properties for the burned gases to be (a) air with constant specific heats at T_0; (b) air with constant specific heats at the average temperature for part (a); (c) air with variable specific heats; (d) stoichiometric C_8H_{18}-air complete combustion products and constant specific heat at T_0; and (e) stoichiometric C_8H_{18}-air products of combustion via combustion charts.

10.6 Using the results of Problem 10.5, calculate the ideal expansion work per unit mass of charge, assuming properties for the burned gases to be (a) air with constant specific heats at T_0; (b) air with constant specific heats at the average temperature for part (a); (c) air with variable specific heats; (d) stoichiometric C_8H_{18}-air complete combustion products and constant specific heat at T_0; and (e) stoichiometric C_8H_{18}-air products of combustion via the combustion charts.

10.7 Consider an Otto cycle model of an SI engine with a 9:1 compression ratio in which 1,630 kJ/kg of heat are added at TDC. Conditions at BDC prior to compression are 101 kPa and 30ºC. Early combustion can be modeled ideally as a constant-volume heat addition process that occurs prior to reaching TDC, followed by compression to TDC of the combustion gases prior to expansion. Assume that early heat addition occurs at a volume equal to twice the volume at TDC, and calculate the ratio of (a) peak pressures; (b) thermal efficiencies; and (c) *IMEPS* for this extended Otto cycle to the basic Otto cycle. Use a constant specific heat air standard cycle analysis.

10.8 Repeat Problem 10.7 for the condition of late combustion, in which case constant-volume heat addition occurs after compression to TDC and the beginning of expansion. Assume that late heat addition occurs at a volume equal to twice the volume at TDC, and calculate the ratio of (a) peak pressures; (b) thermal efficiencies; and (c) *IMEPS* for this extended Otto cycle to the basis Otto cycle. Use a constant specific heat air standard cycle analysis.

10.9 The peak brake power for an automobile engine operating at 4,500 rpm is rated as 250 brake hp. Brake thermal efficiency at this condition is 28%. Assuming a lower heating value of 19,000 Btu/lbm for the fuel, calculate (a) peak load fuel consumption, lbm/hr; (b) peak load torque, ft·lbf; and (c) peak load brake specific fuel consumption, lbm/hp·hr.

10.10 A prototype spark-ignition engine maintains a vehicle at 35 mph on a chassis dynamometer. The engine consumes 2.32 gal/hr of isooctane while the measured volumetric flow rate of air during the test is found to be 50 ft^3/min at *STP*. For these conditions, determine (a) fuel consumption, lbm fuel/hr; (b) *FA* ratio, lbm fuel/lbm air; and (c) fuel economy, mpg.

10.11 A six-cylinder, four-stroke SI engine has been converted to burn liquid methanol and air, with an equivalence ratio of 0.9 at an 8:1 compression ratio. The indicated power developed by the engine is 150 ihp when running at 3,300 rpm. Engine volumetric efficiency is 87%, and conditions on intake can be taken as 14.6 psia and 85ºF. For these conditions, calculate (a) the actual combustion equation *AF* ratio; (b) molar *AF* ratio; (c) fuel-air mixture mass flow rate; (d) heat release per mass of fuel-air mixture at *STP*; (e) indicated thermal efficiency; and (f) indicated specific fuel consumption.

10.12 A spark-ignition internal combustion engine is proposed to burn a blend of methanol and ethanol. Intake conditions are 14.5 psia and 50ºF. At 50ºF, the intake vapor pressure of methanol is 1.08 psia, while that of ethanol is 0.45 psia. Assume that the air-fuel mixture delivered to the engine is a homogeneous vapor, and find (a) the mixture molar *AF* ratio; (b) the mass *FA* ratio; (c) the mixture equivalence ratio; and (d) the percent theoretical air.

10.13 An Otto cycle model for a spark-ignition internal combustion engine has an 8.5:1 compression ratio and burns a stoichiometric mixture of isooctane vapor and air. Conditions at the beginning of the compression process are 14.7 psia and 594ºR. The residual fraction is assumed to be 0.047. For these conditions and using combustion charts, determine (a) *P*, *T*, *v*, and *u* around the cycle; (b) net cycle work, Btu/lbm air; (c) indicated thermal efficiency; (d) exhaust gas temperature at BDC, ºR; and (e) residual fraction.

10.14 An Otto cycle design is based on the combustion of methanol in 15% excess air. The conditions after compression of the air-fuel mixture are given as 270 psia and 1,250ºR. Constant-volume combustion is assumed to occur after spark ignition of the compressed charge, with the resulting temperature after reaction being tripled. Assuming complete combustion, determine (a) the balanced reaction equation; (b) the molar *FA* ratio; (c) the complete combustion product mole fractions; and (d) the peak cycle pressure.

10.15 A four-cylinder, four-stroke IC engine has been modified to run on hydrogen. The 2.5-cm × 2.75-cm engine is running at 1,200 rpm. The engine is designed to burn lean with an equivalence ratio of 0.8. Using JANAF data for the H_2-O_2 reaction system, find the following for a fuel-air Otto cycle analysis: (a) net work, N·m; (b) indicated *MEP*, kPa; (c) indicated thermal efficiency, %; (d) indicated power, ikW; and (e) indicated specific fuel consumption, kg/kW·hr.

10.16 An automobile consumes 3.33 gal of fuel/hr while maintaining a constant speed of 50 mph on a chassis dynamometer. The spark-ignition engine burns a rich isooctane mixture and exhaust gas analysis on a dry volumetric basis is as follows:

9.54% CO_2	0.84% H_2
4.77% CO	2.80% O_2
3.15% CH_4	78.90% N_2

The specific gravity of isooctane is 0.702. Determine (a) *FA* equivalence ratio; (b) *AF* ratio on a mass basis; (c) fuel consumption, mph; and (d) CO production, g/mi.

10.17 A four-cylinder 6.25-cm × 7.5-cm four-stroke spark-ignition engine running at 1,800 rpm burns a mixture of indolene and 20% excess air. The volumetric efficiency of the engine with inlet conditions of 105 kPa and 28ºC is 92%. One of every 12 ignitions results in a misfire. Assuming ideal combustion otherwise with all unburned hydrocarbons produced by misfire, find (a) fuel mass flow rate, g/hr; (b) carbon monoxide mass flow rate, g/hr; and (c) unburned hydrocarbon mass flow rate, g/hr.

10.18 A spark-ignition engine design is required to maintain a 28.2% brake thermal efficiency when burning a variety of fuel alternatives. Determine the required

brake specific fuel consumption when burning (a) normal liquid octane; (b) propane; (c) methanol; and (d) hydrogen.

10.19 An SI engine with a 9.5:1 compression ratio runs on a mixture of *n*-octane and 125% theoretical air. Conditions at BDC can be taken as 104 kPa and 27ºC. Using a JANAF fuel-air Otto cycle analysis, determine (a) conditions at the end of compression; (b) adiabatic flame temperature for complete combustion at TDC, K; and (c) peak cylinder pressure, kPa. Repeat parts (b) and (c), assuming equilibrium conditions at the end of combustion.

10.20 A six-cylinder 6.5-cm × 11-cm four-stroke SI engine running at 2400 rpm burns a mixture of CH_4 in 20% excess air. Assuming a volumetric efficiency of 87% and inlet conditions of 105 kPa and 30ºC, determine (a) fuel mass flow rate, g/sec; (b) charge volumetric flow rate, cc/sec; and (c) ideal carbon monoxide exhaust mass flow rate, g/sec.

10.21 A particular spark-ignition engine is designed such that flame propagation is across the cylinder diameter. When the engine is operating at 600 rpm, a nominal flame speed of 920 m/sec travels across the combustion volume in 0.096 millisec. For these conditions, calculate (a) the distance of flame travel, cm; (b) the crank angle of rotation during combustion; (c) the flame speed required at 1600 rpm to travel the same crank angle as for 600 rpm; and (d) the crank angle at 1600 rpm, assuming the same flame speed as for 600 rpm.

10.22 A four-cylinder 2.5-in. × 3-in. four-stroke SI engine operating at 1800 rpm is using an octane-air rich mixture having an air-fuel ratio of 15:1. Calculate (a) fuel mass flow rate, lbm/hr; (b) ideal CO_2 mass flow rate, lbm/hr; (c) ideal CO mass flow rate for 98% combustion of carbon, lbm/hr; and (d) the mass of UHC if all the emissions resulted from misfire every 12 ignitions, i.e., no combustion, lbm/hr.

10.23 A small air-cooled SI engine is found to produce 32 ikW of power output. Exhaust analysis of dry products of combustion are found to be equal to

CO_2	8.2%
CO	0.8%
O_2	4.5%
N_2	86.5%

The fuel is liquid methanol and enters the engine at 25ºC, with a fuel flow rate 3.5 g/sec. For these conditions, find (a) the heat loss from the engine, kW; (b) the indicated thermal efficiency, %; and (c) the mass flow rate of CO_2, g/sec.

10.24 A pulverized anthracite coal source is to be used to produce synthetic gasoline, $C_{8.5}H_{18.5}$, by hydrogenation. The first step required in the conversion process is to remove the sulfur, oxygen, nitrogen, and ash to produce a stream of carbon and hydrogen. The carbon-hydrogen stream is then further reacted with additional hydrogen to upgrade the material to the specified synthetic fuel conditions. For an ultimate coal analysis of 90% carbon, 3% hydrogen, 2% oxygen, 1% nitrogen, and 3% ash determine (a) the refined coal carbon/hydrogen ratio, kg/kg; (b) the refined coal carbon and hydrogen mole fractions, %; (c) the refined coal ideal hydrogenation reaction; (d) the mass of synthetic fuel/mass of raw coal, kg/kg; and (e) the mass if required hydrogen/mass of raw coal, kg H_2/kg coal.

11

Compression-Ignition Engine Combustion

11.1 INTRODUCTION

Several early pioneers in the development of the spark-ignition internal combustion engine were mentioned briefly in Chapter 10. The modern compression-ignition, or CI, internal combustion engine, however, is the result of the initial efforts by one man, Rudolf Christian Karl Diesel (1858–1913). Diesel's goal was to design and develop a unique reciprocating piston-cylinder combustion engine that would burn considerably less fuel per unit power output than available alternative prime movers of his day. He is credited also with being the first inventor of his time to rely on the use of first principles of thermodynamics rather than experimentation alone to achieve the goal of developing a new heat engine. Much of Diesel's early work was published in his *Rational Heat Power* (1892). Early design work and performance predictions were based on analytical models developed prior to fabricating and testing an engine. His original concept was that of a constant-temperature internal combustion (IC) process that would allow his engine to approach the ideal heat input of a Carnot cycle heat engine. Diesel later modified the thermodynamic model for heat input to his engine to that of his now famous constant-pressure heat addition thermodynamic cycle.

Diesel built an early prototype machine in Augsburg, Germany, which, in February 1894, ran for approximately 1 min at 88 rpm while producing 13.2-ihp (indicated horsepower) output. By 1895, an operating engine was developed that produced 20 ihp at approximately 165 rpm. Diesel technology was introduced to the general public by 1898, when three commercial diesel engines, one each from Krupp, Deutz, and Maschinen-fabrik Augsburg Works (known today as M.A.N.), respectively, were displayed at an exposition of power plants in Munich, Germany.

The simplicity of the diesel's ancillary charge preparation and ignition systems, with its ability to run on far cruder fuels, has made the diesel today a successful IC engine. Compression-ignition engines have been useful in a variety of applications, including: heavy-duty mobility propulsion (locomotive, road transport, off-road earth-

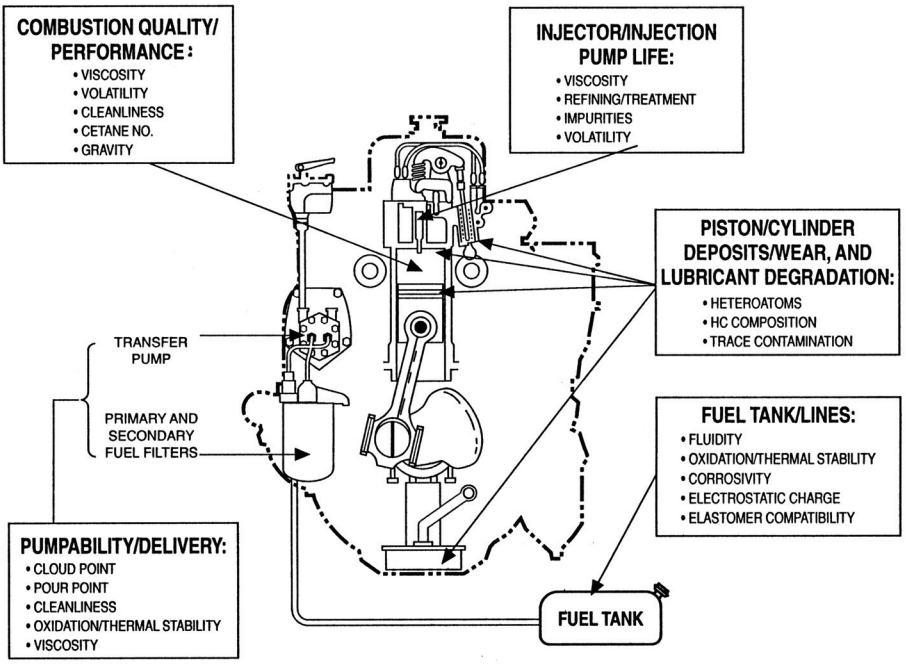

Figure 11.1 Basic CI fuel-engine interface. After Sid Lestz, Report No. AFLRL-164, "Engines/Fuels Workshop," Mann, David M.; Lepera, M. E.; Glance, Paul C.; Munt, Richard; and Mularz, Edward J.; SwRI Fuels and Lubricants Research Lab, San Antonio, TX, 6–8 December 1982.

moving equipment, and marine power); small-scale power generation (standby and emergency generator power sources); and, more recently, hybrid vehicles. The first diesel-powered automobile was built in 1929 by Clessie Cummins, with Mercedes-Benz following suit seven years later in Europe. General Motors began full production of diesel cars in 1977 and, today, automotive and small truck diesels are being built in America, Asia, and Europe.

This chapter will emphasize basic and concurrent fuel engine interface characteristics of compression-ignition engines (see Figure 11.1) and thereby complement the material dealing with spark-ignition fuel-engine interface characteristics presented in Chapter 10. Chapter coverage will include general thermochemical modeling, compatible fuel characteristics, combustion processes, and emission associated with compression-ignition engines.

11.2 THERMODYNAMICS AND COMPRESSION-IGNITION ENGINE MODELING

Dimensionless thermodynamic models for CI engines can be developed as was done for SI engines in Chapter 10. The Classic thermodynamic Otto ($V = c$ heat addition) and/or Diesel ($P = c$ heat addition) cycles do not predict the energy limits of today's intermediate and high-speed diesel engines. The Dual or combined cycle (V and $P = c$ heat

additions) is a more proper thermodynamic model for a modern CI engine. An air standard Dual cycle consisting of the following ideal processes can be used to predict the general energetics of CI engines:

1-2 Isentropic compression from BDC to TDC
2-3 Constant-volume partial heat addition at TDC (valid for high-speed CI engines)
3-4 Constant-pressure partial heat addition during expansion (valid for all CI engines)
4-5 Isentropic expansion to BDC
5-1 Constant-volume heat rejection at BDC

A dimensionless analysis of a compression-ignition engine will be based on the following dimensionless parameters:

$\tau = T_4/T_1$ maximum cycle temperature ratio
$r_v = V_1/V_2$ compression ratio
$r_e = V_4/V_5$ expansion ratio $\neq r_v$
$\alpha = T_3/T_2$ constant-volume heating temperature ratio
$\beta = T_4/T_3$ constant-pressure heating temperature ratio
$\rho = T_5/T_1$ constant-volume cooling temperature ratio
η = indicated thermal efficiency
$\xi = IMEP/P_1$ = dimensionless specific work

Using constant specific heat analysis and the dimensionless parameters listed above, the following dimensionless relationships for temperature now can be written for the Dual cycle:

$$T_2 = T_1 r_v^{\gamma-1}$$

where, from 1–2, $Pv^{\gamma} = \text{const}$

$$T_3 = \alpha T_2 = \alpha T_1 r_v^{\gamma-1}$$
$$T_4 = \beta T_3 = \beta\alpha T_2 = \beta\alpha T_1 r_v^{\gamma-1} = \tau T_1 \tag{11.1}$$

For the Dual-cycle process 3-4, heat addition is at constant pressure during expansion, or

$$P_4 = \frac{RT_4}{v_4} = \frac{RT_3}{v_3} = P_3$$
$$\frac{v_4}{v_3} = \frac{T_4}{T_3} = \beta$$

and, since $v_5 = v_1$,

$$\frac{v_4}{v_5} = \frac{v_4}{v_1} = \left(\frac{v_4}{v_3}\right)\left(\frac{v_3}{v_1}\right) = \left(\frac{v_4}{v_3}\right)\left(\frac{v_2}{v_1}\right) = \frac{\beta}{r_v}$$
$$\frac{T_5}{T_4} = \left(\frac{v_4}{v_5}\right)^{\gamma-1} = \left(\frac{\beta}{r_v}\right)^{\gamma-1}$$

$$\frac{T_5}{T_1} = \left(\frac{T_5}{T_4}\right)\left(\frac{T_4}{T_1}\right) = \frac{\tau\beta^{\gamma-1}}{r_v^{\gamma-1}} = \rho \tag{11.2}$$

Using Equations (11.1) and (11.2), it follows that

$$\alpha\beta r_v^{\gamma-1} = \tau$$
$$\frac{[\alpha\beta r_v^{\gamma-1}]\beta^{\gamma-1}}{r_v^{\gamma-1}} = \rho$$

and thus

$$\rho = \beta^{\gamma}\alpha \tag{11.3}$$

The net work for a Dual cycle w_{net} can be written as

$$\begin{aligned} w_{\text{net}} &= {}_1w_2 + {}_2w_3 + {}_3w_4 + {}_4w_5 + {}_5w_1 \\ &= u_1 - u_2 + P_3(v_4 - v_3) + u_4 - u_5 \\ &= C_v(T_1 - T_2) + C_v(\gamma - 1)(T_4 - T_3) + C_v(T_4 - T_5) \end{aligned}$$

Using the dimensionless parameters cited earlier, w_{net} is then

$$\begin{aligned} w_{\text{net}} &= C_vT_1\left[1 - \left(\frac{T_2}{T_1}\right) + (\gamma - 1)\left\{\left(\frac{T_4}{T_1}\right) - \left(\frac{T_3}{T_1}\right)\right\} + \left(\frac{T_4}{T_1}\right) - \left(\frac{T_5}{T_1}\right)\right] \\ &= C_vT_1\left[1 - r_v^{\gamma-1} + \gamma\left(\frac{T_4}{T_1}\right) - \gamma\left(\frac{T_3}{T_1}\right) - \left(\frac{T_4}{T_1}\right) + \left(\frac{T_3}{T_1}\right) + \left(\frac{T_4}{T_1}\right) - \left(\frac{T_5}{T_1}\right)\right] \end{aligned}$$

or

$$w_{\text{net}} = \frac{RT_1}{(\gamma - 1)}\left[1 - r_v^{\gamma-1} + \gamma\left(\tau - \alpha r_v^{\gamma-1}\right) + \alpha\left\{r_v^{\gamma-1} - \left(\frac{\tau}{\alpha r_v^{\gamma-1}}\right)^{\gamma}\right\}\right] \tag{11.4}$$

Ideal indicated mean effective pressure, *IMEP*, for a Dual cycle, defined as the net work divided by the displacement volume, is then equal to

$$\begin{aligned} IMEP &= \frac{w_{\text{net}}}{v_1[1 - (1/r_v)]} \\ &= \frac{P_1[1 - r_v^{\gamma-1} + \gamma(\tau - \alpha r_v^{\gamma-1}) + \alpha\{r_v^{\gamma-1} - (\tau/\alpha r_v^{\gamma-1})^{\gamma}\}]}{(\gamma - 1)[1 - 1/r_v]} \end{aligned}$$

which, written in dimensionless form as specific work ξ, is given as

$$\begin{aligned} \xi &= \frac{IMEP}{P_1} \\ &= \frac{[1 - r_v^{\gamma-1} + \gamma(\tau - \alpha r_v^{\gamma-1}) + \alpha\{r_v^{\gamma-1} - (\tau/\alpha r_v^{\gamma-1})^{\gamma}\}]}{(\gamma - 1)[1 - 1/r_v]} \end{aligned} \tag{11.5}$$

External heat addition per unit mass consists of both constant-volume heat addition from 2–3 and constant-pressure heat addition from 3–4. The constant-volume heat addition per unit mass $(q_H)_v$ is given as

$$(q_H)_v = {}_2q_3 = C_v[T_3 - T_2]$$

which, in dimensionless form, is

$$\left(\frac{q_H}{C_vT_1}\right)_v = [\alpha r_v^{\gamma-1} - r_v^{\gamma-1}]$$

and the constant-pressure external heat addition from 3–4 is given as

$$(q_H)_P = {}_3q_4 = C_p[T_4 - T_3] = \gamma C_v[T_4 - T_3] \tag{11.6}$$

which, in dimensionless form, equals

$$\left(\frac{q_H}{C_vT_1}\right)_P = \gamma[\tau - \alpha r_v^{\gamma-1}]$$

The total external heat addition now is written as

$$\begin{aligned} q_H &= (q_H)_v + (q_H)_P \\ &= C_vT_1[\alpha r_v^{\gamma-1} - r_v^{\gamma-1} + \gamma(\tau - \alpha r_v^{\gamma-1})] \end{aligned}$$

and

$$\frac{q_H}{C_vT_1} = [(1-\gamma)\alpha r_v^{\gamma-1} + \gamma\tau - r_v^{\gamma-1}] \tag{11.7}$$

An indicated thermal efficiency, η, for the Dual cycle using Equations (11. 4) and (11. 6), is defined as

$$\eta = \frac{\text{net cycle work}}{\text{net external heat addition}}$$

$$\eta = \frac{C_vT_1[1 - r_v^{\gamma-1} + \gamma(\tau - \alpha r_v^{\gamma-1}) + \alpha\{r_v^{\gamma-1} - (\tau/\alpha r_v^{\gamma-1})^{\gamma}\}]}{C_vT_1[\alpha r_v^{\gamma-1}(1-\gamma) + \gamma\tau - r_v^{\gamma-1}]}$$

$$\eta = \frac{[1 - r_v^{\gamma-1} + \gamma(\tau - \alpha r_v^{\gamma-1}) + \alpha\{r_v^{\gamma-1} - (\tau/\alpha r_v^{\gamma-1})^{\gamma}\}]}{[\alpha r_v^{\gamma-1}(1-\gamma) + \gamma\tau - r_v^{\gamma-1}]} \tag{11.8}$$

The classic constant-pressure Diesel cycle can be determined from these relationships if one assumes no constant volume process and heat addition (i.e., $\alpha = 1$, or $T_3 = T_2$). In this instance, the net work for a compression ignition $P = c$ heat addition cycle using Equation (11.4) equals

$$w_{\text{net}} = \frac{RT_1}{(\gamma-1)}\left[1 - r_v^{\gamma-1} + \gamma(\tau - r_v^{\gamma-1}) + r_v^{\gamma-1} - (\tau/r_v^{\gamma-1})^{\gamma}\right]$$

$$w_{\text{net}} = \frac{RT_1}{(\gamma - 1)}\left[1 + \gamma(\tau - r_v^{\gamma-1}) - (\tau / r_v^{\gamma-1})^{\gamma}\right] \tag{11.9}$$

Ideal *IMEP* for the classic Diesel cycle then equals

$$IMEP = \frac{P_1}{(1 - 1/r_v)(\gamma - 1)}\left[1 + \gamma(\tau - r_v^{\gamma-1}) - (\tau / r_v^{\gamma-1})^{\gamma}\right] \tag{11.10}$$

and dimensionless specific work ξ is expressed as

$$\xi = \frac{1}{(1 - 1/r_v)(\gamma - 1)}\left[1 + \gamma(\tau - r_v^{\gamma-1}) - (\tau / r_v^{\gamma-1})^{\gamma}\right] \tag{11.11}$$

External heat addition for the $P = c$ Diesel cycle can be written as

$$\frac{q_H}{C_v T_1} = \gamma(\tau - r_v^{\gamma-1})$$

$$\frac{q_H}{C_p T_1} = (\tau - r_v^{\gamma-1}) \tag{11.12}$$

By combining Equations (11.9) and (11.12), an equation for the Diesel cycle indicated thermal efficiency can be expressed as

$$\eta = \frac{[RT_1/(\gamma - 1)][1 + \gamma(\tau - r_v^{\gamma-1}) - (\tau / r_v^{\gamma-1})^{\gamma}]}{(C_p T_1)(\tau - r_v^{\gamma-1})}$$

or

$$\eta = \frac{[1 + \gamma(\tau - r_v^{\gamma-1}) - (\tau / r_v^{\gamma-1})^{\gamma}]}{\gamma(\tau - r_v^{\gamma-1})} \tag{11.13}$$

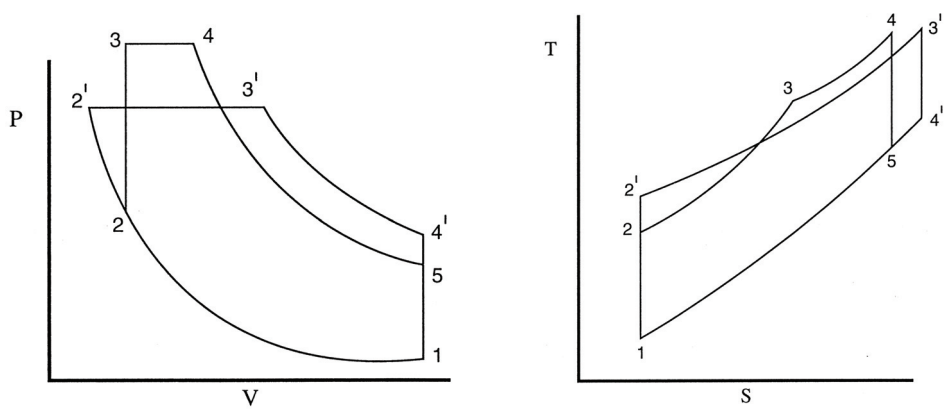

Figure 11.2 Ideal CI air standard *P-v* and *T-s* diagrams.

The ratio v_4/v_3 for the dual cycle $P = c$ combustion stage is termed the *fuel cutoff ratio*. The dimensionless relationships developed for CI cycles in this chapter along with SI cycles from Chapter 10 are summarized in Table 11.1. Figure 11.2 illustrates ideal *P-v* and *T-s* diagrams for air standard CI thermodynamic cycles.

Table 11.1 Dimensionless Thermodynamic Relationships for Air Standard IC Engines

Net work: w_{net}

Otto cycle:

$$= \frac{RT_1}{(\gamma - 1)}\left[1 - r_v^{\gamma-1} + \tau - (\tau / r_v^{\gamma-1})\right] \tag{10. 1}$$

Dual cycle:

$$= \frac{RT_1}{(\gamma - 1)}\left[1 - r_v^{\gamma-1} + \gamma(\tau - \alpha r_v^{\gamma-1}) + \alpha\{r_v^{\gamma-1} - (\tau/\alpha r_v^{\gamma-1})^{\gamma}\}\right] \tag{11.4}$$

Diesel cycle:

$$= \frac{RT_1}{(\gamma - 1}\left[1 + \gamma(\tau - r_v^{\gamma-1}) - (\tau / r_v^{\gamma-1})^{\gamma}\right] \tag{11.9}$$

External heat addition: $\dfrac{q_H}{C_v T_1}$

Otto cycle:

$$= \tau - r_v^{\gamma-1} \tag{10.4}$$

Dual cycle:

$$= [(1 - \gamma)\alpha r_v^{\gamma-1} + \gamma\tau - r_v^{\gamma-1}] \tag{11.7}$$

Diesel cycle:

$$= \gamma(\tau - r_v^{\gamma-1}) \tag{11.12}$$

Specific work: $\xi = \dfrac{IMEP}{P_1}$

Otto cycle:

$$= \frac{[(1 - r_v^{\gamma-1}) + \tau - \tau / r_v^{\gamma-1}]}{(\gamma - 1)[1 - 1/r_v]} \tag{10.3}$$

Dual cycle:

$$= \frac{[1 - r_v^{\gamma-1} + \gamma(\tau - \alpha r_v^{\gamma-1}) + \alpha\{r_v^{\gamma-1} - (\tau/\alpha r_v^{\gamma-1})^{\gamma}\}]}{(\gamma - 1)[1 - 1/r_v]} \tag{11.5}$$

Diesel cycle:

$$= \frac{1}{(1 - 1/r_v)(\gamma - 1)}\left[1 + \gamma(\tau - r_v^{\gamma-1}) - (\tau / r_v^{\gamma-1})^{\gamma}\right] \tag{11.11}$$

Table 11.1 Continued

Indicated thermal efficiency: η

Otto cycle:

$$= 1 - \left(\frac{1}{r_v}\right)^{\gamma-1}$$

Dual cycle:

$$= \frac{[1 - r_v^{\gamma-1} + \gamma(\tau - \alpha r_v^{\gamma-1}) + \alpha\{r_v^{\gamma-1} - (\tau/\alpha r_v^{\gamma-1})^{\gamma}\}]}{[\alpha r_v^{\gamma-1}(1 - \gamma) + \gamma\tau - r_v^{\gamma-1}]} \tag{11.8}$$

Diesel cycle:

$$= \frac{[1 + \gamma(\tau - r_v^{\gamma-1}) - (\tau/r_v^{\gamma-1})^{\gamma}]}{\gamma(\tau - r_v^{\gamma-1})} \tag{11.13}$$

Particular IC engine performance characteristics often are evaluated or compared for various specific design and/or operational purposes. For example, engine configurations may be investigated for the resulting effects in performances with changes in piston speed, displacement volume, compression ratio, heat input, work output, peak pressure, and/or peak temperature. Analytical evaluations can prove useful and complement expensive work necessary with actual engines in the test cell. The relationships in Table 11.1, for example, can be used to compare ideal indicated thermal efficiencies for Diesel, Dual, and Otto cycles. An inspection of Equations (10.5), (11.8), and (11.13) reveals that all three cycles have thermal efficiencies that depend on compression ratio, r_v, and specific heat ratio, γ. Some also depend on the maximum cycle temperature ratio, τ, and the constant-volume heating temperature ratio, α. Using the stated relationships and with the use of a *P-v* and/or *T-s* diagram, such as found in Figure 11.3, one can show that ideal indicated thermal efficiencies for classic air standard Diesel, Dual, and Otto cycles are ordered as follows for the specific conditions indicated below:

Cycle constraint	Thermal efficiency
Fixed heat input and compression ratio	Otto > Dual > Diesel
Fixed heat input and maximum pressure	Diesel > Dual > Otto
Fixed work output and maximum pressure	Diesel > Dual > Otto

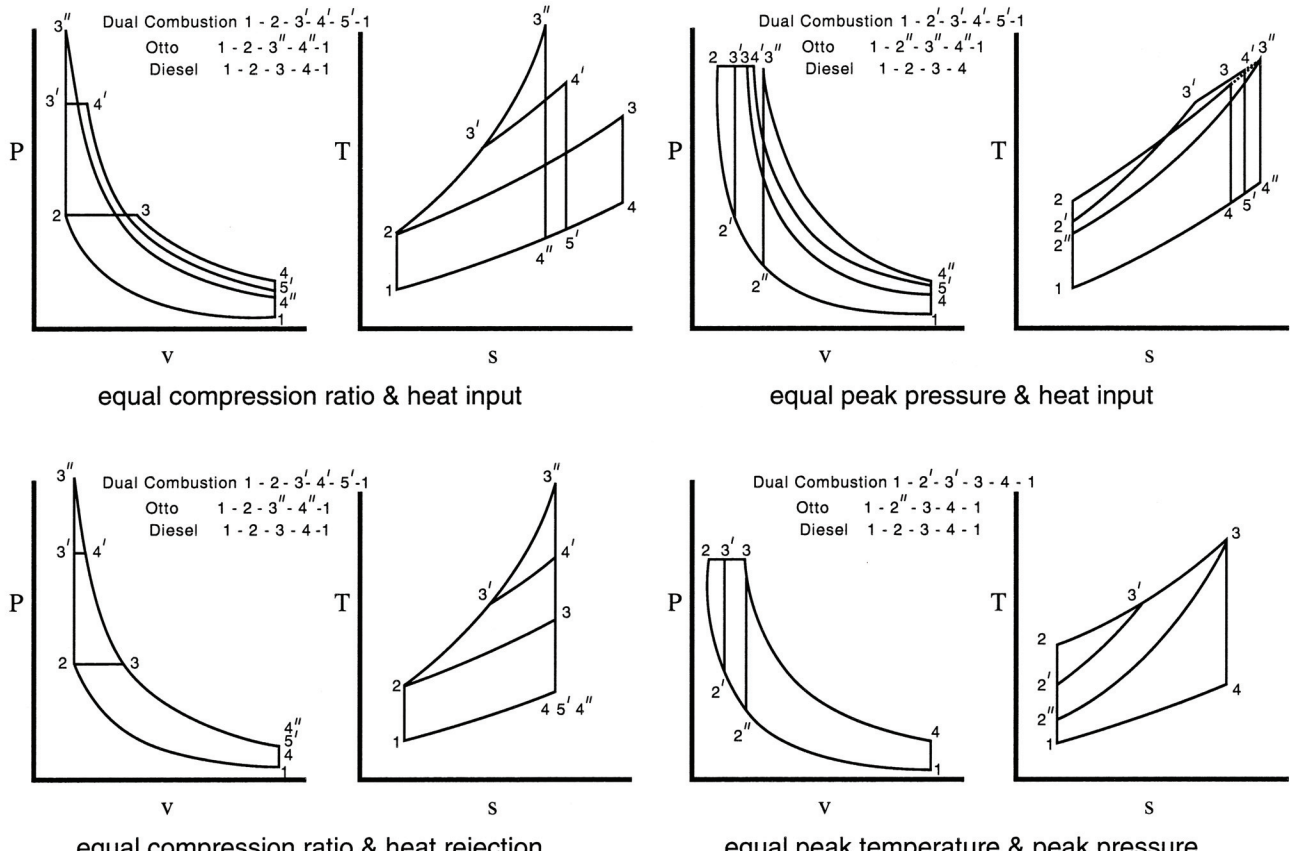

Figure 11.3 Comparison of various air standard cycles. Adapted from Gill, P. W., Smith, J. H., Jr., and Ziurys, E. J., *Internal Combustion Engines*, 4th Edition, U.S. Naval Institute, 1959. With permission.

Frequently, one hears it stated that a diesel has a higher thermal efficiency than an SI engine. This is truly an incomplete and somewhat misleading statement. For equal compression ratios, the Diesel will have a lower efficiency than the Otto and Dual cycles. Diesel engines, however, because of their very different knock limitations and flame chemistry, can be built to operate at higher compression ratios (r_v > 12:1) than knock-limited SI engines (r_v < 11:1). In this way the diesel engine, due chiefly to its higher attainable compression ratio, may be produced having a higher theoretical thermal efficiency than the spark-ignition engine. Note that the additional relationships in Table 11.1 can be manipulated in order to study trends in additional design characteristics, such as indicated mean effective or peak pressures as function of heat input.

Zeroth-order air standard Diesel and Dual cycle modeling can be expanded to include both intake and exhaust processes as developed in Chapter 10. Fuel-air thermochemistry, residual gas influences, use of variable specific heats, and equilibrium chemistry can also be included. Certain diesel combustion engines generate *P-v* indicator cards that under particular operational instances may be fitted to a "combined cycle" diagram. Using simple dual-cycle models, however, is less useful as a general predictive tool for CI engines than the constant-volume modeling is for describing general characteristics of actual SI engines due to heat loss, finite blowdown rates, and physics of heat release in actual diesel engines.

EXAMPLE 11.1 Using a dimensionless Diesel, Dual, and Otto cycle analysis, determine the relative values for thermal efficiencies as a function of compression ratio under the following constraints: $\tau = 10$, fixed peak pressure ratio $P_3/P_1 = 30$, and fixed heat addition per unit mass $q_H / C_v T_1 = 10$. Assume that $\gamma = 1.4$.

Solution:

1. Thermal efficiency, Diesel cycle:

$$\eta = \frac{[1 + \gamma(\tau - r_v^{\gamma-1}) - (\tau / r_v^{\gamma-1})^{\gamma}]}{\gamma(\tau - r_v^{\gamma-1})}$$

2. Thermal efficiency, Dual cycle:

$$\eta = \frac{[1 - r_v^{\gamma-1} + \gamma(\tau - \alpha r_v^{\gamma-1}) + \alpha\{r_v^{\gamma-1} - (\tau / \alpha r_v^{\gamma-1})^{\gamma}\}]}{[\alpha r_v^{\gamma-1}(1 - \gamma) + \gamma\tau - r_v^{\gamma-1}]}$$

3. Thermal efficiency, Otto cycle:

$$\eta = 1 - (1/r_v)^{\gamma-1}$$

4. The constant-volume heating ratio α for the Dual cycle is a function of total heat input, γ, τ, and compression ratio, r_v; see Equation (11. 7). Thus,

$$q_H / C_v T_1 = 10 = [(1 - \gamma)\alpha r_v^{\gamma-1} + \gamma\tau - r_v^{\gamma-1}]$$

or

$$\alpha = \frac{10 - \gamma\tau + r_v^{\gamma-1}}{(1 - \gamma) r_v^{\gamma-1}}$$

5. Cycle thermal efficiency η:

r_c	α	Diesel	Dual	Otto
6	2.3836	0.2626	0.4494	0.5116
7	2.0916	0.3199	0.4711	0.5408
8[a]	1.8528[a]	0.3658[a]	0.4874[a]	0.5647[a]
9	1.6524	0.4036	0.4997	0.5848
10	1.4811	0.4355	0.5088	0.6019
11	1.3322	0.4628	0.5152	0.6168
12	1.2011	0.4865	0.5195	0.6299
13	1.0845	0.5073	0.5218	0.6416
14	0.9798	0.5259	0.5223	0.6520
15	0.8850	0.5425	0.5211	0.6615
16	0.7988	0.5575	0.5183	0.6701
17	0.7197	0.5711	0.5138	0.6780
18	0.6470	0.5835	0.5075	0.6853
19	0.5796	0.5949	0.4993	0.6920
20	0.5171	0.6055	0.4891	0.6983

[a] $\alpha = \dfrac{10 - 14 + 8^{0.4}}{(1 - 1.4)8^{0.4}} = 1.8528$

Diesel:

$$\eta = \frac{1 + 1.4(10 - 8^{0.4}) - (10/8^{0.4})^{1.4}}{1.4(10 - 8^{0.4})} = 0.3658$$

Dual:

$$\eta = \frac{1 - 8^{0.4} + 1.4(10 - 1.8528 \times 8^{0.4}) + 1.8528(8^{0.4} - (10/(1.8528 \times 8^{0.4}))^{1.4}}{1.8528 \times 8^{0.4} \times (1 - 1.4) + 1.4 \times 10 - 8^{0.4}}$$

$$= 0.4874$$

Otto:

$$\eta = 1 - (1/8)^{0.4} = 0.5647$$

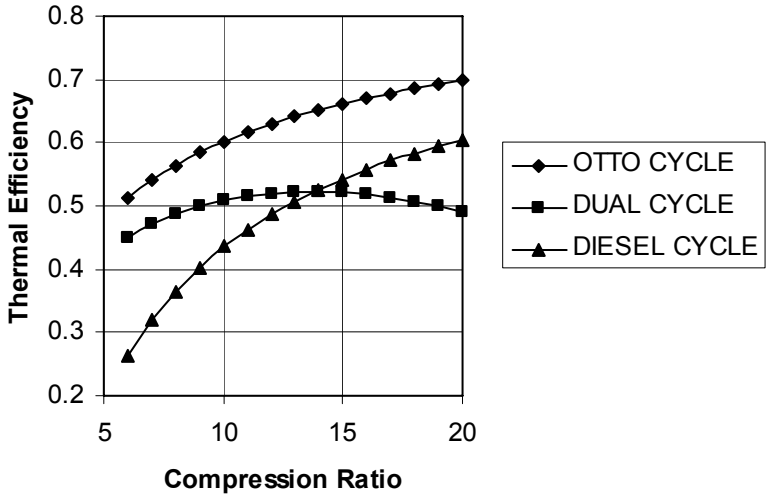

Comments: A review of the results for these *specific* constraints reveal the following facts:

For the same compression ratio, peak cycle temperature, and total heat input,

$\eta_{Otto} > \eta_{Diesel}$ $\eta_{Otto} > \eta_{Dual}$

Thermal efficiencies of the Diesel and Otto cycles increase with increasing compression ratio.

Thermal efficiency for the Dual cycle increases and then decreases with increasing compression ratio.

For the same total heat input, peak cycle temperature, and equal compression ratios,

$\eta_{Diesel} > \eta_{Dual}$ for $r_v > 13$ $\eta_{Diesel} < \eta_{Dual}$ for $r_v < 13$

Thermal efficiency of the Otto cycle at 8:1 compression for the same total heat input, peak cycle temperature can be surpassed by a Diesel cycle having a compression ratio greater than 17:1.

11.3 FUEL THERMOCHEMISTRY AND COMPRESSION-IGNITION ENGINES

Diesel fuels undergo a series of events that enable CI engines to produce useful power output: storage, pumping and handling, filtering, preheating (required for the slow speed engine heavy residual fuels), ingestion, atomization, mixing with air, and finally combustion. These processes and their resulting impact on performance characteristics are governed by thermochemical properties of diesel fuels utilized, engine particularities, and specific CI fuel-engine interactions. Among the more dominant fuel properties are volatility, viscosity, pour point, distillation curve, self-ignition temperature, latent heat, and heat of combustion; see Table 11.2.

Table 11.2 Nominal Properties for Certain CI Fuels[a]

Fuel property	Fuel type			
	Kerosene	Premium diesel	Railroad diesel	Marine distillate diesel
Cetane number	50	47	40	38
Boiling range, °C (°F)	163–288 (325–550)	182–357 (360–675)	176–357 (350–675)	176–250 (350–500) (90%)
Viscosity, SSU at 38°C (100°F)	33	35	36	47
Gravity, °API	42	37	34	26
Sulfur, wt %	0.12	0.30	0.50	1.2
Uses	High-speed city buses	High speed: Buses Trucks Tractors Light marine engines	Medium speed: RR engines Marine engines Stationary engines	Low speed: Heavy marine engines Large stationary engines

[a]Adapted from ASTM D975 Classification of Diesel Fuel Oils. Copyright ASTM International. Reprinted with permission.

Diesel engines can burn a wider range of crude oil distillate liquid fuels than conventional SI engines and are therefore considered by many to be a broad-cut fuel IC engine. Low-speed diesels operate on a variety of hydrocarbon fuels, ranging from heavy residuals to power kerosenes. However, high-speed diesels only are able to utilize a much narrower band of the light distillate fuel oils discussed in Chapter 7.

Fuel viscosity must be low enough to ensure proper fuel pump lubricity and also guarantee that atomization produces a suitable distribution of small droplets. Viscosity, however, should be high enough to prevent fuel oil injector leakage at the end of injection. Diesel fuel viscosity makes injection in large low-speed engines much easier and more efficient than in small high-speed machines, where the number, size, and placement of injection orifices are severely limited. Diesel volatility requirements are stated in terms of a 90% distillation temperature, i.e., a temperature at which 90% of the fuel will vaporize. High-speed engines with less time for fuel chemistry require a more volatile fuel than low-speed CI engines.

Fuel flash point temperatures should exceed 77°C (150°F) to ensure proper fuel compression ignition but, more importantly, to keep fuel safe during storage and handling. The pour point, or congealing temperature of a fuel, is a low-temperature performance factor ensuring fuel flow without the need for preheating, usually less than −17.4°C (0°F). Paraffinic waxes that separate out from fuels at low temperatures are a chief cause of diesel fuel freezing problems. Heat of combustion is the major thermochemical fuel property that controls the power output of a CI engine. Fuel latent heat, i.e., the energy necessary to vaporize diesel liquid fuel droplets, must be provided by heat transfer from hot compressed air. Cold-starting difficulties may sometimes be circumvented by methods that can raise a cold air temperature to ensure proper charge preparation such as the use of Special starting fuels, manifold heaters, and glow plugs, an in-cylinder heater.

Diesel fuel ignition quality is stated in terms of a *cetane index*, an experimental measure of autoignition characteristics that is a complex function of fuel volatility, self-ignition temperature, and combustion chamber geometry. Cetane numbers for diesel fuels, like octane numbers for gasolines, are relative numbers that are obtained using a specific ASTM test and CFR engine; see Chapter 9. Values for the cetane numbers suitable for use in high-speed diesels range from 50 to 60, with a higher scale value being a more easily ignitable fuel. Detonation, or diesel knock, measured by the cetane number is different from SI knock, measured by an octane number. Recall that high octane number fuels resist autoignition, whereas high cetane number fuels have low autoignition characteristics. Note also that straight-chain paraffin compounds with single C–H bonding have high cetane values but low octane numbers, whereas aromatic ring compounds have low cetane but high octane numbers.

EXAMPLE 11.2 The temperature of the air in a diesel engine after compression must be greater than the self-ignition temperature of the injected fuel. Assume that ambient air conditions of 101 kPa and 27°C represent the initial state of the uncompressed air charge. For ideal compression, using both constant and variable specific heats, calculate (a) the compressed air temperature, K; and (b) the compressed air pressure, MPa, as a function of compression ratio. The minimum self-ignition temperature of diesel fuels is approximately 510°C. Determine values of (a) and (b) for this condition.

Solution:

1. Isentropic compression of air, constant specific heats:

$$r_v = \frac{V_{\text{BDC}}}{V_{\text{TDC}}} = \left[\frac{T_2}{T_1}\right]^{1/(\gamma-1)}$$

$$T_2 = T_1 r_v^{\gamma-1} \qquad P_2 = P_1 r_v^{\gamma}$$

2. Isentropic compression of air, variable specific heats:

$$r_v = \frac{V_{\text{BDC}}}{V_{\text{TDC}}} = \frac{V_r\langle T_1\rangle}{V_r\langle T_2\rangle} \qquad V_r\langle T_2\rangle = \frac{V_r\langle T_1\rangle}{r_v}$$

$$T_2 = T_2\langle V_r\rangle \qquad P_2 = \left[\frac{P_r\langle T_2\rangle}{P_r\langle T_1\rangle}\right] \times P_1$$

3. Compressed air properties versus compression ratio:

r_v	T_2	P_2	$V_r \times 10^{10}$	$P_r \times 10^{-10}$	T_2	P_2
8	689	1.86	2,253	25.627	678	1.90
9	723	2.19	2,002	29.078	704	2.15
10	754[a]	2.54[a]	1,802[b]	35.031[b]	736[b]	2.59[b]
11	783	2.90	1,638	39.869	762	2.95
12	811	3.28	1,502	43.961	784	3.25
13	837	3.66	1,386	47.750	803	3.53
14	862	4.06	1,287	54.520	828	4.03
15	886	4.48	1,201	60.207	849	4.45
16	909	4.90	1,126	65.352	868	4.83
17	932	5.33	1,060	69.955	885	5.17
18	953	5.78	1,001	73.746	899	5.45
19	974	6.23	948	81.245	919	6.01
20	994	6.70	901	87.712	936	6.49
21	1,014	7.17	858	94.180	953	6.96
22	1,033	7.65	819	99.506	967	7.36

[a]Constant specific heats
$T_2 = (300\text{K})(10)^{0.4} = 753.56 = 754\text{K}$
$P_2 = (0.101\ \text{MPa})(10)^{1.4} = 2.537 = 2.5\ \text{MPa}$
[b]Variable specific heats, using Example 3.2

$$V_r = \langle 300\rangle \times 10^{10} = 18{,}028 \qquad P_r\langle 300\rangle \times 10^{-10} = 1.366$$

$$V_r\langle T_2\rangle = \frac{18{,}020 \times 10^{-10}}{10} = 1{,}802 \times 10^{-10}$$

$$T_2\langle V_r\rangle = T\langle 1{,}802 \times 10^{-10}\rangle = 736\text{K}$$

$$P_r\langle 736\rangle = 35.031\times 10^{10}$$

$$P_2 = \left[\frac{35.031}{1.366}\right]\times 0.101 \text{ MPa} = 2.59 = 2.6 \text{ MPa}$$

4. Diesel fuel ignition temperature, $T_{\text{ignit}} = 510 + 273 = 783\text{K}$:

$$r_v\langle 783\text{ K}\rangle = 11:1 \text{ (constant specific heats)}$$
$$= 12:1 \text{ (variable specific heats)}$$

Comments: These calculations show that $\gamma = 1.4$ overpredicts the compressed air temperature at TDC. This overprediction increases with compression ratio. Pressure predictions for the two techniques are not that different and suggest that care should be taken when inferring gas temperature from cylinder pressure data.

Use of an *FA* ratio is somewhat nondescript when considering CI combustion. Initially, a nonhomogeneous fuel-rich reactive mixture exists near the injector tip and at specific points throughout the combustion chamber near fuel droplets, with air throughout the remaining volume. Time-dependent injection spray patterns with physics and chemistry producing three-dimensional, unsteady reactive regions make local *FA* ratios quite meaningless. One can speak of an overall *FA* or *AF* ratio and, in this sense, diesel engines operate burning rich mixtures of 20:1 at full load to lean mixtures of 100:1 at light load.

11.4 COMPRESSION-IGNITION I.C. ENGINE COMBUSTION CHEMISTRY

Proper charge preparation, as discussed in Chapter 10 for the case of SI engines, is also necessary for efficient CI engine combustion; see Figure 11.4. Classic SI engine combustion requires a premixed flame that propagates through a homogeneous mixture, whereas classic CI engine combustion is based on diffusion flame chemistry occurring within a heterogeneous mixture and initiates around small burning centers of vaporized droplet of liquid fuel. Very distinct stages of thermochemistry and heat release can be identified in classic CI combustion: (1) a period of ignition delay, (2) a period of ignition and rapid pressure rise, (3) a period of continued combustion and gradual pressure change, and (4) a period of postflame reactions. A pressure-crank angle or pressure-time diagram can be useful to help visualize these various stages of heat release; see Figure 11.5. Heat release rates for CI combustion in low- (under 300 rpm), medium- (300–1,000 rpm), and high-speed (over 1,000 rpm) engines are different. Greater mechanical and kinetic time is available during low-speed heat release (a $P = c$ heat addition thermodynamic model) than during medium- and high-speed heat release (a $V = c$ and $P = c$ heat addition thermodynamic model). The following comments will focus chiefly on high-speed diesel engines to illustrate broadly the principles at work during compression-ignition IC engine combustion chemistry.

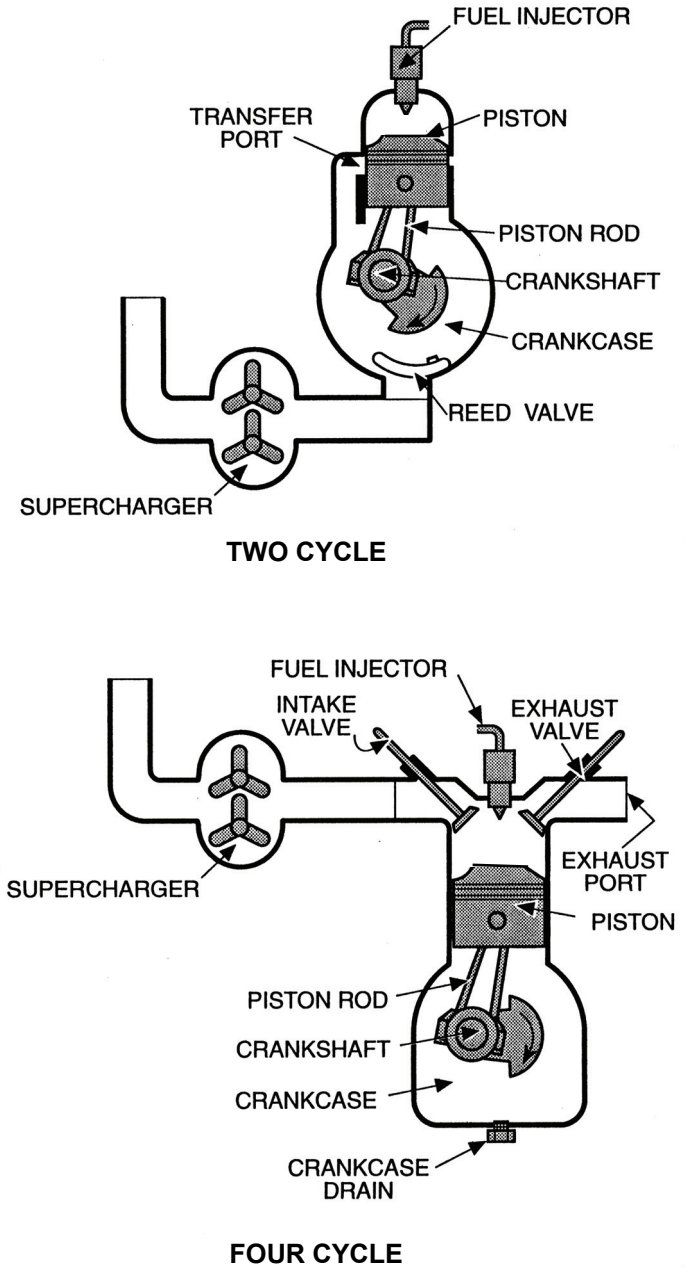

Figure 11.4 Charge preparation and the compression CI engine. After Stephenson, G. E., *Small Gasoline Engines*, Van Nostrand Reinhold Co., New York, 1978.

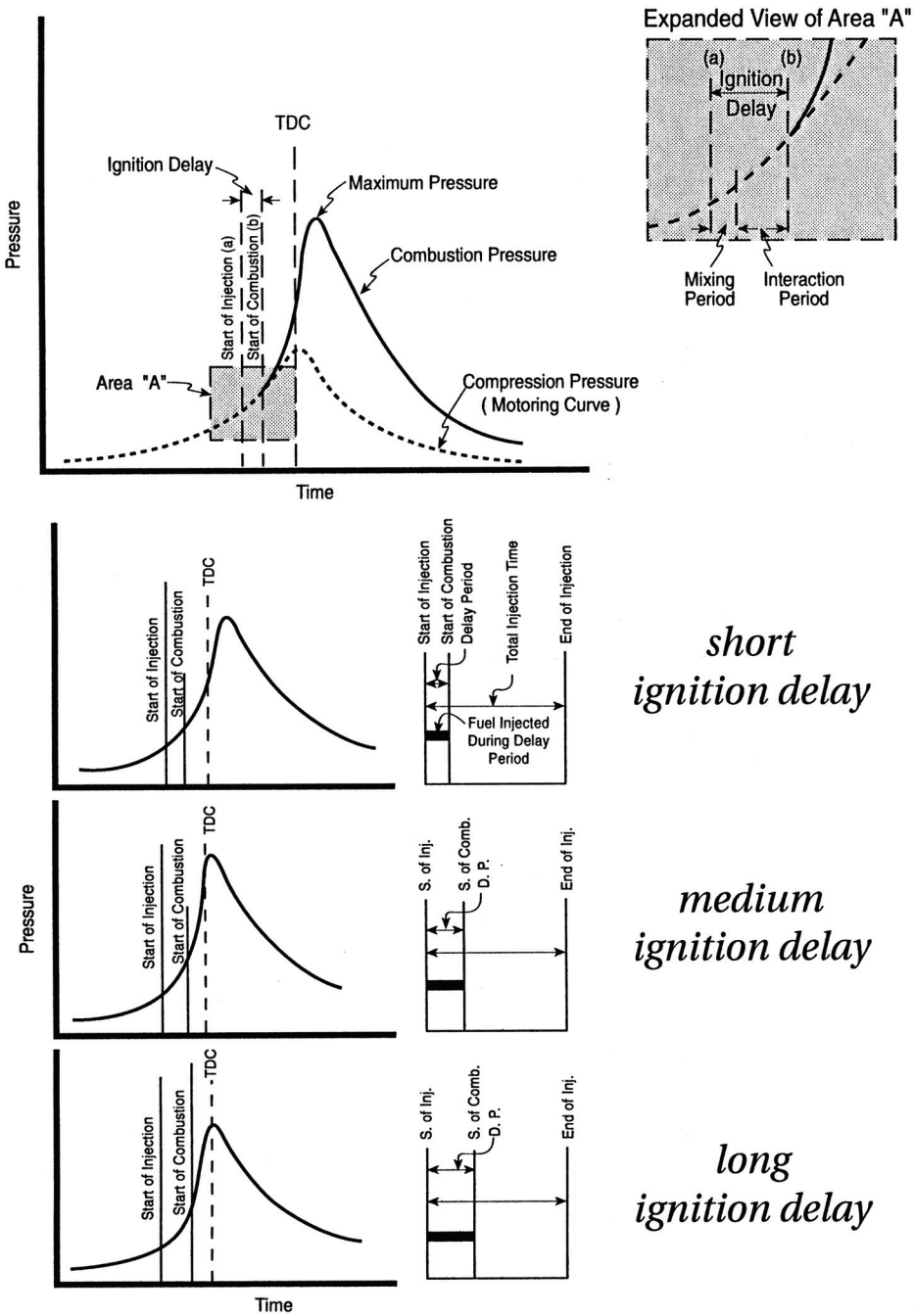

Figure 11.5 Combustion-ignition combustion–pressure–crank angle diagram. Adapted from Gill, P. W., Smith, J. H., Jr., and Ziurys, E. J., *Fundamentals of Internal Combustion Engines*, 4th Edition, U.S. Naval Institute, 1959. With permission.

The first stage of heat release, or *ignition delay*, is a time of charge preparation during which injected liquid fuel is atomized, mixed, and dispersed within hot compressed air. This delay period involves liquid fuel vaporization and a chemical kinetics stage during which fuel pyrolysis reactions begin. During this portion of the overall burn, there is a time of accumulation of unburned fuel and apparent inactivity within the cylinder. Several factors can influence the length of this induction and delay period, which occurs prior to ignition and rapid pressure rise, including:

Compression ratio
Inlet air temperature
Coolant temperature
Piston speed
Injection pressure
Fuel droplet size
Fuel injection rate
Fuel latent heat of vaporization
Fuel cetane number

Increasing the compression ratio will raise the initial charge reaction air temperature, i.e., molecular collisions, and chemical kinetic rates at TDC and shorten the delay. Increasing inlet air temperature for a specified compression ratio may also shorten this delay. Higher coolant temperatures may imply less heat transfer loss to cylinder walls and allow higher charge air temperature and greater wall initiation reactions, resulting in a reduced ignition delay period. Engine speed affects combustion chamber turbulence and indirectly influences the delay period; i.e., a greater piston speed might produce greater turbulence and, hence, shorten delay.

Injection pressure influences the size, velocity, and dispersion of fuel droplets and, in general, higher injection pressures should shorten delay. Fuel droplet size will influence delay; i.e., larger droplets will result in longer delays, while small droplets may have insignificant momentum to provide proper fuel dispersion. Fuel injection rate is also a factor in delay since initial injection occurs in a high-oxygen environment with low reaction rates, whereas at the end of fuel injection, there is a lower-oxygen environment but higher temperatures and reaction rates.

Ignition delay can also be a function of such fuel properties as fuel molecular structure, volatility, and latent heat of vaporization. Cracked hydrocarbon and ring compounds tend to have long delay periods, while straight-run, single-bonded paraffin hydrocarbon chains have short delay periods. Fuel additives such as ethyl nitrate and thionitrate can shorten this delay period.

When sufficient droplets of fuel have vaporized, reached their self-ignition temperature, and undergone pyrolysis, the second stage of combustion begins. Oxidation chemical kinetics is dominated by diffusion flame physics. A sheath of vaporized fuel surrounds atomized droplets, which burn with oxygen from the compressed air diffusing into the vapor layer. This portion of rapid burn increases cylinder temperature and pressure and further accelerates evaporation, ignition, and heat release from the continuing fuel injection process. This second stage of burn is usually designed so that peak cylinder pressure occurs near TDC. The audible sound of CI diesel engine combustion also occurs during this second stage of combustion.

Peak pressure is a function of delay since, in general, the longer a delay, the greater the peak pressure. For an ideal short ignition delay, fuel vaporization is instantaneous, little fuel is accumulated, and major oxidation chemistry consists of degenerate chain-branching reactions. For a long ignition delay, fuel accumulation is severe, a fuel-rich mixture exists, and chemistry consists of chain-branching explosions. It is the long ignition delay and accumulation of unburned fuel that can result in detonation or knock in a diesel engine. Diesel knock can occur at the *beginning of the rapid combustion period* and therefore differs from SI knock, which occurs at the end of combustion.

Autoignition and detonation oxidation chemistry is common to both SI and CI engine combustion. Spark knock is undesirable, but it is the autoignition nature of a diesel fuel that is essential for its proper ignition. Compression-ignition knock can be minimized by early ignition and rapid burning of injected fuel, reducing the amount of accumulated fuel that would be involved in autocatalytic autoignition during the period of rapid pressure rise. A fuel with high volatility and low autoignition temperature will help minimize CI engine knock.

The third and final stage of CI combustion occurs toward the end of fuel injection. Reaction is not completed at TDC, continuing past the peak pressure point but at a lower rate during piston expansion. Cylinder pressure during expansion will be slightly greater than that for a nonreactive adiabatic expansion and will depend on fuel injection advance and cutoff. At the end of fuel injection, the last portion of fuel spray may not completely evaporate, and lower-temperature chemistry will produce a free carbon luminous flame that increases radiation heat transfer losses.

EXAMPLE 11.3 The indicated engine performance of a two-stroke, six-cylinder 4-in. × 4-in. diesel is to be modeled using an air standard cycle analysis. The engine operates at 1400 rpm, and a blower supplies 100% scavenging air at engine inlet conditions of 70°F and 14.7 psi. The heating value of the fuel is 18,500 Btu/lbm, and the overall mass *AF* ratio is 15:1. For a compression ratio of 14:1, calculate: (a) the cycle peak temperature and pressure; (b) the ideal indicated mean effective pressure, psi; (c) the indicated thermal efficiency, %; (d) the ideal indicated engine power, ihp; and (e) the indicated specific fuel consumption, lbm/ihp hr.

Solution:

1. State 1:

$$P_1 = 14.7 \text{ psia}$$

$$T_1 = 530°\text{R}$$

$$V_D = \frac{\pi}{4}\left(\frac{4}{12}\text{ ft}\right)^2\left(\frac{4}{12}\text{ ft}\right) = 0.02909 \text{ ft}^3/\text{stroke}$$

$$V_c = \frac{\pi}{4}\left(\frac{4}{12}\right)^2\left(\frac{4}{12}\right)\left(\frac{1}{13}\right) = 0.00224 \text{ ft}^3/\text{stroke}$$

$$V_1 = V_D + V_c = 0.02909 + 0.00224 = 0.03133$$

$$M_1 = \frac{P_1V_1}{RT_1} = \frac{(14.7 \text{ lbf/in.}^2)(144 \text{ in.}^2/\text{ft}^2)(0.03133 \text{ ft}^3)}{(53.34 \text{ ft}\cdot\text{lbf/lbm°R})(530°\text{R})} = 0.002346 \text{ lbm}$$

$$v_1 = \frac{V_1}{M_1} = \frac{0.03133}{0.002346} = 13.3546 \text{ ft}^3/\text{lbm}$$

2. Process 1–2, $s = c$ compression:

Compression ratio:

$$r_v = \frac{V_1}{V_2} = \frac{0.03133}{0.00224} = 14.0$$

or

$$V_2 = V_c = 0.00224 \text{ ft}^3$$

$$v_2 = \frac{0.00224}{0.002346} = 0.9548 \text{ ft}^3/\text{lbm}$$

$$P_2 = \left(\frac{V_1}{V_2}\right)^{\gamma} P_1 = \left(\frac{0.03133}{0.00224}\right)^{1.4} (14.7)$$

a. $P_2 = 590.6$ psi

$$T_2 = \left(\frac{V_1}{V_2}\right)^{\gamma-1} T_1 = \left(\frac{0.03133}{0.00224}\right)^{0.4} (530°\text{R}) = 1{,}522.5°\text{R}$$

Work of compression:

$$\delta Q - \delta W = dU = MC_v dT$$

$$_1W_2 = MC_v(T_1 - T_2)$$

$$= (0.002346 \text{ lbm})(0.171 \text{ Btu/lbm°R})(530 - 1522.5°\text{R})$$

$$= -0.400 \text{ Btu}$$

3. Process 2–3, $P = c$ heat addition:

$$_2Q_3 = \frac{HV\langle\text{Btu/lbm fuel}\rangle M\langle\text{lbm air}\rangle}{AF\langle\text{lbm air/lbm fuel}\rangle}$$

$$= \frac{(18{,}500)(0.002346)}{(15)} = 2.893 \text{ Btu}$$

$$\delta Q - \delta W = \delta Q - PdV = dU$$

$$\delta Q = dH$$

$$_2Q_3 = MC_p(T_3 - T_2)$$

b. $$T_3 = 1{,}522.5 + \frac{2.893}{(0.240)(0.002346)} = 6{,}661°\text{R}$$

$$P_3 = P_2 = 590.6 \text{ psi}$$

$$V_3 = \frac{MRT_3}{P_3} = \frac{(0.002346)(53.34)(6{,}661)}{(590.6)(144)} = 0.00980 \text{ ft}^3$$

$$v_3 = \frac{0.00980}{0.002346} = 4.1773 \text{ ft}^3/\text{lbm}$$
$${}_2W_3 = PdV = P_3(V_3 - V_2) = (590)(144)(0.0098 - 0.0022)/778 = 0.831 \text{ Btu}$$

4. Process 3–4, $s = c$ expansion:

$$V_4 = V_1 = 0.03133 \text{ ft}^3$$
$$v_4 = v_1 = 13.3546 \text{ ft}^3/\text{lbm}$$
$$T_4 = \left(\frac{V_3}{V_4}\right)^{\gamma-1} T_3 = \left(\frac{0.009780}{0.03133}\right)^{0.4} (6{,}661) = 4{,}184.5$$
$${}_3W_4 = MC_v(T_3 - T_4) = (0.002346)(0.171)(6{,}661 - 4{,}185) = 0.993 \text{ Btu}$$

5. Process 4–1, assuming that $f = 1.0$ (100% scavenging air):

$${}_4Q_1 = MC_v(T_1 - T_4)$$
$$= (0.002346)(0.171)(530 - 4185) = -1.466 \text{ Btu}$$

6. Cycle performance (per cylinder):

$$W_{\text{net}} = {}_1W_2 + {}_2W_3 + {}_3W_4 + {}_4W_1 = -0.400 + 0.831 + 0.993 = 1.424 \text{ Btu}$$
$$Q_{\text{net}} = {}_1Q_2 + {}_2Q_3 + {}_3Q_4 + {}_4Q_1 = 2.893 - 1.466 = 1.427 \text{ Btu}$$

Mean effective pressure:

$$\overline{P} = \frac{W_{\text{net}}}{V_D} = \frac{(1.427 \text{ Btu})(778 \text{ ft}\cdot\text{lbf/Btu})}{0.02909 \text{ ft}^3)(144 \text{ in.}^2/\text{ft}^2)}$$

c. $IMEP = 265$ psi

Thermal efficiency:

$$\eta = \frac{\text{desired energy output}}{\text{required energy output}} = \frac{W_{\text{net}}}{Q_{\text{add}}}$$
$$= 1 + \frac{{}_4Q_1}{{}_2Q_3} = 1 - \frac{1.466}{2.893} = 0.493$$
$$\eta = 49.3\%$$

7. Indicated engine performance:

Indicated power:

$$\dot{W}_1 = \frac{\overline{P}\langle \text{lbf/ft}^2 \text{ stroke}\rangle L\langle\text{ft}\rangle A\langle\text{ft}^2\rangle N\langle\text{rev/min}\rangle C\langle\text{no. cylinders}\rangle}{(33{,}000 \text{ ft}\cdot\text{lbf/hp min})n\langle\text{rev/stroke}\rangle}$$
$$= \frac{(265)(144)(4/12)(\pi/4)(4/12)^2(1{,}400)(6)}{(33{,}000)(1)} = 282.55 \text{ ihp}$$

Indicated specific fuel consumption:

$$\dot{M}_{\text{fuel}} = \frac{M\langle \text{lbm air/stroke}\rangle N\langle \text{rev/min}\rangle C\langle \text{no. cylinders}\rangle}{AF\langle \text{lbm air/lbm fuel}\rangle n\langle \text{rev/stroke}\rangle}$$

$$\dot{M}_{\text{fuel}} = \frac{(0.002346)(1{,}400)(6)}{(14)(1)} = 1.407 \text{lbm fuel/min}$$

Indicated specific fuel consumption:

$$ISFC = \frac{\dot{M}_{\text{fuel}}(\text{lbm/min})}{\dot{W}_I(\text{hp})} = \frac{1.407}{282.55}$$

$$= 0.00498 \text{ lbm/hp} \cdot \text{min} = 0.299 \text{ lbm/hp} \cdot \text{hr}$$

Design requirements for diesel combustors are similar to many of the design objectives set for SI configurations, as discussed in Chapter 10.

Development of turbulence within the charge
Promoting a rapid but smooth rise in pressure versus time (crank angle) during burn
Achieving peak cylinder pressure as close to TDC as possible
Reducing the occurrence of detonation or knock
Promoting complete combustion
Minimizing heat loss

Several illustrative chamber geometries that have been developed in an effort to achieve proper CI combustion are shown in Figure 11.6. These CI combustion chambers may be classified as either *direct-injection* (*open-chamber*) or *divided-chamber* (*indirect-injection*) CI geometries. Particular power applications will dictate which of these CI combustion chambers is more suitable for use. In automotive applications, where a high power-to-weight requirement exists, for example, a high-speed divided-chamber engine is usually needed, whereas in marine and industrial power applications, where weight and size are less critical than fuel economy, large slow-speed open-chamber engines are more often used.

The *open* combustion *chamber* uses space above the piston crown and head for combustion control. Fuel injected directly into this single-chamber combustor requires a high-pressure injection process to ensure proper atomization and penetration of fuel spray throughout the chamber volume. Air motion is relatively nonturbulent, so that intake valve location and piston crown geometries are varied in an attempt to introduce motion and air rotation within a chamber. Chamber geometry is frequently shaped to conform to the fuel spray pattern, with a fuel injector generally positioned close to the piston centerline. Open combustion chamber geometry may have less influence on combustion than air motion. A squish, or reduced area, configuration allows the volume between piston crown and clearance volume at the edge of a piston when at TDC to be quite small. This geometry is an attempt to cause an increased inward motion of a charge at the end of the compression stroke. An open-chamber CI engine requires considerable excess air but, in general, is easy to start. Smaller surface-to-volume ratios for an open chamber result in a lower heat loss than for other geometries. This design is utilized most often in large, low-speed diesel engines that burn diesel fuels having longer ignition delays, i.e., lower

cetane numbers. Open-chamber CI engines generally require compression ratios in a range 12:1–16:1 and have better fuel consumption, higher pressure rise, and less throttling losses of all the CI chambers. High-speed open-chamber CI engines have a tendency to develop diesel knock.

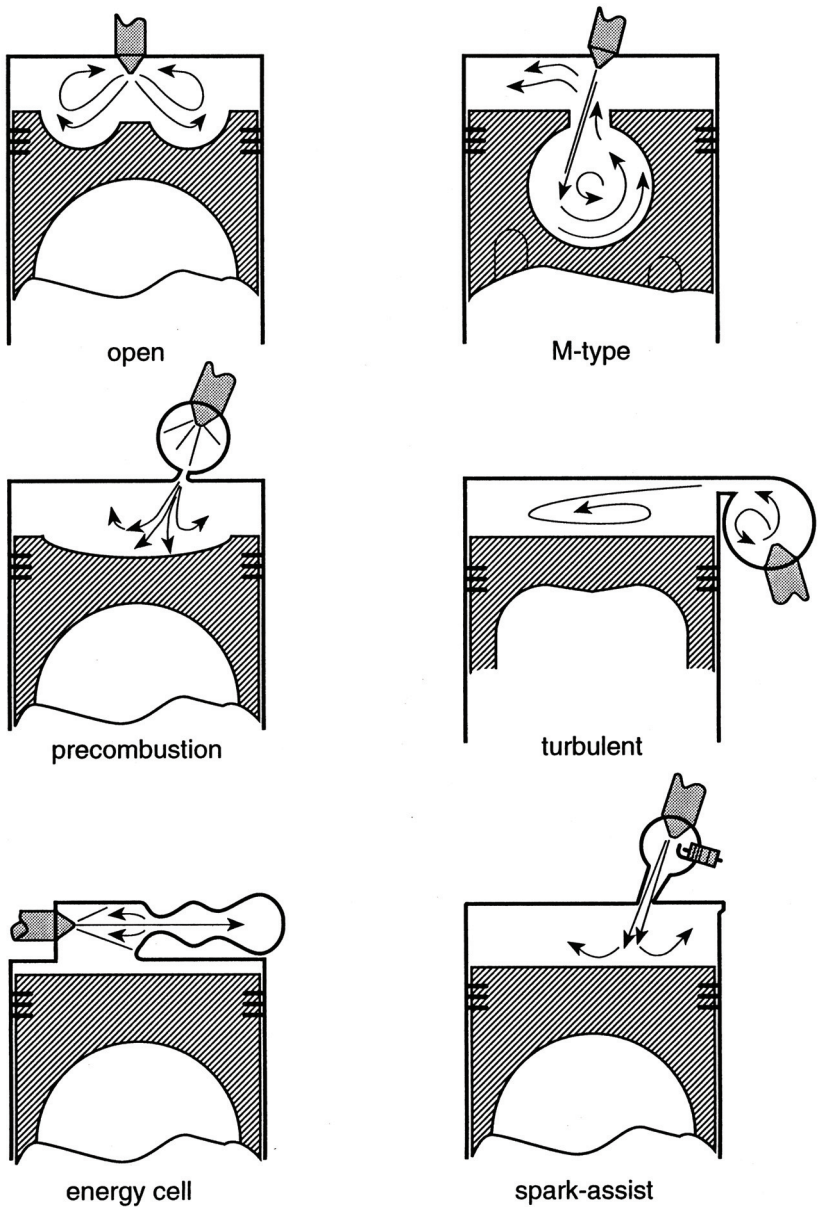

Figure 11.6 Various CI combustion chamber designs.

The *divided combustion chamber* diesel uses two-chamber combustion in an effort to circumvent problems encountered with open-chamber fuel injection designs. A variety of configurations and combustion methods have been developed, including precombustion chambers, swirl or turbulent chambers, and air or energy cell chambers. Divided chambers are most frequently used with small high-speed engine applications in an effort to help shorten the time needed for combustion. The additional chamber volume can be located in the piston crown, cylinder wall, or head. Secondary chamber volumes can be as much as 50% of clearance volume.

Precombustion-chamber CI engines are indirect injection configurations consisting of a main chamber and a separate fuel ignition volume. Air enters the main and prechamber volumes during a compression stroke, but fuel is injected only into the smaller uncooled prechamber. Deep fuel spray penetration is not necessary, allowing a lower injection pressure and shorter ignition delay. Initial ignition occurs in the prechamber and produces a relatively rich homogeneous and turbulent preconditioned charge with jet spray expansion of reactive gases through orifice openings into the main chamber for complete reaction. Prechamber designs do not depend on air motion within their secondary chamber to burn diesel fuels.

A *swirl*, or *turbulent chamber*, is another indirect injection divided-chamber design. Air enters both chambers during compression, and fuel is injected only into the secondary volume, much like the prechamber. However, significant air motion and turbulence are purposely generated within the swirl chamber during compression. Turbulent-chamber diesels reduce stringent fine spray injection atomization requirements needed for open chambers and allow larger fuel droplets to be burned. The boundary distinguishing a prechamber from a turbulent-chamber design is somewhat arbitrary, but, in general, prechamber volumes are relatively smaller and burn only a minor portion of the charge therein, whereas swirl-chamber volumes are larger, with a major portion of the burn occurring therein.

The *air*, or *energy, cell* is a divided combustion chamber configuration but, in this instance, fuel is injected into the main chamber. The air cell is located directly across from an injector, and fuel is sprayed across the main chamber and enters into an energy cell prior to ignition. This method offers benefits of both the open and turbulent geometries. Air-cell engines rely on their small antechamber and the ensuing air motion and charge interaction to reduce the injection pressure required for an open-chamber design. The piston motion during one mechanical cycle causes a turbulent flow to occur between the antechamber and main chamber. The rapid pressure rise and peak pressure in the figure-eight-shaped main is gas dynamically and thermally controlled by the energy cell. Burn in an air-cell engine occurs with slow initial combustion of injected fuel, followed by a rapid secondary burn resulting from flow jetting back into the main chamber during an expansion stroke. Since the energy cell is not cooled, the design regenerates a charge by returning some energy released by combustion to the charge at a later stage in the burn process. Energy-cell CI engines are generally characterized by larger heat losses to the wall, starting difficulties, and lower thermal efficiency but higher *IMEP*. Air- or energy-cell chambers are easier to start than the swirl or turbulent chamber since fuel is injected into the main chamber.

Divided-chamber combustors have larger surface-to-volume ratios, more fluid motion, greater heat transfer coefficients, and, therefore, higher heat loss and lower charge temperatures relative to comparable open-chamber geometries. Indirect injection CI engines usually require compression ratios of 18:1–24:1 to ensure reliable ignition, but they are often smoother-running engines. Additional general characteristics of a divided-

chamber indirect injection CI engine include higher volumetric efficiency, lower peak pressure, lower *IMEP*, lower thermal efficiency, and higher specific fuel consumption. Two-chamber CI configurations are not as compatible with two-stroke or large-displacement volume diesels.

Compression-ignition combustion is slower than SI combustion, which means that maximum engine speeds are lower for diesel engines. Power output, therefore, cannot be raised by increasing engine speed, so that CI engine output is usually increased by turbocharging, a technique that can also produce improvements in fuel economy. Turbocharging may mean that a reduction in compression ratio is required in order to maintain the peak pressure and temperature of the basic engine design. In particular, two-stroke diesel engine designs are often turbocharged.

The higher thermal efficiency and greater fuel economy of diesel engines compared to SI engines are chiefly a result of the higher compression ratios required for diesels. To a lesser degree, diesel performance gains are due to the simplicity of the autoignition process, lower pumping losses as a result of removing the throttle valve, and overall lean *AF* mixtures required for combustion. Diesel engines also have the advantage of being able to maintain a higher sustained torque than a spark-ignition engine.

Diesel engines control load by simply regulating the amount of fuel injected into the combustion air. This approach eliminates throttling as required for SI engine power control. Because of the very localized fuel-rich nature of CI heat release, an engine operating at constant speed, and hence constant airflow rate, can meet a wide range of power demand by simply controlling the rate and amount of fuel injected. Overall rich or stoichiometric conditions are necessary for high power output. In this instance, the rich combustion and high carbon-to-hydrogen ratio of diesel fuels produce carbon atoms and generate black smoke, an objectionable pollutant. Idle engine operation means lower peak reaction temperatures, less air turbulence, incomplete combustion, and the formation of white smoke.

Several types of smoke can be identified with specific CI engine operating conditions. Cold-starting, idle, and low-load engine operation produce white smoke, liquid particulates consisting of unburned, partially burned, or cracked fuel with a small fraction of lubricating oil. Black-gray smoke occurs at maximum loads and rich combustion and consists chiefly of solid carbon particulates resulting from incomplete combustion. Carbon is opaque and will therefore yield black smoke, whereas liquid hydrocarbon droplets have high optical transmissions and, hence, make smoke appear grayer. The intensity of smoke generated by CI engines is influenced by fuel cetane number, injection rate, cutoff, and atomization. Particulate emissions may also include fuel additives and blue smoke, a common characteristic of lubricating oil aerosols. Smoke can be reduced by burning supplementary fuel additives, de-rating (reducing the maximum fuel flow), avoiding engine overload, afterburning the exhaust gases, and proper maintenance.

Variations in CI fuel composition, as specified by an ultimate analysis, will not affect the heat of combustion and heat release as much as it influences the formation of certain undesirable by-products. These by-products can severely impact the status and lifetime of diesel engine components. For example, carbon residue is a prime source of carbon deposits on diesel engine parts and is usually limited to less than 0.01%. Sulfur content in diesel fuels most frequently must be kept to 0.5–1.5% to limit the formation of corrosive combustion products. Ash and sediment, abrasive constituents of fuel mixtures, should be kept to 0.01–0.05% to protect injection systems and piston-cylinder wear. Ash tends to be concentrated when refining heavy residual fuel oil.

11.5 COMPRESSION-IGNITION I.C. ENGINE EMISSIONS

Diesel engine operation depends on a high compression ratio process to raise intake air above the self-ignition temperature of the fuel. Unfortunately, diesel engines run with excess oxygen (i.e., lean) and produce exhaust emissions including carbon monoxide, hydrocarbons HC, odor, particulate matter PM, smoke, sulfur dioxide SO_2, as well as nitrogen oxide NO and small amounts of nitrogen dioxide NO_2 — collectively known as NO_x. Diesel engines are substantial PM and NO_x emitters but discharge relatively small amounts of CO and hydrocarbons HC. Gasoline engines pollute in somewhat the opposite fashion, however, being the greater emitters of CO with modest amounts of PM while exhausting substantial HC and NO_x. Although the NO_x problem is a serious environmental issue for both gasoline and diesel engines, both PM and NO_x from diesel engine powered vehicles are required to meet increasingly tough emissions legislation by the U.S. Environmental Protection Agency and the California Air Resource Board (CARB). It is a matter of record that a large fraction of all NO_x emissions in the western United States come from heavy-duty diesel engines. The required NO_x characteristic of diesel engines is a major factor that impacts operation of future U.S. heavy diesel vehicles. Emission regulations and standards are set for various classes of diesel engines and vehicles at state and national levels; see Chapter 9.

Recall that carbon monoxide is due to insufficient oxygen for complete oxidation of carbon. Since diesel fuel combustion occurs in excess air environments, CO emissions are much lower for CI engines than SI engines.

Unburned hydrocarbons, UHCs are due to specific CI fuel-engine interface characteristics, including: (1) fuel injection, i.e., spray pattern, length of injection, and degree of atomization; (2) particular combustor geometry, i.e., shape of combustion chamber, fuel quenching from spray contacting the wall, and chamber burn pattern; and (3) combustion itself, i.e., fuel structure, locally rich mixture chemistry, and time available for burn. Diesel UHC emissions contain original, decomposed, and recombined diesel fuel constituents and, therefore, differ from those HC compounds generated by SI combustion of automotive fuels. Odor is a by-product of the incomplete burning of diesel fuels. Compression-ignition engine chemistry produces partially oxidized, as well as decomposed and recombined, fuel fractions. The hydrocarbon composition of diesel fuels promotes incomplete combustion, odor-producing, aromatic ring hydrocarbons and oxygenated aldehyde compounds such as formaldehyde.

Volatile organic compounds (VOCs) associated with diesel operation are located in unburned hydrocarbon tailpipe emissions as well as in vehicle evaporative fuel emissions. Due to the lower volatility of diesel fuel, CI engine powered vehicles have extremely low evaporative and cold-start emissions. The unburned hydrocarbon levels depend largely on load and speed of an engine, but with the high overall AF ratios of diesels, hydrocarbon emissions are generally lower than those of comparable SI engines. A portion of the hydrocarbon emissions can be reduced with the oxygen contained in the diesel engine's exhaust discharge by use of a noble-metal catalyst.

Particulate matter (PM) is a term used to identify solid particles and liquid droplets found in the atmosphere. PM can range from mixtures of "coarse" particles to collections of "fine" particles. Coarse PM are designated by EPA as PM_{10}, i.e. 10 microns (0.0004 inch) particles, and are predominantly noncombustion in origin, material including road dust, tire and brake wear debris, and pollen. Fine PM, designated as $PM_{2.5}$, are 2.5 microns (0.0001 inch) particles and result chiefly from a variety of internal and external fuel combustion sources. Particles with diameters of 0.1 micrometers (100 nanometers)

or less are referred to as "ultrafines," while "nanoparticles" have diameters of 50 nanometers or less. So called "secondary" fine particles are also formed in the atmosphere from gases such as sulfur dioxide, NO_x, and VOCs.

Diesel particulate matter is a complex mixture of solid and liquid materials generated within the engine cylinder during combustion consisting of dry carbon particles (i.e., soot), heavy hydrocarbons adsorbed and condensed on the carbon particles (referred to as soluble organic fraction), and a combination of several components of diesel exhaust including hydrated sulfuric acid. PM emissions size distribution is affected by both operating conditions and fuel parameters. Most of the particulate emissions from diesel engines are smaller than 2.5 microns.

Diesel engines in the past had been suspected of causing serious health effects simply because people could see and smell "smoky" exhaust from older diesel engines. Smoke, either a solid or liquid (aerosol) particulate suspended in an exhaust stream, is easily observed and contains certain diesel particulates that are in fact carcinogenic. Ultrafine particle PM emissions from modem diesel engines, however, are not visible but contain fine particulate matter. Control strategies, including incorporating catalytic filters, active traps, and soot afterburning, are but a few of the ongoing aftertreatment approaches being pursued to try to control diesel particulate.

EXAMPLE 11.4 Steady-state operation of a diesel engine test produces the following experimental data:

Engine inlet air temperature	250°C
Fuel inlet temperature	27°C
Exhaust gas temperature	800K
Engine indicated thermal efficiency	58%
Exhaust gas composition, ppm	
CO_2	62,279
CO	14,013
UHC	1,557
H_2	9,861
O_2	28,609
N_2	647,437
H_2O	71,361
NO_x	164,883

Diesel fuel is *n*-dodecane, and the UHC can be assumed to be equivalent to CH_4 and the NO_x equivalent to N_2O. For these conditions, find: (a) the equivalence ratio for the overall fuel-air chemistry; (b) the indicated work, kJ/kg fuel; (c) the overall heat loss as a percent of indicated work, %; and (d) the indicated specific fuel consumption, g/W·hr.

Solution:

1. Stoichiometric equation:

$$C_{12}H_{26} + 18.5[O_2 + 3.76N_2] \rightarrow 12CO_2 + 13H_2O + 69.56N_2$$

$$\overline{AF}_{\text{stoic}} = (18.5)(4.76)/1 = 88.06$$

2. Actual reaction:

$$aC_{12}H_{26} + b[O_2 + 3.76N_2] \rightarrow 62{,}279CO_2 + 14{,}013CO + 1557CH_4 + 9861H_2 + 28{,}609O_2 + 647{,}437N_2 + 71{,}361H_2O + 164{,}883N_2O$$

Carbon balance:

$$12a = 62{,}279 + 14{,}013 + 1557 \qquad a = 6487.4$$

Nitrogen balance:

$$3.76b = 647{,}437 + 164{,}883 \qquad b = 216{,}043$$

$$\overline{AF}_{\text{act}} = 216{,}043 \times \left[\frac{4.76}{6487.4}\right] = 158.52$$

3. Equivalence ratio Φ:

a. $$\Phi = \frac{\overline{AF}_{\text{stoic}}}{\overline{AF}_{\text{act}}} = \frac{88.06}{158.5} = 0.556$$

$$C_{12}H_{26} + (1.8)(18.5)[O_2 + 3.76N_2] \rightarrow 9.6CO_2 + 2.16CO + 0.24CH_4 + 1.52H_2 + 4.41O_2 + 99.8N_2 + 11H_2O + 25.4N_2O$$

4. Energy balance:

$$\bar{q} - \bar{w} = \Sigma N_i \bar{h}_i - \Sigma N_j \bar{h}_j$$

$$\bar{q} - \bar{w} = \{9.6[\bar{h}_f^0 + \Delta\bar{h}\langle 800\rangle]_{CO_2} + 2.16[\bar{h}_f^0 + \Delta\bar{h}\langle 800\rangle]_{CO} + 0.24[\bar{h}_f^0 + \Delta\bar{h}\langle 800\rangle]_{CH_4} + 1.52[\bar{h}_f^0 + \Delta\bar{h}\langle 800\rangle]_{H_2} + 4.41[\bar{h}_f^0 + \Delta\bar{h}\langle 800\rangle]_{O_2} + 99.8[\bar{h}_f^0 + \Delta\bar{h}\langle 800\rangle]_{N_2} + 11[\bar{h}_f^0 + \Delta\bar{h}\langle 800\rangle]_{H_2O_g} + 25.4[\bar{h}_f^0 + \Delta\bar{h}\langle 800\rangle]_{N_2O}\} - \{33.3[\bar{h}_f^0 + \Delta\bar{h}\langle 298\rangle]_{O_2} + (33.3)(3.76)[\bar{h}_f^0 + \Delta\bar{h}\langle 298\rangle]_{N_2} + [\bar{h}_f^0 + \Delta\bar{h}\langle 800\rangle]_{C_{12}H_{26}}\}$$

$$\bar{q} - \bar{w} = 9.6[-94{,}054 + 5453]_{CO_2} + 2.16[-26{,}417 + 3627]_{CO} + 0.24[-17{,}895 + 5897]_{CH_4} + 1.52[0 + 3514]_{H_2} + 4.41[0 + 3786]_{O_2} + 99.8[0 + 3596]_{N_2} + 11[-57{,}798 + 4300]_{H_2O_g} + 25.4[19{,}610 + 5589]_{N_2O} - [-71{,}014 + 126]_{C_{12}H_{26}} = -399{,}293$$

5. Thermal efficiency:

$$\eta = \frac{\bar{w}\langle \text{cal/gmole fuel}\rangle}{LHV\langle \text{cal/gmole fuel}\rangle} = 0.58$$

where

$$LHV\langle \text{cal/gmole}\rangle = HHV - \bar{n}\left\langle \frac{\text{mole } H_2O}{\text{mole fuel}}\right\rangle h_{fg}\langle \text{cal/gmole}\rangle$$

$$LHV = 1{,}931{,}360 \text{ cal/gmole fuel} - \left\{ \frac{\left(\frac{18 \text{ g } H_2O}{\text{gmole } H_2O}\right)\left(\frac{13 \text{ gmole } H_2O}{\text{gmole fuel}}\right)\left(\frac{1050 \text{ Btu}}{\text{lbm } H_2O}\right)\left(\frac{251.98 \text{ cal}}{\text{Btu}}\right)}{(453.6 \text{ g/lbm})} \right\}$$

$$LHV = -1{,}794{,}871 \text{ cal/gmole fuel}$$

and

$$\overline{w} = (0.58)(1{,}794{,}871) = 1{,}041{,}025 \text{ cal/gmole}$$

$$w = (1{,}041{,}025)(4.187 \text{ kJ/kgmole fuel})/(170 \text{ kg/kgmole fuel})$$

b. $w = 25{,}640 = 25{,}640$ kJ/kg fuel

6. Heat loss:

$$\overline{q} - \overline{w} = -399{,}293 \text{ cal/gmole fuel}$$

$$\overline{q} = -399{,}293 + 1{,}041{,}025 = 641{,}732 \text{ cal/gmole}$$

c. $$\% \text{ work} = (q/w) \times 100 = \left[\frac{641{,}732}{1{,}041{,}025}\right] \times 100 = 61.6\%$$

7. Indicated specific fuel consumption:

$$ISFC = \frac{\dot{m}_{\text{fuel}}}{\dot{W}} = \frac{\dot{m}_{\text{fuel}}}{\dot{m}_{\text{fuel}} \eta LHV} = \frac{1}{\eta LHV}$$

$$ISFC = \frac{(170 \text{ g/gmole fuel})(860 \text{ cal/W} \cdot \text{hr})}{(0.58)(1{,}794{,}871 \text{ cal/gmole})}$$

d. $ISFC = 0.140$ g/W · hr

Diesel engines additionally produce unacceptably high levels of NO_x at high speeds and loads. Oxides of nitrogen (NO_x) are a result of excess air and high-compression ratio operation of modern CI engines. The production of NO_x by engine combustion is thus dependent to a large degree on the following three factors:

Post-combustion gas temperatures
Duration of these temperatures
Species in post-combustion gases, with O_2 being most critical

The diesel industry has been attempting to integrate an effective way to reduce NO_x emissions into the diesel infrastructure for many years. Presently only two routes have been identified with potential for commercial success: select catalytic reduction (SCR) and exhaust gas recirculation (EGR). SCR requires significant harsh aggressive chemicals to be introduced on board the vehicle as well as at the fueling stations.

Any reduction in peak temperature or excess air helps to reduce NO_x emissions. In EGR, the exhaust gas from the engine is recycled to the engine intake thereby lowering

the oxygen level and ensuing engine temperature which reduces NO_x emissions. EGR is used in both SI and CI engines as a means of reducing NO_x. EGR provides a dilution mechanism to reduce the first and third production factors cited above. NO_x reductions also are influenced by other factors such as EGR recirculation rate, temperature, and water content, as well as injection timing, and overall air-fuel ratio of the intake charge.

Two major problems with EGR are: (1) recirculation of dirty soot back to the engine and (2) higher engine gas temperature from EGR. Even though EGR has been successful in spark engines, recirculating dirty/corrosive diesel exhaust material with its wear-related problems reduces internal component life and, therefore, compromises diesel engine integrity. EGR puts a significant additional heat load on the engine and introduces the need for heat exchangers to cool the gas. More NO_x production occurs unless cooling is provided for EGR, which introduces ancillary heat exchanger equipment and a pump to circulate cooling water. In addition, even though EGR is effective in reducing NO_x, there are limits to the amount of exhaust gas that can be reintroduced into an engine before power output and fuel economy are adversely affected.

Neither of these approaches, SCR nor EGR, has been seen by the diesel industry as being completely satisfactory, and the industry, therefore, has been slow to embrace either technique as a final solution. In addition, three-way catalysts, used to reduce SI engine NO_x emissions, require stoichiometric or oxygen-deficient exhaust gas compositions in order to work and therefore will not work in oxygen concentrations of diesel engine exhausts.

Sulfur present in diesel fuel will form sulfur oxides, or SO_x during combustion, or

$$S + aO_2 \rightarrow bSO_2 + cSO_3$$

The SO_x concentration in the exhaust depends on the sulfur content of the fuel. Sulfur dioxide is a colorless toxic gas with a characteristic foul odor. Recall from Chapter 6 that sulfur oxides are also major contributors to acid rain.

$$SO_x + aH_2O \rightarrow bH_2SO_4 + cH_2SO_3$$

Significant sulfur emissions reduction from most diesel engines operating throughout the U.S could result from switching to utilization of low sulfur diesel fuels (i.e., less than 0.05% sulfur).

A variety of fuel-engine interface techniques for controlling overall emissions from diesel engines are actively being pursued and include paying attention to the

Combustion chamber design
Fuel injector design
Fuel composition, including additives
Fuel/air ratio
Engine selection
Engine operation conditions

In order to meet all the targeted emissions requirements for current and projected on- and off-road diesel-powered vehicles, it will be a challenge to develop control technologies and/or control system architectures that do not interfere with power and associated fuel economies. Reducing the discharge of emissions from a diesel without de-rating performance will continue to be a goal for the diesel engine designer and manufacturer. Advancements will require more than simply selecting engine types and/or

components, using alternative fuels and additives, or discovering the magic exhaust aftertreatment technique. The Department of Energy/Office of Heavy Vehicle Technologies, for instance, is collaborating currently with industrial partners to achieve very low emissions in heavy trucks. A three-pronged systematic approach is being employed that simultaneously addresses (1) fuel formulation/quality, (2) in-cylinder combustion control, and (3) exhaust treatment to arrive at the most cost-effective emission strategy without sacrificing efficiency.

The complex environmental challenge facing the diesel engine designer is best illustrated by describing an in-cylinder combustion control for keeping both NO_x and PM emissions within their specified regulated limit. Any effort that increases combustion efficiency leads to higher combustion temperatures will reduce PM and, thus, unfortunately higher NO_x emissions. On the other hand, trying to reduce NO_x formation by lowering combustion temperature leads to higher PM emissions. In-cylinder NO_x and PM control characteristics are unfortunately linked by the diesel combustion process. As in-cylinder peak bulk gas temperature is increased, more NO_x is produced but the diffusion flame temperature necessary for PM burnout is also increased, resulting in more oxidized soot and less PM emission. Decreasing peak bulk gas temperature will decrease both NO_x and PM. Adjusting injection to control optimum peak bulk gas temperature by retarding timing results in a tradeoff that affects NO_x, particulate, and power.

11.6 COMPRESSION-IGNITION ENGINE FUEL ALTERNATIVES

Diesel fuels for commercial usage are graded by the American Society for Testing Materials: grade 1-D is a volatile fuel for use in engines that experience frequent speed and load changes; grade 2-D is a low-volatility fuel for use in large mobile and industrial engine applications; and grade 4-D is a fuel oil for low- and medium-speed engines. Special diesel fuels are also available for railroad, bus, marine, and military CI machinery; see Table 11.2. High-speed diesels can burn a gas fuel known as straight-run gas oil, a crude oil fraction that comes directly from the distillation column. Declining quality of crude oil, increased demand for diesel fuel, and greater use of blended distillate fuels containing greater amounts of cracked components have contributed to a lowering of the average cetane number of diesel fuels. Cetane values began declining from their mid-1950 values during the 1960s and are projected to reach values in the 1940s by the twenty-first century. One possible technique for burning low-cetane fuels is to use a *bifue*l engine, a CI engine having dual liquid fuel injection, i.e., a secondary or auxiliary fuel injected separately during the compression stroke and primary fuel injected later near TDC.

Diesel engines have been run on a variety of solid, liquid, and gaseous fuels. By the early 1900s, CI engines had been designed to burn coal dust and even gunpowder. Gasoline also has been used as a CI engine fuel; however, high-octane SI fuels are low-cetane CI fuels, and CI combustion of gasoline results in noisy and rough engine operation. In addition, gasoline, with its lower viscosity, causes wear and seizure of diesel injection pumps. Operation can be improved by using 10–15% diesel fuel/90–85% gasoline blends. Most CI fuel alternatives have been burned in large, slow-speed machines, while their use in intermediate- and high-speed units has not yet proved to be as successful.

Large diesel engines are available that burn natural or synthetic gas as well as fuel oil. Gas fuel engines can operate as a standard CI machine in which compressed gas is injected into hot compressed air. Methane, a gas fuel with a critical compression ratio for autoignition of approximately 12.5:1 measured using a CFR engine, can be used as a spark-ignition engine fuel. These types of gas-fueled SI engines are sometimes grouped with CI engines simply because of their "high" SI compression ratio. Dual-fuel engines compress gas-air mixtures but require a small fraction of injected fuel oil near TDC as a pilot ignition source. Gas diesel combustion is characterized by a lower maximum pressure and slower rate of pressure rise versus crank angle.

Nonpetroleum CI fuels derived from coal, shale, tar sands, and vegetable oils have had limited application, chiefly as a research and development fuel, and will require further fuel-engine interface engineering before they see commercial application as diesel fuels. Water injection in CI combustion has been utilized as a means of controlling peak temperature and NO_x emissions, although some argue that spraying water droplets into the combustion volume can provide additional energetics for the ignition process. Other exotic CI fuel concepts have included pulverized coal-oil and oil-water mixtures.

Alcohol fuels have seen little commercial use in CI engines, chiefly because of their high self-ignition temperatures and low cetane numbers. In addition, alcohols would require extremely high compression ratios to achieve autoignition using conventional CI engines. Alcohols also present potential lubrication problems but show promise of emissions reduction when used with suitable CI combustion systems.

EXAMPLE 11.5 A ten-cylinder, two-stroke low-speed marine diesel operates at a continuous speed of 130 rpm while burning a stoichiometric mixture of liquid dodecane and air. The 30-in. × 55-in. engine has a 13:1 compression ratio with conditions at BDC after air intake of 17.5 psi and 80°F. Fuel is injected at TDC at a temperature of 125°F. Based on the fuel-air Diesel cycle and JANAF data for the engine thermochemistry, determine (a) the ideal indicated net work, ft·lbf; (b) the ideal indicated mean effective pressure, psi; (c) the ideal indicated thermal efficiency; and (d) the ideal indicated specific fuel consumption, lbm/hp hr.

Solution:

1. Engine geometry:

$$V_{\text{displacement}} = \frac{\pi}{4}\left[\frac{30}{12}\text{ ft}\right]^2\left[\frac{55}{12}\text{ ft}\right] = 22.498\ \text{ft}^3$$

$$r_v = \frac{V_{\text{BDC}}}{V_{\text{TDC}}} = \frac{V_D + cV_D}{cV_D} = 13$$

$$c = 0.083333$$

$$V_{\text{TDC}} = (0.08333)(22.498) = 1.875\ \text{ft}^3$$

$$V_{\text{BDC}} = (1.08333)(22.498) = 24.373\ \text{ft}^3$$

2. Conditions at BDC state 1:

$$T_1 = 540°\text{R} = 300\text{K}$$

$$N_{\text{tot}} = \frac{P_1 V_1}{\bar{R} T_1} = \frac{(17.5 \text{ lbf/in.}^2)(144 \text{ in.}^2/\text{ft}^2)(24.373 \text{ ft}^3)}{(1{,}545 \text{ ft} \cdot \text{lbf/lbmole} \cdot °\text{R})(540°\text{R})}$$

$$= 0.0736 \text{ lbmole air/cyl}$$

with

$$U\langle T_1 \rangle = \sum_{i=1}^{N} \bar{x}_i N_{\text{tot}} [\bar{h}_f^0 + \Delta\bar{h}\langle T_1 \rangle - \bar{R} T_1]_i$$

At BDC, assume air only and, using JANAF data from Table B.24 Appendix B for air,

$$U_1\langle 300\text{K} \rangle = \{(0.0736 \text{ lbmole air/cyl})(1.8001)\} \times [0 + 35 - (1.987)(300)] \text{ Btu/lbmole}$$

$$U_1\langle 300\text{K} \rangle = -74.34 \text{ Btu/cyl}$$

3. Process 1–2, isentropic compression of air only:

$$\frac{V_2}{V_1} = \frac{V_r\langle T_2 \rangle}{V_r\langle T_1 \rangle} = \frac{1}{13}$$

Using the material from Example 3.2,

$$V_r\langle 300\text{K} \rangle = 18{,}020 \times 10^{10}$$

$$V_r\langle T_2 \rangle = \frac{18{,}020 \times 10^{10}}{13} = 1{,}386 \times 10^{10}$$

and

$$T_2 = 803\text{K} = 1{,}446°\text{R}$$

$$P_2 = \frac{N_{\text{tot}} \bar{R} T_2}{V_2} = \frac{(0.0736 \text{ lbmole/cyl})(1{,}545 \text{ ft} \cdot \text{lbf/lbmole°R})(1446°\text{R})}{(1.875 \text{ ft}^3)(144 \text{ in.}^2/\text{ft}^2)}$$

$$= 609 \text{ psi/cyl}$$

$$U\langle T_2 \rangle = \Sigma \bar{x}_i N_{\text{tot}} [\bar{h}_f^0 + \Delta\bar{h}\langle T_2 \rangle - \bar{R} T_2]_i$$

Using JANAF data from Table B.24 for air from Appendix B,

$$U\langle 803\text{K} \rangle = \{(0.0736 \text{ mole})(1.8001)\} \times [3{,}667 - (1.987)(803)] \text{ Btu/lbmole}$$

$$= 274.44 \text{ Btu/cyl}$$

4. Process 2–3, P = constant adiabatic flame:

Stoichiometric equation, assume complete combustion:

$$C_{12}H_{26} + 18.5[O_2 + 3.76N_2] \rightarrow 12CO_2 + 13H_2O + 69.56N_2$$

$$\delta Q - P\,dV = dU$$

$$\delta Q = dH = 0 \qquad H\langle T_3\rangle = H\langle T_2\rangle$$

$$H\langle T_3\rangle = \sum_{\text{prod}} N_i[\bar{h}_f^0 + \Delta\bar{h}]_i$$

$$H\langle T_2\rangle = \sum_{\text{react}} N_j[\bar{h}_f^0 + \Delta\bar{h}]_j$$

Using JANAF data for the reactants, including h_{f_g} of the fuel (Table 7.1),

$$H\langle T_2\rangle = \left\{\frac{(0.0736\ \text{lbmole air/cyl})}{(18.5)(4.76)\ \text{lbmole air/lbmole fuel}}\left[-85{,}370 + 53{,}194 + \frac{(110)(170.33)}{(1.8001)}\right] + (0.0736)(3{,}667)\right\}(1.8001)\ \text{Btu/lbmole} = 453\ \text{Btu/cyl}$$

and for the products,

$$453\frac{\text{Btu}}{\text{cyl}} = \left\{\left[\frac{12\ \text{lbmole}\,CO_2/\text{lbmole fuel})(0.0736\ \text{lbmole air/cyl})}{(18.5)(4.76)\ \text{lbmole air/lbmole fuel}}\right]\times [-94{,}054 + \Delta\bar{h}\langle T_3\rangle]_{CO_2} + \left[\frac{(13)(0.0736)}{(18.5)(4.76)}\right][-57{,}798 + \Delta\bar{h}\langle T_3\rangle]_{H_2O} + \left[\frac{(69.56)(0.0736)}{(18.5)(4.76)}\right][\Delta\bar{h}\langle T_3\rangle]_{N_2}\right\}(1.8001)$$

$$2{,}181{,}116 = (12\Delta\bar{h}\langle T_3\rangle)_{CO_3} + (13\Delta\bar{h}\langle T_3\rangle)_{H_2O} + (69.56\Delta\bar{h}\langle T_3\rangle)_{N_2}$$

By trial and error,

$$T_3 = 2{,}752\text{K} = 4{,}954°\text{R}$$

5. Conditions at 3, $P_3 = P_2 = 609$ psi:

$$V_3 = \frac{N_3\bar{R}T_3}{P_3}$$

$$V_3 = \frac{\left(0.0736\frac{\text{lbmole air}}{\text{cyl}}\right)\left(13 + 12 + 69.56\frac{\text{lbmole prod}}{\text{lbmole fuel}}\right)(1{,}545)(4{,}954)}{(18.5)(4.76\ \text{lbmole air/lbmole fuel})(609)(144)}$$

$$= 6.898\ \text{ft}^3$$

$$U_3 = H_3 - P_3V_3 = 382\ \text{Btu} - \frac{(609\ \text{lbf/in.}^2)(144\ \text{in.}^2/\text{ft}^2)(6.898\ \text{ft}^3)}{778\ \text{ft}\cdot\text{lbf/Btu}}$$

$$= -395.5\ \text{Btu/cyl}$$

6. Process 3–4, $s = c$ expansion of products:

$$P_r\langle T_3\rangle = \exp\left\{\frac{\Sigma \bar{x}_i \bar{s}^0\langle T_3\rangle}{\bar{R}}\right\}$$

$$= \exp\left\{\frac{(12/94.56)(78.566)+(13/94.56)(67.280)+(69.56/94.56)(63.001)}{1.987}\right\}$$

$$= 2.1395 \times 10^{14}$$

and

$$V_r\langle T_3\rangle = \frac{\bar{R}T_3}{P_r\langle T_3\rangle} = \frac{(1.987)(2{,}752)}{(2.1395 \times 10^{14})} = 2.556 \times 10^{-11}$$

but

$$\frac{V_r\langle T_4\rangle}{V_r\langle T_3\rangle} = \frac{V_1}{V_3} = \frac{24.373}{6.898} = 3.5333$$

$$V_r\langle T_4\rangle = (3.5333)(92.556 \times 10^{-11}) = 9.031 \times 10^{-11}$$

or

$$P_r\langle T_4\rangle = \frac{\bar{R}T_4}{V_r\langle T_4\rangle} = \frac{1.987\,T_4}{9.031 \times 10^{-11}}$$

where

$$P_r\langle T_4\rangle =$$

$$\exp\left\{\frac{(12/94.56)\bar{s}^0\langle T_4\rangle_{CO_2} + (13/94.56)\bar{s}^0\langle T_4\rangle_{H_2O} + (69.56/94.56)\bar{s}^0\langle T_4\rangle_{N_2}}{1.987}\right\}$$

By trial and error,

$T_4 = 2{,}000\text{K} = 3{,}600°\text{R}$

7. Conditions at 4:

$$V_4 = 24.3728 \text{ ft}^3$$

$$T_4 = 2{,}000\text{K} = 3{,}600°\text{R}$$

$$P_4 = \frac{(0.0736)(94.56)(1{,}545)(3{,}600)}{(18.5)(4.76)(144)(24.373)} = 125 \text{ psi}$$

$$U\langle T_4\rangle = \sum_{i=1} N_i[\bar{h}_f^0 + \Delta\bar{h}\langle T_4\rangle - \bar{R}T_4]_i$$

$$= \left[\frac{(0.0736)(1.8001)}{(18.5)(4.76)}\right] \times \{[(12)(-94{,}054 + 21{,}857 - (1.987)(2{,}000))]_{CO_2}$$
$$+ [(13)(-57{,}798 + 17{,}373 - (1.987)(2{,}000))]_{H_2O}$$
$$+ [(69.56)(+13{,}418 - (1.987)(2{,}000))]_{N_2}\}$$
$$= -1{,}255 \text{ Btu/cyl}$$

8. Ideal indicated work per cylinder:

$$W_{net} = {}_1W_2 + {}_2W_3 + {}_3W_4 + {}_4W_1$$

with process *i–j*,

$$\delta Q - \delta W = dU$$

or

$${}_1W_2 = U\langle T_1\rangle - U\langle T_2\rangle = -74.34 - 274.44 = -348.78 \text{ Btu/cyl}$$

and

$${}_2W_3 = P_3(V_3 - V_2) = (609)(144)(5.023)/778 = 566.19$$
$${}_3W_4 = U\langle T_3\rangle - U\langle T_4\rangle = -395.5 + 1{,}255 = 859.50 \text{ Btu/cyl}$$
$$W_{net} = -348.78 + 566.19 + 859.50 = 1{,}076.9 \text{ Btu/cyl}$$

a. $W_{net} = (1{,}076.9)(778) = 837{,}828 \text{ ft} \cdot \text{lbf/cyl}$

9. Ideal indicated mean effective pressure:

b. $$IMEP = \frac{W_{net}}{V_D} = \frac{837{,}828 \text{ ft} \cdot \text{lbf/cyl}}{(22.498 \text{ ft}^3)(144 \text{ in.}^2/\text{ft}^2)} = 259 \text{ psi/cyl}$$

10. Ideal indicated thermal efficiency:

$$\eta = \frac{W_{net}}{M_{fuel} HV}$$
$$= \frac{(1076.9 \text{ Btu/cyl})(18.5)(4.76 \text{ lbmole air/lbmole fuel})}{(1{,}931{,}360 \times 1.8001 \text{ Btu/lbmole fuel})(0.0736 \text{ lbmole air/cyl})}$$

c. $\eta = 0.370 = 37.0\%$

11. Ideal indicated engine power:

$$\dot{W}_I = \frac{\overline{P}LANc}{33{,}000n}$$
$$= \frac{(259 \text{ psi/cyl})(55/12 \text{ ft/stroke})(\pi/4)(30 \text{ in.})^2(130 \text{ rev/min})(10 \text{ cyl})}{(33{,}000 \text{ ft} \cdot \text{lbf/hp min})(1 \text{ rev/power stroke})}$$
$$= 33{,}055 \text{ ihp}$$

12. Ideal indicated specific fuel consumption:

$$\dot{M}_{\text{fuel}} = \left[\frac{(0.0736\ \text{lbmole air/cyl})(170\ \text{lbm/lbmole})}{(18.5)(4.76\ \text{lbmole air/lbmole fuel})}\right] \times \left[\left(130\frac{\text{rev}}{\text{min}}\right)\left(1\frac{\text{intake}}{\text{rev}}\right)(10\ \text{cyl})\right] = 184.7\frac{\text{lbm fuel}}{\text{min}}$$

$$ISFC = \frac{\dot{M}_{\text{fuel}}}{\dot{W}_I} = \frac{(184.7\ \text{lbm fuel/min})(60\ \text{min/hr})}{(33{,}055\ \text{hp})}$$

d. $= 0.335$ lbm/hp·hr

11.7 ADVANCED SPARK- AND COMPRESSION-IGNITION COMBUSTION CONCEPTS

Advances are being made today to improve the fuel-engine interface characteristics of modern internal combustion engines which are making the differences between SI and CI combustion characteristics less distinct. The constant-volume SI combustion originally envisioned by Otto and constant-temperature CI combustion of Diesel have matured into a number of overlapping combustion concepts, including stratified charge, two-chamber, and direct-chamber fuel-injected spark-ignited engines, as well as homogeneous charge and spark-assisted compression-ignited IC engines.

Many individuals and institutions in industry, government, and universities worldwide are presently directing their collective efforts and knowledge within a variety of fields of applied combustion to help advance IC engine energy conversion. These efforts in basic and directed research and development will help produce new generations of higher-efficiency IC engines having a wider tolerance to a variety of fuel alternatives and minimize the formation of critical pollutants.

Some are encouraged in their pursuit of the goal to develop a generic engine, i.e., one that would burn a wide range of portable fuels, thereby removing a demand on the oil refining industry to produce both SI and CI fuels from the same portion of a barrel of crude oil. Others are pursuing the feasibility of new engines running on nonpetroleum fuels. Improvements in conventional SI, CI, or new nontraditional engine concepts, such as hybrid IC engine configurations, require that engineers understand the rudiments of energy conversion principles of thermochemistry, fuel science, chemical kinetics, and air pollution that are at work in both SI and CI combustion. In addition, future engineering efforts to reduce engine heat loss, to better model engine heat transfer and gas dynamics, and to develop regenerative engine technologies will necessitate including more details of the chemical energy conversion physics.

New configurations are being introduced, such as the hybrid electric-IC engine drive train power system arrangements. Such a concept allows the efficient use of an IC engine, such as a diesel or spark-ignition engine running in a steady condition at its optimum operating point, in order to be matched to a generator configuration to run an electrical generator that is used to drive an electric motor(s) and/or battery, which, in turn, powers a set of wheels of a vehicle.

Chapters 10 and 11 have attempted to provide an overview of the essential fundamentals of applied combustion in SI and CI engines. There are many additional

engineering aspects of this subject that must be understood in the design, fabrication, operation, and maintenance of these machines, including charge preparation and induction systems, intake and exhaust manifold and valve mechanisms, turbochargers and superchargers, along with piston and engine block cooling and lubrication. These areas are but a portion of the complete topic associated with the subject of IC engine technology. The reader is encouraged to continue his or her learning by turning to the literature in these areas for further information.

PROBLEMS

11.1 Consider a CI thermodynamic cycle engine model consisting of the following idealized processes: 1–2 isentropic compression from BDC to TDC; 2–3 isothermal heat addition; 3–4 isentropic expansion to BDC; 4–1 isometric heat rejection at BDC. Using an air standard constant specific heat analysis, develop expressions for (a) net work per unit mass; (b) heat addition per unit mass; (c) *IMEP*; and (d) thermal efficiency as a function of compression ratio and cutoff ratio $r_L \equiv v_3/v_2$.

11.2 Repeat Example 11.1 for (a) a monatomic gas, $\gamma = 1.67$; (b) $\gamma = 1.3$; and (c) $\gamma = 1.2$.

11.3 Repeat Example 11.1 but, instead, solve for the specific work for the three values of γ.

11.4 Repeat Example 11.1 but, instead, solve for the heat rejection for the three values of γ.

11.5 Repeat Example 11.1, but solve for the thermal efficiency for the same constant-pressure heating ratio, $P_3/P_1 = 50$, and heat addition per unit mass, $q_H/C_vT_1 = 10$.

11.6 Diesel engine combustion is measured in terms of the cutoff ratio, $r_L = v_3/v_2$ (volume at the end of heat addition, or fuel injection, to that at the beginning of heat addition, or fuel injection). Show that the indicated thermal efficiency of the diesel cycle can be expressed as

$$\eta = 1 - \frac{1}{r_c^{\gamma-1}}\left[\frac{r_L^{\gamma} - 1}{k(r_L - 1)}\right]$$

11.7 Use Problem 11.6 to determine the effect of varying the cutoff ratio r_L on thermal efficiency for a given diesel cycle with a compression ratio of 18:1. Calculate the thermal efficiency for cutoff ratios of: (a) 1.5; (b) 2; (c) 4; and (d) 6.

11.8 Repeat Problem 11.7, but solve for compression ratios of: (a) 12:1; (b) 14:1; and (c) 16:1.

11.9 Using the results of Problems 11.6, determine the effect of varying the cutoff ratio r_L for the specific work of a given diesel cycle with a compression ratio of 18:1. Calculate the specific work for cutoff ratios of: (a) 1.5; (b) 2; (c) 4; and (d) 6.

11.10 Repeat Problem 11.9, but solve for compression ratios of: (a) 12:1; (b) 14:1; and (c) 16:1.

11.11 Consider the design of a CI engine that has a maximum design limit of 1700°C and 55 atm. If the compression ratio is to be maintained at 16:1 and if ambient

STP conditions are taken to approximate charge conditions at BDC prior to compression, calculate the following for cutoff ratios of 1.5, 3, and 6: (a) specific work ξ; (b) heat input; (c) temperature at the end of the constant-volume burn, K; and (d) thermal efficiency, %.

11.12 Several fuel alternatives for compression-ignition engine utilization are frequently suggested. Using Table 8.6 and assuming that the charge prior to compression is that of air at *STP*, estimate the critical compression ratios for: (a) semibituminous coal dust; (b) hydrogen; (c) methane; and (d) gasoline.

11.13 A limited-pressure diesel engine with a 16:1 compression ratio has a maximum pressure of 900 psi. The equivalent air-fuel ratio is 25:1, and the fuel has a lower heating value of 19,500 Btu/lbm. Intake temperature and pressure are 60°F and 29.92 in. Hg, respectively. Using an open system variable specific heat air standard analysis, calculate (a) the residual fraction; (b) temperature at BDC at the beginning of compression; and (c) thermal efficiency, %.

11.14 A four-stroke, eight-cylinder diesel engine connects directly to an AC generator developing 150 kW full-load generator output (generator efficiency is 91%). The 14-cm × 18-cm engine, running at 1200 rev/ min, uses a 35°API diesel fuel having an ultimate analysis of 84% carbon and 16% hydrogen. Dry exhaust gas analysis yields 9.593% CO_2 and 7.085% O_2. The full-load engine volumetric efficiency is 93%, with an air inlet temperature of 27°C, an exhaust gas temperature of 127°C, and a fuel temperature of 25°C. For these engine test data, find the following: (a) air mass flow rate, kg/hr; (b) brake *AF* ratio; (c) brake mean effective pressure, kPa; (d) brake specific fuel consumption, g/kW hr; and (e) brake thermal efficiency, %.

11.15 A four-stroke 4.75-in. × 6.5-in. diesel engine generates the following test data while running at 1,160 rpm:

Dynamometer load	120 lbf
Brake arm	1.75 ft
Fuel consumption	21 lbm/hr
Friction horsepower	57.3 lbf
Mass *AF* ratio	13.5:1
Fuel oil specific gravity	0.82 at 60°F
Ambient conditions	14.7 psi and 68°F

Using these data, determine the following: (a) heating value of the fuel, Btu/lbm; (b) engine *BHP*, *FHP*, and *IHP*; (c) engine mechanical efficiency, %; (d) brake specific fuel consumption, lbm/hp hr; (e) brake mean effective pressure, psia; (f) engine brake torque, ft·lbf; and (g) brake engine thermal efficiency, %.

11.16 A low-speed, two-stroke research diesel engine operating at full-load conditions burns a stoichiometric mixture of liquid methanol injected into air. The blower supplies 100% scavengine air at 100°F and 15 psi at the beginning of the compression stroke. The compressed air temperature required for compression ignition is 1,650°R. Using a variable specific heat air cycle analysis, calculate (a) ideal compression ratio; (b) peak pressure, psi; (c) peak temperature, °R; (d) net work, ft·lbf/lbm; and (e) thermal efficiency, %.

11.17 An eight-cylinder diesel engine burns #2 fuel oil and requires 200% theoretical air. The fuel, $\text{API}\langle 60°\text{F}\rangle = 32$, has an ultimate analysis of 86.4% carbon, 12.7% hydrogen, 0.4% sulfur, 0.3% oxygen, and 0.2% nitrogen. The engine is rated at a maximum brake power output of 5,220 bhp and a brake specific fuel consumption of 0.284 lbm/hp·hr. For these conditions, calculate: (a) mass *FA* ratio, lbm fuel/lbm air; (b) fuel density, lbm/ft^3; (c) fuel lower heating value, Btu/lbm; (d) fuel consumption, gal/hr; and (e) engine thermal efficiency, %.

11.18 A prototype diesel is designed to burn methanol. The conditions after compression of the air are given as 270 psi and 1,250°R. Constant-pressure combustion occurs after compression ignition of the fuel in air, causing the gas mixture temperature to be tripled. For this engine, assuming ambient *STP* conditions, determine: (a) compression ratio; (b) cutoff ratio; and (c) exhaust gas dew point temperature, °F. Assume overall complete combustion model using CH_3OH, in 45% excess air.

11.19 A four-cylinder, 12-in. × 25-in., single-acting four-cycle gas diesel engine operates at 225 rpm and is designed to burn a variety of gaseous fuels, including: natural, biomass, town, and coal gas fuels. The engine is found to have a 78% mechanical efficiency, a volumetric efficiency of 90%, and an indicated thermal efficiency of 30% when burning methane in 30% excess air. Assuming ambient conditions of *STP*, calculate (a) brake power output, hp; (b) fuel gas consumption, ft^3/hr; (c) *BMEP*, psi; and (d) volume of exhaust gas, assuming 840°F and 14.5 psi, ft^3/hr.

11.20 An expression for estimating the ignition delay in CI engines has been reported by Wolfer as

$$t\langle \text{msec} \rangle = \frac{0.44 \exp\{4{,}650 / T\langle \text{K} \rangle\}}{P\langle \text{atm} \rangle^{1.19}}$$

Using this relationship, estimate the ignition delay for a diesel having the following conditions at the beginning of injection: a cylinder pressure of 48 atm and charge temperature of (a) 500K; (b) 1,000K; (c) 1,500K; and (d) 2,000K.

11.21 Repeat Problem 11.20 for a charge temperature of 1,500K but a charge pressure of (a) 15 atm; (b) 25 atm; (c) 35 atm; and (d) 45 atm.

11.22 A two-stroke diesel engine burns 3.0 lbm/min of fuel. Assuming an ideal 5° crank angle period of constant fuel injection rate, estimate the time available, sec, and injection rate, lbm/°, for an engine speed of (a) 500 rpm; (b) 1,000 rpm; (c) 2,000 rpm; and (d) 4,000 rpm.

11.23 An open-chamber diesel engine of bore *D*, clearance *D*/10, and stroke 2*D* has a half-spherical volume of diameter *D*/2 centered in the face of the piston. For these conditions, determine: (a) the compression ratio; (b) the surface-to-volume ratio; and (c) the ratio of the bowl volume to the clearance volume. Calculate the required clearance in terms of *D* for an open chamber of bore *D* having the same compression ratio but without the bowl. Repeat parts (a), (b), and (c) for this geometry. (Assume that $D = 5$ in.)

11.24 A divided-chamber diesel engine of bore *D*, clearance *D*/10, and stroke 2*D* has a spherical prechamber of diameter *D*/4. For this geometry, determine the following: (a) compression ratio; (b) surface-to-volume ratio; and (c) ratio of the prechamber volume to the main chamber volume. Find the required clearance in

terms D for a simple open chamber of bore D having the same compression ratio but without the prechamber. Repeat parts (a), (b), and (c) for this configuration.

11.25 An eight-cylinder diesel engine burns #2 fuel oil and 200% theoretical air. The fuel, $\text{API}\langle 60 \rangle = 32$, has an ultimate analysis of 86.4% carbon, 12.7% hydrogen, 0.4% sulfur, 0.3% oxygen, and 0.3% nitrogen. The engine is rated at a maximum brake power output of 5220 hp and a brake specific fuel consumption of 0.284 lbm/hp·hr. For these conditions, calculate: (a) FA ratio; (b) fuel density, lbm/ft^3; (c) LHV of the fuel, Btu/lbm; (d) fuel consumption, gal/hr; and (e) brake thermal efficiency, %.

12

Gas Turbine Engine Combustion

12.1 INTRODUCTION

Chapters 10 and 11 discussed essential fuel-engine characteristics of spark- and compression-ignition IC engines. Through the years various attempts have been made to develop unique piston-cylinder prime movers concepts. For example, some nineteenth-century inventors even tried to apply knowledge from gun manufacturing to IC development. Their efforts attempted to adapt the highly explosive nature of gunpowder ignition to intermittent engine combustion chemistry, an illustration of an early attempt at technology transfer.

An important distinction of gas-power engines used for classification purposes is whether they operate utilizing intermittent or continuous combustion. Continuous fluid flow machines such as the basic gas turbine unit shown in Figure 12.1 consist of separate compressor-combustor-turbine components. Windmills are considered by many to be forerunners of today's gas power turbomachines. Historically, windmills were used by different cultures throughout the world, including that of ancient China. Hero of Alexandria, Greece, constructed a steam turbine device that was driven by hot flue gases rising from an open fire. The idea of an efficient power-generating gas turbine machine was envisioned during the Age of Steam, but the earliest recorded patent for a gas turbine was filed by the Englishman John Barber in 1791.

During the nineteenth century, a number of thermodynamic cycles and hot-air piston engines, such as those proposed by Ericsson and Joule, preceded gas turbine engines. Later, some early naval torpedoes were propelled by simple gas turbine devices. By the late 1930s, successful elements needed for an economical gas turbine began to become available. Useful propulsion machinery has resulted from an availability and compatibility of both suitable fuels and engines, a thesis repeatedly stated throughout this text. In addition, an application or need for a particular fuel-engine combination often will exist; manned flight provided an impetus for gas turbine engine development.

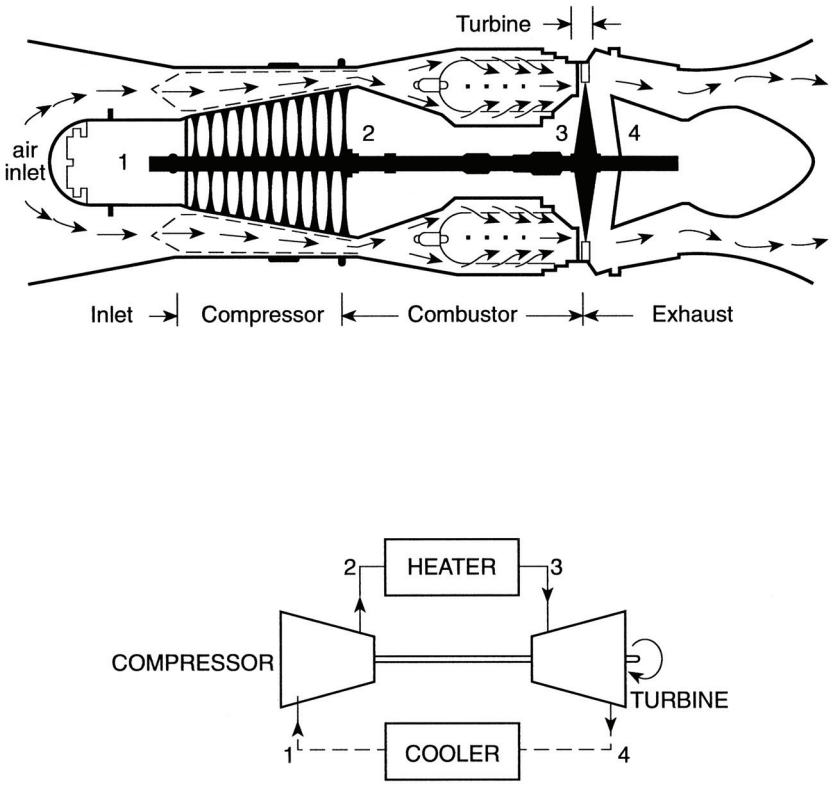

Figure 12.1 Basic gas turbine power system.

The first practical aircraft gas turbine engines appeared during the 1940s, although experimental machinery was operated a decade earlier. Sir Frank Whittle was a leader in developing aircraft turbojet propulsion engines. Work begun in the early 1930s resulted in his W1, a flying engine that operated in 1941 and produced 634 N (859 ft) of thrust. His original unit was built by Rover but, by 1943, Rover was taken over by Rolls-Royce. Several American and German companies also developed and built early jet engines; however, only a few were operational by the end of World War II. Military use of jet engine aircraft was common by the end of the Korean War, and the first commercial use of a jet engine occurred in 1953. Limited success in railroad and automotive applications, most notably Rover and Chrysler, was achieved in the late 1950s. It was not until the 1960s, however, that jet engines entered into satisfactory commercial use. After the 1970s, aircraft-derivative gas turbines began to find a variety of new applications, including marinized aircraft designs for ship propulsion, hovercraft applications, and industrialized designs for stationary power generation.

Many factors helped to slow development of a reliable gas turbine, including the low compressor and turbine component efficiencies of early designs, lack of suitable materials able to withstand locally high temperatures developed in hot sections resulting from continuous combustion, and unacceptably large total stagnation pressure loss across the combustor. Worldwide gas turbine industries today manufacture civilian as well as

military power plants for air, land, and sea applications. Engineering publications and standards are available that support all professional aspects relevant to the science and technology of gas turbine components, including compressors, combustors, turbines, intercoolers, reheaters, and/or regenerators. Reference material also deals with various power and thrust configurations of gas turbine engines, such as turboshaft, turboprop, turbofan, electric power generators, and turbochargers. Efforts are now underway to try to develop new microturbine machinery for unique applications.

Chapter 12 will cover only essential and important fuel-engine energetic characteristics of gas turbine engines; see Figure 12.2. Material discussion, therefore, will focus primarily on the major combustion component, the combustor. This chapter will be limited to the following issues: the thermochemical nature of the reactive mixture, general gas turbine fuel characteristics, basic combustion processes, and related emissions problems generally associated with gas turbine operation, as well as basic combustor design. A brief description of two unique continuous-combustion power systems, the free piston and Stirling engine, will be reviewed as well.

12.2 THERMODYNAMICS AND GAS TURBINE ENGINE MODELING

The Brayton cycle is a zeroth-order thermodynamic model for an ideal basic gas turbine engine. Material can be developed in similar fashion to IC engine cycle developments found in Chapters 10 and 11. An air standard Brayton cycle describes steady-state and steady-flow energy characteristics of turbomachinery components in terms of the following ideal processes:

1–2 Isentropic compression
2–3 Constant-pressure heat addition
3–4 Isentropic expansion
4–1 Constant-pressure heat rejection

Now, the Brayton cycle has thermodynamic processes identical to those Joule proposed in the late nineteenth century for his two-cylinder, reciprocating piston-cylinder, and positive-displacement hot-air engine. The historical success of a gas turbine and the failure of the Joule piston-cylinder engine illustrate a guiding principle of a successful power machinery development program: postulate potentially achievable processes that satisfy principles of energy conservation and conversion; but develop actual hardware that can successfully achieve those postulated events.

A dimensionless Brayton cycle formulation can be expressed based on the following dimensionless parameters:

τ = T_3/T_1 = maximum cycle temperature ratio
r_p = P_2/P_1 = pressure ratio (note $r_p \neq r_v$)
β = T_3/T_2 = constant-pressure heating temperature ratio
ρ = T_4/T_1 = constant-pressure cooling temperature ratio
η = indicated thermal efficiency

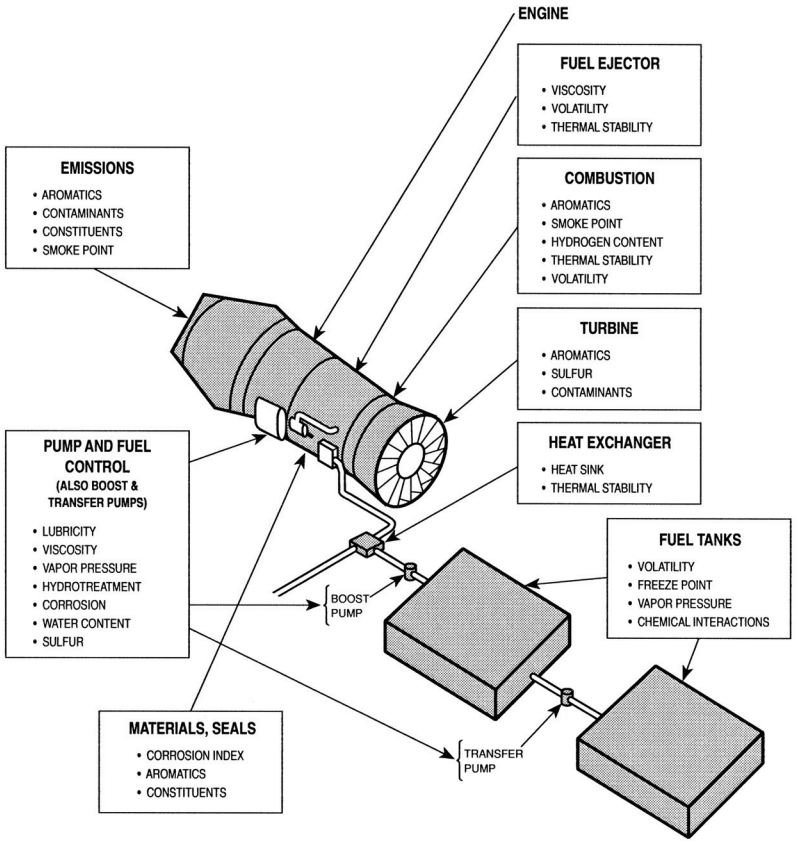

Figure 12.2 Basic gas turbine fuel-engine interface. After Cliff Moses, Report No. AFLRL-164, "Engines/Fuels Workshop," Mann, David M.; Lepera, M. E.; Glance, Paul C.; Munt, Richard; and Mularz, Edward J.; SwRI Fuels and Lubricants Research Lab, San Antonio, TX, 6–8 December 1982.

Using a constant specific heat analysis and the dimensionless relationships shown above, the following equations are valid. Note that, from $1 \rightarrow 2$, $Pv = RT$ and $Pv^{\gamma} = \text{const}$, or

$$T_2 = T_1 r_p^{(\gamma-1)/\gamma} \tag{12.1}$$

and

$$T_3 = \beta T_2 = \beta T_1 r_p^{(\gamma-1)/\gamma} = \tau T_1 \tag{12.2}$$

For an ideal Brayton cycle, $P_3 = P_2$ and $P_4 = P_1$, which means

$$P_4 / P_3 = P_1 / P_2 = 1 / r_p \tag{12.3}$$

and

$$T_4 = (1/r_p)^{(\gamma-1)/\gamma} T_3 = \beta(1/r_p)^{(\gamma-1)/\gamma} T_2 = \rho T_1 \tag{12.4}$$

Net cycle work per unit mass of air flowing through the open compression and expansion components during steady-state and steady-flow operation is expressed as

$$w_{\text{net}} = {}_1w_2 + {}_3w_4 = h_1 - h_2 + h_3 - h_4$$
$$= C_p(T_1 - T_2 + T_3 - T_4)$$

or, in dimensionless form,

$$\xi = \frac{w_{\text{net}}}{C_pT_1} = \left[1 - r_p^{(\gamma-1)/\gamma} + \tau - \rho\right] \tag{12.5a}$$

External heat addition per unit mass flowing, q_H, is

$$q_H = {}_2q_3 = C_p[T_3 - T_2] = C_p[\tau - r_p^{(\gamma-1)/\gamma}]T_1 \tag{12.6}$$

and

$$q_H / C_pT_1 = \left[\tau - r_p^{(\gamma-1)/\gamma}\right] \tag{12.6a}$$

Indicated thermal efficiency η is expressed as

$$\eta = \frac{w_{\text{net}}}{q_H} = \frac{1 - r_p^{(\gamma-1)/\gamma} + \tau - \rho}{\tau - r_p^{(\gamma-1)/\gamma}} \tag{12.7}$$
$$= \frac{\tau - r_p^{(\gamma-1)/\gamma} + 1 - \rho}{\tau - r_p^{(\gamma-1)/\gamma}}$$
$$= 1 + \frac{1 - \rho}{\tau - r_p^{(\gamma-1)/\gamma}}$$

Substituting Equation (12.2) for τ gives the expression

$$\eta = 1 + \frac{1 - \rho}{\beta r_p^{(\gamma-1)/\gamma} - r_p^{(\gamma-1)/\gamma}}$$

and

$$= 1 = \frac{1 - \rho}{r_p^{(\gamma-1)/\gamma}[\beta - 1]}$$

or

$$\eta = 1 - \frac{1}{r_p^{(\gamma-1)/\gamma}}\left[\frac{1 - \rho}{1 - \beta}\right]$$

Recall that $P_3 = P_2$ and $P_4 = P_1$ or $P_3/P_4 = P_2/P_1 = r_p$; then,

$$\frac{T_3}{T_4} = \frac{T_2}{T_1} = r_p^{(\gamma-1)/\gamma} \tag{12.8}$$

or

$$\frac{T_3}{T_2} = \frac{T_4}{T_1} \tag{12.9}$$

and, therefore,

$$\beta = \rho \tag{12.9a}$$

This allows a Brayton cycle thermal efficiency to be written as

$$\eta = 1 - \frac{1}{r_p^{(\gamma-1)/\gamma}} \tag{12.10}$$

EXAMPLE 12.1 Using the dimensionless Brayton cycle relations, determine the dimensionless performance parameters as a function of pressure ratio for: (a) fixed peak temperature ratio, $\tau = 10$; (b) fixed dimensionless net work per unit mass, $\xi = 4.0$; and (c) fixed dimensionless heat addition per unit mass, $q_H/C_PT_1 = 8.0$. For each of these conditions, determine the corresponding values of τ, ξ, and q_H/C_pT_1. Assume that $\gamma = 1.4$.

Solution:

1. Dimensionless Brayton cycle relationships:

$$\xi = [1 - r_p^{(\gamma-1)/\gamma} + \tau - \rho]$$
$$\rho = \beta = \tau / r_p^{(\gamma-1)/\gamma}$$
$$q_H / C_pT_1 = [\tau - r_p^{(\gamma-1)/\gamma}]$$
$$\eta = 1 - 1/r_p^{(\gamma-1)/\gamma}$$

2. Fixed peak temperature ratio, $\tau = 10$:

a.

r_p	ξ	q_H/C_pT_1	η
2	[a]1.5776	[a]8.7810	[a]0.1797
3	2.3253	8.6313	0.2694
4	2.7845	8.5140	0.3270
5	3.1023	8.4162	0.3686
6	3.3381	8.3315	0.4007
7	3.5212	8.2564	0.4265
8	3.6681	8.1886	0.4480
9	3.7888	8.1266	0.4662
10	3.8898	8.0693	0.4821

[a] $\xi = [1 - 2^{0.4/1.4} + 10(1 - \frac{1}{2}^{0.4/1.4})]$
$= 1.5776$
$q_H / C_pT_1 = [10 - 2^{0.4/1.4}] = 8.7809$
$\eta = 1 - \frac{1}{2}^{0.4/1.4} = 0.1719$

3. Fixed dimensionless net work per unit mass, $\xi = 4$:

b.

r_p	τ	q_H/C_pT_1	η
2	[b]23.4827	[b]22.2637	[b]0.1797
3	16.2165	14.8478	0.2694
4	13.7165	12.2305	0.3270
5	12.4353	10.8514	0.3686
6	11.6520	9.9835	0.4007
7	11.1226	9.3790	0.4265
8	10.7409	8.9295	0.4480
9	10.4530	8.5796	0.4662
10	10.2285	8.2979	0.4821

[b] $$\tau = \frac{4 - 1 + 2^{0.4/1.4}}{(1 - \frac{1}{2}^{0.4/1.4})} = 23.4827$$

$$q_H / C_p T_1 = [23.4827 - 2^{0.4/1.4}]$$

$$\eta = 1 - \frac{1}{2}^{0.4/1.4} = 0.1797$$

4. Fixed dimensionless heat addition per unit mass, q_H/C_PT_1, = 8:

c.

r_p	τ	ξ	η
2	[c]9.2190	[c]1.4373	[c]0.1797
3	9.3687	2.1552	0.2694
4	9.4860	2.6164	0.3270
5	9.5838	2.9489	0.3686
6	9.6685	3.2053	0.4007
7	9.7436	3.4119	0.4265
8	9.8114	3.5836	0.4480
9	9.8734	3.7298	0.4662
10	9.9307	3.8564	0.4821

[c] $$\tau = 8.2^{0.4/1.4} = 9.2190$$

$$\xi = [1 - 2^{0.4/1.4} + 9.2190(1 - \frac{1}{2}^{0.4/1.4})]$$

$$\eta = 1 - \frac{1}{2}^{0.4/1.4} = 0.1797$$

Comments: This problem illustrates how the dimensionless relationships of a basic gas turbine cycle can be used in parametric analysis. Results of predictive zero order performance modeling can be easily compared to those for Otto, Diesel, and Dual cycle modeling using material developed in Chapters 10 and 11.

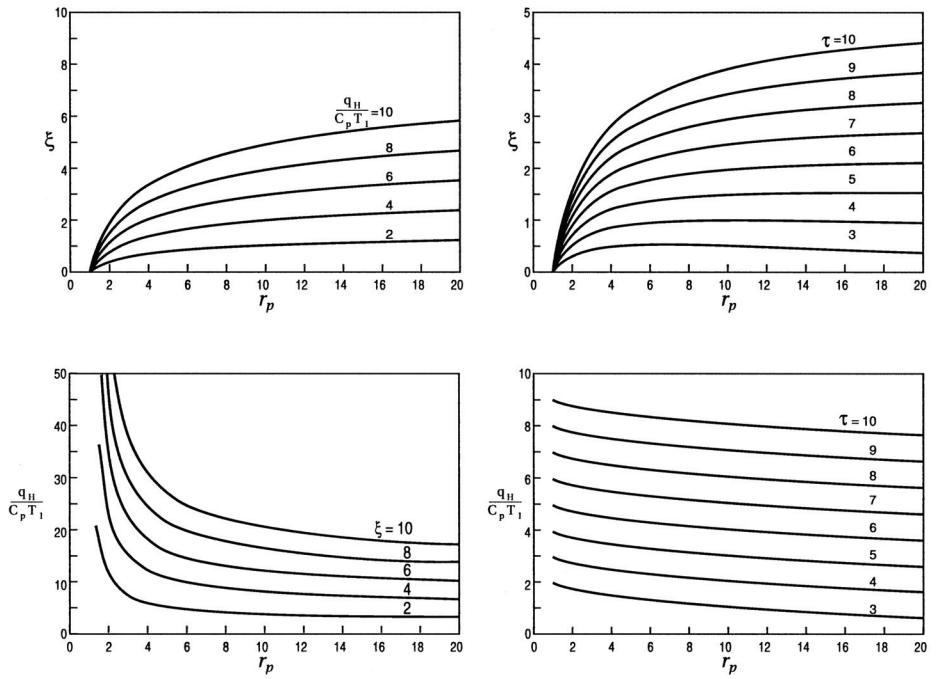

Figure 12.3 Ideal air standard Brayton cycle thermodynamic characteristics.

The previous relationships can be readily utilized during any initial analysis of a basic gas turbine, as was done for both SI and CI engines in Chapters 10 and 11. Figure 12.3 shows dimensionless characteristics of an ideal constant specific heat air standard basic Brayton cycle. Thermodynamic modeling can be expanded to include both variable specific heats and a fuel-air cycle analysis. Adding compressor and turbine component efficiencies, as well as a combustion efficiency, will bring these simple thermodynamic predictions more in line with the actual energetics observed during turbomachinery operation. Modifying the basic engine configuration to include more compressors, turbines, intercoolers, regenerators, and afterburners will impact the gas turbine fuel-engine interface but is not considered in this text.

12.3 GAS TURBINE FUEL THERMOCHEMISTRY

Theoretically, gas turbine engines can burn a wide variety of fuel alternatives. Commercial gas turbine fuels, much like current standard IC engine fuels, are based on specific hydrocarbon crude oil reserves, with turbine fuels coming from crude components that fall between gasoline and power kerosene portions of the distillation curve; see Chapter 7. Many of the IC engine fuel issues discussed in Chapters 10 and 11 are also relevant to the proper operation of gas turbine machinery; however, gas turbine fuels, in addition, should specifically meet the following requirements:

Pump easily, and ensure good flow at all times
Maintain highly efficient combustion
Establish a high heat release rate
Minimize fire hazards associated with fuel handling
Permit easy burner ignition and good relight characteristics
Provide adequate lubrication to moving parts of the fuel system
Prohibit corrosive effects on fuel system components
Minimize harmful effects on the combustor and turbine

An understanding of specific thermochemical properties of gas turbine fuels can help engineers address most of the issues listed above.

Viscosity, for example, impacts both liquid fuel atomization and dispersion processes, essential to complete combustion within any given burner. In addition, pumping characteristics of jet fuel depend on viscosity, and sufficient fluid flow should be maintained down to –50°C (–111°F), the waxing point temperature restriction for most aircraft fuels. This requirement arises from the very low environmental temperatures as well as heat transfer losses from aircraft fuel tanks and fuel lines encountered during flight.

Fuel temperatures, such as pour point, flash point, and self-ignition, are also significant to proper and efficient combustion. Operational considerations and safety constraints will require a minimum flash point to preclude potential fires and/or explosions. Fuel temperature in aviation applications also depends on altitude, rate of climb, duration at altitude, and kinetic heating due to flight speed. Limiting fuel boil-off during rapid climbing, as required for many military aircraft, can be a formidable challenge. When rapid boiling does occur, as it does with a wide-cut gasoline distillate fuel, vapor locking of the engine's fuel system may result. Gas turbine fuel temperature will not vary as greatly in land and/or marine applications and is therefore less of an issue in those operational instances

EXAMPLE 12.2 A marine split-shaft gas turbine has a rated brake thermal efficiency of 23.7% while developing an indicated power output of 15,000 ihp at full load. The unit burns a fuel oil having a specific gravity of 0.92 (at 60°/60°F). The compressor volumetric flow rate measured at the inlet of 64°F and 14.5 psi is 1.16×10^5 ft^3/min. If the combustor has a 95% efficiency and the power plant has a 90% mechanical efficiency, calculate (a) the fuel consumption rate, gal/hr; (b) the *FA* ratio, lbm fuel/lbm air; (c) the brake specific fuel consumption, lbm/bhp·hr; and (d) the minimum tank capacity required for a 10,000-mi. range operating at a constant speed of 20 knots (1 knot = 1.151 mph), gal.

Solution:

1. Brake thermal efficiency:

$$\eta = \frac{\text{desired energy output}}{\text{required energy input}} = \left(\frac{\dot{W}_{\text{net}}}{\dot{Q}_{\text{add}}}\right)_{\text{actual}}$$

or

$$\dot{Q}_{\text{add}} = \frac{(15{,}000\ \text{hp})(2{,}544\ \text{Btu/hp}\cdot\text{hr})}{(0.237)} = 1.610 \times 10^{8}\ \text{Btu/hr}$$
$$= 2.68 \times 10^{6}\ \text{Btu/min}$$

2. Combustor efficiency:

$$\eta_{\text{comb}} = \frac{\dot{Q}_{\text{add}}}{\dot{m}_{\text{fuel}} LHV}$$
$$\dot{m}_{\text{fuel}} = \frac{2.68 \times 10^{6}\ \text{Btu/min}}{(0.95)(LHV\langle\text{Btu/lbm fuel}\rangle)}$$

From Appendix C,

$$SG = 0.92 \qquad \rho = 7.64\ \text{lbm/gal} \qquad LHV = 18{,}030\ \text{Btu/lbm}$$
$$\dot{m}_{\text{fuel}} = \frac{(2.68 \times 10^{6}\ \text{Btu/min})}{(0.95)(18{,}030\ \text{Btu/lbm})} = 156.46\ \text{lbm/min}$$
$$\dot{V}_{\text{fuel}} = \frac{\dot{m}_{\text{fuel}}}{\rho_{\text{fuel}}} = \frac{156.46\ \text{lbm fuel/min}}{7.64\ \text{lbm fuel/gal}}$$

a. $\dot{V}_{\text{fuel}} = 20.5\ \text{gal/min} = 1{,}230\ \text{gal/hr}$

3. Mass *FA* ratio:

$$FA = \frac{\dot{m}_{\text{fuel}}}{\dot{m}_{\text{air}}} = \left(\frac{RT}{P\dot{V}}\right)_{\text{air}} \dot{m}_{\text{fuel}}$$
$$FA = \frac{(53.34\ \text{ft}\cdot\text{lbf/lbm air}\cdot°\text{R})(524°\text{R})(156.46\ \text{lbm fuel/min})}{(14.5\,\text{lbf/in.}^2)(144\,\text{in.}^2/\text{ft}^2)(1.16 \times 10^{5}\ \text{ft}^3/\text{min})}$$

b. $FA = 0.0181\ \text{lbm fuel/lbm air}$

4. Brake specific fuel consumption:

$$BSFC = \frac{\dot{m}_{\text{fuel}}}{(\dot{W}_{\text{net}})_{\text{brake}}} = \frac{\dot{m}_{\text{fuel}}}{(\dot{W}_{\text{net}})_{\text{indicated}} \times \eta_{\text{mech}}}$$
$$= \frac{(156.46\ \text{lbm fuel/min})(60\ \text{min/hr})}{(15{,}000\ \text{hp})(0.90)}$$

c. $BSFC = 0.695\,\text{lbm/hp}\cdot\text{hr}$

5. Tank capacity:

$$V_{\text{tank}} = \frac{(1{,}230\ \text{gal/hr})(10{,}000\,\text{mi.})}{(20\,\text{knots})(1.151\,\text{mph/knot})}$$

d. $V_{\text{tank}} = 534{,}000\ \text{gal}$

Table 12.1 Thermochemical Properties of Aviation Turbine Fuels[a]

	AV gas 100	(Jet B) JP-4	(Jet A) JP-8	JP-5	JP-7
Distillation					
°C	40–136	61–260	167–268	186–258	196–252
(°F)	104–277	142–500	333–514	367–496	385–486
Flammability limits (vol. %)					
lower (lean) limit	1.2	1.3	0.6	0.6	0.6
upper (rich) limit	7	8	4.7	4.6	4.6
Flammability limits (°C)					
lower (lean) limit	–44	–23	53	64	60
upper (rich) limit	–12	18	77	102	100
Average flash point					
°C	—	—	51.2	63.3	70
(°F)	—	—	124	145	157
Autoignition temperature (1 atm.)					
°C	433	246	238	241	241
(°F)	811	475	460	465	465
Heat of combustion					
kJ/kg	43,500	42,800	42,800	42,600	43,500
(Btu/lbm)	18,700	18,400	18,400	18,320	18,700

[a]Data from the *Handbook of Aviation Fuel Properties*, CRC Report #635, 2004.

Effective utilization of any gas turbine fuel is also influenced by both its latent heat and heat of combustion. For an aircraft with fixed fuel tank volume and range as a specifying limiting design factor, one desires to use a fuel with an energy density per unit volume as high as possible to obtain the greatest energy from a unit volume of fuel. However, for cases in which aircraft payload is the limiting factor, fuel energy density per unit mass should be as high as possible to achieve the greatest energy from a minimum weight of fuel.

The ability of turbine fuels to vaporize, i.e., their volatility, is critical, especially at the low temperatures often encountered in jet engine operation. Aircraft turbine engines can burn either a kerosene-base or wide-cut gasoline-base distillate hydrocarbon fuel with the distinctions between the two categories being basically in their volatility. Kerosene fuels have distillation-controlled volatility curves and fuel flash points that allow these fuels to have low vapor pressures and thus to boil only at extremely high altitudes. The wide-cut gasoline-type fuels have distillation-controlled volatility curves with Reid vapor pressures that ensure that fuel will boil off at much lower altitudes.

Gas turbine fuel suitability also requires there be low levels of water, sulfur, and sodium concentrations to minimize corrosion. In addition, minimal mineral materials, such as phosphorous, vanadium, and ash, must be present as well since they can clog or be abrasive to fuel components such as fuel-oil pumps and fuel nozzles, as well as erode power-generating machinery such as turbine blading. Vanadium pentoxide, V_2O_5, and sodium sulfate, Na_2SO_4, are produced in the highly oxidizing gas turbine exhaust and will cause fluxing of all protective oxide films covering hot steel components. These components, if cooled, produce sticky, insoluble deposits on turbine blading. Turbine fuels, when used in aircraft applications, also require precise concentrations of gum and rust inhibitors, as well as anti-icing, antistatic, and antismoke additives to make them more compatible.

Early turbojet fuel development was supported by the military, who helped to establish the JP specifications for those fuels. Table 12.1 lists properties of JP fuels. These fuels are similar in many characteristics but differ dramatically in their volatility, i.e., boiling point range. Commercial jet aircraft utilize fuel specifications set by ASTM. Three ASTM aircraft turbine fuel grades exist and include Jet-A Aviation Turbine Fuel, a kerosene fuel similar to JP-5, with a flash point of 66ºC (150ºF) and a freezing point of –40°C (–40ºF). Jet A-1 fuel is used when turbine operation requires a lower freezing point temperature, –50ºC (–58ºF). Jet B is commercial JP-4.

Kerosenes, with their low viscosities and medium volatilities, provide both efficient atomization and combustion over a wide range of inlet air temperatures, pressures, and velocities and therefore make good jet fuels. Land turbine units can burn a range of fuel phases as well as types, including natural gas, propane, blast-furnace gas, butane, petroleum distillates, residual fuel oil, and alcohols. Continuous combustion allows less expensive gas oils and diesel fuels to be burned in industrial and marinized aircraft-derivative engines. Burning heavy residual fuel oils in gas turbines does result in some negative effects:

Heating required prior to atomizing this highly viscous fuel
Tendency to polymerize and form tar or sludge when overheated
Incompatible with other hydrocarbon oils and potential for forming jellylike substances that can clog fuel systems
High carbon content fuel, producing excessive combustion chamber carbon deposits

Excessive vanadium, alkali metals, and ash, which impact on the reliability and availability of the hot section of the plant

EXAMPLE 12.3 Material constraints require that gas turbine combustion can exhaust temperatures be limited to 2,000ºF. Consider a gas turbine combustor burning a lean *n*-pentane-air mixture. Compressed air enters the can at 90.5 psia and 440ºF while the fuel is injected at 77ºF. For an exhaust gas temperature of 1,880ºF, estimate (a) the required mass fuel-air ratio; (b) excess air, %; (c) the exhaust gas molecular weight and specific heat ratio; and (d) exhaust gas specific volume, ft^3/lbm gas.

Solution:

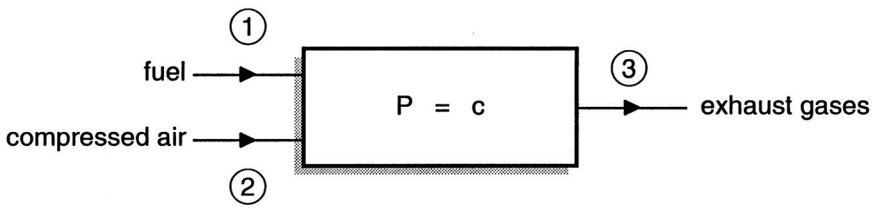

1. Stoichiometric equation:

$$C_5H_{12} + 8O_2 \rightarrow 5CO_2 + 6H_2O$$

2. Actual equation, assume excess air and complete combustion:

$$C_5H_{12} + 8a[O_2 + 3.76N_2] \rightarrow bCO_2 + cH_2O_g + dO_2 + 30.08aN_2$$

Carbon atom balance:

$$b = 5$$

Hydrogen atom balance:

$$12 = 2c \qquad c = 6$$

Oxygen atom balance:

$$16a = 2b + c + 2d \qquad d = 8[a - 1]$$

3. Energy equation, $P = c$ adiabatic combustion:

$$\sum_{j\,\text{prod}} N_j[\bar{h}_f^0 + \{\bar{h}\langle T_j\rangle - \bar{h}\langle T_0\rangle\}]_j = \sum_{i\,\text{react}} N_i[\bar{h}_f^0 + \{\bar{h}\langle T_i\rangle - \bar{h}\langle T_0\rangle\}]_i$$

where

$$\sum_{j\,\text{prod}} N_j\bar{h}_j = 5[\bar{h}_f^0 + \Delta\bar{h}\langle T_3\rangle]_{CO_2} + 6[\bar{h}_f^0 + \Delta\bar{h}\langle T_3\rangle]_{H_2O_g}$$
$$+ 8(a - 1)[\bar{h}_f^0 + \Delta\bar{h}\langle T_3\rangle]_{O_2} + 30.08a[\bar{h}_f^0 + \Delta\bar{h}\langle T_3\rangle]_{N_2}$$

and

$$\sum_{i\,\text{react}} N_i \bar{h}_i = 1[\bar{h}_f^0 + \Delta\bar{h}\langle T_1\rangle]_{C_5H_{12}} + 8a[\bar{h}_f^0 + \Delta\bar{h}\langle T_2\rangle]_{O_2}$$
$$+ 30.08a[\bar{h}_f^0 + \Delta\bar{h}\langle T_2\rangle]_{N_2}$$

$T_1 = T_0 = 537°\text{R}$ $T_2 = 900°\text{R}$ $T_3 = 2{,}340°\text{R}$

Using JANAF data found in Appendix B,

$$5[-94{,}054 + 11{,}988]_{CO_2} + 6[-57{,}798 + 9{,}298]_{H_2O_g}$$
$$+ 8(a - 1)[7{,}971]_{O_2} + 30.08a[7{,}529]_{N_2}$$
$$= [-41{,}890]_{C_5H_{12}} + 8a[1{,}455]_{O_2} + 30.08a[1{,}413]_{N_2}$$
$$a = 3.06$$

4. Mass air-fuel ratio:

$$C_5H_{12} + (8)\,(3.06)\,[O_2 + 3.76N_2] \rightarrow \text{products}$$

or

$$FA = \frac{(1.0)(72.151)\ \text{lbm fuel}}{(8)(3.06)(4.76)(28.97)\ \text{lbm air}}$$

a. $FA = 0.0214$ lbm fuel/lbm air

5. Excess air, %;

Stoichiometric air:

(8) (4.76) = 38.08

Actual air:

(8) (4.76) (3.06) = 116.52
Theoretical air = 306%

b. Excess air = 206%

6. Product molecular weight:

$$MW = \sum \bar{x}_i MW_i$$

where

$$\bar{x}_i = \frac{N_i}{N_{\text{tot}}}$$

$N_{CO_2} = 5$ $N_{H_2O} = 6$

$N_{O_2} = 16.48$ $N_{\text{tot}} = 119.52$

$N_{N_2} = 92.04$

$$MW = \frac{1}{119.52}[(5)(44) + (6)(18) + (16.48)(32) + (92.04)(28)]$$

c. $MW_{prod} = 28.72$ lbm/lbmole

7. Exhaust gas specific volume:

$$P\,V = mR\,T$$

$$v = \frac{(1{,}545 \text{ ft} \cdot \text{lbf/lbmole} \cdot °\text{R})(2{,}340°\text{R})}{(90.5 \text{ lbf/in.}^2)(144 \text{ in.}^2/\text{ft}^2)(28.72 \text{ lbm/lbmole})}$$

d. $v = 9.659 \text{ ft}^3/\text{lbm gas}$

12.4 GAS TURBINE COMBUSTORS

Gas turbine compressed air temperature is raised prior to expansion through a power turbine. The required heat addition to the working fluid may result from either an external or internal combustion process. Most conventional engines inject fuel into the air stream utilizing continuous internal combustion heat release from the mixture as it flows through the burner. Reliable operation, long burner life, and combustion consistency require burner designs that satisfy several conflicting but important issues:

Compact and lightweight geometry, especially in aircraft applications
Minimal stagnation pressure loss across the combustor, i.e., between burner inlet and outlet
Prevention of burner liner erosion during operation
Easy initial and relight ignition characteristics
Uniform combustor exhaust temperature distribution
Continuous flame stability over a wide *AF* range

Isolating and separating combustion from compression and expansion processes by the use of a separate burner give gas turbines their unique fuel-engine interface. For example, there are no octane or cetane detonation indices for the constant-pressure continuous-combustion process as was the case for intermittent burn associated with IC engines discussed in Chapters 9–11. High energy release rates, however, are necessary. For example, most turbojet propulsion machines typically require 373,000–2,980,000 kW/m^3 (10,000–80,000 Btu/ft^3/sec) of heat release, whereas stationary steam power plants have nominal values that range between 22,400 and 112,000 kW/m^3 (600–3,000 Btu/ft^3/sec). Stable burn must occur within flows requiring bulk velocities of 30–60 m/sec (100–500 ft/sec). There are only two fuel-engine design requirements for a combustor configuration to meet in order to assure a high combustor efficiency. To achieve an efficiency of approximately 95%, a burner configuration should:

Sustain complete combustion in a high mass flux environment
Provide sufficient residence time for complete fuel combustion to occur
Prevent combustion processes from continuing into turbine components

Promote combustion reactions that generate no coking or deposition on combustor or turbine surfaces
Produce clean, smokeless exhaust gases having minimal eroding particulates
Limit heat losses from hot reacting gases through burner walls
Prevent hot spots, flameouts, and unreliable light-offs

Furnace combustion is at atmospheric conditions and surrounded by thick walls of firebrick and other materials; whereas high-pressure gas turbine thermochemistry is confined in a burner by a relatively small thickness of metal. A large portion of compressed air must thus bypass the reaction zone and be used to cool burner surfaces as well as to mix with, and to cool, burned gases entering the turbine. Approximately 25% of total airflow by weight is used for burning fuel. Combustor performance depends strongly on the aerothermochemistry of the reacting fluid flow passing through a given burner geometry. Burner configurations have evolved chiefly from experimentation and testing.

An electrically activated igniter, or spark plug, is used to initiate reaction as the fuel-air mixture flows through a burner. After initial ignition, reaction is self-sustaining unless any relighting is required to re-establish a reactive flow after a flameout. This process is different from spark-ignition engine ignition, in which each mechanical cycle requires a separate spark plug firing to continue engine operation.

Gas turbine combustion is basically a two-zone, high-pressure reaction process in which a primary zone is utilized to complete most of the combustion and a secondary zone is required for burner exhaust gas management. Primary combustion is usually a stoichiometric or rich regime and may require 20–30% of the compressed air. The secondary zone does provide for limited chemical kinetics but is predominantly used to produce an acceptable exhaust gas flow having a lower and more uniform temperature profile and is produced by mixing primary zone combustion products with excess air. Sufficient time must be provided within the combustor to ensure fuel droplet vaporization, primary reactant mixing, and kinetics. Combustion aerochemistry further requires proper fluid flow to ensure establishment and stabilization of a stationary primary flame zone that does not get swept downstream and out of the combustor or upstream into the compressor, causing a flameout. Water injection does not improve combustion efficiency; however, it may improve gas turbine performance by increasing total mass flow, while the latent heat of vaporization of water can help control peak temperature.

EXAMPLE 12.4 A gas turbine combustor can with a 6% pressure loss has inlet and discharge conditions as shown below:

$$T_2 = 444\text{K} \qquad P_2 = 40{,}500 \text{ kPa} \qquad V_2 = 61 \text{ m/sec}$$
$$T_3 = 1{,}200\text{K}$$

Assuming that the working fluid is air having mean constant specific heats and an equivalent heat addition of 850 kJ/kg air, calculate (a) the inlet Mach number; (b) the inlet stagnation state; (c) the discharge Mach number; (d) the discharge stagnation state; and (e) the decrease in stagnation pressure across the combustor due solely to heating the air, %.

Solution:

1. Properties for air:

$$T_{\text{mean}} = \frac{(444 + 1{,}200)}{2} = 822\text{K}$$

From Table B.24 in Appendix B,

$$\overline{C}_p\langle 822\text{K}\rangle = 7.633 \text{ cal/gmole}\cdot\text{K}$$

$$\gamma = \frac{\overline{C}_p}{\overline{C}_p - \overline{R}} = \frac{7.633}{(7.633 - 1.987)} = 1.352$$

and

$$C_p = \frac{(7.633 \text{ cal/gmole}\cdot\text{K})\left(4.187 \dfrac{\text{kJ/kgmole}\cdot\text{K}}{\text{cal/gmole}\cdot\text{K}}\right)}{28.97 \text{ kg/kgmole}}$$

$$= 1.103 \text{ kJ/kg}\cdot\text{K} = 1{,}103 \text{ N}\cdot\text{m/kg}\cdot\text{K}$$

2. Inlet Mach number (Example 4.1):

$$c_2 = (\gamma R T_2 g_0)^{1/2}$$

$$= [(1.352)(287\text{N}\cdot\text{m/kg}\cdot\text{K})(444\text{K})(1.0 \text{ kg}\cdot\text{m/N}\cdot\text{sec}^2)]^{1/2} = 415 \text{ m/sec}$$

a. $N_{m_2} = \dfrac{V_2}{c_2} = \dfrac{61}{415} = 0.147$

3. Inlet stagnation conditions (Example 4.2):

b. $T_{0_2} = T_2[1 + N_{m_2}^2(\gamma - 1)/2]$

$$= 444\left[1 + (0.147)^2 \frac{0.352}{2}\right] = 445.7\text{K}$$

$$P_{0_2} = P_2\left[1 + N_{m_2}^2(\gamma - 1)/2)\right]^{\gamma/(\gamma-1)}$$

$$= 40{,}500\left[1 + (0.147)^2 \frac{0.352}{2}\right]^{1.352/0.352}$$

$$= 41{,}095 \text{ kPa}$$

4. Energy:

$${}_2q_3 + \frac{V_2^2}{2g_0} + h_2 = \frac{V_3^2}{2g_0} + h_3$$

$$\frac{V_3^2}{2g_0} = 850{,}000\frac{\text{N}\cdot\text{m}}{\text{kg}} + \left(1{,}103\frac{\text{N}\cdot\text{m}}{\text{kg}\cdot\text{K}}\right)(444 - 1{,}200\text{K}) + \frac{\left(61\frac{\text{m}}{\text{sec}}\right)^2}{(2)\left(1.0\frac{\text{kg}\cdot\text{m}}{\text{N}\cdot\text{sec}^2}\right)}$$

c. $V_3 = 189.7 = 190$ m/sec

5. Discharge Mach number:

$$\begin{aligned} c_3 &= (\gamma RT_3 g_0)^{1/2} \\ &= [(1.352)(287\ \text{N}\cdot\text{m/kg}\cdot\text{K})(1{,}200\text{K})(1.0\ \text{kg}\cdot\text{m/N}\cdot\text{sec}^2)]^{1/2} \\ &= 682\ \text{m/sec} \end{aligned}$$

d. $N_{m_2} = \dfrac{V_2}{c_2} = \dfrac{190}{682} = 0.279$

6. Discharge stagnation conditions:

e. $T_{0_3} = 1{,}200\left[1 + (0.279)^2\dfrac{(0.352)}{2}\right] = 1{,}216\text{K}$

$$\begin{aligned} P_{0_3} &= 38{,}070\left[1 + (0.279)^2\frac{(0.352)}{2}\right]^{1.352/0.352} \\ &= 40{,}113\ \text{kPa} \end{aligned}$$

7. Percent decrease in stagnation pressure:

f. $\% = \left[\dfrac{41{,}095 - 40{,}113}{41{,}095}\right](100) = 2.4\%$

Comments: A pressure loss in a gas turbine will result in a loss in net work and hence in thermal efficiency. From the analysis, approximately 2.4% of the 6% drop in pressure is due solely to heating. A lower velocity would make this stagnation loss less. Additional losses result from mixing and turbulence.

Consider the simple combustor geometry shown in Figure 12.4a. Several limitations are found to exist with this simple arrangement:

Large stagnation pressure loss resulting from the entropy of reaction
Potential flame extinction or movement from the burner exit in high mass flow rate regimes
Possible flame extinction or movement toward the fuel nozzles in low mass flow rate regimes
High heat loss from the combustor because of the steady and highly localized nature of the burn
Stoichiometric *AF* necessary for complete combustion but excess air required to reduce the exhaust gas temperature to acceptable levels at the burner exit
Gas temperatures that can melt even high-alloy steels

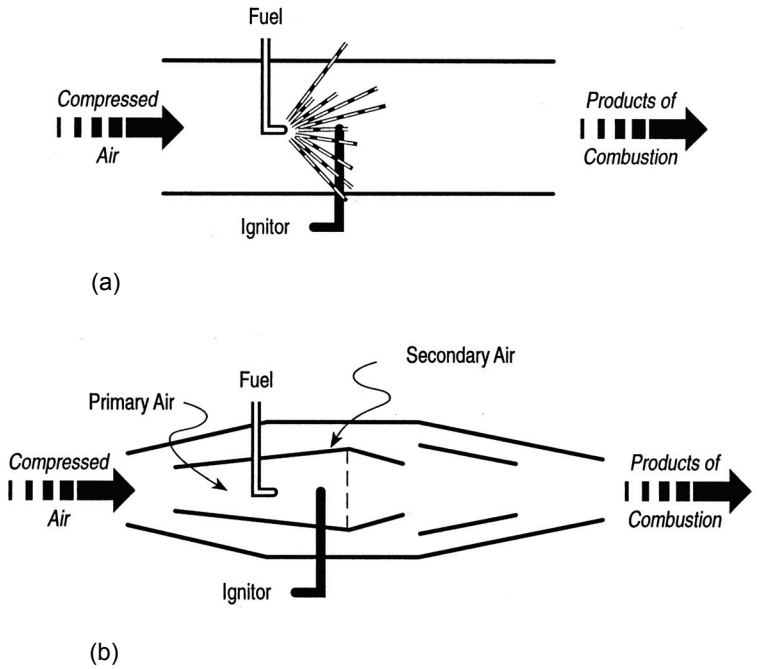

Figure 12.4 Basic gas turbine combustor geometry: (a) simple geometry, (b) modified geometry.

Figure 12.4b illustrates modifications to this simple geometry that may improve the original burner performance. A diffuser is added to reduce supply air inlet velocity. A flame holder is inserted to allow a reaction zone, or flame, to attach and to be stabilized. Geometry provides a stoichiometric reactive gas flow reactant mixture at the nozzles for complete combustion as well as excess air at the combustor exit to provide a lower and more uniform discharge gas temperature. Additional features of this modified burner include:

Outer shell to insulate high-temperature reactive flow
Ports and slots to allow air for stoichiometric burn near the fuel nozzle and excess air after the initial burn
Fuel nozzle designed to provide a conical spray of fuel droplets
Torch or spark-igniter ignition source

Many specific combustors have been developed in an attempt to produce units having superior performance. These various designs are usually classified as *can or tubular, annular, or cannular. Can-type* burners are basically cylindrical-geometry combustors and are compatible with constant-discharge pressure centrifugal compressors that have speed-dependent variable-discharge capacities. Can-type burners are usually found on small gas turbine units. A single fuel nozzle and igniter plug are provided for each

can. Individual cans are often placed around a compressor-turbine power shaft. A gas path through a tubular burner may utilize a once-through or a single reverse pass flow. These combustors can be easily separated from an operating gas turbine unit for maintenance, testing, or modification. Can combustors are mechanically rugged but are usually heavy and bulky configurations. High can strength results from the cylindrical shape although high stagnation pressure losses also occur with this burner geometry. Nonuniform light-off temperature distributions, as well as variations in can-to-can burn characteristics, occur in multican usage. Tubular geometries have smaller diameters than annular chambers.

EXAMPLE 12.5 Natural gas (CH_4) is pumped using the gas turbine configuration shown below. Methane enters the fuel compressor at 22 psia and 77°F, with an inlet volumetric flow rate of 500 ft^3/sec, and discharges from the unit at 88 psia. Air is supplied by a separate air compressor having suction conditions of 14.7 psia and 77°F and a discharge pressure of 88 psia. The combustor burns only a percentage of the total methane supply in 350% theoretical air, being supplied by the air compressor. Exhaust gases expanding through the turbine produce only enough power to run the two compressors. The turbine exhausts to a pressure of 14.7 psia. For ideal conditions, determine (a) the required CH_4 burner bleed, %; (b) the air compressor inlet volumetric flow rate, ft^3/min; (e) the exhaust gas mass flow rate, lbm/hr; and (d) the required turbine and compressor power, hp.

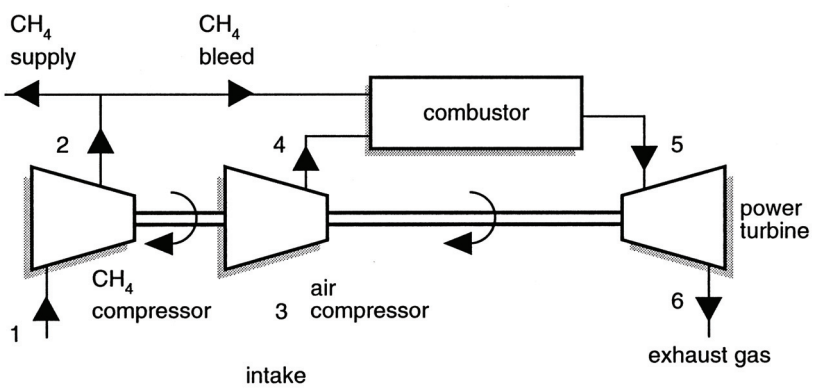

Solution:

1. Methane compressor:

$$P_1 = 22 \text{ psia} \qquad T_1 = 537°\text{R} \qquad \dot{V}_1 = 500 \text{ ft}^3/\text{sec}$$

Mass flow rate:

$$\dot{m} = \frac{P_1 \dot{V}_1}{\overline{R} T_1} = \frac{(22 \text{ lbf/in.}^2)(144 \text{ in.}^2/\text{ft}^2)(500 \text{ ft}^3/\text{sec})(16 \text{ lbm/lbmole})}{(1{,}545 \text{ ft} \cdot \text{lbf/lbmole°R})(537°\text{R})}$$

$$= 30.5 \text{ lbm } CH_4/\text{sec}$$

Isentropic compression process, $1 \rightarrow 2$:

$$\frac{P_r\langle T_2\rangle}{P_r\langle T_1\rangle} = \frac{P_2}{P_1} = \frac{88}{22} = 4$$

Using CH_4 data found in Table B.3 in Appendix B, $\Delta\bar{h}\langle T_1\rangle = 0$

$$P_r\langle T_1\rangle = \exp\left\{\frac{\bar{s}^0\langle 537\rangle}{\bar{R}}\right\} = \exp\left\{\frac{44.490}{1.987}\right\} = 5.2977 \times 10^9$$

or

$$P_r\langle T_2\rangle = (4)(5.2977 \times 10^9) = 2.1191 \times 10^{10}$$

$$\frac{\bar{s}^0\langle T_2\rangle}{\bar{R}} = \ln(2.1191 \times 10^{10}) = 23.7768$$

$$\bar{s}^0\langle T_2\rangle = (1.987)(23.7768) = 47.245$$

Interpolating,

$$\text{At } T_2 = 720°\text{R} \qquad \bar{s}^0 = 47.144 \qquad \Delta\bar{h}\langle T_2\rangle = 923 \text{ cal/gmole}$$

Compressor power:

$$\dot{W}_{CH_4} = \dot{m}[\Delta\bar{h}\langle T_1\rangle - \Delta\bar{h}\langle T_2\rangle]$$

$$= (30.5 \text{ lbm/sec})\left[\frac{(0 - 923) \text{ cal/gmole}}{16 \text{ lbm/lbmole}}\right]\left(1.8001\frac{\text{Btu/lbmole}}{\text{cal/gmole}}\right)$$

$$\dot{W}_{CH_4} = -3167 \text{ Btu/sec}$$

2. Air compressor:

$$P_3 = 14.7 \text{ psia} \qquad T_3 = 537°\text{R} \qquad \Delta\bar{h}\langle T_3\rangle = 0$$

Isentropic compression process:

$$\frac{P_r\langle T_4\rangle}{P_r\langle T_3\rangle} = \frac{P_4}{P_3} = \frac{88}{14.7} = 5.986$$

Using air data found in Example 3.2,

$P_r \times 10^{-10}$	T
3.749	720
8.286	900

$$P_r\langle T_4\rangle = (5.986)(1.288 \times 10^{10}) = 7.710 \times 10^{10}$$

Interpolating, $T_4 = 877°\text{R}$

and for air from Table B.24 in Appendix B,

$$\Delta\bar{h}\langle T_4\rangle = 1{,}349 \text{ cal/gmole}$$

Compressor work:

$$w_{\text{air}} = [\Delta\bar{h}\langle T_3\rangle - \bar{h}\langle T_4\rangle$$
$$= \left[\frac{(0 - 1{,}349) \text{ cal/gmole}}{28.96 \text{ lbm/lbmole}}\right]\left(1.8001\frac{\text{Btu/lbmole}}{\text{cal/gmole}}\right) = -83.85 \text{ Btu/lbm}$$

3. Combustor $P = c$ adiabatic combustion:

Reaction equation, assume complete reaction:

$$CH_4 + (2)(3.5)[O_2 + 3.76N_2] \rightarrow CO_2 + (2)(2.50)O_2 + 2H_2O + 26.32\ N_2$$

$$1 \text{ mole } CH_4 \rightarrow 1 + 5 + 2 + (7)(3.76) = 34.32 \text{ moles product}$$

Product mole fractions:

$$\bar{x}_{CO_2} = \frac{1}{34.32} = 0.0291$$
$$\bar{x}_{O_2} = \frac{5}{34.32} = 0.1457$$
$$\bar{x}_{H_2O} = \frac{2}{34.32} = 0.0583$$
$$\bar{x}_{N_2} = \frac{(7)(3.76)}{34.32} = 0.7669$$
$$MW_{\text{prod}} = \sum \bar{x}_i MW_i = (0.0291)(44) + (0.1457)(32) + (0.0583)(18)$$
$$+ (0.7669)(28) = 28.465 \text{ lbm/lbmole}$$

Combustor energy balance:

$$T_2 = 720°\text{R} \qquad T_4 = 877°\text{R}$$
$$\{1[\bar{h}_f^0 + \Delta\bar{h}\langle T_2\rangle]_{CH_4} + (2)(3.5)[\bar{h}_f^0 + \Delta\bar{h}\langle T_4\rangle]_{O_2}$$
$$+ (2)(3.5)(3.76)[\bar{h}_f^0 + \Delta\bar{h}\langle T_4\rangle]_{N_2}\} = \{1[\bar{h}_f^0 + \Delta\bar{h}\langle T_5\rangle]_{CO_2}$$
$$+ (2)(2.5)[\bar{h}_f^0 + \Delta\bar{h}\langle T_5\rangle]_{O_2} + 2[\bar{h}_f^0 + \Delta\bar{h}\langle T_5\rangle]_{H_2O}$$
$$+ (2)(3.5)(3.76)[\bar{h}_f^0 + \Delta\bar{h}\langle T_5\rangle]_{N_2}\}$$

Using JANAF data found in Appendix B for the reactants and products,

$$\{[-17{,}895 + 923]_{CH_4} + (2)(3.5)[1{,}362]_{O_2} + (26.32)[1{,}323]_{N_2}\}$$
$$= \{[-94{,}054 + \Delta\bar{h}\langle T_5\rangle]_{CO_2} + (2)(2.5)[\Delta\bar{h}\langle T_5\rangle]_{O_2}$$
$$+ 2[-57{,}798 + \Delta\bar{h}\langle T_5\rangle]_{H_2O} + (2)(3.5)(3.76)[\Delta\bar{h}\langle T_5\rangle]_{O_2}\}$$

$$237{,}033 = \Delta\bar{h}\langle T_5\rangle\Big)_{CO_2} + 5\Delta\bar{h}\langle T_5\rangle\Big)_{O_2} + 2\Delta\bar{h}\langle T_5\rangle\Big)_{H_2O} + (2)(3.5)(3.76)\Delta\bar{h}\langle T_5\rangle\Big)_{N_2}$$

where, by trial and error,

$T_5 = 2{,}145°\text{R}$

4. Turbine:

$P_5 = 88$ psia $\quad T_5 = 2{,}145°\text{R}$

Product isentropic expansion:

$$\frac{P_r\langle T_6\rangle}{P_r\langle T_5\rangle} = \frac{P_6}{P_5} = \frac{14.7}{88} = 0.167$$

where

$$\bar{s}^0\langle T_5\rangle = \bar{x}_i\bar{s}_i^0\langle T_5\rangle$$

Using JANAF data from Appendix B for the products,

$$\bar{s}^0\langle T\rangle = [(0.0291)(66.659) + (0.1457)(59.668) + (0.0583)(57.366) + (0.7669)(55.897)] = 56.845 \text{ cal/gmole}\cdot\text{K}$$

and

$$P_r\langle T_5\rangle = \exp\left\{\frac{\bar{s}^0\langle T_5\rangle}{\bar{R}}\right\} = \exp\left\{\frac{56.845}{1.987}\right\} = 2.6576 \times 10^{12}$$

or

$$P_r\langle T_6\rangle = (0.167)(2.6576 \times 10^{12}) = 4.4382 \times 10^{11}$$

$$\frac{\bar{s}^0\langle T_6\rangle}{\bar{R}} = \ln(4.4382 \times 10^{11}) = 26.8187$$

$$\bar{s}^0\langle T_6\rangle = (1.987)(26.8187) = 53.2888$$

$$53.2888 = \sum_{\text{prod}} \bar{x}_i\bar{s}_i^0\langle T_6\rangle$$

By trial and error,

$T_6 = 1{,}384°\text{R}$

Turbine work:

$$\overline{w}_{\text{prod}} = \left[\sum \bar{x}_i \Delta\bar{h}\langle T_5\rangle - \sum \bar{x}_i \Delta\bar{h}\langle T_6\rangle\right]$$
$$= (0.0291)[10{,}521 - 5{,}077] + (0.1457)[7{,}043 - 3{,}538]$$
$$+ (0.0583)[8{,}154 - 4{,}017] + (0.7669)[6{,}651 - 3{,}365]$$
$$= 3{,}430 \text{ cal/gmole products} = \left[\frac{3{,}430 \text{ cal/gmole}}{28.465 \text{ lb/lbmole}}\right]\left(1.8001 \frac{\text{Btu/lbmole}}{\text{cal/gmole}}\right)$$
$$= 216.91 \text{ Btu/lbm products}$$

5. Net power:

$$\left|\dot{W}_{\text{turb}}\right| = \left|\dot{W}_{\text{CH}_4}\right| + \left|\dot{W}_{\text{air}}\right|$$

or

$$\dot{m}_{\text{prod}} w_{\text{turb}} + \dot{m}_{\text{CH}_4} w_{\text{CH}_4} + \dot{m}_{\text{air}} w_{\text{air}}$$

with

$$\dot{m}_{\text{prod}} = \left[\frac{34.32 \text{ moles prod}}{1 \text{ mole CH}_4 \text{ burned}}\right]\left[\frac{28.465 \text{ lbm/lbmole prod}}{16 \text{ lbm/lbmole fuel}}\right] \times \dot{m}_{\text{CH}_4} \text{ burned}$$
$$\dot{m}_{\text{prod}} = 61.057 \dot{m}_{\text{CH}_4} \text{ burned}$$

and

$$\dot{m}_{\text{air}} = \left[\frac{(7)(4.76 \text{ moles air})}{1 \text{ mole CH}_4 \text{ burned}}\right]\left[\frac{28.97 \text{ lbm/lbmole air}}{16 \text{ lbm/lbmole fuel}}\right] \times \dot{m}_{\text{CH}_4} \text{ burned}$$
$$\dot{m}_{\text{air}} = 60.33 \dot{m}_{\text{CH}_4} \text{ burned}$$

substituting for the various terms,

$$(216.91)(61.057)\dot{m}_{\text{CH}_4} = 3{,}167 \text{ Btu/sec} + (83.85)(60.33)\dot{m}_{\text{CH}_4}$$
$$\dot{m}_{\text{CH}_4} \text{ burned} = 0.387 \text{ lbm CH}_4/\text{sec}$$

6. Methane bleed fraction:

$$\%\text{ bleed} = \frac{\dot{m} \text{ burned}}{\dot{m} \text{ supply}} \times 100 = \left[\frac{0.387 \text{ lbm CH}_4 \text{ burned/sec}}{30.5 \text{ lbm CH}_4 \text{ supply/sec}}\right] \times 100$$
$$\text{a. } = 1.3\% \text{ of supply bleed}$$

7. Air compressor volumetric flow rate:

$$\dot{m}_{air} = (60.33)(0.387 \text{ lbm/sec})$$

$$\dot{V}_3 = \frac{\dot{m}RT_3}{P_3} = \frac{(60.33)(0.387 \text{ lbm/sec})(1{,}545 \text{ ft} \cdot \text{lbf/lbmole} \cdot °\text{R})(537°\text{R})}{(22 \text{ lbf/in.}^2)(144 \text{ in.}^2/\text{ft}^2)(28.97 \text{ lbm/lbmole})}$$

$$= 211 \text{ ft}^3/\text{sec} = (211 \text{ ft}^3/\text{sec})(60 \text{ sec/min})$$

b. $\dot{V}_{air} = 12{,}660 \text{ ft}^3/\text{min}$

8. Exhaust gas mass flow rate:

$$\dot{m}_{prod} = (61.093)(0.387 \text{ lbm/sec})(3{,}600 \text{ sec/hr}) = 85{,}115 \text{ lbm/hr}$$

9. Compressor and turbine power:

$$\dot{W}_{CH_4} = \frac{(3{,}167 \text{ Btu/sec})(3{,}600 \text{ sec/hr})}{(2{,}545 \text{ Btu/hr} \cdot \text{hr})}$$

c. $\dot{W}_{CH_4} = 4{,}480 \text{ hp}$

$$\dot{W}_{air} = \frac{(60.33)(0.387 \text{ lbm/sec})(3{,}600 \text{ sec/hr})(83.85 \text{ Btu/lbm})}{(2{,}545 \text{ Btu/hp} \cdot \text{hr})}$$

d. $\dot{W}_{air} = 277 \text{ hp}$

$$\dot{W}_{turb} = \frac{(85{,}115 \text{ lbm/hr})(216.91 \text{ Btu/lbm})}{(2{,}545 \text{ Btu/hp} \cdot \text{hr})} = 7{,}250 \text{ hp}$$

The *annular burner* is a gas turbine combustor design that is most compatible with *axial compressors,* i.e., constant-capacity compressors with a speed-dependent variable-discharge state. These designs are most frequently found on larger gas turbine configurations in which a single annulus is wrapped around the compressor-turbine power shaft. This type of burner arrangement requires multiple nozzles and igniter plugs. Fluid flow can be similar to that for a can, that is, once-through or a single-pass reverse gas flow arrangement. Annular configurations are more compact geometries than cans and have low surface-to-volume ratios. Annular burners require less length, are lighter, and have a lower stagnation pressure loss across the combustor than comparable tubular arrangements. These combustor configurations are easier to light off, but it is more difficult to establish a uniform exhaust gas temperature profile. Burner liners are short-lived components, with outer flame tubes subject to buckling. Unlike can elements, these components are difficult to remove for inspection, maintenance, or modifications. *Can-annular* combustor designs are a compromise between can and annular geometries. Can-annular burners are used with large-pressure ratio gas turbine units. Again, a single annulus is placed around a centerline shafting, but a series of tubular flame tubes are placed inside the annulus. A can-annular configuration is shorter and lighter than a can-shape burner but less compact than an annular configuration. These burners may have a lower stagnation pressure loss than a simple can design. Can-annular systems provide good structural stability for flame tube geometry. With separate tubular flame tubes, these units are less difficult to service, test, or modify than the annular type of burner.

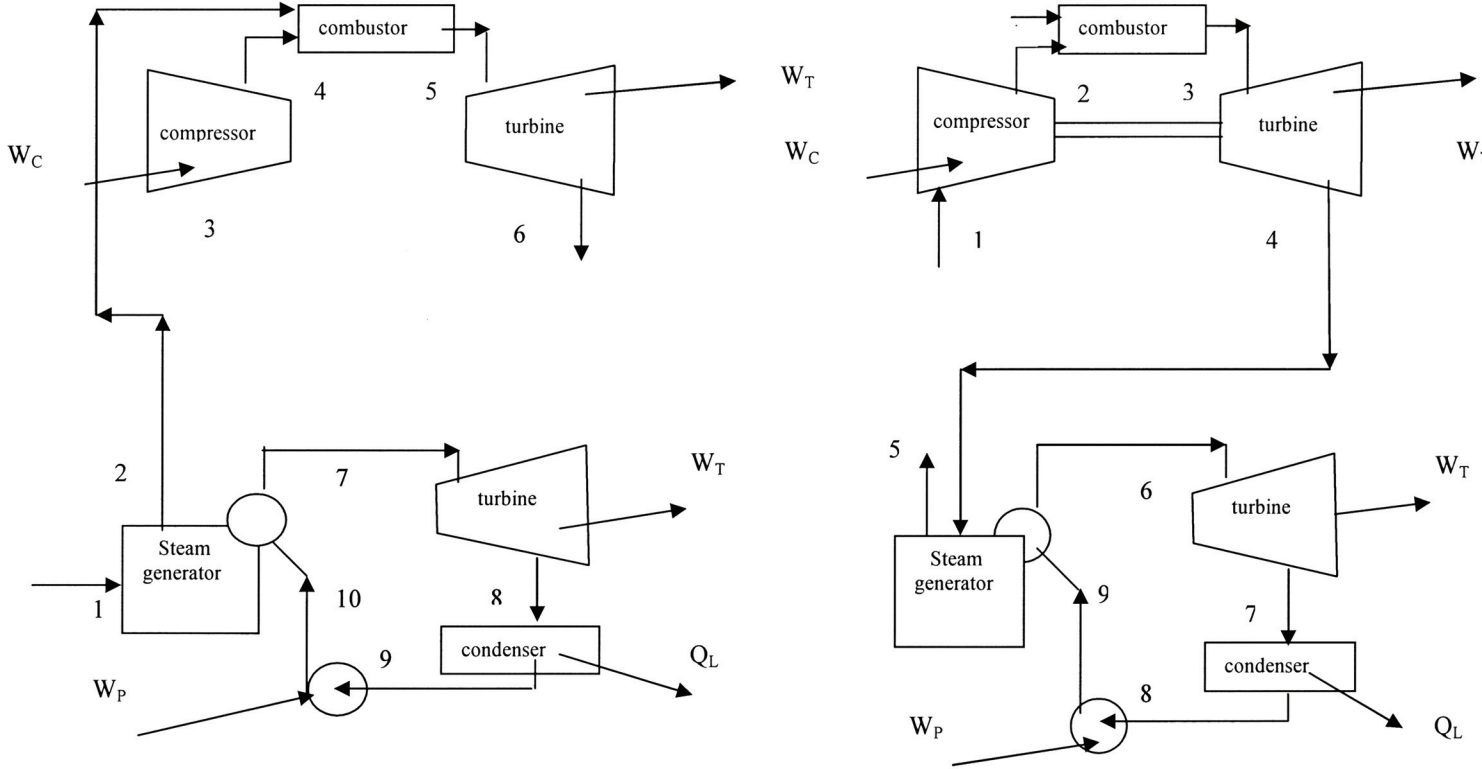

Figure 12.5 Advanced land-based gas turbine technology configurestion.

12.5 GAS TURBINE ENGINE FUEL ALTERNATIVES

Synthetic liquid fuels derived from coal, shale oil, and tar sands may serve as long-term fuel replacements for the crude oil-derived gas turbine fuels currently in use. Alcohol fuels, most probably methanol, might also find some future use in land and/or marine gas turbine engines. Substituting an alcohol fuel in a specific hydrocarbon distillate fueled combustor would result in greater fuel consumption and may partially de-rate the gas turbine engine. Alcohol fuel properties as well as combustion characteristics of alcohols, i.e., viscosity, latent heat of vaporization, specific heats, flame speed, and flammability limits, do not preclude attempting redesigns for optimizing use of alcohol fuels in advanced combustor concepts for particular applications. Water solubility of alcohol would, however, seriously impact its use in a marine environment. Aircraft use would be difficult because of the constant-temperature boiling characteristics of alcohols.

Gas turbine configurations have even been developed that burn solid fuels such as coal and wood. Techniques for burning solid fuels include direct combustion, slurry combustion, fluidized bed combustion, and indirect combustion. Chapter 6 described these combustion techniques as they apply to coal fired steam generating systems. When designing gas turbine combustors for burning solid fuels, such as pulverized coal, numerous fuel–engine interface issues need to be addressed. Coal powder, unlike most of the solid fuel machinery described in Chapter 6, will be introduced into high-pressure and high gas flow rate operating regimes of the gas turbine environment. Note also that any solid fuel would need to completely burn during the short time it resides within a combustor in order to ensure no tar depositing occurs during solid fuel product gas expansion through the hot turbine section.

Chapter 8 described technologies for the gasification of coal. Successful technologies that produce clean energy from coal fired gasification could provide a useable fuel resource for gas turbines supporting electric power generation–distribution systems. Burning solid fuels separately and utilizing heat exchangers instead of using traditional or enhanced combustor components to transfer released energy to the gas turbine airstream might potentially provide a means of protecting the turbine sections from harmful solid combustion products species.

Aero-derivative gas turbine machinery that burns high grade kerosene gas-turbine fuels was initially introduced into the marine, industrial and stationary power generation fields. Greater application of advanced aero-derivative gas turbine technology by the stationary power generating industry, using systems having capabilities of cleanly burning low emission natural gas, heavy oil, and/or coal resources, provides benefits beyond simply augmenting peak load. Unique land-based burner-fuel combinations provide

Increasing fuel alternatives utilization
Increasing utility power output
Increasing thermal efficiencies
Increasing plant flexibility and operability
Increasing flexibility in design

Figure 12.5 illustrates possible arrangements of advanced gas turbine technology based on use of fuel alternatives. In one combined cycle configuration a steam generator, such as a FBC coal combustor, produces a gas product which can then be used as gas turbine fuel for firing in the gas turbine section of the combined plant. In another

combined cycle variation, a gas turbine burning a clean fuel such as natural gas can then use the turbine exhaust gas with supplementary firing as the heat source in the heat recovery boiler section of a combined plant.

Hydrogen's characteristics as a potential long-term fuel resource were considered in Chapter 8. Several properties make hydrogen an attractive prospect as a long-term aviation fuel replacement, including:

Considerably higher specific energy than kerosene fuels
Atomization and vaporization not required if burned as a gas
Good heat sink to help cool engine parts if stored as a liquid
Wide flammability range and high flame speeds, which are both compatible with small combustor designs
Absence of carbon lowers radiant heat loss, smoke, soot, and particulates
No formation of CO, CO_2, UHC
Absence of eroding or corroding containments
No carbon buildup on critical engine components

Note that any of the proposed alternative and/or synthetic turbine fuels, and any of their required system modifications, would still be required to meet the same performance and environmental conditions prescribed that present fuels must meet.

12.6 GAS TURBINE ENGINE EMISSIONS

The principal gas turbine combustion pollutants are carbon monoxide, unburned hydrocarbons, aldehydes, particulates, smoke, and oxides of nitrogen. Carbon monoxide is produced in the stoichiometric or slightly fuel-rich primary combustion zone and results from both incomplete combustion and carbon dioxide dissociation. Unburned hydrocarbons result from unburned fuel and fuel pyrolysis products that exit the combustor without being oxidized. Soot, produced in the primary zone and partially consumed in the secondary zone, is predominantly carbon. Soot formation is a function of fuel structure, with aromatics more prone to soot than paraffin compounds. Smoke emissions contain exhaust soot, water vapor, and hydrocarbon vapors. Conditions that contribute to the production of CO, UHC, and PM include poor fuel atomization and fuel cracking. Oxides of nitrogen such as nitric oxide NO result from three sources: oxidation of the dissociated atmospheric nitrogen, chemical kinetic nitric oxide, and oxidation of fuel nitrogen. Nitrogen dioxide NO_2 is also produced within the combustor, and the total NO_x emission from a gas turbine consists of both NO and NO_2.

Note that pollution control strategies and approaches for gas turbines used in land- and/or marine applications may be very different than for aircraft usage, especially where weight and geometry are driving considerations in the overall engine design envelope. The combustor and its configuration in which low emission reactions are to be achieved is thus the important component in gas turbine emissions control. At a Workshop on Research Needs for Air Quality Compliance for Diesels, Turbines and Ordnance in 1999, Dr. Mel Roquemore from the Air Force Research Laboratory at Wright-Patterson Air Force Base reported that approaches to emissions control have been divided into two broad types: (1) those that may be applied to conventional-appearing combustors and

(2) those that result in non-conventional-appearing combustors. Under each type of combustor, control strategies have been grouped into general categories. For conventional-appearing combustors the general categories have been separated into those affecting emissions of CO and UHCs and those affecting emissions of NO_x. Unconventional combustors have been separated by geometric characteristics for convenience.

Dramatic reductions have been achieved in idle-power CO emissions by increasing the equivalence ratio in the primary zone of the combustor where the flame is held. This action increases the bulk flame temperature and results in improvements in combustion efficiency. Studies have shown CO emissions can also be lowered by improving liquid fuel spray evaporation through enhanced atomization and by intensifying fuel/air mixing. These activities can be difficult to accommodate in practice with operating gas turbine combustor cans. Increasing the pressure drop across a combustor, for example, can enhance air turbulence but promotes adverse impacts on overall engine performance.

Low engine power conditions will discharge unburned hydrocarbons (UHCs) which are primarily unreacted and partially reacted fuel. These UHCs remain entrained in liner cooling air film and exit the combustor frozen within this relatively cool air flow. The reason fuel enters cooling films at low engine power conditions is due chiefly to the conventional recirculation pattern that stabilizes flames in the primary zone. Eliminating the liner film cooling air would largely resolve this particular UHC problem. Industrial power generation gas turbines, in fact, externally cool the liners of ultra-low emission combustors, an approach in the aircraft gas turbine case that is not viable under most circumstances. These UHC difficulties are being addressed by changing the conventional aircraft combustor using new recirculation patterns and with unconventional combustors.

Large amounts of NO_x are produced at high turbine engine power levels and at aircraft engine exhaust nozzle discharge. The NO_x consists mainly of nitric oxide (NO). Thermal NO, produced by the extended Zeldovich mechanism, discussed in Section 5.5 of Chapter 5, is a post-flame phenomenon driven by "time-at-temperature." Initial attempts at NO_x control tried to cut both "time" and "temperature" by shortening the combustor can to reduce residence time. However, with conventional burners having lean stoichiometric primary zones, major NO_x reductions could be achieved by shortening primary zone residence time. Shortening the combustor can to provide the greatest reductions in residence time, unfortunately, also dramatically reduced combustion efficiency to levels considerably less than 90% and also seriously impaired flame stability.

Water has a significant latent heat of vaporization and thereby offers the potential of being a heat sink and means of reducing flame temperatures. Significant NO_x reduction for turbine conditions requires considerable quantities of water flow. It is best to inject water directly into the flame region in the primary zone of the combustor to effectively benefit from the process and to avoid thermal damage to the combustor. The water has to be of boiler feed-water quality to avoid turbine system component failures. The mass added from injected water provides engine thrust augmentation, potentially helpful for hot, high take-offs. Of course, any aircraft would have to carry the additional dead weight of water tanks, supply, distribution, and controls, adding to the initial cost of the power plant and aircraft. Therefore, water injection would only be considered in aircraft application for use at take-off and climb where NO_x formation rates are the most significant. The cooling process provided by water injection has an adverse impact on CO emissions at high engine power levels.

The basic can burner geometry provides a reasonable efficiency of combustion and fuel economy, but meeting emission requirements, even for land-based operations, cannot

be easily achieved by making simple geometric adjustments to the configuration. Any simple action taken in the primary zone to alleviate CO, UHC, and soot, such as stoichiometry and reaction temperature shifts, opposes those efforts that would reduce NO_x. Non-traditional thinking regarding fuel-engine emission issues will be needed in order to fulfill the combustor functions as well as to reduce overall emissions of CO, UHCs, and PM while keeping thermal NO down.

Emission control strategies, such as those used in industrial power generation gas turbines, are not viable to the aircraft gas turbine because of their different operating conditions, the severity of these conditions, and considerations of overall engine reliability and safety that cannot be compromised in the aviation world. Efforts are ongoing to try and introduce new materials having potentials that can help reduce cooling air requirements and allow freedom for shaping the combustor. Development of staged combustion, either through controlled airflow or fuel flow, which can provide more flexibility to conventional-appearing combustors and non-conventional-appearing combustors, is an ongoing activity at government, academic, and industrial centers of excellence.

12.7 THE FREE PISTON AND STIRLING ENGINES

Future combustion science and engine technology will arise from the various machines and mechanisms discussed in the last three chapters. Two unique engine concepts that illustrate how combustion engine characteristics can be categorized in such a manner are the *free piston engine* and the *Stirling engine.* A free piston engine, shown in Figure 12.6, incorporates features of both IC engine combustion and gas turbine power output. A Stirling engine, illustrated in Figure 12.7, combines gas turbine continuous combustion and reciprocating IC engine power output.

The free piston engine is actually a diesel combustion engine gasifier that incorporates a gas turbine expander for power output. A special piston design, consisting of a large compression piston at one end and a small but integral gas expansion piston at the other end, is basic to successful operation of this unique opposed-piston diesel configuration. Two of these special pistons are needed, and they are arranged so that the smaller pistons face inward toward each other. Both large pistons serve a twofold purpose: the inner face is utilized to compress air, and the outer piston face to work with a special closed air-bounce chamber.

One mechanical cycle of a free piston engine begins with air compression. With transfer ports uncovered, air is compressed and moved into a clearance volume defined by the opposed gas expansion pistons. During compression, engine intake and exhaust gas valves are all closed. By the end of compression, air transfer ports are covered by the pistons, and combustion air is centered within the engine. This process helps to scavenge and supercharge this two-stroke type of diesel combustion air. Fuel injection into the high-pressure and high-temperature air results in compression-ignition combustion, with ensuing gas expansion against both small gas expansion pistons. During gas expansion, exhaust ports are exposed, allowing high-pressure gases to expand through a power turbine wheel to produce useful power output. Expansion of the small gas cylinders drives the large compression pistons apart, compressing air trapped in the bounce chambers which, in turn, force the piston assemblies back toward center and thus begin the mechanical cycle again. Exhaust and air intake valves are open while the exhaust

gases expand through the turbine, and a new supply of air is drawn into the engine. Since there are no connecting rods or crankshafts, the pistons are kept in place by means of connecting linkages.

Successful engines must find a niche in which they can provide a viable answer to a real need. In this regard, the free piston engine has not found a suitable application, in part because of the following:

Fixed costs too high to pay for efficiency gains
Mechanical problems associated with starting and control during operation
Synchronization of the pistons in single units and multiunits

The Stirling engine, a positive-displacement engine with external heat addition, was developed by Dr. Robert Stirling, a Scottish clergyman, in 1816, approximately 80 years before the diesel. A Stirling engine is considerably more complex than SI and/or CI IC engines. In its original geometry, two separate cylinders having relatively small communicating passageways were required to run. This path was filled with a wire coil or mesh to allow the region to act as a regenerator when the working fluid was displaced from one cylinder to the other by the pistons. Stirling engines operate as closed loops using a gas, such as helium and/or hydrogen, and therefore require indirect external heating to produce useful power. It is this separation of fuel-air chemistry from events occurring within the engine that allows continuous combustion to be utilized.

A variety of fuels are potentially compatible with Stirling engine combustion, including diesel fuel, unleaded gasoline, alcohol, kerosene, butane, propane, and natural gas. During the 1970s, the U.S. Department of Energy supported pilot projects to stimulate the development of new engine technologies that would be 30% more efficient than the conventional mobility power plants, meet the 1985 federal emissions standards, be capable of burning a wide variety of fuels, and be cost-competitive with standard production engines. Stirling engines were considered by many at that time as a strong candidate to meet those criteria.

The ideal thermodynamic events required for a Stirling engine to produce useful power are as follows:

1–2 $T = c$ Heat rejection during isothermal compression in cylinder 1
2–3 $v = c$ Internal regenerative heat transfer (gain) during flow between cylinders 1 and 2
3–4 $T = c$ External heat addition during isothermal expansion in cylinder 2
4–1 $v = c$ Internal regenerative heat transfer (loss) during flow between cylinders 2 and 1

Cycle performance is strongly influenced by the regenerator heat exchanger design and high effectiveness necessary to return energy from gases during the process 4–1 to the gases during the process 2–3. Mechanical and thermal losses penalize this machine and prevent it from making a breakthrough and finding a general commercial application. The actual P-v diagram from current Stirling engines departs considerably from the ideal processes, yet the maximum operating efficiencies can exceed those for comparable SI and CI engines. This regenerative machine for the ideal events, i.e., $T = c$ heat transfer, would approach the efficiency of the Carnot cycle, the most efficient thermodynamic cycle described in Chapter 1.

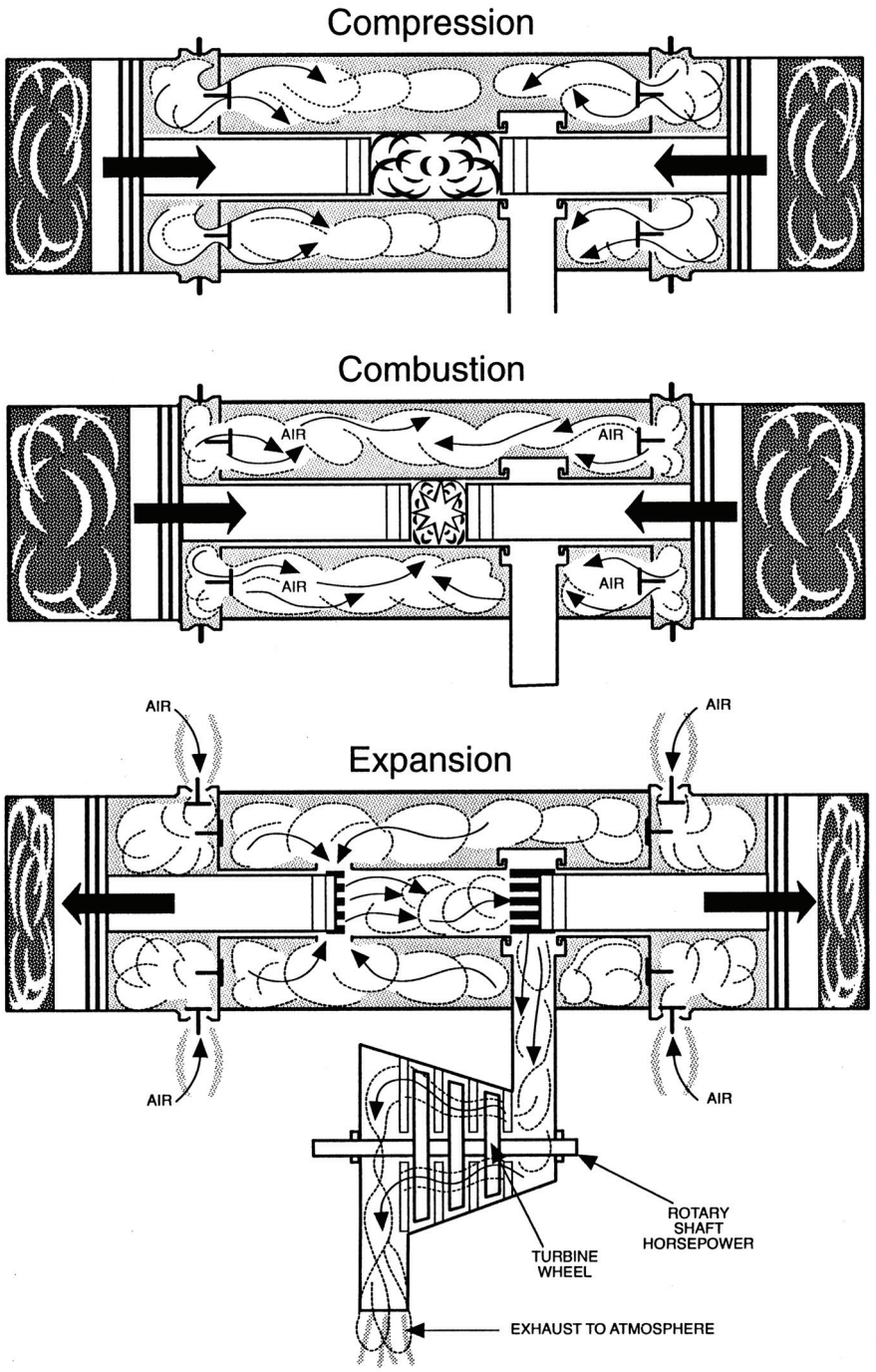

Figure 12.6 The free piston engine. Adapted from Tolboldt, B., *Diesel Fundamentals: Service, Repair*, Goodheart-Willcox, South Holland, Illinois, 1983. With permission.

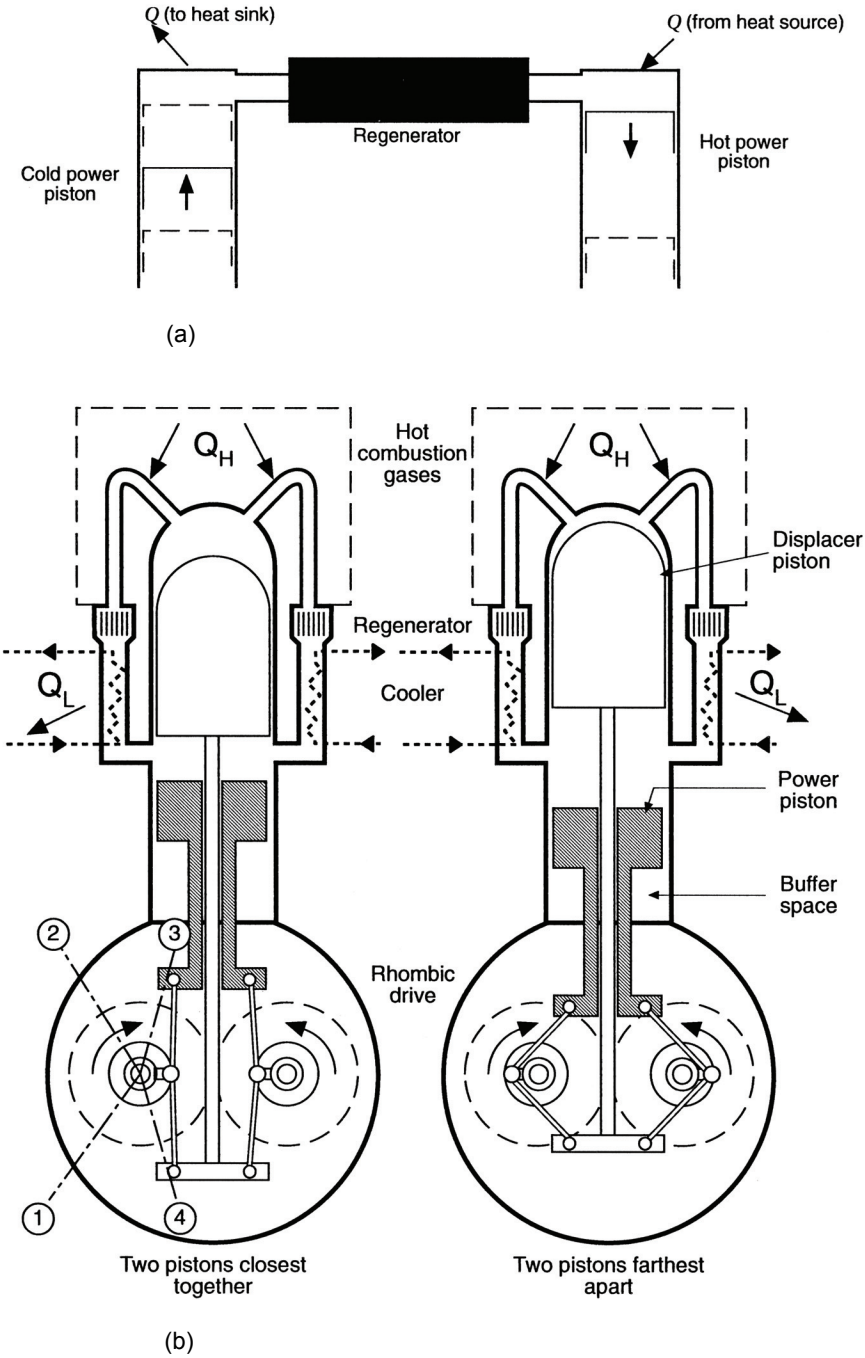

Figure 12.7 The Stirling engine: (a) ideal Stirling cycle engine; (b) practical Stirling cycle engine. After Wood, B. D., *Applications of Thermodynamics*, 2nd Edition, Addison-Wesley, Reading, Massachusetts, 1982.

The advantages of a Stirling engine include:

Decoupling of fuel-air combustion from engine operation
Low emissions (continuous combustion)
Multifuel
Improved fuel economy over Otto cycle
Quiet, low-vibration engine
High thermal efficiency
Can operate with a pressurized burner

The disadvantages of a Stirling engine include:

Complex heat transfer engine
Bulky (50% volume is heat transfer equipment)
Expensive
Seals and gas leakage
Hydrogen leaks and embrittlement
Questionable durability

PROBLEMS

12.1 Repeat Example 12.1 for (a) a monatomic gas, $\gamma = 1.67$; (b) $\gamma = 1.3$; and (c) $\gamma = 1.2$.

12.2 A gas turbine power plant burns a hydrocarbon fuel having an unknown composition. To determine the fuel composition, a sample is burned in air, and the Orsat analysis of the products of combustion yields 10.5% CO_2, 5.3% O_2, and 84.2% N_2. For this fuel, estimate (a) the mass composition of the fuel, % C and % H; (b) the percent of excess air for this reaction, %; and (c) the overall chemical formula, C_xH_y.

12.3 A blend of liquid ethanol and methanol is being proposed as a potential stationary gas turbine fuel alternative. If the fuel mixture consists of 25% ethanol–75% methanol by weight, determine (a) the fuel mixture density at 60°F, lbm/ft^3; (b) the fuel mixture specific gravity at 60°F; (c) the stoichiometric *FA* ratio, lbm fuel/lbm air; and (d) the fuel lower heating value, Btu/gal.

12.4 A propulsion gas power turbine has inlet conditions of 1,440°R and 30 psi, with a discharge temperature of 1,260°R. The burner can exhaust gas composition on a molar basis is 3.6% CO_2, 3.6% H_2O, 16.0% O_2, and 76.8% N_2. For a turbine inlet volumetric flow rate of 119,450 ft^3/min, find (a) the exhaust gas molecular weight, lbm/lbmole; (b) the turbine inlet mass flow rate, lbm exhaust gases/min; (c) the total enthalpy change across the turbine, Btu/lbmole; and (d) turbine power, hp.

12.5 An adiabatic propulsion turbine has the following operational data: inlet conditions $P_3 = 1{,}175$ kPa, $T_3 = 1{,}100$K, $\dot{m} = 66$ kg/sec; discharge conditions $T_4 = 700$K, gas composition (by volume) 6.57% CO_2, 7.12% H_2O, 10.13% O_2, 76.18% N_2. For these conditions, determine (a) the gas mixture molecular weight, kg/kg mole; (b) the gas inlet volumetric flow rate, m^3/sec; (c) the turbine specific work, kJ/kg gas; and (d) the indicated turbine power output, kW.

12.6 Marks' *Handbook* gives an empirical equation for the *LHV* of fuel oils that may be expressed as

$$LHV = 19{,}960 + 1{,}360\ \text{SG}\ \langle 60/60 \rangle - 3{,}780\ \text{SG}^2 \langle 60/60 \rangle \text{ Btu/lbm}$$

Estimate the *LHV* of kerosene having a specific gravity of 50°API gravity using (a) the empirical equation; (b) the relationship in Chapter 7 given by Equation 7.5b; and (c) the tabulated values found in Appendix C.

12.7 The following data are obtained from the test of a gas turbine burner:

Fuel	$(C_4H_{10})g$ at 77°F and 1 atm
Oxidant	300% theoretical air at 77°F and 1 atm
Products	1,160°F and 1 atm
Inlet air velocity	200 ft/sec
Discharge gas velocity	2,200 ft/sec

Assuming complete combustion, determine (a) the net heat transfer per mole of fuel, Btu/lbmole; and (b) net increase in entropy per mole of fuel, Btu/lbmole·°R.

12.8 A fuel with an H/C ratio of 0.16 is burned in a combustor with an *FA* ratio of 0.02 lbm fuel/lbm air. The fuel temperature enters the can at 100°F, and the air inlet temperature is 290°F. The *LHV* of the fuel is 18,500 Btu/lbm, and the specific heat of the fuel is 0.5 Btu/lbm·°R. Calculate (a) the adiabatic or ideal temperature rise across the burner, °F; (b) the ideal temperature entering the turbine, °F; and (c) the combustion efficiency if the actual turbine inlet temperature is 1,995°R, %.

12.9 Liquid C_8H_{18} has a lower heating value at constant pressure of 19,100 Btu/lbm at 68°F. Estimate the product temperature if 60.4 lbm of air at 440°F is supplied to a gas turbine combustion chamber for each pound of liquid C_8H_{18} supplied at 120°F. The specific heat of the fuel is 0.5 Btu/lbm·°R, and the combustion losses are estimated to be 5% of the *LHV* of the fuel.

12.10 JP5, a power kerosene used in military jet aircraft, is burned in a gas turbine combustor at 1,000 kPa. The fuel has an API specific gravity at 15°C of 42 and is supplied to the burner with 400% theoretical air. For ideal complete combustion, find (a) the *FA* ratio, kg fuel/kg air; (b) the exhaust gas molecular weight, kg/kgmole; (c) the exhaust dew point temperature, K; (d) the fuel density at 15°C, kg/m^3; and (e) the fuel *LHV* at 15°C, kJ/kg fuel.

12.11 A gas turbine engine having a 34% brake thermal efficiency develops 450-hp net brake power output. The unit burns a distillate fuel having a specific gravity at 60°F of 0.81. Find (a) the fuel specific gravity at 60°F, API; (b) the fuel density at 60°F, lbm/ft^3; (c) the fuel consumption, gal/hr; and (d) the brake specific fuel consumption, lbm/hp·hr.

12.12 Repeat Example 12.3 using hydrogen as the fuel.

12.13 Repeat Example 12.3 using methanol as the fuel.

12.14 Supercharging is a means of boosting power output from an IC engine by admitting air at a density greater than ambient. One version uses hot exhaust gases from the engine to drive a turbine which, in turn, powers a supercharging compressor. This simple gas turbine with no net power output is termed a constant-pressure turbocharger. Consider such a unit having compressor and turbine conditions as given below:

Turbine:	Compressor:
$T_{in} = 990K$	$T_{in} = 300K$
$T_{out} = 995K$	$P_{in} = 101$ kPa
$P_{out} = 101$ kPa	$\dot{m}_{turbine} / \dot{m}_{compressor} = 1.05$
$r_p = 1.18$	

Neglecting turbomachinery and mechanical efficiencies and assuming air to represent the gas mixture passing through both components, calculate for this operating condition (a) the turbine work output per unit mass flowing, kJ/kg; (b) the compressor boost discharge temperature, K; (c) the compressor boost discharge pressure, kPa; and (d) the turbocharger boost, i.e., density ratio across the compressor.

12.15 A natural gas supply is reported as follows:

$CH_4 = 74.0\%$, $C_2H_4 = 20.6\%$,
$CO_2 = 0.5\%$, $O_2 = 0.3\%$, $N_2 = 4.6\%$

The gas is used as a fuel for a gas turbine in a pipeline pumping station. For this fuel, determine (a) the combustion equation for complete reaction of this gas with 400% theoretical air; (b) the *FA* ratio, lbm fuel/lbm air; (c) the product molecular weight, lbm/lbmole; (c) the adiabatic temperature if the gas enters at 536°R and the air enters at 900°R, °R; and (d) the actual discharge temperature if the combustion chamber has a combustion efficiency of 95%, °R.

12.16 A combustion chamber is supplied with octene, C_8H_{16}, at 77°F and air at 720°R. Exhaust gas analysis of the stack gases generates the following reaction equal for the unit:

$$C_8H_{16} + 48.0O2 + 180.5N_2 \rightarrow 7.6CO_2 + 7.4H_20 + 180.5N_2 + 36.6O_2 + 0.2CO + 0.2H_2 + 0.2CH_4$$

If heat losses from the combustion can are negligible, estimate the combustion efficiency.

12.17 An open cycle gas turbine plant is designed to deliver 4000 bhp under the following conditions:

Atmospheric temperature	80.3°F	Peak temperature	1,400°F
Atmospheric pressure	14 psia	Compressor efficiency	80%
Pressure ratio	5:1	Turbine efficiency	84%
Pressure drop in		Mechanical efficiency	90%
combustion can	5 psi	Fuel *LHV*	18,000 Btu/lbm

Use a variable specific heat analysis for the compressor and turbine and the isentropic tables for air found in Example 3.2. Calculate (a) the internal state points through the unit; (b) the compressor power, ihp; (c) the turbine power, ihp; and (d) the fuel consumption, lbm/hr.

12.18 Clean gasified coal gas having the following molar composition is burned in a gas turbine with 380% theoretical air:

$H_2 = 47.9\%$, $CH_4 = 33.9\%$, $C_2H_4 = 5.2\%$
$CO = 6.1\%$, $CO_2 = 2.6\%$, $O_2 = 0.6\%$, $N_2 = 3.7\%$

Determine the *AF* ratio, m^3 air/m^3 fuel; (b) the *FA* ratio, kg fuel/kg air; (c) mole fractions for the ideal products of combustion; and (d) the molecular weight for the dry products of combustion, kg/kgmole.

12.19 A blend of liquid ethanol and methanol is being proposed as a prospective gas turbine fuel. The fuel mixture would consist of 25% ethanol–75% methanol by weight. Determine the following for these conditions: (a) the fuel mixture density, lbm/ft^3 @ 60ºF; (b) the fuel mixture specific gravity @ 60ºF; (c) the stoichiometric *FA* ratio, lbm fuel/lbm air; and (d) the fuel *LHV*, Btu/gallon.

12.20 A turbojet engine is designed for a speed of 400 mph at 30,000 ft. Intake air is diffused isentropically from a relative velocity of 400 mph at the diffuser inlet to zero velocity at the diffuser exit. Air is then compressed isentropically in a compressor having a pressure ratio of 4. Octane, C_8H_{18}, is introduced into the combustor at a temperature of 540°R and 25% theoretical air. The constant-pressure adiabatic combustion process in the burner goes to completion with negligible dissociation. The products then expand isentropically through a turbine such that power output is equal to the required compressor power input. Exhaust gases then expand through a nozzle reversibly and adiabatically to atmospheric pressure. Use a variable specific heat analysis for the compressor and turbine and the isentropic tables for air found in Example 3.2. Calculate (a) the isentropic compressor discharge temperature, °R; (b) the compressor work, Btu/lbm; (c) the adiabatic flame peak combustor temperature, °R; (d) the turbine discharge temperature, °R; and (e) the nozzle discharge velocity, ft/sec.

12.21 The preliminary design for a 150 MW closed cycle gas turbine power plant is to be made. A coal-fired furnace is proposed to indirectly heat the compressed air discharge using a high temperature heat exchanger. A portion of the turbine gas discharge, using a second heat exchanger, allows exhaust to preheat the combustion air supplied to the furnace. Conditions for the plant are given as follows:

compressor pressure ratio = 12
compressor inlet temperature = 95ºF
compressor inlet pressure = 14.5 psi
compressor efficiency = 88%
turbine inlet temperature = 2,190ºF
turbine efficiency = 91%
flue gas averge $C_p = 0.25$ Btu/lbm·ºR
furnace exhaust temperature = 3,270ºF
flue gas volume = 219.5 ft^3/lbm coal
LHV coal = 13,450 Btu/lbm
furnace efficiency = 0.96

Using a constant specific heat analysis determine the following: (a) the net cycle work, Btu/lbm air; (b) the mass flow of fuel, lbm fuel/min; (c) the cycle thermal efficiency, %; and (d) the heat exchanger gas exit temperature, ºF.

12.22 A natural gas supply is to be used as a low emission fuel source for a peak load gas turbine generator. The gas composition is reported as follows:

$CH_4 = 84.2\%$, $C_2H_4 = 12.5\%$,
$CO_2 = 0.8\%$, O_2 0.2%, $N_2 = 2.3\%$

Fuel enters the combustor at 77ºF while combustion air from the compressor enters the combustor at 465ºF. For 400% theoretical air determine: (a) the compressor pressure ratio for *STP* compressor inlet conditions; (b) the *FA* ratio, lbm fuel/lbm air; (c) the adiabatic flame temperature, ºR; and (d) the mass of water formed per mass of air, lbm H_2O/lbm air.

13

Thermal Destruction

13.1 INTRODUCTION

In earlier chapters, critical fuel-engine interface aspects of important combustion driven heat/power technologies were considered. In this last chapter, attention will be given to fuel-engine issues related to methods and machines being utilized and under development for thermally destructing various waste forms that are generated and discarded in today's industrial societies. Thermal destruction technologies are receiving greater attention now that more emphasis is being placed on the environmentally acceptable disposal of items such as municipal solid waste, by-products from manufactured goods, and hazardous materials.

Wastes with significant organic content are generally considered most appropriate for thermal destruction. Composition and volume reduction occur via high-temperature, thermal-oxidation chemistry in excess of 900ºC (1,650ºF). *Incineration* is the historical engineering field associated with the design and development of thermal-decomposition technology used in the destruction of the organic fraction of waste. Functional characteristics for a variety of thermal destruction systems, including traditional incinerators, can be grouped within the four major subsystems illustrated in Figure 13.1 which include:

Waste preparation and feed
Combustion chamber(s)
Air pollution control
Residue/ash handling

Chapter 13 provides a limited introduction and overview of the broad field of thermal destruction of waste. General thermochemical and reactive characteristics, basic combustion processes, and related issues associated with waste reduction will be discussed. Configurations utilized to achieve specific conversions will also be considered. An overview of general emissions and pollution characteristics of thermal destructors

will be presented along with corresponding air emissions regulations for these units. Advanced thermal destruction technology solutions to waste treatment that not only reduce organic content to benign products but, in addition, produce stable by-products from the inorganics will be briefly highlighted as well.

13.2 THERMAL DESTRUCTION COMBUSTION CHEMISTRY

The thermal destruction of solid waste, including municipal solid waste (MSW), medical waste, or commercial and industrial solid waste, that contains organic materials and moisture takes place in four stages: (1) drying of the material, (2) pyrolysis of the material, (3) gasification of the material, and (4) oxidation of the products. The combustion of liquid organic containing waste requires evaporization of the feed prior to thermal destruction. Any inorganic portion in waste, such as minerals, stones, ceramics, metals, and glass found in solid waste, substantially constitute to residue that remains after thermal destruction of the original material.

Pyrolysis, the first waste destruction stage, is preceded only by drying in solid waste processing and vaporization in liquid waste processing. Recall from earlier chapters that pure pyrolysis, or destructive distillation, is an irreversible chemical change in reactants brought about by the effect of heating in an oxygen-deficient reactive atmosphere. Pyrolysis is an endothermic reaction process in which the thermal decomposition of organic material results in formation of condensable and noncondensable gases as well as solid residue. The products of pyrolytic chemical reactions of solid waste can be solid (char), liquid, or gas. The amount of gas, liquid, and solid formed depends upon the various ongoing processes during pyrolysis. Among other parameters, temperature has a dominant effect in pyrolysis processes.

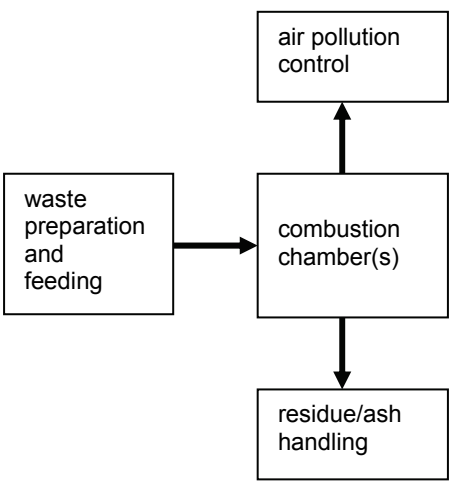

Figure 13.1 Functional elements of thermal destruction.

Gasification is a thermochemical process in which organic substances are converted into combustible gases with the aid of air, oxygen, CO_2, steam, hydrogen or a mixture of these gases. Gasification of solid waste material has an advantage over simple pyrolysis, since it promotes the further reduction of char and conversion to gas thus further reducing the volume of remaining solid residue and thereby releasing the chemical energy available in the char. Gasification is a heterogeneous solid-gas reaction composed of four steps: absorption of the gaseous reactants (gasifying agents) onto the carbon surface; chemical reaction between the absorbed gases and solid material; chemical reaction between the absorbed gas; and desorption of the gaseous products. As an example, during gasification the following principal reactions occur:

$$C + O_2 \rightarrow CO_2$$
$$C + CO_2 \rightarrow 2CO$$
$$C + H_2O \rightarrow CO + H_2$$
$$C + 2H_2 \rightarrow CH_4$$
$$CO + H_2O \rightarrow CO_2 + H_2$$

Thermal destruction promotes reduction in final volume and composition of waste products resulting from pyrolysis and gasification and occurs via oxidation in air in excess of 900°C (1,650°F). Conventional incineration requires equipment to operate at high reaction temperatures, large excess air levels, and long material residence times to complete the destruction process. The overall waste conversion process, i.e., pyrolysis, gasification, as well as oxidation, is accomplished by the dynamics of chemical kinetics introduced in Chapter 5. Chemical transformations occur over time and space throughout the various thermal destruction stages involving both homogeneous and heterogeneous high temperature chemical kinetic reactions. Particular C/H/N/O elementary reactions and chemical kinetic mechanisms can play important roles during specific stages of reduction conversion and post chemistry processes during overall waste destruction.

EXAMPLE 13.1 A waste destruction unit is selected for processing chlorobenzene, C_6H_5Cl. The air-fuel mixture enters the destructor at 25ºC and 101 kPa. The mixture enters the burner at *STP* and 150% theoretical air. For complete combustion, calculate (a) the reaction equation for ideal thermal destruction; (b) the molar $\overline{FA}$ ratio for the reaction, kgmole fuel/kgmole air; (c) the mass of HCl produced per mass of waste burned, kg HCl/kg waste; and (d) an excess air reaction in which the products of combustion contain 7% oxygen by volume.

Solution:

1. Stoichiometric equation for ideal combustion of chlorobenzene in oxygen:

$$C_6H_5Cl + aO_2 \rightarrow bCO_2 + cH_2O + dHCl$$

carbon atom balance	$6 = b$	$b = 6$
chlorine atom balance	$1 = d$	
hydrogen atom balance	$5 = 2c + d$	$c = 2$
oxygen atom balance	$2a = 2b + c$	$a = 7.0$

2. Stoichiometric equation for ideal combustion of chlorobenzene in air:

$$C_6H_5Cl + 7[O_2 + 3.76N_2] \rightarrow 6CO_2 + 2H_2O + HCl + 7(3.76)N_2$$

3. Actual reaction equation for ideal combustion of chlorobenzene in air:

$$C_6H_5Cl + (1.5)(7)[O_2 + 3.76N_2] \rightarrow 6CO_2 + 2H_2O + HCl + (0.5)(7)\,O_2 + (0.5)(7)(3.76)N_2$$

4. Molar $\overline{AF}$ ratio

$$\overline{AF} = \frac{(1.5)(7)(4.76)}{(1)} = 49.98$$

5. The molar $\overline{FA}$ ratio

a. $\overline{FA} = 1/\overline{AF} = 0.02$ kgmole fuel/kgmole air

6. Mass of HCl formed per unit mass of waste destructed.

From reaction equation, one mole of HCl is formed for every mole of C_6H_5Cl destroyed or

b. $$m_{HCl} = \frac{(1.0\text{kgmole HCl})(36\,kg\text{ HCl / kgmole HCl})}{(1\,\text{kgmole waste})(112\,\text{kgmole HCl})} = 0.321\text{kg HCl/kg waste}$$

7. Products for 7% O_2

$$C_6H_5Cl + (a)(7)[O_2 + 3.76N_2] \rightarrow n_1CO_2 + n_2H_2O + n_3HCl + n_4O_2 + 3.76(7+ n_4)N_2$$

where

$n_1 = 6$
$n_2 = 2$
$n_3 = 1$
$N_{tot} = 6 + 2 + 1 + n_4 + 3.76\cdot(7+n_4) = 35.32 + 4.76\cdot n_4$

and the 7% mole fraction of O_2 yields

$$\bar{x}_4 = 0.07 = n_4/(35.32+4.76\cdot n_4)$$

or

$0.07\cdot(35.32+4.76\cdot n_4) = n_4 \qquad n_4=3.708$
$N_{tot} = 6 + 2 + 1 + 3.708 + 3.76\cdot(7+3.708) = 52.97008$
$\bar{x}_1 = 6/52.97008 = 0.113271$
$\bar{x}_2 = 2/52.97008 = 0.037757$
$\bar{x}_3 = 1/52.97008 = 0.018879$
$\bar{x}_4 = 3.708/52.97008 = 0.070002$
$\bar{x}_5 = (3.76\cdot(7+3.708))/52.97008 = 0.760091$

where

$$\bar{x}_1 + \bar{x}_2 + \bar{x}_3 + \bar{x}_4 + \bar{x}_5 = 0.113271 + 0.037757 + 0.018879 + 0.070002 + 0.760091 = 1$$

reaction oxygen atom balance

$$7a = 6 + 1 + 3.078 \qquad a = 10.078/7 = 1.4397$$ or

d. 43.97% excess air

Comment: Waste destruction often involves C/H/O/Cl/S chemistry which influences the ideal products of combustion and overall stoichiometry. One does not simply form CO_2 and H_2O. In addition, actual emission measurements are often corrected to a 7% O_2 dry volume basis for regulatory considerations.

A complete compositional characterization of any particular thermally treated waste stream would require specification of all organic and inorganic feed constituents, often expressed in terms of an ultimate analysis. For single toxic waste compounds such as benzene (C_6H_6), toluene (C_7H_8), or chlorobenzene (C_6H_5Cl), this information is straightforward. In other instances, such as for MSW, the waste stream definition must be based on statistical measurements of the feed with recorded attributes depending on local waste factors such as regional and seasonal aspects as well as sampling size. Recall from Chapter 6 the use of a proximate analysis which was found to be sufficient for engineering consideration to define a solid fuel's combustion characteristics in terms of a measured sample value of combustibles, volatile fraction, moisture, and ash. From a proximate analysis, a great deal of insight can be obtained into the relative energetics associated with the various stages of thermal destruction of a solid waste and/or sludge, i.e., vaporization, pyrolysis, gasification, and oxidation.

EXAMPLE 13.2 A simplified surrogate representation of a municipal solid waste stream is given below with overall material characteristics of the feed provided on a weight basis.

Constituent	Percentage	Surrogate	Formula	Heat of formation
organics	40	cellulose	$C_6H_{10}O_5$	–229,700
plastics	22	polystyrene	C_8H_8	+8,000
moisture	18	water	H_2O	–68,317
noncombustibles	20	—	—	—
	%	compound		cal/gmole

For ideal *STP* stoichiometric combustion of the surrogate materials, calculate: (a) the ashless molar air-fuel ratio, kgmole air/kgmole ashless waste; (b) the actual mass air-fuel ratio, kg air/kg waste; (c) the higher heating value of the waste predicted using DuLong's formula, kJ/kg waste; and (d) the higher heating value of the waste using JANAF data, kJ/kg waste.

Solution:

1. The mass fractions for each constituent of the surrogate waste:

cellulose

Component	N_i	$\bar{x}_i$	MW	$\bar{x}_i MW_i$	mf_i
Cs	6	0.44444	12.0110	5.33817	0.44444
H_2	5	0.37037	2.0160	0.74667	0.06217
O_2	2.5	0.18519	32.0000	5.92608	0.49339

$$\bar{x}_i = \frac{N_i}{\sum N_i} = \frac{6}{13.5} = 0.44444 \qquad mf_i = \frac{\bar{x}_i MW_i}{\sum \bar{x}_i MW_i} = \frac{5.33817}{12.0181} = 0.44444$$

polystyrene

Component	N_i	$\bar{x}_i$	MW_i	$\bar{x}_i MW_i$	mf_i
Cs	8	0.5	12.0110	6.0055	0.85628
H_2	8	0.5	2.0160	1.008	0.14372
O_2	0	0.00000	32.0000	0.00000	0.00000

water

Component	N_i	$\bar{x}_i$	MW_i	$\bar{x}_i MW_i$	mf_i
Cs	0	0.00000	12.0110	0.00000	0.00000
H_2	1	0.66667	2.0160	1.34401	0.11190
O_2	0.5	0.33333	32.0000	10.6666	0.88810

2. The ashless representation of the surrogate waste stream on a weight basis:

Component	%		Cs	H_2	O_2
cellulose	40	0.5	0.44444	0.06217	0.49339
polystyrene	22	0.275	0.85628	0.14372	0.00000
water	18	0.225	0.00000	0.11190	0.88810
ash	20	–	–	–	–
mixture			0.45770	0.09578	0.44652

3. The waste composition of the surrogate waste stream on a mole fraction basis:

Component	mf_i	mf_i	MW_i	mf_i / MW_i	$\bar{x}_i$
cellulose	0.40	0.500	162	0.003086	0.16930
polystyrene	0.22	0.275	104	0.002644	0.14504
water	0.18	0.225	18	0.0125	0.68566
ash	0.20	–	–	–	0.00000

$$\sum mf_i / MW_i = 0.18231$$

$$MW = 1/\sum mf_i / MW_i = 1/0.18231 = 54.85268 = 54.853$$

4. Stoichiometric equation on an ashless basis per mole of mixture of waste is

$$[0.1693\ C_6H_{10}O_5 + 0.14504\ C_8H_8 + 0.68566\ H_2O] + a[O_2 + 3.76N_2] \rightarrow bCO_2 + cH_2O + dN_2$$

Carbon atom balance:

$$6\cdot(0.1693) + 8\cdot(0.14504) = b \qquad b = 2.17612$$

Hydrogen atom balance:

$$10\cdot(0.1693) + 8\cdot(0.14504) + 2\cdot(0.68566) = 2c \qquad c = 2.11232$$

Oxygen atom balance:

$$5\cdot(0.1693) + 0.68566 + 2a = 2(2.17612) + 2.11232$$

$a = 2.4662$

Nitrogen atom balance:

$d = (2.4662)(3.76) = 9.2729$

5. Ashless waste molar air-fuel ratio:

$$\overline{AF} = \frac{(2.4662)(4.76)\ \text{kgmole air}}{1.0\ \text{kgmole ashless waste}}$$

$$\text{a.} = 11.3791\ \text{kgmole air / kgmole ashless waste}$$

6. Ashless waste mass air-fuel ratio;

$$AF = \frac{(11.3791\ \text{kgmoles air})(28.97\ \text{kg / kgmole air})}{(1.0\ \text{kgmole ashless waste})(54.853\ \text{kg/kgmole ashless waste})}$$

$$= 6.2\ \text{kg air/kg ashless waste}$$

7. Actual waste mass air-fuel ratio:

$$AF = \frac{(6.2\ \text{kg air/kg ashless waste})(100 - 20\ \text{kg ashless waste})}{(100\ \text{kg waste})}$$

b. $= 4.96\ \text{kg air/kg waste}$

8. MSW heating value based on DuLong's formula:

$$HHV = 33{,}960\,\text{C} + 141{,}890\left[\text{H} - \frac{\text{O}}{8}\right] + 9{,}420\,\text{S}$$

knowing the waste mixture ashless mass fraction analysis from step 2, the ashless higher heating value is

$HHV = 33{,}960(0.45770) + 141{,}890[(0.09578) - (0.44652/8)] + 9{,}420(0)$
$HHV = 21{,}214.13$ kJ/kg ashless waste

To determine the actual heating value:

$HHV = (21{,}214.13$ kJ/kg ashless waste$)(100 - 20$ kg ashless waste/100 kg waste)
c. $= 16{,}971.3$ kJ/kg waste

9. MSW heating value on an energy balance basis:

$$Q = \sum_{\text{prod}} N_i[\bar{h}_f{}^0 + \Delta\bar{h}]_i - \sum_{\text{react}} N_j[\bar{h}_f{}^0 + \Delta\bar{h}]_j$$

where at $STP\ \Delta\bar{h} = 0$ and

$$\sum_{\text{prod}} N_i[\bar{h}_f{}^0 + \Delta\bar{h}]_i = b[\bar{h}_f{}^0]_{CO_2} + c[\bar{h}_f{}^0]_{H_2O}$$
$$= 2.17612(-94{,}054) + 2.11232(-68{,}317)$$
$$= -348{,}980\ \text{cal/gmole waste}$$

and

$$\sum_{\text{react}} N_j[\bar{h}_f{}^0 + \Delta\bar{h}]_j = \sum_{\text{react}} \bar{x}_j[\bar{h}_f{}^0]_{\text{waste}}$$
$$= 0.1693(-229{,}700) + 0.14504(+8{,}000) + 0.68566(-68{,}317)$$
$$= -84{,}570\ \text{cal/gmole waste}$$
$HHV = H_p - H_r = (-348{,}980) - (-84{,}570) = -264{,}410$ cal/gmole waste

$$HHV = \frac{(-264{,}410)(4.187)\ \text{kJ/kgmole}}{(54.853\ \text{kg/kgmole})} = 20{,}182.8\ \text{kJ/kg ashless waste}$$

Again the actual heating value becomes

$HHV = (20{,}182.8$ kJ/kg ashless waste$)(100 - 20$ kg ashless waste/100 kg waste)
d. $= 16{,}146.2$ kJ kg waste

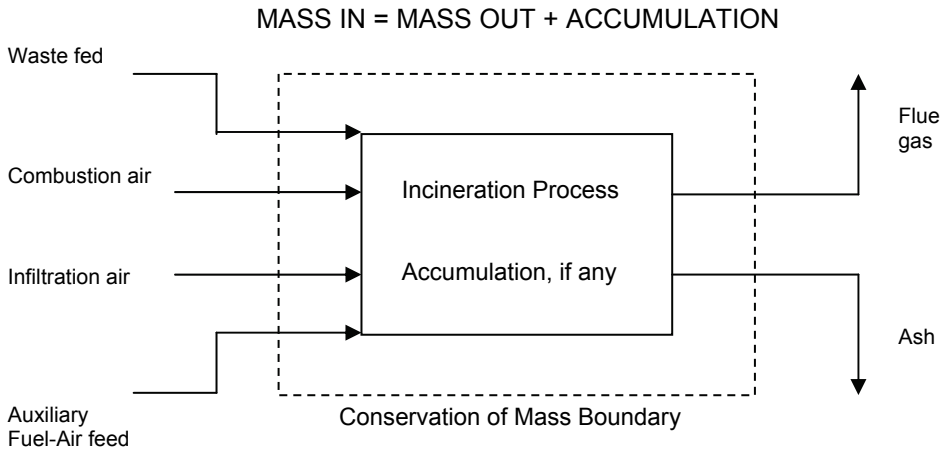

a) Mass Balance

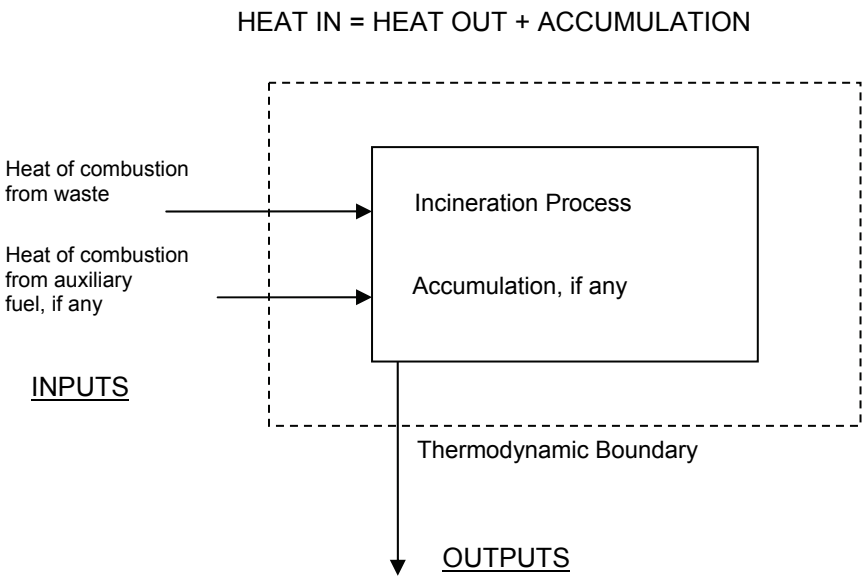

b) Energy Balance

Figure 13.2 Methods utilized for determining incineration performance. After Dan Banks, "Combustion Heat and Mass Balances," 2000 International Conference on Incineration and Thermal Treatment Technologies, Portland, OR, May 2000.

Thermal capacity of an incinerator, kW (Btu/hr), is calculated as the product of the average heating value of the waste being treated, kJ/kg (Btu/lbm), and the waste feed rate, kg/sec (lbm/hr). Heating value correlations other than the classic DuLong equation, which is a relationship based on coal chemistry and does not include atomic species such as Cl, are often needed for waste. Detailed thermal destruction performance characteristics are often based on incinerator mass or energy balances as illustrated in Figure 13.2.

Today, thermochemical analysis of complex waste streams is routinely accomplished with personal computers using spreadsheet and specific programs for design support of incineration and hazardous waste combustors. Excellent packages are available, such as material developed by W. R. Niessen that accompanies his text on combustion processes related to incineration, or the Hazardous Waste Incinerator Program (HWI) developed by Joseph Reynolds and Louis Theodore under sponsorship by the US EPA Air Pollution Training Institute, which is also a part of their hazardous waste incineration text.

Note, when obtaining destruction product compositions and temperatures under frozen and/or equilibrium conditions by performing First and Second Law thermochemical calculations as presented in this text, it is necessary to know heats of formation for waste constituents and use consistent thermochemical data. Sources such as the ASME *Combustion Fundamentals for Waste Incineration* provide enthalpies of formation for numerous organic and inorganic compounds which can be used for waste calculations in circumstances that contain those particular compounds. It is important also to recognize that waste destruction chemistry is more complex than identifying overall percentages of C/H/N/O atomic species in the waste and using complete combustion reactions. Processed material may range from being a simple individual species (compound), to a mixture of species (blends), to a material made up from compounds (composite structure), to mixtures of materials made up from numerous compounds (trash). Each type of waste described above, even if all theoretically had similar overall C/H/N/O atomic mass ratios and formed similar stable products of combustion, would have distinctly different dynamic destruction paths, energetics, and require different thermal destruction configurations.

13.3 BASIC ELEMENTS OF THERMAL DESTRUCTION

In an incinerator, as indicated previously, thermochemical and kinetic processes are occurring concurrently and chaotically throughout any thermal destructor including, to varying degrees, pyrolysis, gasification, as well as subsequent oxidation of evolved gases. Modern incineration technologies achieve destruction of waste through management of the classic three "*T*"s of combustion: time, temperature, and turbulence. The advantages of a well-engineered incineration configuration include defined destructor size, controlled processing, high destruction rates, release of a benign off-gas, as well as discharge of a stable solid residue. In order to support the successful development and operation of new thermal destruction configurations that meet all required design goals one needs to:

Characterize the solid/liquid wastes to be processed
Establish global thermal performance and discharge criteria for the waste throughputs
Select the appropriate thermal destruction system for treatment of the waste
Develop material and heat balances for selected configuration based on performance criteria
Determine flue gas temperatures, air mass flow, cooling exhaust flow, and losses
Evaluate auxiliary equipment requirements

Specific destruction configurations for thermally treating particular wastes are at various stages of commercial and/or advanced technology development. Note that various waste materials selected for processing may have dissimilar compositions, energetics, and/or destruction chemistries, which often require different configurations, overall size, number of components, and even type of incinerator in order to achieve optimum reduction. For instance, MSW incinerator feed can be extremely heterogeneous and highly variable in composition both spatially and temporally. MSW units in general tend therefore to be large in order to establish sufficiency in processing input and promoting completeness in thermal reduction. On the other hand, thermal treatment facilities selected to destroy a specific hazardous solid or liquid toxic compound waste stream may require an alternate design approach. For example, the specified toxic compound might utilize a hazardous waste combustor design that could be much smaller than an MSW configuration, and a toxic waste facility, due to throughput and composition, may require fewer overall components than an MSW plant. Application of chemical kinetic principles can be an important design element used as input to chemical reactor theory when predicting residence time of certain toxic reactants in particular hazardous combustors.

The thermal destruction efficiency for a particular configuration is measured by the completeness of combustion achieved with the burnable fraction of waste. Incomplete combustion and emissions are, therefore, at the very heart of conversion characteristic inefficiencies for any specific thermal destructor arrangement. Modern incineration systems therefore continuously monitor CO to ensure high combustion efficiency and a high destruction and removal efficiency (DRE) for hazardous waste combustors. The presence of carbon monoxide in the stack is an indication of insufficient oxygen for carbon combustion during thermal destruction as well as high temperature dissociation effects of CO_2.

A variety of methods are used in order to provide a method of reporting destruction performance of incinerators, including those established for large incinerators and published by the American Society of Mechanical Engineering (ASME) in their Performance Test Codes. Procedures and practices similar to those established for boilers, as described in Section 6.5 of Chapter 6, are followed for incinerators; see Figure 13.3.

$$\text{EFFICIENCY} = \frac{\text{OUTPUT}}{\text{INPUT}} = \frac{Q_{\text{waste}}}{HHV_{\text{waste}}} \tag{13.1}$$

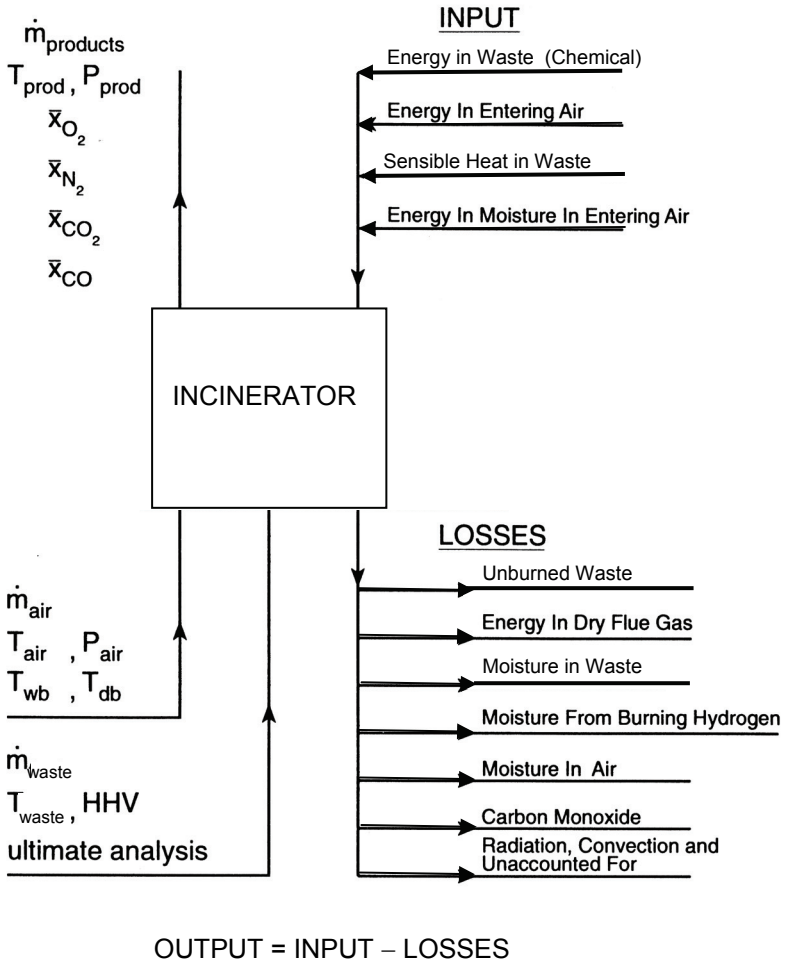

Figure 13.3 Elements of an incinerator energy balance.

Ensuring all design, manufacturing, and operational goals are met prior to startup of any new installation is critical; see Table 1.4. This effort includes operating any particular unit at the factory, or at an approved test facility, prior to being supplied to a customer. Modern development and manufacturing practices today require acceptance-testing incinerator configurations. Incinerator approval testing practices in industry are based in part on measuring critical performance and environmental parameters and can include, but are not limited to, the following items:

Waste feed characterization and acceptance
Offgas composition and secondary wastes
Process effectiveness
Cost/benefit analysis
Permittability
Public acceptance

Thermal destruction technology testing programs can thus range from fundamental testing for demonstrating a new processing concept, to comprehensive testing for validating a fabricated design, through exhaustive trial testing required for permitting an installed facility. Relationships governing performance characteristics of thermal waste treatment devices, such as hazardous waste combustors, are covered today under a myriad of regulations and overlapping authorities.

13.4 THERMAL DESTRUCTION COMPONENTS

Proper waste preparation and feed conditioning can contribute significantly to successful thermal destruction chemistry. For example, during preparation and feed only a small fraction of MSW or medical waste (i.e., glass) breaks down under the traditional solid fuel processing action of crushing as described in Chapter 6. Unlike coal, the majority of solid MSW waste, if subjected to a crushing force, simply distorts, stretches, or compresses into empty spaces in the trash. Considerable energy is absorbed by the deforming material from crushing that could otherwise prove beneficial during preprocessing. It is therefore beneficial to provide a size reduction step using shredders or mills which introduce shearing, ripping, and cutting actions to the feed during solid waste preparation. Sizing waste using such techniques better prepares material than crushing and helps promote improved solid waste destruction.

Depending on the specific configuration, solid waste may be charged mechanically or automatically. During charging every effort should be made to avoid exposing personnel to fire or operating dangers. Hazmat solid waste must be fed to the destructor in sealed containers. Some incinerators place a waste feed hopper system with internal guillotine door against the incinerator for sealing to eliminate exposure to operators. With a feed hopper configuration, the hopper door remains open during loading but closed during the firebox charging. The internal guillotine door between the feed hopper and incinerator remains closed during hopper loading but opens during the firebox charging. Other charging techniques utilize screw auger feed. Large MSW units operate using an overhead crane to batch load waste from a large pit having the capacity of holding several days of delivered waste. In order to try and keep a fairly uniform feed characteristic, waste is selectively gathered from various sections of the pit by a crane operator and delivered into the top of a gravity charging chute leading down into the MSW incinerator.

Liquids and slurries are introduced to appropriate destructors from storage tanks through dedicated burners. Liquid wastes may require attention to leaks, filtering of solids, and mixing feed if several liquids are being introduced for destruction. Liquid waste burner charge preparation requirements include:

Injecting atomized liquid waste droplets into the primary combustion chamber
Vaporizing and pyrolyzing waste
Mixing with sufficient air for combustion
Igniting the waste-fuel mixture

The destruction of some low Btu liquid wastes, as well as certain hazmat combustors, utilizes configurations having auxiliary fuel burners in order to provide sufficient heat release rates and/or preheating in order to maintain proper operating conditions for destruction. Burners and nozzles are incorporated in some of these configurations that allow liquid waste from atomizing nozzles to pass through the flame, helping to promote thermal destruction. In other circumstances liquid wastes are injected using dual-fuel burners. Auxiliary fuel burners are also used with certain low Btu solid waste incinerator applications. Recall liquid fuel combustion and burner requirements were covered in Chapter 7, Section 7.4.

Primary combustion chamber(s) is the location wherein chemical reactions for waste reduction proceed via pyrolysis, gasification, as well as subsequent oxidation of evolved gases. Properly prepared feed mixes with combustion air/oxygen within a refractory-lined or steel shell and cooled chamber. As indicated, auxiliary heat supplied from co-firing using auxiliary fuels may be required to maintain a desired T, P, or reaction conditions. Some configurations utilize a secondary combustion chamber to complete reactions begun under starved air conditions in a primary chamber. The combustion chamber operates under draft, and any flow of cold ambient air must be stopped from entering after charging. Continued inrushing cold air would, for example, quench a solid waste burning process, generate smoke, and impact the interior refractory walls due to rapid cooling. Inlets on solid waste incinerators are equipped with a closure system to limit or stop the flow of cold ambient air.

A forced draft fan delivers combustion air to a variety of locations within the primary combustion chamber, while an induced draft fan downstream of the off-gas cleaning system provides the motive force for mixing combustion air with waste and then transporting the mixture through the thermal destruction system to discharge. Hazardous waste incinerator units are brought up to operating conditions prior to introducing waste into the combustion chamber using an auxiliary fuel such as natural gas, propane, or fuel oil. In order to attain and sustain the required destruction process in the primary combustion chamber, an integrated process control will often be employed utilizing waste input feedback, combustion air controls, draft controls, auxiliary fuel burners, and automatic temperature control devices.

Solid waste combustion can be accomplished using mass-fired burning with grate-type configurations similar to arrangements described for coal in Chapter 6. Mixing the waste, introducing combustion air, and supporting the waste during reaction are accomplished using stationary and traveling grate techniques. Some large MSW incinerators use sloping grate configurations so that ash and unburned material can drop off and be quenched for removal when burn-out is completed. Some older and smaller solid waste incinerators repeatedly open and close their feed door during each operation in order to: (1) spread waste, (2) feed more waste, and (3) occasionally remove ash. Other automated configurations use either a ram feed assembly to simply push waste into the combustion chamber or have auger feed arrangements. Automated feed assemblies may actually reduce processing rates of solid waste unless grinding or shredding of the waste is provided during preprocessing.

Thermal destruction of certain waste such as MSW and medical waste can result in the generation of both fly and bottom ash. Fly ash produced from thermal destruction of waste is discharged with the gas stream, while bottom ash is the inert product stream that is removed from the bottom of the incinerator. Municipal refuse combustion fly ash has been reported to be particularly abrasive, more so than most coal ash. Mechanical erosion/wastage of metal surfaces by fast-moving MSW fly ash particulates can rapidly lead to metal failure. Particulate control from modern incinerators, much like the modern solid fuel power generation pollution control devices described in Section 6.5 of Chapter 6, can include particulate collection, cyclones, venturi scrubbers, baghouses, filtration, and electrostatic precipitator (ESP).

Bottom ash collected in a solid waste incinerator, like coal burner ash, can contain unburned combustible organic material, abrasive and corrosive materials, as well as miscellaneous slag and metals. Batch, continuous, or semi-continuous removal techniques, including gravity drop-out or transport methods, remove hot ash into dry or wet collection and storage systems. Conveyors, augers, or pneumatic devices transfer collected hot ash for cooling and disposal. Collected wet ash passes through a quenching water stream prior to wet storage, while collected dry ash passes onto a screw transfer surface for cooling prior to dry storage.

Groundwater contamination from bottom ash disposal is a concern due to the presence of heavy metals and trace organics contained in the ash. Regulations now require bottom ash to pass specific tests prior to being disposed in regulated sites. Prior to landfill disposal or utilization as a by-product, ash must pass stabilization and solidification characteristic testing such as the Toxicity Characteristic Leaching Procedure (TCLP) Test. After mixing with other solidification and stabilizing materials processed, bottom ash is then disposed in landfills. Advanced techniques are now being considered, such as using plasma arc melters to stabilize both fly and bottom ash in a stabilized solid melt product.

13.5 THERMAL DESTRUCTION CONFIGURATIONS

A number of conventional configurations as well advanced concepts for thermal destruction can be grouped together in terms of various categories, such as (1) according to the type of waste being destructed, hazardous or non-hazardous; (2) according to the operating temperature of the system, low or high temperature destructor; and/or (3) according to the number of combustion stages required, one or two. Solid waste destructors can be accomplished using several different configurations. Grate-type systems pass air through the supported waste. Hearth systems mix air with the introduced waste. Suspension burning systems utilize a high velocity air stream to support conversion chemistry of shredded waste, similar to pulverized coal combustion, or to levitate a fluidized destructor bed. In the following section an introduction to a range of important thermal destruction configurations will be provided.

EXAMPLE 13.3 Hazardous waste incinerator principal organic hazardous constituents, i.e., POHC, require a minimum destruction and removal efficiency (DRE) of 99.99%. For a feed rate of 500 lbm/hr of chlorobenzene calculate: (a) the chlorobenzene discharge requirement for a four nines DRE, lbm chlorobenzene /hr; (b) the HCl discharge rate, lbm HCl /hr; and (c) the HCl removal requirement for a four nines DRE, lbm HCl /hr.

Solution:

1. Chlorobenzene discharge requirement for a four nines DRE:

$$DRE_{C_6H_5Cl} = \left[\frac{\dot{m}_{in} - \dot{m}_{out}}{\dot{m}_{in}}\right] \cdot 100 = 99.99$$

$$\dot{m}_{out} = (1 - 0.9999) \cdot \dot{m}_{in} = 0.0001 \cdot 500 \text{ lbm waste / hr}$$

a) $\dot{m}_{out} = 0.05 \text{ lbm waste / hr}$

2. Stoichiometric reaction equation for ideal combustion of chlorobenzene in air:

$$C_6H_5Cl + 7[O_2 + 3.76N_2] \rightarrow 6CO_2 + 2H_2O + HCl + (7)(3.76)N_2$$

3. Chlorobenzene molar flow rates for a four nines DRE:

$$\dot{N}_{C_6H_{10}O_5})_{out} = (0.05 \text{ lbm waste / hr}) / (112.5 \text{ lbm waste / lbmole waste})$$
$$= 0.000444 \text{ lbmole waste / hr}$$

$$\dot{N}_{C_6H_{10}O_5})_{in} = (500 \text{ lbm waste / hr}) / (112.5 \text{ lbm waste / lbmole waste})$$
$$= 4.444 \text{ lbmole waste / hr}$$

4. Molar discharge rate of HCl:

$$\dot{N}_{HCl})_{out} = \dot{N}_{C_6H_{10}O_5})_{in} = 4.444 \text{ lbmole HCl / hr}$$

5. Mass discharge rate of HCl:

b) $\dot{m}_{HCl} = (4.444 \text{ lbmoles HCl / hr}) \cdot (36.5 \text{ lbm HCl / lbmole HCl})$
$= 162.206 \text{ lbm HCl / hr}$

6. HCl discharge removal requirement for a four nines DRE:

$$DRE_{HCl} = \left[\frac{\dot{m}_{in} - \dot{m}_{out}}{\dot{m}_{in}}\right] \cdot 100 = 99.99$$

$$\dot{m}_{out} = (1 - 0.9999) \cdot \dot{m}_{in} = (0.0001) \cdot (162.26 \text{ lbm HCl / hr}) = 0.0162 \text{ lbm HC}l \text{ / hr}$$

c) $\dot{m}_{removed} = (162.26 - 0.0016) = 162.20 \text{ lbm HCl removed / hr}$

Over the years grate or hearth incinerator configurations have been used to support solid waste during thermal destruction. Rotary kiln hearth incinerator technology is a well established destruction technique that uses a simple positive method of slow rotation for stirring and moving hazardous waste through an inclined combustion zone, as shown in Figure 13.4. Advantages of a rotary kiln thermal destructor include its ability to accept a range of waste forms including solids, sludges, liquids, and fumes. Gases move through the rotating combustion zone in a matter of seconds, whereas solid material can have a residence time in the reaction zone of many minutes based on the motion of the material in the moving bed, i.e., tumbling and/or sliding. A rotary kiln can handle wastes with very high concentrations of inert materials, as well as process wastes with a wide range of heating values. All configurations operate using a secondary combustion chamber to ensure complete combustion. Kilns also incorporate various arrangements of auxiliary burners and may be operated in a slagging or non-slagging mode. Disadvantages of rotary kiln incinerators include high particulate entrainment in the offgas and an ability of particular shaped combustible objects to roll untreated through the combustion zone. In addition, the configuration is mechanically complex having large, heavy, moving parts with difficult rotating seals, and a refractory lining operating under severe conditions.

Modern fixed hearth incinerators, also called controlled air, starved air, or pyrolytic incinerators, employ a two-stage combustion process as illustrated in Figure 13.5. This configuration is utilized for incineration of solids, but it can also handle slurries, liquids, and fumes. The technology is well established and used for treating medical and hazardous wastes. Waste is fed to the first stage or primary chamber and burned using underfire air at roughly 50%–80% of the stoichiometric air requirements. The flow in the first stage is low, and the chamber is maintained in the reducing mode, i.e., less than stoichiometric oxygen supply. The endothermic heat produced by oxidation of the fixed carbon fraction of the waste under starved air condition causes most of the volatile fraction of waste to be vaporized. The smoke and pyrolytic products consisting of methane, ethane, as well as other unburned hydrocarbons, and carbon monoxide pass into the second stage or secondary chamber. Here additional air, in addition to supplementary fuel, if needed, is introduced in order to complete the combustion. Total excess air for a fixed hearth two-stage incinerator is in the 100–200% theoretical air range.

Modern modular, starved-air incinerators operate with a fixed air flow to the primary chamber. As the solid waste burns down, air supply comes into better balance with the bed and the flue gas temperature increases. Thus the use of instrumentation monitoring the primary chamber exit temperature can be used for signaling the need to add more waste. Fixed hearth units tend to be of a smaller capacity because of physical limitations in ram feeding and transporting amounts of waste material through the combustion chamber. Benefits of a two-stage combustion process include low particulate entrainment in the offgas and an ability to readily seal when burning hazardous materials. Disadvantages of controlled air incinerator include having intolerance to large non-combustible objects and being ineffective for processing solids with a high concentration of inert material.

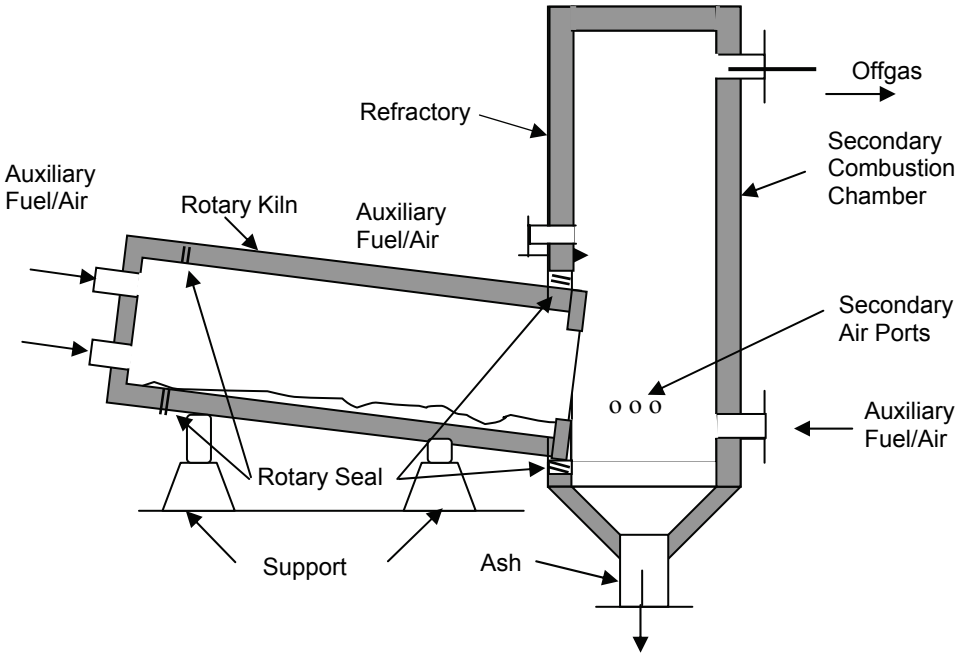

Figure 13.4 Rotary kiln thermal destruction configuration. After Fred J. Kuntz, "Incinerator Systems," 2001 International Conference on Incineration and Thermal Treatment Technologies, Philadelphia, PA, May 2001.

Multiple hearth incinerator technology is a well-established method that has been utilized for processing wastewater sewage sludge. Equipment can be designed having a different number of hearths to handle wastes with very high water content as well as to process liquids, fumes, or solids. Vertical waste processing occurs with feed input at the top hearth for drying, followed by ignition from auxiliary fuel burners, then destruction in the lower combustion zone, continuing down until burnout is achieved, and cooled ash discharges at the bottom. Feed is mechanically moved through the various stages of processing by the continually moving rabble arms. Waste is moved out over the surface of each hearth and dropped to the next lower level by rabble arms attached to a rotating air-cooled shaft. During processing, gaseous products of combustion rise to the top and exhaust to the air pollution control section. Additional auxiliary fuel burners can be located along individual hearths to improve process performance.

Multiple hearth incinerators are large, heavy, mechanically complex configurations having numerous moving parts and subject to potential high temperature failure modes; see Figure 13.6. Any free water in processed solid waste may leak into the combustion zone and damage hot section equipment by thermal shock. In addition, the moving components in the combustion zone are subject to corrosive and high temperature failure. Multiple hearth incinerator technology is, therefore, not well suited for toxic wastes which need high operating temperatures for required DREs and therefore find limited use and applications for hazardous wastes. If processed, volatile organic compounds will have short residence times in the high temperature zone of these units.

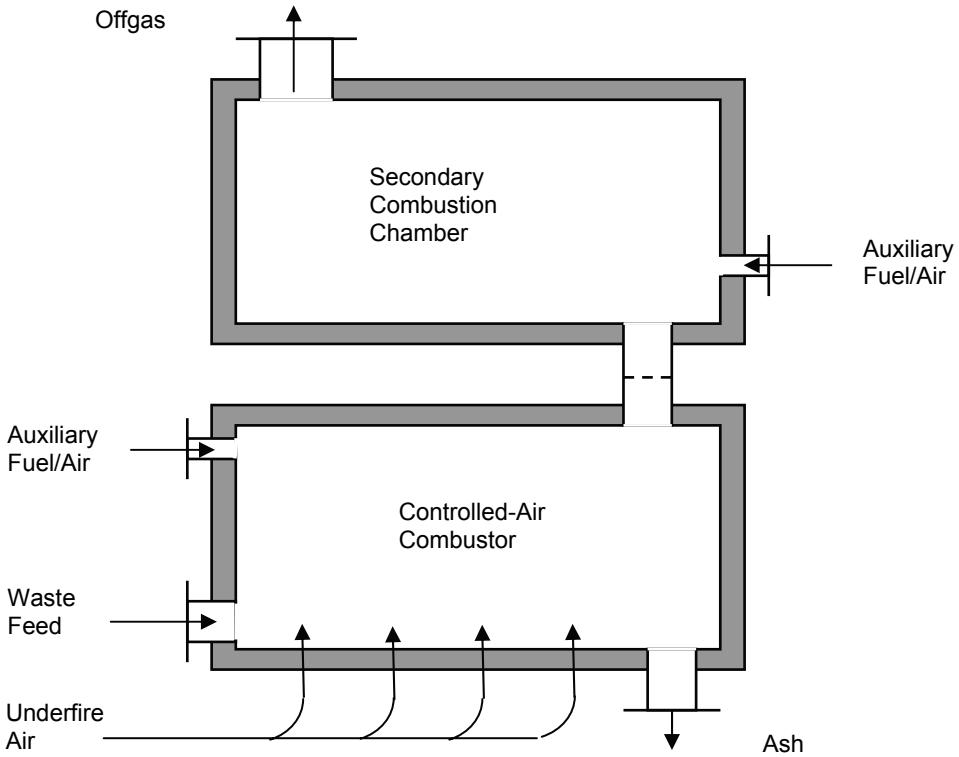

Figure 13.5 Controlled air thermal destruction configuration. After Fred J. Kuntz, "Incinerator Systems," 2001 International Conference on Incineration and Thermal Treatment Technologies, Philadelphia, PA, May 2001.

Thermal destruction of liquids and sludges has been accomplished commercially using a variety of cyclone or vortex incinerator configurations. Cyclone combustor designs inject fuel and air with significant swirl into a chamber that is usually cylindrical in shape. Most configurations discharge combustion products through an exhaust hole centrally located in the wall opposite from injection. Basic vortex designs also have been successfully used to destroy a range of materials that are normally found difficult to burn, including damp refuse, high-ash content solids, as well as high-sulfur content oils.

Swirl burners or tangential entry designs are commonly used to increase the efficient utilization of combustion space. Intense recirculation patterns of swirling flow combustors help promote ignition of the entering waste mixture since burning gases travel back toward the burner, bringing reactive species and thermal energy. Rotation of a vortex flow field has been found to shorten the flame. The recirculation of the swirl or the twisting of the vortex paths increase the post-flame residence time.

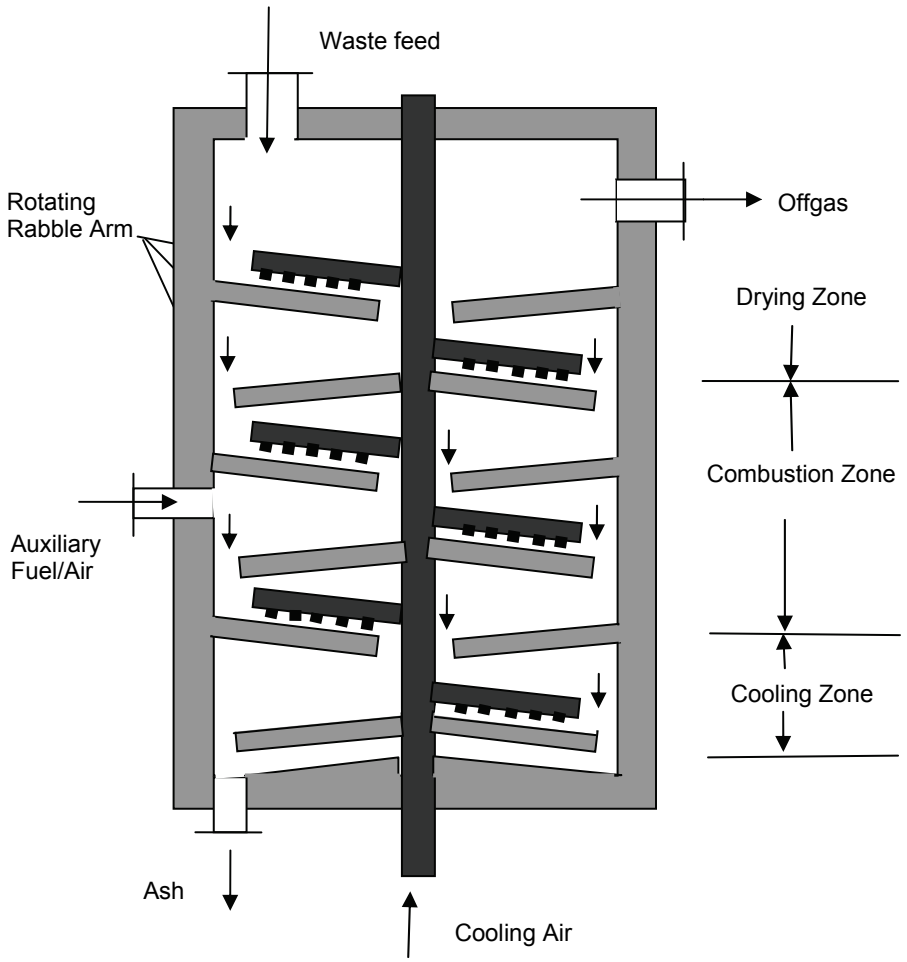

Figure 13.6 Multiple hearth incinerator configuration. After Fred J. Kuntz, "Incinerator Systems," 2001 International Conference on Incineration and Thermal Treatment Technologies, Philadelphia, PA, May 2001.

Due to the limited space available for landfilling and market for composts, a slagging "Vortex Melting System" has been developed for use in Japan to incinerate dried sewage sludge. The Vortex Melter unit was developed on the principle of a cyclone pulverized coal incineration furnace that was used in the 1950s. Dried sludge, reduced to the required feed size using a sieve and pulverizer, is fed to the Vortex Melter by a constant feeder. A swirling motion of vortex air and sludge is generated within the furnace by the flow from a nozzle which is installed tangentially to the cross section of the furnace. Combustibles in the sludge are incinerated, and inorganic materials are melted in the Vortex Melter. Melted ash flows out of the furnace as melted slag. The sludge particles are heated up to a high temperature by high temperature radiant heat from the furnace wall. The inside wall of the furnace is insulated with a refractory, and the entire furnace is cooled by a water jacket.

EXAMPLE 13.4 Highly diluted organic wastewater is thermally processed using an air-cooled vortex incinerator. Feed conditions to the incinerator consist of the following:

organic waste feed:	30 gal/hr (treat as water for the purposes of this analysis)
fuel oil feed:	7 gal/hr of liquid dodecane, $C_{12}H_{26}$
fuel feed supply temperature:	60ºF
incinerator inlet conditions:	*STP*
incinerator burner conditions:	40% excess air
incinerator inlet combustion air:	206.3 acfm
incinerator coolant discharge:	650ºF
incinerator burner temperature:	2,170ºF
incinerator exhaust temperature:	650ºF
incinerator exhaust gas flow:	1,614.9 acfm

For the configuration shown, calculate: (a) organic wastewater processed, lbm/hr; (b) combustion air mass flow rate, lbm/hr; (c) exhaust mass flow rate, lbm/hr; (d) cooling air mass flow rate, lbm/hr; and (e) cooling air volumetric flow rate, acfm.

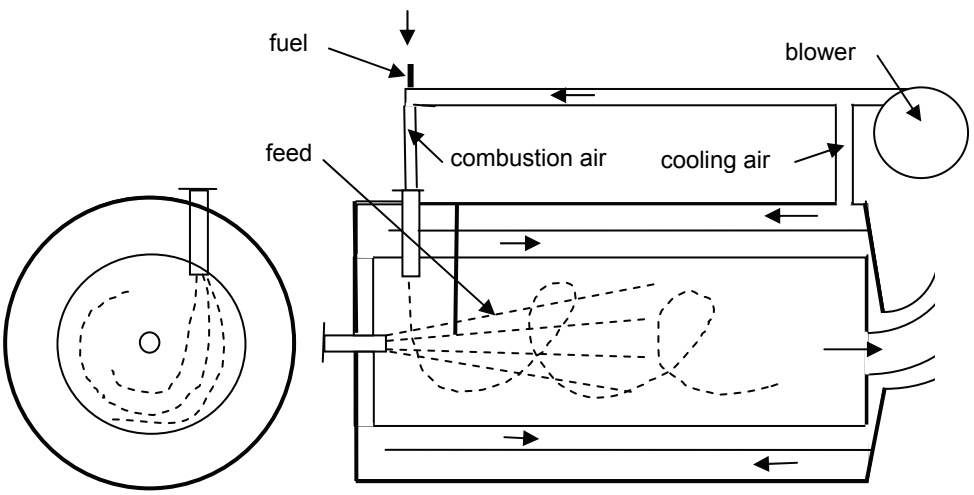

Solution:

1. Burner reaction equation – stoichiometric:

$$C_{12}H_{26} + a[O_2 + 3.76N_2] \rightarrow bCO_2 + cH_2O$$

Carbon atom balance: $b = 12$

Hydrogen atom balance: $c = 13$

Oxygen atom balance: $2.8a = 2b + c = 24 + 13$ $a = 18.5$

1. Burner reaction equation – 40% excess air:

$$C_{12}H_{26} + 25.9[O_2 + 3.76N_2] \rightarrow 12CO_2 + 13H_2O + dO_2 + eN_2$$

Nitrogen atom balance: $3.76 \cdot 25.9 = e$ $e = 97.384$

Oxygen atom balance: $51.8 = 24 + 13 + 2d$ $d = 7.4$

2. Burner air-fuel ratio:

$$\overline{AF} = \frac{(1.4 \cdot 18.5 \cdot 4.76)\text{lbmole air}}{1\,\text{lbmole fuel}} = 123.284 \text{ lbmole air/lbmole fuel}$$

and

$$AF = \frac{(123.284 \text{ lbmole air})(28.97 \text{ lbm air/lbmole air})}{(1 \text{ lbmole fuel})(170.328 \text{ lbm fuel / lbmole fuel})} = 20.96 \text{ lbm air/lbm fuel}$$

3. Liquid mass flow rates:
The density of water from Appendix D is $\rho = 62.25$ lbm/ft^3.

waste: $\dot{m}_w = \left(\dot{V}_w \langle \text{gal/hr} \rangle \cdot 62.25 \text{ lbm/ft}^3\right) / 7.4805 \langle \text{gal/ft}^3 \rangle$

$\dot{m}_w = 30 \text{ gal/hr} \cdot 62.25 \text{ lbm/ft}^3 / 7.4805 \text{ gal/ft}^3$

a) $= 249.65 \text{ lbm waste/hr}$

fuel: $\dot{m}_f = \left(\dot{V}_f \langle \text{gal/hr} \rangle \cdot SG \cdot 62.25 \text{ lbm/ft}^3\right) / 7.4805 \langle \text{gal/ft}^3 \rangle$

From Table 7.1 the specific gravity of liquid dodecane at 60ºF is 0.749.

$$\dot{m}_f = (7 \text{ gal/hr} \cdot 0.749 \cdot 62.25 \text{ lbm/ft}^3) / 7.4805 \text{ gal/ft}^3 = 43.63 \text{ lbm fuel/hr}$$

$$\dot{N}_f = \frac{43.63 \text{lbm/hr}}{170.328 \text{ lbm/lbmole}} = 0.256 \text{ lbmole fuel/hr}$$

4. Combustion air mass flow rate:

$$\dot{m}_{\text{air}} = AF \cdot \dot{m}_{\text{fuel}} = (20.96 \text{ lbm air/lbm fuel}) \cdot (43.63 \text{ lbm fuel/hr})$$
$$= 914.48 \text{ lbm combustion air/hr}$$

5. Gas mass flow rates: $P\dot{V} = \dot{m}RT$

Incinerator combustion air: $\dot{m} = P\dot{V} / RT$

$$\dot{m}_a = \frac{(60 \text{ min/hr}) \cdot P\langle \text{lbf/in}^2 \rangle \cdot (144 \text{ in}^2/\text{ft}^2) \cdot \left(MW_{\text{air}} \langle \text{lbm/lbmole} \rangle \cdot \dot{V}_a \langle \text{ft}^3/\text{min} \rangle\right)}{(1{,}545 \text{ ft} \cdot \text{lbf/lbmole} \cdot {}^\circ\text{R}) \cdot (T_a \langle {}^\circ\text{R} \rangle)}$$

$$\dot{m}_a = \frac{(60\,\text{min/hr})\cdot(14.7\,\text{lbf/in}^2)\cdot(144\,\text{in}^2/\text{ft}^2)\cdot(28.97\,\text{lbm/lbmole})\cdot(206.3\ \text{ft}^3/\text{min})}{(1{,}545\,\text{ft}\cdot\text{lbf/lbmole}\cdot°\text{R})\cdot(537°\text{R})}$$

b $= 914.5\,\text{lbm combustion air/hr}$

6. Vortex incinerator configuration combustion reaction to evaporate and process waste water:

$$(n\text{H}_2\text{O})_\text{w} + (12\text{CO}_2 + 13\text{H}_2\text{O} + 0.4\text{O}_2 + 97.384\text{N}_2)_\text{p} \rightarrow (12\text{CO}_2 + (13+n)\text{H}_2\text{O} + 0.4\text{O}_2 + 97.384\text{N}_2)_\text{e}$$

where

$$n = \frac{(249.65\ \text{lbm waste/hr})\cdot(170.328\ \text{lbm fuel/lbmole fuel})}{(43.63\,\text{lbm fuel/hr})\cdot(18\ \text{lbm waste/lbmole waste})}$$
$$= 54.145\ \text{lbmole waste/lbmole fuel}$$

7. Vortex incinerator energy balance:

$$\dot{Q} = \sum_{\text{out}} \dot{N}_e H_e - \sum_{\text{in}} \dot{N}_p H_p - \sum_{\text{in}} \dot{N}_w H_w$$

where

e – exhaust conditions @ 650ºF
p – burner products @ 2170ºF
w – waste feed conditions @ 212ºF
$\dot{Q}$ – heat transfer rate to cooling air

Using appropriate values for enthalpies for constituents found in tables in Appendixes B and D

Waste feed stream:

$$\dot{N}_w = (54.145\ \text{lbmole waste/lbmole fuel})\cdot(0.256\ \text{lbmole fuel/hr})$$
$$= 13.861\ \text{lbmole waste/hr}$$

$$\sum \dot{N}_w H_w = 13.861\cdot\left[\bar{h}_{fg} + \bar{h}_f^0\langle 212°\text{F}\rangle\right]_{\text{H}_2\text{O}}$$
$$= 13.861\cdot\{-9{,}703 - 68{,}317 + 609\} = -1{,}072{,}994\ \text{cal/hr}$$

Burner product feed stream:

$$\dot{N}_p = (12+13+7.4+97.384\ \text{lbmole product/lbmole fuel})\cdot(0.256\ \text{lbmole fuel/hr})$$
$$= (129.784\ \text{lbmole product})\cdot(0.256\ \text{lbmole fuel/hr}) = 33.225\ \text{lbmole product/hr}$$

$$\sum_{\text{in}} \dot{N}_p H_p = \dot{N}_p\Big\{12\cdot\left[\bar{h}_f^0 + \Delta\bar{h}\langle 2{,}170°\text{F}\rangle\right]_{\text{CO}_2} + 13\cdot\left[\bar{h}_f^0 + \Delta\bar{h}\langle 2{,}170°\text{F}\rangle\right]_{\text{H}_2\text{O}}$$
$$+ 7.4\cdot\left[\bar{h}_f + \Delta\bar{h}\langle 2{,}170°\text{F}\rangle\right]_{\text{O}_2} + 97.384\cdot\left[\bar{h}_f + \Delta\bar{h}\langle 2{,}170°\text{F}\rangle\right]_{\text{N}_2}\Big\}$$
$$= 33.225\{12\cdot[-94{,}054 + 14{,}210] + 13\cdot[-68{,}317 + 2{,}656]$$
$$+ 97.384\cdot[+2{,}246]\}/(129.784) = -403{,}377.8\ \text{cal/hr}$$

Incinerator exhaust stream:

$$\dot{N}_e = (12 + 67.145 + 7.4 + 97.384 \text{ lbmole product/lbmole fuel}) \cdot (0.256 \text{ lbmole fuel/hr})$$
$$= (183.929 \text{ lbmole product}) \cdot (0.256 \text{ lbmole fuel/hr})$$
$$= 47.085 \text{ lbmole exhaust/hr}$$

$$\sum_{\text{out}} \dot{N}_e H_e = \dot{N}_e \left\{ 12 \cdot \left[\bar{h}_f^0 + \Delta\bar{h}\langle 650°\text{F}\rangle \right]_{CO_2} + 67.145 \cdot \left[\bar{h}_f^0 + \Delta\bar{h}\langle 650°\text{F}\rangle \right]_{H_2O} \right.$$
$$\left. + 7.4 \cdot \left[\Delta\bar{h}\langle 650°\text{F}\rangle \right]_{O_2} + 97.384 \cdot \left[\Delta\bar{h}\langle 650°\text{F}\rangle \right]_{N_2} \right\}$$
$$= 45.294 \cdot \{12 \cdot [-94{,}054 + 3{,}280] + 67.145 \cdot [-68{,}317 + 11{,}063]$$
$$+ 7.4 \cdot [+9{,}367] + 97.384 \cdot [+8{,}857]\}/(183.929) = -985{,}466.2 \text{ cal/hr}$$

$$\dot{Q} = -985{,}466.2 - (-403{,}377.8 - 1{,}072{,}994)$$
$$= -490{,}905.6 \text{ cal/hr}$$

8. Vortex incinerator cooling air energy balance:

$$\dot{Q} = \sum_{\text{out}} \dot{N}_c H_{c-out} - \sum_{\text{in}} \dot{N}_c H_{c-in}$$

where

c – cooling air
c-out – cooling air exhaust conditions @ 650ºF
c-in – cooling air inlet conditions @ 77ºF

Using enthalpy values for N_2 and O_2 found in Tables B.18 and B.22 in Appendix B:

$$\dot{Q} = \sum_{\text{out}} \dot{N}_c H_{c-\text{out}} - \sum_{\text{in}} \dot{N}_c H_{c-\text{in}}$$
$$= \dot{N}_c \left\{ \left[\Delta\bar{h}_{O_2}\langle 650°\text{F}\rangle - \Delta\bar{h}_{O_2}\langle 77°\text{F}\rangle \right] + 3.76 \cdot \left[\Delta\bar{h}_{N_2}\langle 650°\text{F}\rangle - \Delta\bar{h}_{N_2}\langle 77°\text{F}\rangle \right] \right\}$$
$$\dot{Q} = \dot{N}_c \cdot \left\{ \left[\Delta\bar{h}_{O_2}\langle 650°\text{F}\rangle \right] + 3.76 \cdot \left[\Delta\bar{h}_{N_2}\langle 650°\text{F}\rangle \right] \right\}$$
$$= \dot{N}_c \cdot (2{,}339.7 + 3.76 \cdot 2{,}246.3) = \dot{N}_c \cdot 10{,}785.79$$
$$\dot{N}_c = (490{,}905.6 \text{ cal/hr})/(10{,}785.79 \text{ cal/lbmole air})$$
$$= 45.51 \text{ lbmole cooling air/hr}$$

Incinerator cooling air mass flow rate:

$$\dot{m}_c = \dot{N}_c MW_{air}$$
$$= \left(45.51 \frac{\text{lbmole cooling air}}{\text{hr}} \right) \cdot (28.97 \text{ lbm air/lbmole air})$$
$$\text{d.} = 1{,}318.425 \text{ lbm cooling air/hr}$$

Incinerator cooling air volumetric flow rate: $\dot{V} = \dot{m}RT / P$

$$\dot{V}_c\left\langle \text{ft}^3/\text{min}\right\rangle = \frac{\left(\dot{m}_c\right)\cdot\left(1{,}545\,\text{ft}\cdot\text{lbf/lbmole}\cdot°\text{R}\right)\cdot\left(T_c\langle °\text{R}\rangle\right)}{\left(60\,\text{min/hr}\right)\cdot P\left\langle \text{lbf/in}^2\right\rangle\cdot\left(144\,\text{in}^2/\text{ft}^2\right)\cdot\left(MW_{\text{air}}\langle\text{lbm/lbmole}\rangle\right)}$$

$$\dot{V}_c = \frac{\left(1{,}318.425\,\text{lbm/min}\right)\cdot\left(1{,}545\,\text{ft}\cdot\text{lbf/lbmole}\cdot°\text{R}\right)\cdot\left(537°\text{R}\right)}{\left(60\,\text{min/hr}\right)\cdot\left(14.7\,\text{lbf/in}^2\right)\cdot\left(144\,\text{in}^2/\text{ft}^2\right)\cdot\left(28.97\,\text{lbm/lbmole}\right)}$$

e. $= 297.3\,\text{ft}^3\text{cooling air/min}$

A variety of wastes, including solids, sludges, liquids, and/or fumes, can be processed using the fluidized bed combustion technology (FBC), depicted in Figure 13.7, and described previously in Section 6.4 of Chapter 6. An FBC bed can tolerate rapid changes in either feed flow rate or heating value of waste being introduced into an FBC for destruction. Recall that the FBC bed materials can neutralize acid gases and an FBC thermal destructor is able to operate effectively even at relatively low destruction temperatures. If excessive bed material is entrained in the off gas stream discharge, the lost bed can be recovered by use of recirculating FBC configurations. Exhaust gas thermal energy from the unit can be used to preheat FBC combustion air or be an input to a waste heat boiler. Any FBC incinerator, however, has certain disadvantages, including intolerance to waste containing components that slag or form low-melting eutectics within the FBC bed material. Therefore, in order for an FBC incinerator unit to be effective when processing solid feed such as MSW, a majority of the non-combustible objects need to removed and combustible input shredded prior to destruction.

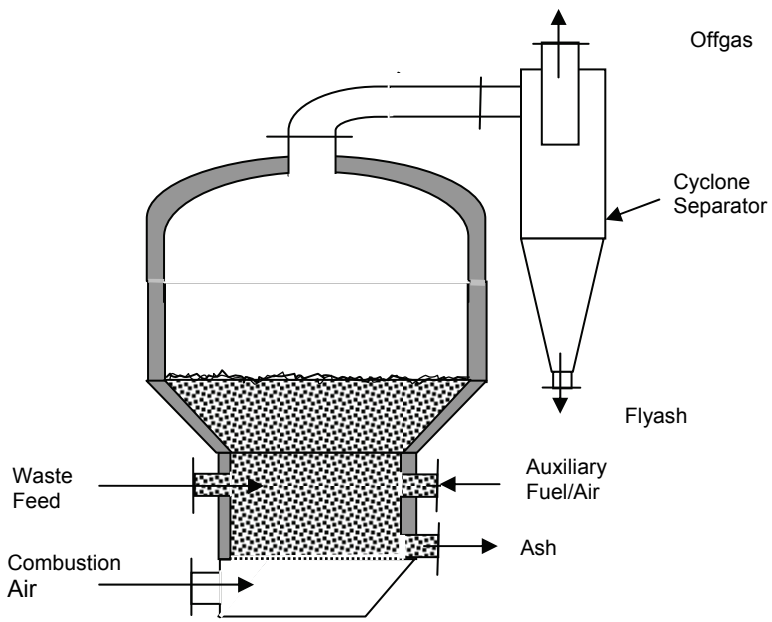

Figure 13.7 FBC thermal destruction configuration. After Fred J. Kuntz, "Incinerator Systems," 2001 International Conference on Incineration and Thermal Treatment Technologies, Philadelphia, PA, May 2001.

The ultra-high heating rates and gas temperatures required by NASA research laboratories during the development of heat shield materials and re-entry vehicle configurations helped to lay the foundation for the development of a whole family of plasma heaters. Plasma is a fourth state of matter, distinct from the more familiar solid, liquid, and/or gas, consisting chiefly of a partially ionized gas containing electrons, ions, atoms, molecules, and free radicals. A plasma state occurs at high temperatures and can be generated within an electric arc created by passing a high energy density current between two electrodes in the presence of an electrically conductive gas. An example of a naturally generated plasma arc is atmospheric lightning. Electrical power in the 100 kilowatt (kW) to 10 megawatt (MW) range has been utilized to produce an electrically neutral, highly ionized, and very high temperature plasma gas. Resistive heating of the plasma gas to extremely high temperatures generates a very hot gas consisting of atoms and their electrons that have been stripped from their orbits. Local temperatures within an arc are typically in the range of 10,000 to 20,000°C (18,030 to 36,030°F), several times hotter than the surface of the sun. The majority of the gas flow is used to stabilize the plasma arc column with typically 1% or less of the gas flow rate being converted into the plasma state. The bulk of the gas is heated to nominal temperatures of 5,000 to 10,000°C (9,030 to 18,030°F).

Today, fundamental plasma torch physics is well developed, and various commercial direct current (DC) and alternating current (AC) torch types are available that can provide a high-energy, radiative heat source for rapid thermal conversion of waste materials. A plasma flame can provide an intense source of heat. High thermal energy transfer rates are available for use with the generation of a low mass, high-enthalpy plasma torch gas. To initiate and sustain the plasma arc column requires the continuous input of ionizing energies into the plasma gas. A long plasma column requires high voltages for sustainment, while short plasma columns require low voltages in order to maintain an arc. Delivery of the highly concentrated power levels of plasma depends, among other variables, on voltage, current, type of gas, and gas flow. Temperatures in the plume of a DC plasma torch have been investigated extensively, both theoretically and experimentally. Typical torch flame temperatures, ranging from 6,730 to 11,730°C (12,140 to 21,140°F), have been measured in argon using optical emission spectroscopy.

Most plasma arc torches in use today can be categorized as either a transferred arc (TA) or a non-transferred arc (NTA) configuration. The transferred arc torch uses a working material to conduct electricity. Here the positive polarity is in the torch electrode, while the negative polarity is in the working piece. This arrangement provides heat suitable for melting, smelting, gasification, annihilation, recovery, and reclamation. For the case of non-transferred arc torch, two internal electrodes are used. A small column of injected gas (argon, oxygen, etc.) creates the plasma plume that extends beyond the tip of the torch. The NTA torch produces more dispersed heat that has found use in processing non-conductive materials such as glass and ceramics. Other designs, such as AC torches or inductively coupled plasma torches, have also been developed.

The idea of using hot thermal plasma as a high energy density heat source is not a new concept. Practical plasma applications started in 1887 when W. Siemens developed his DC electric arc melting furnace. German industry was using plasma heating to produce steel by the end of the late nineteenth century. From 1905 to 1940 Norway utilized plasma heaters to make nitrogen fertilizer from atmospheric air. Plasma-arc technology also has been in use for over 50 years in the manufacture of chemicals. Plasma energy has been used since 1939 at Chemische Werke Hulls in Germany to produce acetylene. Plasma arc torches (PAT) are a cost-effective industrial heat source

now being used by the glass melting and metallurgical industries in the preparation of high purity metals and glass products.

Numerous plasma arc-centered technologies today are being developed and utilized in Japan, Russia, Europe, as well as in the United States. Significant progress is being made toward commercialization of a variety of environmental plasma-arc-centered processes for the thermal remediation, reprocessing, and destruction of numerous types of wastes. Research teams and consortiums at universities, national laboratories, and corporations are involved in these advanced PAT technology waste treatment developmental efforts. Full-scale demonstrations have been reported for the processing and stabilizing of contaminated soils; organic materials containing heavy metals, slurries, and sludges; transuranic (TRU) waste; toxic wastes including hazardous liquids, municipal incinerator ash, medical waste, and asbestos.

A majority of PAT applications have focused on the *vitrification* of wastes. Vitrification is basically a high temperature plasma-arc melt process in which the reduction technique destroys or immobilizes wastes while confining toxic solid waste by-products within a glassy matrix; see Figure 13.8. Glass encapsulation and in-situ melting plasma arc processes have been accepted for their ability to process even Department of Energy (DOE) particular toxic solid waste stream. Vitrification lends itself to processing materials in which the thermal destruction predominantly results in a solid waste by-product. This solid product has been shown to remain stable for geologically long periods of time, thereby reducing human risks. Vitrified solid waste by-products therefore are termed by many as an ultimate waste form. Organic gases that are not converted into a solid residue are treated with appropriate conventional gas cleanup and pollution control devices as needed.

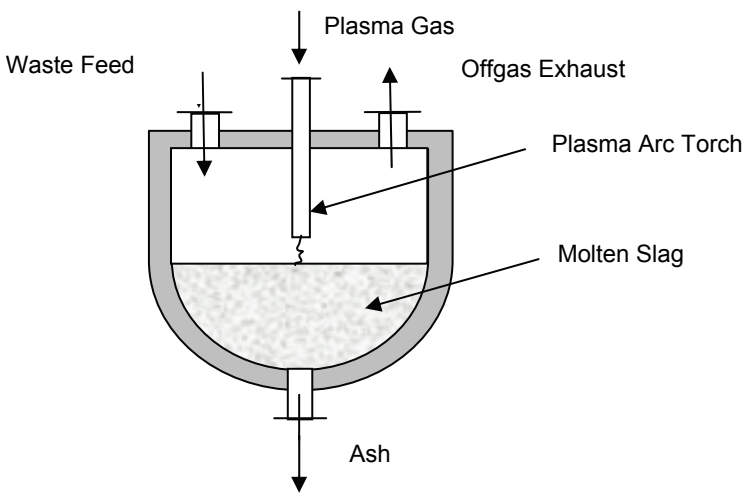

Figure 13.8 PAT thermal destruction configuration. After Fred J. Kuntz, "Incinerator Systems," 2001 International Conference on Incineration and Thermal Treatment Technologies, Philadelphia, PA, May 2001.

PAT can also be effective for wastes that require high operating temperatures for destruction and therefore can also be utilized for the thermal treatment of solids, liquids, or sludges. Gas composition within a primary PAT destruction chamber, unlike conventional incinerators, can be selected from a wide range of oxidizing, reducing, or neutral gases when a PAT provides the destructive energy. The environment in a plasma destruction chamber can therefore operate in either oxygen rich (oxidizing) or oxygen free (reducing) mode. When operated in a reducing mode, plasma destruction produces a gas stream that is approximately 10% of a comparably sized incineration system. In addition, a plasma arc torch requires less than 5% of the mass delivered by a combustion heater in order to deliver the same enthalpy for the destruction process. Because the energy delivered per unit flow rate of plasma gas is so high, there is less exhaust gas from a plasma chamber than from a combustion furnace. This can result in potential benefits of reduced quantities of fly ash and a smaller (and cheaper) gas cleanup associated with the lower gas flow rate. PAT thermal treatment systems do have several disadvantages, including those related to operating at high torch temperature conditions which produce large amounts of NO_x and promote severe and aggressive local reactor interior activity. PAT thermal treatment systems operate as high energy consuming devices and often require size reduction or shredding of solid wastes for effective processing.

Another advanced liquid thermal destruction technology is Supercritical Water Oxidation (SCWO), sometimes referred to as High Temperature Oxidation (HTO), which requires that the liquid waste stream pressure and temperature be maintained at over 220 atm and 347ºC (705ºF), i.e., above the critical point of water. Supercritical water, i.e., water above its critical point, forms a single phase that acts more like a gas than a liquid. Many organic materials such as oils and sludges, which under normal conditions will not dissolve in water, become miscible when in water, which is in the critical state. This occurs because of the reduction of hydrogen bonding leading to an increase in the water's solubility. To enhance the process, solid organic materials are typically treated by particlizing prior to their introduction into the aqueous feed. Entrained waste reacts in high-pressure supercritical water with oxygen. Inorganic material must be removed from the process, since they do not undergo chemical transformation into benign off-gas products. The technology is best suited for the treatment of liquids containing dilute solids and with relatively low concentrations of excess hazardous material.

13.6 ENVIRONMENTAL REGULATIONS AND THERMAL DESTRUCTION

The fairly stable incinerator design world began to undergo changes when air pollution regulations began to emerge in the 1950s. Specific improvements and advancements through the ensuing years have included, but not limited to, development of continuous feed mechanisms, automatic combustion controls, use of multiple combustion chambers, emission control devices, development of hazardous waste incinerators, and unique designs for energy recovery. Specific configurations and approaches to the thermal destruction of wastes, each having their own merits as well as limitations, were described in Section 13.5.

Increased health and environmental awareness today focuses attention on proper handling of all effluent discharged from thermal treatment facilities used for processing various forms of waste. Concerns are related to harmful discharges from equipment into ground and waterways as well as the atmosphere. Air pollutants such as nitric oxides (NO_x), sulfur oxides (SO_x), hydrochloric acid (HCl), unburned hydrocarbons (UHC), carbon monoxide (CO), polynuclear aromatic hydrocarbons (PAH), particulate and volatile metals, the emission of dioxins (PCDD), and furans (PCDF) are receiving increased attention in many countries around the world, including Asia, Europe as well as the United States. At present a number of such specific constituents must achieve high levels of destruction and removal efficiency (DRE) when processed by individual thermal destruction technologies. This trend is expected to grow and become more rigorous with time for thermal destruction systems in use for treating various types of waste, particularly those devices categorized as hazardous waste incinerators.

The Clean Air Act (CAA) of 1963 as amended in 1970 and 1977, as well as the Resource Conservation and Recovery Act (RCRA) of 1976, and amendments, provide authority and legal basis for U.S air pollution laws as well as various related incineration standards. The Environmental Protection Agency (EPA), created by the Clean Air Act Amendments of 1970, establishes pollution performance standards for Maximum Achievable Control Technologies (MACT) for standard and hazmat thermal destruction technology. The Clean Air Act Amendments of 1970 set in motion the categorization of two separate air pollutant categories: National Ambient Air Quality Standards (NAAQS) which established six principal pollutants considered harmful to public health (criteria pollutants), and National Emission Standards for Hazardous Air Pollutants (NESHAPS) established for the regulation of hazardous air pollutants. Hazardous waste incineration regulations were established in 1980 with the RCRA Regulation for Hazardous Waste Incinerators. Table 13.1 lists the National Ambient Air Quality Standards (NAAQS).

Table 13.1 National Ambient Air Quality Standards (NAAQS)

Pollutant	Units	Primary Standards	Averaging Time
Carbon monoxide	ppm	9	8-hr
	ppm	35	1-hr
Lead	$\mu g/m^3$	1.5	3-months
Nitrogen dioxide	ppm	0.053	AAA*
Particulate matter (PM_{10})	$\mu g/m^3$	50	AAA*
Particulate matter (PM_{10})	$\mu g/m^3$	150	24-hr
Particulate matter ($PM_{2.5}$)	$\mu g/m^3$	15	AAA*
Particulate matter ($PM_{2.5}$)	$\mu g/m^3$	65	24-hr
Ozone	ppm	0.08	8-hr
Sulfur dioxide	ppm	0.03	AAA*
	ppm	0.140	24-hr

*Annual arithmetic mean.
Source: U.S. EPA http://www.epa.gov/air/criteria.html, Washington, D.C., 1990.

Table 13.2a MACT Emission Standards for Conventional Waste Incinerators

Pollutant	Units	Municipal Waste Combustor*		Medical Waste Combustor**			Commercial and Industrial Solid Waste Incinerator***
		Small (< 250 TPD)	Large (> 250 TPD)	Small	Medium	Large	
Dioxins/furans	ng TEQ/dscm	13 total mass	13 total mass	125 total or 2.3 TEQ	25 total or 0.6 TEQ	25 total or 0.6 TEQ	0.41
Cadmium	mg/dscm	0.02	0.02	0.16 or 65% RE	0.04 or 90% RE	0.04 or 90% RE	0.004
Lead	mg/dscm	0.2	0.2	1.2 or 70% RE	0.07 or 98% RE	0.07 or 98% RE	0.04
Mercury	mg/dscm	0.08	0.08	0.55 or 85% RE	0.55 or 85% RE	0.55 or 85% RE	0.47
Particulate matter	mg/dscm	24	24	69	34	34	70
Opacity	%	10	10	NA	NA	NA	10
Sulfur dioxide	ppmv	30	30	55	55	55	20
Hydrogen chloride	ppmv	25	25	15 or 99% RE	15 or 99% RE	15 or 99% RE	62
Nitrogen oxides	ppmv	150 or 500	150	250	250	250	388
Carbon monoxide	ppmv	NA	NA	40	40	40	157

All emissions corrected to 7% oxygen dry volume basis.

**Source*: 40 CFR 60 Subpart AAAA and Eb.

***Source*: 40 CFR 60 Subpart Ec.

****Source*: 40 CFR 60 Subpart CCCC.

Table 13.2b MACT Emission Standards for Selected Hazardous Waste Combustors

Pollutant	Units	Hazardous Waste Incinerator		Cement Kiln Combustor	
		(Existing)	(New)	(Existing)	(New)
Dioxins/furans	ng TEQ/dscm	0.2 or 0.4 w/temp <400F at APCD inlet	0.2 or 0.11 for dry APCD or WHB sources	0.2 or 0.4 w/temp <400F at APCD inlet	0.2 or 0.4 w/temp <400F at APCD inlet
Mercury	mg/dscm	130	8.1	Feed ≤30 ppmw and 120 MTEC**; or 120 total emissions	Feed ≤1.9 ppmw and 120 MTEC**; or 120 total emissions
Particulate matter	mg/dscm	29.5	3.4	0.028	0.0023
Opacity	%	NA	NA	20	20
Semivolatile metals	mg/dscm	230	10	7.6E-4 lb/MMBtu*** and 330	6.2E-5 lb/MMBtu*** and 180
Low volatile metals	mg/dscm	92	23	2.1E-5 lb/MMBtu*** and 56	1.5E-5 lb/MMBtu*** and 54
HCl/Cl_2	ppmv	32	21	120	86
CO	ppmv	100	100	100	100
Hydrocarbons	ppmv	10	10	10 or 20	10 or 20 or 50
DRE	%	99.99 or 99.9999*	99.99 or 99.9999*	99.99 or 99.9999*	

All emissions corrected to 7% oxygen dry volume basis.
TEQ = 2,3,7,8-PCDD toxicity equivalents.
* 99.9999% DRE required for dioxin listed wastes; EPA RCRA waste codes F020, F021, F022, F023, F026, or F027.
** MTEC = Maximum Theoretical Emission Concentration, assuming no control of emissions.
*** Mass of polllutant contributed by hazardous waste per million Btu contributed by hazardous waste.
Source: 40 CFR 63 Subpart EEE, as of September 14, 2005.

Best available technologies (BET) for land-based solid waste incinerator units cannot meet existing requirements for regulated gaseous and solid particulate emissions without the use of expensive post-combustion gas cleanup facilities. The high DRE efficiency requirements are guaranteed by the use of large complex exhaust gas management configurations. MSW incineration facilities, for example, require extensive space and machinery for pre-processing the heterogeneous waste input and post-processing of by-products. Proper control of pollutants from discharging can be a significant portion of the overall design cost. Although flue gases from incinerators contain a number of pollutants, air pollution control equipment traditionally directed attention at the primary problem of particulate removal, including finely divided ash material in the stack smoke, as well as unburned, or partially burned, aerosol materials.

Gaseous incineration pollutants are often referred to as products of incomplete combustion, or PICs. Airborne gaseous emissions can in certain instances be mitigated by co-firing with a low-pollutant fuel such as natural gas. Pollutants and their control are strongly a function of the waste and the destructor selected for processing, i.e., the fuel-engine interface.

Certain chlorinated PIC destruction by-products include polychlorinated dibenzo-p-dioxin (PCDDs) and polychlorinated dibenzofuran (PCDFs), hence their common pollution terminology: Dioxin/Furan emissions. The toxic and potential mutagenic characteristics of these compounds are considered to represent a major threat to public health. Over 210 particular dioxin/furan compounds are currently identified that produce significant toxic, carcinogenic, mutagenic, and teratogenic health issues for humans. EPA officials indicate that air deposition of dioxins with bioaccumulation in the food chain is the pathway that affects the most people and the greatest impact on human health. The EPA has expanded regulatory effort to increase the number of dioxin/furan toxic compounds as well as established a 99.999% DRE requirement for dioxin emissions to mitigate the formation of these PICs during combustion system operation. Waste combustion accounts for about 95% of all the known dioxin emissions, with medical and municipal waste combustion being identified as dominant sources. The EPA has focused on waste incinerators as being critical to generation of dioxin/furans and needing regulation in order to reduce their generation levels.

PCDD/PCDF formation chemistry is extremely complex. The chlorine needed for dioxin formation can be supplied by chloro-organic chemicals and also by inorganic salts. Chlorine-based waste stream sources can include PVC plastics, paper, and lead batteries. Dioxins are created within incinerator units by trace kinetic side reactions occurring during thermal destruction. Separate side reactions occur in the gas phase, liquid phase, and on solid surfaces. Some reactions will occur in the flame, others during cool down of post-combustion gases, and still others can occur at lower temperatures in pollution control equipment. The amount of PCDD/PCDF detected in incinerator stack emissions and in the fly ash samples has been found to vary considerably from incinerator to incinerator and from burn to burn.

CPCDD/PCDF chemistry in cooler reformation zones downstream of the combustion zone has a critical need for formed particulates to support catalytic surface reactions. These post combustion particulates to which PCDD/PCDFs can bind may be either non-combustible "fly-ash" or combustion process products, i.e., soot. Current evidence also suggests that surface catalyzed reactions, wherein corrosion processes are determined to be occurring, can also be occurring at relatively low temperatures (250–400ºC) (482–752ºF) and can play an important role in regions. Total dioxin and furan emissions in some cases have been reduced with improvements in combustion control

and the use of electrostatic precipitators. However, even with good combustion control and minimizing particulates to reduce PCDD/PCDF formation, if the reduced particles elude capture by pollution control equipment, overall PCDD/PCDF emissions may actually increase. To this end, the use of air scrubbers having baghouses coupled with injected activated carbon has been found to capture dioxins.

In the incineration of heterogeneous materials such as raw municipal refuse and especially for mass burning configurations, it is common to produce flue gases that fluctuate in composition between oxidizing conditions, i.e., having an excess of oxygen, and reducing conditions, conditions devoid of oxygen and with significant concentrations of reducing gases such as carbon monoxide, hydrogen, or mixed hydrocarbons. The burning of carbon-bearing wastes, conditions of high temperature and low oxygen concentration, lead to the formation of soot. The slow burnout rate of soot makes subsequent control efforts difficult.

Post gas treatment pollution control technologies used with solid fuel combustion configurations, described in detail in Section 6.5 of Chapter 6, are applicable to many of the thermal destruction arrangements described in this chapter. Recall that a variety of methods can be utilized to remove particulate matter from an exhaust gas stream, including mechanical collectors, wet collectors, electrostatic precipitators, and filters.

Thermal destruction technologies will process metals contained in the waste stream. Metals identified of significant public health concern include cadmium (Cd), chromium (Cr), mercury (Hg), and lead (Pb). These materials are discharged after processing either as particulate matter or in a vaporized state. Solid waste incinerators, such as MSW units, due to the waste stream composition, can produce fly ashes of specific activity and may have high concentrations of various metals in the incinerator stack.

NO_x emissions, such as those related to solid waste destruction, much like solid fuel chemistry, are a direct result of several waste-destructor parameters. Emission levels depend on factors such as preparation and particle size of solid waste being burned, percent excess air used in firing, actual reaction temperatures involved, and percent nitrogen originally present in the waste. Burning solid wastes, such as MSW, can generate both thermal NO_x because of high-temperature N-O thermochemistry, and fuel NO_x because of the presence of fuel bound nitrogen in the waste stream. By adjusting primary air using combustion control to promote substoichiometric fuel rich combustion in the incineration's first stage, main combustion zone will reduce the intermediate flame temperature and hence lower NO_x formation. Air staging (see Chapter 6, Section 6.5) using overfire air and separated multilevel injection ports can also achieve burnout at a lower final temperature and prevent additional NO_x formation in MSW incinerators. Flue gas recirculation techniques can return a fraction of the gas either to the incinerator or into the burners in order to reduce NO_x. Post combustion NO_x control approaches can utilize selective noncatalytic reduction (SNCR) or selective catalytic reduction (SCR) technology.

Table 13.2a provides the MACT emission standards for conventional waste incinerators, while Table 13.2b gives the MACT emission standards for selected hazardous waste combustors.

EXAMPLE 13.5 A hazardous waste incinerator is being sized for air enrichment for the thermal destruction of liquid benzene, C_6H_6. Reactant feed conditions are at 25°C and 1 atm total pressure. Determine (a) the adiabatic flame temperature for ideal complete combustion for an equivalence ratio of 1.0, K; (b) the adiabatic flame temperature for

ideal complete combustion for an equivalence ratio of 1.0; (c) the excess air for 30% air enrichment conditions that provides the same adiabatic flame temperature as (a); and (d) the product volumes for parts (a), (b), and (c), %.

Solution:

1. Stoichiometric coefficients for ideal combustion of benzene in oxygen:

$$C_6H_6 + aO_2 \rightarrow bCO_2 + cH_2O$$

carbon atom balance	$6 = b$	$b = 6$
hydrogen atom balance	$6 = 2c$	$c = 3$
oxygen atom balance	$2a = 2b + c$	$a = 7.5$

2. Reaction equation for ideal complete combustion of benzene in air for Φ=1:

$$C_6H_6 + (7.5)[O_2 + 3.76N_2] \rightarrow 6CO_2 + 3H_2O + (28.2)N_2$$

3. Energy balance for ideal complete combustion of benzene in air for Φ=1:

$$P = c \quad H_{\text{prod}} = H_{\text{react}}$$

$$Q = \left\{N_{CO_2}\left[\bar{h}_f^0 + \Delta\bar{h}\right]_{CO_2} + N_{H_2O}\left[\bar{h}_f^0 + \Delta\bar{h}\right]_{H_2O} + N_{N_2}\left[\bar{h}_f^0 + \Delta\bar{h}\right]_{N_2}\right\}_{\text{prod}}$$
$$- \left\{N_{\text{fuel}}\left[\bar{h}_f^0 + \Delta\bar{h}\right]_{\text{fuel}} + N_{O_2}\left[\bar{h}_f^0 + \Delta\bar{h}\right]_{O_2} + N_{N_2}\left[\bar{h}_f^0 + \Delta\bar{h}\right]_{N_2}\right\}_{\text{react}}$$

and for $Q = 0$

$$\left\{6\left[-94{,}054 + \Delta\bar{h}\langle T_2\rangle\right]_{CO_2} + 3\left[-57{,}798 + \Delta\bar{h}\langle T_2\rangle\right]_{H_2O} + 28.2\left[\Delta\bar{h}\langle T_2\rangle\right]_{N_2}\right\}_{\text{prod}}$$
$$= \left\{1\left[-11{,}720\right]_{\text{fuel}}\right\}_{\text{react}}$$

Using values for enthalpies for the product species found in appropriate tables in Appendix B

by trial and error a. $T_2 = 2{,}444.5$ K

4. Energy balance for ideal complete combustion of benzene in oxygen for Φ=1:

$$P = c \quad H_{\text{prod}} = H_{\text{react}}$$

$$C_6H_6 + (7.5)[O_2] \rightarrow 6CO_2 + 3H_2O$$
$$Q = \left\{N_{CO_2}\left[\bar{h}_f^0 + \Delta\bar{h}\right]_{CO_2} + N_{H_2O}\left[\bar{h}_f^0 + \Delta\bar{h}\right]_{H_2O}\right\}_{\text{prod}}$$
$$- \left\{N_{\text{fuel}}\left[\bar{h}_f^0 + \Delta\bar{h}\right]_{\text{fuel}} + N_{O_2}\left[\bar{h}_f^0 + \Delta\bar{h}\right]_{O_2}\right\}_{\text{react}}$$

again for $Q = 0$

$$\left\{6\left[-94{,}054 + \Delta\bar{h}\langle T_2\rangle\right]_{CO_2} + 3\left[-57{,}798 + \Delta\bar{h}\langle T_2\rangle\right]_{H_2O}\right\}_{prod} = \left\{1\left[-11{,}720\right]_{fuel}\right\}_{react}$$

and using enthalpy values for the product species found in appropriate tables in Appendix B

by trial and error b. $T_2 = 3{,}099.3$ K

5. Reaction equation for combustion of benzene in enriched air:

$$C_6H_6 + (1.\,EA)\cdot 7.5[O_2 + neair\ N_2] \rightarrow bCO_2 + cH_2O + dO_2 + eN_2$$

where

neair = moles of nitrogen in enriched air: $0 \leq neair \leq 3.76$

mole fraction of oxygen for 30% enrichment = $0.3 = 1/(1+neair)$
or $neair = 2.333$

$1.EA$ = stoichiometric coefficient multiplier for given excess air value

carbon atom balance	$6 = b$	$b = 6$
hydrogen atom balance	$6 = 2c$	$c = 3$
nitrogen atom balance	$2\cdot(1.\,EA)\cdot a\cdot neair = 2e$	$e = (1.\,EA)\cdot a\cdot neair$
oxygen atom balance	$d = (1.\,EA\cdot a) - (6 + 1.5) = (1.\,EA\cdot 7.5) - 7.5$	

6. Energy balance for ideal complete combustion of benzene in enriched air: $P = c$ $H_{prod} = H_{react}$

$$Q = \left\{N_{CO_2}\left[\bar{h}_f^0 + \Delta\bar{h}\right]_{CO_2} + N_{H_2O}\left[\bar{h}_f^0 + \Delta\bar{h}\right]_{H_2O} + N_{O_2}\left[\bar{h}_f^0 + \Delta\bar{h}\right]_{O_2} + N_{N_2}\left[\bar{h}_f^0 + \Delta\bar{h}\right]_{N_2}\right\}_{prod} - \left\{N_{fuel}\left[\bar{h}_f^0 + \Delta\bar{h}\right]_{fuel} + N_{O_2}\left[\bar{h}_f^0 + \Delta\bar{h}\right]_{O_2} + N_{N_2}\left[\bar{h}_f^0 + \Delta\bar{h}\right]_{N_2}\right\}$$

and for $Q = 0$

$$\left\{b\left[-94{,}054 + \Delta\bar{h}\langle T_2\rangle\right]_{CO_2} + c\left[-57{,}798 + \Delta\bar{h}\langle T_2\rangle\right]_{H_2O} + d\left[\Delta\bar{h}\langle T_2\rangle\right]_{O_2} + e\left[\Delta\bar{h}\langle T_2\rangle\right]_{N_2}\right\}_{prod} = \left\{1\left[-11{,}720\right]_{fuel}\right\}_{react}$$

$$\left\{6\left[-94{,}054+\Delta\bar{h}\langle T_2\rangle\right]_{CO_2}+3\left[-57{,}798+\Delta\bar{h}\langle T_2\rangle\right]_{H_2O}\right.$$
$$+\left[(1.EA\cdot 7.5)-7.5\right]\left[\Delta\bar{h}\langle T_2\rangle\right]_{O_2}$$
$$\left.+\left[(1.EA\cdot 7.5)\right]near\left[\Delta\bar{h}\langle T_2\rangle\right]_{N_2}\right\}_{prod}=\left\{1\left[-11{,}720\right]_{fuel}\right\}_{react}$$

Again using enthalpy values for the product species found in appropriate tables in Appendix B:

by trial and error c. $EA = 0.42$ and $T_2 = 2{,}445.8$

7. Product gas volume – assuming ideal gas behavior $PV = N_{tot}\bar{R}T$

or

$$V = \left(N_{tot}\bar{R}T/P\right)$$

for the combustion in air $N_{tot} = 6 + 3 + 28.8 = 37.8$ kgmoles product/kgmole fuel
for the combustion in oxygen $N_{tot} = 6+3 = 9$ kgmoles product/kgmole fuel
for the combustion in enriched air $N_{tot} = 6 + 3 + 3.15 + 24.85 = 37.00$ kgmoles product/kgmole fuel
The adiabatic product volume for combustion in oxygen then equals

$$V_{air} = \frac{(37.8\ \text{kgmole}\cdot 8{,}314.34\ \text{N}\cdot\text{m/kgmole}\cdot\text{K})(2{,}444.5\text{K})}{(101\ \text{kN/m}^2)(1{,}000\ \text{N/kN})}$$

$$V_{air} = 7{,}606.6\ \text{m}^3/\text{kgmole fuel}$$

The adiabatic product volume for combustion in air then equals

$$V_{oxy} = \frac{(9\ \text{kgmole}\cdot 8{,}314.34\ \text{N}\cdot\text{m/kgmole}\cdot\text{K})(3{,}099.3\text{K})}{(101\ k\text{N/m}^2)(1000\ \text{N/kN})}$$

$$V_{oxy} = 2{,}296.2\ \text{m}^3/\text{kgmole fuel}$$

The adiabatic product volume for combustion in enriched air then equals

$$V_{neair} = \frac{(37\ \text{kgmole}\cdot 8{,}314.34\ \text{N}\cdot\text{m/kgmole}\cdot\text{K})(2{,}445.8\text{K})}{(101\ \text{kN/m}^2)(1{,}000\ \text{N/kN})}$$

$$V_{neair} = 7{,}449.5\ \text{m}^3/\text{kgmole fuel}$$

Comments: Air enrichment holds many potential advantages in the field of thermal destruction of waste if properly used. The presence of varying nitrogen concentrations of enriched air combustion can have two effects on the products at high temperature, including dilution of the product gas mixture by nitrogen, causing the temperature to decrease, lowering of the product mole fractions, and shifting of the species equilibrium concentration in the Gibbs free energy analysis. These simple waste combustion energy calculations for enriched-air chemistry, however, demonstrate that stoichiometry, product composition, product temperature, and flue gas volume are all interrelated. Stoichiometric combustion in oxygen yields a higher temperature than stoichiometric combustion in air. Simply enriching air may not necessarily reduce all critical pollutants,

i.e., NO_x. At the stoichiometric conditions a reduction in flue gas volume is seen with the oxygen burn. Enriching air, with its nitrogen and temperature effects, may not result in reduced flue gas volume. Note that 30% air enrichment and stoichiometric air for the same adiabatic flame temperature yield approximately equal flue gas volumes. Proper application of air enrichment for use in waste treatment is not simply a replacement or reduction of nitrogen with oxygen in combustion air. One must consider First and Second Law effects, dynamic influences such as waste ignition characteristics, flame speed, heat transfer, and economics such as cost and source of oxygen generation.

PROBLEMS

13.1 Consider a stoichiometric mixture of carbon tetrachloride, CCl_4, and air. Calculate for these conditions the (a) reactant mass fractions, *mf*; (b) reactant mixture molecular weight, kg/kgmole; (c) molar $\overline{AF}$ ratio, kgmole air/kgmole fuel; and (d) mass *FA* ratio, kg fuel/kg air.

13.2 Repeat Problem 13.1 for tetrachloroethylene, C_2Cl_4.

13.3 Repeat Problem 13.1 for hexachlorobenzene, C_6Cl_6.

13.4 Repeat Problem 13.1 for chloroform, $CHCl_3$.

13.5 Repeat Problem 13.1 for ethyl chloride, C_2H_5Cl.

13.6 Repeat Problem 13.1 for chlorobenzene, C_6H_5Cl.

13.7 The mass fraction analysis of a liquid hazardous waste mixture is reported as follows:

C_s	0.728%	H_2	0.108%	H_2O	0.026%
O_2	0.106%	Cl	0.032%		

If this waste mixture requires 1 kg methane per 1 kg waste mixture for ideal chemical reaction to achieve proper destruction determine the following: (a) reactant mixture mole fractions, $\bar{x}_i$; (b) reactant mixture molecular weight, kg/kgmole; (c) molar $\overline{AF}$ ratio, kgmole air/kgmole fuel; and (d) mass *FA* ratio, kg fuel/kg air.

13.8 A hazardous liquid waste consists of a mixture containing 44% benzene, 54% toluene, and 12% water. For the combustion of 100 kg/hr of the waste mixture in 125% theoretical air, determine: (a) the reactant mole fractions, $\bar{x}_i$; (b) reactant mixture molecular weight, kg/kgmole; (c) molar $\overline{AF}$ ratio, kgmole air/kgmole fuel; and (d) mass *FA* ratio, kg fuel/kg air.

13.9 A Refuse Derived Fuel (RDF)-coal mixture is being considered for co-firing on a grate fired boiler. The boiler configuration is being designed to burn an RDF-coal mixture that is 80% RDF and 20% coal by weight. Assume that the fuel and air is supplied at *STP* and that ideal products of combustion leave the boiler at 150ºC. The combustion requires 25% excess air by weight. RDF can be considered to be cellulose with properties given in Example 4.2, while coal can be treated as solid carbon. Calculate the following: (a) the fuel-air ratio, kg fuel/kg air; (b) the ideal heat release, kJ/kg air; (c) the actual heat release, kJ/kg air; and (d) the combustion efficiency, %.

13.10 Natural gas, methane, is used to fire a low Btu aqueous waste. The stoichiometric product molecular weight is 26.482 lbm/lbmole. Treating the aqueous waste as water, find (a) the mole fractions of the stoichiometric products, %; (b) the moles of waste per mole of methane, kgmole water/kgmole fuel; (c) molecular weight of the reactive mixture, lbm/lbmole; and (d) the mass FA ratio, lbm waste mixture/lbm air.

13.11 A particular municipal waste incineration facility which processes 200 tons/day will emit particulate beyond the MACT Municipal Waste Combustor particle emission standard unless using control technology. The facility generates 50 dscf per lbm of waste processed and discharges 20 lbm of particulate matter per each U.S. ton of waste burned. For this facility determine: (a) the uncontrolled particulate matter emission, mg/dscm; (b) the appropriate MACT Municipal Waste Combustor particle emission standard, mg/dscm; and (c) the particle DRE necessary to satisfy (b).

13.12 A large Municipal Waste Combustor without particulate control will emit 20 lbm of particulate matter per each U.S. ton of waste burned. The facility generates 50 dscf per lbm of waste processed. For this facility determine: (a) the uncontrolled particulate matter emission, mg/dscm; (b) the MACT large Municipal Waste Combustor particle emission standard, mg/dscm; and (c) the particle DRE necessary to satisfy (b).

13.13 Benzene, C_6H_6, and stoichiometric enriched air are fed to a constant-pressure atmospheric hazardous waste incinerator. Reactants are supplied at 25ºC, and the product adiabatic flame temperature is 4,320ºR. Calculate (a) required air enrichment conditions, %; (b) heat release, Btu/lbm fuel; (c) combustion efficiency, %; and (c) dry exhaust gas volumetric flow rate for a fuel mass flow rate of 75 lbm/hr.

13.14 Consider the surrogate waste described in Example Problem 13.2. For combustion in 100–200% theoretical air calculate the ashless molar air-fuel ratio for the following conditions: (a) waste with no moisture; (b) waste with no plastic; and (c) waste with no cellulose, kgmole air/kgmole ashless waste.

13.15 Consider the surrogate waste described in Example Problem 13.2. For combustion in 100–200% theoretical air calculate the actual mass air-fuel ratio for the following conditions: (a) waste with no moisture; (b) waste with no plastic; and (c) waste with no cellulose, kg air/kg waste.

13.16 Consider the surrogate waste described in Example Problem 13.2. For combustion in 100–200% theoretical air calculate the higher heating value for the following conditions: (a) waste with no moisture; (b) waste with no plastic; and (c) waste with no cellulose, kJ/kg waste.

13.17 Consider the surrogate waste described in Example Problem 13.2. For combustion in 100–200% theoretical air calculate the combustion efficiency for a product temperature of 900K for the following conditions: (a) waste with no moisture; (b) waste with no plastic; and (c) waste with no cellulose, %.

13.18 Consider the surrogate waste described in Example Problem 13.2. For combustion in 180% theoretical air calculate the product volume for a product temperature of 900K for the following conditions: (a) waste with no moisture; (b) waste with no plastic; and (c) waste with no cellulose, m^3/kg waste.

13.19 Consider the surrogate waste described in Example Problem 13.2. For combustion in 100–200% theoretical air calculate the adiabatic flame temperature for the following conditions: (a) waste with no moisture; (b) waste with no plastic; and (c) waste with no cellulose, K.

13.20 Consider the surrogate waste described in Example Problem 13.2. For combustion in 100–200% theoretical air calculate the product volumes at adiabatic flame temperature for the following conditions: (a) waste with no moisture; (b) waste with no plastic; and (c) waste with no cellulose, m^3/kg waste.

Appendixes

APPENDIX A. DIMENSIONS AND UNITS

Combustion calculations require a proper use of all physical laws and, therefore, any particular problem must be correctly formulated both qualitatively, i.e., algebraically, and quantitatively, i.e., numerically.

All fundamental laws and relationships can be expressed algebraically using a consistent set of terms, or *dimensions*. A list of principal dimensions includes:

Force	$[F]$
Mass	$[M]$
Length	$[L]$
Time	$[t]$
Temperature	$[T]$

As an example, velocity has the dimensions of length divided by time, $[L/t]$ or $[Lt^{-1}]$.

Standards for mass, length, time, and temperature have been established and maintained under the supervision of an international body, the General Conference on Weights and Measures. The magnitude of any dimension is expressed numerically in terms of *units*. Some familiar unit choices for the basic dimension of length include:

$[L]$
inches
miles
angstroms
kilometers

Table A.1 Some Systems of Primary Dimensions with Corresponding Units

		Basic Units							
Dimensions		Système International (SI)		Metric (CGS)		English Engineers		British Gravitational	
PRIMARY									
Force	$[F]$	—		—		Pound force	(lbf)	Pound force	(lbf)
Mass	$[M]$	Kilogram	(kg)	Gram	(g)	Pound mass	(lbm)	—	
Length	$[L]$	Meter	(m)	Centimeter	(cm)	Feet	(ft)	Feet	(ft)
Time	$[t]$	Second	(sec)	Second	(sec)	Second	(sec)	Second	(sec)
Temperature	$[T]$	Kelvin	(K)	Kelvin	(K)	Rankine	(°R)	Rankine	(°R)
SECONDARY									
Force	$[M][L]/[t^2]$	Newton	($kg \cdot m/sec^2$)	Dyne	($g \cdot cm/sec^2$)	—		—	
Mass	$[M]$	—		—		—		Slug	
Pressure	$[F]/[L^2]$	Pascal	(N/m^2)	Bar	($dyne/cm^2$)	Psf	(lbf/ft^2)	Psf	(lbf/ft^2)
Energy	$[F][L]$	Joule	($N \cdot m$)	Erg	($dyne \cdot cm$)	ft·lbf		ft·lbf	
Power	$[F][L][t]$	Watt	(J/sec)	—		Horsepower	(ft·lbf/sec)	Horsepower	(ft·lbf/sec)
g_0		$1.0 \dfrac{kg \cdot m}{N \cdot sec^2} = 1.0$		$1.0 \dfrac{g \cdot cm}{dyne \cdot cm^2} = 1.0$		$32.2 \dfrac{lbm \cdot ft}{lbf \cdot sec^2} = 1.0$		$1.0 \dfrac{slug \cdot ft}{lbf \cdot sec^2} = 1.0$	

Table A.1 summarizes several systems of primary dimensions and corresponding units. Two dimension and unit systems are currently used in most engineering and scientific work in combustion: the new International System of Units (SI) and the English Engineers. Length [L] and time [t] are primary dimensions in both these measurement systems; see Table A.1. In the SI, mass [M] is taken as a primary dimension and force [F] is a derived, or secondary, dimension. The Engineers system differs from SI in that force [F] as well as mass [M] are *both* taken as primary dimensions.

Newton's second law defines the interrelationship between force and mass as

$$F \sim Ma \tag{A.1}$$

or, written dimensionally, as

$$[F] \sim [M][L][t^{-2}]$$

Since force, mass, length, and time are distinct dimensions, Newton's second law is more properly written as

$$F = \frac{Ma}{g_0} \tag{A.2}$$

where g_0 is an arbitrary constant necessary to provide both dimensional and unit homogeneity. Thus,

$$g_0 = \frac{[M][a]}{[F]}$$

or

$$[g_0] = [M][L][t^{-2}][F^{-1}] \tag{A.3}$$

Substituting dimensionally for g_0, Newton's second law then yields proper dimensions on both the left and right sides of the equation or

$$[F] = \frac{[M][L][t^{-2}]}{[M]]L][t^{-2}][F^{-1}]} = [F]$$

In the SI, the secondary dimension of force, specified as a Newton [N], is defined as the force that would accelerate 1 kg at a rate of 1 m/sec^2. For the SI, then,

$$g_0 = \frac{Ma}{F} = \frac{(1\,\text{kg})(1\,\text{m}/\text{sec}^2)}{1\,\text{N}} = 1\,\frac{\text{kg}\cdot\text{m}}{\text{N}\cdot\text{sec}^2}$$

Note, however, that the Newton is defined in terms of [M], [L], and [t] as

$$1\,\text{N} \equiv 1\,\text{kg}\cdot\text{m}/\text{sec}^2$$

and

$$g_0 = \frac{\text{kg}\cdot\text{m}}{[\text{kg}\cdot\text{m}/\text{sec}^2]\text{sec}^2} = 1.0$$

For the SI, g_0 has a magnitude of unity and dimensionless character.

For the English Engineers system, force, mass, length, and time are all primary quantities. From physics, the pound force [lbf] is that force that will accelerate a pound mass [lbm] at 32.1740 ft/sec^2. Using the above values, the value of g_0 in the English Engineers system becomes

$$g_0 = \frac{(1\ \text{lbm})(32.1740\ \text{ft}/\text{sec}^2)}{(1\ \text{lbf})} = 32.1740 \frac{\text{lbm} \cdot \text{ft}}{\text{lbf} \cdot \text{sec}^2}$$

It is important to emphasize that g_0 in Engineers units is a dimensional constant having *both* magnitude and dimensions.

Engineering analysis in this text is expressed in either SI or Engineers units of measurement. Often, calculations are compounded by the fact that these two systems of dimensions and units both may appear. Calculations that involve two sets of dimensions and units require conversion factors that allow an easy interchange between units. An equation can be multiplied by a conversion factor without affecting the dimensional characteristics because conversion factors are unities (dimensionless). Two familiar examples are:

$$\frac{2.54\ \text{cm}}{\text{in.}} \equiv 1 \qquad \frac{60\ \text{sec}}{\text{min}} \equiv 1$$

Extensive tables of general conversion factors for combustion analyses are provided in Tables A.2–A.17, while Table A.18 lists specific conversion factors between the English Engineers and SI units. Table A.19 is a set of 16 prefixes for use with the SI units for forming multiples and submultiples of basic SI units.

Useful Conversion Factors

Table A.2 Length Conversion Factors

↓ from to →	Å	μ	cm	m	km	in	ft	yd	mi
angstroms, Å	1	0.0001	1.00000E-08	1E-10	1.00000E-13	3.93701E-09	3.28084E-10	1.09361E-10	6.21371E-14
microns, μ	10000	1	0.0001	1.00000E-06	1.00000E-09	3.93701E-05	3.28084E-06	1.09361E-06	6.21371E-10
centimetres, cm	1.00000E+08	10000	1	0.01	1.00000E-05	0.39370079	0.0328084	0.01093613	6.21371E-06
metres, m	1.00000E+10	1.00E+06	100	1	0.001	39.3700787	3.2808399	1.0936133	6.21371E-04
kilometres, km	1.00000E+13	1.00000E+09	1.00000E+05	1000	1	39370.0787	3280.8399	1093.6133	0.62137119
inches, in	2.54000E+08	25400	2.54*	2.54000E-02	2.54000E-05	1	0.08333333	0.02777778	1.57828E-05
feet, ft	3.04800E+09	3.04800E+05	30.48	0.3048	3.04800E-04	12	1	0.33333333	1.89394E-04
yards, yd	9.14400E+09	914400	91.44	0.9144	9.14400E-04	36	3	1	5.68182E-04
statute miles, mi	1.60934E+13	1.60934E+09	1.60934E+05	1609.344	1.60934E+00	6.33600E+04	5280	1760	1

*To convert from inches to centimeters multiply by 2.54.

Table A.3 Area Conversion Factors

↓ from → to	cm^2	m^2	km^2	in^2	ft^2	yd^2	acre	mi^2	$naut^2$
square centimeters, cm^2	1	0.0001	1E-10	0.15500031	0.001076391	0.000119599	2.47105E-08	3.86102E-11	2.91553E-11
square meters, m^2	10000	1	0.000001	1550.0031	10.76391042	1.195990046	0.000247105	3.86102E-07	2.91553E-07
square kilometers, km^2	10000000000	1000000	1	1550003100	10763910.42	1195990.046	247.1053815	0.386102159	0.29155307
square inches, in^2	6.4516	0.00064516	6.4516E-10	1	0.006944444	0.000771605	1.59423E-07	2.49098E-10	1.88098E-10
square feet, ft^2	929.0304	0.09290304	9.2903E-08	144*	1	0.111111111	2.29568E-05	3.58701E-08	2.70862E-08
square yard, yd^2	8361.2736	0.83612736	8.36127E-07	1296	9	1	0.000206612	3.22831E-07	2.43775E-07
acres, acre	40468564.22	4046.856422	0.004046856	6272640	43560	4840	1	0.0015625	0.001179873
square statute miles, mi^2	25899881103.4	2589988.11	2.58998811	4014489600	27878400	3097600	640	1	0.755118985
square nautical miles, $naut^2$	34299072903	3429907.29	3.42990729	5316366933	36919214.81	4102134.979	847.5485494	1.324294608	1

*To convert from square feet to square inches multiply by 144.

Table A.4 Volume Conversion Factors

from ↓ to →	ml	cm^3	m^3	in^3	ft^3	gal	imp gal	l	yd^3
millilitres, ml	1	1	1.00000E-06	0.061023744	3.5315E-05	2.64172E-04	2.19969E-04	0.001	1.30795E-06
cubic centimetres, cm^3	1	1	1.0000E-06	0.061023744	3.5315E-05	2.64172E-04	2.19969E-04	0.001	1.30795E-06
cubic metres, m^3	1.0000E+06	1.0000E+06	1	6.10237E+04	35.31466672	264.1720524	219.9692347	1000	1.307950619
cubic inches, in^3	16.387064	16.387064	1.63871E-05	1	5.7870E-04	0.004329004	0.00360465	0.016387064	2.14335E-05
cubic feet, ft^3	28316.84659	28316.84659	0.028316847	1728*	1	7.480519	6.228835073	28.31684659	0.037037037
U.S. gallons, gal	3785.411784	3785.411784	0.003785412	231	0.133680556	1	0.832674133	3.785411784	0.004951132
imperial gallons, imp gal	4546.090282	4546.090282	0.0045	277.41945	0.160543663	1.20095	1	4.546090282	0.005946062
litres, l	1000	1000	0.001	61.02374409	0.035314667	0.264172052	0.219969235	1	0.001307951
cubic yards, yd^3	7.64555E+05	7.64555E+05	0.764554858	4.66560E+04	27	201.974026	168.178547	764.554858	1

*To convert from cubic feet to cubic inches multiply by 1728.

Table A.5 Time Conversion Factors

↓ from → to	μsec	msec	sec	min	hr	day	mon	yr
Microseconds, μsec	1	0.001	0.000001	1.66667E-08	2.77778E-10	1.15741E-11	3.80518E-13	3.17098E-14
milliseconds, msec	1000	1	0.001	1.66667E-05	2.77778E-07	1.15741E-08	3.80518E-10	3.17098E-11
seconds, sec	1000000	1000	1	0.016666667	2.77778E-04	1.15741E-05	3.80518E-07	3.17098E-08
minutes, min	60000000	60000	60	1	0.016666667	0.000694444	2.28311E-05	1.90259E-06
hours, hr	3600000000	3600000	3600	60*	1	0.041666667	0.001369863	0.000114155
days, day	86400000000	86400000	86400	1440	24	1	0.032876712	0.002739726
months, mon	2.628E+12	2628000000	2628000	43800	730	30.41666667	1	0.083333333
years, yr	3.1536E+13	31536000000	31536000	525600	8760	365	12	1

*To convert from hours to minutes multiply by 60.

Table A.6 Velocity Conversion Factors

from ↓ to →	cm/sec	m/sec	km/sec	km/hr	ft/sec	ft/min	ft/hr	mi/hr	knots
centimetres per second, cm/sec	1	0.01	1.0000E-05	0.036	0.032808399	1.968503937	118.1102362	0.022369363	0.019438436
metres per second, m/sec	100	1	0.001	3.6	3.280839895	196.8503937	11811.0236	2.236936292	1.94384356
kilometres per second, km/sec	100000	1000	1	3600	3280.839895	1.96850E+05	1.18110E+07	2236.936292	1943.84356
kilometres per hour, km/hr	27.77777778	0.277777778	2.77778E-04	1	0.911344415	54.68066492	3280.839895	0.621371192	0.539956544
feet per second, ft/sec	30.48	0.3048	3.0480E-04	1.09728	1	60*	3600	0.681818182	0.592483517
feet per minute, ft/min	0.508	0.00508	5.0800E-06	0.018288	0.016666667	1	60	0.011364	0.009874725
feet per hour, ft/hr	8.46667E-03	8.46667E-05	8.46667E-08	3.04800E-04	0.000277778	0.016666667	1	1.89394E-04	1.64579E-04
statute miles per hour, mi/hr	44.704	0.44704	4.47040E-04	1.609344	1.466666667	88.0000	5280	1	0.868975825
nautical miles per hour, knots	51.44446912	0.514444691	5.14445E-04	1.852000888	1.687810667	101.26864	6076.1184	1.15078	1

*To convert from feet per second to feet per minute multiply by 60.

Table A.7 Volume Flow Rate Conversion Factors

↓ from → to	cm^3/sec	m^3/sec	m^3/hr	in^3/sec	ft^3/sec	ft^3/min	ft^3/hr	gal/min	gal/hr
cubic centimeters per second, cm^3/sec	1	1.00E-06	0.0036	0.061023744	3.53147E-05	0.00211888	0.1271328	0.015850323	0.951019388
cubic meters per second, m^3/sec	1000000	1	3600	6.1024E+04	35.31466672	2118.880003	127132.8002	15850.32314	951019.3885
cubic meters per hour, m^3/hr	277.7777778	0.000277778	1	16.95104003	0.00980963	0.588577779	35.31466672	4.402867539	264.1720524
cubic inches per second, in^3/sec	16.387064	1.6387E-05	0.05899343	1	0.000578704	0.034722222	2.083333333	0.25974026	15.58441558
cubic feet per second, ft^3/sec	28316.84659	0.028316847	101.9406477	1728.00*	1	60	3600	448.8311688	26929.87013
cubic feet per minute, ft^3/min	471.9474432	0.000471947	1.699011	28.80	0.016666667	1	60	7.480519481	448.8311688
cubic feet per hour, ft^3/hr	7.86579072	7.86579E-06	0.028316847	0.48	0.000277778	0.016666667	1	0.124675325	7.480519481
U.S. gallons per minute, gal/min	63.0901964	6.30902E-05	0.227124707	3.85	0.002228009	0.133680556	8.020833333	1	60
U.S. gallons per hour, gal/hr	1.051503273	1.0515E-06	0.003785412	0.064166667	3.71335E-05	0.002228009	0.133680556	0.016666667	1

*To convert from cubic feet per second to cubic inches per second multiply by 1728.

Table A.8 Mass Conversion Factors

from ↓ to →	grain	gm	kg	slug	oz	lbm	ton	l ton	m ton
grains, grain	1	0.06479891	6.47989E-05	4.44014E-06	0.002285714	1.42857E-04	7.14286E-08	6.37755E-08	6.47989E-08
grams, gm	15.43235835	1	0.001	6.85219E-05	0.035273962	0.002204623	1.10231E-06	9.84207E-07	1.00000E-06
kilograms, kg	1.54324E+04	1000	1	0.068521869	35.27396195	2.20462E+00	0.001102311	9.84207E-04	0.001
slugs, slug	2.25218E+05	14593.88091	14.59388091	1	5.14784E+02	3.21740E+01	1.60870E-02	1.43634E-02	0.014593881
ounces (avoirdupois), oz	437.5	28.34952313	0.028349523	1.94256E-03	1	0.0625	3.12500E-05	2.79018E-05	2.83495E-05
pounds (avoirdupois), lbm	7000	453.59237	4.53592E-01	3.10810E-02	16	1	5.00000E-04	4.46429E-04	4.53592E-04
short tons, ton	1.40000E+07	9.07185E+05	907.18474	6.21620E+01	3.20000E+04	2000*	1	0.892857143	0.90718474
long tons, l ton	1.56800E+07	1.01605E+06	1016.046909	6.96214E+01	3.58400E+04	2240	1.12	1	1.016046909
metric tons, m ton	1.54324E+07	1.00000E+06	1000	68.52186927	3.52740E+04	2204.622622	1.102311311	0.984206528	1

*To convert from short tons to pounds multiply by 2000.

Table A.9 Density Conversion Factors

↓ from → to	gm/cc	gm/m^3	kg/m^3	lbm/in^3	lbm/ft^3	lbm/gal	$slug/ft^3$
grams per cubic centimeter, gm/cc	1	1000000	1000	0.036127292	62.42796058	8.345404452	1.94032326
grams per cubic meter, gm/m^3	0.000001	1	1.00000E-03	3.61273E-08	6.24280E-05	8.3454E-06	1.94032E-06
kilograms per cubic meter, kg/m^3	0.001	1.00000E+03	1	3.61273E-05	0.062427961	0.008345404	0.001940323
pounds mass per cubic inches, lbm/in^3	27.67990471	2.76799E+07	27679.90471	1	1728*	231	53.70796295
pounds mass per cubic feet, lbm/ft^3	0.016018463	1.60185E+04	16.01846337	5.78704E-04	1	0.133680556	0.031080997
pounds mass per U.S. gallon, lbm/gal	0.119826427	119826.4273	119.8264273	0.004329004	7.480519481	1	0.232502004
slugs per cubic feet, $slug/ft^3$	0.515378041	515378.0406	515.3780406	0.018619213	32.174	4.301038194	1

*To convert from pounds mass per cubic inches to pounds mass per cubic feet multiply by 1728.

Table A.10 Mass Flow Rate Conversion Factors

from ↓ to →	gm/sec	kg/sec	slug/sec	lbm/sec	lbm/min	lbm/hr	tons/hr	tons/day	metric ton/day
grams per second, gm/sec	1	0.001	6.85219E-05	0.002204623	0.132277357	7.936641439	0.003968321	0.095239697	0.000001
kilograms per second, kg/sec	1000	1	0.068521869	2.204622622	132.2773573	7936.641439	3.968320719	95.23969726	0.001
slugs per second, slugs/sec	14593.88091	14.59388091	1	32.174	1930.44	115826.4	57.9132	1389.9168	0.014593881
pounds mass per second, lbm/sec	453.59237	0.45359237	0.031080997	1	60	3600	1.8	43.2	0.000453592
pounds mass per minute, lbm/min	7.559872833	0.007559873	0.000518017	0.016666667	1	60	0.03	0.72	7.55987E-06
pounds mass per hour, lbm/hr	0.125997881	0.000125998	8.63361E-06	0.000277778	0.016666667	1	0.0005	0.012	1.25998E-07
tons per hour, tons/hr	251.9957611	0.251995761	0.017267221	0.555555556	33.33333333	2000*	1	24	0.000251996
tons per day, tons/day	10.49982338	0.010499823	0.000719468	0.023148148	1.388888889	83.33333333	0.041666667	1	1.04998E-05
metric tons per day, metric tons/day	1000000	1000	68.52186927	2204.622622	132277.3573	7936641.439	3968.320719	95239.69726	1

*To convert from tons per hour to pounds mass per hour multiply by 2000.

Table A.11 Pressure Conversion Factors

↓ from to →	mmHg	ft H_2O	torr	psi	atm	N/m^2	kPa	MPa	bar
millimeters of mercury, mmHg	1	0.04464804	1	0.019336776	0.001315789	133.3219737	0.133321974	0.000133322	0.00133322
feet of water (@60 F), ft H_2O	22.3974	1	22.3974	0.433093514	0.029470263	2986.065573	2.986065573	0.002986066	0.029860656
torr, mmHg	1	0.04464804	1	0.019336776	0.001315789	133.3219737	0.133321974	0.000133322	0.00133322
pounds force per square inch, psi	51.71492826	2.30897016	51.71492826	1	0.068045958	6894.736305	6.894736305	0.006894736	0.068947363
atmospheres, atm	760	33.93251002	760	14.69595*	1	1.01325E+05	101.3247	0.1013247	1.013247
newtons per square meter, N/m^2	0.007500639	3.34889E-04	0.007500639	1.45038E-04	9.86926E-06	1	0.001	0.000001	1.00000E-05
kilopascals, kPa	7.500639035	0.334888828	7.500639035	0.145038179	0.009869262	1000	1	0.001	0.01
megapascals, MPa	7500.639035	334.8888279	7500.639035	145.0381792	9.869261888	1000000	1000	1	10
bars, bar	750.0639035	33.48888279	750.0639035	14.50381792	0.986926189	1.00000E+05	100	0.1	1

*To convert from atmospheres to pounds force per square inch multiply by 14.69595.

Table A.12 Energy Conversion Factors

from ↓ to →	erg	cal	Btu	J	kJ	MJ	ft·lbf	hp·hr	kW·hr
ergs, erg	1	2.39006E-08	9.48451E-11	1.00000E-07	1.00000E-10	1.00000E-13	7.38056E-08	3.72755E-14	2.77778E-14
calories, cal	4.18400E+07	1	0.003968321	4.184	0.004184	4.18400E-06	3.088025534	1.55961E-06	1.16222E-06
British thermal units, Btu	1.05435E+10	251.99576	1	1054.35026	1.05435E+00	1.05435E-03	778.1693413*	3.93015E-04	2.92875E-04
Joules, J	1.00000E+07	0.239005736	9.48451E-04	1	0.001	0.000001	0.738055816	3.72755E-07	2.77778E-07
kilojoules, kJ	1.00000E+10	2.39006E+02	9.48451E-01	1000	1	1.00000E-03	7.38056E+02	3.72755E-04	2.77778E-04
megajoules, MJ	1.00000E+13	2.39006E+05	9.48451E+02	1.00000E+06	1.00000E+03	1	7.38056E+05	3.72755E-01	2.77778E-01
foot pounds force, ft·lbf	1.35491E+07	0.323831519	0.001285067	1.354911076	1.35491E-03	1.35491E-06	1	5.05051E-07	3.76364E-07
horsepower·hour, hp·hr	2.68272E+13	6.41186E+05	2544.433319	2.68272E+06	2.68272E+03	2.68272E+00	1.98000E+06	1	0.745201092
kilowatt hours, kW·hr	3.60000E+13	8.60421E+05	3414.425108	3.60000E+06	3.60000E+03	3.60000E+00	2.65700E+06	1.341919665	1

*To convert from British thermal units to foot pounds force multiply by 778.1693413.

Table A.13 Specific Energy (Mass) Conversion Factors

↓ from → to	cal/gm	ft·lbf/lbm	Btu/lbm	J/gm	kJ/kg	hp·hr/lbm	kW·hr/kg
calories per gram, cal/gm	1	1399.765807	1.798793312	4.184	4.184	0.000706952	0.001162222
foot pounds force per pound mass, ft·lbf/lbm	0.000714405	1	0.001285067	0.002989071	0.002989071	5.05051E-07	8.30298E-07
British thermal units per pound mass, Btu/lbm	0.55592824	778.1693413*	1	2.326003756	2.326003756	0.000393015	0.000646112
Joules per gram, J/gm	0.239005736	334.5520571	0.42992192	1	1	0.000168966	0.000277778
kilojoules per kilogram, kJ/kg	0.239005736	334.5520571	0.42992192	1	1	0.000168966	0.000277778
horsepower hours per pound mass, hp·hr/lbm	1414.522337	1980000	2544.433319	5918.361457	5918.361457	1	1.643989294
kilowatt hours per kilogram, kW·hr/kg	860.4206501	1204387.405	1547.718911	3600	3600	0.608276467	1

*To convert from British thermal units per pound mass to foot pounds force per pound mass multiply by 778.1693413.

Table A.14 Specific Energy (Volume) Conversion Factors

from ↓ to →	cal/cm^3	Btu/in^3	Btu/ft^3	Btu/gal	ft·lbf/in^3	ft·lbf/ft^3	J/cm^3	J/m^3	kJ/m^3
calories per cubic centimeters, cal/cm^3	1	6.49855E-02	1.12295E+02	1.50117E+01	5.05697E+01	8.73845E+04	4.18400E+00	4.18400E+06	4.18400E+03
British thermal units per cubic inch, Btu/in^3	1.53880E+01	1	1728	231	778.1693413	1344676.622	6.43836E+01	64383562.32	6.43836E+04
British thermal units per cubic foot, Btu/ft^3	8.90512E-03	0.000578704	1	0.133680556	0.45032948	778.1693413	3.72590E-02	3.72590E+04	3.72590E+01
British thermal units per U.S. gallon, Btu/gal	6.66149E-02	0.004329004	7.480519481	1	3.368698447	5821.110917	2.78717E-01	2.78717E+05	2.78717E+02
foot pounds force per cubic inch, ft·lbf/in^3	1.97747E-02	0.001285067	2.22060E+00	2.96851E-01	1	1728	8.27372E-02	82737.21272	8.27372E+01
foot pounds force per cubic foot, ft·lbf/ft3	1.14437E-05	7.43673E-07	0.001285067	0.000171789	0.000578704	1	4.78803E-05	47.88033143	4.78803E-02
Joules per cubic centimeters, J/cm^3	2.39006E-01	1.55319E-02	26.83914865	3.587872303	1.20865E+01	2.08854E+04	1	1.00000E+06	1000
Joules per cubic meters, J/m^3	2.39006E-07	1.55319E-08	2.68391E-05	3.58787E-06	1.20865E-05	2.08854E-02	1.00000E-06	1	1.00000E-03*
kilojoules per cubic meters, kJ/m^3	2.39006E-04	1.55319E-05	0.026839149	0.003587872	1.20865E-02	2.08854E+01	0.001	1.00000E+03	1

*To convert from Joules per cubic meter to kilojoules per cubic meter multiply by 1,000.

Table A.15 Specific Energy (Mass Flux) Conversion Factors

from ↓ to →	cal/gm/sec	ft·lbf/lbm/sec	ft·lbf/lbm/min	ft·lbf/lbm/hr	Btu/lbm/sec	Btu/lbm/min	Btu/lbm/hr	J/gm/sec	kJ/kg/sec
calories per gram per second, cal/gm/sec	1	1399.765807	83985.9484	5039156.904	1.798793312	107.9275987	6475.655923	4.184	4.184
foot pound force per pound mass per second, ft·lbf/lbm/sec	0.000714405	1	60	3600*	0.001285067	0.07710404	4.626242399	0.002989071	0.002989071
foot pound force per pound mass per min, ft·lbf/lbm/min	1.19068E-05	0.016666667	1	60	2.14178E-05	0.001285067	0.07710404	4.98179E-05	4.98179E-05
foot pound force per pound mass per hour, ft·lbf/lbm/hr	1.98446E-07	0.000277778	0.016666667	1	3.56963E-07	2.14178E-05	0.001285067	8.30298E-07	8.30298E-07
British thermal units per pound mass per second, Btu/lbm/sec	0.55592824	778.1693413	46690.16048	2801409.629	1	60	3600	2.326003756	2.326003756
British thermal units per pound mass per minute, Btu/lbm/min	0.009265471	12.96948902	778.1693413	46690.16048	0.016666667	1	60	0.038766729	0.038766729
British thermal units per pound mass per hour, Btu/lbm/hr	0.000154425	0.21615815	12.96948902	778.1693413	0.000277778	0.016666667	1	0.000646112	0.000646112
Joules per gram per second, J/gm/sec	0.239005736	334.5520571	20073.12342	1204387.405	0.42992192	25.79531518	1547.718911	1	1
kilojoules per kilogram per second, kJ/kg/sec	0.239005736	334.5520571	20073.12342	1204387.405	0.42992192	25.79531518	1547.718911	1	1

*To convert from foot pound force per pound mass per second to foot pound force per pound mass per hour multiply by 3600.

Table A.16 Specific Heat and Entropy Conversion Factors

↓ from to →	erg/sec·K	cal/gm·K	ft·lbf/lbm·°R	Btu/lbm·°R	J/gm·K	kJ/kg·K
ergs per second Kelvin, erg/sec·K	1	2.38846E-08	1.85862E-05	2.38846E-08	1.00000E-07	1.00000E-07
calories per gram Kelvin, cal/gm·K	4.18681E+07	1	778.1693413	1	4.186806761	4.186806761
foot pounds force per pound mass Rankine, ft·lbf/lbm·R	5.38033E+04	0.001285067	1	0.001285067	0.005380329	0.005380329
British thermal units per pound mass Rankine, Btu/lbm·°R	4.18681E+07	1	778.1693413*	1	4.186806761	4.186806761
Joules per gram Kelvin, J/gm·K	1.00000E+07	0.238845511	185.8622539	0.238845511	1	1
kilojoules per kilogram Kelvin, kJ/kg·K	1.00000E+07	0.238845511	185.8622539	0.238845511	1	1

*To convert from British thermal units per pound mass Rankine to foot pounds force per pound mass Rankine multiply by 778.1693413.

Table A.17 Power Conversion Factors

from ↓ to →	ft·lbf/sec	ft·bf/min	ft·lbf/hr	Btu/sec	Btu/min	Btu/hr	hp	W	kW
foot pounds force per second, ft·lbf/sec	1	60	3600	0.001285067	0.07710404	4.626242399	0.001818182	1.355818	0.001355818
foot pounds force per minute, ft·lbf/min	0.016666667	1	60	2.14178E-05	0.001285067	0.07710404	3.0303E-05	0.022596967	2.2597E-05
foot pounds force per hour, ft·lbf/hr	0.000277778	0.016666667	1	3.56963E-07	2.14178E-05	0.001285067	5.05051E-07	0.000376616	3.76616E-07
British thermal units per second, Btu/sec	778.1693413	4.66902E+04	2801409.629	1	60	3600	1.414853348	1055.056	1.055056
British thermal units per minute, Btu/min	12.96948902	778.1693413	46690.16048	0.016666667	1	60	0.023580889	17.58426667	0.017584267
British thermal units per hour, Btu/hr	0.21615815	12.96948902	778.1693413	0.000277778	0.016666667	1	0.000393015	0.293071111	0.000293071
horsepower, hp	550*	3.30000E+04	1980000	0.706787033	42.40722199	2544.433319	1	745.6999	0.7456999
watts, W	0.737562121	44.25372727	2655.223636	9.47817E-04	0.056869019	3.412141156	0.001341022	1	0.001
kilowatts, kW	737.5621212	44253.72727	2655223.636	0.947816988	56.86901927	3412.141156	1.341022038	1000	1

*To convert from horsepower to foot pounds force per second multiply by 550.

Table A.18 Engineers-SI Conversion Factors[a]

To convert from English Engineers units	To SI units	Multiply by
acceleration (ft/sec^2)	meter/second^2 (m/sec^2)	3.048 000 E – 01
Btu	joules (J)	1.055 056 E + 03
Btu/gal (U.S. liquid)	kJ/m^3	2,787 200 E + 05
Btu/lbm	joules/kilogram (J/kg)	2.326 000 E + 03
Btu/lbm °R	joules/kilogram Kelvin (J/kg K)	4.184 000 E + 03
Btu/ft^3	joules/meter^3 (J/m^3)	3.725 895 E + 04
Btu/hr	watt (W)	2.930 711 E – 01
degree Celsius	kelvin (K)	tK = t°C + 273.15
degree Fahrenheit	degree Celsius	t°C = (t°F – 32)/1.8
degree Fahrenheit	kelvin (K)	tK = (t°F + 459.67)/1.8
degree Rankine	kelvin (K)	tK = t°R/1.8
foot	meter (m)	3.048 000 E – 01
foot of H_2O	Pascal (Pa)	2.988 980 E + 03
ft^2	meter^2 (m^2)	9.290 304 E – 02
ft^3 (volume)	meter^3 (m^3)	2.831 685 E – 02
ft^3/lbm	meter^3/kg (m^3/kg)	6.242 797 E – 02
ft·lbf	joule (J)	1.355 818 E + 00
ft·lbf/lbm	joules/kilogram (J/kg)	2.989 067 E + 00
ft·lbf/hr	watt (W)	3.766 161 E – 04
ft/sec^2	meter/sec^2 (m/s^2)	3.048 000 E – 01
gallon (U.S. liquid)	meter^3 (m^3)	3.785 412 E – 03
horsepower (550 ft·lbf/sec)	watt (W)	7.456 999 E + 02
inch	meter (m)	2.540 000 E – 02
inch of Hg (32°F)	pascal (Pa)	3.386 380 E + 03
inch^2	meter^2 (m^2)	6.451 600 E – 04
kelvin	degree Celsius	t°C = tK – 273.15
kilowatt hour	joule (J)	3.600 000 E + 06
liter	meter^3 (m^3)	1.000 000 E – 03
mile (statute)	meter (m)	1.609 300 E + 03
mile (U.S. nautical)	meter (m)	1.852 000 E + 03
pound mass (lbm avoirdupois)	kilogram (kg)	4.535 924 E – 01
lbm/ft^3	kilogram/meter^3 (kg/m^3)	1.601 846 E + 01
lbm/hp·hr	kilogram/kilowatt hour (kg/kW·hr)	1.689 659 E – 07
lbm/gal (U.S. liquid)	kg/m^3	1.198 264 E + 02
pound force (lbf)	newton (N)	4.448 222 E + 00
lbf/in^2 (psi)	pascal (Pa)	6.894 757 E + 03
ton (long, 2240 lbm)	kilogram (kg)	1.016 047 E + 03
ton (short, 2000 lbm)	kilogram (kg)	9.071 847 E + 02
velocity, ft/sec	meter/sec (m/sec)	3.048 000 E – 01
volume flow rate, ft^3/sec	meter^3/sec (m^3/sec)	2.831 685 E – 02

[a]From ASTM Standard for Metric Practice E380-76, 1976. Copyright ASTM International. Reprinted with permission.

Table A.19 SI Prefixes

Factor	Prefix	Symbol
10^{18}	exa	E
10^{15}	peta	P
10^{12}	tera	T
10^{9}	giga	G
10^{6}	mega	M
10^{3}	kilo	k
10^{2}	hector	h
10^{1}	deka	da
10^{-1}	deci	d
10^{-2}	centi	c
10^{-3}	milli	m
10^{-6}	micro	μ
10^{-9}	nano	n
10^{-12}	pico	p
10^{-15}	femto	f
10^{-18}	atto	a

APPENDIX B. SOME THERMOCHEMICAL PROPERTIES

Table B.1 Standard State Heats of Formation and Combustion (Higher Heating Value) for Various Compounds

Substance	Formula	Molecular Weight	State	$\bar{h}_f^0$	$-\Delta\bar{H}_c^{0\,a}$
Carbon	C_S	12.0111	solid	0.000	94,054
Carbon	C_g	12.0111	g	170,890	—
Methyl radical	CH_3	15.0350	g	34,820	—
Carbon monoxide	CO	28.0105	g	–26,420	67,636
Carbon dioxide	CO_2	44.0099	g	–94,054	—
Monatomic hydrogen	H	1.00797	g	52,100	—
Hydrogen chloride	HCl	36.465	g	–22,080	—
Diatomic hydrogen	H_2	2.0160	g	0.000	68,317
Water	H_2O	18.016	ℓ	–68,317	—
Water	H_2O	18.016	g	–57,798	—
Hydrogen peroxide	H_2O_2	34.015	g	–32,576	—
Hydrogen sulfide	H_2S	34.080	g	–4,815	—
Monatomic nitrogen	N	14.0067	g	113,000	—
Nitric oxide	NO	30.008	g	21,580	—
Nitrogen dioxide	NO_2	46.008	g	7,910	—
Diatomic nitrogen	N_2	28.0134	g	0.000	—
Ammonia	NH_3	17.036	g	–10,970	—
Hydrazine	N_2H_4	32.045	g	22,790	—
Dinitrogen monoxide	N_2O	44.016	g	19,610	—
Dinitrogen tetroxide	N_2O_4	92.016	g	2,170	—
Monatomic oxygen	O	15.9994	g	59,559	—
Hydroxyl radical	OH	17.0074	g	9,432	—
Diatomic oxygen	O_2	31.9988	g	0.000	—
Ozone	O_3	47.9982	g	34,200	—
Monatomic sulfur	S	32.064	g	66,680	—
Sulfur	S	32.064	solid	0.000	—
Sulfur dioxide	SO_2	64.066	g	–70,947	—
		g/gmole		cal/gmole	

Table B.1 Continued

Substance	Formula	Molecular Weight	State	$\overline{h}_f^0$	$-\Delta\overline{H}_c^{0\,a}$
		Paraffins			
Methane	CH_4	16.041	g	–17,895	212,790
Ethane	C_2H_6	30.067	g	–20,240	372,820
Propane	C_3H_8	44.092	g	–24,820	530,610
n–Butane	C_4H_{10}	58.118	ℓ	–35,390	682,410
n–Butane	C_4H_{10}	58.118	g	–30,150	687,650
iso–Butane	C_4H_{10}	58.118	ℓ	–37,470	680,330
iso–Butane	C_4H_{10}	58.118	g	–32,400	685,400
n–Pentane	C_5H_{12}	72.144	ℓ	–41,890	838,280
n–Pentane	C_5H_{12}	72.144	g	–35,718	844,450
iso–Pentane	C_5H_{12}	72.144	ℓ	–43,590	836,580
iso–Pentane	C_5H_{12}	72.144	g	–37,700	842,470
n–Hexane	C_6H_{14}	86.169	ℓ	–46,850	995,690
n–Hexane	C_6H_{14}	86.169	g	–39,960	1,002,580
n–Heptane	C_7H_{16}	100.198	ℓ	–54,380	1,150,530
n–Heptane	C_7H_{16}	100.198	g	–45,645	1,159,270
n–Octane	C_8H_{18}	114.224	ℓ	–59,740	1,307,550
n–Octane	C_8H_{18}	114.224	g	–49,820	1,317,470
iso–Octane	C_8H_{18}	114.224	ℓ	–62,885	1,304,400
iso–Octane	C_8H_{18}	114.224	g	–55,495	1,311,790
n–Decane	$C_{10}H_{22}$	142.276	ℓ	–72,875	1,619,150
n–Decane	$C_{10}H_{22}$	142.276	g	–60,697	1,631,330
n–Dodecane	$C_{12}H_{26}$	170.328	ℓ	–85,370	1,931,400
n–Dodecane	$C_{12}H_{26}$	170.328	g	–71,014	1,945,760
(increment per above C_6)	C atom	—	g	(~4,925)	(157,440)
		Olefins			
Ethylene	C_2H_4	28.054	g	12,540	337,280
Propylene	C_3H_6	42.081	g	4,879	491,990
n–Butene	C_4H_8	56.108	g	–30	649,450
n–Pentene	C_5H_{10}	70.135	g	–5,000	806,860
n–Hexene	C_6H_{12}	84.162	g	–9,970	964,260
n–Heptene	C_7H_{14}	98.189	g	–14,870	1,121,730
n–Octene	C_8H_{16}	112.208	g	–20,740	1,278,230
n–Nonene	C_9H_{18}	126.243	g	–24,710	1,436,630
n–Decene	$C_{10}H_{20}$	140.270	g	–29,640	1,594,070
(increment per above C_6)	C atom	—	g	(~4,925)	(157,400)
		g/gmole		cal/gmole	

Table B.1 Continued

Substance	Formula	Molecular Weight	State	$\overline{h}_f^0$	$-\Delta\overline{H}_c^{0\,a}$
		Additional Hydrocarbon Fuels			
Acetylene	C_2H_2	26.038	g	54,190	310,620
1–3–Butadiene	C_4H_6	54.092	g	26,330	607,500
Benzene	C_6H_6	78.114	ℓ	11,720	781,000
Benzene	C_6H_6	78.114	g	19,820	789,100
Cyclohexane	C_6H_{12}	84.162	ℓ	–37,340	936,890
Cyclohexane	C_6H_{12}	84.162	g	–29,430	944,800
Toluene	C_7H_8	92.142	ℓ	2,870	934,520
Toluene	C_7H_8	92.142	g	11,950	943,600
Methylcyclohexane	C_7H_{14}	98.189	ℓ	–45,430	1,091,170
Methylcyclohexane	C_7H_{14}	98.189	g	–36,990	1,099,610
Styrene	C_8H_8	104.153	ℓ	24,840	1,050,540
Styrene	C_8H_8	104.153	g	35,220	1,060,920
		Alcohol Fuels			
Methanol	CH_3OH	32.042	ℓ	–57,110	173,580
Methanol	CH_3OH	32.042	g	–48,050	182,640
Ethanol	C_2H_5OH	46.069	ℓ	–66,200	326,860
Ethanol	C_2H_5OH	46.069	g	–56,030	337,030
Propanol	C_3H_7OH	60.096	ℓ	–71,340	484,090
Butanol	C_4H_9OH	74.124	ℓ	–79,540	638,260
		g/gmole		cal/gmole	

Sources:
- ASTM Special Technical Publications No. 109A, 1963, and No. 225, 1958. Copyright ASTM International. Reprinted with permission.
- Selected Values of Physical and Thermodynamic Properties of Hydrocarbons and Related Compounds, American Petroleum Institute Research Project 44, Carnegie Press, 1953.
- Selected Values of Chemical Thermodynamic Properties, National Bureau of Standards, U.S. Circ. 500, 1952.
- JANAF Thermochemical Tables, 2nd Edition, National Bureau of Standards, Publication NSRDS–NBS37, 1971.

[a]The heat of combustion assumes the products are H_2O_ℓ and CO_{2_g}.

NOTE: To convert the molar values above to Btu/lbmole and kJ/kgmole, multiply by 1.8001 and 4.187, respectively. To convert the above molar values to a mass basis, divide by the molecular weight, i.e.,

[MW] = lbm/lbmole (kg/kgmole)

Examples:

$$\left(h_f^0\right)_{H_2O_g} = (-57{,}798 \text{ cal/gmole})(1.8001 \frac{\text{Btu/lbmole}}{\text{cal/gmole}}) = -104{,}040 \text{ Btu/lbmole}$$

$$\left(\Delta H_c^0\right)_{CH_4} = \frac{(212{,}790)\,(4{,}187) \text{ kJ/kgmole}}{16.043 \text{ kg/kgmole}} = 55{,}540 \text{ kJ/kg}$$

Table B.2 Thermochemical Properties of Carbon

Carbon (C_S) March 31, 1961
$MW = 12.011$
$\bar{h}_f^0 = 0.000$ kcal/gmole

T		$\bar{C}_p^0$	$\bar{h}\langle T\rangle - \bar{h}\langle T_0\rangle$	$\bar{s}^0\langle T\rangle$	$\Delta G^0\langle T\rangle$	$\log K_p$
0	0	0.000	–0.252	0.000	0.000	0.000
100	180	0.395	–0.238	0.210	0.000	0.000
200	360	1.202	–0.160	0.720	0.000	0.000
298	536	2.038	0.000	1.359	0.000	0.000
300	540	2.054	0.004	1.372	0.000	0.000
400	720	2.851	0.250	2.075	0.000	0.000
500	900	3.496	0.569	2.784	0.000	0.000
600	1,080	4.038	0.947	3.471	0.000	0.000
700	1,260	4.440	1.372	4.126	0.000	0.000
800	1,440	4.740	1.831	4.739	0.000	0.000
900	1,620	4.970	2.318	5.311	0.000	0.000
1,000	1,800	5.149	2.824	5.844	0.000	0.000
1,100	1,980	5.304	3.347	6.342	0.000	0.000
1,200	2,160	5.430	3.883	6.809	0.000	0.000
1,300	2,340	5.527	4.432	7.248	0.000	0.000
1,400	2,520	5.605	4.988	7.661	0.000	0.000
1,500	2,700	5.669	5.652	8.050	0.000	0.000
1,600	2,880	5.721	6.122	8.417	0.000	0.000
1,700	3,060	5.765	6.696	8.765	0.000	0.000
1,800	3,240	5.803	7.275	9.096	0.000	0.000
1,900	3,420	5.836	7.857	9.411	0.000	0.000
2,000	3,600	5.865	8.442	9.711	0.000	0.000
2,100	3,780	5.891	9.029	9.998	0.000	0.000
2,200	3,960	5.914	9.620	10.272	0.000	0.000
2,300	4,140	5.936	10.212	10.536	0.000	0.000
2,400	4,320	5.956	10.807	10.789	0.000	0.000
2,500	4,500	5.974	11.403	11.032	0.000	0.000
2,600	4,680	5.992	12.002	11.267	0.000	0.000
2,700	4,860	6.009	12.602	11.493	0.000	0.000
2,800	5,040	6.026	13.203	11.712	0.000	0.000
2,900	5,220	6.042	13.807	11.924	0.000	0.000
K	°R	$\frac{\text{cal}}{\text{gmole}\cdot\text{K}}$	$\frac{\text{kcal}}{\text{gmole}}$	$\frac{\text{cal}}{\text{gmole}\cdot\text{K}}$	$\frac{\text{kcal}}{\text{gmole}}$	—

Table B.2 Continued

Carbon (C_S)
$MW = 12.011$
$\bar{h}_f^0 = 0.000$ kcal/gmole

T		$\bar{C}_p^0$	$\bar{h}\langle T\rangle - \bar{h}\langle T_0\rangle$	$\bar{s}^0\langle T\rangle$	$\Delta G^0\langle T\rangle$	$\log K_p$
3,000	5,400	6.057	14.412	12.129	0.000	0.000
3,100	5,580	6.073	15.018	12.328	0.000	0.000
3,200	5,760	6.088	15.626	12.521	0.000	0.000
3,300	5,940	6.103	16.236	12.708	0.000	0.000
3,400	6,120	6.119	16.847	12.891	0.000	0.000
3,500	6,300	6.134	17.460	13.068	0.000	0.000
3,600	6,480	6.150	18.074	13.241	0.000	0.000
3,700	6,660	6.165	18.690	13.410	0.000	0.000
3,800	6,840	6.181	19.307	13.575	0.000	0.000
3,900	7,020	6.197	19.926	13.736	0.000	0.000
4,000	7,200	6.213	20.546	13.893	0.000	0.000
4,100	7,380	6.230	21.168	14.046	0.000	0.000
4,200	7,560	6.247	21.792	14.197	0.000	0.000
4,300	7,740	6.264	22.418	14.344	0.000	0.000
4,400	7,920	6.281	23.045	14.488	0.000	0.000
4,500	8,100	6.299	23.674	14.629	0.000	0.000
4,600	8,280	6.317	24.305	14.768	0.000	0.000
4,700	8,460	6.335	24.937	14.904	0.000	0.000
4,800	8,640	6.354	26.572	15.038	0.000	0.000
4,900	8,820	6.373	26.208	15.169	0.000	0.000
5,000	9,000	6.392	26.846	15.298	0.000	0.000
5,100	9,180	6.412	27.487	15.424	0.000	0.000
5,200	9,360	6.432	28.129	15.549	0.000	0.000
5,300	9,540	6.452	28.773	15.672	0.000	0.000
5,400	9,720	6.473	29.419	15.793	0.000	0.000
5,500	9,900	6.494	30.068	15.912	0.000	0.000
5,600	10,080	6.516	30.718	16.029	0.000	0.000
5,700	10,260	6.538	31.371	16.144	0.000	0.000
5,800	10,440	6.560	32.026	16.258	0.000	0.000
5,900	10,620	6.583	32.683	16.371	0.000	0.000
6,000	10,800	6.606	33.342	16.481	0.000	0.000
K	°R	$\frac{\text{cal}}{\text{gmole}\cdot\text{K}}$	$\frac{\text{kcal}}{\text{gmole}}$	$\frac{\text{cal}}{\text{gmole}\cdot\text{K}}$	$\frac{\text{kcal}}{\text{gmole}}$	—

Source: JANAF Thermochemical Tables, 2nd Edition, National Bureau of Standards, Publication NSRDSNB537, 1971.

Table B.3 Thermochemical Properties of Methane

Methane (CH_4) March 31, 1961
$MW = 16.043$
$\bar{h}_f^0 = -17.895$ kcal/gmole

T		$\bar{C}_p^0$	$\bar{h}\langle T\rangle - \bar{h}\langle T_0\rangle$	$\bar{s}^0\langle T\rangle$	$\Delta G^0\langle T\rangle$	$\log K_p$
0	0	0.000	–2.396	0.000	–15.991	infinite
100	180	7.949	–1.601	35.706	–15.400	33.656
200	360	8.001	–0.805	41.222	–13.909	15.198
298	536	8.518	0.000	44.490	–12.145	8.902
300	540	8.535	0.016	44.543	–12.110	8.822
400	720	9.680	0.923	47.144	–10.066	5.500
500	900	11.076	1.960	49.453	–7.845	3.429
600	1,080	12.483	3.138	51.597	–5.493	2.001
700	1,260	13.813	4.454	53.622	–3.046	0.951
800	1,440	15.041	5.897	55.548	–0.533	0.146
900	1,620	16.157	7.458	57.385	2.029	–0.493
1,000	1,800	17.160	9.125	59.141	4.625	–1.011
1,100	1,980	18.052	10.887	60.819	7.247	–1.440
1,200	2,160	18.842	12.732	62.424	9.887	–1.801
1,300	2,340	19.538	14.652	63.960	12.535	–2.107
1,400	2,520	20.150	16.637	65.431	15.195	–2.372
1,500	2,700	20.688	18.679	66.840	17.859	–2.602
1,600	2,880	21.161	20.772	68.191	20.520	–2.803
1,700	3,060	21.579	22.910	69.486	23.189	–2.981
1,800	3,240	21.947	25.086	70.730	25.854	–3.139
1,900	3,420	22.273	27.298	71.926	28.522	–3.281
2,000	3,600	22.562	29.540	73.076	31.187	–3.408
2,100	3,780	22.820	31.809	74.183	33.851	–3.523
2,200	3,960	23.050	34.103	75.250	36.511	–3.627
2,300	4,140	23.256	36.418	76.279	39.173	–3.722
2,400	4,320	23.441	38.753	77.273	41.833	–3.809
2,500	4,500	23.608	41.106	78.233	44.483	–3.889
2,600	4,680	23.758	43.474	79.162	47.141	–3.962
2,700	4,860	23.894	45.857	80.062	49.791	–4.030
2,800	5,040	24.018	48.253	80.933	52.440	–4.093
2,900	5,220	24.131	50.660	81.778	55.093	–4.152
K	°R	$\frac{\text{cal}}{\text{gmole}\cdot\text{K}}$	$\frac{\text{kcal}}{\text{gmole}}$	$\frac{\text{cal}}{\text{gmole}\cdot\text{K}}$	$\frac{\text{kcal}}{\text{gmole}}$	—

Table B.3 Continued

Methane (CH_4)
$MW = 16.043$
$\bar{h}_f^0 = -17.895$ kcal/gmole

T		$\bar{C}_p^0$	$\bar{h}\langle T\rangle - \bar{h}\langle T_0\rangle$	$\bar{s}^0\langle T\rangle$	$\Delta G^0\langle T\rangle$	$\log K_p$
3,000	5,400	24.233	53.079	82.597	57.736	–4.206
3,100	5,580	24.327	55.507	83.394	60.381	–4.257
3,200	5,760	24.413	57.944	84.167	63.026	–4.304
3,300	5,940	24.493	60.389	84.920	65.669	–4.349
3,400	6,120	24.565	62.842	85.652	68.309	–4.391
3,500	6,300	24.633	65.302	86.365	70.951	–4.430
3,600	6,480	24.695	67.768	87.060	73.589	–4.467
3,700	6,660	24.752	70.241	87.737	76.231	–4.503
3,800	6,840	24.806	72.719	88.398	78.872	–4.536
3,900	7,020	24.855	75.202	89.043	81.511	–4.568
4,000	7,200	24.901	77.690	89.673	84.150	–4.598
4,100	7,380	24.944	80.162	90.288	86.785	–4.626
4,200	7,560	24.984	82.678	90.890	89.429	–4.653
4,300	7,740	25.022	85.179	91.478	92.063	–4.679
4,400	7,920	25.057	87.683	92.054	94.700	–4.704
4,500	8,100	25.090	90.190	92.617	97.335	–4.727
4,600	8,280	25.121	92.701	93.169	99.983	–4.750
4,700	8,460	25.150	95.214	93.710	102.625	–4.772
4,800	8,640	25.177	97.730	94.240	105.268	–4.793
4,900	8,820	25.203	100.249	94.759	107.912	–4.813
5,000	9,000	25.227	102.771	95.268	110.552	–4.832
5,100	9,180	25.250	105.295	95.768	113.198	–4.851
5,200	9,360	25.272	107.821	96.259	115.844	–4.869
5,300	9,540	25.292	110.349	96.740	118.501	–4.886
5,400	9,720	25.311	112.879	97.213	121.145	–4.903
5,500	9,900	25.330	115.411	97.678	123.799	–4.919
5,600	10,080	25.347	117.945	98.134	126.449	–4.935
5,700	10,260	25.364	120.481	98.583	129.106	–4.950
5,800	10,440	25.379	123.018	99.024	131.762	–4.965
5,900	10,620	25.394	125.557	99.458	134.428	–4.979
6,000	10,800	25.409	128.097	99.885	137.081	–4.993
K	°R	$\frac{\text{cal}}{\text{gmole}\cdot\text{K}}$	$\frac{\text{kcal}}{\text{gmole}}$	$\frac{\text{cal}}{\text{gmole}\cdot\text{K}}$	$\frac{\text{kcal}}{\text{gmole}}$	—

Source: JANAF Thermochemical Tables, 2nd Edition, National Bureau of Standards, Publication NSRDSNB537, 1971.

Table B.4 Thermochemical Properties of Carbon Monoxide

Carbon Monoxide (CO) September 30, 1965
$MW = 28.01055$
$\bar{h}_f^0 = -26.417$ kcal/gmole

T		$\bar{C}_p^0$	$\bar{h}\langle T\rangle - \bar{h}\langle T_0\rangle$	$\bar{s}^0\langle T\rangle$	$\Delta G^0\langle T\rangle$	$\log K_p$
0	0	0.000	–2.072	0.000	–27.200	infinite
100	180	6.956	–1.379	39.613	–28.741	62.809
200	360	6.957	–0.683	44.435	–30.718	33.566
298	536	6.965	0.000	47.214	–32.783	24.029
300	540	6.965	0.013	47.257	–32.823	23.910
400	720	7.013	0.711	49.265	–34.975	19.109
500	900	7.121	1.417	50.841	–37.144	16.235
600	1,080	7.276	2.137	52.152	–39.311	14.318
700	1,260	7.450	2.873	53.287	–41.468	12.946
800	1,440	7.624	3.627	54.293	–43.612	11.914
900	1,620	7.786	4.397	55.200	–45.744	11.108
1,000	1,800	7.931	5.183	56.028	–47.859	10.459
1,100	1,980	8.057	5.983	56.790	–49.962	9.926
1,200	2,160	8.168	6.794	57.496	–52.049	9.479
1,300	2,340	8.263	7.616	58.154	–54.126	9.099
1,400	2,520	8.346	8.446	58.769	–56.189	8.771
1,500	2,700	8.417	9.285	59.348	–58.241	8.485
1,600	2,880	8.480	10.130	59.893	–60.284	8.234
1,700	3,060	8.535	10.980	60.409	–62.315	8.011
1,800	3,240	8.583	11.836	60.898	–64.337	7.811
1,900	3,420	8.626	12.697	61.363	–66.349	7.631
2,000	3,600	8.664	13.561	61.807	–68.353	7.469
2,100	3,780	8.698	14.430	62.230	–70.346	7.321
2,200	3,960	8.728	15.301	62.635	–72.335	7.185
2,300	4,140	8.756	16.175	63.024	–74.311	7.061
2,400	4,320	8.781	17.052	63.397	–76.282	6.946
2,500	4,500	8.804	17.931	63.756	–78.247	6.840
2,600	4,680	8.825	18.813	64.102	–80.202	6.741
2,700	4,860	8.844	l9.696	64.435	–82.153	6.649
2,800	5,040	8.863	20.582	64.757	–84.093	6.563
2,900	5,220	8.879	21.469	65.069	–86.028	6.483
K	°R	$\frac{\text{cal}}{\text{gmole}\cdot\text{K}}$	$\frac{\text{kcal}}{\text{gmole}}$	$\frac{\text{cal}}{\text{gmole}\cdot\text{K}}$	$\frac{\text{kcal}}{\text{gmole}}$	—

Table B.4 Continued

Carbon Monoxide (CO)
$MW = 28.01055$
$\bar{h}_f^0 = -26.417$ kcal/gmole

T		$\bar{C}_p^0$	$\bar{h}\langle T\rangle - \bar{h}\langle T_0\rangle$	$\bar{s}^0\langle T\rangle$	$\Delta G^0\langle T\rangle$	$\log K_p$
3,000	5,400	8.895	22.357	65.370	–87.957	6.407
3,100	5,580	8.910	23.248	65.662	–89.878	6.336
3,200	5,760	8.924	24.139	65.945	–91.795	6.269
3,300	5,940	8.937	25.032	66.220	–93.707	6.206
3,400	6,120	8.949	25.927	66.487	–95.609	6.145
3,500	6,300	8.961	26.822	66.746	–97.509	6.088
3,600	6,480	8.973	27.719	66.999	–99.400	6.034
3,700	6,660	8.984	28.617	67.245	–101.286	5.982
3,800	6,840	8.994	29.516	67.485	–103.164	5.933
3,900	7,020	9.004	30.416	67.718	–105.039	5.886
4,000	7,200	9.014	31.316	67.946	–106.908	5.841
4,100	7,380	9.024	32.218	68.169	–108.774	5.798
4,200	7,560	9.033	33.121	68.387	–110.630	5.756
4,300	7,740	9.042	34.025	68.599	–112.483	5.717
4,400	7,920	9.051	34.930	68.807	–114.333	5.679
4,500	8,100	9.059	35.835	69.011	–116.177	5.642
4,600	8,280	9.068	36.741	69.210	–118.012	5.607
4,700	8,460	9.076	37.649	69.405	–119.845	5.573
4,800	8,640	9.084	38.557	69.596	–121.672	5.540
4,900	8,820	9.092	39.465	69.784	–123.497	5.508
5,000	9,000	9.100	40.375	69.967	–125.315	5.477
5,100	9,180	9.107	41.285	70.148	–127.132	5.448
5,200	9,360	9.115	42.196	70.325	–128.941	5.419
5,300	9,540	9.123	43.108	70.498	–130.741	5.391
5,400	9,720	9.130	44.021	70.669	–132.542	5.364
5,500	9,900	9.138	44.934	70.836	–134.336	5.338
5,600	10,080	9.145	45.849	71.001	–136.129	5.312
5,700	10,260	9.153	46.763	71.163	–137.919	5.288
5,800	10,440	9.160	47.679	71.322	–139.698	5.264
5,900	10,620	9.167	48.595	71.479	–141.473	5.240
6,000	10,800	9.175	49.513	71.633	–143.249	5.218
K	°R	$\frac{\text{cal}}{\text{gmole}\cdot\text{K}}$	$\frac{\text{kcal}}{\text{gmole}}$	$\frac{\text{cal}}{\text{gmole}\cdot\text{K}}$	$\frac{\text{kcal}}{\text{gmole}}$	—

Source: JANAF Thermochemical Tables, 2nd Edition, National Bureau of Standards, Publication NSRDSNB537, 1971.

Table B.5 Thermochemical Properties of Carbon Dioxide

Carbon Dioxide (CO_2) September 30, 1965
$MW = 44.00995$
$\bar{h}_f^0 = -94.054$ kcal/gmole

T		$\bar{C}_p^0$	$\bar{h}\langle T\rangle - \bar{h}\langle T_0\rangle$	$\bar{s}^0\langle T\rangle$	$\Delta G^0\langle T\rangle$	$\log K_p$
0	0	0.000	–2.238	0.000	–93.965	infinite
100	180	6.981	–1.543	42.758	–94.100	205.645
200	360	7.734	–0.816	47.769	–94.191	102.922
298	536	8.874	0.000	51.072	–94.265	69.095
300	540	8.896	0.016	51.127	–94.267	68.670
400	720	9.877	0.958	53.830	–94.335	51.540
500	900	10.666	1.987	56.122	–94.399	41.260
600	1,080	11.310	3.087	58.126	–94.458	34.405
700	1,260	11.846	4.245	59.910	–94.510	29.506
800	1,440	12.293	5.453	61.522	–94.556	25.830
900	1,620	12.667	6.702	62.992	–94.596	22.970
1,000	1,800	12.980	7.984	64.344	–94.628	20.680
1,100	1,980	13.243	9.296	65.594	–94.658	18.806
1,200	2,160	13.466	10.632	66.756	–94.681	17.243
1,300	2,340	13.656	11.988	67.841	–94.701	15.920
1,400	2,520	13.815	13.362	68.859	–94.716	14.785
1,500	2,700	13.953	14.750	69.817	–94.728	13.801
1,600	2,880	14.074	16.152	70.722	–94.739	12.940
1,700	3,060	14.177	17.565	71.578	–94.746	12.180
1,800	3,240	14.269	18.987	72.391	–94.750	11.504
1,900	3,420	14.352	20.418	73.165	–94.751	10.898
2,000	3,600	14.424	21.857	73.903	–94.752	10.353
2,100	3,780	14.489	23.303	74.608	–94.746	9.860
2,200	3,960	14.547	24.755	75.284	–94.744	9.411
2,300	4,140	14.600	26.212	75.931	–94.735	9.001
2,400	4,320	14.648	27.674	76.554	–94.724	8.625
2,500	4,500	14.692	29.141	77.153	–94.714	8.280
2,600	4,680	14.734	30.613	77.730	–94.698	7.960
2,700	4,860	14.771	32.088	78.286	–94.683	7.664
2,800	5,040	14.807	33.567	78.824	–94.662	7.388
2,900	5,220	14.841	35.049	79.344	–94.639	7.132
K	°R	$\frac{\text{cal}}{\text{gmole}\cdot\text{K}}$	$\frac{\text{kcal}}{\text{gmole}}$	$\frac{\text{cal}}{\text{gmole}\cdot\text{K}}$	$\frac{\text{kcal}}{\text{gmole}}$	—

Table B.5 Continued

Carbon Dioxide (CO_2)
$MW = 44.00995$
$\bar{h}_f^0 = -94.054$ kcal/gmole

T		$\bar{C}_p^0$	$\bar{h}\langle T\rangle - \bar{h}\langle T_0\rangle$	$\bar{s}^0\langle T\rangle$	$\Delta G^0\langle T\rangle$	$\log K_p$
3,000	5,400	14.873	36.535	79.848	–94.615	6.892
3,100	5,580	14.902	38.024	80.336	–94.587	6.668
3,200	5,760	14.930	39.515	80.810	–94.560	6.458
3,300	5,940	14.956	41.010	81.270	–94.531	6.260
3,400	6,120	14.982	42.507	81.717	–94.495	6.074
3,500	6,300	15.006	44.006	82.151	–94.462	5.898
3,600	6,480	15.030	45.508	82.574	–94.421	5.732
3,700	6,660	15.053	47.012	82.986	–94.379	5.574
3,800	6,840	15.075	48.518	83.388	–94.331	5.425
3,900	7,020	15.097	50.027	83.780	–94.286	5.283
4,000	7,200	15.119	51.538	84.162	–94.237	5.149
4,100	7,380	15.139	53.051	84.536	–94.186	5.020
4,200	7,560	15.159	54.566	84.901	–94.130	4.898
4,300	7,740	15.179	56.082	85.258	–94.072	4.781
4,400	7,920	15.197	57.601	85.607	–94.015	4.670
4,500	8,100	15.216	59.122	85.949	–93.954	4.563
4,600	8,280	15.234	60.644	86.284	–93.885	4.460
4,700	8,460	15.254	62.169	86.611	–93.818	4.362
4,800	8,640	15.272	63.695	86.933	–93.746	4.268
4,900	8,820	15.290	65.223	87.248	–93.678	4.178
5,000	9,000	15.306	66.753	87.557	–93.603	4.091
5,100	9,180	15.327	68.285	87.860	–93.528	4.008
5,200	9,360	15.349	69.819	88.158	–93.450	3.927
5,300	9,540	15.371	71.355	88.451	–93.361	3.850
5,400	9,720	15.393	72.893	88.738	–93.280	3.775
5,500	9,900	15.415	74.433	89.021	–93.190	3.703
5,600	10,080	15.437	75.976	89.299	–93.104	3.633
5,700	10,260	15.459	77.521	89.572	–93.017	3.566
5,800	10,440	15.481	79.068	89.841	–92.918	3.501
5,900	10,620	15.503	80.617	90.106	–92.820	3.438
6,000	10,800	15.525	82.168	90.367	–92.724	3.377
K	°R	$\frac{\text{cal}}{\text{gmole}\cdot\text{K}}$	$\frac{\text{kcal}}{\text{gmole}}$	$\frac{\text{cal}}{\text{gmole}\cdot\text{K}}$	$\frac{\text{kcal}}{\text{gmole}}$	—

Source: JANAF Thermochemical Tables, 2nd Edition, National Bureau of Standards, Publication NSRDSNB537, 1971.

Table B.6 Thermochemical Properties of Acetylene

Acetylene March 31, 1961
$MW = 26.038$
$\bar{h}_f^0 = 54.190$ kcal/gmole

T		$\bar{C}_p^0$	$\bar{h}\langle T\rangle - \bar{h}\langle T_0\rangle$	$\bar{s}^0\langle T\rangle$	$\Delta G^0\langle T\rangle$	$\log K_p$
0	0	0.000	–2.393	0.000	54.325	infinite
100	180	7.014	–1.698	39.002	52.814	–115.418
200	360	8.505	–0.938	44.213	51.383	–56.146
298	536	10.539	0.000	48.004	49.993	–36.644
300	540	10.571	0.020	48.069	49.966	–36.399
400	720	12.065	1.155	51.326	48.567	–26.534
500	900	13.114	2.418	54.139	47.181	–20.622
600	1,080	13.931	3.771	56.604	45.813	–16.687
700	1,260	14.615	5.199	58.805	44.466	–13.882
800	1,440	15.239	6.693	60.798	43.137	–11.784
900	1,620	15.801	8.245	62.625	41.821	–10.155
1,000	1,800	16.318	9.852	64.317	40.622	–8.856
1,100	1,980	16.789	11.507	65.895	39.234	–7.795
1,200	2,160	17.221	13.208	67.375	37.960	–6.913
1,300	2,340	17.613	14.950	68.769	36.690	–6.168
1,400	2,520	17.968	16.729	70.087	35.432	–5.531
1,500	2,700	18.291	18.543	71.338	34.177	–4.979
1,600	2,880	18.582	20.387	72.528	32.923	–4.497
1,700	3,060	18.845	22.258	73.663	31.679	–4.072
1,800	3,240	19.085	24.155	74.747	30.436	–3.695
1,900	3,420	19.302	26.074	75.785	29.199	–3.358
2,000	3,600	19.504	28.015	76.780	27.962	–3.055
2,100	3,780	19.684	29.974	77.736	26.730	–2.782
2,200	3,960	19.853	31.951	78.656	25.493	–2.532
2,300	4,140	20.004	33.944	79.541	24.266	–2.306
2,400	4,320	20.151	35.952	80.396	23.037	–2.098
2,500	4,500	20.282	37.974	81.221	21.804	–1.906
2,600	4,680	20.404	40.008	82.019	20.579	–1.730
2,700	4,860	20.519	42.055	82.791	19.349	–1.566
2,800	5,040	20.625	44.112	83.540	18.124	–1.415
2,900	5,220	20.726	46.179	84.265	16.901	–1.274
K	°R	$\frac{\text{cal}}{\text{gmole}\cdot\text{K}}$	$\frac{\text{kcal}}{\text{gmole}}$	$\frac{\text{cal}}{\text{gmole}\cdot\text{K}}$	$\frac{\text{kcal}}{\text{gmole}}$	—

Table B.6 Continued

Acetylene
$MW = 26.038$
$\bar{h}_f^0 = 54.190$ kcal/gmole

T		$\bar{C}_p^0$	$\bar{h}\langle T\rangle - \bar{h}\langle T_0\rangle$	$\bar{s}^0\langle T\rangle$	$\Delta G^0\langle T\rangle$	$\log K_p$
3,000	5,400	20.820	48.257	84.969	15.674	–1.142
3,100	5,580	20.910	50.343	85.654	14.451	–1.019
3,200	5,760	20.996	52.439	86.319	13.227	–0.903
3,300	5,940	21.078	54.542	86.966	12.000	–0.795
3,400	6,120	21.154	56.664	87.596	10.779	–0.693
3,500	6,300	21.225	58.773	88.211	9.554	–0.597
3,600	6,480	21.297	60.899	88.810	8.331	–0.506
3,700	6,660	21.367	63.032	89.394	7.111	–0.420
3,800	6,840	21.431	65.172	89.965	5.894	–0.339
3,900	7,020	21.494	67.319	90.522	4.675	–0.262
4,000	7,200	21.557	69.471	91.067	3.455	–0.189
4,100	7,380	21.615	71.630	91.600	2.230	–0.119
4,200	7,560	21.670	73.794	92.122	1.017	–0.053
4,300	7,740	21.728	75.964	92.632	–0.205	0.010
4,400	7,920	21.782	78.139	93.133	–1.425	0.071
4,500	8,100	21.835	80.320	93.623	–2.648	0.129
4,600	8,280	21.883	82.506	94.103	–3.858	0.183
4,700	8,460	21.935	84.697	94.574	–5.073	0.236
4,800	8,640	21.985	86.893	95.037	–6.286	0.286
4,900	8,820	22.036	89.094	95.490	–7.500	0.335
5,000	9,000	22.077	91.300	95.936	–8.715	0.381
5,100	9,180	22.129	93.510	96.374	–9.935	0.426
5,200	9,360	22.174	95.725	96.804	–11.144	0.468
5,300	9,540	22.219	97.945	97.227	–12.348	0.509
5,400	9,720	22.263	100.169	97.642	–13.559	0.549
5,500	9,900	22.309	102.397	98.051	–14.767	0.587
5,600	10,080	22.349	104.630	98.454	–15.977	0.624
5,700	10,260	22.393	106.867	98.850	–17.188	0.659
5,800	10,440	22.433	109.108	99.239	–18.394	0.693
5,900	10,620	22.474	111.354	99.623	–19.588	0.726
6,000	10,800	22.521	113.603	100.001	–20.802	0.758
K	°R	$\frac{\text{cal}}{\text{gmole}\cdot\text{K}}$	$\frac{\text{kcal}}{\text{gmole}}$	$\frac{\text{cal}}{\text{gmole}\cdot\text{K}}$	$\frac{\text{kcal}}{\text{gmole}}$	—

Source: JANAF Thermochemical Tables, 2nd Edition, National Bureau of Standards, Publication NSRDSNB537, 1971.

Table B.7 Thermochemical Properties of Ethylene

Ethylene (C_2H_4) September 30, 1965
$MW = 28.05418$
$\bar{h}_f^0 = 12.540$ kcal/gmole

T		$\bar{C}_p^0$	$\bar{h}\langle T\rangle - \bar{h}\langle T_0\rangle$	$\bar{s}^0\langle T\rangle$	$\Delta G^0\langle T\rangle$	$\log K_p$
0	0	0.000	–2.514	0.000	14.578	infinite
100	180	7.952	–1.719	43.125	14.434	–31.544
200	360	8.451	–-0.909	48.721	15.227	–16.638
298	536	10.250	0.000	52.396	16.338	–11.975
300	540	10.292	0.019	52.459	16.361	–11.918
400	720	12.679	1.167	55.745	17.752	–9.699
500	900	14.933	2.550	58.821	19.319	–8.444
600	1,080	16.889	4.143	61.721	21.008	–7.652
700	1,260	18.574	5.918	64.454	22.788	–7.114
800	1,440	20.039	7.851	67.033	24.628	–6.728
900	1,620	21.320	9.920	69.468	26.514	–6.438
1,000	1,800	22.443	12.109	71.774	28.431	–6.213
1,100	1,980	23.427	14.404	73.960	30.373	–6.034
1,200	2,160	24.290	16.791	76.036	32.334	–5.889
1,300	2,340	25.044	19.258	78.011	34.302	–5.766
1,400	2,520	25.706	21.797	79.892	36.282	–5.664
1,500	2,700	26.285	24.397	81.686	38.266	–5.575
1,600	2,880	26.794	27.051	83.399	40.246	–5.497
1,700	3,060	27.242	29.753	85.037	42.237	–5.430
1,800	3,240	27.636	32.498	86.605	44.224	–5.369
1,900	3,420	27.986	35.279	88.109	46.215	–5.316
2,000	3,600	28.296	38.094	89.552	48.204	–5.267
2,100	3,780	28.571	40.937	90.940	50.192	–5.223
2,200	3,960	28.818	43.807	92.275	52.174	–5.183
2,300	4,140	29.038	46.700	93.561	54.163	–5.146
2,400	4,320	29.236	49.614	94.801	56.148	–5.113
2,500	4,500	29.414	52.546	95.998	58.124	–5.081
2,600	4,680	29.575	55.496	97.155	60.109	–5.052
2,700	4,860	29.721	58.461	98.274	62.085	–5.025
2,800	5,040	29.853	61.440	99.357	64.064	–5.000
2,900	5,220	29.973	64.431	100.407	66.047	–4.977
K	°R	$\frac{\text{cal}}{\text{gmole}\cdot\text{K}}$	$\frac{\text{kcal}}{\text{gmole}}$	$\frac{\text{cal}}{\text{gmole}\cdot\text{K}}$	$\frac{\text{kcal}}{\text{gmole}}$	—

Table B.7 Continued

Ethylene (C_2H_4)
$MW = 28.05418$
$\bar{h}_f^0 = 12.540$ kcal/gmole

T		$\bar{C}_p^0$	$\bar{h}\langle T\rangle - \bar{h}\langle T_0\rangle$	$\bar{s}^0\langle T\rangle$	$\Delta G^0\langle T\rangle$	$\log K_p$
3,000	5,400	30.083	67.434	101.425	68.019	–4.955
3,100	5,580	30.184	70.447	102.413	69.996	–4.934
3,200	5,760	30.276	73.470	103.373	71.971	–4.915
3,300	5,940	30.360	76.502	104.305	73.947	–4.897
3,400	6,120	30.438	79.542	105.213	75.920	–4.880
3,500	6,300	30.510	82.590	106.096	77.894	–4.864
3,600	6,480	30.577	85.644	106.957	79.864	–4.848
3,700	6,660	30.638	88.705	107.795	81.844	–4.834
3,800	6,840	30.695	91.772	108.613	83.822	–4.821
3,900	7,020	30.748	94.844	109.411	85.798	–4.808
4,000	7,200	30.797	97.921	110.190	87.775	–4.796
4,100	7,380	30.843	101.003	110.951	89.746	–4.784
4,200	7,560	30.886	104.090	111.695	91.729	–4.773
4,300	7,740	30.926	107.180	112.422	93.703	–4.762
4,400	7,920	30.964	110.275	113.134	95.678	–4.752
4,500	8,100	30.999	113.373	113.830	97.653	–4.742
4,600	8,280	31.032	116.475	114.512	99.643	–4.734
4,700	8,460	31.063	119.579	115.180	101.628	–4.725
4,800	8,640	31.093	122.687	115.834	103.617	–4.718
4,900	8,820	31.120	125.798	116.475	105.608	–4.710
5,000	9,000	31.146	128.911	117.104	107.593	–4.703
5,100	9,180	31.171	132.027	117.721	109.582	–4.696
5,200	9,360	31.194	135.145	118.327	111.574	–4.689
5,300	9,540	31.216	138.266	118.921	113.583	–4.683
5,400	9,720	31.236	141.388	119.505	115.577	–4.677
5,500	9,900	31.256	144.513	120.078	117.583	–4.672
5,600	10,080	31.275	147.639	120.641	119.586	–4.667
5,700	10,260	31.292	150.768	121.195	121.591	–4.662
5,800	10,440	31.309	153.898	121.740	123.597	–4.657
5,900	10,620	31.325	157.030	122.275	125.625	–4.653
6,000	10,800	31.340	160.163	122.802	127.627	–4.649
K	°R	$\frac{\text{cal}}{\text{gmole}\cdot\text{K}}$	$\frac{\text{kcal}}{\text{gmole}}$	$\frac{\text{cal}}{\text{gmole}\cdot\text{K}}$	$\frac{\text{kcal}}{\text{gmole}}$	—

Source: JANAF Thermochemical Tables, 2nd Edition, National Bureau of Standards, Publication NSRDSNB537, 1971.

Table B.8 Thermochemical Properties of *n*-Octane

n-Octane $(C_8H_{18})_g$
$MW = 114.224$
$\bar{h}_f^0 = -49.820$ kcal/gmole

T		$\bar{C}_p^0$	$\bar{h}\langle T\rangle - \bar{h}\langle T_0\rangle$	$\bar{s}^0\langle T\rangle$	$\Delta G^0\langle T\rangle$	$\log K_p$
0	0	0.000	–8.610	0.000	–38.198	infinite
100	180	19.640	–6.633	76.855	–28.733	62.801
200	360	33.837	–3.948	94.896	–24.937	27.252
298	536	45.149	0.000	111.807	3.801	–2.788
300	540	45.368	0.082	111.853	4.228	–3.080
400	720	57.371	5.219	126.555	22.743	–12.427
500	900	68.338	11.523	140.574	41.973	–18.348
600	1,080	77.668	18.813	153.816	61.677	–22.468
700	1,260	85.661	29.975	166.387	81.706	–25.512
800	1,440	92.509	35.907	178.320	101.857	–27.828
900	1,620	98.429	45.477	189.540	122.195	–29.675
1,000	1,800	103.612	55.576	200.202	142.536	–31.154
K	°R	$\frac{\text{cal}}{\text{gmole}\cdot\text{K}}$	$\frac{\text{kcal}}{\text{gmole}}$	$\frac{\text{cal}}{\text{gmole}\cdot\text{K}}$	$\frac{\text{kcal}}{\text{gmole}}$	—

Sources: Tables based on coefficients provided with

- NASA Computer Program for Calculation of Complex Chemical Equilibrium Compositions, Rocket Performance, Incident and Reflected Shocks, in Chapman–Jouquet Detonations, S. Gordon and B. McBride, NASA Lewis Center, 1967.
- Revised NASA Burn Program and Thermodynamic Library, W. Shulman, U.S. Army ARRADCOM Chemical Systems Laboratory, 1981.

Table B.9 Thermochemical Properties of *n*-Dodecane

n-Dodecane $(C_{12}H_{26})_g$
$MW = 170.328$
$\bar{h}_f^0 = -71.014$ kcal/gmole

T		$\bar{C}_p^0$	$\bar{h}\langle T\rangle - \bar{h}\langle T_0\rangle$	$\bar{s}^0\langle T\rangle$	$\Delta G^0\langle T\rangle$	$\log K_p$
0	0	0.000	–12.578	0.000	–54.256	infinite
100	180	29.911	–9.967	96.413	–39.366	86.041
200	360	50.841	–5.914	123.673	–32.469	35.483
298	536	67.000	0.000	148.767	10.413	–7.637
300	540	67.326	0.126	149.207	10.951	–7.978
400	720	85.103	7.752	171.028	38.980	–21.299
500	900	101.294	17.100	191.803	68.022	–29.735
600	1,080	115.031	27.895	211.423	97.716	–35.596
700	1,260	126.751	39.973	230.022	127.872	–39.927
800	1,440	136.751	53.194	247.669	158.199	–43.222
900	1,620	145.399	67.326	264.279	188.734	–45.835
1,000	1,800	152.876	82.256	280.006	219.330	–47.939
K	°R	$\frac{\text{cal}}{\text{gmole}\cdot\text{K}}$	$\frac{\text{kcal}}{\text{gmole}}$	$\frac{\text{cal}}{\text{gmole}\cdot\text{K}}$	$\frac{\text{kcal}}{\text{gmole}}$	—

Sources: Tables based on coefficients provided with

- NASA Computer Program for Calculation of Complex Chemical Equilibrium Compositions, Rocket Performance, Incident and Reflected Shocks, in Chapman–Jouquet Detonations, S. Gordon and B. McBride, NASA Lewis Center, 1967.
- Revised NASA Burn Program and Thermodynamic Library, W. Shulman, U.S. Army ARRADCOM Chemical Systems Laboratory, 1981.

Table B.10 Thermochemical Properties of Methanol

Methanol $(CH_3OH)_g$
$MW = 32.042$
$\bar{h}_f^0 = -48.050$ kcal/gmole

T		$\bar{C}_p^0$	$\bar{h}\langle T\rangle - \bar{h}\langle T_0\rangle$	$\bar{s}^0\langle T\rangle$	$\Delta G^0\langle T\rangle$	$\log K_p$
0	0	0.000	–2.315	0.000	–45.028	infinite
100	180	7.748	–1.771	47.773	–44.171	96.544
200	360	8.883	–0.945	53.458	–44.334	48.450
298	536	10.447	0.000	57.280	–38.813	28.467
300	540	10.482	0.021	57.350	–38.751	28.232
400	720	12.315	1.160	60.614	–35.516	19.407
500	900	14.197	2.485	63.564	–32.077	14.022
600	1,080	15.996	3.996	66.314	–28.490	10.381
700	1,260	17.625	5.679	68.904	–24.807	7.746
800	1,440	19.049	7.514	71.353	–21.064	5.755
900	1,620	20.280	9.482	73.669	–17.263	4.192
1,000	1,800	21.378	11.566	75.864	–13.430	2.935
K	°R	$\frac{\text{cal}}{\text{gmole}\cdot\text{K}}$	$\frac{\text{kcal}}{\text{gmole}}$	$\frac{\text{cal}}{\text{gmole}\cdot\text{K}}$	$\frac{\text{kcal}}{\text{gmole}}$	—

Sources: Tables based on coefficients provided with

- NASA Computer Program for Calculation of Complex Chemical Equilibrium Compositions, Rocket Performance, Incident and Reflected Shocks, in Chapman–Jouquet Detonations, S. Gordon and B. McBride, NASA Lewis Center, 1967.
- Revised NASA Burn Program and Thermodynamic Library, W. Shulman, U.S. Army ARRADCOM Chemical Systems Laboratory, 1981.

Table B.11 Thermochemical Properties of Ethanol

Ethanol $(C_2H_5OH)_g$
$MW = 46.069$
$\bar{h}_f^0 = -056.030$ kcal/gmole

T		$\bar{C}_p^0$	$\bar{h}\langle T\rangle - \bar{h}\langle T_0\rangle$	$\bar{s}^0\langle T\rangle$	$\Delta G^0\langle T\rangle$	$\log K_p$
0	0	0.000	–2.916	0.000	–51.332	infinite
100	180	7.838	–2.325	55.467	–49.512	infinite
200	360	11.791	–1.344	62.109	–49.098	53.656
298	536	15.622	0.000	67.529	–41.427	30.384
300	540	15.699	0.031	67.634	–40.037	29.169
400	720	19.390	1.788	72.662	–34.515	18.860
500	900	22.743	3.898	77.356	–28.720	12.555
600	1,080	25.689	6.323	81.770	–22.744	8.285
700	1,260	28.210	9.021	85.925	–16.633	5.194
800	1,440	30.341	11.952	89.835	–10.459	2.858
900	1,620	32.168	15.080	93.516	–4.220	1.025
1,000	1,800	33.827	18.380	96.992	2.054	–0.449
K	°R	$\frac{\text{cal}}{\text{gmole}\cdot\text{K}}$	$\frac{\text{kcal}}{\text{gmole}}$	$\frac{\text{cal}}{\text{gmole}\cdot\text{K}}$	$\frac{\text{kcal}}{\text{gmole}}$	—

Sources: Tables based on coefficients provided with

- NASA Computer Program for Calculation of Complex Chemical Equilibrium Compositions, Rocket Performance, Incident and Reflected Shocks, in Chapman–Jouquet Detonations, S. Gordon and B. McBride, NASA Lewis Center, 1967.
- Revised NASA Burn Program and Thermodynamic Library, W. Shulman, U.S. Army ARRADCOM Chemical Systems Laboratory, 1981.

Table B.12 Thermochemical Properties of Monatomic Hydrogen

Hydrogen, Monatomic (H) September 30, 1965
$MW = 1.00797$
$\bar{h}_f^0 = 52{,}100$ kcal/gmole

T		$\bar{C}_p^0$	$\bar{h}\langle T\rangle - \bar{h}\langle T_0\rangle$	$\bar{s}^0\langle T\rangle$	$\Delta G^0\langle T\rangle$	$\log K_p$
0	0	0.000	–1.481	0.000	51.631	infinite
100	180	4.968	–0.984	21.965	50.771	–110.954
200	360	4.968	–0.488	25.408	49.714	–54.322
298	536	4.968	0.000	27.392	48.585	–35.612
300	540	4.968	0.009	27.423	48.563	–35.377
400	720	4.968	0.506	28.852	47.361	–25.876
500	900	4.968	1.003	29.961	46.121	–20.158
600	1,080	4.968	1.500	30.867	46.851	–16.336
700	1,260	4.968	1.996	31.632	43.558	–13.599
800	1,440	4.968	2.493	32.296	42.242	–11.539
900	1,620	4.968	2.990	32.881	40.910	–9.934
1,000	1,800	4.968	3.487	33.404	39.562	–8.646
1,100	1,980	4.968	3.984	33.878	38.200	–7.589
1,200	2,160	4.968	4.481	34.310	36.826	–6.707
1,300	2,340	4.968	4.977	34.708	35.441	–5.958
1,400	2,520	4.968	5.474	35.076	34.048	–5.315
1,500	2,700	4.968	5.971	35.419	32.645	–4.756
1,600	2,880	4.968	6.468	35.739	31.236	–4.266
1,700	3,060	4.968	6.965	36.041	29.819	–3.833
1,800	3,240	4.968	7.461	36.325	28.396	–3.448
1,900	3,420	4.968	7.958	36.593	26.970	–3.102
2,000	3,600	4.968	8.455	36.848	25.538	–2.790
2,100	3,780	4.968	8.952	37.090	24.102	–2.508
2,200	3,960	4.968	9.449	37.322	22.659	–2.251
2,300	4,140	4.968	9.945	37.542	21.217	–2.016
2,400	4,320	4.968	10.442	37.754	19.769	–1.800
2,500	4,500	4.968	10.939	37.957	18.316	–1.601
2,600	4,680	4.968	11.436	38.152	16.864	–1.417
2,700	4,860	4.968	11.933	38.339	15.409	–1.247
2,800	5,040	4.968	12.430	38.520	13.949	–1.089
2,900	5,220	4.968	12.926	38.694	12.491	–0.941
K	°R	$\frac{\text{cal}}{\text{gmole}\cdot\text{K}}$	$\frac{\text{kcal}}{\text{gmole}}$	$\frac{\text{cal}}{\text{gmole}\cdot\text{K}}$	$\frac{\text{kcal}}{\text{gmole}}$	—

Table B.12 Continued

Hydrogen, Monatomic (H)
$MW = 1.00797$
$\bar{h}_f^0 = 52{,}100$ kcal/gmole

T		$\bar{C}_p^0$	$\bar{h}\langle T\rangle - \bar{h}\langle T_0\rangle$	$\bar{s}^0\langle T\rangle$	$\Delta G^0\langle T\rangle$	$\log K_p$
3,000	5,400	4.968	13.423	38.862	11.030	–0.803
3,100	5,580	4.968	13.920	39.025	9.565	–0.674
3,200	5,760	4.968	14.417	39.183	8.099	–0.553
3,300	5,940	4.968	14.914	39.336	6.632	–0.439
3,400	6,120	4.968	15.410	39.484	5.164	–0.332
3,500	6,300	4.968	15.907	39.628	3.695	–0.231
3,600	6,480	4.968	16.404	39.768	2.224	–0.135
3,700	6,660	4.968	16.901	39.904	0.753	–0.044
3,800	6,840	4.968	17.398	40.037	–0.722	0.042
3,900	7,020	4.968	17.895	40.166	–2.196	0.123
4,000	7,200	4.968	18.391	40.292	–3.671	0.201
4,100	7,380	4.968	18.888	40.414	–5.144	0.274
4,200	7,560	4.968	19.385	40.534	–6.621	0.345
4,300	7,740	4.968	19.882	40.651	–8.099	0.412
4,400	7,920	4.968	20.379	40.765	–9.575	0.476
4,500	8,100	4.968	20.875	40.877	–11.056	0.537
4,600	8,280	4.968	21.377	40.986	–12.531	0.595
4,700	8,460	4.968	21.869	41.093	–14.010	0.651
4,800	8,640	4.968	22.366	41.198	–15.492	0.705
4,900	8,820	4.968	22.863	41.300	–16.968	0.757
5,000	9,000	4.968	23.359	41.400	–18.447	0.806
5,100	9,180	4.968	23.856	41.499	–19.928	0.854
5,200	9,360	4.968	24.353	41.595	–21.406	0.900
5,300	9,540	4.968	24.850	41.690	–22.887	0.944
5,400	9,720	4.968	25.347	41.783	–24.369	0.986
5,500	9,900	4.968	25.844	41.874	–25.848	1.027
5,600	10,080	4.968	26.340	41.963	–27.326	1.066
5,700	10,260	4.968	26.837	42.051	–28.805	1.104
5,800	10,440	4.968	27.334	42.138	–30.289	1.141
5,900	10,620	4.968	27.831	42.223	–31.768	1.177
6,000	10,800	4.968	28.328	42.306	–33.246	1.211
K	°R	$\frac{\text{cal}}{\text{gmole}\cdot\text{K}}$	$\frac{\text{kcal}}{\text{gmole}}$	$\frac{\text{cal}}{\text{gmole}\cdot\text{K}}$	$\frac{\text{kcal}}{\text{gmole}}$	—

Source: JANAF Thermochemical Tables, 2nd Edition, National Bureau of Standards, Publication NSRDSNB537, 1971.

Table B.13 Thermochemical Properties of Hydrogen

Hydrogen (H_2) March 31, 1961
$MW = 2.016$
$\bar{h}_f^0 = 0.000$ kcal/gmole

T		$\bar{C}_p^0$	$\bar{h}\langle T\rangle - \bar{h}\langle T_0\rangle$	$\bar{s}^0\langle T\rangle$	$\Delta G^0\langle T\rangle$	$\log K_p$
0	0	0.000	–2.024	0.000	0.000	0.000
100	180	5.393	–1.265	24.387	0.000	0.000
200	360	6.518	–0.662	28.520	0.000	0.000
298	536	6.892	0.000	31.208	0.000	0.000
300	540	6.894	0.013	31.251	0.000	0.000
400	720	6.975	0.707	33.247	0.000	0.000
500	900	6.993	1.406	34.806	0.000	0.000
600	1,080	7.009	2.106	36.082	0.000	0.000
700	1,260	7.036	2.808	37.165	0.000	0.000
800	1,440	7.087	3.514	38.107	0.000	0.000
900	1,620	7.148	4.226	38.946	0.000	0.000
1,000	1,800	7.219	4.944	39.702	0.000	0.000
1,100	1,980	7.300	5.670	40.394	0.000	0.000
1,200	2,160	7.390	6.404	41.033	0.000	0.000
1,300	2,340	7.490	7.148	41.628	0.000	0.000
1,400	2,520	7.600	7.902	42.187	0.000	0.000
1,500	2,700	7.720	8.668	42.716	0.000	0.000
1,600	2,880	7.823	9.446	43.217	0.000	0.000
1,700	3,060	7.921	10.233	43.695	0.000	0.000
1,800	3,240	8.016	11.030	44.150	0.000	0.000
1,900	3,420	8.108	11.836	44.586	0.000	0.000
2,000	3,600	8.195	12.651	45.004	0.000	0.000
2,100	3,780	8.279	13.475	45.406	0.000	0.000
2,200	3,960	8.358	14.307	45.793	0.000	0.000
2,300	4,140	8.434	15.146	46.166	0.000	0.000
2,400	4,320	8.506	15.993	46.527	0.000	0.000
2,500	4,500	8.575	16.848	46.875	0.000	0.000
2,600	4,680	8.639	17.708	47.213	0.000	0.000
2,700	4,860	8.700	18.575	47.540	0.000	0.000
2,800	5,040	8.757	19.448	47.857	0.000	0.000
2,900	5,220	8.810	20.326	48.166	0.000	0.000
K	°R	$\frac{\text{cal}}{\text{gmole}\cdot\text{K}}$	$\frac{\text{kcal}}{\text{gmole}}$	$\frac{\text{cal}}{\text{gmole}\cdot\text{K}}$	$\frac{\text{kcal}}{\text{gmole}}$	—

Table B.13 Continued

Hydrogen (H_2)
$MW = 2.016$
$\bar{h}_f^0 = 0.000$ kcal/gmole

T		$\bar{C}_p^0$	$\bar{h}\langle T\rangle - \bar{h}\langle T_0\rangle$	$\bar{s}^0\langle T\rangle$	$\Delta G^0\langle T\rangle$	$\log K_p$
3,000	5,400	8.859	21.210	48.465	0.000	0.000
3,100	5,580	8.911	22.098	48.756	0.000	0.000
3,200	5,760	8.962	22.992	49.040	0.000	0.000
3,300	5,940	9.012	23.891	49.317	0.000	0.000
3,400	6,120	9.061	24.794	49.586	0.000	0.000
3,500	6,300	9.110	25.703	49.850	0.000	0.000
3,600	6,480	9.158	26.616	50.107	0.000	0.000
3,700	6,660	9.205	27.535	50.359	0.000	0.000
3,800	6,840	9.252	28.457	50.605	0.000	0.000
3,900	7,020	9.297	29.385	50.846	0.000	0.000
4,000	7,200	9.342	30.317	51.082	0.000	0.000
4,100	7,380	9.386	31.253	51.313	0.000	0.000
4,200	7,560	9.429	32.194	51.640	0.000	0.000
4,300	7,740	9.472	33.139	51.762	0.000	0.000
4,400	7,920	9.514	34.088	51.980	0.000	0.000
4,500	8,100	9.555	35.042	52.194	0.000	0.000
4,600	8,280	9.595	35.999	52.405	0.000	0.000
4,700	8,460	9.634	36.961	52.612	0.000	0.000
4,800	8,640	9.673	37.926	52.815	0.000	0.000
4,900	8,820	9.711	38.895	53.015	0.000	0.000
5,000	9,000	9.748	39.868	53.211	0.000	0.000
5,100	9,180	9.785	40.845	53.405	0.000	0.000
5,200	9,360	9.822	41.825	53.595	0.000	0.000
5,300	9,540	9.859	42.809	53.783	0.000	0.000
5,400	9,720	9.895	43.797	53.967	0.000	0.000
5,500	9,900	9.930	44.788	54.149	0.000	0.000
5,600	10,080	9.965	45.783	54.328	0.000	0.000
5,700	10,260	10.000	46.781	54.505	0.000	0.000
5,800	10,440	10.034	47.783	54.679	0.000	0.000
5,900	10,620	10.067	48.788	54.851	0.000	0.000
6,000	10,800	10.100	49.796	55.020	0.000	0.000
K	°R	$\frac{\text{cal}}{\text{gmole}\cdot\text{K}}$	$\frac{\text{kcal}}{\text{gmole}}$	$\frac{\text{cal}}{\text{gmole}\cdot\text{K}}$	$\frac{\text{kcal}}{\text{gmole}}$	—

Source: JANAF Thermochemical Tables, 2nd Edition, National Bureau of Standards, Publication NSRDSNB537, 1971.

Table B.14 Thermochemical Properties of Water Vapor

Water Vapor (H_2O) March 31, 1961
$MW = 18.016$
$\bar{h}_f^0 = -57.798$ kcal/gmole

T		$\bar{C}_p^0$	$\bar{h}\langle T\rangle - \bar{h}\langle T_0\rangle$	$\bar{s}^0\langle T\rangle$	$\Delta G^0\langle T\rangle$	$\log K_p$
0	0	0.000	–2.367	0.000	–57.103	infinite
100	180	7.961	–1.581	36.396	–56.557	123.600
200	360	7.969	–0.784	41.916	–55.635	60.792
298	536	8.025	0.000	45.106	–54.636	40.048
300	540	8.027	0.015	45.155	–54.617	39.786
400	720	8.186	0.825	47.484	–53.519	29.240
500	900	8.415	1.654	49.334	–52.361	22.886
600	1,080	8.676	2.509	50.891	–51.156	18.633
700	1,260	8.954	3.390	52.249	–49.915	15.583
800	1,440	9.246	4.300	53.464	–48.646	13.289
900	1,620	9.547	5.240	54.570	–47.352	11.498
1,000	1,800	9.851	6.209	55.592	–46.040	10.062
1,100	1,980	10.152	7.210	56.545	–44.712	8.883
1,200	2,160	10.444	8.240	57.441	–43.371	7.899
1,300	2,340	10.723	9.298	58.288	–42.022	7.064
1,400	2,520	10.987	10.384	59.092	–40.663	6.347
1,500	2,700	11.233	11.495	59.859	–39.297	5.725
1,600	2,880	11.462	12.630	60.591	–37.927	5.180
1,700	3,060	11.674	13.787	61.293	–36.549	4.699
1,800	3,240	11.869	14.964	61.965	–35.170	4.270
1,900	3,420	12.048	16.160	62.612	–33.786	3.886
2,000	3,600	12.214	17.373	63.234	–32.401	3.540
2,100	3,780	12.366	18.602	63.834	–31.012	3.227
2,200	3,960	12.505	19.846	64.412	–29.621	2.942
2,300	4,140	12.634	21.103	64.971	–28.229	2.682
2,400	4,320	12.753	22.372	65.511	–26.832	2.443
2,500	4,500	12.863	23.653	66.034	–25.439	2.224
2,600	4,680	12.965	24.945	66.541	–24.040	2.021
2,700	4,860	13.059	26.246	67.032	–22.041	1.833
2,800	5,040	13.146	27.556	67.508	–21.242	1.658
2,900	5,220	13.228	28.875	67.971	–19.838	1.495
K	°R	$\frac{\text{cal}}{\text{gmole}\cdot\text{K}}$	$\frac{\text{kcal}}{\text{gmole}}$	$\frac{\text{cal}}{\text{gmole}\cdot\text{K}}$	$\frac{\text{kcal}}{\text{gmole}}$	—

Table B.14 Continued

Water Vapor (H_2O)
$MW = 18.016$
$\bar{h}_f^0 = -57.798$ kcal/gmole

T		$\bar{C}_p^0$	$\bar{h}\langle T\rangle - \bar{h}\langle T_0\rangle$	$\bar{s}^0\langle T\rangle$	$\Delta G^0\langle T\rangle$	$\log K_p$
3,000	5,400	13.304	30.201	68.421	–18.438	1.343
3,100	5,580	13.374	31.535	68.858	–17.034	1.201
3,200	5,760	13.441	32.876	69.284	–15.630	1.067
3,300	5,940	13.503	34.223	69.698	–14.223	0.942
3,400	6,120	13.562	35.577	70.102	–12.818	0.824
3,500	6,300	13.617	36.936	70.496	–11.409	0.712
3,600	6,480	13.669	38.300	70.881	–10.000	0.607
3,700	6,660	13.718	39.669	71.256	–8.589	0.507
3,800	6,840	13.764	41.043	71.622	–7.177	0.413
3,900	7,020	13.808	42.422	71.980	–5.766	0.323
4,000	7,200	13.850	43.805	72.331	–4.353	0.238
4,100	7,380	13.890	45.192	72.673	–2.938	0.157
4,200	7,560	13.927	46.583	73.008	–1.522	0.079
4,300	7,740	13.963	47.977	73.336	–0.105	0.005
4,400	7,920	13.997	49.375	73.658	1.311	–0.065
4,500	8,100	14.030	50.777	73.973	2.729	–0.133
4,600	8,280	14.061	52.181	74.281	4.154	–0.197
4,700	8,460	14.091	53.589	74.584	5.576	–0.259
4,800	8,640	14.120	55.000	74.881	6.998	–0.319
4,900	8,820	14.148	56.413	75.172	8.422	–0.376
5,000	9,000	14.174	57.829	75.459	9.844	–0.430
5,100	9,180	14.201	59.248	75.740	11.275	–0.483
5,200	9,360	14.228	60.669	76.016	12.700	–0.534
5,300	9,540	14.254	62.093	76.287	14.135	–0.583
5,400	9,720	14.279	63.520	76.653	15.560	–0.630
5,500	9,900	14.303	64.949	76.816	16.995	–0.675
5,600	10,080	14.328	66.381	77.074	18.426	–0.719
5,700	10,260	14.351	67.815	77.327	19.862	–0.762
5,800	10,440	14.375	69.251	77.577	21.299	–0.803
5,900	10,620	14.398	70.690	77.823	22.736	–0.842
6,000	10,800	14.422	72.131	78.065	24.174	–0.880
K	°R	$\frac{\text{cal}}{\text{gmole}\cdot\text{K}}$	$\frac{\text{kcal}}{\text{gmole}}$	$\frac{\text{cal}}{\text{gmole}\cdot\text{K}}$	$\frac{\text{kcal}}{\text{gmole}}$	—

Source: JANAF Thermochemical Tables, 2nd Edition, National Bureau of Standards, Publication NSRDSNB537, 1971.

Table B.15 Thermochemical Properties of Nitrogen

Nitrogen, Monotomic (N) March 31, 1961
$MW = 14.008$
$\bar{h}_f^0 = 113.000$ kcal/gmole

T		$\bar{C}_p^0$	$\bar{h}\langle T\rangle - \bar{h}\langle T_0\rangle$	$\bar{s}^0\langle T\rangle$	$\Delta G^0\langle T\rangle$	$\log K_p$
0	0	0.000	–1.481	0.000	112.520	infinite
100	180	4.968	–0.984	31.187	111.459	–243.583
200	360	4.968	–0.488	34.631	110.191	–120.405
298	536	4.968	0.000	36.614	108.870	–79.800
300	540	4.968	0.009	36.645	108.845	–79.289
400	720	4.968	0.506	38.074	107.448	–58.704
500	900	4.968	1.003	39.183	106.014	–46.336
600	1,080	4.968	1.500	40.089	104.551	–38.081
700	1,260	4.968	1.996	40.855	103.066	–32.177
800	1,440	4.968	2.493	41.518	101.562	–27.744
900	1,620	4.968	2.990	42.103	100.042	–24.292
1,000	1,800	4.968	3.487	42.627	98.510	–21.528
1,100	1,980	4.968	3.984	43.100	96.967	–19.265
1,200	2,160	4.968	4.481	43.532	95.415	–17.377
1,300	2,340	4.968	4.977	43.930	93.856	–15.778
1,400	2,520	4.968	5.474	44.298	92.289	–14.406
1,500	2,700	4.968	5.971	44.641	90.716	–13.217
1,600	2,880	4.968	6.468	44.962	89.139	–12.175
1,700	3,060	4.968	6.965	45.263	87.556	–11.256
1,800	3,240	4.968	7.461	45.547	85.968	–10.437
1,900	3,420	4.969	7.958	45.815	84.378	–9.705
2,000	3,600	4.969	8.455	46.070	82.784	–9.046
2,100	3,780	4.970	8.952	46.313	81.185	–8.449
2,200	3,960	4.971	9.449	46.544	79.583	–7.905
2,300	4,140	4.972	9.946	46.765	77.979	–7.409
2,400	4,320	4.975	10.444	46.977	76.373	–6.954
2,500	4,500	4.978	10.941	47.180	74.763	–6.535
2,600	4,680	4.982	11.439	47.375	73.151	–6.149
2,700	4,860	4.987	11.938	47.563	71.537	–5.790
2,800	5,040	4.993	12.437	47.745	69.922	–5.457
2,900	5,220	5.001	12.936	47.920	68.303	–5.147
K	°R	$\frac{\text{cal}}{\text{gmole}\cdot\text{K}}$	$\frac{\text{kcal}}{\text{gmole}}$	$\frac{\text{cal}}{\text{gmole}\cdot\text{K}}$	$\frac{\text{kcal}}{\text{gmole}}$	—

Table B.15 Continued

Nitrogen, Monotomic (N)
$MW = 14.008$
$\bar{h}_f^0 = 113.000$ kcal/gmole

T		$\bar{C}_p^0$	$\bar{h}\langle T\rangle - \bar{h}\langle T_0\rangle$	$\bar{s}^0\langle T\rangle$	$\Delta G^0\langle T\rangle$	$\log K_p$
3,000	5,400	5.011	13.437	48.090	66.683	–4.858
3,100	5,580	5.022	13.939	48.254	65.060	–4.587
3,200	5,760	5.035	14.441	48.414	63.435	–4.332
3,300	5,940	5.050	14.946	48.569	61.810	–4.093
3,400	6,120	5.067	15.451	48.720	60.181	–3.868
3,500	6,300	5.086	15.959	48.867	58.551	–3.656
3,600	6,480	5.107	16.469	49.011	56.921	–3.455
3,700	6,660	5.130	16.980	49.151	55.287	–3.265
3,800	6,840	5.156	17.495	49.288	53.653	–3.086
3,900	7,020	5.183	18.012	49.422	52.015	–2.915
4,000	7,200	5.213	18.531	49.554	50.376	–2.752
4,100	7,380	5.245	19.054	49.683	48.735	–2.598
4,200	7,560	5.278	19.580	49.810	47.094	–2.450
4,300	7,740	5.314	20.110	49.934	45.449	–2.310
4,400	7,920	5.351	20.643	50.057	43.803	–2.176
4,500	8,100	5.390	21.180	50.178	42.154	–2.047
4,600	8,280	5.431	21.721	50.297	40.505	–1.924
4,700	8,460	5.473	22.266	50.414	38.853	–1.807
4,800	8,640	5.517	22.816	50.530	37.199	–1.694
4,900	8,820	5.562	23.370	50.644	35.542	–1.585
5,000	9,000	5.608	23.928	50.757	33.883	–1.481
5,100	9,180	5.655	24.491	50.868	32.222	–1.381
5,200	9,360	5.703	25.059	50.978	30.560	–1.284
5,300	9,540	5.751	25.632	51.087	28.894	–1.191
5,400	9,720	5.800	26.210	51.195	27.228	–1.102
5,500	9,900	5.850	26.792	51.302	25.557	–1.016
5,600	10,080	5.900	27.380	51.408	23.884	–0.932
5,700	10,260	5.950	27.972	51.513	22.211	–0.852
5,800	10,440	6.000	28.570	51.617	20.534	–0.774
5,900	10,620	6.050	29.172	51.720	18.853	–0.698
6,000	10,800	6.100	29.780	51.822	17.172	–0.625
K	°R	$\frac{\text{cal}}{\text{gmole}\cdot\text{K}}$	$\frac{\text{kcal}}{\text{gmole}}$	$\frac{\text{cal}}{\text{gmole}\cdot\text{K}}$	$\frac{\text{kcal}}{\text{gmole}}$	—

Source: JANAF Thermochemical Tables, 2nd Edition, National Bureau of Standards, Publication NSRDSNB537, 1971.

Table B.16 Thermochemical Properties of Nitric Oxide

Nitric Oxide (NO) June 30, 1963
$MW = 30.008$
$\bar{h}_f^0 = 21.580$ kcal/gmole

T		$\bar{C}_p^0$	$\bar{h}\langle T\rangle - \bar{h}\langle T_0\rangle$	$\bar{s}^0\langle T\rangle$	$\Delta G^0\langle T\rangle$	$\log K_p$
0	0	0.000	–2.197	0.000	21.456	infinite
100	180	7.721	–1.451	42.286	21.256	–46.453
200	360	7.271	–0.705	47.477	20.984	–22.929
298	536	7.133	0.000	50.347	20.697	–15.171
300	540	7.132	0.013	50.392	20.692	–15.073
400	720	7.157	0.727	52.444	20.394	–11.142
500	900	7.287	1.448	54.053	20.095	–8.783
600	1,080	7.466	2.186	55.397	19.795	–7.210
700	1,260	7.655	2.942	56.562	19.494	–6.086
800	1,440	7.832	3.716	57.596	19.192	–5.243
900	1,620	7.988	4.507	58.528	18.890	–4.587
1,000	1,800	8.123	5.313	59.377	18.588	–4.062
1,100	1,980	8.238	6.131	60.157	18.285	–3.633
1,200	2,160	8.336	6.960	60.878	17.981	–3.275
1,300	2,340	8.419	7.798	61.548	17.678	–2.972
1,400	2,520	8.491	8.644	62.175	17.373	–2.712
1,500	2,700	8.552	9.496	62.763	17.069	–2.487
1,600	2,880	8.605	10.354	63.317	16.765	–2.290
1,700	3,060	8.651	11.217	63.840	16.461	–2.116
1,800	3,240	8.692	12.084	64.335	16.156	–1.962
1,900	3,420	8.727	12.955	64.806	15.853	–1.823
2,000	3,600	8.759	13.829	65.255	15.548	–1.699
2,100	3,780	8.788	14.706	65.683	15.244	–1.586
2,200	3,960	8.813	15.587	66.092	14.941	–1.484
2,300	4,140	8.837	16.469	66.484	14.637	–1.391
2,400	4,320	8.858	17.354	66.861	14.336	–1.305
2,500	4,500	8.877	18.241	67.223	14.033	–1.227
2,600	4,680	8.895	19.129	67.571	13.732	–1.164
2,700	4,860	8.912	20.020	67.908	13.432	–1.087
2,800	5,040	8.927	20.911	68.232	13.132	–1.025
2,900	5,220	8.941	21.805	68.545	12.834	–0.967
K	°R	$\frac{\text{cal}}{\text{gmole}\cdot\text{K}}$	$\frac{\text{kcal}}{\text{gmole}}$	$\frac{\text{cal}}{\text{gmole}\cdot\text{K}}$	$\frac{\text{kcal}}{\text{gmole}}$	—

Table B.16 Continued

Nitric Oxide (NO)
$MW = 30.008$
$\bar{h}_f^0 = 21.580$ kcal/gmole

T		$\bar{C}_p^0$	$\bar{h}\langle T\rangle - \bar{h}\langle T_0\rangle$	$\bar{s}^0\langle T\rangle$	$\Delta G^0\langle T\rangle$	$\log K_p$
3,000	5,400	8.955	22.700	68.849	12.535	–0.913
3,100	5,580	8.968	23.596	69.143	12.237	–0.863
3,200	5,760	8.980	24.493	69.427	11.940	–0.815
3,300	5,940	8.991	25.392	69.704	11.644	–0.771
3,400	6,120	9.002	26.291	69.973	11.349	–0.729
3,500	6,300	9.012	27.192	70.234	11.054	–0.690
3,600	6,480	9.022	28.094	70.488	10.762	–0.653
3,700	6,660	9.032	28.997	70.735	10.470	–0.618
3,800	6,840	9.041	29.900	70.976	10.179	–0.585
3,900	7,020	9.050	30.805	71.211	9.889	–0.554
4,000	7,200	9.058	31.710	71.440	9.598	–0.524
4,100	7,380	9.066	32.616	71.664	9.311	–0.496
4,200	7,560	9.074	33.523	71.882	9.024	–0.470
4,300	7,740	9.082	34.431	72.096	8.739	–0.444
4,400	7,920	9.090	35.340	72.305	8.452	–0.420
4,500	8,100	9.097	36.249	72.509	8.169	–0.397
4,600	8,280	9.105	37.159	72.709	7.888	–0.375
4,700	8,460	9.112	38.070	72.905	7.605	–0.354
4,800	8,640	9.119	38.982	73.097	7.324	–0.333
4,900	8,820	9.125	39.894	73.285	7.040	–0.314
5,000	9,000	9.132	40.807	73.470	6.763	–0.296
5,100	9,180	9.139	41.720	73.651	6.484	–0.278
5,200	9,360	9.145	42.634	73.828	6.207	–0.261
5,300	9,540	9.152	43.549	74.002	6.932	–0.245
5,400	9,720	9.158	44.465	74.173	5.654	–0.229
5,500	9,900	9.164	45.381	74.342	5.383	–0.214
5,600	10,080	9.170	46.298	74.507	5.107	–0.199
5,700	10,260	9.176	47.215	74.669	4.835	–0.185
5,800	10,440	9.182	48.133	74.829	4.566	–0.172
5,900	10,620	9.188	49.051	74.986	4.292	–0.159
6,000	10,800	9.194	49.970	75.140	4.024	–0.147
K	°R	$\frac{\text{cal}}{\text{gmole}\cdot\text{K}}$	$\frac{\text{kcal}}{\text{gmole}}$	$\frac{\text{cal}}{\text{gmole}\cdot\text{K}}$	$\frac{\text{kcal}}{\text{gmole}}$	—

Source: JANAF Thermochemical Tables, 2nd Edition, National Bureau of Standards, Publication NSRDSNB537, 1971.

Table B.17 Thermochemical Properties of Nitrogen Dioxide

Nitrogen Dioxide (NO_2) September 30, 1964
$MW = 46.008$
$\bar{h}_f^0 = 7.910$ kcal/gmole

T		$\bar{C}_p^0$	$\bar{h}\langle T\rangle - \bar{h}\langle T_0\rangle$	$\bar{s}^0\langle T\rangle$	$\Delta G^0\langle T\rangle$	$\log K_p$
0	0	0.000	–2.435	0.000	8.586	infinite
100	180	7.953	–1.640	48.387	9.545	–20.859
200	360	8.218	–0.835	53.954	10.853	–11.859
298	536	8.837	0.000	57.343	12.247	–8.977
300	540	8.850	0.016	57.398	12.274	–8.941
400	720	9.601	0.939	60.046	13.751	–7.513
500	900	10.327	1.936	62.268	15.258	–6.669
600	1,080	10.955	3.001	64.208	16.778	–6.111
700	1,260	11.469	4.123	65.937	18.302	–5.714
800	1,440	11.881	5.291	67.496	19.828	–5.417
900	1,620	12.208	6.496	68.915	21.355	–5.185
1,000	1,800	12.468	7.730	70.215	22.879	–5.000
1,100	1,980	12.677	8.988	71.414	24.400	–4.848
1,200	2,160	12.847	10.265	72.524	25.921	–4.721
1,300	2,340	12.985	11.556	73.558	27.438	–4.612
1,400	2,520	13.099	12.861	74.525	28.951	–4.519
1,500	2,700	13.193	14.176	75.432	30.464	–4.438
1,600	2,880	13.273	15.499	76.286	31.975	–4.367
1,700	3,060	13.340	16.830	77.093	33.484	–4.304
1,800	3,240	13.398	18.167	77.857	34.992	–4.248
1,900	3,420	13.447	19.509	78.853	36.498	–4.198
2,000	3,600	13.490	20.856	79.274	38.002	–4.152
2,100	3,780	13.527	22.207	79.933	39.507	–4.111
2,200	3,960	13.560	23.561	80.563	41.010	–4.074
2,300	4,140	13.588	24.919	81.166	42.514	–4.040
2,400	4,320	13.614	26.279	81.745	44.019	–4.008
2,500	4,500	13.636	27.641	82.301	45.520	–3.979
2,600	4,680	13.656	29.006	82.836	47.025	–3.953
2,700	4,860	13.674	30.373	83.352	48.529	–3.928
2,800	5,040	13.690	31.741	83.850	50.031	–3.905
2,900	5,220	13.705	33.111	84.330	51.540	–3.884
K	°R	$\frac{\text{cal}}{\text{gmole}\cdot\text{K}}$	$\frac{\text{kcal}}{\text{gmole}}$	$\frac{\text{cal}}{\text{gmole}\cdot\text{K}}$	$\frac{\text{kcal}}{\text{gmole}}$	—

Table B.17 Continued

Nitrogen Dioxide (NO_2)
$MW = 46.008$
$\bar{h}_f^0 = 7.910$ kcal/gmole

T		$\bar{C}_p^0$	$\bar{h}\langle T\rangle - \bar{h}\langle T_0\rangle$	$\bar{s}^0\langle T\rangle$	$\Delta G^0\langle T\rangle$	$\log K_p$
3,000	5,400	13.718	34.482	84.795	53.045	–3.864
3,100	5,580	13.730	35.854	85.245	54.551	–3.846
3,200	5,760	13.741	37.228	85.681	56.058	–3.828
3,300	5,940	13.751	38.602	86.104	57.565	–3.812
3,400	6,120	13.760	39.978	86.515	59.075	–3.797
3,500	6,300	13.768	41.354	86.914	60.583	–3.783
3,600	6,480	13.776	42.731	87.302	62.097	–3.770
3,700	6,660	13.783	44.109	87.679	63.613	–3.757
3,800	6,840	13.790	45.488	88.047	65.128	–3.746
3,900	7,020	13.796	46.867	88.405	66.643	–3.734
4,000	7,200	13.801	48.247	88.755	68.158	–3.724
4,100	7,380	13.806	49.627	89.096	69.678	–3.714
4,200	7,560	13.811	51.008	89.428	71.201	–3.705
4,300	7,740	13.816	52.390	89.753	72.727	–3.696
4,400	7,920	13.820	53.771	90.071	74.247	–3.688
4,500	8,100	13.824	55.154	90.382	75.772	–3.680
4,600	8,280	13.828	56.536	90.686	77.304	–3.673
4,700	8,460	13.831	57.919	90.983	78.833	–3.666
4,800	8,640	13.834	59.302	91.274	80.366	–3.659
4,900	8,820	13.837	60.686	91.559	81.894	–3.652
5,000	9,000	13.840	62.070	91.839	83.428	–3.646
5,100	9,180	13.843	63.454	92.113	84.966	–3.641
5,200	9,360	13.846	64.838	92.382	86.501	–3.635
5,300	9,540	13.848	66.223	92.646	88.044	–3.630
5,400	9,720	13.850	67.608	92.905	89.579	–3.625
5,500	9,900	13.852	68.993	93.159	91.128	–3.621
5,600	10,080	13.854	70.379	93.408	92.673	–3.617
5,700	10,260	13.856	71.764	93.654	94.215	–3.612
5,800	10,440	13.858	73.150	93.895	95.767	–3.608
5,900	10,620	13.860	74.536	94.132	97.313	–3.605
6,000	10,800	13.862	75.922	94.365	98.866	–3.601
K	°R	$\frac{\text{cal}}{\text{gmole}\cdot\text{K}}$	$\frac{\text{kcal}}{\text{gmole}}$	$\frac{\text{cal}}{\text{gmole}\cdot\text{K}}$	$\frac{\text{kcal}}{\text{gmole}}$	—

Source: JANAF Thermochemical Tables, 2nd Edition, National Bureau of Standards, Publication NSRDSNB537, 1971.

Table B.18 Thermochemical Properties of Nitrogen

Nitrogen (N_2) September 30, 1965
$MW = 28.0134$
$\bar{h}_f^0 = 0.000$ kcal/gmole

T		$\bar{C}_p^0$	$\bar{h}\langle T\rangle - \bar{h}\langle T_0\rangle$	$\bar{s}^0\langle T\rangle$	$\Delta G^0\langle T\rangle$	$\log K_p$
0	0	0.000	–2.072	0.000	0.000	0.000
100	180	6.956	–1.379	38.170	0.000	0.000
200	360	6.957	–0.683	42.992	0.000	0.000
298	536	6.961	0.000	45.770	0.000	0.000
300	540	6.961	0.013	45.813	0.000	0.000
400	720	6.990	0.710	47.818	0.000	0.000
500	900	7.069	1.413	49.386	0.000	0.000
600	1,080	7.196	2.125	50.685	0.000	0.000
700	1,260	7.350	2.853	51.806	0.000	0.000
800	1,440	7.512	3.596	52.798	0.000	0.000
900	1,620	7.670	4.355	53.692	0.000	0.000
1,000	1,800	7.815	5.129	54.507	0.000	0.000
1,100	1,980	7.945	5.917	55.258	0.000	0.000
1,200	2,160	8.061	6.718	55.955	0.000	0.000
1,300	2,340	8.162	7.529	56.604	0.000	0.000
1,400	2,520	8.252	8.350	57.212	0.000	0.000
1,500	2,700	8.330	9.179	57.784	0.000	0.000
1,600	2,880	8.398	10.015	58.324	0.000	0.000
1,700	3,060	8.458	10.858	58.835	0.000	0.000
1,800	3,240	8.512	11.707	59.320	0.000	0.000
1,900	3,420	8.559	12.560	59.782	0.000	0.000
2,000	3,600	8.601	13.418	60.222	0.000	0.000
2,100	3,780	8.638	14.280	60.642	0.000	0.000
2,200	3,960	8.672	15.146	61.045	0.000	0.000
2,300	4,140	8.703	16.015	61.431	0.000	0.000
2,400	4,320	8.731	16.886	61.802	0.000	0.000
2,500	4,500	8.756	17.761	62.159	0.000	0.000
2,600	4,680	8.779	18.638	62.503	0.000	0.000
2,700	4,860	8.800	19.517	62.835	0.000	0.000
2,800	5,040	8.820	20.398	63.155	0.000	0.000
2,900	5,220	8.838	21.280	63.465	0.000	0.000
K	°R	$\frac{\text{cal}}{\text{gmole}\cdot\text{K}}$	$\frac{\text{kcal}}{\text{gmole}}$	$\frac{\text{cal}}{\text{gmole}\cdot\text{K}}$	$\frac{\text{kcal}}{\text{gmole}}$	—

Table B.18 Continued

Nitrogen (N_2)
$MW = 28.0134$
$\bar{h}_f^0 = 0.000$ kcal/gmole

T		$\bar{C}_p^0$	$\bar{h}\langle T\rangle - \bar{h}\langle T_0\rangle$	$\bar{s}^0\langle T\rangle$	$\Delta G^0\langle T\rangle$	$\log K_p$
3,000	5,400	8.855	22.165	63.765	0.000	0.000
3,100	5,580	8.871	23.051	64.055	0.000	0.000
3,200	5,760	8.886	23.939	64.337	0.000	0.000
3,300	5,940	8.900	24.829	64.611	0.000	0.000
3,400	6,120	8.914	25.719	64.877	0.000	0.000
3,500	6,300	8.927	26.611	65.135	0.000	0.000
3,600	6,480	8.939	27.505	65.387	0.000	0.000
3,700	6,660	8.950	28.399	65.632	0.000	0.000
3,800	6,840	8.962	29.295	65.871	0.000	0.000
3,900	7,020	8.972	30.191	66.104	0.000	0.000
4,000	7,200	8.983	31.089	66.331	0.000	0.000
4,100	7,380	8.993	31.988	66.553	0.000	0.000
4,200	7,560	9.002	32.888	66.770	0.000	0.000
4,300	7,740	9.012	33.788	66.982	0.000	0.000
4,400	7,920	9.021	34.690	67.189	0.000	0.000
4,500	8,100	9.030	35.593	67.392	0.000	0.000
4,600	8,280	9.039	36.496	67.591	0.000	0.000
4,700	8,460	9.048	37.400	67.785	0.000	0.000
4,800	8,640	9.057	38.306	67.976	0.000	0.000
4,900	8,820	9.066	39.212	68.162	0.000	0.000
5,000	9,000	9.074	40.119	68.346	0.000	0.000
5,100	9,180	9.083	41.027	68.525	0.000	0.000
5,200	9,360	9.091	41.935	68.702	0.000	0.000
5,300	9,540	9.100	42.845	68.875	0.000	0.000
5,400	9,720	9.109	43.755	69.045	0.000	0.000
5,500	9,900	9.118	44.667	69.213	0.000	0.000
5,600	10,080	9.127	45.579	69.377	0.000	0.000
5,700	10,260	9.136	46.492	69.539	0.000	0.000
5,800	10,440	9.145	47.406	69.698	0.000	0.000
5,900	10,620	9.155	48.321	69.854	0.000	0.000
6,000	10,800	9.165	49.237	70.008	0.000	0.000
K	°R	$\frac{\text{cal}}{\text{gmole}\cdot\text{K}}$	$\frac{\text{kcal}}{\text{gmole}}$	$\frac{\text{cal}}{\text{gmole}\cdot\text{K}}$	$\frac{\text{kcal}}{\text{gmole}}$	—

Source: JANAF Thermochemical Tables, 2nd Edition, National Bureau of Standards, Publication NSRDSNB537, 1971.

Table B.19 Thermochemical Properties of Dinitrogen Monoxide

Dinitrogen Monoxide (N_2O) December 31, 1964
$MW = 44.016$
$\bar{h}_f^0 = 19.610$ kcal/gmole

T		$\bar{C}_p^0$	$\bar{h}\langle T\rangle - \bar{h}\langle T_0\rangle$	$\bar{s}^0\langle T\rangle$	$\Delta G^0\langle T\rangle$	$\log K_p$
0	0	0.000	–2.290	0.000	20.430	infinite
100	180	7.015	–1.594	43.988	21.573	–47.145
200	360	8.033	–0.849	49.108	23.185	–25.334
298	536	9.230	0.000	52.546	24.896	–18.248
300	540	9.250	0.017	52.603	24.928	–18.159
400	720	10.201	0.992	55.400	26.716	–14.596
500	900	10.953	2.051	57.761	28.514	–12.463
600	1,080	11.565	3.178	59.813	30.311	–11.040
700	1,260	12.070	4.360	61.635	32.097	–10.021
800	1,440	12.486	5.589	63.275	33.873	–9.253
900	1,620	12.830	6.855	64.766	35.638	–8.654
1,000	1,800	13.113	8.153	66.133	37.391	–8.171
1,100	1,980	13.348	9.476	67.394	39.132	–7.774
1,200	2,160	13.544	10.821	68.565	40.863	–7.442
1,300	2,340	13.707	12.184	69.655	42.583	–7.158
1,400	2,520	13.845	13.562	70.676	44.293	–6.914
1,500	2,700	13.961	14.952	71.635	45.996	–6.701
1,600	2,880	14.060	16.353	72.540	47.691	–6.514
1,700	3,060	14.145	17.764	73.395	49.377	–6.347
1,800	3,240	14.218	19.182	74.205	51.054	–6.198
1,900	3,420	14.282	20.607	74.976	52.728	–6.065
2,000	3,600	14.337	22.038	75.710	54.392	–5.943
2,100	3,780	14.385	23.474	76.411	56.049	–5.833
2,200	3,960	14.428	24.915	77.081	57.703	–5.732
2,300	4,140	14.466	26.359	77.723	59.350	–5.639
2,400	4,320	14.499	27.808	78.339	60.993	–5.554
2,500	4,500	14.529	29.259	78.932	62.630	–5.475
2,600	4,680	14.556	30.713	79.502	64.262	–5.401
2,700	4,860	14.580	32.170	80.052	65.894	–5.333
2,800	5,040	14.602	33.629	80.583	67.517	–5.270
2,900	5,220	14.621	35.090	81.095	69.140	–5.210
K	°R	$\frac{\text{cal}}{\text{gmole}\cdot\text{K}}$	$\frac{\text{kcal}}{\text{gmole}}$	$\frac{\text{cal}}{\text{gmole}\cdot\text{K}}$	$\frac{\text{kcal}}{\text{gmole}}$	—

Table B.19 Continued

Dinitrogen Monoxide (N_2O)
$MW = 44.016$
$\bar{h}_f^0 = 19.610$ kcal/gmole

T		$\bar{C}_p^0$	$\bar{h}\langle T\rangle - \bar{h}\langle T_0\rangle$	$\bar{s}^0\langle T\rangle$	$\Delta G^0\langle T\rangle$	$\log K_p$
3,000	5,400	14.639	36.533	81.591	70.757	–5.154
3,100	5,580	14.655	38.018	82.072	72.371	–5.102
3,200	5,760	14.670	39.484	82.537	73.981	–5.052
3,300	5,940	14.784	40.952	82.989	75.591	–5.006
3,400	6,120	14.696	42.421	83.427	77.196	–4.962
3,500	6,300	14.707	43.891	83.853	78.797	–4.920
3,600	6,480	14.718	45.363	84.268	80.400	–4.881
3,700	6,660	14.727	46.835	84.671	81.995	–4.843
3,800	6,840	14.736	48.308	85.064	83.591	–4.807
3,900	7,020	14.745	49.782	85.447	85.183	–4.773
4,000	7,200	14.752	51.257	85.820	86.774	–4.741
4,100	7,380	14.760	52.733	86.185	88.365	–4.710
4,200	7,560	14.766	54.209	86.541	89.951	–4.680
4,300	7,740	14.772	55.686	86.888	91.537	–4.652
4,400	7,920	14.778	57.163	87.228	93.120	–4.625
4,500	8,100	14.784	58.641	87.560	94.703	–4.599
4,600	8,280	14.789	60.120	87.885	96.288	–4.574
4,700	8,460	14.794	61.599	88.203	97.860	–4.550
4,800	8,640	14.798	63.079	88.515	99.441	–4.527
4,900	8,820	14.802	64.559	88.820	101.011	–4.505
5,000	9,000	14.806	66.039	89.119	102.590	–4.484
5,100	9,180	14.810	67.520	89.412	104.156	–4.463
5,200	9,360	14.814	69.001	89.700	105.733	–4.444
5,300	9,540	14.817	70.483	89.982	107.305	–4.425
5,400	9,720	14.820	71.965	90.259	108.872	–4.406
5,500	9,900	14.823	73.447	90.531	110.446	–4.388
5,600	10,080	14.826	74.929	90.798	112.010	–4.371
5,700	10,260	14.829	76.412	91.060	113.575	–4.354
5,800	10,440	14.831	77.895	91.318	115.142	–4.338
5,900	10,620	14.834	79.378	91.572	116.706	–4.323
6,000	10,800	14.836	80.862	91.821	118.267	–4.308
K	°R	$\frac{\text{cal}}{\text{gmole}\cdot\text{K}}$	$\frac{\text{kcal}}{\text{gmole}}$	$\frac{\text{cal}}{\text{gmole}\cdot\text{K}}$	$\frac{\text{kcal}}{\text{gmole}}$	—

Source: JANAF Thermochemical Tables, 2nd Edition, National Bureau of Standards, Publication NSRDSNB537, 1971.

Table B.20 Thermochemical Properties of Monatomic Oxygen

Oxygen, Monatomic (O) June 30, 1962
$MW = 16.000$
$\bar{h}_f^0 = 59.559$ kcal/gmole

T		$\bar{C}_p^0$	$\bar{h}\langle T\rangle - \bar{h}\langle T_0\rangle$	$\bar{s}^0\langle T\rangle$	$\Delta G^0\langle T\rangle$	$\log K_p$
0	0	0.000	–1.608	0.000	58.989	infinite
100	180	5.666	–1.080	32.466	57.989	–126.730
200	360	5.434	–0.523	36.340	56.733	–61.992
298	536	5.237	0.000	38.468	55.395	–40.604
300	540	5.235	0.010	38.501	55.369	–40.334
400	720	5.135	0.528	39.991	53.946	–29.473
500	900	5.081	1.038	41.131	52.485	–22.940
600	1,080	5.049	1.544	42.054	50.995	–18.574
700	1,260	5.029	2.048	42.831	49.486	–15.449
800	1,440	5.015	2.550	43.501	47.960	–13.101
900	1,620	5.006	3.052	44.092	46.422	–11.272
1,000	1,800	4.999	3.552	44.619	44.875	–9.807
1,100	1,980	4.994	4.051	45.095	43.318	–8.606
1,200	2,160	4.990	4.551	45.629	41.755	–7.604
1,300	2,340	4.987	5.049	45.928	40.186	–6.755
1,400	2,520	4.984	5.548	46.298	38.611	–6.027
1,500	2,700	4.982	6.046	46.642	37.032	–5.395
1,600	2,880	4.981	6.544	46.963	35.448	–4.842
1,700	3,060	4.979	7.042	47.265	33.862	–4.353
1,800	3,240	4.979	7.540	47.550	32.271	–3.918
1,900	3,420	4.978	8.038	47.819	30.678	–3.529
2,000	3,600	4.978	8.536	48.074	29.082	–3.178
2,100	3,780	4.978	9.034	48.317	27.484	–2.860
2,200	3,960	4.979	9.532	48.549	25.884	–2.571
2,300	4,140	4.980	10.029	48.770	24.282	–2.307
2,400	4,320	4.981	10.527	48.982	22.679	–2.065
2,500	4,500	4.984	11.026	49.185	21.073	–1.842
2,600	4,680	4.986	11.524	49.381	19.467	–1.636
2,700	4,860	4.990	12.023	49.569	17.859	–1.446
2,800	5,040	4.994	12.522	49.751	16.251	–1.268
2,900	5,220	4.999	13.022	49.926	14.642	–1.103
K	°R	$\frac{\text{cal}}{\text{gmole}\cdot\text{K}}$	$\frac{\text{kcal}}{\text{gmole}}$	$\frac{\text{cal}}{\text{gmole}\cdot\text{K}}$	$\frac{\text{kcal}}{\text{gmole}}$	—

Table B.20 Continued

Oxygen, Monatomic (O)
$MW = 16.000$
$\bar{h}_f^0 = 59.559$ kcal/gmole

T		$\bar{C}_p^0$	$\bar{h}\langle T\rangle - \bar{h}\langle T_0\rangle$	$\bar{s}^0\langle T\rangle$	$\Delta G^0\langle T\rangle$	$\log K_p$
3,000	5,400	5.004	13.522	50.096	13.031	–0.949
3,100	5,580	5.010	14.023	50.260	11.420	–0.805
3,200	5,760	5.017	14.524	50.419	9.807	–0.670
3,300	5,940	5.025	15.026	50.573	8.194	–0.543
3,400	6,120	5.033	15.529	50.724	6.581	–0.423
3,500	6,300	5.041	16.033	50.870	4.967	–0.310
3,600	6,480	5.050	16.537	51.012	3.354	–0.204
3,700	6,660	5.060	17.043	51.150	1.739	–0.103
3,800	6,840	5.070	17.549	51.285	0.125	–0.007
3,900	7,020	5.081	18.057	51.417	–1.492	0.084
4,000	7,200	5.091	18.565	51.546	–3.107	0.170
4,100	7,380	5.103	19.075	51.672	–4.723	0.252
4,200	7,560	5.114	19.586	51.795	–6.339	0.330
4,300	7,740	5.126	20.098	51.915	–7.955	0.404
4,400	7,920	5.138	20.611	52.033	–9.573	0.475
4,500	8,100	5.150	21.126	52.149	–11.189	0.543
4,600	8,280	5.162	21.641	52.262	–12.805	0.608
4,700	8,460	5.174	22.158	52.373	–14.423	0.671
4,800	8,640	5.186	22.676	52.482	–16.041	0.730
4,900	8,820	5.198	23.195	52.589	–17.661	0.788
5,000	9,000	5.210	23.715	52.695	–19.279	0.843
5,100	9,180	5.222	24.237	52.798	–20.896	0.895
5,200	9,360	5.234	24.760	52.899	–22.517	0.946
5,300	9,540	5.246	25.284	52.999	–24.134	0.995
5,400	9,720	5.258	25.809	53.097	–25.755	1.042
5,500	9,900	5.269	26.335	53.194	–27.373	1.088
5,600	10,080	5.280	26.863	53.289	–28.995	1.132
5,700	10,260	5.292	27.392	53.383	–30.616	1.174
5,800	10,440	5.302	27.921	53.475	–32.234	1.215
5,900	10,620	5.313	28.452	53.565	–33.856	1.254
6,000	10,800	5.323	28.984	53.655	–35.476	1.292
K	°R	$\frac{\text{cal}}{\text{gmole}\cdot\text{K}}$	$\frac{\text{kcal}}{\text{gmole}}$	$\frac{\text{cal}}{\text{gmole}\cdot\text{K}}$	$\frac{\text{kcal}}{\text{gmole}}$	—

Source: JANAF Thermochemical Tables, 2nd Edition, National Bureau of Standards, Publication NSRDSNB537, 1971.

Table B.21 Thermochemical Properties of Hydroxyl

Hydroxyl (OH) March 31, 1966
$MW = 17.0074$
$\bar{h}_f^0 = 9{,}432$ kcal/gmole

T		$\bar{C}_p^0$	$\bar{h}\langle T\rangle - \bar{h}\langle T_0\rangle$	$\bar{s}^0\langle T\rangle$	$\Delta G^0\langle T\rangle$	$\log K_p$
0	0	0.000	–2.192	0.000	9.289	infinite
100	180	7.798	–1.467	35.726	9.001	–19.672
200	360	7.356	–0.711	40.985	8.671	–9.475
298	536	7.167	0.000	43.880	8.307	–6.089
300	540	7.165	0.013	43.925	8.299	–6.046
400	720	7.087	0.725	45.974	7.920	–4.327
500	900	7.055	1.432	47.551	7.540	–3.296
600	1,080	7.057	2.137	48.837	7.163	–2.609
700	1,260	7.090	2.845	49.927	6.791	–2.120
800	1,440	7.150	3.556	50.877	6.424	–1.755
900	1,620	7.233	4.275	51.724	6.062	–1.472
1,000	1,800	7.332	5.003	52.491	5.706	–1.247
1,100	1,980	7.439	5.742	53.195	5.353	–1.064
1,200	2,160	7.549	6.491	53.847	5.005	–0.912
1,300	2,340	7.659	7.252	54.455	4.661	–0.784
1,400	2,520	7.766	8.023	55.027	4.318	–0.674
1,500	2,700	7.867	8.805	55.566	3.980	–0.580
1,600	2,880	7.963	9.596	56.077	3.642	–0.497
1,700	3,060	8.053	10.397	56.563	3.307	–0.425
1,800	3,240	8.137	11.207	57.023	2.975	–0.361
1,900	3,420	8.214	12.024	57.467	2.645	–0.304
2,000	3,600	8.286	12.849	57.891	2.313	–0.253
2,100	3,780	8.353	13.681	58.296	1.988	–0.207
2,200	3,960	8.415	14.520	58.686	1.662	–0.165
2,300	4,140	8.472	15.364	59.062	1.336	–0.127
2,400	4,320	8.526	16.214	59.424	1.014	–0.092
2,500	4,500	8.576	17.069	59.773	0.690	–0.060
2,600	4,680	8.622	17.929	60.110	0.372	–0.031
2,700	4,860	8.665	18.794	60.436	0.054	–0.004
2,800	5,040	8.706	19.662	60.752	–0.264	0.021
2,900	5,220	8.744	20.535	61.058	–0.578	0.044
K	°R	$\frac{\text{cal}}{\text{gmole}\cdot\text{K}}$	$\frac{\text{kcal}}{\text{gmole}}$	$\frac{\text{cal}}{\text{gmole}\cdot\text{K}}$	$\frac{\text{kcal}}{\text{gmole}}$	—

Table B.21 Continued

Hydroxyl (OH)
$MW = 17.0074$
$\bar{h}_f^0 = 9{,}432$ kcal/gmole

T		$\bar{C}_p^0$	$\bar{h}\langle T\rangle - \bar{h}\langle T_0\rangle$	$\bar{s}^0\langle T\rangle$	$\Delta G^0\langle T\rangle$	$\log K_p$
3,000	5,400	8.780	21.411	61.355	–0.893	0.065
3,100	5,580	8.814	22.291	61.644	–1.208	0.085
3,200	5,760	8.846	23.174	61.924	–1.519	0.104
3,300	5,940	8.876	24.060	62.197	–1.829	0.121
3,400	6,120	8.905	24.949	62.462	–2.137	0.137
3,500	6,300	8.933	25.841	62.721	–2.446	0.153
3,600	6,480	8.959	26.735	62.973	–2.751	0.167
3,700	6,660	8.984	27.632	63.218	–3.052	0.180
3,800	6,840	9.008	28.532	63.458	–3.355	0.193
3,900	7,020	9.031	29.434	63.693	–3.660	0.205
4,000	7,200	9.053	30.338	63.922	–3.961	0.216
4,100	7,380	9.074	31.245	64.145	–4.256	0.233
4,200	7,560	9.095	32.153	64.364	–4.553	0.237
4,300	7,740	9.115	33.064	64.579	–4.851	0.247
4,400	7,920	9.134	33.976	64.788	–5.144	0.255
4,500	8,100	9.153	34.890	64.994	–5.439	0.264
4,600	8,280	9.171	35.807	65.195	–5.726	0.272
4,700	8,460	9.189	36.725	65.393	–6.018	0.280
4,800	8,640	9.206	37.644	65.586	–6.304	0.287
4,900	8,820	9.223	38.566	65.776	–6.592	0.294
5,000	9,000	9.239	39.489	65.963	–6.882	0.301
5,100	9,180	9.255	40.414	66.146	–7.162	0.307
5,200	9,360	9.271	41.340	66.326	–7.446	0.313
5,300	9,540	9.286	42.268	66.502	–7.722	0.316
5,400	9,720	9.301	43.197	66.676	–8.007	0.324
5,500	9,900	9.316	44.128	66.847	–8.284	0.329
5,600	10,080	9.330	45.080	67.015	–8.563	0.334
5,700	10,260	9.344	45.994	67.180	–8.837	0.339
5,800	10,440	9.358	46.929	67.343	–9.112	0.343
5,900	10,620	9.372	47.866	67.503	–9.385	0.348
6,000	10,800	9.386	48.803	67.661	–9.659	0.352
K	°R	$\frac{\text{cal}}{\text{gmole}\cdot\text{K}}$	$\frac{\text{kcal}}{\text{gmole}}$	$\frac{\text{cal}}{\text{gmole}\cdot\text{K}}$	$\frac{\text{kcal}}{\text{gmole}}$	—

Source: JANAF Thermochemical Tables, 2nd Edition, National Bureau of Standards, Publication NSRDSNB537, 1971.

Table B.22 Thermochemical Properties of Diatomic Oxygen

Oxygen, Diatomic (O_2) September 30, 1965
$MW = 31.9988$
$\bar{h}_f^0 = 0.000$ kcal/gmole

T		$\bar{C}_p^0$	$\bar{h}\langle T\rangle - \bar{h}\langle T_0\rangle$	$\bar{s}^0\langle T\rangle$	$\Delta G^0\langle T\rangle$	$\log K_p$
0	0	0.000	–2.075	0.000	0.000	0.000
100	180	6.958	–1.381	41.395	0.000	0.000
200	360	6.961	–0.685	46.218	0.000	0.000
298	536	7.020	0.000	49.004	0.000	0.000
300	540	7.023	0.013	49.047	0.000	0.000
400	720	7.196	0.724	51.091	0.000	0.000
500	900	7.431	1.455	52.722	0.000	0.000
600	1,080	7.670	2.210	54.098	0.000	0.000
700	1,260	7.883	2.988	55.297	0.000	0.000
800	1,440	8.063	3.786	56.361	0.000	0.000
900	1,620	8.212	4.600	57.320	0.000	0.000
1,000	1,800	8.336	5.427	58.192	0.000	0.000
1,100	1,980	8.439	6.266	58.991	0.000	0.000
1,200	2,160	8.527	7.114	59.729	0.000	0.000
1,300	2,340	8.604	7.971	60.415	0.000	0.000
1,400	2,520	8.674	8.835	61.055	0.000	0.000
1,500	2,700	8.738	9.706	61.656	0.000	0.000
1,600	2,880	8.800	10.583	62.222	0.000	0.000
1,700	3,060	8.858	11.465	62.757	0.000	0.000
1,800	3,240	8.916	12.354	63.265	0.000	0.000
1,900	3,420	8.973	13.249	63.749	0.000	0.000
2,000	3,600	9.029	14.149	64.210	0.000	0.000
2,100	3,780	9.084	15.054	64.652	0.000	0.000
2,200	3,960	9.139	15.966	65.076	0.000	0.000
2,300	4,140	9.194	16.882	65.483	0.000	0.000
2,400	4,320	9.248	17.804	65.876	0.000	0.000
2,500	4,500	9.301	18.732	66.254	0.000	0.000
2,600	4,680	9.354	19.664	66.620	0.000	0.000
2,700	4,860	9.405	20.602	66.974	0.000	0.000
2,800	5,040	9.455	21.545	67.317	0.000	0.000
2,900	5,220	9.503	22.493	67.650	0.000	0.000
K	°R	$\frac{\text{cal}}{\text{gmole}\cdot\text{K}}$	$\frac{\text{kcal}}{\text{gmole}}$	$\frac{\text{cal}}{\text{gmole}\cdot\text{K}}$	$\frac{\text{kcal}}{\text{gmole}}$	—

Table B.22 Continued

Oxygen, Diatomic (O_2)
$MW = 31.9988$
$\bar{h}_f^0 = 0.000$ kcal/gmole

T		$\bar{C}_p^0$	$\bar{h}\langle T\rangle - \bar{h}\langle T_0\rangle$	$\bar{s}^0\langle T\rangle$	$\Delta G^0\langle T\rangle$	$\log K_p$
3,000	5,400	9.551	23.446	67.973	0.000	0.000
3,100	5,580	9.596	24.403	68.287	0.000	0.000
3,200	5,760	9.640	25.365	68.592	0.000	0.000
3,300	5,940	9.682	26.331	68.889	0.000	0.000
3,400	6,120	9.723	27.302	69.179	0.000	0.000
3,500	6,300	9.762	28.276	69.461	0.000	0.000
3,600	6,480	9.799	29.254	69.737	0.000	0.000
3,700	6,660	9.835	30.236	70.006	0.000	0.000
3,800	6,840	9.869	31.221	70.269	0.000	0.000
3,900	7,020	9.901	32.209	70.525	0.000	0.000
4,000	7,200	9.932	33.201	70.776	0.000	0.000
4,100	7,380	9.961	34.196	71.022	0.000	0.000
4,200	7,560	9.988	35.193	71.262	0.000	0.000
4,300	7,740	10.015	36.193	71.498	0.000	0.000
4,400	7,920	10.039	37.196	71.728	0.000	0.000
4,500	8,100	10.062	38.201	71.954	0.000	0.000
4,600	8,280	10.084	39.208	72.176	0.000	0.000
4,700	8,460	10.104	40.218	72.393	0.000	0.000
4,800	8,640	10.123	41.229	72.606	0.000	0.000
4,900	8,820	10.140	42.242	72.814	0.000	0.000
5,000	9,000	10.156	43.257	73.019	0.000	0.000
5,100	9,180	10.172	44.274	73.221	0.000	0.000
5,200	9,360	10.187	45.292	73.418	0.000	0.000
5,300	9,540	10.200	46.311	73.613	0.000	0.000
5,400	9,720	10.213	47.332	73.803	0.000	0.000
5,500	9,900	10.225	48.353	73.991	0.000	0.000
5,600	10,080	10.237	49.377	74.175	0.000	0.000
5,700	10,260	10.247	50.401	74.356	0.000	0.000
5,800	10,440	10.258	51.426	74.535	0.000	0.000
5,900	10,620	10.267	52.452	74.710	0.000	0.000
6,000	10,800	10.276	53.479	74.883	0.000	0.000
K	°R	$\frac{\text{cal}}{\text{gmole}\cdot\text{K}}$	$\frac{\text{kcal}}{\text{gmole}}$	$\frac{\text{cal}}{\text{gmole}\cdot\text{K}}$	$\frac{\text{kcal}}{\text{gmole}}$	—

Source: JANAF Thermochemical Tables, 2nd Edition, National Bureau of Standards, Publication NSRDSNB537, 1971.

Table B.23 Thermochemical Properties of Sulfur

Sulfur (S) December 31, 1965
$MW = 32.064$
$\bar{h}_f^0 = 0.000$ kcal/gmole

T		$\bar{C}_p^0$	$\bar{h}\langle T\rangle - \bar{h}\langle T_0\rangle$	$\bar{s}^0\langle T\rangle$	$\Delta G^0\langle T\rangle$	$\log K_p$
0	0	0.000	–1.053	0.000	0.000	0.000
100	180	3.060	–0.889	2.965	0.000	0.000
200	360	4.639	–0.496	5.622	0.000	0.000
298	536	5.401	0.000	7.631	0.000	0.000
300	540	5.412	0.010	7.665	0.000	0.000
400	720	7.734	1.109	10.674	0.000	0.000
500	900	9.081	2.047	12.768	0.000	0.000
600	1,080	8.200	2.904	14.333	0.000	0.000
700	1,260	7.799	3.704	15.601	0.000	0.000
800	1,440	4.368	17.529	31.363	0.000	0.000
900	1,620	4.396	17.967	31.879	0.000	0.000
1,000	1,800	4.418	18.408	32.344	0.000	0.000
1,100	1,980	4.435	18.851	32.765	0.000	0.000
1,200	2,160	4.450	19.295	33.152	0.000	0.000
1,300	2,340	4.461	19.740	33.509	0.000	0.000
1,400	2,520	4.471	20.187	33.840	0.000	0.000
1,500	2,700	4.480	20.635	34.148	0.000	0.000
1,600	2,880	4.488	21.083	34.438	0.000	0.000
1,700	3,060	4.495	21.532	34.710	0.000	0.000
1,800	3,240	4.501	21.982	34.967	0.000	0.000
1,900	3,420	4.507	22.432	35.211	0.000	0.000
2,000	3,600	4.513	22.883	35.442	0.000	0.000
2,100	3,780	4.518	23.335	35.662	0.000	0.000
2,200	3,960	4.523	23.787	35.873	0.000	0.000
2,300	4,140	4.528	24.240	36.074	0.000	0.000
2,400	4,320	4.632	24.693	36.267	0.000	0.000
2,500	4,500	4.537	25.146	36.452	0.000	0.000
2,600	4,680	4.541	25.600	36.630	0.000	0.000
2,700	4,860	4.545	26.054	36.801	0.000	0.000
2,800	5,040	4.549	26.509	36.966	0.000	0.000
2,900	5,220	4.553	26.964	37.126	0.000	0.000
K	°R	$\frac{\text{cal}}{\text{gmole}\cdot\text{K}}$	$\frac{\text{kcal}}{\text{gmole}}$	$\frac{\text{cal}}{\text{gmole}\cdot\text{K}}$	$\frac{\text{kcal}}{\text{gmole}}$	—

Table B.23 Continued

Sulfur (S)
$MW = 32.064$
$\bar{h}_f^0 = 0.000$ kcal/gmole

T		$\bar{C}_p^0$	$\bar{h}\langle T\rangle - \bar{h}\langle T_0\rangle$	$\bar{s}^0\langle T\rangle$	$\Delta G^0\langle T\rangle$	$\log K_p$
3,000	5,400	4.557	27.420	37.281	0.000	0.000
3,100	5,580	4.561	27.875	37.430	0.000	0.000
3,200	5,760	4.565	28.332	37.575	0.000	0.000
3,300	5,940	4.568	28.788	37.715	0.000	0.000
3,400	6,120	4.572	29.245	37.852	0.000	0.000
3,500	6,300	4.575	29.703	37.984	0.000	0.000
3,600	6,480	4.579	30.160	38.113	0.000	0.000
3,700	6,660	4.583	30.619	38.239	0.000	0.000
3,800	6,840	4.586	31.077	38.361	0.000	0.000
3,900	7,020	4.590	31.536	38.480	0.000	0.000
4,000	7,200	4.593	31.995	38.597	0.000	0.000
4,100	7,380	4.596	32.454	38.710	0.000	0.000
4,200	7,560	4.600	32.914	38.821	0.000	0.000
4,300	7,740	4.603	33.374	38.929	0.000	0.000
4,400	7,920	4.607	33.835	39.035	0.000	0.000
4,500	8,100	4.610	34.296	39.139	0.000	0.000
4,600	8,280	4.613	34.757	39.240	0.000	0.000
4,700	8,460	4.617	35.218	39.339	0.000	0.000
4,800	8,640	4.620	35.680	39.436	0.000	0.000
4,900	8,820	4.624	36.142	39.532	0.000	0.000
5,000	9,000	4.627	36.605	39.625	0.000	0.000
5,100	9,180	4.630	37.068	39.717	0.000	0.000
5,200	9,360	4.633	37.531	39.807	0.000	0.000
5,300	9,540	4.637	37.994	39.895	0.000	0.000
5,400	9,720	4.640	38.458	39.982	0.000	0.000
5,500	9,900	4.643	38.922	40.067	0.000	0.000
5,600	10,080	4.647	39.387	40.151	0.000	0.000
5,700	10,260	4.650	39.852	40.233	0.000	0.000
5,800	10,440	4.653	40.317	40.314	0.000	0.000
5,900	10,620	4.656	40.782	40.393	0.000	0.000
6,000	10,800	4.660	41.248	40.472	0.000	0.000
K	°R	$\frac{\text{cal}}{\text{gmole}\cdot\text{K}}$	$\frac{\text{kcal}}{\text{gmole}}$	$\frac{\text{cal}}{\text{gmole}\cdot\text{K}}$	$\frac{\text{kcal}}{\text{gmole}}$	—

Source: JANAF Thermochemical Tables, 2nd Edition, National Bureau of Standards, Publication NSRDSNB537, 1971.

Table B.24 Thermochemical Properties of Sulfur Dioxide

Sulfur Dioxide (SO_2) June 30, 1961
$MW = 64.066$
$\bar{h}_f^0 = -70.947$ kcal/gmole

T		$\bar{C}_p^0$	$\bar{h}\langle T\rangle - \bar{h}\langle T_0\rangle$	$\bar{s}^0\langle T\rangle$	$\Delta G^0\langle T\rangle$	$\log K_p$
0	0	0.000	–2.522	0.000	–70.341	infinite
100	180	8.013	–1.725	49.932	–70.966	155.088
200	360	8.693	–0.893	55.670	–71.425	78.046
298	536	9.530	0.000	59.298	–71.741	52.585
300	540	9.547	0.018	59.357	–71.746	52.264
400	720	10.395	1.016	62.222	–71.947	39.308
500	900	11.132	2.093	64.623	–71.923	31.436
600	1,080	11.723	3.237	66.707	–71.790	26.148
700	1,260	12.180	4.433	68.550	–71.562	22.342
800	1,440	12.532	5.669	70.200	–72.574	19.825
900	1,620	12.806	6.937	71.693	–70.822	17.197
1,000	1,800	13.022	8.229	73.054	–69.071	15.095
1,100	1,980	13.194	9.540	74.303	–67.326	13.376
1,200	2,160	13.335	10.866	75.458	–65.582	11.943
1,300	2,340	13.451	12.206	76.530	–63.840	10.732
1,400	2,520	13.549	13.556	77.530	–62.102	9.694
1,500	2,700	13.632	14.915	78.468	–60.369	8.795
1,600	2,880	13.704	16.282	79.350	–58.635	8.009
1,700	3,060	13.767	17.656	80.183	–56.905	7.316
1,800	3,240	13.822	19.035	80.971	–55.178	6.699
1,900	3,420	13.872	20.420	81.720	–53.452	6.148
2,000	3,600	13.917	21.809	82.433	–51.731	5.653
2,100	3,780	13.958	23.203	83.113	–50.010	5.204
2,200	3,960	13.995	24.601	83.763	–48.290	4.797
2,300	4,140	14.030	26.002	84.386	–46.573	4.425
2,400	4,320	14.063	27.407	84.984	–44.855	4.084
2,500	4,500	14.093	28.815	85.558	–43.141	3.771
2,600	4,680	14.122	30.225	86.112	–41.426	3.482
2,700	4,860	14.149	31.639	86.645	–39.713	3.214
2,800	5,040	14.175	33.055	87.160	–38.002	2.966
2,900	5,220	14.200	34.474	87.658	–36.288	2.735
K	°R	$\frac{\text{cal}}{\text{gmole}\cdot\text{K}}$	$\frac{\text{kcal}}{\text{gmole}}$	$\frac{\text{cal}}{\text{gmole}\cdot\text{K}}$	$\frac{\text{kcal}}{\text{gmole}}$	—

Table B.24 Continued

Sulfur Dioxide (SO_2)
$MW = 64.066$
$\bar{h}_f^0 = -70.947$ kcal/gmole

T		$\bar{C}_p^0$	$\bar{h}\langle T\rangle - \bar{h}\langle T_0\rangle$	$\bar{s}^0\langle T\rangle$	$\Delta G^0\langle T\rangle$	$\log K_p$
3,000	5,400	14.224	35.895	88.140	–34.575	2.519
3,100	5,580	14.247	37.319	88.607	–32.864	2.317
3,200	5,760	14.270	38.745	89.059	–31.154	2.128
3,300	5,940	14.291	40.173	89.499	–29.446	1.950
3,400	6,120	14.312	41.603	89.926	–27.733	1.783
3,500	6,300	14.333	43.035	90.341	–26.026	1.625
3,600	6,480	14.353	44.469	90.745	–24.313	1.476
3,700	6,660	14.373	45.906	91.138	–22.602	1.335
3,800	6,840	14.392	47.344	91.522	–20.890	1.201
3,900	7,020	14.411	48.784	91.896	–19.183	1.075
4,000	7,200	14.430	50.226	92.261	–17.469	0.954
4,100	7,380	14.448	51.670	92.618	–15.758	0.840
4,200	7,560	14.467	53.116	92.966	–14.047	0.731
4,300	7,740	14.485	54.563	93.307	–12.333	0.627
4,400	7,920	14.502	56.013	93.640	–10.623	0.528
4,500	8,100	14.520	57.464	93.966	–8.908	0.433
4,600	8,280	14.537	58.917	94.285	–7.194	0.342
4,700	8,460	14.554	60.371	94.598	–5.482	0.255
4,800	8,640	14.572	61.828	94.905	–3.769	0.172
4,900	8,820	14.588	63.286	95.205	–2.056	0.092
5,000	9,000	14.605	64.745	95.500	–0.345	0.015
5,100	9,180	14.622	66.207	95.790	1.375	–0.059
5,200	9,360	14.639	67.670	96.074	3.087	–0.130
5,300	9,540	14.655	69.134	96.353	4.806	–0.198
5,400	9,720	14.672	70.601	96.627	6.518	–0.264
5,500	9,900	14.688	72.069	96.896	8.237	–0.327
5,600	10,080	14.704	73.538	97.161	9.952	–0.388
5,700	10,260	14.720	75.010	97.421	11.665	–0.447
5,800	10,440	14.736	76.482	97.677	13.387	–0.504
5,900	10,620	14.753	77.957	97.930	15.099	–0.559
6,000	10,800	14.769	79.433	98.178	16.823	–0.613
K	°R	$\frac{\text{cal}}{\text{gmole}\cdot\text{K}}$	$\frac{\text{kcal}}{\text{gmole}}$	$\frac{\text{cal}}{\text{gmole}\cdot\text{K}}$	$\frac{\text{kcal}}{\text{gmole}}$	—

Source: JANAF Thermochemical Tables, 2nd Edition, National Bureau of Standards, Publication NSRDSNB537, 1971.

Table B.25 Thermochemical Properties of Air

Air[a]
$MW = 28.964$
$\bar{h}_f^0 = 0.000$ kcal/gmole

T		$\bar{C}_p^0$	$\bar{h}\langle T\rangle - \bar{h}\langle T_0\rangle$	$\bar{s}^0\langle T\rangle$	$\Delta G^0\langle T\rangle$	$\log K_p$
0	0	0.000	–2.050	0.000	0.000	0.000
100	180	7.050	–1.359	38.704	0.000	0.000
200	360	6.956	–0.666	43.556	0.000	0.000
298	536	6.947	0.000	46.255	0.000	0.000
300	540	6.949	0.035	46.372	0.000	0.000
400	720	7.010	0.732	48.378	0.000	0.000
500	900	7.122	1.439	49.954	0.000	0.000
600	1,080	7.268	2.158	51.265	0.000	0.000
700	1,260	7.432	2.893	52.397	0.000	0.000
800	1,440	7.598	3.644	53.400	0.000	0.000
900	1,620	7.756	4.412	54.305	0.000	0.000
1,000	1,800	7.893	5.195	55.129	0.000	0.000
1,100	1,980	8.006	5.990	55.887	0.000	0.000
1,200	2,160	8.109	6.796	56.588	0.000	0.000
1,300	2,340	8.203	7.611	57.241	0.000	0.000
1,400	2,520	8.289	8.436	57.852	0.000	0.000
1,500	2,700	8.367	9.269	58.427	0.000	0.000
1,600	2,880	8.437	10.109	58.969	0.000	0.000
1,700	3,060	8.502	10.956	59.482	0.000	0.000
1,800	3,240	8.560	11.809	59.970	0.000	0.000
1,900	3,420	8.612	12.668	60.434	0.000	0.000
2,000	3,600	8.661	13.532	60.877	0.000	0.000
2,100	3,780	8.704	14.400	61.301	0.000	0.000
2,200	3,960	8.743	15.272	61.707	0.000	0.000
2,300	4,140	8.779	16.148	62.097	0.000	0.000
2,400	4,320	8.812	17.028	62.471	0.000	0.000
2,500	4,500	8.842	17.911	62.831	0.000	0.000
2,600	4,680	8.869	18.796	63.178	0.000	0.000
2,700	4,860	8.895	19.684	63.513	0.000	0.000
2,800	5,040	8.918	20.575	63.837	0.000	0.000
2,900	5,220	8.940	21.468	64.150	0.000	0.000
3,000	5,400	8.962	22.363	64.454	0.000	0.000
3,100	5,580	8.987	23.249	64.545	0.000	0.000
3,200	5,760	9.008	24.149	64.740	0.000	0.000
3,300	5,940	9.027	25.051	65.018	0.000	0.000
3,400	6,120	9.047	25.955	65.288	0.000	0.000
3,500	6,300	9.065	26.860	65.550	0.000	0.000
K	°R	$\frac{\text{cal}}{\text{gmole}\cdot\text{K}}$	$\frac{\text{kcal}}{\text{gmole}}$	$\frac{\text{cal}}{\text{gmole}\cdot\text{K}}$	$\frac{\text{kcal}}{\text{gmole}}$	—

[a]78.11% N_2; 20.96% O_2; 0.93% argon by volume

Source: JANAF Thermochemical Tables, 2nd Edition, National Bureau of Standards, Publication NSRDSNB537, 1971.

APPENDIX C. PROPERTIES OF FUEL OIL

Fuel Oil Specific Gravity, Density, and Heats of Combustion

Gravity at 60/60°F		Density at 60°F		Higher Heating Value (Constant Volume)				Lower Heating Value (Constant Pressure)			
5	1.0366	1,036	8.643	4.395	42,450	157,700	18,250	4.164	40,220	149,400	17,290
6	1.0291	1,028	8.580	4.384	42,640	157,300	18,330	4.147	40,335	148,800	17,340
7	1.0217	1,021	8.518	4.365	42,775	156,600	18,390	4.128	40,450	148,100	17,390
8	1.0143	1,013	8.457	4.345	42,890	155,900	18,440	4.111	40,565	147,500	17,440
9	1.0071	1,006	8.397	4.329	43,000	155,300	18,490	4.094	40,680	146,900	17,490
10	1.0000	999.0	8.337	4.309	43,125	154,600	18,540	4.075	40,800	146,200	17,540
11	0.9930	992.0	8.279	4.290	43,240	153,900	18,590	4.058	40,890	145,600	17,580
12	0.9861	985.1	8.221	4.273	43,360	153,300	18,640	4.039	40,985	144,900	17,620
13	0.9792	978.3	8.164	4.253	43,470	152,600	18,690	4.019	41,100	144,200	17,670
14	0.9725	971.6	8.108	4.237	43,590	152,000	18,740	4.002	41,190	143,600	17,710
15	0.9659	965.0	8.053	4.217	43,705	151,300	18,790	3.983	41,285	142,900	17,750
16	0.9593	958.4	7.998	4.200	43,820	150,700	18,840	3.966	41,380	142,300	17,790
17	0.9529	951.9	7.944	4.181	43,940	150,000	18,890	3.947	41,450	141,600	17,820
18	0.9465	945.6	7.891	4.164	44,030	149,400	18,930	3.927	41,540	140,900	17,860
19	0.9402	939.4	7.839	4.147	44,150	148,800	18,980	3.910	41,635	140,300	17,900
20	0.9340	933.1	7.787	4.128	44,240	148,100	19,020	3.891	41,705	139,600	17,930
21	0.9279	927.0	7.736	4.111	44,330	147,500	19,060	3.874	41,775	139,000	17,960
22	0.9218	921.0	7.686	4.092	44,450	146,800	19,110	3.855	41,870	138,300	18,000
23	0.9159	915.0	7.636	4.075	44,540	146,200	19,150	3.838	41,940	137,700	18,030
24	0.9100	909.2	7.587	4.058	44,635	145,600	19,190	3.821	42,030	137,100	18,070
25	0.9042	903.3	7.538	4.041	44,730	145,000	19,230	3.802	42,100	136,400	18,100
26	0.8984	897.5	7.490	4.022	44,820	144,300	19,270	3.785	42,170	135,800	18,130
27	0.8927	891.9	7.443	4.005	44,915	143,700	19,310	3.768	42,240	135,200	18,160
28	0.8871	886.3	7.396	3.988	45,010	143,100	19,350	3.752	42,310	134,600	18,190
29	0.8816	880.8	7.350	3.972	45,080	142,500	19,380	3.732	42,380	133,900	18,220
30	0.8762	875.4	7.305	3.952	45,170	141,800	19,420	3.715	42,450	133,300	18,250
31	0.8708	870.0	7.260	3.936	45,240	141,200	19,450	3.699	42,520	132,700	18,280
32	0.8654	864.6	7.215	3.919	45,330	140,600	19,490	3.682	42,590	132,100	18,310
33	0.8602	859.3	7.171	3.902	45,405	140,000	19,520	3.665	42,635	131,500	18,330
34	0.8550	854.2	7.128	3.885	45,495	139,400	19,560	3.648	42,705	130,900	18,360
35	0.8498	849.0	7.085	3.869	45,565	138,800	19,590	3.632	42,775	130,300	18,390
36	0.8448	844.0	7.043	3.852	45,635	138,200	19,620	3.615	42,820	129,700	18,410
37	0.8398	838.9	7.001	3.835	45,705	137,600	19,650	3.598	42,870	129,100	18,430
38	0.8348	834.0	6.960	3.818	45,775	137,000	19,680	3.582	42,940	128,500	18,460
39	0.8299	829.2	6.920	3.802	45,870	136,400	19,720	3.565	42,985	127,900	18,480
40	0.8251	824.3	6.879	3.785	45,940	135,800	19,750	3.548	43,050	127,300	18,510
41	0.8203	819.5	6.839	3.768	46,010	135,200	19,780	3.531	43,100	126,700	18,530
42	0.8155	814.7	6.799	3.754	46,080	134,700	19,810	3.517	43,170	126,200	18,560
43	0.8109	810.1	6.760	3.738	46,125	134,100	19,830	3.501	43,220	125,600	18,580
44	0.8063	805.5	6.722	3.721	46,195	133,500	19,860	3.484	43,265	125,000	18,600
45	0.8017	800.9	6.684	3.704	46,265	132,900	19,890	3.467	43,310	124,400	18,620
46	0.7972	796.4	6.646	3.690	46,335	132,400	19,920	3.453	43,360	123,900	18,640
47	0.7927	792.0	6.609	3.676	46,380	131,900	19,940	3.437	43,405	123,300	18,660
48	0.7883	787.5	6.572	3.657	46,450	131,200	19,970	3.423	43,450	122,800	18,680
49	0.7839	783.2	6.536	3.643	46,520	130,700	20,000	3.406	43,495	122,200	18,700
API	—	kg/m^3	lbm/gal	$kJ/m^3 \times 10^{-7}$	kJ/kg	Btu/gal	Btu/lbm	$kJ/m^3 \times 10^{-7}$	kJ/kg	Btu/gal	Btu/lbm

Sources: Adapted from National Bureau of Standards Miscellaneous Publication No. 97, Thermal Properties of Petroleum Products, April 28, 1933; and Technical Bulletins from major oil companies, e.g., Exxon, Gulf, Mobil, Shell.

APPENDIX D. PROPERTIES OF SATURATED WATER

SI				
T_{sat}	P_{sat} [a]	C_p [b]	$\rho \times 10^3$ [a]	h_{fg} [a]
0	0.00061	4.217	1.0000	2501.4
10	0.001227	4.193	0.9996	2477.7
20	0.002339	4.182	0.9982	2454.1
30	0.004246	4.179	0.9957	2430.5
40	0.007384	4.179	0.9923	2406.7
50	0.012349	4.181	0.9880	2382.7
60	0.019940	4.185	0.9831	2358.5
70	0.03119	4.190	0.9777	2333.8
80	0.04739	4.197	0.9717	2308.8
90	0.07014	4.205	0.9653	2283.2
100	0.10135	4.216	0.9583	2257.0
110	0.14327	4.229	0.9509	2230.2
120	0.19853	4.245	0.9431	2202.6
130	0.2701	4.263	0.9348	2174.2
140	0.3613	4.285	0.9262	2144.7
150	0.4758	4.310	0.9170	2114.3
160	0.6178	4.339	0.9074	2082.6
170	0.7917	4.371	0.8974	2049.5
180	1.0021	4.408	0.8870	2015.0
190	1.2544	4.449	0.8761	1978.8
200	1.5538	4.497	0.8647	1940.7
210	1.9062	4.551	0.8528	1900.7
220	2.318	4.614	0.8403	1858.5
230	2.795	4.686	0.8273	1813.8
240	3.344	4.770	0.8136	1766.5
250	3.973	4.869	0.7992	1716.2
260	4.688	4.985	0.7840	1662.5
270	5.499	5.130	0.7679	1605.2
280	6.412	5.300	0.7507	1543.6
290	7.436	5.510	0.7323	1477.1
300	8.581	5.770	0.7125	1404.9
°C	MgPa	kJ/kg K	kg/m^3	kJ/kg

Sources: [a]Keenan, J. H., Keyes, F. G., Hill, P. G., and Moore, J. G., *Steam Tables* (S.I. Units), © John Wiley & Sons, Inc., New York, 1969. Reprinted with permission of John Wiley & Sons, Inc..

[b]*Tables on the Thermophysical Properties of Liquids and Gases*, 2nd Edition, N.B. Vargaftik, Hemisphere Publishing Co., Washington, D.C., 1975. With permission.

English Engineers				
T_{sat}	P_{sat}^{a}	C_p^{b}	ρ^{a}	h_{fg}^{a}
32	0.8859	1.007	62.414	1075.4
40	0.12166	1.005	62.422	1070.9
60	0.2563	1.000	62.364	1059.6
80	0.5073	0.998	62.216	1048.3
100	0.9503	0.997	61.996	1037.0
120	1.6945	0.997	61.709	1025.5
140	2.892	0.999	61.376	1014.0
160	4.745	1.001	60.994	1002.2
180	7.515	1.002	60.573	990.2
200	11.529	1.003	60.118	977.9
220	17.188	1.008	59.623	965.3
240	24.97	1.012	59.095	952.3
260	35.42	1.016	58.534	938.8
280	49.18	1.022	57.941	924.9
300	66.98	1.029	57.313	910.4
320	89.60	1.036	56.651	895.3
340	117.93	1.045	55.953	879.5
360	152.92	1.055	55.224	862.9
380	195.60	1.066	54.457	845.4
400	247.1	1.080	53.654	826.8
420	308.5	1.095	52.809	807.2
440	381.2	1.114	51.921	786.3
460	466.3	1.135	50.984	764.1
480	565.5	1.160	49.995	740.3
500	680.0	1.191	48.948	714.8
520	811.4	1.230	47.824	687.3
540	961.5	1.277	46.620	657.5
560	1131.8	1.337	45.310	625.0
580	1324.3	1.415	43.898	589.3
600	5141.0	1.524	42.319	549.7
°R	lbf/in^2	Btu/lbm °R	lbm/ft^3	Btu/lbm

Sources: [a]Keenan, J. H., Keyes, F. G., Hill, P. G., and Moore, J. G., *Steam Tables* (English Units), © John Wiley & Sons, Inc., New York, 1969. Reprinted with permission of John Wiley & Sons, Inc..

[b]*Tables on* the *Thermophysical Properties of Liquids and Gases*, 2nd Edition, N.B. Vargaftik, Hemisphere Publishing Co., Washington, D.C., 1975. With permission.